Proceedings of 2009 12th International Conference on Computer and Information Technology (ICCIT 2009)
21-23 December, 2009, Dhaka, Bangladesh

A Domain Independent Similar-Duplicate Detection Algorithm for Data Cleaning *(Not Presented)*

Kazi Shah Nawaz Ripon, Ashiqur Rahman, Shahariar Monjur
Computer Science and Engineering Discipline, Khulna University, Bangladesh
ripon_cseku@yahoo.com, 2ashiqur@gmail.com, shahariarr@yahoo.com

Abstract

Presence of similar-duplicate records causes over representation of data. If the database contains different representation of the same data, the result of data mining algorithm will be erroneous. Similar-duplicate detection is a hard task, especially when it is domain independent. To date, there are only a few attempts to tackle the domain independent duplicate detection problem. In this paper, we proposed a novel technique for bringing the similar-duplicate records closer. We also presented ideas for making similar-duplicate detection algorithms faster and efficient. A modification of the transitivity rule has also been proposed. Finally, we proposed a domain independent algorithm for similar-duplicate detection. The superiority of the proposed method over some other existing methods is also confirmed by the experimental results.

Keywords: Data cleaning, Domain independent, Similar-duplicate detection, Transitivity rule.

I. INTRODUCTION

Data mining [1] is a knowledge discovery process. It is used for extracting hidden patterns from data. Data mining algorithm assumes that the data will be clean and consistent. One of the major steps of data mining is data preparation. And, data cleaning is one of the steps of data preparation. It is also called data cleansing or scrubbing. It detects and removes errors and inconsistencies from data and improves its quality.

Duplicate record detection and elimination is a part of data cleaning problem. There are several reasons for records to be similarly duplicated which include typing errors, abbreviations, extra word, missing values, word transpositions, illegal values etc. Most of the works in this field focus on domain specific problem. Unfortunately, domain knowledge is not always available. For this reason, domain independent application is very much important.

To date, only a few works are available on domain independent techniques [2]-[4], which use pure transitivity rule. Yet, due to it's affect on the efficiency of duplicate detection algorithm, some authors proposed a modified form of the transitivity rule for domain specific techniques [3]. So far we know, there is no solution for domain independent techniques.

Usually most of the database table contains some unique or primary key field. And due to error in these fields, which contains mostly unique data, it is a common source of error in database. It is because common data are typically entered using drop-down or combo-box, which minimizes the occurrence of error in fields with common values. Still there is no suitable solution for the fields containing mostly unique data. The existing domain independent techniques for bringing similar records closer are not efficient enough for handling such types of problems [4].

This paper presents a domain independent technique for sorting similar records and a modification to the transitivity rule applicable into domain independent cases. It also considers time for performing the de-duplication on real-world data and proposes a new idea for making the duplicate detection algorithms faster for real-world data. In addition, a modification of an existing similar-string matching algorithm [2] has been proposed to make it more efficient. Finally, an algorithm implements all these techniques together. Experimental results show that the proposed schemes work better than the existing domain independent similar-string matching schemes.

The rest of this paper is organized as follows. Section II describes the related works. Section III presents the proposed methods and algorithms. Section IV contains experimental results and finally section V concludes the paper.

II. RELATED WORKS

Hernandez and Stolfo proposed one of the earlier works for similar-duplicate detection [5]. Their proposed Merge/Purge problem gives solution for domain specific problems, and it utilizes a sorting technique based on keys selected by user. Lee et al. proposed another idea for sorting similar records [6]. The efficiency of their method largely depends on user's selection of attributes. Moreover, it assumes that errors in the selected field will be removed using external source files. However, such source files for removing error is not always available and it is partially domain independent.

Monge and Elkan [4] proposed a completely domain independent work. Their proposed sorting method treats each record as one long string and sorts them lexicographically reading from left to right in one pass and right to left in another pass. The authors also proposed a priority queue technique for limiting the

978-1-4244-6283-4/09/$26.00 ©2009 IEEE

number of comparisons. Another work done by Udechukwu et al. [2] is quite related to the work presented in this paper. However, their proposed similar-string matching algorithm does not give an efficient result for some cases. With some modification, it can be made more efficient. The solution for transitivity rule proposed in [3] reduced the effect of transitivity rule during similar-duplicate detection. However, it is also domain specific.

III. OUR PROPOSED METHODS

A. Sorting the Similar Records

The sorting method proposed in [6] is not completely domain independent. In fact, it is partially domain independent, as it requires the user to select the most important fields for sorting the similar records. A completely domain independent technique for sorting the records was proposed in [4]. Still, this technique fails, if the database table contains most unique field in one side and less unique field in the other side. It also fails if error in the most unique field or some record is similarly duplicated for error in the first and last field. Whereas our proposed method works efficiently for solving the problem of error in unique field or when the error is in some other field, which has a high uniqueness value compared to others.

Table I represents the dataset, where data in all records are unique or they become unique due to some error. In this scenario, it is really hard to determine the sorting strategy. However, in a real-world dataset where it is much likely that some records will be similarly duplicated, we can assume that some of it's value will be exactly duplicated as in Table II. In these cases, the uniqueness of the fields will be affected.

For example, in Table I, uniqueness of Field-1, Field-2 and Field-3 are 100%, but in Table II, uniqueness of Field-2 become 75%. In Table II records R1 and R4 may be similar or not. If we use the uniqueness information and sort the dataset using the less unique field, R1 and R4 will be closer as in Table III.

B. Use Two String Matching Algorithms for Measuring the Similarity between Strings

Similar-string matching algorithms are expensive [4]. They need to perform more computations than exact string matching algorithms. In a real world dataset, the number of unique records will be many times greater than the number of duplicate records. Hence, performing an efficient similar-string matching algorithm is not needed when the number of characters in a string is much lower than the number of characters in the second string or the characters in one string does not appear in a certain amount in the second string. Therefore, the use of a fast string matching algorithm (that calls the efficient similar-string matching algorithm when the number of characters and the appearance of characters between two strings pass a threshold value) will save a lot of computational efforts.

Table I Dataset with all unique records

	Field-1	**Field-2**	**Field-3**
R1	A	B	C
R2	D	E	F
R3	G	H	I
R4	J	K	L

Table II Dataset with similar-duplicate records

	Field-1	**Field-2**	**Field-3**
R1	A	B	C
R2	D	E	F
R3	G	H	I
R4	J	B	L

Table III Dataset after sorting using uniqueness

	Field-1	**Field-2**	**Field-3**
R1	A	B	C
R4	J	B	L
R2	D	E	F
R3	G	H	I

C. Modification of the Positional Algorithm

Until now many string matching algorithms are available in the literature [7]. However, most of them do not handle abbreviations efficiently and for many cases, they do not give acceptable measures of similarity. One of the efficient similar-string matching algorithms is the positional string matching algorithm proposed in [2]. It can handle abbreviations efficiently and is able to measure the similarity between two strings much better than the classical string matching algorithms. However for some cases, it also fails to return a good measure of similarity.

For example, consider two strings: A="John" and B="Johnathon". Using the original positional algorithm we get a match score of 1. Whereas, there are 5 characters mismatch between A and B. A match score of 1 usually means that the strings are exact duplicate. Therefore, the match score of 1 is not acceptable. In fact, the original positional algorithm will return a match score of 1, irrespective of the number of characters in the left or right side of "John" in the second string B. This is because during the match score calculation, the algorithm considers only the length of the short string ignoring the length of the second string. As was doing in the original positional algorithm:

match score= (total match score returned by the shorter string / total number of characters in the

shorter string).

Since the match score returned by the shorter string, can also be seen as the match score returned by the longer string, the size of both strings should have effect on the calculation of the final match score. If the mach score is calculated as,

match score = (total match score returned by the shorter string / average number of characters in two strings)

for the above problem, we get a match score of 0.61 which is much more acceptable.

Algorithm 1: DIT

1. Assign PR=1 to the record which creates the window, call it R2.
2. Calculate R1's PR = (similarity between R2 and R1)*(PR of R2) and perform the following operations,

(2a) If R1 is a representative of a set then recalculates the PR of each record of the set with respect to the new PR of R1 in the set of R2.

Move all records from the set of R1 to the set of R2 whose new PR passes the threshold value.

From the remaining records of the set of R1 make a new representative, if any exists, and update the PR of other records with respect to this new representative.

(2b) Otherwise, if R1 is not a representative then if it's PR is higher in the set of R2 then move it to the set of R2 and update it's PR, otherwise not.

(2c) Otherwise, it is the first time, R1 is declaring similarity with some record, simply add it to the set of R2 and record it's PR in the set of R2

D. Domain Independent Transitivity Rule for Similar-Duplicate Detection

Transitivity rule states that if A is equivalent to B and B is equivalent to C then A is equivalent to C. Transitivity rule is used for similar-duplicate detection. In [3], an example was given to illustrate the problem of using transitivity rule for similar-duplicate record detection using one character threshold so that two strings will be similar. If there is only one character mismatch then "Father" is similar-duplicate of "Mather" and "Mather" is similar-duplicate of "Mother". According to the transitivity rule, "Father" is similar-duplicate of "Mother". Since there are two character mismatches between "Father" and "Mother"; "Father" and "Mother" are not similar-duplicates according to our threshold. For these types of problems, a very high threshold is required to separate the values. However, a very high threshold will lower the value of recall. A solution of the transitivity rule for detecting similar-duplicate records was proposed in [3] to obtain a high recall without declaring these types of values similar. However, all their proposed solution was rule based and it requires certainty factor; which in turn requires the user involvement in defining the certainty factors. Moreover, it was domain specific. So far we know, to reduce the effect of the transitivity rule, there is no solution for domain independent cases. Our proposed Domain Independent Transitivity (DIT) rule, described in Algorithm-1, for similar-duplicate detection is totally domain independent, and it does not require any rule or certainty factor or user involvement. In DIT algorithm, SIM stands for similarity and PR stands for power of a record. We call the latest record (the highest numbered record) in a window as the window creator. Input to the algorithm is two records: one is the window creator and the other is the record to which the window creator declares similarity (i.e. passes a threshold value). If the window creator does not declare similarity with some record, then there is no need to invoke the DIT algorithm.

Consider a pre-defined threshold 0.7 for declaring two records as duplicates. If the similarity between records R2 and R1 is ≥ 0.7 then R1 is a duplicate of R2 and a set {R2, R1 (this set is open because it still can grow) will be created. Associate a value PR with each record in the set. This value is the measurement of the ability of a record to bring another similar record in the set to which it belongs. If R2 declare a match with R1 in the dataset then $PR_{R2} = 1$ and PR_{R1} = (similarity between R2 and R1)* (PR_{R2}). If PR_{R1} is above the threshold value then a set {(R2, 1), (R1, PR_{R1}) will be created. Suppose there was another record R which was similar to R1 then PR_R = (similarity between R1 and R) *(PR_{R1}) will be recalculated with respect to R1's new PR in the new set and if the PR of R passes the threshold then it will also be moved to the set where R1 has moved. Otherwise R becomes the representative of the set.

If R1 is a exact duplicate of R2 then $SIM_{R2,R1} = 1$ and $PR_{R2} = 1$. As a result, $PR_{R1} = SIM_{R2,R1}*PR_{R2} = (1)*(1) = 1$. $PR_{R1}>0.7$, so, R1 will be accepted as a duplicate of R2.

If R1 is similar to R2 by half then $SIM_{R2,R1} = 0.5$ and $PR_{R2} = 1$. Hence, $PR_{R1} = SIM_{R2,R1}*PR_{R2} = (0.5)*(1) = 0.5$. $PR_{R1}<0.7$, so, R1 will not be accepted as a duplicate.

If $SIM_{R2,R1} = 0.9$ and $PR_{R2} = 1$ then $PR_{R1} = SIM_{R2,R1}*PR_{R2} = (0.9)*(1) = 0.9$. Since, $PR_{R1}>0.7$, R1 will be accepted as duplicate. Now, if R is exact duplicate to R1 then $PR_R = SIM_{R1,R}*PR_{R1} = (1)*(0.9) = 0.9 = PR_{R1}$. So, in case of exact duplicate PR is preserved.

However, if $SIM_{R2,R1} = 0.9$ and $PR_{R2} = 1$ then $PR_{R1} = SIM_{R2,R1}*PR_{R2} = (0.9)*(1) = 0.9$. $PR_{R1}>0.7$, so, R1 will be accepted as duplicate of R2. If now, $SIM_{R1,R}=0.8$, $PR_R = SIM_{R1,R}*PR_{R1} = (0.8)*(0.9) = 0.72$. Since $PR_R>0.7$, R will be accepted as duplicate in the set where R2 and R1 both exist.

Whereas, If $SIM_{R2,R1} = 0.8$ and $PR_{R2} = 1$ then $PR_{R1} = SIM_{R2,R1}*PR_{R2} = 0.8$. $PR_{R1}>0.7$, so, R1 will be

accepted as duplicate of R2. If now, $SIM_{R1,R} = 0.8$ then $PR_R = SIM_{R1,R} * PR_{R1} = 0.64$. $PR_R < 0.7$, so, R will not be accepted as a duplicate in the set where R2 exists. In order to be duplicate, $SIM_{R1,R}$ must be greater than 0.87. Here the achievement is that, as R1 is diverging from R2, R is needed to be more similar to R1 in order to become the member of the set where R2 exists. From our experimental result, we found that although this method does not compare R2 and R directly, we get the approximate value of matching R2 and R straight away. If there is no similarity at all between R2 and R, then we get a value which is approximately zero or negligible.

Algorithm 2: DIDD

1. Determine the uniqueness of each attribute of the dataset. Uniqueness is a numerical value which returns the number of different data of an attribute.
2. Start sorting with the less unique attribute and sort the dataset using each attribute. If no such attribute can be determined then sort the dataset using any attribute which is more promising to bring the similar-duplicate records nearer than others.
3. Set up a window of length *n*.
4. Perform a less expensive and fast string matching operation between a new (the *n*-th record in the window) record and the remaining (*n-1*) records in the window one by one. If the matching score is below some pre-specified threshold value then continue with step *4*.
5. Perform an expensive but efficient string matching operation only for those records whose similarity is above some pre-specified threshold in step *4*.
6. If the similarity between two records in step *5* is above some pre-specified threshold and any of them already exist in a set of duplicate records then use the modified form of the transitivity rule. If none of them exist in any set then create a new set of duplicate records with these two records.
7. If the last record from any set of duplicate records goes outside the window then close that set of duplicate records. Save this set of duplicate records.
8. Repeat steps *4* to *7* until the last record of the dataset enter the window and is matched using step *4*.
9. Take the set of duplicate records created in step *6* and keep a record from each set and delete the remaining records.

E. Domain Independent Duplicate Detection Algorithm (DIDD)

Our proposed Algorithm-2, Domain Independent Duplicate Detection Algorithm (DIDD), is totally domain independent. All the proposals made in this paper, can be used together using the DIDD algorithm. Any part of the proposal made in this paper is also applicable with existing similar-duplicate detection system, with some simple modification in the existing system. For limiting the number of comparisons any existing system can be used and for cleaning the duplicate records after detection, any existing system can be applied.

IV. EXPERIMENTAL RESULTS

The experiment was performed using 7 tests for comparing the time requirement of the proposed algorithm with two existing domain independent algorithms: Scheme-1 [2] and Scheme-2 [4]. We used desktop computer with Intel Pentium-IV processor, 512 MB RAM, windows XP operating system and Matlab-R2007b. The dataset was created by collecting data from the Internet [8]-[10] and merging them to a database table. Since, the proposed method is domain independent, we are not concerned about the attributes' name. There were total 8 attributes and some attributes contain more than 40 characters data. Table IV contains the description of the dataset and Table V contains the time requirement of the proposed algorithm and the other two algorithms. From Table V, it can be observed that the performance of our proposed algorithm is better than the other two algorithms, when the number of duplicates per record is realistic. Whereas the other two algorithms require more time, when the number of duplicates per records is less. The reason is that they use a priority queue. In a priority queue, when the number of unique records is more, additional comparison per records is required to find a match. If we also make the similar assumption like [4], there will be a maximum of 20 duplicate records per unique records, in that case, the test category falls from test-1 to test-4. In test-4, we require slightly more time. Because, to improve the efficiency, we are using a modified form of the transitivity rule, which requires additional work than the simple transitivity rule.

It is usual that in a real-world dataset the scenario after test-4 will rarely occur. On the other-hand, in a real-world dataset, it is unlikely that every record will have a fixed number of duplicate records. When two records are the exact duplicates, our proposed algorithm needs to perform maximum number of operations. Hence, for time comparison, we used exact duplicates.

Recall (R) and precision (P) of the proposed method and the other two methods are presented in Table VI. It should be mentioned that, Recall = (number of true duplicates detected / the number of total duplicates in the dataset) and Precision = (number of true duplicates detected / the total number of duplicates detected). If the threshold is between 0.1 and 0.4, our precision is better, whereas if the threshold is between 0.5 and 1, our recall is better than the other two algorithms. For comparing the recall and precision, we used a dataset, which contain 3900 unique records with a known number of duplicate records.

Table IV Description of the dataset

Test No.	Description of the dataset
test-1	No duplicates
test-2	800 unique records and 5 exact duplicates for each record
test-3	400 unique records and 10 exact duplicates for each record
test-4	200 unique records and 20 exact duplicates for each record
test-5	100 unique records and 40 exact duplicates for each record
test-6	80 unique records and 50 exact duplicates for each record
test-7	40 unique records and 100 exact duplicates for each record

Table V Required time with varying the number of duplicates

Test No.	Proposed algorithm (sec)	Scheme-1 (sec)	Scheme-2 (sec)
test-1	**50**	490	522
test-2	**300**	460	472
test-3	**450**	**450**	470
test-4	480	**435**	464
test-5	530	**440**	460
test-6	550	**450**	**450**
test-7	670	470	**440**

Table VI Recall and precision for the algorithms

Threshold	Proposed algorithm		Scheme-1		Scheme-2	
	R	P	R	P	R	P
0.1	1	**0.15**	1	0.11	1	0.11
0.2	1	**0.15**	1	0.11	1	0.11
0.3	1	**0.15**	1	0.12	1	0.11
0.4	0.95	**0.59**	1	0.36	1	0.25
0.5	**0.9**	1	0.71	1	0.77	1
0.6	**0.9**	1	0.52	1	0.52	1
0.7	**0.89**	1	0.51	1	0.51	1
0.8	**0.84**	1	0.51	1	0.49	1
0.9	**0.67**	1	0.49	1	0.4	1
1	**0.67**	1	0.46	1	0.33	1

Fig. 1 shows the time requirement with varying the number of duplicate records and Fig. 2, Fig. 3, Fig. 4 shows the Recall and Precision for the algorithms. Efficiency of duplicate detection algorithms depend on the efficiency of the sorting method, as well as the efficiency of the similar-string matching algorithm. From the experimental results, it is clear that the proposed sorting method and the similar-string matching algorithm was more efficient than the other two algorithms for detecting similar-duplicates. When the precision is the same, our sorting method and the modified string matching algorithm is able to detect more duplicates than the other algorithms. At threshold 0.4, our recall is slightly lower than the other two algorithms. However, considering both recall and precision, the overall efficiency of our algorithm is better. When recall is the same, our precision is always better than the other two algorithms. Our proposed Domain Independent Transitivity rule (DIT) plays an important role for making the precision better than the other algorithms. Also, it reduces the number of false positives.

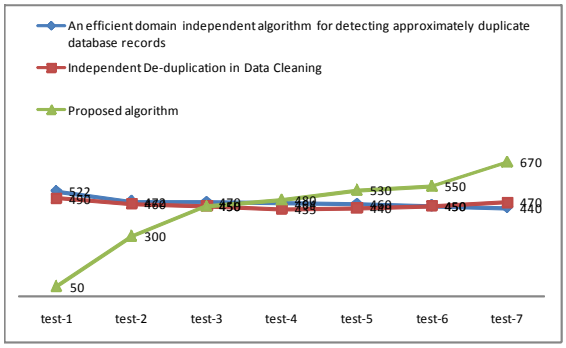

Fig. 1. Time comparison with varying the number of duplicate records.

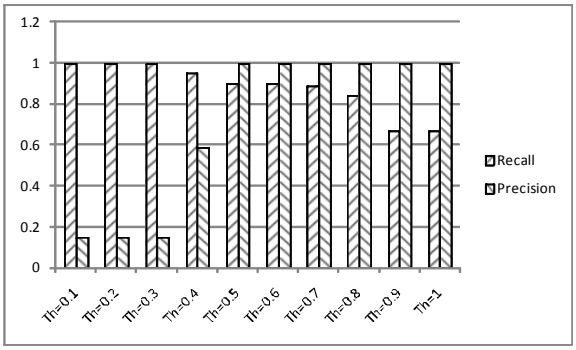

Fig. 2. Recall and Precision for the proposed algorithm.

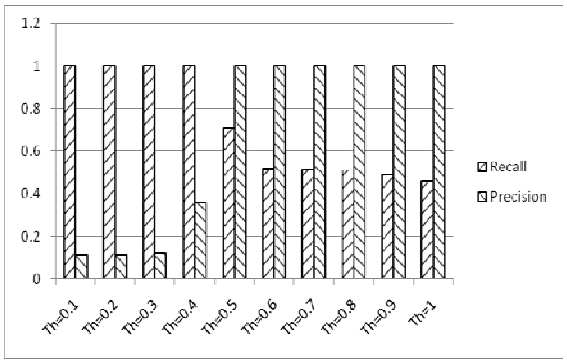

Fig. 3. Recall and Precision for Scheme-1 (Independent de-duplication in data cleaning.)

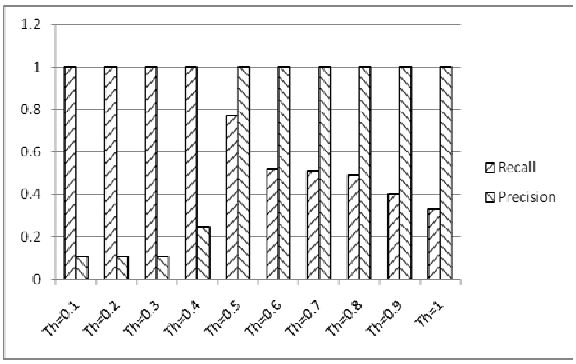

Fig. 4. Recall and Precision for Scheme-2 (An efficient domain independent algorithm for detecting approximately duplicate database records.)

V. CONCLUSIONS

Efficiency of duplicate detection algorithms depends greatly on the efficiency of sorting methods. The sorting method proposed in this paper is a novel technique for bringing the similar records closer and it can sort the records efficiently. The algorithm proposed in this paper also explores the idea to make the duplicate detection algorithms faster and efficient for real life data. A domain independent transitivity rule is also proposed for reducing the effect of transitivity rule for domain independent cases. This paper also outlined an algorithm to implement all the proposed methods together. However, we did not consider the problem of missing values or limiting the number of attributes, because these are usually handled before the duplicate detection phase. We also gave the same importance for each attribute during the calculation of similarity between records. In future, we hope to improve the sorting method to bring the similar records closer.

REFERENCES

[1] http://en.wikipedia.org/wiki/Data_mining

[2] A. Udechukwu, C. Ezeife, K.Barker, "Independent de-duplication in data cleaning," *Journal of Information and Organizational Sciences*, vol. 29, no. 2, 2005.

[3] M. L. Lee, T. W. Ling, W. L. Low "IntelliClean: A knowledge-based intelligent data cleaner," in Proc: the ACM SIGKDD, Boston, USA, 2000.

[4] A. E. Monge, C. Elkan. "An efficient domain independent algorithm for detecting approximately duplicate database records," in Proc: the SIGMOD Workshop on Data Mining and Knowledge Discovery, Arizona, May 1997.

[5] M. A. Hernandez, S. J. Stolfo, "Real-world Data is Dirty: Data Cleansing and The Merge/Purge Problem," *Data Mining and Knowledge Discovery*, vol. 2, no. 1, pp. 9-37, 1998.

[6] M. L. Lee, H. Lu, T. W. Ling, Y. T. Ko, "Cleansing Data for Mining and Warehousing," in Proc: the 10th International Conference on Database and Expert Systems Applications (DEXA), pp. 751 – 760, 1999.

[7] A. K. Elmagarmid, P. G. Ipeirotis, V. S. Verykios, "Duplicate Record Detection: A Survey," *IEEE Transaction on Knowledge and Data Engineering*, vol. 19, no. 1, 2007.

[8] http://flags.skalman.nu/flags/bib_main.html

[9] http://office.microsoft.com/en-us/downloads/

[10] http://www.microsoft.com/downloads/

Proceedings of 2009 12th International Conference on Computer and Information Technology (ICCIT 2009)
21-23 December, 2009, Dhaka, Bangladesh

Steps to Defend Against DoS Attacks

Ahsan Habib, Debashish Roy†
Department of ICT, Metropolitan University, Sylhet, Bangladesh
† Assistant Professor, Department of ICT, Metropolitan University, Sylhet, Bangladesh
ahferoz@gmail.com, ashok96@gmail.com

Abstract

Defending against DoS attacks is extremely difficult; effective solutions probably require significant changes to the Internet architecture. We present a series of architectural changes aimed at preventing most flooding DoS attacks, and making the remaining attacks easier to defend against. The goal is to stimulate a debate on tradeoffs between the flexibility needed for future Internet evolution and the need to be robust to defend attack.

Keywords: Denial-of-Service, DoS Attacks, Defend Against DoS Attacks, Steps to Defend Against DoS Attacks

I. INTRODUCTION

Denial-of-Service (DoS) attacks are one of the most significant problems currently faced in the Internet and by its users. For many users these attacks are merely an irritation - even if they understand the reason for the poor performance they occasionally observe. However, for the Internet to achieve its full potential, it has to be able to offer highly reliable service, even in the face of hostility. We will examine some significant changes to the Internet architecture aimed at making the Internet more robust. Such changes should not be made lightly - any widespread change has real costs associated with it. In writing this paper we are aware that the problem of DoS attacks can not be *completely* solved by the architecture we propose. The problem needs to be tackled on many fronts simultaneously. However we do believe that architectural changes are necessary.

The seven steps discussed in this paper, taken together, provide an enhanced Internet Architecture that is much more resistant to DoS attack than the current Internet. The changes are largely independent of applications, so should permit the Internet to continue to evolve successfully, and the benefits are many. Worms cannot spread rapidly. Reflection DoS attacks are almost completely eliminated, and where they remain feasible, they are only against local targets. Clients are almost completely protected from direct attack and compromise, and they are protected from non-local DoS attacks except by servers with whom they have chosen to communicate. Servers are protected against DoS attack from other servers: as clients now become hard to directly compromise, this provide does not insignificant protection in its own right. The routing architecture means that complete source-address spoofing by clients or servers is not possible, and this in turn means that pushback mechanisms become easier to deploy against known attackers. Client address validation using nonce further reduces the chance of collateral damage from such pushback. The use of middlewalls to validate CPU-puzzles can make the remaining DoS attacks impossible to sustain except through overwhelming numbers of attacking zombie hosts. Even then, if the attacking hosts are readily identified, it should be feasible for middlewalls to do client-address validation, and then use pushback to shut them down. It is noted that with a huge attack this may entail too much filter state in the network, but this architecture would permit the deployment of specialist high-speed filter gateways that can do this filtering. The remaining problems are primarily those in which huge numbers of attacking client zombies cannot be distinguished from legitimate clients. In such cases the proposed design goal will be successful by to forcing the attacker to be indistinguishable from a flash crowd. In fact the researchers have gone rather further than this by removing a number of key vectors for infection that can currently be used to create large DDoS zombie armies in the first place.

II. THE NATURE OF THE PROBLEM

The first step in considering a security problem is to consider the nature of the threat. In [7], the Internet Architecture Board provides a detailed discussion of the nature of DoS attacks on Internet systems, and we strongly recommend this document. Basically all systems are vulnerable to some form of attack, be they clients, servers, firewalls, routers or links. Attacks can attempt to exhaust processing power, memory, bandwidth, quotas, disk-space, and pretty much any other "consumable" that a system requires to perform its job. One modern PC connected to a high-speed network can source around 1Gb/s of traffic, which is enough to saturate many network links and, if the traffic is carefully crafted, enough to overload many large servers. However, traffic from a single machine is relatively easily filtered. Although automated mechanisms to *push-back* such filters towards the source are not widely deployed, there are few technical problems in doing so[9][8]. Unfortunately *source-address spoofing* makes it harder to pushback filters without causing collateral damage. Further, many DoS attacks are *reflection* attacks [11], where the attacker sends traffic to a third party, spoofing the source address of the victim. The third party

978-1-4244-6283-4/09/$26.00 ©2009 IEEE

then replies to the victim, overwhelming them. The attacker can then use many third parties to spread his attack, so now the traffic is "originating" from all over the Internet. In addition, some reflection attacks manage to *amplify* the original attack because the responses sent by the third party are larger or more numerous [4][7] than the original messages sent by the attacker. The biggest DoS problem is caused by *distributed* denial of service (DDoS) attacks, where the attacker compromises a large number of systems and then uses these "zombie" systems to attack the victim. DDoS attacks of sufficient scale provide the firepower needed to overwhelm almost all victims. They can also be combined with spoofing or reflection to make the attack even more difficult to defend against. Currently most DDoS attacks do not bother to spoof the source addresses because, as no automatic push-back mechanism is widely deployed, it takes so long to shut down each zombie that there is no need to hide their identity. DDoS is principally an issue due to widespread exploitation of software vulnerabilities, which permit the control of large numbers of compromised systems. To gain sufficient scale, such exploitation is typically automated using worms, viruses, or automated scanning from already compromised hosts (so called "bots"). Fast-spreading worms are extremely hard to combat in the current Internet Architecture, so these are particular concerns [10]. Although viruses and bots are serious issues, their spread rate is slower, which permits a wider range of defense options.

III. DEFENSE

It is important to begin by recognizing that it is not possible to completely protect all servers against all DDoS attacks. If a sufficiently subtle attacker with sufficiently many compromised hosts at his disposal can mimic legitimate traffic well enough that the victim cannot tell good from bad, there is little that can be done beyond load-shedding, adding server resources, and minimizing collateral damage. However, the ultimate goal is that this is the only way to persistently DoS-attack a server, and that routers and client systems are invulnerable to DoS attacks. Viewing the problem from a high level, there are many tracks that can be taken to make a network architecture that is more resilient to DoS than the current Internet:

- Reducing the ability of worms and viruses to spread quickly will reduce the threat of very large scale DoS attacks. Fast spreading worms are a particular threat, because they outpace the speed of any possible human mediated response.
- Preventing source-address spoofing will aid the shutdown of attacks that occur using push-back mechanisms.
- Preventing reflection attacks will also aid the shutdown of attacks and prevent innocent third parties from being implicated or harmed by reactive defenses.
- Without source-address spoofing and reflection attacks, automated push-back mechanisms would be much more accurate and effective.
- Large-scale wide-area distribution of key services such as DNS would localize attacks, reducing the attacker's advantage and minimizing collateral damage.
- Hosts not wishing to receive incoming connections attempts from the public Internet should not do so.
- Router-to-router traffic should be effectively isolated from all other traffic to reduce DoS threats to routers.

Although this is at least as important as the points above, it is not the main focus of this paper, so it will not be discussed further. In this paper the protocol is not discussed and implementation details needed to ensure that transport protocols and applications are robust to DoS. Instead architectural changes are concentrated on that more widely restrict an attacker's freedom and permit more effective defense.

IV. TOWARDS A DOS-RESISTANT ARCHITECTURE

In this section a set of architectural changes will be proposed, taken together would greatly limit the scope for attack. The aim is to allow all the desired modes of interaction between systems, but to restrict everything else.

A. STEP 1: APPLICATION OF IPV6 ADDRESSES

The IP address space can be divided into a set of client addresses and a set of server addresses. The aim is to allow clients to initiate connections to servers, but not to allow clients to initiate connections to clients, nor servers to initiate connections to servers. The benefits of this depend on where the restriction is enforced. Even if it is only enforced by the recipient, this will immediately reduce the threat from worms. A worm would have to spread from client-server-client, exploiting two separate vulnerabilities. This greatly slows the worm because the server-client phase depends on clients choosing to contact an infected server. Very fast spreading worms would no longer be possible. Worms that attempt to spread via contagion are still possible, but are significantly more likely to be spotted in the client-server phase in time to react by the sort of organized honeypots proposed in [12]. In addition, many reflection DoS attacks on servers (such as bang.c[7]) are prevented. A reflection attack on a server would require server-client-server communication, and most clients are not going to respond to a new connection request from a server. In the current Internet, some of these benefits arise from

the use of Network Address Translators. However, NATs only benefit those clients who chose to use them; attackers simply choose to attack from hosts that are not behind NATs. By formalizing the asymmetry and accepting it as a key part of the architecture, the benefits can be much more widespread, as will be shown below. In addition the downside of NATs not being a consistent part of the architecture can be avoided. Clearly if many hosts have both client and server addresses, some of the benefits are lost; it is hoped that few hosts will need both *globally-reachable* client and globally-reachable server addresses. Typically a server should not be initiating wide-area outgoing connections, and most clients only need to accept incoming connections to permit local management. Obvious exceptions are peer-to-peer applications, and telephony-style applications.

B. STEP 2: CONSTRUCTION OF SOURCE ADDRESS DOMAIN BY DOMAIN

A client address does not need to have any global significance. It only needs to have significance along the path between the client and the server, so that packets from the server can be returned to the client. In fact, a client *wants* its address to not have global significance - this prevents distributed DoS attacks on the client or its access network unless each attacking host can figure out a workable address to route traffic towards the client. One way to allocate client addresses in a non-global manner would be for the source address to be constructed domain-by-domain as the packets travel from client to server. On entry to a domain, a local routing ID (indicating the next domain toward the client) would be pre-pended to the source address. Packets being forwarded back towards the client would then be forwarded by the usual longest-prefix-match forwarding mechanisms within each domain (in this case the prefix is the local ID for the next domain). As the packet leaves each domain heading back towards the client, the local ID is removed. It is likely that such address pre-pending can be done at line-speed in some of today's backbone routers with only firmware upgrades. The goal is that even if one malicious server in the Internet knows a client's address, no-one elsewhere in the Internet who is given that address can easily deduce a workable client address to reach the client from their location. The simple pre-pending scheme above provides this protection to some degree, but it is advisable that more security is required. This can be achieved at the expense of additional forwarding cost by encrypting the client address before pre-pending the local ID in the client-to-server path, and decrypting it in the return path after removing the local ID.

C. STEP 3: PREVENTING THE SERVER FROM ADDRESS SPOOFING

Using path-based client addresses severely restricts source-address spoofing by a client, but it does not restrict spoofing by servers. However, the domain-level symmetry that emerges from using client based addresses means that packets traveling from server-client follow the reverse client-server inter-domain path. This allows domain boundary routers to perform a reverse-path forwarding check on the source address of server-client packets. This check largely prevents a server from spoofing the address of a server in a different domain. When combined with path-based client-addresses, one effect of this is to make it harder to launch blind DoS attacks on ongoing communications, such as injecting a TCP Reset into a connection whose existence can be inferred.

D. STEP 4: CHANGING THE CONNECTION REQUEST PACKET FORMAT

Not all packets are equal. Packets that require the recipient to set up new state are more risky from a DoS point of view than those that don't. It is useful to single these packets out for special handling in a manner that is independent of the upper layer protocol. Packets that will cause transport communication state to be set up (especially connection setup) should set a new state-setup bit in the IP header. Other packets would leave this bit unset. This serves a number of purposes:

- It provides a generic protocol-independent way to identify packets that need special validation. A server receiving a connection setup request with this bit not set would simply discard the packet.
- Stateful firewalls can validate packets with this bit set before instantiating state. What form this validation might take will be discussed.
- Packets without this bit set can be safely dropped by stateful firewalls if no matching state is found. This provides a way for firewalls to permit evolution of network protocols without knowledge of the protocol semantics, and provides a way for firewalls to do some degree of transport-independent validation of encrypted traffic such as IPsec-protected connections.
- Server addresses cannot send packets with the state-setup bit set - all routers would drop such packets. This prevents all unsolicited state-holding DoS attacks initiated from server addresses.
- Sites might rate-limit at their outgoing firewall the number of state-setup packets per second sent by some clients.

E. STEP 5: INCREASING THE FIREWALL'S LEVELS

Mechanisms are needed to validate a client and to add

asymmetric costs to communication so as to tilt the balance of control towards the server. Doing this under heavy load on the server itself is hard, some of this checking are needed to be off-loaded. As the validation point needs to be upstream of links that are vulnerable to saturation attacks, this implies the use of external firewalls to validate flows. The simplest form of validation is that a firewall can validate that the client's address is valid. Although complete client source-address spoofing is not possible with the path-based addresses described above, the client still has some ability to obfuscate the true origin or to launch reflection DoS attacks on clients in the same domain as itself. Thus pushback mechanisms might inflict some collateral damage on clients co-located with an attacker. One feasible mechanism to do address validation would be a simple nonce-echo. On receiving a state-setup packet, a firewall could bounce the packet back to the sender with a nonce appended. The sender would then echo the nonce-packet back, whereupon the firewall would check the nonce, strip it off, instantiate any appropriate state, and forward the packet on towards the intended destination. Such a simple validation could be performed by an edge site's outgoing stateful firewall to validate the source address on an outgoing request. This is in the site's own interest because it would prevent the other clients at that site from suffering collateral damage from any pushback that a DoS attack launched by that client might incur. Going beyond source-validation, transport protocol independent mechanisms can be added to push cost onto the client to limit the sustained attack rate that a client can maintain. CPU puzzles are one such mechanism; the goal is to make the client perform a CPU-intensive task before connection setup is permitted. The hope is that a normal client will not be excessively delayed in solving the puzzle, but that an attacker (who wants to initiate a great many connections and so needs to solve many puzzles) will be CPU limited, and so his rate of attack will be much lower. An example of such a puzzle would be to provide a random bit-string to the client, and require the client to find a text where the first *n* bits of the MD5 hash match the bit-string. Such a puzzle is expensive to solve, but cheap to check. There are also puzzles limited by other resources such as memory bandwidth, which might be more appropriate in some cases. Just as firewalls can validate source addresses, they can also issue puzzles to impose cost on the clients before allowing traffic through. The idea of IP-layer puzzles is not new [6], but architecture provides the right framework to make puzzle deployment safe and effective. In particular, the state-setup bit would provide an appropriate signal to issue a puzzle, and the addressing architecture makes it hard to use malicious puzzle requests or spoofed responses as a DoS attack in their own right. Puzzles at the IP/transport level do not solve application-level DoS problems or complexity attacks, but they at least constrain the rate of incoming connections. The application may well need to do its own DoS prevention; what form this might take depends on the nature of the application itself. Such puzzles also do not prevent *massively* distributed DoS attacks because the connection setup rate from each attacking zombie is so low as to not be CPU constrained. It is hoped to make it much harder to compromise so many client hosts in the first place.

F. STEP 6: PUSHBACK MECHANISMS

Firewalls are normally deployed at site borders, with the goal of limiting the types of traffic allowed into or out of a site to protect the hosts inside. However, in the case of DoS, traditional site firewalls may well be too close to the destination to provide sufficient protection. Pushback mechanisms can provide reactive protection back into the core of the network when an end-system or network link discovers it is under attack. Unfortunately to pushback each source in a large distributed DoS attack is likely to be relatively expensive in terms of network state, and requires each source to be identified and pushed back individually. Such identification may be difficult: it may be hard to tell good traffic from bad if an attack is not too blatant. Non-source-specific pushback is still feasible, but pushes back good and bad traffic alike. It is not desired to re-invent virtual circuits in the Internet, but the only way to throttle requests through a bottleneck is to have some form of access control upstream of that bottleneck. Very simple special-purpose high-speed firewalls are being envisaged to be deployed in the core of the Internet at inter-domain boundaries to serve this purpose. Such *middlewalls* would not normally filter traffic, but a server under stress may issue a middlewall solicitation message to request the assistance of one or more middlewalls. Such a request could be specific - sent along the path back towards a source (another benefit of routing symmetry), or it could be non-specific, flooded in the inter-domain routing information. On receipt of such a request for help, the middlewall would start performing source validation, and issuing puzzles on behalf of the server. The use of middlewalls to perform source-validation or issue puzzles opens up the question of how multiple firewalls in a path should interact. It would be preferred to avoid adding multiple roundtrip times to connection setup, but at this stage this seems simplest. In general though, unlike a site firewall, a middlewall should be transparent unless its help is actively solicited by a server, so the additional delay would not normally be incurred. The economics of middlewalls are not completely clear, but they seem tractable. In the case of a specific request, the middlewall might charge the end-system for the service. Even in the case of a non-specific request, it might still be in a transit ISP's interest for its middlewall to help out because the middlewall

may allow an ISP to avoid forwarding a flood of attack traffic that might disrupt other customers.

G. STEP 7: APPLICATION OF CONGESTION CONTROL

Traditional IP multicast [5] (so called *ASM*) has no wide-area role in a DoS-resistant Internet. The ability for any host anywhere in the Internet to simply start sending and cause routers worldwide to instantiate forwarding state presents an insuperable DoS problem. This is made even worse by the ability of a sender to send to any existing multicast group without the consent of receivers or the other senders. In contrast, Source Specific Multicast (SSM [2]) is relatively robust against DoS attacks. With SSM, a receiver joins explicitly to a specific source address to receive a specific multicast group. This means that there is no way for a multicast sender to be malicious without the active participation of the multicast receivers. However, there are two remaining DoS vulnerabilities with SSM:

- Receivers can join many non-existent multicast groups on many potential sources. This can be a state-holding attack on the routers along the path to these non-sources.
- A receiver can join many high-bit rate groups causing high packet loss on network links towards the receiver.

The latter is really a self-DoS. However, even this can be prevented to a reasonable extent if the router at the congested link simply unsubscribes groups that do not appear to be utilizing congestion control. The former problem is really two separate issues. First, receivers should not be able to join a group where the sender is never going to be active. This can be solved using cryptographically generated addresses (CGA [1] [3]) where a router can validate that the group address must have been chosen by the owner of the sender's key. However, CGA might be too heavy a weight and a DoS risk in its own right. Alternatively, a two-pass multicast join mechanism can first validate group liveness (or the sender's intent to send), then on the second pass actually instantiate forwarding state. This would be done by allowing a join-probe to propagate upstream towards the sender without instantiating any state until it reaches the sender's subnet, or until it reaches a router with active multicast join state. The join-probe would accumulate the entire hop by-hop path, and an affirmative join response traveling the reverse path could be used to instantiate the join state. The same domain-border encryption mechanism used for client addresses could be used to prevent spoofed join responses. Second, it is wanted to make it hard for a receiver to join so many low-rate multicast groups that the routers can't hold the forwarding state. This is mainly an issue close to the receiver itself, because the backbone already needs to transit most of these groups in the absence of any DoS attack. A partial solution is for routers to have a threshold for the number of groups that can be joined. If this threshold is exceeded, then a join-failure message is propagated downstream for all groups. A site firewall or router close to a likely malicious receiver can then use this to trigger a limiting mechanism that reduces the large number of groups that any single receiver has joined. Receivers that have not joined many groups would be unaffected. With our addressing architecture, only server addresses can send multicast traffic and only client addresses can receive it.

V. CONCLUSION

A set of changes to the Internet architecture has been outlined, including the explicit separation of the IP address space into client and server addresses, along with associated rules restricting how those addresses can be used. These changes significantly limit the modes of interaction between Internet systems, in such a way that the vast majority of the desirable interactions are allowed, and a large number of undesirable interactions are disallowed. Taken together, these changes significantly improve the ability to defend against DoS attack. They also increase the difficulty involved in building large DDoS attack networks, and the hope is that the remaining ways to compromise systems are more easily detected or prevented. These changes are not expected to be popular at first, as people have become rather used to the flexibility inherent in the current architecture. It is time to take a hard look at the architecture itself and questions that have been got right and what we cannot live with anymore.

REFERENCES

[1] T. Aura. Cryptographically Generated Addresses (CGA). draft-ietf-send-cga-05.txt, work-in-progress, IETF, Feb. 2004.

[2] S. Bhattacharyya (editor). An overview of source-specific multicast (SSM). RFC 3569, IETF, July 2003.

[3] C. Castelluccia and G. Montenegro. Securing group management in IPv6 with CGA (Cryptographically Generated Addresses). presentation to the IRTF GSEC Research Group, February, 2002.

[4] CERT Advisory CA-1998-01. Smurf IP denial-of-service attacks, Jan. 1998. http://www.cert.org/advisories/CA-1998-01.html.

[5] S. Deering. Host extensions for IP multicasting. RFC 1112, IETF, Aug. 1989.

[6] W. Feng. The case for TCP/IP puzzles. In *Proc. ACM SIGCOMM workshop on Future Directions in Network Architecture*, pages 322–327. ACM Press, 2003.

[7] IAB, M. Handley (editor). Internet denial of service considerations. draft-iab-dos 00.txt, work-in-progress, IETF, Jan. 2004.

[8] J. Ioannidis and S. M. Bellovin. Implementing pushback: Router-based defense against DDoS attacks. In *Proc. Network and Distributed System Security Symposium, San Diego*. ISOC, Reston, VA., February 2002.

[9] R. Mahajan, S. M. Bellovin, S. Floyd, J. Ioannidis, V. Paxson, and S. Shenker. Controlling high bandwidth aggregates in the network. *ACM Computer Communication Review*, 32(3), July 2002.

[10] D. Moore, C. Shannon, G. Voelker, and S. Savage. Internet quarantine: Requirements for containing self-propagating code, Apr. 2003.

[11] V. Paxson. An analysis of using reflectors for distributed denial-of-service attacks. In *ACM Computer Communication Review 31(3)*, July 2001.

[12] cc N. Weaver, V. Paxson, S. Staniford, and R. Cunningham. Large scale malicious code: A research agenda. Darpa sponsored report. http://www.cs.berkeley.edu/~nweaver//largescalemaliciouscode.pdf

Proceedings of 2009 12th International Conference on Computer and Information Technology (ICCIT 2009)
21-23 December, 2009, Dhaka, Bangladesh

A Supervised Spiking Neural Network for Generating Multiple Spikes *(Not Presented)*

Kazi Shah Nawaz Ripon, Farjana Tanha, Farhana Haque
Computer Science and Engineering Discipline, Khulna University, Bangladesh
ripon_cseku@yahoo.com, tanha_040206@yahoo.com, tanni_04@ymail.com

Abstract

Spiking neural networks (SNNs) are considered as the third generation of neural network models. In this paper, we proposed a supervised learning rule for SNNs that can cope with neurons, which can fire multiple spikes. The proposed supervised learning rule is based on the linear algebra method. We implemented the supervised learning rule for approximating the output to the goal time series. Simulation results demonstrate the efficiency of the proposed supervised learning method for generating multiple spikes and for approximating the output spike trains with the goal spike trains.

Keywords: Spiking neurons, Supervised learning, Synapses, Leaky integrate and fire model.

I. INTRODUCTION

Spiking neural network (SNN) has been the subject of significant recent research reflecting the view that spikes have a key role in biological information processing [1]-[3]. Classical artificial neural networks (ANNs) are based on a high abstraction of realistic neurons and only use rate coding to represent neuronal activity. Unlike this, spiking models offer a more detailed description of real biological neuron behavior. It is believed that real neurons use more information than the average firing rate to perform computations. Neuroscientists have carried out many experiments in order to study the chemical interactions between neuron population and the spike generation process. Most simulation of neural networks share the assumption that synaptic efficacy (weight) is considered to be static during the reception of afferent spike trains. However, recent experimental studies of real biological neuron cells show that the synaptic efficacy generating the postsynaptic potential or PSP is a variable quantity, which depends on the presynaptic activity.

Learning is an important feature of the nervous system and it is believed that synapses play a key role in the learning process. Most existing spiking network training algorithms, also referred to as synaptic plasticity, developed to date are unsupervised and based on the classical Hebbian rule or the Spike-Timing Dependent Plasticity (STDP) [4]. These forms of learning are not appropriate when a desired output is known in advance, a task for which supervised training algorithms are more preferred. A supervised training algorithm has been presented in [5]. However, this training algorithm was applicable for generating single spike only.

This paper presents a supervised learning rule for SNN that can cope with neurons, which are able to spike multiple times to train the input spike train with a goal spike train. SNNs are believed to be especially useful for the processing of temporal patterns, such as speech recognition [6]-[8]. These temporal patterns consist of correlating temporal events, such as a series of phonemes in the case of speech. The fact that these temporal events can happen more than once makes temporal patterns actually different from static patterns. So in order to process such patterns with an SNN, they have to be encoded in multiple spikes per input neuron and these neurons should be able to spike more than once.

There have been various studies in the literature introducing learning rules for networks of spiking neurons that spike only once [9]. However, these algorithms are not applicable for learning rules that can cope with neurons that fire multiple spikes. It will be beneficial to have a completely supervised learning algorithm that is designed to cope with multiple spikes per neuron that can learn static data. These motivated us to work with spiking neural network that can deal with multiple spikes. In this work, we proposed a supervised learning rule for SNNs that can cope with neurons, which spike multiple times. We developed this by using the concept of linear algebra in the case of weight learning. Because linear algebra is very useful for SNN to make the neurons learn how to generate multiple spikes. The rest of this paper is organized as follows. Section II, III and IV describe some related basic concepts regarding spiking neuron model, spike coding and synapses respectively. Section V presents our proposed supervised learning method. Experimental results and application of this proposed method are discussed in Section VI. Finally, Section VII concludes the paper.

II. SPIKING NEURON MODELS

A voltage represents the state of a spiking neuron across its cell membrane and a threshold. The neuron sub threshold activity is determined by the integration of its excitatory and inhibitory postsynaptic potential (EPSP, IPSP) [2]. An EPSP causes an increase in the neuron potential while an IPSP decreases it. When its membrane potential reaches certain threshold from below, the neuron generates a spike or action potential;

which is then propagated forward to the next neurons through its axon. When an action potential (the electrical signal which rapidly propagates along a neuron axon to other neurons as a result of a change in membrane potential) is received, the synapse transforms it into a change in postsynaptic neuron membrane potential (post synaptic potential). An action potential, once generated by a presynaptic neuron, takes a certain time to reach the postsynaptic neuron. And, this time is called synaptic delay. Several mathematical models have been proposed to describe neuronal activity. They differ by the level of abstraction and the computation complexity offered by each model. The Hodgkin–Huxley model [2] represents a detailed description of the neuron dynamics where the effects of different ionic channels conductances on the change in the neuron membrane potential are described using a set of ordinary differential equations. The thresholding process (firing when membrane potential reaches a certain threshold) is not explicitly modeled in this model, which is computationally intensive for numerical simulations. In the integrate-and-fire model (IAF) [1], [2], however, a neuron is simulated by an RC-circuit where the voltage represents the membrane potential across the capacitor and an action potential is generated whenever the capacitor voltage reaches a certain threshold. The SRM is another model, which approximates the IAF model by a linear summation of the PSPs caused by the impinging spike trains from predecessor neurons. In this model, neurons are interconnected through a simple scalar weight that modulates the amplitude of the incoming postsynaptic potentials at the receiving neuron. However, in the case of DSs (or weightless synapses) the synaptic strength changes upon the arrival of spike trains. This synapse model is used to connect IAF neurons in a feed forward network, and their computing capabilities are investigated and evaluated.

III. SPIKE CODING

There are many different approaches for using the spike timing information in neural computation. Because of the nature of this paper, we shall only cover two models here: the spike response and the integrate-and-fire model (IAF) [2]. Both are instances of the general threshold-fire model. IAF is commonly used in networks of spiking neurons. Here, it will be covered after the conceptually more simple and general spike-response model. This model is simple to understand and implement. We can therefore ignore the form and characterize these by their firing times $t_i^{(f)}$, where i indicates the neuron and f is the number of the spike. We can then describe the spike-train of a neuron as [5]:

$$F_i = \{t^{(1)},.....,t^{(n)}\} \quad (1)$$

If a neuron's membrane potential crosses threshold value ∂ from below, it generates a spike. We add the time of this event to F_i, defining this set as

$$F_i = \{t \mid u_i(t) = \partial \wedge u_i(t) > 0\} \quad (2)$$

where the variable u_i is used to refer to the membrane potential or internal state of a neuron *i*. When a neuron generates an action potential, the membrane potential suddenly increases and followed by a long lasting negative after-potential. We can model this absolute and negative refractoriness with kernel η:

$$\eta(s) = -n_0 \exp(-\frac{s-\partial^{abs}}{t})H(s-\partial^{abs}) - KH(s)H(\partial^{abs}-s) \quad (3)$$

The duration of the absolute refractoriness is set by ∂^{abs}, during which large constant K ensures that the membrane potential is vastly above the threshold value. Constant n_0 scales the duration of the negative after-potential. Having a description of what happens to a neuron when it fires itself, we need one for the effect of incoming postsynaptic potentials.

$$\varepsilon_{ij}(s) = [\exp[-\frac{s-\Delta^{ij}}{\tau_m}] - \exp[-\frac{s-\Delta^{ij}}{\tau_s}]]H(s-\Delta^{ij}) \quad (4)$$

In (4), Δ^{ij} defines the transmission delay (axons and dendrites are fast, synapses relatively slow) and $0\langle\tau_s\langle\tau_m$ are time constants defining the duration of the effect of the postsynaptic potential. By using the negative value, Kernel ε by default describes the effect of an excitatory postsynaptic potential. We use variable w_{ij} to model the synaptic efficacy or weight; with which we can model inhibitory connections by using values lower than zero. It should be noted that real synapses are either excitatory or inhibitory. Neurons of the second generation work in an iterative, clock-based manner of digital computers, but can deal with analog input values. And, we can quite easily feed input neurons with digitized values from a dataset or a robot-sensor. Due to their iterative nature, these networks are not well suited for temporal tasks. Also they do not use time in their computation, whereas SNNs do. However, such values cannot be fed into a spiking neuron, in some way we will either have to convert this information into spikes, or have to employ a method to alter the membrane-potential directly.

For non-hardware solutions, it might be handier to convert analog signals into spikes that can be fed to the network directly. An often-used solution is to apply a Poisson-process for spike generation by the sensor neuron; a higher input signal correlates with a higher chance for a spike. Such a spike will then be processed and affect the membrane-potential of neurons normally. The current excitation of a neuron is described by

$$u_i(t) = \sum_{t_i^{(f)} \varepsilon F_i} n_i(t - t_i^{(f)}) + h(t) \quad (5)$$

where the refractory state, effects of incoming postsynaptic potentials and eventual external events are

combined. Combined with (1), it forms the spike-response model, which is a powerful but easy to implement model for working with SNNs.

IV. SYNAPSES

There are two classes of ion channel, namely voltage-activated and calcium-activated ion channels. A third type of ion channel, we have to deal with is transmitter-activated ion channels involved in synaptic transmission. Activation of a presynaptic neuron results in a release of neurotransmitters into the synaptic cleft. The transmitter molecules diffuse to the other side of the cleft and activate receptors that are located in the postsynaptic membrane. So called ionotropic receptors have a direct influence on the state of an associated ion channel whereas metabotropic receptors control the state of the ion channel by means of a biochemical cascade of *g*-proteins and second messengers. In any case, the activation of the receptor results in the opening of certain ion channels, and thus, in an excitatory or inhibitory postsynaptic current (EPSC or IPSC) [2]. Instead of developing a mathematical model of the transmitter concentration in the synaptic cleft, we try to keep things simple and describe transmitter-activated ion channels as an explicitly time dependent conductivity $g_{syn}(t)$ that will open whenever a presynaptic spike arrives. The current that passes through these channels depends, as usual, on the difference of its reversal potential E_{syn} and the actual value of the membrane potential,

$$I_{syn}(t) = g_{syn}(t)(u - E_{syn}) \tag{6}$$

The parameter E_{syn} and the function $g_{syn}(t)$ can be used to characterize different types of synapse. Typically, a superposition of exponentials is used for $g_{syn}(t)$. For inhibitory synapses E_{syn} equals the reversal potential of potassium ions (about -75 mV), whereas for excitatory synapses $E_{syn} = 0$.

V. PROPOSED SUPERVISED LEARNING METHOD

Our main goal is to develop a supervised learning rule for SNNs that can cope with neurons that spike multiple times or neurons. In the previous system, a supervised learning algorithm was developed which is applicable for single spike only. For this reason, we would like to develop a supervised learning method, which will be applicable in the case of multiple spikes. This is because, multiple spikes are required in many practical applications, such as speech recognition or signal processing, where we have to process temporal patterns consisting of a series of phonemes.

For performing this task, at first we have to define a spike at time t_1 which has to be a function $s(t_1)$ of time *t* so that $s(t_1)(t)$=1. After that we will be able to define a time series and that will be the finite sum of spikes. i.e.

$$\sum_{i=1}^{N} s(t_i) \tag{7}$$

From here, we are able to define a weighted time series that will be a finite sum of the form

$$\sum_{i=1}^{N} c_i s(t_i) \tag{8}$$

Here, the coefficients c_i and the time t_i can be any real numbers and the number of terms N can be any natural number.

Now to develop the supervised learning rule, we need to take a weighted input time series such as $w_1, w_2, \ldots\ldots, w_k$ and also we have to take a fixed goal time series. An output neuron has to be taken also. The output neuron will be leaky–integrate and fire neuron discussed in [2].

Now we have to train the input time series, which will become the input of the neuron. After finishing the training process of the input time series, the trained time series will be considered as the neuron input. Then we have to find out the values of the weight of the inputs so that the output of the neuron will be as like as or will approximate the goal time series. We used the following supervised learning methods for the inputs and outputs.

A. Iterative Solution

The projection of an error onto the direction of the time series *Sin i* is determined, with *i* randomly chosen in each iteration. The error is defined as the difference between the target and the actual time series. The operation is evaluated until the norm of the error is sufficiently small.

Iteration Method for Input Spike Train

1. Initialize the distance to a very small number.
2. Randomly generate input and goal spike train.
3. Find the distance between input spike train and goal spike train
4. Until the distance becomes small perform the following operation:
   a. Take randomly an input channel
   b. Find out $\Delta w_i = proj_{\sin}(E)$ for that input channel
   c. Update weight by $w_i = w_i + \Delta w_i$
   d. Proceed the network simulation after that read the result as $s_{in}(t)$.

Iteration Method for Output Spike Train

1. Initialize the distance to a very small number.
2. Randomly generate input and goal spike train.
3. Using spike coding scheme generate the output for the randomly taken input time series.
4. Find out the distance between the output spike train and the goal spike train and define the distance as error say *E*.
5. Until the distance or E becomes small with the initially taken distance perform the following operations:
   a. Take randomly an input channel

b. Find out $\Delta w_i = proj_{\sin}(E)$ for that input channel.

c. Update weight by $w_i = w_i + \Delta w_i$

d. Proceed the network simulation after that read the result as $S_{out}(t)$.

VI. EXPERIMENTAL ANALYSIS AND APPLICATION

At first we took an input time series, which was considered as the input to the SNN. We used leaky integrate and fire model for our implementation. After taking an input time series, we trained this series with the help of the supervised learning rule described in the previous section. We used the supervised learning rule for approximating the inputs to the output time series and the output time series approximate the goal time series.

For our implementation, we took 500 input channels; each input channel consists of 10 input spikes. The inputs are taken randomly. The following figure demonstrates the inputs of our algorithm.

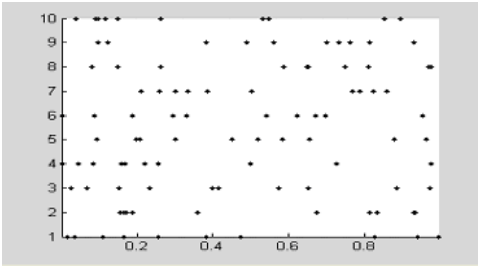

(a)

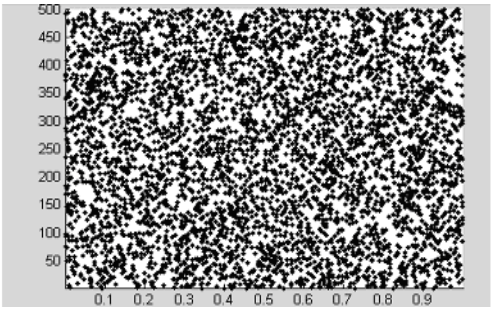

(b)

Fig. 1. Randomly generated inputs for input neuron consisting of (a) 10 and (b) 500 input channels.

Fig. 1(a) shows that the input channels that make up the input neuron consist of 10 and 500 spikes that have been randomly drawn from a uniform distribution in the interval (0,1), we set the initial values of the weights to zero. We applied our algorithm on these inputs for approximating the output to the goal spike train. For that reason we performed 1000 iterations for getting a good result.

The implementation, which we performed, was designed to apply the supervised training algorithm to alter the weights of a spiking neuron that receives the input for the spiking neuron. Here we used leaky integrate and fire neuron with capacitance, resistance, threshold and resting potential equal to $3.03*10^{-8}$ F, 10^{6} ohm, -0.045V, and -0.06V respectively. In fig. 1(b), we showed the randomly generated input time series. With the help of the randomly generated input time series, we will generate the spiking output of the Leaky Integrate and Fire (LIF) neuron [2]. Here we used 500 input channels.

A. Testing

The second set of experiments is designed to apply the iterative training algorithm to alter the input weights $w_1,.....,w_k$ of a spiking neuron that receives the spiking input train as an input to the neuron to produce our goal time series as an output. The neuron is used as a basic LIF neuron; with capacitance, resistance, threshold and resting potential equal to 3.03×10^{-8}F, 10^{6} Ohm, -0.045V, and -0.06V respectively. The time scale of 1/33 is used to match the time constant on which *G* operates. Similar results were obtained with different time scales and parameters.

From fig. 2, we can find our randomly generated goal time series and the spiking output of the LIF neuron after training. This figure shows the result for 500 input channels. The much-increased diversity of the spikes that populate the spiking input train means that there is a much greater likelihood that we will be able to construct our goal spike train with increased accuracy. The trained output is extremely close to our goal.

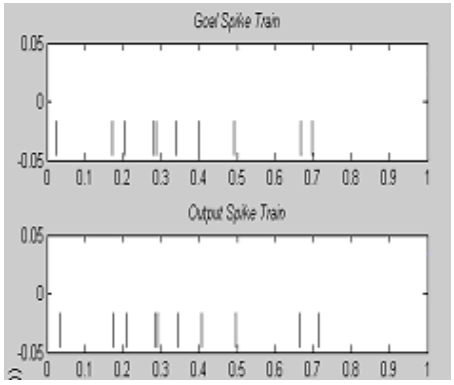

Fig. 2. Randomly generated goal spike trains and the trained output produced by a LIF neuron the associated distance between them.

B. Comparison with Remote Supervised Method (*ReSuMe*)

The approach to which our algorithm is compared is known as the remote supervised method (ReSuMe) [10]. For this comparison, we took 500 LIF neurons.

Each input channel consists of 10 spikes. Again for performing the comparison with ReSuMe, we took 800 input channels. Here the input channels consist of 27 input spikes. The goal time series for our method and gradient descent method consist of 10 spikes. The output spike trains for both methods consist of 10 spikes. But the difference is that ReSuMe takes 100 learning sessions for performing the training of the input spike trains, whereas our method needs 500 learning sessions or iterations for training the input spike trains with the goal spike trains. It indicates that ReSuMe needs a slight less time to perform the job of weight training than our method. The comparison between the two methods is shown in the Table I. However, ReSuMe requires more LIF neurons in comparison to our method.

Table I Comparison with *ReSuMe* method

Methods	**LIF neurons**	**Input spike trains**	**Goal spike trains**	**Output spike trains**	**Learning session**
Proposed Method	500	10	10	10	500
ReSuMe	800	27	10	10	100

C. Application of the Method

We applied our method in case of signal processing. As discussed in the introductory section, for the task of signal processing, we have to deal with multiple spikes because single spike generated with the help of SNN is not suitable for signal processing. For signal processing, we took a series of signals, which we considered as the input signals, and we had a goal signal series. The goal of our method is to process the input signal to approximate with the goal signal series. The input signal which we took, can be considered as a brain signal because SNN deals with the activities of our brain. Now to process the input signals, we generated a series of spikes. And by generating multiple spikes, we performed the job of processing the input signal with the goal series of signal.

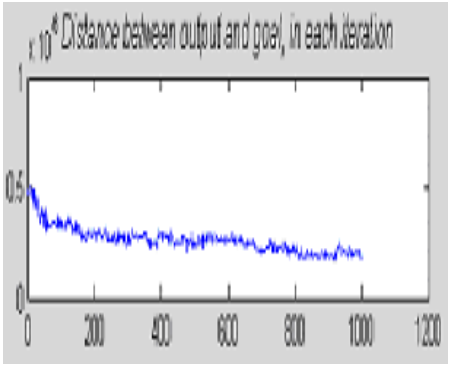

(a)

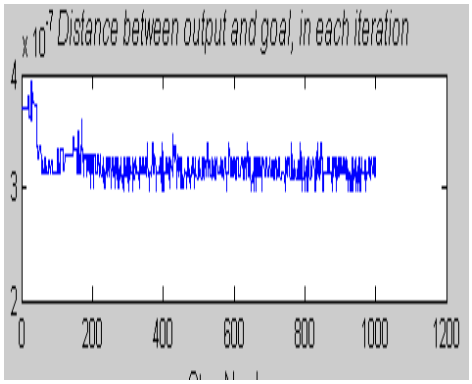

(b)

Fig. 3. (a) The distance of our method for processing the input signals to output signals, (b) the distance of processing the input signals to output signals for single spikes.

The performance of our method for signal processing can be calculated with the help of the distance between the input signals and the output signals. The less the distance between the input signals and the output signals, the more the performance for processing the input signals with the output signals. The distance between the input signals and output signals during the generation of single spike rather than multiple spikes is shown in fig. 3.

Now, it is clear that generating single spike cannot perform efficiently in case of signal processing. The reason is that when we generate single spike, one single spike is used to approximate with the output signals and for this reason, the distance between the input signals and output signals becomes very large. As a result, single spike cannot process signal efficiently. However, the generation of multiple spikes is very much effective for signal processing. In this case, the output signals are generated at once and as a consequence, the distance between the input and output signal is satisfactory. This produces better performance for the multiple spikes than single spikes.

We generated multiple spikes for signal processing, and then applied the generated multiple spikes within two channels, which is known as Sodium (Na) and Potassium (K), channel. The two channels are used to perform signal processing for SNN, which is described in [2]. Applying the generated multiple spikes for signal processing between the two channels as shown in fig. 4; we can find that our method is capable of performing signal processing efficiently. We also applied the single spike between the two channels to show that multiple spikes are capable of performing signal processing nicely. From the experiment, it can be concluded that multiple spikes require less time than the single spike for signal processing.

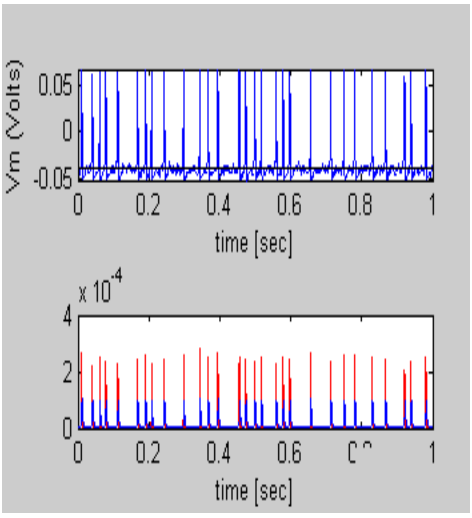

(a)

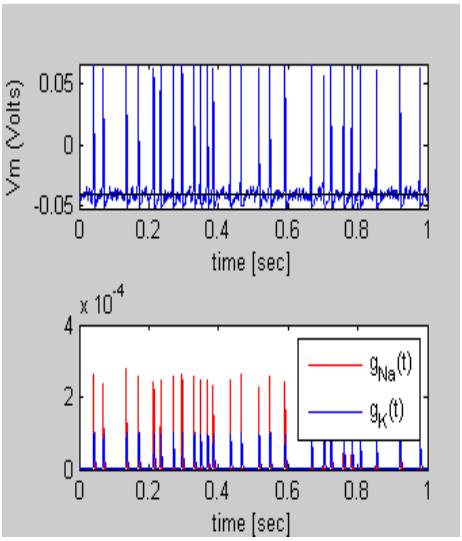

(b)

Fig. 4. Generated spikes for signal processing and the output after performing signal processing through K and Na channels; (a) multiple spikes, and (b) single spike. Our proposed methods.

VII. CONCLUSION

In the last ten years, the aim of neural network research has been shifted to models that are more biologically plausible, such as SNN. In this paper, we developed a supervised learning method for SNNs by using the leaky integrate and fire model and the linear algebra method. The proposed method is simple but effective to train the network for learning any output spike trains or approximating the output to the goal. The algorithm does not restrict the spiking neurons to fire only once like other supervised rules and we can deal with multiple spikes per neuron. The experimental results and the testing segment also justify that the proposed learning method is effective enough to approximate any output spike trains with the goal spike trains, to be exact, the proposed supervised learning method is able to emit multiple spikes. However, the proposed method highly depends on the number of input channels. In some cases, it might take more time for performing the approximation task. In future, we hope to work with the time barrier.

REFERENCES

[1] W. Gerstner, "Time structure of the activity in neural network models", *Phys Rev E*, vol. 51, no 1, 1995, pp. 738–758.

[2] W. Gerstner, W. M. Kistler, *Spiking Neuron Models: Single Neurons, Populations, Plasticity*. Cambridge University Press, 2002.

[3] W. Maass, C. M. Bishop (eds), *Pulsed Neural Network*. The MIT Press, Cambridge, 1999.

[4] S. Song, K. D. Miller et al, "Competitive hebbian learning through spike-timing- dependent synaptic plasticity", *Nature Neuroscience*, vol. 3, no. 9, 2000, pp. 919–926.

[5] A. Belatreche, L. P. Maguire, M. Meinnity, Q. X. Wu, "A method for supervised training of spiking neural networks", in Proc: IEEE Conference Cybernetics Intelligence-Challenges and Advances (CICA'2003), Reading, UK, 2003, pp. 39-44.

[6] S. M. Bohte, J. N. Kok, J. A. La Poutrffe, " Error-backpropagation in temporally encoded networks of spiking neurons", *Neurocomputing*, vol. 48, 2002, pp. 17-37.

[7] J. Hertz, A. Krogh, R. Palmer, *Introduction to the Theory of Neural Networks*. Addison-Wesley, Redwood-City, CA, 1997.

[8] S. M. Moore, *Backpropagation in Spiking Neural Networks*. Master's Thesis, University of Bath, 2002.

[9] B. Ruf, M. Schmitt, "Hebbian learning in networks of spiking neurons using temporal coding", in *Biological and Artificial Computation: from Neuroscience to Technology, Lecture Notes in Computer Science*, vol. 1240, J. Mira, R. Moreno-Diaz, J. Cabestany, Eds. Springer, Berlin, 1997, pp. 380-389.

[10] F. Ponulak, *ReSuMe—New Supervised Learning Method for Spiking Neural Networks*. Technical Report, Institute of Control and Information Engineering, Poznan University of Technology, Poland, 2005.

Proceedings of 2009 12th International Conference on Computer and Information Technology (ICCIT 2009)
21-23 December, 2009, Dhaka, Bangladesh

Biometric Authentication from Low Resolution Hand Images Using Radon Transform

Ahmed Mostayed, Md. Ekramul Kabir†, Saurav Zaman Khan‡, Md. Mynuddin Gani Mazumder
Dept. of Mechanical Engg., The University of Western Australia, Perth, WA, Australia
†Dept. of Applied Physics, Electronics and Communication Engg., University of Dhaka, Dhaka, Bangladesh
‡ALKATEL-LUCENT, Dhaka, Bangladesh
mostayed@mech.uwa.edu.au, ekram_kabeer@yahoo.com, sajib127@hotmail.com, mynudding@mech.uwa.edu.au

Abstract

Biometric authentication refers to the automatic verification of a person's identity from physiological or behavioral characteristics presented by him or her. In this paper an authentication scheme from hand images is presented. Instead of dealing with hand measurements, typically termed as 'hand geometry', this method verifies with entire hand shape. Peg free and position invariant features are calculated using Radon Transform. Low resolution hand images captured by a document scanner are processed to extract feature vectors. The proposed scheme is tested on a data set of 136 images with simple Euclidian norm based match score. The method attained an Equal Error Rate (EER) of 5.1%.

Keywords: Biometric Authentication, Hand Geometry, Morphological Image Processing, Radon Transform.

I. INTRODUCTION

Many physiological and behavioral characteristics of humans are typically invariant over time and unique to each individual. Biometric features such as face, iris, fingerprint, hand geometry, palm-print, etc. have been suggested for secured access control. The most widely studied biometrics has been fingerprint and face (both in 2D and 3D). The reliability of face biometrics has been hampered by the problems caused by pose, expression and illumination. Fingerprint is the most effective identification trait for decades now. However, it also has some limitations as a large group of users, elderly people and manual workers fail to deliver good quality fingerprint images. The surface area of fingerprints is quite small and any cuts or scar mark on this surface generates false minutiae, which undermines the integrity of the system [1]. As a result, other biometric traits are introduced and receiving increased interests. In recent works human gait and iris patterns have attracted many researchers. But the simplicity of hand geometry has made it more favorable. Human hand can be characterized by its length, width, thickness, geometrical composition, shapes of the palm, and shape and geometry of the fingers [2]. The acquisition of hand image is a simple task with no special care needed for illumination or resolution. Moreover, low resolution hand image can be used for integrated hand geometry-palm print authentication system. High resolution hand images can be used in integrated identification/verification system in conjunction with fingerprints [3].

Several patents [4, 5, 6, 7] have been issued for devices that measure hand geometry features for personal verification. In [8] a system is devised for personal authentication using bootstrap technique which effectively utilizes hand geometry features. A similar system using hand geometry features has been described in [9]. Some related work using low-resolution digital hand images appears in [3, 10, 11]. Fixation pegs are used in those works to restrict the hand movement and promising results were obtained.

The method in [3] developed a prototype for hand geometry based verification system for web security system. An image set consisting of around 360 images were tested and a false acceptance rate (FAR) of 2% and a false rejection rate (FRR) of 15% were obtained. Authors of [10] implemented hand geometry verification system using a database of 200 hand images from 20 people and reported 97% success in identification and error rates below 10% in verification. Oden et. al. [11] reported a system for identification and verification using implicit polynomials. Combining their method with geometric features they achieved 95% success in identification and 99% success in verification. The training set they used consists of 40 images. Jain and Duta [12] developed a verification system based on alignment of finger contours and measured the mean alignment error between them. They experimented with 353 images from 50 persons and report FAR of 2% and FRR of 3.5%.

A. Motivation

Convenience acquisition systems along with good identification and verification performance has made hand geometry a popular biometric. Earlier works on hand shape was restricted to its length, width, thickness, geometrical composition, shapes of the palm, and shape and geometry of the fingers for recognition with varying degrees of success. In typical methods Pegs are almost always used to fix the placement of the hand, and anatomical measurements are taken as features [3, 10, 12]. In [13], the outline of the hand is extracted and is represented by a group of salient points, which serve as features in the verification process. Jain et. al. [1] tried to align hand images to a fixed orientation by taking a elliptical shape model. In [2] geometric land marks were identified to get rid of pegs. The objective of this work is to propose a peg free and position invariant method for hand shape verification. One such method is

proposed in [14] based on Higher order Zernike Moments. However, the proposed scheme in this work uses Radon Transform for extracting hand shape feature. One very significant anatomical feature of the hand palm is utilized in this method. The distance between center of mass of the hand palm and the boundary points on the hand is maximum at the middle finger tip. This fact is used to find the optimal parameter for Radon transform and one dimensional position invariant features are extracted from the binary hand silhouettes.

II. PROPOSED METHOD

Peg free hand shape authentication scheme proposed in this work uses Radon Transform to extract position invariant feature vectors. The Radon transform is simply the line integral of an object on the image plane along all the lines from 0 to 360 degrees. But in this paper the radon Transform is taken along an optimal direction only. That optimal angle is found by locating the centroid of hand palm and subsequently locating middle finger tip. In this section several steps of the feature extraction process is described. The discussion begins with a brief introduction of radon Transform.

A. The Radon Transform

Radon transform of an image $f(x,y)$ for a given angle θ can be thought of as computing the projection of the image along that given angle. The resulting projection is a 1 D function which is the sum of the intensities of the pixels in that direction, or in other words a line integral. The Radon Transform of an image $f(x,y)$ for an angle θ is defined as

$$R(\rho,\theta)=\int_{-\infty}^{\infty}\int_{-\infty}^{\infty} f(x,y)\delta(\rho - x\cos\theta - y\sin\theta)\,dxdy \tag{1}$$

where (x,y) denotes spatial coordinates and ρ denotes the radial (perpendicular) distance from the coordinate origin to the line with angle θ. Relation of these parameters with spatial coordinate system is shown in Fig. 1.

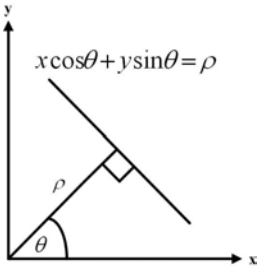

Fig. 1. Parameters for Radon Transform

The Radon Transform possesses some important properties. The most important properties are Linearity, Shifting and Rotation.

Linearity

$$\Re[af_1(x,y)+bf_2(x,y)]=a\Re[f_1(x,y)]+b\Re[f_2(x,y)] \tag{2}$$

Here $\Re[.]$ denotes Radon Transform operator. a and b are scalars.

Shifting

$$\Re[f(x-x_0,y-y_0)]=R(\rho-x_0\cos\theta-y_0\sin\theta,\theta) \tag{3}$$

That means shifting has only effect on the radial distance parameter. This property is very important in the context of this work as it is later used to obtain shift invariant feature vectors.

Rotation

$$\Re[f(x',y')]=R(\rho,\theta-\phi) \tag{4}$$

where $x'=x\cos\phi+y\sin\phi, y'=-x\sin\phi+y\cos\phi$. ϕ is the rotation angle. Note that the change is only on the angle parameter.

B. Image Acquisition

The feature extraction process begins with the hand image acquisition. A document scanner was used to collect low resolution hand images against a dark background. 75 dpi images were taken in 8 bit gray scale format. Each image has a size of 638-by-876 pixels. Fig. 2 shows images taken for one subject. A total of 136 images were taken for 18 subjects. These gray scale images are then converted to binary images by thresholding. The wrist of hand is removed using morphological operators and then the hand boundary was traced to calculate the centroid. Theoretically, the maximum distance point on the boundary from centroid is the middle finger tip. This point along with centroid is used to determine optimal angle for Radon transform.

C. Gray Scale to Binary Conversion

Fig. 3 (a) shows the intensity histogram of the sample image. The images are first converted to double precision format within range [0,1] before calculating its histogram. The threshold problem is substantially simple in this case as the images were taken against dark background. As we can see the foreground (gray) pixels are well separated from the background pixels at an intensity value of 0.15. Thus a threshold value T=0.15 was chosen and this value works well for all the images in the data set. Any intensity value greater than T is assigned the value '1' and any thing lower than that is thresholded to '0'. Fig. 3 (b) shows the thresholded binary image. Small isolated white pixels on the dark background can be noticed. Those pixels are removed while operating the morphological structures to eliminate wrist.

D. Removal of Wrist-Morphological Operation

The success of the proposed method largely depends on the correct location of the palm centroid. For that we must erase the wrist portion from the hand image. This is typically done by morphological operations. A series of morphological opening with disk type structuring element followed by logical 'exclusive or' operation is performed to eliminate wrist. The morphological opening for binary images can be defined as [16],

$$A \circ B = \cup\{(B)_z \mid (B)_z \subseteq A\} \quad (5)$$

where $\cup\{.\}$ denotes the union of all sets inside the braces, and the notation $C \subseteq D$ means that C is a subset of D. The notation $(B)_z$ represents the translation of B to a point $z \equiv (z_x, z_y)$. The morphological opening removes all the foreground pixels that are smaller in size than the structuring element. In this application the disk type structuring element with radius 100 was chosen and was found sufficient for all images used.

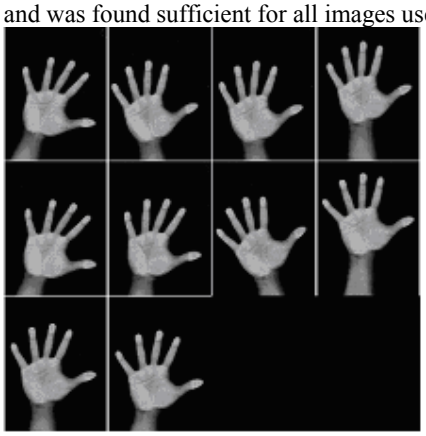

Fig. 2. Example of collected hand images

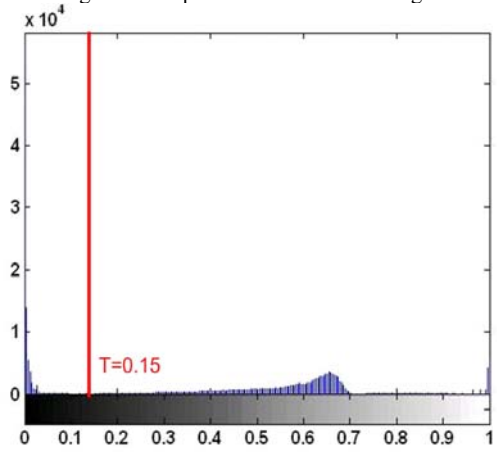

(a)

(b)

Fig. 3. (a) Determination of threshold value from intensity histogram (b) Obtained Binary Image.

E. Finger Tip Identification

Identification of the middle finger tip is an important step of this method. This point along with the centroid, which is the center of mass of the palm, is used to determine the angle parameter for calculation of Radon Transform. That means these two points provide the direction along which the line integral (projection) has to be taken.

Fig. 4. Elimination of wrist after successive morphological operations

The term centroid actually means the geometric center of the object's shape, as above, which is its center of mass or the center of gravity, depending on the context. Centroid of a non-overlapping closed polygon defined by N vertices (x_i, y_i) can be calculated in terms of its area and vertices as below. The area A

$$A = \frac{1}{2}\sum_{i=0}^{N-1}(x_i y_{i+1} - x_{i+1} y_i) \quad (6.1)$$

and its centroid is $C \equiv (C_x, C_y)$ where

$$C_x = \frac{1}{6A}\sum_{i=0}^{N-1}(x_i + x_{i+1})(x_i y_{i+1} - x_{i+1} y_i) \quad (6.2)$$

$$C_y = \frac{1}{6A}\sum_{i=0}^{N-1}(y_i + y_{i+1})(x_i y_{i+1} - x_{i+1} y_i) \quad (6.3)$$

Note that, the polygon has to be closed, that means, the vertex (x_N, y_N) is assumed to be the same as (x_0, y_0).

The palm centroid (C_x, C_y) is calculated as in equation (6.2) and (6.3). Now the maximum centroid distance of the hand boundary corresponds to the middle finger tip. This point will be called 'control point' in the subsequent sections. This point is denoted as $(CTRL_x, CTRL_y)$. In order to calculate centroid distance we first need to trace the hand boundaries. The boundary is traced using eight connected neighborhoods. This process is described in [16] in detail. Fig. 5 (a) shows a traced binary hand image. Fig. 5 (b) shows the centroid and control points marked by red dots. The control point is found by locating the maximum centroid distance as shown in 5 (c).

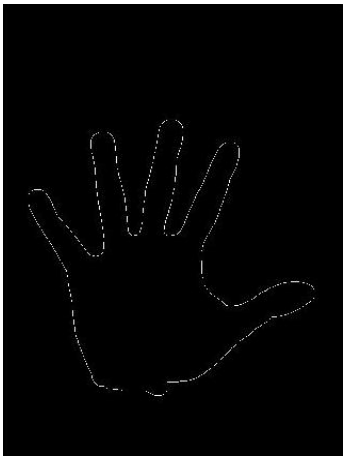

(a)

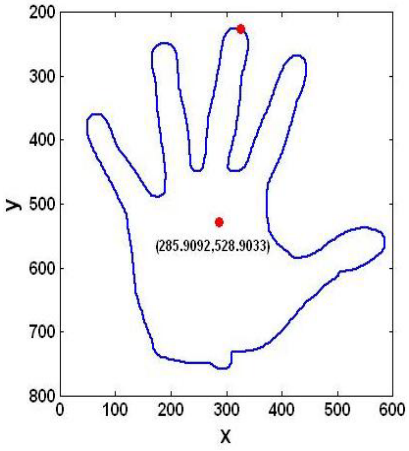

(b)

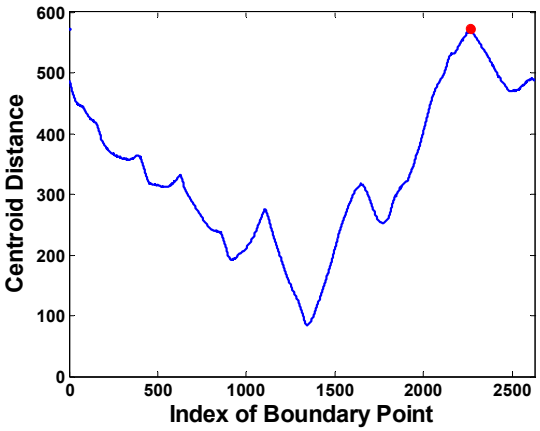

(c)

Fig. 5. (a) Traced boundary of hand (b) Location of palm centroid and control point (c) The centroid distance profile. The red dot corresponds to control point

F. Feature Vector Extraction

The optimal angle for radon transform is found by simply calculating the slope of the line connecting (C_x, C_y) & $(CTRL_x, CTRL_y)$. This can be written mathematically as (in degrees)

$$\theta_{optimal} = \begin{cases} \tan^{-1}\dfrac{B}{A} & when\ B\ and\ A\ have\ same\ sign \\ 180 + \tan^{-1}\dfrac{B}{A} & when\ B\ and\ A\ have\ opposite\ signs \end{cases} \quad (7)$$

with $A = CTRL_x - C_x$ and $B = CTRL_y - C_y$.

The calculation of radon transform of the binary hand image will give rotation invariant feature vectors. But still the complete position invariance is not achieved due to shifting problems in different 'probe' images. This problem is solved by using the shifting property in equation (3) by replacing θ with $\theta_{optimal}$ and assigning $(C_x, C_y) \equiv (x_0, y_0)$. Fig. 6 shows the calculated features for two different hand images.

(a) A hand image

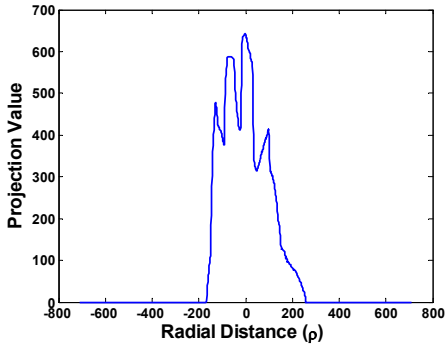

(b) Corresponding feature vector

(c) Another image

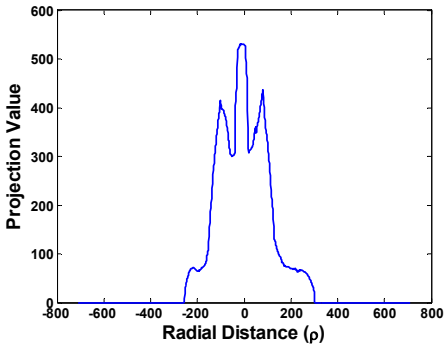

(d) Corresponding feature vector

Fig. 6. Extracted position invariant features

III. PERFORMANCE ANALYSIS

A. Match Score

Usually the similarity between a template image, usually called 'probe', and a data base image, called gallery, is done by setting up a match score of feature vectors. For authentication system, if the similarity score is greater than a predefined threshold, then the probe is accepted as genuine. Otherwise it is rejected. Generally the performance of a proposed algorithm is evaluated by the Receiver Operating Characteristics (ROC) curve which is a plot of False Rejection Rate (FRR) vs False Acceptance Rate (FAR) with changing thresholds. Single valued specification is provided in terms of Equal Error Rate (EER), where FAR and FRR is equal.

In this work the match score for feature vectors is defined as follows

$$S = 1 - \frac{\|X - Y\|}{\|X\|} \tag{8}$$

where **X** and **Y** denotes 'gallery' and 'probe' feature vectors respectively. $\|X - Y\|$ represents Euclidian Distance between them and $\|\|$ denotes Euclidian norm.

B. Results

A total of 136 images were captured. Leaving one gallery image per person, we have a total of 118 probe images. The distribution of FAR and FRR with different threshold is showed in Fig. 7 (a). They cross-over at threshold value 0.82. Fig. 7 (b) shows the ROC curve. The EER value of 5.1% is obtained at threshold value 0.82.

IV. DISCUSSIONS

In [3] around 360 images were tested and a false acceptance rate (FAR) of 2% and a false rejection rate (FRR) of 15% were obtained. A database of 200 hand images from 20 people was tested in [10] and 97% success in identification and error rates below 10% in verification was reported. These two data sets are large enough to be considered impressive. Oden et. al. [11] reported 95% success in identification and 99% success in verification using 40 images. However this population is not that impressive although success rate is very high. Jain and

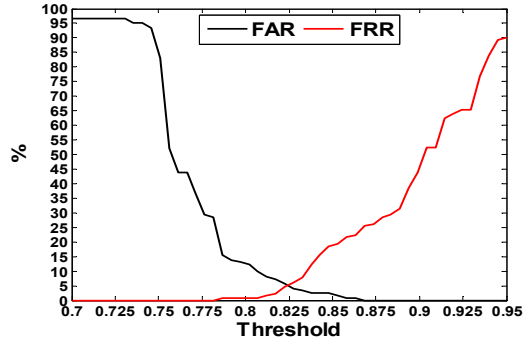

(a)

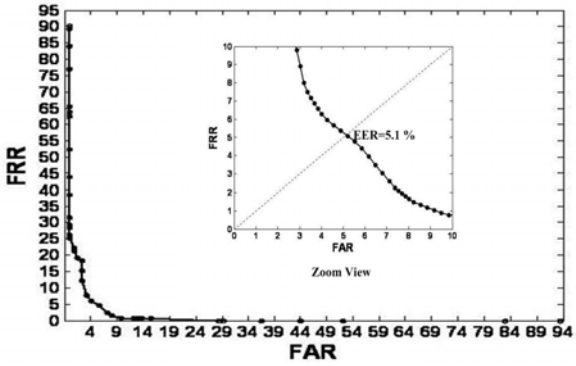

(b)

Fig. 7. (a) Genuine and Imposter Distribution (b) ROC curve. The equal Error Rate is 5.1%

Duta [12] developed a verification system with 353 images based on alignment of finger contours and measured the mean alignment error between them. Their reported FAR and FRR were of 2% and 3.5% respectively. The work presented here established an Equal Error Rate of 5.1 %. Comparing with the work of [3], the FRR is 10% less. It also has better verification result than [10]. However, [12] has showed superior performance. The data set used (134 images) in this work is moderate in size. But similar results are expected for a larger data set. Another issue related to this work is the relative motion of fingers which will clearly hamper the authentication. The subjects were instructed to present their hands according to a particular finger stretching posture (yet no fixation pegs were used—they were free to place their hands at any where in the scanner). Currently the authors are trying to resolve this issue by utilizing fusion of land mark (which are determined automatically from the hand image) based elastic registration with the proposed method.

V. CONCLUSIONS

A novel method for hand shape verification is proposed. Instead of measuring the lengths and widths, this method extracts position invariant features for hand shape using Radon Transform. That also facilitates peg free operation. Low resolution images obtained with a

simple document scanner exhibits an impressive 5.1% error rate for authentication. A data set of 134 images was tested. However, performance analysis against a larger data set is required. Future research is attributed to land mark based elastic registration to counter the problems arise from relative motion of fingers.

REFERENCES

[1] A. Kumar, D. C. Wong, H. C. Shen, and A. K. Jain, "Personal authentication using hand images," *Pattern Recogn. Lett.*, vol. 27, no. 13, 2006, pp. 1478-1486.

[2] A. L. N. Wong, and P. Shi, "Peg-Free Hand Geometry Recognition Using Hierarchical Geometry and Shape Matching," *Proc. IAPR workshop on Machine Vision Applications*, 2002, pp. 281-284.

[3] A.K. Jain, A. Ross, and S. Pankarti, "A prototype hand geometry based verification system," *Proc. 2nd Internat. Conf. on Audio Video based Biometric Personal Authentication*, March 1999, pp. 166–171.

[4] D.P. Sidlauskas, 3D hand profile identification apparatus, US Patent 4736203, 1988.

[5] I.H. Jacoby, A.J. Giordano, and W.H. Fioretti, Personal identification apparatus, US Patent 3648240, 1972.

[6] R.P. Miller, Finger dimension comparison identification system, US Patent 3576538, 1971.

[7] R.H. Ernst, Hand ID system, US Patent 3576537, 1971.

[8] M. Gunther, Device for identifying individual people by utilizing the geometry of their hands, European Patent DE10113929, 2002.

[9] C. C. Han, B. J. Jang, C. J. Shiu, K.H. Shiu, and G.S. Jou, Hand features verification system of creatures, European Patent TW476917, 2002.

[10] R. Sanchez-Reillo, C. Sanchez-Avila, and A. Gonzales-Marcos, "Biometric identification through hand geometry measurements," *IEEE Trans. Pattern Anal. Machine Intell.*, vol. 22, no. 10, 2000, pp. 1168–1171.

[11] C. Oden, A. Ercil, and B. Buke, "Combining implicit polynomials and geometric features for hand recognition," *Pattern Recognition Lett.*, vol. 24, 2003, pp. 2145–2152.

[12] A.K. Jain, and N. Duta, "Deformable matching of hand shapes for verification," *Proc. IEEE International Conference on Image Processing*, Oct. 1999, pp. 857-861.

[13] R. Sanchez-Reillo, "Hand geometry pattern recognition through Gaussian mixture modeling," *Proc. 15th International Conference on Pattern Recognition*, vol. 2, 2000, pp. 937-940.

[14] G. Amayeh, G. Bebis, A. Erol, and M. Nicolescu, "Peg-Free Hand Shape Verification Using High Order Zernike Moments," *Proc. Computer Vision and Pattern Recognition Workshop (CVPRW '06)*, 17-22 June 2006, pp. 40-40.

[15] K.V. Hansen, and P.A. Toft, "Fast Curve Estimation Using Preconditioned Generalized Radon Transform," *IEEE Trans. Image Processing*, vol. 5, no. 12, 1996, pp. 1651-1661.

[16] R. C. Gonzalez, R. E. Woods, and S. L. Eddins, *Digital Image Processing Using Matlab*. Upper Saddle River, NJ: Prentice Hall, 2004, ch. 9.

Proceedings of 2009 12th International Conference on Computer and Information Technology (ICCIT 2009)
21-23 December, 2009, Dhaka, Bangladesh

Phoneme Recognition based on Distinctive Phonetic Features (DPFs) incorporating a Syllable based Language Model

Mohammad Nurul Huda, Manoj Banik†, Ghulam Muhammad‡, Bernd J. Kroger‡‡
Department of CSE, United International University, Dhaka, Bangladesh
† Department of CSE, Ahsanullah University of Science and Technology, Bangladesh
‡College of Computer & Information Science, King Saud University, Saudi Arabia
‡‡Dept. of Phoniatrics and Communication Disorders, University Hospital Aachen, Germany
mnh@cse.uiu.ac.bd, manojbanik@aust.edu, ghulam@ksu.edu.sa, bkroeger@ukaachen.de

Abstract

This paper presents a phoneme recognition method based on distinctive phonetic features (DPFs). The method comprises three stages. The first stage extracts 3 DPF vectors of 15 dimensions each from local features (LFs) of an input speech signal using three multilayer neural networks (MLNs). The second stage incorporates an Inhibition/Enhancement (In/En) network to obtain more categorical DPF movement and decorrelates the DPF vectors using the Gram-Schmidt orthogonalization procedure. Then, the third stage embeds acoustic models (AMs) and language models (LMs) of syllable-based subwords to output more precise phoneme strings. The proposed method provides a higher phoneme correct rate as well as phoneme accuracy with fewer mixture components in hidden Markov models (HMMs).

Keywords: distinctive phonetic features, local features, multilayer neural networks, Inhibition/Enhancement network, hidden Markov models.

I. INTRODUCTION

A new vocabulary word or out-of-vocabulary (OOV) word often causes an "error" or "rejection" and sometimes generates heavy consequence by the lack of a language model (LM) in current hidden Markov models (HMMs)-based systems. To solve this problem, an accurate phoneme recognizer or phonetic typewriter functionality is expected [1, 2].

Though various distinctive phonetic features (DPFs)-based methods were proposed to obtain a more accurate phoneme recognizer [3, 4, 5], they provide a higher phoneme correct rate (PCR) with poor phoneme accuracy rate (PAR). The reason for providing lower phoneme recognition accuracy is the violation of some phonotactic constraints at different places of the output phoneme string of an input utterance. Therefore, it is needed to incorporate syllable-based subword items, which set some grammatical constraints at the recognition stage, for obtaining a phoneme recognizer with higher accuracy.

In this paper, we propose a method, incorporating syllable-based language models, to obtain a more accurate phoneme recognizer that comprises three stages. The first stage extracts three DPF vectors of 15 dimensions each from local features (LFs) of an input speech signal using three multilayer neural networks (MLNs). The second stage incorporates an Inhibition/Enhancement (In/En) network to obtain more categorical DPF movement and decorrelates the DPF vectors using the Gram-Schmidt (GS) algorithm. Then, the third stage embeds acoustic models (AMs) and LMs of syllables at the recognition stage of an HMM-based classifier.

The paper is organized as follows: Section 2 discusses the articulatory features. Section 3 explains the system configuration of the proposed phoneme recognition method. Experimental database and setup are provided in Section 4, while experimental results are analyzed in Section 5. Finally, in Section 6, some conclusions are drawn.

II. JAPANESE ARTICULATORY FEATURES

A phoneme can easily be identified by using its unique articulatory feature or DPF set [6, 7]. The Japanese balanced DPF set [8, 9] for classifying Advanced Telecommunications Research Institute International (ATR) phonemes have 15 elements. These DPF values are mora, high, low, intermediate between high and low <nil>, anterior, back, intermediate between anterior and back <nil>, coronal, plosive, affricate, continuant, voiced, unvoiced, nasal and semi-vowel. Table 1 shows a part of this balanced DPF set. Here, present and absent elements of the DPFs are indicated by "+" and "-" signs, respectively.

Table 1: Japanese Balanced DPF-set.

DPF/Phone	a	e	...	f	r
mora	+	+	...	-	-
high	-	-	...	+	-
low	+	-	...	-	-
nil	-	+	...	-	-
anterior	-	-	...	+	+
back	+	-	...	-	-
nil	-	+	...	-	-
			...		

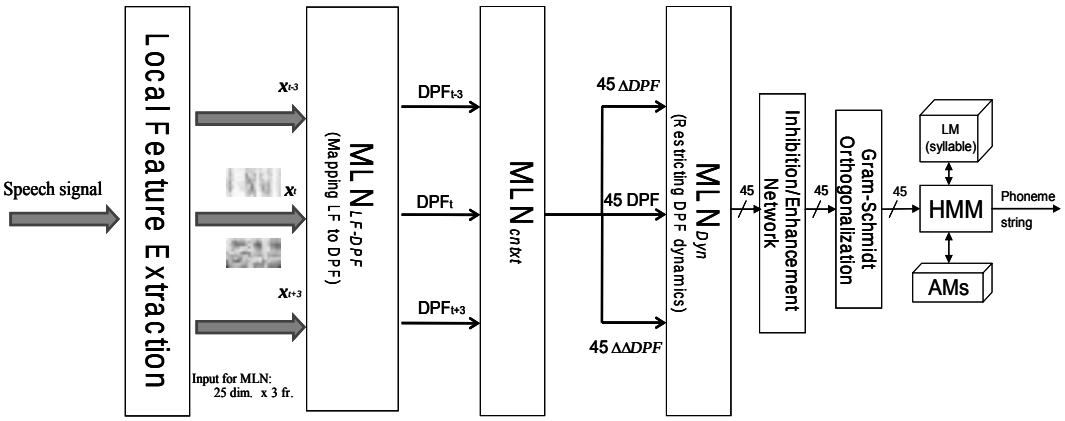

Fig.1: Proposed Phoneme Recognition Method.

III. PROPOSED PHONEME RECOGNITION METHOD

Figure 1 shows the proposed phoneme recognition method. This method comprises three stages. The first stage extracts one 45-dimensional DPF vector from the LFs of an input speech signal using three MLNs. The second stage incorporates In/En functionalities to obtain modified DPF patterns and decorrelates the DPF vector using the GS orthogonalization before connecting it with an HMM-based classifier. Then, the third stage incorporates AMs and LMs of syllable-based subwords at the recognition stage of an HMM-based classifier.

A. DPF EXTRACTOR

In this method, three MLNs instead of a single MLN are used to construct the DPF extractor. The first MLN, $MLN_{LF\text{-}DPF}$, maps acoustic features or LFs [10] onto discrete DPFs [8, 9]. The second MLN, MLN_{cntxt}, reduces misclassification at phoneme boundaries, and the third MLN, MLN_{Dyn}, restricts the DPF dynamics. Here, the $MLN_{LF\text{-}DPF}$ has two hidden layers of 256 and 96 units, respectively and takes three input vectors (t-3, t, t+3) of LFs of 25 dimensions each. It is trained using the standard back-propagation learning algorithm. The 45-dimensional context-dependent DPF vector provided by the $MLN_{LF\text{-}DPF}$ at time t is appended into the MLN_{cntxt}, which consists of five layers including three hidden layers of 90, 180, and 90 units, respectively, and generates a 45-dimensional DPF vector with a small number of errors at phoneme boundaries. This 45-dimensional DPF vector and its corresponding ΔDPF and ΔΔDPF vectors calculated by three-point linear regression (LR) are appended into the subsequent MLN_{Dyn}, which consists of four layers including two hidden layers of 300 and 100 units, respectively, and outputs a 45-dimensional DPF vector with reduced fluctuations and dynamics. Both the MLN_{cntxt} and MLN_{Dyn} are also trained using the standard back-propagation algorithm.

B. INHIBITION/ENHANCEMENT NETWORK

The DPF extractor provides 45 DPF patterns (15 for preceding context, 15 for current context, and 15 for following context) for each input vector along time axis. These patterns may not match with the pattern of input-phoneme string for some phonemes and consequently, some phonemes are incorrectly recognized by the HMM classifier. This phoneme misclassification sometimes occurs when the values of DPF peaks and DPF dips are closer to each other. Therefore, a mechanism, which is called In/En network [3, 4, 5] in this study, is needed to obtain clearly separable DPF peaks and dips. An algorithm for this network is given below:

Step1: For each element of the DPF vectors, find the acceleration (ΔΔ) parameters by using three-point LR.

Step2: Check whether (ΔΔ) is positive (concave pattern) or negative (convex pattern) or zero (steady state).

Step3: Calculate $f(\Delta\Delta)$.

if pattern is convex,

$$f(\Delta\Delta) = \frac{c_1}{1+(c_1-1)e^{\beta\Delta\Delta}}$$

if pattern is concave,

$$f(\Delta\Delta) = c_2 + \frac{2(1-c_2)}{1+e^{\beta\Delta\Delta}}$$

if steady state,

$$f(\Delta\Delta) = 1.0$$

Step4: Find modified DPF patterns by multiplying the DPF patterns with $f(\Delta\Delta)$.

Figure 2 shows the working mechanism of the In/En network using the "anterior" DPF pattern of an input

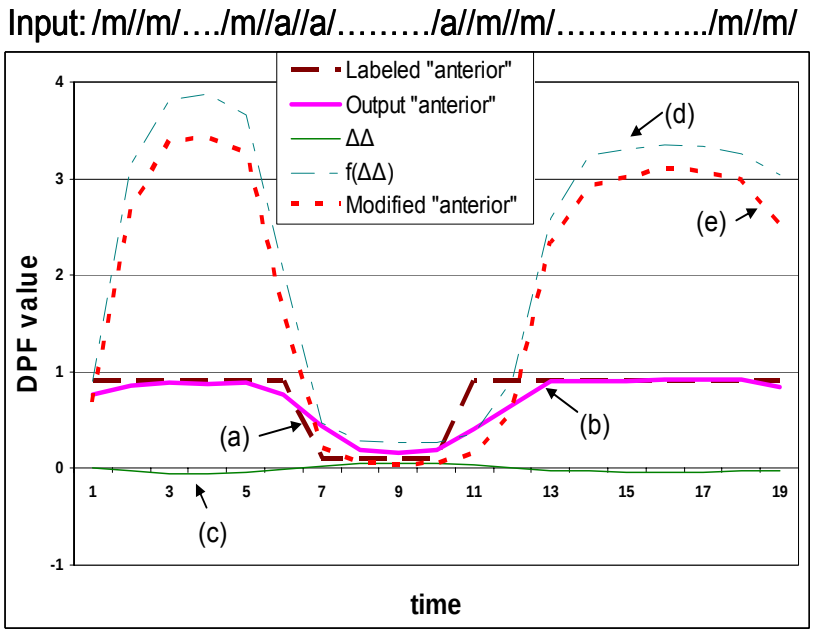

Fig. 2: Working mechanism of the In/En network. Five curves are denoted by (a), (b), (c), (d), and (e), respectively. The curves: a) Labeled "anterior" DPF for input utterance, /mam/, b) Output "anterior" DPF by a neural network, c) ΔΔ for output "anterior", d) f(ΔΔ) for ΔΔ, and e) Modified "anterior" by multiplying curve (b) with curve (d).

utterance, /mam/ along time axis. In the figure, five curves, which represent labeled "anterior" DPF for the input utterance, corresponding output "anterior" generated by a neural network, ΔΔ for the output "anterior" values, f(ΔΔ) for ΔΔ values, and modified "anterior" DPF, are indicated by (a), (b), (c), (d), and (e), respectively. Here, the curve (e) is obtained by multiplying curve (b) with curve (d). After applying the In/En network algorithm on curve (b), the DPF values of frames 1-6 and 13-19 (convex pattern or DPF peak) are enhanced, and frames 7-11 (concave pattern or DPF dip) are inhibited.

C. GRAM-SCHMIDT ORTHOGONALIZATION

Because each of the three 15-dimensional context vectors outputted by the In/En network is not orthogonal to each other, these three context vectors should be decorrelated using the GS orthogonalization [8] with respect to the current context vector.

D. SYLLABLE-BASED LANGUAGE MODEL

The phoneme classification inaccuracy at the acoustic phonetic level is a major weakness in most speech recognition systems. However, the inaccuracy often violates phonotactic constraints at the acoustic phonetic level. Usually, three types of phoneme classification errors appear: (i) phoneme insertions, (ii) phoneme deletions, and (iii) phoneme substitutions. A better performance is expected if a language model is adopted in a recognition system for post-processing phoneme estimates and for making corrections with regard to the grammatical constraints. Words, syllables, and phonological rules, etc. of a language provide some constraints on a phoneme sequence generation, but a language has a large number of words and knowledge-based rules. On the other hand, since the number of syllables of a language is limited, they can be used to enhance the phoneme recognition performance.

IV. EXPERIMENTS

A. SPEECH DATABASES

Since open tests are done, different training data sets are used for the neural network-based and HMM-based classifiers. The following five clean data sets are used in our experiments.

D1. Training data set for $MLN_{LF\text{-}DPF}$

A subset of the Acoustic Society of Japan (ASJ) Continuous Speech Database [11] comprising 4503 sentences uttered by 30 different male speakers (16 kHz, 16 bit) is used.

D2. Training data set for MLN_{cntxt}

This data set contains 5000 sentences that are taken from Japanese Newspaper Article Sentences (JNAS)

[12] Continuous Speech Database; the sentences have been uttered by 33 different male speakers (16 kHz, 16 bit).

D3. Training data set for MLN_{Dyn}

This data set contains 5000 JNAS [12] sentences uttered by 33 different male speakers (16 kHz, 16 bit). Speakers of this data set are different from the D2 data set.

D4. Training data set for HMM classifier

This data set takes 5000 JNAS [12] sentences uttered by 33 different male speakers (16 kHz, 16 bit). Speakers of this data set are different from the D2 and D3 data set.

D5. Test data set

This test data set comprises 2379 JNAS [12] sentences uttered by 16 different male speakers (16 kHz, 16 bit).

B. EXPERIMENTAL SETUP

The frame length and frame rate are set to 25 ms and 10 ms, respectively, to obtain acoustic features from an input speech signal. LFs are a 25-dimensional vector consisting of 12 delta coefficients along time axis, 12 delta coefficients along frequency axis, and delta coefficient of log power of a raw speech signal.

Since our goal is to design a more accurate phoneme recognizer, PCR and PAR for D5 data set are evaluated using an HMM-based classifier. The D4 data set is used to design 38 Japanese monophone HMMs with five states, three loops, and left-to-right models. Input features for the classifier are DPFs. In the HMMs, the output probabilities are represented in the form of Gaussian mixtures, and diagonal matrices are used. The mixture components are set to 1, 2, 4, 8, and 16.

In our experiments of the three-MLN, the non-linear function is a sigmoid from 0 to 1 (1/(1+exp(-x))) for the hidden and output layers.

For the In/En network, the value of the enhancement coefficient, C1, is set to 4.0 after evaluating the proposed method, DPF(3-MLN+In/En+GS,dim:45), for different values of C1 , such as 2, 4, and 6, and the value of the steepness coefficient, β, is set to 80. The value of inhibitory coefficient, C2, is fixed to 0.25 after observing the DPF data patterns to keep the values of f(ΔΔ) between 0.25 and 1.0.

For the experiments incorporating LMs, the Julius 3.5.3 version is used to embed acoustic models and tri-gram subword models (short and long syllables) as LMs. It is a two-pass system, where the first pass is a bigram and the second one is a trigram to set more constraints on the output phoneme sequence. Syllable structures are CV, CVV, CV1V2, CVN, and CVQ. Weight/Insertion penalties are 5.0/-1.0 and 6.0/00 for the first and second passes, respectively.

To investigate the effect of syllable-based subword LM, we have designed the following phoneme recognition tests, where the DPF extractor inputs a 45-dimensional orthogonalized DPF vector to the HMM.

(a) 3-MLN+In/En+GS [5]
(b) 3-MLN+In/En+GS+LM [Proposed]

V. EXPERIMENTAL RESULTS AND DISCUSSION

Figure 3 shows the phoneme correct rate of the proposed method before and after adding syllable-based subword language model. For all the mixture components investigated, the method with LM provides higher PCR. For example, at mixture component 16, the method without LM shows 84.50% PCRs, while the corresponding value for the method with LM is 87.40%.

On the other hand, the method with LM outperformed the method without LM for phoneme accuracy, which is shown in Fig. 4. By using the mixture components 1 an-

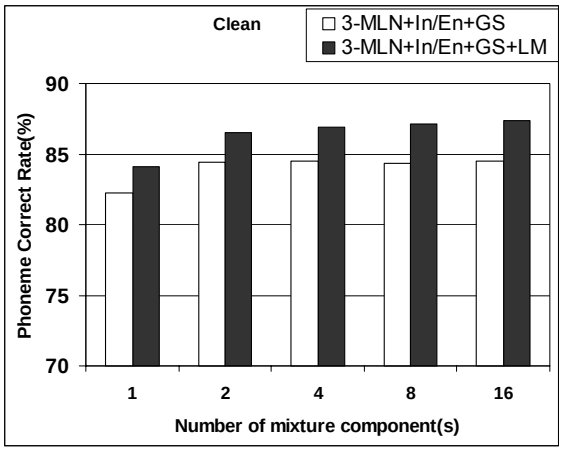

Fig. 3: Comparison of phoneme correct rate before and after adding LM.

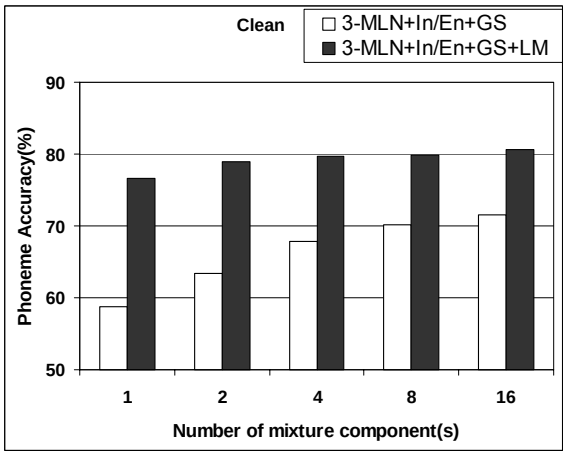

Fig. 4: Comparison of phoneme accuracy before and after adding LM.

d 2, the syllable knowledge leads to correction of the highest number of phonemes and shows the highest level improvement. Again, the addition of syllable knowledge shows the highest accuracy (80.54%) at mixture component 16. Therefore, language constraints resist misclassification of phonemes and consequently, provide higher phoneme recognition performance in a clean acoustic environment.

VI. CONCLUSION

In this paper, a DPF-based phoneme recognition method is presented incorporating a specific syllable-based language model. The method with language model does not increase phoneme correct rate in a large scale, but the effectiveness of the syllable-based language model is observed significantly for improving phoneme recognition accuracy. In future research, an evaluation of Bengali phoneme recognition accuracy will be tried using the method proposed in this paper.

REFERENCES

[1] I. Bazzi and J. R. Glass, "Modeling OOV words for ASR," Proceedings of ICSLP, Beijing, China, p. 401-404, 2000.

[2] O. Scharenborg and S. Seneff, "A two-pass for strategy handling OOVs in a large vocabulary recognition task," Proc. Interspeech, 2005.

[3] M. N. Huda, H. Kawashima, and T. Nitta, "Distinctive Phonetic Feature (DPF) extraction based on MLNs and Inhibition/Enhancement Network," IEICE Trans. Inf. & Syst., Vol.E92-D, No.4, April 2009.

[4] M. N. Huda, H. Kawashima, K. Katsurada, and T. Nitta, "Distinctive phonetic feature (DPF) based phoneme recognition using MLNs and Inhibition/Enhancement network for noise robust ASR," Proc NCSP'09, Honolulu, Hawaii, USA, March 2009.

[5] M. N. Huda, H. Kawashima, and T. Nitta, "Distinctive phonetic feature extraction based on 3-stage MLNs and Inhibition/Enhancement network," Proc Technical Report of IEICE, SP08, December 2008.

[6] S. King and P. Taylor, "Detection of Phonological Features in Continuous Speech using Neural Networks," Computer Speech and Language 14(4), pp. 333-345, 2000.

[7] E. Eide, "Distinctive Features for Use in an Automatic Speech Recognition System," Proc. Eurospeech 2001, vol.III, pp.1613-1616, 2001.

[8] T. Fukuda and T. Nitta, "Orthogonalized Distinctive Phonetic Feature Extraction for Noise-Robust Automatic Speech Recognition," The Institute of Electronics, Information and Communication Engineers (IEICE) Transactions on Information and Systems, Vol. E87-D, No.5, pp. 1110-1118, 2004.

[9] T. Fukuda, W. Yamamoto, and T. Nitta, "Distinctive Phonetic feature Extraction for robust speech recognition," Proc. ICASSP'03, vol.II, pp.25-28, 2003.

[10] T. Nitta, "Feature extraction for speech recognition based on orthogonal acoustic-feature planes and LDA," Proc. ICASSP'99, pp.421-424, 1999.

[11] T. Kobayashi, et. al, "ASJ Continuous Speech Corpus for Research," Acoustic Society of Japan Trans. Vol.48, No.12, pp.888-893, 1992.

[12] JNAS: Japanese Newspaper Article Sentences. http://www.milab.is.tsukuba.ac.jp/jnas/instruct.html

.

Proceedings of 2009 12th International Conference on Computer and Information Technology (ICCIT 2009)
21-23 December, 2009, Dhaka, Bangladesh

A Crosstalk Free Routing Algorithm of Optical Multistage Interconnection Networks

Arjuman Sultana, Md. Naimul Hasan†
Dept. of Computer Science & Engineering, Khulna University of Engineering & Technology, Khulna, Bangladesh
† Dept. of Electrical and Electronic Engineering, Bangladesh University of Engineering & Technology, Dhaka, Bangladesh
arjucse03@yahoo.com, anik_ieee@yahoo.com

Abstract

Crosstalk is an intrinsic drawback of optical networks and avoiding crosstalk is important for making fruitful application of optical switching networks. Rearrangeable optical Multistage Interconnection Networks (MINs) are feasible since they have lower complexity than their strictly counterparts. In this paper, we propose a crosstalk free routing algorithm of optical MINs and we apply it to three examples of optical MINs, the Generalized Recursive Network (GRN), the Banyan Network and the Benes Network. The routing algorithm is derived based on the idea of the semi-permutation and it completes the decomposition of a permutation.

Keywords: Crosstalk, Optical Switch, Routing Algorithm and Semi-permutation.

I. INTRODUCTION

Communications among processors in a parallel computing system are always the main design issue when a parallel system is built or a parallel algorithm is designed. Fiber optic communications offer a combination of high bandwidth, low error probability, and gigabit transmission capacity. Multistage interconnection networks have an important interconnecting scheme for parallel computing systems [1]. Two major problems in designing optical switch networks are signal loss and crosstalk. There are two ways in which optical paths can interact in planar switching networks. First, two optical channels on different waveguides may cross each other in order to obtain a particular topology. This is called channel crosstalk. Alternatively, two paths sharing a switching element will experience some undesired coupling from one path to the other. This is called optical crosstalk [3]. Therefore, the main objective of this paper is to propose a crosstalk free routing algorithm of the optical MINs and apply the algorithm on three optical MINs as examples.

This paper is organized as follows. In section II, we give an overview idea of preliminaries. In section III, we discuss details about the semi-permutations. In section IV, we propose a crosstalk free routing algorithm of optical MINs. In section V, we discuss realizing semi-permutations in optical MINs and we also show simulation results of three networks. Finally, Section VI concludes the paper.

II. PRELIMINARIES

There are mainly two types routing centralized routing and distributed routing. Centralized routing means control of switches is centralized; the decision about how to send the input signal to its desired output is taken at a central location for any input. Distributed routing means control units may be distributed among several switches. Self-routing means every switching elements in the architecture can decide about the routing without having any information of other switches states [4]. Self-routing reduces the connection complexity for the control lines [3]. As the control function is distributed among different switching modules, the network is less susceptible to faults of a switch. Most of the existing switch networks are not self-routing for all permutations.

A. Limitation of Optical MINs

There are two major problems in designing optical switch networks are signal loss and crosstalk. When two optical paths interact to each other, then crosstalk occurs. The number of crosstalk switches along a path of a signal from input to output is a representative measure of crosstalk of the switch architecture [3]. The number of switching elements in a signal path is a measure of signal loss. Clearly signal loss is proportional to the number of switches that has to be crossed by a signal before reaching the output. The total number of switches required, is called switch count, to build a network is a representative measure of the hardware complexity of the network [4].

B. Approaches to Solving Crosstalk Problem

One way to solve the crosstalk problem is a space domain approach, where a MIN is duplicated and combined to avoid crosstalk. But this approach uses more than double of the original network hardware to achieve the same permutation capability. Another way to implement this idea is a time domain approach [6]. A set of connections is partitioned into several subsets such that the connections in each subset can be established simultaneously in a network without crosstalk. In our work, we will consider the idea of time domain approach. Because each switch can only pass one signal at a given time. In this paper, we will consider how to

978-1-4244-6283-4/09/$26.00 ©2009 IEEE

realize permutations in an optical MIN efficiently using the time domain approach. Any permutation in an optical MIN requires at least two passes.

III. SEMI-PERMUTATIONS

We consider an $n \times n$ multistage interconnection network with n inputs and n outputs where $n = 2^m$. A permutation for a network is a pairing of its inputs and outputs such that each input appears in exactly one pair and each output appears also in exactly one pair. In other words, a permutation is a full one-to-one mapping between the network inputs and outputs. For an $n \times n$ network, suppose input x_i is mapped to output y_i, where $x_i = i$ and $y_i \in \{0, 1…., n\text{-}1\}$ for $0 \le i \le n\text{-}1$, we denote this permutation as,

$$\begin{pmatrix} x_0 & x_1 & ..... & x_{n-1} \\ y_0 & y_1 & ..... & y_{n-1} \end{pmatrix}$$

Apparently, a crosstalk-free optical network can not realize a permutation in a single pass, since at least the two input links on an input switch or the two output links on an output switch cannot be active in the same pass. For an optical network consisting of 2×2 switches, it is useful to introduce the following definition,

A partial permutation, $\begin{pmatrix} x_0 & x_1 & ..... & x_{n/2-1} \\ y_0 & y_1 & ..... & y_{n/2-1} \end{pmatrix}$ of an n-element set $\{0, 1, ……, n-1\}$, where n is an even integer, $x_i, y_i \in \{0, 1, ….., n-1\}$ and $x_0 < x_1 < ……. < x_{n/2-1}$, is referred to as a semi-permutation of n-element set $\{\lfloor x_0/2 \rfloor, \lfloor x_1/2 \rfloor, ..., \lfloor x_{n/2-1}/2 \rfloor\} = \{0,1,….,n/2\text{-}1\}$ and $\{\lfloor y_0/2 \rfloor, \lfloor y_1/2 \rfloor, ..., \lfloor y_{n/2-1}/2 \rfloor\} = \{0,1, ….., n/2\text{-}1\}$

Example 1 For n = 16, partial permutation

$$\begin{pmatrix} 1 & 2 & 5 & 7 & 8 & 10 & 12 & 14 \\ 2 & 0 & 13 & 11 & 9 & 6 & 5 & 15 \end{pmatrix}$$

is a semi-permutation, since we have

$\left\{\frac{1}{2}, \frac{2}{2}, \frac{5}{2}, \frac{7}{2}, \frac{8}{2}, \frac{10}{2}, \frac{12}{2}, \frac{14}{2}\right\} = \{0, 1, 2, 3, 4, 5, 6, 7\}$, and

$\left\{\frac{2}{2}, \frac{0}{2}, \frac{13}{2}, \frac{11}{2}, \frac{9}{2}, \frac{6}{2}, \frac{5}{2}, \frac{15}{2}\right\} = \{1, 0, 6, 5, 4, 3, 2, 7\} = \{0, 1, 2, 3, 4, 5, 6, 7\}$

Clearly, a semi-permutation is a partial permutation that ensures that there is only one active link passing through each input switch and output switch, that is, it eliminates crosstalk in the first and last stages in the network, and thus it has the potential to be realized in an optical network under the constraint of avoiding crosstalk. Of course, to ensure the entire network crosstalk free, we need to eliminate crosstalk in the switches in the intermediate stages as well.

A. BIPARTITE GRAPH

A bipartite graph (BG) is a graph whose vertices can be divided into two disjoint sets V_1 and V_2 such that every edge connects a vertex in V_1 and one in V_2; that is, there is no edge between two vertices in the same set [1]. Given a permutation of the form (1), in which input x_i is mapped to output y_i, where $0 \le i \le n\text{-}1$. Define $A_j^{[1]}$ and $A_j^{[2]}$ both as the two-element set $\{2j, 2j+1\}$ for $0 \le j \le n/2\text{-}1$, where $A_j^{[1]}$ and $A_j^{[2]}$ correspond to the inputs and outputs, respectively.

Now we construct an undirected bipartite graph $G = (V_1, V_2, E)$. The vertex sets of G are defined as $V_1 = \{A_0^{[1]}, A_1^{[1]}, ……, A_{n/2-1}^{[1]}\}$, $V_2 = \{A_0^{[2]}, A_1^{[2]}, …… , A_{n/2-1}^{[2]}\}$ and the edge set E of G is defined as: for any one-pair mapping $\begin{pmatrix} xi \\ yi \end{pmatrix}$ in the permutation. If $x_i \in A_{j1}^{[1]}$ and $y_i \in A_{j2}^{[2]}$, then there is an edge between vertex $A_{j1}^{[1]}$ and vertex $A_{j2}^{[2]}$ in E. We also assign each edge in E a label representing the corresponding one-pair mapping in the permutation. Here n is an integer value. This bipartite graph has the following properties. This graph may have parallel edges and each vertex of the graph has degree two. The graph may consist of more than one connected component. It's vertexes $|V_1| = |V_2| = n/2$ and $|E| = n$. From graph theory, we know that for a component of a graph in which each vertex has an even degree, there exists an Euler tour which traverses each edge exactly once [5].

B. DECOMPOSITION ALGORITHM OF BG

- Construct a bipartite graph G for the given Permutation.
- For each connected component of G, start from a vertex of this component in V_1, traverse through an unvisited edge to the neighbor vertex in V_2, back and forth until return to the starting vertex. (During the traversing, a visited edge is marked "forward" if the traverse direction on this edge is from V_1 to V_2; and the marked "backward" if the direction is opposite.)
- Take all one-pair mappings corresponding to the edges marked with "forward", to form one semi-permutation; let the remaining one-pair mappings, corresponding to the edges marked with "backward", form another semi-permutation.

The above algorithm is correct because from the properties of the bipartite graph G listed above, the set of all edges marked with "forward" is a perfect matching of the bipartite graph G, and so is that marked with "backward". Also, it is easy to see that the time to construct the bipartite graph is proportional to the number of pairs in the permutation, i.e., $0(n)$, and the time to traverse all edges is $0(|E|) = 0(n)$. Hence, the complexity of the decomposition algorithm is $0(n)$. Let's apply the

above algorithm to Example 2. The bipartite graph and edge traverses are shown in Fig. 1, where

Example 2 The decomposition of a permutation into two semi-permutations and the bipartite graph for this permutation is shown in Fig. 1

$$\begin{pmatrix} 0 & 1 & 2 & 3 & 4 & 5 & 6 & 7 & 8 & 9 & 10 & 11 & 12 & 13 & 14 & 15 \\ 8 & 2 & 0 & 12 & 4 & 13 & 3 & 11 & 9 & 1 & 6 & 7 & 5 & 10 & 15 & 14 \end{pmatrix}$$

$e_0 = \begin{pmatrix} 0 \\ 8 \end{pmatrix}$, $e_1 = \begin{pmatrix} 1 \\ 2 \end{pmatrix}$, $e_2 = \begin{pmatrix} 2 \\ 0 \end{pmatrix}$, $e_3 = \begin{pmatrix} 3 \\ 12 \end{pmatrix}$, $e_4 = \begin{pmatrix} 4 \\ 4 \end{pmatrix}$,

$e_5 = \begin{pmatrix} 5 \\ 13 \end{pmatrix}$, $e_6 = \begin{pmatrix} 6 \\ 3 \end{pmatrix}$, $e_7 = \begin{pmatrix} 7 \\ 11 \end{pmatrix}$, $e_8 = \begin{pmatrix} 8 \\ 9 \end{pmatrix}$, $e_9 = \begin{pmatrix} 9 \\ 1 \end{pmatrix}$,

$e_{10} = \begin{pmatrix} 10 \\ 6 \end{pmatrix}$, $e_{11} = \begin{pmatrix} 11 \\ 7 \end{pmatrix}$, $e_{12} = \begin{pmatrix} 12 \\ 5 \end{pmatrix}$, $e_{13} = \begin{pmatrix} 13 \\ 10 \end{pmatrix}$,

$e_{14} = \begin{pmatrix} 14 \\ 15 \end{pmatrix}$, $e_{15} = \begin{pmatrix} 15 \\ 14 \end{pmatrix}$

Take the pairs e_1, e_2, e_5, e_7, e_8, e_{10}, e_{12} and e_{14} that correspond to the edges with traversing direction being from v_1 to v_2 to form the forward pair and take the pairs e_0, e_3, e_4, e_6, e_9, e_{11}, e_{13} and e_{15} that correspond to the edges with traversing direction being from v_2 to v_1 to form the backward pair.

$$\text{Forward} = \begin{pmatrix} 1 & 2 & 5 & 7 & 8 & 10 & 12 & 14 \\ 2 & 0 & 13 & 11 & 9 & 6 & 5 & 15 \end{pmatrix} \quad (1)$$

$$\text{Backward} = \begin{pmatrix} 0 & 3 & 4 & 6 & 9 & 11 & 13 & 15 \\ 8 & 12 & 4 & 3 & 1 & 7 & 10 & 14 \end{pmatrix} \quad (2)$$

We can again decompose the "forward" pair from (1), according to bipartite graph. The bipartite graph for the semi-permutation shown in (1) is depicted in Fig. 2. Then take the pairs e_1, e_7, e_{10} and e_{14} to form the forward pair and take the pairs e_2, e_5, e_8 and e_{12} to form the backward pair.

$$\text{Forward} = \begin{pmatrix} 1 & 7 & 10 & 14 \\ 2 & 11 & 6 & 15 \end{pmatrix} \quad (3)$$

$$\text{Backward} = \begin{pmatrix} 2 & 5 & 8 & 12 \\ 0 & 13 & 9 & 5 \end{pmatrix} \quad (4)$$

Now we can again decompose the "forward" pair from (3), according to bipartite graph. Then take the pairs e_1, and e_{14} to form the forward pair and and take the pairs e_7 and e_{10} to form the backward pair. The bipartite graph is depicted in Fig. 3. Similarly, we can also decompose the "Backward" pair of (4), according to bipartite graph. Then take the pairs e_2, and e_8 to form the forward pair and take the pairs e_5 and e_{12} to form the backward pair. The graph is depicted in Fig. 4.

$$\text{Forward} = \begin{pmatrix} 1 & 14 \\ 2 & 15 \end{pmatrix} \text{ and Backward } = \begin{pmatrix} 7 & 10 \\ 11 & 6 \end{pmatrix}$$

$$\text{Forward} = \begin{pmatrix} 2 & 8 \\ 0 & 9 \end{pmatrix} \text{ and Backward } = \begin{pmatrix} 5 & 12 \\ 13 & 5 \end{pmatrix}$$

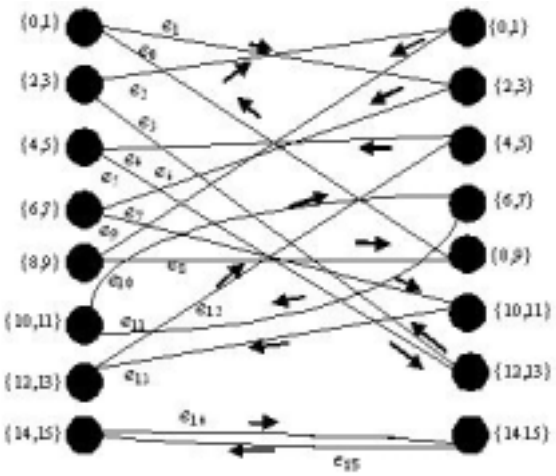

Fig. 1. The bipartite graph and edge traverses of the decomposition for 16 × 16 inputs/outputs

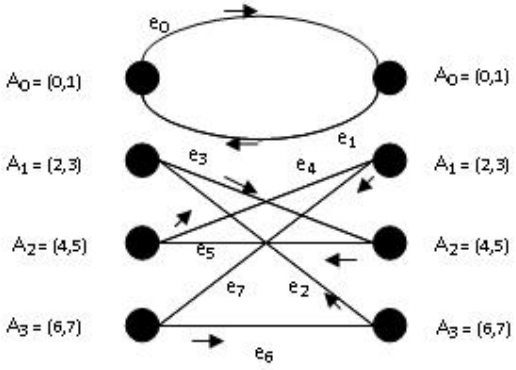

Fig. 2. The bipartite graph and edge traverses of the decomposition for 8 × 8 inputs/outputs

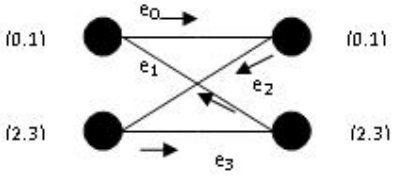

Fig. 3. The bipartite graph and edge traverses of the decomposition for 4 × 4 inputs/outputs

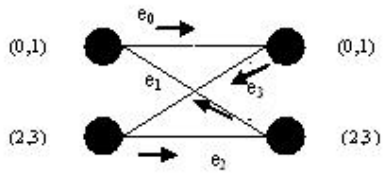

Fig. 4. The bipartite graph and edge traverses of the decomposition for 4 × 4 inputs/outputs

IV. ROUTING ALGORITHM OF OPTICAL MINS

To make a network crosstalk free decompose the permutation according to the proposed routing algorithm until the network become crosstalk free.

Routing Algorithm (integer N, SEMI-PERM semi-perm)**:**

Step 1: If N is 2, make the connection in the 2 × 2 switch according to semi-perm; exit.

Step 2: Construct the bipartite graph $G = (V_1, V_2, E)$ corresponding to the permutation.

Step 3: Decompose the permutation according to the decomposition algorithm of bipartite graph**.**

Step 4: Take all one-pair mappings corresponding to the edges marked with "forward" to form one semi-permutation and take all one-pair mappings corresponding to the edges marked with "backward" to form another semi-permutation.

Step 5: Then at a time, for any semi-permutation make a connection pass through the corresponding input switch and output switch.

Step 6: Recursively call Routing Algorithm (integer N, SEMI-PERM semi-perm) until the network becomes crosstalk free.

END

V. REALIZING SEMIPERMUTATIONS IN OPTICAL MINS

This section describes the realization of semi permutations in GRN, in Banyan and in Benes network.

A. REALIZING SEMIPERMUTATIONS IN GRN

In GRN architecture, any $M \times N$ non-blocking switch network can be built with building blocks of given size $m \times n$, where M, N, m, n are all powers of integers. The switches of GRN maintain the connection pattern of shuffle-exchange fashion. If the size of the building block is $m \times n$, then the number of building blocks required is M/m and the Number of switching elements required is $n((M/m) - 1)$. The number of recursions in GRN is $\log(N/n)$. An $M \times N$ GRN constructed from $m \times n$ strictly non-blocking building blocks is also a strictly non-blocking network. There are three stages in GRN. The stages are input stage, output stage, and building-block-stage. In $M \times N$ GRN, with building block size of $m \times n$, a signal has to cross $\log(N/n)$ input stage switches, and $\log(M/m)$ output stage switches in addition to one building block. Since the input stage switches are 1×2 switches, they do not contribute to crosstalk. Likewise, the output stage switches are 2×1 and they do not have to bear signals at both of their inputs at the same time. So, they do not contribute to crosstalk as well. The only possible elements that contribute to crosstalk are the building blocks.

The whole routing mechanism of GRN from an input to an output is divided into three steps: routing in the input stage, routing in the building-block-stage, and routing in the output stage. Starting from the left, the first log (N/n) bits are used by the input stage switches. In this stage the signal is routed from the leaf to the root of the output tree. The last log (M/m) bit is used by the output stage switches. Building block use the remaining middle bits for it's own routing. Suppose that the signal at input (source address) 0001 requests to be connected with output (destination address) 1000. So, the header in the request message has TAG = 10001000. Here the tag format is,

$$d_{q-1}\, d_{q-2} \ldots d_0\, s_0\, s_1 \ldots\ldots s_{p-1}$$

d_0 = LSB bit of destination address
d_{q-1}= MSB bit of destination address
S_0 = LSB bit of source address
S_{p-1}= MSB bit of source address

When $m = n = 4$, $M = N = 16$, thereby $\log(N/n) = \log(M/m) = 2$. That is, the first (from left) two bits, 10, will be used by the SE at the only input stage and the last two bits, 00, will be used by the SE at the only output stage. The leaf building block will use the middle 4 bits, 0010, for its internal routing. Only for the input stage, the bits will be interchanged i.e., 01. Now for the 0 bit it will follow the upper line and for the 1 bit it will follow the lower line for it's routing in the input and output stage. Consider the above permutation, where the output sequence is generated randomly:

$$\begin{pmatrix} 0 & 1 & 2 & 3 & 4 & 5 & 6 & 7 & 8 & 9 & 10 & 11 & 12 & 13 & 14 & 15 \\ 8 & 2 & 0 & 12 & 4 & 13 & 3 & 11 & 9 & 1 & 6 & 7 & 5 & 10 & 15 & 14 \end{pmatrix}$$

Then, decompose the permutation according to the proposed routing algorithm and obtain two semi-permutations those are shown in (1) and (2). In Fig. 5, the realization of the this permutation is shown in 16 × 16 GRN network where the 4 × 4 switch is used as building block. Fig. 5(a) shows that semi-permutation shown in (1) can not be realized in a single pass, and Fig. 5(b) shows that semi-permutation shown in (2) can be realized in a single pass.

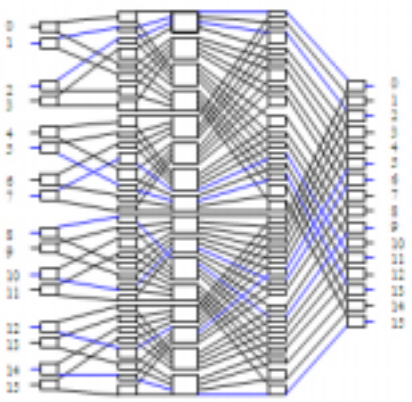

(a)

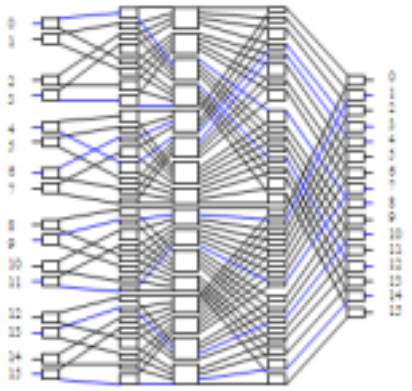

(b)

Fig. 5. Realizing semi-permutations in an 16 × 16 GRN network (a) forward pair and (b) backward pair

The bold boxes in Fig. 5(a) indicate the switch where two signals come at the same time. So, there is a possibility to occur crosstalk in this switch. According to the routing algorithm if we again decompose the semi-permutation then we again get another two semi-permutations. Those are shown in (3) and (4). After applying these two semi-permutations the network would be crosstalk free because two signals do not come in a single switch at the same time. So, there is a no possibility to occur crosstalk and hence the whole network is crosstalk free.

B. REALIZING SEMIPERMUTATIONS IN BANYAN NETWORK

Banyan networks were first introduced by Goke and Lipovski [9] using graph methods. In a simplifying approach, any multistage network for which there is a unique path from each network input to each network output is called a banyan network. The banyan network considered in this paper is an $n \times n$ network composed of 2×2 switches, where $n = 2^m$. The network has m stages of switches and the switches in the consecutive stages are linked by recursively applying butterfly interconnection patterns. Due to the unique path nature of a banyan network, a semi-permutation is routed through the network in a fixed switch setting. Consequently, some semi-permutations can be realized in a banyan network in a single pass while others cannot. In Fig. 6, we apply the above example for an 16 × 16 banyan network. The bold boxes in Fig. 6(a) and in Fig. 6(b) indicate that the network is not crosstalk free. If we again apply the routing algorithm on the forward and backward pair then the network will be crosstalk free.

C. REALIZING SEMIPERMUTATIONS IN BENES

A Benes network can be constructed by concatenating a banyan network and a reverse banyan network with the center stages overlapped. In Fig. 7 we will show that Benes networks also have good properties to support permutations in optical networks. The bold boxes in Fig. 7(a) and in Fig. 7(b) indicate that crosstalk occurs in those switches. After applying the routing algorithm on the forward pair and backward pair for the second time the network will be crosstalk free.

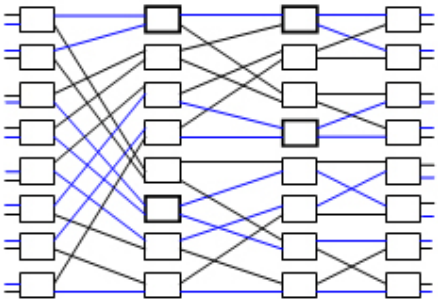

(a)

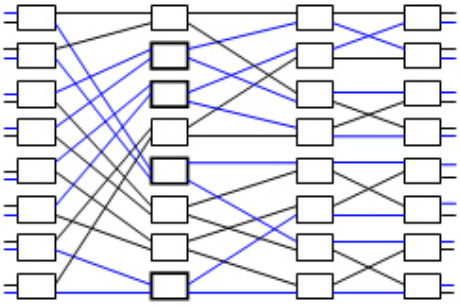

(b)

Fig. 6. Realizing semi-permutations in an 16 × 16 Banyan network (a) forward pair and (b) backward pair

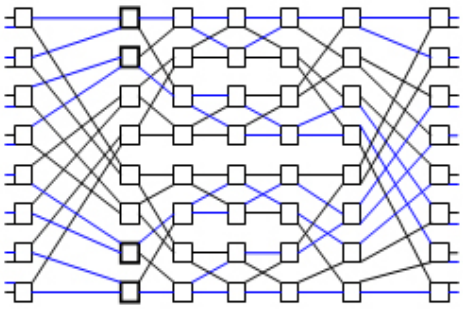

(a)

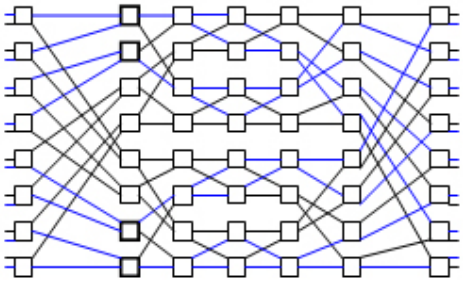

(b)

Fig. 7. Realizing semi-permutations in an 16 × 16 Benes network (a) forward pair and (b) backward pair

VI. CONCLUSION

We have proposed a crosstalk-free routing algorithm of optical MINs and we apply it on three optical MINs as examples. We show that each switch can only pass one signal at a given time. Therefore, there is no possibility to occur crosstalk in the switch. This algorithm is derived based on the idea of the semi-permutation, and the main advantage of our proposed routing algorithm is that it makes the optical MINs crosstalk free.

REFERENCES

[1] Yuanyuan Yang, Jianchao Wang and Yi Pan, "Permutation Capability of Optical Multistage Interconnection Network-s," *Journal of Parallel and Distributed Computing*, vol.60, no.1, pp.72-91, Jan.2000.

[2] M.R Khandker, X.Jiang, H.Shen and S.Horiguchi, "Crosstalk Free Permutation in Photonic Rearrangeable Networks Built on a Combination of Horizontal Expansion and Vertical Stacking of Banyan Networks," *IEICE Trans. On Information and Systems*, Vol.E86-D, No.9, pp.1525-1533, 2003.

[3] M.R. Khandker, X.Jiang, H.Shen and S.Horiguchi, "Generalized Recursive Network: a new architecture for self-routing non-blocking optical switch networks," *Optics Communication*, Vol.208, No.4-6, pp.299-308, 2002.

[4] M.R. Khandker, X.Jiang, and S.Horiguchi, "New Non-blocking Optical Switch Network," *Proc. Of the First workshop of International Joint Research: parallel computing, data mining and optical networks*, Tatsunokuchi, Japan, pp.87-97, 2001.

[5] J. A. Bondy and U. S. R Murty, "Graph Theory with Applications," Am. Elsevier, New York, 1976.

[6] C. Qiao, and R. Melhem, "A time domain approach for avoiding crosstalk in optical blocking multistage interconnecttion networks," *J. Lightwave Technology,* vol.12.no. 10, pp.1854-1862, Oct, 1994.

[7] C. Qiao, "A two-level process for diagnosimg crosstalk in photonic dilated Benes network," *Journal of Parallel and Distributed Computing*, vol. 41, no.1, pp.53-56, 1997.

[8] D. K. Hunter and I. Andonovic, "Guided wave optical switch architectures," *International Journal of Optoelectronics,* vol. 9, no. 6, pp. 477-487, 1994.

[9] L.R. Goke and G.J. Lipovski, "Banyan networks for partitioning multiprocessor systems," *Proc. of the First Annual Symposium on Computer Architecture,* 1973, pp.21-28.

Proceedings of 2009 12th International Conference on Computer and Information Technology (ICCIT 2009)
21-23 December, 2009, Dhaka, Bangladesh

Novel Adaptive Step Power Control Algorithm for 3G WCDMA Cellular System

Abdullah Al Mamun, Saiful Islam, Farzana Yesmin, Masuma Akter, Shaikh Afsana Jahan
Electronics and Communication Engineering Discipline, Khulna University, Khulna 9208, Bangladesh
ronee_ece04@yahoo.com, sunny.kln@hotmail.com, urmieceku@yahoo.co.uk, keya_ece04@yahoo.com, afsana0401@yahoo.com

Abstract

Power control is an essential radio resource management method in CDMA cellular communication systems, where co-channel and adjacent-channel interferences are the primary capacity limiting factors. Power control intends to control the transmission power levels in such a way that required quality of service for the users is guaranteed with lowest possible transmission powers. In this paper, a modulation of power control algorithm is proposed for the 3G WCDMA system. The algorithm is figured on a modification of the transmitted power update step size. Instead of the fixed value presently suggested, the step size is modified dynamically in order to obtain more adapted power variations as well as the step is also represented as a function of the difference between the target and estimated SIR of the MS to obtain more stability of the system. A general form of this algorithm is presented and it is then studied in a simple simulation. Performance of the algorithm was evaluated with the outage percentage, which is the percentage of the number of MS's whose received SIR falls below the fixed threshold. The focused requirement, which had been tried to achieve by this algorithm, is the stability, which was studied and represented through simulation.

Keywords: ASPC, Average outage percentage, Novel ASPC, Signal to Interference ratio, WCDMA.

I. INTRODUCTION

The WCDMA air interface is organized in frames of 10 ms duration. A frame contains 15 time slots and each slot includes one PC command (up or down), which gives a PC update rate of 1500 b/s. The transmitted power has a fixed value during a given time slot. Power control in WCDMA is a closed-loop PC that is a combination of outer and inner closed loop control (figure 3.1). The inner (also called fast) closed loop PC adjusts the transmitted power in order to keep the received Signal-to-Interference Ratio (SIR) equal to a given target. This SIR target is fixed according to the received BLER (Block Error Rate) or BER (Bit Error Rate). The setting of the SIR target is done by the outer loop PC, which is part of the Radio Resource Control Layer (layer 3), in order to match the required BLER [13]. Outer loop PC update frequency is 10-100 Hz. The BLER target is a function of the service that is carried. Ensuring that the lowest possible SIR target is used results in greater network capacity. This target SIR is estimated on the basis of received BER and estimated BER for the system and this is an input to the inner loop power control. The inner closed-loop PC measures the received quality, defined as the received Signal-to-Interference Ratio (SIR) and sends commands to the transmitter (i.e., the mobile in the case of uplink) for the transmitted power update. For updating the mobile station's power different algorithms may be used. Main purpose of the inner loop power control is to get the individual SIR of the MS's towards the targeted SIR value that have been determined by the outer loop power control.

II. POWER CONTROL ALGORITHM IN WCDMA

In order to estimate the received SIR, the receiver estimates the received power of the connection to be power controlled and the received interference. The obtained SIR estimate, noted SIR_{est}, is then used by the receiver to generate PC commands according to regular step power control algorithm or producing commands one time among five. In regular step power control algorithm, the transmitted power is updated at each time slot (10/15 ms). It is increased or decreased by a fixed value:

- If $SIR_{est} > SIR_{target}$ then the TPC command to transmit is "0", requesting a transmit power decrease;
- If $SIR_{est} < SIR_{target}$ then the TPC command to transmit is "1", requesting a transmit power increase.

The power control step size is a parameter of the fast (inner) closed-loop PC. In the case of the uplink, it is equal to 1 or 2 dB in WCDMA system. Values smaller than 1 dB can be emulated by taking larger PC update periods. It depends on the requirements of the individual system.

A. System Model

We use a very simple system model to realize our algorithm. Uplink of FDD WCDMA 3G system is considered. In a FDD-CDMA system, a physical channel is defined by its code and its frequency. The methods proposed in this paper could be applied to downlink and TDD systems after some slight adaptations. Power control is only applied at Layer 1 (inner closed-loop PC). Circuit-switched systems (e.g., voice service) are considered. A rather simple simulation model is used. This allows comparisons between the PC algorithms. A maximal transmitted power limitation is considered. For each mobile, the best-received base station is selected as its corresponding one. A discrete event simulation is considered. At a given instant, M mobiles are

978-1-4244-6283-4/09/$26.00 ©2009 IEEE

transmitting information sharing a common radio channel (CDMA). Each mobile should communicate with one of the B base stations. The index of the base to which mobile m is assigned is a_m. A mobile is connected to the best-received power level BS, which is not always the closest one due to fading. Mobile m transmitted power is p_m and the link gain from mobile m to base b is noted g_{bm}, so matrix $\mathbf{G} = (g_{bm})$ is of the size (B × M).

Mobile m received SIR on base b, noted $\gamma_{m,b}$, can be calculated the way below:

Signal to Interference ratio (SIR) for mobile m on base station b, $\gamma_{m,b} = \frac{S}{I}$

Here, S = desired signal power at base station b for mobile m

I = Interference or Unexpected signal power at base station b which may cause for the signal power arrived at base station b for the mobiles except m and the noise power also.

Thus for mobile m and base station b, $S = g_{bm}\, p_m$

And for the same case,

$$I = \sum_{j=2, j\neq m}^{M} g_{bj} p_f + n_b$$

Where n_b is the receiver noise, also called thermal noise, at the base b.

Mobile m received SIR on base b, noted $\gamma_{m,b}$, can be given as:

$$\gamma_{m,b} = \frac{g_{bm} P_m}{\sum_{f=1, f\neq m}^{M} g_{bj} p_j + n_b} \quad \ldots\ldots\ldots\ldots\ldots\ldots\ldots\ldots\ldots\ldots (1)$$

The received SIR of mobile m on its assigned BS is noted γ_m, so one can write: $\gamma_m = \gamma_{m,\, a_m}$. A mobile is in outage state when its SIR falls below the range ω_0. Paging or synchronization channels are not included in the simulation. Performance of the algorithm is evaluated with the outage probability, which is the probability that the received SIR falls below the fixed threshold. Call dropping is not considered in our simulations.

B. An Introduction to ASPC (Adaptive Step Power Control)

Received quality-based power control out performs received power level-based power control [13]. The two power control algorithms of WCDMA described are based on received quality level. The transmitted power range may be up to more than 70 dB. For the present version of power control algorithm of WCDMA, transmitted power update step is around 1 dB. Frequent variations occur in the mobile network due to communications starts and ends, to mobiles movements and to propagation channel changes. Radio channel modification may be due to multi path and to obstacles movements. Thus, a fast power control is needed. The aim of the algorithm proposed in this algorithm is to converge faster than the present WCDMA power control algorithms. The value of the fixed step may be too small or too large for the transmitted power adjustment needed. In the following, it was proposed to replace the fixed power update step by an adaptive step in the inner closed-loop one-bit (information) PC of 3G WCDMA systems. We call Adaptive-Step Power Control this variant the (ASPC). It is based on the following principle. If the transmitter detects several simultaneous up commands, the step is increased. This is also done for several simultaneous down commands. The update step is decreased if an alternative succession of up and down appears, showing that the update step is probably too large. Using this basic principle, the algorithm may have many forms.

III. The ASPC Algorithm

Generally, the algorithm works as follows. The initial value of the power update step is Δ_0, expressed in dB. The APSC works in up or down commands as in the case of WCDMA algorithms with the difference that the power update step may change in some cases. These cases are given in the following:

1. The update step is multiplied by μ when n_0 successive up commands are received.
2. The update step is multiplied by ν when n_1 successive down commands are received.
3. This value is divided by λ when the power update command sequence is an alternate sequence of n_{01} up and down commands.

In this algorithm the scaling factor μ, ν and λ are arbitrary constants which may be assigned by the system designer as to make the best convenience to control the outage probability as fast as possible.

A. Simulation Result

In figure 1, we see the simulation result of the algorithm just held above. The same simulation result will be observed in case of algorithm 2. Here we assume the power update step for both up command and down command as 1.67 dB or 50 dBm.The output graph of the simulation is presented in terms of average outage performance vs. iteration number. Outage percentage is here the percentage of the number of MS whose SIR_{est} level is below the SIR_{target} level.

A.1 Simulation Result of ASPC Algorithm

Here again notice, the total system model under which the simulation model was considered will be given later. In figure 2, we see the simulation result of the algorithm ASPC. Here we assume the power update step Δ_0 as 1.67 dB or 50 dBm and the multiplier for the up command step, μ is 24, the multiplier for the down command step, ν is 6 and the divider of the step when the power update sequence is an alternate sequence, λ is 10. We assume also $n_1 = n_0 = n_{01} = 2$ in the simulation. Here the output graph of the simulation is presented in terms of average outage performance vs. iteration number also. Outage percentage is defined here as the percentage of the number of MS whose SIR_{est} level is below the SIR_{target} level.

A.2 Considerable Features of ASPC Algorithm (superiority over Regular Step Algorithm)

From Figure 1 and 2, we can see that in case of algorithm (1) the average outage percentage decreased to 22% at the time of iteration number 20 and this is decreasing exponentially with the increasing iteration number becoming 1% at the time of iteration number 100, when we terminated our simulation. While in case of ASPC algorithm the average outage percentage decreased to 0% at the time of iteration 20 that is an excellent improvement in terms of outage.

A.3 Drawbacks of ASPC Algorithm

We can see from the result figure 2 of ASPC algorithm that faster convergence of the outage percentage is been got at the cost of some instability in the outage percentage. It is the main draw back of this algorithm, because in telecommunication system instability problem is very undesirable. Often it is reported that the customers like to not get connection rather than getting the connection cut a few after the establishment of the connection. Another problem is that the additional features of multiplication and division will bring extra circuitry operations for this algorithm that indicates to the additional increment of the circuit complexity of the receiver.

IV. AN INTRODUCTION TO NASPC (*NOVEL ADAPTIVE STEP POWER CONTROL*)

Considering the qualitative reason of the instability of ASPC algorithm, we can realize that the instability comes from the hopping up or down of the power level of MS's at a large amount because of the multiplier of update step occurring the SIR_{est} being above or below of the SIR_{target} at alternate iterations. Thus we thought to adapt the power. Update step on the basis of the difference between the SIR_{target} and SIR_{est}, so that the SIR_{est} of the MS's do not jump down or up crossing the SIR_{target} level rather it step ahead to the SIR_{target} level in a convergent manner sensing how long the step should be according to the distance between SIR_{target} and SIR_{est}.

A. Algorithm Steps of NASPC Algorithm

In NASPC algorithm the power update step is been determined on the basis of the difference between SIR_{target} and SIR_{est} that means the step is been adapted according to how long the path to cross to embrace the SIR_{target} level.

The algorithm works in the following way:

1. The difference between the SIR_{target} and SIR_{est}, Δ_{diff} would be measured in case of each mobile station, which is expressed in dB.
2. The update step would be α times Δ_{diff} when n_0 successive up commands are received.
3. The update step would be β times Δ_{diff} when n_1 successive down commands are received.
4. This value is divided by λ when the power update command sequence is an alternate sequence is an alternate sequence of n_{01} up and down commands.

B. Simulation Model

The numerical hypothesis of the simulated system model for the mobile network is now given. The NASPC Algorithm is evaluated in simulation. The simulated service is 8 kbps circuit-switched services with voice activity 100%. Class 3 mobile stations are considered. The maximum transmitted power is 24 dBm and the minimum transmitted power is -50 dBm as specified in [13]. The receiver thermal noise for base station is -103 dBm. A receiver thermal noise is considered in order to have absolute values for transmitted powers computed by the PC algorithms. The initial transmitted powers have random value between the minimum value and 10% of the (real) value of maximum transmitted power. In 3G proposed systems, the outer-loop sets the SIR target. In this paper, we consider a unique SIR target for all links, where we assume that all communications have the same data rate. The target SIR range for all mobiles, on the uplink, is $\omega_0 = -17 \pm 0.5$ dB. A perfect estimation of the received SIR is assumed. A CDMA system with 16 BS (4x4) is considered. The base stations are placed on a rectangular grid. The side of the average square cell is 41m. Mobiles are uniformly distributed. The link gain between mobile *j* and base *i* is modeled as:

$$g_{ij} = \frac{c_s}{d_{ij}^n}$$

Where coefficient c_s corresponds to obstacles (shadow fading) and d_{ij} is the mobile-to-base distance given in cm and n is the path gain factor whose value ranges from 2 to 5 which is about 4 at practical environment but we assume $n = 2$ for sake of the ease of calculation. Coefficient c_s is a zero-mean log-normal random variable whose standard deviation is $\sigma = 6$dB. In our simulations, we consider $n_0 = n_1 = n_{01} = 2$ for the simulation. Average values are evaluated by Monte Carlo simulation for an independent configuration (mobiles distributions). Admission control is not addressed in this work, i.e., an 'admit-all' policy is considered, the outage probability being the performance evaluation criterion. The association of the proposed algorithm with an admission control policy is an interesting topic of research. We consider a simulation with fixed-position mobiles. The number of mobiles in the simulated zone is 40 (18 mobiles per cell in average). The update step of WCDMA PC algorithms is $\Delta = \Delta_{diff} \times \eta$ dB, where we use $\eta = 32000$ for up step which is noted by α and $\eta = 1600$ for down step which is noted by β. The average outage percentage is the percentage of mobiles that's SIR is smaller than the SIR target. It is plotted as a function of the iteration step in order to discuss the convergence speed and the stability factor of NASPC algorithms.

C. Simulation Result of NASPC Algorithm

We can see from Figure 3 that the average outage percentage decreased to only 5% exponentially with smoother curve at the time of iteration number 20 that then maintains a constant value up to iteration 56 and then decrease to 0% at iteration number 60 with a slope of about 45^0.

This NASPC algorithm that can be realized from the simulation result of section achieves the objective with which we started to walk through this algorithm to obtain more stability as well as lower outage percentage quite successively.

D. Complexity Estimation of the Algorithm

The analysis is a major task. Suppose M is an algorithm and suppose n is the size of the input data. The time and space used by the algorithm M are the two main measures for the efficiency of M. Hence the complexity of an algorithm M is a function *f(n)* which gives the running time or storage space requirement of the algorithm in terms of the size of input data. Frequently, the storage space required by an algorithm is simply a multiple of the data size n. accordingly, if not stated otherwise; the term 'complexity' shall refer to the running time of the algorithm.

D.1 Complexity in terms of running time

Here we assume we will execute the algorithm (run the simulation) to r iterations. Let denote the number of iteration by i and the size of input data by n. In each iteration the program will run throughout the loop n times. So in the worst case the complexity, *C(n) = nr*. Accordingly the number of running can be any of the numbers 1, 2, 3, ……., r and each number occurs with probability p = 1/n. then we get the complexity for average case,

$$C(n) = 1n\frac{1}{r} + 2n.\frac{1}{r} + ... + rn.\frac{1}{r}$$

$$= (1 + 2 + 3 + ... + r)\frac{n}{r}$$

$$= \frac{r(r+1)}{2}.\frac{n}{r}$$

$$= \frac{n(r+1)}{2}$$

D.2 Complexity in Terms of Rate of Growth (Big O notation)

Suppose M is an algorithm and suppose n is the size of the input data. Clearly the complexity *f(n)* of M increases as n increases. It is usually the rate of increase of *f(n)* that we want to examine. This is usually done by comparing *f(n)* with some standard function, such as *log n, n, n log n,* n^2 etc. the rate of growth of these functions is given in the following table.

g(n)	log n	n	nlog n	n^2	n^3
5	3	5	15	25	125
10	4	10	40	100	1000
100	7	100	700	10^4	10^6
1000	10	1000	10000	10^6	10^9

Table 1: rate of growth of standard function

One way to compare the function *f(n)* with these standard functions is to use the functional O notation. One can glance at the appendix B to be introduced with it. As we can see that the run time increases with the size of input *n* linearly as *nr* where *r* is the number of iteration so for our algorithm complexity *f(n) = O(n)*.

V. DISCUSSION

Comparing the algorithms ASPC, NASPC and regular step power control algorithm, we could realize that each has some better aspects regards to the other. For convenience, the comparison is held in the tables given below. As ASPC has arrived from regular step algorithm, they has been compared in table VI and ASPC and NASPC in table VII as NASPC is step forward of ASPC.

Factors	NASPC	ASPC
1. Outage percentage at the time of iteration 20	Outage percentage 5%	Outage percentage 0%
2. Stability of the system	It holds a smoother convergence of the output curve, which indicates more stability of the system.	It shows quite abrupt up and down in its output curve, which indicates instability of the system
3. Circuit complexity	Has to perform additional subtraction operation, which may increase the circuit complexity of the receiver.	Has more complexity than that of regular step power control algorithm but less than NASPC.
4. Algorithm complexity	Need more execution time hence more complexity than ASPC	Need less execution time hence more complexity than NASPC
5. Iterations needed to bring outage to 0%	60 iterations	20 iterations

Table 2: Comparison between NASPC and ASPC

To visualize this factor graphically, here we have presented the figures obtained by simulation side by side for graphical comparison. Hence it can be claimed that our algorithm NASPC gives far better stability to the communication system than that of ASPC at the

expense of increased complexity. Moreover the outage percentage has to wait some extra iteration to be pulled down to zero.

In this case, a positive point should be noticed that the outage percentage attains a small value within 20 iterations and then carry a constant value throughout most of the rest iteration before it reduced to zero that may not be much annoying to the customer of the cellular system.

VI. Future Work

As was discussed before, our proposed algorithm has a problem of delay to attend zero outage; we would like to work on this issue so that faster speed could be obtained with satisfactory stability. Modifying the step in some other way may help in this intention. Besides we considered our model as with mobile stations of fixed position and the call dropping and hand-offs were neglected. The total system modeled and simulated with the consideration of all these factors will give more realistic and practically efficient realization of this algorithm. All the ideas may be interesting topics to work further on this algorithm.

References:

[1] Abdurazak Mudesir, "Power Control Algorithm in CDMA systems," International University Bremen, 11 May, 2004.

[2] Bo Bernhardsson, "Power Control In CDMA-Background," Dept. of Automatic Control, Lund Institute of Technology.

[3] Saleh Faruque, "Cellular Mobile Systems Engineering." Artech House Inc, Norwood.

[4] *http://www2.ing.unipi.it/ew2002/proceedings/177.pdf*, 9 pm, 4 November, 2008.

[5] *http://www.pearsonhighered.com/samplechapter/0130871125.pdf*, 8 pm, 16 December, 2008.

[6] *http://lib.tkk.fi/Diss/2005/isbn9512278987/*, 2.30 pm, 16 December, 2008.

[7] *http://www.utdallas.edu/~torlak/wireless/projects/krishna.pdf*, 2.18 pm, 3 March, 2009.

[8] *http://services.eng.uts.edu.au/~kumbles/paper/WISTS2006.pdf*, 11 pm, 5 march, 2009.

[9] I. Virtej, H. Koivo, "Application of gain scheduling concept in power control of WCDMA system," in Proc. of IEEE Vehicular Technology Conference 1999 Fall, VTC-99F, Sept 2000.

[10] Louis C. Yun and David G. Messerschmitt, "Power Control for Variable QOS on a CDMA Channel," Dept. of Electrical Engineering and Computer Sciences. University of California at Berkeley, Berkeley, CA 94720, 11 May, 2008.

[11] Matti Rintamaki, "Adaptive Power Control in CDMA Cellular Communication Systems." Report 53, Dept. of Electrical and Communications Engineering, Helsinki University of Technology, 2005.

[12] Theodore S. Rappaport, "Wireless Communication Principles and Practice." Second Edition, Prentice- Hall India Ltd.

[13] 3G TS 25.214 v4.1.0 (2001-06), "Physical layer procedures (FDD) (Release 4)" 3rd Generation Partnership Project; Technical Specification Group Radio Access Networks, March 2001.

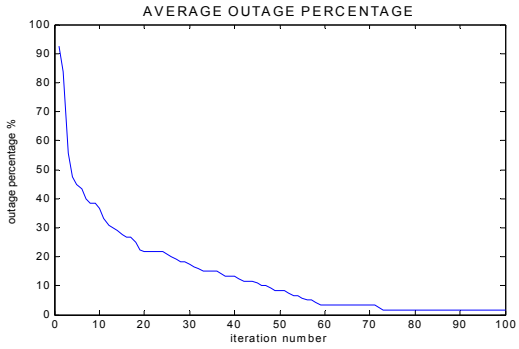

Figure 1: Convergence speed of the regular step power control.

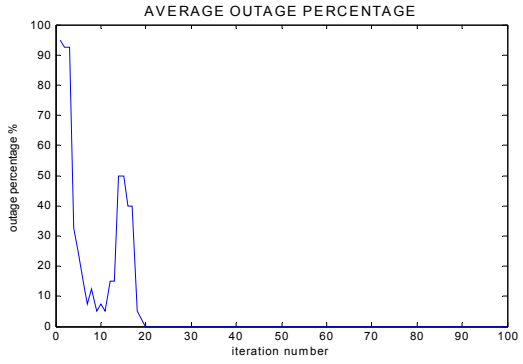

Figure 2: Convergence speed of the ASPC.

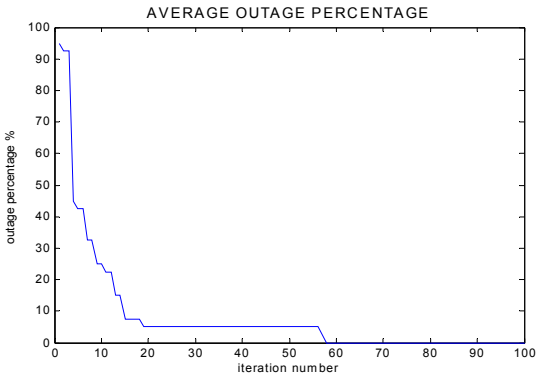

Figure 3: Convergence speed of the NASPC.

Proceedings of 2009 12th International Conference on Computer and Information Technology (ICCIT 2009)
21-23 December, 2009, Dhaka, Bangladesh

Packing Identical Circles in a Minimized Circular Container by Monotonic Basin Hopping Heuristic Approach

A. R. M. Jalal Uddin Jamali, A. Grosso‡, M. Locatelli‡, F. Schoen†
Dept. of Mathematics, Khulna University of Engineering & Technology, Khulna 9203, Bangladesh
‡ Dept. of Computer Science, University of Turin, Italy
† Dept. of Computer Science, University of Firenze Italy

armjamali@yahoo.com, grosso@di.unito.it, locatelli@di.unito.it, Fabio.schoen@unfi.it

Abstract

Packing problems have mathematical as well as practical application point of interest. We present, here, Monotonic Basin Hopping heuristic approach to solve the problem of packing identical circles within a minimum size of circular container. Extensive computational experiments have been performed for analyzing the problem as well as for choosing an appropriate way the parameter values for the proposed methods. Several improvements with respect to the best results reported in the literature have been detected.

Keywords: Circle Packing, Monotonic Basin Hopping, Multistart.

I. INTRODUCTION

The problem of optimally placing *N* non overlapping and possibly of different size objects belonging to R^d within a smallest container is a classical mathematical problem and have a spectrum of application including production and packing for the textile, apparel, naval, automobile, aerospace and food industries, news paper, web pages design, in particular, to problems related to cutting and packing [1]. They are bottleneck problems in Computer Aided Design (CAD) and Computer Aided Manufacturing (CAM) where design's plans are to be generated for industrial plants, electronic modules, nuclear and thermal plants, etc. In particular, we consider in this paper, the Identical Circle Packing in a Circular Container (ICPCC) problems. The ICPCC problems can be described by the several equivalent problems [1]. One of the settings is given bellow:

Problem: To find the minimum circular container radius D_n which contains *n* identical and non-overlapping circles of radius one. Mathematically,

$$\min \; r$$

Subject to

$$x_i^2 + y_i^2 - 1 \le r^2 - 2r \; ; \quad i \in I$$

$$(x_i - x_j)^2 + (y_i - y_j)^2 \ge 4 \; ; \quad i, j \in I \quad \ni i \ne j$$

$$1 \le r < \quad \infty$$

As the problem might be shown to be NP-hard [2], there do not exist an algorithm that is both rigorous and fast [2]. Hence researchers are searching for the efficient heuristic approximation algorithms to solve the problems. There is a long history of solving packing problems in literature. A survey about this problem can be found in a recent book [3] that has been dedicated to the subject. But literature of circular container packing problems is not so rich. And also history of circular container packing problem is relatively recent [4]. Benchmark results for the problem of packing equal circles in a container whose shape is a square, a circle or an equilateral triangle are reported and continuously updated in E. Specht's web site [5]. Finally, we also refer to the paper [6] where a detailed survey about methods and applications of packing problems can be found.

In [7] authors investigated the problem of packing equal circles in the unit square and proposed a quite successful method for the problem. The problem is, in fact, equivalent to that of minimizing the edge length of a square container into which we want to pack *n* equal circles with unit radius. In this paper we investigate a related problem: packing circles with unit radius into a circular container of minimum radius. Except for the shape of the container (unit square container, here a circular container) the two problems are quite similar and we do expect that the extension of the method employed in [7] also gives very good results for this problem (this is indeed confirmed by the computational results). But the aim of this paper is not merely to apply a method, proved to be successful for one problem, to a closely related one. The aim of the paper is also (and, actually, mainly) to perform a more detailed computational investigation both of the problem at hand and of the proposed method, in order to better understand how to choose its most relevant parameters.

II. PROPOSED MONOTONIC BASIN HOPPING ALGORITHM

In Section (I) we have discussed about the mathematical formulation of ICPCC problems. As the problem is a NP-hard global optimization one, the number of local minimizers tends to increase quite quickly with the number *n* of circles. When dealing with global optimization problems for NP-hard problem, an obvious and simplest approach is the Multistart (MS) one. In such an approach we simply start different local searches from randomly generated initial points and

978-1-4244-6283-4/09/$26.00 ©2009 IEEE

return the best local minimizer. However, the rapid increase in the number of local minimizers suggests that Multistart can not be an efficient method for this problem. The method we are going to propose is quite close to Multistart (they are both based on multiple local searches and they only differ in the mechanism for the generation of the initial points) but at the same time also dramatically more efficient than Multistart. In the field of global optimization such method has been (to the authors' knowledge) first applied to molecular conformation problems (see [8]) under the name of Monotonic Basin Hopping (MBH), but in fact it can also be viewed as a special case of the Iterated Local Search (ILS) approach (see, e.g., [8]), which is usually employed in the field of combinatorial optimization problems. Since our problem belongs to the global optimization field, we will refer to this method with MBH. Its description is rather simple. The main ingredients of the method are: (i) Initialization (Init), (ii) local search procedure (LS), (iii) perturbation move (PM), (iv) Acceptance Rule (AR) and (v) stopping rule (SR). Let operator τ and ξ denote LS and PM respectively. Also let $f(X)$ denotes the objective value of the configuration X. Then the pseudo code of MBH approach is as follows:

Monotonic Basin Hopping
Step 1 :Let X_0 be randomly generated initial solution
// Initialization procedure
Step 2: Let $X := \tau(X_0)$ be a local minimum
// local search procedure
While SR not satisfied
Step 3 : Let $Y := \xi(X)$
// perturbation procedure
Step 4: Let $X := \tau(Y)$
// local search procedure
Step 5: If $f(X') < f(X)$, then $X := X'$
// acceptance rule
EndIf
EndWhile
Return X

As we have remarked before that the main difference between MS and MBH is the technique of generation of initial solution of each LS. We know that, in MS, the initial solution of each LS is randomly generated. On the other hand in proposed MBH, only the first initial solution X_0 is generated randomly within large enough region, $R^2_{reg,}$ and all the other subsequence initial solutions of LS are generated by the PM, a simple but efficient procedure. Since our problem can be viewed as a non-convex one with objective and constraint functions continuously differentiable infinitely many times. So, any local search method for this kind of problems can be employed. However, our past experience (see [1]) suggests that SNOPT [5] is particularly well suited for these problems. The acceptance rule, for updating, is very simple just compare the objective values of the existence configuration and newly obtained configuration and upload new one if better objective value obtain. Since PM as well as SR are the core components of MBH approach we would like to discuss it in following section in some details.

A. Perturbation move

One of the keys of the success of the existing MBH or ILS methods is often the perturbation move. A good rule is to choose it in such a way that the structure of the current local minimizer is not completely disrupted. The basic idea is that the method should move between different but "close" local minimizers. In the case of equal circles we proposed three very simple perturbation move, based on a uniform random perturbation of each coordinate of each center of the circle within some interval $[-\Delta, \Delta]$. The single parameter Δ on which the perturbation depends is of great importance. If Δ is too small, the starting point will be very likely in the basin of attraction of the current local minimizer (we are not disrupting at all the structure of the current local minimizer); on the other hand, if Δ is too large, the method becomes basically equivalent to a Multistart method (which disrupts the structure too much). In Section III we will further discuss the choice of Δ and perform experiments in order to select an appropriate value for it. The proposed perturbation move are (i) Full Jerk (FJ) , (ii) Random Partial Jerk (RPJ) and (iii) Fixed Partial Jerk (FPJ) perturbation move. All the proposed three PMs are very similar, just different in the sense of move technique. Full Jerk perturbation move technique is very simple – all the center of the circles are randomly and uniformly move within $(-\Delta, \Delta)$. The proposed RPJ perturbation move is very similar to FJ perturbation move – at first, a partial number of the center of the circles are randomly selected. Then by using uniform distribution, perturb each coordinate of them within $(-\Delta, \Delta)$. All the other circles are being unchanged during PM operations. The proposed FPJ perturbation move is very similar to RPJ perturbation move – at first, a fixed number of the center of the circles are randomly selected. Then by using uniform distribution, perturb each coordinate of them within $(-\Delta, \Delta)$. In FPJ we initially fixed up the number of circles which are perturbed during perturbations operation where as in RPJ, the number of circles which are perturbed is not fixed up initially rather random in each PM operation. It is worthwhile to remark that the initial configuration produced by PM operation may be unfeasible. But, if possible, LS procedure makes it feasible and finally the configuration converges to any local optimum configuration.

B. Stopping rule

Ideally we would like to stop a method as soon as no more progress can be expected. For the Multistart method, for which under mild assumptions, it can be proved that it is able to detect the global minimizer with probability one if we allow for an infinite number of local searches. This would mean stopping when the global minimizer has been detected. Instead, a single

run of MBH does not necessarily lead to a global minimizer and might get stuck into a local minimizer from which it is unable to escape. In such case what we

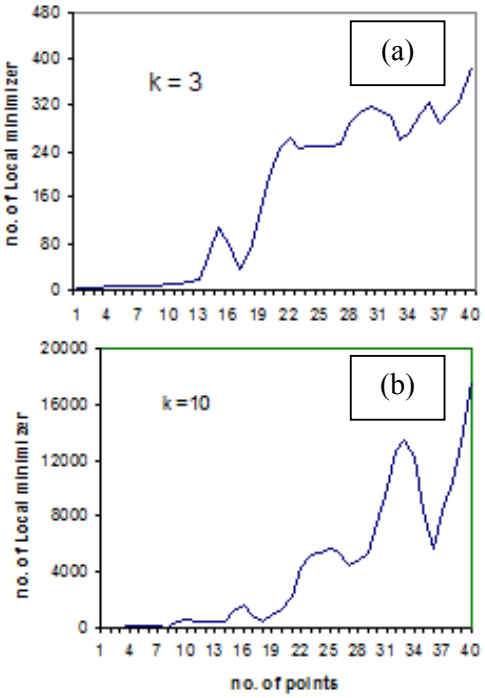

Fig. 1 : Empirically determine local minima, with threshold 10^{-8}.

can do is simply to restart MBH from a new random starting point (a sort of Multistart where local searches are substituted by MBH runs). In practice, if no special information is available, we are unable to stop when we are really sure that no more progress will be possible. The best we can do is to stop when no improvement has been observed for a sufficiently large number of iterations (of course, this is just a heuristic rule with no guarantee that improvements are not possible any more). The number of iterations, after which the algorithms are stop (with assuming that there is no further improvement), is denoted by the parameter MaxNonImp. The choice of this parameter is particularly important: we should not stop too early (which could mean that we are not patient enough to reach the global minimizer) or too late (which would mean a waste of computational effort). The choice of this parameter will be computationally investigated in Section III.

III. COMPUTATIONAL EXPERIMENTS AND DISCUSSION

Our first set of experiments aims at showing how the number of local minimizers increases with the number n of circles by considering 50,000 randomly generated local searches for n up to 40. In order to recognize distinct local minimizers we consider their objective function values with *threshold value 10-8.* We notice [see Fig. 1] that local minimizer increasing exponentially w.r.t. n from the very beginning (for both the dimensions: k=3 and k=10). It will be worthwhile to remark that, we also measure the local minimizer with *threshold value* 10^{-11}. We observed that though the number of local minimizers are increased but the shape of the curves are similar for each case. We also notice that number of local minimizer increasing rapidly w.r.t. k too. So it is confirmed that MS is not good at all for the problem.

Our next experiment is the investigation of the appropriate stopping parameter MaxNonImp. For the experiments we consider Full Jerk (FJ) perturbation technique with fixed Δ, Δ=0.8. Anyway we tested the following set of MaxNonImp values: {50, 100, 200, 300, 400, 500} with 5 MBH runs. Experimental results are reported in the Table I. Note that where there are at lest three successes for each MaxNonImp value and there are no any improved value, then result is not displayed in the table I. We remark that in 19 cases we could obtain an improvement with respect to [5]. At the same time, we also have some failures. In particular, we have 13 failures with MaxNonImp = 50 but these is immediately drop down to 9 with MaxNonImp=100 and progressively decrease to 4 with MaxNonImp=500.

As a further test we decided to enlarge the number of MBH runs from 5 to 50 for the 9 cases where the failures occurred with MaxNonImp=100. The experimental results are reported in the Table II. We notice that n = 31 turns out to be an extremely hard case for MBH: only with MaxNonImp=500 a single success could be obtained. In all the other cases we always have at least one success (with the only exception of the failure for n =83 with MaxNonImp=50) and in three cases, namely n =78, 83 and 92, we have a further improvement with respect to [5]. It is worthwhile to mention here that reference [5] i.e. Packomania website is always updating the latest information regarding packing problem, mainly packing configuration. Though there is no any optimal MaxNonImp value, tt seems that MaxNonImp = 100 or 200 is better choice for over all problems.

Our next experiment is to investigate the range of perturbation move i.e. to find the appropriate value of Δ for each perturbation strategy namely FJ, RPJ and FPJ. In the experiments we observed that MBH(FJ) performed better for Δ =0.8, MBH(RPJ) performed better for Δ. = 1.2 and MBH(FPJ) performed better for Δ. = 2.2 with 10% circles under perturbation in each PM operation. It is interesting to remark that number of perturbed circles is inversely proportional with the range of perturbation [-Δ, Δ]. We would like to mention here that the setting of value of each perturbation moves are fixed up by performing several experiments in each perturbation moves. For detail we refer [11].

We have performed another experiment for the comparison of the perturbation strategies of MBH

approaches as well as compare with MS approach. From the experimental results which is reported in the table III, it seems that all the three version of MBH methods are comparable each other whereas MS approach, all most always produced worse results though computationally very costly. We also perform another experiments with MBH(RPJ) for the 9 cases where MBH(FJ) hardly got the global optima. We notice that in this experiments with these hard instances, MBH(RPJ) has a significance better performance relative to MBH(FJ) as well as MBH(FRJ).

IV. CONCLUSION

In this study, we have performed several experiments to setup every parameters in an appropriate way. We also investigate the efficiency of the proposed algorithm for solving packing identical circles in minimum circular container. From these primary experiments we notice that all the three version of MBH algorithms able to detect the global optima efficiently. More over, we also observed that for the hard instances whose global structure of packing is not regular at all, MBH (RPJ) outperform over all other two version of the proposed algorithms.

Table I: Over all result for 5 MBH (FJ) runs with different MaxNonImp values.

			NrSuccesses						
n	**BestKnown**	**OurBestResult**	**50**	**100**	**200**	**300**	**400**	**500**	**CPU Time**
31	6.291502622129	*6.352805480965*	0	0	0	0	0	0	130.14
45	7.572912326368	7.572912326368	0	2	3	3	3	3	482.36
49	7.886870958803	7.886870958803	1	1	1	1	2	2	775.54
50	7.947515274784	7.947515274784	2	2	4	4	4	4	655.69
53	8.179582826841	8.179582826841	1	2	3	3	3	3	807.84
54	8.203982383469	8.203982383469	2	3	3	3	3	3	701.10
60	8.646219845458	8.646219845458	0	5	5	5	5	5	1168.12
62	8.829765408972	8.829765408972	2	3	4	4	4	4	1400.12
64	8.961971108486	8.961971108486	0	1	1	1	1	1	1266.97
66	9.096665836768	**9.096279426824**	3	3	3	3	4	4	1813.23
67	9.169119588389	**9.168971881784**	1	1	2	2	2	2	2563.13
68	9.229773746751	*9.234077340100*	0	0	0	0	0	0	1390.52
70	9.346055334486	**9.345653194048**	1	2	3	3	3	3	2391.79
71	9.416206538907	**9.415796896871**	4	5	5	5	5	5	2487.81
73	9.540509504650	**9.540346152138**	1	1	1	1	1	2	2806.35
74	9.589239461626	**9.589232764339**	1	2	2	2	2	2	2543.33
75	9.672029634515	**9.672029631947**	1	2	2	2	2	2	3034.33
76	9.729596802162	9.729596802162	1	1	1	1	2	3	3927.92
77	9.798987497420	**9.798911924507**	1	1	3	4	4	4	3694.47
78	9.857712212603	**9.857709899885**	0	0	0	0	0	2	4852.32
79	9.905063467661	*9.909306621540*	0	0	0	0	0	0	3590.06
80	9.968151813153	*9.969802931195*	0	0	0	0	0	0	4032.13
81	10.010864241201	10.010864241201	2	2	2	3	3	3	5293.59
82	10.050824223451	10.050824223451	1	3	4	4	4	4	5432.51
83	10.116864426926	**10.116857875102**	0	0	1	2	2	2	7914.08
86	10.298701310984	**10.298701053110**	3	4	5	5	5	5	5128.90
87	10.363209161980	**10.363208505078**	2	5	5	5	5	5	4927.78
88	10.432342147160	**10.432337692732**	4	4	4	4	4	4	5578.01
89	10.500627671551	**10.500491814574**	2	2	2	3	3	3	4874.01
91	10.566772233506	10.566772233506	2	3	3	3	3	3	6113.41
92	10.684689759023	*10.687984877108*	0	0	0	0	0	0	10041.70
93	10.733386127679	**10.733352600260**	0	1	2	3	3	3	7251.63
94	10.778032163883	**10.778032160252**	1	2	2	2	2	2	7831.68
95	10.840205021597	10.840205021597	0	0	0	0	1	1	13635.10
96	10.883669894312	10.883669894312	1	1	1	1	1	1	9701.68
97	10.938791648300	**10.938590110073**	1	1	1	2	2	2	9259.48
98	10.979383128207	10.979383128207	0	0	0	2	5	5	19099.90
99	11.037197388568	**11.035161062993**	4	5	5	5	5	5	7533.95
100	11.082527292540	**11.082149724310**	1	2	4	5	5	5	15311.60
Total Improvement			16	17	18	18	18	**19**	
Toal Failure			13	9	8	7	6	5	

Table II: Overall results for 50 MBH(FJ) runs with different MaxNoImp values over some hard Instances.

			NrSuccesses					
n	**BestKnown**	**OurResult**	**50**	**100**	**200**	**300**	**400**	**500**
31	6.291502622129	6.291502622129	0	0	0	0	0	1
68	9.229773746751	9.229773746751	10	16	18	19	21	21
78	9.857712212603	**9.857709899885**	4	6	9	16	18	21
79	9.905063467661	9.905063467661	1	1	2	2	2	2
80	9.968151813153	9.968151813153	3	3	3	3	4	4
83	10.116864426926	**10.116857875102**	0	3	9	13	19	21
92	10.684689759023	**10.684645847916**	1	3	3	4	5	5
95	10.840205021597	10.840205021597	4	9	15	17	18	19
98	10.979383128207	10.979383128207	12	22	28	35	41	41

Table III: Comparison among Different perturbations based MBH methods (with MNI=200, R=5) as well as MS approaches.

	BestKnown	**OurBestResult**	**Number of Success**				
n	**(literature)**	**(MBH method)**	**FJ (0.8)**	**RPJ (1.2)**	**FPJ (2.2)**	**MS (L)**	**MS (D)**
60	8.646219845458	8.646219845458	5	5	5	4	5
61	8.661297575540	8.661297575540	5	5	5	50	86
62	8.829765408972	8.829765408972	3	3	3	1	1
63	8.892351537551	8.892351537551	5	4	5	1	1
64	8.961971108486	8.961971108486	2	1	3	0	0
65	9.017397323209	9.017397323209	1	3	5	2	5
66	9.096665836768	**9.096279426924**	5	5	2	0	0
67	9.169119588389	**9.168971881784**	1	0	0	0	0
68	9.229773746751	9.229773746751	1	2	1	0	0
69	9.269761266641	9.269761266641	1	5	1	0	0
70	9.346055334486	**9.345653194084**	2	2	1	0	0
71	9.416206538907	**9.415796896871**	4	2	1	0	0
72	9.473890856713	9.473890856713	1	5	4	0	0
73	9.540346152138	**9.540346152138**	2	1	0	0	0
74	9.589239461626	**9.589232764339**	2	2	1	0	0
75	9.672029634515	**9.672029631947**	1	0	3	0	0
76	9.729596802162	9.729596802162	3	4	2	1	1
77	9.798987497420	**9.798911924507**	1	4	1	0	0
78	9.857712212603	**9.857709899885**	0	2	0	0	0
79	9.905063467661	9.905063467661	0	1	1	0	0
80	9.968151813153	9.968151813153	0	2	0	0	0
Improvement		**08**	**8**	**8**	**6**	**0**	**0**
Total No. of Success		**21**	**18**	**19**	**17**	**6**	**6**
Total Failure		**0**	**3**	**2**	**4**	**15**	**15**
Total elapsed time (hrs)			**4.6**	**7.6**	**5.8**	**25.8**	**40.1**

Table IV: Comparison among MBH(FJ), MBH(RPJ) and MBH(FRJ) approaches in Hard Instances (with MNI=500, R=50).

n	**BestKnown**	**OurBestResult**		**Number of Success**	
	(literature)	(MBH method)	**FJ (0.8)**	**RPJ (1.2)**	**FRJ (2.2)**
31	6.291502622	6.291502622129	1	24	1
68	9.229773747	9.229773746751	21	37	18
78	9.857712213	**9.857709899885**	21	19	16
79	9.905063468	9.905063467661	2	7	6
80	9.968151813	9.968151813153	4	20	11
83	10.11686443	**10.116857875102**	21	23	5
92	10.68468976	**10.684645847916**	5	4	2
95	10.84020502	10.840205021597	19	20	10
98	10.97938313	10.979383128207	41	39	36
Total Success			135	193	105

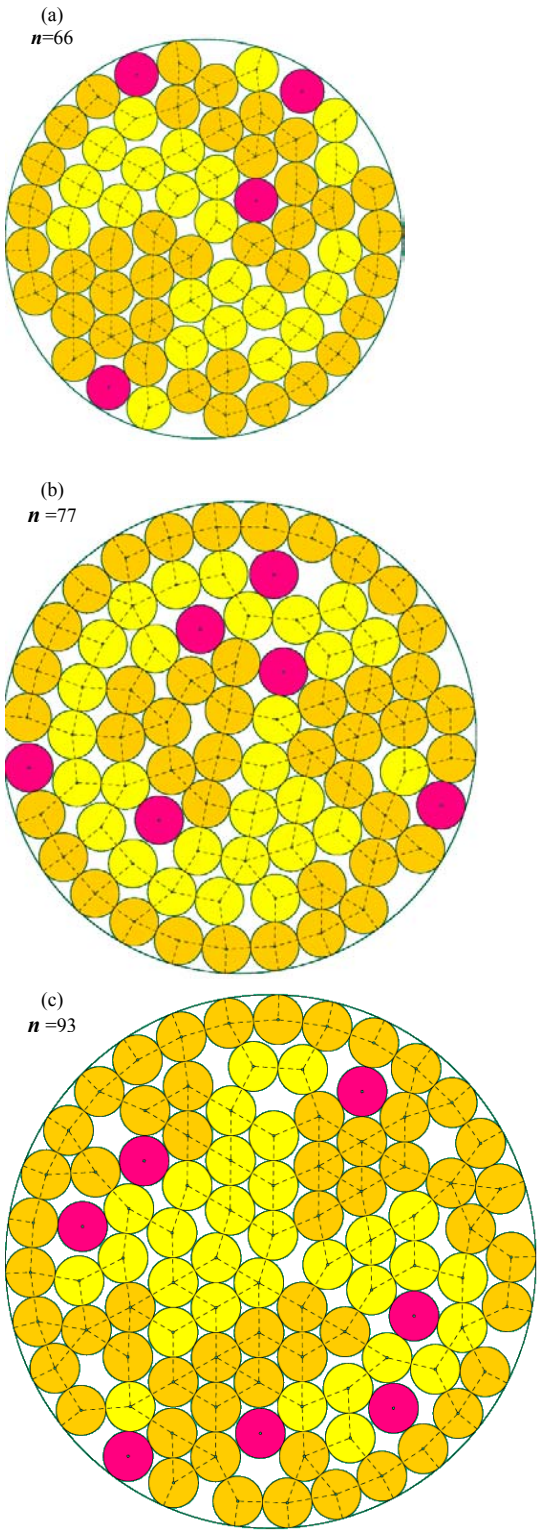

Fig. 2: Few examples of the overall best known solutions (which are improved by our proposed method) for ICPCC problems .

We would like to conclude with remark that MBH approach is able to apply in packing identical circle in circular container problem efficiently. We also mention here without details that, population basin hopping approach - a extension of MBH approach-perform better for extremely hard case w.r.t. MBH [11].

We have observed that our proposed MBH approach able to improved 19 solutions, by considering n = 30 – 100, compare to the existence ones in the literatures. Few of them are displayed, in a schematic view, in the Fig. 2. We would like to again remark that all the best packing (including our improved results) are available in the website *www.packomania.com* [5] which is maintaining by E. Specht , the Otto von Guericke University of Magdeburg, Denmark.

REFERENCES

[1] H. Dyckhoff, "A typology of cutting and packing problems", *Eur. J. Oper. Res, Elsevier, vol. 44*, 1990, pp. 145-159.

[2] M. R. Garey, D. S. Johnson, "*Computers and intractability: a guide to the theory of NP-completeness"*, San Francisco: Freeman, 1979.

[3] M. C. Szabot, T. Csendes, E. Specht., L. G., Casado, P. G. Garcia, I. Mark "*New approaches to circle packing in a square, optimization and its applications"*, Springer, 2007.

[4] D. Lubachevsky, R. L. Graham, "Curved hexagonal packing of equal disks in a circle*"*, *Discrete & Computational Geometry*, 1997, pp. 179194.

5] Packomania web site maintained by E.Specht, *www.packomania.com* , 2009.

[6] I. Castillo, F. J. Kampas, J. D. Pinter, "Solving circle packing problems by global optimization: numerical results and industrial applications*"*, *European Journal of Operational Research*, vol. 191 (3), Elsevier, 2008, pp. 786-802

[7] B., Addis, M. Locatelli, F. Schoen, "*Disk packing in a square: a new global optimization approach"*, INFORMS: Journal on Computing, vol. 20849(4), 2008, pp. 516-524.

[8] R. H, Leary, "Global optimization on funneling landscapes", *J. Global Optim*, vol. 18, 2000, pp. 367-383

[9] H. R. Lourenco, O. Martin, T. Stutzle, "*Iterated local search*," In: F. Glover and G. Kochenberger, editors, Handbook of Metaheuristics, Kluwer Academic Publishers, Norwell, MA, 2002, pp. 321-353.

[10] P. E. Gill, W. Murray, M. A. Saunders, "SNOPT: an SQP algorithm for large-Scale constrained optimization*", SIAM J. Optim.,* vol. 12, 2002, pp. 9791006.

[11] A. R. M. Jalal Uddin Jamali, "*Heuristic approaches for maximin distance and packing problems"*, Ph.D. Dissertation, University of Turin, Italy, 2009.

Proceedings of 2009 12th International Conference on Computer and Information Technology (ICCIT 2009)
21-23 December, 2009, Dhaka, Bangladesh

An Empirical Assessment of Customer Satisfaction with Internet Banking Applications: An Australian Experience

Md Mahbubur Rahim and JieYing Li
Caulfield School of Information Technology, Faculty of IT, MONASH University, Australia
E-mail: mahbubur.rahim@infotech.monash.edu.au

Abstract

In recent years, Internet-based Banking (IB) applications are gaining popularity among retail banking customers. The long term success of these applications is however influenced by customer satisfaction because it affects customers' perceptions about banks' innovative ability and customer caring intentions. Hence, measuring customer satisfaction with IB applications is important. In this article, we report the development of an instrument to operationalise customer satisfaction following a rigorous mixed approach, and then apply that instrument to measure customer satisfaction with IB applications in Australia. Several interesting findings have emerged which are useful to research and practice alike.

Keywords: internet banking, satisfaction, instrument evaluation, mixed approach, e-commerce

I. INTRODUCTION

Internet banking refers to an online facility which provides an alternative channel for delivering banking/financial services and enables individuals to access their accounts anytime and anywhere through a bank's web site [1]. It is important for the bank management to assess customer satisfaction because it largely determines the success of their IB offerings. There is evidence to suggest that retention of existing customers to a very large extent is influenced by their satisfaction with bank's online initiatives [2]. According to Molina et al. [3], customer satisfaction is a key element for the success of financial institutions which are facing increased competition and frequent market changes now-a-days. Unfortunately, inadequate attention has been paid to understand the dimensions comprising customer satisfaction with IB offerings. In addition, little research has been conducted to measure customer satisfaction with IB offerings. This is particularly true for Australia in which IB applications are gaining increased popularity [4]. Against this background, we report the development of a model to measure customer satisfaction with internet banking and derive an initial instrument from that model. We then describe how that instrument was refined using a rigorous process. We further report a pilot survey in which the refined instrument was administered among 150 staff and students of a large Australian university. The findings indicate that five dimensions such as *user friendliness, response time, up-to-date information, information tailored to customer preferences, and customisation and online support* contribute to the formation of customer satisfaction with IB applications. Another finding is that the overall satisfaction level of the survey participants is high although there is a variation in their perceptions towards each of the five dimensions underlying customer satisfaction. We thus contribute to literature by developing and empirically evaluating a theory driven instrument which the bank management can use as a measurement tool to diagnose how well their internet banking applications are doing in creating a satisfied customer community.

II. BACKGROUND LITERATURE

We have consulted three relevant streams of literature to help develop an improved understanding of customer satisfaction with internet banking: End-User Computing (EUC) satisfaction literature, Business-to-Consumer (B2C) eBusiness satisfaction literature and Internet banking satisfaction literature. Each stream is briefly described below and the gaps in these streams from methodology perspective are identified.

End-User Computing satisfaction literature: The pioneering work within this stream was conducted by Doll and Torkzadeh [5] who developed End-User Computing Satisfaction (EUCS) framework specifically for measuring end-users' satisfaction with intra-organisational computer based applications. There are five major factors which act as the foundation of the EUCS framework: content, accuracy, format, ease of use and timeliness. Since its inception, this framework has gained strong popularity among many practitioners and researchers [6,7]. This is because the EUCS framework concentrates on evaluating user satisfaction regarding one application in a parsimonious way [8]. In general, the EUCS framework has received broad support from various scholars. For example, McHaney et al. [9] and Abdinnour-Helm et al. [10] have confirmed the test-retest reliability and validity of the EUCS measure. We believe that many of the factors included in the EUCS are likely to be relevant for measuring customer satisfaction with IB applications.

978-1-4244-6283-4/09/$26.00 ©2009 IEEE

Our view is confirmed by Pikkarainen et al. [8] and Afzaal et al [11] who have in recent years referred to this framework for measuring consumer satisfaction with online banking applications. However, despite the popularity of the EUCS framework, it has also been criticised for its lack of measure of the IT department's service quality [12].

Business-to-Consumer eBusiness satisfaction literature: This stream of literature has investigated consumer satisfaction from three perspectives: web site quality, service quality, and total retail purchasing process. Typical studies exploring the relationship between web site quality and consumer satisfaction include those of Szymanski and Hise [13], Heiner et al. [14], Hsuehen [15]. On the other hand, scholars like Yang and Fang [16], Zhang et al. [17] and Ha [18] have examined user satisfaction in the context of online services. They found such factors as perceived convenience and perceived security to be major factors that affect satisfaction level of the users of online retail services. Finally, Liu et al. [19] have examined consumer satisfaction from their total purchasing experience viewpoint. We believe that some of these factors are also likely to influence the formation of customer satisfaction with IB applications.

Internet banking satisfaction literature: Within this stream, three distinct lines of investigation are reported. One group of scholars has proposed a number of factors to be included as components comprising customer satisfaction with internet banking applications. These scholars (e.g. Pikkarainen et al. [8] and Afzaal et al. [11]) have fundamentally drawn from the EUCS framework [5]. However, online banking applications are different from those of end-user oriented IT applications in many respects (e.g. channel of delivery, type of user characteristics, and security concerns). These differences are recognised by some scholars of this group who have included several additional factors as dimensions of customers' satisfaction with internet banking. For example, Buys and Brown [20] and Hwang, et al. [21] have added such new factors as security, customer support, transaction capability and trust. We have however noted a difference in the focus of this group of scholars. For example, some scholars have focused on web appearance while others have emphasised more on transaction support.

The second group of scholars (e.g. Arunachalam and Sivasubramanian [22]) regard user satisfaction to be a dimension of user experience with internet banking. They have not however developed an instrument to empirically measure customer satisfaction and their experience with internet banking. Yet another group of scholars (e.g. Chung and Paynter [23] and Floh and Treiblmaier [24]) have measured overall customers' satisfaction with internet banking. They have used a single satisfaction item for evaluating the effectiveness and performance of retail internet banking services. Unlike the first group of scholars, these scholars did not produce a comprehensive measurement scale for customer satisfaction with internet banking, because satisfaction is considered to be based on cumulative experiences of customers. They argue that customer satisfaction is not affected by successful online transaction and hence operationalising satisfaction with multiple factors is restrictive.

Gaps in the existing literature: We acknowledge the contribution of all scholars mentioned in the above-mentioned three streams of literature. However, we argue that many of these studies suffer from several weaknesses which call for further research attention. For example, most studies have not reported how they have followed a rigorous qualitative approach for producing a reliable instrument. According to methodology gurus, both qualitative and quantitative evaluations are necessary for developing precise satisfaction instruments. This aspect has been ignored by most scholars. We specifically address this particular weakness and report our experience of evaluating an instrument following a rigorous mixed approach, thus bridging a gap in the existing literature. Another weakness which is particularly inherent in the IB satisfaction literature is that although some scholars [20-21] have added new factors which are relevant for internet banking satisfaction, they still did not consider the influence of other important characteristics (e.g. customisation, web appearance, information tailored to customer needs, response time) of internet banking applications which are likely to influence satisfaction of customers.

III. SATISFACTION MODEL

Drawing on the factors identified in the existing literature and a broad understanding developed through a review of literature, a research model on customer satisfaction is proposed which includes 13 dimensions: *user-friendliness, ease of navigation, customisation, website appearance, online customer support, support for transactions, accuracy, up-to-date, sufficient, information tailored to specific needs, security capacity, response time and perceived convenience*. In the following section, we now briefly present our arguments in support of the inclusion of these dimensions.

User friendliness: Doll and Torkzadeh [5] identified user-friendliness to be a major element that affects end-user computing satisfaction. For internet banking, it can be argued that customers would be dissatisfied

when they find the application hard to use. This line of argument is empirically supported by several scholars [5, 8, 21].

Ease of navigation: Applications which are easy to navigate are likely to create positive feelings in the minds of users towards that application. This view is supported by Liao and Chung [1], who argued that users' satisfaction about website quality is improved when those sites are easy to navigate. Hence, for internet banking applications, ease of navigation can help improve customer satisfaction.

Customisation: It refers to the ability of a website to be shaped so as to better the meet needs of individual users. Customisation has been found to be one of the factors which influence user satisfaction with online systems [26,27]. As internet banking applications are likely to be used by a diverse range of customers, strong customisation capabilities would help creating satisfied customers.

Web appearance: According to Kim and Stoel [28], "web appearance" emphasises how well a website guides its users for its use. The importance of website appearance is also highlighted in several e-commerce studies [2, 29]. According to these studies, consumers prefer uncluttered and easy-to-navigate sites. For internet banking context, we argue that an attractive website appearance will help in advancing satisfaction of customers.

Online customer support: In the competitive market environment, customers who are not happy with the services offered by a business are likely to seek satisfying their needs elsewhere [24]. In their study, Yang and Peterson [30] measure service quality of online business in terms of three capabilities: a) the abilities of companies to provide customers with wide ranges of product/service packages, b) the abilities of companies to provide customers with products/services with the features they want, and c) the quality of companies' customer services. In the context of internet banking, banks need to provide wider range and higher quality of services in order to satisfy internet banking user's expectations. In their study, Buys and Brown [20] found customer support to be of distinct importance in the context of internet banking. This is due to the fact that many users are not confident with the Internet and the general complexity of the e-banking application itself, lack of support or failure of providing appropriate support from the banks may be an obstacle for increasing customer satisfaction.

Support for transactions: Banks must support the ability to provide feedback on each transaction completed by customers via their internet banking applications. In the absence of any bank employees, customers would be anxious to know the status of their transactions performed online. Hence, internet banking applications need to assure customers (by such means as pop-up messages) that their online transactions have been acted on. Such feedback helps improve customer confidence in the internet banking applications which in turn contributes to increased customer satisfactions.

Accuracy, Up-to-date and Sufficient: In their study, Tojib et al. [31] highlighted the importance of accurate, up-to-date and adequate information for measuring employee satisfaction with B2E portals. Their observation also applies to the internet banking scenario. We believe that the ability of internet banking applications to provide customers with accurate, up-to-date and sufficient information that exactly match their needs positively affects customer perceived value from internet banking [20] which in turn helps create satisfied customers.

Information tailored to specific needs: A diverse range of customers with varying taste and needs use internet banking applications. Hence, there is an expectation on the part of the customers that they would not want to be overloaded with too much information from their banks owing to easy connectivity via these applications. They expect to receive only those information which are relevant to their specific needs. This line of argument is supported by several scholars [2, 29].

Security capacity: Technological capacity of websites representing online service delivery is a major contributor of customer satisfaction. The key construct to measure technological capacity is security capacity. Customers consider security as one of the most important concerns, especially in the area of internet banking [32]. Security measures customers' perceptions of online channel reliability and safety [33]. In their study, Hwang, et al. [21] asserted that customer satisfaction with internet banking has a high correlation with security.

Response time: Another important feature of technological capacity is "response time of internet banking" which has roots in the concept of "timeliness" drawn from the end-user satisfaction literature. Doll and Torkzadeh [5] indentified that "timeliness" is one of the most significant factors affected end-user computing satisfaction. In their study, Sugianto and Tojib [31] defined timeliness as "the ability to deliver requested information with a reasonable response time". Response time also refers to the loading time of the website and the waiting time between users' actions and the website's response [32]. Consumers tend to be highly sensitive to the speed of service delivery [1]. As a result,

response time is also one of the important factors which should be considered in order to help raise customer satisfaction.

Perceived convenience: Today's customers demand greater conveniences and accessibility, the quality attribute of time and location convenience is likely to be significant in differentiating internet banking from traditional retail banking [1, 34]. Consequently, the ability to access internet banking at anytime and from anywhere is likely to influence customers' satisfaction with internet banking applications. Furthermore, customers interacting with their bank using the Internet without the need to directly interface with bank employees can be valuable in advancing satisfaction because it reduces communication apprehension which may be caused by the profound cultural diversity [33].

IV. RESEARCH APPROACH

A survey approach was considered appropriate due to three reasons: a) in light of Neuman's [35] advice, our research is considered to be exploratory in nature as it aims to explore the existence of various dimensions comprising customer satisfaction with IB applications, b) in terms of Yin's [36] classification, our research can be categorised as theory building in nature because it helps build a theoretical model on customer satisfaction with IB offerings, and c) we are concerned with measuring 'how much' type of questions because our participants are required to indicate their level of agreement/disagreement on a scale of 1 to 5 for a series of items which operationalise various dimensions of customer satisfaction with IB applications. A total of 47 items were developed from the existing streams of literature. These items were then adapted for the internet banking context to operationalise the 13 dimensions included in the model. Several items were however developed by the authors in support of such dimensions as 'Support for transactions' and 'Customisation'. These 47 items collectively formed the foundation of the initial theory driven instrument.

A two-stage process was followed to refine the instrument: qualitative and quantitative. The qualitative stage involved execution of three specific activities: deliberations with several domain experts [37], item-factors association analysis [38] and pre-testing [39]. Following the suggestions of Kitchenham and Pfleeger [37], a total of 3 domain experts were consulted who collectively offered 69 suggestions for improving the initial instrument. These suggestions were analysed using two criteria proposed by Eklim and Rahim [40]: *completeness of factors* and *comprehensiveness of items operationalising those factors*. As a result, 28 items were revised, 2 items were relocated, 16 items were removed and 1 new item was added. A revised survey questionnaire was thus prepared which contained 32 items.

The revised instrument was then given to a group of participants for evaluating item-factor association. According to the recommendations of Nielsen [41], a total of 5 participants (including 2 IT post-graduate students having prior job experience, 1 undergraduate student, 1 academic staff and 1 administration staff) were selected for evaluating item-factor association. They were required to associate each item with a factor which they think represents the best match. Their responses were captured on a scale of 1 to 5, where 1 represents strongly unrelated, 3 represents neutral and 5 represents strongly related. The participants were found to associate 13 items with more than one factor. As a result, 7 items were removed and another 6 were revised to improve the clarity of the items. The resultant instrument thus contained 25 items.

The 25-item instrument was then subject to pre-testing by a group of 14 postgraduate students who were randomly selected from a tertiary institution. This group was targeted because they match the profile of the typical Internet banking users [20]. During the pre-testing stage, the participants expressed their views about their difficulties in interpreting the meaning of several items for which further changes were incorporated in the instrument. Based on their feedback, several items were rephrased to improve clarity and one item was removed resulting in a 24-item instrument which was then distributed through a pilot survey among 400 staff and students of a leading Australian university.

A total of 150 responses received from the pilot survey (resulting in a response rate of 37.5%) were analysed using SPSS software. Two techniques such as item purification analysis using corrected item-total correlation [42] and exploratory factor analysis using varimax approach [43] were applied to help improve validity of the instrument. In addition, Cronbach's alpha [44] was calculated for each item to establish reliability. Following the suggestions of Churchill [42], we have removed 5 items for which corrected item-total correlation were less than 0.3. The remaining 19 items were then subject to several rounds of factor analysis which eventually resulted in a five-factor solution with 14 items. During factor analysis, using the suggestions of Hair et al. [43], 5 more items were removed which loaded onto more than one factor. The resultant dimensions are: user friendliness, response time, up-to-date information, information tailored to customer preferences, and customisation and online support.

V. EMPIRICAL FINDINGS

Profile of the survey participants: Male dominance is observed. Most participants are young (i.e. less than 29 years old) and most have undergraduate degrees.

Dimensions of satisfaction: The mean scores of the participants' responses for each of the five dimensions indicate that the participants in general are not dissatisfied with any of the five dimensions of customer satisfaction. They believed that the internet banking applications which they use are user friendly (mean score: 4.04), have fast response time (mean score: 3.83), provides up-to-date information (mean score: 3.82), provides somewhat information tailored to their preferences (means core: 3.54). However, the opinion of the participants regarding customisation and online support (mean score: 3.01) is just above neutral. We thus argue that bank management needs to pay greater attention to include functionalities that would help customers customise the contents and offer superior online customer support for their internet banking applications.

Customer satisfaction: The average satisfaction level of the participants (i.e. 50.39) is much greater than the neutral satisfaction level (i.e. 3 x 14 = 42 in which 3 means neutral on a scale of 1 to 5 for each of the 14 items) suggesting that participants in general are satisfied with the internet banking applications. Out of 150 participants, 132 have an overall satisfaction level which is greater than the neutral level (i.e. > 42). Student t-tests suggest the absence of any significant differences in both overall satisfaction and each of the five dimensions of satisfaction based on gender. Likewise, no significant differences were observed based on participants' age. (*The detailed results of these two student t-tests are not shown due to page constraints*)

VI. DISCUSSION

Even though 13 distinct dimensions were identified from the literature and were included in the measurement of overall customer satisfaction with internet banking, our study empirically confirms that only five dimensions are relevant. These dimensions include: user friendliness, response time, up-to-date information, information tailored to customer preferences, and customisation and online support. The qualitative evaluation stage helped removed 4 dimensions (i.e. ease of navigation, website appearance, sufficient, perceived convenience), while the quantitative evaluation stage further identified 2 dimensions (i.e. support for transactions, accuracy) for removal and two other dimensions were merged into one new dimension labelled as customisation and online support.

The items which were derived from the existing literature to measure 13 dimensions (originally included in the initial theory driven instrument) also evolved. Initially, a total of 47 items was generated (from literature analysis) to operationalise the 13 dimensions comprising customer satisfaction. A total of 23 items were then removed, modified, and some new items were added during the qualitative stage of instrument refinement process. The quantitative process has then further removed 14 items through item purification and factor analysis. The resultant instrument has thus 14 items measuring 5 dimensions which together are significant for measuring customer satisfaction.

We now compare these five dimensions (i.e. user friendliness, response time, up-to-date information, information tailored to customer preferences, and customisation and online support) with those reported in the existing B2C and EUCS literature. Our satisfaction instrument has some similarities and differences with the EUCS framework developed by Doll and Torkzadeh [5]. Dimensions like 'user-friendliness' and 'timeliness' are similar to our 'ease of use' and 'response time'. Likewise, 'content' factor present in the EUCS framework has somewhat similar meanings of such dimensions as 'up-to-date content' and 'Information tailored to specific needs'. However, customisation dimension which is important in our study does not have an equivalent component in the EUCS model. Moreover, unlike the accuracy and security aspects mentioned in the B2C satisfaction literature [17,18], we did not find their relevance with regard to satisfaction towards IB applications. One possible explanation is that customer's concerns for security and accuracy may be more important at their IB adoption decision making stage. These two dimensions perhaps lose their significance once customers use these applications on a regular basis. The lack of 'perceived convenience' to act as a dimension for customer satisfaction with IB can be explained by the fact that once customers develop a habit of using internet banking this factor too (which is initially important at the adoption decision making stage) is regarded irrelevant by the customers. Our analysis further provides indicate evidence that commonly cited demographic characteristics of customers (e.g. age and gender) are not associated with customer satisfaction with internet banking. This observation is similar to those of Haytko and Simmers [45] who found no gender effect in the overall satisfaction for online banking services. One possible explanation for the lack of gender influence on satisfaction is that female customers are now growingly using online shopping and hence they equally feel satisfied in the use of IB applications. We have however reservations about the influence of age because the sample is from a tertiary educational institutional setting in which both staff and students

regardless of their age are more likely to be familiar with many online activities (e.g. online delivery of teaching and research materials, online training). Further investigations are required to address this aspect.

VII. CONCLUSION

We have reported development of an instrument by following a rigorous mixed approach. Several interesting findings have emerged from our study; these were then discussed in light of the existing literature. However, our interpretation of the findings should be treated with caution due to the selection of a convenient and small sample. Despite this limitation, our findings are useful to both practice and research. Bank management can use our instrument as a diagnostic tool for not only to measure overall customer satisfaction with internet banking initiatives but also to identify those dimensions of satisfaction which are more closely related to customer loyalty. This in turn helps them in preparing appropriate strategies on how to minimise customer complaints. Our contribution to theory is the explicit demonstration of the application of a mixed approach for validating an initial theory driven satisfaction instrument. In addition, we also highlight that certain well-known factors such as perceived security and convenience which are significant at the IB adoption decision stage of customers may lose their importance at a later post-adoption stage. This is an important discovery which is not mentioned in the existing literature.

There are several ways to extend our work. There is a need to validate the instrument involving corporate customers. This may help researchers identify other important dimensions of customer satisfaction. Further studies should employ our instrument to understand the influence of satisfaction on customer retention and loyalty. Further studies are also required to replicate this work in other cultural contexts.

REFERENCES

[1] Z. Liao, and M. Cheung, "Internet-based e-banking and consumer attitudes: an empirical study", *Information and Management*, Vol. 39, pp. 283-259, 2002.

[2] C. F. Ho, and W. H. Wu, "Antecedents of Customer Satisfaction on the Internet: An Empirical Study of Online Shopping", *Proceedings of the 32nd Hawaii International Conference on System Sciences*, pp. 1-12, 1999.

[3] Arturo Molina, David Martin-Consurgra, and Agueda Esteban, "Relational benefits and customer satisfaction in retial banking", *International Journal of Bank Marketing*, Vol.25, No. 4, pp.253-271, 2007.

[4] Deanie Sultana, "Aussie consumers choose Internet banking over ATM, phone and branch", ACNielsen, http://au.nielsen.com/news/20070426.shtml, 2007

[5] W. J. Doll, and G. Torkzadeh, "The Measurement of End-User Computing Satisfaction", *MIS Quarterly*, Vol. 12, No. 2, pp.259-274, 1998.

[6] Wynne W. Chin, and Peter R. Newsted, "Research Report—The Importance of Specification in Causal Modeling: The Case of End-User Computing Satisfaction", *Information Systems Research*, Vol. 6, No. 1, pp. 73-81, 1995.

[7] W. J. Doll, and W. Xia, "Confirmatory factor analysis of the end-user computing satisfaction instrument: A replication". *Journal of End User Computing*, Vol. 9, No. 2, pp.24–31, 1997.

[28] K. Pikkarainen, T. Pikkarainen, H. Karjaluoto, and S. Pahnila, "The measurement of end-user computing satisfaction of online banking services: empirical evidence from Finland", *International Journal of Bank Marketing*, Vol.24, No. 3, pp.158-172, 2006.

[9] V. McKinney, K. Yoon, and F. M. Zahedi, "The measurement of web customer satisfaction: An exception and disconfirmation approach." *Information Systems Research*, Vol. 13, No. 3, pp.296–315, 2002.

[10] Sue F. Abdinnour-Helm, Barbara S. Chaparro, and Steven M. Farmer, "Using the end-user computing satisfaction (EUCS) instrument to measure satisfaction with a web Site", Decision Science, Vol. 36, No. 2, pp.341-364, 2005.

[11] S. Afzaal and M. M. Rahim, "Customer Satisfaction with Internet Banking in Brunei Darussalam: Evaluating the Role of Demographic Factors", *Submitted to Journal of Electronic Commerce in Organizations*, 2008.

[12] W. J. Kettinger, and Choong C. Lee, "Perceived service quality and user satisfaction with information services function", *Decision Sciences*, Vol. 25, No.5/6, pp.737-750, 1994.

[13] D. M. Szymanski, and R. T. Hise, R.T., "E-satisfaction: an initial examination", *Journal of Retailing*, Vol. 76 No. 3, pp. 309-22, 2002.

[14] E. Heiner, R. I. Gopalkrishnan, H. Josef, H. and A. Dieter, "E-satisfaction: a re-examination", *Journal of Retailing*, Vol. 80, No. 3, pp. 239-47, 2004.

[15] H. Hsuehen, "An empirical study of web site quality, customer value, and customer satisfaction based on e-shop", *The Business Review*, Vol. 5 No. 1, pp. 190-3, 2006.

[16] Z. Yang, and X. Fang, "Online service quality dimensions and their relationships with satisfaction: a content analysis of customer reviews of securities brokerage services", *International Journal of Service Industry Management*, Vol.15, No 3, pp. 302-26, 2004.

[17] X. Zhang, V. Prybutok, and A. Huang, "An empirical study of factors affecting e-service satisfaction", *Human Systems Management*, Vol. 25, No. 4, pp. 279-91, 2006.

[18] H.Y. Ha, "An integrative model of consumer satisfaction in the context of e-services", *International Journal of Consumer Studies*, Vol.30, No.2, pp. 137-49, 2006.

[19] X. Liu, M. He, F. Gao, and P. Xie, "An empirical study of online shopping customer satisfaction in China: a holistic perspective", *International Journal of Retail &*

Distribution Management, Vol. 36, No.11, pp.919-940, 2008.

[20] M. Buys and I. Brown, "Customer satisfaction with internet banking web sites: an empirical test and validation of a measuring instrument", *Proceedings of the 2004 annual research conference of the South African institute of computer scientists and information technologists on IT research in developing countries*, Stellenbosch, Western Cape, South Africa, pp. 44-52, 2004.

[21] H. G. Hwang, R. F. Chen, and J. M. Lee, "Measuring customer satisfaction with internet banking: an exploratory study", *International Journal of Electronic Finance*, Vol.1, No.3, pp.321-335, 2007.

[22] L. Arunachalam and M. Sivasubramanian, "Theoretical framework to measure the user satisfaction in internet banking", *Academic Open Internet Journal*, Vol. 20, 2007.

[23] W. Chung and J. Paynter, "An Evaluation of Internet Banking in New Zealand", *Proceedings of the 35th Hawaii International Conference on System Sciences*, pp.2410- 2419, USA. 2002.

[24] A. Floh and H. Treiblmaier, "What keeps the e-banking customer loyal? A multigroup analysis of the moderating role of consumer characteristics on e-loyalty in the financial service industry", *Journal of Electronic Commerce Research*, 7(2), 2006.

[25] S. Lichtenstein, and K. Williamson, "Understanding Consumer Adoption of Internet Banking: An Interpretive Study in the Australian Banking Context", *Journal of Electronic Commerce Research*, Vol.7, No. 2, pp. 50-66, 2006.

[26] T. A. Horan, and Abhichandani T. "Evaluating user satisfaction in an e-government initiative: results of structural equation modeling and focus group discussions", *Journal of Information Technology Management*, Vol. XVII, No. 4, 2006.

[27] Y.S. Wang, Y. M. Wang, H. H. Lin, and T. I. Tang, "Determinants of user acceptance of Internet banking: an empirical study", *International Journal of Service Industry Management*, Vol.14, No.5, pp.501-519, 2003.

[28] S. Kim, and L. Stoel, "Apparel retailers: website quality dimensions and satisfaction", *Journal of Retailing and Consumer Services*, Vol.11, No.2, March, 2004, pp.109-117, 2004.

[29] J. H. Huang, C. Yang, C., B. H. Jin, and H. Chiu, "Measuring satisfaction with business-to-employee systems", *Computers in Human Behavior*, Vol.20, No. 1, pp.17-35, 2004.

[30] Z. Yang, and R. T. Peterson, "Customer Perceived Value, Satisfaction, and Loyalty: The Role of Switching Costs", *Psychology & Marketing*, October, Vol. 21, No. 10, pp.799-822, 2004.

[31] L. D. R. Tojib, F. Sugianto, and S. Senjaya, "User satisfaction with business-to-employee portals: conceptualization and scale development", *European Journal of Information Systems*, Vol. **17,** pp.649–667, 2008.

[32] W. Chung and J. Paynter, "An Evaluation of Internet Banking in New Zealand", *Proceedings of the 35th Hawaii International Conference on System Sciences*, pp.2410- 2419, USA. 2002.

[33]R. Awamleh, R., and C. Fernandes, "Internet Banking: An empirical investigation into the extent of adoption by banks and the determinants of customer satisfaction in the United Arab Emirates", *Journal of Internet Banking and Commerce*, Vol. 10, No. 1, 2005.

[34] S. S. Alam, R. S., Shaharudin, I. Ahmad, and N. Ahsan, "Internet Banking Adoption: Non-Internet Banking Users Perspective", *The 2008 International Joint Conference on e-Commerce, e-Administration, e-Society, and e-Education*, Bangkok, March 27-29, 2008.

[35] W. L. Neuman, *Social research methods: Qualitative and quantitative approaches*. Boston: Allyn and Bacon., 2003.

[36] R. K. Yin, C*ase study research: Design and methods*. Thousand Oaks, CA: Sage, 2003

[37] B. Kitchenham, and S. L. Pfleeger, "Principles of survey research4 questionnaire evaluation", *Software Engineering Notes*, Vol. 27, No. 3, pp.20-23, 2002.

[38] G. Santos, "Card sort technique as a qualitative substitute for quantitative exploratory factor analysis", *Corporate Communications*, Vol. 11, No. 3, pp.288-302, 2006.

[39] N. M. Bradburn, S. Sudman, S. and B. Wansink, *Asking Questions: The Definitive Guide to Questionnaire Design*, California: Jossey-Bass, 2004.

[40] S. Eklim, and M. M. Rahim, "An Instrument to measure organizational motivations for inter-organizational systems adoption: A qualitative evaluation", *International Journal of Business and Information*, Vo3, No1, pp.53-85. 2008

[41] J. Nielsen, "Card sorting: How many users to test", Jakob Nielsen's Alertbox, Retrieved April 1, 2005 from http://www.useit.com/alertbox/20040719.html, 2005

[42] G.A. J. Churchill, "A paradigm for developing better measures of marketing constructs", *Journal of Marketing Research*, Vol. XV, pp.64-73, 1979.

[43] J. F. Hair, R. E. Anderson, R. L. Tatham, and W. C. Blake, Multivariate Data Analysis, Prentice Hall: Englewood Cliff, N.J. 4th edition, 1995.

[44] Nunnally, J. C. *Psychometric Theory*, 2nd Edition, New York: McGraw-Hill, 1978.

[45] S. Haytko, and C. Simmers, "What's your preference? An exploratory examination of the effect of human vs ATM vs online interactions on overall consumer satisfaction with banking services", *Management Research*, Vol. 32, No.4, pp.337-353. 2009.

[46] M. David, "Culture, context, and behaviour", *Journal of personality*, Vol.75, No.6, pp.1285-1320, 2007.

Proceedings of 2009 12th International Conference on Computer and Information Technology (ICCIT 2009)
21-23 December, 2009, Dhaka, Bangladesh

Heuristic Algorithm of the Multiple-Choice Multidimensional Knapsack Problem (MMKP) for Cluster Computing

Md. Iftakharul Islam, Md. Mostofa Akbar

Department of Computer Science and Engineering,
Bangladesh University of Engineering and Technology (BUET), Dhaka-1000, Bangladesh
tamim@csebuet.org, mostofa@cse.buet.ac.bd

Abstract

This paper presents two heuristic algorithms of the MMKP (a variant of 0-1 knapsack problem) for cluster computing. We present an architecture of a cluster, such that algorithm requires small message passing. The algorithms divide the problem among computational nodes. Each node solves its sub problem using a sequential heuristic. This naïve divide and conquer approach cannot achieve good revenue. The revenue is the value achieved by the solution of MMKP. To improve the revenue, it accumulates the unused resources from every node, and assigns to the node, which gives maximum revenue over all nodes. This is the residue exploitation (RE) strategy. The solution quality can be improved by a novel resource-division policy rather than equal division. The policy divides the resource among all nodes such that total revenue increases. A sequential heuristic calculates the solution incrementally for different amounts of resource capacity, and the best combination is taken as the solution. This is the resource adjustment (RA) strategy. We experiment the algorithm using MPI (Message Passing Interface). The proposed algorithms show encouraging results.

Keywords: Admission control architecture, Heuristic algorithm, Knapsack problem, Parallel processing.

I. INTRODUCTION

This paper will present two distributed heuristics of the MMKP for cluster computing. In the MMKP, a set of groups is given. Each group has some items. Each item, requiring multiple resources, gives a nonnegative revenue. The problem is to select an item from every group, such that the resource constraints of knapsack are not violated, and the revenue is maximized. Let there be n groups. Each group is denoted as $J_l, l = 1, \dots, n$. Group J_l has r_l items. Each item $j, j = 1, \dots, r_l$ of group J_l has a value v_{lj}, and requires m resources $W_{lj} = (w_{lj}^1, w_{lj}^2, \dots, w_{lj}^m)$. $C = (C^1, C^2, \dots, C^m)$ be the resource bound of the knapsack. The objective of the MMKP is to pick exactly one item from each group for maximum total revenue of the collected items, subject to the resource constraints of the knapsack. That is, the problem is to find $max \sum_{l=1}^{n} \sum_{j=1}^{r_l} x_{lj} v_{lj}$ such that $\sum_{l=1}^{n} \sum_{j=1}^{r_l} x_{lj} w_{lj}^k \leq C_k$ for $k = 1,2, \dots, m$ where $x_{lj} \epsilon \{0,1\}$ and $\sum_{j=1}^{r_l} x_{lj} = 1$.

Many real-world problems, for example, admission control and resource scheduling for multimedia system can be formulated in terms of MKPP [8]. We will propose a cluster architecture, such that the algorithm requires small message passing. We will show the architecture in the context of admission control of multimedia server. The remainder of the paper is organized as follows. In Section 2, we present different solutions for MMKP. Section 3 describes the cluster architecture. Section 4 presents the algorithms. In Section 5, we evaluate the performance of the algorithms. Section 6 concludes the paper.

II. RELATED WORKS

To solve the MMKP, an approach was designed based on Lagrange multipliers [10]. An algorithm has been proposed (named HEU) based on the aggregate resources [9]. A preprocessing and post processing is augmented to the HEU is called M-HEU is presented in [1]. It helps the algorithm to go out of local optima. An incremental version of M-HEU, called I-HEU, is also proposed in [1]. Guided Local Search (GLS) algorithm is a recent approach for solving MMKP [5]. The Linear Programming Relaxation (LPR) of MMKP, called HMMKP, is described in [4]. Another heuristic, based on convex hull, is proposed in [2]. Later, Reactive Local Search (RLS) based approach is used for MMKP [6]. Dividing the computation of M-HEU among multiple processors, a parallel heuristic for MMKP is proposed for shared memory architecture [11]. This paper presents heuristic solutions of MMKP for distributed memory architecture.

III. CLUSTER ARCHITECTURE

In the section, we discuss a cluster computing architecture for solving the MMKP, in an admission controller of a multimedia server. In a trivial cluster architecture, all the requests come to a server. The server takes the help of other nodes to solve the admission control problem. If the server divides the problem among all nodes, huge message passing will be required. In our proposed architecture, we will divide the problem while posing to the server. So, no overhead will be required for dividing the problem. Fig. 1 illustrates the architecture.

978-1-4244-6283-4/09/$26.00 ©2009 IEEE

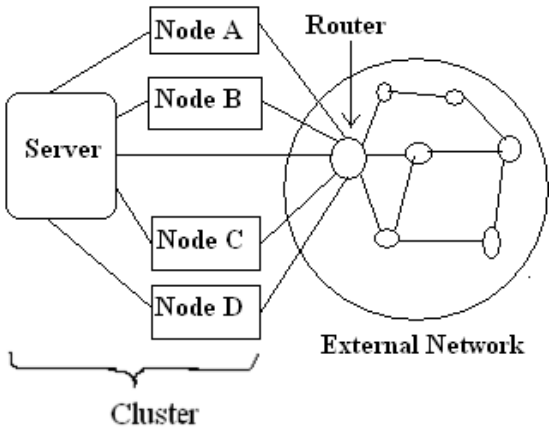

Fig. 1. Cluster computing architecture of an admission controller for multimedia server.

Node A, B, C, D, and the server form the cluster. A router is connected to every node using point to point links. The router intelligently divides the MMKP among all nodes. When a request (also called group in terms of MMKP) arrives at the router, router destines it to a node in a round robin fashion. So, every node has almost equal number of groups. A parallel-heuristic algorithm solves the whole problem. At the end of the computation, every node sends the list of selected items to the server. Thus, the messages include only one item per group instead of a whole group. In this way, we reduce the cost of message passing significantly.

Besides the network architecture, many other issues affect the performance. Some issues of ethernet cluster are studied in [7]. In our study, we adopt static task assignment policy. Scattered subdivision is chosen for dividing the problem among nodes. In scattered subdivision, packet i is assigned to the node $i \bmod p$, where p is the total number of nodes.

IV. ALGORITHM

We propose two algorithms. In the first algorithm, only Residue Exploitation (RE) is used. In the second algorithm, both Resource Adjustment (RA) and Residue Exploitation (RE) are used. Both of the algorithms divide the problem among nodes. The algorithms are abbreviated as DCRE and DCRARE respectively, where 'DC' stands for Divide and Conquer.

A. DCRE ALGORITHM

The steps of the DCRE algorithm are the following:

1. Server divides resources equally (almost) among all nodes.
2. Each node calculates a local solution using a sequential heuristic.
3. In most of the cases, some resources are not totally used while one or more other resources are finished. Each node calculates the unused resources.
4. Each node sends the amount of unused resources to the server.
5. The server calculates the total unused resources, and sends it to every node.
6. Each node tries to increase its revenue using the unused resources.
7. Each node calculates its revenue increment based on the unused resources, and sends it to the server.
8. Server finds the node, which obtains maximum revenue increment.
9. The solution of that node is updated.
10. Finally, each node sends its solution to the server.

B. DCRARE ALGORITHM

The algorithm divides the resources among nodes. Each node calculates local solutions for the different amounts of resources incrementally. Then, an amount of resources is chosen for each node that gives maximum total revenue. Finally, it collects the unused resources, and allocates to a node, as it is done in DCRE.

To demonstrate the allocation of resources, we introduce two parameters: λ (a positive odd number) and δ (0< δ<1). λ indicates the number of allocation levels of the assigned resources. δ indicates the difference between the two consecutive allocation levels. If we consider λ=7 and δ=0.05, then the fractions of allocation are: 0.85, 0.90, 0.95, 1.0, 1.05 and 1.10, 1.15. The fraction to be allocated at level t is indicated by the following expression:

$$1.0 + \left(t - \left\lceil \frac{\lambda}{2} \right\rceil\right) * \delta \quad \text{where } (1 \le t \le \lambda)$$

λ is considered as an odd value with the following levels: i) Level $1, \ldots, \left\lceil \frac{\lambda}{2} \right\rceil - 1$ indicates the pessimistic allocation. Each of these levels is less than 1.0 in terms of fraction of assigned resources. ii) Level $\left\lceil \frac{\lambda}{2} \right\rceil$ indicates the exact allocation. It is analogous to the fraction 1.0. iii) Level $\left\lceil \frac{\lambda}{2} \right\rceil + 1, \ldots, \lambda$ indicates the optimistic allocation. Each of the levels is higher than fraction 1.0.

The algorithm starts with the minimum fraction, and increases the fraction by δ amount in every iteration. In the first iteration, local solution is obtained by a sequential heuristic. In the next iterations, the solution of the previous iteration is upgraded, taking it as the initial solution. The algorithm is presented in Algorithm 1.

The procedure *allocate_resource* is described in procedure 1. Line 1of *allocate_resource* initializes the solution for fraction 1.0. Line 4 and 6 finds the node, which are most suitable for up-gradation and down-gradation respectively. Line 10-12 update the solution to increase revenue.

Time complexity of the algorithms depends on the sequential algorithm, which is used to find local solutions. Both DCRE and DCRARE uses divide and conquer strategy. So, both are very high throughput algorithm. DCRARE calculates local solutions incrementally for λ times. It calculates an initial

solution, and then upgrades it. Time complexity will not increase considerably for this incremental fashion. Time complexity of *allocate_resource* is $O(\lambda p^2)$.

Algorithm 1: DCRARE (λ, δ)

1. Server divides the resources among nodes
2. Each node calculates a minimum fraction of assigned resource which is discussed before.
3. Each node calculates the solutions for each fraction of resources incrementally.
   - 3.1. Calculate the solution for the initial fraction of resource using a sequential heuristic. The solution of each iteration will be the input of the next iteration.
   - 3.2. Calculate the solutions for subsequent fractions of resources. It takes the solution of previous step as an initial solution, and upgrades it. This step will be repeated for $\lambda - 1$times.
   - 3.3. Each node forms a $1 \times \lambda$ matrix where each entry holds the revenue for the different fractions.
   - 3.4. This matrix is send to the server.
4. Server forms a $p \times \lambda$ matrix M from the $1 \times \lambda$ matrix of each node.
5. Call the procedure *allocate_resource* (M)
6. Solution obtained by *allocate_resource*(M) is updated.
7. Apply residue exploitation procedure of DCRE.

Procedure 1: allocate_resource (M)

Input: M is a $p \times \lambda$ matrix , M_{it} indicates the revenue, which is earned by the ith node for level t.

Output: $H = (H_1, \dots, H_p)$ where M_{iH_i} holds revenue of the ith node that gives better global revenue.

1. $H_i \leftarrow \lceil \lambda/2 \rceil$ **for** $1 \le i \le p$
2. **for** $t = 1, \dots, \lceil \lambda/2 \rceil - 1$ **do**
3. **while**(**true**) **do**
4. $a_0 \leftarrow \underset{1 \le a \le p}{argmin} \{M_{aH_a} - M_{a(H_a - t)}\}$
5. $a_0\_revenue \leftarrow M_{a_0 H_{a_0}} - M_{a_0 (H_{a_0} - t)}$
6. $b_0 \leftarrow \underset{1 \le b \le p, b \ne a_0}{argmax} \{M_{b(H_b + t)} - M_{bH_b}\}$
7. $b_0\_revenue \leftarrow M_{b_0 (H_{b_0} + t)} - M_{b_0 H_{b_0}}$
8. **if**($a_0 = null$ *or* $b_0 = null$) **then**
9. **break**;
10. **if** ($b_0\_revenue > a_0\_revenue$)**then**
11. $H_{a_0} \leftarrow H_{a_0} - t$
12. $H_{b_0} \leftarrow H_{b_0} + t$
13. **else**
14. **break**;
15. **end while**.
16. **end for**.
17. **return** $(H_1, \dots, H_p)$

V. EXPERIMENTAL RESULTS

PVM (Parallel Virtual Machine) and MPI (Message Passing Interface) facilitate the implementation of parallel applications on multiprocessor environments (especially for distributed memory architecture). PVM supports heterogeneity, portability, and fault tolerance while sacrificing performance. MPI does not provide much flexibility as PVM, but demonstrates high performance [3]. To achieve better performance, we have implemented our algorithm using MPI. We tested our algorithms on a cluster of thirteen nodes connected by a Myrinet GM network. Every node is a Pentium IV, 1.7 GHz processor, 128 Mb RAM with Linux operating system. The algorithms have been coded using C programming language. We vary the number of nodes to observe the effect. We have tested the two algorithms on the benchmark instances, found in http://www.laria.u-picardie.fr/hifi/OR-Benchmark/MMKP/MMKP.html. Here, I01,… I06 are small problems, and I07, I08, … , I13, Ins01, Ins02, … , Ins20 are medium and large problems. Our algorithms need a sequential heuristic to solve MMKP locally. We have taken MRLS as the sequential heuristic, as it demonstrates better performance among all the existing heuristics and standard package, for example, Cplex Solver [6]. Table I shows the parameters related to the performance of MRLS with their associated values for better revenue [6].

Table I: Parameters of sequential heuristic

Number of iterations	Number of solutions can be upgraded	Length of memory list for detection of cycling
50n	5	$[2n, 2n + 10]$

Limited experiment shows that as number of node increases, computation time decreases with slight minor solution. For small problem (I01,… I06), search space reduces quickly with increase of the number of nodes (p). So, revenue also reduces quickly. For larger problems, search space does not become too small after dividing into sub problems. So, solution quality does not reduce much. It supports the reason of parallelization that we need parallelization mainly for large problem. For small problem, we should use sequential algorithm rather than DCRE or DCRARE.

Fig. 2 shows how the number of nodes affects solution quality and time requirement. The result of DCRE algorithm is represented as a dotted line. The data with one node represents the result of sequential heuristic MRLS. The data with more than one node represents the result of parallel heuristics DCRE and DCRARE. This experiment is conducted on large and medium sized problems (I07, I08, … , I13, Ins01, Ins02, … , Ins20) of the benchmark. Here, the revenues and times are taken as average. For DCRE, as p increases, computation time reduces with reduced quality of solution. From the figure, it is clear that it is highly scalable algorithm. As p increases, the number of messages increases. These messages create heavy traffic in the server. As a result,

communicational overhead increases with the increase of p. Again, residue exploitation step is common in all case (do not depend on number of node). So, time requirement will not decrease linearly with the increase of p. Note that, the revenue is very close to the sequential heuristic, up to $p = 5$, and the computation time is much less than that. But, after a certain level, revenue decreases exponentially. The level depends on the size of problem. So, DCRE gives a good quality solution only up to certain number of node. The choice of p depends on the required revenue and computation time.

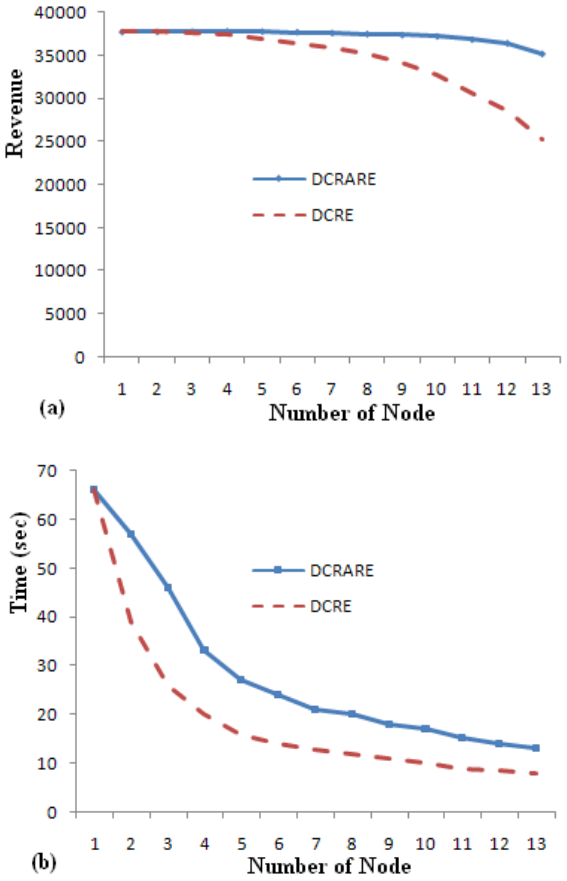

Fig. 2. (a) Average revenue Vs number of nodes (b) Average time Vs number of nodes

In DCRARE approach, we calculate solutions for different amount of resource capacity cumulatively. The solution of each iteration is treated as the initial solution for next iteration. For this cumulative process, time complexity will not increase significantly. Let the initial fraction be η. Note that, η is calculated as a function of λ and δ. Limited computational result shows that if η is less than 0.9, it gives an inferior solution with small resource capacity. It also increases computation time. If η is very close to 1.0, then it is almost equivalent to DCRE. So, value of η should be taken 0.90. This imposes a constraint on the value of λ and δ. Table II shows the revenues and time requirements for different values of λ and δ. This experiment is done for different values of p. The table shows a tradeoff between running time and revenue. For small value of λ, the algorithm solves for small number of combinations. This will increase throughput but decrease revenue. For (λ, δ) = (21, 0.01), revenue increase with increasing running time significantly. A reasonable choice is (λ, δ) = (11, 0.02).

As p increases, the combination of local solutions increases. This helps to find a better global solution. Again, search space decreases with increase of p. So, revenue of local solution decreases with increase of p. Thus, two conflicting effect falls on a global solution with increase of p. Fig. 2 describes how the revenue and computation time changes with the number of node. The result of DCRARE algorithm is represented as a solid line. As p increases, revenue increases (very small amount) until $p = 4$. In this situation, size of the sub problem does not become too small. Rather, a better global solution can be found from the combination of local solutions. So, revenue increases. Thus, DCRARE gives better revenue than MRLS. If we increase p more, revenue decreases slowly as the size of the sub problems reduces. From the figure, it is clear that revenue achieved by DCRARE is much better than DCRE. Again, computation time also decreases with increase of p. It is a highly scalable algorithm, but it's time requirement is greater than DCRE.

Table II. The behavior of algorithm DCRARE for different value of λ, δ

λ	δ	Avg. Time (sec)	Avg. Revenue
21	0.01	55	60011
11	0.02	42	59998
7	0.03	36	59636
5	0.04	32	59195

VI. CONCLUSION

Both DCRARE and DCRE achieve good quality of solution within very small time. DCRARE achieves more revenue than DCRE, but requires more time than it (DCRE). DCRARE and DCRE can be employed to develop an admission control and resource scheduling framework for distributed multimedia server. The algorithms are the first algorithm of the MMKP for cluster computing. Many issues of these distributed algorithms are still open. In DCRE, the solution quality reduces greatly for large number of nodes. Research should be made to address this problem. We experiment the algorithms with a cluster of thirteen nodes. A survey should be conducted with a large cluster for extensive set of problem instances. These algorithms should be experimented for several real life applications. We experiment our algorithms with static task assignment strategy. Research should be conducted on dynamic task

assignment and dynamically varying the number of nodes.

VII. ACKNOWLEDGEMENT

The authors would like to thank the Computer Science and Engineering (CSE) department of BUET (Bangladesh University of Engineering and Technology) for the support to conduct the experiment.

REFERENCES

[1] M. M. Akbar, E. G. Manning, G. C. Shoja and S. Khan, "Heuristic Solutions for the Multiple-Choice Multi-Dimension Knapsack Problem", International Conference on Computational Science, (ICCS 2001) vol. 2074 of Lecture Notes in Computer Science, pp 659-668, Springer, 2001.

[2] M.M. Akbar, M. S. Rahman, M. Kaykobad, E.G. Manning, and G.C. Shoja, "Solving the Multidimensional Multiple-Choice Knapsack Problem by Constructing Convex Hulls", Computers & Operations Research, Elsevier Science, 2006.

[3] G. A. Geist, J. A. Kohl, P. M. Papadopoulos, "PVM and MPI: a Comparison of Features," Calculateurs Paralleles Vol. 8 No. 2 (1996).

[4] R. Parra-Hernandez and N. Dimopoulos, "A new Heuristic for Solving the Multi-choice Multidimensional Knapsack Problem", IEEE Transaction on Systems, Man and Cybernetics, Part A: Systems and Humans,2005.

[5] M. Hifi, M. Michrafy and A. Sbihi, "Algorithms for the multiple-choice multi-dimensional knapsack problem", Journal of the Operational Research Society, vol. 55, pp. 1323-1332, 2004.

[6] M. Hifi, M. Michrafy and A. Sbihi, "A Reactive Local Search-Based Algorithm for the Multiple-Choice Multi-Dimensional Knapsack Problem", Computational Optimization and Applications, 33, 271–285, 2006.

[7] M. Hamdi, Y. Pan, B. Hamidzadeh, F. M. Lim, "Parallel Computing on an Ethernet Cluster of Workstations: Opportunities and Constraints", The Journal of Supercomputing, 13, 111-132,1999.

[8] S. Khan, "Quality adaptation in a multisession multimedia system: Model, algorithms and architecture," Ph.D. dissertation, Department of Electrical and Computer Engineering, University of Victoria, Victoria, BC, Canada, 1998.

[9] S. Khan, K. F. Li, E. G. Manning, M. M. Akbar. "Solving the Knapsack Problem for Adaptive Multimedia System", Studia Informatica, 2002.

[10] M. Moser, D. P. Jokanovic and N. Shiratori, "An Algorithm for the Multidimensional Multiple-Choice Knapsack Problem", IEICE Transactions on Fundamentals of Electronics, pp 582-589, Volume 80(3), 1997.

[11] A. Z. M. Shahriar, M. M. Akbar, M. S. Rahman, and M. A. H. Newton, "A Multiprocessor based Heuristic for Multi-dimensional Multiple-Choice Knapsack Problem". The Journal of Supercomputing, Volume 43, 2008.

Proceedings of 2009 12th International Conference on Computer and Information Technology (ICCIT 2009)
21-23 December, 2009, Dhaka, Bangladesh

Microstrip Antenna Array with Four Port Butler Matrix for Switched Beam Base Station Application

Muhammad Mahfuzul Alam
Department of Electronics & Communication Engineering
Khulna University of Engineering & Technology, Khulna-9203, Bangladesh
Email: mahfuz04_ece@yahoo.com

Abstract

In this paper, the design of a microstrip antenna array with four port Butler matrix is presented. The Butler matrix is used as a beamforming network and it produces orthogonal beams that can be steered in different directions. Simulated butler matrix has 10 dB return loss bandwidth of 20%. This matrix feeds four single element microstrip antennas that can be operated from 2.412GHz to 2.484GHz. The circuit is designed by considering a single layer microstrip structure that makes it simpler. The design of wide band microwave devices such as branch-line coupler; cross-coupler and phase-shifters are also incorporated. The switched beam antenna is designed for 2.4GHz band Wi-Fi (Wireless Fidelity) system.

Keywords: *Butler matrix, beamforming network, orthogonal beams, single layer structure.*

I. INTRODUCTION

Smart antennas have been characterized as one of the most prominent devices in wireless communication. Nowadays, there is a considerable work in prototype and test beds of such system [1].The use of "Smart antenna" can improve wireless performance [2]. Smart antenna may contain switched-beam or fully adaptive configuration that electronically steer the pattern toward an individual user. An adaptive antenna array aims to reject automatically interference signals by modifying its radiation pattern using adaptive algorithms. This pattern modification allow to steer the main lobe in the desired signal direction and to create pattern nulls in directions of interfaces, which results in better signal to noise ratio. Implementation of this algorithm is more complex than the switched-beam system. Switched beam system produces multiple narrow beams and selects from them the appropriate beam that gives the strongest signal level [3]. The switched beam systems are the solution in the current transition phase between the scarce and full integration of the smart antenna technology. The benifite of the switched beam antenna is that only fairly simple RF signal processing is required,which makes it possible to apply the techniques also in existing wireless system. The draw–back of the system is that it has limited adaptabilty [4]. One of the most crucial parts of a switched beam antenna system is the antenna feeding network [5]. Implementation of such a switched beam antenna is based on a Butler matrix. This paper details the realization of a 4×4 Butler matrix with four single patch antenna array and its constituting components. In order to minimize the space occupied by the microwave circuit and for easy circuit implementation we consider single layer microstrip structure. This configuration can be used in smart antenna system for wireless application based on swicthed beam system.The system can produce narrow multi-beams in different directions instead of omni-directional patterens. The beam scanning can be obtained by different feedings with phase increment provided by the Butler matrix. Therefore,it would increase the performance of the system in terms of antenna's gain,and as a result ,it would reduce the possible power usage. By doing that, the reliability and and capacity of the system can be enhanced. Generally wideband system need double/multilayered configuration or complex design[1],[5],[7] but here illustration of a butler matrix on a single layer structure is given, that is easy to fabricate and as well as maintained wideband operating frequency. In simulation RT/duroid 5880 (ε_r=2.2) is considered for substrate with height of 1.58mm. Least number of bends is used in transmission line for the reduction of microstrip discontinuity [10]. Also the overall dimension of the structure has kept compact. This type of matrix incorporated with antenna can be used in base stations for 2.4GHz band Wi-Fi (IEEE 802.11b/g/draft-n) system.

II. QUADRATURE (90^0) HYBRID

Quadrature hybrids are 3dB directional couplers with 90^0 phase difference in the outputs of the through and coupled arms. This type of hybrid is often made in Microstrip or stripline and is also known as branch-line hybrid. The basic operation of the branch-line coupler is as follows. With all ports matched, power entering port 1 is evenly divided between ports 2 and 3, with a 90^0 phase shift between these outputs. No power is coupled

978-1-4244-6283-4/09/$26.00 ©2009 IEEE

to ports 4. Thus, the $[S]$ matrix will have the following form [6]:

$$[S] = \frac{-1}{\sqrt{2}}\begin{bmatrix} 0 & j & 1 & 0 \\ j & 0 & 0 & 1 \\ 1 & 0 & 0 & j \\ 0 & 1 & j & 0 \end{bmatrix} \quad (1)$$

Simulated Return loss and Phase difference of the two ports of quadrature hybrid are given in Figure 2. 3dB power division in ports 2 and 3 is obtained in operating frequency. Also perfect isolation and return loss at ports 4 and 1 is found at the designed frequency. The hybrid junction has a frequency bandwidth of 820MHz, which is about 33% of its center frequency.

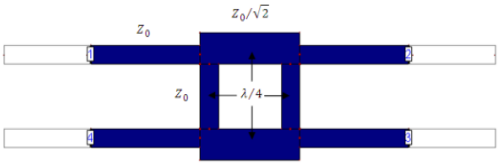

Fig. 1. Branch line coupler

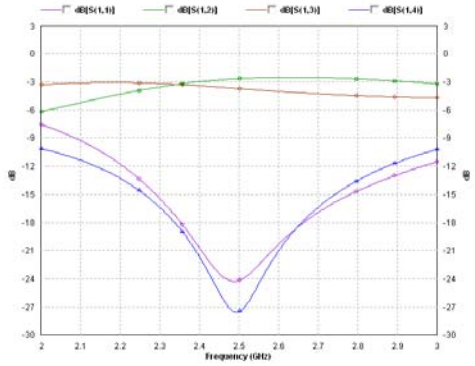

(a)

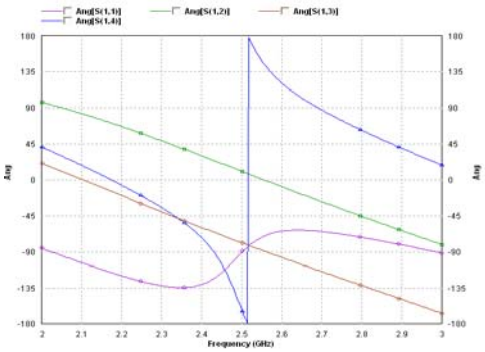

(b)

Fig. 2. (a) S parameter versus frequency for the branch-line coupler and (b) Phase Angle.

III. CROSS-COUPLER

These devices, also known as 0 dB couplers, are an efficient means of crossing two transmission lines with a minimal coupling between them [7]. It is possible to make a cross–coupler by connecting two 90 degrees hybrids. But more advanced and area efficient is when two parallel arms with 50 Ohm in the middle of the structure is replaced by a single 25 Ohm. The $[S]$ matrix of cross−coupler will have the following form [6],[7]:

$$[S] = \begin{bmatrix} 0 & 0 & j & 0 \\ 0 & 0 & 0 & j \\ j & 0 & 0 & 0 \\ 0 & j & 0 & 0 \end{bmatrix} \quad (2)$$

Figure 4 shows the simulated return loss of the cross-coupler. The cross-coupler has a frequency bandwidth of 810MHz which is about 33% of its centre frequency.

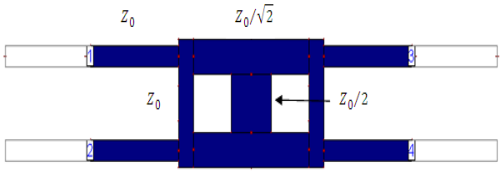

Fig. 3. Cross-coupler or 0dB coupler.

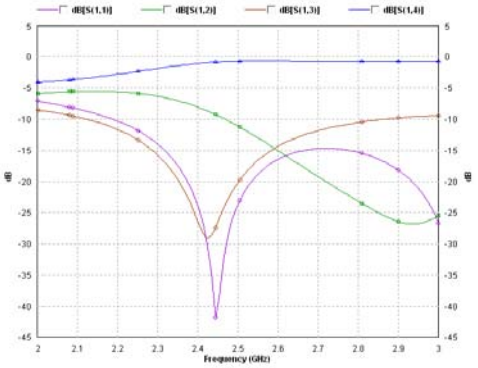

Fig. 4.S-parameters versus frequency at port 1.

IV. PHASE SHIFTER

For designing a 4×4 butler matrix we need two phase shifter, this thing can be easily made by microstrip transmission lines. Changing the length of transmission line desired phase shift can be found. Two 45^0 phase shifter is required. Simple calculations are needed to design these things.

$$\phi = \beta l = \sqrt{\varepsilon_e} k_0 l \quad (3)$$

Here $k_0 = 2\pi f/c$, ϕ is the phase shift , l is length of the transmission line, β is the propagation constant and ε_e is the effective dielectric constant[6].The length of the 45^0 phase shifter 11.134mm.

V. BUTLER BEAM-FORMING ARRAY OR BUTLER MATRIX

Butler matrix is an analog RF beam-forming network. It consists of 3-dB directional couplers (hybrid junctions) and fixed phase shifter to form *N* contagious beams with an *N*-element linear array. The number N is an integer expressed as some power of 2, that is $N = 2^p$ [8] .The 3-dB coupler is a four-port junction, as we discussed in the previous sections. The block diagram of 4×4 butler beamforming matrix is given in Figure 5. The Butler matrix is a four-element array that produces four independent beams. It utilizes four directional couplers and two fixed phase shifters. Butler matrix has 2^p input and 2^p outputs. The number of hybrid junctions/directional couplers required for *N*-element array is equal to $(N/2)\ \log_2 N$, number of fixed phase shifts is $(N/2)(\log_2(N) - 1)$. The Butler matrix is theoretically lossless in that no power is intentionally dissipated in terminations. There will always be, however, a finite insertion loss due to inherent losses in directional couplers, phase shifters and in transmission lines that make up the network. The low cross-over level of a butler matrix is one of its disadvantages [8].

Using the universal variable $u = (d/\lambda)(\sin\theta - \sin\theta_i)$, where d/λ is the element spacing in wavelength and θ_i is the axis of the ith beam measured from broadside, the Butler beam patterns are as follows:

$$F(u) = \frac{\sin(N\pi u)}{N \sin(\pi u)} \qquad (4)$$

All beams have the same shape u space. For half-wave spacing and large *N* (number of array elements) the beam are orthogonal. Beam position for any spacing are given by following equation –

$$\sin\theta_i = \pm\frac{i\lambda}{2Nd} \ , i=1, 2, 3\ldots, (N\text{-}1) \qquad (5)$$

The corresponding inter-element phase shift with spacing $d = \lambda/2$ is

$$\alpha_i = \beta d \sin\theta_i = i\frac{\pi}{N} \qquad (6)$$

where $\beta = \frac{2\pi}{\lambda}$ is the wave number [9].

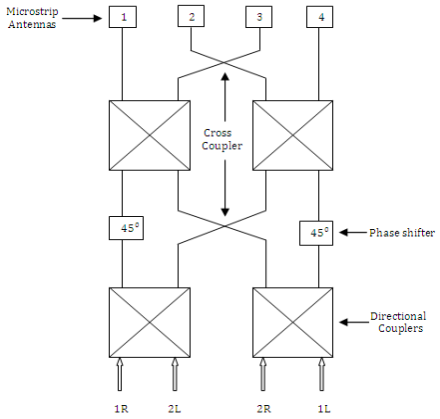

(a)

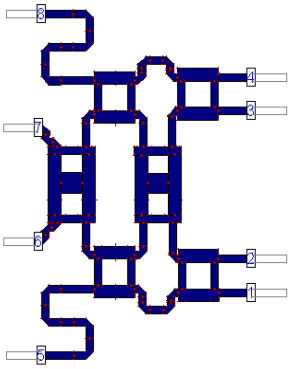

(b)

Fig. 5.(a)Block diagram of four-element Butler beam-forming matrix and (b) layout.

The phase shift between the inputs and corresponding outputs that are given in Table 1(simulation results). Some phase errors have been found but these are tolerable.

Table 1. Input-output phase shift (degrees) of the Butler matrix at 2.45 GHz

Ports	Ant.1	Ant.2	Ant .3	Ant .4
1R	130.04	88.25	40.20	-3
2L	43.75	-178.20	-41.35	88.75
2R	88.12	-43.18	177.96	43.78
1L	-1.10	46.50	92.05	133.25

Figure 6 given below gives the detailed S-parameters of the matrix. In almost all cases the return loss is -10dB or below except for some cases where return losses are deviated from the desired value. Operating frequency range for different ports is between 2.15-3.0GHz. So about 500MHz operating frequency is obtained in different ports and it is 20% of the centre frequency.

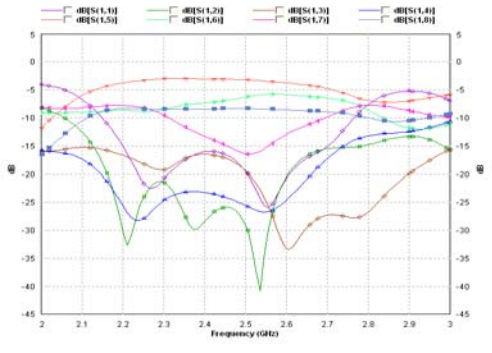

(a)

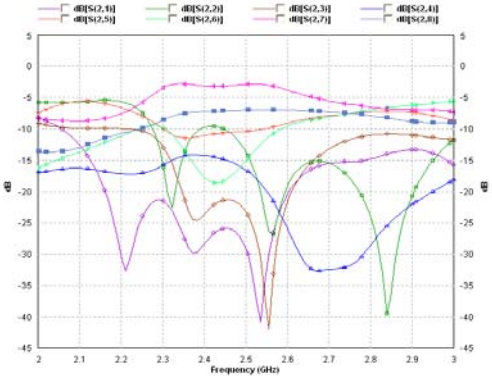

(b)

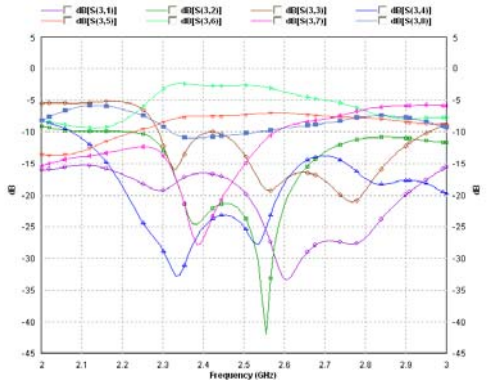

(c)

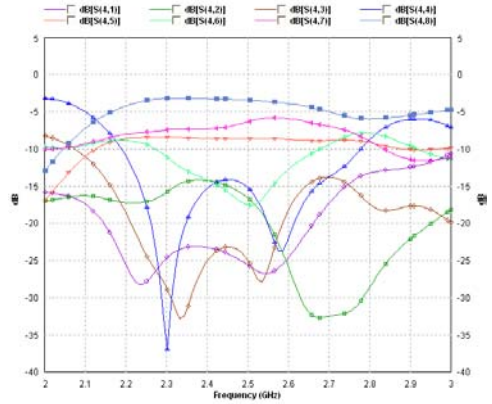

(d)

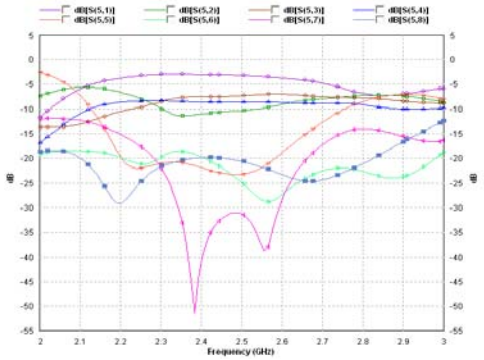

(e)

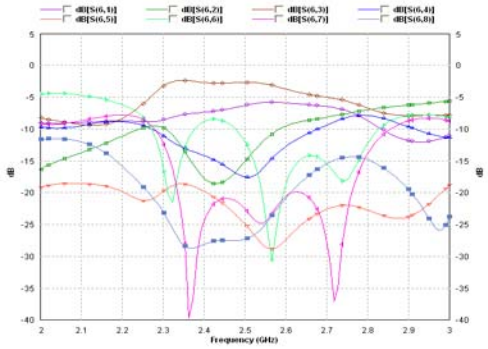

(f)

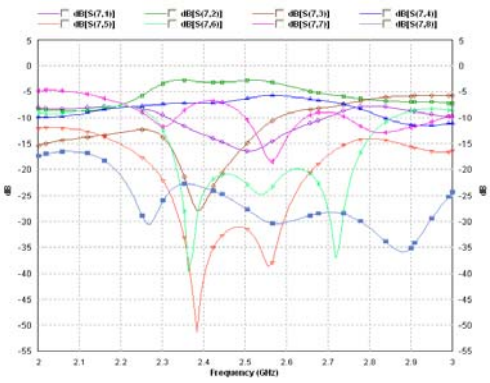

(g)

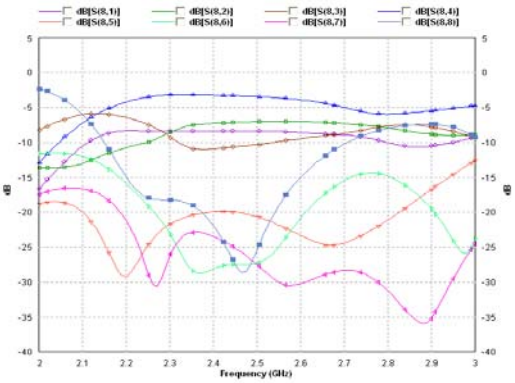

(h)

Fig. 6 . (a) to (h) illustrates the simulated S-parameters of the 8 different ports.

VI. MICROSTRIP ARRAY ANTENNA WITH BEAM FORMING NETWORK

Single element microstrip antenna of operating frequency 2.45GHz is considered for array element. Inset-feeding techniques is used for better impedance matching at the inputs of the radiating elements. Four single element patch antenna are inserted into the four port of the butler matrix, this configuration gives a switched beam antenna system. Fig. 7 shows the layout of the simulated antenna. Total dimension of the structure is 244mm×195mm. Dimensional parameters of the antenna are given in Table 2. Fig. 8 shows the detailed s-parameters of the butler matrix with antenna at different ports. All cases the return loss is −10dB or below at resonance frequency but in port 1L this condition is not maintained, which is somewhat shifted. In Fig. 9 four different beam patterns of the butler matrix are shown, a little amount of phase errors have been found. Theoretically the angle of four beams when feeding in port 1R ,2L ,2R and 1L are found 15^0,45^0,-45^0 and -15^0 respectively but after simulation 16^0,41^0, -42^0 and -19.5^0 have been found in different ports. It is acceptable as the phase error is within 10^0. From the beam pattern curves, we also see that for ports 2R, 1L and 2L side lobe levels (SSL) is lower than 13.32dB than main lobe. But for port 1R side lobe level is 9dB lower than the main lobe. This is due to the mutual coupling effects between the radiating elements as well as the slightly mismatches between the feeding network and the antennas. Gain of the antenna varies from 8.73085dBi to 11.1075dBi when feeding at different ports.

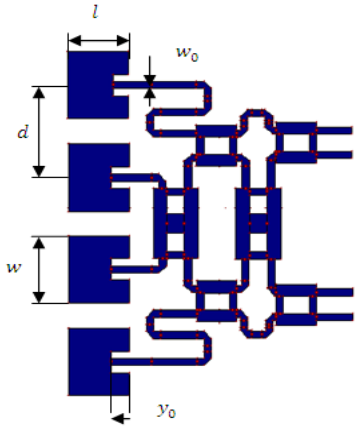

Fig. 7. The proposed Microstrip antenna array with butler matrix Layout.

Table 2. Dimensional parameters of the single patch

w	l	d	w_0	y_0
48.4mm	40.49mm	65mm	5.02mm	14.2mm

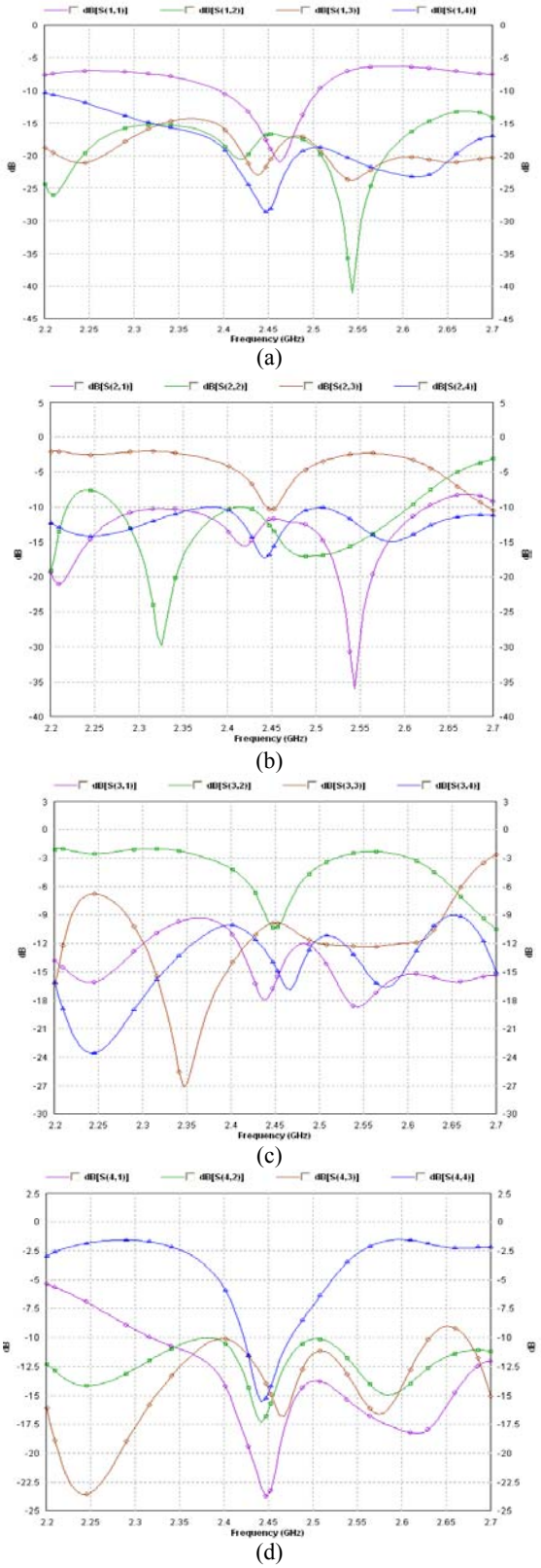

Fig. 8. (a) to (d) illustrates simulated S-parameters of four different ports.

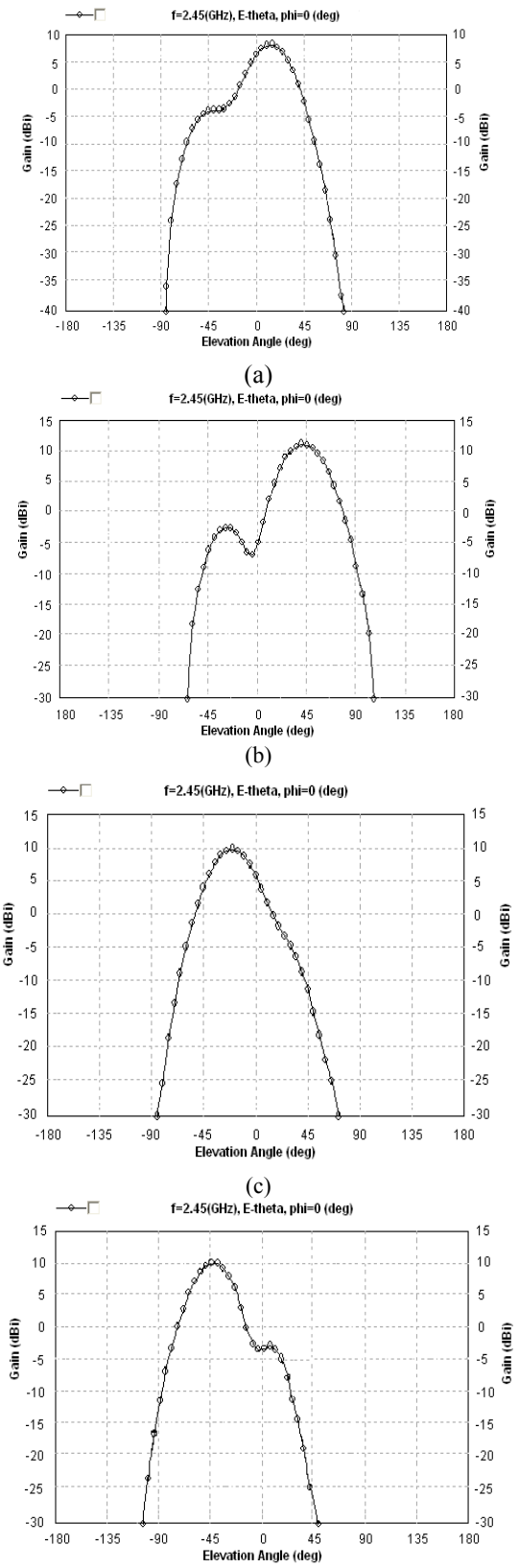

Fig. 9. Beam patterns at four different ports (a)1R ,(b)2L,(c)1L and (d)2R.

VII. CONCLUSION

Wide band 4×4 Butler matrix has been designed for the excitation of microstrip array antenna to steer the beams in different desired directions. Most important thing about the simulated structure is that it can be easily implemented using current photolithographic technology with minimum cost and it requires simple materials for construction. The simulated butler matrix has wideband operating frequency range from 2.15GHz to 3.0GHz. At last simulation has been done by incorporating butler matrix and four microstrip antennas. This structure gives operating frequency range from 2.412GHz to 2.484GHz.

REFERENCES

[1] Theodoros N. Kaifas and John N. Sahalos ," A 4×4 Butler matrix optimization for UMTS application", *Microwave and Optical Technology Letters*,Vol. 40 ,No.3 , March 2007

[2] Eleftheria siachalou, Elias vafiadis, Sotirious S. Groudos, Theodoros Samaras, Christos S. Koukurlis and Stavros Panas , "On The design of Switched-Beam Wideband Base Station". *IEEE Antenna and propagation Magazine*, vol. 46, No. 1, February 2004.

[3] Tayeb A. Denidni and Taro Eric Libar , "Wide band Four−port Butler Matrix for Switched Multibeam Antenna Arrays", The 14th IEEE 2003 International Symposium on Personal, Indoor and Mobile Radio Communication Proceedings, pp.2461-2464, 2003.

[4] John D .Kraus, Ronald J. Marhefka, Ahmed S.Khan, *ANTENNAS FOR ALL APPLICATION*, 3rd ed, 2006.

[5] Theodoros N. Kaifas and John N. Sahalos,"On the Design of a Single-Layer Wideband Butler Matrix for Switched-Beam UMTS System Application ", *IEEE Antenna and Propagation Magazine*, vol. 48 , No. 6 ,December 2006.

[6] D.Pozar, *Microwave Engineering,* wiley, 3rd ed, 2005.

[7] Jean-Sebastien Neron and Gilles-Y. Delisle , "Microstrip EHF Butler Matrix Design and Realization", *ETRI Journal* ,Vol.27, Number 6. December 2005.

[8] Merrill I. Skolnik, *Introduction to RADAR System*, 3rd ed, 2001.

[9] R.C.Hansen, *Phased Array Antenna,* Willey, New Yoke 1998.

[10] K.C.Gupta, Ramesh Garg, Inder Bahl, Prakash Bhartia, "*Microstrip Lines and Slotlines*",Artech House,2nd,1996.

Proceedings of 2009 12th International Conference on Computer and Information Technology (ICCIT 2009)
21-23 December, 2009, Dhaka, Bangladesh

A Modified MAP in Performance Evaluation of Asynchronous Packet Traffic

Anupam Roy, Md. Jweel Hossain, Md. Imdadul Islam
Department of Computer Science and Engineering, Jahangirnagar University, Savar, Dhaka-1342, Bangladesh
anupamroy132@gmail.com, jewelh3@gmail.com, imdad@juniv.edu

ABSTRACT

Markov Arrival Process (MAP) is the most widely used traffic model to analyze performance of a node of an asynchronous packet traffic. Recent literatures make transition between overload and underload states of a node without arrival but sometimes transition may take place from underload to overload with an arrival which deviates our analysis from the present literature of Markov Modulated Poisson Process (MMPP) traffic model. In this paper two different rates of packet 'arrival' and 'non arrival' is incorporated in state transition of underload to overload and a comparison is made with previous literatures.

Keywords: Generator matrix, MMPP, PH distribution, sojourn time and transition probability matrix.

I. INTRODUCTION

In teletraffic engineering two most important traffic parameters are inter arrival time and service time of call arrival. In circuit switching traffic both of the parameter follows exponential or Poisson's probability density function (pdf). Therefore most of the circuit switching traffic follows *M/M/n/k* traffic model. In packet switching traffic packet arrival rate may follows negative exponential probability density function, but service time distribution is either deterministic or non-exponential. Since Markov Arrival Process (MAP) has non-exponential distribution of sojourn time of a probability state, therefore it is well suited for packet traffic like ATM and BISDN explained in [1]-[2].

In Phase Type (PH) distribution (the most generalized pdf of packet traffic) one vector, $\boldsymbol{\alpha} = [\alpha_1, \alpha_2 \ldots \alpha_m]$, a transition matrix **T** of $m \times m$ and a column vector $\mathbf{T_0} = -\mathbf{Te}$ are used to represent the probability density function. Here $\boldsymbol{e}$ is a unit column vector summarized in [3]-[4]. Markov Arrival Process (MAP) is like PH distribution and is represented by two matrices **C** & **D** shown in next section of the paper.

We are more interested about Markov Modulated Poisson Process (MMPP) which is a doubly stochastic process, where arrival of any state depends on the face or state of the continuous time Markov chain [5]-[6]. MMPP is a special case of Phase Type distribution, where $\boldsymbol{\alpha} = \mathbf{I}$, $\mathbf{T_0} = \mathbf{D}$, $\mathbf{T} = \mathbf{R}-\mathbf{D}$. Here **R** is the generator matrix of MMPP.

In this paper a traffic model of asynchronous data traffic is developed considering transition between underload and overload state of MMPP considering both 'with' and 'without' arrival. Traffic load of a network varies with time can be represented by two state Markov chain where one state is the condition of underload state and another is that of overload state, with arrival of any packet / frame in underload condition the network may stay in that state or make a transition to overload state. But when the network is in overload state it will make a transition to underload state after some sojourn time $1/r_1$ known as transition without arrival. In view of above, in this paper a Markov chain of packet traffic is proposed and its performance is compared with existing model. The paper is organized like, section II describes proposed traffic model, section III and IV describes methodologies of evaluation of probability density function, section V depicts the result of entire analysis and finally section VI concludes the analysis the paper.

II. TRAFFIC MODELING

A stochastic process $\{N(t), t \geq 0\}$ is said to be a *counting process* if $N(t)$ represents the total number of *events* that have occurred up to time t. Again a continuous-time stochastic process $\{J(t) \geq 0\}$ with integer state space is called Markov process if it satisfies, $P(J(t+h) = n \mid J(t) = m, J(u) = x(u), 0 \leq u < t) = P(J(t+h) = n \mid J(t) = m)$. Markovian arrival processes consists of two processes; continuous-time Markov process $j(t)$ and a counting process $N(t)$.

Let us consider a counting process $N(t)$ provides the number of arrival of packet in $(0,t]$ and $J(t)$ indicates the state of the Markov chain at time t. Now $\{N(t), J(t)\}$ on state space called Markov Arrival Process (MAP) is analyzed using the generator matrix [8]-[9],

$$\mathbf{Q} = \begin{bmatrix} \mathbf{C} & \mathbf{D} & 0 & 0 \ldots\ldots \\ 0 & \mathbf{C} & \mathbf{D} & 0 \ldots\ldots \\ 0 & 0 & \mathbf{C} & \mathbf{D} \ldots\ldots \\ \ldots & \ldots & \ldots & \ldots \end{bmatrix} \quad (1)$$

For $1 \leq J(t) \leq m$, both **C** and **D** are $m \times n$ matrices, **C** has negative diagonal elements and nonnegative off-diagonal elements and **D** has nonnegative elements. The Markov modulated Poisson process (MMPP) is a double stochastic Poisson process where arrival rate of any traffic depends on its probability state which forms a continuous time Markov chain. In a continuous time

978-1-4244-6283-4/09/$26.00 ©2009 IEEE

Markov chain, sojourn time/life time in any state *i* is exponentially distributed with parameter λ_i. At the end of sojourn time in state *i,* a transition takes place to another state or to the same state. The transition may or may not correspond to an arrival. Let us consider the simples case of two sate MMPP system where the arrival rate λ_i; *i=1, 2* appears alternately with exponentially distributed life time r_i^{-1}; *i=1, 2*. The transition between state-*1* and *2* occurs without any arrival. The two state *MMPP* is characterized by **(Q, D)** where **Q** is the infinitesimal generator and **D** is a 2×2 arrival matrix. The generator matrix **Q**, expressed as sum of another two matrices **C** and **D**. For the proposed state transition chain of fig.1, the matrices are,

$$\mathbf{C} = \begin{bmatrix} -\lambda_1 - r_1 - R_1 & r_1 \\ r_2 & -\lambda_2 - r_2 \end{bmatrix} \quad (2)$$

$$\mathbf{D} = \begin{bmatrix} \lambda_1 & 0 \\ 0 & \lambda_2 \end{bmatrix} \quad (3)$$

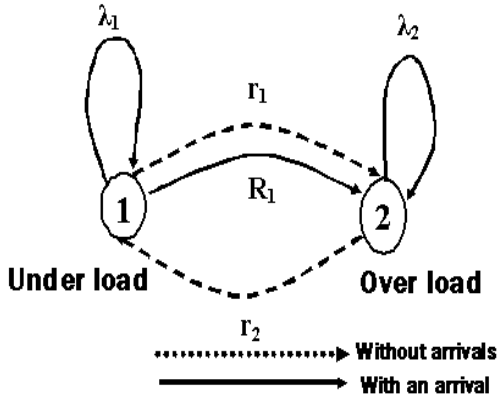

Fig.1 State transition for MMPP (2)

Here r_1 and r_2 are the rate of transition without arrival and R_1 is that of with arrival.

III. METHODOLOGY 1

The Eigen values of **C** matrix evaluated like,

$\beta_1 = x + y$ and $\beta_2 = x - y$

Where

$$x = \left(-\frac{1}{2}(r_1 + \lambda_1 + R_1 + \lambda_2 + r_2) \right) \text{ And}$$

$$y = \frac{1}{2}\left\{2r_1 g + r_1^{\,2} + h + r_2^{\,2} + k + j\right\}^{\frac{1}{2}}$$

Where

$$2r_1(r_2 - \lambda_2 + \lambda_1 + R_1) = g$$

$$2r_2(-\lambda_1 - R_1 + \lambda_2) = h$$

$$2\lambda_1(-\lambda_2 + R_1) = k$$

$$\lambda_1^{\,2} + R_1^{\,2} + \lambda_2^{\,2} - 2R_1\lambda = j$$

Now the Diagonal matrix,

$$\mathbf{D} = \begin{bmatrix} x+y & 0 \\ 0 & x-y \end{bmatrix}$$

Let us consider a unitary matrix,

$$\mathbf{U} = \begin{bmatrix} a & b \\ c & d \end{bmatrix} \quad (4)$$

∴ The inverse of **U**,

$$\mathbf{U}^{-1} = \begin{bmatrix} \frac{d}{ad-bc} & \frac{-b}{ad-bc} \\ \frac{-c}{ad-bc} & \frac{a}{ad-bc} \end{bmatrix} \quad (5)$$

Now the **C** matrix based on the concept of [11],

C = U. D. U^{-1} =

$$\begin{bmatrix} a(x+y)\frac{d}{ad-bc} - b(x-y)\frac{c}{ad-bc} & -a(x+y)\frac{b}{ad-bc} + b(x-y)\frac{a}{ad-bc} \\ c(x+y)\frac{d}{ad-bc} - d(x-y)\frac{c}{ad-bc} & -c(x+y)\frac{b}{ad-bc} + d(x-y)\frac{a}{ad-bc} \end{bmatrix} \quad (6)$$

Values of *a, b, c,* and *d* can be evaluated by the following relations:

$$\begin{aligned} a(x+y)\frac{d}{ad-bc} - b(x-y)\frac{c}{ad-bc} &= -\lambda_1 - r_1 - R_1 \\ -a(x+y)\frac{b}{ad-bc} + b(x-y)\frac{a}{ad-bc} &= r_1 \\ c(x+y)\frac{d}{ad-bc} - d(x-y)\frac{c}{ad-bc} &= r_2 \\ -c(x+y)\frac{b}{ad-bc} + d(x-y)\frac{a}{ad-bc} &= -\lambda_2 - r_r \end{aligned} \quad (7)$$

Now the time dependent probability density matrix,

P (t) = U. e^{Dt}. U^{-1}=

$$\begin{bmatrix} a.\exp[(x+y).t+b].\frac{d}{ad-bc} & -[a.\exp.[(x+y).t]+b].\frac{b}{ad-bc} \\ -[a+b.\exp[(x-y).t]].\frac{c}{ad-bc} & +[a+b.\exp[(x-y).t]].\frac{a}{ad-bc} \\ [c.\exp[(x+y).t+d].\frac{d}{ad-bc} & -[c.\exp[(x+y).t+d]].\frac{b}{ad-bc} \\ +[c+d.\exp[(x-y).t]].\frac{c}{ad-bc} & +[c+d.\exp[(x-y).t]].\frac{a}{ad-bc} \end{bmatrix} \quad (8)$$

Where,

$$P_{00}(t) = W\text{-}T \quad (9)$$

$$P_{11}(t) = U\text{-}V \quad (10)$$

Where

$$a \,.\, \exp[(\quad x + y\,).\, t + b\,].\ \frac{d}{ad - bc} = W$$

$$[\,a + b \,.\, \exp[(\quad x - y\,).\, t\,]].\ \frac{c}{ad - bc} = T$$

$$[\,c \,.\, \exp[(\quad x + y\,).\, t + d\,]].\ \frac{b}{ad - bc} = v$$

$$[\,c + d \,.\, \exp[(\quad x - y\,).\, t\,]].\ \frac{a}{ad - bc} = U$$

If $P_{00}(t) > P_{11}(t)$ then the system is stable, i.e. the system is in under load state, in most of the time of observation period.

IV. METHOLODOLOGY 2

The transition probability matrix [12],

$$\mathbf{F(t)} = \int_0^1 e^{Cx} dx D = (I - e^{Ct})(-C)^{-1} D \qquad (11)$$

To evaluate e^{Ct}, let us first determine the Eigen values β_1 and β_2 of **C** matrix. Let us write the system equations,

$$e^{\beta_1 t} = \psi_1(t) + \psi_2(t)\beta_1$$
$$e^{\beta_2 t} = \psi_1(t) + \psi_2(t)\beta_2$$

Solving the equations,

$$\psi_1(t) = \frac{-\beta_2 e^{\beta_1 t} + \beta_1 e^{\beta_2 t}}{\beta_1 - \beta_2} \qquad (12)$$

$$\psi_2(t) = \frac{e^{\beta_1 t} - e^{\beta_2 t}}{\beta_1 - \beta_2} \qquad (13)$$

$$Now, e^{Ct} = \psi_1(t).\mathbf{I} + \psi_2(t).C \qquad (14)$$

Where **I** is the identity matrix.

From equation (11) & (14) the probability density function $F(t)$ of states can be evaluated.

V. RESULTS

Taking traffic parameters, $\lambda_1 = 1.2$ packet/unit time, $\lambda_2 = 1.3$ packet/unit time, $r_1 = 0.2$ per unit time, $r_2 = 0.7$ per unit time and $R_1 = 0.08$ packet/unit time, the **C** matrix,

$$\mathbf{C} = \begin{bmatrix} -1.48 & 0.2 \\ 0.7 & -2 \end{bmatrix}$$

The Eigen values of **C** matrix are found -1.284 and -2.196

Now the **C** matrix for without arrival case,

$$\mathbf{C} = \begin{bmatrix} -1.4 & 0.2 \\ 0.7 & -2 \end{bmatrix}$$

The Eigen values of **C** matrix are found -1.22 and -2.18.

$\therefore$ The transition probability matrix at $t = \infty$ is,

$$\mathbf{T} = (-\mathbf{C}^{-1}).\mathbf{D} = \begin{bmatrix} 0.902 & 0.098 \\ 0.316 & 0.684 \end{bmatrix}.$$

The elements of transition probability matrix **F (t)** with $t \to \infty$ is formed, $P_{00}(t) = 0.902$, $P_{01}(t) = 0.098$, $P_{10}(t) = 0.316$ and $P_{11}(t) = 0.684$.

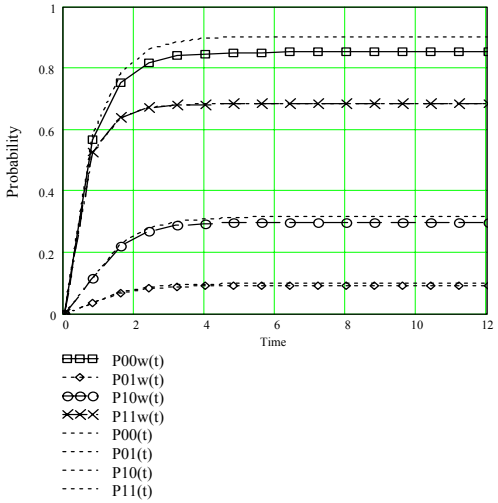

Fig. 2 Comparison of profile of probability states and their transition of MAP for 'with' and 'without' arrival cases ($R_1 = 0.08$/unit time).

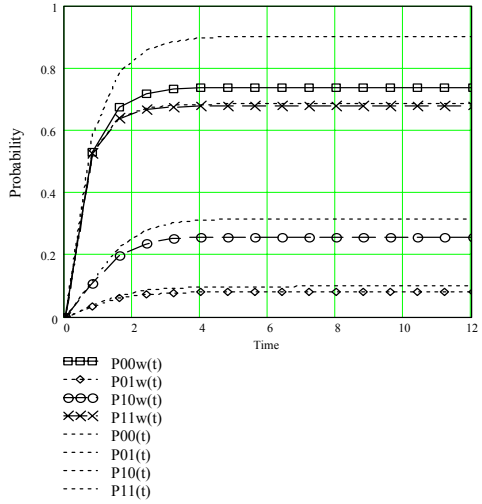

Fig. 3 Comparison of profile of probability states and their transition of MAP for 'with' and 'without' arrival cases ($R_1 = 0.3$/unit time).

Probability of staying in underload and overload states are $P_{00}(t)$, $P_{11}(t)$ respectively. Here the transition probabilities $P_{01}(t)$ and $P_{10}(t)$ are the probability of changing states from 1 & 2 and 2 & 1 respectively. All the four probability are plotted in fig. 2 for both the cases with and without arrival between transition states. Except $P_{11}(t)$ all the state has higher probability with incorporation of R_1. Here $P_{00}(t)$ is affected most severely but it is the real condition of a network. Incorporation of an arrival rate in the direction of underload to overload state will make rapid transition towards overload state hence reduce the probability of staying in underload condition. Therefore the analysis validates this convention of teletraffic engineering. For successful observation of the network $P_{00}(t) >> P_{11}(t)$ but the situation will deteriorate with increase in packet arrival rate. Similarly the condition will improve with increase in packet termination rate. Increasing R_1 to 0.3, the profile of $P_{11}(t)$ is found very close to $P_{00}(t)$ like fig. 3 and further increase in R_1 the condition of unstable i.e. $P_{11}(t) > P_{00}(t)$ will take place.

VI. CONCLUSION

Incorporation of additional arrival in Markov chain deteriorates the probability of staying in underload condition but the situation is not so harmful for the overload state. Although degradation of performance of the network is visualized from the result section but it reveals the realistic situation of the network. A practical network faces different load condition at different 'times slot' of observation time and we can get the condition of traffic at different 'time slots' incorporating some intermediate states in the state transition chain of our proposed model.

REFERENCES

[1] Bing Zheng and Mohammed Atiquzzaman, 'Traffic Management of Multimedia over ATM Networks,' IEEE Communications Magazine, pp.33-38, January 1999.

[2] Md. Imdadul Islam and J. K. Das, 'Performance Evaluation of Wireless ATM Network Based on Two States Absorbing Markovian Chain,' Jahangirnagar University Journal of Science, vol.30, No.2, 215-228, Dec'2007.

[3] Mark William Fackrell, 'Characterization of Matrix-exponential Distributions', Thesis Doctor of Philosophy, the University of Adelaide, November 8, 2003.

[4] Shoji Kasahara, 'Studies on Queuing Models With Vacations and Their Applications' Thesis of Doctor of Engineering, Kyoto University, Kyoto 606-01, Japan. December 1995.

[5] Seok K. Hwang, Dongsoo S. Kim, 'Markov model of link connectivity in mobile ad hoc networks,' Springer, Telecommun Syst (2007) 34:51–58.

[6] Sheldon M. Ross, 'Introduction to Probability Models' 7th Edition, ISBN-81-7867-055-0, pp.216-225, Academic Press, A Harcourt Science and Technology Company, San Diego, USA, 2001.

[7] Reinhard German,' Performance Analysis of Communication Systems: Modeling with Non-Markovian Stochastic Petri Nets' John Wiley & Sons; 1 edition (May 17, 2000).

[8] Muhammad El- Ta ha, 'Queuing Networks' Class Lecture, Department o f Mathematics and Statistics, University of Southern Maine, Portland, ME 04104-9300, August 8, 2007.

[9] Andrzej Chydzinski, 'Buffer Overflow Period in a MAP Queue,' Mathematical Problems in Engineering, Article ID 34631, pp.1-18, Volume 2007.

[10] Sang H. Kang, Yong Han Kim, Dan K. Sung and Bong D. Choi, 'An application of Markovian Arrival Process (MAP) to modeling superposed ATM cell stream,' IEEE Transaction on Communications, vol.50, no.4, pp.633-642, April 2002.

[11] M. F. Neuts, "Models based on Markovian arrival process" IEICE Trans, Commun, vol. E75-B, pp. 1255-1265, Dec. 1992.

Proceedings of 2009 12th International Conference on Computer and Information Technology (ICCIT 2009)
21-23 December, 2009, Dhaka, Bangladesh

A New Image Compression Scheme Using Repeat Reduction and Arithmetic Coding

Md. Rafiqul Islam, Abdullah-Al-Baki, Md. Shahidul Haque Palash

Computer Science and Engineering Discipline, Khulna University, Khulna-9208, Bangladesh
dmri1978@yahoo.com, bakigm@gmail.com, palash.cseku@gmail.com

Abstract

Based on some simple arithmetic operation, an efficient lossless image compression technique is proposed. We use repeat reduction and arithmetic coding to improve the results of compression. We get better results than Log-Exp based compression and Arithmetic modulo based compression. From the experimental results, it can be seen that the performance of proposed method is better for all standard images. The complexity of our proposed method with respect to compression ratio has also been analyzed. The proposed method is most applicable for those images where lossy compression is to be avoided.

Keyword: Image compression, difference snakescan, repeat reduction, arithmetic coding, and compression ratio.

I. INTRODUCTION

Image compression requires higher performance due to increasing use of multimedia technologies (such as videoconferencing, internet and facsimile transmission) and database systems [1, 2]. Although many efficient image compression techniques with different features have been developed to address needs of multimedia and internet application, still research is going on to achieve better result with better image quality. Reconstructed image is identical to original image in lossless compression technique but compression ratio is very less. On the contrary, lossy compression technique does not reconstruct original image and gives better compression ratio with satisfactory quality of reconstruct image. Human Visual System (HVS) facilitates some tolerance to distortion of image depending upon the image and viewing condition [9]. For the reason HVS can not detect the difference between the original image and the reconstructed image. Neighboring pixels of image are highly correlated that means image contain a large amount of interpixel redundancy where neighbor pixels have almost the same value [1]. This redundancy can be used by lossy compression technique to get high compression ratio. Image compression is essential for reduction of storage space, reduction of transmission time and save bandwidth. The basic measures for the performance of image compression systems are picture quality and the compression ratio *i.e.* ratio between original data size and compressed data size. In this paper we have proposed a lossless image compression method using repeat reduction and arithmetic coding, which gives better performance than the existing related methods.

II. RELATED WORKS

While many different compression methods are employed to compress the image, they can be separated into two categories: lossless and lossy. In lossy compression algorithm should achieve trade off between compression ratio and picture quality. Higher compression ratios will produce lower picture quality and vice versa. Transform is a basic step classically needed for lossy image compression. JPEG (Joint Photographic Experts Group) is an international compression standard for continuous-tone still image, both grayscale and color was proposed by G. K. Wallace [4]. This standard is designed to support a wide variety of applications for continuous-tone images. Because of the distinct requirement for each of the applications, the JPEG standard has two basic compression methods. The DCT-based method is specified for lossy compression, and the predictive method is specified for lossless compression. The DCT compresses an image into 8×8 blocks and places them consecutively in the file. In this compression process, the blocks are compressed individually, without reference to the adjoining blocks. This results in "blockiness" associated with compressed JPEG files. A simple lossy technique called baseline, which is a DCT-based method, has been widely used today and is sufficient for a large number of applications [6].

The JPEG2000 compression algorithm was released by an ISO standardization committee in January 2001. This wavelet-transformation algorithm offers improved image quality at very high compression ratios. JPEG2000 is said to produce as much as a 20% improvement in compression efficiency over the current JPEG format. JPEG2000 proposed by G. K. Wallace at the core of the JPEG 2000 structure is a new wavelet based compression methodology that provides for a number of benefits over the Discrete Cosine Transformation (DCT) compression method, which was used in the JPEG format [4]. However, much of the detail that makes for a pleasing, continuous image is lost. In contrast, wavelet compression converts the image into a series of wavelets that can be stored more efficiently than pixel blocks. Although wavelets also have rough edges, they are able to render pictures better by eliminating the "blockiness" that is a common feature of DCT compression. Not only does this make for smoother color toning and clearer edges where there are

978-1-4244-6283-4/09/$26.00 ©2009 IEEE

sharp changes of color, it also gives smaller file sizes than a JPEG image with the same level of compression. Discrete Wavelet Transform (DWT) is used instead of DCT in JPEG2000 [7]. It has mainly been developed for use on the Internet.

A Novel Lossless Image Compression Algorithm Using Arithmetic Modulo Operation proposed by S. K. Pattanaik *et al.*, is an efficient lossless image compression technique based on some simple arithmetic calculation. This technique is designed for high quality still image compression, especially Peak Signal to Noise Ratio (PSNR) value above 34 [3]. This algorithm is most applicable for those images where lossy compression is avoided such as medical and scientific images [3]. The encoding and decoding procedure is very fast. Where for reducing the redundancy of the pixel values, pixels values are divided by a base number and only the division value is stored and the reminder is truncated to locate pixel values in a small and continuous range.

A Novel Image Compression Algorithm by Using LOG-EXP Transform called the logarithmic and exponential transform was proposed by S. C. Huang *et al* [1]. This image compression algorithm is designed based on the logarithmic number system (LNS) properties. In this compression technique 8 bit image represent with 7 bit after log transform where first 3 bit for integer part and last 4 bit for fractional part. For gray level image, the pixel value is usually represented in integer format [1].

For simplicity of our discussion we denote novel lossless image compression algorithm using arithmetic modulo operation by ICAUAMO and a novel image compression algorithm using LOG-EXP transform by ICAULET.

A. Drawbacks of the Existing Algorithms

The JPEG process is a widely used form of lossy image compression that centers on the Discrete Cosine Transform (DCT) [4]. The main drawbacks of JPEG are block artifacts and low throughput. JPEG based on the DCT transform [4], the block artifacts make large distortion in the image quality, especially in the zoom view for the region of interest (ROI) access. Comparing with Huffman and arithmetic coding, the modified algorithm that was proposed by I. Brailovskiy and D. Plotkin [10], the binary interval transform algorithm compression ratio is high but speed of compression is slow.

The main drawbacks of JPEG2000 image compression algorithm is, only recent workflows or computer applications can deal with JPEG2000 compression [7]. If there are need to distribute data, this can be a real showstopper. Compressing data requires lots of CPU-horsepower and compression time is more than any other compression algorithm.

Compression method ICAUAMO proposed by S. K. Pattanaik *et al* is very much useful of those images where the information content is very large *i.e.* redundant data is very less, but when the redundant data or information are used, this method does not work properly.

To overcome the above drawbacks in JPEG, S. C. Huang *et al* proposed ICAULET based still image compression algorithm [1]. The speed of this algorithm is limited because of the presence of Huffman coding block and use of logarithm and exponential operation. If the color value is large, the design of the Huffman code is quite complex and the compression achieved is very less.

III. A New Image Compression Scheme Using Repeat Reduction and Arithmetic Coding

By exploiting the methods proposed by S. K. Pattanaik [3] and by S. C. Huang *et al*. [1] we proposed an image compression scheme using repeat reduction and arithmetic coding, which gives better compression ratio. In this scheme we use compression ratio as the major measurement issue of performance for lossless image compression. We also get less compression time due to computational plainness. After repeat reduction we use arithmetic coding because it can represent a pixel with fractional number of bits. On the contrary any other coding needs integer number of bits for encoding [8]. In our proposed method, we work in 8 bit gray-scale image containing up to 256 different shades of gray with values from 0 to 255. Sometimes one can interpret the pixel values of gray-scale images as indices to colors in a color palette. Here, pixel values of gray-scale images are regarded as shades of gray from black to white [2].

The proposed algorithm is described below:

1) At first step we read the pixel value of gray level image.
2) Divide pixel values by base and take only integer part.
3) Perform snake scan and calculate the difference of neighbor pixel values.
4) Perform repeat reduction. Repeat reduction gives output of nonrepeat data and repeat trace bit.
5) Apply arithmetic coding on repeat data and nonrepeat data in the following way:
    i) Apply run length coding on repeat trace bit and after that apply arithmetic coding on run length coded data.
    ii) Apply arithmetic coding also on nonrepeat data.

After arithmetic coding we get compressed data. We decompress data in reverse strategies of compression technique. The decoding process decodes the encoded data from compressed file by arithmetic decoding. After getting decoded data, we apply repeat restoring process to get repeated data. Then difference addition processes are applied on total data. Next the data are rearranged in such way that data form an image (inverse process of

snake scan). After multiplying the values by the base the original pixel values are found. Block diagram of the proposed compression and decompression system is shown in Fig. 1(a) and Fig. 1(b) respectively.

After reading pixel values from image, each pixel value is divided by the base where base is a number that should be the power of 2 and only integer part is taken after division. After this operation, a lot of repeated pixel values are produced. This process is useful for the repeat reduction process. When the pixel values are processed in sequential scan and go from current line to the next line, there will be large neighboring differences. To avoid such kind of large neighboring difference, the snake scan is used.

The difference between two adjacent pixel values is called neighboring difference [3]. The neighbor pixels usually represent the same object so that the values of the pixels are similar or same. By applying the differences between the neighbor pixels, the pixel values will be very small and generate many same pixel values. The procedure of neighboring differences is shown in Fig 2.

After dividing each pixel by the base we found a large number of redundancies in the form of repeated values in adjacent pixels and also generate repeated values after performing snakescan difference. This redundancy can be reduced by performing the run length coding on the transformed data. Repeat reduction process transmits 1 for repeated pixel values and 0 for non repeated values and stores the repeated pixel value only once. The procedure of repeat reduction is shown in Table I. After repeat reduction, run length coding has been applied on repeat trace bit in the following way. As for example,

Repeat trace bit: 0 0 1 1 1 0 1 0 0 0 0 1 1 1 1 1 0 1 0
Run length coded data: 2 3 1 1 4 5 1 1 1
Now we apply arithmetic coding on run length sequence. Arithmetic coding is useful for lossless data compression. Arithmetic coding encodes a message into another representation that represents frequently used characters using fewer bits and infrequently used characters using more bits, with the goal of using fewer bits in total [8].

A. Performance Analysis with Respect to Compression Ratio

Here we analyze the performance of our proposed method Compression ratio can be defined as the ratio of total number of bits to represent the compressed information and the total number of bits in original information. For the 8 bit gray level image of size $M \times N$, the total number of pixel is,

$$T = M \times N \quad (1)$$

So the total number of bits required to represent the 8 bit gray image is,

$$T_b = M \times N \times 8$$

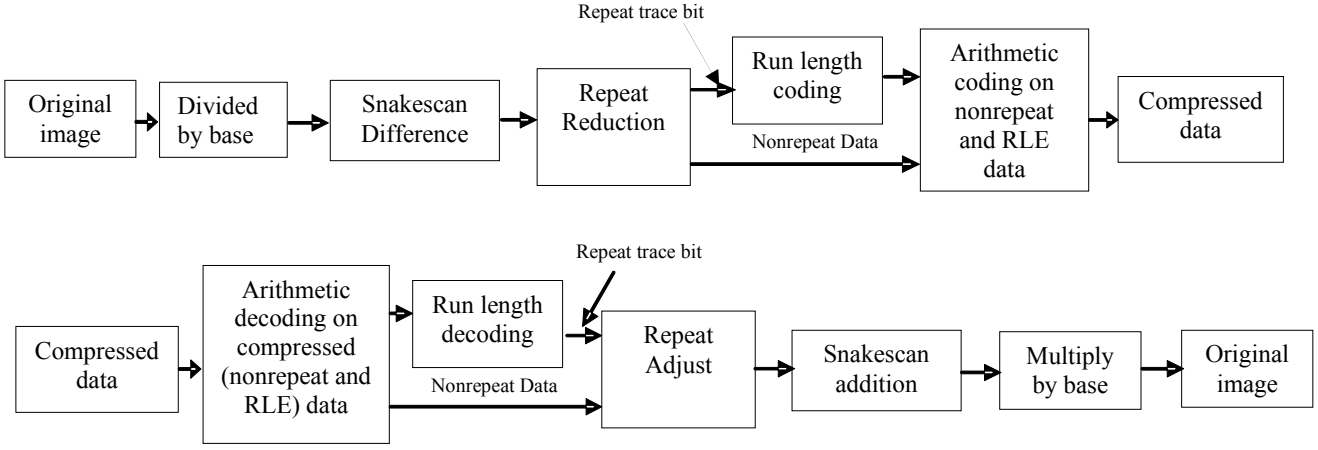

Fig. 1(a) Block diagram of our proposed Compression process
Fig. 1(b) Block diagram of our proposed Decompression process

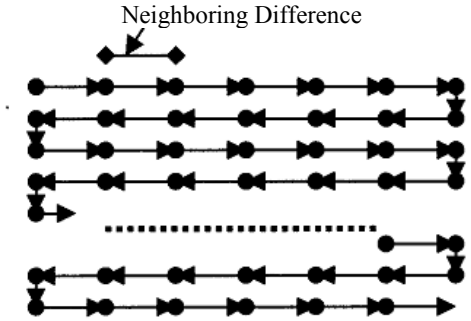

Fig. 2 Neighboring Difference and Snake Scan

TABLE I. REPEAT REDUCTION

Snakescan Difference	Data	Repeat trace bit
40	40	0
35	35	0
35		1
35		1
31	31	0
31		1
32	32	0

In our proposed method we divide the pixel values by the base, *b* where *b* is a number that should be the power of 2 and we take only integer part after division. Here a lot of same pixel values are generated and pixel values will be very small in range. Next, neighboring difference is done on pixel values that also produce same pixel value in small range. To reduce repeated pixel values we apply repeat reduction process. So, after performing division by base and neighboring difference, a lot of repeated data is produced. Let the number of repeated data is R. So total number of data remain (nonrepeat data) after repeat reduction is,

$$T_{nr} = T - R$$
$$T_{nr} = M \times N - R \quad (2)$$

For repeated data we use one bit for each pixel. So for $M \times N$ pixels $M \times N$ bits are required to keep trace of repeated data. Let r be the number of repeated bits. After applying run length coding, total number of data is,

$$T_{rc} = M \times N - r \quad (3)$$

Now arithmetic coding is applied on both outputs of run length coding and nonrepeat data found at the stage of repeat reduction.

For nonrepeat data T_{nr}, let the number of each distinct data is f_i for $l_{nr} \le i \le h_{nr}$ where $l_{nr} = min\left(\frac{P_I}{b}\right)$ and $h_{nr} = max\left(\frac{P_I}{b}\right)$ and P_I is the original pixel values of image. So the probability of each distinct data is $p_i = \frac{f_i}{T_{nr}}$. By arithmetic coder, the number of bits is produced for each distinct data according to their probability information. If the probability of each distinct data is p_i, then the numbers of bits are produced for each distinct data is $-log(p_i)$ [16]. Here $0 \le p_i \le 1$ and log of any fractional value for 0 < value < 1 produces negative value. Preceding negative of log is used to get positive value. So for the nonrepeat data, suppose probability of 1^{st} distinct data is p_1, then numbers of bits are produced for each data is $-log(p_1)$. If the number of 1^{st} distinct data is N_1, then total numbers of bits are produced for the 1^{st} distinct data,

$$S_1 = -log(p_1) \times f_1$$

Similarly for the 2^{nd} distinct data,

$$S_2 = -log(p_2) \times f_2$$

And for the i^{th} distinct data,

$$S_i = -log(p_i) \times f_i$$

Therefore, the total number of bits required for all non repeat data is,

$$S_{nr} = S_1 + S_2 + \dots + S_i$$
$$S_{nr} = -\sum_{i=l_{nr}}^{h_{nr}} log(p_i) \times f_i$$
$$S_{nr} = -\sum_{i=l_{nr}}^{h_{nr}} log\left(\frac{f_i}{T_{nr}}\right) \times f_i$$
$$S_{nr} = -\sum_{i=l_{nr}}^{h_{nr}} log\left(\frac{f_i}{M \times N - R}\right) \times f_i \quad (4)$$

For output of run length coding T_{rc}, let the number of each distinct data is k_j for $l_{rc} \le j \le h_{rc}$ where $l_{rc} = min(T_{rc})$ and $h_{rc} = max(T_{rc})$. So the probability of each distinct data is $p_j = \frac{k_j}{T_{rc}}$. So total number of bits required for all repeat data is,

$$S_{rc} = -\sum_{j=l_{rc}}^{h_{rc}} log(p_j) \times k_j$$
$$S_{rc} = -\sum_{j=l_{rc}}^{h_{rc}} log\left(\frac{k_j}{T_{rc}}\right) \times k_j$$
$$S_{rc} = -\sum_{j=l_{rc}}^{h_{rc}} log\left(\frac{k_j}{M \times N - r}\right) \times k_j \quad (5)$$

So total number of bits required to compress the image is,

$$T_p = S_{nr} + S_{rc}$$
$$T_p = -\sum_{i=l_{nr}}^{h_{nr}} log\left(\frac{f_i}{M \times N - R}\right) \times f_i - \sum_{j=l_{rc}}^{h_{rc}} log\left(\frac{k_j}{M \times N - r}\right) \times k_j$$

$$T_p = -\left\{ \sum_{i=l_{nr}}^{h_{nr}} log\left(\frac{f_i}{M \times N - R}\right) \times f_i + \sum_{j=l_{rc}}^{h_{rc}} log\left(\frac{k_j}{M \times N - r}\right) \times k_j \right\}$$

$$T_p = \sum_{i=l_{nr}}^{h_{nr}} log\left(\frac{M \times N - R}{f_i}\right) \times f_i + \sum_{j=l_{rc}}^{h_{rc}} log\left(\frac{M \times N - r}{k_j}\right) \times k_j \quad (6)$$

IV. EXPERIMENTAL RESULTS AND PERFORMANCE EVALUATION

The experiment is performed on Microsoft Windows XP Dual core 2 GHz processor having 1 GB RAM. The programs are implemented using Matlab 7.5.0 (R2007b) and tested with the standard grayscale images namely, house, peppers, Barbara, Lena, Boat, Baboon, Fingerprint, Flintstone and so on. Each image is of 8 bit resolution. The performance of our proposed algorithm is compared with ICAUAMO (A Novel Image Compression Algorithm using Arithmetic Modulo Operation) and ICAULET (A Novel Image Compression by Using LOG-EXP Transform) on basis of compressed bits and bit reduced in percentage. Experimental results are shown in Table II, III and IV. Table II, III and IV show the values of compressed bits and bit reduced in percentage of our proposed method, ICAUAMO and ICAULET on the basis of base and fraction digit (FD). From the Tables it can be seen that the compressed bits and bits reduced in percentage is obtained using our proposed method is better than those obtained using ICAUAMO and ICAULET. For all the images it is found that our proposed one is performing better. For the small base, bits reduction is few but image quality is better and for the large base, bits are reduced more but image quality is degraded. Similarly for the large FD, bits reduction is few but image quality is better and for the small FD bits are reduced more but image quality degrades.

TABLE II. COMPRESSED BITS AND DATA REDUCTION IN PERCENTAGE FOR BASE 4

Image	Original Size	Original Bits	Base 4				FD 4	
			Proposed Method		ICAUAMO		ICAULET	
			Compressed Bits	Bits Reduced%	Compressed Bits	Bits Reduced%	Compressed Bits	Bits Reduced%
Lena	512×512	2097152	625822	70.16	884227	57.84	960117	54.22
Baboon	200×200	320000	148642	53.55	176807	44.75	189882	40.66
Peppers	256×256	524288	175365	66.55	233485	55.47	252317	51.87
Barbara	512×512	2097152	815982	61.09	1115074	46.83	1134356	45.91
House	256×256	524288	129556	75.29	182721	65.15	207574	60.40
Boat	512×512	2097152	716148	65.85	986678	52.95	1079525	48.52
Fingerprint	512×512	2097152	1014533	51.62	1116260	46.77	1220215	41.82
Flinstones	512×512	2097152	865212	58.74	1072924	48.84	1137846	45.74

TABLE III. COMPRESSED BITS AND DATA REDUCTION IN PERCENTAGE FOR BASE 8

Image	Original Size	Original Bits	Base 8				FD 3	
			Proposed Method		ICAUAMO		ICAULET	
			Compressed Bits	Bits Reduced%	Compressed Bits	Bits Reduced%	Compressed Bits	Bits Reduced%
Lena	512×512	2097152	428081	79.59	654545	68.79	697391	66.75
Baboon	200×200	320000	106093	66.85	140277	56.16	146420	54.24
Peppers	256×256	524288	125042	76.15	176493	66.34	186491	64.43
Barbara	512×512	2097152	583637	72.17	856004	59.18	854920	59.23
House	256×256	524288	93720	82.12	140806	73.14	143166	72.69
Boat	512×512	2097152	485400	76.85	754600	64.02	810762	61.34
Fingerprint	512×512	2097152	746487	64.40	884574	57.82	932796	55.52
Flinstones	512×512	2097152	646467	69.17	850194	59.46	833021	60.28

TABLE IV. COMPRESSED BITS AND DATA REDUCTION IN PERCENTAGE FOR BASE 16

Image	Original Size	Original Bits	Base 16				FD 2	
			Proposed Method		ICAUAMO		ICAULET	
			Compressed Bits	Bits Reduced%	Compressed Bits	Bits Reduced%	Compressed Bits	Bits Reduced%
Lena	512×512	2097152	276519	86.81	446720	78.69	502689	76.03
Baboon	200×200	320000	68806	78.49	105985	66.88	114136	64.33
Peppers	256×256	524288	86563	83.49	127096	75.76	137763	73.72
Barbara	512×512	2097152	391614	81.33	617015	70.58	150978	68.96
House	256×256	524288	56219	89.28	84768	83.83	112051	78.63
Boat	512×512	2097152	309229	85.25	529914	74.73	603785	71.21
Fingerprint	512×512	2097152	489838	76.64	665491	68.27	724539	65.45
Flinstones	512×512	2097152	453403	78.38	641909	69.39	693629	66.93

V. CONCLUSION

Arithmetic modulo based image compression technique is known to yield reconstructed image with better subjective quality. In this paper we presented an image compression method using repeat reduction and arithmetic coding. Repeat reduction is employed before the encoding process and achieved good results for different images especially for face images. For more redundant data our proposed method shows better results than those of existing methods but for less redundant data our proposed method shows minor improvement of the results of the existing methods. It is found that proposed method improves the compression results of ICAUAMO without altering PSNR. This is very much useful for those images where the information content is very large *i.e.* redundant data is very less [3].

REFERENCES

[1] S. C. Hung, L.G. Chen and H. C. Chang," *A novel Image Compression Algorithm by using LOG-EXP Transform*", IEEE Sym. Circuits and Systems, pp. 17-20, 1999.

[2] R. C. Gonzalez, R. E. Woods, Digital Image Processing, Pearson Education 2nd Edition 2004.

[3] S. K. Pattanaik, K. K. Mahapatra, G. Panda, "*A Novel Lossless Image Compression Algorithm using Arithmetic Modulo Operation*", IEEE Trans., Cybernetics and Intelligent Systems, 2006.

[4] G. K. Wallace, "*The JPEG Still-Picture Compression Standard*", Communications of ACM, pp. 30-44, April 1991.

[5] P. G Howard, and J. S. Vitter, "*Arithmetic Coding for Data Compression*", IEEE proc, vol. 82, no. 6, 1994.

[6] N. Ahmed, T. Natarajan, and K. R. Rao, "*Discrete cosine transform*," IEEE Trans. Comput. Vol. C-23, pp. 90–93, Jan.1974.

[7] Charilaos Christopoulos, Athanassios Skodras, Touradj Ebrahimi, "*The JPEG2000 still image coding system: An overview*", Published in IEEE Transactions on Consumer Electronics, Vol. 46, No. 4, pp. 1103-1127, November 2000.

[8] Alistair Moffat, Radford M. Neal and Ian H. Witten, *"Arithmetic Coding Revisited",* ACM Transactions on Information Systems, Vol. 16, No. 3, July 1998, Pages 254-294.

[9] Ayant, N-Johnston, J. Safranek, "Signal Compression Based in Models of Human Perception", Proc. Of IEEE 81 (1993), 1385-1422.

[10] I. Brailovskiy, D. Plotkin*,"Modified JPEG algorithm with Binary Interval Transform coding with improved compression ratio,"* Thesis #2296, Moscow state University, Moscow, Russia.

Proceedings of 2009 12th International Conference on Computer and Information Technology (ICCIT 2009)
21-23 December, 2009, Dhaka, Bangladesh

A Practical Approach of Designing Synchronous Replicated Heterogeneous Distributed Database System *(Not Presented)*

Mohammad Shahinur Islam, Md. Fokhray Hossain†, Mohammad Zahidur Rahman‡

University of Greenwich, UK
† Department of Computer Science and Engineering, Daffodil International University, Dhaka, Bangladesh
‡ Department of Computer Science and Engineering, Jahangirnagar University, Savar, Dhaka, Bangladesh
mislam.gre@gmail.com, drfokhray@daffodilvarsity.edu.bd, rmzahid@juniv.edu

Abstract

Data replication is a central technique to increase availability and performance of distributed systems. In this paper we present a Hybrid Replication (Multi-master and Materialized View) approach for managing replicated data in wide area distributed networks. Our solution is based on synchronous replication that ensures or guarantees both the primary and remote sites are 100% synchronized and managed in a decentralized manner. Based on a real Greeting Cards retails business we present the involved concepts and for practical purpose we used Oracle and SQL server.

Keywords: Data replication, Distributed system, Synchronous replication, Hybrid Replication, Multi-Master, Materialized View

I. INTRODUCTION

"Online Transaction Processing (OLTP) was born just before two decades and with the invention of OLTP system the computing infrastructure alters from large centralized mainframes with dumb terminal to decentralized client/server computing running on personal Computers and accessing database on other machines over a network using graphical user interfaces (GUIs)." Most firms today use a diverse set of multi-vendor hardware and software platform, within this environment, they run several business applications. And much of that data that supports these applications is redundantly stored. The challenge for these firms is to ensure that all applications and business users make decisions with consistent copies of this redundantly stored data. This begs the question of why do firms store data redundantly. Basically we thought there are four major reasons account for this phenomena:

- firms use a wide range of hardware and software platforms
- firms are becoming more distributed
- firms need a disaster recovery solution, and
- the basic fact that humans do not like to share

II. LITERATURE REVIEW

From the last decade distributed database and data warehousing is the hot research topic in the Computing research arena. Replication is the central technique that improves and increases the availability and performance of distributed services. According to the dictionary Replication means duplicated copy of data [1], but data replication is much more than simply copying data between data stores, it encompasses the analysis, and design, implementation, administration and monitoring of service that guarantees data consistency across multiple resource mangers in a distributed environment [1].

To reduce risk, all redundantly stored data either must be totally consistent with all other copies at all times or must have an acceptable level of inconsistency for short periods of time. Because an inconsistent copy can be made consistent by synchronizing the data with what has been designated as its primary source. A replication service is the principle driver to maintain data consistency in distributed database. One of the major problems of replication mechanisms in distributed database is the localization of data copies. To maintain the data copies for small environment is very easy because there are small numbers of copies but it is very difficult for large scale environments because there could be unreliable nodes and some times hundreds or thousands of replicas [2]. In a nutshell, we the following challenges are found for replication systems:

- Robustness, i.e. supporting updates even if the primary owner of a given data object fails without risking consistency, [2]
- Scalability, the number of replicas in order to support settings with hundreds or thousands of replicas. [2]

To maintaining the replicated data there are basically there are two classes of algorithms. The optimistic method that is based on "optimistic" assumption and in this method problem occurred rarely [5]. The main task of optimistic replication system is to detection and resolution of the conflicts. But Gray et, al [3] mentioned that optimistic approaches are not good for large system.
However the traditional pessimistic algorithms that work on a single copy [4] and basically commercial systems are based on primary copy system and in this system data object is managed by its own master node [5].

978-1-4244-6283-4/09/$26.00 ©2009 IEEE

III. ISSUES ASSOCIATED WITH THE DESIGNING

The design technique we are using for distributed database system for Clinton Cards is Heterogeneous Distributed System design. The design is shown in figure1.

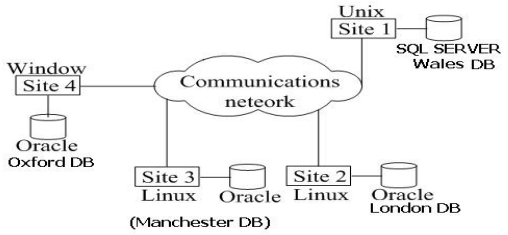

Figure1: Heterogeneous Distributed Database for Clinton Cards Group

We choose Heterogeneous design because some of the branches uses different database not the same (Homogeneous distributed system). In the figure1 Wales site using SQL Server that is diverse rather than other site's database. Basically each site operates independently and they are storing their information in their own database. The main objective of distributed database system is that it will provides all the features of centralized system to the user but the user are not aware of where a piece of data is physically stored. In distributed database system data can be distributed if different way it could be distributed through either replication process or fragmented process (Horizontal or Vertical or Mixed or Hybrid fragmentation).

IV. A COMPREHENSIVE EXAMPLE

To design the database at first we have design the Entity Relationship Diagram (ERD) for the OLTP system. Figure 2 represents the basic ER model for the Clinton Cards Group.

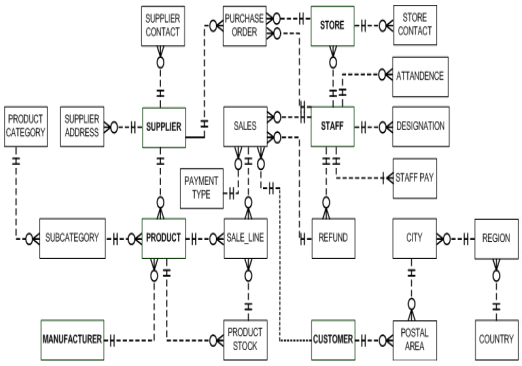

Figure 2: Basic ER model of OLTP system for the Clinton Cards Group

Our OLTP database is fully normalized database.

According to the user requirements and based on the OLTP database model we are creating the entire tables for the Clinton Cards Group. Not only that we have creating Triggers for each table and indexes also.

V. REPLICATION STRATEGY

There are three different ways that we can replicate data and are as follows:

- Multi-master Replication
- Materialized View Replication
- Hybrid Replication (Multi-master and Materialized View)

In our research project we are using Multi-master Materialized View Hybrid Configuration technique because in Multi-master Replication technique if updates made in one master site then that master site propagated update of data to all other master sites. That's means every master site using the same table and contains similar records. In materialized view replication process a materialized view contains a complete or partial copy of a target master from a Single point in time. According to the requirements of the users of the Clinton Cards they wants to store all sites replicas at London Site that is the headquarter of the Clinton Cards. So, if we use Multi-master techniques then when one site insert data or update data then it will appeared in other sites. So every records of each table are replicated that is not the concept of distributed database it is the concept of replicated database because of replicated database and distributed database concept are not same. In a distributed database, data is available at many locations, but replication means that the same data is available at multiple locations. Replication uses distributed database technology to share data among different sites,

For that reason we are using hybrid replication environment (combination of multi-master and materialized view replication) that suite our organizational architecture of the business. In this case The London Site is our Master definition site and Oxford Site is our Master site. Manchester and Wales Sites are our Snapshot or Materialized View Sites. Figure 3 represents the concepts of Hybrid Replication:

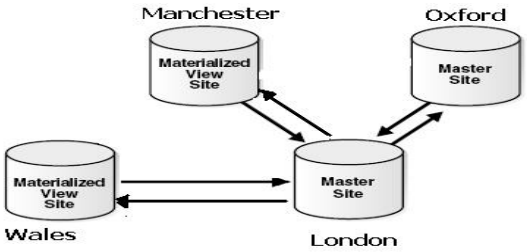

Figure 3: Hybrid Replication technique for Clinton Cards Group

In the figure 3 the London is our Master Definition site and Oxford is our Master Site. Though London our headquarter and according to the requirements all replicated copies will be available at headquarter so if any this is changed at Oxford site then it will be automatically updated at London site and also vise-versa. And the Manchester and Wales are Materialized view sites and if the update is occurred any of these sites then it will update the target Master Site that is our London site. In this environment if any node or site is down due to the failure then it will not interrupt the other sites and other sites can perform their operation(s) smoothly.

VI. CREATING ENVIRONMET FOR REPLICATED DISTRIBUTED SYSTEM

Creating database schema for London is LondonDB, Oxford is OxfordDB, Manchester is ManchesterDB and Wales is WalesDB. After creating Database then we need to configure the Oracle TNS file to propagated bio-directional communication with each site.

A. Setup Oracle Network

We need to configure the tnsnames.ora Network Configuration File and need to write the following

```
MANCHESTERDB =   (DESCRIPTION =
 (ADDRESS = (PROTOCOL = TCP)(HOST = ACS)(PORT = 1521))
   (CONNECT_DATA =
   (SERVER = DEDICATED)
   (SERVICE_NAME = manchesterdb)
   )   )
OXFORDDB =   (DESCRIPTION =
   (ADDRESS = (PROTOCOL = TCP)(HOST = workstation5)(PORT
= 1521))
   (CONNECT_DATA =
    (SERVER = DEDICATED)
    (SERVICE_NAME = oxforddb)
   )  )
LONDONDB =   (DESCRIPTION =
   (ADDRESS = (PROTOCOL = TCP)(HOST = lcbit1)(PORT =
1521))
   (CONNECT_DATA =
    (SERVER = DEDICATED)
    (SERVICE_NAME = londondb)
   )  )
```

B. Setting up Master Definition Site

The master definition site is the central repository for a master group and the entire base objects that will be replicated at the remote sites are belong to the master definition site. In our case our LondonDB is the master definition site. Master definitions site is the control center for the management of group and the objects in that master group. In simple word all changed are performed at the master definition site and propagated to all other master sites.

B.1 Create the Replication Administrator at LondonDB

Our first task is to create a replication administrator and provide that administrator necessary privileges that can create and manage replication environment. The following command is the examples of creating replication administrator.

```
CONNECT SYSTEM/MANAGER@londondb;
CREATE USER clinton_repadmin IDENTIFIED BY
clinton_repadmin;
```

B.2 Providing Necessary Privileges to Administrator

Using the following procedure we are giving more powerful privileges to the rapadmin user

```
BEGIN
DBMS_REPCAT_ADMIN.GRANT_ADMIN_ANY_SCHEMA (
                username => 'clinton_repadmin');
END;      /
```

Here "DBMS_REPCAT_ADMIN" is a package for creating administrator account for replication and "GRANT_ADMIN_ANY_SCHEMA" is the procedure or subprogram that will give privileges or administer permission on any replication group at the current site. We are also providing necessary privileges to our clinton_repadmin that this user can also be able to create materialized view logs for any replicated table using the following commands:

```
GRANT COMMENT ANY TABLE TO clinton_repadmin;
GRANT LOCK ANY TABLE TO clinton_repadmin;
```

And not only that we are also giving privileges to clinton_repadmin user to connect to the Replication Management tool using the following privileges

```
GRANT SELECT ANY DICTIONARY TO clinton_repadmin;
```

B.3 Register propagator at LondonDB

We need to grant the Replication Administrator for the propagate privileges because the propagator is responsible for propagating the deferred transaction (is a transaction that is queued for delivery to one or more remote databases) queue to other master sites that means if any change occurred in Master definition sites that will be appeared in other remote sites.

```
BEGIN  DBMS_DEFER_SYS.REGISTER_PROPAGATOR (
                username => 'clinton_repadmin');
END;
```

B.4 Register the Receiver at LondonDB

We also need to register receive because the receiver will receives the deferred transaction that is sent by the propagator. And the task of receiver is to receive the

deferred transaction queue and applies them to the local objects. The following diagram represents the above two (propagator and receiver) concept:

Register receiver, the receiver receives the propagated deferred transactions sent by the propagator from other master sites. Figure 4 represents how propagator and receiver communicate each other.

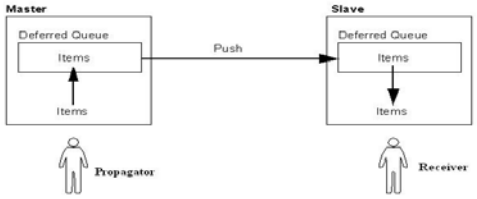

Figure 4: Communication between Propagator and Receiver [6]

```
BEGIN
DBMS_REPCAT_ADMIN.REGISTER_USER_REPGROUP (
            username => 'clinton_repadmin',
            privilege_type => 'receiver',
            list_of_gnames => NULL);
      END;
```

B.5 Schedule a Job at Master site LondonDB

We need to purge the successfully completed deferred transaction to keep the size of the queue in check. This is an automated process and this procedure will be executed at the replication administrator site at the master definition site.

```
BEGIN
DBMS_DEFER_SYS.SCHEDULE_PURGE (
                next_date => SYSDATE,
                interval => 'SYSDATE + 1/24',
                delay_seconds => 0);
END;
      /
```

B.6 Setup Proxy Materialized View site at LondonDB

Though we are using hybrid replication architecture so we need to create proxy master site users at out LondonDB master definition site and this proxy will correspond to users at the materialized view sites

```
CONNECT SYSTEM/MANAGER@londondb
CREATE USER proxy_manchester_clinton_mviewadmin IDENTIFIED BY proxy_manchester_clinton_mviewadmin;
```

B.7 Register Proxy Materialized view Administrator

```
BEGIN
DBMS_REPCAT_ADMIN.REGISTER_USER_REPGROUP (
    username => 'proxy_manchester_clinton_mviewadmin',
    privilege_type => 'proxy_snapadmin',
    list_of_gnames => NULL);
END;
GRANT SELECT_CATALOG_ROLE TO proxy_manchester_clinton_mviewadmin;
```

B.8 Setup Proxy Refresher

The proxy refresher performs tasks at the master site **on behalf of the refresher at the materialized view site.**

```
CREATE USER proxy_refresher IDENTIFIED BY proxy_refresher;
GRANT CREATE SESSION TO proxy_refresher;
GRANT SELECT ANY TABLE TO proxy_refresher;
```

B.9 Create the DB Link Between the Master Sites

Now we need to create the database link to communicate among the master site(s) because the database links will provide us the necessary distributed facility that will allow us to replicate data in different sites. But we need to create the PUBLIC database links before creating any private database link and another important thing is that we need to create a database link for all replication administrators that are participating in our design as master sites.

```
CONNECT SYSTEM/MANAGER@londondb
CREATE PUBLIC DATABASE LINK oxforddb USING 'oxforddb';
CONNECT CLINTON_REPADMIN/CLINTON_REPADMIN@londondb
CREATE DATABASE LINK oxforddb CONNECT TO clinton_repadmin IDENTIFIED BY clinton_repadmin;
```

B.10 Define a Schedule for each Database Link

Now we need to create a schedule link for the database link that we create before because the schedule link determines how often our deferred transaction queue will be propagated to other master sites. In our case we are using asynchronous replication mechanism for real-time replication .

```
CONNECT
clinton_repadmin/clinton_repadmin@londondb;
BEGIN
DBMS_DEFER_SYS.SCHEDULE_PUSH (
    destination => 'oxforddb',
    interval => 'SYSDATE + (1/144)',
    next_date => SYSDATE,
    parallelism => 1,
    execution_seconds => 1500,
    delay_seconds => 1200);
END;
```

C. Crating Master Site OxfordDB

After creating the master definition site LONDONDB now we need to create or define the other sites that will be participate in our replication environment. In our case we need to setup the OXFORDDB because this is our master site. The steps are same that we follow for the master definition site.

C.1 Create Master Replication Group on LondonDB

After setup the master site(s) now we are ready to build the Master Replication group in our Master Definition Site at LONDONDB.

CREATE_MASTER_REPGROUP procedure is used for crating a new, empty and quiesced master group and definitely we need to create by replication administrator.

```
CONNECT clinton_repadmin/clinton_repadmin@londondb;

BEGIN

DBMS_REPCAT.CREATE_MASTER_REPGROUP (
    gname => 'clinton_repg');
END;
```

C.2 Add Objects to the Replication Group on Master

For adding object(s) to the Replication group we use CREATE_MASTER_REPOBJECT procedure to add an object to our master group. Using this procedure we will add tables, indexes and triggers but it is also possible to add procedures, views and synonyms and so on.

C.2.1 Adding Tables

We need to add the all table name that we are using in our database. Here we are showing one example how to add a table to the replication group.

```
BEGIN
DBMS_REPCAT.CREATE_MASTER_REPOBJECT (
    gname => 'clinton_repg',
    type => 'TABLE',
    oname => 'SUPPLIER',
    sname => 'clinton',
    use_existing_object => TRUE,
    copy_rows => FALSE);
END;
/
```

C.2.2 Adding Indexes

We also need to add the indexes that we have created for our table objects that we already added in the replication group. Here we are showing one example how to add an index in replication group**.**

```
BEGIN
DBMS_REPCAT.CREATE_MASTER_REPOBJECT (
    gname => 'clinton_repg',
    type => 'INDEX',
    oname => 'SHELF_ID_PK',
    sname => 'clinton',
    use_existing_object => TRUE,
    copy_rows => FALSE);
END;
```

C.2.3 Adding Triggers

Triggers are also need to add in the replication group. Here we are showing one example how to add trigger in replication**.**

```
BEGIN
DBMS_REPCAT.CREATE_MASTER_REPOBJECT (
    gname => 'clinton_repg',
    type => 'trigger',
    oname => 'ATTANDENCE_TRIGGER',
    sname => 'clinton',
    use_existing_object => TRUE,
    copy_rows => FALSE);
END;
```

C.3 Adding Additional Master Site OxfordDB

In this step we need to add that all the master site (s) that are participate in our replication environment. In our case we have one Master site OXFORDDB. So, we are adding one master site. To add master site we use ADD_MASTER_DATABASE procedure.

```
BEGIN
DBMS_REPCAT.ADD_MASTER_DATABASE (
    gname => 'clinton_repg',
    master => 'oxforddb',
    use_existing_objects => TRUE,
    copy_rows => FALSE,
    propagation_mode => 'SYNCHRONOUS');
END;
```

We can check that our adding master site in the replication group or not using the following command.

```
SELECT DBLINK FROM DBA_REPSITES WHERE GNAME = 'clinton_repg';
```

Here ‘clinton_repg’ is our Replication Group name.

C.4 Activate Replication Support for each added Table on Master

We need to add support for the objects that we added on Master Definition site. The following one as an example**.**

```
BEGIN
DBMS_REPCAT.GENERATE_REPLICATION_SUPPORT (
    sname => 'clinton',
    oname => 'PRODUCT',
    type => 'TABLE',
    min_communication => TRUE);
```

END;

C.5 Start the Replication on the Master

All setup are done so our system is ready for the replication. From the Master Definition site we need to start the replication process. But the important thing is that we should need to be waiting until DBA_REPCATALOG view is empty before resuming master activity. We can see the status of DBA_REPCATALOG using the following command

CONNECT

clinton_repadmin/clinton_repadmin@LONDONDB;

SELECT COUNT(*) FROM DBA_REPCATLOG WHERE GNAME = 'clinton_repg';

We can also check the status, object name and message using the following command.

SELECT onam, status, message FROM DBA_REPCATLOG ;

When DBA_REPCATALOG view is empty then we need to Resume the activity using the following procedure.

BEGIN

DBMS_REPCAT.RESUME_MASTER_ACTIVITY (

gname => 'clinton_repg');

END;

We can check the status of the DBA_REPGROUP using the following command.

SELECT SNAME, MASTER, STATUS FROM DBA_REPGROUP;

At first the status will be **quiesced** but the system is not ready for the replication until the status is NORMAL. And another interesting thing is that before '**Normal'** that means when the status is **quiesced** at that time no DDL command is accepted.

D. Setting up Materialized View Sites

In Our example for the Greeting Cards Company, Manchester and Wales sites are the Materialized view site. The steps are same that we follow for the master definition site. Except the following

D.1 Create Materialized View Logs on Master

Here we are showing one as an example

CREATE MATERIALIZED VIEW LOG ON clinton.SHELF

WITH PRIMARY KEY

INCLUDING NEW VALUES;

D.2 Create a Refresh Group

BEGIN

DBMS_REFRESH.MAKE (

name => 'clinton_mviewadmin.clinton_refg',

list => '',

next_date => SYSDATE,

interval => 'SYSDATE + 1/24',

implicit_destroy => FALSE,

rollback_seg => '',

push_deferred_rpc => TRUE,

refresh_after_errors => FALSE);

END;

D.3 Add Objects on the Materialized View Group

Here we are showing one as an example

CREATE MATERIALIZED VIEW CLINTON.STORE

REFRESH FAST WITH PRIMARY KEY FOR UPDATE

AS select * from CLINTON.store@londondb where store_id='CLISTO19102008000002';

D.4 Add Objects to the Refresh Group

Here we are showing one as an example

BEGIN

DBMS_REFRESH.ADD (

name => 'clinton_mviewadmin.clinton_refg',

list => 'CLINTON.STORE',

lax => TRUE);

END;

VII. IMPLEMENATION

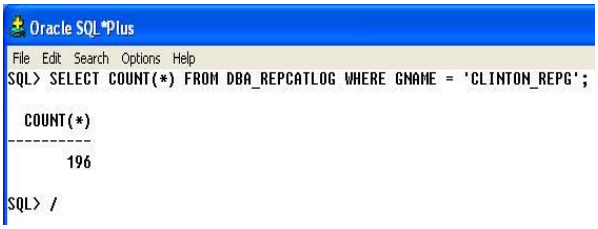

Figure 6: shows the number of objects in the DBA_REPCATLOG.

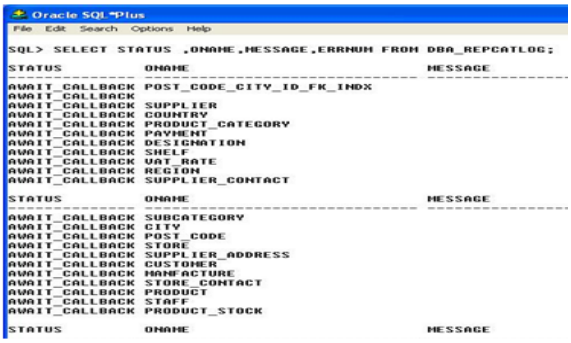

Figure7: Partial output that showing the status of the object in the DBA_REPCATLOG

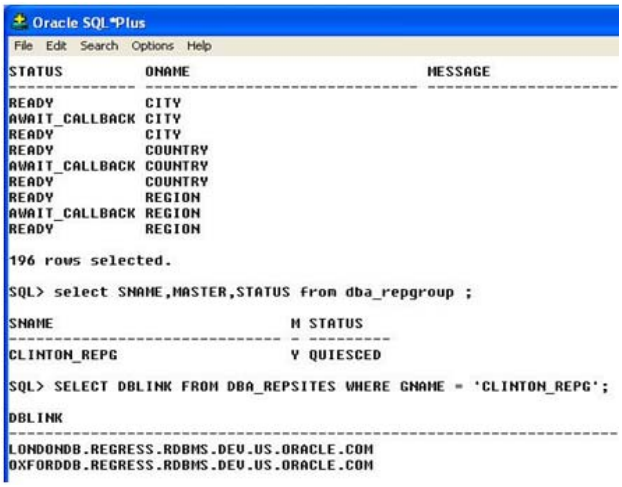

Figure 8: showing the database link and how many master sites are exists and also showing the status of the DBA_REPGROUP

VIII. CONCLUSION

Replication is one of the main techniques to improve avail ability and performance in distributed systems. In this paper we have introduced Synchronous Hybrid replication technique for managing massively distributed replicas. We have shown how Hybrid technology work in real life base of a real case study of a Greeting Card's Company and all experiments reported in this paper were performed using ORACLE environment. The main strength of Hybrid replication is that if one node is failed then others node will be active and can work without interruption and zero data loss is guaranteed in Synchronous approach because of a data storage write is not committed back to an application until both the primary and secondary storage nodes have acknowledged the writes.

REFERENCES

[1] *Data Replication Tools and Techniques for Managing Distributed Information, Marie Buretta*, Wiley Computer Publishing,

[2] Bhagwan, R., Moore, D., Savage, S., and Voelker, G. *Replication strategies for highly available peer-to-peer storage*. In Fudico (2003).

[3] Gray, J., Helland, P., O'Neil, P., and Shasha, D. *The dangers of replication and a solution, In ACM SIGMOD* (1996), pp. 173{182. [18] Page, T. W., Jr., Guy, R. G., Heidemann, J. S.

[4] Ratner, D. H., Reiher, P. L., Goel, A., Kuenning, G. H., and Popek, G. *Perspectives on optimistically replicated peer-to-peer* { Practice and Experience 11, 1 (1997).

[5] Saito, Y., and Shapiro, M. *Optimistic replication. Computing Surveys* 37, 1 (2005)

[6] Martin Zahn, *Oracle Replication Survival Guide* , Akadia AG, 25.09.2005

Proceedings of 2009 12th International Conference on Computer and Information Technology (ICCIT 2009)
21-23 December, 2009, Dhaka, Bangladesh

Design of Meandering Probe Fed Microstrip Patch Antenna for Wireless Communication System

Mohammad Tariqul Islam, Mohammed Nazmus Shakib†, Norbahiah Misran†
Institute of Space Science (ANGKASA), Universiti Kebangsaan Malaysia, 43600 UKM Bangi, Selangor Darul Ehsan, Malaysia
†Dept. of Electrical, Electronic & Systems Engineering, Universiti Kebangsaan Malaysia, 43600 UKM Bangi, Selangor Darul Ehsan, Malaysia
titareq@yahoo.com, engmdns@yahoo.com, bahiah@vlsi.eng.ukm.my

Abstract

A wideband, low cross-polarization patch antenna fed by meandering probe is presented in this paper. The patch antenna consists of inverted patch structure with air-filled dielectric, slotted patch and meandering probe. The composite effect of integrating these techniques and by introducing the proposed patch, offer a low profile, broadband, high gain, and low cross-polarization level. The results for the VSWR and co-and cross-polarization patterns are presented. The antenna operating the band of 1.84-2.29 GHz shows an impedance bandwidth (2:1 VSWR) of 22% and a gain of 10.6 dBi with a gain variation of 1.02 dBi. Good radiation characteristics, including cross-polarization level in xz- and yz-plane are -50dB and -23 dB respectively, have been obtained.

Keywords: Microstrip antenna, meandering probe, broadband antenna, low cross-polarization.

I. INTRODUCTION

The explosive growth of wireless system and booming demand for a variety of new wireless application, it is important to design broadband antennas to cover a wide frequency range. The design of an efficient wide band small size antenna, for recent wireless applications, is a major challenge. Microstrip patch antennas have found extensive application in wireless communication system owing to their advantages such as low-profile, conformability, low-cost fabrication and ease of integration with feed-networks [1]. However, conventional microstrip patch antenna suffers from very narrow bandwidth, typically about 5% bandwidth with respect to the center frequency. This poses a design challenge for the microstrip antenna designer to meet the broadband techniques [2], [3].There are numerous and well-known methods to increase the bandwidth of antennas, including increase of the geometry [4]-[6]. However, the bandwidth and the size of an antenna are generally mutually conflicting properties, that is, improvement of one of the characteristics normally results in degradation of the other.

Recently, a patch antenna, which is low in cross-polarization level and wide in impedance bandwidth, designated as the suspended probe-fed plate antenna [7], has been proposed. The antenna has an impedance bandwidth of 20%. However, it was pointed out [7] that using a higher patch height could cause a higher cross-polarization level. Also, the antenna gain is only 5 dBi, which is lower than other wide-band patch antennas [4], [5]. Some other techniques as utilizing the shorting pins or shorting walls on the unequal arms of a U-shaped patch, U-slot patch, or L-probe feed patch antennas, wideband and dual-band impedance bandwidth have been achieved with electrically small size in [8], [9]. However, these techniques result in high cross-polarization radiation. High cross-polarization not only leads to a distortion in the co-polarization pattern, but also reduces the gain of the antenna.

In this paper, a new patch antenna incorporated as a W-shape patch with meander probe fed is investigated for enhancing the impedance bandwidth, low cross-polarization and high gain characteristics. The design employs contemporary techniques namely, the meander probe feeding, inverted patch, and proposed patch techniques to meet the design requirement. A better cross-polarization is achieved compared to the design reported in [10].

II. ANTENNA DESIGN AND ANALYSIS

Fig. 1 depicts the geometry of the proposed patch antenna. The inverted rectangular patch is designed according to the specified central frequency by using the following equations [11]:

$$w = \frac{c}{2f_o}\sqrt{\frac{\varepsilon_r + 1}{2}} \tag{1}$$

$$l = \frac{c}{2f_o\sqrt{\varepsilon_e}} - 2\Delta l \tag{2}$$

Where w is the width of the patch, l is the length of the patch, f_O is center frequency, c is the speed of light in a vacuum and the effective dielectric constant can be calculated by the equation:

978-1-4244-6283-4/09/$26.00 ©2009 IEEE

$$\varepsilon_e = \frac{\varepsilon_r + 1}{2} + \frac{\varepsilon_r + 1}{2}\sqrt{\left(1 + \frac{10h}{w}\right)} \qquad (3)$$

Where ε_r is the dielectric constant of the superstrate, ε_e is the effective dielectric constant and h is the thickness of the substrate. The fringing field around the periphery of the patch electrically makes the antenna larger than its physical dimensions. Δl takes this effect in account and can be expressed as:

$$\Delta l = 0.412h\frac{(\varepsilon_r + 0.3)(w/h + 0.264)}{(\varepsilon_e - 0.258)(w/h + 0.8)} \qquad (4)$$

The location of the probe point example, if (x_1, y_1) for matching to 50 ohm can be determined as

$$x_1 = \frac{w}{2} \qquad (5)$$

$$y_1 = \frac{l}{\pi}\cos^{-1}\frac{w\sqrt{5(\varepsilon_r - 1)}}{3\varepsilon_r l} \qquad (6)$$

where $0 \le y_1 < l/2$ [12].

While for a microstrip antenna, it is found that the patch length can still be designed using formulas (1) to (6) for the required resonant frequency. However, the patch width calculated by formula (1) usually needs to be widen to ensure the excitation and matching using the probe feed.

In this design, the inverted rectangular patch is supported by a low dielectric superstrate with dielectric permittivity ε_r and thickness h. An air-filled substrate is sandwiched between the superstrate and a ground plane. The proposed patch slots are on the same radiating element appear like a W-shape patch. The proposed patch slots are shown in Fig. 1(a), where, l and w are the length and width of the slots. The slots (outer widths as w_1) are embedded in parallel on the radiating edge of the patch symmetrically with respect to the centerline (x-axis) of the patch for enhancing the antenna bandwidth. The extra slot (outer width as w_2) is included to reduce the size of the patch. The proposed patch is fed by a meandering probe along the centerline (x-axis) of the patch as shown in Fig. 1(b).Table 1 shows the optimized design parameters obtained for the proposed patch antenna. A dielectric substrate with dielectric permittivity, ε_r of 2.2 and thickness, h of

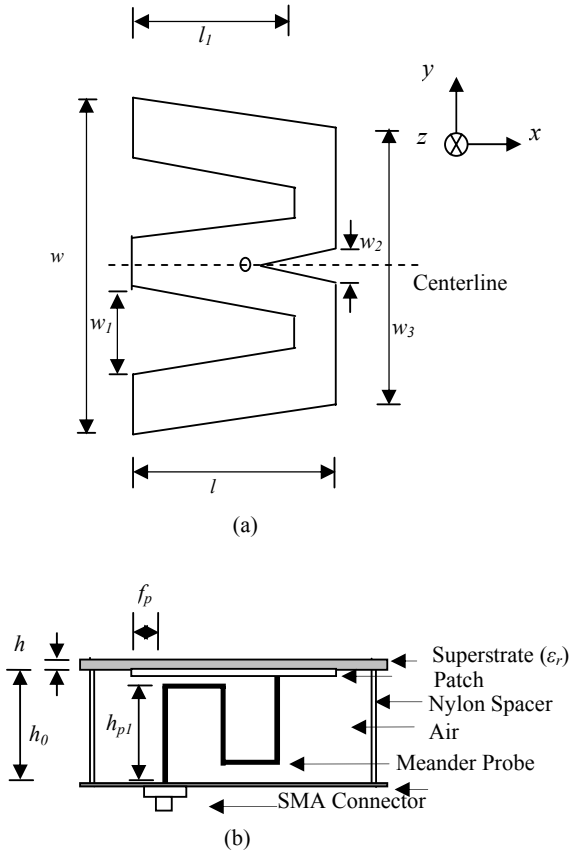

Fig. 1. Geometry of the Proposed Antenna: a) Top view, b) Side view.

Table I Proposed patch antenna design parameters

Dimensions (mm)	w	l	w_1	l_1	w_2
	76	50	18	40	6
Dimensions (mm)	w_3	h	h_0	h_{p1}	f_p
	66	1.5748	16	14	8

1.5748mm has been used in this research. The thickness of the air-filled substrate, h_o is 16 mm. An aluminum plate with dimensions of $1.393\,\lambda_0 \times 1.254\,\lambda_0$ (where λ_0 is the guided wavelength of the centre operating frequency) and thickness of 1 mm is used as the ground plane. The proposed patch has a simple structure with dimension of $0.516\,\lambda_0 \times 0.38\,\lambda_0$. The proposed antenna is designed to operate at 1.84 GHz to 2.29 GHz region. In this design, the use of a thick air-filled substrate in between the radiating patch and the ground plane provides the bandwidth enhancement, while the application of superstrate with inverted radiating patch offers a gain enhancement. The use of superstrate on the other hand would also provide the necessary protections for the

patch from the environmental effects. The use of meandering probe fed reduces cross-polarization level. In the design, the vertical portions of the meandering probes excite constructively to co-polarization but destructively to cross-polarization. The horizontal portions of the meandering probe incorporated with the radiating patch and the ground plane introduce capacitances. These capacitances can suppress some of the inductance contributed by the vertical portions of the probe and hence, achieve low cross-polarization. In addition, the antenna has better cross-polarization in comparison with the slotted antenna described in [10].

III. RESULTS AND DISCUSSIONS

The resonant properties of the proposed antenna have been predicted and optimized using of a commercial software package HFSS™ v11. It is measured by an Agilent 8753ES analyzer. Fig. 2 shows the simulated and measured results of VSWR of the proposed patch antenna. The two closely excited resonant frequencies at 1.88 GHz and at 2.16 GHz as shown in the figure gives the measure of the wideband characteristic of the patch antenna. The measured impedance bandwidth of 21.79% from 1.84 GHz to 2.29 GHz is achieved at 10 dB return loss (VSWR≤2) while the simulated patch gives an impedance bandwidth of 24.88% (1.83-2.35GHz). The slightly mismatch in between simulation and measured results at second resonant occurs due to fabrication complexity of meandering probe feed. The wide-band characteristic is due to large separation

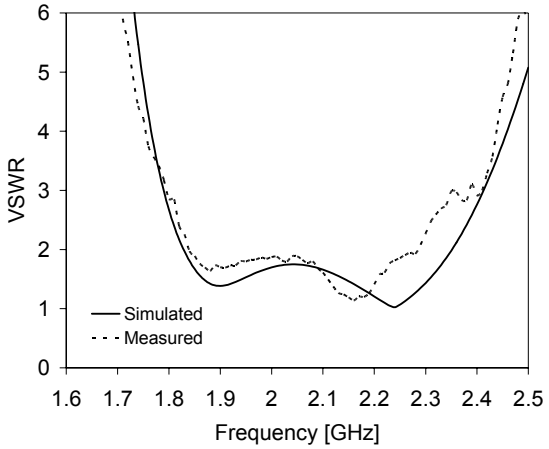

Fig. 2. VSWR of proposed antenna.

between the radiating patch and the ground plane, and due to the use of a low permittivity substrate with the proposed design. Fig. 3 shows the simulated *xz*-plane and *yz*-plane radiation pattern of the proposed antenna at 1.88 GHz. For the sake of brevity, only simulated radiation pattern for first resonant frequency is given in this paper. As shown in figure, the designed antenna displays good broadside radiation patterns in the *xz*-plane and *yz*-plane. It can be seen that 3-dB beamwidth of 64º and 58º for *xz*-plane and *yz*-plane respectively at 1.88 GHz. The peak cross-polarization level of the antenna is observed to be about -50dB and -23dB below the copolarization level of the main lobe at *xz*-plane and *yz*-plane respectively at the frequency of 1.88 GHz. The proposed patch antenna exhibits better cross polarization than the design reported in [10]. Notable, the radiation characteristics of the proposed patch antenna are better to those of the conventional patch antenna. The radiation patterns at other bands, which are similar to those at 2.16 GHz, are not presented here in detail

.

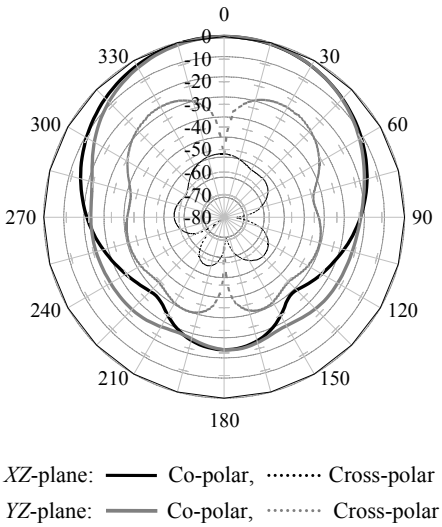

Fig. 3. Radiation pattern of the proposed antenna at 1.89 GHz.

The simulated gain of the proposed patch antenna at various frequencies is shown in Fig. 4. As shown in the figure, the maximum achievable gain is 10.6 dBi at the frequency of 2.27 GHz and the gain variation is 1.02 dBi between the frequency ranges of 1.84 GHz to 2.29GHz.

In Fig. 5, a parametric study on the proposed antenna has been performed to investigate the effects of the antenna parameters on the impedance matching. The width of the slot (w_1) on the patch equals 18 mm is used in the reference model. It can be observed that the upper and lower resonant frequency are matched with increasing of slot width. But, with decreasing slot width experiences lowest resonant at the expense of reducing the upper edge frequency. Hence, an optimal value of w_1 =18 is chosen in this design.

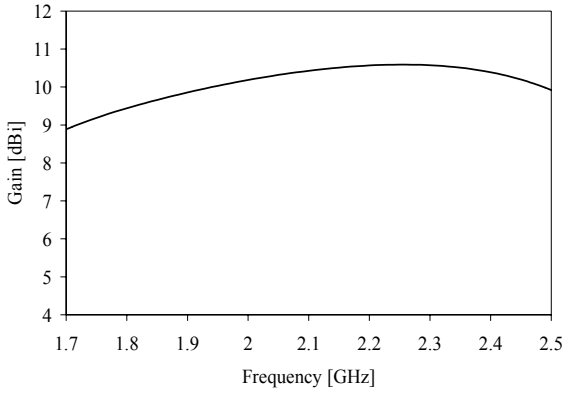

Fig. 4. Gain of proposed patch antennas at different frequencies.

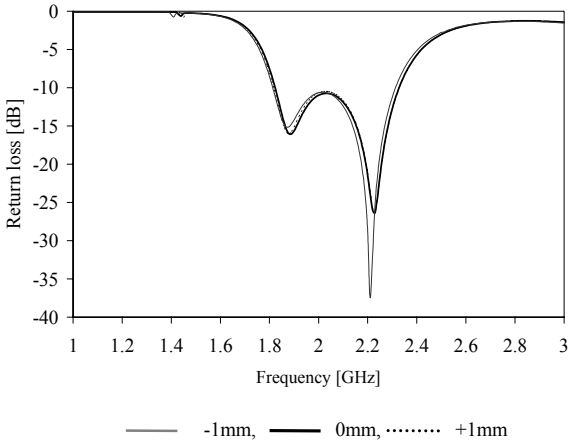

Fig. 5. Effect on return loss of different slot width *(w_1)* of the proposed patch.

IV. CONCLUSIONS

In this paper, a meandering probe fed patch antenna has been designed and developed. Results indicate that a 21.79% fractional impedance bandwidth is achieved with respect to the centre frequency of 2.065 GHz. In addition, good antenna gain and radiation characteristics have also been obtained. The proposed patch has a simple structure with dimension of $0.516\,\lambda_0 \times 0.38\,\lambda_0$. Techniques for microstrip broadbanding, size reduction, and cross-polarization reduction are applied with significant improvement in the design by employing proposed patch design, inverted patch, and meandering probe feeding.

V. ACKNOWLEDGEMENT

The authors would like to thank Institute of Space Science (ANGKASA), Universiti Kebangsaan Malaysia (UKM) and the MOSTI Secretariat, Ministry of Science, Technology and Innovation of Malaysia, e-Science fund: 01-01-02-SF0376, for sponsoring this work.

REFERENCES

[1] W. He, R. Jin, and J. Geng, "E-Shape patch with wideband and circular polarization for millimeter-wave communication," *IEEE Trans. Antennas Propag.*, vol. 56, no. 3, 2008, pp. 893-895.

[2] K. L. Lau, K. M. Luk, and K. F. Lee, "Design of a circularly-polarized vertical patch antenna," *IEEE Trans. Antennas Propag.*, vol. 54, no. 4, 2006, pp. 1332-1335.

[3] H. W. Lai and K. M. Luk, "Wideband patch antenna with low cross-polarization," *Electron. Lett.*, vol. 40, 2004, pp. 159–160.

[4] M. M. Matin., B. S. Sharif, and C. C. Tsimenidis, "Probe fed stacked patch antenna for wideband applications," *IEEE Trans. Antennas Propag.*, vol. 55, no. 8, 2007, pp. 2385-2388.

[5] S. H. Wi, Y. B. Sun, I. S. Song, S. H. Choa, I. S. Koh, Y. S. Lee, and J. G. Yook, "Package-Level integrated antennas based on LTCC technology," *IEEE Trans. Antennas Propag.*, vol. 54, no. 8, 2006, pp. 2190-2197.

[6] S. H. Wi, J. M. Kim, T. H. Yoo, H. J. Lee, J. Y. Park, J. G. Yook, and H. K. Park, "Bow-tie-shaped meander slot antenna for 5 GHz application," in *Proc. IEEE Int. Symp. Antenna Propag.*, vol. 2, 2002, pp. 456–459.

[7] Z. N. Chen and M. Y. W Chia, "Broad-band suspended probe-fed plate antenna with low cross-polarization levels," *IEEE Trans. Antennas Propag.*, vol. 51, 2003, pp. 345–346.

[8] R. Chair , C. L. Mak, K. F. Lee, K. M. Luk, and A. A. Kishk, "Miniature wide-band half U-slot and half E-shaped patch antennas," *IEEE Trans. Antennas Propag.*, vol. 53, 2005, pp. 2645-2652.

[9] C. L. Mak, K. M. Luk, K. F. Lee, and Y. L. Chow, "Experimental study of a microstrip patch antenna with an L-shaped probe," *IEEE Trans. Antennas Propag.*, vol. 48, 2000, pp. 777–783.

[10] M. Tariqul Islam, N. Misran, and K. G. Ng, "A 4×1 L-probe fed Inverted Hybrid E-H Microstrip Patch Antenna Array for 3G Application," American Journal of Applied Sciences, vol. 4, no. 11, 2007, pp. 897-901.

[11] K. Hirasawa, *Analysis, Design, and Measurement of Small and Low- Profile Antennas. Norwood*, MA: Artech House, 1991, ch. 4.

[12] W. L. Stustzman and G. A. Thiele, *Antenna Theory and Design*. New York: Wiley, 1998.

Proceedings of 2009 12th International Conference on Computer and Information Technology (ICCIT 2009)
21-23 December, 2009, Dhaka, Bangladesh

Evaluation of Performances of Digital Adaptive Filters in Acoustic Echo Cancellation

Md. Anamul Haque, A.K.M. Kamrul Islam, Md. Imdadul Islam
Department of Computer Science and Engineering, Jahangirnagar University, Savar, Dhaka-1342, Bangladesh
kamrul@iubat.edu, imdad@juniv.edu

Abstract

Wireless network link is debilitated by fading, attenuation, non-linear distortion and noise. Analogically sound system in a conference room shows similar phenomena due to the fact that the reflected feedback signals resemble the multi-path propagation of wireless communication; exception is that the noise level is very low. The signal path of the feedback signal is a non-linear system can be replaced by a finite impulse response filter. The aim of the paper is to compare the performance of three well known adaptive filters (Frequency Domain Adaptive Filter, Least Mean Square Filter, Kalman Filter) in context of echo cancellation under adaptive white Gaussian noisy environment.

Keywords: Predictor-corrector algorithm, FDAF, near and far-end signal and Kalman equation.

I. INTRODUCTION

In wireless communication, the transmitted signal from any source may traverse through multiple paths towards the receiver. Such propagation happens by the obstruction or reflection of natural barriers such as ground, buildings, vehicles, hills at different atmospheric levels [1]-[2]. As a result of such propagation, the receiver receives multiple copies of same signal each of different physical length. Each signal experiences different noise, attenuation, phase shift and delay [3]-[4]. Sound system in a conference room resembles the consequences of wireless transmission [5]. A voice signal been sent by one participant come out from the speaker propagates through multiple paths and echoed back from the conference room walls crossing multiple directions yield the distortion of root voice signal of the microphone. The distinguishing feature between the two analogous systems is that the feedback signal in acoustic echo cancellation retains less signal length and also low strength. The goal of the paper is to learn the performances of digital adaptive filters through evaluation. Frequency domain adaptive filter (FDAF) has an adaptable feature riding which the coefficients of the signal continually adjust. At every time state the input signal is estimated and after processing error signal is generated and refine the coefficients of the estimated signal. Least mean square (LMS) filter uses the instantaneous estimates of its weights where FDAF uses weight vector gained from all the previous estimates. Kalman Filter is widely used due to its recursive strategy to estimate the current state of the process from the previous measurement update in a way that would keep the mean square error minimized.

II. ADAPTIVE FILTER THEORY

A. Least Mean Square Filter Concept

LMS is based on the steepest descent algorithm. Two basic processes work behind the LMS filtering algorithm [6]: *filtering process*- calculates the output response of the filter relating to the input signal and generates an estimation signal subtracting the output from the desired signal and *adaptive process* adjusts the parameters based upon the error signal [7]. Weight update vector at time *k+1* should be as follows:

$$W_{k+1} = W_k - \mu \nabla_k \quad (1)$$

Where W_k is the *k*-th weight vector, ∇_k is the gradient vector composed in (1) and μ controls the rate of convergence. Replacing the value of ∇_k ,

$$W_{k+1} = W_k + 2\mu (P - RW_k) \quad (2)$$

But as LMS uses the instantaneous estimates [6] *P* and *R* of (2) will be substituted by the values:

$$P = y_k X_k \qquad R = X_k X_k^T$$

Corresponding weight update W_{k+1} is:

$$W_{k+1} = W_k + 2\mu (y_k X_k - X_k X_k^T W_k)$$

$$= W_k + 2\mu X_k (y_k - W_k^T X_k)$$

$$= W_k + 2\mu e_k X_k$$

Where $e_k = y_k - W_k^T X_k$ (3)

Iteratively, it learns signal characteristics and keeps the error (3) minimized. In this way, with the lapse of time it provides good adaptability.

B. Theory of Frequency Domain Adaptive Filter

Some essential development likely in 'Acoustic Echo Cancellation in Teleconferencing' a long impulse response apparently mixes with the echo duration [8]. This claims to have a long memory and increases the complexity of computation. LMS filter cannot resolve this problem [7]. Transforming the system of interest to the frequency domain simply by Fourier transform

mapping reduce the computational complexity. A mathematical implementation of block FIR filter has adopted below [9]:

Let *L* is the length of the block and *M* is the length of tapped weight vector.

Data matrix,

$$A(k) = \begin{bmatrix} u(kL).....u(kL-1).....u(kL-M+1) \\ u(kL+1).....u(kL).....u(kL-M+2) \\ ..... \\ u(kL+L+1)..u(kL+L-2)....u(kL+L-M) \end{bmatrix} = \begin{bmatrix} G(kM) \\ G(kM+1) \\ ... \\ G(kM+L-1) \end{bmatrix} \quad (4)$$

A(k) is a $L \times M$ matrix [9] shown in (4) and length of vector $G^T(kM)$ is *M*. Let the weight vector,

$$\hat{W}(k) = [w_0(k) \quad w_1(k) ... \quad ... \quad ... \; w_{L-1}(k)]^T \quad (5)$$

Output vector of the filter written in (6), would be the multiplication of *A(k)* and weight vector $\hat{W}(k)$ written in (4) and (5) respectively,

$$[y(kL)..... y(kL+1)..... y(kL+L-1)]^T = A(k).\hat{W}(k) \quad (6)$$

For individual element,

$$y(kL) = G(kM).\hat{W}(k)$$

$$y(kL+1) = G(kM+1).\hat{W}(k)$$

……

$$y(kL+i) = G(kM+i).\hat{W}(k)$$

$$= [w_0(k) \quad w_1(k) \quad w_2(k) ... \quad ... \quad ... \; w_{L-1}(k)] \cdot$$

$$[u(kL+i) \quad u(kL+i-1) \quad ... \quad u(kL+i+M-1)]^T$$

$$= \sum_{j=0}^{M-1} w_j(k).u(kL+i-j) \quad (7)$$

y(kL+ i) is the i-th output vector disposed in (7). Let the desired response of *(kL+i)*th element is *d(kL+i)*. Therefore the error signal, *e(kL+i) = d(kL+i) - y(kL+i).* In matrix form,

$$e(k) = \begin{bmatrix} d(kL) \\ d(kL+1) \\ d(kL+2) \\ ... \\ ... \\ ... \\ d(kL+L-1) \end{bmatrix} - \begin{bmatrix} y(kL) \\ y(kL+1) \\ y(kL+2) \\ ... \\ ... \\ ... \\ y(kL+L-1) \end{bmatrix} = \begin{bmatrix} e(kL) \\ e(kL+1) \\ e(kL+2) \\ ... \\ ... \\ ... \\ e(kL+L-1) \end{bmatrix} \quad (8)$$

The cross correlation vector is the multiplication of the error vector *e(k)* in (8) with the transpose of data matrix A^T,

$$\Phi(k) = A^T(k)e(k) \quad (9)$$

The update equation of weight vector can be achieve by adding constant multiplication of correlation vector (9),

$$\hat{W}(k+1) = \hat{W}(k) + \mu\Phi(k) \quad (10)$$

By continuing this technique, all the vector coefficients will be updated for each *(k+i)* th term as stated in (10) for *(k+1)* th.

C. Kalman Filter Concepts

One step predictor is the key of mathematical formulation of Kalman filter [10]. It predicts state space while introducing new observation *y(n)* in the input [10]. At the end of processing of *y(n),* it calculates the error covariance of prediction and updates the mean square estimation for the imminent operation. As an inherent part of correction of predict, Kalman gain *G(n)* works along with the new observation *α(n)*. For this reason, Kalman filter is also known as the predictor-corrector algorithm [10]. Mathematical equations of Kalman Filter which are also known as kalman equations mentioned below along with their respective details.

Kalman gain equation in (11) is:

$$G(n) = F(n+1,n)K(n,n-1)C^H(n)R^{-1} \quad (11)$$

Where error correlation matrix *k(n, n-1)* can be defined by the expectation of the error correlation matrix of previous time unit.

$$K(n,n-1) = E[\in(n,n-1) \in^H (n,n-1)] \quad (12)$$

ε (n, n-1) is the predicted state-error vector at time *n* [10]

The inverse of the correlation matrix of innovations $R^{-1}(n)$ in (13) is described by multiplication of the previous error vector *k(n, n-1)*(12) with correlation of measurement matrix[10] *C(n)* in presence of relevant Gaussian measurement noise (A white noise added by Gaussian distribution). Explicitly it is:

$$R^{-1}(n) = [C(n)K(n,n-1)C^H(n) + Q_2(n)]^{-1} \quad (13)$$

As a detection of the *innovation* i.e. the new information of observation *y(n)* can be calculated as in (14):

$$\alpha(n) = y(n) - C(n)\hat{x}(n \mid y_{n-1}) \quad (14)$$

Time state update of one unit for current use is the result of multiplication of a transition matrix *F(n+1, n)* and previous time state $\hat{x}(n \mid y_{n-1})$ incorporating Kalman gain *G(n)* and innovation *α(n)* as shown in (15). This is the basic prediction equation.

$$\hat{x}(n+1 \mid y_n) = F(n+1,n)\hat{x}(n \mid y_{n-1}) + G(n)\alpha(n) \quad (15)$$

Correction of error correlation matrix of the current time can be obtained by (16):

$$K(n) = K(n,n-1) - F(n,n+1)G(n)C(n)K(n,n-1) \quad (16)$$

In the final part of the calculation, we need to *update the measurement* of the future error correlation matrix *k(n+1, n)*. As an integral part of this, white Gaussian process noise $Q_1(n)$ will be added to it. Mathematical equation has composed in (17)

$$k(n+1,n) = F(n+1,n)K(n)F^H(n+1,n) + Q_1(n) \quad (17)$$

III. ACOUSTIC ECHO CANCELLATION

An acoustic echo cancellation is noise cancellation of a recorded speech signal. A recorded speech signal from the loud speaker returns to the microphone as an echo reflecting from the room and mingled with original speech signal. This signal is also called far-end speech signal. The speaker signal, i.e. the near-end speech signal at the microphone input thus is not uniform and distorted [8]. During the processing of the distorted signal adaptive filter produces the best estimation of the noisy signal. Subtraction of this noisy signal from original signal will solve the problem. Concurrently an error signal will be generated mirroring the difference between the actual signal and our approximation and hence coefficients will be updated.

A. Experimental Setup

Signal inserted in microphone of a hall room is the direct speech signal $d(n)$ of the speaker and echoed signal $\hat{d}(n)$ that arises from the reflection of walls shown in Fig.1. Direct speech signal is called near-end signal (NES) and the echoed signal is called far-end signal (FES). The combined input signal of the microphone, $\mu(n) = d(n) + \hat{d}(n)$. Objective of an echo canceller is to remove the far-end signal so that only near-end signal is sent to the loud speaker. The path or channel between loud speaker and the microphone is represented by a long finite impulse response filter. For an instance, Room environment of an acoustic echo canceller depicted in Fig. 1.

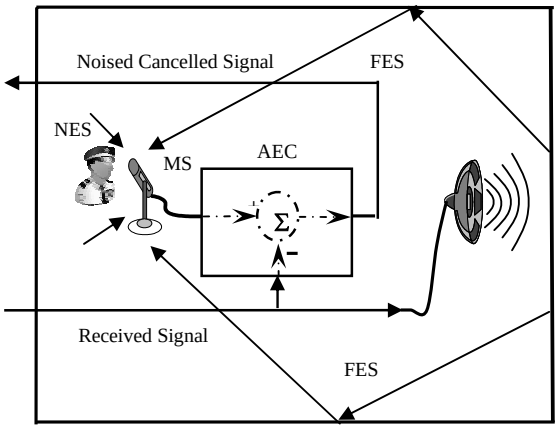

Fig.1: Room environment of Acoustic Echo Canceller

IV. RESULTS

We used *chebyshev2* filter to have the basic channel impulse response of the room. The filter is assumed to be fourth order *(N=4)* and sampling frequency f_s as 8000. Stop-band ripple presumed as 20 and edge frequency W_n will be in the range (*0.1 < Wn < 0.7*). Let us consider number of time sequences *M = 4001*. The time domain and frequency domain views of the system are show in Fig. 2 and 3 respectively.

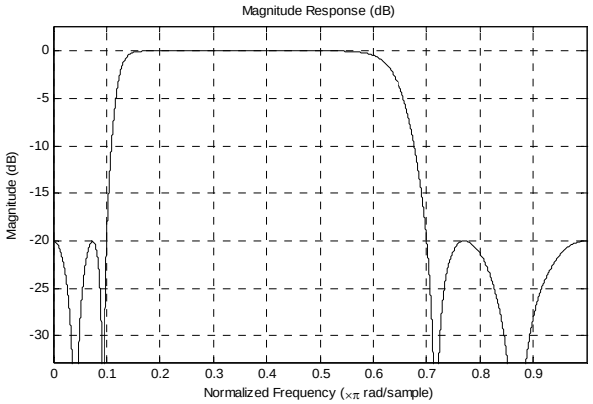

Fig.2: Impulse response of the room (Frequency domain)

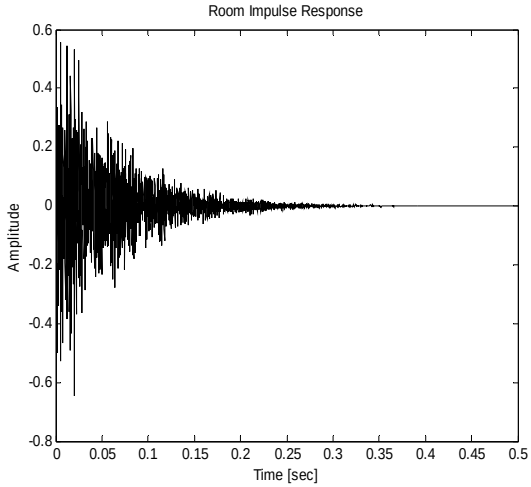

Fig.3: Impulse Response of the room (Time Domain)

Let us observe the performance of three filters considering the signal to noise ratio (*SNR = 45*) and number of samples *15000*. For LMS filter the amplitude of the filtered wave and mean square error estimation illustrated in Fig. 4 and 5 respectively.

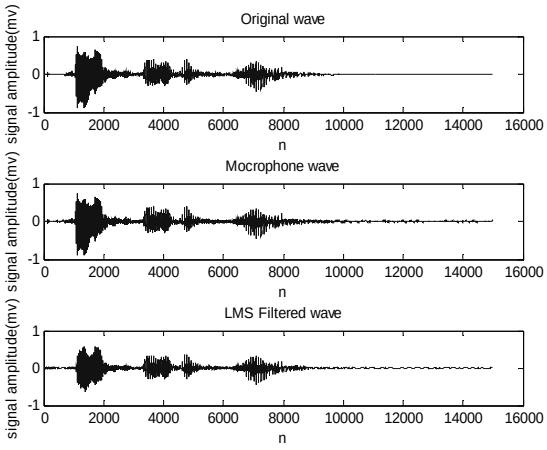

Fig.4: Amplitude comparison of Filtered wave relating to original wave (in milivolts)

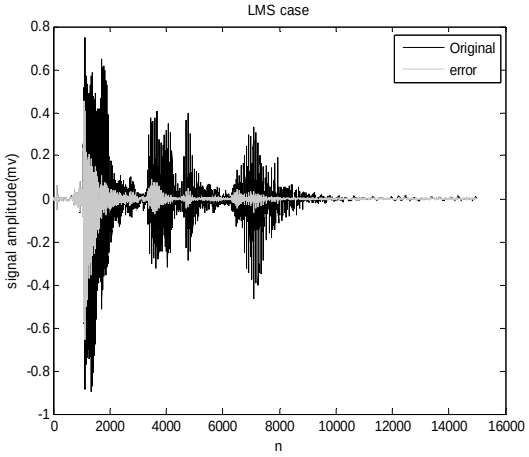

Fig.5: Error in estimation of clean wave relating to original wave (mean error =5.5602×10^{-4}).

The amplitude of the filtered wave and mean square error in error estimation depicted in Fig. 6 and 7 respectively for FDAF.

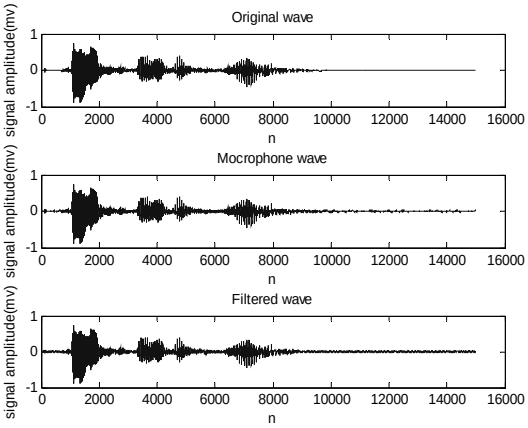

Fig.6: Amplitude comparison of Filtered wave relating to original wave (in milivolts).

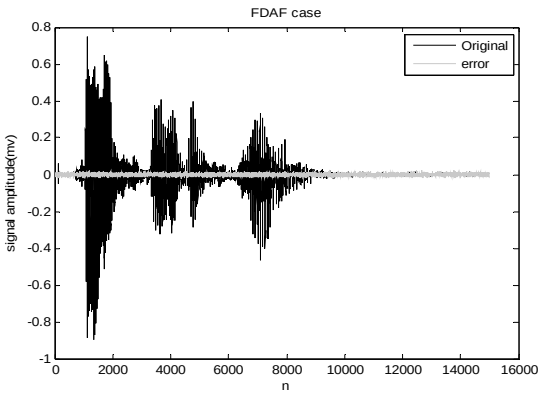

Fig.7: Error in estimation of clean wave relating to original wave (mean error =3.1702×10^{-5}).

The amplitude of the filtered wave and mean square error in error estimation had shown in Fig. 8 and 9 respectively for Kalman filter.

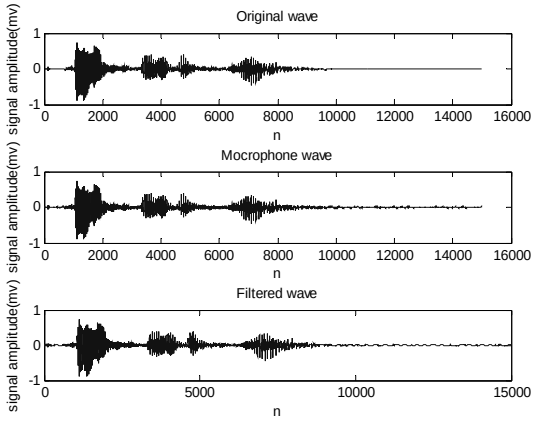

Fig.8: Amplitude comparison of Filtered wave relating to original wave (in milivolts)

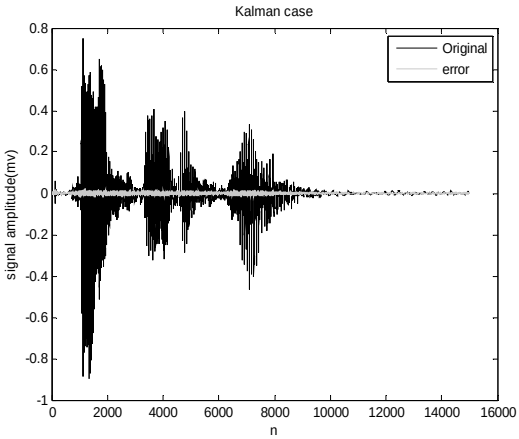

Fig.9: Error in estimation of clean wave relating to original wave (mean error = 1.383×10^{-5}).

Table. I, II and III demonstrates the results of observations of three filters. We portrayed only the observation at *SNR = 45* whereas the table shows the results of sev-

eral *SNR* from 45 to 30. However, all the results conclude the equal inference.

Table I Performances of LMS filter with varying signal to noise (SNR) ratio

SNR(db)	Errors in LMS Filter			
	Max	Min	SD	ET
45	0.4555	5.56e-4	0.0236	0.81
40	0.4541	5.57e-4	0.0236	0.79
35	0.4532	5.64e-4	0.0238	0.79
30	0.4555	5.63e-4	0.0237	0.79

Table II Performances of FDAF filter with varying signal to noise (SNR) ratio

SNR(db)	Errors in FDAF Filter			
	Max	Min	SD	ET
45	0.0234	3.17e-5	0.0056	3.35
40	0.0383	1.00e-4	0.0100	0.43
35	0.0863	3.23e-4	0.0180	0.39
30	0.1213	9.97e-4	0.0316	0.39

Table III Performances of kalman filter with varying signal to noise (SNR) ratio

SNR(db)	Errors in Kalman Filter			
	Max	Min	SD	ET
45	0.0230	1.38e-5	0.0037	3.96
40	0.0344	3.71e-5	0.0061	3.26
35	0.0578	8.63e-5	0.0093	3.15
30	0.0918	2.03e-4	0.0143	3.18

According to the analysis, change in Max error, Mean error and standard deviation (SD) of the mean error of FDAF and Kalman filter with the increase of SNR are mutually related. At the time of *SNR = 45 db* Max error of Kalman filter is *0.0230* which prescribes its good performance whereas for *FDAF* and *LMS* it is *0.0234* and *0.4555* respectively. One important thing to notice is that both FDAF and LMS require less execution time (ET) than Kalman. As the noise increases the max error also increases and ET decreases due to the adaptability. For Kalman filter and FDAF filter max error is inversely proportional to the *SNR*; both of them retain strong convergence but for FDAF, ET falls sharply at SNR *40.* However, in LMS filter error behaviors are unexpected at the starting but at the end its adjustment is good with much less ET.

V. CONCLUSION

We can conclude this paper with subtle differences on the performances of three filters regarding acoustic echo cancellation technique. Besides its aptitude in almost all system; Kalman filter performs best in a heavily noisy system. The only shortcoming of the Kalman filter is its lengthy process time. On the contrary, FDAF and LMS filter both takes comparatively much little time for processing. FDAF uses recurrence relation of all previous observed data and provides good convergence. LMS filter, which contains an easy operational algorithm, is easy to implement than other two. A significant fact is that, at first LMS takes time to adjust its coefficients appropriately but later it provides remarkable performance. Considering all these, in our low noisy acoustic echo cancellation system, thus the best filter is either the Frequency Domain Adaptive Filter or the Least Mean Square Filter.

REFERENCES

[1] Marvin K. Simon, Mohamed-Slim Alouini, "Digital Communication over Fading Channels: A Unified Approach to Performance Analysis", Copyright © 2000 John Wiley & Sons, Inc. ISBN 0-471-31779-9, pp.4-10, pp.15-20.

[2] D. Molkdar, "Review on radio propagation into and within buildings," *IEE Proc. H*, vol. 138, February 1991, pp. 61–73.

[3] Zhiwei Zeng, "Digital Communication via Multipath Fading Channel", Cpre537x Final Project, November 2000, pp.17-22.

[4] J. K. Cavers and P. Ho, "Analysis of the error performance of trellis coded modulations in Rayleigh fading channels*," IEEE Trans. Commun.*, vol. 40, January 1992, pp. 74–80.

[5] P. Yegani and C. McGlilem, "A statistical model for the factory radio channel," *IEEE Trans. Commun.*, vol. COM-39, October 1991, pp. 1445–1454.

[6] E. R. Ferrara, Jr., "Fast Implementation of LMS Adaptive Filter," *IEEE Trans. Acoust.,Speech, Signal Processing*,vol. ASSP-28, pp. 474-475 (1980).

[7] Alexandar D. Poularikas, Zayed M. Ramadan, "Adaptive Filtering Primer with Matlab", CRC-Taylor and Francis, ISBN 0-8493-7043-4, 1999, pp.55-58, pp.101-2

[8] Satoru Emura, Yoichi Haneda, and Shoji Makino, "Enhanced Frequency-Domain Adaptive Algorithm for Stereo Echo Cancellation", *IEEE Transc.* Vol-II, pp.1901-03

[9] J. S. Soo and K. K. Pang, "Multidelay Block Frequency Domain Adaptive Filter," *IEEE Trans. Acoust. Speech, Signal Processing*, vol. ASSP-38, pp. 373-376 (1990).

[10] Greg Welch and Gary Bishop, "An Introduction to the Kalman Filter", TR 95-041, Department of Computer Science University of North Carolina at Chapel Hill, April 5, 2004, pp.3-7.

Proceedings of 2009 12th International Conference on Computer and Information Technology (ICCIT 2009)
21-23 December, 2009, Dhaka, Bangladesh

Automatic Speech Recognition for Bangla Digits

Ghulam Muhammad, Yousef A. Alotaibi, and Mohammad Nurul Huda†
College of Computer & Information Sciences, King Saud University, Riyadh, Saudi Arabia
†Computer Science and Engineering, United International University, Dhaka, Bangladesh
ghulam@ksu.edu.sa, yaalotaibi@ksu.edu.sa, mnh@cse.uiu.ac.bd

Abstract

In this paper, we introduce a system for Bangla digit automatic speech recognition (ASR). Though Bangla is one of the largely spoken languages in the world, only a few works on Bangla ASR can be found in the literature, especially on Bangladeshi accented Bangla. In this work, the corpus is collected from natives in Bangladesh. Mel-frequency cepstral coefficients (MFCCs) based features and hidden Markov model (HMM) based classifiers are used for recognition. Experimental results show comparatively high recognition performance (more than 95%) for first six digits (0 – 5) and low performance (less than 90%) for the next four digits (6 – 9). We notice two confused pairs of digits: one with '৬' (6) and '৯' (9), and the other with '৭' (7) and '৮' (8), in the experiments. We also find that different dialects in Bangladesh have a greater role on this confusion.

Keywords: Automatic speech recognition, Bangla digit, Bangla phoneme, hidden Markov model.

I. INTRODUCTION

There have been many literatures in automatic speech recognition (ASR) systems for almost all the major languages in the world. Unfortunately, only a very few works have been done in ASR for Bangla (can also be termed as Bengali), which is one of the largely spoken languages in the world. More than 215 million people speak in Bangla as their native language. It is ranked seventh based on the number of speakers [1]. A major difficulty to research in Bangla ASR is the lack of proper speech corpus. Some efforts are made to develop Bangla speech corpus to build a Bangla text to speech system [2]. However, this effort is a part of developing speech databases for Indian Languages, where Bangla is one of the parts and is spoken in the eastern area of India (West Bengal). But most of the natives of Bangla (more than two thirds) reside in Bangladesh, where it is the official language. Although the written characters of standard Bangla in both the countries are same, there are some sounds which are produced differently in different pronunciations of standard Bangla. Therefore, there is a need to do research on the main stream of Bangla, which is spoken in Bangladesh, ASR.

Some developments on Bangla speech processing or Bangla ASR can be found in [3]-[10]. For example, Bangla vowel characterization is done in [3]; isolated and continuous Bangla speech recognition on a small dataset using hidden Markov models (HMMs) is described in [4]; recognition of Bangla phonemes by Artificial Neural Network (ANN) is reported in [7]-[8]. Continuous Bangla speech recognition system is developed in [9], while [10] presents a brief overview of Bangla speech synthesis and recognition. However, most of these works are mainly concentrated on simple recognition task on a very small database, or simply on the frequency distributions of different vowels and consonants.

In this paper, we build an ASR system for Bangla digit. For this purpose, we first develop a medium size (compared to the exiting size in Bangla ASR literature) Bangla digit speech corpus comprises of native speakers covering almost all the major cities of Bangladesh. Then we build a Bangla digit ASR system using hidden Markov model toolkit (HTK) [11]. The results are investigated, and a group of confused Bangla digits in terms of ASR is analyzed. It is claimed that this is the first ever work done on Bangla digit ASR.

The paper is organized as follows. Section 2 briefly describes an approximate phonetic scheme for Bangla digits; Section 3 explains about Bangla digit speech corpus; Section 4 gives experimental setup, results and discussion on Bangla digit ASR. Finally, Section 5 draws some conclusions with future direction.

II. PHONETIC SCHEME FOR BANGLA DIGITS

A. Bangla Phonemes

Phonetic inventory of Bangla consists of 14 vowels, including seven nasalized vowels, and 29 consonants. An approximate phonetic scheme in IPA is given in Table I. In Table I (a), only the main 7 vowel sounds are shown, though there exists two more long counterpart of /i/ and /u/, denoted as /i:/ and /u:/, respectively. These two long vowels are seldom pronounced differently than their short counterparts in modern Bangla. There is controversy on the number of Bangla consonants. Apart from the 29 consonants mentioned in the table, we use another one /ɾ/(/ɻ/), which is palatial in place of articulation and approximant in manner.

Native Bangla words do not allow initial consonant clusters: the maximum syllable structure is CVC (i.e. one vowel flanked by a consonant on each side) [12].

Table I. Bangla phonetic scheme in IPA.[1]

(a) Vowel

	Front	Central	Back
Close	i (ই)		u (উ)
Close-mid	e (এ)		o (ও)
Open-mid	æ (অ্যা)		ɔ (অ)
Open		a (আ)	

(b) Consonants

		Labial	Dental	Alveolar	Apico-Postaveolar	Lamino-Postaveolar	Velar	Glottal
Nasal		m (ম)		n (ন)			ŋ (ং)	
Plosive	Voice less	p (প) pʰ (ফ)	t̪ (ত) t̪ʰ (থ)		t (ট) tʰ (ঠ)	ʧ (চ) ʧʰ (ছ)	k (ক) kʰ (খ)	
	Voiced	b (ব) bʰ (ভ)	d̪ (দ) d̪ʰ (ধ)		ɖ (ড) ɖʰ (ঢ)	ʤ (জ) ʤʰ (ঝ)	g (গ) gʰ (ঘ)	
Fricative				s (স)		ʃ (শ)		h (হ)
Liquid				l (ল) r (র)	ɽ (ড়)			

[1]Some parts are extracted from http://en.wikipedia.org/wiki/Bengali_phonology

Table II. Bangla digit pronunciation.

English Digit	Bangla Digit	Pronunciation (Bangla)	IPA
0	০	শূন্য	/ʃu:nno/
1	১	এক	/æk/
2	২	দুই	/d̪ui/
3	৩	তিন	/t̪in/
4	৪	চার	/ʧar/
5	৫	পাঁচ	/pãʧ/
6	৬	ছয়	/ʧʰɔ̯/
7	৭	সাত	/sat̪/
8	৮	আট	/at/
9	৯	নয়	/nɔ̯/

Sanskrit words borrowed into Bangla possess a wide range of clusters, expanding the maximum syllable structure to CCCVC. English or other foreign borrowings add even more cluster types into the Bangla inventory.

B. Bangla Digits

The Bangla script has 10 digits corresponding to the arabic numerals. Table II lists Bangla digits with their written forms and the corresponding ipa. From the table, we can see that '০' (0) and '২' (2) have long /u:/ and short /u/, respectively, though they can be perceived similarly. '৫' (5) has /ã/, which is a nasalized vowel of /a/.

III. BANGLA DIGIT SPEECH CORPUS

At present, a real problem to do experiment on Bangla digit ASR is the lack of proper Bangla digit speech corpus. In fact, such a corpus is not available or at least not referenced in any of the existing literature. Therefore, we develop a medium size Bangla digit speech corpus, which is described below.

A. Speakers

We have selected 50 male (m01-m50) and 50 female (f01 – f50) - a total of 100 speakers for the corpus. All of the speakers are Bangladeshi residents and native speakers of Bangla. The age of the speakers ranges from 16 to 60 years. We have chosen the speakers from a wide area of Bangladesh: 20 from Dhaka (central region), 10 from Comilla – Noakhali (East region), 10 from Chittagong (South-East region), 20 from Rajshahi (West region), 20 from Dinajpur – Rangpur (North-West region), 10 from Khulna (South-West region), and the rest from Sylhet (North-East region). Though all of them speak in standard Bangla, they are not free from their regional accents.

B. Recording

Recording was done in three quiet rooms located at Dhaka, Rajshahi and Dinajpur. All of the three rooms bore the same type of environment. A laptop was used to record the voices using a head mounted close-talking microphone. All of the speakers spoke ten Bangla digits starting from '০'. We recorded 10 trials of each digit from each speaker: 5 trials in quiet condition and 5 trials in typical Bangladeshi office environment, where ceiling fans were switched on and windows were open, and some low level street or corridor noise could be heard. These two types of trials were recorded in two sessions. A total of 50 utterances were recorded from each speaker in quiet condition (5 trials and 10 digits) and 50 utterances in office environment. The experiment of this paper involves only quiet condition utterances.

GoldWave software was used to record the voices [13]. The speech was sampled at 11025 Hz and quantized to 16 bit coding without any compression. The number of channels was 2, and no filter was used on the recorded voice.

IV. BANGLA DIGIT ASR

Research works on Bangla speech recognition starts from the beginning of this new century. Most of these works involve with vowel and consonant characterization, small vocabulary isolated word recognition, small vocabulary continuous speech recognition, and classification using neural networks. All of the experiments are performed on a small size database, not exceeding 15 speakers [3]-[10].

In this section, we present the first ever Bangla digit ASR on a comparatively larger size database with 100 speakers. The following subsections describes the platform, database, parameters, experiments, and results of Bangla digit ASR.

A. Platform

HMMs are a well-known and widely-used statistical method for characterizing the spectral features of speech frame. HMMs provide a natural and highly reliable way of recognizing speech for a wide range of applications. HTK was used in all the experiments reported here.

B. Database

We divide 100 speakers into training and testing sets. 37 male (m01 – m37) and 37 female (f01 – f37) speakers are used as training set and the rest as testing set. All the five trials for each digit in quiet condition are included in corresponding training and testing sets. Hence we have a total of 2×37×5 instances for each digit in the training set and 2×13×5 in the testing set. In both the training and the testing sets, a balanced representation of speakers from different regions (see Section 3) is maintained.

C. Parameters

The system uses the following parameters: 11.025 kHz sampling rate with 16 bit sample resolution, 25 ms Hamming window with a step size of 10 ms, 13 MFCC features with their first and second order derivatives and 0.97 as the pre-emphasis coefficients.

In addition to these monophones, 'silB' and 'silE' are also used to represent silence at the beginning and at the end of an utterance, respectively. As the size of vocabulary is limited to only 10, we use word models for recognition. Training data set is used to design 10 Bangla digit-HMMs with left-to-right organization. A speaker independent Bangla digit recognition test is then carried out using the testing data set. The test is open as no speaker from the training set is used in the testing set. In the experiment, we vary the number of states from nine to 19, and Gaussian mixture components from one to 12 in each state. We find the optimum result with 13 states excluding nonemitting start and end states, and eight mixture components in each state. We fix these parameters for subsequent experiments.

D. Results And Discussion

We evaluate the system based on digit correct rate (%). Fig. 1 shows digit correct rate (%) of the 10 Bangla digits in the system with 13-state HMMs and varied number of Gaussian mixture components. The correct rate increases with the number of mixture components, however after eight components, it again drops in most of the cases. The following description involves with eight mixture components per state. Fig. 1 demonstrates two categories: one that includes the first six digits with correct rate of over 95% and the other, which includes the last four digits, with correct rate of less than 90%. The highest correct rate (100%) is obtained with the digit '২' (2), while the lowest correct rate (84%) is found with '৮' (8). The low accuracy of the second category is due to the confusion of the system between the members of this category, which is described later.

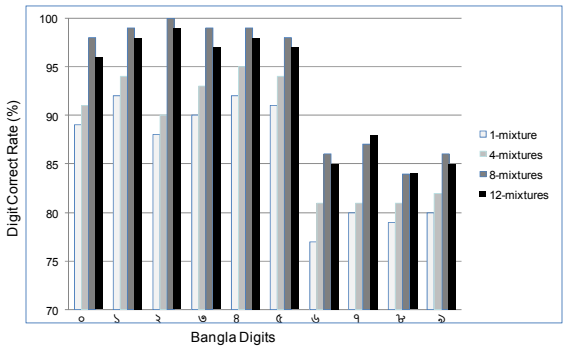

Fig 1. Digit correct rate (%) of Bangla digits in the system.

Table III. 10-digit confusion matrix. The most two confused pairs are: '৬' (6) and '৯' (9); and '৭' (7) and '৮' (8).

Input \ Output	০	১	২	৩	৪	৫	৬	৭	৮	৯
০	98									2
১		99							1	
২			100							
৩				99						1
৪					98			1	1	
৫						98		1	1	
৬							86			14
৭		1						87	12	
৮		2						14	84	
৯			1				13			86

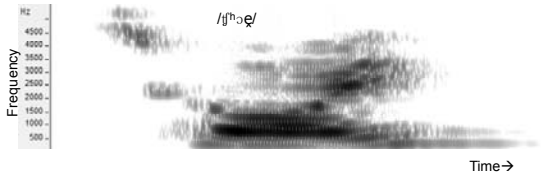

(a) Spectrogram of '৬' (6).

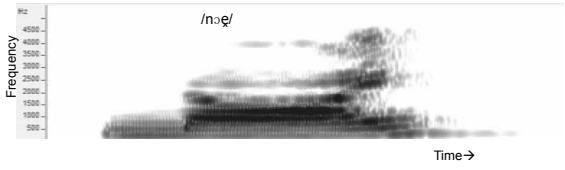

(b) Spectrogram of '৯' (9).

Fig 2. Spectrograms of two confused Bangla digits '৬'(6) and '৯' (9).

Digit '০' (0) has correct rate of 98%, which was reduced to 96% (not shown) while using long /u:/ for its transcription. Optimization of pronunciation dictionary for this digit is thereby justified.

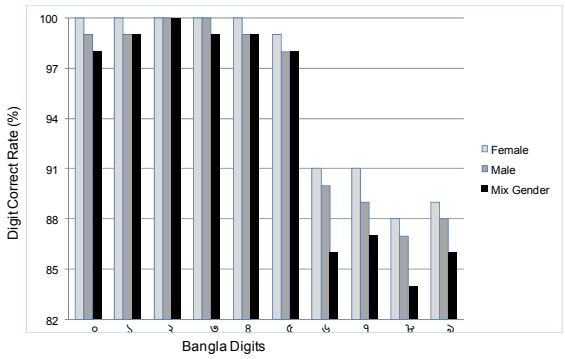

Fig 3. Digit correct rate (%) of Bangla digits in the system (gender dependent). Mix gender result corresponds to the 3rd bar of Fig. 1.

Table III shows confusion matrix generated by the system for all the 10 digits. From the table, we find two most confusing digit pairs: one including digits '৬' (6) and '৯' (9), and the other including digits '৭' (7) and '৮' (8). 14% of '৬' is misclassified as '৯' and 13% of '৯' is misclassified as '৬'. Both of the digits contain long durational phoneme /ɔ/, which contributes most part of the utterances, and different short durational unvoiced parts /ʧ ʰ/ (for '৬') and /n/ (for '৯'). Many of the speakers speak digit '৬' softly without emphasizing the unvoiced parts and this may be a cause for confusion between this pair. Even human listeners sometimes find it difficult to distinguish between softly spoken '৬' and '৯' from long distance. Fig. 2 shows spectrograms of confused pair '৬' and '৯'. From the spectrograms we can see that both digits contain similar phoneme /ɔ/ for most of the part.

Another confusing pair is digits '৭' and '৮'. 12% of '৭' is confused as '৮' and 14% is confused in the reverse direction. Most part of these two utterances has almost similar pattern /at̪/ and /at/. The unvoiced part /s/ in '৭' is very short in duration, and hence sometimes remains undetected. This is one of the reasons for confusion between these two digits.

Fig. 3 gives digit correct rate (%) for gender dependent Bangla digit ASR. 'Mix Gender' in the figure corresponds to the result shown in Fig. 1 with '8-mixtures'. It is obvious than gender dependent ASR has higher correct rate than that with gender independent ASR. In case of female speakers, correct rate for first five digits reaches to 100%, while for male speakers only digits '২' and '৩' have 100% correct rate. From the figure, we can find that, in case of gender dependent, though there is an increase of correct rate for the last four digits, it is still not reaching to the level of the first six digits. Even for some digits within first six, gender dependent cases do not have correct rate of 100%. These observations inspire us to look more insight the last four digits in terms of dialectical difference.

A careful listening of digits uttered by different dialects reveals some clues to improve digit correct rate by the system. For example, many of the natives from

northern part of Bangladesh (Dinajpur – Rangpur) pronounce digit '৪' (4) with nasal voice, which means they pronounce it like /ʧãr/ rather than /ʧar/. In fact, most of the speakers of that region have a tendency to utter with nasalized sound for other digits as well, specially with /a/ sound, for example, /sã͡t/, /ãt/, /æ̃k/. This dialectical difference causes comparatively lower accuracy in ASR for these digits. A preliminary experiment excluding all the utterances from northern region shows a significant improvement of correct rate specially for the digits '৫', '৭', and '৮' (results not shown in figure or table). Therefore, adaptation of different dialects in Bangla digit ASR is our near future goal.

V. CONCLUSION

A Bangla digit ASR system was proposed after developing a medium size Bangla digit speech corpus. The first six digits showed higher accuracy than that of the last four digits. We found two confusing pairs ('৬' (6) and '৯' (9)), and ('৭' (7) and '৮' (8)) in the system. Dialectical difference caused a part of performance degradation. In case of gender dependent experiments, female spoken digits had higher correct rates than those by male spoken digits. In a future work, we will work on adaptation of different dialect in Bangla digit ASR.

REFERENCES

[1] R. Gordon, "Ethnologue: Languages of the World," 15th Ed., SIL International, Texas, 2005.

[2] S. P. Kishore, A. W. Black, R. Kumar, and Rajeev Sangal, "Experiments with unit selection speech databases for Indian languages," Carnegie Mellon University.

[3] S. A. Hossain, M. L. Rahman, and F. Ahmed, "Bangla vowel characterization based on analysis by synthesis," Proc. WASET, vol. 20, pp. 327-330, April 2007.

[4] M. A. Hasnat, J. Mowla, and Mumit Khan, " Isolated and Continuous Bangla Speech Recognition: Implementation Performance and application perspective, " in *Proc. International Symposium on Natural Language Processing* (*SNLP*), Hanoi, Vietnam, December 2007.

[5] R. Karim, M. S. Rahman, and M. Z Iqbal, "Recognition of spoken letters in Bangla," in *Proc. 5th International Conference on Computer and Information Technology (ICCIT02)*, Dhaka, Bangladesh, 2002.

[6] A. K. M. M. Houque, "Bengali segmented speech recognition system," Undergraduate thesis, BRAC University, Bangladesh, May 2006.

[7] K. Roy, D. Das, and M. G. Ali, "Development of the speech recognition system using artificial neural network," in *Proc. 5th International Conference on Computer and Information Technology (ICCIT02)*, Dhaka, Bangladesh, 2002.

[8] M. R. Hassan, B. Nath, and M. A. Bhuiyan, "Bengali phoneme recognition: a new approach," in *Proc. 6th International Conference on Computer and Information Technology (ICCIT03)*, Dhaka, Bangladesh, 2003.

[9] K. J. Rahman, M. A. Hossain, D. Das, T. Islam, and M. G. Ali, "Continuous Bangla speech recognition system," in *Proc. 6th International Conference on Computer and Information Technology (ICCIT03)*, Dhaka, Bangladesh, 2003.

[10] S. A. Hossain, M. L. Rahman, F. Ahmed, and M. Dewan, "Bangla speech synthesis, analysis, and recognition: an overview," in *Proc. NCCPB,* Dhaka, 2004.

[11] S. Young, et al, The HTK Book (for HTK Version. 3.3), Cambridge University Engineering Department, 2005. http:///htk.eng.cam.ac.uk/protdoc/ktkbook.pdf.

[12] C. Masica, *The Indo-Aryan Languages*, Cambridge University Press, 1991.

[13] GoldWave v5.25, available at http://www.goldwave.com/

Proceedings of 2009 12th International Conference on Computer and Information Technology (ICCIT 2009)
21-23 December, 2009, Dhaka, Bangladesh

A Modified 2-D Logarithmic Search Technique for Video Coding With Reduced Search Points

Tahmina Akhtar†, Rahima Akter†, Chhalma Sultana Chhaya†, Ashfaqur Rahman‡
† Military Institute of Science and Technology/Dept of CSE, Dhaka, Bangladesh
‡ Central Queensland University/Centre for Intelligent and Networked Systems, QLD, Australia
rekha_antor@yahoo.com, rahima_akter@live.com, s_chhaya_20@yahoo.com, a.rahman@cqu.edu.au

Abstract

Video coding is a process for representing video sequences in a compact manner. A significant step in video coding is searching for similar segments in previous frames and use only the difference information for reconstruction thus reducing space requirement. Different search techniques including Full search and 2-D logarithmic search etc. are used in the current literature. Full search restricts its application because of its computational load. 2D logarithmic search is computationally less expensive although there are some spaces for improvement. In this paper we propose a new search technique by modifying the 2-D logarithmic search that requires less search points with insignificant loss in visual quality. Experimental results demonstrate the effectiveness of the proposed technique.

Keywords: *video coding, 2-D logarithmic search.*

I. INTRODUCTION

Video is a sequence of still images representing scenes in motion. A video is created by capturing a numbers of still images in a short time interval. When these still images are displayed very quickly, it represents the motion of the object in the images.

Video represent the huge amount of data. In order to transfer video data from one place to another efficiently it is required to compress the size of video data. One way to compress the size of video data is *video coding* [1]**Error! Reference source not found.**. The principal goal in the design of a video-coding system is to reduce the transmission rate subject to some picture quality constraint. In transmission side, the first frame (normally called the reference frame) is transmitted as it is and the remaining frames are sent as a function of the reference frame. The frame to be sent is divided into a number of blocks and the best match for the block is looked for in the search window of the reference frame. This processing is called the *search technique* in video coding literature.

There exist a number of video coding techniques including MPEG-1/2/4 **Error! Reference source not found.**[7], H.26X [8] etc. uses search techniques like Full search [1], 2-D logarithmic search **Error! Reference source not found.**, Coarse-Fine-Three-Step search **Error! Reference source not found.**, Conjugate Direction search **Error! Reference source not found.**, and Pyramid search **Error! Reference source not found.**. Each of these search techniques has merits and demerits in their favor. Full search finds the best match for a block as it searches all the candidate positions in the search window. Full search however is computationally expensive and renders difficulty for real time implementation. Some variants exist that applies some heuristics to reduce the candidate search points and reduce the computational complexity although compromising the image quality a bit.

2-D logarithmic search is one such search technique that reduces the search points to a subset of the search window (to be detailed in literature review) and finds the near-optimal best match with reduced computational complexity. Although computationally inexpensive it contains some redundancy in the search space. We aim to reduce this redundancy and aim to find a modified 2-D logarithmic search technique with even reduced computational load. Experimental results demonstrate that the proposed technique reduces the number of search points and thus reduces search time with insignificant sacrifice of image quality.

The paper is organized as follows. In Section II we elaborate some related works. In Section III we present our proposed search approach. Some experimental results to demonstrate the effective of the proposed approach is presented in Section IV. Finally Section V concludes the paper.

II. RELATED WORKS

In this section we present full search technique and the logarithmic search technique. In both cases the frame to be coded is divided into a number of non-overlapping equal size blocks of size $p \times q$. The best match is looked for in a search window of size $(2d+1) \times (2d+1)$ in the reference frame .

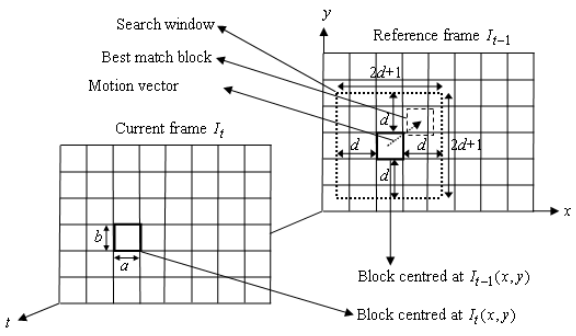

978-1-4244-6283-4/09/$26.00 ©2009 IEEE

Fig 1: Block matching process in video coding that uses search techniques.

A. FULL SEARCH

In Full search [1] finds the best match by inspecting all the $(2d+1)\times(2d+1)$ candidate positions within the search window. Full search procedure is brute force in nature. The advantage of Full Search is that it delivers good accuracy in searching for the best match. The disadvantage is that it involves a large amount of computation.

B. 2-D LOGARITHMIC SEARCH

Jain and Jain **Error! Reference source not found.** developed a 2-D logarithmic search technique that successively reduces the search area, thus reducing the computational burden. The first step computes the similarity for five points in the search window. These five points are as follows: the central point of the search window and the four points surrounding it, with each being a midpoint between the central point and one of the four boundaries of the window. Among these five points, the one corresponding to the minimum dissimilarity is picked as the winner. In the next step, surrounding this winner, another set of five points are selected in a similar fashion to that in the first step, with the distances between the five points remaining unchanged. The exception takes place when either a central point of a set of five points or a boundary point of the search window gives a minimum dissimilarity. In these circumstances, the distances between the five points need to be reduced. The procedure continues until the final step, in which a set of candidate points are located in a 3x3 2-D grid. The steps in a 2-D logarithmic search technique are presented in Fig 2.

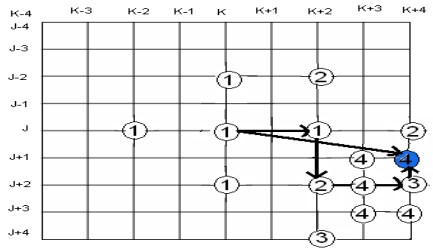

Fig 2: The 2-D logarithmic search technique. The circle numbered *n* is searched at the *n*-th step. The arrows indicate the points selected as the center of the search for the next pass.

The 2-D logarithmic search hits a maximum of 18 points and a minimum of 13 search points. The advantage of this technique is that it successively reduces the search area, thus reducing the computational burden. One of the disadvantages is that some points are searched more than once thus leave some space for improvement. Moreover, it follows a greedy approach by selecting the minimum dissimilar point at each step thus posing a threat to follow a local minimum trend. Considering these facts we propose to modify the 2-D logarithmic search to overcome the local minimum problem and also eliminate the redundant computing as described in the following section.

III. PROPOSED SEARCH TECHNIQUE

We mainly modified the 2-D logarithmic search technique to eliminate the redundancy and local minimum problem associated with it. The search technique is elaborated next under the light of 2-D logarithmic search technique.

Our proposed search technique starts with the five points in the search window where the one is at the center and other four surrounds center point (Fig 3(a)). Unlike 2-D logarithmic search, our proposed technique selects two points min_1 and min_2 (Fig 3(b)) that has dissimilarity scores lower than the other three points. We then select a point as the center of search for the next pass that lies on the line in between min_1 and min_2. This selection reduces the local minimum effect as it simply does not follow the minimum point. Moreover, the five points selected in the next pass does not match with any of the previous points thus eliminates the redundancy that exists in 2-D logarithmic search. Centered at the point selected at the next pass the search continues (Fig 3(d)-Fig 3(f)). The steps of the search are portrayed in Fig 3.

Following are some of the merits of our proposed technique:

- Successively reduces the search area with no point searched twice
- Maximum search points are 12 and minimum search points are 5 – an improvement over 2-D logarithmic search.

IV. RESULTS AND DISCUSSION

We have conducted a comparative analysis of Full Search, 2-D logarithmic Search and our proposed search technique as presented next. All the experiments were conducted on MPEG sequences using MATLAB. We used sequences like *garden*, *Akiyo*, *Table Tennis*, *Car*, and *coastguard*. Full search, 2-D logarithmic search and our proposed technique applied in these standard MPEG file and we computed the ASNR (Average Signal to Noise Ratio) and Computational load (i.e. number of search points). The results on different sequences are presented next.

***Akiyo Sequence*:** Each frame of the *Akiyo* sequence is of 352×288 pixels, recorded at 25 frames per second and there are a total of 398 video frames. Fig 4 shows the reconstructed 20th frame of *Akiyo* sequence coded using Full search, 2D-logarithmic search and proposed search technique. In this video only face portion is moving. Search point comparison for these three search techniques is presented in Fig 5 and ASNR is reported

in Fig 6. ASNR achieved using the proposed search technique is almost equal 2D logarithmic search but at reduced number of search points (Fig 5). Number of search points remains almost similar over the different frames. ASNR value shown in Table 1.

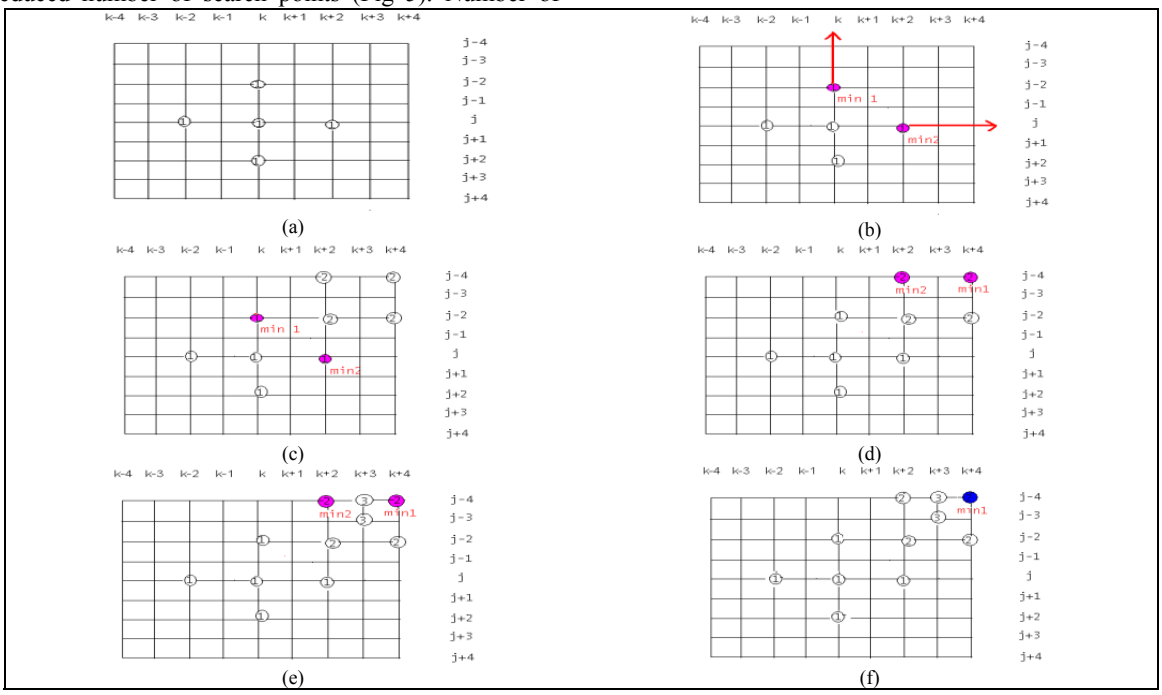

Fig 3: The different steps of our proposed 2-D logarithmic search technique. (a) five points of search window, (b) the direction of the search in between the direction offered by the two points min_1 and min_2. (c) Search at step 2, (d) min_1 and min_2 at step 2, (e) Search points at step 3, and (f) Search ends at the blue point.

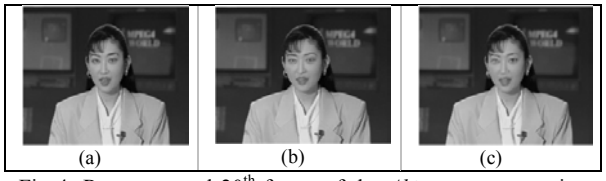

Fig 4: Reconstructed 20th frame of the *Akiyo* sequence using (a) Full search, (b) 2-D logarithmic search, and (c) Our proposed search technique.

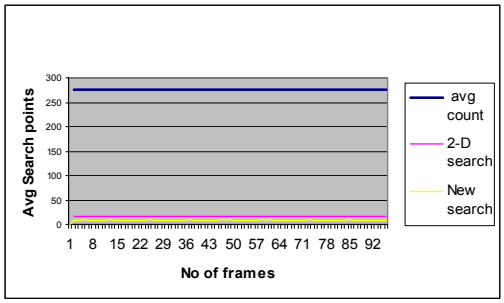

Fig 5: Comparison of # of search points for *Akiyo* sequence.

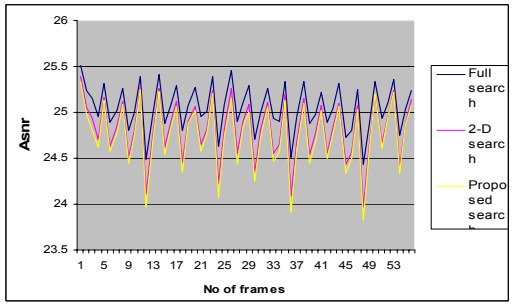

Fig 6: Comparison of ASNR for *Akiyo* sequence.

Table 1: ASNR value of different search for Akiyo sequence

Frame No	Full Search	2D logarithmic Search	Proposed Search
1st	25.86188	25.55678	25.46245375
5th	24.84504	23.77938883	23.57562323
10th	24.37532	23.01043038	22.67351877
15th	24.38495	22.98908004	22.5831958
20th	24.4424	22.90227928	22.56886825
25th	24.44956	23.03416597	22.51615637

***Car Sequence*:** Each frame of the *Car* sequence is of 320×240 pixels and recorded at 25 frames per second and there are a total of 398 video frames. The reconstructed 20th frame of *Car* sequence using the three search techniques is presented in Fig 7. In this video sequence the car moves but background is still. Here each repeated two times. Average no of search point is

almost 10.46 for repeated frames and 11.50 for new frames. Here number of search points vary significantly compared to *Akiyo* sequence. Overall the proposed technique has reduced search points (Fig 8) although the ASNR is bit low (Fig 9). ASNR value of some frames shown in Table 2.

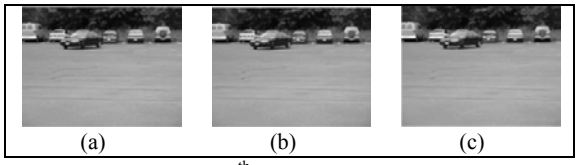

(a) (b) (c)

Fig 7: Reconstructed 20th frame of the *Car* sequence using (a) Full search, (b) 2-D logarithmic search, and (c) Our proposed search technique.

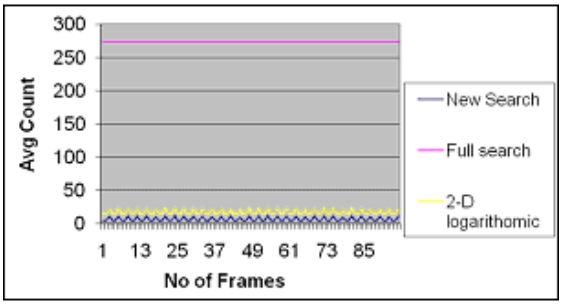

Fig 8: Comparison of # of search points for *Car* sequence.

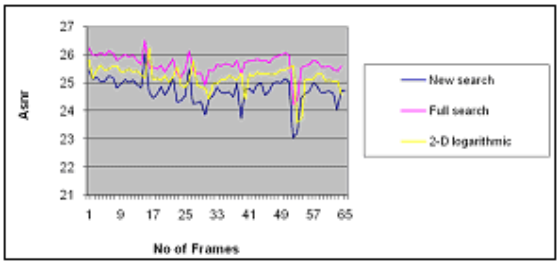

Fig 9: Comparison of ASNR for *Car* sequence.

Table 2: ASNR value of different search for Car sequence

Frame No	Full Search	2D logarithmic Search	Proposed Search
1st	27.13312	26.5682	26.08265
5th	26.68718	25.75123	25.16904
10th	26.10589	25.12647	24.27394
15th	26.31185	25.16266	24.54981
20th	26.28613	25.41915	24.61234
25th	25.86261	25.02255	24.12599

***Garden Sequence*:** Each frame of the *Garden* sequence is of 352×240 pixels and recorded at 30 frames per second and there are a total of 59 video frames. Fig 10 represents the reconstructed 20th frame of this sequence coded using the three search techniques. In this video the motion is due to camera movement. Fig 11 and Fig 12 reveals that the new search technique reduces the number of search points with minor loss in ASNR. ASNR value of some frames shown in Table 3.Here Average no of search point for each frames required almost same. In frame 20th average no of search point is 11.6053 and ASNR is 18.22931.

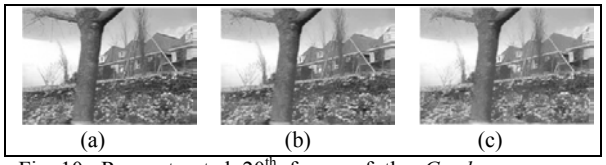

(a) (b) (c)

Fig 10: Reconstructed 20th frame of the *Garden* sequence using (a) Full search, (b) 2-D logarithmic search, and (c) Our proposed search technique.

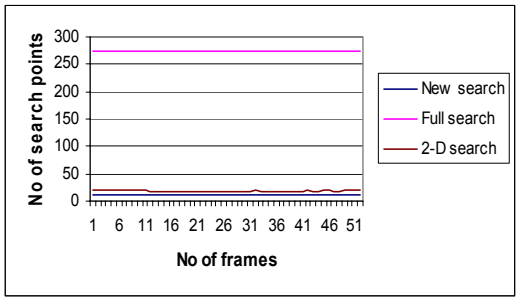

Fig 11: Comparison of # of search points for *Garden* sequence.

Fig 12: Comparison of ASNR for *Garden* sequence.

Table 3: ASNR value of different search for Garden sequence

Frame No	Full Search	2Dlogarithmic Search	Proposed Search
1st	24.27663	24.27663	23.5971
5th	21.6078	21.6078	20.49847
10th	20.71779	20.71779	19.34323
15th	19.9641	19.9641	18.69269
20th	19.6754	19.6754	18.22931
25th	19.39791	19.39791	18.05226

***Coastguard Sequence*:** Each frame of the *Coastguard* sequence is of 320×240 pixels and recorded at 25 frames per second and there are a total of 378 video frames. Here the boat and the camera are moving. Fig 13 represents a reconstructed frame of this sequence coded using the three search techniques. Fig 14 represents the search point required by the three techniques. Our proposed technique shows periodic nature in terms of search points. This is due to the repetitive nature of motion in the video. Fig 15 represents a comparison of ASNR obtained using different techniques. Table 4 shown ASNR of some frames.

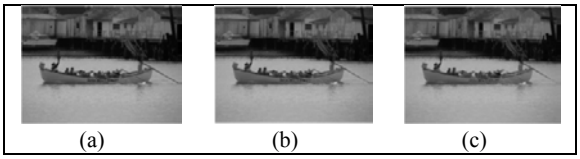

(a) (b) (c)

Fig 13: Reconstructed frame of the *Coastguard* sequence using (a) Full search, (b) 2-D logarithmic search, and (c) Our proposed search technique.

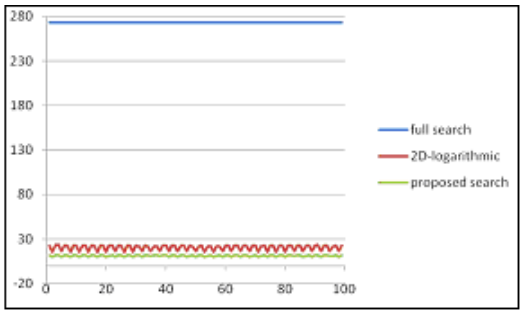

Fig 14: Comparison of # of search points for *Coastguard* seq.

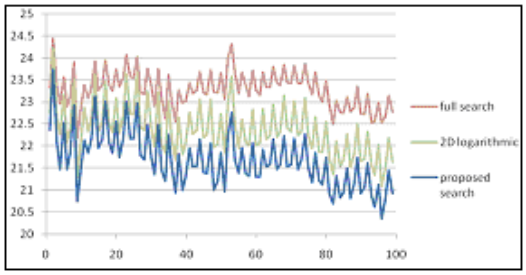

Fig 15: Comparison of ASNR for *Coastguard* sequence.

Table 4: ASNR value of different search for Coastguard seq.

Frame No	Full Search	2D logarithmic Search	Proposed Search
1st	24.78771	24.33338	23.61801
5th	24.31753	23.35416	22.54516
10th	23.90367	23.03317	22.07546
15th	24.36529	23.44171	22.66604
20th	24.38658	23.26823	22.50994
25th	24.54524	23.91583	22.91885

***Table tennis Sequence*:** Each frame of the *Table tennis* sequence is of 352×240 pixels and recorded at 30 frames per second and there are a total of 9 video frames. Here ball is moving fast. The reconstructed frames, number of search points, and ASNR of the three search techniques are presented in Fie 16, Fig 17, and Fig 18.Some ASNR of Table tennis sequence shown in table 5.

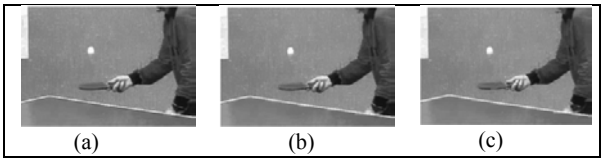

(a) (b) (c)

Fig 16: Reconstructed frame of the *Table tennis* sequence using (a) Full search, (b) 2-D logarithmic search, and (c) Our proposed search technique.

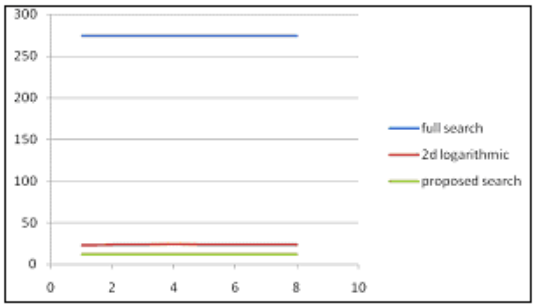

Fig 17: Comparison of # of search points for *Table tennis* sequence.

Overall the result of ASNR for Full Search is best in all cases but number of search point is so high. The result of ASNR for 2-D logarithmic and our proposed search is almost same but the number of search point of our proposed search is smaller than the 2-D logarithmic search and thus an improvement over the existing technique.

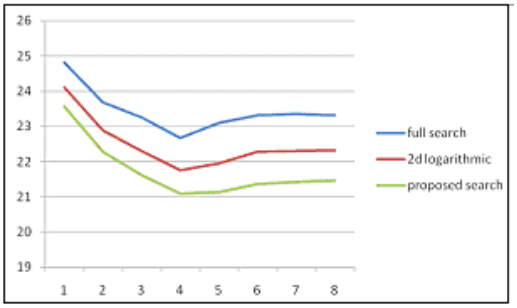

Fig 18: Comparison of ASNR for *Table tennis* sequence.

Table 5: ASNR value of different search for *Table tennis* seq

Frame No	Full Search	2D logarithmic Search	Proposed Search
1st	25.2698	24.56416	23.90544
3rd	23.60795	22.69326	21.81273
5th	23.43996	22.35007	21.29301
7th	23.71878	22.71607	21.58383

V. CONCLUSION

In this paper we have presented a new search technique for video coding that is a modification of the existing 2-D logarithmic search. The proposed technique reduces the search time of 2-D logarithmic search by reducing the redundant search points. Although ASNR is sacrificed to some extent it had insignificant visual impact as observed from the experimental results.

REFERENCES

[1] Shi and H. Sun, "*Image and Video Compression for Multimedia Engineering*", Fundamentals, Algorithms and Standards, 2nd Edition.

[2] P.N. Tudor, "*MPEG-2 Video Compression*", IEEE J Langham Thomson Prize, Electronics and Communication Engineering journal, December 1995.

[3] J. R. Jain and A. K. Jain, *"Displacement Measurement and Its Application in Interframe Image Coding*", IEEE Transactions on Communications, vol. com-29, no. 12, December 1981.

[4] T. Koga, K. Linuma, A. Hirano, Y. Iijima, and T. Ishiguro, "*Motion-compensated interframe coding for video conferencing*," Proc. NTC'81, G5.3.1-G5.3.5, New Orleans, LA, Dec. 1981.

[5] R. Srinivasan and K. R. Rao, "Predictive coding based on efficient motion estimation," Proc. of ICC, 521-526, May 1984.

[6] D. Tzovaras, M. G. Strintzis, and H. Sahinolou, "*Evaluation of multiresolution block matching techniques for motion and disparity estimation*," Signal Process. Image Commun., 6, 56-67, 1994.

[7] MPEG-4, http://en.wikipedia.org/wiki/MPEG-4, last accessed in December 2008.

[8] H.264, http://en.wikipedia.org/wiki/H.264, last accessed in December 2008.

Proceedings of 2009 12th International Conference on Computer and Information Technology (ICCIT 2009)
21-23 December, 2009, Dhaka, Bangladesh

Implementation of E-Commerce in Developing Countries: Bangladesh Perspective *(Not Presented)*

S. A. Ahsan Rajon, Abdullah-Al-Nahid†, Abu Shamim Mohammad Arif‡

Department of Computer Science and Engineering, Bangladesh University of Engineering and Technology, BUET, Dhaka, Bangladesh

† Electronics and Communication Engineering Discipline, Khulna University, Khulna-9100, Bangladesh

‡ Computer Science and Engineering Discipline, Khulna University, Khulna-9100, Bangladesh

ahsan.rajon@gmail.com, nahidku@yahoo.com, shamimarif@yahoo.com

Abstract

In this paper, we describe an effective framework for adapting electronic commerce and e-commerce services in developing countries like Bangladesh. A comprehensive model of establishing e-commerce infrastructure in developing countries has also been integrated in this paper. This paper focuses on the socio-economic aspects of e-commerce infrastructure building along with e-commerce service establishment policy with detailed overview on the prospects and corresponding problems of the same from Bangladesh perspective. This paper also investigates various ways of integrating existing infrastructure in implementing electronic commerce in low-income countries. We especially present the adaptability of e-commerce in the possible sectors and provide a methodical study on the strategies of business process re-engineering improving the socio-economic aspects and service delivery with their participation in overall trade and commerce.

Keywords: Electronic Commerce, Digital Divide, Developing Countries, E-Commerce, Information and Communication Technology.

I. INTRODUCTION

Current century is the era of Information and Communication Technology. The prime concern of this decade of electronic revolution is to establish and ensure a better way of management, communication and development with the use of information and information-oriented services based on computer and information technology. Crossing the boundary of personal computations and communications, the uses of digital media for greater levels of management has been initialized early in the century. Electronic Commerce or e-commerce may simply be considered as an extension of this trade. With the enhanced facilities of technology for providing smart and easy living, E-commerce has become a prime demand in the world for ensuring better and quicker product marketing, wider and comprehensive representation, stable and competitive pricing throughout the various sectors of business and commerce including other e-services.

An overall study on the impact of e-commerce for the uplift of the economy of developing countries by enhancing the product presentation style over e-market has been focused in this paper. Here, we consider Bangladesh perspective as the representative analysis-base and try to investigate the same for developing countries.

The main contribution of the paper is, it provides an effective framework of implementing e-commerce in developing countries considering Bangladesh as a test-bed. Secondly, it demonstrates the inter-relation of existing infrastructure and e-commerce implementation policy for countries with relatively weak economy. Moreover, this paper compares the existing models of implementing e-commerce for developing countries and analyzes the suitability (and unsuitability) of those from the socio-economic perspective of Bangladesh.

II. E-COMMERCE

The term *commerce* indicates the activity of distributing products and services to the interested parties who possess the capability and intention to buy the materials or products [1], [2]. In the most simplified form, when this type of business or commercial transaction involves digital communication using internet and web-oriented services for information transfer, the overall process is termed as e-commerce [1], [5]. More specifically, electronic commerce may be defined as the process of adapting electronic means especially information and communication technology for providing better, faster and greater services to the consumer as well as facilitating a comprehensive managerial innovative framework encompassing both the customers and suppliers. For electronic commerce, this involvement of internet and internet-oriented services may be complete or partial.

In [3], *e-commerce* has been broadly defined as, "An electronic transaction is the sale or purchase of goods or services, whether between businesses, households, individuals, governments, and other public or private organizations, conducted over computer mediated networks. The goods and services are ordered over those networks, but the payment and the ultimate delivery of the goods or service may be conducted on or off-line".

The rapid application of e-commerce has tremendously affected the overall business processes from the early 1990. With the evolution of e-marketplace in the place of physical-marketplace has gradually mobilized the overall process of production, presentation and mar-

978-1-4244-6283-4/09/$26.00 ©2009 IEEE

keting enlarging the spread of marketing. Crossing the geographical boundary, e-transactions has placed a new horizon in world economy by virtue of e-commerce.

The prime objective of e-commerce is to establish a user-friendly, trust-worthy, effective and efficient approach of providing internet centered business transactions [6, 7, 8]. In order to initiate e-commerce in developing countries, there should have legible and reliable implications of the effectiveness of e-commerce and e-commerce services. The only means to ensure this in a feasible, credible and efficient way is to ensure minimum overhead of implementation because; it is the only way through which a low-income person can explicitly become interested with the new technology and different aspects of business and commerce.

Research Methodology:

In our research, we carried out structural questionnaires in order to have an impartial survey on the e-commerce development issue of Bangladesh. The researchers went to the people of villages and towns and collected their opinion. An intra-network survey was also made to collect information from the students and teachers of Khulna University to have a comprehensive analysis on the concerned issue. The two way survey was made in order to have a balanced analysis from the technology aware university personnel and relatively facility-deprivated and updated technology-unaware village people. The questions were divided into three sections. Section 1 comprised of two subsections namely subsection A and subsection B. Subsection A was designated to collect direct information related to the perception of electronic commerce like the feasibility of implementing electronic marketing, architecture of effective customer support service system in Bangladesh. Subsection B aimed to gather information regarding the feasible and cost-effective hierarchical structure of electronic commerce with ordering and delivery subsystem components in point of view of Bangladesh. Section 2 was made up of dichotomous type which required the respondents to answer yes or no only. Questions regarding their current feelings and matchmaking between electronic commerce and traditional commerce focusing on agriculture and agro-based products was the main content of this section. Section 3 was devoted to collect information regarding the factors that hinders the implementations of electronic commerce as well as the key barriers in getting perceived benefits from electronic technologies.

III. E-COMMERCE INFRASTRUCTURE IN BANGLADESH

There are a number of literatures available emphasizing the development issues of e-commerce. Most of the researches provide a framework for implementing e-commerce in domain specific areas. There is also a wide range of papers describing the features, advantages, challenges and other concerned issues of electronic commerce and electronic markets as well. Though a number of studies regarding the potential sectors of implementing electronic commerce in developing countries and assumed outcome of electronic commerce for the same has been made, a little research is available dedicated to explore the framework of implementing e-commerce in those developing countries. Its is the novelty of this research that, this paper focuses on the e-commerce implementation framework from the point of view of developing countries considering Bangladesh as the pioneer. An overall analysis on the adapted framework for implementing e-commerce in other countries is also incorporated in this paper along with comparative analysis and feasibility study of those schemes. A detailed overview on the components, status, potential and constraints of e-commerce in Bangladesh has been presented in [14] and [15]. Overview on the existing legislation with comparative analysis of required legislations are also described in this paper. Identifying the challenges, Najmul [15] recommends a couple of remedies. In [16] and [19], players, procedures and problems of implementing e-commerce with Legal and regulatory framework for e-commerce has been discussed. Actions to be taken at national level has also been described in this paper. An Exploratory study on the Barriers to Adopting ICT and e-commerce with SMEs in Developing Countries considering Sri Lanka has been presented by Kapurubandara and Lawson in [17]. A Secure E-commerce Model for Bangladesh using various local pre-paid and debit cards has been proposed by Chowdhury *et al.* where they focus on solely the payment infrastructure in [2]. In [18], the impact of e-Commerce in the way of Business in Thailand has been conveyed.

Bangladesh, a small developing country with enormous prospects realizes the importance of implementing e-commerce in Bangladesh. However, because of its financial backwardness and the lack of dedicated technical expertise, it is still now in the initializing step of implementing e-Commerce. Though there are some unformatted steps in implementing e-commerce in Bangladesh, still now the total achievements are not mention-worthy. Being a country with lower income, and lower literacy rate, the concept of e-commerce has not got complete implementation. Although Bangladesh is an agricultural country, because of the shortage of agro-industry, marketing of agro-products as well as primary agricultural products has also not seen the light of increased marketing span. However, this situation may be radically changed by adapting proper and multidimensional use of existing infrastructure.

IV. EMERGENCE OF E-COMMERCE FOR DEVELOPING COUNTRIES

Electronic commerce is a revolution in the field of trade and commerce. The establishment of electronic

commerce has added new dimension in the total scheme of business ensuring smarter and faster service in concerned sectors. In fact, these criteria have established e-commerce as an essential demand of time rather than an additional service.

The economical backwardness of the developing countries focuses the prime essence of implementing e-commerce in developing countries. Without e-commerce it is completely impossible to have global reach of the product, and without wide-spanned market, it is never possible to have greater profit. Secondly, most of the developing and under-developed countries of the world including Bangladesh are agricultural country. There may be a number of agro-products, which possess greater possibility to be marketed crossing the geographical barrier. The scope to eradicating middlemenship in the overall marketing process by adapting e-commerce is also giving rise to the necessity of e-commerce implementation. Moreover, scope of better management and monitoring is leading the world to rush towards e-commerce. The necessity of e-commerce for especially developing countries has been extensively conveyed in the literatures [3], [4], [5], [6], [7] and [8]. Most of these researches focus on the current e-commerce situations of e-commerce with necessity of e-commerce and effectiveness of the same for developing countries in Asia without framework details.

V. IMPLEMENTATION OF ELECTRONIC COMMERCE IN BANGLADESH

We have presented an approach to implement e-commerce in Bangladesh ensuring the maximum and effective use of existing infrastructure in figure 1. The overall implementation plan of e-commerce should must focus on current ICT infrastructures along with optimal precedence on security issues and monitoring aspects. The total infrastructure may be considered as software infrastructure, hardware infrastructure and other related

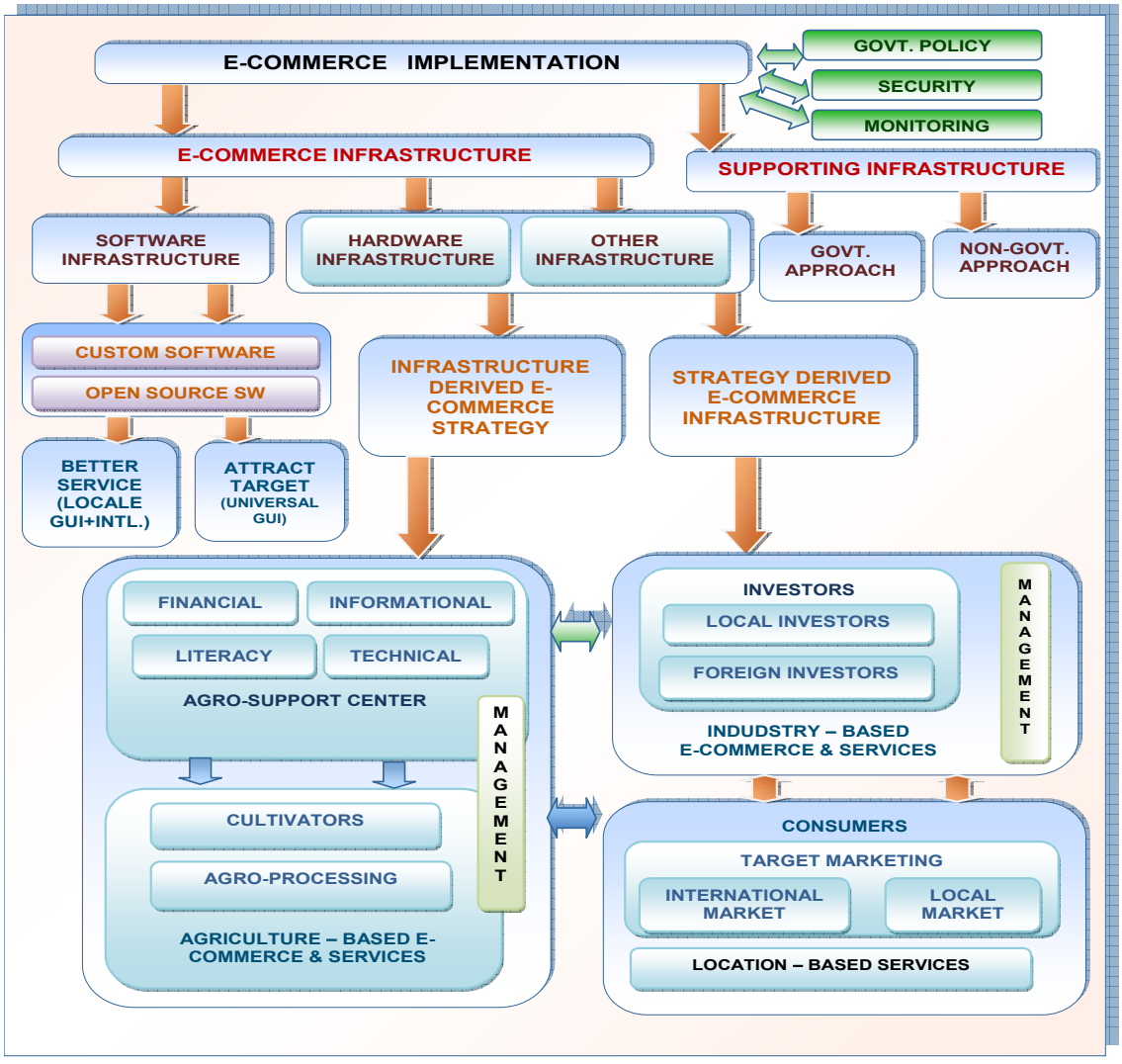

Fig. 1. Proposed Scheme for implementing e-Commerce in Developing Countries from Bangladesh perspective

infrastructure. The total infrastructure should be viewed in terms of strategy execution. The hardware infrastructure should be taken into consideration with ultimate care because of being a country with lower information and communication peripherals support. As there are two different streams exist parallelly in developing countries including both agricultural and industrial sector, we are to consider them from the view of potential use of existing infrastructure. The prime question that comes in establishing e-commerce for agricultural products and agro-based products is the support for hardware infrastructure to get access in information and communication technology and corresponding services. As in maximum cases, the overall income of the rural people engaged in agriculture is too poor to adapt e-commerce technology with solely their own interest. Again, it is also troublesome to have the total support from and by government to implement robust and efficient e-commerce and corresponding e-services. But, for industry based e-commerce implementation may have a different view. In industry based e-commerce, where the involved parties are in most cases private groups with ultimate aim to profit maximization may be moved to implement e-commerce with newer technology, better and improved infrastructure and developed architecture. Because of this difference in infrastructure and both-side limitations for agro-based e-commerce with both-side possibilities for industry-based e-commerce, it is a must to have distinct strategy in implementing e-commerce in developing countries like Bangladesh.

VI. FRAMEWORK FOR IMPLEMENTING E-COMMERCE

We have proposed two aspects namely agro-based e-commerce and industry based e-commerce from the infrastructural point of view in order to ensure faster, better and effective implementation of e-commerce in Bangladesh. We propose current infrastructure derived strategy for agro-based e-commerce and strategy based infrastructure for industry based e-commerce. The overall running of agro-based industry should be driven by Agro-Support center that will inherently support the village people who are directly related to agriculture and agricultural production in terms of capacity building, logistic support, informational support and other technical cooperation and coordination. This also includes literacy programs, awareness building and supporting measures to equip the cultivators and other stakeholders to have their robust and meaningful presence in e-commerce. The following is a glimpse of some of those points with greater details in section VI.

A. Stage-Setting Steps for Establishing E-Commerce

In order to facilitate E-Commerce, we must have proper physical infrastructure. This infrastructure support must be affordable and effective for the country. It is true that, Bangladesh has already joined in the information super highway; the establishment of total fiber-optic based ICT-infrastructure requires a large amount of time as well as subject to huge expense. But, it may be the fastest and most cost effective to establish Broadband over Power Line Communication because the maximum infrastructure already exists. In this stage-setting step, we also intend to emphasize on awareness building. E-Commerce is aimed for better and faster customer support, and this enhanced customer support is aimed at the overall uplift of the national economy. This necessity and functionality of E-Commerce should be communicated to the people so that they may realize and evaluate E-Commerce.

One of the main issues for implementing E-Commerce in developing countries is expense. The huge expense of implementing E-Commerce often turns the E-Commerce implementation project into an abandoned one. However, this may be easily handled by involving universities and other organizations in implementation process. The universities and other ICT related organizations may provide major support by providing their experienced IT-experts and concerned human resource. This may also bring a new dimension of research in the organizations. As in Bangladesh, there are more than hundred universities (both public and private) among which about all the universities possess courses and degrees regarding computer science and information technology, there is a great scope to engage large amount of human resource into the design and development of E-Commerce system for all possible sectors. Selecting renowned universities to perform this job with the supervision of honorable experienced teachers may ensure a successful, effective and efficient design, development and implementation of E-Commerce system. The universities may also be benefited with the scope of E-Commerce analysis and implementation related research support.

B. Design issues for implementing Electronic Commerce

The design and implementation of E-Commerce should must take the social, economical and educational issues into concern. The adaptability and effectiveness of the E-Commerce depends mainly on the citizens, as they are the stakeholders of E-Commerce. It should be taken into consideration that, the first language of Bangladesh is Bengali. So that, it would be most effective to ensure the use of Bengali in implementation of E-Commerce for conveying information. The use of Unicode in representation of Bengali text is also expected to facilitate uniform and massively accessible platform. The integration of the facility to provide comments and other information through internet may guarantee the participation of citizens in decision-making and various multi-

dimensional service-oriented processes. We propose to use a Phonetic based encoding scheme for obtaining the information from the concerned parties. Figure 5 presents a typical screenshot of proposed phonetic based approach of Bengali text composition.

Being a developing country, the development of E-Commerce should must focus on open source software development. As a research contribution there is a great scope of developing rich, effective and efficient applications as open source software development that will comprehensively promote new dimensions in the Information and communication arena of Bangladesh. The main advantage of open source software development is that, it may bring new idea in incorporating various indirect or secondary sectors into a common e-commerce platform which may ensure a robust electronic commerce.

E-Commerce is a large-scale activity which requires large scale data warehouses to be implemented. For faster, reliable and consistent database applications regarding development of E-Commerce, distributed database management may be the most effective. It is also necessary to consider WAP-support for all levels of design and development of services relating E-Commerce. For designing E-Commerce applications in most cases the best suited process model may be prototyping because of its adaptive nature. As, the users of E-Commerce varies from all levels of people, the software design will must consider the acceptability of the software or software components to the mass people. The overall Software development project management should also be reviewed to cope with overall aspects.

C. Support for implementing E-Commerce

E-commerce requires proper infrastructure for implementation. This an inseparable major issue of the exercise of E-Commerce too. For developing countries, this is a dire point of concern. In order to facilitate E-Commerce, the essential infrastructure involving computer, internet and human resource is still now a great problem for Bangladesh. If we plan to employ E-Commerce with completely individuals' interest, it is absolutely impossible to see the light of E-Commerce. Conversely, it is also not possible to provide separate infrastructure for E-Commerce because the economical framework would not support that. The only feasible as well as optimal solution is to arrange the total infrastructure combining the previous two sectors with the use of existing resources. As, in most areas, including rural areas we have secondary schools or madrasas and within the last few years government with the help of various non-governmental sources has already distributed computers and computer peripherals, we may use these schools or madrasas as a information center or service point for facilitating the citizens to have free access to E-Commerce. Basic awareness building may also be motivated from these centers. Besides these, distinct and sophisticated Information Centers equipped with IT-peripherals and support personnel may be established for providing E-Commerce support.

D. E-Commerce to M-Commerce: The Journey Begins

Increase of mobile communication in Bangladesh has made a silent revolution in all the sectors. The spread of the networks has now reached even into the extreme-rural areas. As, people are now more flexible with mobile oriented services, the adoption of m-governance which is to some sense a bridge between E-Commerce and mobile communication with the use of WAP or SMS. M-Governance is also a great concern because of its extreme growth, availability and flexibility. Considering mobiles as a communication tool for all types of service-request and information possessing from citizens may mobilize the E-Commerce process [3].

E. Analysis of proposed E-Commerce Framework

In figure 1, we have presented our proposed framework for implementing e-commerce in developing countries in Bangladesh. For the proposed model, we consider the developing countries as mainly agriculture based countries. Implementation of e-commerce has been considered on two basements namely, e-commerce infrastructure and supporting infrastructure. Being a multi-dimensional activity, it is in-fact impossible to implement e-commerce without the support of related aspects. Moreover, the implementation of e-commerce is directed through the government policy, security concerns and is operated soundly through the effective monitoring of both levels of administration. E-Commerce infrastructure is formed with the integration of software infrastructure and hardware infrastructure. For any developing country, this both software and hardware infrastructure are tough to manage because of the financial backwardness as well as lack of technical personnel. Consequently, on the two main streams of software sources, it is the most feasible and effective for any developing country to adapt open source software. However, there arises the question of required level of customization for making the software user-friendly though integration of locale graphical user interfaces (GUI). It is still now a great point of debate to determine the possible level of service which may be provided through easing the understandable GUI. At this point, the most important concern is strategy and infrastructure. The concerned elements i.e. e-commerce strategy may be derived on the basis of existing infrastructure in order to minimize the establishment cost which is the prime concern for developing countries like Bangladesh and other under-developing countries. For this infrastructure derived e-commerce strategy, as existing resources are given the most priority, it is quite common that, the main focus would be agriculture. That is, agro-based e-commerce may be the best vehicle to run e-commerce for this scheme. Similarly, whenever the scheme for e-commerce implementation is strategy

derived, that is, there is a distinct and dedicated large-scale investment for e-commerce, the total strategy should must emphasize the investors choice and themes including foreign investors and local investors. This assimilation may also explore the large-scale global market and the technical architecture, robustness, design and other concerned components also varies with this degree of involved parties. It is a key point to note that, for infrastructure derived electronic commerce strategy as well as strategy derived e-commerce strategy, socio-economic aspects like financial status of the people, information-awareness, literacy skill and technical adaptability of inhabitants is very much important which essentially focuses on target marketing and market targeting. The total scheme presented here definitely takes technology-aware management into concern which in terms focuses consumers in all levels.

VII. CONCLUSION

In this paper, we have presented an overview on the sectors for adapting E-Commerce from the point of view of the developing countries Bangladesh. We also describe the specific issues of implementing e-commerce ensuring effective utilization of existing infrastructure. The overall analysis on the usefulness and effectiveness to establish e-Commerce and e-Commerce services has been elaborately provided here. A detailed approach for implementing E-Commerce has also been presented in this paper. We also provide specific recommendations for designing, developing and managing the E-Commerce system in developing countries. The implementation of E-Commerce is the only way left to uplift the socio-economic infrastructure of the country into a glittering one. .

REFERENCES

[1] Efraim Turban, Jae Lee, David King, H. Michael Chung, *Electronic Commerce: A Managerial Perspective*, Pearson Publications, Second Edt. 2006.

[2] Md. Shahidul Islam, M. Ismail Jabiullah, M. Lutfar Rahman, "M-Commerce Infrastructure Design and Development: Bangladesh Perspective", *Proceedings of 7th International Conference on Computer and Information Technology*, 26-28 December 2004, Dhaka, Bangladesh

[3] John Humphrey, Robin Mansell, Daniel Paré, Hubert Schmitz , "The Reality of E-commerce with Developing Countries". *Interdepartmental Program in Media and Communications*, Institute of Development Studies, UK, March 2003.

[4] Judith E. Payne, "E-Commerce Readiness for SMEs in Developing Countries: A Guide for Development Professionals", *LearnLink*, Academy for Educational Development , Washington, D.C., USA

[5] Zorayda Ruth Andam, "*E-Commerce and e-Business*", Report, e-ASEAN Task Force, UNDP, APDIP, May 2003.

[6] Laura Männistö, "Electronic Commerce in Asia", Research Report, International Telecommunication Union, *Asia and the Future of the World Economic System*, 18 March 1999, London.

[7] Laura Männistö, "Internet commerce in developing countries", *Internet Journal*, January 1999.

[8] Wolfgang Koenig, R. T. Wigand, R. Beck, "Globalization and e-commerce: Environment and policy in Germany", *Communications of the Association for Information Systems* (Vol.10, 2003) 33-72.

[9] Murali Raman, , Richard Stephenaus, Nafis Alam, Mudiarasan Kuppusamy, "Information Technology in Malaysia: E-service quality and Uptake of Internet banking". *Journal of Internet Banking and Commerce*, August 2008, vol. 13, no.2.

[10] Mohammed Quaddus, "A Partial Least Square Approach to Modelling Electronic Commerce Success in Australia", *Information & Decision Systems*, Curtin University of Technology, Australia.

[11] Dr. Md. Abdul Mottalib, Sheikh Faridul Hasan, Syed Khairuzzaman Tanbeer, "BPLC: Proposed Approach to Implement E-governance in Remote Areas of Developing Countries", *International Academy of CIO* (IAC), Japan, 2006

[12] K. K. Bajaj, D. Bajaj. "*Electronic Commerce*". Tata McGraw Publishing Company, 2006.

[13] S. A. Ahsan Rajon, "On the design and implementation of E-Commerce in Bangladesh". Research Report-CSE-ec-03/2008, Computer Science and Engineering Discipline, Khulna University, Khulna, Bangladesh, 2008.

[14] E-Governance Horizon Scan Report: "An assessment study of e-Governance in Bangladesh", Access To Information (A2I) Program, Chief Adviser's office, Government of the People's Republic of Bangladesh, December 2007.

[15] E-Commerce in Bangladesh: Status, Potential and Constraints, Draft Final Report, JOBS/IRIS Program of USAID, December 2000.

[16] Mr Rajiv Rastogi, "Initiatives for, India: Country Report On E-Commerce Initiatives, E-Commerce Capacity-Building of Small and Medium Enterprises", India.

[17] Mahesha Kapurubandara, and Robyn Lawson, "Barriers to Adopting ICT and e-commerce with SMEs in Developing Countries: An Exploratory study in Sri Lanka", *CollECTeR '06,* Adelaide, 9 December 2006.

[18] Somnuk Keretho, "E-Commerce The Way of Business in Thailand", *National Electronics and Computer Technology Center* (NECTEC), 2002.

[19] Zaharah Abd Rashid, E-Perolehan – A Breakthrough for E-Commerce, In The Malaysian Government, *Public Sector ICT Management Review*, October 2006 – March, 2007 Vol. 1 No. 1.

Proceedings of 2009 12th International Conference on Computer and Information Technology (ICCIT 2009)
21-23 December, 2009, Dhaka, Bangladesh

FM-Chord: Fault-tolerant Chord Supporting Misspelled Queries

Md. Rakibul Haque, Reaz Ahmed†
Dept. of Computer Science & Engineering, Military Institute of Science & Technology (MIST), Bangladesh
† Dept. of Computer Science & Engineering, Bangladesh University of Engineering & Technology, Bangladesh
rakibul_haq@yahoo.com, reaz@cse.buet.ac.bd

Abstract

Searching with partial knowledge and misspelled keywords is a challenging problem in Peer-to-Peer networks. This paper presents FM-Chord, a novel searching mechanism for information retrieval with queries containing spelling and pronunciation mistakes in keywords using a widely-used structured overlay Chord. FM-Chord uses Double Metaphone encoding and 3-grams of keywords to reduce the effect of edit distance between the advertisement and query keywords. FM-Chord replicates advertisement to achieve fault tolerance to node failures. We evaluate the performance of our proposed mechanism in FM-Chord with necessary simulation results.

Keywords: Chord, distributed systems, P2P networks, spelling mistakes.

I. INTRODUCTION

Searching is the vital operation in any P2P networks. Lack of knowledge about the advertised objects is very common in distributed systems. Query success rate is very low in currently deployed P2P networks. Besides lack of knowledge about advertised information, another major reason behind this low success rate is the misspelling in the keywords. According to [14] about 34% queries in Napster [4] networks contain at least one misspelled keywords. There are many reasons for misspelling in query keywords such as typing mistakes, inconsistency between spelling and pronunciation in English language, difference of spelling in different dialects of English languages, *etc*. For example, 'colour' in British English is 'color' in American English.

Chord [20] only supports exact-match keywords with high efficiency. Moreover, Chord is not resilient to node failures at all. This paper presents a searching framework *FM-Chord* (Fault-tolerant Chord supporting Misspelled queries), which can efficiently search queries containing partial and misspelled keywords, and increases the availability of the advertised information during frequent node failures.

The rest of this paper is organized as follows. Section II presents related work. The searching framework of FM-Chord is presented in Section III. In Section IV, we present the performance evaluation of FM-Chord. Finally, we conclude and outline our future research goals in Section V.

II. RELATED WORKS

One of the key issues in fully decentralized P2P networks is how to efficiently search the flexible queries. Unstructured systems like Gnutella [2], Kazaa[3], Freenet[9], [13] support partial matching keywords but they are inefficient in bandwidth consumption. The reason behind this is adopting blind searching mechanism like flooding, random-walk etc. as file locations in these systems are totally unrelated to the overlay topology. Some research activities ([16], [10], and [12]) adopt hint based routing strategies for reducing query traffic volume but do not guarantee on search completeness.

Structured search techniques such as Chord [20], CAN [17], Kademlia [15], etc. are DHT (Distributed Hash Table)-based, and provide a mapping between file identifiers and node identifiers in the network. Structured systems are popular for low bandwidth consumption and high success rate for exact-match queries. Many research proposals including [8], [18], and [21] adopt additional layer on Chord or CAN to support partially specified query keywords. Squid [18] adopts space-filling-curves to map similar keywords to numerically close keys and uses Chord [20] for routing. pSearch [21] adopts CAN for routing and distributes document indices based on document semantics generated by Latent Semantic Indexing (LSI). In general, these extensions to the DHT routing support prefix matching only and do not support spelling mistakes in query keywords. Some non-DHT based search techniques (like [11], [7], and [19]) provide partial keyword searching but could not handle the spelling mistakes in queries.

In real world scenarios, between 10% and 47% of user-entered queries contain spelling mistakes in keywords [14]. But none of the existing search techniques address the problem of queries containing misspelling in keywords. We propose FM-Chord based on Chord for its high success rate, low query traffic volume and low maintenance overhead.

III. MODEL OF FM-CHORD

A. CORE CONCEPT

The basic concept of *FM-Chord* is advertising files using a set of words (W_{adv}) computed from the keywords associated with the files and searching files with a set of

978-1-4244-6283-4/09/$26.00 ©2009 IEEE

words (W_{qry}) computed from the query keywords. Since Chord [20] efficiently search queries with exact-match keywords, hence it is always possible to discover the requested files as long as the following condition hold:

$$W_{adv} \cap W_{qry} \neq \phi$$

The computation of W_{adv} and W_{qry} are discussed in Section III-C. *FM-Chord* increases the availability of advertised information by maintaining replica which is explained in Section III-D.

B. FRAMEWORK

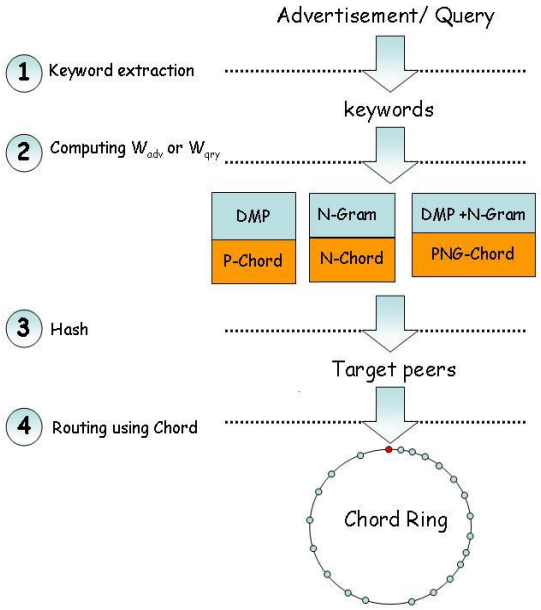

Fig. 1. Framework of FM-Chord

Advertisement and searching process in *FM-Chord* consists of the following four steps as depicted in Figure 1.

1) Keyword Extraction:
   Keywords from the file or query description are extracted, and then the popular keywords are filtered out to avoid hot-spot problem in the network.
2) Computing W_{adv} and W_{qry}:
   W_{adv} and W_{qry} are the set of words used to identify targets on the Chord overlay for advertisement and search, respectively. W_{adv} and W_{qry} are computed from the keywords selected in the earlier step. The computation of W_{adv} and W_{qry} are explained in Section III-C.
3) Hash:
   Each word in W_{adv} or W_{qry} is hashed to identify target nodes on the network as in Chord.
4) Routing:
   FM-Chord uses Algorithms 1 and 2 for advertisement and search, respectively.

C. COMPUTING W_{ADV} AND W_{QRY}

In this section we present the following three strategies for computing W_{adv} and W_{qry} which are depicted in Figure 1:

1) *P* approach (P-Chord):
   W_{adv} or W_{qry} includes keywords and their double metaphone codes [1]. For example, for the keyword 'Jhon Abraham', W_{adv} or W_{qry} = {'Jhon Abraham', 'JNPR', 'ANPR'}.
2) *NG* approach (N-Chord):
   W_{adv} or W_{qry} includes 3-grams which are generated from the selected keywords. For example, for the string 'beethoven', W_{adv} or W_{qry} = {'beethoven', 'bee', 'eet', 'eth', 'tho', 'hov', 'ove', 'ven'}.
3) *PNG* approach (PNG-Chord):
   W_{adv} or W_{qry} is consists of the selected keywords, double metaphone codes and 3-grams generated from the keywords.

For optimizing the bandwidth consumption during query resolution, *FM-Chord* randomly selects 70% 3-grams for computing W_{qry} in *NG* and *PNG* approaches which is explained in Section IV-C. We evaluate the three approaches with different performance metrics in Section IV and finally choose *PNG* for computing W_{adv} and W_{qry} given a high priority on search flexibility.

D. HANDLING NODE FAILURE

FM-Chord achieves high search completeness during node failures. *FM-Chord* replicate index to the two successor nodes and two predecessor nodes of the target nodes which is depicted in Figure 2. The value of *avg-Rep* (number of replica) is chosen as four which is explained in Section IV-D. *FM-Chord is* able to return requested files as long as the replicated nodes are alive.

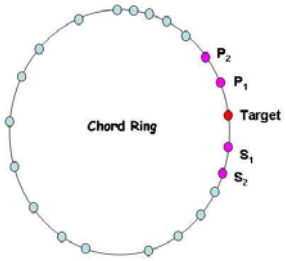

Fig. 2. Handling node failure in FM-Chord

For example in Figure 2, if the target node and successor S_1 fails, then predecessor P_1 will serve the requested file. Similarly, S_2 and P_2 serve if the target peer, S_1 and P_1 fails.

We provided mechanisms for advertisement and searching in Algorithm 1 and 2, respectively based on the Chord [20] lookup algorithm. The complexities of Algorithms 1 and 2 are similar to the complexity of routing algorithm specified in Chord.

Algorithm 1 Advertise (*n*, *id*, *keyword*, *avgRep*)

Inputs:
n : Node initiates the advertisement
id : id which is used to advertise
keyword : keyword which is to be advertised
avgRep : Number of redundant replica
Externals:
findSuccessor(*id*): Chord lookup algorithm
Start
target = *n.findSuccessor*(*id*)
target.store(*keyword*)
s = *target*
p = *target*
for *i* = 1 *to* $\left\lceil \frac{avg\,\mathrm{Re}\,p}{2} \right\rceil$ **do**
    s=s.successor
    p=p.predecessor
    s.store(keyword)
    p.store(keyword)
end for
End

IV. SIMULATION RESULT AND EVALUATION

In this section, we present the experimental results obtained by simulating the proposed searching framework with three strategies explained in Section III-C. In these experiments we have varied spelling mistakes in query keywords, network size, and failure rate to measure the search flexibility, scalability and robustness of *FM-Chord* in varied dynamic environments.

A. SIMULATION SETUP

We have used Peersim [6], a well-known P2P simulator for our experimental evaluation of *FM-Chord*. We have collected keywords for the experimental dataset of these experiments from the online database of movie information at http://www.imdb.com/Search/keywords [5]. We selected keywords of length 6~10 for our experiments.

Algorithm 2 Search (*n*, *id*, *keyword*, *avgRep*)

Inputs:
n : Node initiates the advertisement
id : id which is used to advertise
keyword : keyword which is to be advertised
avgRep : Number of redundant replica
Externals:
findSuccessor(*id*): Chord lookup algorithm
Start
target = *n.findSuccessor*(*id*)
if *keyword* ∈ *target.db* **then**
    return *target*
else
    s = *target*
    p = *target*
    i = 0
    while *i* < $\left\lceil \frac{avg\,\mathrm{Re}\,p}{2} \right\rceil$ **do**
        s = *s.successor*
        if *keyword* ∈ *s.db* **then**
            return *s*
        end if
        p=p.predecessor
        if *keyword* ∈ *p.db* **then**
            return p
        end if
        i = *i* + 1
    end while
end if
End

B. SEARCH FLEXIBILITY

Our major contribution in this paper is searching with queries containing misspelled keywords. We evaluated the proposed three strategies for computing W_{adv} and W_{qry} with varied edit distances between the advertised and queried keywords. We did not compare *FM-Chord* with Chord, since Chord only support exact-matched keywords. In our experimental graphs, E(i, j) refers to the spelling mistakes due to i and j number of errors in vowels and consonants, respectively.

We have measured search completeness for varied edit distances between the advertisement and query keywords by varying spelling mistakes due to vowels and consonants, which are depicted in Figures 3, 4 and 5. From Figure 3, it is observed that search completeness is very close to 98.6% and 84% for *PNG*, *NG* strategies respectively for both E(2, 0) and E(0, 2). However, *P* approach shows different level of search completeness which are 46% and 14% for E(2, 0) , E(0, 2), respectively. The reason behind the varied performance in *P* approach is that errors in vowels have less effect than errors in consonants. It is also evident that *PNG* approach achieves high search completeness as compared to the others.

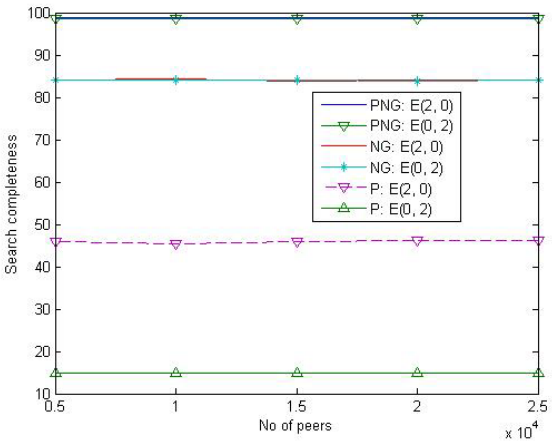

Fig. 3. Search completeness for edit distance two

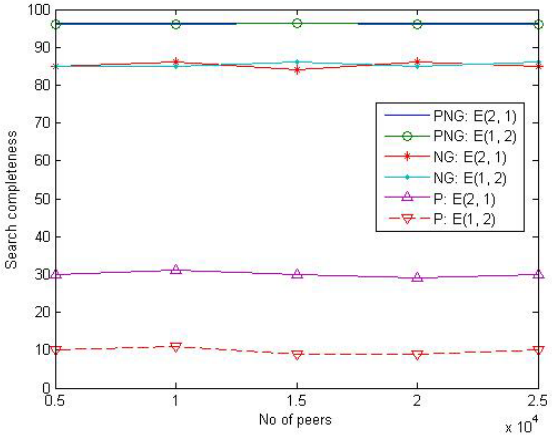

Fig. 4. Search completeness for edit distance three

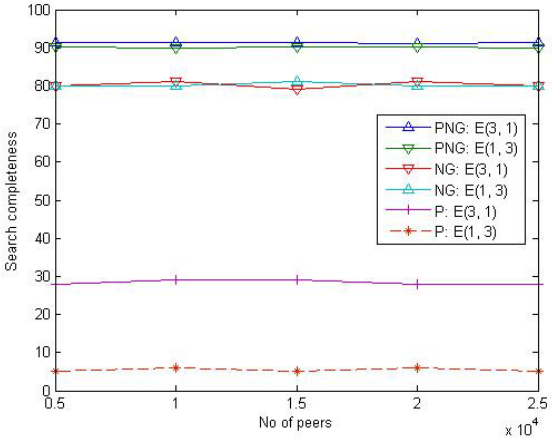

Fig. 5. Search completeness for edit distance four

From Figure 4, we observed that search completeness is about 96.2%, 85% for E(2, 1), E(1, 2) in *PNG* and *NG* approach, respectively. *P* achieves poor performance which is about 30% and 10% for E(2, 1), E(1, 2) respectively. In Figure 5, we found that *PNG*, *NG* approach achieved about 91%, 80%, respectively for E(3, 1), E(1, 3). In these cases, *P* approach has search completeness 28% and 5% for E(3, 1) and E(1, 3), respectively.

From Figures 3, 4 and 5, it is observed that *PNG* approach performs best among the three approaches. Spelling mistakes whether by errors in vowels or consonants has great impact on performance of *P* approach. *PNG* and *NG* approach react in a similar manner for errors with vowels and consonants.

We have estimated the search completeness with the following function:

$$Completeness = \frac{100}{N}\sum_{i=0}^{N}\frac{d_f(i)}{d_a(i)}$$

Here, N is the total number of keywords used for searching. $d_a(i)$ is the actual number of documents with the i^{th} keyword, and $d_f(i)$ is the number of documents from $d_a(i)$ as returned by the search mechanism.

C. IMPACT OF QUERY CONTENT ON SEARCH COMPLETENESS

In this experiment, we measure the impact of query content on search completeness. We search queries using varied % of 3-gram randomly chosen from W_{qry} to observe the impact of query content on search completeness and traffic volume for edit distance one to four, which is depicted in Figure 6 and Figure 7, respectively. From Figure 6, it is observed that search completeness increases slightly with the increase of query content (i.e., % 3-grams) for 10% to 70% 3-grams, and becomes constant for beyond 70% 3-grams. On the other hand, Figure 7 shows that search traffic volume increases with the increase of query content. From these observations, we can optimize the bandwidth consumption during query resolution by making queries with 70% randomly selected 3-grams from W_{qry}.

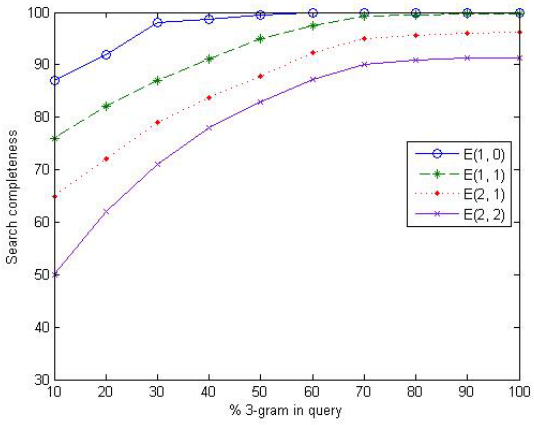

Fig. 6. Effect of query contents on search completeness

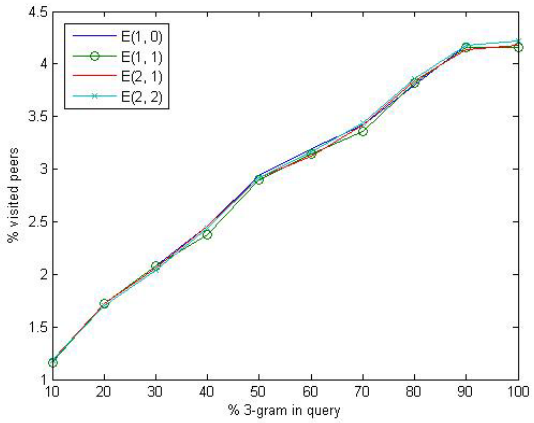

Fig. 7. Effect of query contents on routing efficiency

D. FAULT TOLERANCE

Chord is not fault tolerant to node failure, and achieves poor search completeness if the node containing the advertised information fails. *FM-Chord* maintains replica of advertised information to a number of peers. We varied the value of *avgRep* and found different level of search completeness in varied level of node failures which is depicted in Figure 8. From this figure, it is evident that *FM-Chord* achieved high level of search completeness for increased value of *avgRep*. On the other hand, increased value of *avgRep* causes higher level of replication factor (replication per file) which is depicted in Figure 9. Using these observations, we choose four as the optimal value of *avgRep* for achieving high fault resilience with low replication factor.

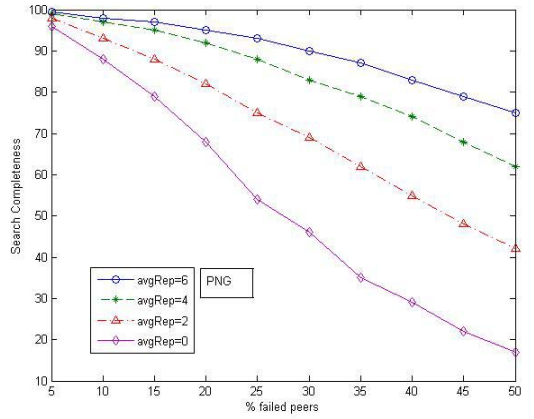

Fig. 8. Fault resilience of FM-Chord

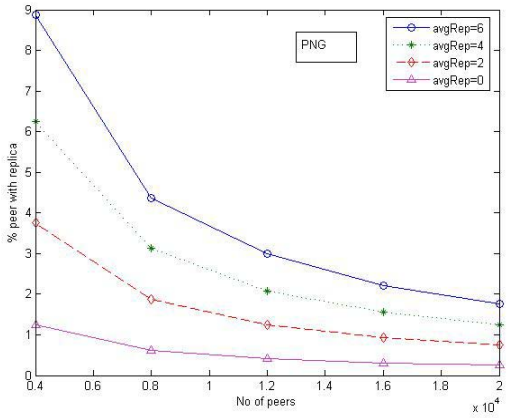

Fig. 9. Replication factor of FM-Chord

V. CONCLUSION AND FUTURE WORK

In this paper we have addressed the P2P search problem in presence of misspelled query keywords. This paper presents *FM-Chord*, which is a modified Chord protocol to solve this problem efficiently. We adopted the concept of double Metaphone encoding and 3-gram for minimizing the effect of edit distance between the advertised and queried keywords. *FM-Chord* achieves high search flexibility and increased availability during node failures. *FM-Chord* attains search completeness about 98.5%, 96.2%, 90% for edit distance two, three and four, respectively. *FM-Chord* exhibits search completeness above 80% for below 30% node failures.

In future research work, we want to optimize the advertisement and searching process in *FM-Chord*, which will require low bandwidth consumption and less index storage on nodes in the network. In addition, we intend to compare the search flexibility with the other search techniques providing partial-keyword searching like Squid [18].

REFERENCES

[1] Data management group (DMG) website, http://www.datamanagementgroup.com/resources/articles/introductiontodoublemetaphone.asp.

[2] The Gnutella website, http://www.gnutella.com.

[3] The KaZaA website, http://www.kazaa.com/.

[4] The Napster website, http://www.napster.com/.

[5] On line database of popular movie keywords, http://www.imdb.com/search/keywords/.

[6] Peersim Peer-to-Peer simulator, http://peersim.sourceforge.net/.

[7] A. Amir, E. Porat, and M. Lewenstein. Approximate subset matching with don't cares. In *Proc. of Annual ACM-SIAM Symposium on Discrete Algorithms (SODA)*, pages 305–306, 2001.

[8] M. Bawa, T. Condie, and P. Ganesan. LSH forest: Self-tuning indexes for similarity search. In *in Proc. of WW0W Conference*, May 2005.

[9] Ian Clarke, Oskar Sandberg, Brandon Wiley, and Theodore W. Hong. Freenet: A distributed anonymous information storage and retrieval system. *Lecture Notes in Computer Science (LNCS)*, 2009:46–66, 2001.

[10] E. Franconi, G. Kuper, A. Lopatenko, and I. Zaihrayeu. The coDB robust Peer-to-Peer database system. In *Proc. of Workshop on Semantics in Peer-to-Peer and Grid Computing at the International World Wide Web Conference (WWW)*, May 2004.

[11] Omprakash D Gnawali. A keyword set search system for Peer-to-Peer networks. Masters thesis, Massachusetts Institute of Technology, June 2002.

[12] J. Kim and G. Fox. A hybrid keyword search across Peer-to-Peer federated databases. In *Proc. of East-European Conference on Advances in Databases and Information Systems (ADBIS)*, September 2004.

[13] Qin Lv, Pei Cao, Edith Cohen, Kai Li, and Scott Shenker.Search and replication in unstructured Peer-to-Peer networks. In *Proc. of the International Conference on Supercomputing (ICS)*, 2002.

[14] S. Saroiu M. A. Zaharia, A. Chandel and S. Keshav. Finding content in file-sharing Networks When you Can't Even Spell. In *International workshop on Peer-To-Peer Systems*, February 2007.

[15] Petar Maymounkov and David Mazireres. Kademlia: A Peer-to-Peer information system based on the XOR metric. Pages 53–65. Springer-Verlag, march 2002.

[16] W. Siong Ng, B. Chin Ooi, K. Lee Tan, and A. Zhou. PeerDB: A P2P-based System for Distributed Data Sharing. pages 633– 644, 2003.

[17] S. Ratnasamy, P. Francis, M. Handley, R. Karp, and S. Schenker. A scalable content-addressable network. pages 161–172, 2001.

[18] C. Schmidt and M. Parashar. Enabling flexible queries with guarantees in P2P systems. *IEEE Internet Computing*, 8(3):19–26, June 2004.

[19] Shuming Shi, Guangwen Yang, Dingxing Wang, Jin Yu, Shaogang Qu, and Ming Chen. Making Peer-to-Peer keyword searching feasible using multi-level partitioning. In Proc. *of International Workshop on Peer-to-Peer Systems (IPTPS)*, pages 151–161. Springer, 2004.

[20] I. Stoica, R. Morris, D. Liben-Nowell, D. R. Karger, M. F. Kaashoek, F. Dabek, and H. Balakrishnan. Chord: a scalable Peer-to-Peer lookup protocol for Internet applications. *IEEE/ACM Transaction on Networking (TON)*, 11(1):17–32, 2003.

[21] Chunqiang Tang, Zhichen Xu, and Mallik Mahalingam. pSearch: information retrieval in structured overlays. *ACM SIGCOMM Computer Communication Review*, 33(1):89–94, 2003.

Proceedings of 2009 12th International Conference on Computer and Information Technology (ICCIT 2009)
21-23 December, 2009, Dhaka, Bangladesh

STP: In-network Aggregation through Proximity Queries in a Sensor Network

Md. Rakibul Haque, Mahmuda Naznin†, Md. Asaduzzaman†, Rakib Uddin Ahmed†

Dept. of Computer Science & Engineering, Military Institute of Science & Technology (MIST), Bangladesh
† Dept. of Computer Science & Engineering, Bangladesh University of Engineering & Technology, Bangladesh
rakibul_haq@yahoo.com, mahmudanaznin@cse.buet.ac.bd, parvez_ku_01@yahoo.com, rakib007@gmail.com

Abstract

Event detection and notification is a common task in a Wireless Sensor Networks (WSN). Efficient data aggregation and minimization of energy consumption are the great research challenges in WSN. In WSN, aggregated event information is more important than individual event information for energy saving and reliability. Proximity queries or query approximation can be used to reduce the complexity of data aggregation and energy consumption. This paper presents an efficient and scalable hybrid framework for processing spatial and temporal proximity queries in WSN which we call STP. STP builds tree structure with less overhead, and reduces the event propagation cost through proximity queries. STP reduces energy consumption by reducing the number of aggregator nodes, which ultimately increases the network life time. STP eliminates the unnecessary aggregation of events using a tunable temporal proximity threshold. We compare STP's performance with another spatial query processing method and we show that, STP performs better.

Keywords: Aggregation, proximity, sensor network, spatial and temporal query.

I. INTRODUCTION

Advances in wireless technology, micro-fabrication and integration, embedded microprocessors, ad-hoc nature and easy deployment have established sensor network as a very popular network for a range of commercial and military applications. One of the major applications of sensor network is monitoring task. An event is generated when a particular condition is satisfied by a sensor node. Proximity query allows reporting events those are observed by sensor nodes placed within a certain distance from each other. We can reduce the unnecessary event notifications to the base station, and increase the network life time by in-network aggregation of the events through proximity queries. This paper presents *STP* (*Spatial and Temporal Proximity query processor*), which can efficiently aggregate proximity events, and provide alarms to the base station with low energy consumption. *STP* provides an aggregation mechanism, which selects small number of *aggregator* nodes based on the spatial and temporal proximity of the nodes.

Combining the proximity events carefully, *STP* can simultaneously handle a large number of proximity queries without flooding the large portion of the network, which ultimately keeps sensors less busy and saves the energy of the sensors.

The rest of the paper is organized as follows. Section II presents related work. We define the spatial and temporal proximity query in Section III. The framework of *STP* is explained in Section IV. In Section V, we present the performance evaluation of *STP* and compare with another proximity query processing method [21]. Finally, we conclude and outline our future research goals in Section VI.

II. RELATED WORK

One of the fundamental issues in proximity query processing is data aggregation. Due to inherent redundancy in raw data collected from sensors, data aggregation can reduce communication cost by eliminating redundancy and forwarding only the useful information extracted from the raw data. For these reasons, it is crucial for a sensor network to support in-network data aggregation [8]. Various aggregation approaches ([3], [8], [10], [22], and [19]) have been proposed for data gathering applications and event raised applications. Most of these approaches use tree based structure for aggregation and utilize the multi-hop communication links to reduce the computation of expensive queries ([15], [16]). Some methods try to reduce cost of data aggregation using probabilistic techniques [18] or decentralized algorithms ([6], [10], and [11]). Some research proposals ([2], [7], [4], and [14]) advance the in-network data aggregation mechanism. Although, these researches with the techniques for data aggregation, none of them utilizes the concept of proximity query where events are related with some aspects.

The concept of proximity query was introduced in [21]. Yannis uses the *Routing Indices* (*RI*) method for minimizing packet forwarding in the large portion of the network. Although, it depends on the tree structure generated through the proximity query registration phase, it does not take the full advantage of the tree structure, and it does not consider the timing of event generation for the event aggregation. The target that is responsible for generating events does not move rapidly from one place to another in the network. If a target is detected by a node s at time t, the target should be detected either by s or w (any neighbor of s) at time $t+1$. As a result, there is an opportunity for the sensor w to utilize the routing

978-1-4244-6283-4/09/$26.00 ©2009 IEEE

structure generated by *s*. The RI method does not utilize the routing structure. The RI method [21] does not bind any time constraint with the proximity event. For a proximity query *Q(X, Y, d)* in [21], proximity alarm is unnecessary if the events *X* and *Y* are aggregated at node *z* after a long time or the time difference between the detection of *X* and *Y* is very high.

III. PROXIMITY QUERY

Given a set of predefined event types $\Psi = \{A, B, C...\}$, *proximity query* can be defined as $Q = (X, Y, d, t)$ where *X* and *Y* are members of Ψ , and *d*, *t* is the *spatial* and *temporal proximity* threshold, respectively. When two events *X* and *Y* are occurred within a distance *d* and within the time *t*, then a *proximity event* is generated, and the base station should be alarmed. The idea can be extended to multiple events scenario. A set of proximity queries is registered on the sensor nodes from the base station. When a node detects or hears an event, it propagates the event information to its neighbor nodes with a hope for potential proximity event in the other nodes of the network. Figure 1 shows a scenario where a proximity event is generated due to two events *X* at node n_1 and *Y* at node, where the distance between n_1 and n_2 is not greater than the defined proximity threshold, *d*. The potential *aggregator* nodes hear about the events within very short time after events (event *X* and *Y*) detection propagation by the source nodes n_1 and n_2. By '*aggregator*', we refer to the node which is selected to send the proximity event to the base node.

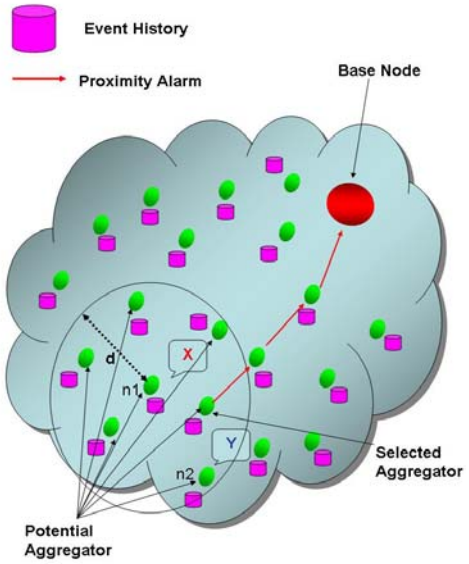

Fig. 1. A scenario showing proximity event

IV. FRAMEWORK OF STP

In this section, we have explained the framework of *STP*. The framework of *STP* consists of two main phases: *query registration* and *event propagation*. The first phase is responsible for establishing the routing structure that is used in the second phase. We assume a sensor network architecture that has one base station which may be a powerful sensor node, or may be located outside of the sensor network that can communicate with a subset of sensors in the network.

A. QUERY REGISTRATION

The base station acts as an initiator of the proximity query processing. The user registers the proximity queries in the base station. The base station informs all the nodes in the sensor network about these queries. The simplest approach is to broadcast the packet to the nodes in the sensor network. This approach leads to flooding which may generate several problems. To minimize the impact of broadcasting, *STP* adopts random waiting time [9]. It is a simple technique, for achieving temporal convergence, in which when a node receives a packet it waits for a random period of time. During this time period, if it receives another query packet, it combines both queries into a single packet, and forwards the combined packet to other nodes. In order to further reduce the impact of broadcasting, if a node receives a packet more than once, it discards the later packets. In this approach, queries will be reached to all of the nodes in the network.

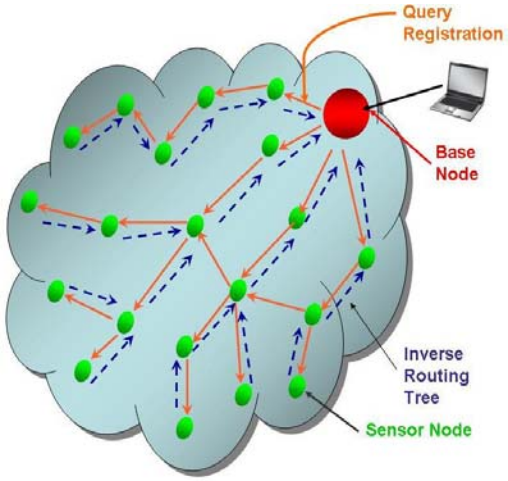

Fig. 2. Inverse routing tree

Each *query packet* contains *proximity events*, *distance threshold*, *hop count* and *time threshold*. If a node receives query packet from multiple neighbors, it should select one of them as a next hop to reach to the base station. The *hop count* (*hp*) is used as metric for this purpose. This process forms an *inverse routing tree* which is depicted in Figure 2. All the nodes in the network know the next neighbor for forwarding a message to the base node in the shortest path. This inverse routing tree is used for sending proximity alarm.

B. EVENT PROPAGATION

Algorithm 1 processEvent(X, n_1, t_X, h_p)

Parameters:
X: Event needs to be processed
n_1: Source node detecting the event X
t_X : Detection time of X
h_p: Hop counter
Update *eventHistory*
if hasSeen (X, n_1, t_X, h_p) **then**
  Return
end if
if $h_p > 0$ **then**
  Broadcast *eventDetected* Message $M(X, n_1, t_X, h_p - 1)$
end if
for all event y in the *eventHistory* **do**
  if there is a proximity query like $Q(X, y, d_{Xy}, t_{Xy})$ **then**
    if distance $(n_1, n_2) \le d_{Xy}$ and
     $| t_X - t_y| \le t_{Xy}$ and
     $|t_c - min\ (t_X, t_y)| \le t_0$ **then**
      Raise Proximity Event $PE(X, n_1, y, n_2)$
    end if
  end if
end for

When a node detects an event, normally, it informs the base station about the event. In general, events are propagated independently to the base station. The number of event notification to the base station is reduced by the processing of proximity queries efficiently. *STP* takes the advantages of in-network aggregation of events which requires less effort (in terms of bandwidth, battery power, etc.) than the general method. When a node detects an event, it sends an *EventDetected* message to its neighbors hoping that the event would be aggregated in other nodes. An *Event-Detected* message contains about the event information, source node, event time and hop counter (h_c), *etc*. For limiting the event propagation, hop count (h_c) can be used as a bound. The source node initializes the h_c as follows:

$$h_c = \max\left(\left\lceil \frac{d_{xy}}{2} \right\rceil \right), \text{ for events } y \text{ registered with event } x \quad (1)$$

When another node receives the *EventDetected* message, it runs the process specified in Algorithm 1. The node updates its event history with the received message, and checks whether the event will cause aggregation or not. If the h_c received in the message is not zero, it decreases the h_c by one, and transmits the message to its neighbors. For optimizing the number of messages, *Random-Walk* [5] or *modified-BFS* [20] can be used.

C. EVENT HISTORY

Each node maintains a cache, *EventHistory*. Each entry of the cache corresponds to a proximity event detected or heard from neighboring nodes. Each node refreshes its cache after a certain period of time. For example, consider the following proximity queries (X, Y, d_1, t_1), (X, W, d_2, t_2), (Y, Z, d_3, t_3), (X, Z, d_4, t_4) and in the network, all nodes receive above proximity queries from the base station. If a node receives an event X, then it stores this event information for the amount of time that is the maximum of the threshold times among the registered queries where event X is involved. We call this time as $T_{refresh,x}$ for X and it is calculated as follows:

$$T_{refresh,x} = max(t_1, t_2, t_3, t_4) \quad (2)$$

D. AGGREGATION

In this section, we describe the mechanism of *event aggregation*. For example, a node $n1$ detects an event X, and propagates the *EventDetected* message to its neighbors. Similarly, node n_2 detects an event Y, and it also propagates the message. These two messages may meet each other at some nodes in the network. From Figure 1, the nodes within the bounded area may be potential *aggregator* if the event detection time within the temporal proximity threshold. To become a potential *aggregator* node the following conditions are to be held:

$$Distance\ (n_1, n_2) \le d_{xy}\ and \quad (3)$$
$$|t_x - t_{y|} \le txy \text{ and} \quad (4)$$
$$|t_c - min\ (t_x, t_y)\ | \le t_0 \quad (5)$$

Equations 3 and 4 are required to meet the conditions of proximity query, and Equation 5 is used to avoid the unnecessary proximity alarms. In Equation 5, t_c is the current time at the potential *aggregator* node, and t_0 is the time threshold, which refers to the *maximum allowed time* for event propagation.

E. SELECTION OF AGGREGATOR

STP selects *aggregator node* efficiently to reduce the redundant proximity alarms to the base station which causes less energy, bandwidth consumption than RI method [21]. The *aggregator selection problem* is similar to the leader selection problem in WSN. There are many research ([13], [12], *etc*.) are performed to resolve this problem. We adopt the leader selection mechanism from [12] to select *aggregator* node efficiently. In [12], leaders are selected efficiently based on the some parameters like available energy, number of neighbors, distance from the source and base node, *etc*. The rotation of *aggregator* node among the potential *aggregator* nodes can be used to save the battery power of the nodes and proper load distribution.

F. SENDING PROXIMITY ALARM

The selected *aggregator* nodes send the proximity alarm to the *base node* using the inverse routing tree which is depicted in Figure 2. The *aggregator* node suppresses the same proximity event for a small amount of time to avoid the redundant proximity alarms.

G. ROUTE MAINTENANCE

As long as the inverse routing tree is maintained, aggregator node can easily send alert to the base station. The inverse routing tree should be fault resilience to the node failure. If a node in the inverse routing tree fails, the ancestor in the failed path to the base station can easily determine the link failure through periodic neighbor discovering protocol. To repair the link, the ancestor broadcasts a packet requesting for an alternative path. When a neighboring node receives the packet it sends an *Acknowledgement* packet to the ancestor node. It may happen that several nodes having the routes to the base station send the acknowledgement to the ancestor. The ancestor will selects the node which has the minimum hop count distance to the base station.

Figure 3 describes the link failure and alternative path establishment procedure.

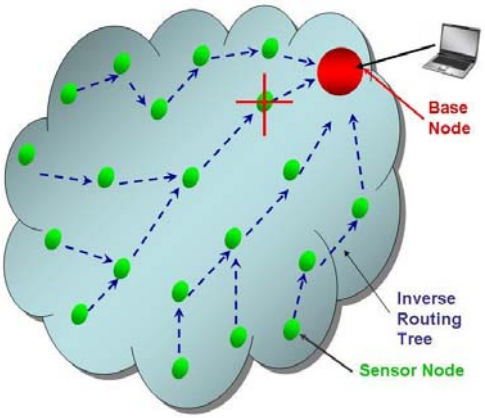

Fig. 3(1). Path failure

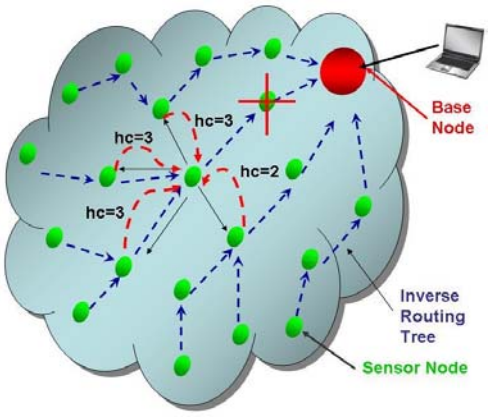

Fig. 3(2). Discovering a new path

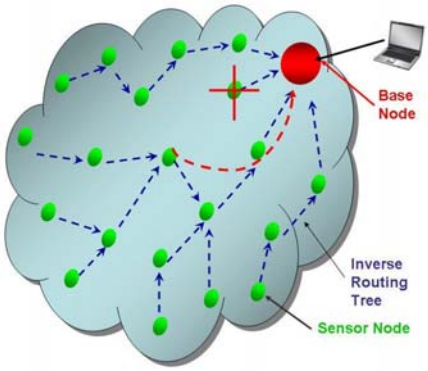

Fig. 3(3). Established a new path

V. SIMULATION RESULTS AND EVALUATION

In this section, we evaluate the framework of *STP w.r.t.* RI method [21] with the experimental results obtained by simulation. In these experiments, we have varied the spatial and temporal proximity threshold and network sizes to compare the total cost and number of aggregator nodes. The total cost is calculated as follows [21]:

Total Cost = 1.41 x (No. of transmitted messages)
+ (No. of received messages)
+ (No. of idle listened messages)

The total cost includes all the cost handling each event in the network except the cost for query registration phase.

A. SIMULATION SETUP

We have developed a simulator using Java to evaluate *STP w.r.t.* RI method on various aspects. The major classes of the simulator program are *Network*, *Node*, *Initializers*, *Observers*, *Dynamics*, *Target*, *Event*, *Message*, *Base*, and *Aggregator,* where *Base* and *Aggregator* class inherits the *Node* Class. We have model the network in this experiment as two dimensional (*n*x*n*) grids for simplicity. We assumed that, all sensor nodes have similar properties in the simulated network.

B. EFFECT OF SPATIAL PROXIMITY

We have measured the impact of varied spatial proximity threshold on the total cost which is depicted in Figure 5(a). We consider the hop distance between nodes as the spatial proximity. From Figure 5(a), it is evident that total cost increases as the spatial proximity threshold increases in both *STP* and RI method. The total cost increases because, the event propagation cost and the number of aggregator nodes increases when the spatial proximity increases. The rate of increase of total cost in our *STP* method is less than the rate of increase in RI method [21]. The reason behind this is that *STP* selects aggregator node (explained in section IV-E) among the potential aggregator nodes efficiently, and the number of selected aggregator nodes is less than the number of

aggregators in RI method, which is depicted in Figure 5(b).

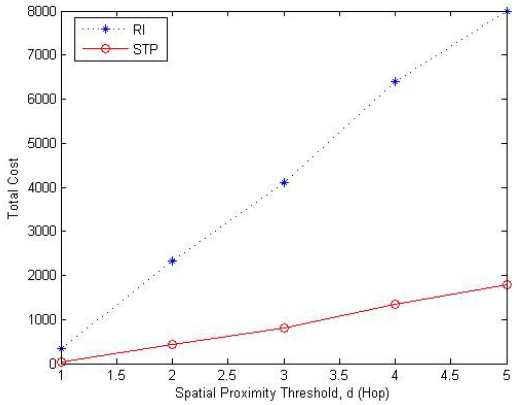

Fig. 5(a). Effect of spatial proximity threshold

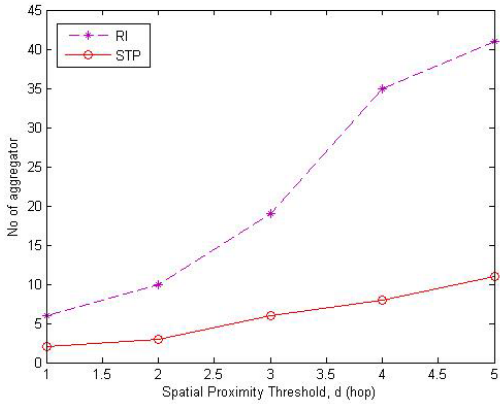

Fig. 5(b). Number of aggregators

C. EFFECT OF TEMPORAL PROXIMITY

We have also measured the effect of temporal proximity threshold on the total cost and number of aggregator nodes which are depicted in Figure 6(a) and Figure 6(b), respectively. From these two figures, it is observed that the total cost and number of aggregator in RI method is almost constant since RI method did not consider the concept of temporal proximity. In *STP*, the total cost and the number of aggregator increase slightly as the temporal proximity threshold increases, and become constant for higher value of proximity threshold. The reason behind this is that the number of proximity events and number of potential aggregator node increases when the temporal proximity threshold increases (see Equation 4). From Figure 6(a) and Figure 6(b), it is evident that the total cost and the number of aggregator node is less in *STP* than those in RI method.

D. NETWORK SIZE

We have estimated the total cost in the networks of different sizes varied from (5x5) to (25x25) nodes, which is depicted in Figure 7. From this figure, it is observed that the rate of increase of total cost is less in *STP* than in RI method. The reason behind is that the number of aggregator nodes increases more in RI method when the network size increases.

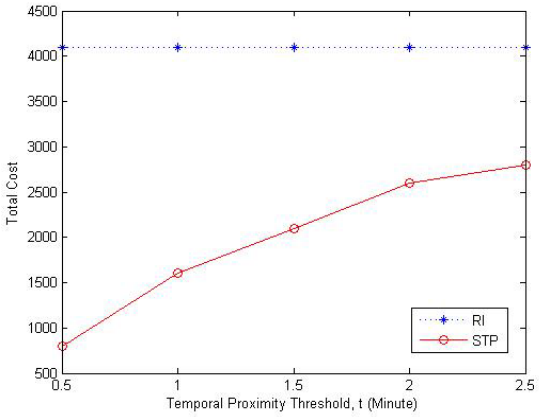

Fig. 6(a). Effect of temporal proximity threshold

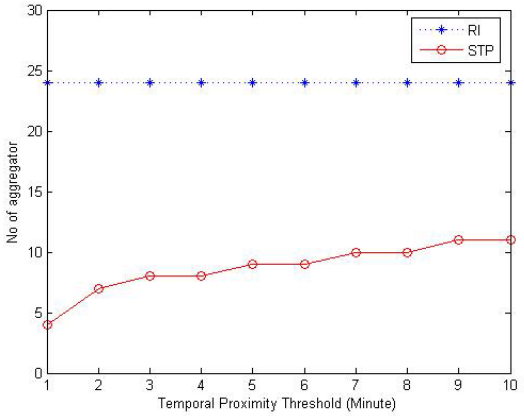

Fig. 6(b). Number of aggregators

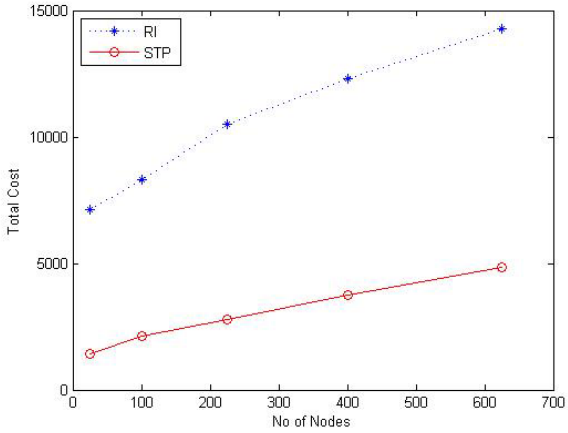

Fig. 7. Effect of network size

VI. CONCLUSION AND FUTURE WORK

In this paper, we have presented *STP*, a framework for in-network aggregation of events through proximity queries in sensor network for the monitoring applications where aggregated event information is more im-

portant than individual event information. *STP* reduces the cost for query registration and event propagation. *STP* eliminates unnecessary proximity events through temporal proximity threshold. *STP* reduces the cost for sending proximity alarms to the base node by selecting small number of aggregator nodes. Simulation results show that *STP* performs better than RI [21] method.

In this paper, we have simulated *STP* and RI methods assuming the network of *nxn* grids and homogeneous nodes. We intend to compare other method E-SPAN [1] using other network simulator NS2 [17]. We plan to measure the effect of target movement, and effect of concurrent events on the performance of *STP*. In addition, we will investigate the applications of sensor networks where the proximity query is efficiently applicable for in-network aggregations.

REFERENCES

[1] M. Lee, V.W.S. Wong. "An energy-aware spanning tree algorithm for data aggregation in wireless sensor networks". PACRIM, 2005.

[2] A. Brayner, A. Lopes, D. Meira, R. Vasconcelos, R. Menezes. "An adaptive in-network aggregation operator for query processing in wireless sensor networks". Journal of Systems and Software, Vol.1 Issue.3 Pages.328-342, 2008.

[3] A. Deshpande, C. Guestrin, S. Madden, J.M. Hellerstein, and W. Hong. "Model-Driven Data Acquisition in Sensor Networks". In Proc. of the 13th International Conference on Very Large Data Bases (VLDB), Toronto, Canada, 2004.

[4] Albath, Julia G. M. "Energy Efficient Clustering and Secure Data Aggregation in Wireless Sensor Networks". Ph.D. Dissertation, Computer Science, Missouri University of Science and Technology, 2008.

[5] C. Lv, P. Cao, E. Cohen, K. Li, and S. Shenker. "Search and Replication in Unstructured Peer-to-Peer Networks". In ICS, 2002.

[6] D. Kempe, A. Dobra, and J. Gehrke. "Gossip-Based Computation of Aggregate Information". In Proc. of the 44th IEEE Annual Symposium on Foundation of Computer Science (FOCS), 2003.

[7] H. Chan, A. Perrig, D. Song. "Secure hierarchical in-network aggregation in sensor networks". Proceedings of the 13th ACM conference on Computer and communications security, USA, 2006.

[8] J. Considine, F. Li, G. Kollios, and J. Byers. "Approximate Aggregation Techniques for Sensor Databases". In Proc. of the 20th International Conference on Data Engineering (ICDE), Washington DC, USA, 2004.

[9] J. Gao, L. Guibas, and J. Hershbinger. "Sparse Data Aggregation in Sensor Networks". In Proc. of the 6th International Symposium on Information Processing in Sensor Networks (IPSN), Cambridge, MA, USA, 2007.

[10] K. Fan, S. Liu, and P. Sinha. "On the potential of Structure-free Data Aggregation in Sensor Networks". In Proc. of the 25th IEEE International Conference on Computer Communication (INFOCOM), Bercelona, Spain, 2006.

[11] K. Fan, S. Liu, and P. Sinha. "Structure-free Data Aggregation in Sensor Networks". IEEE Transactions on Mobile Computing, vol. 6, no. 8, pp. 929-943, 2007.

[12] K. Kifayat, M. Merabti, Q. Shi and D. Llewellyn-Jones. "An Efficient Multi-Parameter Group Leader Selection Scheme for Wireless Sensor Networks". IFIP, 2008.

[13] Kim, J, S. Park, Y. Han, T. Chung. CHEF: Cluster Head Election mechanism using Fuzzy logic in Wireless Sensor Networks. Advanced Communication Technology ICACT 2008, pp. 654- 659, 17-20 Feb. 2008.

[14] L. Xiaoming, M. Spear, K. Levitt, N. S. Matloff, S. F. Wu. "Using Soft-Line Recursive Response to Improve Query Aggregation in Wireless Sensor Networks". ICC apos'08. IEEE International Conference on Communications.

[15] M. Bawa, H. Garcia-Molina, A. Gionis, and R. Motwani. "Estimating Aggregates on a Peer-to-Peer Network", Technical Report, Stanford University, CA, USA, 2003.

[16] M. Ding, X. Cheng, and G. Xue. "Aggregation Tree Construction in Sensor Networks". In Proc. of the 58th IEEE Vehicular Technology Conference, vol. 4, pp. 2168-2172, 2003.

[17] The network simulator ns2. http://www.isi.edu/nsnam/ns/.

[18] R. Cheng and S. Prabhakar. "Managing Uncertainty in Sensor Databases."ACM SIGMOD Record, vol. 32, no. 4, pp. 41-46, 2003.

[19] S. Madden, M. J. Franklin, J. M. Hellerstein, and W. Hong. "Tag: A Tiny Aggregation Service for Ad-hoc Sensor Networks". ACM SIGOPS Operating Systems Review, vol. 36, pp. 131-146, 2002.

[20] V. Kalogeraki, D. Gunopulos, and D. Zeinalipour-Yazti. "A Local Search Mechanism for Peer-to-Peer Networks". In CIKM, 2002.

[21] Y. Kotidis. "Processing Proximity Queries in Sensor Networks", In Proc. of the 3rd International-Workshop on Data Management for Sensor Networks (DMSN), Seoul, South Korea, 2006.

[22] Y. Kotidis. "Snapshot Queries: Towards Data-Centric Sensor Networks". In Proc. of International Conference on Data Engineering (ICDE), Tokoyo, Japan, 2005.

Proceedings of 2009 12th International Conference on Computer and Information Technology (ICCIT 2009)
21-23 December, 2009, Dhaka, Bangladesh

Improvement of Speech Enhancement Techniques for Robust Speaker Identification in Noise

Md. Rabiul Islam, Md. Fayzur Rahman†, Muhammad Abdul Goffar Khan†
Department of Computer Science & Engineering, Rajshahi University of Engineering & Technology, Rajshahi, Bangladesh
† Department of Electrical & Electronic Engineering, Rajshahi University of Engineering & Technology, Rajshahi, Bangladesh
rabiul_cse@yahoo.com, mfrahman3@yahoo.com, qmagk@yahoo.com

Abstract

This paper presents an approach of speech enhancement techniques to improve the performance of the robust speaker identification under noisy environments. Start-end points detection, silence part removal, frame segmentation and windowing technique have been used to pre-process and wiener filter has been used to remove the silence parts from the speech utterances. To extract the features from the speech various speech parameterization techniques that is LPC, LPCC, RCC, MFCC, ΔMFCC and ΔΔMFCC have been simulated. Finally, to measure the performance of the proposed speech enhancement techniques, genetic algorithm has been used as a classifier for the noise robust automated speaker identification system and various experiments have performed on genetic algorithm to select the optimum parameters. According to the NOIZEOUS speech database, the highest identification rate of 70.31 [%] for text-dependent and of 61.26 [%] for text-independent speaker identification system have been achieved.

Keywords: Genetic Algorithm, Noise Robust Speaker Identification, Speech Parameterization, Speech Pre-processing.

I. INTRODUCTION

Automatic speaker recognition (ASR) systems are increasingly employed in real-world applications such as voice authentication, surveillance and forensics [1]. Significant amount of research has been conducted in finding speech features that would yield maximum information about the identity of the speakers, thereby increasing the accuracy of the speaker identification system. With only usable portions of speech being input to the speaker identification system, there is an increase in the accuracy of the identification [2]. A number of usable speech measures for using in the usable speech extraction system, have been developed [3, 4, 5].

Current ASR system works very well under noiseless environments. However, in the presence of background noise the recognition performance of such systems degrades significantly, especially at low SNRs. Most published works in the areas of speech recognition and speaker recognition focus on speech under the noiseless environments and few published works focus on speech under noisy conditions [6, 7, 8, 9].

This work deals mainly the effective speech feature enhancement techniques that can be used successfully on speaker identification purpose in noisy environments. To measure the performance of the proposed techniques, genetic algorithm has been used as a classifier. The performance of this system was measured for both the text dependent and text-independent speaker identification system in noiseless and noisy environments according to the NOIZEOUS speech database.

II. PARADIGM OF SPEECH PARAMETERIZATION TECHNIQUES

Fig.1 shows the block diagram of the noise robust speaker identification system on the basis of the proposed speech enhancement techniques. For the noise robust speaker identification purpose wiener filter has been used which can remove the background noise from the speech. Finally GA has been used to measure the performance of this system.

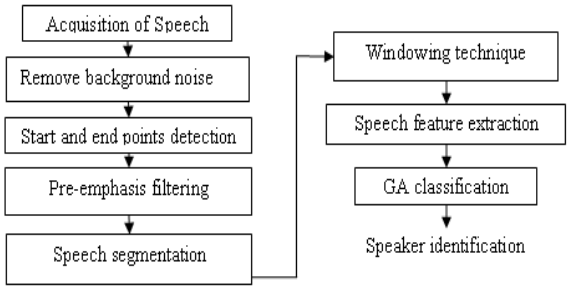

Fig.1. Paradigm of speech enhancement techniques for the proposed speaker identification system

III. SPEECH SIGNAL PRE-PROCSEEING

A. Acquisition of Speech Utterances and Removing the Background Noises

Speech utterance acquisition for this system has been done using high quality microphone. To increase the accuracy of this system, it is necessary to keep speech acquisition process noise free. The length of the speech is about 3 seconds. Sampling frequency 8000 Hz, sampling resolution 16 bits, mono recording channel and recorded file format *.wav have been considered when recorded the speech utterances.

To remove the background noises from the speech utterance, wiener filter [10, 11, 12] has been used. For

implementing of the wiener filter the following equations has been calculated:

$$\phi(f) = \frac{|S(f)|^2}{|S(f)|^2 + |N(f)|^2} \quad (1)$$

Since, $|S(f)|^2 + |N(f)|^2 \approx |C(f)|^2$, we get,

$$\phi(f) \approx \frac{|S(f)|^2}{|C(f)|^2} \quad (2)$$

Where, $|C(f)|^2$, $|S(f)|^2$ and $|N(f)|^2$ are the power spectrum of *C*, *S*, *N* and *C, S, N* are the Fourier transform of the measured signal *c(t)*, original source signal *s(t)* and background noise *n(t)*.

The best filter is one where the following integral is a minimum at every value of f of the equation:

$$\int_{-\infty}^{\infty} |R(f)|^{-2} |S(f)|^2 |1-\phi(f)|^2 + |N(f)|^2 |\phi(f)|^2 \, df \quad (3)$$

Where *R(f)* is the Fourier transform of *r(t)* and *r*(*t*) be the known response of the convolution.

Fig.2 shows the output after applying the wiener filtering technique.

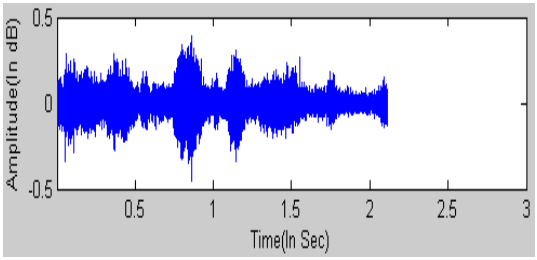

(a) Speech utterance with background noise.

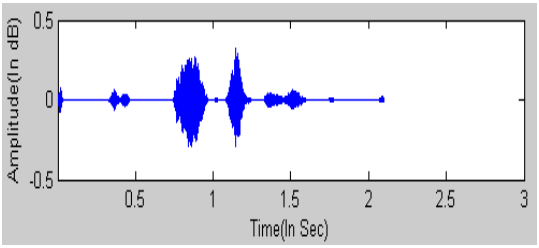

(b) Utterance after applying wiener filter.

Fig.2. Effects of wiener filter on noisy speech utterance.

B. Start and End Points Detection

Speech endpoints detection was used to detect the presence of speech and to remove the silences in background noises [13, 14, 15, 16]. The start and end points detection algorithm [17] has been used to detect the end points of the speech and finally short-time energy is implemented to remove the silence parts by using the equation:

$$E_i = \sum_{t=n_i}^{n_i+N-1} S^2(t) \quad (4)$$

Where *s(t)* is the data sample, *i* is the frame number, E_i is the frame energy, *N* corresponds to the frame length and n_i is the index of first data sample in the frame.

C. Speech Pre-emphasizing

The Pre-emphasizing filter has been used here as a noise reduction system to increase the amplitude of the input signal at frequencies where signal-to-noise ratio (SNR) is low.

Pre-emphasis has been used to balance the spectrum of voiced sounds that have a steep roll-off in the high frequency region [18, 19, 20]. This process is usually performed by a first order digital high pass filter. The transfer function of the filter used in the experiments is

$$H(z) = (1 - az^{-1}) \quad (5)$$

D. Speech Segmentation

In this step the continuous speech signal has been blocked into frames of *N* samples, with adjacent frames being separated by *M (M<N)*. The purpose of the overlapping analysis is that each speech sound of the input sequence would be approximately centered at some frame [21, 22]. In all the experiments to be presented, a frame length of 15-30 milliseconds was used and 65% frame overlapping has been considered for speech segmentation.

E. Windowing Technique

In this work, the purpose of using windowing is to reduce the effect of the spectral artifacts that results from the framing process [23, 24, 25]. A Hamming window, which tapers at its edges rather than having a sharp discontinuity, introduces fewer artifacts and is therefore used. The hamming window has been implemented by the following equation [26]:

$$w[k+1] = 0.54 - 0.46\cos(2\pi \frac{k}{n-1}), k = 0,1,\ldots\ldots\ldots n-1 \quad (6)$$

IV. FEATURE EXTRACTION

This stage is very important in the robust speaker identification system because the quality of the speaker modeling and pattern matching strongly depends on the quality of the feature extraction methods. Different types of speech feature extraction methods [27, 28, 29, 30, 31, 32] such as LPC, LPCC, RCC, MFCC, ΔMFCC and ΔΔMFCC have been applied to extract the features from the speech.

In linear prediction coding (LPC), the current speech sample, say *s(n)* is estimated by a linear combination of the past *p* samples. i.e.

$$S(n) = \sum_{k=1}^{P} a_k S(n-k) + e(n) \quad (7)$$

Where, *e(n)* is the error term and the $(a_k)^P_k = 1$ values are referred to as the linear prediction coefficients (LPCs).

To compute the linear prediction cepstral coefficients (LPCCs), we have at first compute n^{th} order LPC vec-

tors from preprocessed speech. The following equation transforms the LPC set into cepstral coefficient set.

$$lpcc(n) = \begin{cases} In\,G & ;\ n=0 \\ a_n + \sum_{k=1}^{n-1} \left(\frac{k}{n}\right) c(k) a_{n-k} & ;\ 0<n\le p \\ \sum_{k=n-p}^{n-1} \left(\frac{k}{n}\right) c(k) a_{n-k} & ;\ n>p \end{cases} \quad (8)$$

To compute the Real Cepstral Coefficients (RCCs), at first the signal is transformed from the time domain into the frequency domain by applying Fourier Transform.

$$x(t) * y(t) = X(\omega) Y(\omega)$$
$$X(\omega) * Y(\omega) = x(t) y(t) \quad (9)$$
$$S(m,\omega) = E(m,\omega) H(m,\omega)$$

The symbol * denotes the convolution operator.

$$\log|S(m,\omega)| = \log|E(m,\omega)| + \log|H(m,\omega)| \quad (10)$$

The inverse Fourier Transform is linear and therefore works individually on the two components

$$c_s(m,t_0) = c_e(m,t_0) + c_k(m,t_0) \quad (11)$$

Here $c_s(m,t_0)$ is called the cepstram or real-cepstram coefficient of $c(n,t_0)$.

The calculation of the mel frequency cepstral coefficients that is MFCCs are calculated in the same way as the Real Cepstral Coefficients expect that the frequency scale is warped to correspond to the mel scale. The mel scale is generally mapping below 1000Hz and logarithmically spaced above. The mapping is usually done using an approximation, taken from

$$Mel(f) = 2595 \log\left(1 + \frac{f}{700}\right) \quad (12)$$

By calculating the MFCC coefficients some tasks must be performed. Fig.3 shows the block diagram of the MFCC coefficients.

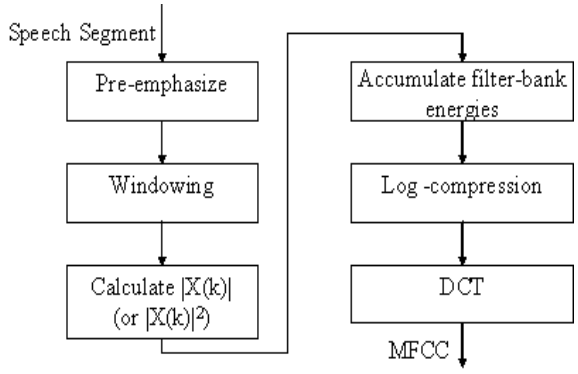

Fig.3. Block diagram to calculate the MFCC coefficients.

To calculate the ΔMFCC and ΔΔMFCC, if log energy is requested then we get the first element of each row followed by the delta and then the delta-delta coefficients. Fig. 4 shows the features after applying different types of feature extraction techniques.

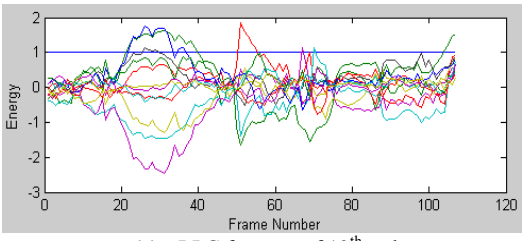

(a) LPC features of 12th order

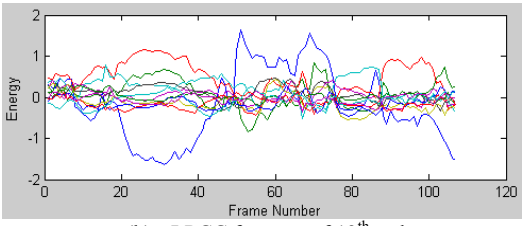

(b) LPCC features of 12th order

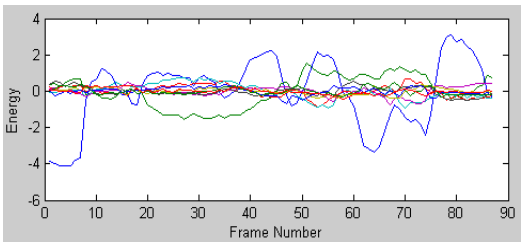

(c) RCC features with 15 coefficients

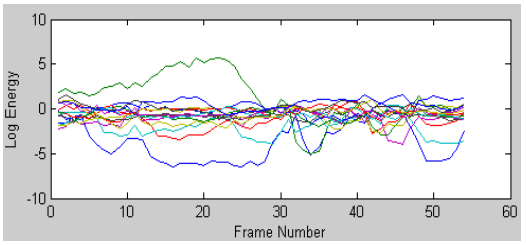

(d) MFCC features with 15 coefficients

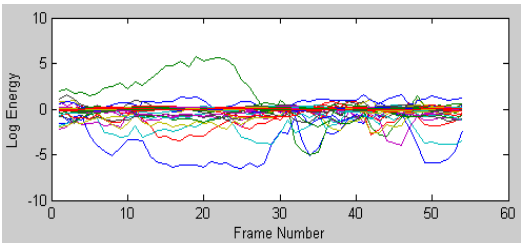

(e) ΔMFCC features with 15 coefficients

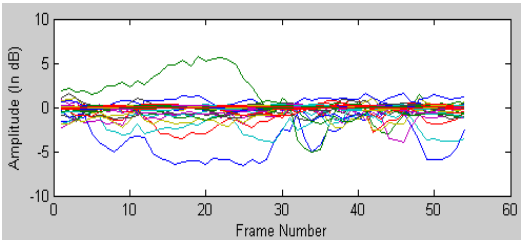

(f) ΔΔMFCC features with 15 coefficients

Fig. 4. Feature extraction form of speech.

V. PARAMETERS SELECTIONS ON GENETIC ALGORITHM

Genetic algorithm has been used as a classifier for this proposed system. In GA processing selection, crossover and mutation operators have been used here. The fitness function is expressed as,

fitness = sum (unknown speech features × each stored speech features) (13)

There are some critical parameters (such as crossover rate and number of generation) that affect the performance of the developed system. A trade off is made to explore the optimal values of the above parameters and experiments were performed using those parameters. The optimal values of the above parameters were chosen and finally found out the results.

A. Experiment on the Crossover Rate

In this experiment, crossover rate has been changed in various ways such as 1, 2, 5, 7, 8, 10, 12, 14, 16, 18, 20. The highest speaker identification rate of 96[%] was found at crossover point 8 which is shown in the Fig. 5.

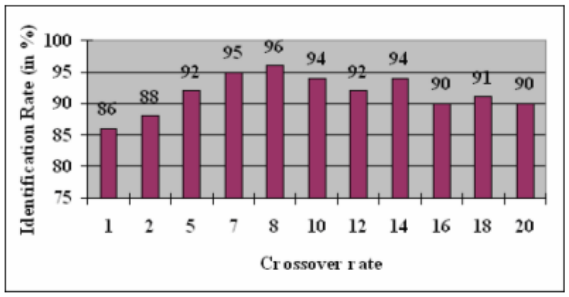

Fig.5. Performance measurement according to the crossover rate.

B. Experiment on the Number of Generations

In this experiment, crossover rate has been changed in various ways such as 1, 2, 5, 7, 8, 10, 12, 14, 16, 18, 20. The highest speaker identification rate of 96[%] was found at crossover point 8 which is shown in the Fig. 6.

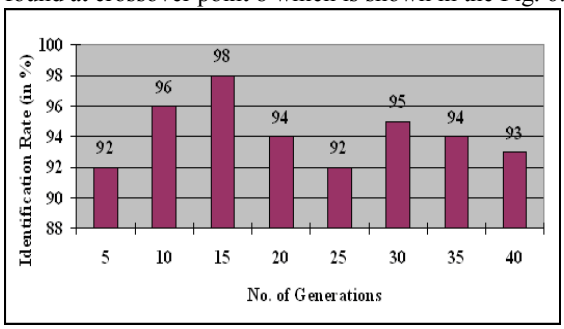

Fig.6. Accuracy measurement according to the no. of generations.

VI. EXPERIMENTAL RESULTS AND PERFORMANCE ANALYSIS

The optimal values of the critical parameters of the GA are chosen carefully according to various experiments. In noiseless environment, the crossover rate and number of generation have been found 8 and 15 respectively. The performance analysis has been counted according to the text-dependent and text independent speaker identification system.

To measure the performance of the proposed system, NOIZEOUS speech database [37, 38] has been used. In NOIZEOUS speech database, eight different types of environmental noises (i.e. Airport, Babble, Car, Exhibition, Restaurant, Street, Train and Train station) have been considered with four different SNRs such as 0dB, 5dB, 10dB and 15dB. All of the environmental conditions and SNRs have been accounted on the following experimental analysis.

A. performance Analysis according to the Text-dependent Speaker Identification System

In this experiment, the highest average speaker identification rate was achieved to be 70.31[%] for ΔMFCC which is shown in Table I.

B. Performance Analysis according to the Text-independent Speaker Identification System

The performance of the proposed speaker identification techniques were also been measured in text-independent case. In the close set text-independent system, the highest speaker identification rate has been counted 61.26[%] for ΔMFCC which is shown in Table II.

VII. CONCLUSION AND OBSERVATION

To find out the best performance of this proposed speech enhancement techniques, the optimal values of the GA parameters have been selected effectively. Two experiments (according to crossover rate and no. of generations) have been performed for this purpose. The highest identification rate has been achieved at ΔMFCC and the rates are 70.31[%] and 61.26[%] in text-dependent and text-independent case respectively. Therefore, this can satisfies a major amount of practical demand in the field of speaker identification. Though the performance of the speech enhancement techniques were measured using GA, the system performance can also be populated by using Hidden Markov Model (HMM), Support Vector Machine (SVM), and so on. The performance of this system can also be tested by using hybrid system as a classifier.

Table I Overall text-dependent speaker identification rate (%) for NOIZEOUS speech corpus

Method / Various Noise	MFCC	ΔMFCC	ΔΔMFCC	RCC	LPCC
Airport Noise*(Average of 15dB, 10dB, 5dB and 0dB)*	70.83	75.62	50.83	56.83	55.29
Babble Noise*(Average of 15dB, 10dB, 5dB and 0dB)*	68.92	68.83	44.56	48.33	60.29
Car Noise*(Average of 15dB, 10dB, 5dB and 0dB)*	65.67	65.87	50.17	50.50	58.92
Exhibition Hall Noise*(Average of 15dB, 10dB, 5dB and 0dB)*	69.67	75.17	49.89	65.17	64.17
Restaurant Noise*(Average of 15dB, 10dB, 5dB and 0dB)*	65.59	68.54	35.63	60.67	65.33
Street Noise*(Average of 15dB, 10dB, 5dB and 0dB)*	67.65	70.33	43.17	59.29	64.89
Train Noise*(Average of 15dB, 10dB, 5dB and 0dB)*	68.92	68.92	56.29	58.33	62.33
Train Station Noise*(Average of 15dB, 10dB, 5dB and 0dB)*	60.00	69.17	30	50.33	58.29
Average Identification Rate (%)	67.16	70.31	45.07	56.18	61.19

Table II Overall text-independent speaker identification rate (%) for NOIZEOUS speech corpus

Method / Various Noise	MFCC	ΔMFCC	ΔΔMFCC	RCC	LPCC
Airport Noise*(Average of 15dB, 10dB, 5dB and 0dB)*	58.56	66.89	42.87	45.17	48.29
Babble Noise*(Average of 15dB, 10dB, 5dB and 0dB)*	57.92	60.87	40.56	42.83	49.17
Car Noise*(Average of 15dB, 10dB, 5dB and 0dB)*	55.67	53.33	38.29	40.29	50.17
Exhibition Hall Noise*(Average of 15dB, 10dB, 5dB and 0dB)*	55.92	62.29	40.33	52.5	45.87
Restaurant Noise*(Average of 15dB, 10dB, 5dB and 0dB)*	53.59	58.34	33.33	49.5	56.33
Street Noise*(Average of 15dB, 10dB, 5dB and 0dB)*	55.33	62.17	39.92	50	53.29
Train Noise*(Average of 15dB, 10dB, 5dB and 0dB)*	60.29	60.29	48.17	46.33	50
Train Station Noise*(Average of 15dB, 10dB, 5dB and 0dB)*	51.17	65.87	30	40.33	49.87
Average Identification Rate (%)	56.06	61.26	39.18	45.87	50.37

REFERENCES

[1] A. El-Solh, A. Cuhadar and R.A. Goubran, "Evaluation of Speech Enhancement Techniques for Speaker Identification in Noisy Environments," *Ninth IEEE International Symposium on Multimedia 2007 – Workshops.*

[2] S. Khanwalkar, B. Y. Smolenski and R. E. Yantorno, "Speaker Identification Enhancement under Co-Channel Conditions using Sinusoidal Model based Usable Speech Detection," *IEEE international Symposium on Intelligent Signal Processing and Communication Systems (ISPACS 2004).*

[3] K. Krishnamachari and R. E. Yantorno, "Spectral autocorrelation ratio as a usability measure of speech segments under cochannel conditions," *IEEE Inter. Symposium on Intelligent Signal Processing & Comm. Systems*, 2000, pp. 710–713.

[4] J. M. Lovekin, K. R. Krishnamachari and R. E. Yantorno, "Adjacent pitch period comparison as a usability measure of speech segments under co-channel conditions," *IEEE International Symposium on Intelligent Signal Processing and Communication Systems*, 2001, pp. 139–142.

[5] N. Chandra and R. E. Yantorno, "Usable speech detection using modified spectral autocorrelation peak to valley ration using the lpc residual," *4th IASTED Int. Conference Signal and Image Processing*, 2002, pp. 146–150.

[6] Reynolds, D.A., "Experimental evaluation of features for robust speaker identification," *IEEE Transactions on SAP,* Vol. 2, 1994, pp. 639-643.

[7] Sharma, S., Ellis, D., Kajarekar, S., Jain, P. & Hermansky, H., "Feature extraction using non-linear transformation for robust speech recognition on the Aurora database," *Proc. ICASSP2000*.

[8] Wu, D., Morris, A.C. & Koreman, J., "MLP Internal Representation as Disciminant Features for Improved Speaker Recognition," *Proc. NOLISP2005*, Barcelona, Spain, 2005, pp. 25-33.

[9] Konig, Y., Heck, L., Weintraub, M. & Sonmez, K., "Nonlinear discriminant feature extraction for robust text-independent speaker recognition," *Proc. RLA2C, ESCA workshop on Speaker Recognition and its Commercial and Forensic Applications,* 1998, pp.72-75.

[10] Simon Doclo and Marc Moonen, "On the Output SNR of the Speech-Distortion Weighted Multi-

channel Wiener Filter," *IEEE Signal Processing Letters*, vol. 12, no. 12, 2005.

[11] Wiener, N., *Extrapolation, Interpolation and Smoothing of Stationary Time Series with Engineering Applications*, Wiely, Newyork, 1949.

[12] Wiener, N., Paley, R. E. A. C., *Fourier Transforms in the Complex Domains,* American Mathematical Society, Providence, RI, 1934.

[13] Koji Kitayama, Masataka Goto, Katunobu Itou and Tetsunori Kobayashi, "Speech Starter: Noise-Robust Endpoint Detection by Using Filled Pauses," *Eurospeech 2003*, Geneva, pp. 1237-1240.

[14] S. E. Bou-Ghazale and K. Assaleh, "A robust endpoint detection of speech for noisy environments with application to automatic speech recognition," *Proc. ICASSP2002*, vol. 4, pp. 3808–3811.

[15] A. Martin, D. Charlet, and L. Mauuary, "Robust speech / non-speech detection using LDA applied to MFCC," *Proc. ICASSP2001*, vol. 1, 2001, pp. 237–240.

[16] Sarma, V., Venugopal, D., "Studies on pattern recognition approach to voiced-unvoiced-silence classification," *IEEE International Conference on ICASSP '78.* , vol. 3, 1978, pp. 1-4.

[17] Kaushik Roy and M. Ganger Ali, "Implementation of Speech Recognition System using Artificial Neural Network," *Third International Conference on Electrical, Electronics and Computer Engineering,* Dhaka, Bangladesh, 2003.

[18] Harrington, J., and Cassidy, S., *Techniques in Speech Acoustics,* Kluwer Academic Publishers, Dordrecht, 1999.

[19] Makhoul, J., "Linear prediction: a tutorial review," *Proceedings of the IEEE 64*, 4 (1975), pp. 561–580.

[20] Picone, J., "Signal modeling techniques in speech recognition," *Proceedings of the IEEE 81*, 9 (1993), pp. 1215–1247.

[21] Clsudio Beccchetti and Lucio Prina Ricotti, *Speech Recognition Theory and C++ Implementation*, John Wiley & Sons. Ltd., 1999, pp.124-136.

[22] L.P. Cordella, P. Foggia, C. Sansone, M. Vento., "A Real-Time Text-Independent Speaker Identification System," *Proceedings of 12th International Conference on Image Analysis and Processing*, IEEE Computer Society Press, Mantova, Italy, 2003, pp. 632 - 637.

[23] J. R. Deller, J. G. Proakis, and J. H. L. Hansen, *Discrete-Time Processing of Speech Signals,* Macmillan, 1993.

[24] F. Owens., *Signal Processing Of Speech,* Macmillan New electronics, Macmillan, 1993.

[25] F. Harris, "On the use of windows for harmonic analysis with the discrete fourier transform," *Proceedings of the IEEE 66,* vol. 1, 1978, pp. 51-84.

[26] J. Proakis and D. Manolakis, *Digital Signal Processing, Principles, Algorithms and Aplications,* Second edition, Macmillan Publishing Company, New York,1992.

[27] D. Kewley-Port and Y. Zheng, "Auditory models of formant frequency discrimination for isolated vowelsm," *Journal of the Acostical Society of America*, 103(3), 1998, pp. 1654–1666.

[28] D. O'Shaughnessy, *Speech Communication - Human and Machine,* Addison Wesley. 1987.

[29] E. Zwicker., "Subdivision of the audible frequency band into critical bands (frequenzgruppen)," *Journal of the Acoustical Society of America*, 33, 1961, pp. 248–260.

[30] S. Davis and P. Mermelstein, "Comparison of parametric representations for monosyllabic word recognition in continuously spoken sentences," *IEEE Transactions on Acoustics Speech and Signal Processing*, 28, 1980, pp. 357–366.

[31] S. Furui., "Speaker independent isolated word recognition using dynamic features of the speech spectrum," *IEEE Transactions on Acoustics, Speech and Signal Processing*, 34, 1986, pp. 52–59.

[32] S. Furui, "Speaker-Dependent-Feature Extraction, Recognition and Processing Techniques," *Speech Communication*, vol. 10, 1991, pp. 505-520.

[33] Koza, J .R., *Genetic Programming: On the programming of computers by means of natural selection,* Cambridge: MIT Press, 1992.

[34] D.E. Goldberg, *Genetic Algorithms in Search, Optimization and Machine Learning,* Addison-Wesley, Reading, MA, 1989.

[35] Z. Michalewicz, *Genetic Algorithms + Data Structures = Evolution Programs,* Third Edition, Springer-Verlag, New York, USA, 1999.

[36] Rajesskaran S. and Vijayalakshmi Pai, *G.A., Neural Networks, Fuzzy Logic, and Genetic Algorithms- Synthesis and Applications,* Prentice-Hall of India Private Limited, New Delhi, 2003.

[37] Hu, Y. and Loizou, P., "Subjective comparison of speech enhancement algorithms," *Proceedings of ICASSP-2006*, Toulouse, France, pp. 153-156.

[38] Hu, Y. and Loizou, P., "Evaluation of objective measures for speech enhancement," *Proceedings of INTERSPEECH-2006*, Philadelphia, PA.

Proceedings of 2009 12th International Conference on Computer and Information Technology (ICCIT 2009)
21-23 December, 2009, Dhaka, Bangladesh

Adaptive Energy Detection for Cognitive Radio: An Experimental Study

James Y. Xu, Fakhrul Alam†
School of Engineering and Advanced Technology, Massey University, Auckland, New Zealand
jyxu@jamesyxu.com, F.Alam@massey.ac.nz

Abstract

A cognitive radio (CR) is able to sense spectral environment over a wide range of frequencies, and provide opportunistic access to frequency bands temporarily unoccupied by an incumbent. Accurate channel sensing is the first important task for a CR, and energy detector is often used for this purpose. While a normal energy detector works well with well chosen window size based on prior knowledge about possible primary users, it often fails with signals that are narrow compared to the detector window, or if only a fraction of the signal is inside the detector window. We propose an adaptive energy detector that can adjust its detection window, and evaluate such detector's performance using experimental results obtained through a real time implementation.

Keywords: channel sensing, cognitive radio, energy detection, energy detector model, labview

I. INTRODUCTION

Unlicensed spectrum is becoming increasingly scarce, especially those under 3 GHz. The Federal Communications Commission (FCC)'s spectrum allocation chart shows that many frequency bands are being allocated to multiple incumbents, overlapping each other [1]. While most frequency bands are licensed, studies from [1] and [2] suggest utilization rate between 15% and 85%. Cognitive radio (CR) has been highlighted as a possible candidate in improving spectrum utilization by providing opportunistic spectrum access [3, 4]. A cognitive radio can be defined as a radio that is able to sense the spectral environment over a wide frequency, and exploit this information to opportunistically provide wireless links that best meet the user's communication requirements [1]. In order to provide access to a frequency band as a secondary user, a CR must first be able to sense and identify frequencies (spectrum sensing) that are temporarily unoccupied by an incumbent. These "free" areas are termed as "holes" in [5].

For spectrum sensing, energy detector is a popular technique [1, 6]. In this paper, we focus on the detection of signals that are narrow compared to the detector window (narrow signals), and on the detection of signals where only a small portion of the signal is captured in the detector window. A real time detector with adaptive detection window is proposed and implemented. The performance of such detector is then investigated using data obtained from a real time experiment.

The paper is organized as follows: Section 2 briefly discusses related work done by other research groups. In Section 3, we provide an overview of the energy detector model, and our problem statement. Section 4 describes our adaptive detection strategy in detail. Section 5 presents our testbed set up and experimental data. And Section 6 presents some limitations of our detector and energy detectors in general. Finally Section 7 summarizes the work done and concludes the paper.

II. RELATED WORK

There are many researches being done on energy detectors. The hidden terminal problem in detection was discussed in [1], where the CR is behind a building with high penetration loss, and may not see the primary user. However as the CR starts to transmit, the primary user will be interrupted. A suggestion of an extra 30-40dB SNR sensitivity requirement was made for the CR to combat this effect. The article also defined a term "local spectrum sensing", where a CR must independently detect primary users, due to the lack of a direct way of measurement between the primary transmitter and receiver. In [6], theoretical analysis of pilot detection and energy detection are presented. The models for the detectors were derived, and experimental results were presented to support the theory. Detailed discussions of the limitations of each detection strategy were also included. In [8], a practical energy detector was presented. The article starts by detailing the model of the energy detector, and then moves on to the derivation of threshold calculations. Finally some experimental data were used to evaluate the performance of the detector under various conditions. In [9], the concept of an SNR wall for systems trying to detect low power signals (<< 0dB SNR) was derived as a fundamental limit of an energy detector. For a detector with N_x noise uncertainty, there exist a $SNR_{wall} = 10\log_{10}\left[10^{\left(\frac{N_x}{10}\right)} - 1\right] dB$ under which the signal becomes impossible to detect. In [7], a complete system using software radio is presented. The radio uses a Genetic Algorithm (GA) that is able to search through a large combination of possible system parameters, and find the one that is best for the current channel conditions. The demonstration system is able to stream video continuously under heavy interference by adjusting the operating parameters of the radio.

978-1-4244-6283-4/09/$26.00 ©2009 IEEE

III. ENERGY DETECTION AND PROBLEM STATEMENT

A. ENERGY DETECTOR MODEL

An energy detector can be used to determine if a given window contains only noise (1), or signal plus noise (2). This goal can be simplified to the following hypotheses test [6, 8]:

$$H_0: y[n] = w[n] \quad (1)$$

$$H_1: y[n] = x[n] + w[n] \quad (2)$$

where y is the signal received by the CR, x is the transmitted signal, and w is presumed to be Additive White Gaussian Noise (AWGN). The test statistic for an energy detector is:

$$T = \sum_n^N (y[n])^2 \quad (3)$$

With large numbers of samples (M number), by central limit theorem this can be modeled as:

$$T_{H_0} \sim N(BP_n, \frac{(BP_n)^2}{M}) \quad (4)$$

$$T_{H_1} \sim N(BP_n + P_s, \frac{(BP_n + P_s)^2}{M}) \quad (5)$$

where B is the window bandwidth of the detector, P_n is the noise power spectral density, and P_s is the power of the signal. The probability of false alarm is the probability that noise is large enough to be detected as a signal. With estimated noise power, we can derive a model for the probability of false alarm:

$$P_{fa}[X > \gamma] = Q(\frac{\gamma - BP_n}{BP_n/\sqrt{M}}) \quad (6)$$

Where Q is the normal cumulative distribution function. Using (6) we can specify a target false alarm rate, and calculate the corresponding threshold [8]:

$$\gamma = BP_n(\frac{Q^{-1}(P_{fa})}{\sqrt{M}} + 1) \quad (7)$$

Given a threshold, the energy detector itself can be implemented easily by squaring the magnitude data of an FFT, and normalizing over bin size to obtain the power spectral density (PSD). The detector then integrates over the entire window, obtaining total power within the window. Comparing this with the threshold from (7), the detector then makes a decision, indicating whether the current window is free or not. When using this method, we can modify the frequency resolution of the FFT by increasing the number of points for the FFT. The tradeoff for this is increased processing time. We can also average a number of PSDs to smooth out the effect of noise. This improves detection, again at a cost of processing time.

B. PROBLEM STATEMENT

Regarding the energy detector from Section 3.A, experiments from [6, 8], and our preliminary experimental data have shown that this energy detector model is accurate. The detector described is set to work at a particular window size. First a frequency band is selected and filtered. An FFT is computed, and the energy detection is performed subsequently. In practice, various operation parameters are met by changing the number of averages taken, and sometimes by changing the frequency resolution [6].

A cognitive radio is often "blind", in the sense that it has no prior knowledge about incumbents. This often means that the window size chosen for the energy detector described in Section 3.A may not be appropriate. As a result, the energy detector often fails if the signal is narrow (compared to the detector window), or if only a small fraction of the signal is captured within the window. We can alleviate this problem by adjusting the window used for energy detection. But an increased number of energy detection also leads to an increase in sensing time. An energy detector that can selectively subdivide large windows into finer ones can trade the minimum detectable bandwidth with possible increase in detection time. This is more effective than decreasing the detection window across the board, especially in areas where a small number of narrow signals are expected.

IV. ENERGY DETECTOR WITH ADAPTIVE WINDOW SIZE

A weakness of the conventional energy detector when detecting narrow or partial signals is demonstrated in Fig. 1. The PSD in Fig. 1 is captured in real time by our workbench, and shows a frequency band of 195 MHz to 203 MHz (TV3 in New Zealand).

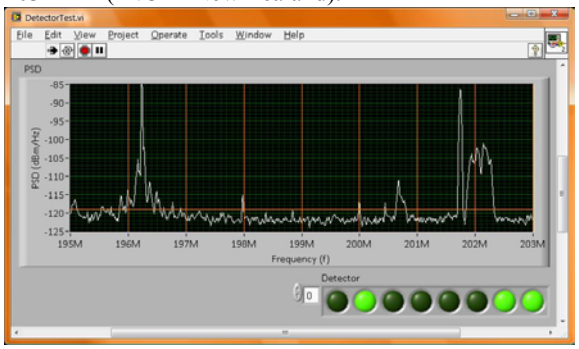

Fig. 1. Energy detector performance on narrow band signals

Assuming no prior knowledge of the incumbents, the system uses a 1 MHz window for energy detection, and the results suggest that windows 1, 3, 4, 5 and 6 are free. However, we can clearly see that there are signals present in those window positions. While these signals are present, they occupy a band that is narrow compared to the energy detector. As the integration in (3) completes for each window, the total power in window is not enough to rise above the threshold. Three possible ways to combat this problem are to lower the threshold, to choose a window similar in size to the signal under detection, or to narrow the detector window. Lowering the threshold increases P_{fa} significantly according to Eq.

(6), resulting in an unusable radio system. Choosing a window size closer to the signal under detection (6-8 MHz in case of a TV signal) requires prior knowledge of incumbents, something the CR often does not have. Using a narrow detector window alleviates the problem, at a cost of increased sensing time.

We propose an adaptive energy detector based on the third method. The detector normalizes the γ threshold obtained in Eq. (7) to dBm/Hz, does a preliminary scan of the PSD within the detector window, and performs a window subdivision if necessary. Fig. 2 describes the workflow of this adaptive energy detector.

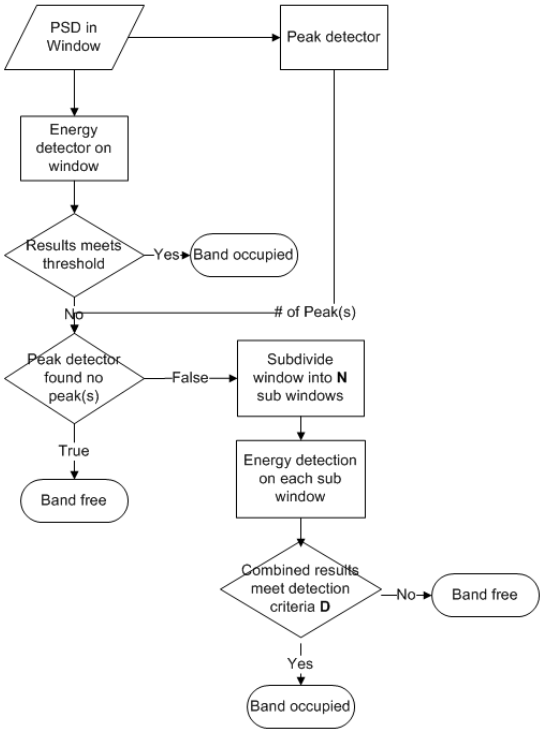

Fig. 2. Adaptive energy detector workflow

If there are peaks above the normalized threshold, and wider than the minimum detectable bandwidth, then the detector automatically subdivides the current window into N numbers of sub windows. We note that the minimum detectable signal bandwidth is limited by the frequency resolution (f_r) of the FFT, and thus the subdivision is limited also by the frequency resolution. Our proposed detector sets minimum detectable narrow signal to the frequency resolution of the FFT, and subdivides the current window into:

$$N = \frac{B}{f_r} \tag{8}$$

The decision variable then becomes:

$$D = E_0 \vee E_1 \vee \ldots \ldots \vee E_{N-1} \tag{9}$$

Where D is the final decision variable, and E_i is the decision on the ith window.

V. EXPERIMENTAL RESULTS

A. TESTBED DESCRIPTION

Fig. 3 showcases our CR work bench. The bench consists of: a National Instruments PXI-5661 Vector Signal Analyzer (consisting of PXI-5600 RF Down converter and PXI-5142 OSP Digitizer) housed in a PXI chassis [11]; two computers with LabVIEW [12] for interfacing with the VSA (including one PXI-8106 embedded controller in the PXI chassis); a Universal Software Radio Peripheral (USRP) with both RX and TX daughter boards; an Agilent 33120 Signal Generator; an HP 54600B Oscilloscope; and an Agilent 35670A Dynamic Signal Analyzer.

For this experiment, only the PCs and the NI VSA were used. The VSA has a range of 30 kHz to 2.7 GHz, with 20 MHz of real time bandwidth. It uses a 3 stage super heterodyne design, and can return data in both I/Q and Frequency domain through the on board signal processor. The PCs are running LabVIEW for interfacing with the VSA, through the CRLibs library we developed especially for cognitive radio applications.

Currently our library supports various spectrum measurements, channel sensing and energy detection with a flexible bandwidth from 1 kHz to 1GHz. Spectrum averaging, windowing and other signal processing functions are also included. It is used for a range of applications from wideband 802.22 channel sensing similar to [10], to UWB communication system simulations.

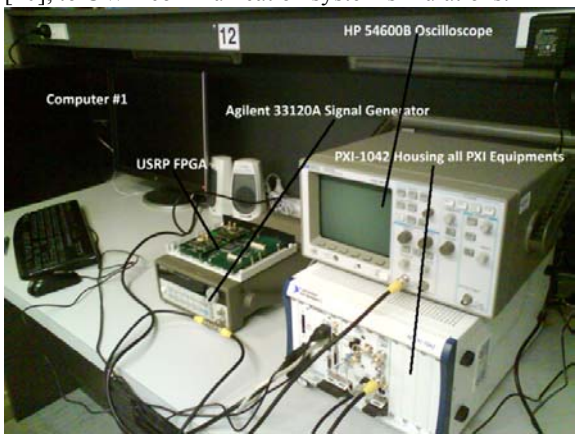

Fig. 3. Cognitive radio work bench

B. ADAPTIVE ENERGY DETECTOR SETUP

The adaptive energy detector is implemented completely in software under LabVIEW, based on periodogram [1]. First, the VSA is initialized with system parameters such as resource handles and application specific parameters such as frequency scan range. Once in acquisition mode, we configured the onboard signal processor to return a PSD waveform in dBm/Hz. A noise floor is estimated, and the appropriate threshold is computed using (7). The detector then follows the steps described in Fig. 2, finally reaching a decision for the current win-

dow. This adaptive energy detector is now a part of the CRLibs, and can be used as a subVI in LabVIEW. It offers programmable FFT frequency resolution, number of averages, and windowing functions. The detector's sensing time performance can be seen in Fig. 5.

C. EXPERIMENTAL SETUP

Using our CRLibs with the VSA, we can perform the energy detection correctly on signals from 9 kHz to 2.7 GHz, with 1 kHz to 1 GHz of bandwidth. We decided to investigate the VHF/UHF range due to the frequency band's connection to 802.22, and the readily available public broadcast signals at known locations. The VSA is connected with a TV antenna, and has the following parameters:

Table I. Experimental system parameters

FFT resolution bandwidth	15 kHz
Energy detector window size	1 MHz
Number of averages	60

We then collected sets of data for both the normal energy detector, and the adaptive detector. To provide accurate experimental data, each measurement was repeated 10,000 times.

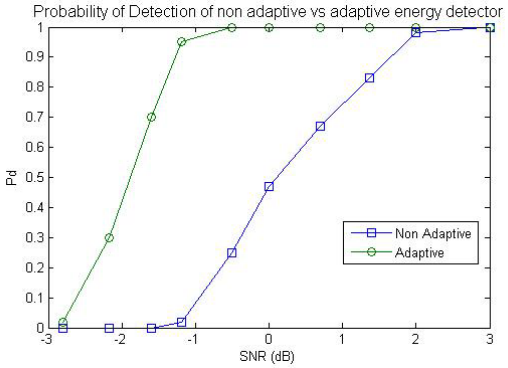

Fig. 4. Detection performance

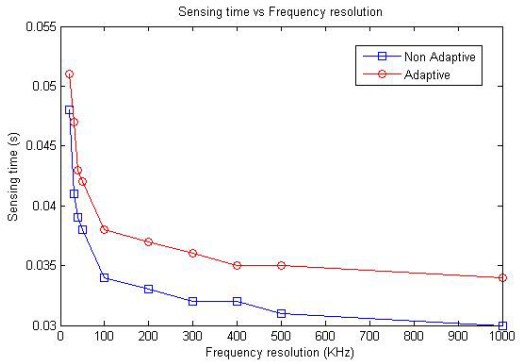

Fig. 5. Sensing time performance

D. RESULTS

First, we evaluate the cumulative distribution function (CDF) of the probability of detection for our adaptive detector. While the signal power within each of the detector windows may be small, the regions that rise above the threshold are enough for the adaptive energy detector to adjust the window size, and make a more accurate decision. Fig. 4. shows that for the same probability of detection, the adaptive energy detector requires 1 to 2dB less SNR. We note that none of the detectors were able to make correct decisions with signals that are lower than -3dB SNR. This is expected from a detector using a relatively small number of samples (M = 60) and is in line with results obtained by [8].

Then, we compare our detector's sensing time performance against a normal energy detector. While the PC based detectors do not have fast response times, Fig. 5. still demonstrates the relatively longer sensing time our adaptive method takes compared to a normal detector. This is to be expected, as our adaptive method has to first make a preliminary scan of the window, and then sub divide the window and perform multiple energy detections when necessary.

VI. LIMITATIONS

For a general energy detector with N_x dB of noise uncertainty, there exists a wall $SNR_{wall} = 10\log_{10}\left[10^{\left(\frac{N_x}{10}\right)} - 1\right] dB$ under which a signal is impossible to detect [6, 9]. Also, studies have shown that weak signals with power << 0dB require $O(1/SNR^2)$ samples to detect, which can increase sensing time significantly [6, 9].

Apart from the fundamental limits discussed above, our adaptive detector also has a limitation in terms of the minimum detectable signal bandwidth, and further increase in detection time. In Section 5 we noted that the minimum detectable signal bandwidth decreases with a decrease of frequency resolution of the FFT. This limits what we can detect, as decreasing the frequency resolution increases sensing time. Together with the time required to do a preliminary scan of the window, the total extra time is compounded on top of the time needed to gather the number of samples required to detect weak signals. The sensing time performance of our adaptive detector can be seen in Fig. 5.

While FPGA implementations are much faster than our generic PC setup, our CRLibs subVI library provides a flexible testbed that can be configured to do most spectral measurement tasks with minimum set up and tear down time. For example, the set up can be used to test ultra wideband CR systems, M-ary modulated communication systems and energy detector systems all using the CRLibs with no code modification. A theoretical model can be evaluated quickly using our setup, and once it is confirmed to be working, deployment onto a FPGA can start.

VII. CONCLUSION

Without a properly chosen window size, energy detectors often fail to detect signals that are narrow compared to the detector window, or if only a fraction of the signal

is captured within the detector window. We proposed an adaptive energy detector that can subdivide its detection window into sub windows, and evaluated such detector's performance. We carried out experiments on the VHF/UHF band using a real time implementation, and found that given the same parameters, our detector can meet a probability of detection with 1 to 2 dB lower SNR compared to the normal energy detector.

We are now evaluating other models for channel sensing such as entropy detection, and looking at stochastic channel selection strategies. Interested readers can follow the project at: http://cr.jamesyxu.com.

VIII. ACKNOWLEDGEMENT

The authors would like to thank Dr. James Chang and Dr. Tom Moir for their support and technical knowledge.

REFERENCES

[1] D. Cabric, et al., Implementation issues in spectrum sensing for cognitive radios, *Signals, Systems and Computers Conference,* 2004, pp. 772-776.

[2] FCC, Spectrum Policy Task Force Report, *ET Docket No. 02-155*, 2002

[3] FCC, Notice of Proposed Rule Making and Order, *ET Docket No. 03-322,* 2003

[4] D. Chen, et al., Cooperative Spectrum Sensing under Noise Uncertainty in Cognitive Radio, *Wireless Communications, Networking and Mobile Computing Conference,* 2008, pp. 1-4.

[5] Z. Tian, et al., Performance Evaluation of Distributed Compressed Wideband Sensing for Cognitive Radio Networks, *Information Fusion Conference,* 2008, pp. 1-8.

[6] D. Cabric, et al., Spectrum Sensing Measurements of Pilot, Energy and Collaborative Detection, *Military Communications Conference,* 2006, pp. 1-7.

[7] B. Fette, *Cognitive Radio Technology,* Newnes Elsevier, 2006

[8] S. Shellhammer, Performance of the Power Detector, *IEEE Doc: 802.22-06/0075r0,* 2006

[9] A. Sahai, et al., Some Fundamental Limits on Cognitive Radio, *Allerton Conference on Communication, Control, and Computing,* 2004, pp. 1-5.

[10] V. Blaschke, et al., A Cognitive Radio Receiver Supporting Wide-Band Sensing, *International Conference on Communications,* 2008, pp. 499-503.

[11] National Instruments, NI PXI-5661, July 2009, http://sine.ni.com/nips/cds/view/p/lang/en/nid/203038

[12] National Instruments, LabVIEW, July 2009, http://www.ni.com/labview/

Proceedings of 2009 12th International Conference on Computer and Information Technology (ICCIT 2009)
21-23 December, 2009, Dhaka, Bangladesh

Examining Branch and Bound Strategy on Multiprocessor Task Scheduling

M Mostafizur Rahman, Muhammad Foizul Islam Chowdhury*

Dept. of Computer Science & Engineering, Leading University, Bangladesh
Computer Science Dept. University of Western Ontario, Canada*
mmrbappy@gmail.com, umel81@gmail.com*

Abstract

The multiprocessor task graph scheduling problem has been extensively studied as academic optimization problem which occurs in optimizing the execution time of parallel algorithm with parallel computer. The problem is already being known as one of the NP-hard problems. There are many good approaches made with many optimizing algorithm to find out the optimum solution for this problem with less computational time. One of them is branch and bound algorithm. In this paper, we studied the branch and bound algorithm for the multiprocessor scheduling problem.

Keywords: A Multiprocessor scheduling problems, Branch and Bound, Lower Bound, Upper Bound, Task Graph Scheduling.

I. INTRODUCTION

The computing system is becoming more complex and researchers are trying to find out efficient solution for allocating the resource of computer system. One of the interesting and major problems is the task scheduling in multiprocessor environment. The utilization of parallel processing systems in various applications is the result of numerous breakthroughs over the last two decades. The development of parallel and distributed systems has lead to there use in several applications including information processing, fluid flow, weather modeling, database systems, real-time high-speed simulation of dynamical systems, image processing. The data for these applications can be distributed evenly on the processors of parallel and distributed systems. The maximum benefits from these systems can be obtained by employing efficient task partitioning and scheduling strategies [1]. The multiprocessor task schedule problem is *NP-hard*. Although it is possible to formulate and solve the problem using heuristics, the feasible solution space quickly becomes intractable for larger problem instance. When the structure of the parallel program such as number of task, execution time of tasks, dependency constraints, communication cost, and the number of processors are known beforehand, a schedule is determined statically at compile time. Except for a few special cases, no polynomial-time algorithm that finds the schedule with a minimum length exists. For that reason, many heuristic algorithms [1-3, 10-12] have been developed to obtain suboptimal solutions for scheduling problems but very few research has been made with Branch and Bound algorithm. In this paper, we have considered the Branch and Bound algorithm to solve the multiprocessor task graph scheduling. The critical problem that is found for solving the *Multi Processor Scheduling* is the delay between communications of the data from one task to other task; defining precedence relationship for the set of task, being predecessor and successor. Our concern is on the problem of scheduling dependencies tasks onto multiprocessor system with processors connected in an arbitrary way, while explicitly accounting for the time required to transfer data between the tasks allocated to different processors. The delay in communication therefore occurs whenever two pair of tasks (predecessor, successor) is assigned to different processors. Each processor can perform single task at a time. The problem is defined as a directed acyclic graph (DAG) where the vertices represent the tasks and an (directed) arc indicates a direct one-way communication between a predecessor and successor pair of modules.

II. MULTIPROCESSOR TASK SCHEDULING PROBLEM

Multiprocessor task scheduling problem (MTSP): Let P = $\{P_1, \ldots, P_m\}$ be the set of *m* identical processor, $m > 1$, connected by a complete interconnection network, where all links are identical [2]. Each processor has its own memory and can execute only one task at a time. During the execution of task, processor will communicate exclusively by message passing through the interconnection network. There are *n* tasks need to be scheduled on a set of *m* identical processors. Each task is associated with a cost that represents the execution time of the task and also a number of precedence constrains. It's more convenient to use a weighted acyclic *task digraph* to represent the problem [3]. A task graph is a weighted DAG with G = (*T*, *E*), where the set of nodes corresponding to tasks and *E* is a set of communication edges. *W* is the set of node weights, and *C* is the set of edge weights. Given a task graph TG and *m* number of processors, MTSP requires to distribute the tasks in TG -which is fully connected- onto *m* computational processors. There is no pre-emption or duplication of task in this case [2-3]. The vertices represent the set of tasks $T = \{t_1, \ldots, t_n\}$ and each arc represents the precedence relation between two tasks. An arc $(t_1, t_2) \in E$ represents the fact that at the end of its execution, t_1 sends a message whose contents are required by t_2 to start execution. In this case, t_1 is said to be an immediate predecessor of t_2, and t_2 itself is said to be an immediate successor of t_1. We suppose that t_1 is the only task without any immediate predecessor. A

path is a sequence of nodes $< t_1, \ldots, t_k >$, $1 < k < n$. A task t_i is a *predecessor* of another task t_k if there is a path $< t_i, \ldots, t_k >$ in *D*. For every task t_i, there is an associated value representing its duration.

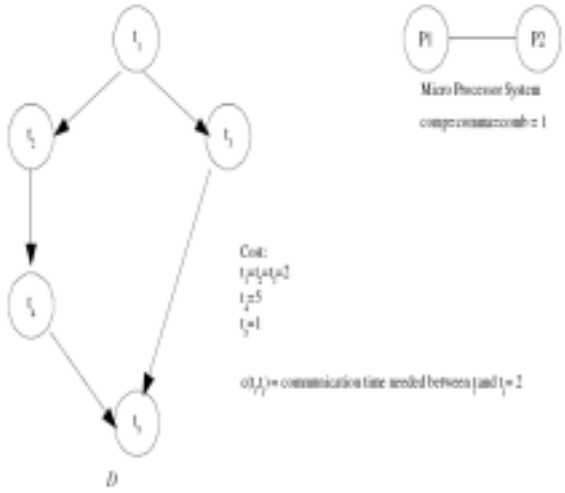

Fig 1: Task graph to be scheduled on processor P_1 and P_2

It is also assumed that the duration of all communications is known at compile-time. Thus, for every arc $(t_i, t_k) \in E$ there is an associated cost representing the transfer time of the message sent by t_i to t_k. If both -message source and destination- are scheduled on same processor, then the cost associated with this arc becomes null [2-3]. There are some other attributes for the parallel machine, "comp", "comma" and "comb". "*comp"* is the performance factor of the machine, means if a task (a node of the graph) costs x, than it's execution time will be *comp* *x. "*comma"* and "*commb"* are the communication's parameters. "*commb"* represents the time to start a communication between two nodes and "*comma"* represents the time (without start-up time) to communicate a data, e.g. if nodes *a* must send *h* data to node *b* then node *b* can not start before the end of execution of *a* plus *comma* *x+ *commb* time's units, if the tasks *a* and *b* are scheduled to different processor. A schedule can be represented by $S = \{s_1, \ldots, s_n\}$ where $s_j = \{ t_i, \ldots, t_k\}$, where s_j is the set of tasks scheduled on processor P_j. The execution time yielded by a schedule is known as "*make span"*. Our objective was to develop a Branch and Bound algorithm for searching an optimum solutions (having minimum "*make span"*) form the search space, by making less branches and creating minimum numbers of nodes.

III. BRANCH AND BOUND TECHNIQUE

Branch and bound (BnB) is a general algorithm for finding optimal solutions of various optimization problems, especially in discrete and combinatorial optimization. It consists of a systematic enumeration of all candidate solutions, where large subsets of fruitless candidates are discarded en masse, by using upper and lower estimated bounds of the quantity being optimized.

A. General Description

For definiteness, we assume that the goal is to find the minimum value of a function f(x) (e.g., the cost of manufacturing a certain product), where x ranges over some set S of admissible or candidate solutions (the search space or feasible region). Note that one can find the maximum value of f(x) by finding the minimum of $g(x) = - f(x)$. A branch-and-bound procedure requires two tools. The first one is a splitting procedure that is given a set S of candidates, returns two or smaller sets whose union covers S. This step is called branching, since its recursive application defines a tree structure (the search tree) whose nodes are the subsets of S. Another tool is the procedure that computes upper and lower bounds for the minimum value of f(x) within a given subset of S. This step is called bounding. The key idea of the BnB algorithm is: if the lower bound for some tree node (set of candidates) say A is greater than the upper bound for some other node say B, then A may be safely discarded from the search. This step is called pruning, and is usually implemented by maintaining a global variable say m (shared among all nodes of the tree) that records the minimum upper bound seen among all sub regions examined so far. Any node whose lower bound is greater than m can be discarded. The recursion stops when the current candidate subset of S is reduced to a single element; or also when the upper bound for the subset of S matches the lower bound.

B. Effective Subdivision

The efficiency of the method depends strongly on the node-splitting procedure and on the upper and lower bound estimators. All other things being equal, it is best to choose a splitting method that provides non-overlapping subsets. Ideally the procedure stops when all nodes of the search tree are either pruned or solved. At that point, all non-pruned sub regions will have their upper and lower bounds equal to the global minimum of the function. In practice the procedure is often terminated after a given time; at that point, the minimum lower bound and the minimum upper bound, among all non-pruned sections, define a range of values that contains the global minimum. Alternatively, within an overriding time constraint, the algorithm may be terminated when some error criterion, such as (max - min)/(min + max), falls below a specified value. The efficiency of the method depends critically on the effectiveness of the branching and bounding algorithms used; bad choices could lead to repeated branching, without any pruning, until the sub-regions become very small. In that case, the method would be reduced to an exhaustive enumeration of the domain, which is often impractically large. There is no universal bounding algorithm that works for all problems; therefore the general paradigm needs to be implemented separately

for each application, with branching and bounding algorithms that are specially designed for it. Branch and bound methods may be classified according to the bounding methods and according to the ways of creating/inspecting the search tree nodes. This method naturally lends itself for parallel and distributed implementations. It may also be a base of various heuristics. For example, one may wish to stop branching when the gap between the upper and lower bounds becomes smaller than a certain threshold. Many applications use this technique to solve searching problems [4, 5].

IV. BRANCH AND BOUND ALGORITHM FOR MTSP (MULTIPROCESSOR TASK SCHEDULING PROBLEM)

In this section, we propose a branch and bound algorithm for searching the optimal solution for the problem described in the section 2. For branching, i.e., for selecting a node to generate branches, the depth-first rule is used. That is, a node with the most unit-jobs included in the associated partial schedule is selected for branching. In case of ties, a node with the lowest lower bound is selected. When child nodes are generated from a selected parent node, it is checked whether or not schedules associated with the child nodes are dominated by using dominance properties that can be obtained by observing the lower bound and upper bound given for every child node. Nodes with lower bounds that are greater than the upper bound, i.e., the solution value of the current incumbent solution, are deleted from further consideration (fathomed). In addition with that a global variable *bestUB* is maintained (shared among all nodes of the tree) that records the minimum upper bound seen among all sub regions examined so far. Any node whose lower bound is greater than *bestUB* can be discarded. The recursion stops when the current candidate set is reduced to a single element; or when the upper bound of the selected node matches the lower bound and the entire tasks are scheduled.

A. Branching Scheme

As described in section 2, there are $T = \{t_1, \ldots, t_n\}$ set of tasks to be schedule on $P = \{P_1, \ldots, P_m\}$ processors by maintaining the precedence relationship between tasks. C_{ti} is the cost of the task t_i. CC is the communication cost of an arc; $CC_{ij} = (t_i, t_j) \in E$ represents the fact that at the end of its execution, t_i sends a message whose contents are required by t_j to start execution. In this case, t_i is said to be an immediate predecessor of t_j, and t_j itself is said to be an immediate successor of t_i.

Creating partial solutions: Each node say α in the search tree is defined by $\alpha = (S_{\alpha 1}, \ldots, S_{\alpha m})$. $S_{\alpha i}$ represents a sequence of scheduled tasks on the processor i for node α. T_α is the list of all the unscheduled job at node α. k_α is the list of computational time (end time) of all scheduled tasks in $(S_{\alpha 1}, \ldots, S_{\alpha m})$. μ(α) is the set of all the child nodes of the node α, which are also known as the open nodes means the nodes not yet been expended. Branching out from a node α is carried out by creating a new node and coping all the information form the node α. Scheduling is done by taking a task t_j form the list of T_α for which all the predecessor are already been scheduled, and appending it to the tail of sequence $S_{\alpha i}$. Let the newly created node be β and the related sequence be $S_{\beta i}$. T_β be the new list of unscheduled task after scheduling the task t_j. Which shows that β is the partial schedule with one more task scheduled then the node α [1-2]. We add all the newly created children nodes from the parent node α in the μ(α) as a open node. After creating all the possible children from the parent node, the parent node is immediately removed from the list of open nodes. A node α can be selected again depending on the branching rule for next expansion, in this case the node which has lowest bound. The bounding paradigm is given bellow.

B. Bounding Scheme

For the branch and bound algorithm we have used two heuristics value for every created node. One is upper bound *UB* and another is lower bound *LB*

Upper Bound:

Upper bounds are tested by calculating using simply greedy heuristics lowest starting time first (LSTF).

UB With Greedy LSTF:

1. **while** (number of unscheduled task >0)
   i. select a task which all the predecessors are already scheduled
   ii. get the CPU P_i for which the task has the lowest starting time
   iii. Schedule the task to P_i in the sequence of S_β
   iv. Update k_β
   b. End While
2. compute make span
3. return make span as the upper bound of the node

Algorithm for upper bound using LSTF

Lower Bound:

For the Branch and Bound algorithm, researchers gave several lower bounds. Carlier [6] presents some lower bounds based on machine load. Carlier and Pinson [7] introduce the concept of pseudo-pre-emptive schedule and Gharbi and Haouari [8] derive several lower bounds from the lower bound proposed by Webster [9] for the parallel machine problem with resource availability constraints, but there is no such proved lower bound for the specific problem that we are addressing in this paper. A simple lower bound LB of every newly created node is calculated in the following function:

$$LB_\beta = \frac{\sum C_{T_\beta}}{m} + \textit{partial schedule time}$$

C_{T_β} is cost of all unscheduled tasks in the node β

m is the number of processor where $m \geq 1$

C. Example of the application of BnB Algorithm in a DAG

Figure 2 shows the optimum solution found by the branch and bound algorithm of the DAG shown above. The detail search iteration is shown next in the figure 3.

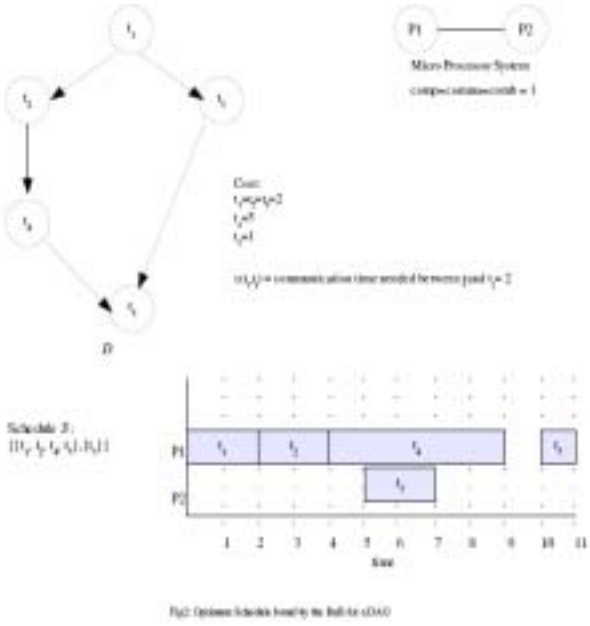

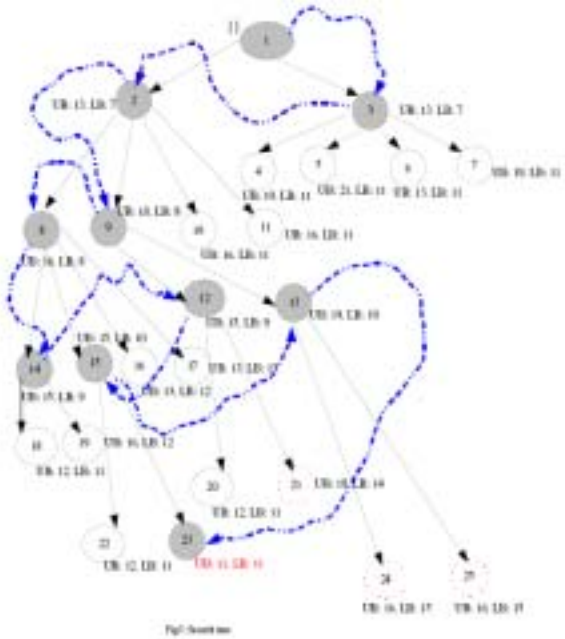

In the search tree shown in figure 3 we can see that node 1 which is the root node having partial solution as null { }. At this stage only task 1 is ready to execute, so from that node the BnB algorithm makes two child nodes one for scheduling the task 1 to processor one and another for task 1 to processor 2, having upper bound as 13 and lower bound as 7 for both, and then they are added to the list of open nodes and the root node marked as a closed node. As LB (lower bound) of all the nodes in the list of open nodes is equal, the algorithm selects node number 3 for expending next. As task 1 is scheduled and task 2 and 3 become free to be scheduled to processor 1 or 2. From the node 3 there are four new child nodes are created for the combination of 2 jobs to 2 processors, having (UB, LB) as (19,11), (21,11), (13,11), (19,11) and they are added in the list of open list. For expending next the algorithm selects the node 2 as it has the lowest lower bound among all the nodes that are in the list of open nodes. This is how it proceeds for further expansion. When it comes to node number 23 the algorithm found that the upper bound and lower bound are equal for that partial schedule node, there it stops the algorithm and prints the upper bound of the node as a found optimum solution. During the creation of the child nodes when ever the algorithm computes the upper bound and lower bound for a partial solution node it will check if the lower bound of the node is grater then the upper bound of the node or not, if it matches then this newly created node is deleted from the open list. The algorithm maintains a global variable for storing the best known upper bound. During the creation of a new node the algorithm compare the upper bound of the node with the best known upper bound and then it update the best known upper bound with the upper bound of the new node and delete all the nodes having lower bound greater than the best known upper bound. In figure 3, nodes 21, 24 and 25 are deleted from the list of all the open nodes having lower bound greater than the best known upper bound.

V. EXPERIMENTAL RESULTS

The proposed Branch and Bound algorithm was implemented in visual C++ 2008; all the experiments were conducted on Intel 1.6 GHz processor with 2 GB RAM in windows vista operating system. In order to assess the effectiveness of the proposed branch and bound algorithm, we conduct experiments on some randomly generated *task graph* DAG. Table1 shows the output with the lower bound method.

Using Lower Bound Method (LB)					
Number of task *n*	Number of processor *m*	Number of node created with out pruning	Number of node after pruning	Number of Branch made	Average CPU time in milliseconds
4	2	19	9	7	5
	3	34	10	8	8
	4	53	11	9	12
	5	73	12	10	16
6	2	55	27	21	10
	3	88	28	22	12
	4	125	29	23	16
	5	116	30	24	19
8	2	1327	662	452	125
	3	2089	683	473	203
	4	2913	702	492	250
	5	3706	717	503	359
10	2	1381	701	313	203
	3	1936	718	282	312
	4	5073	934	633	608
	5	6356	822	634	780
15	2	2424	1230	549	356
	3	3398	1260	495	548
	4	8903	1639	1256	1067
	5	11155	1443	1317	1369

Table 1

From Table-1, we obtain the following graphs where we can see that the numbers of nodes are increasing with respect to the number of task.

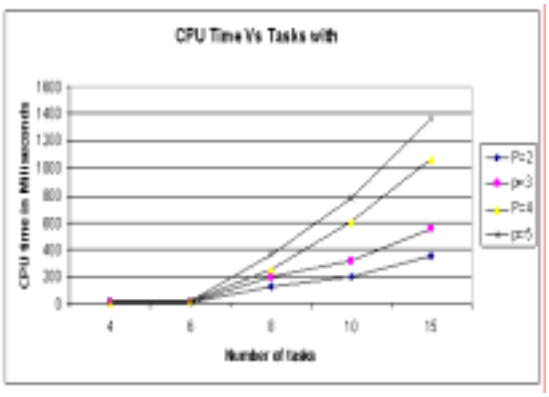

The following graphs show how efficient our system is with respect to the memory complexity.

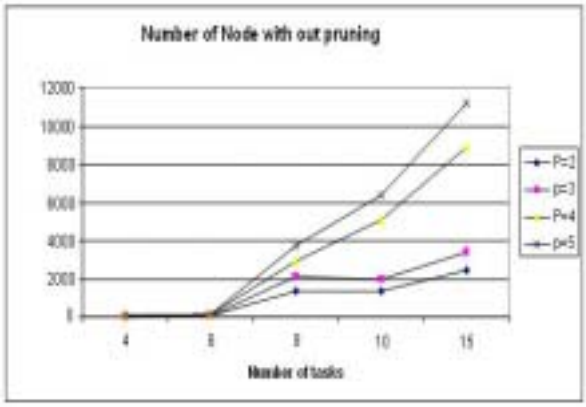

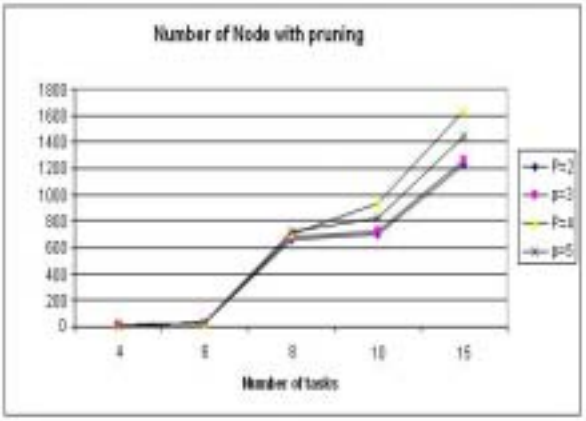

We have done several experiments with the bigger and complex DAG such as ssc, celbow and cstanford. These graphs come from an arm controller from [13]. Table-2 shows the comparison results (make span) between BnB, Ant Colony (ACO), and Genetic Algorithm (GA):

DAG	BnB Best Known Upper bound (make span)	ACO	GA
ssc2	10	----	----
cstanford	603	663	627
celbow	6210	6637	6630

Table-2

VI. CONCLUSION AND FUTURE WORK

We have tested the algorithm in a small set of problem with less number of task and processor. For the future work, we believe that there is a need of further improvement to find out a new lower bound that will work better, and also improvement of coding may save memory and CPU time which will help to deal with large set of problems. New branching scheme can also

be proposed for betterment of the searching. An interesting research can be made to find out the best solution using a hybrid algorithm, combining genetic algorithms and integer programming branch and bound approaches.

REFERENCES

[1] Reakook Hwanga, Mitsuo Genb, Hiroshi Katayamaa. "A comparison of multiprocessor task scheduling algorithms with communication costs" Science Direct Computers & Operations Research 35 (2008) 976 – 993.

[2] Correa, R.C, Ferreira, A, Rebreyend, Pascal. "Integrating list heuristics into genetic algorithms for multiprocessor scheduling". Parallel and Distributed Processing, 1996. Eighth IEEE Symposium on IEEE Comput. Soc. Press.

[3] Correa, R.C, Ferreira, A, Rebreyend. " Scheduling multiprocessor tasks with genetic algorithms". Parallel and Distributed Systems, IEEE Transactions on IEE/IEEE, 1999. Issn: 10459219.

[4] Parallel Lower and Upper Bounds for Large TSPs, a summary of André Rohe's thesis (in English), will appear in ZAMM Volume 77, Supplement 2, pp. 429-432, 1997.

[5] A recursive branch and bound algorithm for the multidimensional knapsack problem Wiley Periodicals. 2008. Volume 22 Issue 2, Pages 341 – 353

[6] Carlier J. Scheduling jobs with release dates and tails on identical parallel machines to minimize the makespan. European Journal of Operational Research 1987;29:298–306.

[7] Carlier J, Pinson E. Jackson's pseudo preemptive schedule for the P|ri, qi |Cmax. Annals of Operations Research 1998;83:41–58.

[8] Gharbi A, Haouari M. Minimizing makespan on parallel machines subject to release dates and delivery times. Journal of Scheduling 2002;5:329–55.

[9] Webster S-T. A general bound for the makespan problem. European Journal of Operational Research 1996;89:516–24.

[10] Sang-Oh Shim,Yeong-Dae Kim. "A branch and bound algorithm for an identical parallel machine scheduling problem with a job splitting property" Computers & Operations Research 35 (2008) 863 – 875.

[11] Mohammad Mahdavi Mazdeha, Mansoor Sarhadia, Khalil S. Hindi"A branch-andbound algorithm for single-machine scheduling with batch delivery and job release times" Computers & Operations Research 35 (2008) 1099 – 1111

[12] Rabia Nessah□, FaroukYalaoui, Chengbin Chu.A "branch-and-bound algorithm to minimize total weighted completion time on identical parallel machines with job release dates." Computers & Operations Research 35 (2008) 1176 – 1190

[13] Kasahara & Narita, Practical multiprocessor scheduling algorithms for efficient parallel processing. IEEE Transactions on Computer, Vol C-33, No 11, Novembrer 1984, pp 1023-1029

Proceedings of 2009 12th International Conference on Computer and Information Technology (ICCIT 2009)
21-23 December, 2009, Dhaka, Bangladesh

Impact of Optical Fiber Dispersion and Self Phase Modulation on the Performance of DS-OCDMA

Md. Jahedul Islam*, Mostafezur Rahman Talukdar, and Md. Rafiqul Islam
Department of Electrical & Electronic Engineering, Khulna University of Engineering & Technology,
Khulna-9203, Bangladesh
jahed_eee@yahoo.com*

Abstract

The performance of direct sequence optical code division multiple access with cascaded optical amplifiers is analytically investigated in presence of fiber group velocity dispersion (GVD) and self phase modulation (SPM). In our analysis, Gaussian-shaped optical orthogonal codes are employed as address sequence and avalanche photodiode is used in an optical correlator receiver. The signal to noise power for the proposed system is evaluated on account of receiver, optical amplifier and multiuser access interference noises. The system performance is determined as a function of optical signal power, code length, code weight, number of simultaneous users, and fiber length. The power penalty suffered by the system is evaluated at bit error rate (BER) of 10^{-9}. The numerical results show that the BER performance of the system is highly dependent on the signal input power, bit rate, and fiber length. It is found that the performance of the proposed system can be improved by the combined effect of GVD and SPM.

Keywords: DS-OCDMA, GVD, SPM, IM/DD.

I. INTRODUCTION

In recent years, research interests are highly concentrated in all-optical fiber-based access networks to meet the future demand for high-speed and high performance communications [1]. Communication capacity can be enhanced dramatically by optical networks employing multiple access techniques that allow multiple users to share the fiber bandwidth. Among the various multiple accesses, optical code division multiple access (OCDMA) enjoys from many features that are of immense interest, for example, simplified and decentralized network control, enhanced information security, improved spectral efficiency and increased robustness in multi-rate services [2]. Until now, research on OCDMA mainly focused on direct time spread OCDMA, spectral encoding–decoding, pulse position modulation OCDMA, asynchronous phase-encoding OCDMA [3], and frequency hopping(FH) OCDMA [4]. The bit error rate (BER) performance of OCDMA systems considering only group velocity dispersion (GVD) has been reported in previous studies [4]-[5]. It was found that the system performance degrades due to interchip interference caused by dispersion-induced spreading and overlapping of chips. Consequently, transmission distance is significantly reduced due to reduction of received optical power, which can be increased by incorporating optical amplifiers as a repeater in the system [6]. When optical amplifiers are used in cascade, the maximum allowable input power and the amplifier spacing are limited by fiber nonlinear effect known as self phase modulation (SPM) [6]. Recently, the performance of FH-OCDMA [7] and SPECTS-OCDMA [8] system is investigated in presence of both GVD and SPM. It is well established that the direct sequence (DS) OCDMA has some advantages over FH- OCDMA, such as; it allows greater privacy, security, and greater flexibility in assignment of users. Most of previous researches on DS-OCDMA system are carried out considering only the effect of dispersion as reported so far [3]-[5]. To best of our knowledge, there is no study on DS-OCDMA considering the combined effect of GVD and SPM.

In this paper, an analytical approach is presented to investigate the performance of DS-OCDMA with inline cascaded optical amplifiers taking into combined effect of GVD and SPM for a single mode fiber (SMF) operating at 1550 nm. In our analysis, Gaussian-shaped optical orthogonal code (OOC) is used as the user address. Avalanche photodiode (APD) is selected as the system receiver [9]. The BER performance of the system is determined as a function of bit rate, fiber length, and transmitted input signal power considering the effects of APD receiver noises, optical amplifier noises and multiuser access interference (MAI). It is found that for a particular input signal power the proposed system suffers minimum penalty when the combined effect of GVD and SPM is considered.

978-1-4244-6283-4/09/$26.00 ©2009 IEEE

II. SYSTEM DESCRIPTION

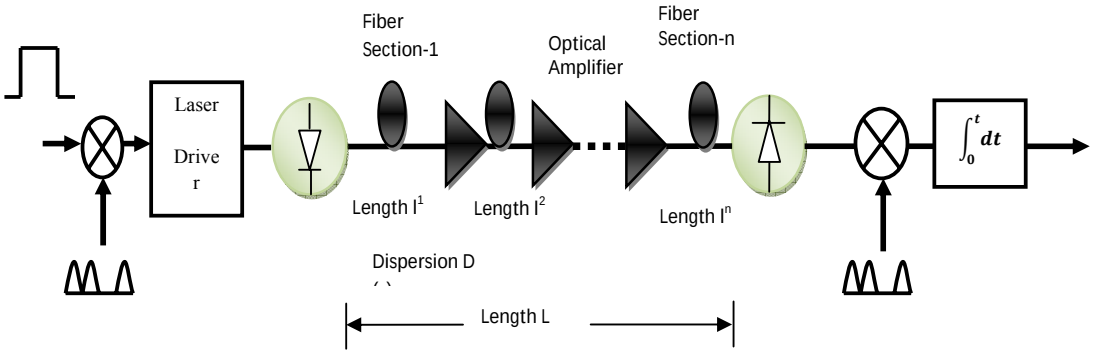

Fig. 1: Schematic configuration of proposed DS-OCDMA system.

The schematic configuration of the proposed system is shown in Fig. 1. Here, the total length of fiber is L, consisting of n fiber sections and n-1 optical amplifiers in which CDMA technique is used to transmit and receive data. P_i is the peak optical power launched into the i-th fiber section, l^i is the length of the i-th fiber section, D(z) is the fiber dispersion, and z is the distance from the transmitter. In the transmitter, a user's binary data is modulated by Gaussian-shaped chip. The composite signal is then transmitted through a SMF operating at 1550 nm. The loss of optical signal in the fiber is taken to be 0.2 dB/Km.To compensate signal attenuation in each fiber section, erbium doped fiber amplifier (EDFA) is used. The output signal is detected by intensity modulation direct detection (IM/DD) technique using APD. A particular user data is received by correlating the user chip with the photodetected signal.

III. SYSTEM ANALYSIS

In this analysis, the effects of shot noise, surface leakage current and thermal noise current associated with APD receiver are considered. Furthermore, we assume that all users have the same effective power at any receiver, the identical bit rate and signal format. For an OCDMA system with N transmitter and receiver pairs (users), the received signal $y_{out}(t)$ is the sum of N user's transmitted signals, which can be given by

$$y_{out}(t) = P_r \sum_{n=1}^{N} \sum_{i=1}^{F} B_n A_n(i) \int_{\tau_n + iT_c}^{\tau_{n+(i+1)T_c}} G(1 - \tau_n - iT_c)dt \quad (1)$$

where P_r is the received pulse peak power, B_n is the n-th user's binary data bit (either "1" or "0") with duration T_b at time t ($0 < t \leq T_b$), $A_n(i)$ is the i-th chip value (either "1" or "0") of the n-th user address code with code length $F = \frac{T_b}{T_c}$ and code weight W, τ_n is the time delay associated with the n-th user's signal. Without loss of generality, we assume that user 1 is the desired user, all delays τ_n at the receiver are relative to the first user delay only, i. e., $\tau_1 = 0$. $G(t)$ is the Gaussian function with period T_c, and satisfies the normalization condition. All users are assumed chip synchronous, i.e., $\tau_n = jT_c$, and $0 \leq j < F$ is an integer. In that case, the MAI will be maximum and the BER will be an upper bound on the BER for the chip asynchronous case.

At the receiving terminal, the correlation operation between signal $y(t)$ and a replica of the desired user's address code is carried out by an optical correlator receiver for decoding the desired signal. The output signal is obtained by integrating the decoded signal throughout the bit period. Output photocurrent X_1 sampled at time $t = T_b$ can be written as

$$X_1 = I' + I'' + I_n + I_A \quad (2)$$

where $I'$is the desired user's signal current, I'' the interference signal current offered by MAI, I_n the APD noise currents which includes shot noise current, bulk dark current, surface leakage current and thermal noise current, and I_A optical amplifier noises (i.e. signal-spontaneous beat noise, spontaneous-spontaneous beat noise). We assume that the (F, W, 1) OOC's selected as user address codes. By the correlation definition of OOC's, each interference user can contribute at most one hit during the correlation time. If γ denotes the total number of hits from interference users, the probability density function of γ is given by

$$P(\gamma) = \binom{N-1}{\gamma} K^{\gamma} \rho^{N-1-\gamma} \quad (3)$$

where $K = W^2/2F$, $\rho = 1 - K$ and γ is an integer ($0 \leq \gamma \leq N - 1$). If code length F, code weight W and γ are given, the first two terms in (2) can be

determined. We assume that the APD noise current has Gaussian nature. The output photocurrent X_1 can be regarded as a Gaussian random variable. Its average I_1 and variance σ_1^2 for bit "1" and "0" are determined as follows [9]. Since the received signal is multiplied by the user address code, i.e., (0,1) sequence. During the bit "1" interval of the desired signal, photons fall on the APD only during the W mark intervals and are totally blocked during the $F-W$ space intervals. During the W chip intervals of the desired signal, the total number of pulses (either marks or spaces) due to N users is WN. Among these WN pulses, there are $W+\gamma$ mark pulses with power level $\sigma_d P_r$, and $WN-(W+\gamma)$ space pulses with power level $\sigma_d r P_r$. Here, σ_d includes the effect of SMF dispersion and self phase modulation, r is the extinction ratio of APD receiver. Therefore, I_1 and σ_1^2 are given by

$$I_1 = M(R_0 P_t^l + I_{BD}) + I_{SL} \quad (4)$$

$$\sigma_l^2 = 2eM^{2+x}(R_0 P_t^l + I_{BD})B_e + 2eI_{SL}B_e + \frac{4\kappa_B T}{R_L} + \frac{4GI_S^1 I_{SP} L^2 B_e}{B_0} + \frac{(I_{SP}L)^2 B_e(2B_0 - B_e)}{B_0^2} \quad (5)$$

where the exponent x varies between 0 and 1.0 depending on the APD material and structure, M the average APD gain, R_0 the unity gain responsivity, e an electron charge, I_{BD} the average bulk dark current, which is multiplied by the avalanche gain, I_{SL} the average surface leakage current, which is not affected by avalanche gain, B_e the receiver electrical bandwidth, B_0 the optical bandwidth, κ_B the Boltzmann's constant, T the receiver noise temperature and R_L the receiver load resistor.

$$P_t^1 = (W+\gamma)\sigma_d P_r + (WN - W - \gamma)\sigma_d r P_r \quad (6)$$

$$I_{SP} = N_{SP}(G-1)eB_0 \quad (7)$$

$$I_S^1 = \frac{eP_t^l 2r}{(hv(r+1))} \quad (8)$$

$$\sigma_d = \frac{\sigma_0}{\sigma} \quad (9)$$

where, broadening factor due to the combined influence of GVD and SPM is

$$\frac{\sigma}{\sigma_0} = \sqrt{1 - \frac{\Gamma(1/2)}{\Gamma(3/2)}\frac{\alpha\beta_2 L}{t_0^2} + \frac{(1+\alpha^2)(\beta_2 L)^2}{t_0^4}} \quad (10)$$

Here N_{SP} is the spontaneous emission factor, G is the gain of amplifier, β_2 is the average GVD of the transmission fiber, t_0 the FWHM of the Gaussion-sheped pulse and $\alpha = \alpha_0 + \alpha_{SPM}$.

Where $\alpha_{SPM} = -\frac{v\kappa P_{in}}{a}\left(\frac{n+1}{2} - \frac{1}{al}\right)$ (11)

Here α_0 the original α-parameter of the transmitter, v is the fiber nonlinear coefficient, κ is the waveform factor, P_{in} is the input signal power, a is the attenuation coefficient, n is the number of fiber section and l is the length of the each fiber section. For data bit "0", average I_0, variance σ_0^2 of photocurrent X_1 can be determined in the same way as for data bit "1". In this case, I_0 and σ_0^2 can be written as

$$I_0 = M(R_0 P_t^0 + I_{BD}) + I_{SL} \quad (12)$$

$$\sigma_0^2 = 2eM^{2+x}(R_0 P_t^0 + I_{BD})B_e + 2eI_{SL}B_e + \frac{4\kappa_B T}{R_L}B_e + \frac{4GI_S^0 I_{SP} L^2 B_e}{B_0} + \frac{(I_{SP}L)^2 B_e(2B_0 - B_e)}{B_0^2} \quad (13)$$

where

$$P_t^0 = \gamma\sigma_d P_r + (WN - \gamma)\sigma_d r P_r \quad (14)$$

$$I_S^0 = \frac{eP_t^l 2}{(hv(r+1))} \quad (15)$$

For the desired user's data bit "1" or "0", the conditional probability density function of the output photocurrent X_1 can be expressed as

$$\mathrm{P_{X_1}(I|\gamma,1)} = \frac{1}{\sqrt{(2\pi\sigma_1)}}\exp\frac{-(\mathrm{I}-\mathrm{I_1})^2}{2\sigma_1^2} \quad (16)$$

$$\mathrm{P_{x_1}(I|\gamma,0)} = \frac{1}{\sqrt{(2\pi\sigma_0)}}\exp\frac{-(\mathrm{I}-\mathrm{I_0})^2}{2\sigma_0^2} \quad (17)$$

For a given threshold level Th, the probability of error for bit "1" and "0" are calculated by

$$P_e^{(1)}(\gamma) = \int_0^{Th} P_{X_1}(I|\gamma,1)dI = \frac{1}{2}\mathrm{erfc}\left(\frac{\mathrm{I_1}-\mathrm{Th}}{\sqrt{2}\sigma_1}\right) \quad (18)$$

$$P_e^{(0)}(\gamma) = \int_{Th}^{\infty} P_{X_1}(I|\gamma,0)dI = \frac{1}{2}\mathrm{erfc}\left(\frac{\mathrm{Th}-\mathrm{I_0}}{\sqrt{2}\sigma_0}\right) \quad (19)$$

The probability of error per bit, depended on the threshold level Th, is defined as

$$P_e(\gamma) = \frac{1}{2}[P_e^{(1)}(\gamma) + P_e^{(0)}(\gamma)] \quad (20)$$

The threshold level Th, is defined as

$$Th = \frac{\sigma_0 I_1 + \sigma_1 I_0}{\sigma_0 + \sigma_1} \quad (21)$$

Here, we assume that the bit "1" and "0" have the identical probability. The total probability of error P_e per bit is given by

$$P_e = \sum_{\gamma=0}^{N-1} P_e(\gamma)\binom{N-1}{\gamma} K^{\gamma}\rho^{N-1-\gamma} \quad (22)$$

IV. RESULTS AND DISCUSSION

Following the analytical formulations, the BER performance of DS-OCDMA system is evaluated in presence of GVD only. The results are compared with results reported in [5] and found to be in good

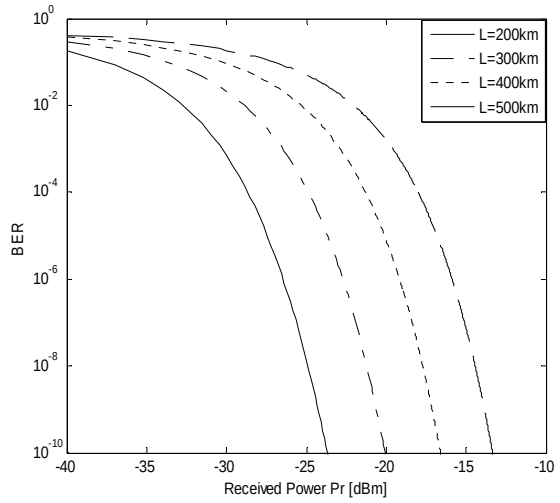

Fig. 2: Plot of BER versus received power for different fiber lengths when bit rate = 10 Gb/s, and input signal power P_{in}=-15 dBm.

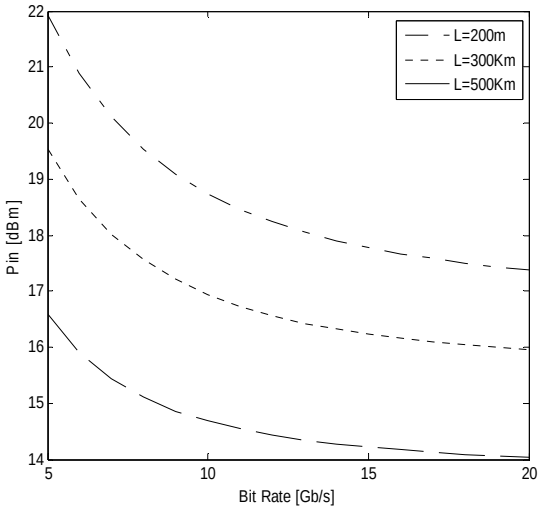

Fig. 4: Variation of optimum input signal power as a function of bit rate for different fiber lengths in presence of GVD and SPM.

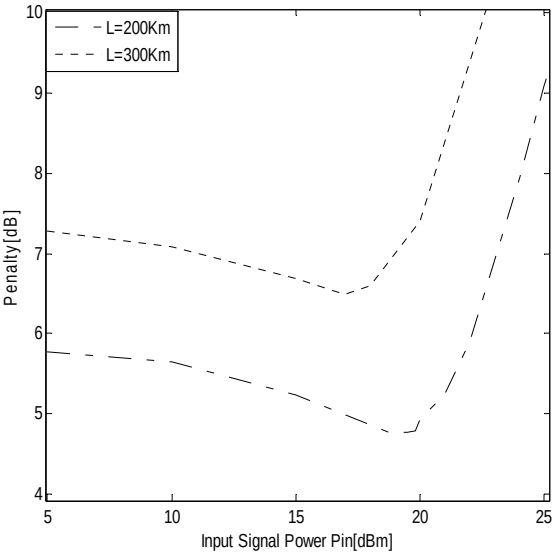

Fig. 3: Power penalty evaluated for different fiber lengths at BER of 10^{-9} considering the effects of GVD and SPM at bit rate 10Gb/s.

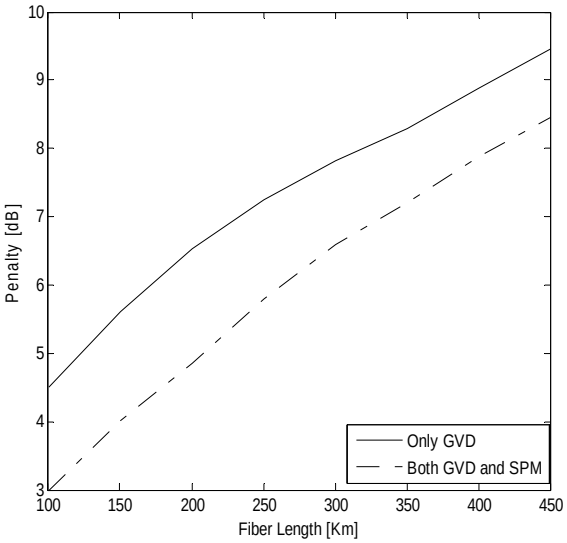

Fig. 5: Plots of power penalty versus fiber length in presence of GVD, and GVD and SPM at bit rate 10 Gb/s.

agreement. In this paper the BER performance for the proposed system is evaluated with the combined effect of GVD and SPM at different bit rates, fiber length, and transmitted input signal power. The dispersion parameter of a SMF operating at 1550 nm is taken as 18 ps/km.nm. In the numerical calculation, we assume that OOC's with code length F = 255 and weight W = 4, the number of simultaneous users N = 10. The InGaAs APD is selected as the system receiver, its primary parameters are taken as follows: mean gain M = 20, excess noise index x = 0.7, bulk dark current I_{BD} = 2 nA, surface leakage current I_{SL} = 10 nA. Other parameter are receiver load resistor R_L = 1000 Ω, extinction ratio is r =0.05, spontaneous emission factor N_{SP} =1.4, and the gain of each EDFA which adjusted to compensate the fiber attenuation in each fiber section .Fig. 2 shows the BER versus received power curves plotted for different values of fiber length and constant input signal power $P_{in} = -15$dBm. It is found that higher received signal power is needed with increasing fiber length in order to maintain a BER of 10^{-9}. At constant transmitted signal power, the received signal power is reduced with increasing fiber length due the effect of dispersion. For particular value of fiber length, with the increase of received power, SNR is increased and hence the system BER performance

is improved. We have also studied the BER performance as a function of input signal power keeping the fiber length constant. The power penalty suffered by the system is determined at BER of 10^{-9} and plotted as a function of input signal power which is shown in Fig. 3. It is found that for a particular transmitted input signal power (18.75 dBm at L=200km), the power penalty is minimum (4.77 dB). This is because GVD and SPM at this point oppose each other. This particular point is the optimum value of the transmitted input signal power at which the system BER performance is improved. If the fiber length is increased (L=300km), the optimum value of the transmitted input signal power is decreased (P_{in}=16.96 dBm) but power penalty is increased (6.48 dB) as seen in Fig. 3. The optimum transmitted input signal power is also highly dependent on bit rate. Fig. 4 shows optimum transmitted input signal power as a function of bit rate for different fiber length. It is also found in Fig. 4 that the signal power decreases rapidly up to 15 Gb/s and decreases gradually when bit rate is above 15 Gb/s. Fig. 5 depicts plots of power penalty versus fiber length at BER 10^{-9} for bit rate 10 Gb/s. It is found that power penalty reduced when the combined effect of GVD and SPM is considered rather than the effect of GVD alone if the system is operated at optimum transmitted input signal power. It is observed in Fig. 5 that the SPM- and GVD- induced penalty is reduced with fiber length. This is may be due to the fact that the α_{SPM} parameter is proportional to the transmitted signal power. The optimum input signal power decreases with fiber length as seen in Fig. 3. As a result α_{SPM} parameter is reduced which lead to decrease power penalty for longer fiber length due to reduction of pulse broadening.

V. CONCLUSION

We have analytically studied the performance of DS-OCDMA in presence of GVD and SPM. The analysis is carried out by OOC's with Gaussian-shaped chip and APD receiver. The effect of receiver, amplifier and MAI noises are considered to evaluate the BER performance. The power penalty suffered by the system at BER of 10^{-9} is determined as a function of fiber length, bit rate and transmitted input signal power. The results show that system suffers minimum power penalty at a particular input signal power. This is because GVD and SPM oppose each other at this transmitted input signal power. The typical value of input signal power is evaluated to be 16.96dBm for 300 km fiber length and 18.75 dBm for 200 km fiber length and the corresponding power penalties suffered by the system are evaluated to be 6.48 dB and 4.77 dB respectively. The optimum transmitted input signal power at which the system penalty is minimum is also found to be highly dependent on the bit rate.

REFERENCES

[1] J. Ratnam, "Optical CDMA in broadband communication: Scope and applications," *J. Opt. Commun.*, vol. 23, no. 1, pp. 11–21, Jan. 2002.

[2] Kambiz Jamshidi,and Jawad A. Salehi ,"Performance Analysis of Spectral-Phase-Encoded Optical CDMA System Using Two-Photon-Absorption Receiver Structure for Asynchronous and Slot-Level Synchronous Transmitters,'' *J. Lightw. Technol*., vol. 25, no. 6, pp. 1634–1645, June 2007.

[3] M. Wehuna *et al.*, "Performance analysis on phase-encoded OCDMA communication system," *J. Lightw. Technol.*, vol. 20, no. 5, pp. 798–805, May 2002.

[4] Chao Zuo, "The Impact of Group Velocity on Frequency-Hopping Optical Code Division Multiple System,'' *J. Lightw. Technol*., vol. 19, no. 10, Oct. 2001.

[5] S.P. Majumder, Member, IEEE, Afreen Azhari, and F.M. Abbou "Impact of fiber chromatic dispersion on the BER performance of an optical CDMA IM/DD transmission system"; *IEEE photonics technology letters,* vol. 17, No. 6, June2005.

[6] Nobuhiko Kikuchi and Shinya Sasaki, *Member, IEEE, "*Analytical Evaluation Technique of Self- Phase-Modulation Effect on the Performance of Cascaded Optical Amplifier Systems", *J. Lightw. Technol,* vol. 13, no. 5, May 1995.

[7] Ng Wai Ling, F. M. Abbou, A. Abid, H. T Chuah, "Performance Evolution of FH-OCDMA in presence of GVD and SPM", *IEICE Electronic Express,* Vol. 2, No23, December 10, 2005.

[8] F. M. Abbou, H. Y. Wong, L. H. Hiap, A. Abid H. T. Chuah, "Performance of Walsh Code and m-Sequence Spectral Phase-encoded Time Spreading OCDMA in the Presence of GVD and SPM,'' *Journal of Optical Communications,* 2007, vol. 28, no2, pp. 145-147.

[9] Xiaoqiang An, Kun Qiu: "Influence of Single-mode fiber dispersion and pulse linear chirp on direct-detection optical CDMA systems"; *Journal of Optical Communications,* 27(2006)1, 20-25.

Proceedings of 2009 12th International Conference on Computer and Information Technology (ICCIT 2009)
21-23 December, 2009, Dhaka, Bangladesh

OSDT: Outer Shape Detection Technique for Recognition of Bangla Optical Character

Md. Al Imran, Jobed Hossain, Tanay Dey, Bijan Kumar Debroy, Ahsan Habib Abir
Dept. of Computer Science & Engineering, Khulna University of Engineering & Technology, Khulna, Bangladesh
swim_imran_cse@yahoo.com, jobedhossain@gmail.com, dtanay2004@yahoo.com,bijan0507kuet@yahoo.com, abircse2k5kuet@yahoo.com

Abstract

Optical Character Recognition is one of the challenging fields in recognition of printed Bangla text. The main difficulties are that there are no precise techniques or algorithms for separating lines, words, and characters from printed Bangla text and efficiently recognize these separate characters. In this paper, we introduce new methods to separate lines, words, and characters from printed Bangla text. We also propose Outer Shape Detection Technique (OSDT), a new technique to recognize each character based on its outer shape which is unique. To successfully accomplish this, proposed technique scans each character both from its left side and right side. Finally our experimental results are compared with some prevalent ones which precisely show that our approach performs smoothly on different font sizes and number of characters.

Keywords: Optical Character Recognition, Filtering, Segmentation, Outer Shape Detection Technique.

I. INTRODUCTION

OCR means Optical Character Recognition. Bangla OCR System converts printed Bangla text into electronic version [1]. Recognition of printed Bangla text is a subject of interest for us and also very important for Bangla language processing [2]. Bangla OCR has many application potentials like reading aid for the blind (OCR and speech synthesis), automatic text entry into the computer, desktop publication, library cataloging and ledgering, automatic reading for sorting of postal mail, bank cheques and other documents [1]. However, there are no precise methods or algorithms for segmentation of lines, words, and characters from printed Bangla text. Another problem is the complexity of the shape of each character. Although some limited research works have been done on this field but they are not sufficient to segment the printed Bangla text properly. In our technique to recognize the shape of a character, we used the outer shape of every character which is unique. For the segmentation purpose some new methods have been taken to improve the performance. There were few problems to segment characters from a word when characters in a word are overlapped with one another and contain no minimum gap between them. For those special cases, we used some algorithms for separating them. The remaining part of the paper is organized as follows: related work is briefly discussed in Section II. In Section III, we discuss our proposed Bangla optical character recognition process in details. In Section IV, we measure our performance through simulation and compare with prevailing ones. Finally, some conclusions are drawn in Section V.

II. RELATED WORK

Bangla is one of the richest languages of the world. So analysts and scientists all over the world are trying to computerize the Bangla language for further processing convenience. In [3] it uses superimposed matrices; some use Neural Networks [2], [4], [5]. The main problem of Neural Network technique is that first we need to train up the characters with the system to get a effective output. Suppose we can consider a Bangla word 'চালাক'. If we put this word as input of that software which uses neural network, it can not recognize the characters. First we have to train up each character i.e., চ, া, ল, ক with the system. Then if we use these characters as input of that software, it can successfully recognize those characters. How much times we run the software, every time we do need to train up the characters firstly. Otherwise it can not recognize that characters totally. But in case of our software, it does not need to train up the characters rather it depends on the unique shape of every character. In Bangla OCR Apona Pathak [6], uses Neural Network and faces the same problem as described above. Bangla OCR of BRAC [7] uses the Hidden Markov Model technique which also incorporates the character train up technique for its recognition process. It is quite amazing that 'Apona Pathak' software does not work properly with their own given examples which are given in site [6].

III. PROPOSED BANGLA OPTICAL RECOGNITION TECHNIQUE

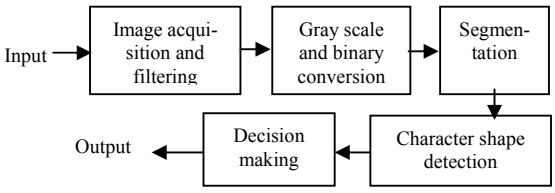

Fig.1. Process sequence block diagram

Throughout our recognition process we followed the following process sequence:

A. Image Acquisition & Image Filtering

We started whole process by getting an image document

containing Bangla text. This image may be stored in any format e.g. jpg, jpeg, bmp etc. To remove garbage from image we used image filtering.

B. Gray Scale Conversion and Binary Conversion

The image is converted into gray scale image for our processing convenience. Then we convert the gray scale image into binary formatted image by considering the pixel as 1(black) or 0(white). When we get pixel, it is considered as binary 1(if black) and otherwise considered binary 0(if white). As a result we get a full image structured with 1 and 0.

C. Segmentation of Text Image

To segment the whole binary image containing Bangla characters into separate characters, we firstly, separated each line. Then we departed each word from each line. Finally characters belonging to each word were separated. Each of the steps is sustained below:

C.1 Line Segmentation

In our system we first, separated the line from the binary image. We considered the binary image as a two dimensional array. From this array, we got the starting binary data and ending binary data i.e. 1 of the line.

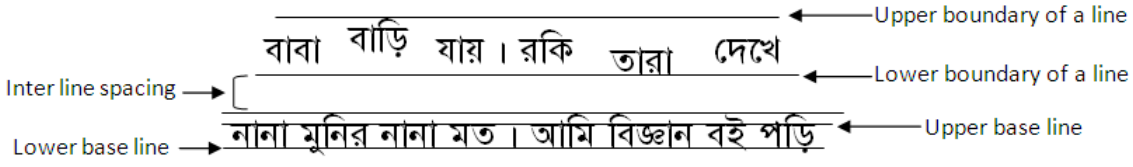

Figure 2: Segmentation of line from text

We scanned horizontally each pixel until a horizontal line containing all zero (white) pixels is found. Then we assumed, there was a separation between two lines. From the figure 2, we see that there is a separation between lower boundary of first line and upper boundary of second line. Sometimes some words may exist in little bit upper or lower position according to the base label of a line. But in our new technique, we also considered it and solve this problem very successfully. In figure 2, we can see that two words, "ewo" and "Zvi" exist little bit upper and lower position respectively with respect to upper and lower base level of a line. From the binary image, we detected that distortion of a word and solved it successfully. All of these cases base line helps to identify the average word position in a line and also to detect special character inside a word such as "ৗ "," " etc.

C.2 Word Segmentation

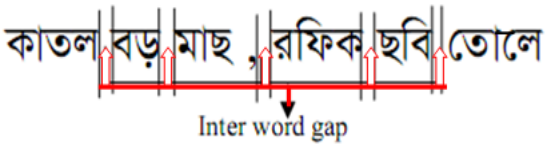

Figure 3: Segmentation of word from line

There must have some number of columns contain 'zero' between two words of a particular line. So we scanned vertically each pixel until a vertical line containing all zero (white) pixels is found. If we count a certain numbers of (may vary with font size) vertical lines containing all zero (white) pixels then it specifies the end of a word.

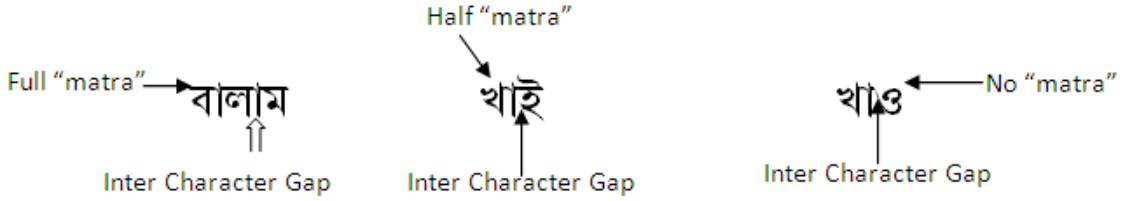

Figure 4: Classification of words considering "matra"

In figure 3, there are several consecutive vertical lines containing zero (white) pixels between the words "**KvZj**" and "**eo**". After the segmentation of each word, we store the width of each word into a separate array for further processing.

C.3 Character Segmentation

To segment characters from a word, we tried to find out and remove 'matra' from the word. But words may have half 'matra' and some may have no 'matra' which is shown in figure 4. So, firstly we started scanning horizontally from the beginning of each word in each line. After completing the scanning of the first line of a word we calculate the number of 1s in that line. If the number of 1s in a horizontal line greater than a certain percentage of word width under the condition of font size used

and match with some conditions then our algorithm took decision that was there a "matra" or half 'matra' or no 'matra' in the word. We used some segmentation techniques to separate characters for special cases such as what number of currently scanned, total number of line will be scanned for a word etc.

Generally, there are at least one vertical column contains white pixels that means all data are zero in that column between two character of a word. We scanned vertically each pixel (binary information) until a vertical line containing all zeros were found. If we found a vertical line containing all zeros, we considered it as a separation between two characters in a word.

C.4 Character Shape detection using Outer Shape Detection Technique (OSDT)

We know that Bangla characters are complex. At the beginning of our analysis, we tried to find the similarities among characters. After a long analysis, we found that the shape of each character is unique except few ones. By analyzing, we expressed each character with few turns such as left, right, vertical etc. In our recognition technique, we tried to detect these turns and then made a final decision to determine what character was. Firstly, we stored binary format of the image into a two dimensional array. From following figure5 (a), (b) we see that many consecutive 1s make a character," e". We made two layers of a binary formatted character. One is outer layer and another is inner layer. In figure 5 we can easily observe these two layers. Figure 5 contains 1s in the most outer side construct the outer shape of the character.

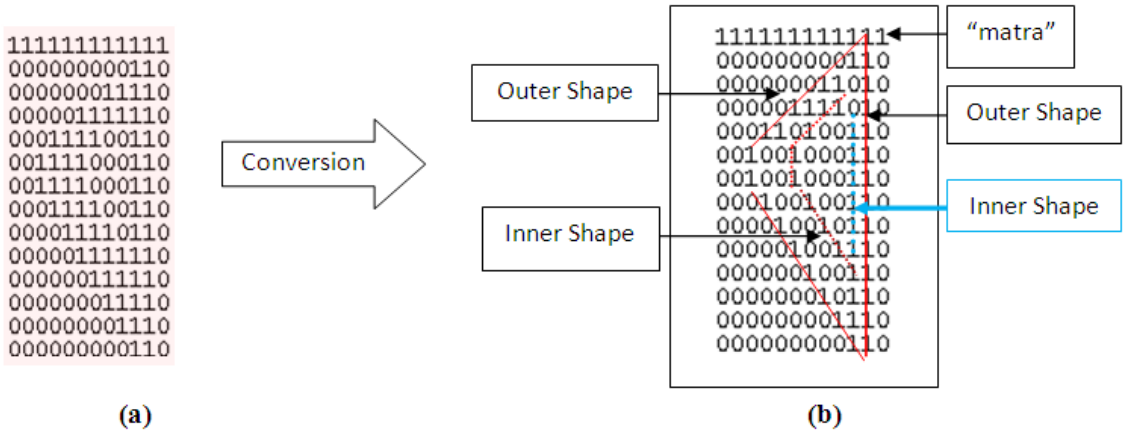

Figure 5: (a) Binary representation of a character (b) Inner and Outer Shape of a character

It also contains 1s in the most inner side construct the inner shape of the character. Inside outer and inner shape 1s are made zero applying some condition for OSDT computing. We use outer shape to recognize a character. So, the proposed technique is named "Outer Shape Detection Technique".

C.4.1 Scanning Procedure

With our outer shape detection technique, we scanned left outer shape of each character horizontally from left to right to take a decision and also scanned right outer shape from right to left to take another decision. After checking these two decisions we get the final decision. Some of characters and their shapes are given below in the table 1. Here we use some symbolic letters such as 'L', 'R', 'V' and 'S' where 'L' means left turn, 'R' means right turn, 'V' means vertical line and 'S' means straight vertical line which is bigger than 'V'.

Table 1: Some characters with their corresponding shapes in OSDT

Character	scanning from left to right	scanning from right to left
e	LR	S
h	RLR	S
K	LR	RLV
Á	LVR	RVLV
R	LSVRV	RLSV
Ù	SRLVR	S
I	LVR	RSVL
¨	VLSVL	VLSL

The starting and ending indexes of each character is stored in character segmentation section. Firstly we removed unnecessary binary data and resized each character. To scan from left to right we started form first index e.g. (0, 0) of resized 2D array of each character. We scanned horizontally until a black pixel (binary data 1) of that row was found. Then we went first index of next line. We again started our process with last scanned index of previous row and continue until a black pixel of current row was found. By this process we scanned all 1s of a binary data of each character and took a decision with some letters i.e., 'LR', 'RV' etc.

Let i be row index and j be column index of the array. If the index of first 1 is [1,4] i.e., i = 1 and j = 4 and the next index of black pixel(e.g. 1) is [2,3] i.e., i = 2, j= 3, we observed that 'j' was decreasing row by row. So, we took the decision that it was left turn (L). Otherwise if 'j' increases we decide that it was right turn(R). From figure 6(a) we get consecutive left turn (L) and right turn (R) while scanning from left to right. So, here was the decision LR. In the case of scanning from right to left we started our scanning from the index in the top right corner. From this index we scanned the binary data of characters horizontally until a black pixel is found.

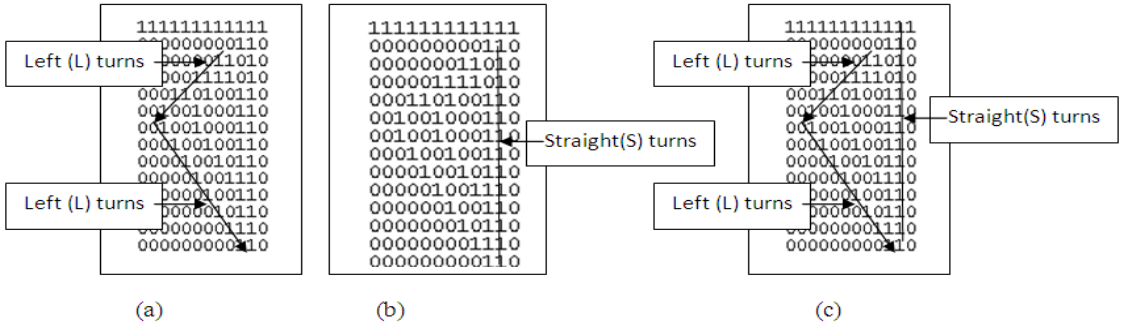

Figure 6: (a) Left to right Scanning (b) Right to left scanning (c) Complete shape of character

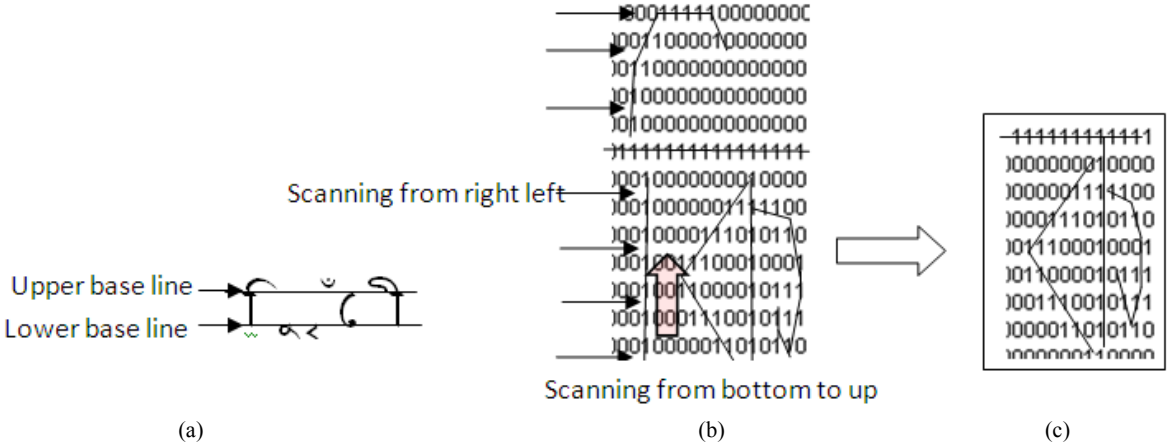

Figure 7: (a) Some special characters in Bangla language (b) A special character "ৗ" with a main character "K" (c) After separating "ৗ" we got main character "K"

Then we went to the index of next line from its most right corner and continued our process until a 1 is found. By this process we scanned all 1s of the binary data of a character and took a decision based on S, V etc. From figure 6(b) we took decision that it was a straight (S) line. So, here the decision was S. But some may think what the need for scanning from right to left is. To detect a character accurately we need this right to left scanning as well as left to right scanning e.g. if we closely examine two Bangla characters " e " and " K", we can observe that the shape of left side of both characters are same. But only difference is its right side. So scanning horizontally only from left to right will give the same decision for both "e" and "K". To identify both figure 7(a). These characters must be with an alphabet within a word. For these cases we applied our own algorithm to segment properly. For example: from figure 7(b) we can easily see an alphabet "K" with "ৗ ". By scanning from left to right we got the shape of ৗ which character uniquely and precisely we need further process i.e. scan from right side to left side. After scanning from right to left we will get another decision for each character. Like this, character e and h has same decision for right to left scanning but totally different in left to right scanning. The decision for right scanning of "e" and " h" is 'S'. The final decisions of this character are respectively 'LR' and 'RLR'. From the figure 6(c) we see the complete shape of character. So we can say that the character (from Table 1) is "e". We check these two decisions precisely to recognize each character. We also considered some special characters like has unique shape. After detecting "ৗ " we remove it and continue our process with the alphabet " K". To detect this character we manipulated different types of algorithm. To describe the entire process in a nut shell an algorithm is stated below.

D. Algorithm

The following algorithm will illustrate the procedure discussed above:

1. Image acquisition

2. Gray scale conversion and Binary Conversion

3. Line Splitting from binary data of text image

4. Word Splitting from line

Trying to delete Horizontal Line from a Word considering condition

5. Character Splitting from a Word

"Akar (ু)" splitting if it is closely coupled with a character

6. Mapping characters position inside binary data of a text

7. Resizing each character from main Mapping of character inside binary data of a text

8. Shape Detection

Finding "matra" or " rashee-kar(ি)" or special character closely coupled with main chracter

Remove special character and send the main character to step 9

9. First do Left and then right scanning for each character by using OSDT

If the shape of currently scanned character matches with the shape of other characters then

Apply vertical scanning from top to down then down to up

10. Repeat step 3 to 9 until shape of all character in the text is detected

IV. PERFORMANCE SIMULATION

A. Image Acquisition & Image Filtering

To perform the simulation we implemented our algorithm in C# .NET. The simulation parameters are shown in Table 2.

Table 2: Simulation parameters

Parameter	Value
Platform	C# .NET
Input File Format	JPG, JPEG, BMP
Output File Format	.doc, .docx, .txt
Font Name	SutonnyMJ
No. of characters	50 to 300
Font size	20pt, 28pt, 36pt

B. Results

Our system has been tested with several image file with different font size, number of character in the image. The system accuracy is calculated as [4]

$$Accuracy = \frac{Total\ No.of\ recornize\ character\ from\ inputed\ image\ of\ text\ document}{Total\ No.of\ character\ in\ inputed\ image\ of\ text\ document} * 100\% \quad (1)$$

For different images file we got different performances. The summary of the simulation results is shown in Table 3.

Table 3: Summary of simulation results

Font Size	Total number of characters in the document	No. of recognized characters in the document	Execution time(s)	Accuracy
36	*200*	*197*	*2.91*	***98.50%***
36	*250*	*240*	*3.53*	***96.00 %***
36	*300*	*299*	*4.11*	***99.66%***
20	200	143	3.10	***71.50%***
20	300	190	4.20	***63.33%***
28	250	215	3.77	***86.00%***

C. Comparison with other Bangla OCR Techniques

To compare the performance with other prevalent Bangla OCR software available in the web we ran the simulations as a common form of input to different techniques. Figure 8 is the corresponding graph to the total execution time over different number of characters inputted Figure 8 shows that our technique takes shortest time to get the output which relates to the total execution time over number of character inputted. As our proposed OSDT, uses the outer shape of a character to detect each character uniquely. So it incurs less cost as the technique incorporates less complex technique. On the other hand some OCR software such as "Apona Pathak", "BRAC OCR" integrates neural networks and hidden markov model technique respectively which are complex methods. So they incur immense execution time compare to OSDT.

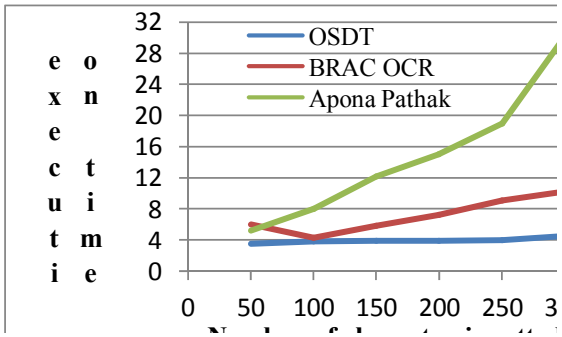

Figure 8: Total execution time(second) over different number of characters inputted

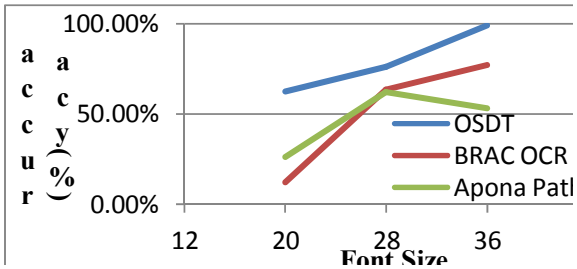

Figure 9: Accuracy of techniques over different size of the font

Figure 9 represents the accuracy of the different techniques over different size of the font. For accuracy calculation we used equation (1). Table 3 shows the accuracy result at different font sizes in case of our techniques. Most of the OCR techniques depend on the size of the font through out the recognition process. But in contrast our technique depends on the outer shape of every character which is unique whether it is small or large. So our technique preserve myriad accuracy compared to the other techniques over the different font sizes.

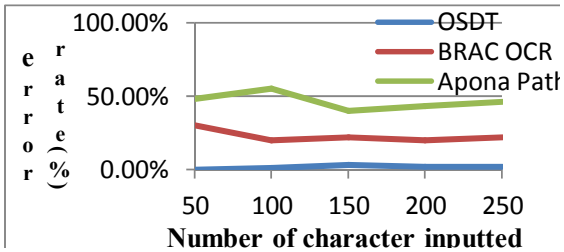

Figure 10: Error rate (%) observed over different number of characters inputted

Figure 10 shows the graph of error rate (%) over the number of character inputted to out OSDT technique and the other compared techniques. For error calculation we used the following equations:

$$error\ rate = 100\% - Accuracy \qquad (2)$$

Our technique is not perfect for all characters recognition but so far we got other techniques for simulations were full of bug. None of them were not usefully to find out most of the Bangla character efficiently. As the accuracy of our technique is immense (figure 9) compared to the other techniques, so consequently it will incur low error rate (%). From figure 10 it can be easily perceivable that our technique costs low error rate compared to the other techniques which is desired for any Bangla OCR. From the figure 9 and 10, it can easily perceivable that our OSDT performs efficiently.

REFERENCES

[1] B. B. Chaudhuri and U. Pal, "A complete Bangla OCR System", *Pattern Recognition, Vol 31*, 1998.

[2] Md. Al Mehedi Hasan, Md. Abdul Alim, Md. Wahedul Islam , " A New Approach to Bangla Text Extraction And Recognition From Texual Image" , *ICCIT, Proceedings of 8th International Conference on Computer and Information Technology,* December 2005, Bangladesh.

[3] Ahmed Shah Mashiyat, Ahmed Shah Mehadi , kamrul Hasan Talukder , " Bangla-off-line Handwritten Character Recognition Using Superimposed Matrices ", *ICCIT, Proceedings of 7th International Conference on Computer and Information Technology,* December 2004, Bangladesh.

[4] Amin Ahsan Ali, Syed Monowar Hossain, " Optical Bangla Digit Recognition Using Back-propagation Neural Networks" , *CS 407 Project Works & Project Report* ,Department of Computer Science, University of Dhaka, Bangladesh.

[5] Gil Cohen, Barak Hermesh , " ISLAB OCR project using a neural network" [Online],Available: http://www.cs.technion.ac.il/labs/Isl/Project/Prjects/done/NN/OCR/ocrcodezip

[6] Alamgir Mohammed, "Bangla OCR Apona Pathak" [Online], Available: http://www.apona-bd.com/bangla-ocr/2.html

[7] Md. Abul Hasnat, S M Murtoza Habib and Mumit Khan, "Segmentation free Bangla OCR using HMM: Training and Recognition", *Proc. of 1st International Conference on Digital Communications and Computer Applications (DCCA2007*), Irbid, Jordan, 2007.

[8] U. Bhattacharya, B. B. Chaudhuri, "A Majority Voting Scheme for Multiresolution Recognition of Hand printed Numeral", *Document Analysis and Recognition, Proceedings, Seventh International Conference*, 3-6 August 2003.

[9] A. M. Shoeb Shatil and Mumit Khan, "Minimally Segmenting High Performance Bangla OCR using Kohonen Network", *Proc. of 9th International Conference on Computer and Information Technology (ICCIT 2006)*, Dhaka, Bangladesh, December 2006.

Proceedings of 2009 12th International Conference on Computer and Information Technology (ICCIT 2009)
21-23 December, 2009, Dhaka, Bangladesh

Adaptation of ATAM[SM] to Software Architectural Design Practices for Organically Growing Small Software Companies

S. M. Saiful Islam, M. Rokonuzzaman†
School of Engineering & Computer Science ,Independent University, Bangladesh (IUB), Dhaka, Bangladesh and,
PyxisNet Ltd., Dhaka, Bangladesh
† School of Engineering & Computer Science, Independent University, Bangladesh (IUB), Dhaka, Bangladesh
shaikatdsbd@yahoo.com, †zaman.rokon@yahoo.com

Abstract

The architecture of a software application determines the degree of success of both operation and development of software. Adopted architectural options not only affect the functionality and performance of the software, but they also affect delivery related factors such as cost, time, changeability, scalability, and maintainability. It is thus very important to find appropriate means of assessing benefits as well as liabilities of different architectural options to maximize the life-time benefit and reduce the overall cost of ownership of a software application. The Architecture Tradeoff Analysis Method (ATAM[SM]) developed by Software Engineering Institute (SEI) is that kind of tool. Considerably this is a very big framework for dealing with architectural tradeoff issues faced by large companies for developing large as well as complex software applications. The practicing of full blown ATAM without taking into consideration of diverse forces affecting the value addition from its practice does not maximize benefits from its adoption. Related forces faced by small software companies are significantly different than those faced by large software companies. Therefore, ATAM should be adapted to make it suitable for the practice by small software companies. This paper presents the information about the architectural practice level of organically grown small software companies within the context of ATAM followed by the gap analysis between the industry practices and ATAM, and adaptation recommendations. Both literature review and field investigation based on key informant interview have been performed for this purpose. Based on the findings of this study an adaptation process of ATAM for the small companies has been proposed.

Keywords: ATAM, software architecture, small software companies, value optimization, project forces, and adaptation of ATAM.

I. INTRODUCTION

The software architecture is the key to software quality. The right software architecture can pave the way for successful system development, while the wrong architecture results in a system that fails to meet critical requirements and incurs high maintenance costs [2]. It would then make sense to validate the architecture of a system as early on as possible in the development process in order to ensure that it is going to be on the right track [1]. For evaluating the architecture, Software Engineering Institute of Carnegie Mellon University (SEI) has developed a framework named Architecture Tradeoff Analysis Method[SM] (ATAM). The purpose of the ATAM is to assess the consequences of architectural decisions in light of quality attribute requirements [5]. A good amount of literatures and resources is available on providing the guideline for applying well generic ATAM. But these guidelines for ATAM applying process need to be tailored according to existing project forces faced by the small companies. The research identifies typical nature of practice level of architecture trade-off process in small software companies and the challenges in defining software architecture in a structured and disciplined manner using ATAM. Based on such findings, a recommended ATAM adaptation process for their best benefit has been proposed.

The objectives of this research article are:

1. To identify the gap of existing architecture design practice in small software companies with ATAM recommended practices along with their implications on software companies and other related stakeholders.
2. To propose an ATAM adaptation process by fusing the knowledge and concern of the practitioners and global standards and best practices, instead of full-blown ATAM, that best serves the need of the small software companies.

II. PROBLEM STATEMENT

To achieve the major objectives of this research work stated in the previous section, key informant interviews among the architects of small companies were performed. Through the key informant interview, architecture evaluation practices for different companies in the context of ATAM were identified at different level. Moreover, published literature has been reviewed to assess related situations faced by global small software companies [8, 16]. Finally, how ATAM can be practiced adapting to the existing practices of small companies is identified, which is the core part of the research.

Small software organizations—independently financed and organized companies with fewer than 50 employees—are fundamental to many national economies' growth [8]. To persist and grow, small software companies need efficient, effective software engineering practices. Considering the large percentage of small software organizations across the globe, relatively few publications present software engineering solutions focusing specifically on small software companies [8]. Small companies aren't just scaled-down versions of large firms. Tight finances also constrain many small businesses, so they can't always afford to buy required expertise [8]. Most of the small software companies deliver small and medium sized solutions to the customers. They do not concern most about the architectural solutions to the problems. Therefore, they suffer in the later phases of the software development life cycle, which leads to heavy rework and restructuring of the project.

The purpose of evaluating the architecture of a software system is to design the best architecture to validate the quality requirements, improve stakeholder communication and eliminate system risk [9]. The ATAM appears to be one of the best and proven available frameworks for ensuring the right architectures for the large and complex projects. In this article, considering the typical characteristics and limitations, how small organizations can tailor ATAM to improve software quality and productivity without introducing unacceptable overhead has been addressed.

III. METHODOLOGY

Study has been conducted on a number of research papers and available standards to develop a clear understanding of global practices of architectural evaluation with special reference to ATAM. Literature review reveals that there is a need for defining a process of adapting ATAM for the small companies. Therefore, the research proposed an ATAM adaptation process considering the existing practice of architectural design.

Key informant interviews were performed with 5 software architects from 5 different software companies of Bangladesh, who have years of experience in developing and designing contract projects. Face-to-Face interview technique was used to obtain information from each of the key informants. For collecting the data about the practice level of architecture evaluation process in the context of ATAM, two sets of questionnaire were created following ATAM steps and sub steps. First set of questions focuses on high level understanding and the use of ATAM and the other one focuses on detailed level practice and knowledge areas.

IV. LITERATURE REVIEW

The software architecture of a program or computing system is the structure or structures of the system, which comprises software elements, the externally visible properties of those elements, and the relationships among them [3]. In large software systems, the achievement of qualities such as performance, availability, security, and modifiability is dependent not only upon code-level practices (e.g., language choice, detailed design, algorithms, data structures, and testing), but also upon the overall software architecture. Quality attributes of large systems can be highly constrained by a system's software architecture [14]. Architectural decisions take different quality attributes into account and they are the key factors in exposing risks and sensitivity points of the architecture while the evaluation is in progress [10]. Furthermore, architectural styles play an important role during evaluation [11, 12] to extract and derive the possible combination of design decisions from earlier experience [13].

The process of analyzing and deducting the architectural potential for implementing a system capable of supporting the major business requirements and identifying major risks and trade-offs is evaluation's main concern [15]. Different research groups have taken initiatives and are proposing various methods for software architecture quality evaluation [6]. A number of methods [7] have been developed to evaluate quality related issues at the Software Architecture level. These methods includes Scenario based Architecture Analysis Method (SAAM) , Architecture Tradeoff Analysis Method (ATAM), Active Reviews for Intermediate Design (ARID), and integrating SAAM in domain-Centric and Reuse-based development (ISAAMCR)[7].

Over the past several years, the Software Engineering Institute (SEI) has developed the Architecture Tradeoff Analysis Method[SM] (ATAM) and validated its usefulness in practice [4]. ATAM helps to identify the architectural approaches used and, by means of scenarios, exposes areas of risk [9]. ATAM method consists of four phases: presentation, investigation and analysis, testing, and reporting. Each phase is a collection of steps[6]. The major steps and sub steps of ATAM are Step 1: Present the ATAM, Step 2: Present business drivers, Step 3: Present architecture, Step 4: Identify architectural approaches, Step 5: Generate quality attribute utility tree, Step 6: Analyze architectural approaches, Sub-Step 6.1: Investigation of Architectural Approach, Sub-Step 6.2: Creation of Analysis Questions, Sub-Step 6.3: Answers to the Analysis Questions, Sub-Step 6.4: Find the Risk, Non-Risks, Sensitivity and Tradeoff Points, Step 7: Brainstorm and prioritize scenarios, Step 8: Analyze architectural approaches, and Step 9: Present results.

V. DATA ANALYSES AND RESULTS

The data were gathered from the 5 companies in two levels - high level and detailed level following defined methodology. The key informants were asked a number of questions (high level 60, detail level 117) against each ATAM steps. The narrative answers of the companies were accumulated in the tabular format. Then the narrative answers were carefully converted to quantita-

tive points for further analysis. For each question, weightage range was 0 to 10.

All the narrative answers, both in high level and detailed level were taken into consideration and converted to the quantitative value, which is called earned points following the conversion method. These data are provided in Table I along with the average earned points and total available points. The average points earned for the high level is 271 out of 600 (45%) and 441 out of 1170 (38%) for detailed level practice.

Table I Combined Status of ATAM Practice Level

ATAM Steps	Company A		Company B		Company C		Company D		Company E		Average		Total Point	
	HLP	DLP	HLP	DLP	HLP	DLP	HLP	DLP	HLP	DLP	HLP	DLP	HLP	DLP
1	16	23	17	20	18	26	22	20	18	21	18	22	40	50
2	18	20	14	28	14	24	15	32	20	33	16	27	30	60
3	33	36	25	37	30	38	28	45	40	42	31	40	60	80
4	17	10	16	17	16	14	16	18	20	18	17	15	30	40
5	27	32	19	50	30	39	26	52	28	52	26	45	80	170
6	9	19	7	22	8	22	3	22	4	17	6	20	20	40
6.1	29	42	24	57	25	41	28	55	30	56	27	50	60	130
6.2	40	42	36	70	40	49	33	75	50	80	39	63	80	170
6.3	6	9	7	10	6	10	6	11	7	12	6	10	10	20
6.4	9	18	5	11	8	20	9	13	6	13	7	15	30	90
7	41	42	28	62	30	42	40	62	34	66	34	55	80	140
8	20	25	20	39	20	24	20	39	20	41	20	34	30	80
9	22	42	18	45	20	43	22	45	24	46	21	44	50	100
Total	287	360	236	468	265	392	268	489	301	497	271	441	600	1170

HLP: High Level Point DLP: Detail Level Point

The comparative practice status of ATAM has been analyzed based on the earned points as percentage of available points as shown in Table II. The result indicates that at the higher level, the practice level is much higher than that of the detail level. It is also evident that for some steps the practice level is much higher than the other steps. There is a significant variation among the practice levels of the companies.

Table II Comparative Status of ATAM Practice Level (% of available points)

ATAM Steps	Company A		Company B		Company C		Company D		Company E		Average	
	HLP%	DLP %	HLP%	DLP%	HLP %	DLP%	HLP%	DLP %	HLP%	DLP%	HLP%	DLP%
1	40	46	43	40	45	52	55	40	45	42	46	44
2	60	33	47	47	47	40	50	53	67	55	54	46
3	55	45	42	46	50	48	47	56	67	53	52	50
4	57	25	53	43	53	35	53	45	67	45	57	39
5	34	19	24	29	38	23	33	31	35	31	33	26
6	45	48	35	55	40	55	15	55	20	43	31	51
6.1	48	32	40	44	42	32	47	42	50	43	45	39
6.2	50	25	45	41	50	29	41	44	63	47	50	37
6.3	60	45	70	50	60	50	60	55	70	60	64	52
6.4	30	20	17	12	27	22	30	14	20	14	25	17
7	51	30	35	44	38	30	50	44	43	47	43	39
8	67	31	67	49	67	30	67	49	67	51	67	42
9	44	42	36	45	40	43	44	45	48	46	42	44
All	48	31	39	40	44	34	45	42	50	42	45	38

HLS: High Level Point DLS: Detail Level Point

The Fig. 1 gives the better visibility of the average practice level of all the ATAM Steps and Sub-Steps in comparative manner. It shows that the ATAM Sub-Step 6.3 "Answers to the analysis questions" is the highest practiced step (52% in detail level) and the ATAM Sub-Step 6.4 "Find the risks, non-risks, sensitivity points and tradeoff points" is the least practiced step (17% in detail level).

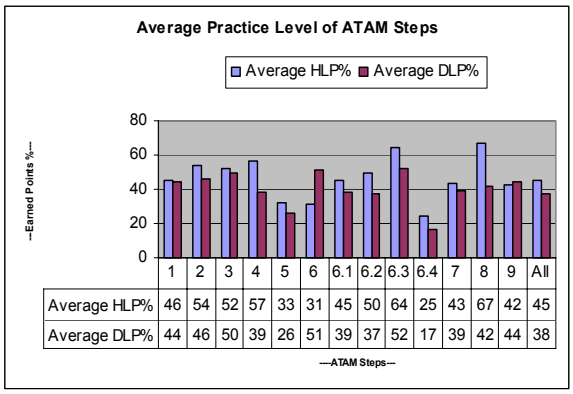

Fig. 1. Average Practice Level of ATAM Steps

The Fig. 2 depicts the average practice level of ATAM of the companies. It is evident that the variation among the higher level and detailed level is significant. This might happen due to the understanding about the process and practice was clearer when detailed level investigation was done. The variations among the companies are not very significant. It is found that average practice level in detailed level is only 38%, where the lowest is 31% and highest is 42%. So, it is evident that the companies perform some practices in the context of ATAM which is at very primary stage.

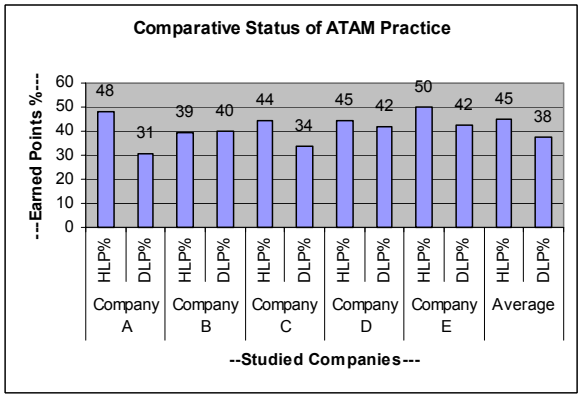

Fig. 2. Average Practice Level of the Companies

VI. ATAM ADAPTATION

ATAM adaptation is meant here as the process of adopting and adapting ATAM in the industry to bring the disciplined approach in their architectural design practices.

The guidelines provided here help to determine what to do at what step of ATAM for the Small companies. This is described following the ATAM Steps.

ATAM Step 1: Present the ATAM

This Step is very relevant for the architectural practices to the small companies. The companies usually have some sort of architectural meeting when new projects are started. That should be formalized and methodical. Following points should be considered for practicing this step:

1. Provide the functionality and plenty of knowledge about the project before meeting.
2. Involve the related stakeholders of the project who are directly involved to the project or might be affected by the project decisions.
3. Try to involve client's representatives in the evaluation process if possible.

ATAM Step 2: Present the Business Drivers

The business drivers are not well considered but this is very important and relevant to the architecture evaluation process. So, this should be practiced by the companies. Following points should be considered for practicing this step:

1. Identify and present the business goals and business drivers which are crucial for the success of the project.
2. Consider business process fitting and flexibility, customizability, security, performance, requirement complexity, lack of domain knowledge and technological uncertainty.
3. Clearly describe the intended system functions to all the participants.

ATAM Step 3: Present the Architecture to be evaluated

This is very relevant and required practice for architectural practices. Following points should be considered for practicing this step:

1. Define the alternative architectures and architectural approaches providing the good reasoning for selecting that approach for the project beforehand.
2. Present the Layered diagram, Layer to Layer communication diagram, sequence diagrams and deployment diagram for giving the clear visibility and understandability to the participants.
3. Address all constraints and uncertainty, all quality attributes like reliability, performance, security, availability, plugability and future enhancement which are deemed to be relevant at the initial level.

ATAM Step 4: Identify the Architectural Approach

This is very relevant and required practices should be followed properly. Following points should be considered for practicing this step:

1. Explain the flow of control of the architecture to the team.
2. Determine the flow of controls following the different business workflows considering the best and worst case scenarios.

3. Address the critical and the complex business requirement and algorithmic complexity for the business goal.
4. Provide the explanation and establish how the critical goal will be met by the identified architectural approach.

ATAM Step 5: Generate the Quality Attribute Utility Tree

The companies usually do not identify the quality attribute goals consciously and completely and do not make quality attribute tree as well. This would be pretty overhead for the small companies. So, the companies can skip this step of making quality attribute utility tree in detail and instead practicing something simpler will do the job. Its recommended that they identify quality attributes within the context of different scenarios that may arise. Following points should be considered for practicing this step:

1. Identify the quality goals clearly and specifically.
2. Consider the common quality goals like security, performance, functionality and reliability at least.
3. Determine the quality attributes, find out the importance to the project, and prioritize them accordingly.
4. Consider the different scenarios which may happen in the project.
5. Consider the different use case scenarios as minimum. Then look into the growth scenarios if possible. The exploratory scenarios can be avoided depending on the project nature.

ATAM Step 6: Analyze the Architectural Approach

The companies usually analyze the architectural approach in high level. This is very relevant practice for evaluating the architecture. Following points should be considered for analyzing the architectural approaches:

1. Identify the relevant and required quality attributes for the project that should be met.
2. Consider the quality attributes such as security, modifiability, reliability, conceptual integrity, functionality, performance, reusability, framework expandability, validation, consistency, modifiability, and integrity .
3. Investigate how architectural approach support these quality attributes if relevant.
4. Consider the cost and time implication to achieve these goals.
5. Thoroughly analyze and discuss the answers and explanations to the questions in the meeting.
6. Criticize the answers and explanations from different angles by the different stakeholders to figure out if there are flaws.
7. Identify the project risks and non-risks properly. The most of the risks are project dependent. Consider unavailability of client resource, failure of meeting the performance goals, quality requirements, requirement complexity, technological uncertainty etc. as risk.
8. Figure out the sensitivity points of the project if any. The sensitivity points are dependent on the project and client.
9. Check if there is any trade off points. Make the right allocation of resources to the different points based on the tradeoff, priority, importance and complexity.

ATAM Step 7: Brainstorm and Prioritize Scenarios

The brainstorm and prioritization are done to some extent as the quality attributes and scenarios are not well identified. But, no voting process is mandatory for prioritizing the scenarios. This can be done by the majority consensus. Following points should be considered for practicing this step:

1. Involve all the major stakeholders to the evaluation and decision making process.
2. Consider all the scenarios which deemed to be more likely to happen. Consider complex work flows, work flows with huge transaction, work flows with multiple accesses, workflows with distributed transaction process, etc.
3. Prioritize every scenario based on application functionality, complexity, business driver and stability of requirement.

ATAM Step 8: Analyze the Architectural Approaches

This is the same step discussed in Step 6. This is usually not required and relevant unless any new thing comes up from the previous exercise.

ATAM Step 9: Report the ATAM

The architecture evaluation team produces the report based on the evaluation meeting. This is absolutely required for finalizing the architecture. Following points should be considered for reporting the ATAM:

1. Provide the list of quality attributes and business drivers that were considered along with their priority.
2. Describe all the scenarios that were considered during the evaluation process by grouping into appropriate category.
3. Provide the list of architectural approaches that were considered in the evaluation process.
4. Describe all the risks, non-risks, sensitivity points and tradeoff points that were identified in evaluation process.
5. Describe the final Architectural approach that was selected and that is fulfilling all the business and quality requirements.

The full-blown ATAM produces number of items which all are not relevant for the adapted ATAM. But following items should be produced along with the practices of ATAM:

1. Business drivers and quality attributes
2. List of scenarios produced by the stakeholders
3. List of architectural approaches considered

4. All the risks, non-risks, sensitivity points and tradeoff points.
5. Analysis result
6. Selected architectural approach and architecture Outline

VII. SUMMARY AND PROPOSITION FOR FUTURE WORK

The study reveals the nature of the architecture design process is in practice in the small software companies. Basically, the Architectural practices small software companies are not well evident. They use some common style of architecture without considering of its merits or demerits in detail. They sometimes do the evaluation without following any structured framework or methodology like ATAM. The study records and analyzes the high level and detailed level gaps of practice within the context of standards and recommended practices. The analysis result depicts that the average practice level of ATAM in the local companies is very low and only one third of the steps and activities are performed in the companies to a some extent. The full blown ATAM cannot be practiced blindly in the small software companies without increasing significant overhead. As the full blown ATAM is not the solution for the small software companies, the study defined the ATAM adaptation process by combining the academic knowledge, global standards, and industry practitioners' knowledge and concerns.

As the ATAM framework itself is a big topic, therefore the participants were not very interested to provide enough inputs. Besides these, narrow knowledge of software architecture and architectural practices of the concerned practitioners, lack of architecture evaluation concept, lack of thorough understanding and knowledge on tradeoff analysis process among the architects have limited the progress of the study. However, the study was conducted only on 5 selected companies of Bangladesh. Therefore, the finding of this study is likely to have limited accuracy.

The study should be conducted to the larger community, i.e. involving the practitioners from the different category of software companies like local, outsourcing, offshore development center, etc. and of different sizes employing effective and efficient market research approach. The practitioners can be provided with preliminary knowledge of architectural practices and ATAM framework itself so that they can relate the real life practices with the theoretical ones. Future related works should investigate more deeply into the further modification of the entire adaptation process from the cost benefit analysis perspective i.e. value creation ability from the ATAM practices.

REFERENCES

[1] M. N. Ambe, F. Vizeacoumar, Evaluation of two architectures using the Architecture Tradeoff Analysis Method (ATAM)

[2] Using the Architecture Tradeoff Analysis Method^{SM} (ATAM^{SM}) to Evaluate the Software Architecture for a Product Line of Avionics Systems: A Case Study. http://www.sei. cmu.edu/ pub/documents/03. reports/ pdf/ 03tn012.pdf

[3] L. Bass, P. Clements, R. Kazman, Software Architecture in Practice, 2nd edition. Boston, MA: Addison-Wesley, 2003.

[4] P. Clements, R. Kazman, M. Klein, Evaluating Software Architectures: Methods and Case Studies. Boston, MA: Addison-Wesley, 2002.

[5] R. Kazman, M. Klein, P. Clements, ATAM: Method for Architecture Evaluation (CMU/SEI-2000-TR-004, ADA382629). Pittsburgh, PA: Software Engineering Institute, Carnegie Mellon University, 2000.

[6] Scenario-Based Software Architecture Evaluation Methods: An Overview. http://www. win.tue.nl/ oas/architecting/aimes/ papers/ Scenario-Based% 20SWA %20Evaluation % 20 Methods.pdf

[7] A Framework for Classifying and Comparing Software Architecture Evaluation Methods. http://www. cse. unsw. edu.au/~limingz/ publication/ASWEC2004_Zhu.pdf

[8] I. Richardson, G.V. Wangenheim, Why Are Small Software Organizations Different? http:// www. computer.org/ portal/ cms_ docs_ software/ software/homepage/2007/s1018.pdf

[9] T. Kim, I. Ko, S. Kang, D. Lee, "Extending ATAM to Assess Product Line Architecture**.",** Proceedings of the 5th Working IEEE/IFIP Conference on Software Architecture, pp. 45 - 56.

[10] L. Bass, P. Clements, R. Kazman, Software Architecture in Practice, Second Edition. Addison-Wesley Professional, April 2003.

[11] L. Zhu, M.A. Babar, D.R. Jeffery, Distilling scenarios from patterns for software architecture evaluation - a position paper. In EWSA (2004), pp. 225–229.

[12] L. Zhu, M.A. Babar, D.R. Jeffery, Mining patterns to support software architecture evaluation. In WICSA '04: Proceedings of the Fourth Working IEEE/IFIP Conference on Software Architecture (WICSA'04) (Washington, DC, USA, 2004), IEEE Computer Society, pp. 25.

[13] A. Jansen, J. Bosch, Software architecture as a set of architectural design decisions. In WICSA '05: Proceedings of the 5th Working IEEE/IFIP Conference on Software Architecture. (WICSA'05) (Washington, DC, USA, 2005), IEEE Computer Society, pp. 109–120.

[14] M.R. Barbacci., S. J. Carriere, P. H. Feiler, R. Kazman, M. H. Klein, H. F. Lipson, T. A. Longstaff, C. B. Weinstock, "Steps in an Architecture Tradeoff Analysis Method: Quality Attribute Models and Analysis", http://www.sei.cmu.edu/ publications/ documents/97.reports/97tr029/97tr029title.htm

[15] A. Vasconcelos, P. Sousa, J. Tribolet, Information System Architecture Evaluation: From Software to Enterprise Level Approaches. http://www.inesc-id.pt/ficheiros/publicacoes/ 2548.pdf

[16] L. Bass, R. Nord, W. Wood, D. Zubrow, I. Ozkaya, "Analysis of architecture evaluation data.", Journal of Systems and Software, Volume 81, Issue 9, pp. 1443-1455 (September 2008)

Proceedings of 2009 12th International Conference on Computer and Information Technology (ICCIT 2009)
21-23 December, 2009, Dhaka, Bangladesh

Potential Consequences of E-Commerce Application

(Not Presented)

Tarun Kanti Bose, Abdullah Al Nahid[†]
Business Administration Discipline, Khulna University, Khulna, Bangladesh
[†] Electronics and Communication Engineering Discipline, Khulna University, Khulna, Bangladesh
tarun84ku@yahoo.com, nahidku@yahoo.com

Abstract

E-commerce application for enhancing small community business success is one of the most discussed issues that have been raised by contemporary researchers. This study aimed to investigate the probable outcome of e-commerce application for the small business operation mainly from the perspective of online business conduction in Bangladesh. Qualitative and quantitative data derived from field interviews with small business network directors and members has been used to identify potential relationships among those constructs. With insight from the interviews, hypotheses has been derived and tested with quantitative data gathered via a direct survey instrument with 150 small business stakeholders who has the potentiality to get influenced directly if the system can be established among small business communities across four divisions of Bangladesh. Owner's perceptions about the successful and the likelihood of growing the business have also been taken into consideration. Results of the study focuses that e-commerce application can bring new times in SME operation in Bangladesh and can improve the performance drastically. The study will contribute significantly regarding members' future participation plans, thus furthering the likelihood of e-commerce network continuance.

Keywords: E-commerce, Communities, SME, Consequence.

I. INTRODUCTION

For the past few decades substantial interest has been developed regarding SMEs all over the world [1]-[3]. Although the economic uniqueness of the small enterprises has been acknowledged globally, in Bangladesh this sector began to get some momentum during 1990s. Since then the government of Bangladesh started devising policy instruments to guard the sector from any sort of undue intervention.

This shift in prioritization of different sectors of the economy by the government did not come all of a sudden, such a discernible move was rather imminent due to the facts that on the one hand agriculture sector, the mainstay of the economy, has long been suffering from low productivity problem and was employing some 60 percent of the labor force to produce a meager one–third of the national income [4].

Many small businesses radiate a unique charm that attracts consumers to main streets. Small enterprises as a whole are a major employer and an essential contributor to community civic environments. However, research suggests there is a significant correlation between a business's location and its growth, with firms operating in rural areas less likely to grow. Rural areas have been described as periphery to the cities and are often seen as poor environments for the creation and cultivating of business. E-commerce is even more difficult in rural areas in compare to that of urban areas. Now is e-commerce networking a big issue or a significant success factor variable of SME's? This study is directed toward the successful answering of that question.

In Bangladesh the most noted thing is most often than not SME's sustainable growth are a rare phenomenon. They rise quickly and disappear quickly as well. Researchers of small business often blame the government policy as well as global factors for these incidents. However, this study is aim to find whether an e-commerce networking in small business operation can improve the scenario and enhance the overall position of the small business operation.

II. LITERATURE REVIEW

Concerned research coverage

Small business success has social as well as economic consequences for communities and geographic regions. Business success in developing new products and ways of doing business adds value to the economy and improves the quality of life in communities [5].If small businesses are vitally important to a community's economic and societal health, the question then become one of 'How can small businesses overcome the limitations that often accompany the rural or small community environment?' The goal of this research is to explore whether online business operation helps to overcome several of the limitations and challenges associated with scale and often remote locations of small firms operating in small and rural communities. Specifically we have examined whether the e-commerce can play a key role in enhancing the position of and change the color of the fate of small business owners.

E-commerce

Electronic Commerce consists of the buying and selling of products or services over electronic systems such as the Internet and other computer networks. The amount of trade conducted electronically has grown extraordinarily with widespread Internet usage. The use

978-1-4244-6283-4/09/$26.00 ©2009 IEEE

of commerce is conducted in this way, spurring and drawing on innovations in electronic funds transfer, supply chain management, Internet marketing, online transaction processing, electronic data interchange (EDI), inventory management systems, and automated data collection systems.

Modern electronic commerce typically uses the World Wide Web at least at some point in the transaction's lifecycle, although it can encompass a wider range of technologies such as e-mail as well. A large percentage of electronic commerce is conducted entirely electronically for virtual items such as access to premium content on a website, but most electronic commerce involves the transportation of physical items in some way. Online retailers are sometimes known as e-tailers and online retail is sometimes known as e-tail. Almost all big retailers have electronic commerce presence on the World Wide Web.

Electronic commerce that is conducted between businesses is referred to as business-to-business or B2B. B2B can be open to all interested parties (e.g. commodity exchange) or limited to specific, pre-qualified participants (private electronic market). Electronic commerce that is conducted between businesses and consumers, on the other hand, is referred to as business-to-consumer or B2C. This is the type of electronic commerce conducted by companies such as Amazon.com. Electronic commerce is generally considered to be the sales aspect of e-business. It also consists of the exchange of data to facilitate the financing and payment aspects of the business transactions.

Small and Medium Enterprises

Across the world, the SMEs are defined on the basis of two criteria: volume of turnover and number of person employed in a particular organization. Small firms are comprised of wide variety of firms ranging from the single proprietor business, independent business owners who employ a handful of workers. European Commission has defined SME sector as the businesses with fewer than 500 employees, and broken that definition down into three subcategories namely micro-enterprise with between 1 to 9 employees, small-enterprises with between 10 to 99 employees and Medium-enterprises with between 100 to 499 employees. On the other hand, the central bank of Bangladesh defines any business having a “Net-Worth” of up-to Tk. 10 Million or number of employees between 10 to 50 persons as small and business having a “Net-Worth” between Tk. *10 to 100 Million*, or employees between *50 to 100* persons as Medium enterprises.

Small & Medium Enterprise Development in Bangladesh

Historically, Bangladesh followed a development strategy in which private investment was controlled through a host of regulations involving investment sanctioning, credit disbursement, import licensing, foreign exchange allocation etc. While these regulatory barriers threaten private investment in general, the impact fell unevenly on SMEs. This was because of the relative inability of the SMEs to cope with the regulations compared to their large-scale counterparts. Thus, the policy regime was largely biased against the SMEs although, paradoxically, promoting SME development was a stated objective of successive governments. The creation and development of SMEs is seen as an important element of overall economic policy, especially for promoting employment, reducing poverty and enhancing overall growth. Arguably, when faced with as many odds as Bangladesh encounters, the development options available to her are limited and hence development of a strong, dynamic and vibrant SME sector is not a luxury but it is rather a dire necessity. Though efficient and productive agriculture is a precondition for rapid sustainable growth, agriculture is unlikely to be engine of growth in future. As the economy already faces huge challenge to absorb some two million people entering the labor force annually, on top of the large number of existing unemployed .exports and job oriented manufacturing, especially in the SME sector must hold the key to national development over the next quarter century or so .

Reference [6] shows that the factors that are acting as constraints in case of SME market development are: quality and standards, marketing, investment and working capital, shortage of skilled workers, lack of entrepreneurship and management skills, physical infrastructure, transport costs, trade policy and incentives, information, legal and regulatory framework, domestic environment etc.

Reference [7] shows that it is necessary to review the Government’s industrial policy and technology policy to outline the Government’s measures to support SMEs in technological up gradation. Reference [19] shows, some similar issues in case of Pakistani SME sector, those are: inadequate infrastructure, financial barriers and disincentives, adverse government policies, shortage of skilled personnel, technological constraints and lack of innovation and entrepreneurial handicap.

Reference [20] shows that in case of United States, entrepreneurship development and competitive environment generated through the presence of strong SMEs are quoted to be the leading factors behind the country’s recent success in the rivalry against Europe and Japan.

Analysis indicates three important cases within the American success story:

a) Big companies, such as General Electric, adapted/reengineered themselves, became leaner-with the sales and profit rising sharply.

b) New, small high-tech start-ups have been expanding from traditional industrial sectors to internet based and e-commerce (Amazon.com, Netscape, AOL, E-Bay etc.)

c) Thousands of new, micro and small firms have been founded, many by women, minorities and immigrants.

Studies on E-commerce

The impact of business and e-commerce networks on economic life has been studied by scholars working independently and collaboratively across several countries. There has been a large concentration of small business network research conducted outside the USA in Belgium and Finland, Denmark, Sweden and Norway, Italy .Japan and the UK [11].
Several scholars have conducted matched studies examining structures and activities and activities of e-commerce specifically across entrepreneurs in Norway Sweden , Scotland, Northern Ireland , Japan ,and Canada .These studies discovered that some elements of e-commerce in small and medium business operation are universal, and though not highlighted, small firms operating in small communities were represented among the sample populations in these studies.

Theoretical Evidences and Hypotheses

Theoretical Evidences and Hypotheses

There are some literal elements of commerce that are necessary for any transactions to take place, which are as true for regular bricks-and-mortar commerce as they are for e-commerce. First, whether someone is doing business online or in the real world, he or she have to have a product to sell or a service to offer. Then, it must have a place from which to do business. In the traditional world of commerce this can be a physical store or, in a more figurative sense, a catalog or phone number. In the world of e-commerce the place from which to do business is the Web site [11].

Most businesses already exist in the bricks-and-mortar world of commerce. Adding a Web site is a means to enhance their business. For Internet startups, the Web site is the only place that they do business. In both regular commerce and e-commerce it is needed to find a way to attract customers to your place of business. This is embodied by marketing strategy, and everything from advertising to word of mouth fits into this category [12].

In order to do business, you also need a way to take orders and process payment. In a retail store there are no orders. Customers simply find the products they want, get in a line at the register, and pay the cashier. In e-commerce, orders have to be placed and items shipped. Orders are usually handled through interactive, online forms. Money is another issue easily handled in traditional commerce. Customers in a retail store pay by check, cash, or credit or debit cards. Online customers cannot pay by cash or check, only through electronic means. Also, there are issues of security that surround online payment that do not come into play in the traditional bricks-and-mortar world. E-commerce transactions have to take place through secure electronic connections and special merchant accounts for accepting payment [11].

Once payment is collected, delivery of the product must take place. Fulfillment in traditional stores is as easy as putting the item in a bag and handing it over to the customer. Fulfillment in the world of e-commerce is more difficult, requiring shipping and transportation similar to catalog and mail order businesses. For businesses that integrate e-commerce into their existing business plan, fulfillment is as easy as hiring an extra employee to ship online orders. In Internet startup businesses, fulfillment must often be outsourced to a facility that can handle order processing and shipping in a more timely and professional manner [10].

Hypothesis

Hypothesis

In review of the above-mentioned research outcomes the study anticipates the following hypotheses:
H1: E-Commerce Application among SME Communities in Bangladesh is positively related to service Promptness.
H2: E-Commerce Application among SME communities in Bangladesh is positively related to customer convenience
H3: E-Commerce Application among SME Communities in Bangladesh is positively related to producer convenience
H4: E-Commerce application among SME communities in Bangladesh is positively related to global phenomenon.
H5: E-Commerce application among SME communities in Bangladesh is positively related to cost curtail.
H6: E-Commerce application among SME communities in Bangladesh is positively related to easiness in delivery.
H7: E-Commerce application among SME Communities in Bangladesh is positively related to advertising facilities.
H8: E-Commerce application among SME communities in Bangladesh is positively related to International business entry.
H9: E-Commerce application among SME communities in Bangladesh is positively related to handling rivalry.

III. METHODOLOGY

Research Design, Sample, and Procedure

A descriptive research design was used to test the hypotheses, proposed for examining the effects of various factors to the stakeholders' intention with data collected from different parties in Bangladesh through a self administered structured survey instrument. The survey questions were adopted from the literature and exploratory techniques. A convenient sampling method was used to select the sample considering the total citizens of Bangladesh as population of the study. The sample for this study is selected from the prospective stake-

holders of 4 divisions in Bangladesh such as Dhaka, Rajshahi, Khulna and Sylhet. Different types of people have been included in the sample, which is stated in the sample profile, to make the sample representative. A total of 150 surveys were conducted in March, 2009-May 2009.

IV. Data Analysis Data Analysis

To address nine independent variables of the study 28 items were generated, that were purified and validated through the factor analysis and internal consistency of the items were examined using cronbach alpha.

For the purposes of this study, items measuring the independent variables were simultaneously subjected to a principal components factor analysis with varimax rotation. The result yielded a 9 factor solution with eigen values greater than 1.0 (as shown in Table 2). The factor analysis further reveals that all the items were retained within the 9 factors those are anticipated for the study that cumulatively explained 66.79% of the total variance.

V. RESEARCH FINDINGS

Table 1 shows the demographic profile of the respondents.

DESCRIPTION	**F**	**Percent**
Respondents Age		
Below 25 years	22	14.67
25 to 45 years	90	60
46 to 60 years	30	20
Above 60 years	8	5.33
Occupation		
Student	15	10
Government Job	35	23.33
Private Job	85	56.67
Business	12	8
Others	3	2
Gender		
Male	125	83.33
Female	25	16.67
Marital Status		
Married	105	70
Single	45	30
Education		
HSC or below	30	20
Graduate	80	53.33
Post Graduate	40	26.67
Area		
Dhaka Division	30	20
Rajshahi Division	32	21.33
Khulna Division	70	46.67
Sylhet Division	18	12

Table: 2 Regression Statistics

Variables	**Standardized**	**Alpha**
Service	.248**	..589
Customer	..252**	..701
Producer	..11	..781
Global Phe-	..002	..526
Cost Curtail	-..231	..757
Easiness in	..256**	.658
Advertising	..102	..812
International	.006	..865
Handling	-..174*	..632
R^2	.232	
F Value	4.458**	
Durbin-Watson	1.952	

** p <.001, * p<.05

		Component								
		Service Promptness	**Customer Convenience**	**Producer Convenience**	**Global Phenomenon**	**Cost Curtail**	**Easiness in Delivery**	**Advertising Facilities**	**International Business Entry**	**Handling Rivalry**
1	Q15	.443	.029	.040	-.225	.600	.081	.021	.145	.65
2	Q18	.280	-.079	.035	-.139	.721	.089	-.0045	.023	.111
3	Q20	.107	.359	.120	-.031	.656	-.031	-.031	.048	-.65
4	Q01	.0045	.820	.072	-.025	.030	.047	.062	.111	-.048
5	Q12	.002	.658	.019	.121	.054	.182	-.028	.026	-.065
6	Q21	.185	.601	.045	.169	.444	-.222	-.015	-.014	-.098
7	Q15	.135	.698	.062	-.047	.069	.039	-.005	-.058	.112
8	Q10	.222	-.039	.163	.686	-.185	.225	.0078	.112	.068
9	Q7	-.054	.042	-.115	.632	-.111	-.024	-.058	-.058	.069
10	Q8	-.111	-.018	-.020	.669	-.120	.048	.180	.236	.142
11	Q11	.062	.169	.220	.631	.335	.026	.041	.048	-.232
12	Q12	.698	.021	-.063	-.333	.362	.032	-.021	.111	-.047
13	Q8	.664	-.020	-.030	.111	.222	.114	.054	.232	.058
14	Q9	.747	.085	.059	.182	-.054	-.068	-.085	-.0048	-.039
15	Q5	.654	.223	-.032	-.122	.222	-.006	.111	.113	.021
16	q4	-.126	-.009	.654	.041	.030	.115	.063	.168	.032
17	Q5	.285	.061	.630	-.006	-.098	.032	.121	-.336	.108
18	Q6	-.108	.232	.732	-.093	.002	.184	.124	.094	.066
19	Q17	.058	.002	.715	.065	.111	-.121	.034	.042	.045
20	Q16	.126	-.014	.120	-.026	-.065	.065	.45	.098	-.060
21	Q19	-.0368	.010	.150	.221	.045	.021	.635	.112	.158
22	q11	.0027	.057	.020	.115	-.025	.822	.004	-.045	.179
23	q10	.1160	.186	.049	-.018	.035	.657	-.031	.165	-.132
24	q12	-.1233	-.079	.169	.161	.060	.666	.111	-.223	.148
25	Q2	.079	.066	.159	.111	.118	-.135	.136	.731	.069
26	q3	.279	.056	-.032	.223	-.080	.058	.120	.698	.093
27	q20	-.053	.114	.035	.152	.052	.062	.115	-.035	.786
28	Q13	.189	-.020	.263	-.060	.020	.178	-.201	.202	.693

VI. DISCUSSION

The regression analysis have indicated significant correlations between service promptness, customer convenience, producer convenience, global phenomenon, cost curtail with the e-commerce application which means that the positive perceptions of these five characteristics or attributes led to higher purchase intention. On the other hand, handling rivalry is negatively correlated with tour intention, which means that the perceptions of rivalry were not really big concern. . Although the handling rivalry is observed significant in tourists' destination selection, disagree with previous researches as most of the researches explain the significant positive relation in between rivalry and SME business conduction.

Easiness of delivery has emerged as the strongest factor in terms of degree and magnitude affecting the perceptions of the stakeholders. The issue of delivery is significant as people normally reckon through e-commerce they can get their product available in a very easy way in compare to the old manual system.

International business entry also has as an important factor affecting the perceptions of the Bangladeshi stakeholders of SME. This is due to the fact that for the sake of attaining the global business entry it is obligatory that they have the access of modern up to date technique of selling.

Cost Curtail variable has also found to be a significant one as the common perception is through the application of e-commence a great deal of costs that is both variable as well fixed costs will be cut down as it will reduce the transaction cost and transportation cost by a huge margin.

The survey outcome and variable analysis also shows the fact that the SME business man will get a huge advantage for going for advertising through internet or online operation, because the area of coverage is huge and it will cover almost everything of relative business boundary that is the customer segments of all levels.
The research study and its outcome clearly indicate that e-commerce application can increase the performance level of SME business drastically. There is every likelihood that it can bring new times in the SME sector of our country. Only proper guideline and materials or ingredients is the ultimate requirement from the proper or concern authority.

VII. CONCLUSIONS AND IMPLICATIONS

Over the last few years, Bangladesh is investing a lot for giving a boost to its economic development through utilizing country's resources and expertise particularly in SME sector. Many people reckon, SME sector has the potentiality to become a major area that can bring new times in the country's export business. The indigenous culture, climate, geographic location, currency exchange rate, price of essential commodities and services and quality of products are extremely favorable for developing an organized and professional SME industry in Bangladesh that can contribute a substantial amount of money each year in the national exchequer. It will also generate huge employment opportunities that will ultimately help develop country's overall economic environment. Although the SME sector has the potentials of contributing a substantially large amount of money in national economy, the government's initiative, people's perception on the SME, and country's culture hinder the development of the sector up to a certain extent.

The political instability, strike, blockage and ban in different issues and the emergence of political and religious rebellions and terrorism are to be considered as major barriers of emerging a strong SME industry in Bangladesh. Infrastructures like technological, legal, financial, human resources are also to be considered as important influencer in Bangladesh. The government should provide a positive look at developing the human resource infrastructure required for developing SME sector in the country. Highly professional and technical human resource competent in SME can contribute positively to satisfy diversified needs of different requirements of SEM business operation. A specialized institution thus may be established for small business education in Bangladesh. Besides the above mentioned supports and services the entrepreneurs in the field of this industry should be supported and encouraged by establishing government's grants and subsidies and adopting country's SME policy that may be used as the guideline for the rapid expansion of this sector. The study is believed to be supported by its academic proponents and professionals.

REFERENCE

[1] Birch, D. L. (1979). "The Job Generation Process MIT Program on Neighborhood and Regional Change, Bambridge, Mass: MIT.

[2] Anderson, D. (1982). "Small Industries in Development Countries: A Discussion of Issues," *World Development*, Vol.10 (11), pp. 913-948.

[3] Gibb, A. A. (1993). 'Small Business Development in Central and Eastern Europe-Opportunity for Rethink?' *Journal of Business,* Venturing, Vol. 8: 461-486.

[4] McIntire, John (1998). "The Prospects for Agricultural Growth". In Faruqee, Rashid (ed.). "Bangladesh Agriculture in the 21th Cen tury". Dhaka University Press Ltd.

[5] Dabson, B. (2001). 'Supporting Rural Entrepreneurship', in Exploring Policy Options for a New Rural America, Kansas City, MO: Center for the Study of Rural America, Federal Reserve Bank of Kansas City, URL pp. 35–47

[6] Razzaque, A., (2003). "Market Development for Bangladesh's SMEs: An Analysis of Issues and Constraints" paper presented at the request of the Bangladesh Enterprise Institute (BEI) on December 24, 2003, Google Website, Retrieved August03, 2007 from http://www.gogle.com./

[7] Ahmed, M. U. (2004). "Promoting Busi ness and Technological Incubation for Improved Competitiveness of Small and Medium-sized Industries Through Application of Modern and Efficient Technologies in Bangladesh", Presented at General Economics Division, Planning Commission, Dhaka, Bangladesh on May 05, 2005, Google Website, Retrieved August13, 2007 from http://www.gogle.com./

[8] Bari, F. & heema, A. & Haque, E. U., (2005). "SME Development in Pakistan: Analyzing the Constraints to Growth", Pakistan Resident Mission Working Paper Series, No. 3, October.

[9] Hübner, W. (2000). 'SME Development in Countries of Central Asia (Kazakhastan, Kygyzstan and Uzbekistan): Constraints, Cultural Aspects and Role of International.

[10] Neergaard, H. (2005). 'Networking Activities in Technology-based Entrepreneurial Teams', *International Small Business Journal* 23(3): 257–8.

[11] Raynor, M. E. and Weinberg, H. S. (2004). 'Beyond Segmentation', *Marketing Management* 13(6): 22–8.

[12] Rip, A. and Kemp, R. (1998). 'Technological Change', in S. Rayner and E. L. Malone (eds) *Human Choice and Climate Change*. Columbus, OH: Battelle Press.

Proceedings of 2009 12th International Conference on Computer and Information Technology (ICCIT 2009)
21-23 December, 2009, Dhaka, Bangladesh

An Approach to Improve Collusion Set Detection Using MCL Algorithm

Md. Nazrul Islam, S. M. Rafizul Haque†, Kaji Masudul Alam‡, Md. Tarikuzzaman‡
Computer Science and Engineering Discipline, Khulna University, Bangladesh
nazrulcsebd@gmail.com, rafizulku@gmail.com†, km.alam@ku.ac.bd‡, litondb_03@yahoo.com‡

Abstract

Many malpractices in stock market trading e.g. price manipulation, circular trading, use the modus-operandi of collusion. Generally, a set of traders is a candidate collusion set when they are "trading heavily" among themselves in cross trading or circular trading. In real life not all colluders always trade with each other. In a perfectly circular collusion set of size 4, trader A will trade with B, B with C, C with D and D with A; there will be no cross trading among these traders. An existing method using shared, mutual nearest neighbor and collusion graph clustering algorithm fails to detect purely circular trading which is also a collusion set. In this paper, we have proposed a new approach to detect collusion sets using Markov Clustering Algorithm (MCL). Proposed method can detect purely circular collusions as well as cross trading collusions. We have used MCL at various strength of "residual value" to detect different cluster sets from the same stock flow graph. We have combined our collusion clusters with the existing method using Dempster Schafer theory of evidence. The experimental result shows that MCL algorithm provides better collusion clusters and the performance improved significantly.

Keywords: Collusion Cluster, *Expansion*, *Inflation*, MCL, Stochastic Matrix, Sparse Graph.

I. INTRODUCTION

It is a well known unfortunate fact that there are unscrupulous organizations and groups of individuals, which attempt to influence the activities on stock exchanges with the intention of making profits through unfair ways. Continued prevalence of such malpractices can have disastrous long term consequences for the stock exchange, investors, financial institutions, government and the economy, in general.

To facilitate fair transactions, the competent authorities keep developing various laws and guidelines to be followed by all participants in stock market activities. Enforcing the laws and guidelines requires continuous surveillance of stock market activities through analysis of the associated databases. Online surveillance systems are generally unable to detect or prevent occurrences of complex types of malpractices because they can only analyze short term trading data in the limited time.

Many different types of malpractices may happen in stock market trading such as circular trading, price manipulation, etc [1]. In price manipulation, a group of individual traders try to act together artificially to increase the price of a security by circulate a fixed number of shares in a large volume among themselves and try to achieve interest of other traders to buy these shares. When the price of these shares sufficiently increases, the traders "exit" the group and sell their original shares. Since the price is not tenable, the price crashes back to its original level or below.

We group these malpractices together in a class called collusion based malpractices as because they trade in a group to increase the price of a target security. In collusion based malpractices, the individual transactions are usually innocuous (superficially legal); the malpractice is visible only when the transactions are appropriately grouped together. Evidence for such malpractices is often hidden deep inside the trading databases. That is why surveillance of stock market databases for detecting collusion based malpractices is an important, complex and knowledge intensive task.

For detecting such type of trading collusion set Palshikar and Apte [2] proposed graph clustering algorithm which is mainly based on cross trading. If purely circular trading happens then this method fails to detect collusion. So, efficiency of the method is low.

In this paper, we have proposed a new approach using MCL algorithm which can detect both circular and cross trading collusion sets. MCL algorithm is very efficient and unsupervised. It does not require quantifying the number of candidate collusion sets or heavy trading.

In section II, we provide survey of some related works. In section III, we define collusion set, data preparation and the notion of a stock flow graph. In section IV, we discuss existing method and their limitations. In section V, we discuss our proposed method and how to apply it to detect collusion sets. Section VI provides combined results of all algorithms and brief description of how to detect evidence using Dempster Schafer theory. Section VII and VIII describes performance and accuracy analysis respectively. At last section IX provides the conclusion.

II. RELATED WORK

Most approaches to fraud detection use the supervised learning framework, where a set of training examples containing both fraudulent and normal transactions is assumed to be available. But such training set is very difficult to obtain. Hence, we have not chosen this assumption for frauds in stock market trading. Thus we need unsupervised learning algorithms that are specialized to separate normal trading from fraudulent trading. There have been a few attempts to formally characterize frauds in stock market trading.

Palshikar and Arun [1] proposed a pattern recognition based approach for surveillance, on the premise that each type of malpractice leaves a telltale trace in the trading databases, which can be approximately specified

978-1-4244-6283-4/09/$26.00 ©2009 IEEE

as a temporal pattern by investigation experts. They describe a fuzzy temporal logic notation to specify such pattern and a fuzzy temporal logic tools *SNIFFER*, which detects where and how strongly the given surveillance pattern occurs in the given temporal databases. In real life it is very difficult to specify any pattern that can be match later one. Investigative experts should be needed to characterize each type of malpractice in terms of approximation. The pattern should be dynamic in behavior, which is also a difficult task.

Rubin [3], Bapeswara and Sankara [4] proposed a procedure to determine whether Hamilton paths or circuits exist in a given graph, and will find one or all of them. A combined procedure is given for both directed and undirected graphs. The search consists of creating partial paths and making deductions which determine whether each partial path is a section of any Hamilton path. Honkanen [5] presents an algorithm for determining the circuits of a graph in a mechanical manner. How ever these procedures are computationally infeasible.

In this paper, we have proposed a method using MCL [11], [12] that is capable of detecting both circular and cross trading collusion set. We have shown that using MCL the performance of collusion set detection increases.

III. PRILIMINARIES

A. Case Study

SEBI (Securities and Exchange Board of India) [13] has published a report on its web site containing an example of collusion in the trading of the DSQ Industries. Three traders were involved in this collusion, which occurred in the period 1st January, 2001 to 8th January, 2001 (in 6 trading sessions). The three traders traded the same 10000 shares among themselves many times and raised the price of these shares 32% after seven days trading.

B. Data Pre Processing

Actual trading data contains various things; e.g., trader and client details, order details such as IDs, placement times, quantities and prices quoted in the order etc. Each record in this trading database refers to a single trading transaction. We assume that the input trading data consists of records having the following form:

Stock ID	Time stamp	Seller ID	Buyer ID	Quantity	Price	Value

We have prepared a summary of the above trading data as follows:

1. Select records for a specific stock, which fall in a specific time period.
2. Summarize the transactions between each pair of seller (trader) and buyer (trader) into a single record.

C. Stock Flow Graph

Using the summary trading database, we construct a directed edge labeled graph called the stock flow graph for a particular stock-IDs, denoted $GS = (V, E, \varphi)$, where V is the set of vertices (each vertex is labeled by a trader ID), E is the set of directed edges and φ is the function that associates a label for each edge. Label of a directed edge (u, v) is the total number of shares (total quantity) sold by u *to* v (as per the given trading summary database). A stock flow graph can have parallel edges in opposite directions but cannot have self-loops and any isolated vertices. Stock flow graph can be disconnected. Note that the user has to select the time period for which the summary database is created**.** Fig. 1 shows an example of a stock flow graph with 9 vertices and 23 edges.

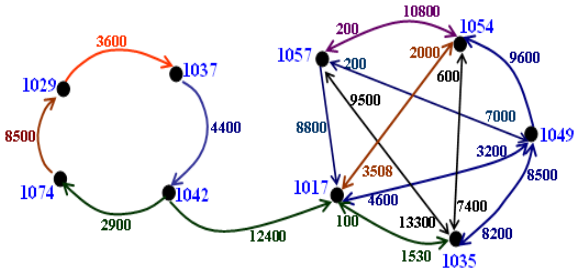

Fig.1. An example of a stock flow graph with 9 vertices and 23 edges

IV. EXISTING METHOD

The Existing Method [2] is based on graph clustering and here Shared Nearest Neighbors (*shared_NN*), Mutual Nearest Neighbor (*mutual_NN*) and Collusion Clustering (*collusion_clustering*) algorithm are used to detect collusion sets. Each algorithm of this method initially selects those vertices that have at least k number of out degrees of all vertices $kNN(u)$ compare to heavy trading with others. For k=3 using the graph of the Fig.1 the following sets of traders is found.

Table I *3NN* list for vertices in Fig. 1

1017{1035,1049,1054}	1054{1017,1035,1057}
1035{1049,1057,1054}	1057{1017,1035,1054}
1049{1017,1035,1054}	

shared_NN algorithm takes two parameters, k (number of nearest neighbor) and kt (common nearest neighbor between two clusters). When k=3 and kt= 2 then from Table I we find $3NN(1017)$ = {1035,1049,1054} and $3NN(1049)$ = {1017,1035,1054}. This algorithm then merges this two clusters on the basis that, 3NN(1017) ∩3NN(1049) >=kt and 1017∈ $3NN(1049)$ and 1049∈ $3NN(1017)$. $3NN(1017)$ and $3NN(1049)$ satisfied this two condition and merge. This process is continued until merge is possible. Complexity of this algorithm is $O(kN^2)$ where N is the number of vertices.

mutual_NN algorithm takes one parameter, k. It merges the selected cluster on the basis of average mutual neighborhood value (*mnv*). The value of *mnv* is the sum of the ranks of the two points in each other's sorted k-

NN list. Sorting is done on the basis of heavy treading between traders. Using Table I for k=3 average *mnv* between clusters {1017,1035} and {1049,1054}= average{*mnv*{(1017,1049), (1017,1054), (1035,1049), (1035,1054)}} = average{ {(2+1),(3+1), (1+2), (3+2)} = 15/4 = 3.75. In this way it merges two clusters which have minimum *mnv* among all pairs of clusters and so on. Complexity of this algorithm is $O(kN^2)$.

collusin_clustering algorithm takes three parameters, k, m, h. If C and D are two clusters, then m is the number of times C in D and D in C and h is the number of common points between C and D at percentage (%). This algorithm at first calculates the collusion level, $L(C)$= internal trading of a cluster, $I(C)$/external trading, $E(C)$ and sorted all selected cluster in descending order accordingly $L(C)$. Then it merges first two ordered cluster if they are (*k, m, h)* compatible and then second two clusters and so on. When k=3, m=1, h=0.6, 1017 and 1049 (from Table I) are (k, m, h) compatible. Because 1017 and 1049 are both is in their cluster one time and common points are 2 and so they are merged. Complexity of this algorithm is $O(kN^3)$.

A. Limitation of the Existing Method:

Definition: Informally, a graph with relatively few edges is sparse, and a graph with many edges is dense [14]. Consider, a graph G= (V,E) with N nodes. A graph is sparse when E= Θ ($|V|$) and it is dense when E= Θ ($|V|^2$). If the out-degree of each vertex in G some fixed constant then it is a sparse graph, because $|E| = k|V| = \Theta(|V|)$. If the out-degree of each vertex in G some fraction f on N, $0< f \leq N$ (e.g. if N =16, f =0.25 then out-degree = 4) then it is dense graph, because $|E| = f|V^2| = \Theta(|V|^2)$.

From above discussion we see that each of the algorithm first select those vertices that have at least k number of out degrees and other vertices are discarded. All the three algorithms have the property that, $k\geq 2$ at least. From the definition we can see that, only dense graph have the property that, $k \geq N*f$. In a purely circular graph out-degree (k) is not ≥ 1. So, purely circular graph is a sparse graph. Thus, the Existing Method cannot detect purely circular collusion sets and so the number of detection rate is low.

To overcome this problem and increasing the detection performance we proposed a new approach using MCL algorithm that can work on both dense and sparse graphs.

V. PROPOSED METHOD

This paper uses Markov Clustering Algorithm (MCL) to detect collusion clusters. The algorithm starts by creating a Markov matrix from the stock flow graph. Markov matrix is an adjacency matrix that is normalized to one [11]. Elements in a column / node can be interpreted as decision probabilities of a random walker being at that node. Then adjacency matrix is added diagonal elements to include, self loops for all nodes, i.e., probabilities that the random walker stays at a particular node.

After this initialization, the algorithm works by alternating two operations named *expansion* and *inflation* and iteratively recomputed the set of transition probabilities. The *expansion* step corresponds to matrix multiplication (on stochastic matrix); the *inflation* step corresponds with a parameterized *inflation* operator *Hadamard power r*, which acts column wise on (column) stochastic matrix.

The *inflation* operator transforms a stochastic matrix into another one by raising each element to a positive power r and renormalizing columns to keep the matrix stochastic. The effect is that larger probabilities in each column are emphasized and smaller ones deemphasized. On the other side, the matrix multiplication in the *expansion* step creates new nonzero elements, i.e., edges. The algorithm converges very fast, and the result is an idempotent Markov matrix, $M = M \times M$, which represents a hard clustering of the graph into components. *Expansion* and *inflation* have two opposing effects. While *expansion* flattens the stochastic distributions in the columns and thus causes paths of a random walker to become more evenly spread, *inflation* contracts them to favored paths.

A straightforward implementation of MCL will have time and space complexity respectively $O(N^3)$ and $O(N^2)$, where N is the number of nodes of the input graph. We have used MCL in prune mode and in every iteration if K number of values are alive and rest of the probability values becomes zero then the time and space complexity is reduced to $O(N^2 \log(K))$ and $O(N*K)$ respectively. But these are worst case estimation, in section VII we have showed the actual running times that given MCL is very efficient.

After running the algorithm we find an idempotent matrix. The diagonal vertices are considered as circular trading cluster and other are cross trading cluster.

From Fig.1 if we consider four vertices 1017, 1035, 1049 and 1054 then we have found the weighted matrix which is given in Table II. After this we have converted it to a column stochastic matrix is as, $M_{ij}= M_{ij}/\Sigma M_{ij}$.

Table II Weighted Matrix of 1017, 1035, 1049, 1054

	1017	1035	1049	1054
1017	0	1530	3200	2000
1035	100	0	8500	600
1049	4600	8200	0	9600
1054	3508	7400	0	0

Table III Stochastic Matrix of Table II

	1017	1035	1049	1054
1017	0	0.08932	0.27350	0.16393
1035	0.01218	0	0.72649	0.04918
1049	0.56043	0.47869	0	0.78688
1054	0.42738	0.43199	0	0

Then run the MCL algorithm for above stochastic matrix set the parameters r= 2, *maxResidual* = 0.01, *zeroMax* = 0.1 and finally find collusion cluster, {1017, 1035, 1049, 1054}.

If we run the MCL algorithm to use the graph of Fig.1 and set the parameters r = 2, *maxResidual* = 0.01, *zeroMax* = 0.01 then the results are as follows: (1029, 1037, 1042, 1074) and (1049, 1054, 1035, 1017, 1057). Thus from above experiment we can see that MCL can detect circular cluster and also cross trading cluster.

algorithm *MCL*
input stochastic matrix ($M \times M$)
input *Hadamard power r, maxResidual, zeroMax*
output collusion cluster of set of vertices

G is a graph // Directed Graph
add loops to *G* // Create a Weighted Matrix
set Γ to some value // Stochastic Matrix
set $M = \Gamma$ to be the matrix of random walks on *G*
//Check whether the Matrix is in idempotent stage
while(*residual* > *maxResidual*)
$M_1 = M \times M$ //expand by multiplying $m * m$
$M = M_1 \times\hat{}\ r$ // inflate by Hadamard potentiation
//Search value from *M* and replace it with zero if
// it is < zeroMax
Prune(*find*(*M*) < *zeroMax*)
$M_{ij} = M_{ij} / \Sigma M_{ij}$ // column re-normalization
maxs = Max(*M*) // Find max value from all M_{ij}
sqsums = sum($M \times\hat{}\ 2$) //take the square sum of Matrix
residual = *maxs* - *sqsums* //difference between *M*, M_1
end while

From the above algorithm we can see that if the value of *maxResidual* is high then the numbers of clusters are increasing for fixed value of r and *zeroMax*. Again when *zeroMax* is increases for fixed value of *maxResidual* then number of cluster is decreasing.

VI. COMBINING THE RESULTS

To combine the results of the four algorithms we have used Dempster Schafer theory which is based on Rich and Knight [9], [10]. Dempster Schafer theory has two parameters [*Bel* , *Pl*], where *Bel* measures the strength of evidence in favor of statement s and *Pl* is the plausibility which measures the extent to which evidence in favor of $\neg s$ leave room for belief in s. *Bel* = 0 or 1 and *Pl(s)* = 1 − *Bel*($\neg s$).

Let Θ, the frame of discernment; denote the set of all possible hypotheses. If T = {1017, 1029, 1035, 1037, 1042, 1049, 1054, 1057, 1074} is the set of nine traders, then Θ contains all possible subsets of T and so Θ contains 2^9 elements, where each element of Θ can be a candidate collusion set.

Let X and Y are two subset of Θ to which m_1 and m_2 assigns a nonzero value respectively. The new belief function m_3 after combination m_1 and m_2 is defined as:

$$m_3(z) = \frac{\sum_{X \cap Y = Z} m_1(X) \times m_2(Y)}{1 - \sum_{X \cap Y = \phi} m_1(X) \times m_2(Y)}$$

Let collusion coefficient $\gamma(C)=\omega(\hat{H}_{G(C)})/I(C)$, where C is a given set of traders of a graph G, $\omega(\hat{H}_{G(C)})$ denoted the largest weight ($\hat{H}_G$) among weights of all Hamiltonian circuits in G and $I(C)$ is the internal trading of C. If G is not Hamiltonian then let Γ denote the set of all Hamiltonian circuits of maximum size among all sub graphs of $G(C)$. If $\tau = \phi$ then the collusion coefficient $\gamma(C)$=0, otherwise, $\gamma(C) = \omega(\Gamma)/ I(C)$.

Let G (1017, 1035, 1054, 1049) denotes the stock flow graph in Fig.1; G is Hamiltonian and it is largest all other circuit in G. So, ω(1017, 1035, 1054, 1049) = 4,600 and $\gamma(C)$ = 4,600/ 49238 = 0.09342.

Suppose from *mutual_NN* algorithm for k =3 in Fig.1 getting the candidate collusion set A = {1017, 1035, 1049, 1054}. The collusion coefficient $\gamma(A)$ as a measure of belief that A is a collusion set. This results in an update of m_1 as follows, {1017, 1035, 1049, 1054} (0.09342), {Θ} (0.90658).

Suppose from *collusion_clustering* algorithm with k = 3, m = 1, = 0.60, getting the candidate collusion set {1049, 1057, 1054}. This results in a new m_2 function: {1049, 1057, 1054} (0.007194), {Θ} (0.9928) the belief function m_3 that combines the results of both these experiments (e.g., m_1 and m_2), according to the Dempster Schafer rule of combination, is as follows,

Table IV Detecting evidence using Dempster theory

	{1049, 1057, 1054} (0.007194)	{Θ}(0.996)
{1017, 1035, 1049, 1054} (0.09342)	{1049, 1054} (0.0006721)	{1017, 1035, 1049, 1054} (0.09305)
{Θ} (0.90658)	{1049, 1057, 1054} (0.00652)	{Θ}(0.90295)

In this way successively we have revised the belief function after each experiment and obtain the final belief function m at the end of the experiment.

Table V The final belief function for Table VI

(0.154836), ϕ	0.000567, {1017, 1054}	0.124254, {1017, 1035, 1049, 1054}
0.000699, {1054}	0.001658, {1017, 1054, 1057}	0.039584, {1017, 1049, 1054, 1057}
0.016686, {1049, 1054}	0.002919, {1049, 1054, 1057}	0.044716, {1017, 1035, 1049, 1054, 1057}
0.005615, {1035, 1054}	0.005204, {1017, 1035, 1054}	0.121814, {1029, 1037, 1042, 1074}
0.134067, {1035, 1049, 1054}	0.013541, {1017, 1049, 1054}	0.473340, {1017, 1029, 1035, 1037, 1042,
0.000122, {1054, 1057}	0.015213, {1017, 1035, 1054, 1057}	1049, 1054, 1057, 1074}

Table VI Candidate collusion sets identified in different experiments for the graph in Fig. 1

Algorithm	Parameters	Collusion Set, *C*	$\omega(\hat{H}_G)$	$I(C)$	$\gamma(C)$
shared_NN	k=4, kt=2.5	1035,1049,1054,1057,1017	3200	99038	0.03231
	k=3, kt=2	1017,1035,1049,1054,1057	3200	99038	0.03231
		1017,1035,1049,1054	4600	49238	0.09342
mutual_NN	k =2	1035,1049,1054,1057	7400	75300	0.09827
		1042,1017	$\tau = \varnothing$	12400	0
	k=3	1017,1035,1049,1054	4600	49238	0.09342
collusion_ clustering	k=3, m=1, h=0.6	1017,1035,1049,1054	4600	49238	0.09342
		1017,1035, 1054,1057	2000	49738	0.0402
		1049,1057,1054	200	27800	0.007194
	k=4, m=1 ,h=0.70	1017,1035,1049,1054,1057	3200	99038	0.03231
MCL	maxResidual=0.1, zeroMax =0.01, r=2	1029,1037,1042,1074	2900	19400	0.1495
		1042,1017	$\tau = \varnothing$	12400	0
		1054,1049,1035	7400	34300	0.2157
	maxResidual=0.01, zeroMax =0.01, r=2	1029,1037,1042,1074	2900	19400	0.1495
		1017,1035,1049,1054,1057	3200	99038	0.03231

Bel(p), is defined as the sum of the values of the belief function *m* for *p*(set of hypothesis) and for all its subsets. Using Table V we have obtained that,
Bel {1017, 1049, 1054, 1057} = 0.36012,
Bel{1017, 1035, 1049, 1054} = 0.320536 and
Bel{1017,1035,1049,1054,1057} = 0.404836
These collusion sets include all other collusion set except {1029, 1037, 1042, 1074} but this collusion set have a higher belief value except other. So, we can summarize that {1017, 1035, 1049, 1054, 1057} and {1029, 1037, 1042, 1074} are the candidate collusion sets.

VII. PERFORMANCE ANALYSIS

Fig.2 shows the performance of the existing method and MCL algorithm on synthetic trading data. We randomly generate stock flow graph, on the basis of following rules:
1. N (no. of vertices): from 100 to 1,000 in steps of 100.
2. μ_d (the average degree for the vertices): $0.15 * N$
3. μ_v (average volume (edge label) for the edges): 1000.
We assumed that the degrees and volume of the vertices are distributed exponentially around the given average degree μ_d and μ_v, with the additional restriction that degree of each vertex has to be $\leq (N-1)$. We used the following parameters for each of the algorithms:

MCL	shared_ NN	mutual_ NN	collusion_ clustering
r = 2, maxResidual = .01, zeroMax = 0.01	k = 4, kt = 2	k = 4	k = 4, m = 1, h = 0.70

For MCL when the number of vertices greater than 100 then we have broken the vertex into 100x100 matrix and run the MCL for each matrix. Each time we have run MCL and taken the Time (seconds) needed to detect collusion cluster.

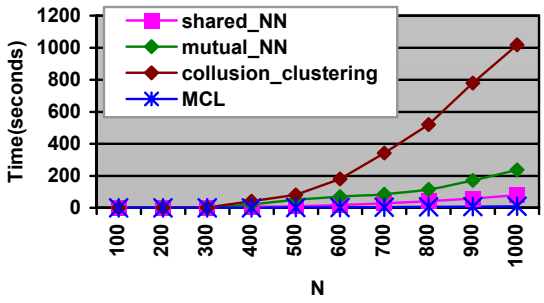

Fig. 2. Performance of existing method and MCL

For each value of *N*, we generated the stock flow graph 10 times, and averaged the running time of each algorithm over these 10 runs. From Fig. 2 we see that MCL algorithm performs almost linearly compared to others.

VIII. ACCURACY OF COLLUSION SET DETECTION

In the second experiment, we attempted to validate the accuracy of the existing method and MCL algorithms in detecting known collusion sets. For this purpose, we followed the same procedure as above for generating synthetic data. In addition, we induced one collusion set of known size *C* in the synthetic data. For cross trading collusion set (containing *C* traders) we selected *C* vertices and introduced $C*(C-1)$ edges between every pair of them and for circular trading we induced a purely circular collusion set of size *C* and volume of each edge are exponentially distributed with mean = $30*\mu_v$. Thus the collusion set had substantially larger trading within itself, as compared with its trading with others. In our experiments, we varied the size *C* of the induced collusion set from 3 to 10. For *shared_NN*, *k* = $2*C$ and *kt* =2 and for *mutual_NN*, *k* = $2*C$ and for

collusion_clustering, $k = 2 * C$, m = 1 and h = 0.7 was set. For MCL we set r = 2, *maxResidual* = 0.01, *zeroMax* = 0.01 and taking 100x100 synthetic trading data. For each value of C, we generated the stock flow graph and induced a collusion set of size C and tested whether each graph clustering algorithm was able to detect the induced collusion set (in a single cluster) or not (see Table VII). Following table gives, for a specific value of C, the number of times out of 10, the algorithm detected the collusion set.

Table VII Accuracy of existing method and MCL algorithm on inducing cross and pure circular trading

C	shared_NN		mutual_NN		collusion_ clustering		MCL	
	cross	Circular	cross	circular	cross	circular	cross	circular
3	2	0	10	0	10	0	10	10
4	4	0	10	0	10	0	10	10
5	7	0	10	0	10	0	10	10
6	9	0	10	0	10	0	10	10
7	10	0	10	0	10	0	10	10
8	10	0	10	0	10	0	10	10
9	10	0	10	0	10	0	10	10
10	10	0	10	0	10	0	10	10

The accuracy of *shared_NN* algorithm is 100% when $C \geq 7$ and *mutual_NN* and *collusion_clustering* are always 100% for all values of C in case of cross trading. But these three algorithms always fail to detect pure circular cluster. But, the accuracy of MCL algorithm is always 100% for all values of C and for both cross and circular trading. So, the efficiency of MCL algorithm of collusion set detection is higher than Existing Method.

IX. CONCLUSION

In this paper, we stated and formalized the important practical problem of detection of collusions among the traders in stock market. The Existing Method performs well for detecting cross trading but it cannot detect purely circular trading. We proposed here an approach using MCL algorithm that can detect both purely circular trading as well as cross trading collusions. We have applied Dempster Schafer theory of evidence to combine candidate collusion sets detected by existing algorithms and MCL algorithm. We have also used randomization to validate the accuracy of collusion set detection. The idea formalizes our intuitive understanding that more the experiments that report a trader as part of a candidate collusion set, more is our belief that he is indeed likely to be a colluder. From the experimental results we find that collusion clusters provided by MCL algorithm gets higher evidence. Performance and accuracy analysis of our proposed and existing methods conclude that MCL algorithm offers better efficiency than existing method.

REFERENCES

[1] G. K. Palshikar, Arun Bahulkar, *Fuzzy temporal patterns for analyzing stock market databases*, in Proc. Int. Conference on Advances in Data Management (COMAD-2000),2000,Pune, India, Tata-McGraw Hill,pp.135-142.

[2] Girish Keshav Palshikar, Manoj M. Apte *Collusion set detection using graph clustering*, Journal of the ACM, Volume 16, Issue 2, Pages: 135 - 164, April 2008.

[3] Frank Rubin *A Search Procedure for Hamilton Paths and Circuits*, Journal of the ACM, Volume 21, Issue 4, Pages: 576 - 580, October 1974.

[4] V. V. Bapeswara Rao and K. Sankara Rao, *Enumeration of Hamiltonian Circuits in Digraphs*, Proc. IEEE, vol. 73, pp. 1524-1525, Oct. 1985.

[5] P. A. Honkanen, *Circuit enumeration in an undirected graph*, Proc. 16th ACM Southeast Regional Conference, pp. 49 – 53, 1978.

[6] R. A. Jarvis, E. A. Patrick, *Clustering using a similarity measure based on shared nearest neighbors*, IEEE Transactions on Computers, Vol. C-22, No. 11, November 1973.

[7] K. C. Gowda, G. Krishna, *Agglomerative clustering using the concept of mutual nearest neighborhood*, Pattern Recognition, Vol. 10, pp.105-112, 1978.

[8] A.K. Jain, M.N. Murty, P.J. Flynn, *Data clustering: a review*, ACM Computing Surveys, vol. 31, no. 3, Sep. 1999, pp. 264-323.

[9] S. Le Hegarat-Mascle, D. Richard, C. Ottle, *Multi-scale data fusion using Dempster-Shafer evidence theory*, Integrated Computer-Aided Engineering, 10 (2003), pp. 9–22.

[10] G. Shafer, *A mathematical theory of evidence*, Princeton University Press, 1976

[11] Van Dongen, *Graph Clustering by Flow Simulation*. PhD thesis, University of Utrecht (2000). http://www.library.uu.nl/digiarchief/dip/diss/1895620/inhoud.htm

[12] Stijn van Dongen. *A cluster algorithm for graphs*. Technical Report INS-R0010, National Research Institute for Mathematics and Computer Science in the Netherlands, Amsterdam, May 2000. http://www.cwi.nl/ftp/CWIreports/INS/INS-R0010.ps.Z.

[13] http://www.sebi.gov.in, SEBI Order against DSQ Holdings dated 10th December 2004. Order no.CO/109/ISD/12/2004

[14] Bruno R. Preiss, *Data Structures and Algorithms with Object-Oriented Design Patterns in Java*, John Wiley & Sons, 1999.

Proceedings of 2009 12th International Conference on Computer and Information Technology (ICCIT 2009)
21-23 December, 2009, Dhaka, Bangladesh

Young Consumers' M-banking Choice in Urban Bangladesh: Preliminary Indication

Saifullah M Dewan, Ahsanullah M Dewan†
Integrated Solutions Ltd, Dhaka, Bangladesh
† Graduate School of Business, Curtin University of Technology, Perth, Australia.
s.dewan@isl.com.bd, a.dewan@postgrad.curtin.edu.au

Abstract

With banking channels changing rapidly and multi-channeling becoming increasingly widespread, there is a need to understand consumers' choice of channel and the banking tasks for the channel. Using the example of banking services in urban Bangladesh, where multi-channeling is expected to become a norm, this research reports on an initial study comparing young consumers' choice of banking channels. Based on the results of a survey among 500 young adults between 18 and 30 years of age in Dhaka city, this study finds that although majority of the respondents did not use mobile banking (m-banking), most of them are interested to do banking on mobile phones. They are interested to do a range of banking related tasks on mobile phones if services are made available. Clearly young consumers in urban Bangladesh are in favour of m-banking and thus, m-banking has a chance to be a success story in Bangladesh.

Keywords: Consumers' choice, m-banking, technology acceptance, Bangladesh.

I. INTRODUCTION

In an increasingly competitive banking sector, m-banking can be seen as an attempt to provide the needed added value for consumers by offering more opportunities for conducting different banking tasks [1]. M-banking is defined as a channel whereby the consumer interacts with a bank via a mobile device, such as a mobile phone [2-3]. In its simplest form, m-banking enables consumers to receive information about account balances via SMS [4]. Today m-banking services enable consumers in many countries, for example, to request their account balance and the latest transactions in their accounts, to transfer funds between accounts, to trade stocks, to send / receive remittance and to receive portfolio and price information. In that sense, electronic banking (e-banking) can be seen as a concept covering all the electronic modes of conducting banking tasks, and m-banking as a subset of e-banking [1, 5]. In the presence of mobile and electronic trends, there is a growing need to understand consumers' choice of electronic channels and the tasks for which one channel may be chosen ahead of another (m vs. i) [6]. According to Motorola (2008), more than 80 percent of the world's population already lives in an area covered by the wireless networks (CNNMoney.com). There are an estimated 1.5 billion cell phones now in use in the developing world. That figure will grow to at least 3 billion over the next five years. Therefore, further empirical work is needed to enhance understanding of consumers' choice among channels, particularly between two electronic banking channels (m-banking and i-banking) and tasks for relatively new mobile channel. This study is one of the first few studies to include choice among tasks using alternative and complementary banking channels, rather than limiting it to a single behavior.

II. M-BANKING SERVICES IN BANGLADESH

Developing countries, for example Bangladesh, where the penetration rate of mobile phones is high and the penetration of internet is low, provision of innovative mobile services, such as m-banking, may be the way to go. In countries like Australia, UK and US, m-banking has not been widely adopted yet despite high penetration of computer, internet and mobile phones. However, in Japan and Korea applications on both mobile and internet channels are popular. There are suggestions that m-banking is likely to be successful in both developed and developing countries because consumers want convenience and they want banking services to be as ubiquitous as possible [7]. However, m-banking is likely to be more successful in developing countries, for example in Bangladesh, where mobile phone penetration rate is high and alternative / complementary channels are not always or easily accessible. Already, the number of mobile subscribers in Bangladesh has crossed 40 million in June 2008 [8]. The number of mobile subscribers per 100 population reached 20 in 2007 from 0.2 per 100 population in 2000 which makes mobile phone growth rate one of the highest in the world [9]. At the same time, the number of fixed phone line has increased from 0.4 per to 0.8 only per 100 population. The mobile phone as a share of total phone lines per 100 population has increased from 36.2 in 2000 to 94.4 in 2006 [9]. It appears that the rapid development of mobile phone networks in Bangladesh has stifled the expansion of fixed-line systems.

The adoption of internet by consumers in Bangladesh is extremely slow despite being introduced earlier than mobile phones. The number of internet users per 100 population has increased to only 0.3 in 2006 from few thousands in 1999. While lack of infrastructure is a ma-

978-1-4244-6283-4/09/$26.00 ©2009 IEEE

jor issue for internet banking success, there is an already established mobile phone network which is a prerequisite for the success of mobile applications. So, Wireless Application Protocol (WAP) services, such as m–banking has the potential to succeed in Bangladesh.

Several m-banking and related services already exist in Bangladesh, though in a limited scale, such as credit transfer from one mobile account to another, pay utility bills, purchase products and services from stores having affiliation with mobile phone companies and mobile phone based market (for example CellBazaar). Some of these are described below.

SMS Banking allows checking account balance, recent transaction details, credit card details etc through SMS. AKTEL, for example, a mobile phone operator in Bangladesh, has partnered with banks, namely BRAC Bank and Standard Chartered Bank to offer this banking service to their subscribers.

CellBazaar is Grameenphone's, country's largest mobile phone operator to date, exclusive provider of community-based, user-generated product and service market on the mobile phone. It is an electronic marketplace (similar to eBay) that enables buyers and sellers to be in contact. It works on four synchronized platforms – SMS (texting), WAP, internet and IVR (interactive voice response) which allows users call to hear the latest news [10]. The system at this stage does not handle transactions.

Balance Transfer allows both pre-paid and post-paid subscribers to transfer balance for cell phone to any account.

Table I Operators and subscribers

Operator	**Subscribers (millions)**
Grameen Phone Ltd. (GP)	20.31
Orascom Telecom Bangladesh (Banglalink)	9.46
TMIB (Aktel)	7.85
Warid Telecom International L.L.C (Warid)	3.31
PBTL (Citycell)	1.70
Teletalk Bangladesh Ltd.	1.07
Total	43.70

Source: Bangladesh Telecommunication Regulatory Commission Website, 2008

Mobile phone operators offer premium and discount services. GrameenPhone's offer is called *thankyou Crown* and Aktel's offer is called *Club Magnate*. It allows loyal customers to receive discount for purchasing products and services from selected partner stores, hotels, restaurants and hospitals both at home and abroad. It makes use of mobile phone to verify and receive instant discounts and top up credits in subscriber's account.

In summary, mobile phone has the potential to become a remote control to every consumer for his or her banking needs. There are six mobile phone operators in Bangladesh. The operator names and the number of subscribers are listed in table I.

III. PREVIOUS RESEARCH

This section presents a summary of previous research to provide a preliminary understanding of consumer choice in relation to banking channels and banking tasks.

A. CONSUMERS' CHOICE

For many years, adoption models such as Fishbein and Ajzen (1975)'s Theory of Reasoned Action (TRA), Ajzen (1991)'s Theory of Planned Behavior (TPB) and Davis (1989)'s Technology Acceptance Model (TAM) have been widely used to predict a single application usage in which no alternative or complement is observed [11-15]. Researchers have long recognized that the accuracy of predicting behavior with the presence of alternatives is higher than without them [16]. Very few researchers have examined the usage of a technology with its alternatives [17-20]. Lin et al. (2006) applied TPB for predicting the choice of one of the two instant messaging technologies [17]. Szajna (1994) applied TAM for predicting the selection of different database technologies [18] and Chan et al. (2004) used TAM for predicting the usage of different browsers [19]. Dabholkar (1994) applied the TRA to evaluate the choice between using touch-screen technology menu orders and normal orders [20]. Barely any researchers studied these theories in the context of choice. Thus, adding the dimension of choice in traditional adoption model is necessary [18], particularly in the context of multi-channel banking environment where consumers can choose from a number of channels.

Multi-channeling in consumer banking is becoming a norm and the reliance on a single channel is likely to be the exception rather than the rule in future. While conventional forms of banking in branch and on ATM machine will continue for the foreseeable future, the consolidation of channels such as mobile phone and internet on personal computers would suggest that for many consumers, the traditional channels may cease to be the outlet of first choice. A common assumption that is made in many writings that the choice of channel can be seen in the same conceptual framework as choice of product [21]. While this position might be a useful starting point, and while consumer choice models may provide useful insights, they do not readily deal with task-channel interactions in which type of banking tasks affect the channel considered [21-22]. Accordingly, there is case for further research to consider the choice among banking channels [21, 23-24].

Few acceptance studies considered the effects of rival

products when they examined the acceptance of a specific product [17]. For instance, a study that examines respondents' usage of the Internet Explorer browser may inadvertently cause the respondents to also consider its rivals, Mozilla or Firefox. Subsequently, when answering the questionnaire regarding the intention to choose Internet Explorer, the respondents may compare their evaluations with other alternatives. Therefore, measuring user intention of a specific product alone may yield an incomplete picture. Researchers in the field of psychology and marketing have widely recognized this issue [17]. However, barely any study in adoption literature of Information Systems (IS) examined this issue. Moreover, given that there are similar products for many different product ranges such as operating systems (e.g. Linux, MacOS, and Microsoft Windows), office software packages (e.g. Microsoft Office, IBM SmartSuite, and StarOffice), and graphics software (e.g. Photoshop, Corel Draw), additional research that examines more than one similar application is important.

Degeratu et al. (2000) conceptualized how different store environments (online and traditional stores) can differentially affect consumer choices [25]. In the first stage choice model, they used a binary probit model of store choice (online vs. offline), with utility for shopping online vs. offline being a function of household income. In the second stage, they used a multinomial logit model of brand choice with observed and unobserved heterogeneity. They claimed the errors from the binary probit model are likely to be correlated with the unobserved heterogeneity in price sensitivity (i.e., heterogeneity not induced by differences in observed characteristics, such as income) during brand choice. Xin et al. (2007) identified several demographic features with significant effects on the choice of service alternatives through a multinomial logit model [26].

B. CHOICE OF CHANNEL

Very few studies addressed the issue of young consumers' channel choice in relation to banking channels. Moreover, barely any research attempted to explicitly consider variations in consumer preferences across banking channels. Consumer choice has been typically investigated in relation to store choice [27-28]. The majority of research relating to new channels has focused on issues to do with adoption of new channels. Telephone and internet have tended to dominate this area of research. Eastlick and Liu (1997) researched television shopping and its attributes relative to other distribution channels [29]. Gehrt and Yale (1996) studied decision choice to shop via catalogue [30]. Liang and Huang (1998) developed a transactions cost based model to explore the extent to which internet would be acceptable as a distribution channel for a set of products which included books, shoes, toothpaste, microwaves and flowers [31].

Early channel adoption literature in financial services marketing focused on ATMs [32-33] and then there was a shift in interest towards telephone banking [34] and electronic banking in general [35]. Recent studies focused on internet banking [36-38] and studies on m-banking have also started to emerge [1, 6]. Albesa (2007) investigated consumer channel preferences and the motives that induce consumers to use a particular channel [39]. However, Albesa (2007)'s research focused on counter, ATM and internet but did not include mobile phone channel [39]. Albesa (2007) stated that it is not enough simply to have the necessary technology i.e. hardware, software and telecommunications and companies must investigate consumer channel preferences [39].

C. CHOICE OF BANKING TASK

To a large degree, the assumption is that choice of banking channel is generally a logical corollary of choice of banking tasks. Fang et al. (2006) extended TAM [14] to the mobile commerce context and identified three categories of tasks for wireless handheld devices: a) general tasks that do not involve transactions and gaming, b) gaming tasks, and c) transactional tasks. The survey respondents ranked and rated their future intention to perform each task on a wireless handheld device. Fang et al. (2006) selected five transactional tasks, such as purchasing movie tickets, banking online, purchasing books, purchasing clothes, and trading stocks [40]. Lee et al. (2007) studied the suitability of three insurance tasks: recruiting new contracts, post-contract customer services and tax and legal information services for the Personal Digital Assistant (PDA) [41]. This study identified ten banking related tasks for mobile phones: 1) enquire balance, 2) request statement, 3) receive alert, 4) find branch or ATM location, 5) transfer fund 6) pay utility bills, 7) trade stocks, 8) purchase phone card, 9) send / receive remittance and 10) receive credit card alert (see table III).

IV. RESULTS

A paper-based questionnaire was used in the survey. A convenience sample of young urban mobile phone users between 18 and 30 years of age in Bangladesh was used. The survey was conducted to gain a preliminary understanding of banking choice of young and educated urban population. The survey was conducted among students and their friends in a private university environment in Bangladesh. In the end, 500 responses were used and the profile of the respondents is summarized below.

- Over two thirds (68%) of the respondents were males.
- More than 90% of respondents had HSC or higher degree awarded.

- Over two thirds (72%) of the respondents earned tk. 5,000 or less per month.
- Nearly 19% of respondents used mobile banking. Over 76% never used mobile banking and over 5% were unsure if they used mobile banking.
- Nearly 60% of respondents will use mobile banking. Nearly 22% will not use mobile banking and the rest (about 19%) are still undecided.

Table II Comparison of channel choice

Channel	Most preferred
Mobile Phone	29.1%
Bank Branch	27.4%
ATM	23.6%
Internet	13.8%
Phone	6.0%

The study found that among young consumers, mobile phone is the most preferred banking channel, followed by traditional branch (see table II). Currently, consumers use mobile phones the most to make and receive calls and the least for banking (see fig. 1). One of the reasons for least current use of m-banking could be it is still in its initial adoption stage in Bangladesh. However, nearly half of the respondents are willing to do a range of m-banking tasks on their mobile phones (see table III) and their preference (most preferred) to do banking on mobile phones is strong compared to doing the same on internet. The reason may be mobile phone is more ubiquitous compared to computers and provides easy access to banking services [42] and young tech-savvy consumers are excited about 'new' self-service technology.

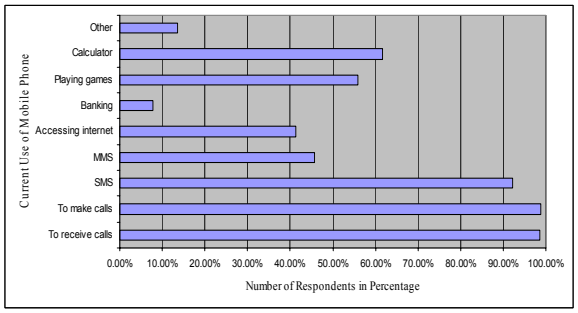

Fig. 1. Consumers' current use of Mobile Phones.

Table III Comparison of mobile vs. internet as most preferred channel for banking (percentage of respondents)

Task	Mobile Phone	Internet
Enquire balance	45.57%	13.53%
Find branch/ATM location	45.25%	17.71%
Purchase phone card	44.93%	11.92%
Receive credit card alert	43.80%	14.98%
Request statement	42.42%	12.24%
Receive alert	41.71%	17.39%
Trade stocks	37.58%	23.19%
Transfer fund	36.39%	15.94%
Pay utility bills	36.39%	13.71%
Send/receive remittance	33.33%	14.01%

V. CONCLUSION

Banks need to continue to produce more advanced personal electronic services in order to survive. Such a strategy must, however, go hand in hand with efforts to focus on the consumer and differentiate service delivery strategies on the basis of identified and recognized consumer motives. Banks need to be much smarter in assessing their consumers' motives to choose certain services for certain channels, particularly the banking tasks which the consumers deem suitable to do on mobile phones. It follows then that research efforts towards unearthing the consumers' choice motives should receive more attention in the banking sector. This preliminary study found that young consumers in Bangladesh are likely to choose m-banking. But further research needs to be done for other demographics. Also, future research can be done to understand the factors that influence consumers' choice of banking channels.

REFERENCES

[1] Laukkanen, T., et al., *Segmenting bank customers by resistance to mobile banking.* International Journal of Mobile Communications, 2008. 6(3): p. 309-320.

[2] Barnes, S.J. and B. Corbitt, *Mobile banking: concept and potential.* International Journal of Mobile Communications, 2003. 1(3): p. 273-288.

[3] Scornavacca Jr, E. and S.J. Barnes, *M-banking services in Japan: a strategic perspective.* International Journal of Mobile Communications, 2004. 2(1): p. 51-66.

[4] Mallat, N., M. Rossi, and V.K. Tuunainen, *Mobile banking services.* Communications of the ACM, 2004. 47(5): p. 42-46.

[5] Suoranta, M. and M. Mattila, *Mobile banking and consumer behaviour:New insights into the diffusion pattern.* Journal of Financial Services Marketing, 2004. 8(4): p. 354-366.

[6] Laukkanen, T., *Internet vs mobile banking: comparing customer value perceptions.* Business Process Management Journal, 2007. 13(6): p. 788-797.

[7] Yoon, C. and S. Kim, *Convenience and TAM in a ubiquitous computing environment: The case of wireless LAN.* Electronic Commerce Research and Applications, 2007. 6(1): p. 102-112.

[8] BTRC, *Country Paper on Information Society Statistics: Core ICT Indicators.* Bangladesh Telecommunication Regulatory Commission, 2008.

[9] BTRC, *Country Paper on Information Society Statistics: Core ICT Indicators*. Bangladesh Telecommunication Regulatory Commission, 2007.
[10]Quadir, K. and N. Mohaiemen, *CellBazaar: A market in your pocket*, in *Innovations / Mobile World Congress*. 2009.
[11]Fishbein, M. and I. Ajzen, *Belief, attitude, intention, and behavior: an introduction to theory and research*. 1975.
[12]Thompson, R.L., C.A. Higgins, and J.M. Howell, *Personal Computing: Toward a Conceptual Model of Utilization*. MIS Quarterly, 1991. 15(1): p. 125-143.
[13]Ajzen, I., *The theory of planned behavior*. Organizational Behavior and Human Decision Processes, 1991. 50(2): p. 179-211.
[14]Davis, F.D., *Perceived Usefulness, Perceived Ease of Use, and User Acceptance of Information Technology*. MIS Quarterly, 1989. 13(3): p. 319-340.
[15]Davis, F.D., R.P. Bagozzi, and P.R. Warshaw, *User Acceptance of Computer Technology: A Comparison of Two Theoretical Models*. Management Science, 1989. 35(8): p. 982-1003.
[16]Sheppard, B.H., J. Hartwick, and P.R. Warshaw, *The Theory of Reasoned Action: A Meta-Analysis of Past Research with Recommendations for Modifications and Future Research*. The Journal of Consumer Research, 1988. 15(3): p. 325-343.
[17]Lin, J., H.C. Chan, and K.K. Wei, *Understanding Competing Application Usage With the Theory of Planned Behavior*. Journal of the American Society for Information Science and Technology 2006. 57(10): p. 1338-1349.
[18]Szajna, B., *Software Evaluation and Choice: Predictive Validation of the Technology Acceptance Instrument*. MIS Quarterly, 1994. 18(3): p. 319-324.
[19]Chan, H.C., et al., *The Technology Acceptance Model for Competitive Software Products*. Proceedings of the Eighth Pacific Asia Conference on Information Systems, 2004: p. 1848–1855.
[20]Dabholkar, P.A., *Incorporating choice into an attitudinal framework: Analyzing models of mental comparison processes*. Journal of Consumer Research, 1994. 21(1): p. 100.
[21]Black, N.J., et al., *Modelling consumer choice of distribution channels: an illustration from financial services*, in *Marketing*. 2002. p. 173.
[22]Tauber, E.M., *Why Do People Shop?* Journal of Marketing, 1972. 36(4): p. 46-49.
[23]Pieterson, W. and J.V. Dijk. *Channel choice determinants: an exploration of the factors that determine the choice of a service channel in citizen initiated contacts*. in *Proceedings of the 8th annual international conference on Digital government research*. 2007.
[24]Sridhar Balasubramanian, R.R.V.M., *Consumers in a multichannel environment: Product utility, process utility, and channel choice*. Journal of Interactive Marketing, 2005. 19(2): p. 12-30.
[25]Degeratu, A.M., A. Rangaswamy, and J. Wu, *Consumer choice behavior in online and traditional supermarkets: The effects of brand name, price, and other search attributes*. International Journal of Research in Marketing, 2000. 17(1): p. 55-78.
[26]Xin, D., R. Verma, and Z. Iqbal, *Self-service technology and online financial service choice*. International Journal of Service Industry Management, 2007. 18(3): p. 246-268.
[27]Black, N.J., et al., *Modelling consumer choice of distribution channels: an illustration from financial services*. Marketing, 2002. 161: p. 173.
[28]Teo, T.S.H. and Y. Yu, *Online buying behavior: a transaction cost economics perspective*. Omega, 2005. 33(5): p. 451-465.
[29]Eastlick, M.A. and M.M. Liu, *The influence of store attitudes and other nonstore shopping patterns on patronage of television shopping programs*. Journal of Direct Marketing, 1997. 11(3): p. 14-24.
[30]Gehrt, K.C., L.J. Yale, and D.A. Lawson, *The convenience of catalog shopping: Is there more to it than time?* Journal of Direct Marketing, 1996. 10(4): p. 19-28.
[31]Liang, T.P. and J.S. Huang, *An empirical study on consumer acceptance of products in electronic markets: a transaction cost model*. Decision Support Systems, 1998. 24(1): p. 29-43.
[32]Rugimbana, R., *Predicting automated teller machine usage*. International Journal of Bank Marketing, 1995. 13(4): p. 26-32.
[33]Prendergast, G.P. and N.E. Marr, *The Future of Self-Service Technologies in Retail Banking*. The Service Industries Journal, 1994. 14(1): p. 94-114.
[34]Holland, C.P., A.G. Lockett, and I.D. Blackman, *Global strategies to overcome the spiral of decline in universal bank markets*. Journal of Strategic Information Systems, 1998. 7(3): p. 217-232.
[35]Barczak, G., P.S. Ellen, and B.K. Pilling, *Developing typologies of consumer motives for use of technologically based banking services*. Journal of Business Research, 1997. 38(2): p. 131-139.
[36]Rotchanakitumnuai, S. and M. Speece, *Barriers to Internet banking adoption: a qualitative study among corporate customers in Thailand*. Marketing, 2007. 2003: p. 312-323.
[37]Liao, Z. and M.T. Cheung, *Measuring consumer satisfaction in internet banking: a core framework*. 2008.
[38]Liao, Z. and M.T. Cheung, *Internet-based e-banking and consumer attitudes: An empirical study*. Information & Management, 2002. 39(4): p. 283-295.
[39]Albesa, J.G., *Interaction channel choice in a multichannel environment, an empirical study*. The International Journal of Bank Marketing, 2007. 25(7): p. 490-506.
[40]Fang, X., et al., *Moderating Effects of Task Type on*

Wireless Technology Acceptance. Journal of Management Information Systems, 2006. 22(3): p. 123-157.

[41] Lee, C.C., H.K. Cheng, and H.H. Cheng, *An empirical study of mobile commerce in insurance industry: Task-technology fit and individual differences.* Decision Support Systems, 2007. 43(1): p. 95-110.

[42] Calisir, F. and C.A. Gumussoy, *Internet banking versus other banking channels: Young consumers' view.* International Journal of Information Management, 2008. 28(3): p. 215-221.

Proceedings of 2009 12th International Conference on Computer and Information Technology (ICCIT 2009)
21-23 December, 2009, Dhaka, Bangladesh

Neural Network Ensembles based on Artificial Training Examples

M. A. H. Akhand, Pintu Chandra Shill, K. Murase†
Dept. of Computer Science & Engineering, Khulna University of Engineering & Technology (KUET), Bangladesh
† Dept. of Human and Artificial Intelligence Systems, University of Fukui, Japan
akhand@cse.kuet.ac.bd, pintu98cse@yahoo.com

Abstract

Ensembles with several neural networks are widely used to improve the generalization performance over a single network. Proper diversity among component networks is considered an important parameter for ensemble construction so that failure of one may be compensated by others. Data sampling, i.e., different training sets for different networks, is the most investigated technique for diversity than other approaches. This paper presents a data sampling based neural network ensemble method where individual networks are trained on the union of original training set and a set of some artificially generated examples. Generated examples are different for different networks and are the element to produce diversity among the networks. The effectiveness of the method is evaluated on a suite of 20 benchmark classification problems. The experimental results show that the performance of this ensemble method is better or competitive with respect to the existing popular methods.

Keywords: Artificial training example, diversity, generalization, neural network ensemble, bagging, AdaBoost, negative correlation learning.

I. INTRODUCTION

The goal of ensemble construction with several classifiers is to achieve better generalization ability over a single classifier. The inspiration for building an ensemble is the same as for establishing a committee of people: each member of the committee should be as competent as possible, but the members should be complementary to one another. If the members are not complementary, i.e., if they always agree, then the committee is unnecessary as any one member is could perform the task of the committee. If the members are complementary, then when one or a few members make an error, there is a high probability that the remaining members can correct his error. Thus, for ensemble construction, proper diversity among component classifiers is considered to be an important parameter so that failure of one may be compensated by others.

Among classifiers, artificial neural networks (NNs) and decision trees (DTs) are the two popular tools. Starting in the early 90s a number of ways have been investigated, for creating diverse NNs or DTs for ensembles, and among them data sampling, i.e., different data/examples for different classifiers, is found to be the most effective approach [1]-[2]. This is because it is the training data that determines the function it (a classifier) approximates. The most popular algorithms that explicitly or implicitly use different training data for different classifiers in an ensemble are the bagging [3], AdaBoost [4] and negative correlation learning (NCL) [6]-[7].

Both bagging and AdaBoost algorithms explicitly manipulate the original training data to create a separate training set for each classifier in an ensemble [10]. Bagging creates the separate training set by forming bootstrap replicas of the original training data, while AdaBoost creates it by the same method but with adaptation [4],[8]-[9]. Both the methods use different training sets to build different DT or to train different NNs for constructing ensemble of DTs or NNs.

Although bagging and AdaBoost are the general techniques that can be used with any type of classifier (i.e., DTs or NNs), NCL is applicable only to construct ensembles of NNs. Like bagging and AdaBoost, NCL [6-7] does not create separate training sets explicitly for NNs in an ensemble. The NCL rather uses a correlation penalty term in the error function of the NNs by which networks can maintain training time interaction. The training method used in NCL is simultaneous where all NNs in the ensemble are trained on the same original training data at the same time. Since NCL provides training time interaction among NNs, it can produce diverse NNs for the ensemble.

A new scheme, called DECORATE algorithm [5], recently has been proposed for DT that sequentially produces a relatively large number of DTs to select several DTs for constructing an ensemble. It firsts create a DT based on the original training set and select it for ensemble. The algorithm uses different training sets for other DTs; a particular training set is the union of the original training data and randomly created artificial patterns. A DT considers for the ensemble when ensemble's performance does not degrade with this DT. The aim of using artificial training data is to create diverse DTs for the ensemble. To generate an artificial example, it randomly generates a set of input feature and then defines the class label of the pattern. It first checks the class probability of the feature set passing through the existing ensemble and then inversely defines class probability to use in training. Due to inverse relabeling, the method is called Diverse Ensemble Creation by Oppositional Relabeling of Artificial Training Examples (DECORATE).

Based on artificial training examples, the DECORATE algorithm is found an effective ensemble method when compared with other DT based ensemble methods, such as bagging and AdaBoost. According to our best knowledge, there is no neural network ensemble (NNE) me-

978-1-4244-6283-4/09/$26.00 ©2009 IEEE

thod based on such artificial training examples. As a classifier, NNs have been extensively applied across numerous domains and show better classification ability. In some situations a single NN is a better classifier than an ensemble of DTs [5]. Therefore, investigation of artificial training examples for NNE construction might be interesting and is a current demand. But the idea of example in DECORATE cannot apply directly on ensemble of NNs because NN defers from DT various points of view. NNs work on preprocessed training data that contain all information in numeric form. The focus of this study is to evaluate a neural network ensemble method based on artificial training examples.

The rest of the paper is organized as follows. Section II gives a description of the artificial training example creation for neural networks and training of the networks for the ensemble. Section III presents an experimental study. Section IV concludes the paper with a brief summary.

II. ARTIFICIAL TRAINING EXAMPLE BASED NEURAL NETWORK ENSEMBLES (ATENNE)

For ensemble construction, proper diversity among component NNs is an important parameter so that failure of one may be compensated by others. Artificial training examples, that are different for different NNs, may motivate different NNs towards different functional spaces and may promote diversity among the NNs. But the random artificial examples might not be always positive to improve overall NNE performance though they promote diversity. For this reason, a selection scheme requires to build NNE with appropriate NNs.

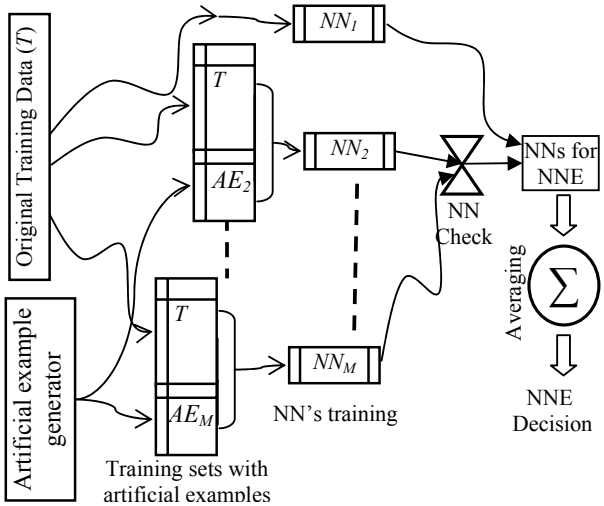

Fig.1. Graphical representation of ATENNE.

Figs. 1 and 2 show the graphical representation and the pseudo code, respectively for the artificial training example based NNE (ATENNE) method. According to Fig.1 first NN is trained with the original training set (*T*) and by default the NN is consider for final NNE. For each of other NNs, the method generates a unique set of training examples, i.e., the artificial training set. The training set on which a NN is trained therefore is the union of the original training set and the generated examples. After training a NN, it checks the NNE's performance including the NN and discards the NN if performance degrades. Therefore, to include more NNs in the final ensemble, it follows a trial-and-test with a relatively large number of trained NNs. Fig. 2 shows the ATENNE algorithm to construct an NNE of maximum M networks from N_{max} trained NNs. To observe NNE's performance, the algorithm measures ensemble error, i.e., the number of examples on which NNE gives wrong classification. When ensemble error decreases for a network, the NN is consider for final ensemble.

1. Let N_{max} be the number of NNs to be trained for an NNE and M the desired number of NNs.

   Take original training set $T= \{(x(1), d(1)),\ldots\ldots, (x(N), d(N))\}$ with class label $d(n) \in K = \{1,2,\ldots,k\}$

   Take R_{Size} -factor that determines number artificial examples for a network

   i=1 (for NN in NNE) and *trials* =1 (for trial NN)

   Train network NN_i with T (i.e., first NN is trained with original training data)

   Initialize ensemble, $NNE = \{NN_i\}$

   Compute ensemble error, $\varepsilon = \left(\sum_{(x(n),d(n)) \in T: NNE(x(n)) \neq d(n)} 1 \right) / N$

2. *while trials* < N_{max} and $i < M$ {

   a. Generate $R_{Size} \times |T|$ artificial training examples, AE_i

   b. Label examples in R with probability of class labels inversely proportional to predictions of *NNE*

   c. Prepare training set T_i, $T_{i=} T \cup AE_i$ and train network NN_i with T_i

   d. $NNE = NNE \cup \{NN_i\}$

   e. Compute ε' based on Step 1

   f. *if* $\varepsilon' \leq \varepsilon$ *then* $i = i + 1$ *and* $\varepsilon = \varepsilon'$, *otherwise* $NNE = NNE - \{NN_i\}$

   g. *trials = trials +1*

   }

3. Ensemble decision is made in simple average way

Fig. 2. ATENNE algorithm.

The artificially generated training examples in the training of different NNs are the main attraction of ATENNE. The diversity among the NNs is solely depends on the artificial examples. The size of artificial examples set (*AE*) is also an element of diversity. The size of *AE* is defined by the factor R_{Size} i.e., the size ratio of *AE* to the original training set (*T*). To create an artificial training example, ATENNE first generates the Gaussian number for each input attribute with the mean and the standard deviation of the attribute values of *T*. To define the class label of the pattern, it first checks the

class probability of it passing through the existing NNE and then inversely defines class probability to use in training. Thus, desired output values for artificial example does not 0 or 1, it might be any value in between 0 and 1. On the other hand, each original example contains one output node as 1 representing a particular class while others set to zero for a problem having *C* distinct classes.

The main problem of this algorithm is seen from the above description is that it trains relatively large number of NNs for an ensemble. Also it uses relatively larger training set (i.e., original training set plus generated examples) to train a NN. Both the factors increase training time. However, it might not be guaranteed to build NNE with desired number of NNs due to selection scheme of NNs.

III. EXPERIMENTAL STUDIES

This section first gives description of benchmark problems on which ATENNE was applied to evaluate its performance. It was also compared with the popular methods bagging, AdaBoost and NCL on the basis of achieved performance. Finally, the effect of different parameters on the performance of ATENNE was investigated.

A. BENCHMARK DATA AND GENERAL EXPERIMENTAL METHODOLOGY

Twenty real-world classification problems from the University of California, Irvine (UCI) machine learning benchmark repository were used for experiments. The characteristics of the problems are summarized in Table 1, and show a considerable difference in the number of patterns, input features and classes. These problems, therefore, provide a suitable experimental test bed. The UCI web site (http://www.ics.uci.edu/~mlearn/) contains detailed descriptions of these problems.

The UCI benchmark repository contains only raw data that require preprocessing to use in any NN. We followed the benchmark methodology suggested in [13] for preprocessing the data sets of different problems. In this work, the continuous input feature values were rescaled between 0 and 1 with a linear function. For discrete features, the number of inputs was selected as the number of distinct values in the data set in general. As an example, the ACC problem has 6 continuous and 9 discrete input features and after manipulation it was feed to a neural network as 51 inputs.

Three layered feed-forward architectures were used for NNs in ensembles. The number of nodes in the input and output layers was set equal to the number of processed inputs and classes of a given problem, respectively. We chose the number of hidden nodes based on the number of input and output nodes [9], one hidden node for every output node plus one hidden node for every 10 input nodes. The minimum number of hidden nodes was set at 5. The common logistic sigmoid function, $\phi(y) = 1/(1+\exp(-y))$, was used as the activation function for nodes in the hidden and output layers.

Table 1. Characteristics of benchmark datasets.

Dataset	Example	Class	Input Features		NN Architecture	
			Cont.	Disc.	Input	Hidd. Node
Australian Credit Card (ACC)	690	2	6	9	51	10
Breast Cancer Wisconsin (BCW)	699	2	9	-	9	5
Car (CAR)	1728	4	-	6	21	10
Diabetes (DBT)	768	2	8	-	8	5
Heart Disease Cleveland (HDC)	303	2	6	7	35	5
Hepatitis (HPT)	155	2	6	13	19	5
House Vote (HSV)	435	2	-	16	16	5
Hypothyroid (HTR)	7200	3	6	15	21	5
Ionosphere (INS)	351	2	34	-	34	10
Iris Plants (IRP)	150	3	4	-	4	5
King+Rook vs. King+Pawn (KRP)	3196	2	-	36	74	10
Lymphography (LMP)	148	4	-	18	18	10
Lungcancer (LNG)	32	3	-	56	56	10
Page Blocks (PGB)	5473	5	10	-	10	5
Promoters (PRM)	106	2	-	57	228	10
Soybean(SBN)	683	19	-	35	82	25
Segmentation(SGM)	2310	7	19	-	19	10
Sonar (SNR)	208	2	60	-	60	10
Waveform (WVF)	5000	3	21	-	21	10
Zoo(ZOO)	101	7	15	1	16	10

The learning rate of back-propagation (BP) is a parameter on which the performance of any algorithm may vary [11]. Based on a few trail runs, the value was selected 0.1-0.15 for the experiments. The number of NNs for ensembles was set to 20 for all problems. It has been reported that an ensemble consisting of 20 NNs is sufficient to reduce the testing set error. The initial weights of NNs were set randomly between -0.5 and 0.5.

B. EXPERIMENTAL RESULTS

This section presents experimental results of ATENNE along with bagging, AdaBoost and NCL. The results were compared based on testing error rate (TER). The TER refers to the rate of wrong classifications produced by the trained ensemble on the testing set; the lower TER value represents the better generalization ability. For comparison, an NNE method without data sampling, called simple NNE (sNNE), is also considered in this study. In sNNE, only initial random weight sets are different for different NNs and all the NNs are trained with the same original training set. A previous study revealed that in some cases sNNE also gives results

comparable to data sampling based methods [9]. By default; a data sampling based method also randomly initializes weights of a NN which makes for variation in weight sets in different NNs. Considering sNNE as a base line, ATENNE is compared with the popular methods.

For ensemble construction 20 NNs were trained, except for ATENNE. To be comparable to other methods, the maximum number of NNs per NNE in ATENNE was defined as 20 and maximum trial NNs as 30. The number of epochs for training NNs was set 50. It was observed that a minimum TER was found with a particular value of R_{Size} for ATENNE. This value was found not to be the same for all problems. We, therefore, selected the value of R_{Size} for a particular problem after some trial runs, and this value was selected in the range of 0.5 to 1. The number of training epochs per NN is a component getting better TER and the number is different for different problems as well as NNE methods. Therefore, an ensemble method was tested for a problem using three different training epochs per NN; 50, 75 and 100. For a specific problem the best TER among the three individual runs was used to compare with TERs of other ensemble methods. The built-in parameters of ATENNE and NCL are also found to have an important effect on TER. To minimize the effect of these parameters on a problem, ATENNE was tested with R_{Size} values of 0.5, 0.75 and 1; NCL was tested with λ values of 0.25, 0.5 and 0.75. Thus, for a particular problem, the best result for ATENNE and NCL among the nine individual runs was used to compare with the other methods. On the other hand, the results presented for sNNE, bagging and AdaBoost is the best among three independent runs i.e., for training epochs per NN equal 50, 75 and 100.

It is known that a different arrangement of patterns in training and testing sets may produce different performance, even when the numbers of patterns are kept the same for the training and testing sets. Therefore, 10-fold cross validation was used for creating the training and testing sets with different arrangement of patterns. In

Table 2. TERs comparison over five standard 10-fold cross-validation runs. A plus (or minus) sign indicates that TER is found significantly better (or worse) than sNNE by *t*-test. A single and double plus/minus is for 95% and 99% confidence interval, respectively. The bottom of the table contains a pair wise Win/Draw/Loss summary and method Best/Worst summary.

Problem	sNNE	Bagging	AdaBoost	NCL	ATENNE(NN/NNE)
ACC	0.1519	0.1409 +	0.1556	0.1432	**0.1356(5.62)** ++
BCW	0.0333	0.0331	0.0333	**0.0278** +	0.0319(5.38)
CAR	0.1128	0.0995 ++	**0.0799** ++	0.1036 +	0.1203(2.00)
DBT	0.2379	0.2321	**0.2305**	0.2308 +	0.2342(1.14)
HDC	0.1613	0.1607	0.1613	0.16	**0.1507(6.92)** +
HPT	0.1587	0.1533	0.18 -	0.1547	**0.152(1.02)**
HSV	0.0489	**0.0372** ++	0.0437 ++	0.0396 +	0.0442(5.68)
HTR	0.0531	0.0518 ++	**0.0263** ++	0.0522 +	0.0528(1.02)
INS	0.1343	0.1297	0.1034 ++	0.1366	**0.0606**(12.9) ++
IRP	**0.0267**	0.0293	0.028	**0.0267**	**0.0267**(1.00)
KRP	0.076	**0.0214** ++	0.0894	0.0765	0.0557(9.14) ++
LMP	0.1571	0.1543	0.1829 -	0.1571	**0.1357(4.96)** ++
LNG	0.5	**0.4067** +	0.4533	0.4933	0.4667(16.50)
PGB	0.0582	0.0563	**0.0499** ++	0.0589	0.0577(1.02)
PRM	0.068	0.068	0.072	0.068	**0.066**(20.00)
SBN	0.0541	**0.0517**	0.0535	0.0544	0.0559(10.5) -
SGM	0.07	0.0648	**0.0432** ++	0.0677 +	0.0761(3.14) -
SNR	0.195	0.194	0.181	0.195	**0.166**(7.58) ++
WVF	0.1327	**0.1297** +	0.132	0.1312	0.1308(4.18)
ZOO	0.11	0.1	**0.038** ++	0.11	0.098(16.52) +
Average	**0.127**	**0.1157**	**0.1169**	**0.1244**	**0.1159**

NNE	Pair Wise Win/Draw/Loss Summary				
Method	sNNE	Bagging	AdaBoost	NCL	ATENNE
sNNE	-	18/1/1	12/2/6	11/5/4	16/1/3
Bagging		-	9/0/11	4/1/15	10/0/10
AdaBoost			-	10/0/10	11/0/9
NCL				-	12/1/7
Best/Worst	1/9	5/1	6/7	2/4	8/3

10-fold cross validation, the patterns of the original data set were divided into 10 equal or nearly equal sets. By rotation, one set was reserved for testing while the remaining nine sets were used for training.

Table 2 shows the average TERs over five standard 10-fold cross-validation (i.e., 5*10=50) runs. For each problem, the best TER among the five methods is shown in bold-face type. Considering sNNE as a base line, pair two tailed *t*-test was conducted between sNNE and other NNEs individually to determine the significance in the variation of results for each problem. If TER of an NNE method is found significantly better than sNNE by *t*-test, it is marked with a plus (+) sign with TER. On the other hand, a minus (-) sign indicates TER of an NNE method is significantly worse than sNNE for a particular problem.

According to Table 2, among the data sampling based ensemble methods none is able to achieve better TER with respect to sNNE and other data sampling based methods for all the problems. However, on the basis of average TER for all the problems, any data sampling based method (i.e., bagging/AdaBoost/NCL/ATENNE) is better than sNNE. Among 20 problems, sNNE achieved the best TERs jointly with others for only one problem. On the other hand, bagging, AdaBoost, NCL and ATENNE have the best TERs for 5, 6, 2 and 8 problems, respectively. In this point of view ATENNE is the best among the methods. Also on the basis of average TER over 20 problems, ATENNE is better than sNNE, NCL and AdaBoost and competitive to bagging. According to Table 2, average TER achieved by ATENNE is 0.1159 whereas the TERs for sNNE, bagging, AdaBoost and NCL are 0.127, 0.1158, 0.1169 and 1244, respectively.

Bootstrap based data sampling (i.e., bagging or AdaBoost) creates different training sets for different NNs from the original available examples. The problems where bagging or AdaBoost performed better generally contain sufficient training examples such as, CAR, DBT, and SGM (Table 1). With respect to sNNE, bagging and AdaBoost outperformed in 18 and 12 problems, respectively; the results are found significant by *t*-test for seven for each of bagging and AdaBoost. Besides explicit creation of training sets for different NNs, NCL trains all the NNs in an NNE with the same original training examples. However, NCL encourages different NNs to produce different hypothesis adding a penalty term into the error function of a NN. On the basis of Table 2, NCL appears better than sNNE for 11 problems (in which in six cases the TERs were significantly better).

ATENNE creates some artificial training examples that are unique for individual NNs. Due to example creation, it might not suffer from the limitation of examples like bootstrap sampling based methods. From Table 2 it can be seen that ATENNE is shown best suited to the NNE method for problems with a limited number of examples, such as HPT, INS, LMP, and PRM problems. LMP has 148 training examples and the TER achieved by ATENNE is 0.1357; however TERs for sNNE, bagging and AdaBoost are 0.1571, 0.1543, and 0.1829, respectively. With respect to sNNE, out of 20 problems ATENNE is better in 16 problems, and among these the TERs for seven problems are significantly better.

Due to the NN selection scheme, ATENNE builds adaptive ensembles with different sizes for different problems. To select a second NN for the final ensemble, ATENNE trains NNs with an artificial training set having the opposite class definition of the first NN. Therefore the second NN might show higher diversity than the first one and combining it with the first one might degrade NNE performance, rather than improving or maintaining previous performance (i.e., the condition to add a NN in the NNE). This might be the reason ATENNE failed to build an ensemble and return a single NN for several problems. When it built ensembles, ATENNE selected few NNs from a large number of trained NNs. Out of 20 problems in only 10 cases did it build NNEs with more than five NNs and only once (i.e., for PRM) meet the desired NNE size. The selection scheme of ATENNE guaranteed to improve the ensemble performance from a single NN. Therefore, the problems in which ATENNE built NNE with a relatively larger number of NNs showed a better TER. For example, for the INS problem ATENNE built an ensemble with 12.9 NNs on average and achieved the best TER among the five methods. The achieved TER of ATENNE for this problem was 0.0606; however, TERs were 0.1343, 0.1297 and 0.1034 for sNNE, bagging and AdaBoost, respectively. Out of 20 problems, ATENNE has the best TER for eight problems. At a glance, ATENNE is an effective NNE method for small sized problem and also competitive with other methods for large problems.

C. EXPERIMENTAL ANALYSIS OF ATENNE

Performance of a method may vary depending on its parameter values, and better TER may be achieved at a certain range or point. This subsection investigates the effect of R_{Size} (the ratio of artificial generated pattern set with original training set) on TER and diversity of ATENNE. For better TER it is necessary to maintain proper diversity among component NNs, as we said earlier. Simply, diversity means disagreement among component NNs. Many diversity measuring techniques have been proposed. Among them the pairwise plain disagreement technique [12] is the most popular and is the one employed in this study. For two NNs *i* and *j*, the plain disagreement is equal to the proportion of the patterns on which the NNs make different class predictions. It can be expressed as

$$div_{i,j} = \frac{1}{N}\sum_{n=1}^{N} Diff\ (C_i(n), C_j(n)), \qquad (1)$$

where N is the number of patterns in the testing set and $C_i(n)$ is the class assigned by the NN i for the pattern n.

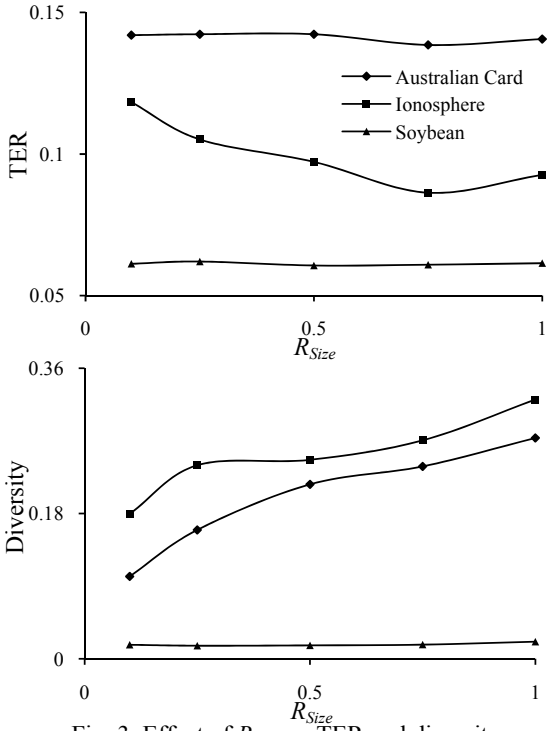

Fig. 3. Effect of R_{Size} on TER and diversity.

Diff(a, b) = 0, if *a* = *b*; otherwise *Diff(a, b)* = 1. The diversity for a NNs pair varies from 0 to 1. This measure is equal to 0, when the NNs return the same classes for each pattern, and it is equal to 1 when the predictions are always different. The NNE diversity is the average of all the NN pairs' diversity.

Fig. 3 presents experimental results over five 10-fold cross validation runs for three problems Australian Card, Ionosphere, and Soybean. R_{Size} was varied from 0.1 to 1.0. For NNE construction, 20 NNs (i.e., N_{max}) were trained to select a maximum of 10 NNs. In an NNE each NN was trained for 50 epochs. According to Fig. 3, TER and diversity varied for the variation of R_{Size}. The effects of R_{Size} are more visible for Australian Card and Ionosphere (those are two-classed problems) than for Soybean problem that have 19 classes. For the Australian Card and Ionosphere problems diversity increased greatly with respect to R_{Size} but TER reduced at a certain level. For the Australian Card and Ionosphere problems the lowest TERs occur at R_{Size} =0.75. On the other hand, minimum TER for Soybean problem occurs when R_{Size} equals 0.5. For this reason, R_{Size} value was varied in between 0.5 to 1 for experimental results

IV. CONCLUSION

In this study an artificial training example based NNE (ATENNE) is investigated. ATENNE is tested on a large number of benchmark problems and is compared with the popular NNE methods such as bagging, AdaBoost and NCL. ATENNE constructed problem dependent adaptive NNE that was smaller than the other methods. ATENNE is showed the best TERs with respect to bagging and Adaboost for small sized problems; bagging and boosting suffer shortage of examples for small sized problems. Also for any other problem, ATENNE was found competitive.

In case of ATENNE, the resulting TER has a relation with the final NNE size, i.e., selected NNs for final NNE. When ATENNE was able to select several NNs for the final NNE, it gave a better TER. For NN addition, much trial was required for the second NN due to high diversity with the first one; the problem was common for large R_{Size} values. Also the value of R_{Size} selection required trail-and-test. To overcome these problems an adaption scheme might be interesting and remain as future study.

REFERENCES

[1] G. Brown, J. Wyatt, R. Harris, and X. Yao, "Diversity Creation Methods: A Survey and Categorization," *Information Fusion,* vol. 6, 2005, pp. 99-111.

[2] T. G. Dietterich, Ensemble Learning, *The Handbook of Brain Theory and Neural Networks*, 2002, pp. 405-408.

[3] L. Breiman, "Bagging predictors," *Machine Learning*, vol. 24, 1996, pp. 23-140.

[4] Y. Freund and R. E. Schapire, "Experiments with a new boosting algorithm," *in Proc. of the 13th Int. Conf. on Machine Learning*, 1996, pp. 148-156.

[5] P. Melville and R. J. Mooney, "Creating diversity in ensembles using artificial data," *Information Fusion*, vol. 6, 2005, pp. 99-111.

[6] Y. Liu and X. Yao, "Ensemble learning via negative correlation," *Neural Networks*, vol. 12, 1999, pp. 1399–1404.

[7] Y. Liu and X. Yao, "Simultaneous Training of Negatively Correlated Neural Networks in an Ensemble," *IEEE Trans. Systems, Man, and Cybernetics – Part B*, vol. 29, 1999, pp. 716-725.

[8] E. Bauter and R. Kohavi, "An Empirical Comparison of Voting Classification Algorithms: Bagging, Boosting, and Variants," *Machine Learning*, vol. 36, 1999, pp. 105-142.

[9] D. W. Opitz and R. Maclin, "Popular ensemble methods: An empirical study," *Journal of Artificial Intelligence Research*, vol. 11, 1999, pp. 169-198.

[10] R. Polikar, "Bootstrap Inspired Techniques in Computational Intelligence," *IEEE Signal Processing Magazine*, vol. 24, 2007, pp. 59-72.

[11] S. Haykin, *Neural Networks – A Comprehensive Foundation*, 2nd ed., Prentice Hall, 1999.

[12] A. Tsymbal, M. Pechenizkiy and P. Cunningham, "Diversity in search strategies for ensemble feature selection," *Information Fusion*, vol. 6, 2005, pp. 83-98.

[13] L. Prechelt, *Proben1- A Set of Benchmarks and Benching Rules for Neural Network Training Algorithms*, Tech. Rep. 21/94, Fakultat fur Informatik, University of Karlsruhe, Germany, 1994.

Proceedings of 2009 12th International Conference on Computer and Information Technology (ICCIT 2009)
21-23 December, 2009, Dhaka, Bangladesh

Application of Greedy Sequential Grammar Transform on Dynamic Markov Compression: A Way to Produce More Amenable Compression *(Not Presented)*

Sajib Kumar Saha, Ratna Saha, Beroza Paul†, Md. Masudur Rahaman‡
Dohatec New Media, Dhaka, Bangladesh
† EVOKNOW Inc., Dhaka, Bangladesh
‡ Khulna University, Khulna, Bangladesh
to_sajib_cse@yahoo.com, li_ratna@yahoo.com, beroza07@gmail.com, masud_cse02@yahoo.com

Abstract

A method of lossless data compression has been proposed based on greedy sequential grammar transform and dynamic markov model. Greedy sequential grammar transform can be used to generate smallest grammar of the input file and can therefore be used as a basis for data compression. To this end, greedy sequential grammar transform can be coalesced with dynamic markov compression to fabricate more prevailing method of data compression. Experimental results reported here indicate that the proposed model achieves much better data compression than that observed with competing methods on typical computer data.

Keywords: Arithmetic coding, dynamic markov compression (DMC), greedy sequential grammar.

I. INTRODUCTION

The compression technique DMC [3] is very prominent in the field of lossless data compression but not generally used because of seizing considerable amount of computation and large amount of memory. The anticipated methodology reduces the memory requirement of DMC by applying greedy sequential grammar transform on the input data to generate shorter context and then pass it to DMC. The method enhances the compression performance, reduces memory requirement while keeps the compression time comparable. The comparison with greedy sequential grammar transform based compression proposed in [1] and DMC proposed in [3] indicate that the proposed method is a good alternative in the field of lossless data compression.

II. LITERATURE SURVEY

A. Review of Grammar-based Codes

Very recently, a new type of lossless source code called a grammar-based code has developed [5]. Grammar based codes can be viewed as a generalization of the well-known Lempel–Ziv lossless codes. These codes compress a data sequence x, by first transforming it into a context free grammar G, and then compress G through arithmetic coding algorithm.

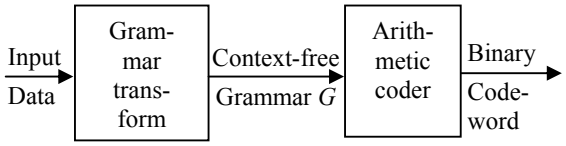

Fig. 1. Structure of a grammar-based code

As described in [2] let A be our source alphabet with cardinality greater than or equal to 2. Let A^* be the set of all finite strings drawn from A, including the empty string λ, and the A^+ set of all finite strings of positive length from A. The notation $|A|$ stands for the cardinality of A, and for any $x \in A^*$, $|x|$ denotes the length of x. For any positive integer n, A^n denotes the set of all sequences of length n from A. Similar notation will be applied to other finite sets and finite strings drawn from them. To avoid possible confusion, a sequence from A is sometimes called an A-sequence. Let $x \in A$ be a sequence to be compressed. As shown in Figure 1, in a grammar-based code, the sequence x is first transformed into a context-free grammar (or simply a grammar) G from which x can be fully recovered, and then compressed indirectly by using a zero-order arithmetic code to compress G. To get an appropriate G, string matching is often used in some manner. It is clear that to describe grammar-based codes, it suffices to specify grammar transforms.

B. Grammar Transforms/ Greedy Grammar Transforms

A grammar transform converts x from A into an admissible grammar G from which x can be fully recovered. The grammar transform proposed in [2] starts from the grammar G consisting of only one production rule $s_0 \rightarrow x$, and applies repeatedly reduction rules 1–5 as described in [2] in some order to reduce into an irreducible grammar G'. To compress x, the corresponding grammar-based code then uses a zero-order arithmetic code to compress the irreducible grammar G'. After receiving the codeword of G', one can fully recover G' from which x can be obtained via parallel replacement. Greedy grammar transform produces the smallest grammar for the inputted string.

978-1-4244-6283-4/09/$26.00 ©2009 IEEE

C. Dynamic Markov Model

Dynamic Markov compression (DMC) is a lossless data compression algorithm. It predicts and codes one bit at a time. DMC [3] consists of two components – a predictor and a coder. And the predictor is the foundation of DMC, which is dynamic Markov model. It's a finite state model that counts the characteristics of the next input. The probability of occurrence of the next input bit can be calculated from the current state of the model by using the frequency count. This probability is then supplied to the arithmetic coder that generates code for it. It has been shown that the arithmetic coder will generate codes which are nearly as good as the entropy of the text with respect to the model used [6].

Initial model is assumed as one state fsa with transitions 0/1 and 1/1. In general, the transitions are marked by $0/p$ or $1/q$ where p and q denote non-zero counts of number of transitions from that state (not including the next bit) from a given state with input 0 or 1, respectively. The initial count is set to 1 to take care of the "zero frequency" problem. The estimate of probability of a 0 being the next input is $p/(p+q)$ and 1 being the next state is $q/(p+q)$. These probability values are used by a background entropy coder (such as an arithmetic coder) to estimate the interval in the cumulative probability space for the next symbol in the input. If the next symbol is zero, it will change then the count to $(p+1)$, make the appropriate state change and continue. Similarly, for a 1 input it will change the value of q to $(q+1)$.

An important concept of dynamic Markov model is Adaptation or Cloning. If a transition to a particular state t from some previous state u is heavy, that is more frequent, in order to capture this skewed context, the state t is cloned. Both encoder and the decoder must agree upon a threshold value of the count value for cloning and it is defined as two parameters MIN_CNT1 and MIN_CNT2. The cloned state is designated as t'.

For example, consider figure 2. Before cloning, when the current state is D, it is not known what are the states (A or B) before C. To capture this information, a new state C' can be cloned from C so that it is now possible to know which state was visited before. Such information will help the model make a more accurate prediction of the next occurring bit and allow the coder to compress the file more effectively.

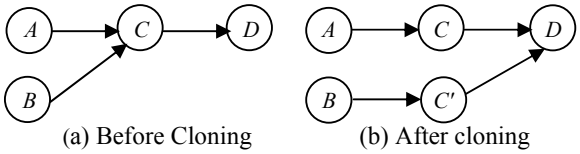

(a) Before Cloning (b) After cloning

Fig. 2. Example of Cloning

There are several factors affecting the performance of DMC as initial model, threshold value in case of cloning, as well as the amount of memory available for the creation of new states.

III. THE PROPOSED MODEL

In our proposed compression, we first construct a grammar based upon the input data using greedy sequential grammar and then compress that grammar using DMC. Since the generated grammar is diminutive compared to the actual data DMC can be used without any hassle of memory related quandary, which is very common for basic DMC as proposed in [3].

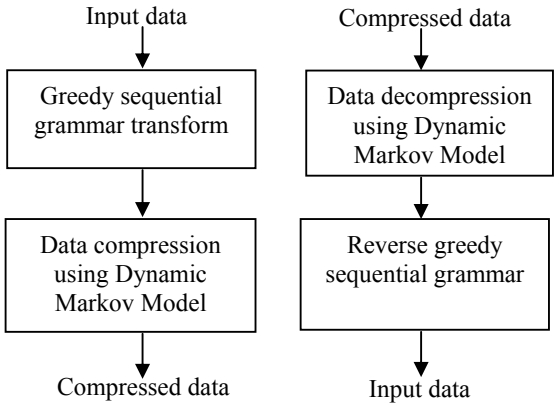

(a) (b)

Fig. 3. Proposed model (a) Compression (b) Decompression.

A. Proposed Compression Technique

The proposed compression algorithm consists of two phases:

1. Greedy sequential grammar transform
2. Applying DMC

Greedy Grammar Transform [2]

Let $x = x_1x_2 \ldots x_n$ be a sequence from A which is to be compressed. It parses the sequence x sequentially into non-overlapping substrings $\{x_1, x_2 \ldots x_{n_2}, \ldots, x_{n_{i-1}+1} \ldots x_{n_t}\}$ and builds sequentially an irreducible grammar for each $x_1, \ldots, x_{n_t}$ where $1 \le i \le t$, $n_1 = 1$, and $n_t = n$. The first substring is x_1 and the corresponding irreducible grammar G_1 consists of only one production rule $s_0 \rightarrow x_1$. Suppose that $x_1, x_2 \ldots x_{n_i}, \ldots, x_{n_{i-1}+1} \ldots x_{n_i}$ have been parsed off and the corresponding irreducible grammar G_i for $x_1, \ldots, x_n$ has been built. Suppose that the variable set of G_i is equal to

$$S(j_i) = \{s_0, s_1, \ldots, s_{j_i - 1}\}$$

Where $j_1 = 1$. The next substring $x_{n_i+1} \ldots x_{n_{i+1}}$ is the longest prefix of $x_{n+1} \ldots x_n$ that can be represented by s_j for some $0 < j < j_i$ if such a prefix exists.

Otherwise, $x_{n_i+1} \ldots x_{n_{i+1}} = x_{n_i+1}$ with $n_{i+1} = n_i + 1$. If $n_{i+1} - n_i > 1$ and $x_{n+1} \ldots x_n$ is represented by s_j, then append s_j to the right end of $G_i(s_0)$; otherwise, append the symbol x_{n+1} to the right end of $G_i(s_0)$. The resulting grammar is admissible, but not necessarily irreducible. Apply reduction rules 1–5 proposed in [2] to reduce the grammar to an irreducible grammar G_{i+1}. Then G_{i+1}

represents $x_1 \ldots x_n$. Repeat this procedure until the whole sequence is processed. Then the final irreducible grammar G_t represents x. Since only one symbol from S (j_i) U A is appended to the end of $G_i(s_0)$, not all reduction rules can be applied to get G_{i+1}.Furthermore, the order via which reduction rules are applied is unique.

Dynamic Markov Compression

Dynamic markov compression consists of two phases. In phase one dynamic markov model [3] is used to calculate the probability for the upcoming bit.

Dynamic Markov Model Algorithm [8]

Two data structure T and C are defined. Each is a table with rows equal to number of states s and two columns corresponding to input 0 or 1. The first table is just the 'next' state transition table and is denoted as $T[1{:}s][0,1]$ and C is the count table giving the number of transitions for a given state for input 0 or 1 and is designated as $C[1{:}s][0,1]$.

1. s:=1 /* The current number of states */
2. t:=1 /* the current state */
3. $T[1][0]=T[1][1]$:=1 /* initial model*/
4. $C[1][0]=C[1][1[$=1 /* initial count to avoid zero frequency problem*/
5. For each input bit e do
   a) u:=t
   b) t:=$T[u][e]$ /* Follow the transition*/
   c) Code e with probability $C[u][e] / (C[u][0] + C[u][1])$
   d) $C[u][e] = C[u][e]+1$
   e) If cloning threshold are exceeded then,
      s:=s+1 /* new state */
      $T[u][e]= s$
      $T[u][e] := s$
      $T[s][0] := T[t][0]$
      $T[s][1] := T[t][1]$, and
      Move some of the counts from $C[t]$ to $C[s]$

In phase two Guazzo encoding algorithm proposed in [3] is used to produce the compressed data based on the probability calculated in phase one.

B. Proposed Decompression Technique

The proposed decompression algorithm consists of two phases:

1. Reverse greedy sequential grammar transform
2. Applying Dynamic Markov Model

IV. EXPERIMENTAL RESULTS

We have taken *bib*, *book1*, *book2*, *news*, *paper1*, *paper2* files from the *Calgary Corpus*; *alice29.txt*, *plrabn12.txt*, *lcet10.txt*, *kennedy.xls* files from *Canterbury Corpus*; *Chntxx.seq, Chmpxx.seq* files from *Dna*; *Mj*, *Sc* files from *Protein Corpus*; *bible.txt, E.Coli, world192.txt* files from *Large Centerbury* for experiment. The experimental result is given on Table I through Table V.

Table I Comparison with greedy sequential grammar based compression, and the proposed model for files from *Calgary Corpus*

File Name	Original Size (bytes)	Using Greedy Sequential Grammar Transform based Compression (bytes)	Using DMC proposed in [3] (bytes)	Using the Proposed Model (bytes)
Bib	1,11,261	36,864	**30,262**	30,768
book1	7,68,771	2,94,912	2,09,105	**1,90,812**
book2	6,10,856	2,04,800	1,66,152	**1,56,918**
News	3,77,109	1,47,456	1,52,573	**1,48,361**
paper1	53,161	17,980	**14,459**	16,617
paper2	82,199	27,567	22,358	**21,844**
Total	20,03,357	7,29,579	5,94,909	**5,65,320**

Table II Comparison with greedy sequential grammar based compression, and the proposed model for files from *Canterbury Corpus*

File Name	**Original Size** (bytes)	**Using Greedy Sequential Grammar Transform based Compression** (bytes)	**Using DMC proposed in [3]** (bytes)	**Using the Proposed Model** (bytes)
Alice29.txt	1,55,648	51,020	49,496	**49,381**
plrabn12.txt	4,81,861	1,82,049	1,73,231	**1,65,988**
Lcet10.txt	4,26,754	1,39,748	1,35,707	**1,30,622**
kennedy.xls	10,29,744	**2,03,795**	3,27,458	2,05,336
Total	20,94,007	5,76,612	6,85,892	**5,51,327**

Table III Comparison with greedy sequential grammar based compression, and the proposed model for files from *Dna*

File Name	**Original Size** (bytes)	**Using Greedy Sequential Grammar Transform based Compression** (bytes)	**Using DMC proposed in [3]** (bytes)	**Using the Proposed Model** (bytes)
Chntxx.seq	1,55,844	**39,625**	41,909	43,677
Chmpxx.seq	11,67,360	2,92,905	3,11,768	**2,69,341**
Total	13,23,204	3,32,530	3,53,677	**3,13,018**

Table IV Comparison with greedy sequential grammar based compression, and the proposed model for files from *Protein Corpus*

File Name	**Original Size** (bytes)	**Using Greedy Sequential Grammar Transform based Compression** (bytes)	**Using DMC proposed in [3]** (bytes)	**Using the Proposed Model** (bytes)
Mj	4,48,779	1,45,927	**1,24,311**	1,24,971
Sc	29,00,352	11,63,336	11,02,133	**11,00,720**
Total	33,49,131	13,09,263	12,26,444	**12,25,691**

Table V Comparison with greedy sequential grammar based compression, and the proposed model for files from *Large Centerbury Corpus*

File Name	Original Size (bytes)	Using Greedy Sequential Grammar Transform based Compression (bytes)	Using DMC proposed in [3] (bytes)	Using the Proposed Model (bytes)
bible.txt	40,47,392	11,39,752	11,21,127	**10,79,920**
World192.txt	24,73,400	7,37,908	**6,85,131**	7,03,413
Total	65,20,792	18,77,660	18,06,258	**17,83,333**

V. CONCLUSION

This paper has aimed at providing a sketch on how greedy sequential grammar transform can be used in conjunction with Dynamic Markov compression (DMC). Though both of them [1], [3] are complete compression technique the juxtaposition of greedy sequential grammar transform with DMC shows more amenable results. The projected methodology implements the fundamental operation of DMC while perform greedy sequential grammar transform on input data first and tentatively shows better compression than any of the two methods keeping akin compression time.

REFERENCES

[1] En-hui Yang and Da-Ke He , *Efficient universal lossless data compression algorithms based on a greedy sequential grammar transform—Part two: With context models*, IEEE Trans. Inform. Theory, vol. 49, no.11, November 2003.

[2] E.-h. Yang and J. C. Kieffer, Efficient universal lossless data compression algorithms based on a greedy sequential grammar transform—Part one: Without context models, IEEE Trans. Inform. Theory, vol. 46, pp. 755–788, May 2000.

[3] Gordon Cormack and Nigel Horspool, Data Compression using Dynamic Markov Modelling, Computer Journal 30:6 (December 1987).

[4] K. S. Trivedi, Probability and Statistics with Reliability, Queuing and Computer Science Applications. Pren-tice-Hall, Englewood Cliffs, N.J. (1982).

[5] J. C. Kieffer and E.-H. Yang, Grammar based codes: A new class of universal lossless source codes, IEEE Trans. Inform. Theory, Vol.IT-46, No. 3, pp. 737--754, May 2000.

[6] Witten, I. H., Neal, Radform M., Cleary, J. G. (1987), Arithmetic Coding for Data Compression, Communica-tions of the ACM, Vol 30 No 6 : 520 – 540.

[7] NG JUN PING, ONG GHIM HWEE, NUROP – Applying Dynamic Markov Modeling To Chinese Texts for Data Compression.

[8] Read Sayood, DMC(Dynamic Markov Compression), pp.174-176, Bell et. Al., Managing Gigabytes,pp.69-72.

Proceedings of 2009 12th International Conference on Computer and Information Technology (ICCIT 2009)
21-23 December, 2009, Dhaka, Bangladesh

Migration to the Next Generation Passive Optical Network

Md. Shamim Ahsan†, Man Seop Lee†, S. H. Shah Newaz†, Syed Md. Asif ‡
† Korea Advanced Institute of Science and Technology, 119, Munjiro, Yuseong-gu, Daejeon, 305-732, South Korea
‡ Sylhet International University, Shamimabad, Bagbari, Sylhet-3100, Bangladesh
Shamim@kaist.ac.kr, leems1502@kaist.ac.kr, newaz@kaist.ac.kr, asif_ece04@yahoo.com

Abstract

Due to the rapid growth of Internet with new generation of services and applications, demand for faster and cheaper access network has been rising. To address the present and future demand, broadband fiber access technologies such as passive optical networks (PONs) are a potential solution. Mostly, time division multiplexed (TDM)-PON is deployed in all parts of the world. In order to mitigate the future demand, some next-generation PON systems have been investigated by the researchers. In this paper, we examine the current status of PONs and investigate the probable future PONs. We also explain the smooth migration process from the current status to the future technologies. Architecture of a self-restored tree-type hybrid wavelength division multiplexed/TDM-PON (WDM/TDM-PON) has been proposed, for migrating from TDM to WDM-PON. Due to the restorable capacity of the architecture, the availability of the system is increased. In addition, cost analysis of different PON architectures are performed and compared with the cost of the proposed architecture. It is found that, the proposed architecture provides more cost effective solution.

Keywords: BSWDM FILTER, FTTXS, PON, TDM, WDM.

I. INTRODUCTION

Due to the expansion of multimedia services, such as video on demand, videoconferencing, high-definition TV (HDTV), e-learning, interactive games and VOIP, users will require more than 30 Mb/s of guaranteed bandwidth per user in the near future. New services favoring greater bandwidth appear persistently, and many service providers are planning to provide networks capable of 50 Mb/s, 100 Mb/s or higher, per customer. Fig. 1 shows the historic and future projections for average data rates through the access network [1].

In order to provide broadband access services, there is a strong competition between several technologies: digital subscriber loop, coaxial cable, wireless, and FTTx (Fiber to the x, where x stands for node, curb, building, home, and premise etc.). The bandwidth of copper wire and wireless access technologies is limited due to physical media constraints. To satisfy the future bandwidth demand, service providers will have to deploy optical access networks. According to the FTTH Council, presently there are 32 million FTTH connections worldwide. More than 27 million connections are accounted by the Asian region.

Depending on the use of passive or active devices, an FTTx network can be classified as Passive Optical Network (PON) and Active Optical Network (AON).

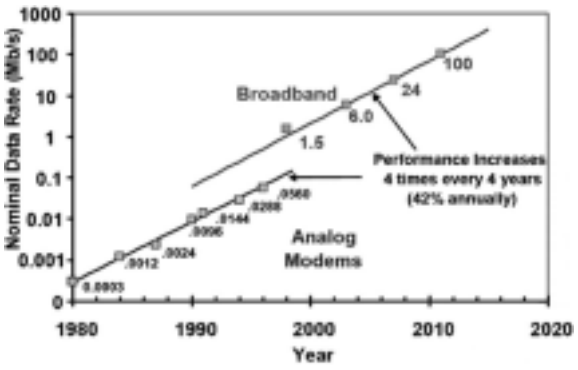

Fig. 1. Broadband evolution in access networks [1].

From topological point of view, FTTx can be categorized also into two types: Point-to-Point (P2P) and Point-to-Multi-Point (P2MP) systems. Fig. 2 shows a simple architecture of a P2MP based AON and PON systems. Here, the feeder fiber runs from the Optical Line Terminal (OLT) of the Central Office (CO) up to a splitting point in the path. From this point, distribution fibers extend to several Optical Network Units (ONUs) at end points.

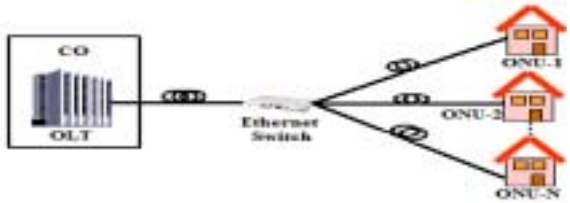

(a)

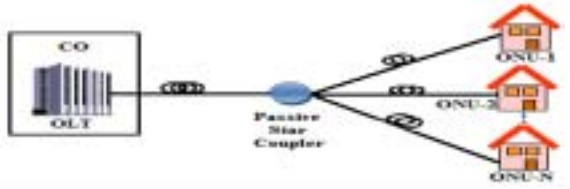

(b)

Fig. 2. Optical Networks. (a) Active Optical Network (AON); (b) Passive Optical Network (PON)

In the rest of the paper, we focus on PONs as an essential FTTx architecture. At first, we review the TDM-PONs (designated as current generation PONs). Next, we review the next generation PON systems, which we

978-1-4244-6283-4/09/$26.00 ©2009 IEEE

categorize into short-term and long-term future generations. The process of smooth migration of the current generation PONs to the future generation PONs will be discussed also. Architecture of a self-restored tree-based hybrid WDM/TDM-PON has been proposed with duplex fiber system against the fiber failure. It has a hybrid OLT to support both TDM and WDM-PON. The proposed structure provides protection for both feeder fiber and distribution fibers with a minimum addition of looses in the transmission path.

We quantified the performance of the proposed architecture by calculating the system availability, which is defined as the probability of service delivery upon request. It is found that the proposed scheme provides more system availability due to its protection scheme.

We also perform the cost analysis for different PONs and found the proposed architecture more cost effective.

II. OVERVIEW OF PASSIVE OPTICAL NETWORKS

PON was first introduced in 1980s. The search for a TDMA system over a PON was proposed in 1987 by researchers at BT Laboratories via the TPON and the first TDMA-based system was developed and demonstrated in this field in 1989 [2]. We categorize the PONs as current generation PONs and next generation PONs. The next generation PONs are also sub-categorized as short-term and long-term future generation PONs. They are explained briefly in this section.

A. Current Generation PONs

One of the most important events in the development of the PON systems was the founding of Full Service Access Network (FSAN) group in 1995. The mission of FSAN was to drive applicable standards, where already exist, into the services and products in the optical access systems industry in an economical way by promoting common standards and the result is A-PON. It provides 155 Mb/s symmetric (both downstream and upstream) bandwidth up to maximum 32 subscribers.

In order to deliver a full set of telecommunications services, both narrowband and broadband, FSAN has produced the initial recommendations for broadband-PON (B-PON) since 1996, which were adopted by ITU-T as ITU-T G.983.x series since 1998. Some researchers consider A-PON and B-PON as same. The main difference is the 622 Mb/s downstream, and 155 Mb/S or 622 Mb/s aggregate upstream data rates. It also provides maximum 32 split with a maximum reach of 20 km.

In 2001, the IEEE 802.3 working group initiated a task force, called 802.3ah to draft a standard to address Ethernet in the First Mile (EFM). One of their goals was to standardize the transport of Ethernet frames (1000Base-x) on PONs. The result was the Ethernet-PON (E-PON) that began with existing Ethernet devices and standardized in 2004. It operates at bit rates of 1.25 Gb/s with a split ratio of maximum 32.

In 2001 the FSAN start a new effort for standardizing networks operating at bit rates of above 1 Gb/s. In 2003, the FSAN proposed the first recommendation for gigabit capable PON (G-PON) which is described in ITU-T G.984.x series. It operates at bit rates of 2.5 Gb/s and 1.5 Gb/s in downstream and upstream respectively. The maximum split ratio is 64.

B. Short-term Future Generation PONs

Both FSAN/ITU-T and IEEE are working on PONs with 10 Gb/s data rate. In 2007 the IEEE 802.3av task force was established to develop 10 GE-PON systems. The targeted systems include 10 Gb/s symmetric system (10G/10G) and an asymmetrical system with 10 Gb/s downstream and 1 Gb/s upstream (10G/1G). The standardization will be done in 2009.

The FSAN group is considering many different upgrade systems. Among them the most important considerations are based on 10 Gb/s (XG-PON1 and XG-PON2).The XG-PON1 is the primary focus of FSAN and supported by ITU-T. In XG-PON1, the downstream is at 10 Gb/s and the upstream is at 2.5 Gb/s. In XG-PON2, the downstream and upstream bit rates are 10 Gb/s (10G/10G). This symmetric system may be considered as the ultimate version of TDMA by FSAN and supported by IEEE.

C. Long-term Future Generation PONs

WDM-PON is found to be the only realistic solution for long term even though it is not standardized yet. WDM-PONs have been reported with up to 32 users at 1.25 Gb/s to 2.5 Gb/s per user/wavelength, offering both great security and protocol transparency [3], [8]-[9]. WDM-PON provides an optical point-to-point link by allocating a pair of bidirectional wavelengths between each ONU and OLT connected to the PON as in Fig. 3.

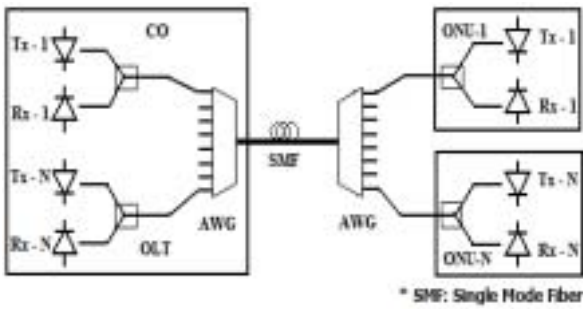

Fig. 3. Basic WDM-PON architecture.

An Arrayed Waveguide Grating (AWG) is used to demultiplex the downstream wavelengths and multiplex the upstream wavelengths. In OLT, there are an array of transmitters (Txs) and receivers (Rxs). In each ONU, there is a passive splitter to separate transmitter and the receiver.

Table I Comparison of different PONs

	TDM-PONs							Long-term Future Generation PON
	Current Generation PONs				Short-term Future Generation PONs			
	A-PON	B-PON	E-PON	G-PON	10 GE-PON	XG-PON1	XG-PON2	WDM-PON
Standards	ITU-T G.983.1	ITU-T G.983.x	IEEE 802.3ah	ITU-T G.984.x	IEEE 802.3av (draft)	FSAN	FSAN	No Standard
Framing	ATM	ATM	Ethernet	GEM	Ethernet	GEM	GEM	Protocol independent
Maximum Bandwidth	155 Mb/s (↓↑)	622 Mb/s (↓↑)	1.25 Gb/s (↓↑)	2.5 Gb/s(↓) 1.5 Gb/s (↑)	10 Gb/s (↓↑)	10 Gb/s (↓) 2.5 Gb/s (↑)	10 Gb/s (↓↑)	1-10 Gb/s per channel
User per PON	16-32	16-32	16-32	32-64	≥ 64	≥ 64	≥ 64	16-32
Bandwidth per user	10-20 Mb/s	20-40 Mb/s	30-60 Mb/s	40-80 Mb/s	≥ 100 Mb/s	≥ 100 Mb/s	≥ 100 Mb/s	1-10 Gb/s
Line Coding	Scrambled NRZ	Scrambled NRZ	8b10b	Scrambled NRZ	64b66b	Scrambled NRZ	64b66b	
Video	RF/IP	RF/IP	RF/IP	RF/IP	RF/IP	RF/IP	RF/IP	
Cost	Low	Low	Low	Medium	High	High	High	Very high

The main limitation of WDM-PON is its higher cost due to the requirement of a wavelength specific laser for each ONU. Several approaches have been demonstrated for the implementation of cost-effective colorless ONUs in WDM-PONs. The most important enabling technologies for WDM-PON are based on injection-locked Fabry-Perot (FP) lasers [3], tunable components [4], spectral slicing [5], and centralized light sources (CLSs) [6]. Hybrid WDM/TDM-PONs are also attractive for migration from existing TDM-PON to the WDM-PON and are discussed in the next section. A comparison between different PONs is shown in Table I.

III. MIGRATION TECHNIQUES FROM CURRENT STATUS TO FUTURE PON SYSTEMS

For migrating from current generation PONs to the next generation PONs and providing interoperability between them, we can discuss about the following two proposals [7]: OLT add scenario and OLT replace scenario. Both scenarios are discussed from WDM and TDMA approach. In the first case, the addition of next generation OLT (NG-OLT) with the present OLT is proposed. They work parallel with each other. In the second case, replacement of present OLT with a NG-OLT has been proposed as shown in Fig. 4.

With "OLT add and WDM approach," only C/L band are available for NG-PON wavelength allocation. But with "OLT replace and TDMA approach," O band is also available with C/L band for NG-PON wavelength allocation. Both these approaches are good for migration and interoperability purposes, but the second one helps the cost reduction of optics. On the other hand, in "OLT add and TDMA approach", individual E/G-OLT and NG-OLT are needed to be synchronized with each other, which is technically difficult. With "OLT replace & WDM approach," NG-OLT requires transmitter and receiver for current PON also, which is more expensive than "OLT replace & TDMA approach," but may become practical within few years.

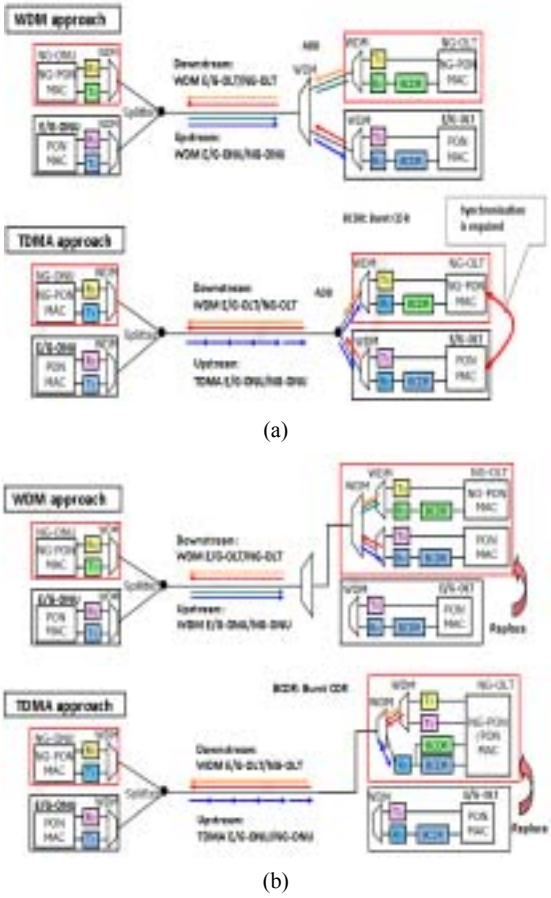

Fig. 4. PON migration Scenario from Current status to Next Generation PON Systems. (a) OLT add Scenario; (b) OLT replace Scenario [7]

In this paper, we proposed the architecture of a hybrid WDM/TDM PON based on "OLT add and WDM approach."

IV. PROPOSED SELF-RESTORED TREE-BASED HYBRID WDM/TDM PON

As we already understand, migration from the TDM-PON to WDM-PON will be essential for long term future. Many researchers reported different ways of migration using hybrid WDM/TDM-PON architectures [8]-[9]. A self-restored tree-based hybrid WDM/TDM-PON with duplex fiber system has been proposed here.

A. System Architecture

The architecture of the proposed system is shown in Fig. 5. The proposed architecture can serve multiple TDM and WDM-PONs using a single OLT. 1×16 AWGs are used in the OLT and in the second stage remote node (RN) for WDM-PONs. Each output from AWGs are separated by an optical circulator (OC), which is connected to the transmitter (Tx) and Receiver (Rx), to separate upstream and downstream transmission. 1×4 band splitting wavelength division multiplexing (BSWDM) filters have been used in the OLT, as well as in the first stage RN, which de-multiplexes and multiplexes downstream and upstream signals. The BSWDM filter can be realized, by cascading two AWGs and can be fabricated in a single chip, based on a planer light wave circuit (PLC) technology. The bandwidth and the number of splitting points are determined by connection configuration between AWGs. The BSWDM filter for the proposed architecture, consisted of one input and multiple outputs for multiple channels. It separates several channels and can be assigned to different subscriber groups. The advantages of using BSWDM filter are the independency of insertion loss with the splitting ratio; and the transmission pass-band of each port has wide bandwidth. A pair of 1:16 passive splitter is used at the second stage RN, for TDM-PON to de-multiplex and multiplex signals at a channel level, respectively.

Here we use the four ITU-T channels λ_1 - λ_4 (λ_1 = 1530 nm, λ_2 = 1550 nm, λ_3 = 1570 nm and λ_4 = 1590 nm), each of which can incorporate up to 16 dense wavelengths to address all ONUs of a PON. For providing downstream service to TDM-PON 1, the Tx in the OLT utilize the dense wavelength, positioned at the centre of the channel λ_1, to address all ONUs connected to TDM-PON 1, in a broadcasting manner, although it can use any wavelength within the same pass-band. For providing downstream service to WDM-PONs, each Tx of any WDM-PON will employ one of the 16 dense wavelengths for each channel λ_2 - λ_4. To avoid the need for laser sources at the ONUs, CLSs with reflective semiconductor optical amplifiers (RSOAs) can be used to implement colorless transceivers. One broadband light source (BLS) is placed in the OLT; it provides optical signals to ONUs, where the optical signals are modulated with the upstream data and are sent back to the OLT. The coupling device (CD) consists of 1 optical circulator and 1 WDM filter.

Single mode fibers (SMFs) are used as feeder and distribution fibers. To provide protection against fiber fault, one 1×2 optical circulator (OC) is used at OLT to split the signals into two paths: one of which will follow the working fiber and the other will follow the restoring fiber. Each ONU, has a 1×2 OS to select connecting the working or restoring fibers. Even though the ONU receives the downstream signal from restoring fiber path in normal state in parallel from the connecting fiber path, the OS automatically block the signals from the restoring fiber path. When the fault is occurred in the feeder fiber (from OLT to second stage RN), all ONUs will switch to reconnect the restoring fiber; but when the fiber fault is occurred in any distributed fiber (from second stage RN to each ONU), the OS of that particular ONU will switch only. To provide protection inside OLT, 1×2 optical switches (OSs) are added. In this way, protection against all kinds of fault is achieved.

B. Analysis of System Availability

The performance of the proposed system is quantified by calculating the system availability. The System un-availability U can be obtained as follows:

$$U = MTTR / MTBF \quad (1)$$

The System availability A can be obtained as follows:

$$A = 1 - U \quad (2)$$

where, MTTR and MTBF represents mean-time-to-repair and mean-time-between-failure respectively. The model for calculating the system availability is shown in Fig. 6. The values for calculating MTTR and MTBF are found in Table II [10]-[11].

For non-restorable WDM-PON (Fig. 6(a)), overall un-availability of a channel is calculated by the sum of the un-availabilities of an OLT, a feeder fiber, an AWG, a distribution fiber, and an ONU. Un-availability of OLT is calculated by the sum of the un-availabilities of a transceiver, a WDM filter, an AWG, 1 BLS, and a bidirectional coupling device (CD), which consists of 1 optical circulator and 1 WDM filter. So, un-availabilities are of non-restorable WDM-PON are as follows:

$$U_{OLT\text{-}WDM} = U_{TRx} + U_{OC} + U_{AWG} + U_{BLS} + U_{CD} = 67\times10^{-7}$$

$$U_{Overall\text{-}WDM} = U_{OLT} + U_{FF} + U_{AWG} + U_{DF} + U_{ONU} = 765\times10^{-7}$$

So, the availability of non-restorable WDM-PON is,

$$A_{Overall\text{-}WDM} = 1 - U_{WDM\text{-}Overall} = 0.9999235$$

For non-restorable hybrid WDM/TDM-PON (Fig. 6(b)),

$$U_{OLT\text{-}NR} = U_{TRx} + U_{OC} + U_{AWG} + U_{BSWDM} + U_{BLS} + U_{CD} = 75\times10^{-7}$$

$$U_{Overall\text{-}WDM/TDM\text{-}NR} = U_{OLT} + U_{FF} + U_{BSWDM} + U_{AWG} + U_{DF} + U_{ONU} = 781\times10^{-7}$$

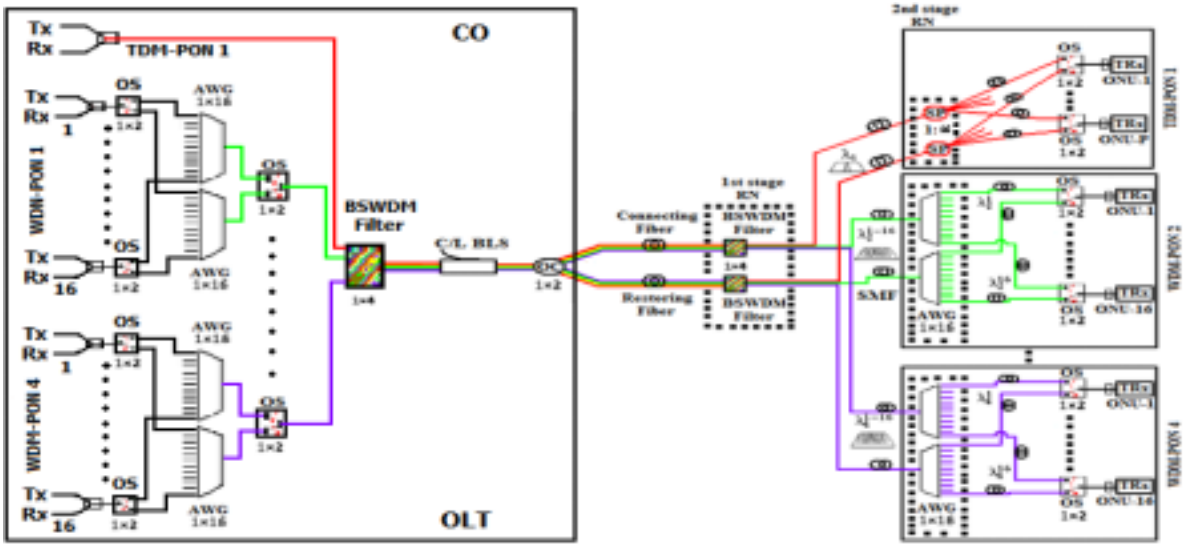

Fig. 5. Architecture of the proposed self-restored tree-based hybrid WDM/TDM-PON with duplex fiber.

Therefore, the availability of non-restorable WDM/TDM-PON is as follows:

$A_{WDM/TDM\text{-}NR} = 1 - U_{WDM/TDM\text{-}Overall} = 0.9999219$

Table II
MTTR, MTBF and Un-availability of Elements

Elements	MTTR (hours)	MTBF (Years)	Un-availability
Tx	2	630	3.62×10^{-7}
Rx	2	1630	1.4×10^{-7}
Optical switch (OS)	2	570	4×10^{-7}
AWG	2	570	4×10^{-7}
Optical circulator (OC)	2	570	4×10^{-7}
WDM filter	2	229	9.97×10^{-7}
BLS	2	57	40×10^{-7}
Feeder Fiber (20+5 km)	24	50	547.9×10^{-7}
Distribution Fiber (5 km)	24	200	137×10^{-7}

For the proposed self-restored tree-based hybrid WDM/TDM-PON (Fig. 6(c)):

$$U_{OLT\text{-}Proposed} = U_{TRx} + U^2_{AWG} + U_{BSWDM} + 2U_{OS} + U_{BLS} + U_{CD} + 2U_{OC}$$
$$= 83\times10^{-7}$$

$$U_{Overall\text{-}Proposed} = U_{OLT} + (U_{FF} + U_{BSWDM} + U_{AWG} + U_{DS})^2 + U_{OS} + U_{ONU}$$
$$= 96\times10^{-7}$$

So, the availability of the proposed architecture is,

$A_{Overall\text{-}Proposed} = 1 - U_{Proposed\text{-}Overall} = 0.9999904$

It is found that, the availability of the proposed architecture of Fig. 5, has increased by a factor of 8.

tecture (with and without protection), to provide services to the same number of users. Some components are essential for both cases. We consider the price of ONUs of WDM-PONs as X for all cases. On the other hand, we consider that, there are 16 users in each individual PON. The cost of the equipments and other related items are shown in Table III. They are collected from [11] and other sources. The cost for existing non-restorable architectures is calculated as follows:

$$C_{ENR} = 3\times C_{WDM\text{-}PON} + C_{TDM\text{-}PON}$$
$$= X + 3\times(2\times C_{AWG} + 16\times C_{TRx} + C_{BLS\&CD} + C_F + C_{BF} + C_{CO}) + (C_{TRx} + 16\times C_{ONU} + C_{SP\text{-}16} + C_F + C_{BF} + C_{CO})$$
$$= X + \$\ 174{,}200$$

The cost for existing architectures with restorable capability is calculated as follows:

$$C_{ER} = 3\times C_{WDM\text{-}PON\ (Restorable)} + C_{TDM\text{-}PON\ (Restorable)}$$
$$= X + 3\times(4\times C_{AWG} + 16\times C_{TRx} + 33\times C_{OS} + C_{BLS\&CD} + C_{OC1\times2} + 2\times C_F + 2\times C_{BF} + C_{CO}) + (C_{TRx} + 16\times C_{ONU} + 2\times C_{SP\text{-}16} + C_{OC1\times2} + 16\times C_{OS} + 2\times C_F + 2\times C_{BF} + C_{CO})$$
$$= X + \$\ 246{,}850$$

Now the cost for the proposed restorable tree-type hybrid WDM/TDM-PON is calculated as follows:

$$C_P = X + 12\times C_{AWG} + 49\times C_{TRx} + 115\times C_{OS} + 3\times C_{BSWDM} + C_{BLS\ \&\ CD} + C_{OC\_1\times2} + 2\times C_{SP\text{-}16} + 16\times C_{ONU} + 2\times C_F + 2\times C_{BF} + C_{CO}$$
$$= X + \$\ 176{,}250$$

From cost analysis, we found that the proposed architecture can provide protection with the same cost of existing non-restorable architectures. It provides more cost effective solution, if restorable capability is added with existing architectures. Besides these, it uses less space for central office compared to existing architectures.

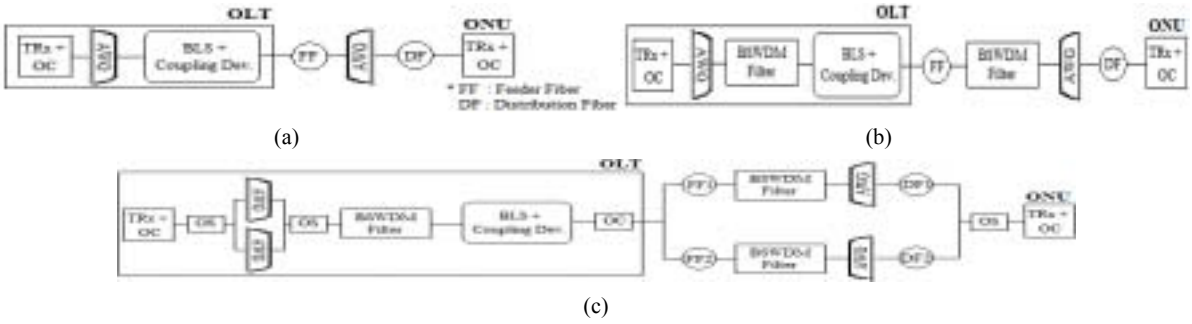

Fig. 6. The Schematic Architectures for calculation of availability. (a) The non-restorable WDM-PON; (b) The non-restorable hybrid WDM/TDM-PON; (c) The proposed self-restored tree-based hybrid WDM/TDM-PON

Table III
Tentative Costs of Different Equipments and Other Items

Name	Symbol	Cost (US $)
Transceiver and OC in OLT	C_{TRx}	650
AWG (1×16)	C_{AWG}	5,000
BLS and CD	$C_{BLS\&CD}$	5,000
Passive Splitter (1: 16)	$C_{SP\text{-}16}$	650
Optical Circulator (1×2)	$C_{OC1\times2}$	50
Optical Switch	C_{OS}	100
BSWDM Filter	C_{BSWDM}	10,000
ONU	C_{ONU}	400
Optical Fiber	C_F	2.5/km
Burying cost of fiber	C_{BF}	250/km
Office for OLT (CO)	C_{CO}	15,000

V. CONCLUSION

In order to mitigate the demand of present and future services, PON has become a promising solution for access networks. Even though, the current generation PONs, like E-PON and G-PON are sufficient for current services, some TDM-PONs with higher bit rates such as 10 GE-PON, XG-PON1, and XG-PON2 are considered for short-term future generation PONs. In order to provide much higher bandwidth to individual users, WDM-PON is considered for long-term future generation PONs. The proposed self-restored tree-based hybrid WDM/TDM-PON, provides cost effective solution with increased availability compared to other architectures. So, it can become a suitable solution for interoperability and migration from TDM-PON to WDM-PON.

REFERENCES

[1] C. H. Lee, W. V. Sorin, and B. Y. Kim, "Fiber to the home using a PON infrastructure," *J.Lightw. Technol.*, vol. 24, no. 12, Dec. 2006, pp. 4568-4573.

[2] P. Chanclou, S. Gosselin, J. F. Palacios, V. L. Alvarez, and E. Zouganeli, "Overview of the optical broadband access evolution: A joint article by operators in the IST network of excellence e- Photon/ONe," *IEEE Commun. Mag.*, vol. 44, no.8, Aug. 2006, pp. 29-35.

Gb/s) capacity based on wavelength-locked Fabry-perot Laser diodes," *Opt. Express*, vol. 16, no. 15, Jul. 2008, pp. 11361-11368.

[4] H. Suzuki, M. Fujiwara, T. Suzuki, N. Yoshimoto, H. Kimura, and M. Tsubokawa, "Demonstration and performance of colorless ONU for coexistence-type WDM-PON using a wavelength-tunable L-Band DWDM-SFP transceiver," *IEEE Photon. Technol. Lett.*, vol. 20, no. 19, Oct. 2008, pp. 1603-1605.

[5] D. K. Jung, S. K. Shin, C.-H. Lee, and Y. C. Chung, "Wavelength-division-multiplexed passive optical network based on spectrum-slicing techniques," *IEEE Photon. Technol. Lett.*, vol. 10, no. 9, Sep. 1998, pp. 1334-1336.

[6] H. Takesue and T. Sugie, "Wavelength channel data rewrite using saturated SOA modulator for WDM networks with centralized sources," *J. Lightw. Technol.*, vol. 21, no. 11, Nov. 2003.

[7] H. Mukai, "Physical layer requirements for smooth migration from the current FTTH," *Joint ITU-T/IEEE Workshop on Next Generation Optical Access Systems*, Jun. 2008,[Online]. Available: http://www.itu.int/dms_pub/itu-t/oth/06/13/T061 30000300002PDFE.pdf

[8] M. Zhu, W. Guo, S. Xiao, Y. Dong, W. Sun, Y. Jin, and W. Hu, "Design and performance evaluation of dynamic wavelength scheduled hybrid WDM/TDM PON for distributed computing applications," *Opt. Express*, vol. 17, no. 2, Jan. 2009, pp. 1023-1032.

[9] C. Bock, J. Prat and S. D. Walker, "Hybrid WDM/TDM PON using the AWG FSR and featuring centralized light generation and dynamic bandwidth allocation," *J. Lightw. Technol.*, vol. 23, no. 12, Dec. 2005, pp. 3981-3988.

[10] S. Verbrugge, D. Colle, M. Pickavet, P. Demeester, S. Pasqualini, A. Iselt, A. Kirstädter, R. Hülsermann, F. –J. Westphal, and M. Jäger, "Methodology and input availability parameters for calculating OpEx and CapEx costs for realistic network scenarios," *J. Opt.Netw.*, vol. 5, no. 6, Jun. 2006, pp. 509-520.

[11] J. Chen and L. Wosinska, "Analysis of protection schemes in PON compatible with smooth migration from TDM-PON to hybrid WDM/TDM-PON," *J. Opt. Netw.*, vol. 6, no. 5, May 2007, pp. 514-526.

Proceedings of 2009 12th International Conference on Computer and Information Technology (ICCIT 2009)
21-23 December, 2009, Dhaka, Bangladesh

Raman Gain Spectrum Equalization by Using Polarization-diversity Loop Filter

Md. Azmal Hossain, Md. Fahad Chowdhury†, and Feroz Ahmed‡

Department of Computer Science and Engineering, Military Institute of Science and Technology, Mirpur Cantonment, Dhaka, Bangladesh
†Grameenphone BD ltd., Gulshan, Dhaka, Bangladesh
‡School of Engineering and Computer Science, Independent University, Bangladesh, Baridhara, Dhaka, Bangladesh
azmal1002@yahoo.com, fahmed@secs.iub.edu.bd

Abstract

Raman amplifier plays an important role in wavelength division multiplexing (WDM) systems. The drawback of Raman amplifier is that the Raman gain spectrum is flat for very small narrowband. So, it is necessary to equalize the Raman gain spectrum to achieve the desire performance for the WDM systems. This paper has proposed an extrinsic gain equalization technique by using Polarization-diversity Loop Filter. It is found that by using PDLF, an equalize bandwidth of 90nm (1550nm – 1640nm) can be achieved with a gain ripple of 0.5dB.

Keywords: Raman amplifier, FRAs, WDM, Raman gain spectrum, PDLF, gain ripple.

I. INTRODUCTION

Fiber Raman amplifier (FRA) has attracted a considerable interest because of their potential applications as a discrete and distributed amplifiers in Wavelength-Division-Multiplexing (WDM) transmission systems. Besides their large bandwidth, the advantages of the Raman amplifier over other optical amplifiers include the possibility of operating in any wavelength region and superior noise performance of distributed amplification.

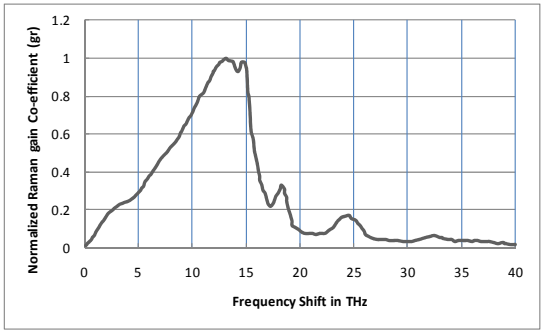

Figure 1: Normalized Raman Gain Co-efficient (g_r) Vs Frequency Shift (THz)

Raman gain spectrum in a conventional Single-Mode Fiber (SMF) has a gain bandwidth of 40THz; the spectrum is flat only over a narrow range of wavelengths. So, there is a significance power deviation among the amplified signals. Raman gain spectrum in a conventional Single-Mode Fiber (SMF) is shown in Figure 1, which needs to be equalized for the utilization in a long-haul WDM transmission network. Practically, gain flattening in Raman amplifier is achieved by using different intrinsic and extrinsic techniques. Usually, this is done by using properly chosen multiple pump wavelengths with specific power level.

Fiber design is one of the intrinsic gain flattening mechanisms and have reported in [1]-[2], in which refractive index of the fiber is control to achieve the goal. Pumping at different wavelengths and the use of available optical filters are two major extrinsic gain equalization methods. Such types of gain flattening technique have reported in [3]-[5]. Polarization-independent interferometric filter (PIIF) can flatten the gain within ±0.5% over a bandwidth of 43nm at the centre wavelength of 1550nm [5]. However, a simple approach of gain flattening technique for FRA with large bandwidth is still in demand. In this paper, a simple method for the equalization of Raman gain spectrum is proposed by means of Polarization Diversity-loop Filter (PDLF) and is achieved an equalized bandwidth of 90nm (1550nm-1640nm) with a gain ripple of 0.5 dB.

II. PROPOSED MODEL FOR THE EQUALIZATION OF RAMAN GAIN SPECTRUM USING POLARIZATION DIVERSITY LOOP FILTER

The schematic diagram of the proposed Fiber Raman amplifier is shown in figure 2. The model is constructed by interfacing RAs with a Polarization-diversity Loop Filter (PDLF).

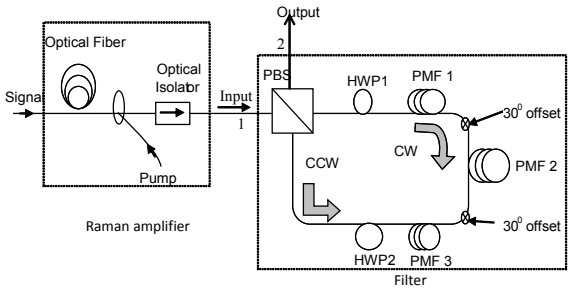

Figure 2: Proposed schematic for the broadband Raman gain flattened amplifier.

Broadband Raman gain flattened amplifier is constructed in association with Raman amplifier with

backward pumping configuration and PDLF, where PDLF is arranged at the output of the amplifier section in order to get equalized amplification of the WDM channels, and Optical Isolator prevents the backward flow of the optical signals. The filter consists of three sections of Polarization Maintaining Fiber (PMF1, PMF2, & PMF3) of equal length, two half wave plates (HWP1 & HWP2), and Polarization Beam Splitter (PBS). At the input of the filter (Port 1 of PBS), the PBS separates the amplified Optical signals into horizontally polarized and vertically polarized components. This separated polarized is then flows in clockwise (CW) and counter clockwise (CCW) direction respectively through the three sections of Polarization Maintaining Fiber (PMF1, PMF2, & PMF3) & two Half Wave Plates (HWP1 & HWP2) and thereby maximize the filter transmittance, t_{filter}. As a result, an equalized amplified output can be achieved at the output of the filter (port 2 of PBS).

The transmittance, t_{filter} of the filter can be expressed as follows [6]:

$$t_{filter}=\frac{9}{8}\left[\cos\left(2\theta_{h1}-2\theta_{h2}+\frac{\pi}{3}\right)\cos\Gamma+\frac{1}{6}\cos(2\theta_{h1}-2\theta_{h2})+\frac{\sqrt{3}}{2}\sin(2\theta_{h1}-2\theta_{h2})\right]^2\times(\cos\Gamma)$$

$$+\frac{9}{8}\left[\cos\left(2\theta_{h1}+2\theta_{h2}-\frac{\pi}{3}-2\theta_{p1}\right)(\cos\Gamma+\frac{1}{3})\right]^2(1-\cos\Gamma) \quad \text{-- (1)}$$

Where θ_{h1}, θh_2, and θ_{P1} are the field orientation (with respect to x axis) by HWP1, HWP2, PMF1, PMF2, and PMF3, respectively, and $\Gamma=2\pi BL/\lambda$, that is generated due to birefringence, B, Length, L of one PMF, and λ is the wavelength in vacuum.

The resultant Raman gain spectrum for the proposed scheme can be calculated using the following relationship:

Output (dB) = $10\log(g_r) + 10\log(t_{filter})$ ---------- (2)

Where, g_r is the Raman gain co-efficient and t_{filter} is the filter transmission parameter (transmittance).

III. RESULTS AND DISCUSSION

For the proposed scheme, the WDM signals are amplified by the Raman amplifier and the amplified signals are then passed through the PDLF, where these signals can be equalized by properly adjusting the filter's parameters.

In this paper, the Raman gain spectrum equalization is verified by writing simulation program in MATLAB® for the filter transmittance, t_{filter}, which is then combined with the normalized Raman gain co-efficient, g_r in order to achieve the desired equalized output. The filter parameters θ_{h1}, θh_2, and θ_{P1} & length of PMF and birefringence of PDLF are adjusted in such a way, so that the filter transmission parameter is higher for the lower values of Raman gain co-efficient and the transmission parameter becomes relatively smaller for higher values of Raman gain co-efficient. Such transmission characteristics of the filter can be found in figure 3, which is achieved by fine adjusting the field orientation for HWP1, HWP2, and PMF fiber length of 0.02m with birefringence value of $3.84\text{x}10^{-4}$.

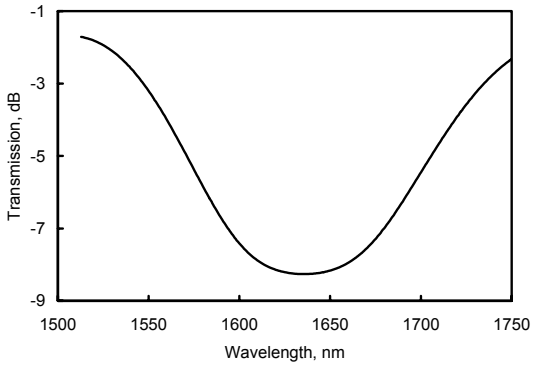

Figure 3: Filter Transmission Characteristic

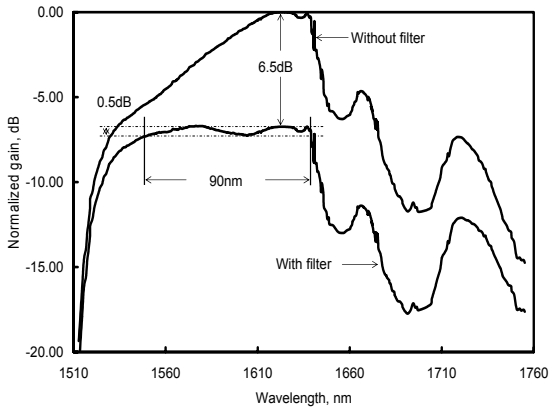

Figure 4: Comparison of the Raman gain spectrums: with and without using PDLF.

Figure 4 shows a plot of normalized Raman gain co-efficient as a function of wavelength for the Raman amplifier without filter and with filter. After the fine tuning of filter parameters, such as the field orientation for HWP1, HWP2, and PMF fiber length of 0.02m with birefringence value of $3.84\text{x}10^{-4}$, it is found that the 3dB Raman gain spectrum as large as 115nm (1530nm-1645nm) and 0.5dB Raman gain spectrum as large as 90nm (1150nm-1640nm) can be achieved for the filter with transmission characteristics (transmittance, t_{filter}) as like as shown in the figure 3. Here, the peak Raman gain coefficient is reduced by 6.5dB. The gain reduction and variation can significantly be reduced by adjusting the filter parameters for different wavelengths. However, there is a trade-off between gain flattened bandwidth and the values of Raman gain co-efficient. Higher the values of Raman gain co-efficient smaller the flattened bandwidth that can be achieved.

IV. CONCLUSION

A method for the equalization of Raman gain spectrum

has been proposed by means of Polarization-diversity Loop Filter (PDLF). An equalized bandwidth of 90nm (1550nm-1640nm) has been achieved with a gain ripple of 0.5dB for the reduction of normalized Raman peak gain of 6.5 dB. PDLF would be the most promising gain equalizer for long-haul & ultra-long haul fiber optic communication systems.

REFERENCES

[1] K. Thyagarajan and Charu Kakkar, "Fiber Design for Broad-Band Gain-Flattened Raman Fiber Amplifier", *IEEE Photonics Technology Letters*, vol. 15, No. 12, December 2003.

[2] Huai Wei, Zhi Tong, Muguang Wang, Shusheng Jian, "All optical method to achieve gain-clamping in broadband distributed fiber Raman amplifiers", *Optica Applicata*, vol. XXXIV, no. 3, 2004.

[3] Jonathan Hu, Brain S. Marks, Curtis R. Menyuk, " Flat-gain Fiber Raman Amplifiers Using Equally spaced Pumps", *Journal of Lightwave technology*, vol. 22, No. 6, Jun 2004.

[4] G. Ravet, A.A Fotiadi, M. Blondel, P. Mergret, V.M. Mashinsky, E.M. Dianov, "Gain Distribution in a short Raman fiber amoplifier", *Proceedings symposium ieee/leos, Benelux* Chapter, 2005, Mons.

[5] Andrew A. B. Tio, P. Shum, "Wide bandwidth flat gain Raman amplifier by using polarization-independent interferometric filter", *Optics Express*, vol.11, No. 23, Nov 17, 2003.

[6] Yong Wook Lee, Hyun-Talk Kim, and Yong Wan Lee, " Second-order All-fiber Comb Filter Based on Polarization-diversity Loop Configuration", *Optics Express*, vol.16, No. 6, March 17, 2008.

[7] Md. Azmal Hossain, "Study on Multi-wavelength Raman amplifier with Gain Equalization by Using Polarization-diversity Loop Filter", *Master's Thesis*, May 2009.

[8] R. C. Jones, "New calculus for the treatment of optical systems," *J. Opt. Soc. Am*. 31, 488-492 (1941).

[9] R. H. Stolen and E. P. Ippen, "Raman gain in glass optical waveguides," *Appl. Phys. Lett.*, vol. 22, no. 6, 1973.

[10] S. Namiki and Y. Emori, "Ultrabroad-band Raman amplifiers pumped and gain-equalized by wavelength-division-multiplexed high-power laser diodes," *IEEE J. Select. Topics Quantum Electron.*, vol. 7, Jan.–Feb. 2001.

[11] Y. Emori, Y. Akasaka, and S. Namiki, "100 nm bandwidth flat-gain Raman amplifiers pumped and gain-equalized by 12-wavelegnth-channel WDM laser diode unit," *Electron. Lett.*, vol. 35, pp. 1355–1356, 1999.

Proceedings of 2009 12th International Conference on Computer and Information Technology (ICCIT 2009)
21-23 December, 2009, Dhaka, Bangladesh

Cleaning and Clustering of Sensor Data by K-Means Algorithm for Efficient Query Processing *(Not Presented)*

Md. Muhidul Islam Khan, A.S. M. Latiful Hoque
Bangladesh University of Engineering & Technology, Dhaka-1000, Bangladesh
muhit_smart@yahoo.com, asmlatifulhoque@cse.buet.ac.bd

Abstract

The way of collecting sensor data will face a revolution when newly developing technology of sensor network will become fully functional. The program/stack memory and the battery life of sensor nodes are not suitable for complex data mining in runtime. Effective data mining can be implemented on the central base station, where the computational power is not generally constrained. Real-world sensor databases contain noisy, missing, and inconsistent data because of extraction from multiple, heterogeneous sources. Low-quality data will lead to low-quality mining results. We have designed a complete mining technique for Wireless Sensor Network (WSN) data. We have used Approximate Duplicate Record Detection method to remove noisy data from sensor data set. K-Means Algorithm has been used for data clustering. Simulation results have shown that our proposed mining technique for WSN Data improves the performance of query processing.

Keywords: Sensor Data, Cleaning, Clustering, K-Means Algorithm, Query Processing etc.

I. INTRODUCTION

Data mining is required for efficiently data retrieving from data sources. Sensor nodes are limited to battery power and memory space. A suitable technique is required for mining sensor data. Dirty data is a challenge for efficient mining and hence preprocessing is required. Various mining techniques can be applied to the preprocessed data. Clustering is required to make the searching efficient. Searching data from a huge database is not suitable. We need high quality data for high quality mining. Sensor networks collect information from sensor nodes which may be faulty. Data transmission errors, limited memory are also challenges for clean data. Duplicate records can hamper the preprocessed tasks. A suitable technique is required for cleaning the duplicate records. After preprocessing, clustering can be applied to data. If we can cluster the data it will make the query processing more efficient. In this paper, we have proposed data cleaning system based on Approximate Duplicate Record Detection method.

We have designed clustering system based on K-Means algorithm. Queries can be performed on the clustered data that improves the query performance. There are some limited works on mining technique for sensor data. Section 2 mentions some related works on this. Section 3 discusses the proposed mining technique. Result and discussion is given in section 4. Section 5 is the conclusion.

.

II. RELATED WORKS

Several works and studies have been performed regarding data mining in WSN Data. These are Artificial Neural Network based approach [1], Kohonen Map Implementation [2], Adaptive Modular Approach [3], Local Hill Climbing Approach [4]. Artificial Neural Network Implementation [1] presents two possible implementations of the ART and FuzzyART neural networks algorithms. It is unsupervised learning methods for categorization of the sensory inputs. They are tested on data obtained from a set of several motes, equipped with several sensors. A framework for building and deploying predictors in sensor networks that pushes most of the work out to the sensors themselves. Kohonen Map Implementation [2] enables sensors to respond to changes in data by relearning when their local predictive accuracy changes. This creates new possibilities, such as allowing sensors to predict only some target classes. Adaptive Modular Approach [3] is a two-layer modular architecture to adaptively perform data mining tasks in large sensor networks. Lower layer performs data aggregation and upper layer performs local learning technique. Local Hill Climbing Approach [4] shows that in some cases hill climbing can be solved using a local algorithm. Local algorithms are important for sensor networks because they have superb message pruning capabilities and because they perform their entire computation in-network.

978-1-4244-6283-4/09/$26.00 ©2009 IEEE

In Artificial Neural Network Implementation, two models are presented for categorization of sensory inputs. There is no clustering and cleaning technique. In Kohonen Map Implementation, it allows sensors to predict only some target classes. It is not a proper data mining technique. In Adaptive Modular Approach, it gives a structure only. Data mining technique is not purely defined. In Local Hill Climbing Approach, it develops local algorithms for sensors which is capable of solving only the centralized problem. It solves a particular problem. Nothing is mentioned about clustering technique.

III. PROPOSED MINING TECHNIQUE:

Our proposed mining technique works on preprocessed data. The features of the proposed mining technique are as follows:

- Preprocessing of sensor data. Approximate duplicate record detection is used to identify and remove the duplicate records.
- Data Clustering is performed on both clean and dirty data based on K-Means Algorithm. It reduces the query response time over the network.

A. Proposed Technique for Data Cleaning

Data cleaning is also called data cleansing or scrubbing. To state it simple, it means to clean the errors and inconformity, i.e. to detect and clean the wrong, incomplete and duplicated data by means of statistics, data mining or predefined cleaning rules, so as to improve data quality. The principle of data cleaning is illustrated in Figure 1.

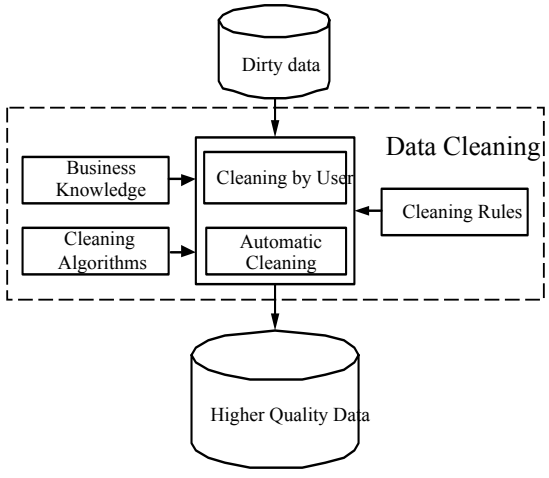

Figure 1: The Principle of Data Cleaning

In order to reduce the redundant information from the electronic data acquisition, it is important to clean approximately duplicated records. The approximately duplicated records refer to the same real-world entity, which cannot be confirmed by the system of database for its differences of formatting and spelling. Figure2 shows the principle of approximately duplicated records cleaning.

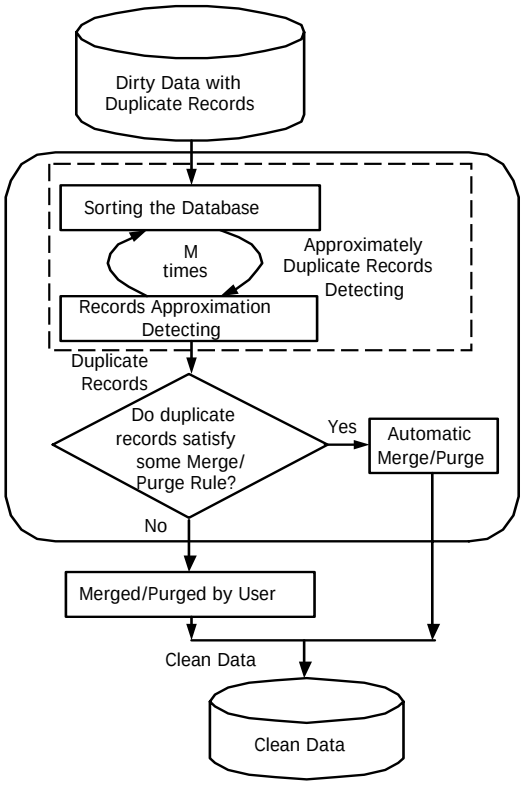

Figure 2: The Principle of Approximately Duplicated Records Cleaning

The process of approximately duplicated records cleaning can be described as follows:

Firstly, the data to be cleaned was input into system. Then, data cleaning is performed. The module of sorting the database introduces sorting algorithm for uncleaned records to sort the database. Having sorted the database, the module of records approximation detecting introduces approximation detecting arithmetic from arithmetic base. Approximation detecting is done in the neighboring scope so as to 1) calculate the approximation of records, 2) to determine whether the records are approximately duplicated ones. To detect more approximately duplicated records, sorting the database once is inadequate. It is necessary to adopt multi-round sorts, multi-round contrasts, with a different key for a different round, before the integration of all the detected approximately duplicated records. In this way, the

detection of approximately duplicated records is completed. Finally, the integrated disposal of approximately duplicated records was completed according to the predefined purge/merge rules for each detected group of approximately duplicated records.

The key steps of approximately duplicated records cleaning:

From Figure 2, the key steps of approximately duplicated records cleaning can be summarized as: sorting the database → records approximation detecting → purge/merge of approximate duplicate records, the functions which include the following functions:

(1) Sorting the database

To locate all the duplicated records in data source, it is essential that each possible record pair be contrasted. However, the detection of approximately duplicated records becomes a costly operation. When the amount of acquired electronic data increases enormously, this will result in an invalid and unpractical approach. To decrease the number of record contrasts, and to increase the effectiveness of detection, the general approach is to contrast the records within a limited range, i.e. to sort the database first, then to contrast the records in the neighboring range.

(2) Records approximation detecting

It is an essential step to detect the approximation of records in approximately duplicated record cleaning. By detecting the approximation of records, we can determine whether two records are approximately duplicated records.

(3) Approximately duplicated record purge/merge

Having completed the detection of approximately duplicated records, the detected duplicated records should be processed. For a group of approximately duplicated records, two methods are applied:

Method 1: regard one record true in the approximately duplicated records, the rest false. The mission is, therefore, to delete the duplicated records in the database. In this situation, the following measures can be taken:

Manual rules

Manual rules refers to find the most accurate record to store manually from a group of approximately duplicated ones and delete all the rest from the database. This is the easiest.

Random rules

Random rules refers to select any one record to store randomly from a group for approximately duplicated ones and delete all the rest from the database.

The latest rules

In many cases, the latest records can better represent a group of approximately duplicated records. For example, the more up-to-date the information is, the more accurate it may be. The address of daily used accounts is more authorized than that of the retired accounts. So it means to choose the latest record from a group of approximately duplicated records and delete the others.

Integrated rules

Integrated rules refers to choose the most integrated record to store from a group of approximately duplicated ones and delete the others.

Practical rules

The more repeated the information is, the more accurate it may be. For instance, if, in three records, the phone numbers of two suppliers are the same, it is most likely that the repeated numbers are accurate and reliable. According to this, practical rules refers to choose the record whose matching number is the largest to store and delete the other duplicated records.

Method 2: regard each individual approximately duplicated record as a portion of the whole information source, the purpose of which is to integrate a group of duplicated records to produce another more complete group of new records. This approach is generally manually done.

It is very important to complete data cleaning quickly. Therefore, it is essential to improve the efficiency of approximately duplicated records detection. From the previous analysis, it is clear that approximate detection between records still remains a major problem in approximately duplicated records detection. The key steps lie in the approximate detection between each field, whose efficiency has an impact on the whole algorithmic efficiency.

Generally, edit distance is applied. Since the complexity of distance editing is $O(m \times n)$, without an effective filtration to reduce

unnecessary edit distance when the quantity of data is enormous, this may lead to over-length of detecting. Therefore, to increase the efficiency of approximately duplicated records detection, the technique of length-filtering method can be adopted to reduce unnecessary edit distance. Length-filtering method is based on the following theorem:

Given any two character strings, *x*, *y*, the length of which are respectively |*x*|, |*y*|. If the maximum edit distance is *k*, the difference between the lengths of the two character strings cannot exceed *k*, i.e. $\|x| - |y\| \le k$.

Figure 3 shows the Approximate Duplicate Record Detection Algorithm.

Input: two records: R1 and R2, the threshold of the two fields is δ1, the threshold of the two records is δ2. (the two values are to determine whether the two records are approximate)
Output: True/False
Approximate Duplicate Record Detection Algorithm:

Step 1: Assign initial value for record distance Rdist = 0
Step 2: Find the field number of Record R1 and assign it to n
Step 3: For i=1 to n repeat steps 4,5 and 6
Step 4: If R1.Field[i] == NULL OR R2.Field[i] == NULL
Decrease the field number by 1
continue
Step 5: Assign s_int = length(R1.Field[i]) and t_int = length(R2.Field[i])
If (s_int - t_int) > δ1
Return False
Else
Find the distance between field of R1and R2
Step 6: If (distance) > δ1
Return False
Else
Add this distance to the record distance
Step 7: Divide record distance by record field number
Step 8: If record distance < δ 2
Return True
Else
Return False

Figure 3: Approximate Duplicate Record Detection Algorithm

The distance between two fields can be calculated by Euclidean distance.

Euclidean: $dis(t_i, t_j) = \sqrt{\sum_{h=1}^{k} (t_{ih} - t_{jh})^2}$

B. Clustering Technique

Clustering is similar to classification in that data are grouped. The groups are not predefined. The grouping is accomplished by finding similarities between data according to characteristics found in the actual data. Elements from different clusters are not alike. The distance between points in a cluster is less than the distance between a point in the cluster and point outside it.

K-means is an iterative clustering algorithm in which items are moved among sets of clusters until the desired set is reached.

A high degree of similarity among clusters is obtained, while a high degree of dissimilarity among elements in different clusters is achieved simultaneously.

The cluster $k_i = \{ t_{i1}, t_{i2}, \ldots\ldots t_{im} \}$ mean can be defined as $m_i = \frac{1}{m} \sum_{j=1}^{m} t_{ij}$.

Algorithm:
Input:
$D = \{t_1, t_2, \ldots\ldots t_n\}$ (set of elements)
K (number of desired clusters)
Output:
K (set of clusters)
K-means algorithm:

Assign initial values for means
$m_1, m_2, \ldots m_k$;
repeat
Assign each item t_i to the cluster which has the closest mean;
Calculate new mean for each cluster;
until convergence criteria is met;

Figure 4: K-Means Algorithm

IV. RESULT AND DISCUSSION:

We have implemented Approximate Duplicate Record Detection Algorithm in Java platform. We have used both dirty and clean data for our experiment purpose.

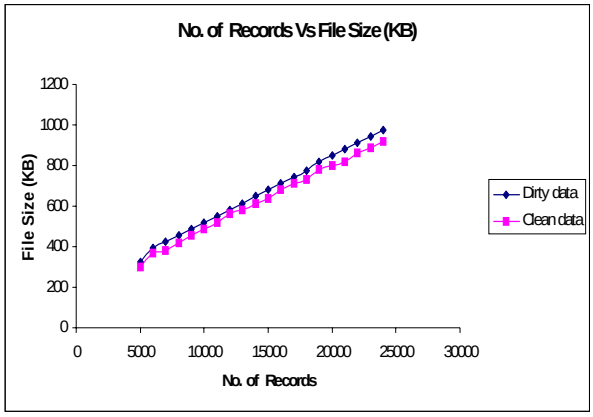

Figure 5: No. of Records Vs File Size (KB)

We have applied K-Means Clustering technique to cluster sensor data. The data set that we have used is available on the site www.engr.udayton.edu.

	Initial Cluster centers			
	1	2	3	4
V4	-99.00	60.30	92.50	28.10

Iteration History

Iteration	Change in Cluster Centers			
	1	2	3	4
1	.000	.205	11.720	11.595
2	.000	.461	3.112	3.979
3	.000	.057	.901	1.178
4	.000	.185	.163	.435
5	.000	.168	.000	.214
6	.000	.134	.041	.122
7	.000	.168	.054	.149
8	.000	.119	.054	.087
9	.000	.045	.014	.040
10	.000	.060	.000	.073

Figure 6: K-Mean applied to Dirty Data

	Initial Cluster centers			
	1	2	3	4
V4	.00	61.80	92.50	31.10

Iteration	Change in Cluster Centers			
	1	2	3	4
1	.000	.556	11.322	10.120
2	.000	.524	3.068	3.407
3	.000	.080	.903	.949
4	.000	.003	.292	.323
5	.000	.055	.128	.073
6	.000	.018	.020	.000
7	.000	.000	.000	.000

Figure 7: K-Mean applied to Clean Data

The clustering technique as in figure 5 has been applied for both noisy and clean data. The simulation result has shown that the number of iterations required is less for clean data than for noisy data.

For same number of clusters and same number of data we get better performance for clean data.

For Noisy data-

- The number of Iterations required is 10
- The minimum distance between initial clusters is 32.200

For Clean data-

- The number of Iterations required is 7
- The minimum distance between initial clusters is 30.700

Less iterations is required for clean data cause after removing dirty data, K-Means has been applied to reduced size of data. As the size of data has been reduced the minimum distance between initial clusters is also less than dirty data.

So, data cleaning can improve the effectiveness for data mining. SPSS is used as a simulator.

We have performed clustering algorithm both on noisy and clean data. Figure 8 shows comparison between non clustered dirty data and non clustered clean data. Figure 9 shows comparison between clustered dirty data and clustered clean data.

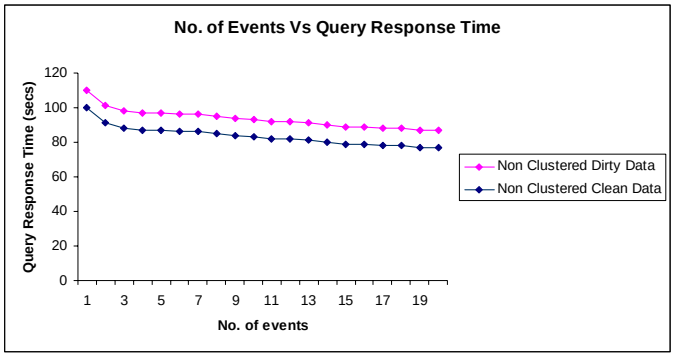

Figure 8: No. of Events Vs Query Response Time

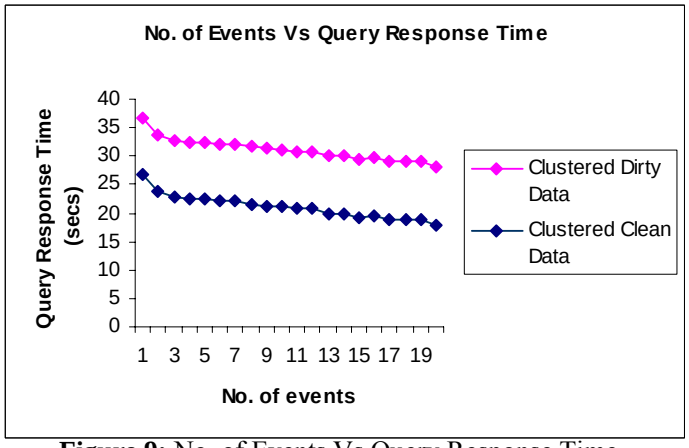

Figure 9: No. of Events Vs Query Response Time

The query response time has been decreased with the increasing number of events cause we have applied both clustered and non clustered data on the WSN protocol A-sLEACH. In the A-sLEACH cluster head takes the charge of query response after some rounds and they handle the operations. So, query response time has been decreased with the increasing of events.

V. CONCLUSION

For efficient mining of sensor data clean data plays an effective role. In this paper, redundant data has been removed by approximately duplicated records detection and the K-mean algorithm has been applied which will discover knowledge from pre-processed sensor data with less time requirement. Approximately Duplicate Record Detection has been applied on both dirty and clean data. Clean data has reduced the file size in every cases. Clustering technique has been applied both on dirty and clean data. Comparisons have been performed for clustered and non clustered data. The number of iterations both for dirty and clean data has also been compared. Better results have come for cleaned and clustered data.

REFERENENCE

[1] C. Virginio, L. Luca and L. Paolo, "Challenges for data mining in distributed sensor networks", European Commission-Joint Research Centre, IPSC, TP210 via Fermi 1,21020 Isapa, Italy. Pattern Recognition, 2006. ICPR 2006. 18th International Conference on Volume 1, Issue , 0-0 0 Page(s):1000 – 1007.

[2] K. Andrea and D. Danco, "Data mining in wireless sensor networks based on artificial neural-networks algorithms", Computer Science Department, Faculty of Electrical Engineering, Skopje, Macedonia. 2005 SIAM International Conference on Data Mining, Sutton Place Hotel, New Port Beach, CS, April 21-23, 2005.

[3] M. Sabine and S. David, ''A distributed approach for prediction in sensor networks'', School of Computing, Queen's University. 2005 SIAM International Conference on Data Mining, Sutton Place Hotel, New Port Beach, CS, April 21-23, 2005.

[4] B. Gianluca and B. Yann-Ael, "An adaptive modular approach to the mining WSN data", ULB Machine Learning Group, Universite Libre de Bruxelles, Belgium. 2005 SIAM International Conference on Data Mining, Sutton Place Hotel, New Port Beach, CS, April 21-23, 2005.

[5] Computer Science Dept., Technion-Israel, "Local hill climbing in sensor networks", 2005 SIAM International Conference on Data Mining, Sutton Place Hotel, New Port Beach, CS, April 21-23, 2005.

[6] For data files- http://www.engr.udayton.edu

Proceedings of 2009 12th International Conference on Computer and Information Technology (ICCIT 2009)
21-23 December, 2009, Dhaka, Bangladesh

Data Exchange: Algorithm for Computing Maybe Answers

(Not Presented)

S. M. Masud Karim
Computer Science and Engineering Discipline, Khulna University, Khulna 9208, Bangladesh
masud@ku.ac.bd

Abstract

The accuracy and completeness of data exchange largely depend on the semantics of the data exchange problem and are best verified by answering queries over target instances in such a way that is semantically consistent with the source data. The concept of certain answers is used in the definition of the semantics of answering queries. But as certain answers are defined as a relation without null values, the approaches for answering queries over databases do not always lead to semantically correct answer. In this paper, an algorithm is presented that produces all possible semantically correct answers to simple positive queries under the closed world assumption. In order to obtain all possible semantically correct answers, maybe answers are considered along with certain answers. As there may be infinitely many maybe answers, sophisticated and restricted representation techniques are used to represent them compactly. Then using the compact representation, an algorithm to compute possible answers incrementally is designed. Finally the algorithm is implemented for a fragment of relational algebra.

Keywords: Close World Assumption, Data Exchange, Maybe Answers, Query Answering.

I. INTRODUCTION

Data exchange, also known as *data translation* is the problem of transforming a given instance of a source database schema to an instance of a target database schema by satisfying a set of constraints and reflecting the given source data as accurately as possible. As huge amount of data are to be transferred over the web and web-data are stored in different formats (e.g., relational database schemas, semi-structured schemas, various scientific formats etc.), the tract of data exchange has expanded recently. A Detail overview of the recent advances in schema mapping, data exchange and metadata management is provided in [7].

Combining the specifications provided in [1, 4, 7, 8, 9], it can be stated that a *data exchange setting* is a triple $E = (\sigma, \tau, \Sigma)$, where σ is the *source* schema, τ is the *target* schema and Σ is a set of constraints. The goal of a *data exchange problem* associated with a data exchange setting is to find a target instance *T* of a given source instance *S* such that *S* and *T* satisfy all constraints in Σ and produce answers to the queries written over τ in such a way that is semantically consistent with the information in *S* over σ. The target instance *T* is called a *solution* of the data exchange problem.

One of the most crucial observations of data exchange problem is that a given instance of data exchange problem may have *infinitely many solutions*; again there may be *no solution*. Another crucial observation of data exchange problem is the conceptual difficulty associated with the *context of query answering*. As there may be many solutions for a given instance of data exchange problem, each will produce its own answer for a specific query, that means, there will be as many answers for a specific query as the solutions. Therefore, the question comes into attention that what makes an answer 'right'?

According to [7], a solution that carries *no more and no less* information is the desired solution. In [3], an algebraic specification is given to select the 'most general possible' and preferred solution, universal solution among all solutions. Fairly general and practical conditions that ensure the existence of a universal solution are identified and algorithm for efficiently computing a *canonical universal solution* using the well known *chase procedure* is developed. They extend their work in [4] and proposed the 'best' universal solution as the best solution for data exchange. The notion of core of a structure and the concept of *isomorphism* are used to get the best solution, *core of universal solution* (in short, *core*).

The concept of *certain answers*, the answers that occur in the intersection of all possible answers is used in the definition of the semantics of answering queries. It was shown in [3, 4] that the canonical universal solution and the core are good for answering conjunctive queries with inequalities. But as certain answers are defined as a relation without *null values*, approaches for answering queries over databases lead to semantically incorrect answers. In [8], the concept of both *maybe answers* (the union of all possible answers) and certain answers are combined at the levels of individual solutions and all solutions.

In [3, 4], *Open World Assumption* (OWA) is used, while *Closed World Assumption* (CWA) is considered as the standard assumption for data exchange in [8]. While OWA permits new facts to be added to the databases, CWA does not allow adding new facts to database except those consistent with one of the incomplete tuples in the database. In [5], an alternative approach based on the concept of *locally-controlled open world database* is introduced. In this approach, portions of a database in the traditional closed world database can be defined as open. This concept is used in [9] as a standard for schema mapping and data exchange.

The purpose of this paper is to present an algorithm that

produces all possible semantically correct answers to queries posed against relational schemas under the closed world assumption. This purpose is associated with specific objectives: (i) As maybe answers are inherently infinite, a sophisticated and restricted finite representation has been developed in order to provide the user an upper approximation for a query, (ii) an algorithm has been designed to compute possible answers incrementally, and (iii) finally the algorithm has been implemented for a fragment of relational algebra (i.e. a simple set of SQL queries).

II. LITERATURE REVIEW

A. Data Exchange Problem

A data exchange setting is a triple $E = (\sigma, \tau, \Sigma)$, where σ is the *source* schema, τ is the *target* schema (it is assumed that there is no common relation names in σ and τ) and Σ is a set of constraints. The set Σ is a combination of two sets, denoted $\Sigma = \Sigma_{st} \cup \Sigma_t$, where Σ_{st} provides the specification of the relationship between the source and the target schemas (i.e., source-to-target dependencies, in short STDs) and Σ_t expresses data dependencies on the target schema. The focus of attention is restricted only to two types of constraints: tuple-generating dependencies (TGDs) and equality-generating dependencies (EGDs). The data exchange setting in consideration is assumed to be associated with a finite set of TGDs as Σ_{st} (i.e., STDs) and a finite set of EGDs and target TGDs as Σ_t. When writing a TGD or EGD, the universal quantifiers are usually omitted.

Definition 2.1 (Data Exchange Problem): A *data exchange problem* associated with a data exchange setting *E* is the function problem: find a target instance *T* of a given source instance *S* such that *S* and *T* satisfy all constraints in σ, provided that such a target instance exists. •

The target instance *T* is called a *solution* of *S* under the data exchange setting *E*. It is showed in [7] that, if there is no constraint (dependency in the form of EGDs and TGDs) on target schema, then solutions always exist.

B. Database with Incomplete Information

The most common concept used for modeling incomplete information in the context of relational databases is *null value*. A null value is placed for an attribute of a relation whose value cannot be represented by an ordinary constant. The *unknown* null value represents that the attributes value is missing or not known. The *nonexistent* null value represents that value of an attribute in a tuple does not exist. Most of the researchers consider the null values as existent but unknown in the context of data exchange. Assume that CONSTANT is the set of all ordinary values (constants). Let NULL be an infinite set of values, called marked null values such that CONSTANT ∩ NULL = ∅. A database instance with incomplete information is an instance whose domain is a subset of CONSTANT ∪ NULL. The source instances are complete relational databases, i.e., their domains are subsets of CONSTANT and target instances are relational databases with incomplete information.

C. Valuation

A *valuation* is a partial map v: NULL → CONSTANT. If *T* is an instance with incomplete information and *v* is a valuation defined on all the nulls in *T*, then $v(T)$ be the instance of the same schema over CONSTANT in which every null $\perp$ present in *T* is replaced by $v(\perp)$. Then a potential infinite object $\text{REP}(T)$ can be defined as

$$\text{REP}(T) = \{v(T)\}, \text{ where } v \text{ is a valuation}$$

D. Universal Solution

The notation of homomorphism is used to provide the algebraic specifications of universal solution and core.

Definition 2.2 (Homomorphism): For any two instances T_1 and T_2 over any arbitrary schema, where domains of instances are subsets of CONSTANT ∪ NULL, a *homomorphism* $h: T_1 \to T_2$ is defined in [3] as a mapping function from CONSTANT ∪ NULL (T_1) to CONSTANT ∪ NULL (T_2) such that:

- For every constant $c \in$ CONSTANT, $h(c) = c$.
- For every fact $P(t)$ of T_1, there is a fact $P(h(t))$ in T_2, where for any $t = (x_1, x_2, ..., x_n)$, $h(t)$ is defined as $(h(x_1), h(x_2), ..., h(x_n))$. •

This definition of homomorphism also implies mapping from NULL to CONSTANT ∪ NULL. In order to obtain the same complete instances as $\text{REP}(T)$, this definition of homomorphism is slightly modified in [8] by assuming the mapping from NULL only to NULL and then a partial valuation is performed.

Definition 2.3 (Universal Solution): A solution *T* for a source instance *S* is called a *universal solution* for *S*, if for every solution T' for *S*, there is homomorphism $h: T \to T'$. •

The canonical universal solution of a given source instance *S* is denoted as $\text{CANSOL}(T)$. The concept of universal solution suffers from the fact that there may be multiple, non-isomorphic universal solutions for a source instance under a given data exchange setting. Therefore, the notation of cores of universal solutions is defined in [4] and it is denoted as CORE(*T*) for solutions *T*.

E. Data Exchange Solutions under CWA

In [8], CWA is chosen as the standard assumption for data exchange and *CWA-solutions* are considered as the solutions. The concept of *justification* is taken into account in [8, 9] for generating the CWA-solutions. This can easily be verified that CWA-solutions are universal solutions in the terminology of [3]. For every CWA-solution *T*, the following inclusions hold:

$$\text{REP}(\text{CORE}(T)) \subseteq \text{REP}(T) \subseteq \text{REP}(\text{CANSOL}(T)).$$

F. Certain Answers and Maybe Answers

The *certain answers* of a query Q are the tuples that occur in the intersection of all $Q(T)$ on all the solutions T. If the collection of all solutions for S under the data exchange setting E is defined as SOLUTION(E, S), the certain answers of Q on T with respect to E, denoted CERTAIN(Q, S), is a set

$$\text{CERTAIN}(Q, S) = \cap \{Q(T) \mid T \in \text{SOLUTION}(E, S)\}.$$

On the other hand, the *maybe answers* of a query Q are the tuples that occur in the union of all answers of the query $Q(T)$ on all the solutions T in SOLUTION(E, S). The maybe answers of Q on T with respect to E, denoted MAYBE(Q, S), is a set

$$\text{MAYBE}(Q, S) = \cup \{Q(T) \mid T \in \text{SOLUTION}(E, S)\}.$$

To evaluate Q on an instance T with nulls, the set $\{Q(R) \mid R \in \text{REP}(T)\}$ is normally considered. The lower and upper approximations are defined respectively as

$$\nabla Q(T) = \cap \{Q(R) \mid R \in \text{REP}(T)\},$$

$$\Delta Q(T) = \cup \{Q(R) \mid R \in \text{REP}(T)\}.$$

G. Semantics of Query Answering

There are primarily two different ways to obtain the answers to queries over different solutions: (i) by computing the certain answers which are true for all solutions (this semantics used in [2]) and (ii) by collecting tuples true in some solutions. The combination of certain and maybe answers at the levels of individual solutions and all solutions give rise to four reasonable semantics for query answering. For a source instance S under a data exchange setting E, these are defined in [8] as *certain answers semantics*, *potential certain answers semantics*, *persistent maybe answers semantics* and *maybe answers semantics*.

III. PROPOSED METHOD

In the query answering scenarios, the two extremes semantics $\text{CERTAIN}_{\nabla}(Q, S)$ and $\text{MAYBE}_{\Delta}(Q, S)$ are used for providing approximation to query answers. Since both can be computed over CANSOL(S) [8], and the CANSOL(S) is a database instance formed with naive evaluation; the query answering can be easily done for positive queries. Simple positive SQL queries considered for the experiment are of the following general format:

SELECT *Attribute-list*

FROM *Relation-list*

WHERE *Predicate*.

Relation-list consists of any n relations R_i with $1 \le i \le N$. *Attribute-list* has one or more of $A_{ij}(s)$, where A_{ij} stands for the j-th attribute from R_i. The value of j depends on the arity of the associated relation R_i and it may be different for different relations, i.e., for different values of i. *Predicate*, denoted by P consists of $p_1 \wedge p_2 \wedge \cdots \wedge p_m$, i.e., conjunction of m atomic expressions of the form p: X **op** Y, where **op** is any binary operator from the set $\{=, >, <, \ge, \le\}$. One of the two operands X and Y of p: X **op** Y must be an attribute from any R_i. In order to distinguish between projection and predicate attributes, a superscript is used: s for projection-attributes (attributes in SELECT clause) and w for predicate-attributes (attributes in WHERE clause). The other operand may be either any constant value from C_k with $1 \le k \le m$ or another attribute from any R_i. When both operands are of the form A_{ij}^{w}, they might be either from the same relation or two different relations.

A. Computing Certain Answers

When a positive relational query Q is posed over a schema τ, the certain answers $\nabla Q(T)$ are computed using the naive evaluation method [6] on the canonical solution T over τ. The null variables are treated as constants and general query evaluation is applied to T in order to get $Q(T)$. Finally, the tuples with nulls are discarded to get $\nabla Q(T)$.

B. Computing Maybe Answers

The system is initialized with a canonical solution and a pre-processing metadata (the pre-processing is explained later). All the attributes stored in the relational databases are of type *text* (or *varchar*). The constants are inserted in its original form in texts. Each null is represented by distinct text with a common prefix pattern $\_n\_$. Nulls of an attribute domain are distinguished by numbering (1, 2, ...) and nulls of different attribute domains are by naming.

B.1. Pre-processing

In order to reduce the work load during the computation of maybe answers, pre-processing can be applied to a canonical solution T. Pre-processing may include identification of null/constant presences for attributes, computation of the common attributes in relations etc. Pre-processing on the attributes uses two Boolean parameters, *hasNull* and *hasConstant*, confirming whether a specific attribute has null values and constant

values, respectively. Note that, out of the four combinations for the possible values of these two parameters, (TRUE, TRUE) is most common in data exchange. The combination (FALSE, FALSE) is an impossible one and hence is never used. The attributes with no nulls, having parameters value (FALSE, TRUE) and with only nulls with parameters value (TRUE, FALSE) are vital in data exchange.

B.2. Query Rearrangement

As *Q*s are simple positive queries, they can easily be rearranged to obtain better performance in join operation. In order to reduce the storage complexity during the join operations, the projection can be pushed in, i.e., projection is performed before join operation. The concept of restriction will be useful during the query rearrangement process.

Definition 3.1 (Restriction): The set of all atomic expressions p_l with $1 \le l \le m$ is called the *restriction* of P to R_i, if all the attributes used in the atomic expressions are only from R_i. •

Restriction of P to R_i is denoted by $\text{REST}_P(R_i)$. This definition can be extended for a relation-pair.

Definition 3.2 (Extended Restriction): The extended restriction of P to a relation-pair (R_i, R_j) with $i \neq j$ is the set of all atomic expressions p_l in P that include only attributes of $R_i \cup R_j$. •

When a query Q is posed to any n relations of an instance T with N relations $R_1, R_2, \cdots, R_N$,

- First projection operation is performed on each of the n relations using $A_{ij}^s \cup A_{ik}^w \cup A_{il}^c$, where A_{il}^c are the attributes in R_i that also present in at least one of the $(n-1)$ relations (superscript c stands for common attributes in different relations). Note that three different j, k, l are used to avoid ambiguity, but they can also represent the same value(s).
- Then, the restrictions of P to relations and extended restrictions of P to relation-pairs are identified. Finally, each of the $p \in \text{Rest}_P(R_i)$ is applied to R_i using valuation to compute the tuples incrementally upon which $p \in \text{Rest}_P(R_i)$ holds.

B.3. Join Operations

The basic idea for the null variables in the join operation as follows: should look like:

- Nulls of different attribute domains are different i.e., $\perp_{ik} \neq \perp_{jl}$ for any $i \neq j$ and any k, l,
- Nulls of the same attribute domain are same i.e., $\perp_{ki} \neq \perp_{kj}$ for any $i \neq j$ and any fixed k.

Now join operation, referred to as *join around nulls*, in short JAN and denoted by $\otimes$ can be described as (i) to perform the Cartesian product on the targeted relations, and (ii) to discard the tuples with different constant values for the common attribute(s).

B.4. Compact Representation

After performing query rearrangement and join operation, a combined relation is obtained. Then extended restrictions of P to relation-pairs are applied on the combined relation. Finally by performing projection operation using projection attributes on the combined relation, an *intermediate representation*, W of maybe answers $\Delta Q(T)$ is obtained. Finally, $\Delta Q(T)$ can be expressed as

$$\cup \{ \text{REP}_x(\bar{t}) \mid \bar{t} \in W \} = \Delta Q(T).$$

B.5. Putting All Together

First, the query Q is analyzed and decomposed to get A_{ij}^s, A_{ik}^w, A_{il}^c of all n query-relations.

Next, for each relation R_i of the n query-relations, where $1 \le i \le N$, do the followings:

- Perform projection operation on R_i using $A_{ij}^s \cup A_{ik}^w \cup A_{il}^c$, where j, k, l are integers.
- Identify the restriction of P to R_i, i.e., $\text{REST}_P(R_i)$ and apply each atomic expression $p \in \text{REST}_P(R_i)$ on R_i using valuation. For the valuation, each constant of the allowed domain of constants is associated with a counter that indicates the number of appearances of that constant in valuation.
- Identify the extended restrictions of P to relation-pairs.

A set of n relations is produced with possibly less arity, where all tuples of a relation are satisfied by corresponding restriction of that relation. Then n relations are combined into a single relation by applying JAN. Next, each of the atomic expression p of the restrictions of P to relation-pairs is checked on the combined relation using valuation. Finally, the intermediate representation is obtained by performing projection operation on the combined relation using $\cup \{A_{ij}^s\}$ of all relations $R_i \in n$-query-relations. Valuation on W is applied to get the maybe answers $\Delta Q(T)$.

IV. EXPERIMENTAL RESULT

The proposed algorithm is implemented in a restricted setting. It is assumed that all the queries posed to the system are syntactically correct. When both the operands of any arbitrary atomic expression are attributes from relations, they are with the same attribute-domain. The operation process of the described algorithm are experimented using different

scenarios of data exchange setting, couple of them are given below:

Example 4.1 (Tabulation): Consider a simple canonical solution given in Table I, which shows marks of a particular course.

Table I: Relation *marks*

roll	test1	test2	test3
970227	29	27	29
970232	_n_test1_1	23	25
970239	_n_test1_2	_n_test2_1	29

The result of the preprocessing is given in Table II.

Table II: Preprocessing for Tabulation

Attribute	type	rela-tions	hasNull	hasConstant
roll	String	marks	FALSE	TRUE
test1	Integer	marks	TRUE	TRUE
test2	Integer	marks	TRUE	TRUE
test3	Integer	marks	FALSE	TRUE

Now "to list the students who have obtained 27 in the second test", the SQL expression is written as

SELECT *marks.roll*, *marks.test2*
FROM *marks*
WHERE *marks.test2* = 27.

As it is a single relation, query rearrangement only drop attributes of other than the set {*roll*, *test2*} and no join operation is needed. The maybe answers computed are given in Table III.

Table III: Maybe Answers for Tabulation

marks.roll	marks.test2
970227	27
970239	27

In Table III, the first tuple is also a certain answer; the last one is obtained by applying valuation.

Example 4.2 (People-Person): Consider another canonical solution is given in Table IV.

Table IV: Canonical solution for People-Person

name
Tanisha
_n_name_1

(a) people

name
Tanisha
_n_name_1

(b) person

Table V shows the result of the preprocessing.

Table V: Preprocessing for People-Person

Attri-bute	type	relations	hasNull	hasConstant
name	String	person, people	TRUE	TRUE

If the following SQL statement is executed on the canonical solution,

SELECT *person.name*, *people.name*
FROM *person*, *people*
WHERE *person.name* = *people.name*;

output (in Table VI) is produced after applying query rearrangement and join operation using valuation.

Table VI: Maybe Answers for People-Person

people.name	person.name
Tanisha	Tanisha
Tanisha	_n_name_1
_n_name_1	Tanisha
_n_name_1	_n_name_1

V. PERFORMANCE ANALYSIS

Implemented system is evaluated using a combination of *goal-based evaluation* and *IT-system as such* [2]. Using a combination of *criteria-based evaluation* and *IT-system as such* [2], it is ensured that no invalid criterion is assumed. The results of each phases like query rearrangement, join operation etc are compared with the definitions and each time expected outcomes are obtained. The proposed algorithm generated a finite intermediate representation W of this infinite object, which is defined as

$$\cup \{ \ \text{REP}_x(t) \mid t \in W \} = \Delta Q(\ \ \text{CANSOL}(S)) .$$

It is claimed in [8] that, a *fair representation* of $\Delta Q(T)$ can be constructed in polynomial time for a positive relational algebra query. Fair representation is defined as a table in the similar manner as the intermediate representation. Initial results using queries consist of only equality (i.e., =) on attributes with nulls and others operators (e.g., $>, <, \geq, \leq$) on attributes without nulls justify this claim.

But this claim fails in case of queries including $>, <, \geq, \leq$ on attributes with nulls. The main reason of this failure is that a simple table is not enough to represent maybe answers in such situations. For example, the output maybe answers are generated (given in Table VII) for the query "to list the students who have obtained at least 27 in the first test" for Tabulation in Example 4.1.

Table VII: Intermediate representation for queries on marks in Tabulation

marks.roll	marks.test1
970227	29
970232	_wn_test1_1
970239	_wn_test1_2

(a) W

attribute	*condition*
test1	_wn_test1 >= 27

(b) C

The first tuple has a constant (i.e., 29) which satisfies the predicate and hence it is included in the representation. The second and third tuples have marked null va-

riables (_n_test1_1 and _n_test1_2 respectively) and applying valuation, sometimes constants are mapped which satisfy the predicate (for constant values greater than or equal to 27) and sometimes does not satisfy (for constant values less than 27). A simple marked null variable cannot be used in the representation and for every valuation, correct answer is not obtained. Using the concept of adding condition to the conditional-table [6], a slightly modified null variable, termed as *weighted marked null variable* is used instead in *W* (see Table VII(a)). A separate table *C* given in Table VII(b) is used to add the condition. When a weighted marked null variable is encountered in a tuple of *W* during valuation, first the condition is checked in *C* for the attribute and if the condition is satisfied, the tuple is included as a maybe answer. The intermediate representation will be these two tables (*W* and *C*).

Theorem 4.1: If a positive relational query *Q* is executed on a canonical solution *T*, an *intermediate representation*, *W* of $\Delta Q(T)$ can be constructed in polynomial time, where *Q* consists of only equality (i.e., =) on attributes with nulls and others operators (e.g., $>,<,\geq,\leq$) on attributes without nulls. For a generalized positive relational query *Q*, another condition table *C* is needed to form the representation. •

In the algorithm, answers are obtained by assigning constant to null (if only one of the operands of '=' is null) and renaming two nulls to a new null variable (if both operands are null). The main idea behind this operation is that the infinitely many maybe answers form equivalence-classes. The implemented algorithm returns each of these equivalence-classes only once, as nulls are renamed considering equivalent (i.e., using the isomorphic property). The experimental results show that the implemented algorithm is *complete*, produces all the maybe answers and *sound*, does not produce any wrong maybe answers. The implementation uses no relational database software-specific macro, hence it can be implemented on any system.

VI. FUTURE WORKS

The restricted implementation setting under CWA is tested with simple positive relational queries. This can be extended for all types of queries, e.g., on self-joined relations. The queries with inequalities can be considered. More generalized data exchange setting with target dependencies can also be used to get all possible answers. To allow extending the target instance beyond the source instance, a combination of CWA/OWA can be considered.

VII. CONCLUSION

Maybe answers play a vital role in the study of data exchange. The maybe answers semantics provide an upper approximation for the answers to the queries. In this paper, a novel algorithm is presented to compute the maybe answers incrementally under CWA. The results show that the algorithm generates all possible answers. There are situations where there exists no certain answer, the maybe answers help to get an idea about the possible answers to the queries.

REFERENCES

[1] S. Abiteboul, P. Kanellakis and G. Grahne. On the Representation and Querying of Sets of Possible Worlds. Theoretical Computer Science 78 (1991), pp. 159-187.

[2] S. Cronholm and G. Goldkuhl. Strategies for Information Systems Evaluation - Six Generic Types. Electronic Journal of Information Systems Evaluation Volume 6 Issue 2 (2003), pp.65-74.

[3] R. Fagin, P.G. Kolaitis, R. Miller, L. Popa. Data Exchange: Semantics and Query Answering. In ICDT 2003, pp. 207-224.

[4] R. Fagin, P.G. Kolaitis, L. Popa. Data Exchange: getting to the Core. PODS 2003, pp. 90-101.

[5] G. Gottolob and R. Zicari. Closed World Databases Opened Through Null Values. VLDB 1988, pp. 50-61.

[6] T. Imielinski and W. Lipski. Incomplete Information in Relational Databases. Journal of the Association for Computing Machinery, Vol. 31, No.4, October 1984, pp. 761-791.

[7] P.G. Kolaitis. Schema Mappings, Data Exchange and Metadata Management. PODS 2005.

[8] L. Libkin. Data Exchange and Incomplete Information. PODS 2006. June 26-28, 2006.

[9] L. Libkin and C. Sirangelo. Data Exchange and Schema Mappings in Open and Closed Worlds. ACM SIGMOD/PODS 2008. June 9-12, 2008.

[10] W. Lipski. On Semantic Issues Connected with Incomplete Information in Database. ACM Trans. Database Systems 4 (1979), pp. 262-296.

Proceedings of 2009 12th International Conference on Computer and Information Technology (ICCIT 2009)
21-23 December, 2009, Dhaka, Bangladesh

Bangla Hand Written Digit Recognition Using Supervised Locally Linear Embedding Algorithm and Support Vector Machine

Saleh Ahmed, Md. Rashedul Islam, Md. Shafiul Azam
Dept. of CSE, Leading University, Sylhet, Bangladesh
sumon.edu@gmail.com, rashed.cse@gmail.com, shahincseru@gmail.com

Abstract

This paper presents Bangla numeral Character Recognition System using supervised locally linear embedding algorithm and Support Vector Machine (SVM). The locally linear embedding (LLE) algorithm is an unsupervised technique proposed for nonlinear dimensionality reduction. In this paper, we describe its supervised variant (SLLE). Where class membership information is used to map overlapping high dimensional data into disjoint clusters in the embedded space. we combined it with support vector machine (SVM) for classifying handwritten digits from the On-Line Handwritten Bangla Numeral Database.

Keywords: LLE, SLLE, SVM, Bangla Handwritten, Digit Recognition.

I. INTRODUCTION

Bangla Hand Written digit recognition system attempts to recognize a hand written Bangla numeral character on the basis of individual bitmap information of a character image. This system can be either Unsupervised and supervised. The key idea is to recognize the numeric character classes using any human written document. Dimensionality reduction is an important preprocessing step before classifying multidimensional data. The locally linear embedding (LLE) algorithm [3] [4] has been recently proposed for this purpose. Its attractive properties are: 1) only two parameters to be set, 2) optimizations not involving local minima, 3) preservation of local geometry of high dimensional data in the embedded space, 4) a single global coordinate system of the embedded space. In this paper, we describe a supervised variant of LLE, called the supervised locally linear embedding (SLLE) algorithm [2]. Unlike LLE, SLLE projects high dimensional data to the embedded space using class membership relations. This allows obtaining well-separated clusters in the embedded space (if the dimensionality of the embedded space is less by one than the number of classes [2]); moreover, each cluster is represented by only one point in the embedded space. To test SLLE, we coupled it with support vector machine (SVM) [5], since SVM has provided excellent results in many tasks. SVM performs classification by mapping data into a high dimensional space where classes are linearly separable by hyper planes. The combination of SLLE and SVM was applied for recognizing handwritten digits of the On-Line Handwritten Bangla Numeral Database [1]. Our results bring open questions for further research, which are also briefly discussed.

II. LOCALLY LINEAR EMBEDDING ALGORITHM

As an input, LLE takes a matrix X of size D × N consisting of N columns representing feature vectors. Its output is a matrix Y of size d × N (d << D), where columns are coordinates of the feature vectors in the embedded space. Further, the term point will stand for a vector either in RD or Rd space, depending on the context. The LLE algorithm contains the following three steps:

Step 1. K nearest neighbors are found for each point Xi in RD, i = 1, 2, N by using Euclidean distances to measure similarity. Then the proximity matrix A of size K × N is built and its i -the column holds indices of K points, which are the nearest to Xi (A1i corresponds to the highest proximity).

Step 2. Assigning a weight to every pair of neighboring points. The weights representing contributions to the reconstruction of a given point from its nearest neighbors can be found by solving the optimization task [3]:

$$\in (W) = \sum_{i=1}^{N} \left\| X_i - \sum_{j=1}^{N} W_{ij} X_j \right\|^2 \quad (1)$$

subject to constraints Wij= 0, if Xi and Xj are not neighbors and $\sum_{j=1}^{N} W_{ij} = 1.$ The latter condition enforces rotation, translation, and scaling invariance of Xi and its neighbors.

Step 3. Computing embedded coordinates Yi for each Xi. Projections are found by minimizing the embedding cost function for the fixed weights [3]:

$$\delta(Y) = \sum_{i=1}^{N} \left\| Y_i - \sum_{j=1}^{N} Wij Y_j \right\|^2 \quad (2)$$

under the following constraints: $\frac{1}{N}\sum_{i=1}^{N} Y_i Y_i^{'}$ (normalized unit covariance) and $\sum_{i=1}^{N} Y_i = 0$ (translation-

invariant embedding), which provide a unique solution. To find the matrix Y, a new matrix
M = (I − W)'(I − W) is constructed and its d bottom eigenvectors starting from the second one are computed. These eigenvectors span rows of Y.

III. SUPERVISED LOCALLY LINEAR EMBEDDING ALGORITHM

The essence of SLLE consists of the following. The whole data set Ψ is divided into subsets Ψ1,Ψ2, ...,Ψm sothat

Ψ = Ψ1□Ψ2□...□Ψm and Ψi∩Ψj =Ø, $\forall i \neq j$. Each Ψi holds the data of one class only and m is the total number of classes known a priori. Let each Ψi be associated with its own data matrix Ξi, which contains a set of Ni D-dimensional feature vectors.

Each Ψi is treated separately from others as follows. For each data point Xi □ Ψ1, we seek its K nearest neighbors belonging to Ψ1, i.e., Xi and its neighbors are contained in the same class, while the nearest neighbors are chosen from arbitrary classes in the LLE algorithm. When applied to all Xjs □ Ψ1, this procedure leads to a construction of the matrix A1 of size K ×N1, where columns correspond to the points and rows correspond to the nearest neighbors. By repeating the same for Ψ2, ...,Ψm, matrices A2, ...,Am are generated.

To distinguish points belonging to different classes, we add a shift to values of all elements of the matrices starting from A2. The shift for all elements of A2 is equal to N1, the shift for all elements of A3 is N1 + N2, ..., and the shift for all elements of Am is $\sum_{i=1}^{m-1} N_i$. Such a procedure guarantees that no two matrices Ai and Aj will make reference to the same point. Having set elements of all matrices, we concatenate Ai's into a single matrix A whose size is K × N, where now $N = \sum_{i=1}^{m} | N_i$. We also concatenate Ξ_i 's into a single matrix X whose size is D × N. After that, operations are carried out as in case of LLE starting from Step 2.

At a first glance, it may be difficult to estimate the influence of the changed procedure for the selection of nearest neighbors on the final embedding. The change is small, yet significant, since the matrix A is used to construct another matrix, W, which, in turn, determines embedded coordinates. As a result, embeddings obtained with the unsupervised and supervised LLE are different.

IV. REOGNITION OF HANDWRITTEN DIGIT

The On-Line Handwritten Bangla Numeral Database of handwritten digits [1] was used in experiments. It consists of ten di□erent classes of grayscale images (from '0' to '9', each of 28×28 pixels in size) together with their class labels. The present database consists of 6000 samples of online handwritten Bangla numerals. In each class there are 600 samples. A few samples from this database are shown in the Figure 1.

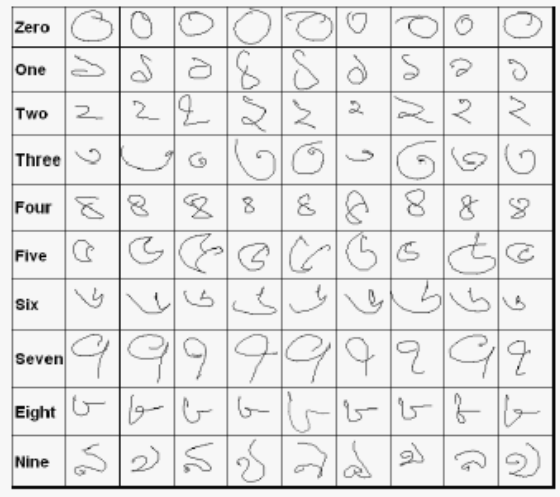

Fig. 1. Sample Data from On-Line Handwritten Bangla Numeral Database.

The training and test sets consist of 6,000 and 1,000 images, respectively. The number of images in the training set varies from 542 to 600 per class and it is about 600 images per class in the test set. Each image was transformed into a D-dimensional feature vector (D = 28 × 28 = 784), where pixels values were used as features. From the previous work [2] we learnt that for good data separation the dimensionality of the embedded space, d, should be less by one than the number of classes, L. Since we have ten classes, it is obvious that d should be set to 9. Moreover, there is no significant influence of the parameter K on good data separation by SLLE; K = 18 was used in the experiments. The meaning of "good separation" is that all points from the same class in the high dimensional space are mapped into one point in the embedded space.
A procedure of the application of SLLE+SVM for classification

1) Map the training set into d-dimensional space (d = L − 1) by using SLLE.
2) Train SVM on L d-dimensional vectors, each of which represents a certain class.
3) Map the test set by applying the non-parametric generalization [4].
4) Use the projection obtained in the previous step and the trained SVM to classify the test data.

Table I Confusion matrix in % when classifying in the original space

Classes	০	১	২	৩	৪	৫	৬	৭	৮	৯
০	99.3	0	0.1	0.2	0	0.1	0.1	0	0.2	0
১	0	99.4	0.2	0.1	0	0.1	0.1	0.1	0.1	0
২	0.7	0.1	97.7	0.1	0.1	0	0.4	0.6	0.4	0
৩	0	0	0.3	97.7	0	0.5	0	0.5	0.7	0.3
৪	0.1	0	0.4	0	98.4	0	0.2	0	0	.09
৫	0.2	0	0	1.0	0.1	97.8	0.3	0.1	0.2	0.2
৬	0.5	0.2	0.2	0	0.2	0.5	98.1	0	0.2	0
৭	0	0.6	0.9	0.1	0.1	0	0	97.5	0.1	0.8
৮	0.4	0	0.2	0.4	0.3	0.2	0.1	0.4	97.6	0.3
৯	0.2	0.4	0	0.4	0.9	0.4	0	0.4	0.3	97.0

Mathematically, it means that the best solution for the minimization problem (2) was found, i.e., $\delta(Y) = 0$.

The SVM with a polynomial kernel $\left[\gamma\left\langle X_i, X_j\right\rangle + c\right]^{\xi}$ was then used for data classification in the high and low dimensional spaces, where ξ's were set to 2 and 1 for the original and embedded spaces, respectively, γ's and c's were set to 1 in both cases.

We first trained the SVM classifier using 60,000 images in the original space. Then 10,000 images were fed to the classifier and the confusion matrix shown in Table 1 was obtained (the average accuracy of recognition is 98.05%).

Next, we combine SLLE and SVM (see Figure 2) for classification. In this case, the SVM training was very fast since L << N and the output of SLLE immediately gave us support vectors. Table 2 represents the confusion matrix obtained for the classification in the embedded space (the average accuracy is equal to 97.06%).

To compare the performances of SVM and SLLE + SVM on a more difficult data, the training and test sets were interchanged, i.e. the number of images in the training set was 6 times less than that in the test set. Moreover, the number of classes was reduced to five ('৫', '৬', '১', '৯' and '২'). These digits are the most difficult to recognize due to their shape similarity. SVM was applied to the data lying in the original space and in the 4D embedded space obtained by SLLE, respectively. In the latter case the unseen data points were mapped into the embedded space by the non-parametric generalization algorithm [4].

Table II Confusion matrix in % when classifying in the embedded space.

Classes	০	১	২	৩	৪	৫	৬	৭	৮	৯
০	99.3	0.6	0	0	0	0	0	0.1	0	0
১	0	99.7	0.2	0.1	0	0	0	0	0	0
২	0.6	1.3	97.3	0	0	0	0.1	0.7	0.1	0
৩	0	2.4	0.1	96.2	0	0.4	0	0.6	0.3	0
৪	0.1	1.3	0	0	97.0	0	0.3	0.1	0	1.1
৫	0.1	3.0	0	0.3	0	96.3	0.1	0.1	0	0
৬	0.2	1.2	0	0	0.1	0.1	98.4	0	0	0
৭	0	1.9	0.5	0	0.1	0	0	97.1	0	0.4
৮	0.2	4.4	0.2	0.4	0	0.1	0	0.2	94.2	0.3
৯	0.2	3.2	0	0.2	0.8	0	0	0.5	0.1	95.0

The achieved accuracies were 96.59% and 95.86%, respectively.

Despite of these unfavorable circumstances, the combination SLLE + SVM has its merits. SLLE arranges all points of the same class lying in the original space into one point of the embedded space, i.e. a unique representation is obtained for each class in the embedded space. This fact allows a cheaper way to train SVM, since only one vector of dimensionality d per class is needed for this stage. In our experiments when SVM was trained on the D-dimensional data, 7749 and 957 support vectors were found for ten and five class' problems, respectively, whereas these numbers are 10 and 5 after preprocessing with SLLE. Moreover, in the latter case the data are linearly separable, i.e. only a linear SVM is needed, which means that a problem-dependent kernel tuning is avoided.

One can see from the results of the two series of experiments that when the recognition task becomes more difficult and the number of support vectors significantly decreases, the accuracy of SVM falls more rapidly (98.05%−96.59% =1.46%) than that of SLLE + SVM (97.06%−95.86% = 1.2%). Furthermore, the difference between the accuracies of SVM and SLLE + SVM becomes smaller: 0.99% and 0.73% for 10 and for 5 classes, respectively. However, more research on different data sets would be needed to confirm these observations.

V. CONCLUSION

The original LLE assumes that data lie on one manifold embedded in a high dimensional space. In this paper, we extended the concept of LLE to the case of multiple disjoint manifolds by proposing a supervised variant of LLE. It can be used as a preprocessing step before classification in order to obtain a compact representation for classes while reducing dimensionality. SLLE allows computing support vectors for SVM without training SVM on the huge amount of data. By comparing the performance of SVM and SLLE + SVM for recognition of Handwritten digits, SLLE + SVM failed to overcome SVM alone operating in the high dimensional space. Perhaps, this indicates that the effect known as the curse of dimensionality did not manifest itself in the large extent for the task considered. It also implies that further research is definitely needed to establish how much SLLE (mapping + generalization) contributes to the classification accuracy.

LLE (and moreover, SLLE) is a new technique and its efficient implementation for large-scale problems (N 105 and higher) did not yet come into existence. This is concerning both the nearest neighbor search and Eigen decomposition. If an efficient solution for these two problems will be found, the time spent on dimensionality reduction can be significantly shortened.

REFERENCES

[1] On-Line Handwritten Bangla Numeral Database. http://www.isical.ac.in/~ujjwal/download/numeral-online.html

[2] O. Kouropteva, O. Okun, A. Hadid, M. Soriano, S. Marcos, and M. Pietik¨ainen. Beyond locally linear embedding algorithm. Technical Report MVG-01-2002, Machine Vision Group, University of Oulu, 2002.

[3] [3] S.T. Roweis and L.K. Saul. Nonlinear dimensionality reduction by locally linear embedding. Science, 290(5500):2323–2326, 2000.

[4] L.K. Saul and S.T. Roweis. Think globally, fit locally: unsupervised learn-ing of nonlinear manifolds. Technical Report MS CIS-02-18, University of Pennsylvania, 2002.

[5] V. Vapnik. The nature of statistical learning theory. Springer Verlag, 1995. [6] Dick de Ridder, Olga Kouropteva, Oleg Okun, Matti Pietik¨ainen and Robert P.W. Duin “Supervised locally linear embedding”

[6] Robert Burbidge, Bernard Buxton “An Introduction to Support Vector Machines for Data Mining”

[7] Christopher j.c. Burges “A Tutorial on Support Vector Machines for Pattern Recognition”, Data Mining and Knowledge Discovery, 2, 121–167 (1998).

[8] Panu Erasto “Support Vector Machines - Backgrounds and Practice”, Rolf Nevanlinna Institute. 2001

[9] Andrew W. Moore Associate Professor School of Computer Science Carnegie Mellon University “Support VectorMachines”, ISBN-412-268-7599.

Proceedings of 2009 12th International Conference on Computer and Information Technology (ICCIT 2009)
21-23 December, 2009, Dhaka, Bangladesh

Improved Needham-Schroeder Protocol for Secured and Efficient Key Distributions

Shamima Sultana, Md. Ismail Jabiullah† and Md. Lutfar Rahman‡
Department of Computer Science and Engineering, Dhaka City College, Dhaka, Bangladesh
† Department of Software Engineering, Daffodil International University, Dhaka, Bangladesh
‡Department of Computer Science and Engineering, Dhaka University, Dhaka, Bangladesh
shamima819@yahoo.com, mij1964iii@yahoo.com, lrahman44@gmail.com

Abstract

A key distribution procedure is an essential constituent of secured exchange of information between the participants. In this paper, a fast symmetric key distribution technique with additional security services is presented. The aim of the proposed technique is to improve the conventional Needham and Schroeder five-message protocol in four aspects. First aspect is to introduce an additional authentication level in originator's identity. Second aspect is to provide the integrity of the originator's message. Third aspect is to reduce the time needed to distribute session-key between pair of entities. And the fourth aspect is to develop the key freshness security issue. A comparative analysis between conventional and proposed technique is presented to visualize the improvements of the proposed one. C programming language is used to implement the technique and running time is measured by using the time function and it is found that proposed technique is faster than the conventional one. For the purpose of threat analysis, several attacks, such as altering the message information, are applied by force on the proposed technique to check whether it will provide the security services or not. And the result of threat analysis is that the proposed technique provides all the security services. Hence, the proposed technique will bring a new dimension in key distribution paradigm.

Keywords: Key Distribution, Secret Key, Entity Authentication, Key Confirmation, Message Integrity and Security.

I. INTRODUCTION

Key Distribution refers to the means of delivering a key between two parties who wish to exchange data, without allowing others to see the key. Symmetric schemes require both parties to share a common secret key. But the issue is how to distribute this key securely. Two parties A and B have various key distribution alternatives, as follows [2]:

1. A can select key and physically deliver to B.
2. Third party can select & deliver key to A & B.
3. If A & B have communicated previously can use previous key to encrypt a new key.
4. If A & B have secure communications with a third party C, C can relay key between A & B.

Physical delivery (option 1 & 2) is simplest - but only applicable when there is personal contact between recipient and key issuer. A third party is a trusted intermediary, whom all parties trust, to mediate the establishment of secure communications between them. As numbers of parties grow, some variant of option 4 is only practical solution and widely adopted. In this proposed work, option 4 is used with the Centralized Key Distribution Center (KDC) as the trusted third party.

II. KEY DISTRIBUTION MODELS

Two Simple Key Distribution Models are:

1. Point-to-Point Key Distribution Model
2. Centralized Key Distribution Model

Point-to-Point Key Distribution model involves two parties communicating directly and Centralized Key Distribution Model uses a Trusted Third Party (TTP) to distribute key between users.

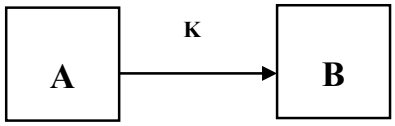

Fig.1. Point-to-Point Key Distribution Model

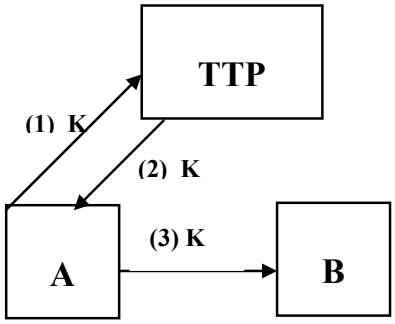

Fig.2. Centralized Key Distribution Model

III. CONVENTIONAL KEY DISTRIBUTION TECHNIQUE

Many existing authentication protocols are derived from the Needham-Schroeder protocol (1978). As in Fig. 3,

978-1-4244-6283-4/09/$26.00 ©2009 IEEE

only A makes contact with the server, who provides A with the session key, $K_{ab,}$ and a certificate encrypted with B's key conveying the session key and A's identity to B. Then B decrypts this certificate and carries out a nonce handshake with A to be assured that A is present currently, since the certificate might have been a replay.

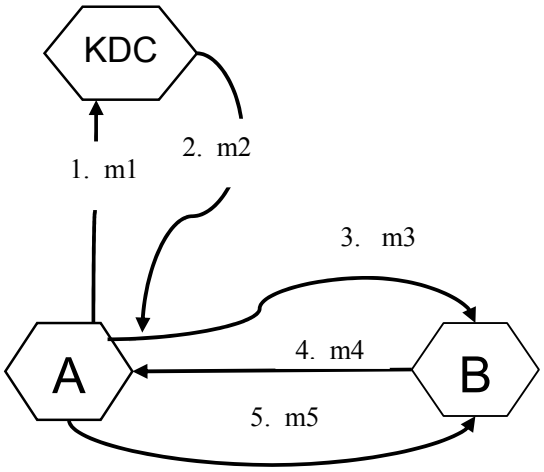

Fig.3. Conventional Needham-Schroeder Key Distribution Protocol

Where,

m_1 = (IDA, IDB, n_A)

n_A = code for the request made by user A.

IDA= identifier of user A.

IDB= identifier of user B.

$m_2 = E_{Ka}(K_{ab}, n_{A,}$ IDB, $E_{Kb}(K_{ab}$, IDA))

Where, K_{ab} = secret key generated by the KDC for secure communication between user A and B.

$C_1 = E_{Kb}(K_{ab}$, IDA)

K_a = private key of user A.

$m_3 = C_1$

$m_4 = C_2 = E_{kab}(n_B)$

Where, n_B = a random number generated by user B.

$m_5 = C_3 = E_{kab}(n_B\text{-}1)$.

The procedure is as follows:

Step1. A->KDC:

m1= IDA, IDB, n_A

Step2. KDC->A:

$m2=E_{Ka}(K_{ab}, n_{A,}$ IDB, $E_{Kb}(K_{ab}$, IDA)

Step3. A->B:

$m3=E_{Kb}(K_{ab}$, IDA)

Step4. B->A:

$m4=E_{Kab}(n_B)$

Step5. A->B:

$m5=E_{Kab}(n_B - 1)$

The working process of conventional technique is as follows:

1. User A sends a request message m_1 to the KDC indicating that it wants to establish a secure logical communication channel with user B. The message contains a code for the request n_A, the user identifier of A (ID_a) and the user identifier of B (ID_b). This message is transmitted from user A to KDC in plaintext form.
2. On receiving m_1, the KDC extracts from its table the keys K_a and K_b, which corresponds respectively to the user identifiers ID_a and ID_b in the message. It then creates a secret key K_{ab} for secure communication between user A and B. By using K_b the KDC encrypts the pair (K_{ab}, ID_a) to generate the cipher text $C_1 = E((K_{ab}, ID_a), K_b)$. Finally it sends a message m_2 to user A that contains $n_{A,,}$ ID_a , K_{ab} , C_1 . The message m_2 is encrypted with the key K_a so that only user A can decrypt it.
3. On receiving m_2 user A decrypts it with its private key K_a and checks whether n_A and ID_a of the message match with the originals to get confirmed that m_2 is the reply for m_1. If so, user A keeps the key K_{ab} with it for future use and sends a message m_3 to user B. This message contains cipher text C_1. Note that only user B can decrypt C_1 because it was generated using key K_b.
4. On receiving m_3 user B decrypts C_1 with its private key K_b and receives both K_{ab} and ID_a. At this stage both the users have the same key K_{ab} that can be used for secure communication between them because no other user has this key. Now user B needs to verify if user A is also in possession of the key K_{ab}. Therefore, user B initiates an authentication procedure that involves sending a nonce to user A and receiving a reply that contains some function of the recently sent nonce. For this, user B generates a random number n_B, encrypts n_B by using key K_{ab} to generate cipher text $C_2 = E(n_B, K_{ab})$ and sends C_2 to user A in message m_4. The random number n_B is used as a nonce.
5. On receiving m_4 user A decrypts C_2 with the key K_{ab} and retrieves n_B. It then transforms n_B to a new value $N_t = n_B\text{-}1$ by a previously defined function *f*. User A encrypts N_t by using K_{ab} to generate the cipher text $C_3 = E(N_t , K_{ab})$ and sends C_3 to user B in message m_5.
6. On receiving m_5 user B decrypts C_3, retrieves N_t, and applies the inverse of function *f* to N_t to check if the value obtained is n_B. If so, user B gets confirmed that a secure channel has been created between user A and user B by using key K_{ab}. This is enough to achieve mutual confidence and from now on the exchange of actual message encrypted with key K_{ab} can take place between user A and B.

IV. PROPOSED KEY DISTRIBUTION TECHNIQUE

The replay attack of the original protocol is removed in the following proposed method and three additional security services as: Authentication of Originator's Identity, Originator's Message Integrity and Key-Freshness are introduced. Another major point is parallel transfer of symmetric key by the KDC server to the pair of nodes (as in Fig. 4). This parallel transfer of symmetric key saves much time than to distribute symmetric key sequentially from the KDC server to the initiator node and then the symmetric key is sent to the responder node (from the initiator) to which the initiator wants to communicate.

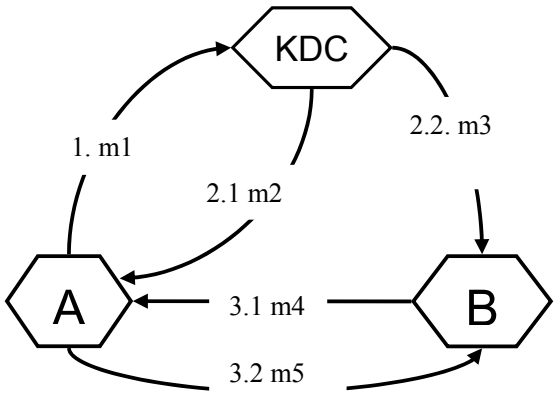

Fig.4. Proposed Key Distribution Technique

Where,

m1=IDA, IDB, E_{Ka}(IDA, IDB ,n_A)

n_A = code for the request made by user A.

IDA= identifier of user A.

IDB= identifier of user B.

K_a = private key of user A.

m2 = E_{Ka} (K_{ab}, n_r, n_A)

Where, K_{ab} = secret key generated by the KDC for secure communication between user A and B.

n_r= Common nonce

m3 = E_{Kb} (K_{ab}, n_r, IDA)

K_B = private key of user B.

m4 = E_{Kab} (n_r)

m5 = E_{Kab} (n_r)

The procedure is as follows:

Step1. A->KDC:

m1=IDA, IDB, E_{Ka}(IDA, IDB ,n_A)

Step2. KDC->A:

m2=E_{Ka}(K_{ab}, n_r, n_A)

KDC->B:

m3=E_{Kb} (K_{ab}, n_r, IDA)

Step3. B->A:

m4=E_{Kab} (n_r)

A->B:

m5=E_{Kab}(n_r)

The working process of proposed technique is as follows:

1. User A sends a request message m_1 to the KDC indicating that it wants to establish a secure logical communication channel with user B. The message contains the user identifier of A (ID_a), the user identifier of B (ID_b) and a cipher text of (IDA, IDB and a code for the request $n_{A)}$ which is encrypted by the private key K_a. This message (m1) is transmitted from user A to KDC.
2. On receiving m_1, the KDC extracts from its table the keys K_a and K_b, which corresponds respectively to the user identifiers ID_a and ID_b in the message. KDC decrypts the cipher text part of m1 with the private key K_a and checks whether ID_a and ID_b of the message match with the originals to get confirmed that m_1 is sent by the valid originator A and also checks the integrity of message m_1. It then creates a secret key K_{ab} for secure communication between user A and B. It then generates a random number n_r which will be used by A and B to authenticate each other. It then creates two messages m_2 and m_3, for A and B respectively, and sends them simultaneously. The message m_2 contains K_{ab}, n_r, n_A and is encrypted by the key K_a so that only user A can decrypt it. The message m_3 contains K_{ab}, n_r, IDa and is encrypted by the key K_b so that only user B can decrypt it.
3. On receiving m_2 user A decrypts it with its private key K_a and checks whether n_A of the message match with the originals to get confirmed that m_2 is the reply for m_1. If so, user A keeps the key K_{ab} with it for future use and sends a message m_5 to user B. This message contains cipher text = E_{Kab} (n_r). User A also saves a copy of n_r. The message m_5 indicates the readiness of user A. By this message user A also indicates to user B that it is in possession of the common key K_{ab} and is ready for secure communication with B.
4. On receiving m_3 user B decrypts it with its private key K_b and receives K_{ab}, n_r and ID_a. At this stage both the users have the same key K_{ab} that can be used for secure communication between them because no other user has this key. User B sends a message m_4 to user A. This message contains cipher text= E_{Kab} (nr). User B also saves a copy of n_r. The message m_4 indicates the readiness of user B. By this message user B also indicates to user A that it is in possession of the common key K_{ab} and is ready for secure communication with A.

5. On receiving m_4, user A decrypts it by K_{ab}, retrieves n_r and compares its value with the stored n_r value. If the values are equal then user A gets confirmed that user B is in possession of the common key K_{ab}. On receiving m_5, user B also does the same thing.

V. IMPROVEMENT WORKS

Improvement Work 1:
Existing Needham-Schroeder Key Distribution Technique does not provide Authentication of Originator's Identity. But, Proposed Technique provides Authentication of Originator's Identity by using encryption function on message m1. If IDA is changed by attacker, then KDC could recognize it by matching IDA with the decrypted IDA and terminates the communication.

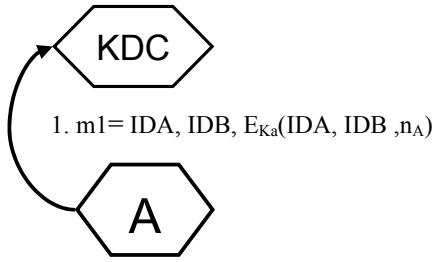

Fig.5. Authentication of Originator's Identity

Improvement Work 2:
Existing Needham-Schroeder Key Distribution Technique does not provide Originator's Message Integrity. Since m1 is in plaintext form, any parameter in m1 may be altered by the attacker. But, Proposed Technique provides Originator's Message Integrity by using encryption function on message m1. Any alternation in m1 could be identified by matching IDA, IDB with the decrypted IDA and decrypted IDB respectively.

Improvement Work 3:
Proposed Technique provides Key Freshness property by creating and distributing Kab and Nr from KDC. But Key Freshness property is absent in conventional technique.

Improvement Work 4:
In Proposed Technique, message m2 and message m3 can pass in parallel. Also, message m4 and message m5 can pass in parallel. Hence, it is faster than the Existing one.

VI. IMPLEMENTATION

For implementation C programming language is used. The three communicating entities in the proposed technique are: initiator (A), trusted server (KDC) and the responder (B). Each entity has the capability to create messages and several remote procedure calls are used to establish communication link and also for the purpose of message passing among entities. KDC stores the identity of initiator and responders. It also generates secret key for secure communication between user A and B. Key freshness and message freshness is checked by matching the nonce value. To measure the time in each operation, the time function in C language is used.

Running time in different machines is given in the following table:

Table I Running Time in Different Machine

Processor's speed	**Running time needed for Conventional technique (mili-seconds)**	**Running time needed for Proposed technique (mili-seconds)**
1.73 GHz	5055.555556 mili-seconds	3000.000000 mili-seconds
700 MHz	5111.111111 mili-seconds	3011.111111 mili-seconds
400 MHz	5611.111111 mili-seconds	3555.555556 mili-seconds

VII. COMPARATIVE ANALYSIS

Efficiency and Security Services provided by the Proposed and Conventional Technique is summarized in the Table II. Three additional security services as Originator's identity authentication, Originator's message integrity and Key-freshness are introduced in the proposed technique.

Table II Comparative Analysis between Proposed and Conventional Technique

Security Services	**Proposed Technique**	**Conventional Technique**
1.Authentication of Originator's Identity	√	×
2. Originator's Message Integrity	√	×
3. Originator's Message Freshness	√	√
4. Key Freshness	√	×
5. Key Authentication	√	√
6. Key Confirmation	√	√
7. Entity Authentication	√	√
8. Efficiency (time)	3000.00000 mili second	5055.555556 mili second

VIII. THREAT ANALYSIS

By force attacks are applied on the proposed technique to check its functionalities. Message m1, m2, m3 and m4 (as in Fig.4) are altered by force for the purpose of checking authentication of originator's identity, message integrity, message freshness, key freshness and confirmation.

Attack 1: Checking message integrity

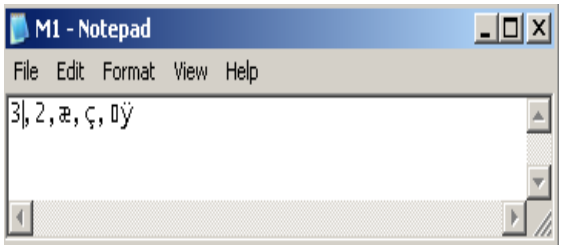

Fig.6. Changing IDA in message m1

KDC matches IDA and finds that the message is altered, so KDC will not generate any session key and terminate the session.

Attack 2: checking message freshness

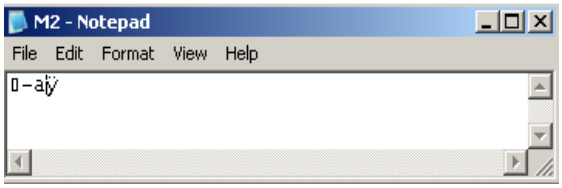

Fig.7. Changing nonce n_A in message m2

On receiving message m2, A matches n_A and finds that this is not the reply of m1 and terminate the communication.

Attack 3: checking key freshness

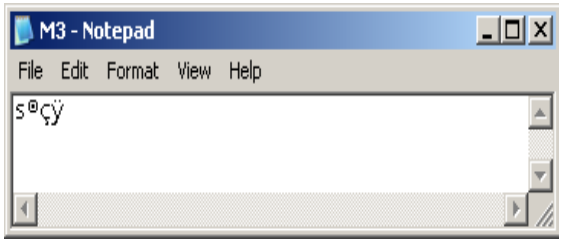

Fig.8. Changing session key K_{ab} in message m3

B receives message m3 and creates message m4 by using changed K_{ab}. A receives m4 and but can not decrypt m4 by its K_{ab}, so A stops communication.

Attack 4: checking key confirmation and entity authentication

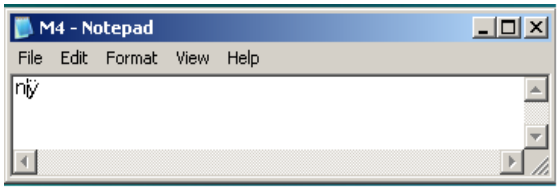

Fig.9. Changing session key n_r in message m4

On receiving message m4 by A, the nr provided by KDC to A is not matched with the nr in m4. So, entity authentication is not provided.

IX. DISCUSSIONS

A session-key is a key used for encrypting one message or a group of messages in a single communication session. Security solutions require that the secret session-keys to be kept out of reach from the adversaries. KDC generates the secret key and common nonce for several verifications. When designing or selecting a key establishment technique for use, it is important to consider what assurances and properties an intended application requires. The fundamental security services of key distribution protocol are: authentication of the originator's identity, originator's message-integrity, originator's message-freshness, key authentication, entity authentication, key freshness and key confirmation. In the proposed technique, the replay attack of the original Needham and Schroeder five- message protocol is removed and three additional security services as: authentication of originator's identity, originator's message integrity and key-freshness are introduced (these three security services are absent in conventional Needham and Schroeder five- message protocol). Moreover, the time needed for distributing keys between pair of nodes in the proposed technique is reduced.

X. CONCLUSION

The motivation of the proposed work is to improve the security issues of the conventional Needham-Schroeder five-message protocol and another is to make the key distribution faster. From the above discussion, the following conclusions can be drawn:

- The proposed technique gives all the benefits (Security Services) that the conventional Needham-Schroeder five-message protocol can provide.
- It provides an additional authentication level in originator's identity.
- It enhances the Security Services by providing the integrity of the originator's message.
- It removes the replay attack by establishing key freshness security issue.
- It reduces the time needed to distribute session-key between pair of entities and It is found that for all cases the proposed technique is about 40% faster than the conventional protocol.

Hence, it is concluded that the Proposed Key Distribution Technique that will perform better than the Conventional one.

REFERENCES

[1] A. Menezes, P. van, Oorschot, and S. Vanstone, "Handbook of Applied Cryptography", CRC Press, 1996.

[2] William Stallings, "Cryptography and Network Security", Third Edition.

[3] Pradeep K. Sinha, "Distributed Operating Systems Concepts and Design", IEEE Press, ISBN-81-203-1380-1.

[4] Maithili Narasimha, "Applied Cryptography".

[5] R. Needham and M. Schroeder, "Authentication Revisited. Operating Systems Review", January 1987.

[6] D. Otway and O. Rees, "Efficient and Timely Mutual Authentication. Operating Systems Review", 1987.

[7] Lawrence C. Paulson, "Mechanized Proofs of Security Protocols".

[8] M. Backes and C. Jacobi, "Cryptographically Sound and Machine-assisted Verification of Security Protocols".

[9] Lawrence C. Paulson, "Relations between Secrets: Two Formal Analyses of the Yahalom Protocol. J. Computer Security", 2001.

[10] M. Satyanarayanan, "Integrating Security in a Large Distributed System. ACM Transactions on Computer Systems",1989.

[11] Charlie Kaufman, Radia Perlman, Mike Speciner, "Network Security: Private Communication in a Public World", 2nd Edition.

[12] Jason Coombs, "Programming Public Key Crypto Streams", Part 1.

[13] D. Boneh, C. Gentry, B. L. and Shacham, "H. Aggregate and Verifiably Encrypted Signatures from Bilinear Maps", in Eurocrypt '03, LNCS 2656, Springer-Verlag, 2003.

[14] Goel, S., Robson, M., Polte, M., and Sirer, E. G. Herbivore, "A Scalable and E_cient Protocol for Anonymous Communication", Technical Report TR2003-1890, Cornell University Computing and Information Science, 2003.

[15] Juels, A. and Brainard, J. G. Client puzzles, "A cryptographic countermeasure against connection depletion attacks", in NDSS, The Internet Society, 1999. ISBN 1-891562-04-5, 1-891562-05-3.

[16] Kagal, L., Finin, T., Cost, R. S., and Peng, Y, "A Framework for Distributed Trust Management", in Second Workshop on Norms and Institutions in MAS, Autonomous Agents, May 2001.

[17] Mui, L., Mohtashemi, M., and Halberstadt, A, "A Computational Model of Trust and Reputation for E-businesses", in HICSS, page 188, 2002.

[18] R. Kemmerer, C. Meadows, and J. Millen, "Three Systems for Cryptographic Protocol Analysis", Journal of Cryptology, 7(2):79–130, 1994.

Proceedings of 2009 12th International Conference on Computer and Information Technology (ICCIT 2009)
21-23 December, 2009, Dhaka, Bangladesh

Secure E-cash Model Using Java based Smartcard

Kaafi Mahmud Sarker, Israt Jahan, Mohammad Zahidur Rahman
Dept. of Computer Science and Engineering, Jahangirnagar University, Savar, Dhaka, Bangladesh
kaafimahmud@gmail.com, isratju1@yahoo.com, rmzahid@juniv.com

Abstract

Association of a true observer guaranties electronic cash not to be double-spent by any means. Java card is a smartcard which represents one of the smallest computing platforms. A major challenge influencing the design and implementation of e-cash observer in Java card is the limited availability of computing resources in it. In this paper, we show a new methodology of blending and associating high-level CORBA based bank server, user wallets and resource-constrained Java based observer. We choose a realistic e-cash scheme and show its successful implementation. We also analyze performance of Java card with various lengths of secret keys used for generating electronic coins.

Keywords: Binary Tree, Blending Technique, Java card, Observer.

I. INTRODUCTION

Electronic cash or e-cash refers to cash and associated transactions performed with it on an open communication network. Special protocols are used to manage secure e-cash transactions. Ideal e-cash system should be independent, anonymous, unforgeable, divisible, unlinkable, undouble-spending, transferable and of course, offline [1]. Though cryptography solves some of the problems such as anonymity, offline etc., double-spending cannot be prevented only through cryptography. Most of the e-cash authors suggested use of a temper-proof hardware as an observer of the system [1]-[7]. If user spends same coin twice or manipulates information inside observer, the observer drops working [7]. On the other hand, the observer cannot send or receive information alone without contribution of user's wallet. Both the wallet and the observer must confirm mutually when they work together. A true e-cash observer should compute electronic coins by itself and should not allow their manipulations by any means, even if the issuer authority (bank) attempts so. Smartcard is the best candidate to be observer, but implementation of very efficient and secured e-cash protocols with the observer cannot come into reality due to limited resources of smartcard.

Java card is a resource constrained device and we tried to overcome this limitation by blending and associating Java card with wallet and CORBA-based high-level bank server. Bank server is powered by LiDIA libraries. LiDIA can handle larger integers essential for e-cash security, and can suitably be implemented in bank and wallet components. Length of secret keys generated by Java card does not match with those generated by the bank and the wallet. However, without compromising security issues, the key published by bank, random numbers, observer's secret key, and different computational parameters exchanged among bank, wallet and Java card are synchronized in this paper. The processing cost and response time of Java card is optimized by distributing some processing to card hosts. Parameters are reduced in size using one way hashing and matching when they are being participated in various calculations inside the observer. We refer this technique as *blending technique*. We choose a realistic e-cash protocol [7] and carefully analyze performance of Java card with various lengths of secret keys used for generating electronic coins.

II. REVIEW OF MAJOR E-CASH PROTOCOLS WITH OBSERVER

E-cash is similar to paper cash and should guarantee anonymity. David Chaum [8] proposed an anonymous payment protocol in 1988 introducing the concept of e-cash. To prevent illegal copies of coins Chaum also described a method of preserving a list of all coins spent. Bank can verify any coin before it is being reused. But the verification needs to be performed online; otherwise, the payment will not be a valid payment. However, this limitation was corrected by Chaum, Fiat and Naor [9]. They proposed an offline e-cash model where transactions can be done online even the bank remains offline. RSA [10] public key based blind signatures and use of one way hash function are the strength of their protocol. The major drawback of these protocols is bank can detect double-spending when coins are deposited back to the bank which might incur huge losses.

Okamoto and Ohta [11] added divisibility property to e-cash based on binary tree, and hardness of the factorization and quadratic residues problems. Though binary tree representation efficiently handles large value of coins, anonymity is compromised in this scheme. Ferguson [3] proposed single-term scheme, where RSA signatures are combined with random blind signatures. He added a secret-sharing concept with which it is possible to know who commits fraud, but unfortunately, the security of this protocol was not guaranteed [12]. S. Brands's [5] scheme superseded others and considered as practical single-term e-cash. Earlier Chaum and Pedersen [13] introduced almost similar protocol. Yet the time between a fraud incident and its detection still do not guarantee banks for their financial losses.

978-1-4244-6283-4/09/$26.00 ©2009 IEEE

Recently, Liu, Luo, Si Ya-li, Wang and Li Feng [1] worked with *N*, *K* [6] based payment protocol with observer, where *N* denotes total coins value and *K* denotes payment times. It solves double-spending effectively with the prior restraint smartcard. But it demands huge storage when large value of e-cash needs to be withdrawn. However, Israt Jahan and M. Zahidur Rahman [7] proposed an elegant method with binary tree representation of coins, where large valued e-cash can be efficiently handled. Use of a prior-restraint smartcard not only protects reuse at the time a coin is being spent but also lightens the burden of the bank. Fig. 1 shows the basic model.

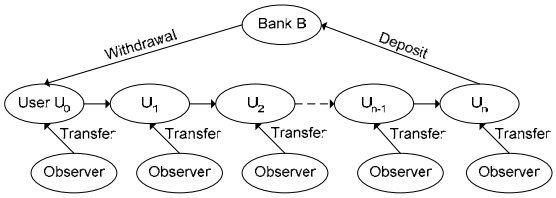

Fig. 1. Model of offline transferable e-cash with observer.

III. PROTOCOL DESCRIPTION

We worked for the divisible protocol described in [7]. Here p, q, g, g_1, g_2 and H are the system parameters published by the bank where the orders of g, g_1, g_2 is q. x and x_t are the secret key of bank. x will be used for issuing digital cash and x_t will be used for issuing coin extension. $h = g^x$ and $h_t = g^{x_t}$ are the public keys of the bank.

A. Bank's Setup, Account Opening and Withdrawal of E-cash by User U_0 from Bank

Bank setup, account opening and withdrawal of e-cash by user U_0 appears in Fig. 2. While opening an account and issuing the observer to the user, in *Setup1()*, bank chooses $oa_0 \in Z_q^*$ as the secret key of the observer. In *Calculate1()* the observer computes $AO_0 = g_1^{oa_0}$ and sends it to the host. Let u_0 is the secret key of the user which may be stored in user's wallet. The wallet calculates $I_0 = OAg_1^{u_0}$ in *Setup2()* and sends this value to the bank. The user sends the withdrawal amount, ω_l to the bank. The wallet performs computation and forms a binary tree rooted with the amount ω_l. At the same time, in *Calculate2()* the observer performs calculation and forms the tree by itself. It sends the encrypted value of nodes and the root to the wallet. The bank deducts ω_l amount from user's account balance and calculates z_0, a_0, b_0 in *Calculate3()* and sends to the wallet. The wallet generates c_0 and sends it to the bank. Bank calculates r_0 and sends the value to the wallet. At last, the wallet obtains, verifies and stores the signature in it.

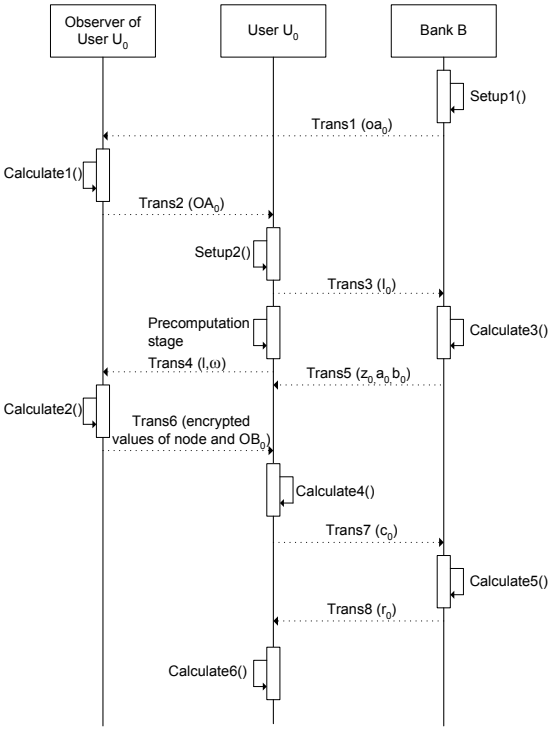

Fig. 2. Bank's setup, account opening and withdrawal of e-cash by user U_0.

B. Withdrawal of Coin Extension by User U_1 to Receive Transferred E-cash

Withdrawal of coin extension is almost similar to withdrawal protocol described in the earlier section. Only difference is here user pre-withdraws zero-valued coins from bank. Fig. 3 elaborates the protocol. In *Calculate2()* the smartcard chooses $O \in_R Z_q^*$ and calculates $OB_1 = g_1^{O_1}$.

C. Coin Transfer from User U_0 to U_1

Fig. 4 shows coin transfer protocol between users. In *Calculate1()* the user's wallet U_0 reveals $n_{0j_1j_2\ldots j_k}$'s contribution of its corresponding ancestor nodes as $\beta_{0j_1j_2\ldots j_k} = g_1^{\gamma_{0j_1j_2\ldots j_k,1}} g_2^{\gamma_{0j_1j_2\ldots j_k,2}} \bmod p$. In the next step the user U_0 reveals other related nodes. User U_0 forms the transcript $Tr_0 = \{m_0', T, A_0, Sign(m_0', T), a_k, a_{k-1}, \ldots, a_2, a_1, \beta_{0j_1j_2\ldots j_k}\}$ and sends to user U_1. In *Calculate2()* user calculates

ϕ_0 and sends it to U_0. In *Calculate3()* U_0 calculates ϕ_0' and sends ϕ_0' and corresponding node of the coin to the observer of U_0. If the node is found then it is erased. The observer calculates $\rho_0' = \phi_0' oa_0 + O_0 \bmod q$. In the last step it checks if any node exists; if not, then erases O_0.

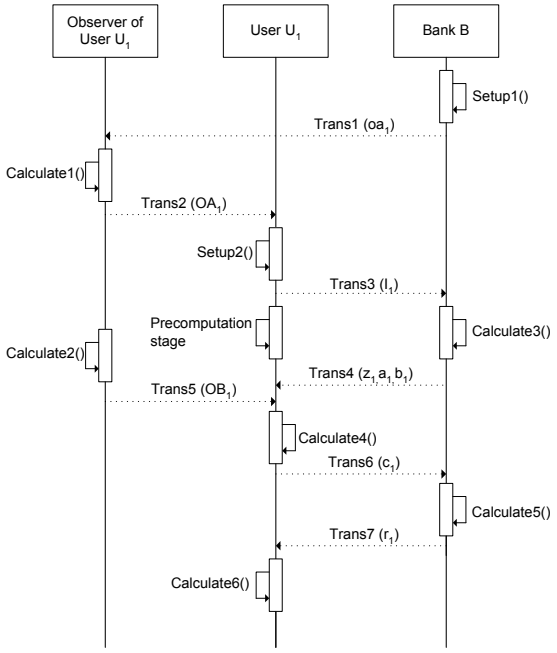

Fig. 3. Withdrawal of coin extension by user U_1.

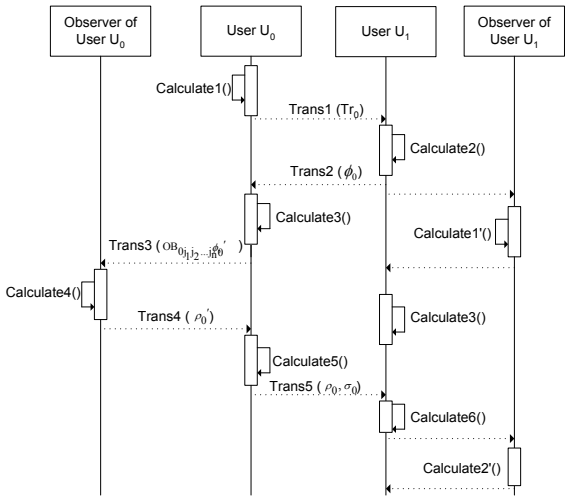

Fig. 4. User U_0 spends his coin to user U_1.

D. Deposit

User deposits his coin to the bank. If the coin is not deposited previously it is deposited to the account.

IV. IMPLEMENTATION OF OBSERVER IN JAVA CARD

Major system components of the protocol [7] are bank server, wallets and one observer with each wallet. The bank and wallet are designed on the distributed and object-oriented CORBA architecture using LiDIA libraries. The observer is implemented in Java platform. The observer has a client part which runs in association to the wallet, and a server part which is the card system itself. The server of the observer accepts commands from the client part and performs the requested action. Fig. 5 shows components' architecture and their interfaces. Fig. 6 shows an interfacing code segment.

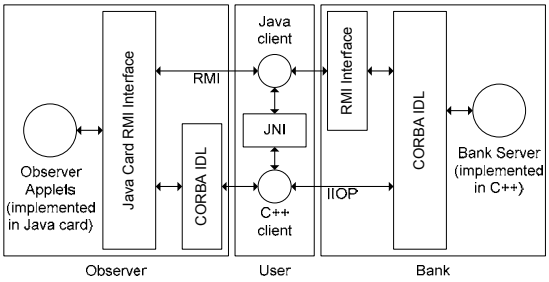

Fig. 5. Wallet with Java card observer and bank server component architecture.

```
...
...
Account_ptr
Bank_impl::create()
Account_impl * ai = new Account_impl;
Account_ptr aref = ai->this();
assert (!CORBA::in_nil (aref));
...
...
```

Fig. 6. Code segment shows pointer for bank interface.

V. DESIGN ISSUES

Bank issues Java based smartcards to users. The smartcard contains the observer for e-cash transactions. User performs e-cash transactions through ATM or his PC. If ATM is used to perform e-cash transactions, ATM carries out the tasks those the user's wallet does. If e-cash transactions are not performed through ATMs, the user's PC runs the wallet. In this case, a smartcard reader device is attached to the user's PC. Both the ATM and the wallet, running in user's PC, are connected to the bank component. The wallet, running in ATM or user's PC, performs e-cash loading, spending and depositing to bank in presence of respective observer.

In this design, we use *ATM* as both the smartcard reader and the execution platform of the wallet application. The term *User* is used to represent the wallet. *Observer* of the e-cash system is the smartcard system.

A. Use Cases:

Following are the use cases of the system.

Use Case 1: Bank setup and account opening

Precondition	Customer inserts Observer (smartcard) into the ATM.
Successful outcome	h and h^t are stored in Observer and ejects the Observer to customer.
Primary actor	ATM
Secondary actor	User, Observer and Account
Main scenario	1. User inputs x and x^t into the Bank system. 2. Bank generates h and h^t, and stores them into the Observer.
Post scenario	h and h^t are stored in the Observer and ejects the Observer to customer.

Use Case 2: Withdrawal of e-cash by user U_0

Precondition	Customer has balance in his account maintained in the bank and has a valid Observer (smartcard) inserted into the ATM.
Successful outcome	Coins are generated into the wallet and transferred to the Observer.
Primary actor	ATM, User and Observer
Secondary actor	Account
Main scenario	1. Customer inputs withdrawal amount. 2. Bank creates coins and stores them into the Observer.

Use Case 3: Withdrawal of coin extension by user U_1

Precondition	Customer has an account in the bank.
Successful outcome	Blank coins are generated into the Observer.
Primary actor	ATM, User and Observer
Secondary actor	Account
Main scenario	Bank creates blank coins and stores them into the Observer.

B. Parameters

p, q, g, g_1, g_2, H : System parameters published by the bank

x, x^t : Secret keys of bank

h, h^t : Public keys of bank

u_0, u_1 : Users' secret keys

oa_0, oa_1 : Observers' secret keys

I_0, I_1 : Identity of users

$\{m, T, z, a, b\}$: Generated coin using binary tree based divisibility

$\{A, B, z, a, b\}$: Coin extension

$\{m, T, I, Date, Time\}$: Transferred coin to other user

Use Case 4: Coin transfer from user U_0 to user U_1

Precondition	1. Two Observers inserted into ATM. 2. Two Users communicate to each other.
Successful outcome	Coins are transferred from one User to other User.
Primary actor	1. Spending User 2. Observer of spending User 3. Receiving User 4. Observer of receiving User
Main scenario	1. Spending User inputs amount to be transferred. 2. Spender's Observer validates input and erases required number of coins. 3. Spending User creates a transcript and transfers it to receiving User. 4. Receiving User stores the received transcript into receiver's Observer.

Use Case 5: Deposit

Precondition	Customer inserts Observer (smartcard) into the ATM.
Successful outcome	Coins are deposited to customer's account in his bank.
Primary actor	ATM
Secondary actor	User, Observer and Account
Main scenario	1. Customer inputs amount to be deposited. 2. User generates a transcript and sends it to the ATM. 3. ATM validates the transcript. 4. Observer erases required coins if the Bank sends acknowledgement.
Post scenario	h and h^t are stored in the Observer and ejects the Observer to customer.

C. Implementation Classes

Since APIs, supporting blending technique, are not specified in Java card specification [14], we designed blending APIs to perform various actions inside Java

card. Classes and interfaces related to blending keys and parameters those used in Java card are as follows:

• javacard.security.BlendRandom - This class helps generating random values.

• javacard.security.BlendBigInt - This class helps blending large integers of bank server and unmatched integers inside Java card observer.

• javacard.security.BlendBigMod - This class helps calculating blended modulus for large parameters of bank server and unmatched parameters inside Java card.

• javacard.security.BlendPower - This class helps calculating blended power for large integers of bank server and unmatched integers inside Java card.

• javacard.security.BlendGenerateTree - This class helps constructing binary tree for blended values of coin inside Java card.

Fig. 7 shows sample code to using APIs related to blending technique.

```
...
...
BlendBigInt coinCount = (BlendBidInt)(wl/l);
byte[] buffer = new byte[coinCount];
BlendRandom random = BlendRan-
dom.getInstance(BlendRandom.RAND);
...
BlendGenerateTree tree = BlendGenerate-
Tree.setCoin(totalValue,treeDepth);
...
...
```

Fig. 7. Sample code using APIs related to blending technique.

VI. RESEARCH APPROACH

In Java card, the Java Card Runtime Environment (JCRE) requires a fair amount of computational power in order to work properly. Experiments were carried out in Java card simulator using 16K of ROM, 8K of EEPROM, and 256 bytes of RAM. We used Java Card API specification [14] provided by Sun Microsystems Inc. It requires Java card Workstation Development Environment (WDE). We developed the card services using new classes to run on Java card platform RMI API, and the card services ran on simulated environment using T=1 protocol. The card services used port number 9011 and 9022 with interfaces to bank and wallets. Bank and wallet components were developed in CORBA architecture using LiDIA library sets in C++ language. The Bank server and wallet ran on two separate PCs with 1.7 GHz processor each. The experiments were carried out in Linux environment.

VII. RESULTS

We used various sizes of keys in the observer with fixed key size of bank and wallet. Sample output of compiling, loading and execution of applets is given in Fig. 8.

```
Received ATR = 0x3b 0xf0 0x11 0x00 0xff 0x00
...
...
CLA: 80, INS: 30, P1: 00, P2: 00, Lc: 01, 64,
Le: 00, SW1: 90, SW2: 00
CLA: 80, INS: 50, P1: 00, P2: 00, Lc: 00, Le:
02, 00, 64, SW1: 90, SW2: 00
CLA: 80, INS: 40, P1: 00, P2: 00, Lc: 01, 32,
Le: 00, SW1: 90, SW2: 00
CLA: 80, INS: 50, P1: 00, P2: 00, Lc: 00, Le:
02, 00, 32, SW1: 90, SW2: 00
CLA: 80, INS: 30, P1: 00, P2: 00, Lc: 01, 80,
Le: 00, SW1: 6a, SW2: 83
CLA: 80, INS: 50, P1: 00, P2: 00, Lc: 00, Le:
02, 00, 32, SW1: 90, SW2: 00
CLA: 80, INS: 40, P1: 00, P2: 00, Lc: 01, 33,
Le: 00, SW1: 6a, SW2: 85
CLA: 80, INS: 50, P1: 00, P2: 00, Lc: 00, Le:
02, 00, 32, SW1: 90, SW2: 00
CLA: 80, INS: 40, P1: 00, P2: 00, Lc: 01, 80,
Le: 00, SW1: 6a, SW2: 83
CLA: 80, INS: 50, P1: 00, P2: 00, Lc: 00, Le:
02, 00, 32, SW1: 90, SW2: 00
...
...
```

Fig. 8. Snapshot of the output of Applet Compilation and Loading.

Table I shows processing time for various sizes of keys generated by the observer while the number of tree nodes were 63.

Table I Processing time for the combination of various lengths of keys

Length of Keys generated by bank and wallet	Length of keys generated by Observer	Processing Time (msec)
310	8	165.882
310	10	254.156
310	22	478.521

VIII. SECURITY

Inherent security mechanism of Java card prevents coin tempering inside it. Java has a clear separation between the card operating system (COS) and applications running on it to ensure distributed and secured execution environment [15]. Moreover, adoption of Schnorr identification scheme [16] guaranties efficiency of the secret keys.

Java card and the user's personal computer compose the user's electronic wallet, and they participate in transactions together. Only keys and calculation parameters are exchanges via open network; no coins are transmitted out of Java card or even allowed to get into it from the outer world. When user spends any coins, he needs to activate Java card by any means. Java card erases the coin trace from its coins' tree by itself. Any illegal attempts can be traced instantly by the observer during spending coins. On the other hand, Java card cannot be activated without active command issued from the wallet. Thus, this protocol not only prevents double-spending but also ensures that the card is useless if stolen or theft.

IX. CONCLUSION

The Java card is a tinny, resource-constrained and passive device whose association and synchronization with the high-speed bank servers is yet a dream. We show a way how to make use of latest generation, but still very low performance Java card in comparison to very high-end CORBA-based server. The limitation of this work is the limited availability of the card reader devices. It would be more realistic if the protocol can be implemented in mobile phones. Recently, Java enabled subscriber's identification modules (SIM), used in mobile phones, are getting most benefits of smartcards. SIMs might play a vital role in e-cash domain, specially, in peer-to-peer spending in small scale network with Bluetooth technology. A similar work can also be carried on with recently manufactured .NET card [17]. Moreover, when a single Java card would be used to serve more than one purpose (e.g., e-banking, shopping, traveling, peer-to-peer spending etc) security among applets inside the card should be the major concern. Thus, another work might be planned to develop protocols those ensure security for applets resided in Java cards for ever.

REFERENCES

[1] L. Wen-yuan, L. Yong-an, S. Ya-li, W. Bao-wen and L. Feng, "Offline divisible e-cash scheme based on smart card", in *Eighth ACIS International Conference on Software Engineering, Artificial Intelligence, Networking, and Parallel/Distributed Computing,* pp. 799-804, IEEE, 2007.

[2] D. Chaum and T. Pederson, "Wallet database with observer", pp. 89-105, Spriger-Verlag, Berlin Heidel-berg, 1993.

[3] N. Ferguson, "Single term offline coins", in *Advances in Cryptology: Eurocrypt '93, Proceedings, Lecture Notes in Computer Science no. 765*, pp. 318-328, Springer-Verlag, 1993.

[4] R. Cramer and T. Pedersen, "Improved privacy in wallets with observers", in *Advances in Cryptology: Eurocrypt '93, Proceedings, Lecture Notes in Computer Science no. 765*, pp. 329-343, Springer-Verlag, 1993.

[5] S. Brands, "Untraceable off-line cash in wallets with observers", in *Advances in Cryptology: Pre-Proceedings of Crypto '93*, 1993.

[6] X. Hou and C. Tan, "Fair traceable off-line electronic cash in wallets with observers", in *Proceedings of the 6th International Conference on Advanced Communication Technology*, pp. 595-599, 2004.

[7] I. Jahan and M. Z. Rahman, "A realistic divisible transferable electronic cash for general use", *Journal of Discrete Mathematical Science and Cryptography*, vol. 10 (2007), No. 1, pp. 125-150, 2007.

[8] D. Chaum, "Blind signature for untraceable payments", in *Proceedings of Advances in Cryptology -Crypto '83*, pp. 199-203, 1983.

[9] D. Chaum, A. Fiat, and M. Naor, "Untraceable electronic cash", in *Proceedings. Crypto '88 - Advances in Cryptology, Santa Barbara, California, Lecture Notes in Computer Science*, vol. 403, pp. 319-327, Springer, Berlin, 1990.

[10] R. Rivest, A. Shamir, and L. Adleman, "A method for obtaining digital signatures and public key cryptosystems", *ACM*, vol. 21, pp. 120-126, 1978.

[11] T. Okamoto and K. Ohta, "Disposable zero-knowledge authentication and their applications to untraceable electronic cash", in *Advances in Cryptology - Crypto '89, Proceedings (Lecture Notes in Computer Science, no. 435)*, pp. 481-496, Springer-Verlag, Santa Barbara, California, 1990.

[12] Y. Tiannis, *Efficient Electronic Cash: New Notations and Techniques*. PhD Thesis, North-eastern University Boston, Massachusetts, 1997.

[13] D. Chaum and T. Pederson, "Wallet databases with observers", in *E. Brickell editor, Advances in Cryptology - Crypto '92, Proceedings, Lecture Notes in Computer Science*, pp. 89-105, Springer-Verlag, New York, 1993.

[14] Sun Microsystems Inc., *Java Card 2.2.2*, *Application Programming Interface specification*, 2005.

[15] Z. Chen, *Java Card Technology for Smart Cards*, Addison-wesley, 2000.

[16] C. P. Schnorr, "Efficient signature generation by smart cards", *Journal of Cryptography*, vol. 4, pp. 161-174, 1991.

[17] Gemalto NV, *.NET Card*, available at http://www.gemalto.com/products/dotnet_card/, last visited on March 2009.

Proceedings of 2009 12th International Conference on Computer and Information Technology (ICCIT 2009)
21-23 December, 2009, Dhaka, Bangladesh

Performance Evaluation of MIMO System Incorporating Water Filling Model and Minimum Eigenvalue Constraints

Nur Afroza Khurshid†, Md. Imdadul Islam†, and M. R. Amin‡
†Department of Computer Science and Engineering, Jahangirnagar University, Savar, Dhaka 1342, Bangladesh
‡Department of Electronics and Communications Engineering, East West University, 43 Mohakhali, Dhaka 1212, Bangladesh
imdad@juniv.edu, ramin@ewubd.

Abstract

In this paper, both equal power and water filling models are simulated for comparison of their performance in a multiple-input multiple-output environment. The effects of fast fading and the shadowing effects have been incorporated in the models. Minimum eigenvalue required for successful transmission for individual link is evaluated from the probability density functions of eigenvalue and equivalent uncoupled multiple-input multiple-output link. Impact of the number of antenna elements of an array on the minimum eigenvalue of an uncoupled channel is analyzed based on probability density function of eigenvalue of the channel matrix. The analysis shows that the cutoff eigenvalue decreases with increase in the number of antenna elements and signal to noise ratio of the received signal.

Keywords: Antenna elements, channel capacity, MIMO, Rayleigh fading, shadowing effects and SNR.

I. INTRODUCTION

In wireless communication systems, the multiple-input multiple-output (MIMO) system provides benefits of spatial diversity with additional channel capacity without increasing the required bandwidth of the communication system [1]. A space diversity technique employs multiple transmit or receive antennas with spacing between adjacent antennas. Usually the separation between two adjacent antenna elements are kept half of the wavelength or slightly greater. To alleviate different types of fading in wireless communication systems, spatial diversity and spatial multiplexing techniques are widely used and incorporation of MIMO is a simpler solution [2], [3].

In a spatial multiplexing technique, MIMO channels offer a linear increase in capacity without requiring any additional power or bandwidth. This gain referred to as spatial multiplexing gain, is realized by transmitting independent data signals from the individual antennas. Under favorable channel conditions, such as rich scattering, the receiver can separate the different streams, which results a linear increase in capacity [4]. A space diversity technique, at both the transmitter and the receiver ends, provides the basis for a channel capacity enhancement. In this MIMO system, the signals on the transmitter antennas on one end and the receiver antennas on the other end are combined in such a way so that the quality or BER (Bit Error Rate) or data rate of the communication for each MIMO user will be improved [5]. A MIMO approach is to transmit and receive two or more unique data streams through a single radio channel, i.e. the system can deliver two or more times the data rate per channel. By allowing for the simultaneous transmission of multiple data streams, MIMO multiplies wireless data capacity without using additional frequency spectrum [6], [7]. Therefore, MIMO systems play an unparallel role in the advancement of the state-of-the-art wireless systems in the areas of signal processing, communication, and networking. Moreover, a MIMO system offers a good quality-of-service (QoS) in building wireless link for wireless wide area network (WWAN) in non-line-of-sight (NLOS) environment [8], [9]. MIMO offers a higher data rate for users who demand to use bandwidth hungry applications such as online gaming, streaming audio and video services.

The areas of influence for MIMO systems spread over different layers of protocol stack, from the physical and data link layers to network, transport, and application layers. The MIMO gains are achieved in existing wide-area networks without changing the existing protocols. The improvement of substantial performance can be achieved with adaptive array signal processing techniques at the base station combined with similar processing at the mobile terminal. In fact, it indicates that, this is the optimal approach where many of the channel conditions are common in wide-area networks.

The impulse response of the uncorrelated equivalent MIMO link is the square root of the eigenvalue of the squared modulus of the channel matrix. The throughput of a MIMO link depends on the condition of the channels. If the eigenvalue of a link falls below a threshold, the omission of the channel brings better results because of reduction in the frequent acknowledgment of erroneous frames of that fading channel. The analysis is relevant to water filling model of power constraint. The minimum eigenvalue of a link depends on both the number of antenna elements and SNR value of the received signal.

This paper is concentrated to observe the profile of minimum eigenvalue against the number of antenna elements and SNR. The Rayleigh fading along with the shadowing effects have been incorporated in the model [7].

978-1-4244-6283-4/09/$26.00 ©2009 IEEE

The reminder of this paper is organized as follows. Section II gives the overview of a MIMO system with its capacity formula, the MIMO model in water filling transmission and the minimum eigenvalue constraint in the MIMO system. Section III illustrates the simulation results of the channel capacity, channel outage probability and comparison of approximate and equal probability density function (pdf) of eigenvalues of the channel matrix. Finally the conclusion of the work is drawn in Setion IV.

II. CAPACITY OF A MIMO SYSTEM

A. Capacity of a MIMO System

A MIMO system consists of several transmit and receive antennas. A system with N_t transmit and N_R receive antennas can be considered here. The channel of this system is defined by an $N_r \times N_t$ matrix, which is denoted by $\mathbf{H}$ and is a complex matrix. The transmitted signal is represented by an $N_t \times 1$ column matrix, denoted by symbol $\mathbf{x}$, whereas the received signal is represented by an $N_r \times 1$ column matrix, denoted by symbol $\mathbf{r}$. Here, the $N_t \times 1$ vector is as follows

$$\mathbf{x}(n) = \left[\hat{x}_1(n),\ \hat{x}_2(n),\ \cdots\cdots,\ \hat{x}_{N_t}(n)\right]^T, \qquad (1)$$

which represents the complex signal vector transmitted by N_t antennas at discrete time n, the superscript T represents transpose. Here the vector $\mathbf{x}(n)$ is assumed to have zero mean and common variance σ_x^2 and the total transmitted power is defined as $P = N_t\sigma_x^2$.

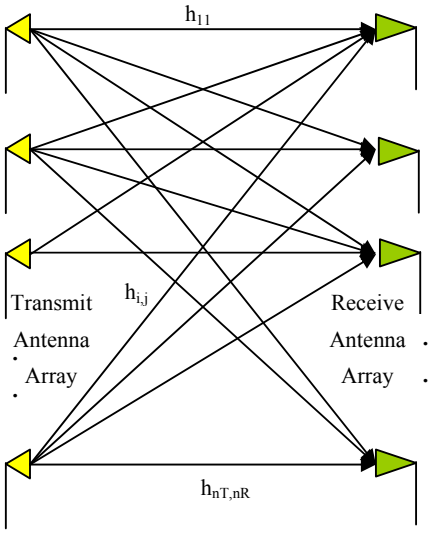

Fig. 1. MIMO channel for wireless network.

The system equations can be expressed as the following matrix form

$$\mathbf{r}(n) = \mathbf{H}(n)\mathbf{x}(n) + \mathbf{n}(n), \qquad (2)$$

where $\mathbf{H}(n)$ is the $N_r \times N_t$ channel matrix and $\mathbf{n}(n)$ is the complex noise vector with dimension $N_r \times 1$:

$$\mathbf{n}(n) = \left[\tilde{n}_1(n), \tilde{n}_2(n), \ldots\ldots\ldots, \tilde{n}_{Nr}(n)\right]^T \qquad (3)$$

Equation (2) depicts the basic complex channel model for MIMO wireless communications, specifically for a flat-fading channel. To simplify Eq. (2), the dependency on time n can be suppressed by the following expression

$$\mathbf{r} = \mathbf{H}\mathbf{x} + \mathbf{n}. \qquad (4)$$

The log–det formula for the ergodic capacity of the MIMO link can be found from any standard text [3], and it is given by the following formula [10]

$$C = E\left[\log_2\left\{\frac{\det\left(\mathbf{R}_n + \mathbf{H}\mathbf{R}_x\mathbf{H}^\dagger\right)}{\det\left(\mathbf{R}_n\right)}\right\}\right], \qquad (5)$$

where E is the statistical expectation operator; $\mathbf{R}_x$ and $\mathbf{R}_n$ are respectively the correlation matrices of the transmitted signal vector and the noise vector and the superscript † indicates Hermitian conjugate. Now, if we let $N_t = N_r = N$ for a MIMO link, the above capacity formula becomes

$$C = \log_2\left[\det\left(\mathbf{I}_N + \frac{1}{\sigma_n^2}\mathbf{R}_x\mathbf{H}\mathbf{H}^\dagger\right)\right], \qquad (6)$$

where σ_n^2 is the variance of the noise vector and $\mathbf{I}_N$ is the $N \times N$ identity matrix.

Let $\mathbf{D} = \mathbf{U}^\dagger\mathbf{H}^\dagger\mathbf{H}\mathbf{U}$, where $\mathbf{D}$ is a diagonal matrix made up of the eigenvalues of $\mathbf{H}^\dagger\mathbf{H}$, and $\mathbf{U}$ is a unitary matrix whose columns are the associated eigenvectors with property $\mathbf{U}^\dagger\mathbf{U} = \mathbf{I}_N$, then it can be easily shown that $\mathbf{H}^\dagger\mathbf{H} = \mathbf{U}\mathbf{D}\mathbf{U}^\dagger$. Therefore, the capacity formula, Eq. (6), can be expressed as follows

$$C = \log_2\left[\det\left(\mathbf{I}_N + \frac{1}{\sigma_n^2}\mathbf{D}\overline{\mathbf{R}}_x\right)\right], \qquad (7)$$

where $\overline{\mathbf{R}}_x = \mathbf{U}^\dagger\mathbf{R}_x\mathbf{U}$. The receiver is ready to receive if the channel capacity is equal or above the threshold information rate of transmitting source.

B. Water-filling model in MIMO

In water filling model each antenna element is considered as a bottle where the height of the bottom (black portion) is the noise level of corresponding uncorrelated MIMO link. White portion of the bottle is the power of the corresponding link. The level μ comes from power constraint i.e. the sum of the white portion of the bottle

is const. Here λ_i is the i-th eigenvalue and σ_n^2 is the noise variance.

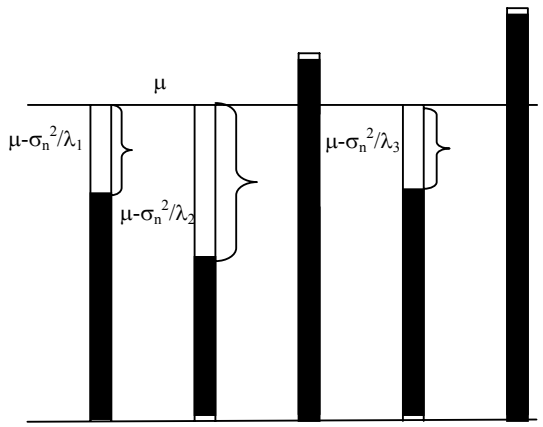

Fig. 2. Water–filling procedure, shows optimization process.

C. Minimum Eigenvalue Constraint in MIMO

MIMO channel **H** is modeled as multiplication of Rayleigh fast fading channel matrix and a scalar s counts for shadowing effect and is a random variable with $N(0,\rho^2)$. Following reference [7], the cumulative distribution function of λ can be written as

$$F(\lambda)=\int_0^{\infty}\int_0^{\lambda/s} r(s)\,g(t)\,dt\,ds\,, \tag{8}$$

where

$$r(s)=\frac{10}{\rho\log_{10}\sqrt{2\pi}}\cdot\frac{1}{s}e^{-(10\log_{10}s)^2/2\rho^2}\,, \tag{9}$$

$$g(t)\approx\frac{1}{2\pi}\sqrt{\frac{4}{tM}-\frac{1}{M^2}}\;;\; t\in(0,4M)\,, \tag{10}$$

and $N_t=N_r=M$. By differentiating $F(\lambda)$ with respect to λ, we obtain the pdf of λ as

$$f(\lambda)=\frac{10}{\rho\log_{10}\sqrt{2\pi}}\int_0^{\infty} g\left(\frac{\lambda}{s}\right)\frac{1}{s^2}e^{-(10\log_{10}s)^2/2\rho^2}\,ds\,. \tag{11}$$

Now, the optimal power adaptation is

$$P(\lambda)=\left(\Gamma_0^{(\sigma_n^2,M)}-\sigma_n^2/\lambda\right)^+,$$

where a^+ denotes $\max\{0,a\}$, and the optimal cutoff value $\Gamma_0^{(\sigma_n^2,M)}\equiv\mu$, as shown in Fig. 2, can be found by numerically solving the following power constraint equation:

$$M\int_{\sigma_n^2/\Gamma_0^{(\sigma_n^2,M)}}^{\infty}\left(\Gamma_0^{(\sigma_n^2,M)}-\frac{\sigma_n^2}{\lambda}\right)f(\lambda)\,d\lambda=\overline{P}\,, \tag{12}$$

where $\overline{P}$ is the average power constraint.

III. SIMULATION RESULTS

A simulation work based on MATLAB 7.0 is run for both equal power and water filling case. For each point on the curve of Fig. 3, the simulation is run 200 times and the average value is taken on each point. It is visualized from Fig. 3 that the normalized channel capacity of water filling model is much better than that of equal power case.

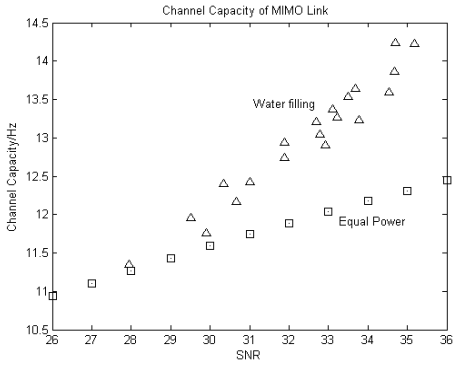

Fig. 3. Channel capacity versus SNR (μ=1.7).

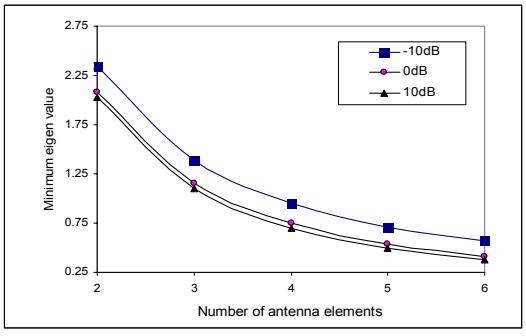

Fig. 4. Number of antenna elements against minimum eigenvalue.

The difference between two curves increases with the increase in SNR. Here the water level μ=1.7 is taken for the simulation. The variation of minimum eigenvalue against the number of antenna elements, taking the SNR value of the received signal as a parameter is shown in Fig. 4. It is observed from Fig. 4 that the minimum eigenvalue decreases with increase in both the number of antenna elements and SNR value of the received signal.

IV. CONCLUSIONS

In this paper, the channel capacity for water filling and equal power case of MIMO system are compared. The appropriate MIMO model applied here incorporating both the Rayleigh fading as well as the shadowing effects. It has been found that the channel capacity of water filling model is much better than that of the equal power case. Here, channel capacity increases with the increase of the SNR value. Minimum eigenvalue of any uncoupled link decreases with the increase of the number of antenna elements as well as with the SNR. The work can be extended incorporating the channel coding technique, such as space time block code, which repeats the symbols and finally decreases the bit error rate (BER) at the expense of the throughput.

REFERENCES

[1] Lizhong Zheng and D.N.C. Tse, "Diversity and Multiplexing: A Fundamental Tradeoff in Multiple-Antenna Channels", IEEE Trans. Inform. Theory, vol. 49, no. 5, pp. 659-664, May 2003.

[2] G. J. Foschini and M.J. Gans, "On limits of wireless communications in a fading environment when using multiple antennas", Wireless Personal Communications, vol. 6, no. 3, pp. 311-335, March 1998.

[3] Simon Haykin and Michael Moher, 2005. Modern Wireless Communications. 1st Edn., Pearson Education, Singapore, ISBN: 81-297-1000-5, 2005.

[4] H. Bolcskei, D. Gesbert, and A. J. Paulraj, 2002, "On the capacity of OFDM-based spatial multiplexing systems", IEEE Trans. Comm., vol. 50, no. 2, pp. 225-234, Feb. 2002.

[5] Ajay R. Misra, "Advanced Cellular Network Planning And Optimisation 2G/2.5G/3G - Evolution to 4G", 1st Edition, John Wiley & Sons, New York. ISBN: 978-0-470-01471-4, 2007.

[6] R. W. Heath Jr., M. Airy, and A.J. Paulraj, "Multiuser diversity for MIMO wireless systems with linear receivers" In the 35th Asilomer Conference on Signals, Systems and Computers, vol. 2, pp. 1194 - 1199, 2001.

[7] Z. Shen, R.W. Heath, J.G. Andrew and B.L.Evans, "Space-Time Water Filling Composite MIMO Fading channel", EURASIP Journal on Wireless Communications and Networking, vol. 2006, pp. 1-8, 2006.

[8] A. J. Paulraj, D. A. Gore, R. U. Nabar and H. Bolcskei, "An Overview of MIMO Communications – A key to gigabit wireless", In Proc. IEEE, 92 (2): 198-218, 2004.

[9] K. K. Wong, "Performance analysis of single and multiple MIMO diversity channels using Nakagami-distribution", IEEE Trans. Wireless Commun., vol. 3, no. 4, pp. 1043-1047, July 2004.

[10] Peter Smith and Mansoor Shafi, "An approximate capacity distribution for MIMO syatems", IEEE Trans. Commun., vol. 52, no. 6, pp. 887-890, June 2004.

Proceedings of 2009 12th International Conference on Computer and Information Technology (ICCIT 2009)
21-23 December, 2009, Dhaka, Bangladesh

WiMAX Security Analysis and Enhancement

Muhammad Sakibur Rahman, Mir Md. Saki Kowsar
Department of Computer Science and Engineering
Chittagong University of Engineering and Technology
Chittagong-4349, Bangladesh
sakib_cse_cuet@yahoo.com, sakikowsar@cuet.ac.bd

Abstract

The importance of IEEE 802.16, Worldwide Interoperability for Microwave Access (WiMAX) is growing and will compete with technologies such as 3G. The acceptance and adoption of technologies also depend on security. Therefore, this article shows security vulnerabilities found in WiMAX and gives possible solutions to eliminate them. We find the initial network procedure is not effectively secured that makes man-in-the-middle attack possible. Focusing on this attack, we propose Diffie-Hellman (DH) key exchange protocol to enhance the security level during network initialization. We modify DH key exchange protocol to fit it into mobile WiMAX network as well as to eliminate existing weakness in original DH key exchange protocol. Finally we found that the proposed algorithm shows 2.5 times better performance in comparison with existing systems.

Keywords: Key Generation, Man-in-the-Middle, Sealing Function, WiMAX.

I. INTRODUCTION

IEEE 802.16 is the Standard to state the radio frequency of fixed Broadband Wireless Access (BWA). WiMAX is the trade name of "IEEE 802.16 Standard". IEEE 802.16 was first planned to offer the last mile for Wireless Metropolitan Area Network (WMAN) with the line of sight (LoS) of 30- 50 km. It was designed to facilitate WISP's (Wireless Internet Service Provider) Backhaul, Broadband internet connectivity to proprietary and standards-based Wi-Fi mesh networks, hotspots, residences and businesses. It is featured with QoS for Voice and Video, real-time video conferencing and other services with up to 280 Mbps per base stations. Revised Standard 802.16d, 2004 provides extended support for non-line-of-sight (NLoS) in 2-11GHz spectrum with mesh connections for both fixed and nomadic users. Latest IEEE 802.16e Standard, released on February 28, 2006 intends to facilitate mobility in 2-6GHz spectrum within a range of 2-5 km.

Mobile WiMAX introduces new features like different handover types, power saving methods and multi- and broadcast support. Furthermore IEEE 802.16e eliminates most of the security vulnerabilities discovered in its predecessors [1]. It uses EAP-based mutual authentication, a variety of strong encryption algorithms and packet numbers to protect against replay attacks and reduced key lifetimes.

But in current standard of WiMAX consists some vulnerabilities and these vulnerabilities are the main cause to introduce unauthenticated messages which are susceptible to forgery and the unencrypted management communication which reveals important management information.

In this paper, we present an overview of WiMAX protocol layer and security scheme. We focus the security vulnerabilities found in mobile WiMAX and introduce Diffie-Hellman (DH) key exchange protocol to eliminate these security leaks. Furthermore, we also introduce a new thought to eliminate man-in-the-middle problem arises in DH key exchange protocol.

II. WIMAX SECURITY ARCHITECTURE

EEE 802.16 PROTOCOL LAYER

IEEE 802.16 WiMAX standard consists of a protocol stack with well-defined interfaces. The WiMAX protocol layer contains MAC layer and PHY layer. MAC layer includes three sub-layers shown in Figure 1: The Service Specific Convergence Sub-layer (MAC CS), the MAC Common Part Sub-layer (MAC CPS) and the Security Sub-layer or Privacy Sub-layer.

Two main protocols work in security sub layer, one is an encapsulation protocol for encrypting packet data across the fixed BWA, and the other is a Privacy and Key Management Protocol (PKM) providing secure distribution of keying data from Base Stations (BS) to Subscriber Stations (SS) or Mobile Stations (MS). Security sub layer is responsible for all security related activities. It also enables BS to impose conditional access to network services.

WiMAX security process is divided into three steps:

01. Authentication
02. Data Key exchange.
03. Data Encryption.

978-1-4244-6283-4/09/$26.00 ©2009 IEEE

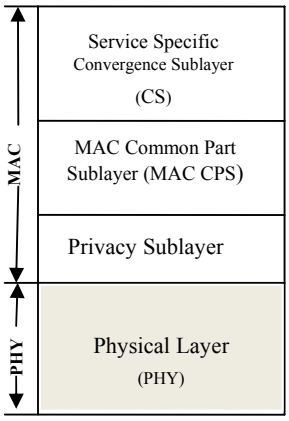

Fig. 1. IEEE 802.16 MAC and Physical Layer.

The PKM protocol uses, RSA public key algorithm, X.509 digital certificates, and strong encryption algorithm to carry out key exchanges between SS and BS [2]. This Privacy protocol has been enhanced to accommodate stronger cryptographic methods such as AES to fit into the IEEE 802.16 MAC [3].
The main objective of the privacy sub layer is to protect service providers against theft of service, rather than guarding network users. Privacy sub layer is above the physical layer, so it only guards data at the data link layer but does not protect physical layer from intercepted. It is necessary to include technologies to secure physical layer

III. VULNERABILITIES IN IEEE 802.16

With the publication of the Mobile WiMAX amendment, most of these vulnerabilities were solved. The security of IEEE 802.16e was only analyzed by a few papers, and [4] examined the 3-way TEK exchange and the authorization process and could not find any security leak. Also [5] analyzed the key management protocol using protocol analyzing software and did not detect any problem. But [6] shows, in mobile WiMAX there are some unauthenticated and unencrypted management messages which threat system reliability. This section explains vulnerabilities found in Mobile WiMAX.
These vulnerabilities are:

• Unauthenticated messages:

Mobile WiMAX includes some unauthenticated messages. Their forgery can constrict or even interrupt the communication between mobile station and base station.

• Unencrypted management communications:

The complete management communication between mobile station (MS) and base station (BS) is unencrypted. If an adversary listens to the traffic, he can collect lots of information about both instances.

A. UNAUTHENTICATED MESSAGES

Most of the management messages defined in IEEE 802.16e are integrity protected. This is done by a hash based message authentication code (HMAC) [7] or alternatively by a cipher based message authentication code (CMAC). However, some messages are not covered by any authentication mechanism. This introduces some vulnerability. A couple of management messages are sent over the broadcast management connection. Since in WiMAX security architecture, there is no common key which can be used as the authentication of broadcasted management messages, so the authentication of these messages is difficult. Furthermore, a common key would not completely protect the integrity of the message as mobile stations sharing the key can be generated by unauthenticated BS.

B. UNENCRYPTED MANAGEMENT COMMUNICATION

The topic of unencrypted messages has already been discussed in some papers for Fixed WiMAX. In Mobile WiMAX management messages are still sent in the clear. The risk introduced by the management messages when they sent without encrypted will be discussed in this section.

When a MS performs initial network entry it negotiates communication parameters and settings with the BS, a lot of information is exchanged like security negotiation parameters, configuration settings, mobility parameters, power settings, vendor information, MS's capabilities, etc. Since the management messages are unencrypted, so an attacker can be accessed the mentioned information just by listening on the channel.

Initial network entry contains four processes: initial Ranging process, SS Basic Capability (SBC) negotiation process, PKM authentication process, and registration process. Initial network entry is the most security sensitive processes in Mobile WiMAX network not only because it is the first gate to establish a connection to the network, but also because many physical parameters, performance factors, and security contexts between SS and serving BS are determined during this process. The initial network process and MS Basic Capability negotiation is illustrated in Figure 2.

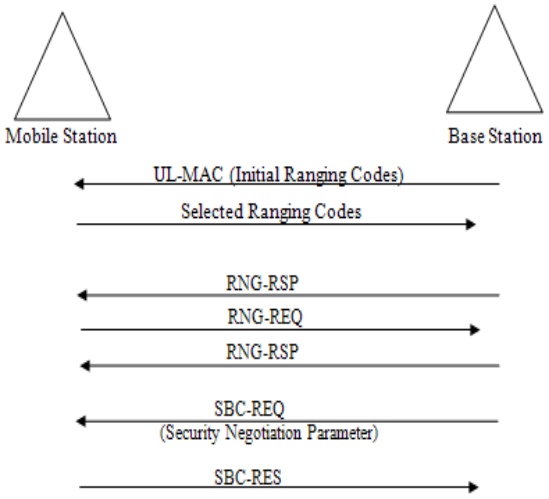

Fig. 2. WiMAX Initial Network Entry Procedure.

After initial network entry, the management communication over the basic and primary management connections remains unencrypted. As most of the management messages are sent on these connections, nearly all management information exchanged between MS and BS can be accessed by a listening adversary.

The only messages which are encrypted are key transfer messages. But in this case only the transferred key is encrypted, all other information is still sent in the clear. An adversary collecting management information can create detailed profiles about MS's including capabilities of devices, security settings, associations with base stations and all other information described above. Using the data offered in power reports, registration, ranging and handover messages, a listening adversary is able to determine the movement and approximate position of the MS as well. Monitoring the MAC address sent in ranging or registration messages reveals the mapping of connection identifier (CID) and MAC address, making it possible to clearly relate the collected information to user equipment.

IV. SOLUTION AND IMPROVEMENT

There are not appropriate methods to protect these messages. In order to eliminate the security vulnerabilities during initial network entry, we can encrypt the initial management massages based on Diffie-Hellman (DH) key exchange protocol [8]. DH key agreement is a key management method to share an encryption key with global variables known as prime number 'P' and 'G', 'G' is a primitive root of P. 'a' is the private key of MS, and 'b' is the private key of BS.

SS's public key is $PK_{MS} = G^a \bmod P$, and

BS's public key is $PK_{BS} = G^b \bmod P$.

The DH key exchange protocol is described as follows where both BS and MS exchange keys:

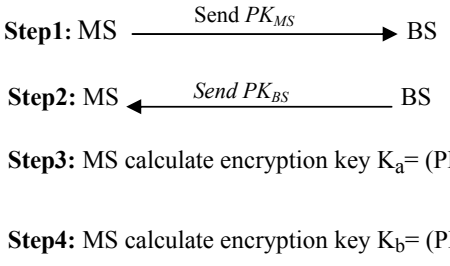

Algebraically it can be shown that $K_a = K_b$. So, the encryption will be symmetric key encryption process. And it is suggested to use 'Vernam Cipher' encryption process rather than DES or AES to encrypt initial management communication where the key will be used as a random number for encryption. Because of the use of symmetric key encryption as well as Vernam Cipher which required only to performed bitwise Exclusive-OR operation [9], it will not introduce any traffic overhead in the network. Encryption process is described as follows:

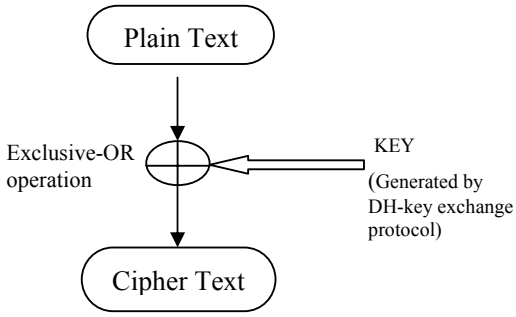

Fig. 3. Encryption Process by using Key, Generated by DH Algorithm.

A. MAN-IN-THE-MIDDLE VULNERABILITIES

A man-in-the-middle attack is one in which the attacker intercepts messages during the process of communication establishment or a public key exchange and then retransmits them, tampering the information contained in the messages, so that the two original parties still appear to be communicating with each other.

In Diffie-Hellman key exchange process [10], it is possible to man-in-the-middle attack. Figure: 5 illustrated this type of vulnerability in DH key exchange protocol.

In man-in-the-middle attack, a legitimate MS sends its public key to an evil MS. This evil MS acts as a BS to a legitimate MS. It also acts as a MS to a legitimate BS. This way, it can exchange its public key to both MS and BS. A legitimate MS and evil MS exchange keys and both generate the same symmetric key for encryption and evil SS uses this key to communicate with the MS but it also generate another symmetric key to communicate with legitimate BS. When traffic received

from legitimate MS, the evil MS just decrypt the message by the symmetric key generated by DH key exchange protocol and listen the message and finally, again encrypt the message by the symmetric key generated by DH key exchange protocol between legitimate BS and evil MS and send to the legitimate BS.

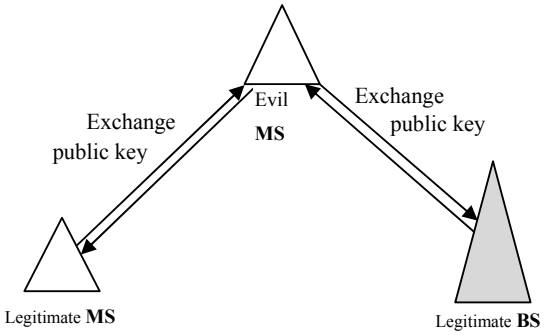

Fig. 4. Man-in-the-middle Attack

It is possible to overcome the man-in-the-middle vulnerability by using cryptographic sealing functions. In this process every MS has an International Subscriber Station Identity (ISSI) and a cryptographic function as a seal of legitimate MS. The security process is as follows:

Step1: MS alleges that it is a legitimate subscriber.

Step2: BS sends a random number, R_{BS} as a challenge to MS.

Step3: MS calculates the value of the function for this random number and sends the value and its ISSI number to BS.

Step4: MS sends a random number, R_{SS} as a challenge to BS that it is a legitimate BS.

Step5: BS calculates the value of the function by this random number for the corresponding ISSI and sends to BS.

Step6: Only the legitimate BS knows the function which is used by the given ISSI but not the evil MS. So the evil MS is not able to produce correct value for the given random number. Then MS checks BS's identity using the response that it receives, if the BS is legitimate, the shared key is established and MS continues to communicate with BS; otherwise, MS ceases the communication.

Suppose a MS's ISSI number is: 0346AE2D and it consists the cryptographic function:

$$f(x)= x^3 + x-5$$

Now, the initial communication will be as follows:

Step1: MS says that: "I am a legitimate subscriber".

Step2: Suppose, BS sends a random number $R_{BS} = 3$ to MS as challenge to MS.

Step3: MS calculate the value of f(x) =25, and send the value as well as the ISSI number.

Step4: BS also calculates the value of f(x) for the given ISSI number and finds that it is a legitimate MS.

Step5: Suppose, MS also sends a random number $R_{MS}=5$ to BS as a challenge to BS.

Step6: BS calculates the value of f(x) =125, send to MS.

Step7: MS verify the value and continue to communicate with BS if the value of the cryptographic function matches with MS's calculated value. Otherwise MS ceases the communication.

Afterward, both MS and BS exchange their public key and generate a common key by DH algorithm for exchanging management information and other messages which verify the message authenticity and enhance system reliability that gives no information to attackers.

B. PERFORMANCE ANALYSIS

After employing the proposed system, it is sure that the system runs as a secured system without any probability of attacks on the management communications. Even this system eliminates the possibility of man-in-the-middle attacks in initial network entry procedure and makes authentication process more easy and reliable. Moreover, the proposed encryption process required less execution time than the existing process which does not introduce any traffic overhead in the network. The comparative analysis of the performance between proposed system and the existing system is described in the following table I.

Table I Comparative analysis between proposed system and existing system

Existing System	Proposed System
01. After negotiation with the network MS sets up a security association (SA). This SA manages the keys for all encryption processes. So the initial negotiation process remains unencrypted.	01. In proposed system, keys are not managed only by the SA; rather keys also have been generated by Diffie-Hallman algorithm [8] before negotiation and this key generation provides the opportunity to encrypt the messages required for negotiation.
02. If the management information remains unencrypted it makes possible to get user's ranging information, channel information, vendor information and registration information etc. which threats user secrecy and interrupt the communication.	02. The proposed system allows the network to establish a shared key and this is used to encrypt all management messages. So it is not possible for an attacker to listen the user's ranging information, channel information, user's vendor information, etc. and communication continues without any interruption.

Authentication process of the proposed system is too much simple and required only four steps to send and receive the random numbers and corresponding function values. But in the existing systems, authentication process is very much complex and not sufficient to eliminate man-in-the –middle attacks because the authentication process is performed only by the BSs not by MSs.

Proposed system required four steps for authentication process:

1. BS sends a random number to MS
2. MS calculates and sends the function value for the corresponding random number and ISSI number to BS
3. Again BS receives a random number from MS and calculates the function value for the given ISSI number.
4. MS received function value from BS for the given random number.

Existing system's authentication process required steps are:

1. MS sends Authentication-Inf-Mess (manufacturer X.509 certificate) to BS
2. MS sends Authentication-Req-Mess (X.509 cert, Capability, Basic CID, SAID) to BS.
3. BS sends Authentication-Rep-Mess (AK-Seq, Life time, SA-Descriptor) by encrypting MS's public key.
4. MS calculates KEK and message authentication keys HMAC_ Keys (HMAC_Key_U, HMAC_Key_D) and sends response by using these keys.

Here, we found that the BSs have to calculate Authorization Key (AK), life lime, and to generate security association descriptor and also have to perform encryption by using MS's public key. Again MSs have to calculate key encryption key (KEK), Authorization keys (HMAC_Key_U, HMAC_Key_D). So this complex but one-way authentication required total three keys calculation and one key generation and RSA encryption and one SA-Descriptor generation processes. So we found that the proposed authentication process is very simple and required only two operations (calculate two functions value) where existing system is very much complex and required five operations (three key generations, one descriptor generation and one encryption process). The operation time depends on vendor's capability. The following figure 5: shows the comparative analysis of the number of operations have to process for N subscribers and we found that the proposed systems require 2.5 times less operations and perform authentications for both BSs and MSs.

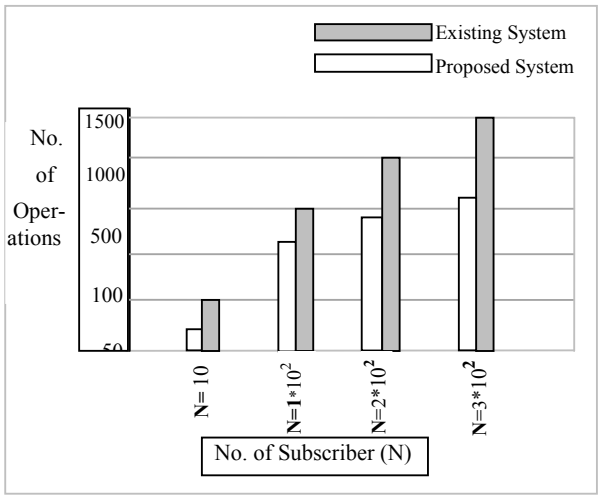

Fig. 5. Comparative analysis of Authentication Process (Operations vs. Subscribers)

V. CONCLUTION

In this paper, an overview of security scheme in IEEE802.16 based mobile WiMAX is presented. We investigate various vulnerabilities in mobile WiMAX network and we propose DH key exchange protocol to enhance the security level during the initial network entry procedure to reduce unauthenticated messages and to encrypt the initial management communication. We modify DH protocol to fit mobile WiMAX to eliminate man-in-the-middle attack by using cryptographic sealing function. Verily it could eliminate the possibilities of the man-in-the-middle attacks as well as resist DoS attacks toward mobile WiMAX.

REFERENCES

[1] Johnston D., Walker J.: Overview of IEEE 802.16 Security, IEEE Computer Society, 2004.

[2] Xu, S., Matthews, M. & Huang, C. (2006). *Security Issues in Privacy and Key Management Protocols of IEEE802.16,* retrieved on 1st May, 2006.

[3] Eklund, C., Marks,R.B., Stanwood, K.L., & Wang, S.(2002) *IEEE Standard 802.16: A Technical Overview of the WirelessMAN™ Air Interface for Broadband Wireless Access,* retrieved on 1st May, 2006.

[4] Datta A., He C., Mitchell J.C., Roy A., Sundararajan M.: 802.16e Notes, Electrical Engineering and Computer Science Departments, Stanford University, CA, USA, 2005
Yuksel E.: Analysis of the PKMv2 Protocol in IEEE 802.16e-2005 Using Static Analysis Informatics and Mathematical Modeling, Technical University Denmark, DTU, 2007.

[5] Andreas Deininger, Shinsaku Kiyomoto, Jun Kurihara, Toshiaki Tanaka: Security Vulnerabilities

and Solutions in Mobile WiMAX, IJCSNS International Journal of Computer Science and Network Security, VOL.7 No.11, November 2007.

[6] Krawczyk H., Ballare M., Canetti R.: HMAC: Key-Hashing for Message Authentication, RFC 2104.

[7] Whitfield Diffie and Martin E. Hellman: New Directions in Cryptography, Invented Paper.

[8] Charles P. Pfleeger, "Security in Computing" VOL No. 2

[9] Tao Han, Ning Zhang, Kaiming Liu, Bihua Tang, Yuan'an Liu: Analysis of Mobile WiMAX Security: Vulnerabilities and Solutions, IEEE Xplore.

Proceedings of 2009 12th International Conference on Computer and Information Technology (ICCIT 2009)
21-23 December, 2009, Dhaka, Bangladesh

Speaker Identification System Using PCA & Eigenface

Md. Rashedul Islam*, Md. Shafiul Azam, Saleh Ahmed*****
Dept. of Computer Science & Engineering, Leading University, Sylhet, Bangladesh
Dept. of Computer Science & Engineering, University of Rajshahi, Bangladesh
*rashed.cse@gmail.com, **shahincseru@gmail.com, ***sumon.edu@gmail.com

Abstract

This paper presents a speech-based speaker identification system and an efficient approach for selection of acoustic parameters closely related to the vocal track shape of the speaker. Speech endpoint detection algorithm is developed in order to discard the room noise and non-speech signal to achieve high accuracy of the system. Windowing and Fast Fourier Transform (FFT) are used to determine the spectrum of the speech signal and PCA has been used to extract feature of speech of individual speaker. Eigenface algorithm has been used here as a classification and recognation tool. Eigenspace of individual speaker is generated by the feature of the speech signal. The experimental results show the noticeable performance of the proposed system.

Keywords: Endpoint detection, Hamming window, FFT, PCA, Eigenface , Eigenvectors.

I. INTRODUCTION

Speaker identification system attempts to recognize a speaker on the basis of individual information included in speech signal. The system can be either text-dependent (constraint on what is spoken) or text-independent (no constraint what is spoken). The idea is to identify the inherent differences in the articulator organs and the manner of speaking [1], [2]. Speaker identification technology makes it possible to a the speaker's voice to control access to restricted services, for example, phone access to banking, database services, shopping or voice mail, and access to secure equipment. Features like vocal track system characteristics, pitch, and intonation pattern for a particular text carry speaker information [3]. Biometrics systems are the automated methods for verifying a person's identity based on physiological characteristics like handwriting, fingerprints, and voice. Some techniques are expensive, and others are invasive. Voices of different individuals do not sound alike and may be the most natural and inexpensive biometrics system to be used for personal identity verification. Speaker recognition could be useful in many services, and can play a major role in security system. A general model for speaker identification is shown in Fig. 1.

The speaker identification problem can be broadly divided into two components: speech analysis (feature extraction) and Classification [2], [4]. The feature space ultimately determines the separability of the desired classes (speakers), whereas the classifier must be tuned to model and differentiate the classes in a given feature space. Spectrum, MFCC, LPCC are usually used for feature extraction. And Hidden Markov Model (HMM)[2], [5], ANN [2], [6]-[8], dynamic time wrapping (DTW) [2], [5], [8] and Gaussian Mixture Model (GMM) [2], [9] are usually used classification tools in speaker identification. In our proposed system PCA used for feature extraction and feature space is mapped into eigenspace for classification and identification. The selected features have enough information within it to identify each speaker class uniquely. Here a class label is assigned to each unknown speaker by examining the extracted features and comparing them with classes learnt during training phase.

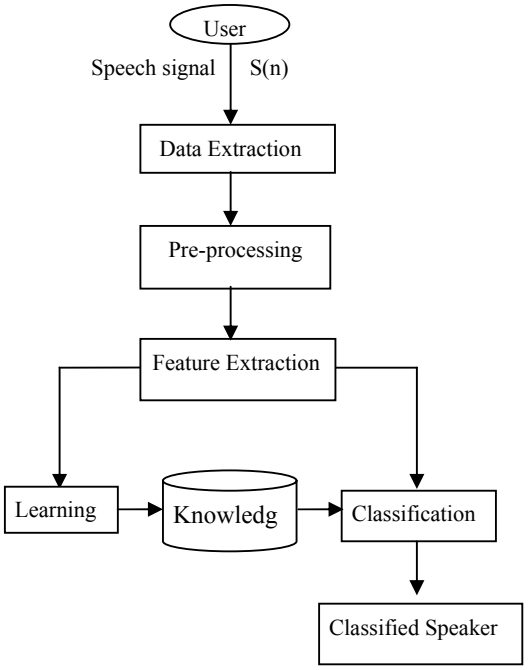

Fig. 1 Block diagram of a Speaker Identification System.

II. PREPROCESSING OF SPEECH

Preprocessing is to adjust the recorded speaker's utterance to have a better quality and to prepare the signal for the better processing in the following steps. It covers mainly the digital filtering and the endpoint detection. Filtering is to filter out the any surrounding noise using the application of digital filters. Endpoint detection is a process to clamping only a desired speech interval. Although this approach probably causes error with too small loudness of speech, protection of this error can be done during a speech recording process.

A. ROOM NOISE MEASUREMENT

Speech is recorded for each speaker in a laboratory environment, which always include some background noise. The noise depends on the sensitivity of the microphone and room environment. Noise measure has been done with both microphone and speaker keeping on. The knowledge of this background noise energy is very important for speech endpoint detection and, in turn, to success of the speaker identification system.

B. SOURCES OF BACKGROUND NOISE

During recording our speech signal the talker produces some noise like lip smacks, heavy breathing, and mouth clicks and pops. Besides this, other environmental noise may also be included in our speech signal. Fig. 2 shows a typical mouth click produced by opening the lips (prior to speaking) when the mouth is relatively dry, thereby causing the lips to pops (i.e., produce a high frequency, transient sound) and a high level of breath noise produced at the end of speaking, caused by speaker's heavy breathing.

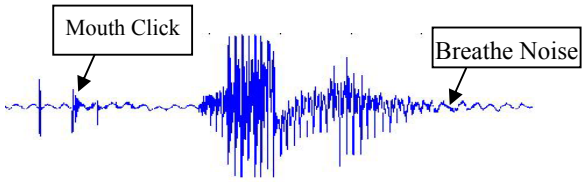

Fig. 2 Speech Signal with Mouth Click and Breathe Noise.

In order to implement a good speaker identification system, it is required to consider this noise and some method to eliminate it.

C. ENDPOINT DETECTION

Detecting the presence of speech in a background noise is an important task to achieve high accuracy in speaker identification. For the detection of the endpoint of speech signals [10][11], several algorithms have been proposed. Simple endpoint uses the short-time energy and zero-crossing rate algorithms.
Sophisticated endpoint detection employs the short-time energy, pattern comparison, and a decision rule for noisy environments. Short-time energy is used to distinguish among voiced, unvoiced, or background silence speech.

The zero-crossing rate also provides a rough voiced/unvoiced classification feature since unvoiced speech has a much higher zero-crossing than voiced speech. In speaker recognition systems, speech endpoints are used to remove silence, pauses, and other unwanted unvoiced speech thereby detecting speech signal. It in turns helps to reduce the amount of processing of the speech data.

The endpoint detection algorithm as follows[10]:

- The algorithm removes any DC offset in the signal.
- Compute the average magnitude and zero-crossing rate of the signal as well as the average magnitude and zero-crossing rate of background noise.
- At the beginning of the signal, we search for the first point where the signal magnitude exceeds the previously set threshold for the average magnitude.
- From this point, search backwards until the magnitude drops below a lower magnitude threshold.
- From here, we search the previous twenty-five frames of the signal to locate if and when a point exists where the zero-crossing rate drops below the previously set threshold. This point, if it is found, demonstrates that the speech begins with an unvoiced sound and allows the algorithm to return a starting point for the speech, which includes any unvoiced section at the start of the phrase.
- The above process will be repeated for the end of the speech signal to locate an endpoint for the speech.

The following Fig. 3 illustrate signal before and after endpoint detection for a sample speech signal.

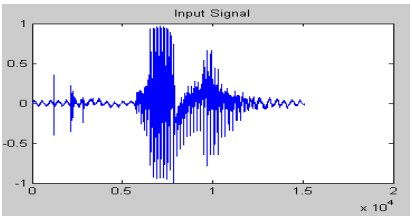

(3.a) Input speech signal.

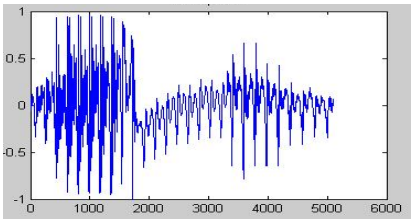

(3.b) Speech after silence

III. FEATURE EXTRACTION

The data set used for training and testing the system consists of selected words for several speakers. The training feature set is generated for each speaker. A set of features are extracted for each speaker for both one syllable and two syllable words. Speech feature, namely the principal component of the speech is obtained by winding with overlapping, Fast Fourier Transformation and PCA. The process of the calculation of speech feature is shown in Fig. 4.

After overlapped framing the signal of each frame is multiplied by Hamming window of frame length to

reduce the spectral discontinuity. Then the fast Fourier transform is applied on the windowed frame to compute the signal coefficients in frequency domain. Finally the magnitude spectra converted to Spectral Image and submitted to PCA module for acquiring feature of a speaker's speech characteristics.

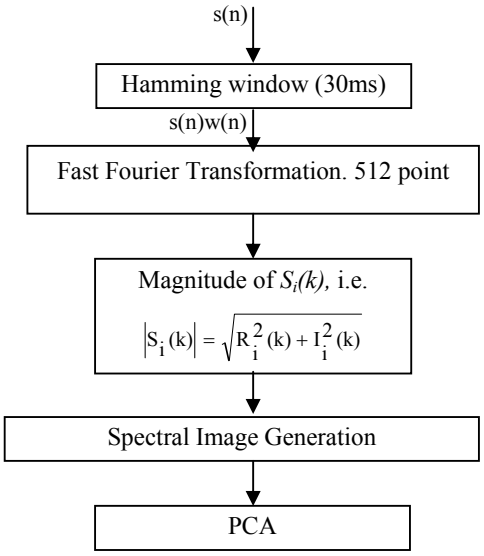

Fig. 4 Acquire data for 30ms speech.

A. Frame Overlapping

In order to obtain good DFT spectral analysis results many contiguous DFT outputs must be computed and averaged. If the window and the FFT are applied to non-overlapping portions of the sequence, as shown in Fig.5(a), a significant part of the series is ignored due to the window's exhibiting small values near the boundaries.

For instance, if the transform is being used to detect short-duration tone-like signals, the non-overlapped analysis could miss the event if it occurred near the boundaries.

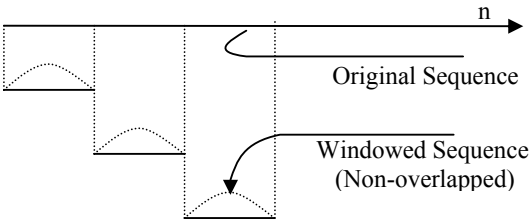

Fig. 5(a) Partition of sequence for non-overlapped processing.

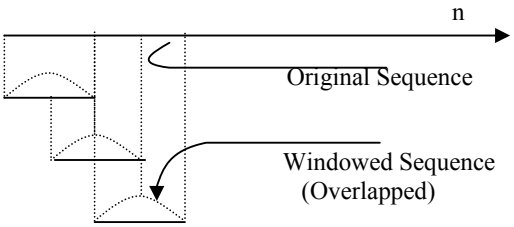

Fig. 5(b) Partition of sequence for overlapped processing.

B. Hamming Window

Windows are used to modify the DFT frequency output response characteristics. Windows are used in conjunction with DFT spectral analysis to reduce spectral leakage, reduce scalloping loss and provide variable resolution. In speech processing it is used to divide continuous speech into segments, which are assumed to be stationary in a short period of time. Several commonly used windows include rectangular, Hanning, Hamming, and Blackman-Harris windows.

The Hamming window of length N, is defined as:

$$w[k+1] = 0.54 - 0.46\cos\left(2\pi\frac{k}{n-1}\right),$$

$k=0...,n-1$

….. (1)

The Fig. 6 illustrate the effect of Hamming window over a frame of speech.

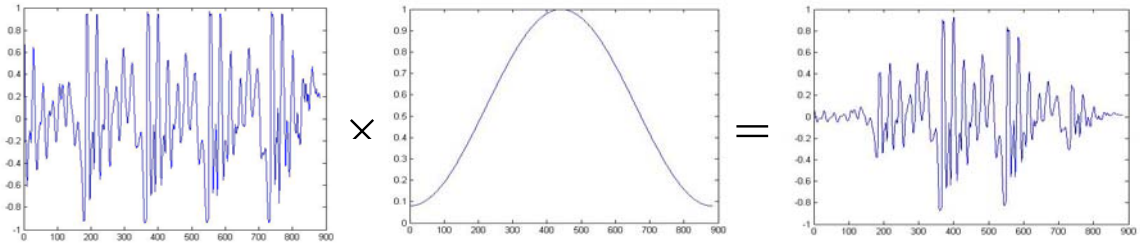

Fig. 6 Effect of Hamming Window

T data, the transforms are usually applied to the overlapped partition sequences as shown in Fig. 5(b)

C. FAST FOURIER TRANSFORM:

A fast Fourier transform (FFT) [12] is an efficient algorithm to compute the discrete Fourier transform (DFT) and its inverse. FFTs are of great importance to a wide variety of applications, from digital signal processing to solving partial differential equations to algorithms for quickly multiplying large integers.

If x(n) is the discrete sequence obtained by sampling the continuous signal *x(t)*, its Fourier Transform (FT) and Inverse Fourier Transform (IFT) are defined as [12]:

(FT)
$$X(\varpi)=\sum_{n=-\infty}^{\infty}x(n)e^{-j\varpi n} \quad \ldots\ldots(2)$$

(IFT)
$$x(n)=\frac{1}{2\pi}\int_{-\pi}^{\pi}X(\varpi)e^{j\varpi n}d\varpi \quad \ldots\ldots(3)$$

We have acquired the magnitude spectra from FFT. Here 512 point FFT have been used. After Calculate the magnitude, we get 256 point. The acquired magnitude data of all frame using FFT. From the total data we can get fixed set of data using Peak detection in difference frequency range. Using the set of all peak value we can generate a spectral image.

D. Spectral Image generation:

A Spectral data matrix is generated based on the N feature values for each of the speech. Then the data matrices are mapped onto a 2-D plane for generating an image called Spectral image. Then using PCA[15] we can get Feature from this Image. Fig. 7 shows training image for sample speech signal.

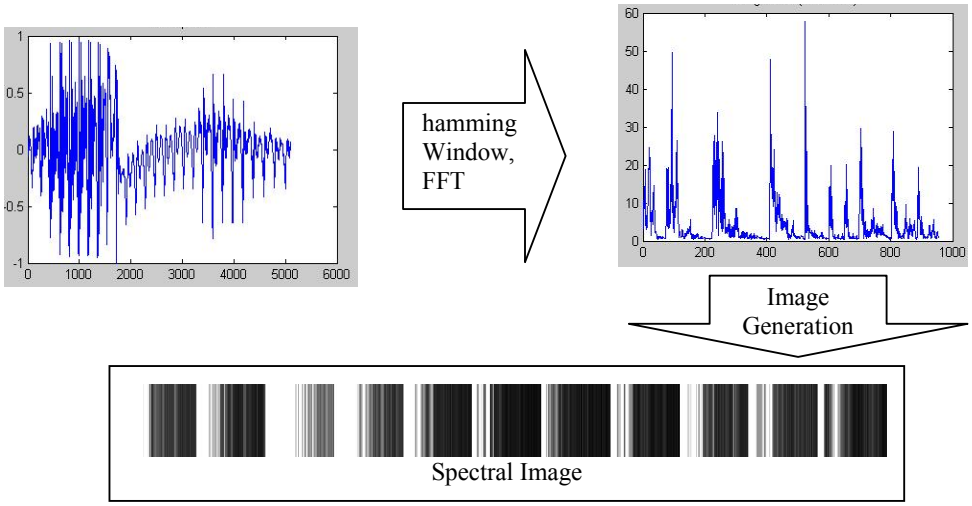

Fig. 7 Spectral Image for a sample speech signal.

E. PCA Method

1. In this step, the spectral image constituting the training set (Γ_i *i*) should be prepared for processing.
2. The average matrix Ψ has to be calculated, then subtracted from the original spectral image (Γ_i) and the result stored in the variable Φ_i :

$$\Psi=\frac{1}{M}\sum n-1M\Gamma_n \quad \ldots\ldots (4)$$

$$\Psi_i=\Gamma_i-\Psi \quad \ldots\ldots (5)$$

The following Fig. 8 illustrates Average image for some training spectral images.

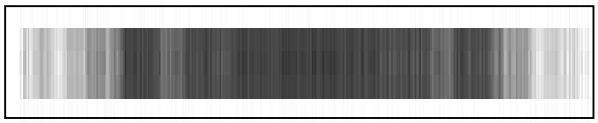

Fig. 8 Average image for some training spectral images.

3. In the next step the covariance matrix *C* is calculated according to

$$C=\frac{1}{M}\sum_{n-1}^{M}\Phi_n\Phi_n^T \quad \ldots\ldots (6)$$

4. Calculate the eigenvectors and eigenvalues of the covariance matrix
5. From *M* eigenvectors (eigenfaces) *ui*, only *M'* should be chosen, which have the highest eigenvalues. The higher the eigenvalue, the more characteristic features of a feature image does the particular eigenvector describe. Eigenfaces with low eigenvalues can be omitted, as they explain

only a small part of characteristic features of the feature image. After *M'* eigenfaces *ui* are determined, the "training" phase of the algorithm is finished.

The following Fig. 9 illustrates Eigenface for some training spectral images.

Fig. 9 Eigen face for some training spectral image.

IV. EIGENFACE RECOGNITION PROCEDURE

In previous generally ANN is used for speaker identification. But in this paper Eigenface [13] is used for for voice pattern recognition in speaker identification system. In this section, the original scheme for recognition of a speaker will be presented.

A. RECOGNITION

1. A spectral image of a new speaker Γ_{new} is transformed into its eigenface components. First we compare our input feature with our mean and multiply their difference with each eigenvector of the Ψ matrix. Each value would represent a weight and would be saved on a vector Ω_{new}^{T}.

$$\omega_k = u_k^T(\Gamma_{new} - \Psi) \qquad \text{K=1....M} \qquad \ldots\ldots (7)$$

$$\Omega_{new}^{T} = [\omega_1\ \omega_2\ .....\ \omega_M] \qquad \ldots\ldots (8)$$

2. We now determine which face class provides the best description for the input image. This is done by minimizing the Euclidean distance.
3. The input feature is consider to belong to a class if εk is bellow an established threshold θ. Then the feature image is considered to be a known face. If the difference is above the given threshold, but bellow a second threshold, the feature can be determined as a unknown feature image
4. If the feature is found to be an unknown feature, you could decide whether or not you want to add the feature to your training set for future recognitions. You would have to repeat steps 1 trough 4 to incorporate this new feature.

V. EXPERIMENTAL AND RESULTS

In this experiment, the proposed Speaker Identification system is evaluated with 30 speaker (3 speech for each speaker) by speech. The speech recorded at normal noise less environment. The speech signal is sampled at a rate of 22050 samples per second (Fs=22050Hz).

Table 1. Some Speech sample for Training

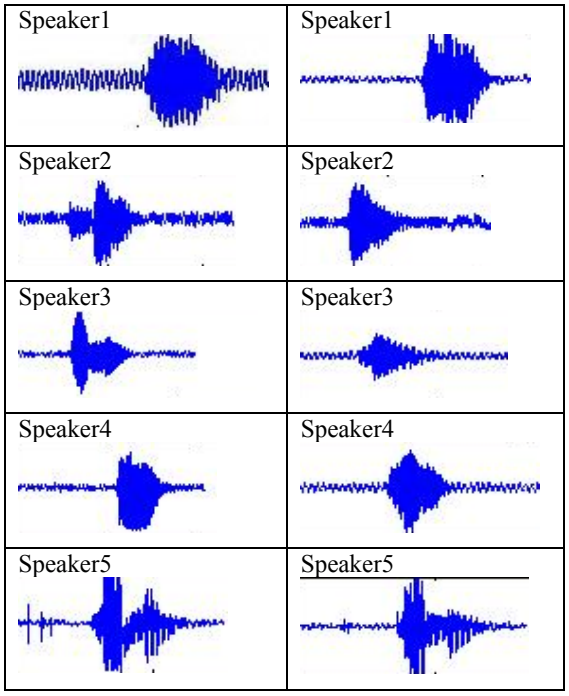

Table 2. Some Speech sample for Test

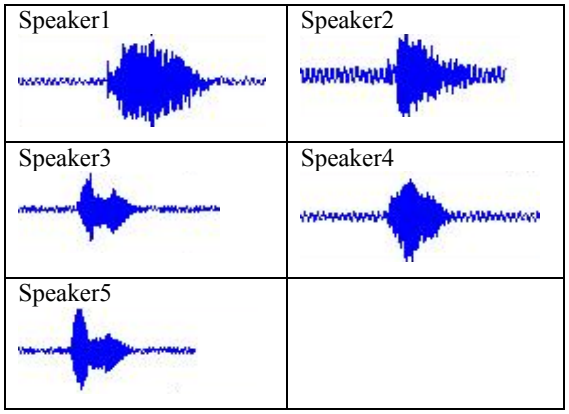

In this new approach using PCA and Eigenface method, we have got much better performance. I think the performance is better then previously used normal Fourier spectrum analysis and Artificial Neural Network (ANN).

Table 3. Average Speaker Identification rate for 30 speaker.

Speaker tests	Identified	Do not identified	Accuracy (%)
30	27	3	90%

In this approach speaker identification rate (Accuracy) might be changed over the number of speaker increase in training set. The following figure reveals the expected changes of accuracy for increasing the number of speaker trained.

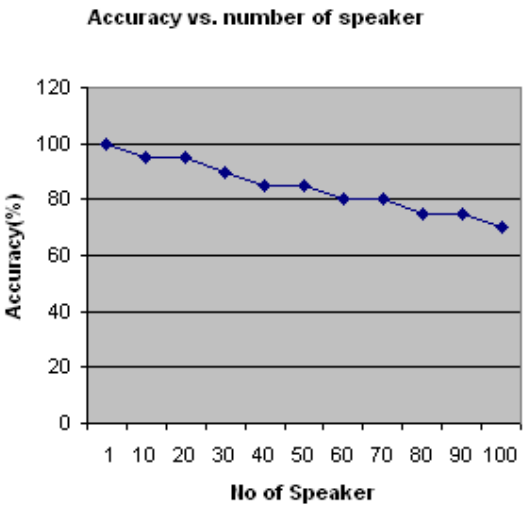

Fig. 10 Expected graph of accuracy vs. number of speaker.

VI. CONCLUSION

Speaker Identification System for speech using PCA and Eigenface technique is proposed here. The goal of this study is to use the Eigenface for recognition speaker. Fourier spectrum and PCA method are used for feature extraction. This system can be termed as a language and text independent speaker identification system. This system will identify speaker by a word what ever it is. Using the proper normalization of speech signal, speech processing (adaptive filtering, noise elimination), better method in feature extraction and changing Eigenface parameter this system can achieve better performance. In near future, it is very important to extend this technique so that more accurate and real-time speaker identification becomes possible.

REFERENCES

[1]. R. J. Mammone, X. Zhang, R. Ramachandran, "Robust Speaker Recognition", IEEE Signal processing Magazine, September 1996

[2]. Md. Khademul Islam Molla, Keikichi Hirose, Nobuaki Minematsu "On the Effectiveness of MFCCs and their Statistical Distribution Properties in Speaker Identification " Preprint: Submitted to IEEE Transaction on Instrumentation & Measurement

[3]. Lawrence R. Rabiner and Ronald W. Schafer, "Digital Processing of Speech Signal," Prentice-Hall Inc., Englewood cliffs, New Jersey

[4]. D. A. Raynolds, "Experimental Evaluation of Features for Robust Speaker Identification", IEEE Transaction on Speech and Audio Processing, Vol. 2, No. 4, Oct 1994

[5]. K. Yu, J. Mason, J. Oglesby, "Speaker Recognition using Hidden Markov Model, Dynamic Time Warping and Vector Quantization", IEE Proc. Visual Image Signal Processing, Vol. 142, No. 5, Oct 1995.

[6]. S. Sae-Tang, C. Tanprasert, "Feature Windowing-Based for Thai Text-Dependent Speaker Identification using MLP with Backpropagation Algorithm", International Symposium on Circuits and Systems (ISCAS), 2000.

[7]. P. Premakanthan, W. B. Michael, "Speaker Verification/Recognition and the Importance of the Selective Feature Extraction: Review", ISCAS 2001

[8]. S. Sakuriya et. al. "Text-Dependent Speaker Identification via Telephone based on DTW and MLP", Twentieth IASTED International Conference on Modeling, Identification and Control (MIC2001), 2001

[9]. Y. Shao, D. Wang, "Co-Channel Speaker Identification using Usable Speech Extraction based on Multi-pitch Tracking", ICASSP 2003.

[10]. Speaker Verification Endpoint Detection, http://www.owlnet.rice.edu/~elec301/Projects99/wrcocee/endpt.htm

[11]. M.H. Savoji, "A Robust Algorithm for Accurate Endpointing of Speech Signal," Speech Communication 8, 1989.

[12]. Matlab help "Fast Fourier Transformation"

[13]. Eigenface-based facial recognition, Dimitri, PISSARENKO, February 13, 2003.

[14]. *Natasha Singh-Miller, Michael Collins, Timothy J. Hazen* "Dimensionality Reduction for Speech Recognition Using Neighborhood Components Analysis"

[15]. Tetsuya Takiguchi, Yasuo Ariki "PCA-Based Speech Enhancement for Distorted Speech Recognition"

Proceedings of 2009 12th International Conference on Computer and Information Technology (ICCIT 2009)
21-23 December, 2009, Dhaka, Bangladesh

Integrated Data Warehousing for Telecommunication Industries

Md. Mosharaf Hossain, Tawseef Azim, Md. Yasser Karim, A. S. M. Latiful Hoque
Department of Computer Science and Engineering
Bangladesh University of Engineering and Technology, Dhaka-1000, Bangladesh
mosharafc@gmail.com, salues.351@gmail.com, sunnycse117@yahoo.com, asmlatifulhoque@cse.buet.ac.bd

Abstract

Data warehousing provides an excellent opportunity in transforming operational data into useful and reliable information to support the decision making process in any organization. Data Warehouse (DW) generalizes and consolidates multidimensional (MD) data. Hence, DW has become an important platform for Online Analytical Processing (OLAP) which is based on a MD data model. In this paper, we propose an integrated data warehouse system for the telecommunication companies in Bangladesh .Our integrated DW provides a common framework based on temporal data from different telecommunication operators rendering their services. We develop a dimensional model architecture, data extraction methodology, transformation and loading techniques which provides analytical options with the implementation of relational OLAP.

Keywords: Data Warehousing, Dimensional modeling, CDR, ETL, OLAP

I. INTRODUCTION

The extremely challenging business environment of today necessitates many telecommunications carriers to measure their success by the extent and augmentation of their turnover margins. Consequentially, carriers are under tremendous amount of pressure to reduce or eliminate the major threats to these margins which traditionally arise from revenue leakage, erroneous inter-carrier billing and churn. Carriers depends on observation of terabytes of Call Detail Record (CDR) data to enable them to make critical management decisions that will aid them in the realization of their profit aspirations. High-end DWs and powerful Business Intelligence (BI) solutions are thus becoming crucial tools to help carriers meet profit goals [1].

Data warehousing is an approach of data integration in which integrated information is stored in a data warehouse for direct querying and analysis by the users [2]. The main difference between this approach and the traditional data integration one is that relevant data are extracted from data sources and integrated information is stored in the data warehouse in advance of approach so that queries can be answered and data analysis can be performed more quickly and efficiently since integrated information is directly available at the DW.

II. RELATED WORKS

Korea Telecom's Call Data Analysis Team made SIMS (Strategic Information Management System), a prototype DW System for telecommunications pricing strategy [3]. Telecom Italia has their own DW project IBDA which now consists of 52 databases [4]. LGR Telecommunications, a specialized solutions provider to the global telecommunications industry, offering a unique business solution that taps directly into the source of each customer interaction with the network by accessing the CDRs it creates. LGR's approach intelligently captures CDR data in real-time, appends additional business information to the record, stores the data within a comprehensive Oracle data warehouse solution, and provides real-time analysis to the telecom service provider [5]. Other telecom companies using Oracle's DW includes Telefonica Germany, Turkcell Telecommunications, Mobiltel (Bulgaria), Anhui Telecom Company Ltd (China) and others [6].

III. SYSTEM ARCHITECTURE

Data is extracted from relational database system of telecom operators and transported into a staging area (See Figure 1). The staging area is likely a temporally holding place where data comes here that needs to be changed, converted and made ready in a format that is suitable to be loaded into warehouse and finally querying and analysis. Three major functions need to be performed for getting the data ready. These functions are extraction, transformation and loading take place in the staging area which are very common in every DW system and popularly known as ETL. This area may be some set of flat files or temporally staging tables in the warehouse. In our experiment, we have extracted a flat file from each of the operational system who has a relational database contains CDRs. The time period of the extraction process vary for different systems. It may be a fixed time interval or at the end of the business event such as the end of the day or week. It depends on which and how much data to be extracted and transported. In the telecommunication network millions of CDRs are generated daily. So our system extracts and loads the data as daily basis to improve performance.

978-1-4244-6283-4/09/$26.00 ©2009 IEEE

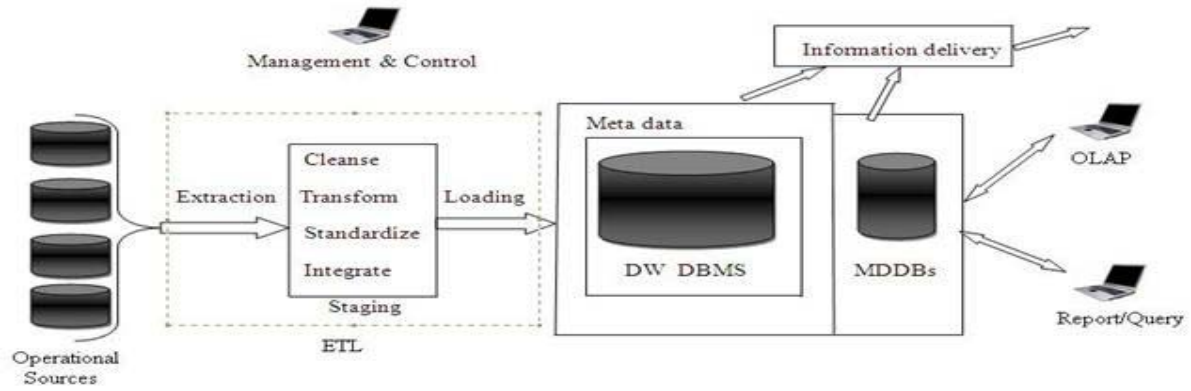

Fig. 1. System Architecture

Data transformation function includes cleansing the data, standardization, integration, calculation of attribute values and some other necessary jobs (See Figure 1). Cleaning may be just misspelling or providing default values for missing data element or elimination of duplicate data.

It should be needed standardization of data types and fields length for same data element retrieved from the various sources. Semantic standardization is also important which includes synonyms and homonyms [7]. Multiple sources data are finally integrated. The refined and standard data is now loaded into the DW. Once the data is loaded into the DW, further processing to integrate it with existing data, update the indexes, refresh the materialized view needs to take place.

The data storage of the DW is a separate read-only repository stores large volume of historical data. Also these repositories contain the data structured in highly normalized formats for fast and efficient processing. Our DW also employs multidimensional database (MDDB) management systems. Data extracted from the data warehouse storage is aggregated in many ways and the summary data is kept in MDDBs.

For the users, the strength of our DW architecture is mainly concentrated in the robustness and flexibility of the information delivery component. It provides OLAP and also report generation opportunities. The primary DW feeds data to proprietary MDDBs where summarized data is kept as multidimensional cubes of information (See Figure 1). The users perform complex multidimensional analysis using the information cubes in the MDDBs.

IV. A DIMENSIONAL MODEL

According to Ralph Kimball, "dimensional model is a specific discipline for modeling data that is an alternative to entity relationship modeling" [8]. The star sche-

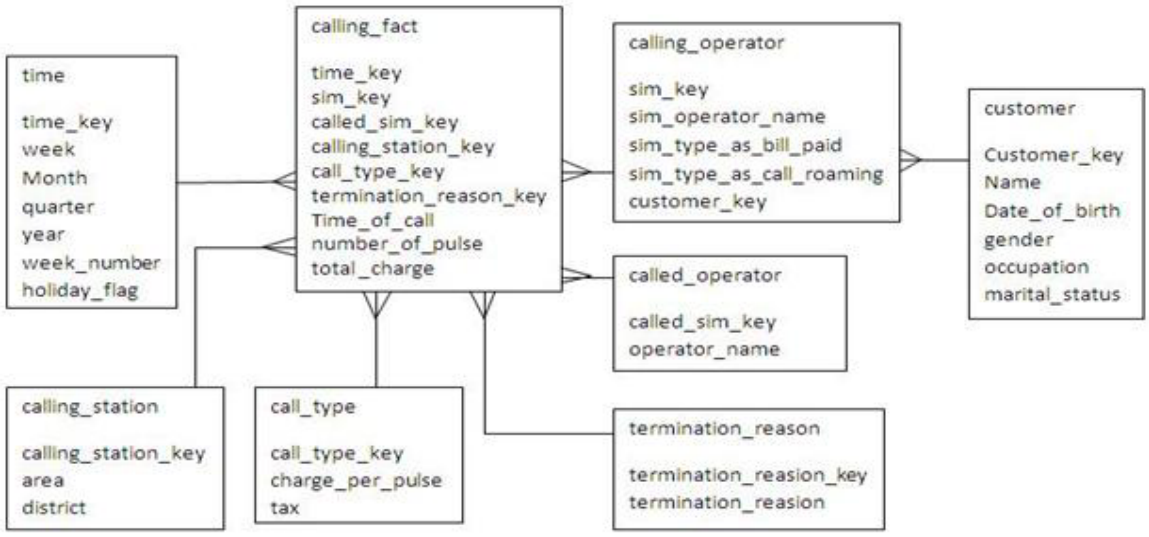

Fig. 2. Call-event Star schema

ma or dimensional model has been recognized as an effective structure for organizing many DW components. The star schema is characterized by a center fact table, which contains numeric information that is used in summary reports. Radiating from the fact table are dimension tables that provide a rich query environment. Figure 2 contains a fragment from call event transaction-oriented star schema discussed in this paper.

A. The fact Table

The most appropriate facts are additive numeric data items that can be summed, averaged, or combined in other ways to form summary statistics. As Kimball points out, "The best and most useful facts are numeric, continuously valued, and additive" [9]. We have modeled calling_fact as a fact table that contains useful additive facts time_of_call, number_of_pulse and total_charge (See Figure 2).

B. Dimensions

Dimensions are important concept in DW, which are the same type of data collection and represent the factors used for analyzing the measures. In general terms, dimensions are also characterized by attributes usually called dimension attributes. Time, calling_operator, called_operator and calling_station are very important dimensions in our DW. We have included other necessary dimensions those are call_type and termination_reason.

V. IMPLEMENTATION

A. Physical database design methodology

Physical database design is a crucial aspect for the data warehousing. Some important issues in physical database design, in particular, the relevance of partitioning for managing history and for performance issues that has been taken into account of our DW project. The main type of partitioning used in DW design is range partitioning (there are also hash, list and composite partitioning). A table is usually partitioned on a date column (partition key) and each partition contains rows that fall in a range expressed by a start_date and end_date [10]. The fact table **calling_fact** is partitioned by month, and if a query asked for sales from February 2010, the optimizer would know which partition the data was stored in and would just read from that partition. All other partitions would be eliminated from its search. In the SQL statement bellow (See Figure 3), we have shown only three partitions of the fact table though the fact table has 24 partitions for the two years of data it contains.

```
CREATE TABLE calling_fact(
      time_key date ,
      sim_key varchar2(18) ,
      called_sim_key varchar2(15) ,
      calling_station_key varchar2(14) ,
      call_type_key varchar2(6) not null,
      termination_reasion_key number(2, 0),
      time_of_call varchar2(10),
      number_of_pulse number(3, 0),
      total_charge number,
 PARTITION by RANGE (time_key)
 (PARTITION jan2010
      VALUES LESS THAN (TO_DATE('01-FEB-
2010', 'DD-MON-YYYY'))
      TABLESPACE  jan1010 ,
 PARTITION feb2010
      VALUES LESS THAN (TO_DATE('01-MAR-
2010', 'DD-MON-YYYY'))
      TABLESPACE  feb1010 ,
 PARTITION mar2010
     VALUES LESS THAN (TO_DATE('01-APR-
2010', 'DD-MON-YYYY'))
     TABLESPACE  mar1010 );
```

Fig. 3. Partitioning of fact table

B. Summery table and refreshing

Since the data would be selected, joined, sorted, and aggregated over and over again for each user it needs to reexecute each query repeatedly. So the result is precomputed and saved in a table. Such precomputed results are often called summary tables. A database object, known as Materialized View (MV) of oracle, which store precomputed results, such as a summary table [11]. First we have created MV log of tables for fast refresh. Without a MV log, Oracle Database must re-execute the MV query to refresh the MV. Figure 4 shows a sample materialized view (actually there are a lot of MVs are created in our DW project) including the logs which indicates monthly total calls, total pulse, average charge per day and total charge for each mobile user. **ON COMMIT** option is used to refresh the MV with details data at the end of each transaction.

```
CREATE MATERIALIZED VIEW LOG ON time
WITH SEQUENCE, ROWID(time_key)
INCLUDING NEW VALUES;

CREATE MATERIALIZED VIEW LOG ON call-
ing_fact WITH SEQUENCE,ROWID
(time_key, sim_key, called_sim_key)
INCLUDING NEW VALUES;

CREATE MATERIALIZED VIEW LOG ON call-
ing_operator WITH SEQUENCE, ROWID(sim_key)
INCLUDING NEW VALUES;

CREATE MATERIALIZED VIEW
monthly_call_mv
PCTFREE 0 TABLESPACE mview
STORAGE (initial 64k next 64k pctincrease 0)
BUILD IMMEDIATE
REFRESH FAST ON COMMIT
ENABLE QUERY REWRITE
AS
SELECT t.month_name, t.year, cf.sim_key as call-
ing_number,
      COUNT (cf.total_charge) as total_calls,
      SUM (cf.number_of_pulse) as total_pulse,
      AVG (cf.total_charge) as avg_charge_per_day,
      SUM (cf.total_charge) as total_charge
FROM time t,calling_fact cf, calling_operator cg
WHERE t.time_key = cf.time_key AND
     cg.sim_key = cf.sim_key
GROUP BY t.month_name, t.year, cf.sim_key;
```

Fig. 4. monthly_call_mv Materialized View

C. ETL IMPLEMENTATION

Everyday the telecom operators generate a large number of data from switching systems, which are produced for every phone call through a telephone network. **CDR** is the fingerprint of how many seconds and at what time a customer is using phone. However every telecom company maintains an relational database for temporary saving the CDRs .We have actually followed the four telecom companies in Bangladesh (Grameenphone, BanglaLink, AKTEL and WARID) and their relational databases. We have generated random data for those operational databases. Finally , we have extracted data from those operational databases into **dat** files by sql procedures. Figure 5 shows a SQL package which extracts data from a relational database into a **dat** file with coma separated data.

```
CREATE OR REPLACE DIRECTORY EXTR AS
'F:\dwdata\
CREATE OR REPLACE PACKAGE csv_n AS
PROCEDURE generate (p_dir     IN
VARCHAR2,p_file    IN  VARCHAR2,p_query   IN
VARCHAR2);
END csv_n;

CREATE OR REPLACE PACKAGE BODY csv_n
AS
g_sep        VARCHAR2(5)  := ',';
PROCEDURE generate (p_dir     IN  VARCHAR2,
                p_file    IN  VARCHAR2,
                p_query   IN  VARCHAR2) AS
 l_cursor    PLS_INTEGER;
 l_rows      PLS_INTEGER;
 l_col_cnt   PLS_INTEGER;
 l_desc_tab  DBMS_SQL.desc_tab;
 l_buffer    VARCHAR2(32767);
 l_file      UTL_FILE.file_type;

BEGIN
 l_cursor := DBMS_SQL.open_cursor;
 DBMS_SQL.parse(l_cursor, p_query,
DBMS_SQL.native);
 DBMS_SQL.describe_columns (l_cursor, l_col_cnt,
l_desc_tab);
 FOR i IN 1 .. l_col_cnt LOOP
         DBMS_SQL.define_column(l_cursor, i,
l_buffer, 32767 );
 END LOOP;
 l_rows := DBMS_SQL.execute(l_cursor);
 l_file := UTL_FILE.fopen(p_dir, p_file, 'w', 32767);
FOR i IN 1 .. l_col_cnt LOOP
          IF i > 1 THEN
                UTL_FILE.put(l_file, g_sep);
         END IF;
         UTL_FILE.put(l_file,
l_desc_tab(i).col_name);
 END LOOP;
 UTL_FILE.new_line(l_file);

LOOP
         EXIT WHEN
DBMS_SQL.fetch_rows(l_cursor) = 0;
         FOR i IN 1 .. l_col_cnt LOOP
                IF i > 1 THEN
                      UTL_FILE.put(l_file, g_sep);
                END IF;
          DBMS_SQL.COLUMN_VALUE(l_cursor, i,
l_buffer);
         UTL_FILE.put(l_file, l_buffer);
         END LOOP;
         UTL_FILE.new_line(l_file);
 END LOOP;
 UTL_FILE.fclose(l_file);
EXCEPTION
    WHEN OTHERS THEN
```

```
    IF UTL_FILE.is_open(l_file) THEN
        UTL_FILE.fclose(l_file);
    END IF;
    IF DBMS_SQL.is_open(l_cursor) THEN
        DBMS_SQL.close_cursor(l_cursor);
    END IF;
    RAISE;
END generate;
END csv_n;
```

Fig. 5. Extraction methods

Package **csv_n** includes a procedure **generate** which takes three parameters. First parameter is a directory in where the **dat** file is created, second is the file name and third is the query that tells which attribute's data of the tables of operator's relational database will be extracted.

The extracted data is raw data and it can not be loaded into the DW. First, all the extracted data must be made usable in the DW. Having information that is usable for strategic decision making is the underlying principle of the DW. The data in the operational systems is not usable for this purpose. So, before moving the extracted data into our DW, it inevitably has been performed various kinds of data transformations such as format revisions, decoding of fields, calculated and derived values, splitting of single fields, merging of information, character set conversion and deduplication.

Finally, the extracted and transformed data is saved into dat file for Loading into the DW. We used SQL* Loader for loading. Actually, we loaded data into the fact table **calling_fact** and the dimension tables are also updated. Before loading data, all the referential integrity constraints must be disabled and after completion of loading the constraints are enabled. To load data into the **dat** file by SQL* Loader a control file need to be created, describing which **dat** file would be loaded into which partition of the fact table. Actually, loading into a partitioned table, it requires partitionwise load in SQL*Loader. Figure 6 is a sample for loading data into the partition **JAN2010** of **calling_fact** table.

```
OPTIONS (DIRECT=TRUE)
UNRECOVERABLE LOAD DATA
INFILE 'E:\loadingtest\callingfact1.dat'
BADFILE 'E:\loadingtest\callingfact1.bad'
APPEND
INTO TABLE CALLING_FACT
PARTITION (JAN2010)
FIELDS TERMINATED BY ","
(TIME_KEY,SIM_KEY,CALLED_SIM_KEY,
CALLING_STATION_KEY,CALL_TYPE_KEY,
TERMINATION_REASION_KEY,TIME_OF_CALL
,
NUMBER_OF_PULSE,TOTAL_CHARGE)
```

Fig. 6. Data loading into JAN2010 partition of the fact table

VI. RESULTS AND DISCUSSION

The experiments run on a Intel Celeron(R) 2.00GHz processor with 768MB RAM running Windows xp operating system. All the results presented in this paper are obtained using randomly generated data. At first we have extracted 20000 data from the sources in 13 seconds and next we have extracted more data. Time consumption is shown in the graph bellow (See Figure 7). The curve is approximately linear.

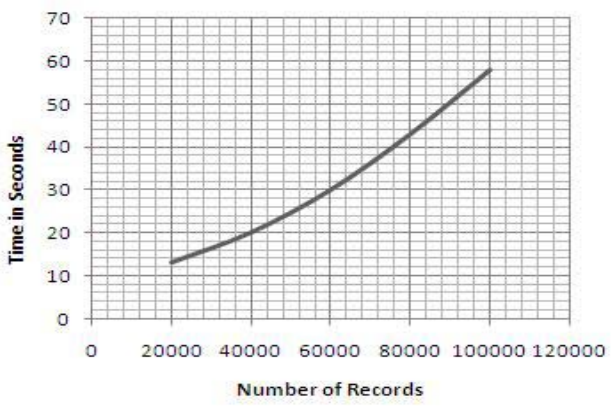

Fig. 7. Performance of Data Extraction

Four **dat** files are created after transforming the four extracted files of the four operational sources. And finally, the four transformed **dat** files are integrated to generate one single file. Time required for total transformation process starting at sample data 20000 is given bellow (See Figure 8).

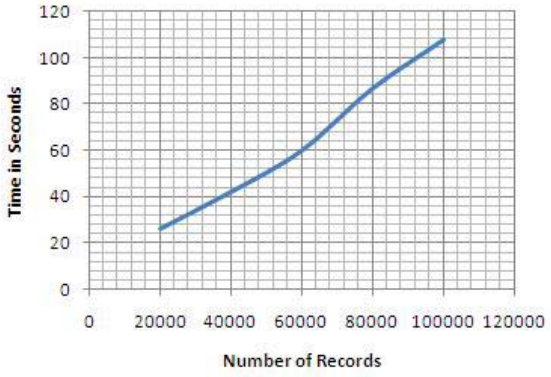

Fig. 8. Performance of Data Transformation

Oracle 10g is used in all our experiments. Loading time is got from the log file created after execution of the sql command **sqlldr userid=userame/password control=callingfact1.ctl**. The time graph is shown bellow for the same sample data as used before (See Figure 9). The curve of loading data into DW is found nearly linear

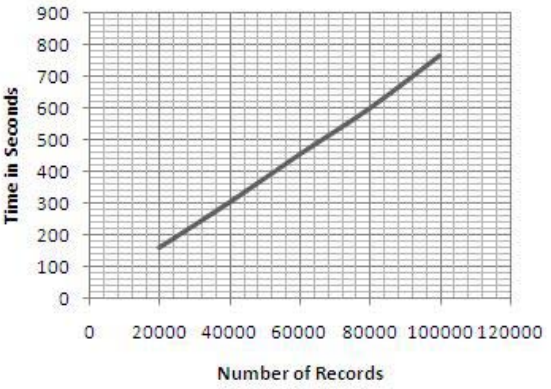

Fig. 9. Performance of Data Loading

VII. CONCLUSION

In this paper, a dimensional DW design of telecom companies for Bangladesh has been described. We have implemented the data staging area in a efficient way which clearly describes the data extraction, data transformation and data loading methodologies. We have partitioned the fact table so that the data retrieval from the DW is performed faster. Oracle Materialized Views are created for saving precomputed result to protect from re-execution of queries. The performance graphs of our experiments have been explained which show significant achievement of our experiments. Finally, multilevel aggregations within the Data Warehouse database have been performed using CUBE, ROLLUP and GROUPING SETS with OLAP.

In the future, we plan to develop an advanced **ETL** processing which incorporates any type of data sources and a data mining tool which will analyze data from different perspectives and summarize it into useful information.

REFERENCES

[1] Koustuv Dasgupta, Rahul Singh, Balaji Viswanathan, Dipanjan Chakraborty, Sougata Mukherjea, Amit A. Nanavati IBM India Research Lab," Social Ties and their Relevance to Churn in Mobile Telecom Networks", In the Proceeding of ACM 11th international conference on Extending database technology (Nantes, France) pp. 668-677, 2008.

[2] W.H. Inmon, Building the Data Warehouse, 4th ed., Indianapolis, Indiana: John Wiley & Sons, 2005.

[3] Seungjae Shin, Gilju Park, Wonjun Lee, Sunmi Lee Korea Telecom R&D Group, Telecom Economic Research Lab, "Case Study : How to Make Telecom Pricing Strategy Using Data Warehouse Approach", In the Proceeding of 31st Hawaii international conference (Kohala Coast, HI, USA), Vol. 6, pp. 55-60, 1998.

[4] Stefano M. Trisolini, Maurizio Lenzerini, Daniele Nardi, "Data Warehousing and Integration in Telecom Italia", In the Proceedings of the 1999 ACM SIGMOD international conference on Management of data(Philadelphia, Pennsylvania, United States) pp. 538 – 539, 1999.

[5] Oracle Customer Snapshot: http://www.oracle.com/customers/snapshots/lgr-telecommunications-db-business-benefits-case-study.pdf.

[6] Oracle Data Warehousing Customers list: http://www.oracle.com/customers/products/data-warehouse.html.

[7] Paulraj Ponniah, DATA WAREHOUSE FUNDAMENTAL, New York: John Wiley & Sons, 2001, pp.27-35.

[8] Ralph Kimball, Richard Mertz, The Data Warehouse Lifecycle Toolkit, New York: John Wiley & Sons, 2000.

[9] R. Kimball, The Data Warehouse Toolkit, New York: John Wiley& Sons, 1996.

[10] Robert Wrembel, Christian Koncilia, Data Warehouses and OLAP: Concepts, Architectures and Solutions, Hershey: IRM Press, 2007, ch. IV.

[11] Lilian Hobbs, Susan Hillso, Shilpa Lawande, Pete Smith, Oracle Database 10g Data Warehousing, Burlington: Elsevier Digital Press, 2005.

Proceedings of 2009 12th International Conference on Computer and Information Technology (ICCIT 2009)
21-23 December, 2009, Dhaka, Bangladesh

Multiple-Case Outlier Detection in Least-Squares Regression Model Using Quantum-Inspired Evolutionary Algorithm

Mozammel H. A. Khan, Salena Akter
Department of Computer Science and Engineering, East West University, 43 Mohakhali C/A, Dhaka 1212, Bangladesh
mhakhan@ewubd.edu, s_lina_cse@yahoo.com

Abstract

In ordinary statistical methods, multiple outliers in least-squares regression model are detected sequentially one after another, where smearing and masking effects give misleading results. If the potential multiple outliers can be detected simultaneously, smearing and masking effects can be avoided. Such multiple-case outlier detection is of combinatorial nature and $2^N - 1$ *sets of possible outliers need to be tested, where* N *is the number of data points. This exhaustive search is practically impossible. In this paper, we have used quantum-inspired evolutionary algorithm (QEA) for multiple-case outlier detection in least-squares regression model. An information criterion based fitness function incorporating extra penalty for number of potential outliers has been used for identifying the most appropriate set of potential outliers. Experimental results with four datasets from statistical literature show that the QEA effectively detects the most appropriate set of outliers.*

Keywords: Information criterion based fitness function, least-squares regression model, multiple-case outlier detection, quantum-inspired evolutionary algorithm

I. INTRODUCTION

If substantial error is associated with data, least-squares regression is used to model the trend of the data, which minimizes the discrepancy between the data points and the fitted straight line. In least-squares regression, a straight line is fitted to a set of paired data points: (x_1, y_1), (x_2, y_2), … , (x_N, y_N), where N is the number of data points. The equation of the fitted straight line is

$$\hat{y} = a_0 + a_1 x, \tag{1}$$

where $\hat{y}$ is the approximated value of the dependent variable y, x is the independent variable, a_0 and a_1 are coefficients representing the intercept and the slop, respectively. The true value of the depended variable y is related with the fitted line by the equation

$$y = a_0 + a_1 x + e, \tag{2}$$

where e is the error, or residual, between the model and the true value, which can be represented as

$$e = y - a_0 - a_1 x. \tag{3}$$

Thus, the error, or residual, is the discrepancy between the true value of y and the approximate value $\hat{y}$ predicted by the model. The least-squares regression model minimizes the sum of the squares of the residual between the true value y and the approximate value $\hat{y}$ predicted by the model

$$S_r = \sum_{i=1}^{N} e_i^2 = \sum_{i=1}^{N} (y_i - a_0 - a_1 x_i)^2. \tag{4}$$

The coefficients a_0 and a_1 are computed using the following equations [1]:

$$a_1 = \frac{N\sum_{i=1}^{N} x_i y_i - \sum_{i=1}^{N} x_i \sum_{i=1}^{N} y_i}{N\sum_{i=1}^{N} x_i^2 - \left(\sum_{i=1}^{N} x_i\right)^2} \tag{5}$$

$$a_0 = \frac{\sum_{i=1}^{N} y_i}{N} - \frac{a_1 \sum_{i=1}^{N} x_i}{N}. \tag{6}$$

The standard deviation for the regression line, or the *standard error of the estimate*, is determined with two degree of freedom as [1]

$$s_{y/x} = \sqrt{S_r/(N-2)}. \tag{7}$$

The distribution of the squares of the residuals e_i^2, for $i = 1, \cdots, N$, is normal $N\left(\overline{S_r}, s_{y/x}^2\right)$, where $\overline{S_r}$ is the mean of the squares of the residuals and $s_{y/x}^2$ is the *variance of the estimate*.

In statistical data analysis, outliers, or aberrant observations, are observations that are somehow different from the majority of the data [2]. If outliers occur in the data, the residuals can be thought to have a distribution different from normal. The presence of outliers in the data may result into misleading least-squares regression model, which is biased towards the outliers. There are several statistical methods for outlier detection [3], where the outliers are detected sequentially one by one. There are also several ways of taking the detected outliers into account in the analysis. For example, the outliers can be removed from the data altogether or they can be incorporated into the statistical model [3]. There are two problems in practical outlier detection known as smearing and masking. Smearing means that an outlier causes another non-outlier observation to be considered as an outlier by an outlier detection method. Masking means that an outlier prevents another outlier being detected by an outlier detection method. One by one or sequential detection of outliers may, therefore, be misleading, if the detection of one outlier causes the subsequent detection of other outliers to be flawed, due to either smearing or masking, or both. Multiple-case, or simultaneous, outlier detection method can overcome the limitations of the sequential outlier detection method. The simplest multiple-case outlier detection method would be to consider all possible permutations of the data points into outliers and non-outliers groups and

decide which of these is the best combination based on some criterion. This method is combinatorial in nature and requires $2^N - 1$ possible combinations to be considered, where N is the number of data points. As the exhaustive search of $2^N - 1$ possible combinations is practically impossible, evolutionary algorithms may be very useful in detecting multiple-case outliers.

Genetic algorithm (GA) was used to detect multiple-case outliers in [4]. In this work, subsets of data points with cardinality k, for $k = 2, \cdots, \lfloor N/2 \rfloor$, where N is the number of data points, were separately identified to be potential outliers and they are omitted from the data-set to calculate three different measures of outlyingness. Then post analysis was used to identify the outlier set. In this GA, ordered-based integer encoding of the chromosome, a variant of two-parent uniform ordered-based crossover (UOX) [5], and a mutation that replace a randomly chosen point with a unique random value were used. This approach suffered from two drawbacks – (i) the GA was run $\lfloor N/2 \rfloor - 1$ times separately, where N is the number of data points, to identify $\lfloor N/2 \rfloor - 1$ separate subsets of potential outliers, which was time consuming and (ii) the post analysis to identify the outlier set from $\lfloor N/2 \rfloor - 1$ sets was somewhat misleading.

Another attempt of using GA for outlier detection and variable selection in linear regression models was presented in [2]. This work dealt with multiple-case outlier detection in multivariate linear regression models. Additional dummy variables were used corresponding to potential outliers. These dummy variables are by definition binary in nature. Binary encoded chromosome was used to represent dummy variables corresponding to potential outliers. The 1s of the chromosome represented the dummy variables and the variables were created before the GA was run and used in the regression model to determine the fitness of the solution. The fitness of the solution was calculated using a modified BIC information criterion from [6]. The used fitness function was

$$\mathrm{BIC}' = \log(\hat{\sigma}^2) + (1+p)\log(N)/N + km_d \log(N)/N \quad (8)$$

where, N was the sample size, $\hat{\sigma}^2 = \sum_{i=1}^{N} e_i^2 \Big/ N$ was the residual sum of squares, 1 was for constant in the model, p was number of independent variables, m_d was the number of outlier dummies, and $k\ (k > 1)$ was extra penalty given to outlier dummies. A solution with lowest BIC′ value was selected. The selection of parents was biased towards the fitness values and a two point classical crossover and classical mutation were used.

In the above works, GAs were used to detect multiple-case outliers in linear regression models. However, other evolutionary techniques may be equally or more suitable for this purpose. In this work, we have used quantum-inspired evolutionary algorithm (QEA) for detecting multiple-case outliers in least-square regression model.

II. THE PROPOSED QUANTUM-INSPIRED EVOLUTIONARY ALGORITHM

QEA has been proposed by Han and Kim [7] and experimentally shown that the QEA is better than classical GAs for solving 0/1 knapsack problem. Latter, in [8], they have proposed extension of the basic QEA such as termination criterion, a modified version of the variation operator, and a two-phase scheme to improve the performance of the QEA. Besides, applications of the QEA in different application areas such as disk allocation problem [9], multiobjective 0/1 knapsack problem [10], and face detection [11] have been reported. The basic QEA structure presented in [7] is based on the concept and principle of quantum computing. As the QEA is found to be effective for other combinatorial problems, it is also likely that it will be very suitable for multiple-case outlier detection, since the problem is combinatorial in nature.

The proposed QEA for multiple-case outlier detection in least-squares regression model maintains three data structures as discussed below:

Population of Q-bit individuals: A Q-bit in a QEA is a classical equivalent of a qubit in a quantum system. A Q-bit is represented as a tuple (α, β) such that $\alpha^2 + \beta^2 = 1$, where α^2 is the probability that the Q-bit is in state 0 and β^2 is the probability that the Q-bit is in state 1. A Q-bit can be visualized as a two-dimensional unit vector, where α is the projection of the unit vector on the x-axis and β is the projection of the unit vector on the y-axis. When the unit vector lies on the x-axis, it represents a 0 and when it lies on the y-axis, it represents a 1. The probabilities of a Q-bit being in state 0 or 1 can be changed by rotating the Q-bit. If a Q-bit is rotated towards *y*-axis, it converges towards state 1 and if it is rotated towards *x*-axis, it converges towards state 0. A Q-bit individual of length N is represented as

$$q = \left[(\alpha_1, \beta_1)(\alpha_2, \beta_2)\cdots(\alpha_N, \beta_N)\right], \quad (9)$$

where N is the number of data points. A Q-bit individual of length N eventually represents 2^N binary individuals in superposition. The population of Q-bit individuals at generation t is denoted by $Q(t)$. Readers can see [7] for more details of Q-bit individuals.

Population of observed binary solutions: The multiple-case outlier detection problem can be encoded as a binary string of length N

$$x = (x_1 x_2 \cdots x_N), \quad (10)$$

where N is the number of data points and if $x_i = 0$, then the *i*th data point is considered as a potential outlier, otherwise considered as a non-outlier. The population of binary solutions at generation t is denoted by $X(t)$. The sizes of the population of Q-bit individuals and the population of binary solutions are same. The population of binary solutions $X(t)$ is generated by probabilistic observation of the population of Q-bit in-

dividuals $Q(t-1)$. In the probabilistic observation process, the binary value of x_i of an observed binary solution is set to 1 if and only if random$[0\cdots1] < \beta_i^2$ for the corresponding Q-bit individual, otherwise it is set to 0.

The best binary solution: The best binary solution is denoted by $b = (b_1 b_2 \cdots b_N)$, where N is the number of data points, which stores the best binary solution so far generated.

The structure of the QEA for multiple-case outlier detection is given below:

Procedure QEA for multiple-case outlier detection
Begin

$t \leftarrow 0$
(i) initialize $Q(t)$
(ii) make $X(t)$ by observing $Q(t)$
(iii) repair $X(t)$
(iv) evaluate $X(t)$
(v) store best solution among $X(t)$ into b
while (t < MAX_GEN) **do**
begin
$t \leftarrow t+1$
(vi) make $X(t)$ by observing $Q(t-1)$
(vii) repair $X(t)$
(viii) evaluate $X(t)$
(ix) update $Q(t)$
(x) store the best solution among $X(t)$ and b into b
end
end

The procedure is discussed below step wise:

Step (i): The Q-bits of all Q-bit individuals of $Q(0)$ are initialized to $\alpha = \beta = 1/\sqrt{2}$, which implies that the probabilities of a Q-bit being in state 0 or 1 are equal.

Step (ii): The population of binary solutions $X(0)$ is generated by probabilistic observation of the population of Q-bit individuals $Q(0)$.

Step (iii): We have assumed that the maximum number of outliers in a dataset can be $\lfloor N/2 \rfloor$, where N is the number of data points. If the number of 0s in an observed binary solution is more than $\lfloor N/2 \rfloor$, then the excess 0s are randomly selected and converted into 1s.

Step (iv): The evaluation of a binary solution is the most important part of the QEA for multiple-case outlier detection. We have used the following information criterion based fitness function for a binary solution x similar to (8):

$$f(x) = \log\left(S_r/(n-2)\right) + (1 + p + Km)\log(n)/N, \quad (11)$$

where N is the number of data points, n is the number of 1s in the binary solution x, i.e., the number of non-outlier data points, m is the number of 0s in the binary solution x, i.e., the number of potential outlier data points, $n + m = N$, 1 is for the constant in the model, $p = 1$ is the number of independent variable, S_r is calculated using (4) for only the n non-outlier data points, and K ($K \geq 1$) is extra penalty given to the number of potential outliers m. Readers can easily recognize from (7) that $S_r/(n-2)$ is the variance of the estimate of least-squares fit of n non-outlier data points. Selection of the value of K will be discussed in the experimental result section. A smaller value of $f(x)$ means that elimination of the potential outlier data points from the dataset will produce a better least-squares fit of the remaining non-outlier data points.

Step (v): The binary solution x among $X(0)$ having the lowest $f(x)$ value is stored into b. The while loop runs the subsequent generations of the QEA.

Step (vi): The population of binary solutions $X(t)$ is generated by probabilistic observation of the population of Q-bit individuals $Q(t-1)$.

Step (vii): The binary solutions in $X(t)$ are repaired as in Step (iii).

Step (viii): The repaired binary solutions in $X(t)$ are evaluated as in Step (iv).

Step (ix): In this step, the Q-bit individuals are updated to converge towards the stored best solution b by rotating each Q-bit θ radian. If $f(x) < f(b)$ for a binary solution x, then the Q-bits of the corresponding Q-bit individual are not rotated, i.e., rotated 0 radians. If $f(x) \geq f(b)$ for a binary solution x, then there are three situations: (i) if $x_i = b_i$, then the corresponding Q-bit is not rotated, (ii) if $x_i = 0$ and $b_i = 1$, then the corresponding Q-bit is rotated θ radians towards *y*-axis to converge the Q-bit towards 1, and (iii) if $x_i = 1$ and $b_i = 0$, then the corresponding Q-bit is rotated θ radians towards *x*-axis to converge the Q-bit towards 0. We have used $\theta = 0.01\pi$ radians as rotation angle for our experiments. Readers can see [7] for more details of updating Q-bit individuals.

Step (x): The binary solution x among $X(t)$ and b having the lowest $f(x)$ value is stored into b.

III. EXPERIMENTAL RESULTS

We have implemented the QEA for multiple-case outlier detection in least-squares regression model using C language on a PC. We have used MAX_GEN = 500 and the population sizes have been chosen depending on the problem sizes. For each dataset, the QEA has been run 100 times with different seeds and for all datasets the same set of seeds has been used. We have experimented with four datasets from [12].

We have first experimented with *Belgium* dataset from [12], which has 24 data points and shows the number of international calls from Belgium between 1950 and 1973. For this dataset, the last two digits of the year is the independent variable and the number of calls is the dependent variable. The value of the extra penalty K

given to the number of potential outliers in (11) is very important. If a K value detects 100% times $\lfloor N/2 \rfloor$ number of outliers, then we call it *under penalty*. If a K value detects 100% times zero outliers, then we call it *over penalty*. For this dataset, we have used population size 100. We have run the QEA for several K values from under penalty to over penalty and then identify the number of outliers detected by most number of K values. The number of outliers detected versus % of times detected for Belgium dataset is shown in Fig. 1. From Fig. 1, we see that seven outliers have been detected by seven different values of K and eight outliers have been detected by four different values of K. Therefore, we have taken seven as the number of potential outliers for this dataset. The dataset, outliers, and least-squares fits with and without outliers are shown in Fig. 2. The six data points indicated by (o) are reported as outliers in [12] and are also detected by our QEA. Besides these six known outliers, the data point ((70, 4.3) indicated by (*) is also detected as outlier by our QEA. To test whether the data point (70, 4.3) is a potential outlier, we have calculated e_i^2 of the data point; and $s_{y/x}^2$ and $\overline{S_r} + 3s_{y/x}^2$ for 18 data points except those indicated by (o) and tabulated in Table I. From Table I, we see that the square of the residual for the data point (70, 4.3) lies outside the normal distribution of the squares of the residuals. Therefore, the data point (70, 4.3) is an outlier, which is detected by our QEA. However, the sequential outlier detection method could not detect this data point as outlier due to smearing and/or masking. In this dataset, it is interesting to see that four outliers have been detected by $K = 3$, six outliers have been detected by $K = 2$, seven outliers have been detected by $K = 1$, and 15 outliers have been detected by $K = 1$. Therefore, each potential outlier set is detected once. But the outlier set with six outliers has been detected 92% by $K = 2$. Therefore, we have taken six as the number of potential outliers in the dataset. The dataset, outliers, and least-squares fits with and without outliers are shown in Fig. 4. The four data points indicated by (o) are reported as outliers in [12] and are also detected by our QEA. Besides these four known outliers, the two data points (3.84, 4.65) and (4.26, 5.57) indicated by (*) are also detected as outliers by our QEA. We have calculated e_i^2 of the data points (3.84, 4.65) and (4.26, 5.57); and $s_{y/x}^2$ and $\overline{S_r} + 3s_{y/x}^2$ for 43 data points except those indicated by (o) and tabulated in Table I. The data from Table I show that these two data points lie outside the normal distribution of the squares of the residuals and they are outliers, though the sequential outlier detection method could not detect them due to smearing and/or masking.

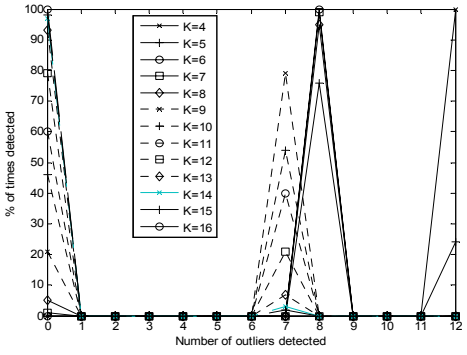

Fig. 1. Determination of number of potential outliers in Belgium dataset.

The second dataset that we have experimented with is the *Hertzsprung-Russel diagram of the CYG OB1 star cluster* from [12], which is an often analyzed dataset in statistical literatures. The data is taken from 47 stars in the direction of Cygnus. The independent variable is the log of the effective temperature at the surface of each star and the dependent variable is the log of the star's light intensity. We will refer to this dataset as *CYG* dataset. For this dataset we have used population size 100. The number of outliers detected versus % of times detected for this dataset is shown in Fig. 3. From Fig. 3,

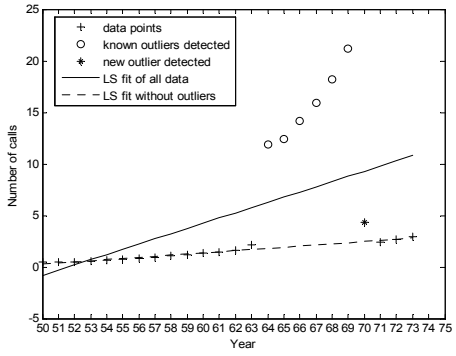

Fig. 2. The dataset, outliers, and least-squares fits with and without outliers for Belgium dataset.

Table I Data related to newly detected outliers.

Problem	$s_{y/x}^2$	$\overline{S_r} + 3s_{y/x}^2$	**Data point**	e_i^2
Belgium	0.193	0.751	(70, 4.3)	2.310
SYG	0.157	0.628	(3.84, 4.65)	0.718
			(4.26, 5.57)	0.824
Brain	270894.4	1061906.02	(2547, 4603)	4038227.59
			(62, 1320)	1145544.56

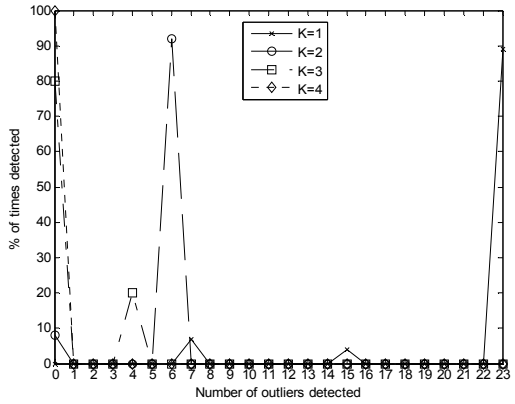

Fig. 3. Determination of number of potential outliers in CYG dataset.

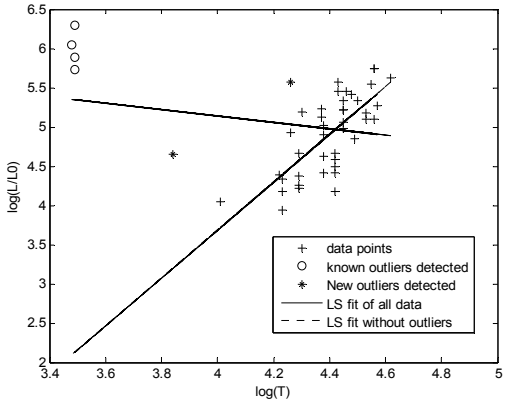

Fig. 4. The dataset, outliers, and least-squares fits with and without outliers for CYG dataset.

We have also experimented with *China* dataset from [12], which is a record of the annual rates of growth of average prices in the main free cities of free China from 1940 to 1948. The dataset has nine data points. The independent variable is the last two digits of the year and the dependent variable is the growth of price. For this dataset we have used population size 10. The number of outliers detected versus % of times detected for this dataset is shown in Fig. 5. From Fig. 5, we see that one outlier has been detected by three K values (26 to 28) and two outliers have been detected by 14 K values (12 to 25). Therefore, we have taken two as the number of potential outliers in the dataset. The dataset, outliers, and least-squares fits with and without outliers are shown in Fig. 6. The two data points indicated by (o) are reported as outliers in [12] and are also detected by our QEA.

Finally, we have experimented with *Brain* dataset from [12], which contrasts body weight against the brain weight of 28 different animal species. The independent variable is the body weight and the dependent variable is the brain weight. For this dataset we have used population size 100. The number of outliers detected versus % of times detected for this dataset is shown in Fig. 7. From Fig. 7, we see that two outliers have been detected by six K values, three outliers have been detected by two K values, five outliers have been detected by eight K values, six outliers have been detected by one K value, seven outliers have been detected by one K value, nine outliers have been detected by two K values, and 11 outliers have been detected by four K values. Therefore, we have taken five as the number of potential outliers in the dataset. The dataset, outliers, and least-squares fits with and without outliers are shown in Fig. 8. The three data points indicated by (o) are reported as outliers in [12] and are also detected by our QEA. Besides, our QEA detected two more data points (2547, 4604) and (62, 1320) as outliers indicated by (*). We have calculated e_i^2 of the data points (2547, 4604) and (62, 1320); and $s_{y/x}^2$ and $\overline{S_r} + 3s_{y/x}^2$ for 25 data points except those indicated by (o) and tabulated in Table I. The data from Table I show that these two data points lie outside the normal distribution of the squares of the residuals and they are outliers, though the sequential outlier detection method could not detect them due to smearing and/or masking.

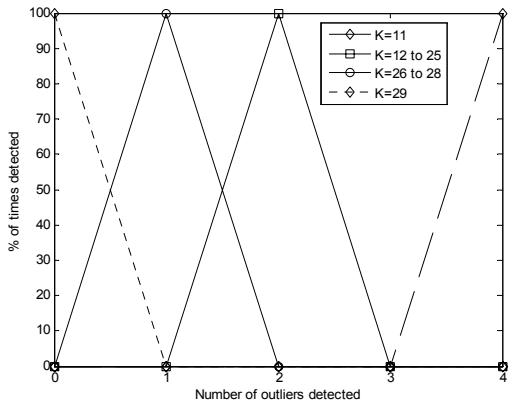

Fig. 5. Determination of number of potential outliers in China dataset.

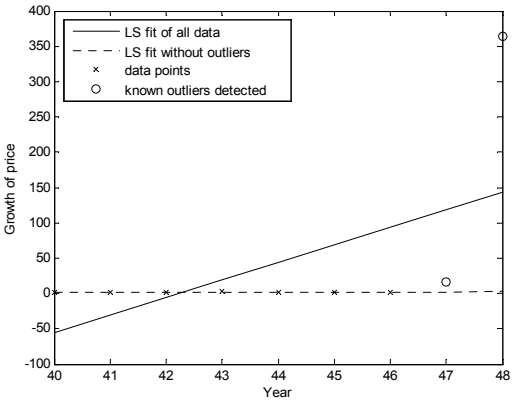

Fig. 6. The dataset, outliers, and least-squares fits with and without outliers for China dataset.

The method of determining number of potential outliers may now be summarized as:

- Run the QEA for a range of K values from under penalty (a K value that detects $\lfloor N/2 \rfloor$ number of

outliers 100% of times or $K = 1$) to over penalty (a K value that detects zero outliers 100% of times).

- Select the number of outliers that is detected by most K values. Break the tie by selecting the number of outliers that is detected most of the times.

This rule is incorporated in our proposed QEA for multiple-case outlier detection.

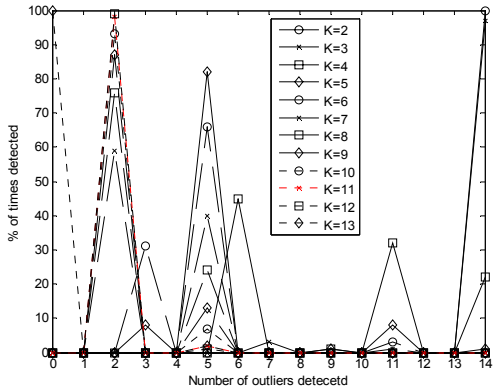

Fig. 7. Determination of number of potential outliers in Brain dataset.

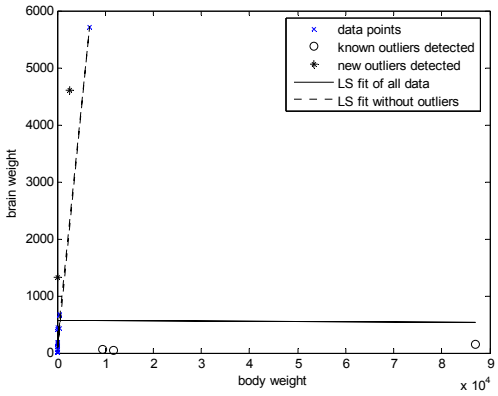

Fig. 8. The dataset, outliers, and least-squares fits with and without outliers for Brain dataset.

IV. CONCLUSION AND FURTHER WORK

Quantum-inspired evolutionary algorithm (QEA) for multiple-case outlier detection in least-squares regression model is presented here. Experimental results with four datasets from statistical literature [12] shows that the proposed QEA has detected all outliers previously detected using sequential outlier detection methods. Moreover, the QEA also has detected some more potential outliers that were not detected by sequential outlier detection methods due to smearing and/or masking. From this observation, we can conclude that the proposed QEA is completely able to avoid the potential problems of smearing and masking.

Multiple-case outlier detection is combinatorial in nature and requires testing of $2^N - 1$ subsets of data points as potential outliers, where N is the number of data points. For this practical limitation, multiple-case outlier detection is not used for large datasets. The superb performance of QEA for multiple-case outlier detection will allow us to handle this practical limitation of large dataset very effectively.

In this paper, we have considered two-variable least-squares regression model. Currently we are working to extend the proposed QEA for multiple-variable linear regression model and experimenting with more datasets.

REFERENCES

[1] S.C. Chapra and R.P. Canale, *Numerical Methods for Engineers With Software and Programming Applications*, 4th edn. New Delhi, India: Tata McGraw-Hill Publishing Company Limited, 2002.

[2] J. Tolvi, "Genetic algorithms for outlier detection and variable selection in linear regression models," *Soft Computing*, vol. 8, 2004, pp. 527-533.

[3] V. Barnett and T. Lewis, *Outliers in Statistical Data*, 3rd edn. Chichester: John Wiley, 1994.

[4] K.D. Crawford and R.L. Wainwright, "Applying genetic algorithms to outlier detection," *Proceedings of the 6th International Conference on Genetic Algorithms (ICGA-95)*, Pittsburgh, PA., Larry Eshelman, Editor, Morgan Kaufmann Publisher, July, 1995, pp. 546-550.

[5] L. Davis, *Handbook of Genetic Algorithms*. New York: Van Nostrand Reinhold, 1991.

[6] G. Schwarz, "Estimating the dimension of a model," *The Annals Stat*, vol. 6, 1978, pp. 461-464.

[7] K.-H. Han and J.-H. Kim, "Quantum-inspired evolutionary algorithm for a class of combinatorial optimization," *IEEE Transactions on Evolutionary Computation*, vol. 6, no. 6, Dec. 2002, pp. 580-593.

[8] K.-H. Han and J.-H. Kim, "Quantum-inspired evolutionary algorithms with a new termination criterion, H_ϵ gate, and two-phase scheme," *IEEE Transactions on Evolutionary Computation*, vol. 8, no. 2, April 2004, pp. 156-169.

[9] K.-H. Kim, J.-Y.Hwang, K.-H. Han, J.-H. Kim, and K.-H. Park, "A quantum-inspired evolutionary computing algorithm for disk allocation method," *IEICE Transactions on Information and Systems*, vol. E86-D, no. 3, March 2003. pp. 645-649.

[10] Y. Kim, J.-H. Kim, and K.H. Han, "Quantum-inspired multiobjective evolutionary algorithm for multiobjective 0/1 Knapsack problems," *Proceedings of the 2006 IEEE Congress on Evolutionary Computation*, July 2006, pp. 9151-9156.

[11] J.-S. Jang, K.-H. Han and J.-H. Kim, "Face detection using quantum-inspired evolutionary algorithm," *Proceedings of the 2004 IEEE Congress on Evolutionary Computation*, June 2004, pp. 2100-2106.

[12] P.J. Rousseeuw and A.M. Leroy, *Robust Regression & Outlier Detection*. New York: John Wiley & Sons, 1987.

Proceedings of 2009 12th International Conference on Computer and Information Technology (ICCIT 2009)
21-23 December, 2009, Dhaka, Bangladesh

Present Status and Critical Success Factors of E-Commerce in Bangladesh

Md. Raihan Jamil, Nafis Ahmad†
TID, University Grants Commission of Bangladesh, Agargaon, Dhaka, Bangladesh
† Department of IPE, BUET, Dhaka, Bangladesh
jamilraihan@yahoo.com, nafis@ipe.buet.ac.bd

Abstract

Online trading between businesses or individuals has employed attention of corporations worldwide as they are challenged to remain viable through difficult economic conditions. Despite the losses of so many businesses two years ago when the "dot-com bubble" burst, no serious business analyst disagrees that electronic commerce is steadily transforming how business is done, hence changing the business environment globally. Businesses everywhere need to understand if, when and how to use electronic commerce. The organizational factors, which are critical to the success of e-commerce, are investigated in this research. Different pieces of literature report different factors as key to success and generally based on subjective, perceptual data. A synthesis of existing literature is a basis for survey questions. The data is collected from Bangladesh e-commerce based organizations who are offering their goods & services on electronic channels, using postal questionnaires and Interview technique. The top factors found to be most critical for the success in e-commerce are: quick responsive products/services, organizational flexibility, services expansion, systems integration and enhanced customer service. An important lesson from this research is that organizations need to view the e-commerce initiative as a business critical area rather that just a technical issue. They need to give attention to internal integration, which may include channels, technology and business process integration, and improving the overall services to their customers.

Keywords: Critical Success Factors, dot-com bubble, electronic commerce, systems integration.

I. INTRODUCTION

There have been significant developments in the structure of the Asia online transaction services sector in the past 12 years. Kalakota and Whinston define e-commerce as 'the buying and selling of information, products and services via computer networks' [1]. It is changing the way organizations carry out their responsibilities, cooperate with customers and running their business usually. According to Tuunainen e-commerce consists of transaction oriented Internet base functions (e.g. on-line catalogs, purchasing and payment). In particular, Electronic Commerce provides a new means of creating, sustaining and escalating competitive advantage by driving down the cost of transacting business, deepening customer relationships and creating new markets in the MarketSpace through virtualization.

The combined effects of the aftermath of the Dot com crash and the current recessionary worldwide economy put even more pressure on firms to find cost-cutting measures. A number of developing countries have adopted e-commerce hoping that it would boost their economies and competitiveness to a new level. The current status of E-commerce is not really significant in Bangladesh compared to developed countries. In 1998 e-commerce generates $39 billion and in 1999 it was 114 billion and in 2004 it generated well over $100 billion in retail business and over 1.5 trillion business-to-business traffic [2]. Forrester forecasts that shopping supposed to grow to $204 billion in 2008. By 2009 online shopping will reach $235 billion, by 2010 it will reach $267 billion and by 2012 online shopping is expected to reach $334 billion. On the contrary, in the context of 'Internet availability and infrastructure' Bangladesh is ranked 73 in the world [3]. Business-to-Consumers (B2C) e-commerce is practically less practiced in Bangladesh, while a very limited level of Business-to-Business (B2B) and Business-to-Government (B2G) transactions exists. In Bangladesh there are approximately 5,000 technical professionals engaged in the e-commerce industry and the size of the domestic market has been estimated to be more than Tk. 300 crore in a year [4].

This paper is a presentation and discussion of the results of a questionnaire survey, which was conducted to investigate the Critical Success Factors (CSFs) in e-commerce. The survey targeted the e-commerce sector in the Bangladesh. A number of medium and large size organizations in the Bangladesh EC sectors were invited to participate. The focus was mainly on the 'what' factors, for which survey research is considered suitable (Oppenheim, 1992).

This paper consists of four main parts. In the first part, the paper's context in current literature will be presented. In the second part, the research framework will be described briefly. The third part is the statistical analysis and discussions. The final part provides a summary of the results and a discussion on the implications of the research. The statistical analyses performed for this phase of the research are similar to those applied by Han and Noh (1999-2000).

II. CRITICAL SUCCESS FACTORS IN E-COMMERCE

The concept of critical success factor (CSF) was developed to help managers define the key information

needed by top-level management. CSFs have been defined in several ways depending on the purpose for which they were used. For the purpose of this paper, Rockart's (1979) definition will be used. He defines CSFs as "the limited number of areas in which results, if they are satisfactory, will ensure successful competitive performance for the organization". CSFs can be used to direct an organization's effort in developing strategic plans, establish guidelines for monitoring a corporation's activities, identify critical issues associated with implementing a strategic plan and can be used by manager and organizations to help achieve high performance. In the context of this research, CSFs theory will be used to pinpoint some areas that are critical for success of the e-commerce.

The following are some of the most critical success factors of the Internet based services reported in the literature. These factors formed the basis for questions included in our data collection instrument.

According to critical success factors for E-Commerce companies which identified by Sung [5], there are customer relationship, privacy of information, low cost operation, ease of use, E-Commerce strategy, technical E-Commerce expertise, stability of systems, security of systems, plenty of information, variety of goods/services, speed of systems, payment process, services, delivery of goods/services, low price of goods/services, and evaluation of E-Commerce operations.

Based on the theoretical model of consumer acceptance of virtual stores proposed by Chen et al. [6], the critical success factors are product offerings, usability of storefront, perceived service quality, and perceived trust.

Regan and Macaluso (2000) and Storey et al. (2000) see excellent customer services as a key factor in the success of e-commerce.

For E-Commerce success, Turban et al. [7] listed CSFs which are user-friendly Web interface, delivery of specific and high-value services or products.

Dubelaar et al. [8] stated that the CSFs presented by the companies succeed in B2C e-business adoption is the combination of strong customer attention, clearly defined performance measures, a clear link between value proposition and measures, and incremental development process.

Viehland [9] identified six factors critical to the success of the e-business strategy as to create a consumer-centric strategy, to accept outsourcing to improve business performance, to act like a new entrant, to utilize information management to differentiate company's product, to be part of an e-business community, and to require executive leadership.

Eid et al. [10] grouped the CSFs for business-to-business international Internet marketing successful implementation into five related factors, which are marketing strategy related factors, web site related factors, global related factors, internal related factors, and external related factors. Each group comprised of several factors.

Jennex et al. [11] discussed the key infrastructure factors for setting up B2B e-commerce enterprise in developing countries. They are people factors, technical infrastructure factors, client interface factors, business infrastructure factors, and regulatory environment factors.

G.Yan and J.C. Paradi [12] identified the five critical success factors for financial institutions to compete in E-Commerce market. They involve E-Commerce strategy, innovation, risk tolerance, communication network and size of company assets.

N. Madeja and D. Schoder [113] investigated the web characteristics as significant success factors for web sites. Their investigation found that interactivity and immediacy are success factors for B2B web sites.

Liu and Arnett [14] obtained four major factors: information and service quality, system use, playfulness and system design quality.

Hahn and Noh (1999-2000) explored the factors that inhibit the growth of e-commerce. They categorized variables into six CSFs: lower level of data security, inconvenient use, unstable systems, lack of information mind, dissatisfied purchasing, and social disturbance.

Although the publications reviewed above identify one or more CSFs, it is evident that CSFs in e-commerce have not been specifically studied in the context of developing country like Bangladesh and most of the factors reported above were presented with little empirical evidence. This study will investigate CSFs of e-commerce empirically, to find out which factors are really critical to the success of this channel in Bangladesh.

III. RESEARCH FRAMEWORK

The research presented in this paper proceeded as follows: first, a list of possible success factors (see Table 2) in e-commerce was extracted using the literature review process. Second, a questionnaire was developed. Third, a survey was conducted using postal questionnaires. Finally, various statistical methods including descriptive statistics, factor analysis and t-tests were applied using the SPSS/Win 9.0 statistical package to analyze the data collected.

A. Development of Survey Questionnaire and Pilot Study

In our quest for a suitable existing questionnaire for the research, we have searched the literature and posted an enquiry to the IS world members' email list. Failing to find any suitable instrument we developed a questionnaire. The questions ask one thing at a time and their internal cohesiveness was one of the main objectives of 'validation testing' of the instrument during pre-pilot and pilot study. The consistency of the attributes was achieved by dividing the instrument into different sec-

tions and special attention was paid to validity and linearity issues during the design and testing stages of the instrument development. Likert Scales (1-7) were used to measure the criticality of different attributes, with 1 being least critical and 7 representing maximum criticality.

Once a workable instrument was ready, a testing strategy similar to that of Han and Noh (1999-2000) was used. It was tested on 2 PhD and 3 Msc. Engineering students within the Department of Computer Science & Engineering University, which resulted in several changes. Few e-commerce consultants participated in a separate field test. Their comments led to a refinement of the questionnaire instrument. Their contribution is gratefully acknowledged.

B. Research Method

The questionnaire was sent to 325 medium & large size e-commerce organizations, software firm, government officials and expert personnel. It is important to note that this sample therefore, represented a purposive, non-probabilistic population, rather than a random one. Senior IT managers are generally considered to be the most likely people to be aware of issues related to e-commerce. For this reason, the questionnaire was targeted at them with a request to pass it to anybody they considered to be more suitable to answer the questions in the survey instrument. The organizational background of the respondents is summarized in Table I.

Table I Organizational backgrounds of the respondents

Organization Type	Number	Percentage of total responses
E-Commerce based Company	18	18.75
Software firm	28	29.12
Bank	22	22.92
Expert Personnel	28	29.12
Total	96	

Out of 325 questionnaires sent, a total of 96 were returned giving a 29.5% response rate. This level of response is common for similar surveys in the Developing countries. Out of 96 responses, 73 were usable (22.4%). Table I presents a breakdown of 'valid respondents' by type of organization. 23 responses were not usable. This unusually high number (23.96% of total responses) of unusable responses was due to the fact that Internet based transaction services are a relatively new area and many organizations are not yet offering such services. Therefore, they returned the questionnaire, stating that they do not take part in e-commerce. Also, some companies were no longer operating from the address given, and these questionnaires were returned uncompleted.

C. Data Analysis

This section is a presentation of statistical analyses, which were applied to the data collected from the survey. First the factors were ranked using the mean scores to see if there was an indication of consensus about the relative weighting of the factors. Second, a factor analysis was performed (see Table III and IV) which shows a possible relationship between different factors by categorizing them into six different categories. Finally, an Independent Sample t-test was performed to compare the data from different size organizations.

Table II Descriptive statistics for each variable in the order of importance (v stands for variable)

Ranking of the Item	Description of variable	Mean	Std. Deviation
V8	Light and faster website	5.947	1.057
V9	Secure website and other related systems	5.869	1.258
V11	Fast responsive customer service (better that usual)	5.684	1.200
V13	promotion of electronic e-commerce within organization	5.602	1.349
V7	All time availability of services	5.453	1.426
V4	Rapid delivery of services	5.450	1.406
V5	Fast and integrated business processes	5.419	1.506
V1	Share Information	5.287	1.465
V10	Customer Database	5.260	1.337
V12	Flexible workforce	5.145	1.734
V6	Personalizing services	5.095	1.667
V2	Flexible organizational structure	5.082	1.598
V3	Web-specific marketing	5.080	1.412
V14	Business solution	4.932	1.879

IV. DESCRIPTIVE STATISTICS OF CSF IN E-COMMERCE

The main aim of this analysis was to describe the importance of each variable in order of importance given to it by the survey respondents. Results are presented in descending mean value (order of mean importance) in Table II. The relative ordering of adjacent factors in the Table II is not significant but across the table as a whole there are some indications of significant differences between the factors at the top and bottom of the table. This could imply that factors at the top are significantly more critical than the factors at the bottom of the table.

V. FACTOR ANALYSIS

Factor analysis was performed using a Principal Component Analysis (PCA) and the Varimax with Kaiser Normalization rotation method until the Eigen value of each factor was greater than 1. The rotation converged in 14 iterations. The reasons for PCA selection are given in the following paragraph.

Rotation is ordinarily used after the factor extraction to maximize the potential high correlations and minimize low correlations.

The results of the factor analysis appear in Table III, which shows that variables are grouped into 6 factors, with the highest score of each variable given in the bold type face highlighting the membership of each variable within 6 factors.

Factors were tested using reliability analyses to calculate their Cronbach's Alpha, results of which are given in Table IV. The factors are derived from the combination of their variables.

Four of these factors had a score of more than 0.6 in the Cronbach's α reliability test (see TableIV). The fifth factor was selected even though its Cronbach's α was 0.52 because 'customer service' was felt to be important. However, since the internal consistency of this factor is weak, care must be taken in interpreting it. The Cronbach's α value of factor 4 is not large enough to indicate whether this factor is reliable. It was included because it was thought to be important by the researchers. The sixth factor was eliminated because of its very low Cronbach's α value of just 0.2.

A. Organizational Flexibility (α =0.72)

The working of the items constituting this factor (see factor 2 in Table IV) portrays the concept of flexibility in different aspects of an organization. The first element is structural flexibility, which is about organizing different functions of an organization around business processes, rather than traditional hierarchical structures, so that a structure changes according to the changes in business environments and objectives (Kalakota and Robinson, 1999).

Having a policy of selecting best of breed products and an ability to integrate them, adds another dimension to

Table III Results of factor analysis

Variables	Components					
	1	2	3	4	5	6
V1	**.495**	-3.294E-02	-3.968E-02	.454	.108	-4.115E-02
V2	.231	**.583**	.196	.314	-.218	-.147
V3	.237	.149	.152	**.732**	.206	.112
V4	.191	.289	-.104	**.475**	.450	-.331
V5	.242	.249	.258	**.397**	.247	-.274
V6	.321	.142	.405	**.409**	.287	-7.357E-03
V7	**.544**	.236	.371	.259	-1.466E-02	3.835E-02
V8	**.739**	7.029E-02	.165	5.090E-02	9.751E-02	5.263E-02
V9	.254	-8.519E-02	4.355E-03	6.098E-02	**.781**	5.625E-02
V10	4.575E-02	5.166E-02	**.592**	.426	9.828E-02	2.358E-02
V11	-.159	**.241**	.223	-2.285E-03	-5.583E-02	9.093E-02
V12	.144	**.658**	.263	8.799E-02	.102	.107
V13	.394	**.724**	-1.357E-02	5.595E-03	-4.554E-02	-.109
V14	-9.284E-02	**.731**	5.627E-02	.120	.211	.247

the organization's business freedom. This enables it to choose the systems components according to its business requirements, rather than building the business around its systems capabilities.

B. Fast and Responsive Products/Services (α = 0 .78)

This factor is comprised of variables (see factor 1 in Table IV) which mainly involve Web-specific marketing, rapid delivery of products/services, personalized marketing, fast responsive and integrated business processes, and having sufficient human/financial resources to do these things. Effective Web-specific marketing and personalizing products to individual needs, requires gathering relevant data about customers and using it to build long-term relationships. Integrated business processes and systems create opportunities to trace the trails of each transaction by a customer. If that transaction is aggregated with the customer's other transactions and analyzed, it may yield invaluable historical information about consumer preferences and how the organization may cater for and influence those preferences. If the customer's transaction history is analyzed with that of other customers, the organization

Table IV Cronbach's α for each critical factor in e-commerce

Factors	Number of variables	Cronbach's α Score	Success factors and their variables
1	3	0.72	**Organizational flexibility** Share Information All time availability of services Light and faster website
2	5	0.78	**Fast and responsive products/services** Fast responsive customer service (better that usual) promotion of electronic e-commerce within organization Flexible workforce Flexible organizational structure Business solution
3	1	0.69	**Expansion of services** Customer Database, 24 x 365 days availability of service, attractive website.
4	4	0.65	**Systems and services integration** Rapid delivery of services Fast and integrated business processes Web-specific marketing Personalizing services
5	1	0.52	**Enhanced customer service** Secure website and other related systems
6	0	0.20	Eliminated from analysis because of too low score

may discover a segment preference that can be satisfied by new products and services (Kalakota and Frei, 1998)..

C. Expansion of Services (α = 0.69)

In e-commerce expansion of services starts from development of an interactive and user-friendly website. The website along with associated functions or services has to be available 24 hours every day of the year. Some organizations, such as CellBazaar and Hutbazar are offering extra services such as job circular or other advertisements on their website, through their partner organizations. Not only does this result in extra revenues from new services, it often results in increased sales of existing products.

D. Systems and Services Integration (α = 0. 65)

Integration is not only necessary for cost savings in processing, but also to develop the ability to gather/analyze customer related data for marketing purposes and the ability to deliver integrated products in real time across channels. It involves the elimination of redundant systems, integrating remaining legacy and new systems so that they work like a single system.

E. Enhanced Customer Service (α = 0.52)

This factor is mainly concerned with improving customer service to accommodate ever rising expectation and addressing their fears about the security of their personal data and transactions. Once they become aware of the integrated and secure services available somewhere, they are likely to switch to the providers of such services (Kalakota and Frei, 1998).

VI. SUMMARY AND CONCLUSIONS

This section is a summary of the main findings of the survey. E-commerce is a key issue for many organizations in the financial industry. However a number of organizations are finding it difficult to exploit this relatively new way of conducting business (Dewan and Seidmann, 2001).

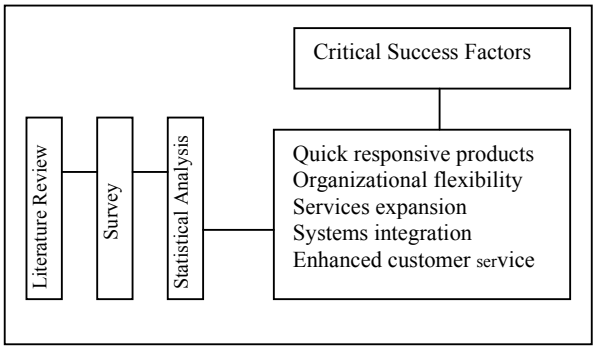

Figure1. The process and results of postal survey research

This study addresses this issue by attempting to explain the factors, which are critical to the success in e-commerce. The process and results of this study so far, are summarized in Figure 1

In this paper, two major types of statistical analyses were conducted, descriptive statistical analyses and factor analysis. In descriptive analyses, the factors (or variables) were ranked in order of their mean score, the highest score being the most important and so on. The top six factors in order of importance were: user-friendly website, systems security, support from top management, fast responsive customer service (better that usual), promotion of electronic commerce within

organization, all time availability of services and rapid delivery of services.

The findings of the survey are in line with theoretical predictions from general e-commerce literature reviewed earlier in the paper. One of the main contributions of this research was that it brought together a diverse range of factors which were scattered across many publications and had them validated by the practitioners in the field. The resulting list of factors is by no means exhaustive or final. Managers may find it useful in the strategic planning of e- commerce and to channel resources towards the most critical aspects of e- commerce management. The theoretical framework based on CSFs proposed by this research, is useful in demonstrating the presence of critical factors in the e-commerce environment and their positive relationship with the success of such services. It is concluded that factors found by this research may be applicable in retail e-banking in general but only with some context specific changes. The factors found in this research are also likely to be applicable to many other areas, but further research is required to address these issues. Regarding the research method, surveys offer some advantages and some disadvantages. In the context of this research, one of the main advantages of the survey research approach was the ability to collect information from a large number of samples which in this case were all medium and large size organizations in Bangladesh. Thus, the researcher was able to explore the opinions of a large group of people, dispersed all over the country. The second advantage of the survey is that results can often be generalized but this was not the main aim of this research. However, a relatively good response rate of this survey and rigorous application of best practice in this research area means that results presented in this paper may be viewed as reliable for the whole sample. The third advantage of this survey is that it lends itself to future replication by other researchers because the questions and sampling were tightly controlled. Thus this survey may be repeated after few years to assess the degree of change over a given period of time.

REFERENCES

[1] Laosethakul, K., Boulton, W., "Critical Success Factors for E-commerce in Thailand: Cultural and Infrastructural Influences", Electronic Journal of Information Systems in Developing Countries, Vol-30(2), pp 1-22, 2007.

[2] Awad, E. M., "Electronic Commerce From Vision to Fulfillment", Prentice-Hall of India Private Limited, pp 5-45, 3rd Edition, 2007.

[3] Kirkman,G.S., Cornelius, P.K., Sachs, J.D., Schwab,K., , "The Global Information Technology Report 2001-2002: Readiness for the Networked World", Oxford University Press, pp. 168-169, 2002.

[4] Bangladesh Association of Software and Information Services, "Basis News & Views", Vol- 3(4), BASIS, 2007.

[5] T.K. Sung, "E-Commerce critical success factors: east vs. west", Technological Forecasting and Social Changes, In Press, Corrected Proof, Available online 5 October 2004.

[6] L. Chen, M.L. Gillenson, and D.L. Sherrell, "Consumer acceptance of virtual stores: a theoretical model and critical success factors for virtual stores", ACM SIGMIS Database, vol.35, issues.2, Spring 2004.

[7] E. Turban, D. King, J. Lee, M. Warkentin, and H.M. Chung, "Electronic commerce 2002 A Managerial Perspective", pp.4, 689-690, 718 , Prentice-Hall, New Jersey, 2002.

[8] C. Dubelaar, A. Sohal, and V. Savic, "Benefits, impediments and critical success factors in B2C E-business adoption", Technovation, In Press, Corrected Proof, Available online 8 October 2004.

[9] D.W. Viehland, "Critical success factors for developing an e-business strategy", Available Online at: http://www.massey.ac.nz/~dviehland/ebusinesscsf.html, 2000.

[10] R. Eid, M. Trueman, and A.M. Ahmed, "A cross-industry review of B2B critical success factors", Internet Research: Electronic Networking Applications and Policy, vol.12, no.2, pp.110-123, 2002.

[11] M.E. Jennex, D. Amoroso, and O. Adelakun, "E-Commerce Infrastructure Success Factors for Small Companies in Developing Economics", Electronic Commerce Research, vol.4, pp.263-286, 2004.

[12] G. Yan, and J.C. Paradi, "Success Criteria for Financial Institutions in Electronic Commerce", Proceeding of the 32nd Annual Hawaii International Conference on System Sciences, vol.5, pp.5007, January 1999.

[13] N. Madeja and D. Schoder, "Designed for Success - Empirical Evidence on Features of Corporate Web Pages", Proceeding of the 36th Annual Hawaii International Conference on System Sciences, track 7, pp.188, January 2003.

[14] C. Liu and K.P. Arnett, "Exploring the factors associated with Web site success in the context of electronic commerce", Information & Management, vol.38, issue 1, pp.23-33, October 2000.

Proceedings of 2009 12th International Conference on Computer and Information Technology (ICCIT 2009)
21-23 December, 2009, Dhaka, Bangladesh

Design and Analysis of Smart Antenna System for DECT Radio Base Station in Wireless Local Loop

Muhammad Mahfuzul Alam, Md. Majharul Islam Rajib†, and Sumon Kumar Biswas
Dept. of ECE, Khulna University of Engineering & Technology, Bangladesh
†Dept. of ECE, Northern University Bangladesh
mahfuz04_ece@yahoo.com, majhar951@yahoo.com, skbiswas_ece04@yahoo.com

Abstract

Digital Enhanced Cordless Telecommunication (DECT) can be a latent solution for wireless local loop (WLL) based communication system planning. In this paper, the design and simulation of a 8×8 *planar microstrip antenna array and signal processing techniques of smart antenna systems for DECT radio base stations are presented.* ***MU****ltiple* ***SI****gnal* ***C****lassification (MUSIC) and Least Mean Square (LMS) signal processing algorithm techniques are analyzed and simulated for smart antenna system. Simulation results of the radiation characteristics, gain and return loss of the fixed beam planar array antenna have been produced by EM simulation software Zeland IE3D. Signal processing simulations were run in MATLAB. This smart antenna system is designed and simulated for DECT system in 1.88−1.90GHz frequency band.*

Keywords: *DECT, LMS, MUSIC, WLL, Planar array, Smart antenna System.*

I. INTRODUCTION

To exploit the dramatic advent of information and communication technology (ICT) into distant areas Wireless Local Loops (WLL) plays a vital role besides mobile communication. In contrast to Plain Old telephone System (POTS) or broadband internet connection where copper wires are used to connect end users to backbone network, WLL uses wireless link as the last mile solution. Consequently it can provide very cost effective and rapid deployment over vast area which is particularly essential to extend the ICT sector in developing countries like Bangladesh, India, Kenya etc. Several technologies are used for WLL like CDMA, DECT, and LMDS etc. DECT has the advantage of low cost equipment at both user and service provider end. Moreover, it doesn't require the valuable cellular spectrum as operates in 1880-1900 MHz band. A simplified model of DECT used as WLL described in [1]. DECT is recognized by the ITU as fulfilling the IMT-2000 requirements and thus qualifies as a 3G system [7]. It is the leading cordless technology [8]. However, DECT requires Line of Sight (LOS) communication which might not be as feasible in sub-urban areas as in rural areas. To significantly improve the communication link in multipath scenario Smart Antenna System can be deployed. Many works have been done on smart antenna system [2], [3], [4], [5]. Design of smart antenna system combines the technology of antenna design and signal processing algorithms. Smart antenna system consists of an array of radiating elements able to steer the main lobe beam towards the desired signal and to locate suitable nulls of the radiation pattern in the direction of interferences. One essential component of smart-antenna is its sensors or antenna elements. These antenna elements play an important role in shaping and scanning the radiation patterns and constraining the adaptive algorithm used by digital signal processor [6]. Different types of radiators are found such as dipoles, monopoles, loops, horns, reflectors, microstrip and so on. Microstrip antennas gain popularity for its simple and inexpensive manufacturing using modern printed-circuit technology. This type of antenna is mechanically robust when mounted on rigid surfaces. As microstrip antenna has many advantages, we considered microstrip antenna for antenna array design. We designed a 64 element planar array antenna for the smart antenna system. The simulated smart antenna signal processing system use MUSIC algorithm and LMS algorithm for Direction of Arrival (DOA) estimation and adaptive beamforming respectively. The total system is simulated for a DECT radio Base Station smart antenna system that can be used in WLL Communication System. In this paper we consider DECT system for outdoor application; it may be university campus, industrial area in remote places or rural area.

II. ANTENNA ARRAY DESIGN

The corporate–feed network is used to provide power splits of 2^n (i.e., n=2, 4, 8, 16, 32, etc.). This is accomplished by using either tapered lines or using quarter wavelength impedance transformers. With this method the designer has more control of the feed of each element both in amplitude and phase. The array factor of planar array antenna with element spacing in the x and y directions are d_x and d_y respectively can be expressed in following equation [9], [10].

$$FA = (\sin^2(N\pi(d_x/\lambda)\sin\theta_a)/N^2\sin^2(\pi(d_x/\lambda)\sin\theta_a)).$$

978-1-4244-6283-4/09/$26.00 ©2009 IEEE

$\left(\sin^2\left(M\pi\left(d_y/\lambda\right)\sin\theta_e\right)/M^2\sin^2\left(\pi\left(d_y/\lambda\right)\sin\theta_e\right)\right)$ (1)

where $N=$ number of radiating elements in vertical direction of array that gives rise to the azimuth angle θ_a and M =number of radiating elements in horizontal direction that gives rise to the elevation angle θ_e. The radiated fields of the E-plane for a single element patch can be expressed using following formula given in [6] as.

$E=+jk_0\ WV_0e^{-jk_0r}/\pi r\left\{\sin\left(\frac{k_0h}{2}\cos\phi\right)/\frac{k_0h}{2}\cos\phi\right\}.$
$\cos\left(\frac{k_0L_e}{2}\sin\phi\right)$ (2)

Here W is the width of the patch antenna,L_e is the extended length, V_0 =hE_0 is the voltage across radiating slot, h is the substrate height, k_0=$2\pi/\lambda$ and r is the far field distance from the antenna.

Substrate of this antenna is considered R03010 ($\epsilon_r=10.2$), high dielectric constant is taken for size reduction because the operating frequency of the antenna is 1.88GHz −1.90GHz. In these range of frequency antenna size is usually large unless high dielectric constant substrate is not used for antenna design. Recessed microstrip line feeding techniques is used as this gives a good impedance matching at inputs of the radiating elements. Feed networks in general have certain undesired characteristics that must be carefully monitored in order to minimize any adverse effects on array performance. These characteristics include conductor and dielectric losses, surface wave loss, and spurious radiation due to discontinuities such as bends, junctions and transitions. These losses constitute the overall insertion losses of the feed system affecting the maximum obtainable gain of the array [11]. For this simulated antenna, chamfered bend is used to compensate for excess capacitance [12].

Simulated antenna layout is shown in Fig.1 and dimensional parameters of the simulated antenna are given is Table. In Fig. 1(b) c indicates chamfered bend and antenna dimension: $700(l)\times691(w)\times1.58(h)mm$.

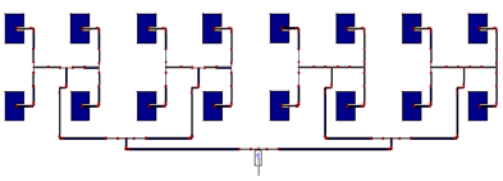

(a)

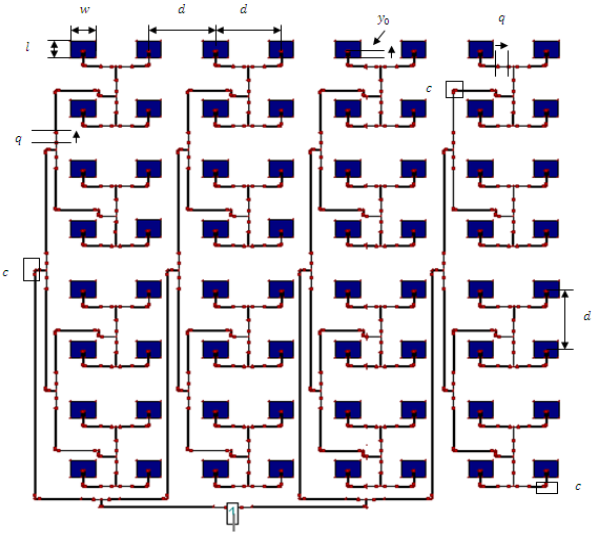

(b)

Fig. 1: Layout of the simulated antenna.

Table: Dimensional parameters of the antenna.

w	l	d	q	y_0
34mm	25mm	88mm	15.6mm	10.13mm

After Simulation we found that return loss is −33.10dB at 1.88GHz. Return loss of -10dB or below is found from 1.855GHz to 1.907 GHz, so it is suitable for use in 1.88/1.90GHz frequency band. 2.77% bandwidth is found for this antenna. Figure 2 shows the return loss curve. Side lobe level (SLL) of the antenna is more than 15dB lower than main lobe. Figure 3 gives the radiation pattern of the simulated antenna. Fig. 4 gives the gain of the antenna at different frequencies. Simulated gain and directivity of the antenna is 21.0dBi and 23.39dBi respectively.

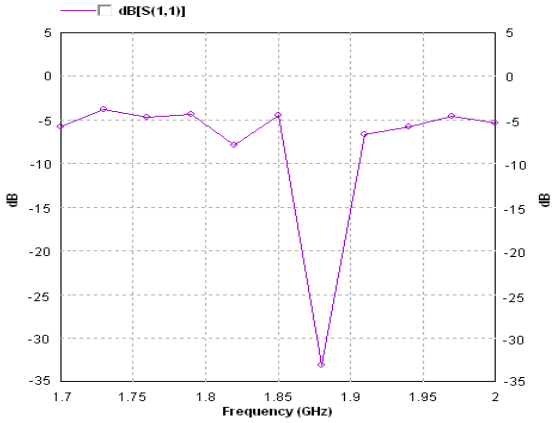

Fig. 2. Return loss of the array antenna (64 elements).

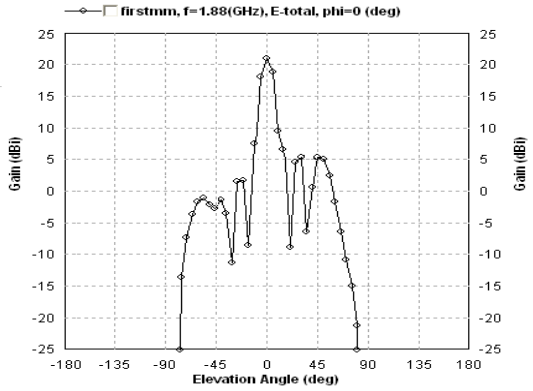

Fig. 3. Radiation pattern of the array antenna.

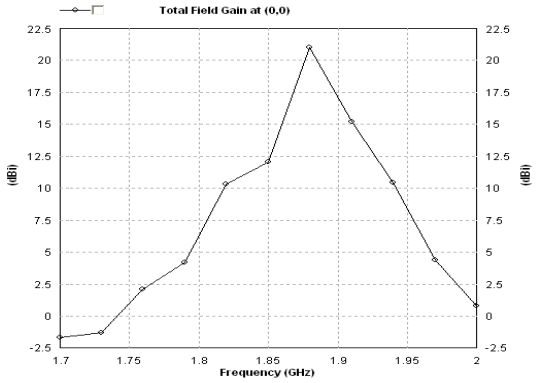

Fig. 4. Simulated gain of the antenna at different frequencies.

III. DECT SYSTEM in WLL AND RAYLEIGH-FADIANG CHANNEL

DECT system may have various different physical implementations depending on its actual use. Different DECT entities can be integrated into one physical unit; entities can be distributed, replicated etc. A good DECT system architecture model is given in ref. [1], [13]. DECT system use GFSK modulation techniques (BT=0.5).It's bit rate is 1.152Mbps, frame cycle time is 10ms and TDD duplex method is used. Wireless communication systems are characterized by time-varying multipath propagation channels, which are typically modeled as fading channels. In mobile radio channels, the Rayleigh distribution is commonly used to describe the statistical time varying nature of the received envelope of a flat fading signal, or the envelope of an individual multipath component [14]. Figure 5 shows a typical Rayleigh fading envelope at 1890MHz, frequency within DECT range and receiver speed is $15km/h$. The BRE of GFSK (Gaussian Frequency Shift Keying) modulation is evaluated over an AWGN channel where received signal is corrupted only by additive white Gaussian noise as shown in Fig. 6. DECT has been used for Fixed Wireless Access as a substitute for copper pairs in the "last mile" in countries such as India and South Africa. DECT is considered WLL, when a public network operator provides wireless service directly to the user via this technology. By using directional antennas, DECT cell coverage can be extend up to 2000m.

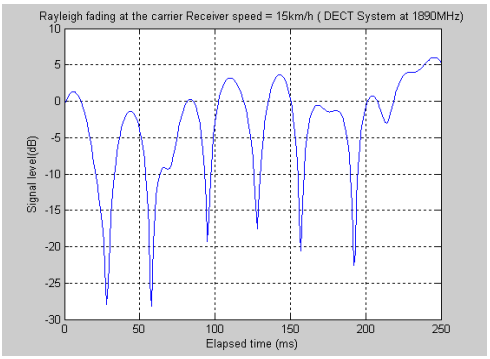

Fig. 5. Rayleigh fading envelope at 1890MHz

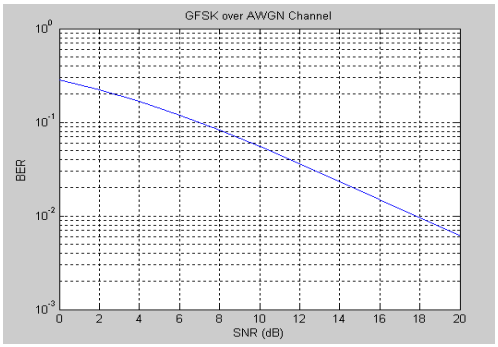

Fig. 6. BRE over AWGN channel for GFSK modulation

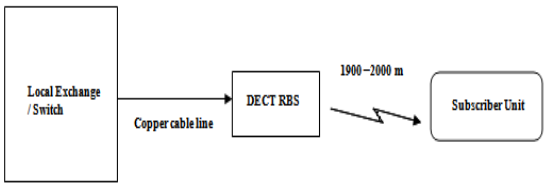

Fig. 7. Block of DECT system for last mile solution.

Signal processing techniques is used to combat multipath fading and interference reduction. Smart antennas (adaptive array) work in the following way: First digital signal processor receives signals collected from each antenna element, it computes the direction - of-arrival (DOA) of the signal of interest (SOI).It then uses adaptive beamforming algorithms to produce a radiation pattern that focuses on the SOI, at the same time as tuning out any signal not of interest (SNOI). Fig. 8 shows the functional block diagram of a smart antenna system.

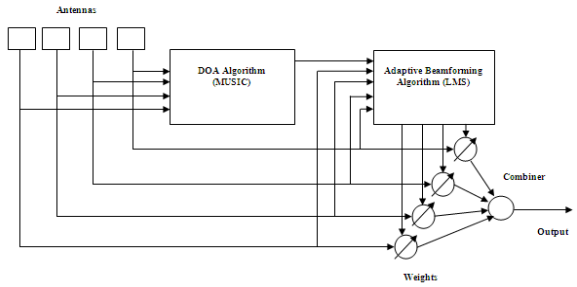

Fig. 8. Block Diagram of a Smart Antenna System.

IV. DOA ESTIMATION ALGORITHM

Subspace-based methods exploit the structure of the received data, resulting in an impressive improvement in resolution. **MU**ltiple **SI**gnal **C**lassification (MUSIC) algorithm fall into this category [6]. MUSIC is the first subspace-based DOA estimation approach (Schmit, 1986). MUSIC promises to provide unbiased estimates of the number of signals, the angle of arrival and the strengths of the waveforms. It makes the assumption that the noise in each channel is uncorrelated making the noise correlation matrix diagonal and the incident signals may be somewhat correlated creating a nondiagonal signal correlation matrix [15].Music algorithm can be described in the following way:

Considering the number of signals is *D* and number of array elements is *M*. So the number of signal eigenvalues and eigenvectors is *D* and the number of noise eigenvalues and eigenvectors is *M−D(M>D)*. Now $M \times M$ array correlation matrix can be written as follows,

$$\bar{\boldsymbol{R}}_{xx} = \boldsymbol{E}[\bar{x}.\bar{x}^H] = \boldsymbol{E}[(\bar{A}\bar{s} + \bar{n})(\bar{s}^H\bar{A}^H + \bar{n}^H)]$$
$$= \bar{A}\boldsymbol{E}[\bar{s}.\bar{s}^H]\bar{A}^H + \boldsymbol{E}[\bar{n}.\bar{n}^H] = \bar{A}\bar{\boldsymbol{R}}_{\boldsymbol{ss}}\bar{A}^H + \bar{\boldsymbol{R}}_{\boldsymbol{nn}}$$
$$= \bar{A}\bar{\boldsymbol{R}}_{\boldsymbol{ss}}\bar{A}^H + \sigma_n^2\bar{\boldsymbol{I}} \qquad (3)$$

Where $\bar{\boldsymbol{R}}_{\boldsymbol{ss}} = D \times D$ source correlation matrix, $\bar{\boldsymbol{R}}_{\boldsymbol{nn}} = \sigma_n^2\bar{\boldsymbol{I}} = M \times M$ noise correlation matrix and $\bar{\boldsymbol{I}} = N \times N$ identity matrix.

After this we can write $M \times (M - D)$ dimensional subspace spanned by the noise eigenvectors that is as follows,

$$\bar{\boldsymbol{E}}_{\boldsymbol{N}} = [\bar{e}_1 \quad \bar{e}_2 \quad \ldots\ldots \quad \bar{e}_{M-D}] \qquad (4)$$

The noise subspace eigenvectors are orthogonal to array steering vector at angles of arrival $\theta_1, \theta_2, \ldots, \theta_D$. At last MUSIC pseudo spectrum is defined as,

$$\boldsymbol{P}_{\boldsymbol{MU}}(\theta) = \frac{1}{|\bar{a}(\theta)^H\bar{\boldsymbol{E}}_{\boldsymbol{N}}\bar{\boldsymbol{E}}_{\boldsymbol{N}}^{\boldsymbol{H}}\bar{\boldsymbol{a}}(\theta)|} \qquad (5)$$

The MUSIC algorithm in general can apply to any arbitrary array regardless of the position of the array elements [14]. We use MUSIC algorithm for uplink condition. We consider signal arrival from four different directions in different angles (Fig .9 and Fig.10). For simulation we use 64 element planar array antenna. Operating frequency is 1.88GHz and element spacing is 88mm. Fig. 11 illustrates the different possible radiation pattern of the spatial beamformer.

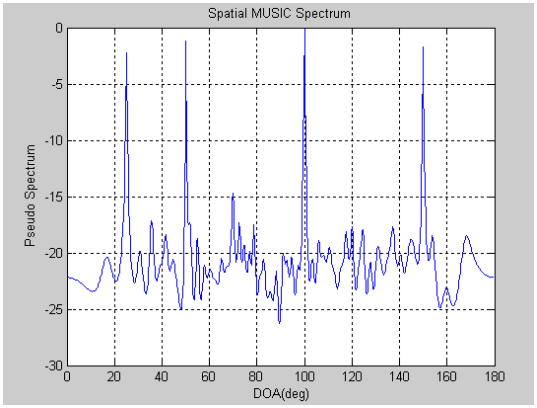

Fig. 9. Pseudo Spectrum of MUSIC with angle, Signal arrival at $25^0$and 50^0, 100^0 , 150^0 and SNR is 18dB.

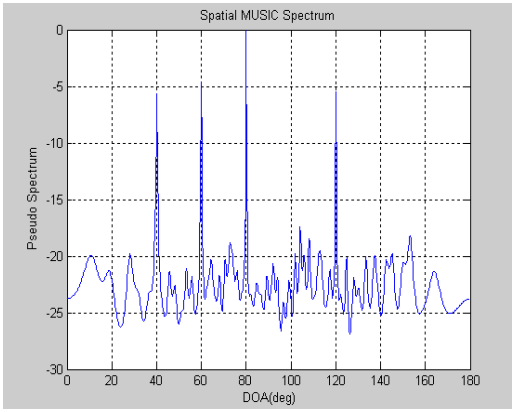

Fig.10. Pseudo Spectrum of MUSIC with angle, Signal arrival at 40^0,60^0, 80^0 and 120^0 SNR is 16dB.

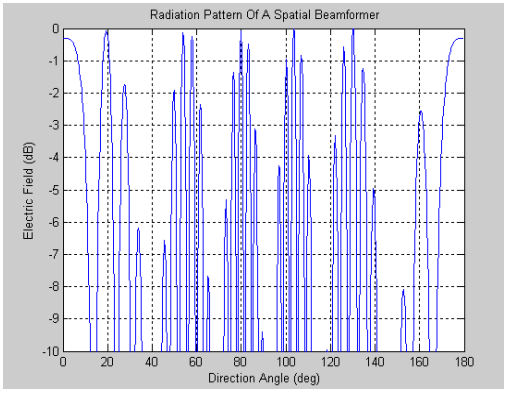

(a)

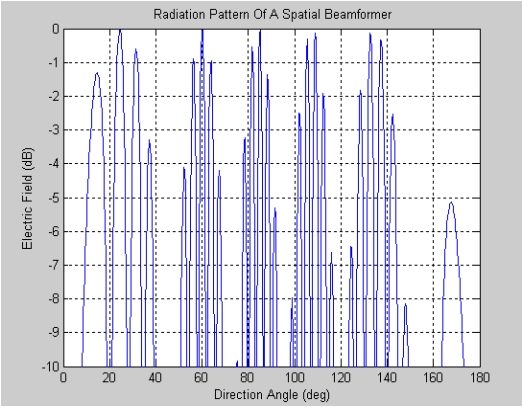

(b)

Fig. 11. Possible Radiation of Spatial beamformer Signal arrival at 40^0 , 60^0 , 80^0 and 120^0 and SNR is 16dB.

V. ADAPTIVE BEAMFORMING TECHNIQUES

In adaptive beamforming, the target is to adapt the beam by adjusting the amplitudes and phases of signals such that an enviable pattern is formed. One of the simplest algorithms that are commonly used to adapt the weights is the Least Mean Square (LMS) algorithm. The LMS algorithm is a low complexity algorithm that requires no direct matrix inversion and no memory. It is an approximation of the steepest descent method using an estimator of the gradient instead of the actual value of the gradient, since computation of the actual value of the gradient is impossible because it would require knowledge of the incoming signals. As a result, at each iteration in the adaptive process, the estimate of the gradient is a follows [6].

$$\hat{\nabla}[J(\boldsymbol{w})]_k = \begin{bmatrix} \frac{\partial J(\boldsymbol{w})}{\partial w_0} \\ \vdots \\ \frac{\partial J(\boldsymbol{w})}{\partial w_L} \end{bmatrix} \tag{6}$$

Where the $J(\boldsymbol{w})$ is the cost function. We can obtain this by following mathematical analysis,

x_k is a vector from each antenna array element at time step k,

$$x_k = [x(k)_1\ x(k)_2 \ldots\ x(k)_L]^T \tag{7}$$

respectively, we also get a weight vector w

$$w = [\, w_1\ w_2 \ldots \ldots\ w_L\,] \tag{8}$$

Then the output $y(k)$ for time step k is

$$y(k) = w^H\, x(k) \tag{9}$$

ε_k is the error between the desired signal d_k and the output signal of the array y_k, can be expressed as,

$$\varepsilon_k = d_k - \boldsymbol{w}^H x_k \tag{10}$$

MSE (Mean Square Error) based cost function,

$$J_{MSE}(E[\varepsilon_k^2]) = d_k^2 - 2\boldsymbol{w}^H E[d_k \boldsymbol{x}_k] + \boldsymbol{w}^H E[\boldsymbol{x}_k \boldsymbol{x}_k^H]\boldsymbol{w} \tag{11}$$

$$J_{MSE}(E[\varepsilon_k^2]) = d_k^2 - 2\boldsymbol{w}^H r_{xd} + \boldsymbol{w}^H R_{xx}\boldsymbol{w} \tag{12}$$

where $\boldsymbol{r}_{xd} = E[d_k \boldsymbol{x}_k]$ and $\boldsymbol{R}_{xx} = E[\boldsymbol{x}_k \boldsymbol{x}_k^H]$.Using steepest descent method, the iterative equation updates weights at each iteration; this can be expressed by following equation,

$$\boldsymbol{w}_{k+1} = \boldsymbol{w}_k - \mu\bar{\nabla}[J(\boldsymbol{w})]_k \tag{13}$$

where μ is the step size related to the rate of convergence. LMS algorithm minimizes the MSE (Mean Square Error) cost function and it solves the Wiener-Hopf equation iteratively without the need for matrix inversion. The Wiener-Hopf equation is as follows,

$$\boldsymbol{w}_{opt} = \boldsymbol{R}_{xx}^{-1}\boldsymbol{r}_{xd} \tag{14}$$

The LMS algorithm computes the weights iteratively as,

$$\boldsymbol{w}_{k+1} = \boldsymbol{w}_k + 2\mu x_k(d_k - x_k^T \boldsymbol{w}_k) \tag{15}$$

In order to assure convergence of the weights,$\boldsymbol{w}_k$, the step size μ is bounded by the following condition

$$0 < \mu < \frac{1}{\lambda_{max}} \tag{16}$$

Where λ_{max} is the maximum eigenvalue of the covariance matrix, R_{xx} given is equation (3). Fig. 12 shows the simulated result of actual and estimated system output using LMS algorithm. Four weights are considered for simulation. Fig. 13 illustrates the error curve that deals with the error of actual value and estimated value. At last Fig. 14 describes the comparison of actual weights and estimated weights.

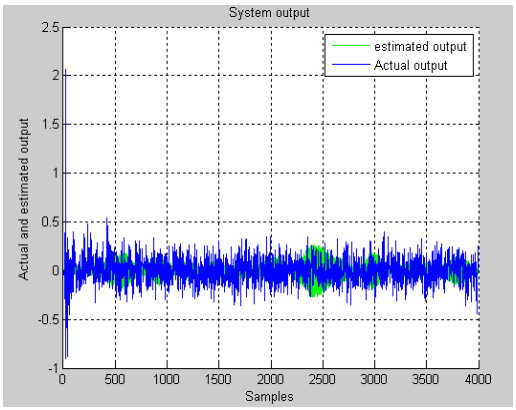

Fig. 12. System output comparison of Actual value and estimated value.

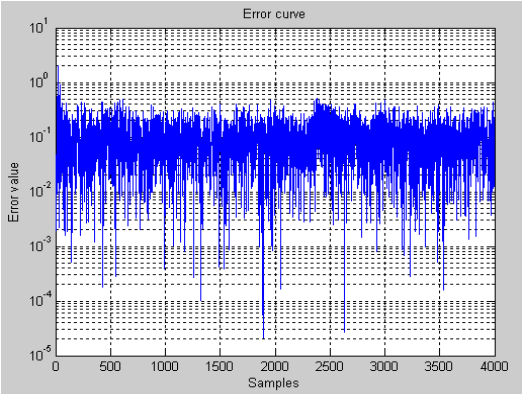

Fig. 13. Error value between actual and estimated output.

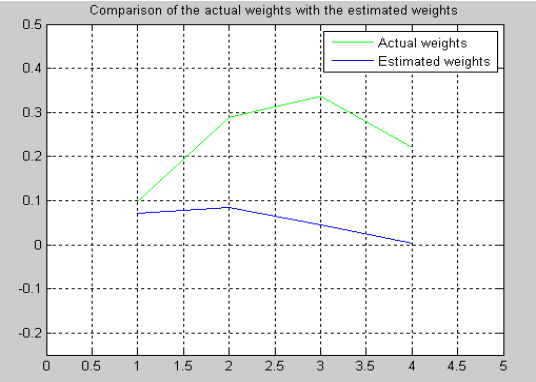

Fig. 14. Comparison of Actual weights and the estimated weights (consider four weights) iteratively computes using equation (15).

VI. CONCLUSION

A smart antenna system for the minimization of the adverse effect of time-varying multipath propagation channel and improve the signal communication link of the DECT RBS in WLL system has been designed. For signal processing we exploit MUSIC algorithm because of its simplicity and LMS algorithm for its low complexity. MUSIC algorithm gives us different possible radiation of spatial beamformer. Using LMS algorithm we can calculate the weights for adaptive beamforming. Simulation of 64 element microstrip antennas is very time consuming specially using low processing speed computer, Intel core 2 due CPU T8100 @ 2.10GHz , 2.09GHz is used for this task. Only 11 frequency points are taken from 1.7-2.0GHz for processing as more frequency points require more time. In this simulation each frequency point takes approximately 2800sec and a total of 9 hours for 11 frequency points.

REFERENCES

[1] Saifur Rahman, and Manisa Pipattanasomporn, "Alternate Technologies for Telecommunications and Internet Access in Remote Locations", *In Proc. of 3rd Mediterranean Conference and Exhibition on Power Generation, Transmission, Distribution and Energy Conversion*, Greece, November 2002.

[2] Salvatore Bellofiore, Jeffrey Foutz,Ravi Govindarajual, İsrafil Bahçeci, Constantine A. Balanis , Fellow , IEEE, Andreas S.Spanias, Jeffrey M.Capone, Member , IEEE, and Tolga M. Duman, "Smart Antenna System Analysis, Integration and Performance for Mobile Ad-Hoc Networks (MANETs)", IEEE Transactions on Antennas and Propagation, Vol.50, No.5, May 2002.

[3] A. Kundu, S Ghosh, B.K.Sarkar and A. Chakrabarty,"Smart Antenna based DS-CDMA system design for third generation mobile communication" ,*Progress In Electromagnetics Research M,Vol.4,67-80,2008* .

[4] S.N.Shahi, M.Emadi and K.Sadeghi,"High Resolution DOA Estimation in Fully Coherent Environments", *Progress In Electromagnetics Research C,* Vol.5, 135-148,2008 .

[5] L.Lizzi, F.Viani, M.Benedetti, P.Rocca , and A.Massa ,"The *M-DSO-ESPRIT* Method for Maximum Likelihood DOA Estimation", *Progress In Electromagnetics Research,* PIER 80,477-497,2008

[6] C.A. Balanis, *Antenna Engineering,* wiley, 3rd ed, 2005.

[7] http:// www.dect.org

[8] Friedhelm Hillebrand,"*GSM and UMTS : The Creation of Global Mobile Communication*", John Wiley & Sons Ltd, 2001.

[9]Merrill I. Skolnik, *Introduction to RADAR System*, 3rd ed, 2003.

[10]Hubregt J. Visser Array and Phased Array Antenna Basics , John Wiley & Sons Ltd, 2005.

[11] Ramesh Garg, Prakash Bhartia, Inder Bahl, Apisak Ittipiboon, *Microstrip Antenna Design Handbook,* 2001 ARTECH HOUSE, INC.

[12] K.C.Gupta,Ramesh Garg, Inder Bahl, Prakash Bhartia, "Microstrip Lines and Slotlines",Artech House,2nd,1996.

[13] Jochen Schiller "Mobile Communications", 2nd ed. Pearson education Limited 2003.

[14] Theodore S. Rappaport, "Wireless Communication Principles and Practice"Prentice Hall, 2nd ed, 2004.

[15] Frank Gross, "Smart Antenna for Wireless Communication with MATLAB" The McGraw-Hill Companies, Inc. 2005

Proceedings of 2009 12th International Conference on Computer and Information Technology (ICCIT 2009)
21-23 December, 2009, Dhaka, Bangladesh

A Probabilistic Position-based Routing Scheme for Delay-Tolerant Networks

Farzana Yasmeen, Shigeo Urushidani†, Shigeki Yamada†
Department of Informatics, The Graduate University for Advanced Studies, Tokyo, Japan
† National Institute of Informatics, Tokyo, Japan
bonhomie@nii.ac.jp, urushi@nii.ac.jp, shigeki@nii.ac.jp

Abstract

Observably, participants in realistic scenarios repeatedly navigate specific locations based on routine behavior, leading to inherently structured movement patterns. In this paper we propose a delay-tolerant routing scheme, called Probabilistic Routing with Minimum Proximity (PRMP), which aims to utilize prior movement patterns of peers to predict future probability of forwarding messages to a location proximal to a destinations home address. A source considers next-hop forwarding based on a probabilistic benefit-metric; which takes into account a nodes frequented trajectories and current position, its spatial distance from a destinations stationary home location and the probability of any of its immediate trajectories minimizing the spatial distance to the destinations home. Delivering a message to a nodes' home address in the network is synonyms to delivering mail to an individual's designated mailbox. The protocol avoids flooding completely in efforts to optimize use of network resources. Simulations of PRMP reflect low buffer occupancy at both high and low loads in the network. It also maintains resource optimization in varying node densities compared to two prominent DTN flooding protocols – Epidemic and PRoPHET.

Keywords: DTN, Intermittent Connectivity, Routing Protocol, Location-based Routing.

I. INTRODUCTION

Delay-tolerant Networking (DTN) [1] is gradually emerging as the de-facto standard for providing communication solutions in intermittently connected networks and challenged environments. These environments usually consist of wireless, mobile nodes where there may be frequent, long-duration partitions in the network causing excessive delivery latency and high error rates in transmissions. Presumably, in such scenarios establishment of an end-to-end connection between a traffic source and its destination, prior to message forwarding is unattainable, rendering many tested ad hoc routing protocols [2]-[4] impracticable. DTN networks, therefore, require special attention considering the problem of routing. The DTN architecture model [5] proposes asynchronous message switching in a store-and-forward manner along with custodial transfer of bundles (message aggregates) to allow for communication in intermittent networks. Applications such as nomadic networks and connectivity constrained networks can benefit from such an opportunistic forwarding architecture [6], [7].

Recent studies on the distribution of inter-contact time of participants [8] and mobility characteristics of nodes [10] in challenged networks provide sound evidence that routing in constrained environments may improve performance-wise by considering the underlying behavior patterns of network participants. In this paper, we introduce a novel DTN routing protocol for non-random, location-aware contexts. It has been often quoted "Mobility is two faced"; in our case message delivery depends on the mobility of nodes but successful delivery can also be hampered due to a destinations constant movement, especially in disruptive situations where no end-to-end path exists and the addressing space is flat [11]. To increase reliability of message deliverance, an intended message for the final recipient is forwarded to its' stationary home location, as obtaining the contemporaneous location of a roaming destination in remote situations and without any hierarchical infrastructure is convoluted. The local decision of selecting a forwarder depends on available information from previous node roaming and currently achievable space minimization to the intended destinations home. The protocol focuses improving network performance by achieving a steady state of resource consumption, even during very high event generation in the network.

The remainder of this paper is organized as follows: Section II presents an overview of related DTN routing protocols. Section III states the underlying assumptions of our protocol and describes necessary metrics along with explanation of the routing mechanism. A quantitative evaluation of our protocol is given in Section IV, comparing with two mainstream DTN routing protocols – Epidemic and PRoPHET. Finally, Section V concludes the paper by outlining future work.

II. RELATED WORKS

In recent years numerous routing protocols have been proposed for DTNs, each with solutions depending on, but not limited to, the amount of tolerable delay

978-1-4244-6283-4/09/$26.00 ©2009 IEEE

by the application, link characteristics, contact types, and resource availability. Different mechanisms are applied depending on whether the network is primarily of mobile ad-hoc nature (e.g., mobile devices carried by humans) or is based upon a (fixed or mobile) infrastructure (e.g., space networks, bus networks). Mixed networks exist as well (e.g., mobile users supported by infrastructure nodes). Ad-hoc DTNs usually apply variants of reactive protocols. Flooding protocols such as Epidemic [12] rely on the theory of flooding algorithms by doing pair-wise exchange of bundles among contacting nodes for eventual delivery to the destination. This technique performs well in weak connectivity scenarios and is scalable to large network sizes, but performs poorly considering network resource utilization [13]. Predictive protocols, such as PRoPHET [14], utilize past encounter of nodes to predict future suitability of forwarding - when two nodes meet, they exchange and update encounter summary vectors containing the delivery predictability information stored at the nodes. For large number of nodes in high load scenarios, this imposes problems in case of communication overhead and resource utilization.

DTN routing protocols also differ in replication strategies, i.e., how many copies of a message they create which, in turn, has a direct impact on the load incurred on the network. Some protocols generate just a single copy [15], others a fixed number limited by the sender [16] while others create an "infinite" number of messages [14]. Utilizing patterns of node mobility in ad hoc like scenarios is not new in DTN [17]. However, we believe that our method of using historical position information with an intention to minimize distance to the destination with emancipation from the dependency of per-contact links is a first in DTN. In the following section we describe our position-based probabilistic routing scheme which intends to be scalable in both small and large-scale networks and also improves network performance in resource constrained environments [6], [7].

III. THE PROPOSED PROTOCOL

We propose a new protocol for DTNs called Probabilistic Routing with Minimum Proximity (PRMP).

As our system model we assume nodes move to specific locations repetitively at recurring time intervals; for example – most people take the same path to route to their respective workplace 5 days a week and to the church only once a week, thus roaming some locations more than others. This can be modeled, in the network, as a recurring set of locations (grids) for a determinable frequency in a limited time span for any itinerant node. We can determine a probability distribution from the frequencies of all previous visitations. The source generating a bundle for a destination tries to forward the bundle through successive one hops to a destinations assigned agent (DAA) permanently residing at its home location. Our introduced *minimity* metric determines *mini*mum proxi*mity* obtainable to the home agent (DAA) and a benefit metric measures the probabilistic maximum benefit of selecting a node to forward to that agent. With probabilistic predictions of a future forwarding direction, bundles are less likely to wander aimlessly in the network, consenting for faster delivery. Furthermore, single-copy forwarding ensures evident resource utilization over multi-copy methods.

A. Assumptions

We consider a wireless, ad hoc DTN environment for PRMP with the following assumptions:

1) *Active nodes - Mobile nodes generating message events and actively participating in bundle forwarding:* Active nodes move in a predictable fashion based on repeating behavioral patterns and keep periodical traces of their physical movement in a record-tuple <*longitude, latitude, UTC time*>. These nodes are the primary forwarders and event generators in the network.

2) *Passive nodes - Stationary DAA nodes act as temporary recipients for bundles at a nodes home location:* We assume each node *A* is associated to a home location upon system initialization. A destination associated agent (DAA) is a fixed node stationed at a node *A's* home location, acting as a temporary acceptor of bundles intended for *A*. Thus, *A* may be roaming anywhere in the network but still receive intended bundles form its' DAA upon returning to its home. This is synonymous to the real-world situation where postal packages arrive at resident mailboxes, irrelevant of the actual recipients' immediate presence. This, however, is in contrast to the concept of Post Offices (PO) proposed in [9] where a message from a source to the destination requires going through the sources own PO first, then onto the destination PO. In our scheme, a source can send directly to a destinations PO (in our case the DAA). DAA's do not generate message events; they only act as one-hop forwarders to the associated destination *A*. Binding with the home node persists until an interrupt is sent for home relocation. Mapping of nodes to their respective DAA's are obtainable by presumed location services such as in [18], and extensive discussion is out of the scope of this paper. It is mentionable that the cardinality between a single node *A* and its DAA is one-to-one, but relationship between a DAA and the set of all *n* nodes in the network $N_i \in \{1 \ldots n\}$ may be one-to-many; as more than one node may share the same home location.

3) *Common features for all nodes:* Nodes implement the bundle protocol for asynchronous message for-

warding with EIDs as identifiers. Nodes have finite amount of storage capacity. Each node is equipped with a wireless radio-interface and is aware of its geographical position (i.e. via GPS). We assume lower layers handle peer discovery. Peers exchange data when they are in joint communication range.

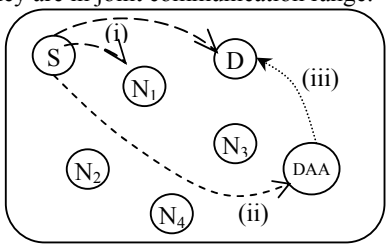

Fig. 3.1: Node role-based communication in PRMP

We foresee three combinations of communication between nodes depending on node roles, shown in Fig 3.1: (i) Active-Active: source to next hop candidate; source to final destination; (ii) Active-Passive: source to DAA; and (iii) Passive-Active: DAA to destination. Case (ii) and (iii) are self-explanatory, as direct forwarding suffices. We emphasize on case (i).

B. Preliminaries

In this section, we define postulates necessary for our proposed protocol.

Home: The home of a node N_i is considered to be a location; □*(n)* which is most frequented by N_i and it resides there for a significant pause time, τ. A single location □*(n)* can be the home of one or multiple network participants.

Distance: Assuming the network topology to be 2-dimensional, we define distance to be an L_m order Minkowski distance between two nodes P and Q, computed as: $\left(\left|p_x - q_x\right|^m + \left|p_y - q_y\right|^m\right)^{1/m}$

where, $P = \left(p_x, p_y\right)$; $Q = \left(q_x, q_y\right)$ and m= 2.

This is equivalent to the Euclidian distance of the nodes: $\sqrt{(p_x - q_x)^2 + (p_y - q_y)^2}$

Grid Transposition: We project the network area as an overlay on an *m*×*m* square grid. Each cell is assigned a unique grid-id, g(X, Y), given by the mapping: g(X, Y) = (Y − 1)m + X. This numbering is equivalent to assigning successive numbers to grids from left to right, top to bottom, beginning with the origin id, (1,1).

C. The PRMP Protocol

Routing in PRMP operates as follows. When a source *S* (with a bundle for destination *D*) encounters an active peer node N_i; it first checks if N_i is *D* itself. If so the is bundle forwarded directly. However, if N_i is not the destination then it receives a PRMP request from *S* along with the destinations DAA location. N_i uses this location to calculate the maximum benefit it can provide and sends this information to *S* in a PRMP request reply. *S* may receive more than one PRMP reply if it is communicating with multiple nodes contemporaneously. *S* also appends it own maximum benefit to the list of replies. Depending on the outcome *S* may decide to forward the bundle to N_i, choose to retain the bundle (if there are no peers providing better benefit values than *S*). We now progressively show how the *minimity* and *maximum benefit* metrics are calculated in PRMP from previous motion paths and current distance to the DAA.

C.1. *Segments and Segmentation*

We define a *segment* to be a trajectory traversed by a node N_i for activity-offset durations and is represented as a successive array of grids:

$S^i(n) = \text{g(x, y)[1….t]}$

where, $\left\{g_t(x,y) : x \in X; y \in Y\right\}$; $\left|t\right| = m^2$;

and $n \in \{1,2,3...k\}$ for k segments of a node N_i.

Segments are delimited by a significant pause time, τ; i.e. there is a pause τ between the beginning of segment S^i2 and end of segment S^i1. Further segmentation of a segment (into smaller segments) may occur when two segments overlap. A concept of path segments and their segmentation is show in Fig 3.2.

C.2. *Probability Distribution of Segment Visitation*

We consider for a node N_i an association of its traversed segments onto recurring frequency of those segments as $\{S^i_{1\ldots n}{:}f_i\}_{[T]}$; where f_i denotes the repetitive visits to a segment S_k during a trace duration T. This association is reassessed after every T time units. From the associative frequencies f_i, each node also calculates the probability of visitations to S_k as:

$$\Phi^i(k) = \left[\frac{f_i}{\Sigma f_i}\right] \quad \text{where,} \quad \Phi^i(k) = \left[0,1\right]. \qquad (1)$$

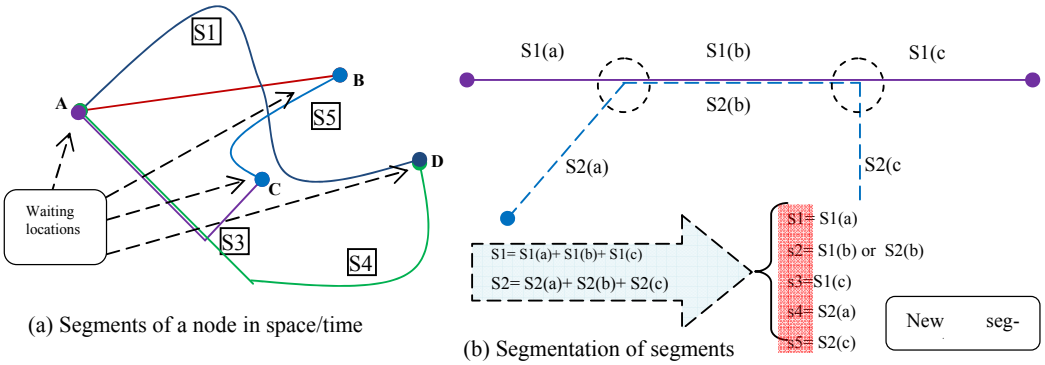

(a) Segments of a node in space/time

(b) Segmentation of segments

Fig. 3.2: Segments and Segmentation

The likeliness of node N_i's future repetition of segment S_k can be predicted from obtained $\Phi^i(k)$ values. A maximum value of 1 indicates that S_k is the only segment recurrently traversed by N_i within the previous trace duration T.

We assume collective locations in a single grid-bin are represented by the *point-of-interest* (POI), which is calculated at the center of the grid-bin. This creates a deviation from the actual visitation. A smaller grid-bin resolution assures greater accuracy of reflecting the actual visited location. Intuitively, grid-bin resolution depends on the radio-range capabilities of nodes and the network area.

We consider the finite set $M = \{S_1, S_2 \ldots S_m\}$, called a matching set, representing m segments each containing the location N_i is currently traversing. Fig. 3.3 shows a node's matching sets. N_i can be traveling any one of the m segments in $\{M\}$ with a uniform probability $P(M) = \frac{1}{m}$.

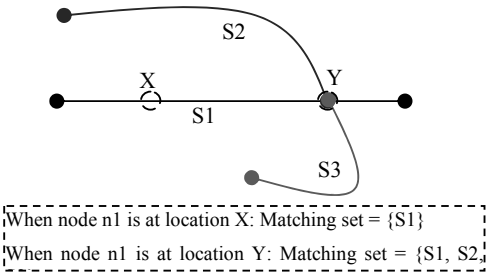

Fig 3.3: Determining the matching

For $\forall S_m \in \{M\}$:

i) $S_m = g_{1\ldots k}(x,y) = [POI_1, POI_2 \ldots POI_k]$: array of points-of-interest of grid-bin's form a segment

ii) $POI_k(x,y)$: location of k-th POI in a segment S_j; $j = \{1,2,\ldots m\}$.

The shortest *remaining* Euclidian distance achievable to $DAA(x,y)$ from any segment S_j is the *minimity*:

$$\upsilon(S_j) = (\min_j \left| \{d_1, d_2, d_3) \ldots d_k\} \right|) \forall j = \{1,2,\ldots..m\} \quad (2)$$

Here, $\upsilon(S_j) = [0,\infty]$, $d_k = POI_i(x,y) - DAA(x,y)$; $i = \{1,2,\ldots k\}$ $\forall$k POI's forming the segment S_j.

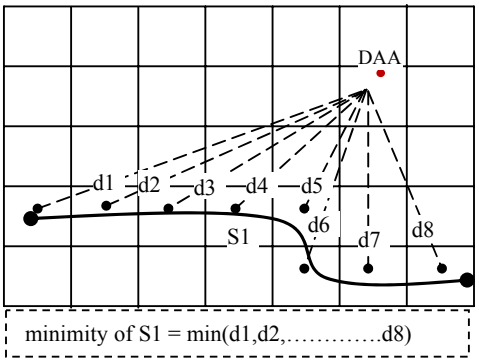

Fig 3.4: Finding the minimum proximity

Let, *probability* of j[th] segment = $P(S_j)$ be $\Phi(S_j) = [0;1]$, from (1); *minimity* of j[th] segment= $d_{min}(S_j)$ be $\upsilon(S_j) = [0,\infty]$, from (2) and D_{max} = maximum possible distance to a destination (i.e. = network area diagonal). Then, we define the *benefit metric* of segment S_j, as b_{Sj}:

$$bs_j = P(S_j)\left[1 - \frac{d_{\min}(S_j)}{D_{\max}}\right] \ldots \forall j = \{1,2\ldots.m\} \quad (3)$$

Here, m = no. of segments in matching set {M}.

We define *maximum benefit* of node N_i (usage benefit as potential next-hop), B_{Ni} as:

$$B_{N_i} = \max_i(bs_j) = \max_i\left(P(S_j)\left[1 - \frac{d_{\min}(S_j)}{D_{\max}}\right]\right) \quad (4)$$

Here, $j = \{1,2,\ldots m\}$ $\forall S_m \in \{M\}$ and $i = \{1,2,\ldots n\}$ $\forall N_i \in \{C\}$ where, {C} = all nodes currently in communication range of source *S*. The maximum benefit achievable by B_N, would be when $P(S_j) = 1$ and $d_j = 0$. It represents the ideal case of a node hav-

ing a segment within direct proximity of the DAA.

C.3 *Forwarding to Next-hop*

Source S receives PRMP replies from all n peers $N_i \in \{C\}$ and stores them in a vector $\left\langle P_{B(|\nu|+1)} \right\rangle$, where $|\nu|$ = size of set {C}. The vector shows the maximum benefit affordable by individual communicating peers. Upon receiving all peer replies, S appends its own benefit, using (4), to the vector and chooses the next optimal hop for forwarding as: $MAX\left\langle P_{B(|\nu|+1)} \right\rangle$. Based on the outcome, S may forward the bundle or keep it (S itself provides maximum benefit).

IV. EXPERIMENTAL EVALUATION

In this section, we provide an analytical comparison of our PRMP protocol with two existing DTN protocols, Epidemic and PRoPHET, discussed in section II. PRMP exploits the movement structure of network peers. If peers move randomly, which is the case in Epidemic, then no peer is any better at delivering a message than any other, hence the need for flooding. Again, routing assuming non-random behavior patterns of real users, as in PRoPHET, but delivering messages based on peer meeting probability alone (not considering peer location), is not significantly better either [19]. Through simulation results we show the improvements of using a non-random, location-aware approach over non-location-aware approaches; such as that of Epidemic and PRoPHET.

A. Simulation Environment

For the quantitative evaluation of our protocol, we use the Opportunistic Network Environment (ONE) Simulator [20] for generating mobility traces, running DTN messaging and implementing pre-defined movement models to evaluate the protocols.

We consider a simulation area of 4500 x 3500 meters with nodes having a wireless transmission range of 100 meters. A grid-cell is the squared value of twice the transmission range of a node; i.e. 200 m x 200 m. Data transmission speed is 2Mbps with total simulation time of 10k seconds for each run. Three node models have been used: (1) Pedestrian: walking speed .5 to 1.5 meter/sec; (2) Car: 10 to 50 km/hour; and (3) Tram: 7 to 10 meter/sec. 500kB - 1MB size messages were generated for the whole duration of simulation, except first 1000 sec as warm up time. Each node is equipped with a 10MB buffer.

B. Results and Analysis

We present simulation results of Epidemic, PRoPHET, and our proposed PRMP protocol in Fig 4.1. In Fig. 4.1 (a) we see that Epidemic and PRoPHET buffers' saturate before 30% of the total runtime.

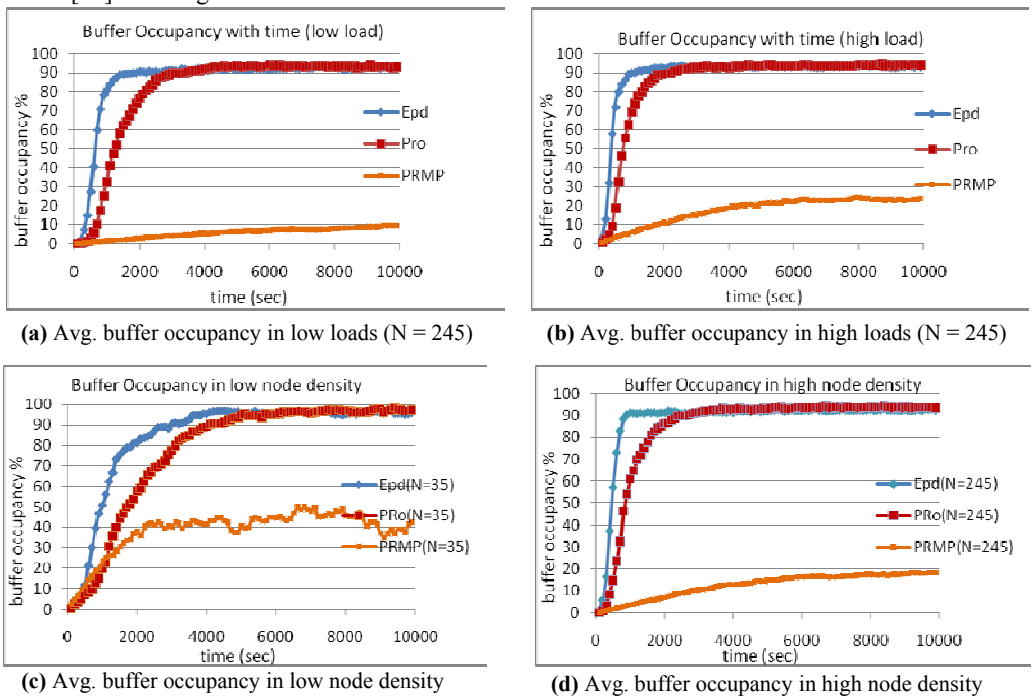

(a) Avg. buffer occupancy in low loads (N = 245)

(b) Avg. buffer occupancy in high loads (N = 245)

(c) Avg. buffer occupancy in low node density

(d) Avg. buffer occupancy in high node density

Fig. 4.1: Simulation results of protocols in ONE

In (b) the situation worsens when higher events occur in the network, buffers for both deplete much rapidly

than in the case of low loads. On the other hand, in both (a) and (b) PRMP maintains a steady depletion rate and has enough buffers for forwarding messages throughout the whole simulation run. We considered figure (c) and (d) for high loads with messages generated every 5 to 10 seconds. We see that the number of nodes negatively impact the performance of Epidemic and PRoPHET, due to their resource hungry nature. However, PRMP scales surprisingly well to high load, high density scenarios, as observed in (d). This is because in PRMP the same numbers of messagess get distributed to more nodes in high node den sities, while in PRoPHET and Epidemic; with the increase in node density the numbers of messages also increase in the network, leading to rapid resource depletion.

V. CONCLUSION

In future, we will perform a comprehensive evaluation of PRMP with other performance metrics; i.e. delivery ratio, throughput and latency. It can be fairly expected that the delivery ratio of PRMP will be higher than that of Epidemic and PRoPHET. This is because buffers are always available for new messages, and ideally no message drops. We also plan to extend the development of home agents to contain naming, addressing and access infrastructure issues.

REFERENCES

[1] V. Cerf, S. Burleigh, A. Hooke, L. Torgerson, R. Durst, K. Scott, K. Fall, H. Weiss, "Delay- Tolerant Network Architecture", DTN Research Group, Internet-Draft, March 2003.

[2] Charles E. Perkins , Pravin Bhagwat, "Highly Dynamic Destination-Sequenced Distance-Vector Routing (DSDV) for Mobile Computers", In Proc. of conference on Communications Architectures, Protocols and Applications, p.234-244, August 31-September 02, 1994.

[3] Charles E. Perkins , Elizabeth M. Royer, "Ad-hoc On-Demand Distance Vector Routing"; In Proc. of the 2nd IEEE Workshop on Mobile Computer Systems and Applications, p.90, Feb. 25-26, 1999.

[4] J. Broch, D.B. Johnson, D.A. Maltz; "The Dynamic Source Routing Protocol for Mobile Ad hoc Networks"; IETF MANET Working Group, Internet-Draft, October 1999.

[5] Kevin Fall, "A Delay-Tolerant Network Architecture for Challenged Internets"; Proc. ACM SIGCOMM 2003.

[6] A. Doria, M. Uden, D. Pandey, "Providing connectivity to the Saami nomadic community"; In Proc. of 2nd Int. Conf. on Open Collaborative Design for Sustainable Innovation, Dec 2002.

[7] A. Pentland, R. Fletcher, A. Hasson, "DakNet: Rethinking Connectivity in Developing Nations"; IEEE Computer, vol. 37, no. 1, pp. 78-83, January 2004.

[8] A. Chaintreau, P. Hui, J. Crowcroft, Christophe Diot, R, Gass, J. Scott, "Impact of Human Mobility on the Design of Opportunistic Forwarding Algorithms"; In Proc. of IEEE INFOCOM 2006.

[9] S. Paul, Roy Yates, Dipankar Raychaudhuri, Jim Kurose, "The Cache-and-Forward Network Architecture for Efficient Mobile Content Delivery Services in the Future Internet"; First ITU-T Kaleidoscope Academic Conference, pp. 367-374, May 2008.

[10] M. Kim, D. Kotz, S. Kim, "Extracting a Mobility Model from Real User Traces";Proc. IEEE INFOCOM 2006.

[11] K. Scott, S. Burleigh, "Bundle Protocol Specification"; IETF RFC 5050, Experimental, Nov. 2007.

[12] A. Vahdat, D. Becker, "Epidemic routing for partially connected ad hoc networks"; Technical Report CS-200006, Duke University, April 2000.

[13] A. Islam, M. Waldvogel, "Reality-Check for DTN Routing Algorithms"; In Proc. of 28th Int. Conference on Distributed Computing Systems Workshops, pp. 204-209, 17-20 June, 2008.

[14] A. Lindgren, A. Doria, O. Schelen, "Probabilistic Routing in Intermittently connected Networks"; In Proc. of SAPIR04.

[15] T. Spyropoulos, K. Psounis, C. S. Raghavendra, "Single-copy routing in intermittently connected mobile networks"; In Proc. Sensor Ad Hoc Communications and Networks, pp. 235–244, Oct 2004.

[16] T. Spyropoulos, K. Psounis, C. S. Raghavendra, "Spray and Wait: An Efficient Routing Scheme for Intermittently Connected Mobile Networks"; In Proc. of ACM SIGCOMM, WDTN 2005.

[17] Jérémie Leguay, Timur Friedman, Vania Conan, "DTN routing in a mobility pattern space"; In Proc. of ACM SIGCOMM Workshop on Delay-Tolerant Networking, WDTN 2005.

[18] J. Li, J. Jannotti, D. De Couto, D. Karger, R. and Morris, "A scalable location service for geographic ad hoc routing"; Proc. of 6th ACM Int. Conference on Mobile Computing and Networking,, pp.120-130, August 2000.

[19] J. Davis, A. Fagg, B. Levine, "Wearable computers and packet transport mechanisms in highly partitioned ad hoc networks"; In Proc. of Intl. Symposium on Wearable Computers, October 2001.

[20] Project page - ONE simulator. http://www.netlab.tkk.fi/tutkimus/dtn/theone

Proceedings of 2009 12th International Conference on Computer and Information Technology (ICCIT 2009)
21-23 December, 2009, Dhaka, Bangladesh

Design and Analysis of Online Testability of Reversible Sequential Circuits

Moshaddek Hasan, A.K.M. Tauhidul Islam, Ahsan Raja Chowdhury
Dept. of Computer Science and Engineering, Faculty of Engineering and Technology,
University of Dhaka, Dhaka, Bangladesh
moshaddekhasan@yahoo.com, k_tauhid03@yahoo.com, farhan717@cse.univdhaka.edu

Abstract

Reversible logic plays an important role in the synthesis of circuits having application in quantum computing, low power CMOS design and nanotechnology-based system. In this paper, we have proposed the online testability of reversible sequential circuits, which is first ever proposed in literature. On the way to propose the online testability of reversible sequential circuits, we have proposed an improved Rail-check circuit that significantly improves the performance of the overall circuit in terms of gate cost and garbage cost parameters. We have also used our improved and efficient rail-check circuit to realize the testability of different benchmark circuits.

Keywords: Benchmark circuits, Online testability, Rail-check circuit, Testable block.

I. INTRODUCTION

Testing of reversible circuits is a major challenge in today's world because the levels of logic are significantly higher than the standard logic [1]. Online testability is a unique feature of a circuit, which ensures the testing of the circuit at the time the computation is performed. Our proposed work concentrates on the design of online testable reversible circuits rather than fault tolerant circuits [2, 3]. The online testability of reversible combinational circuits has already been proposed in [4]. This paper proposes the online testability of sequential reversible circuits like R-S, J-K, T, D, Master Slave flip-flops. Rest of our paper is organized as follows: Section II discusses on background study and proposed idea is thoroughly explained in Section III along with the examples of each method. Section IV highlights the Experimental results of our proposed method performed over several well-known benchmark circuits. Section V concludes the paper.

II. BACKGROUND STUDY

In this section, we define the important terms and the existing method briefly.

Definition1: Online Testability is the ability of a circuit to test a reversible block at the time the circuit is performing the operation. It is the unique feature of reversible circuit first proposed in [4]. Online testable Reversible gates R1 and R2 [5] are two complementary gates which are paired to achieve the online testability [4] feature. The first gate R1 is used for implementing arbitrary functions while the R2 gate is employed to incorporate the online testability feature.

Example 1: Authors of [4] have proposed the structure of the online testable block, which is shown in Fig. 1.

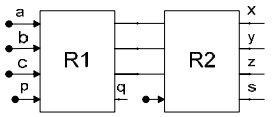

Fig. 1. Online testable block of [4]

From the above figure we can see that first three outputs of R1 gate is just propagated through R2 gate (i.e., as output of the R2 gate). Final output of R2 is the desired output of the total online testable block's output.

Definition 2: Railcheck Circuit is a novel circuit, which is used for the purpose of checking the output of the online testable block. In fact, the fault free railcheck circuit will produce the complementary outputs if the inputs are complement to each other.

Example 2: First Railcheck circuit, proposed in [4] using R gates [5], is shown in Fig. 2. From the figure, we can see that whenever the circuit works correctly, it will produce the complementary output in e1 and e2.

Now we discuss some of the existing techniques of Online Testing. Authors of [4] primarily deal with the combinational circuits. Here, the online testability feature is proposed as well as the universality of the R1 and R2 gate has been showed. Authors of [5] have shown that a testable block can be formed by using R1 and R2 gate. These gates are efficient in "universality" feature i.e. they can perform all functions by controlling inputs and their total design [4] achieve this feature. But the overhead regarding gate, garbage cost are very high for sequential circuits.

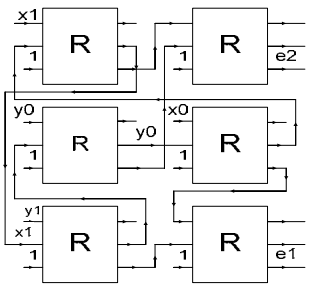

Fig. 2. Railcheck Circuit

Authors of [6] have shown the online testable reversible adders with the new OTG gate. The approach is good

978-1-4244-6283-4/09/$26.00 ©2009 IEEE

for particular combinational circuit like online testable reversible adder. But it is not efficient for higher logic level circuits like sequential circuits. Moreover, their proposed circuit also loses some of the universality features. All these existing designs discussed so far are within the combinational paradigm. We tend to propose online testability of reversible circuits in the sequential domain.

III. PROPOSED IDEA

In this paper, we have proposed a new Railcheck using Fredkin gate and Feynman gate [7, 8], which is very efficient than the existing one [4], followed by proposing Online Testable Reversible Sequential Circuits. We have used the transformation based approach [9] to implement our proposed circuits.

A. Improved Railcheck Circuit

The improved railcheck circuit, consists of Feynman gate and Fredkin gate [7, 8], is shown in Fig. 3 where the Correctness of our proposed railcheck is shown in Table I. The improved railcheck significantly reduces the gate cost and garbage cost than the existing one. Rest of the paper, the proposed rail checker will be termed as IRC (Improved Rail Checker).

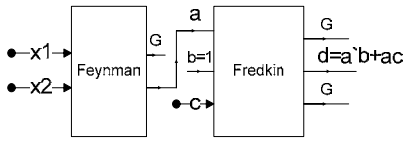

Fig. 3. Improved railcheck circuit with Feynman Gate and Fredkin Gate (* G stands for garbage output)

Table I Correctness of the improved railcheck

a	b=1	c	a`b+ac	a`+c (b=1)
0	1	0	1	1
0	1	1	1	1
1	1	0	0	0
1	1	1	1	1

When a = 0, i.e., x_0 and x_1 are identical which indicates wrong for the incoming input of the Feynman gate or when c = 1, it indicates that one or more faults occur in the input of Fredkin gate. From the above truth table we can observe that output (d) of IRC will be 1 only if a=0 or c=1 or both. It means when d=1, it indicates a fault anywhere in the circuit. The truth table also shows that once IRC generates a wrong output it will propagate the error through out the circuit.

We have taken a sample combinational circuit (ab + cd) for showing the improvement that we have achieved in modifying the existing railcheck circuit. Fig. 4 shows the online testable circuit for the considered function. It should be noted that, TB is considered as Testable Block and IRC stands for improved railcheck. Considered expression is tested with [4] and comparative result is shown in Table II.

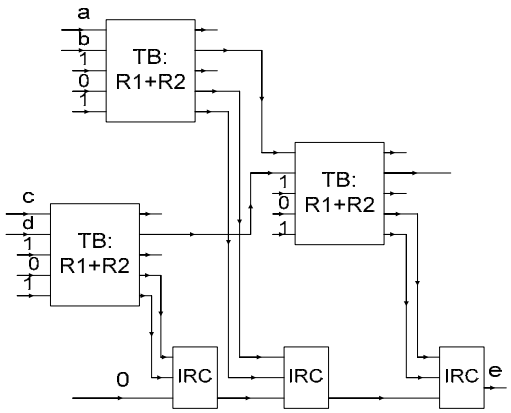

Fig. 4. Online testability of combinational function (ab+cd) with improved railcheck

Table II Comparative study for function (ab+cd)

Cost	Existing [4]	Proposed	Improvement Ratio%
Gate	18	12	150
Garbage	22	15	147

Now we propose the construction procedure of Improved Railcheck Circuit (IRC) in algorithm form (Algorithm 1)

Algorithm 1: IRC (X1, X2, C)

Input: Complementary outputs of testable block (TB), Output of earlier IRC or C=0 for initial case.
Output: A binary digit D
Begin
Step 1: A= $x1 \oplus x2$
Step 2: A=A`
Step 3: D=A+C (output of earlier IRC, D or 0 for initial case)
Step 4: Return D.
End.

Now, we evaluate the proposed algorithm in terms of Theorems.

Theorem 1: *n* IRC circuits can be realized by at least 2*n* gates.

Proof: For performing the EX-OR operation in order to check that the incoming input is either complementary or not from the testable blocks, we need to have the Feynman gate. In other case, Fredkin gate is needed for testing the pervious IRC at its input 'C'. So, at least two gates are necessary for realizing the IRC circuits and hence, *n* IRC can be realized by 2*n* gates.

Theorem 2: *n* IRC circuits can be realized by at least 3*n* garbage outputs.

Proof: For all input combinations in the input of Feynman gate we get the unique output after EX-OR operation. We know that the Feynman gate is the least cost garbage-producing gate for EX-OR operation, so we need single garbage for the first case. We need Fredkin gate for the testing of the previous IRC's output and we know that, Fredkin gate will produce at least two garbage outputs. So, the number of garbage output to real-

ize an IRC circuit is 1+2=3.So, *n* IRC circuit can be realized by 3*n* garbage outputs.

Lemma 1: A testable block can achieve online testability with pairing itself with an IRC circuit.

Proof: From Table I and Fig. 3, we can see that when two inputs of the Feynman gates are identical it means error has occurred somewhere in the previous testable blocks. So, it can be inferred that a Feynman gate is a must for checking the testability of the testable block at the same time Fredkin gate is used for checking the testability of previous IRC. So, to ensure the complete online testability of a circuit we need a testable block-IRC pair.

Theorem 3: *n* testable block-IRC pairs can be realized by exactly 4*n* gates.

Proof: From [4], we know that, a testable block can be realized by 2 gates. So, n testable blocks can be realized by 2*n* gates. From Theorem 1, we know that *n* IRC circuits can be realized by 2*n* gates. So, from [4] and from Theorem 1, a testable block-IRC pair can be realized by 2*n*+2*n*=4n gates.

Theorem 4: *n* testable block-IRC pairs can be realized by exactly 5*n* garbage outputs.

Proof: From [4] we know that a testable block can be realized by 2 garbage output. So, *n* testable blocks can be realized by 2*n* garbage outputs. From Theorem 2, we know that, *n* IRC circuits can be realized by 3*n* garbage outputs. So, from [4] and Theorem 2, *n* testable block-IRC pair circuits can be realized by 2*n*+3*n*=5*n* garbage outputs.

B. Proposed Online Testable Sequential Circuits

In this section, we have shown the novel online testable sequential circuits, first ever proposed in literature. We have shown the online testability of the reversible sequential circuits like R-S FF, J-K FF, T FF, D FF, MS FF. On the way to propose the online testable sequential circuits, we have used our proposed railcheck. Though the online testable sequential circuits are yet to be proposed, we have considered the existing technique of online testable combinational circuit [5] to realize the sequential circuits in order to show the comparative study with the newly proposed one. We have used the transformation-based approach [9] to design the sequential circuits.

Here we propose the procedure of online testable unit operation in algorithm form (Algorithm 2)

Algorithm 2: Online_Testable_OP

Input: Xn, Yn, OPn (where OP=NAND, OR, EXOR, NOT, COPY), C.(n=integers)
Output: Xn OPn Yn, C
Begin:
Step 1: Compute Xn OPn Yn using testable block
Step 2: Compute two complementary outputs q, s (where q, s used for ensuring online test ability).
Step 3: C= IRC (q, s, C)
Return Xn OPn Yn, C.
End.

Here we propose the procedure of online testable pair (unit of sequential operation) in algorithm form (Algorithm 3) and Algorithm 4 realizes the final circuit.

Algorithm 3: Online_Testable_Pair

Input: X1, X2, Y1, Y2, OP1, OP2
Output: Result1, Result2, C.
Begin:
Step1: Result1=Online_Testable _OP(1)
Step2: Result2 = Online _Testable_OP(2)
Return Result1, Result2;
End.

Algorithm 4:**Online_Testable_Reversible_Sequential _circuit**

Input: Clock, Name, In1, In2
Output: Reversible sequential circuit (where sequential circuit=R-S/J-k/D/T/ M-S FF)
Begin:
Step 1: If i=3 or 4 then n = i;
Else n=4, m=3;
Step 2: if init_OP=NOT then
Call Online_NOT
flag = 1;
Else if init_OP=Clock_COPY then
Call Online_Clock_COPY
Step 3: For (j=1 to n)
Result = Online_Testable_Pair
if n = 3 then
if flag =1 then
print(D flipflop)
else
print(R-S flipflop)
if n =4 then
If flag =1 then
print (T flipflop)
else
print (J-K flipflop)
Step 4: If (!m) return Result
Step 5: Call Online_Clock_COPY
Step 6: For (j=1 to m)
Result= Online_Testable_ Pair
print (M-S flipflop)
Return Result
End.

As the realizations of online Testability of sequential circuits are first proposed in this paper, we have considered the existing Railcheck circuit to realize the online testability sequential circuit for comparison purposes. Comparison is shown at the end of this section.

B.1 Online Testable R-S FF

R-S (stands for Reset-Set) FF is one of the preliminary forms of sequential circuits. By using the transformation-based approach, we have implemented the online

testable R-S FF, which requires six testable blocks and six Rail Check circuits. The online testable reversible R-S FF is shown in Fig. 5, where IRC stands for Improved Rail-check circuit and OP: NAND/COPY stands for NAND/COPY operation in the testable block. The proposed circuit is mainly composed of two types of blocks: One is the online testable block which composed of the R1 and R2 gates to ensure the online testability as well as NAND functionality, the other is the Railcheck Circuit (RC). The first four online testable blocks (R1+R2) of the circuit (from left) functions the NAND whereas the last two blocks function the copy operation. The railcheck circuit ensures the online testability of the above testable blocks. In this way, the total circuit (R-S flip-flop) becomes an online testable reversible sequential circuit.

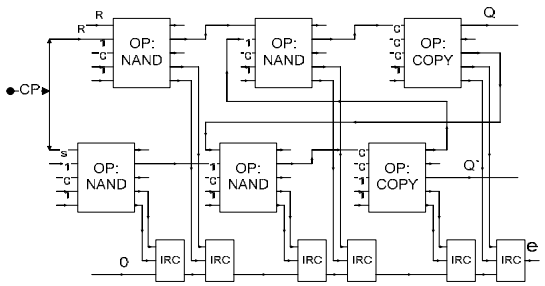

Fig. 5. Online Testability of R-S FF

Lemma 2: *n* RS flip-flop circuits can be realized by 24*n* gates.

Proof: We can see from Fig. 5 that an R-S flip-flop requires six testable block-IRC pair circuits to complete its operation. So, from Theorem, 3 we can say that an R-S flip-flop can be realized 6*4=24 gates.So, *n* RS flip-flops can be realized by 24*n* gates.

Lemma 3: *n* RS flip-flop circuits can be realized by 28*n* garbage outputs.

Proof: We can see from Fig.5 that six testable block-IRC pair circuits are necessary to realize an R-S flip-flop. From theorem 4, we came to know that a testable block-IRC pair can be realized by five garbage outputs. So, six testable block-IRC pair should be realized by 6*5=30 garbage output. Two garbage outputs have been reduced due to the copy operation. So, the total number of garbage output is 30-2=28. So, *n* RS flip-flop circuits can be realized by 28*n* garbage outputs.

B.2 Online Testability of J-K FF

The J-K FF performs the same functionality of R-S FF except the toggle feature. So, its online testability also changed according to its change in the operation. The online testable J-K FF is shown in Fig. 6. In Fig. 6 the operation of the circuit starts from the clock pulse, and then the first two blocks perform the NAND operation. Next two blocks perform the (*jcp*)`+*q* operation and the (*kcp*)`+*q* operation. Operation OR is performed in the 3rd next 2 blocks from the left. From these two, the lower block has got an input from the upper copy block, which reduces one of the garbage outputs of that block.

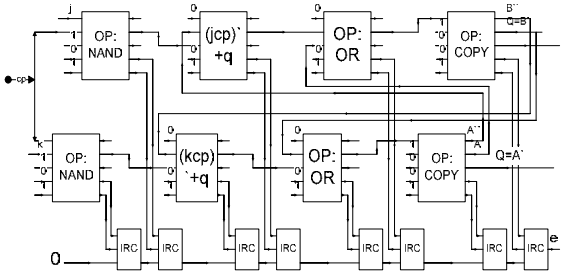

Fig. 6. Online Testability of J-K FF

Lemma 4: *n* J-K flip-flop circuit can be realized by 32*n* gates.

Proof: We can see from Fig.6 that J-K flip-flop requires eight testable block-IRC pairs to complete its operation. So, from theorem 3 we can say that a J-K flip-flop can be realized 8*4=32gates. So, *n* J-K flip-flops can be realized by 32*n* gates.

Lemma 5: *n* J-K flip-flop circuits can be realized by 36*n* garbage outputs.

Proof: We can see from Fig.6 that eight testable block-IRC pair circuits are necessary to realize a J-K flip-flop. According to Theorem 4, we know that a testable block-IRC pair can be realized by 5 garbage outputs. So, eight testable block-IRC pair should be realized by 8*5=40 garbage outputs. 4 garbage outputs have been reduced due to the copy operation. So, the total number of garbage output is 40-4=36 and hence, *n* J-K flip-flop circuits can be realized by 36*n* garbage outputs.

B.3 Online Testable D FF

The online testable reversible D FF consists of seven testable blocks and seven rail-check circuits, which are shown, in Fig. 7. First of these seven blocks performs the NOR function, then the next four blocks perform the NAND function and the final two blocks are the copy function block. This is the novel online testable D flip-flop, which is first ever proposed in literature.

Lemma 6: *n* D flip-flop circuits can be realized by 28*n* gates.

Proof: We can see from Fig.7 that D flip-flop requires seven testable block-IRC pairs circuit to complete its operation. So, from theorem 3 we can say that a D flip-flop can be realized 7*4=28 gates. So, *n* D flip-flops can be realized by 28*n* gates.

Lemma 7: *n* D flip-flop circuits can be realized by 33*n* garbage outputs.

Proof: We can see from Fig. 7 that seven testable block-IRC pair circuits are necessary to realize a D flip-flop. From Theorem 4, we know that a testable block-IRC pair can be realized by five garbage outputs and so, seven testable block-IRC pair should be realized by 7*5=35 garbage output. Two garbage outputs have been reduced due to the copy operation. So, the total number of garbage output is 35-2=33. So, *n* J-K flip-flop circuits can be realized by 33*n* garbage outputs.

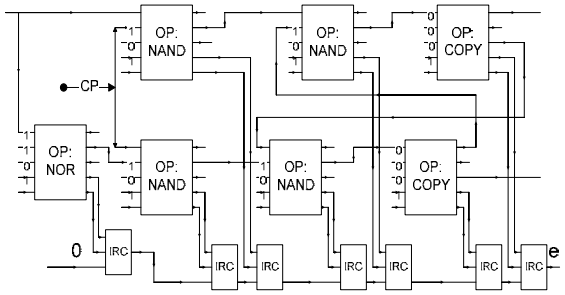

Fig. 7. Online testability of reversible D FF

B.4 Online Testability of T FF

The online testable T FF consists of nine testable blocks and nine rail-check circuits. First block performs the NOT operation. Next two performs the NAND operation, the last but two blocks performs the OR again and finally the copy operations are performed in the remaining blocks. Online testable T-FF is shown in Fig. 8.

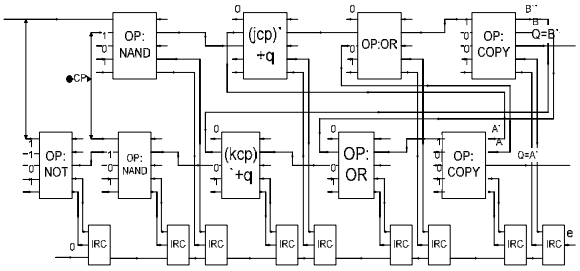

Fig. 8. Online testability of reversible T FF

Lemma 8: *n* T flip-flop circuits can be realized by 36*n* gates.

Proof: We can see from Fig. 8 that T flip-flop requires nine testable block-IRC pair circuits to complete its operation. So, from theorem 3 we can say that a T flip-flop can be realized 9*4=36 gates. So, *n* T flip-flops can be realized by 36*n* gates.

Lemma 9: *n* T flip-flop circuits can be realized by 41*n* garbage outputs.

Proof: We can see from Fig. 8 that nine testable block-IRC pair circuits are necessary to realize a T flip-flop. From Theorem 4, we came to know that a testable block-IRC pair can be realized by five garbage outputs. So, nine testable block-IRC pair should be realized by 9*5=45 garbage output. Four garbage outputs have been reduced due to the copy operation. So, the total number of garbage output is 45-4=41. So, *n* J-K flip-flop circuits can be realized by 41*n* garbage outputs.

B.5 Online Testable Master Slave FF

In this section, we have designed a little bit complex circuit; Master Slave FF. Due to the larger circuit, realization of the testable master slave FF is a bit complex and requires sixteen testable blocks along with sixteen railcheck circuit. So, total sixteen testable block-IRC pairs are needed to realize the Online testable Master-Slave FF. The figure is shown in Fig. 9.

Lemma 10: *n* M-S flip-flop circuits can be realized by 64*n* gates.

Proof: We can see from Fig. 7 that M-S flip-flop requires sixteen testable block-IRC pairs circuit to complete its operation. So, from Theorem 3 we can say that an M-S flip-flop can be realized 16*4=64 gates and hence, *n* M-S flip-flops can be realized by 64*n* gates.

Lemma 11: *n* M-S flip-flop circuit can be realized by 73*n* garbage outputs.

Proof: We can see from Fig. 9 that sixteen testable block-IRC pairs are necessary to realize an M-S flip-flop. From Theorem 4, we know that a testable block-IRC pair can be realized by five garbage outputs and hence sixteen testable block-IRC pair should be realized by 16*5=80 garbage outputs. Seven garbage outputs have been reduced due to the copy operation. So, the total number of garbage output is 80-7=73. So, *n* M-S flip-flop circuits can be realized by 73*n* garbage outputs.

After proposed all the above Online Testable Reversible Sequential Circuit, we are going to show the comparison with existing technique. As the proposed technique is a newly proposed one, we have considered the rail-check circuit of [4] to realize the Reversible online sequential circuits. Experimental result is shown in Table III. Table III clearly highlights the supremacy of the proposed design method in terms of improvement ratio.

IV. Experimental Results

This paper not only highlights the realization of sequential circuits but also experiments some of the existing Benchmark circuits [10]. We have used few benchmark functions in order to compare our circuits with the existing circuits. Hwb4, Mod5adder, 4mod5, 5mod5, Hwb5, 4_49, Hwb5, Xor5, Rd32, 2or5, Rd53, ham3, 3_17 have been used as inputs and the experimental results of our work have been listed in Table IV. It is found from the experimental result that, in both aspects (Number of gates and Number of Garbage Outputs) Performance of the proposed circuit is satisfactorily better than that of the existing ones [4].

V. Conclusion

In this paper, we have presented the online testability of reversible sequential circuits, which is first ever proposed in literature. We have also proposed a modified railcheck circuit that is also very efficient for the realization of Online Testability of sequential circuits. While presenting the online testability of our proposed circuits, we have developed algorithms to define their working principle and we used appropriate theorems and lemmas to prove the correctness of our algorithm. We have used the transformation-based approach to realize the proposed circuits. Comparative studies reflect the betterment of the proposed method and experimental results for Benchmark circuits proves the supremacy of the proposed method greatly.

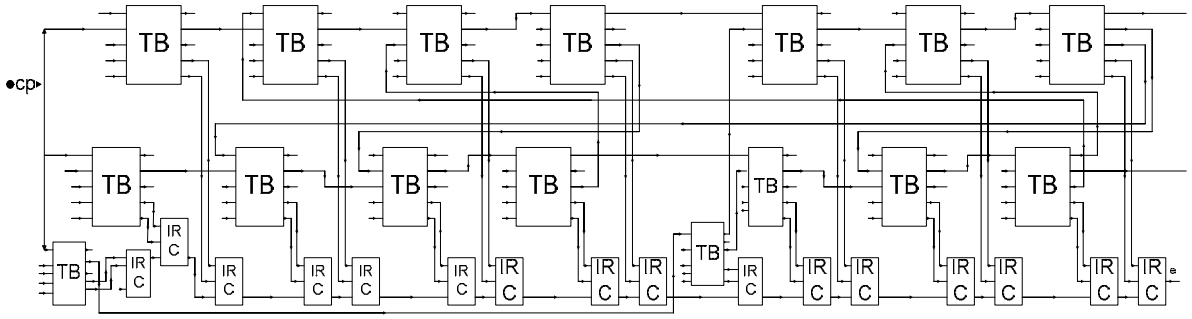

Fig. 9. Online testability of reversible M-S FF

Table III Comparison of the proposed design with the existing railcheck [4] with sequential blocks

Flip flops with online testability	Gate cost			Garbage cost		
	Existing	Proposed	Improvement %	Existing	Proposed	Improvement %
R-S FF	42	24	175	50	28	179
J-K FF	58	32	182	68	36	189
D FF	50	28	179	60	33	182
T FF	66	36	183	78	41	190
Master Slave FF	122	64	182	145	73	189

Table IV Comparison of the proposed design with the existing railcheck [4] with sequential blocks

Benchmark with online testability	Gate cost			Garbage cost		
	Existing	Proposed	Improvement %	Existing	Proposed	Improvement %
Hwb4	178	92	194	208	101	206
Mod5adder	490	248	198	587	285	206
Xor5	26	16	163	32	20	160
Ham7	386	196	197	451	214	211
4mod5	66	36	184	79	42	189
Rd32	82	44	187	98	51	193
5mod5	306	156	197	368	181	204
4_49	242	124	196	286	139	206
Hwb5	578	292	198	686	329	209
2or5	290	148	196	349	172	203
Rd53	306	156	197	367	180	204
Ham3	66	36	184	76	39	195
3_17	106	56	190	125	63	199

References

[1] D. P. Vasudevan et al., "Online Testable Reversible Circuit Design using NAND blocks", Proc of Symposium on Defect and Fault Tolerance, , Oct 2004, pp. 324-331.

[2] K. N. Patel, J. P. Hayes and I. L. Markov, "Fault Testing for Reversible Circuits", IEEE transaction on CAD, 23(8), Aug 2004, pp. 1220-1230.

[3] P.O. Boykin and V.P.R. Chowdhury, "Reversible Fault Tolerant Logic", Proc of International Conference on Dependable systems and Networks. DSN 2005, June 2005, pp. 444-53.

[4] D. P. Vasudevan et al. "Reversible Logic Design with Online Reliability", IEEE Transaction on Instrumentation and Measurement, Vol 55, no. 2, April 2006, pp. 406-414.

[5] D. P. Vasudevan et al., "A Novel Approach for Online Testable Reversible Logic Circuit Design", Proc of the 13th Asian Test Symposium, 2004, pp. 325-330.

[6] H. Thapliyal and A. P Vinod, "Designing Efficient Online Testable Reversible Adders with New Reversible Gate", In Proc of ISCAS, May 2007, pp. 1085-1088.

[7] E. Fredkin and T.Toffoli , "Conservative logic", International Journal of Theoretical Physics, Vol. 21, 1982, no. 3-4, pp. 219-253.

[8] T. Toffoli, "Reversible Computing", Tech memo MIT/LCS/TM-151, MIT lab for computer science (1980).

[9] D. Maslov, D. M. Miller, G. W. Dueck, "A Transformation Based Algorithm for Reversible Logic Synthesis", In Proc of Design Automation Conference, 2003.

[10] http//www.iqc.cs/~dmaslov/research.html.

Proceedings of 2009 12th International Conference on Computer and Information Technology (ICCIT 2009)
21-23 December, 2009, Dhaka, Bangladesh

Computational Intelligence Approach to Load Forecasting - A Practical Application for the Desert of Saudi Arabia

Suman Ahmmed, Dewan Md. Fayzur Rahman, Md. Khairul Hasan†, Ahmed Yousuf Saber‡, and Mohammad Zahidur Rahman*

Department of Computer Science and Engineering, United International University, Dhaka, Bangladesh
†Department of Computer Science and Engineering, Ahsanullah University of Science and Technology, Bangladesh
‡Real-Time Power and Intelligent Systems Laboratory, Missouri University of Science and Technology, USA
*Department of Computer Science and Engineering, Jahangirnagar University, Dhaka, Bangladesh
suman@uiu.ac.bd, fayzur@ieee.org, khairul271276@aust.edu, aysaber@ieee.org, rmzahid@juniv.edu

Abstract

This paper presents the development of an Artificial Neural Networks and Particle Swarm Optimization (ANN-PSO) based short-term load forecasting model with improved generalization technique for the Regional Power Control Center of Saudi Electricity Company, Western Operation Area (SEC-WOA). Weather, load demand, wind speed, wind direction, heat, sunlight, etc. are quite different in a desert land than other places. Thus this model is different from a typical forecasting model considering inputs and outputs. In this research paper two steps have been introduced, first load forecasting made by mapping mechanism and then optimization technique applied to improve its accuracy. This paper includes ANN and PSO models for 24-hours ahead load forecasting. ANN is an effective mathematical tool for mapping complex relationships. It is also successful for doing forecasting, categorization, classification, and so forth. On the other hand, PSO is the most promising optimization tool. It has better information sharing and conveying mechanism; it has better balance of local and global searching abilities; and can handle huge multi-dimensional optimization problems efficiently with hundreds of thousands of constraints. Thus PSO is chosen as the optimization model of the weight matrix of ANN. Results show that the proposed ANN-PSO performs much better than ANN for the load forecasting in a desert like Saudi Arabia.

Keywords: Computational intelligence, short-term load forecasting, neural networks, particle swarm optimization, desert of Saudi Arabia.

I. INTRODUCTION

In recent years load forecasting have become one of the major areas of research in electrical engineering because they are practically used in power system for unit commitment, real-time dispatch, maintenance, optimization of power systems and so on. Load forecasting and its optimization are challenging tasks depending on previous real data. Depending on the time horizon, load forecasting can be generally divided into short-term, mid-term, and long-term. Short-term load forecasting [1], ranging from an hour to a week, on the other hand mid/long-term load forecasting, covering from a few weeks to several years. Unit commitment uses this forecast load demand as input and generates proper schedule for available units with minimum cost. In this research a forecasting model has been proposed for the Western Area of Saudi Arabia, which is shown in Fig. 1. As there are no existing computer aided systems in this area and thus planning and scheduling of this area are done manually. Approximate total load demand is 10,000 MW; there are about 110 thermal generating units; weather is uncertain; and load mainly depends on weather and Islamic events (Hajj, prayer, holidays, etc.). The manual operation of this large system obviously involves higher operating cost than near optimum.

Fig. 1. The Main Network of Western Saudi Arabia

Many researchers have addressed load forecasting. Load forecasting is a difficult task of many input attributes and huge practical data complex mapping. Firstly the load series is complex and exhibits several levels of seasonality. Secondly the load at a given hour is dependent not only on the load at the previous hour, but also on the load at the same hour on the previous day. There are also many important exogenous variables that must be considered, specially the weather-related variables [2]. Load forecasting plays an important role in power system planning, operation, dispatch, maintenance and so on. Basic operating functions such as unit commitment, economic dispatch, fuel scheduling, and unit maintenance and so on can be performed efficiently with an accurate load forecast [3]. Various statistical forecasting techniques have been applied to short term load forecasting (STLF). Examples of such methods including, time series [4], similar-day approach [5], regression methods [6], expert systems [7]. In general, these methods are basically linear models and the load pattern is usually a nonlinear function of the exogenous variables [2]. On the other hand, artificial neural network (ANN) has been proved as powerful alternative for STLF that it is not rely on human experience. ANN is data-driven method, in the sense that it is not necessary for the researcher to postulate tentative models and then estimate their parameters. Given a sample of input and output vectors, ANN simply maps the relationship [8]. However, the researchers want to include optimization for practical input load data with corresponding errors and weight matrix

978-1-4244-6283-4/09/$26.00 ©2009 IEEE

of ANN, as ANN is not an optimization method.

In recent years, AI-based techniques [9] such as neural networks [10] have been used to obtain promising results. Neural networks have the capability to approximate any continuous nonlinear function, and can adapt to a changing forecasting environment through self-learning. However, it is often difficult to decide whether the obtained neural network is the best due to the tedious and trial-and-error tuning process, and model overfitting that may occur and results in less satisfactory forecasting accuracy [2]. Some variants of neural networks have been applied for the short term load forecasting such as fuzzy neural networks [11], adaptive neural networks [12], Bayesian neural network [13], and Back propagation neural networks [14]. Among them, the fuzzy neural network is one of the popular load forecasters. Some techniques have also been combined with neural network to find highest accuracy such as gradient methods [15], fuzzy expert system [16], and wavelet transformation [17]. Other techniques such as fuzzy logic [18], GA [19], support vector machines (SVMs) [20] and simulated annealing [21] have also been applied to load forecasting. Wavelet-based techniques [17] have also been applied to load forecasting, typically in conjunction with neural networks.

The advantage of using particle swarm optimization (PSO) [22-24] algorithm over other techniques is that it can be computationally inexpensive, easily implementable, and does not require gradient information of an objective function, but only its values. Therefore, the particle swarm optimization algorithm is applied to the neural network in the training phase, to obtain a set of weights that will minimize the error function in competitive time.

The main limitation of the ANN in STLF is that it always depends on the backpropagation algorithm to train the ANN. It does not consider the randomness nature to escape from local optima. On the other hand PSO has the guided randomness property. That's why it can explore more search spaces and can avoid local optima gradually. So we have chosen ANN for forecasting and after forecasting we have chosen PSO for optimization for better results.

This paper presents a hybrid approach of ANN and PSO model of STLF, typically, next 24-hours, for the Western Area of Saudi Arabia. A significant improvement has found after applying PSO on ANN. Temperature, and load related inputs are considered in this model. One year of historical dependent data are used. A special design for the forecasting system that copes with the features of Saudi Arabia (SECWOA) electrical load is presented. This is the first paper to explore this desert dataset for STLF using ANN and PSO. It is found that the error is in acceptable range for the proposed method. To find out the robustness of the proposed method, seven days results are also forecasted. The proposed ANN-PSO method performs much better with respect to ANN for that case as well. Based on the forecast results, some suggestions have placed to the Saudi Arabia power market providers.

II. PROBLEM FORMULATION

Given the day of the week (D_i), pervious 24 hours load (Y_{i-1}) and previous 24 hours temperature (T_{i-1}) where is the 24 hours load of the day to be forecast (i), the predictor has the general form $(Y_i = f(Y_{i-1}, T_{i-1}, D_i)$, in other words one may use data from the past load and temperature history as well as the week day type of the forecasted day. At midnight of previous day $(i-1)$, it is required to provide a prediction for the 24 hours of next day (i). This prediction will be used for scheduling the power generators to be activated in the following working day (i). Typical load for two days are presented in Fig. 2.

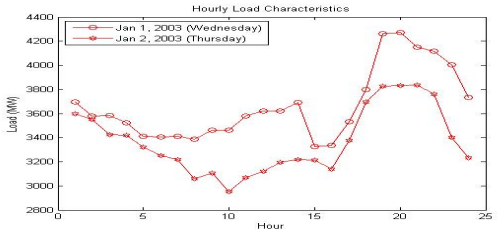

Fig. 2. Hourly Load Characteristics

III. PROPOSED MODEL

A. Major Components of the Model

A.1 ANN for Load Forecasting

The ANN model implemented consists of a totally-connected two-layer network (input, hidden and output layers) having the following structural characteristics. Forty-nine inputs, namely:

- 24 hourly load values of the day preceding the forecast day $(L_{(i-1,tj)}, where \ \ j = 1, \ldots \ldots, 24)$; For example, $L_{(i-1,t1)}$ implies that the first hourly $(t1)$ load of the day proceeding $(i-1)$ the forecast day (i). Here mention that i implies the forecast day.
- 24 hourly temperature values of the day preceding the forecast day $(T_{(i-1,tj)}, where \ \ j = 1, \ldots \ldots, 24)$; For example, $T_{(i-1,t14)}$ implies that the fourteenth hourly $(t14)$ temperature of the day proceeding $(t-1)$ the forecast day (i) and so on. Here mention that i implies the forecast day.
- 1 digit integer code known as day of the week (D_i) flagging the day of the forecast (i.e., 1 implies Saturday and 7 implies Friday).

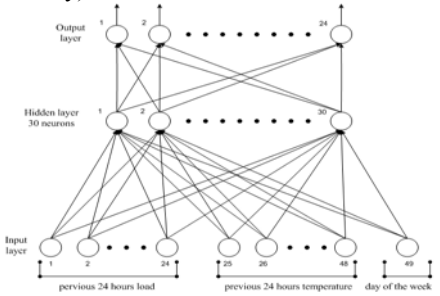

Fig. 3. ANN for 24-hours ahead load forecasting

The number of hidden neurons was parametrically optimized to 30. The number of outputs was set at 24, comprising the simultaneous forecast of the load of the day concerned. Fig. 3 reports the schematic of the architecture of the ANN, as implemented. A simplified form of the proposed ANN model can thus be summarized as follows:

$$Y_i = f(Y_{i-1}, T_{i-1}, D_i) \quad (1)$$

A.2 Particle Swarm Optimization for Weight Optimization of ANN

Particle Swarm Optimization is a heuristic approach first proposed by Kennedy and Eberhart in 1995 [22] as an evolutionary computational method developed for dealing with the optimization of continuous and discontinuous function decision making. The PSO algorithm is based on the biological and sociological behavior of animals such as schools of fish and flocks of birds searching for their food. PSO imitates this behavior by creating a population with random search solution and each potential solution is represented as a particle in a population (called swarm). The social sharing of information among the particles of a population may provide an evolutionary advantage. Each particle is flown through the multidimensional search space with random and adaptable velocity in order to find the lower function values (global minimum).

In standard PSO algorithm, particles are manipulated according to (2) and (3) where each particle tries to adjust its velocity according to best positions ever visited that is stored in its memory called personal best ($pbest$) and according to the best previous position attained by any particle in its neighborhood called global best ($gbest$) trying to search for a better position. Thus, particles communicate with each other and distribute their information among each other during their search.

$$v_i(t+1) = w_i(t) + r_1 c_1 [pbest - x_i(t)] + r_2 c_2 [gbest - x_i(t)] \quad (2)$$

$$x_i(t+1) = x_i(t) + v_i(t+1) \quad (3)$$

Here w is an inertia weight, which provides a balance between the local and global exploration. $v_i(t)$ and $v_i(t+1)$ are current and modified velocity for each iteration, respectively. c_1 and c_2 are positive numbers, used to control the particle's movement at each iteration. They represent cognitive and social components, respectively. r_1 and r_2 are uniform distribution numbers in the range [0, 1]. $x_i(t)$ and $x_i(t+1)$ are the current and modified position for each iteration, respectively. N is number of particles.

In this paper the connection weights between input to hidden and hidden to output layers are represented in two matrices ω_1 of size $m_1 \times n_1$ and ω_2 of size $n_1 \times m_2$ respectively. The current position $x_i(t)$ for each particle is represented by $\omega_i(t) = \{\omega_1, \omega_2\}$. Therefore, the position of each particle represents a set of weights for the current iteration. Thus, using equations (2) and (3), updated velocity and then position for each particle is determined to minimize the error of the network. The dimension of the search space for each particle is the number of weights associated with the network. The fitness value for each particle is determined based on the new position value of each weight matrix.

B. Proposed Algorithm

The major steps of the algorithm are summarized as follows:

Step 1: To select the ANN structure initially a fully connected three layered feedforward ANN is taken. The numbers of input and output neurons are determined by the input factors and the number of targeted outputs. To determine the number of hidden neurons various experiments of STLF are performed and finally fixed the number which shows the best result.

Step 2: Train the ANN by BP algorithm for selected dataset. The dataset is divided into three different sets like training, validation and testing datasets. Training dataset is used to train the ANN. Validation dataset is used for determining the stopping criteria of the ANN and the Testing dataset is used for determining STLF performance. After training completion we store the weight matrix for further updates.

Step 3: STLF is done by using the present ANN found in Step 2.

Step 4: A number of matrix sets that means candidate particles are generated from the stored weight matrices in Step 2. This step explores the opportunity of randomness and generates more search spaces.

Step 5: Initialize local best ($pbest$), global best ($gbest$), and other PSO parameters w, c1 and c2 using standard PSO rules.

Step 6: STLF is done using the ANN having the new weight matrices.

Step 7: If the performance of step 6 is better than the previous one, then go to Step 8, otherwise go to Step 9.

Step 8: Update $pbest$ and $gbest$ parameters based on the performances of current solutions.

Step 9: In this step the present solutions (particles) are updated based on equations (1–2). Thus a new set of solutions is obtained and the new search spaces are explored.

Step 10: Check whether the stopping criterion is met or not. If met then the global best weight matrix set is taken as the solution of the proposed method, and go to next step, otherwise go to step 6 for further exploration.

Step 11: The updated weighted matrix is put in the ANN structure. Thus the new ANN is constructed applying PSO. Therefore the STLF is done by this new ANN and the performance is treated as the performance of the proposed method.

Step 12: Compare the performance of Step 3 and Step 11.

Step 13: Print the results.

In this research, the authors are proposing a hybrid method for STLF. Here this proposed model is able to forecast next 24-hours load. Thus this technique can be used to forecast 24-fours ahead load efficiently. Flowchart is shown in Fig. 4. This work is done on the data set of Saudi Arabia.

The performance is measured in terms of mean absolute percentage error (MAPE) defined as:

$$MAPE = 100/N \sum_{i=1}^{N} \left(\left| Actual(i) - Forecast(i) \right| \right) / Actual(i) \quad (4)$$

where N is the number of test data.

IV. SIMULATION RESULTS AND DISCUSSIONS

All calculations have been run on Intel(R) Core(TM)2 Duo 2.66GHz CPU, 2.96 GB RAM, Microsoft Windows XP OS and Matlab compiler for coding. ANN delivers two weight matrices. PSO is applied to tune these weight matrices to achieve more accuracy in forecasting. n (30) number of matrix sets that means candidate particles are generated from the main matrix set by multiplying each element with a different random number ranged from 0-1. Initialize the values of PSO parameters, is decreasing in each iteration from 1.0 to 0.4 uniformly, and $c_1 = 1.5$ and $c_2 = 0.5$. The maximum number of iterations, m = 500.

A. Selection of Data Set

Saudi Arabia's dataset has been used in this experiment. For each test case January 1 to November 30, 2003 data is used for training and 1-7 of December 2003 data is used for Testing. Due to space limitation sample data are not presented here.

B. ANN Training

Firstly, the network uses the Levenberg-Marquardt algorithm for training. Input vectors and target vectors are randomly divided into two sets so that 80% are used for training and 20% are used to validate that the network is generalizing and to stop training before overfitting. The training stops when the performance goal that is Mean Square Error (MSE = 0.001) is met or when the training error decreases but the validation error increases or the upper limit of iterations is reached.

C. Determination of ANN Structure

Initially a fully connected ANN is chosen for doing the STLF. The number of input nodes is determined by the number of inputs those are responsible for determining forecasting. Forty nine input characteristics are found (one for day type, twenty four represents immediate past twenty four hours actual load, and remaining twenty four represents immediate past twenty four hours actual temperature) those are key factors for load forecasting. So the number of input determines at forty nine (49). As the target is to forecast the load for next twenty four hours so the number of output nodes becomes twenty four (24). The number of hidden neurons is determining by a wide variety of the number of hid den neurons from 20 to 40 and simulates the performances and thus based on performance 30 hidden neurons are optimal. Therefore the ANN structure determines having 49X30X24 for the STLF of Jeddah, KSA data.

D. Results

The Table I shows the performance of the method. For training ANN uses eleven months data (January 01, 2003 – November 30, 2003) and for testing it uses December 01-07, 2003 data Table I shows average MAPE using ANN is 4.08017%. However, the average MAPE is 0.65754% for proposed method. Accuracy is improved by 3.42263%.

The following three diagrams, Fig. 5–7, are drawn based on the load forecasting results of test case 03 (test_03), i.e., for December 03, 2003, Wednesday.

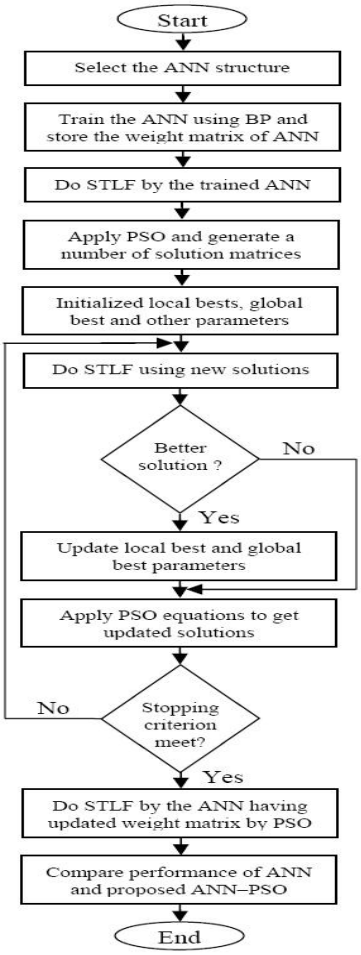

Fig. 4. Flowchart of the Proposed Algorithm

In Fig. 5, red, green and the blue curves represent the actual load, forecasted load by ANN and ANN–PSO respectively for the 24 hours of December 03, 2003 on Wednesday. It is clearly visible that the actual load and ANN–PSO method's forecasted loads are very close, whereas the only ANN based forecasted load is apart from the actual load.

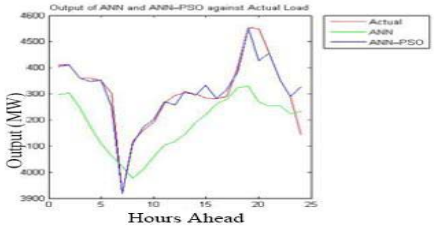

Fig. 5. Load comparison for the day 03 Dec, 2003

Table I Performance of ANN, ANN–PSO and achieved improvements

		1-12-03 (Mon)	2-12-03 (Tue)	3-12-03 (Wed)	4-12-03 (Thu)	5-12-03 (Fri)	6-12-03 (Sat)	7-12-03 (Sun)	
		Test_01	Test_02	Test_03	Test_04	Test_05	Test_06	Test_07	Average
MAPE	ANN	2.8362	2.8223	3.1377	2.8766	4.8911	6.53	5.4673	4.08017
	ANN–PSO	0.9387	0.4584	0.5368	0.3765	0.4847	0.7354	1.0723	0.65754
	Improvement	1.8975	2.3639	2.6009	2.5001	4.4064	5.7946	4.395	3.42263
MIN	ANN	0.0061	0.1003	0.1963	0.0127	0.1089	0.0506	0.005	0.06856
	ANN–PSO	0	0.0019	0	0.0038	0	0	0.0012	0.00099
	Improvement	0.0061	0.0984	0.1963	0.0089	0.1089	0.0506	0.0038	0.06757
MAX	ANN	9.5797	6.5264	6.1325	6.8234	10.141	15.663	21.0762	10.8489
	ANN–PSO	7.9972	2.8764	4.3778	2.8844	2.7557	6.5816	9.0296	5.21467
	Improvement	1.5825	3.65	1.7547	3.939	7.3855	9.0816	12.0466	5.63427
STD	ANN	2.4688	1.6818	1.5592	2.2229	3.2896	4.8753	6.1222	3.17426
	ANN–PSO	1.8568	0.7406	1.0193	0.6719	0.7454	1.4715	2.1937	1.24274
	Improvement	0.612	0.9412	0.5399	1.551	2.5442	3.4038	3.9285	1.93151

Note: 1-12-03 means 1st December, 2003; Test_01 means test no. 1; MAPE means mean absolute percentage error; STD means standard deviation;

In Fig. 6, the green and blue colored curves represent the percentage of errors occurred by applying ANN and ANN–PSO methods respectively when load forecasting is done for 24 hours for December 03, 2003 on Wednesday. ANN produces an average error of 3.1377% with a maximum error of 6.1325%. Whereas the proposed ANN–PSO's average error is 0.5368% and the maximum error is 4.3778%.

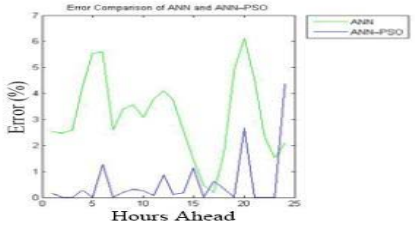

Fig. 6. Percent error comparison for the day 03 Dec, 2003

In Fig. 7, the curve shows how the MAPE decreases in each iteration of ANN–PSO exploration. It is observed that the major performance improvement occurs during 200 – 300 iterations. Why convergence does not start at the beginning, but at this stage will be a subject to research in future.

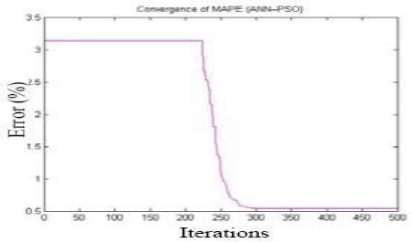

Fig. 7. Convergence of MAPE for the day 03 Dec, 2003

Fig. 8 is drawn based on the load forecasting results of test case 07 (test_07), i.e., for December 07, 2003, Sunday. This test case is chosen based on the performance results of the proposed method. The test case is selected to show the worst performance (MAPE) of the proposed method which is also within a tolerable range. The green and blue colored curves represent the absolute percentage error distributions occurred by applying ANN and ANN–PSO methods respectively when load forecasting is done for 24 hours for December 07, 2003 on Sunday. The ANN-PSO curve shows that 90% of the time the error is within 2% whereas only 45% of the time the error is within 2% in case of only ANN.

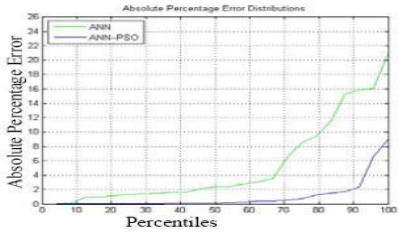

Fig. 8. Absolute % error distributions for 07 Dec, 2003

E. Robustness of The ANN–PSO Method

To establish the robustness of the proposed method the authors extended the simulation for ten individual separate cases. Table II compared the performances between ANN and proposed ANN–PSO method for ten separate test cases occasions. For training ANN uses eleven months data (January 01, 2003 – November 30, 2003) and for testing it uses December 01-07, 2003 data. Table II shows average MAPE using ANN is 4.7936%. However, the average MAPE is 3.08172% for proposed method. Accuracy is improved by .71188%.

From Table II, it is seen that the MAPE values of the proposed ANN–PSO model are always better than the MAPE values of ANN method. This means that ANN–PSO is more

Table II Performance of ANN and ANN–PSO and achieved improvements

		Tst_01	Tst_02	Tst_03	Tst_04	Tst_05	Tst_06	Tst_07	Tst_08	Tst_09	Tst_10	Avg.
MAPE	ANN	4.4135	5.4014	5.2286	5.4458	5.5159	4.364	4.2711	4.2116	4.4106	4.6735	4.7936
	ANN - PSO	3.0292	2.8564	3.0015	3.0464	3.0011	2.8429	3.3584	3.0177	3.3054	3.3582	3.08172
	Improvement	1.3843	2.545	2.2271	2.3994	2.5148	1.5211	0.9127	1.1939	1.1052	1.3153	1.71188
MIN	ANN	0.0061	0.003	0.0989	0.0169	0.0182	0.0414	0.0077	0.0416	0.078	0.0414	0.03532
	ANN - PSO	0.009	0.0031	0	0.0005	0.0006	0.0058	0	0.0031	0.0015	0.001	0.00246
	Improvement	-0.003	-1E-04	0.0989	0.0164	0.0176	0.0356	0.0077	0.0385	0.0765	0.0404	0.03286
MAX	ANN	18.338	22.543	22.362	25.3	27.434	16.318	17.343	19.402	17.075	18.4	20.4515
	ANN - PSO	15.536	12.412	14.52	12.72	12.765	13.945	13.868	12.84	15.902	16.073	14.058
	Improvement	2.8016	10.131	7.842	12.58	14.669	2.3736	3.4743	6.5618	1.1733	2.3277	6.39342
STD	ANN	3.0193	3.5601	3.6968	3.7003	3.5935	3.2914	3.2216	3.0464	3.1786	3.3076	3.36156
	ANN - PSO	2.767	2.4785	2.4718	2.6969	2.5119	2.5172	2.7624	2.3656	2.7326	2.6493	2.59532
	Improvement	0.2523	1.0816	1.225	1.0034	1.0816	0.7742	0.4592	0.6808	0.446	0.6583	0.76624

Note: Test_01 means test no. 1; MAPE means mean absolute percentage error; STD means standard deviation.

accurate than ANN. Also the better STD values indicate that the ANN–PSO is more consistent. Moreover, in case of maximum error ANN–PSO always performs better than that of ANN. This is also true for minimum error except for the two test cases (Tst_01 and Tst_02). This may happen occasionally because PSO is a stochastic process having random nature. The authors will investigate further to control the number of this type of occurrence.

The Fig. 9–10, are drawn based on the load forecasting results of test case 10 (Tst_10) for 7 days, i.e., December 01–07, 2003.

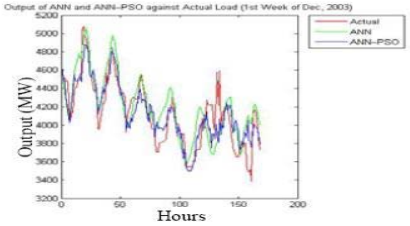

Fig. 9. Load comparison for the week December 01-07, 2003.

In Fig. 9, red, green and the blue curves represent the actual load, forecasted load by ANN and forecasted load by ANN–PSO respectively for a week, 168 (24x7) hours, from December 01 – 07, 2003. It is clear in the figure that the actual load (red) and ANN–PSO load (blue) are very close to each other, whereas the ANN is apart from the actual load curve. The main reason of this performance enhancement is the application of PSO. PSO explores the randomness nature for broaden solution spaces and a guided search mechanism of it converges into best solution for every cases.

In Fig. 10, the green and blue colored curves represent the percentage of errors occurred by applying ANN and ANN–PSO methods respectively when load forecasting is done for 24 hours for the week December 01-07, 2003. ANN produces an average error of 4.6735% with a maximum error of 18.4%. Whereas the proposed ANN–PSO's average error is 3.3582% and the maximum error is 16.073%.

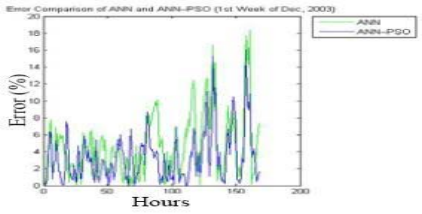

Fig. 10. Percent error comparison for Dec, 01-07, 2003

V. CONCLUSION

This paper presents 24-hour ahead load forecasting using ANN and PSO for the Western Area of Saudi Arabia. ANN is very common to use in the arena of forecasting. On the other hand, PSO is used to optimize the input and output weight matrices of ANN. It is a short term load forecasting using the hybrid approach of ANN and PSO. A significant improvement has found after applying PSO on ANN. The authors have applied first time this hybrid method on Saudi Arabia's data to forecast its STLF. Average MAPE is 0.65754% where maximum, minimum and standard deviation of results are tolerable. For robustness of the proposed method, results for seven days have also been forecasted. The ANN–PSO performs much better with respect to ANN for that case as well. The load depends on uncertain desert weather and events of Saudi Arabia and thus in future a fuzzy representation will be included in this model.

REFERENCES

[1] S. Rahman and I. Drezga, "Identification of a standard for comparing short-term load forecasting techniques," *Electric Power Systems Research*, vol. 25, no. 3, pp. 149-158, Dec 1992.

[2] H. S. Hippert, C. E. Pedreira, and R. C. Souza. "Neural networks for short-term load forecasting: A review and evaluation," *IEEE Trans. Power Syst.*, vol. 16, no. 1, pp. 44-55, Feb 2001.

[3] O. A. Alsayegh, "Short-term load forecasting using seasonal artificial neural networks," *International Journal of Power and Energy Syst.*, vol. 23, no. 3, pp. 137-142, 2003.

[4] K. Lru, S. Subbarayan, R. R. Shoults, M. T. Manry, C. Kwan, F. L. lewis, and J. Naccarino, "Comparison of very short term load forecasting techniques," *IEEE Trans. Power Syst.*, vol. 11, no. 2, pp. 877-882, May 1996.

[5] I. Drezga and S. Rahman,, "Short-term load forecasting with local ANN predictors," *IEEE Trans. Power Syst.*, vol. 14, no. 3, pp. 844–850, Aug 1999.

[6] D. Alex and C. Timothy, "A regression-based approach to short term system load forecasting," *IEEE Trans. Power Syst.*, vol. 5, no. 4, pp. 1535–1550, Nov 1990.

[7] S. Rahman and O. Hazim, "A generalized knowledge-based short-term load forecasting technique", *IEEE Trans. Power Syst.*, vol. 8, no. 2, pp. 508-514, May 1993.

[8] H. Chen, C.A. Canizares, and A. Singh. "ANN-based short-term load forecasting in electricity markets", *Proceedings of the IEEE Power Engineering Society Transmission and Distribution Conference*, 2:411–415, 2001.

[9] R. C. Ebehart, P. K. Simpson, and R. W. Dobbins, "Compuational intelligence," in *PC Tools*. New York: Academic Press Professional, 1996.

[10] M. N. Kandil, R. Wamkeue, M. Saad, and S. Georges, "An efficient approach for short term load forecasting using artificial neural networks," *International Journal of Electrical Power & Energy Systems*, vol. 28, no. 8, pp. 525-530, Oct. 2006.

[11] H. Y. Yang, H. Ye, G. Wang, J. Khan, and T. Hu, "Fuzzy neural very-short-term load forecasting based on chaotic dynamics reconstruction," *Chaos, Solitons & Fractals*, vol. 29, no. 2, pp. 462-469, Jul 2006.

[12] T. S. Dillon, S. Sestito, and S. Leung, "Short term load forecasting using an adaptive neural network," *International Journal of Electrical Power & Energy Systems*, vol. 13, no. 4, pp. 186-192, Aug 1991.

[13] P. Lauret, E. Fock, R. N. Randrianarivony, and J. Manicom-Ramsamy, "Bayesian neural network approach to short time load forecasting," *Energy Conversion and Management*, vol. 49, no. 5, pp. 1156-1166, May 2008.

[14] Z. Xiao, S. Ye, Bo Zhong, C. Sun, "BP neural network with rough set for short term load forecasting," *Expert Systems with Applications*, vol. 36, no. 1, pp. 273-279, Jan 2009.

[15] L. Mohan Saini, M. Kumar Soni, "Artificial neural network-based peak load forecasting using conjugate gradient methods," *IEEE Trans. Power Syst.*, vol. 17, no. 3, pp. 907 - 912, Aug 2002.

[16] D. Srinivasan, S. S. Tan, C. S. Chang, and E. K. Chan, "Parallel neural network-fuzzy expert system for short-term load forecasting: System implementation and performance evaluation," *IEEE Trans. Power Syst.*, vol. 14, no. 3, pp. 1100–1106, Aug 1999.

[17] C. Kim, I. Yu, and Y. H. Song, "Kohonen neural network and wavelet transform based approach to short-term load forecasting," *Elect. Power Syst. Res.*, vol. 63, no. 3, pp. 169-176, 2002.

[18] S. C. Pandian, K. Duraiswamy, C. Christober, Asir Rajan, and N. Kanagaraj, "Fuzzy approach for short term load forecasting," *Electric Power Systems Research*, vol. 76, no. 6-7, pp. 541-548, Apr 2006.

[19] D. E. Goldberg, *Genetic Algorithms in Search, Optimization & Machine Learning*. Reading, MA: Addision-Wesley, 1989.

[20] B. J. Chen, M. W. Chang, and C. J. Lin, "Load forecasting using support vector machines: A study on EUNITE competition 2001," *IEEE Trans. Power Syst.*, vol. 19, no. 4, pp. 1821–1830, Nov 2004.

[21] P. Pai and W. Hong, "Support vector machines with simulated annealing algorithms in electricity load forecasting," *Energy Conversion and Management*, vol. 46, no. 17, pp. 2669-2688, Oct 2005.

[22] Kennedy and R. C. Eberhart, "Particle swarm optimization," *in Proc. IEEE Int. Conf. Neural Networks*, 1995, vol. 4, pp. 1942–1948.

[23] A. Y. Saber, T. Senjyu, A. Yona, and T. Funabashi, "Unit commitment computation by fuzzy adaptive particle swarm optimization," *IET Gen. Transm. Dist.*, vol. 1, no. 3, pp. 456-465, May 2007.

[24] A. Y. Saber, S. Chakraborty, A. Razzak, and T. Senjyu, "Optimization of economic load dispatch of higher order general cost polynomials and its sensitivity using modified particle swarm optimization," *Electric Power Systems Research*, vol. 79, no. 1, pp. 98-106, Jan 2009.

Proceedings of 2009 12th International Conference on Computer and Information Technology (ICCIT 2009)
21-23 December, 2009, Dhaka, Bangladesh

Control of the Speed of a DC Motor by Employeeing Pulse Width Modulation (PWM) Technique *(Not Presented)*

Mohammad Tafiqur Rahman, Fahad Faisal, Munawwar Mahmud Sohul, Farruk Ahmed

Department of Electrical Engineering & Computer Science, North South University, Dhaka, Bangladesh
m.tafiqur.rahman@gmail.com, m.fahad.faisal@gmail.com, mmsohul@northsouth.edu, farruk@northsouth.edu

Abstract

This paper is mainly focused on the technique of pulse width modulation for controlling the speed of a 12 volt DC motor more efficiently. A potentiometer was used to generate a wide variety of pulses. The output of the controlling circuit (Pulse Width) was connected to the second circuit as input for direction control. Here a single push switch was used to change the state (stop-forward-stop-reverse) of the DC motor. These two circuits were combined into one for ease of use. Third circuit was designed to measure the speed of the motor by employing an opto-electronic sensor, an amplifier and a two blade fan to interrupt the signal transmission of the sensor. Finally, the output of the sensor was connected with an oscilloscope through an amplifier and a train of square was found. By measuring the time period of the square waves, the duty cycle and Rotation per Minute (RPM) was calculated. After calculating the result from the observation proves that pulse width modulation is an efficient technique for controlling DC motor rather than other conventional technique.

Keywords: DC Motor, IED, PWM, RPM.

I. INTRODUCTION

Modulation is the process of varying some characteristic of a periodic wave with an external signal. It is utilized to send an information bearing signal over long distances. Modulation is an essential process in communication since it enables multiple signals to be transmitted simultaneously over a common medium or communication channel.[1] Digital communication systems can be implemented using a variety of different modulation schemes, one of which is based on Pulse Width Modulation (PWM) methods. PWM is an attractive scheme for transmission of analogue and data signals compared with purely digital modulation techniques. In PWM the width of a constant amplitude pulse carrier is changed according to the sample values of the modulating signal. [2], [3].

A conventional linear output stage applies a continuous voltage to a load. This can waste plenty of power. On the other hand, PWM applies a pulse train of fixed amplitude and frequency, only the width is varied in proportion to an input voltage. The end result is that the average voltage at the load is the same as the input voltage; but with less wasted power in the output stage. Pulse-width modulation control works by switching the power supplied to the motor on and off very rapidly. The DC voltage is converted to a square-wave signal, alternating between fully on (nearly 12V) and zero, giving the motor a series of power "kicks". If the switching frequency is high enough, the motor runs at a steady speed due to its fly-wheel momentum. [4] By adjusting the duty cycle of the signal (modulating the width of the pulse, hence the 'PWM') i.e., the time fraction it is "on", the average power can be varied and hence the motor speed. [5], [6].

A PWM circuit works by making a square wave with a variable on-to-off ratio, the average on time may be varied from 0 to 100 percent. In this manner, a variable amount of power is transferred to the load. The main advantage of a PWM circuit over a resistive power controller is the efficiency, at a 50% level, the PWM will use about 50% of full power, almost all of which is transferred to the load, a resistive controller at 50% load power would consume about 71% of full power, 50% of the power goes to the load and the other 21% is wasted heating the series resistor. Load efficiency is almost always a critical factor in solar powered and other alternative energy systems which we are using in our daily life. [7], [8].

II. FEEDBACK SYSTEM

Pulse Width Modulation (PWM) is used to control the electrical power delivered to the motor. The reason behind this idea is that a closed loop controller will regulate the power delivered to the motor to reach the required velocity.

If the motor is to turn faster than the required velocity, the controller will deliver less power to the motor. Closed-loop control systems typically operate at a fixed frequency. The frequency of changes to the drive signal

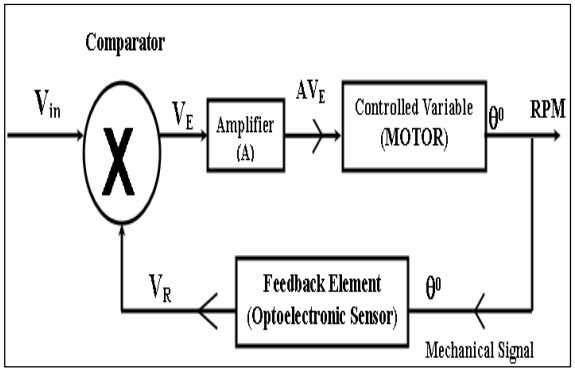

Fig. 1. Flowchart of closed loop feedback control system

is usually the same as the sampling rate, and certainly

not any faster. For example, if the feedback system indicates that your car is going too quickly, the cruise control system can temporarily reduce the amount of fuel fed to the engine.[9],[10] The closed loop feedback system concept is used to control the speed of the 12 volt DC motor, where the input is a voltage signal and the output is Rotation per Minute (RPM).

In figure 1, at the first stage a comparator is used to compare the input signal (Vi) with the voltage signal (VR) from the feedback element (optical sensor). Then the comparator checks whether the input voltage (Vi) is greater than (VR) or not. The result of the comparator VE is then amplified to the control variable (Motor). Finally, based on the motor rotation we can decide that how the mechanical signal will be changed.

III. FUNCTIONAL DESCRIPTION

The whole experiment design phase is divided into 3 parts. As the main concern of this experiment is to develop a system for controlling the speed of a motor, in first stage a system for PWM to control the speed was made, then the system for control the direction was developed and finally, a small system to calculate the rotation of the motor was designed.

A. Controlling the Speed of the Motor

The PWM circuit required a steadily running oscillator to operate. The first and fourth OPAMP of IC LM324N formed a square/triangle waveform generator with a frequency of around 400 Hz. From the circuit we got saw-tooth wave coming from the output pin on fourth OPAMP of IC LM324N. It generates a frequency about 130 Hz with the components where the amplitude is swinging between 3.5 V and 9.5V on a 12V supply. We found that the reference voltage system was designed to apply a level ranging from 3V to 7.5V to the comparator. At 3V the fan was getting power all the time, at 7.5V about 30% of the time (when the sawtooth wave went over 7.5V). The pulse power applied to the fan at the minimum setting, which was just enough to keep my test fan spinning.

Third OPAMP of IC LM324N was used to generate a 6 Volt reference current which was used as a virtual ground for the oscillator and it was necessary for the oscillator to run off of a single supply instead of a +/- voltage dual supply. Second OPAMP of IC LM324N was wired in a comparator configuration and was the art of the circuit that generates the variable pulse width. IC LM324N's pin 6 received a variable voltage from the R6, VR1, and R7 voltage ladder. This was compared to the triangle waveform from fourth output pin 14. When the waveform was above the pin 6 voltage, IC LM324N produces a high output. Conversely, when the waveform was below the pin 6 voltage, IC LM324N produces a low output. By varying the pin 6 voltage, the on/off points were moved up and down the triangle wave, producing a variable pulse width. Resistors R6 and R7 were used to set the end points of the VR1 control, the values shown allowed the control to have a full on and a full off setting within the travel of the potentiometer. These part values were varied to change the behavior of the potentiometer. Finally, the N channel MOSFET worked as the power switch, it received the modulated pulse width voltage on the gate terminal and switched the load current on and off through the Source-Drain current path. When the N channel MOSFET was on, it provided a ground path for the load and when it was off the load's ground was floating. The load had the supply voltage on the positive side at all times. LED gave a variable brightness response to the pulse width.

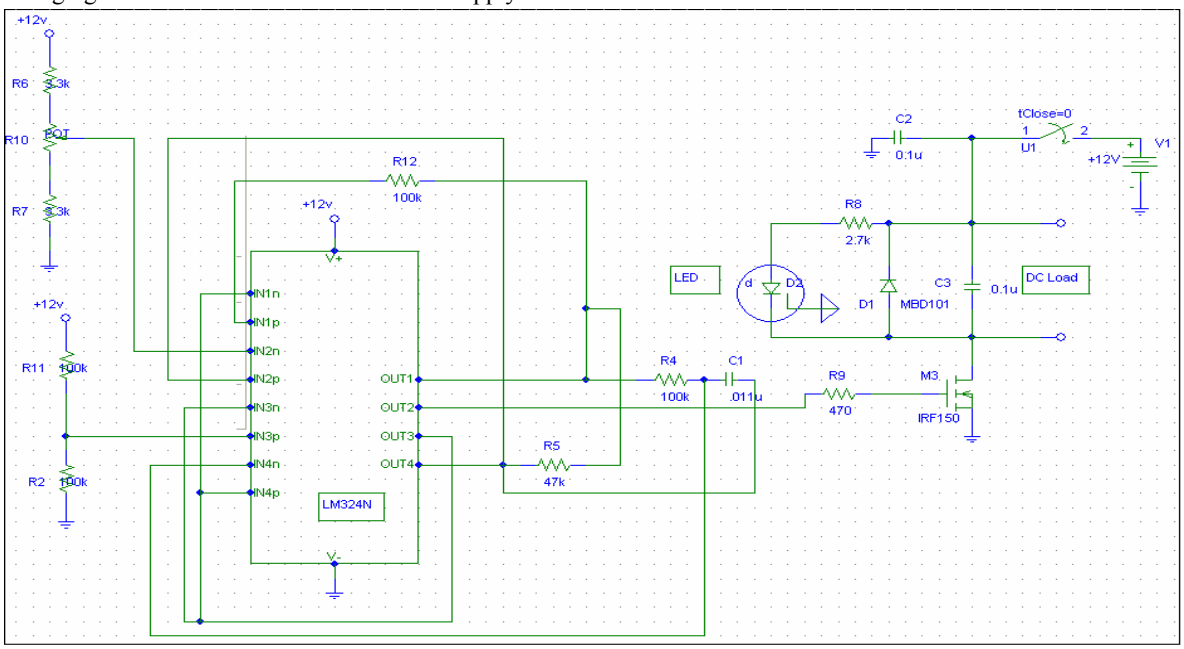

Fig. 2. Circuit Diagram of the Motor Speed Controller

Capacitor C3 smoothed out the switching waveform and removed some RFI, Diode D1 was a flywheel diode that shorted out the reverse voltage kick from inductive motor loads. The speed controller worked by varying the average voltage sent to the motor, which was done by simply adjusting the voltage sent to the motor.

The time that it took a motor to speed up and slow down under switching conditions was dependant on the inertia of the rotor means the weight of it and how much friction and load torque there was. If the supply voltage was switched fast enough, it won't have time to change speed much, and the speed would be quite steady. This was the principle of switch mode speed control. Thus the speed was set by Pulse Width Modulation.

B. Controlling the Direction of the Motor

We can run the DC motor in clockwise or anti-clockwise direction and stop it using a single switch. It provided a constant voltage for proper operation of the motor. The glowing of LED1 through LED3 indicated that the motor was in stop, forward rotation and reverse conditions, respectively. Here, timer IC1 was wired as a monostable multivibrator to avoid false triggering of the motor while pressing switch S1. Its time period was approximately 500 milliseconds (ms). Suppose, initially, the circuit was in reset condition with Q0 output of IC2 being high. Since Q1 and 3 outputs of IC2 were low, the outputs of IC3 and IC4 were high and the motor doesn't rotate. LED1 glowed to indicate that the motor was in stop condition. When you momentarily press switch S1, timer 555 (IC1) provided a pulse to decade counter CD4017 (IC2), which advanced its output by one and its high state shifted from Q0 to Q1. When Q1 went high, the output of IC3 at pin 3 went low, so the motor started to indicate that the motor was running in forward direction. By pressing S1 again, the high output of IC2 shifted from Q1 to Q2. The low Q1 output of IC2 made pin 3 of IC3 high and the motor did not rotate. LED1 glowed (via diode D2) to indicate that the motor was in stop condition. Pressing switch S1 once again shifted the high output of IC2 from Q2 to Q3. The high Q3 output of IC2 made pin 3 of IC4 low and the motor started running in anti-clockwise (reverse) direction. LED3 glowed to indicate that the motor was running in reverse direction. If S1 was pressed again, the high output of IC2 shifted from Q3 to Q4. Since Q4 was connected to reset pin 15, it reset the decade counter CD4017 and its Q0 output went high, so the motor did not rotate. LED1 glowed via diode D1 to indicate that the motor was in stop condition. In Fig. 3 the circuit diagram is given.

C. Speed Measurement

The optical coupler was used to measure the speed of the motor. The optical sensor had very little space between the emitter and the detector through which the blades of a small fan attached with the motor can pass. The opto-interrupter consists of an Infrared Emitting Diode (IED) and a photo-detector. A constant current (a constant voltage difference) was supplied across the terminals of the IED, which emitted a light with a constant intensity. With no obstruction between the IED and photo - detector, the opposing photo - detector received this constant intensity light and outputs a constant current (or constant voltage difference), say IC, across its two leads. When an opaque object is placed between the IED and the photo-detector, the photo-detector output goes essentially to zero. When the small

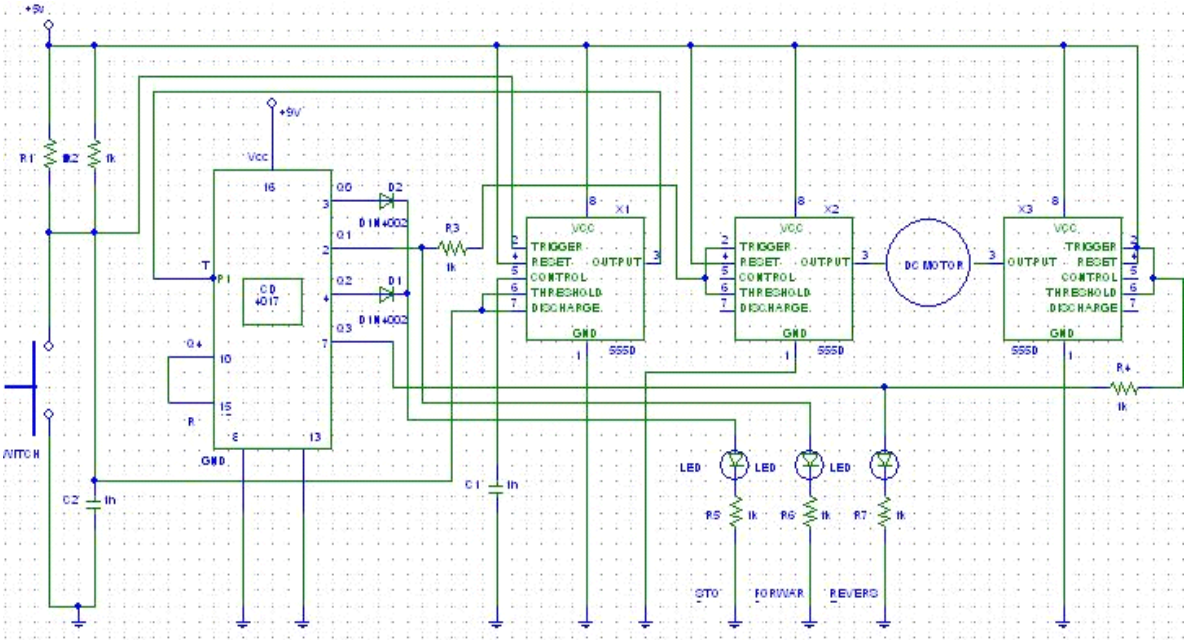

Fig. 3. Direction Controller Circuit of the DC Motor

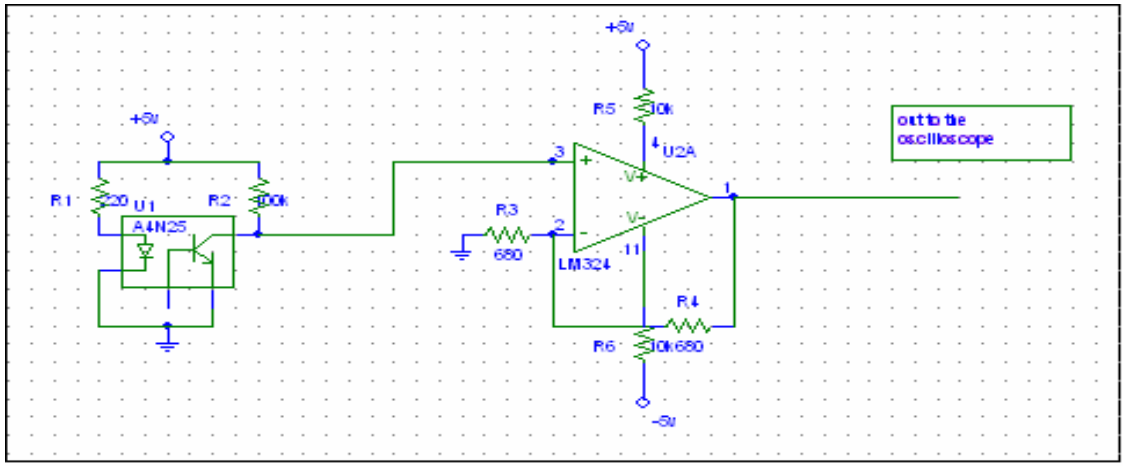

Fig. 4. Circuit Diagram for calculating the RPM

fan with two blades attached to the motor shaft, rotating at a constant RPM, is passed between the IED and the photo-detector, the photo-detector output becomes periodic. The photo-detector output signal peaks occurred once every revolution of the single blade, when the light from the IED is passed to the photo-detector through the center of the blade. Ideally these periodic signals would have very sharp rise and fall edges associated with the pulses. In actuality, these periodic pulses were fairly rounded, or mound shaped. This rounding of the pulses was primarily due to the finite width of the blade. When the leading edge of the blade just passed in front of the IED, the photo detector current output began to climb. The photo detector output current continued to climb as more of the IED was "seen" by the photo-detector. When the center of the IED was aligned with the center of the blade, the photo-detector current was at a maximum, or was at its peak. As the trailing edge of the blade began to pass the IED, the photo-detector output current began to decrease. The photo-detector current dropped to zero, when the trailing edge of the blade passed the IED completely. The photo-detector current remained zero until the leading edge of the blade was again "seen". The time between peaks was equal to the time for one revolution of the two blades fan. The output came from the cathode terminal of the sensor. A UA741 operational amplifier was used to receive and amplify the produced signal. The output terminal was directly connected to the positive input of the operational amplifier. The operating voltage of the operational amplifier was feed (+5V in pin 7 and -5Vin pin 4) through 10kΩ resistor individually to drop some voltage across it for getting the desired output voltage. The negative input terminal was grounded through a 680Ω (R_G) resistor. It was also connected to the output of the operational amplifier through another 680Ω (R_F) resistor. In this part of the experiment same value had been chosen for R_G and R_F to make the sensor's output signal double.

Operational amplifier follows the following formula for gain in its output,

$$Vo=[1+(RG/RF)]\times Vi \quad (1)$$

The output of the operational amplifier was then connected to the oscilloscope to view the output graph. The time period (ΔT) was calculated from the oscilloscope and it was multiply by two as the fan. Finally, the speed i.e. the Rotation per Minute (RPM) is then calculated by following the formula,

$$RPM=60/(\Delta T\times 2) \quad (2)$$

IV. GRAPHICAL VIEW OF THE RESULT AND PERFORMANCE OF THE SYSTEM

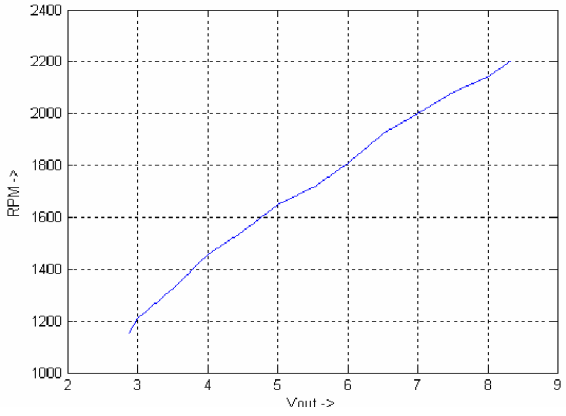

Fig. 5. Actual graph for V_{out} vs RPM

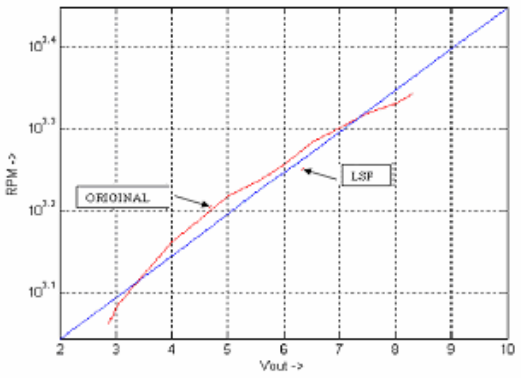

Fig. 6. Least Square Fit graph for V_{out} vs RPM

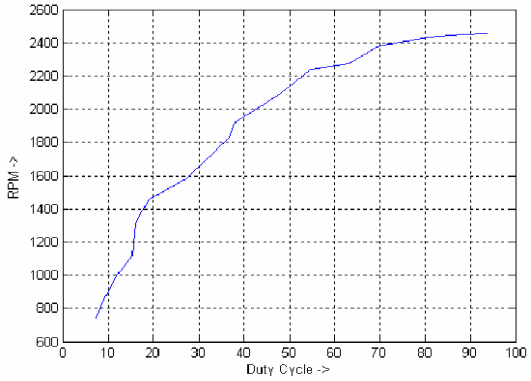

Fig. 7. Actual graph for Duty Cycle vs RPM (Forward Direction)

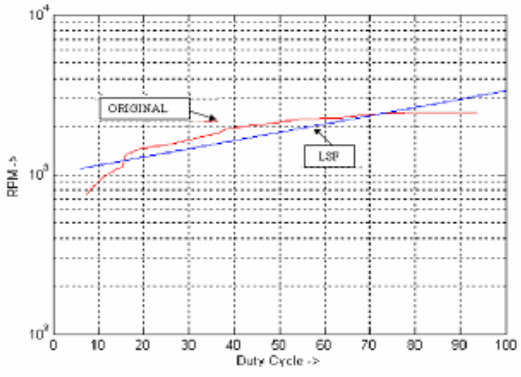

Fig. 8. Least Square Fit graph for Duty Cycle vs RPM (Forward Direction)

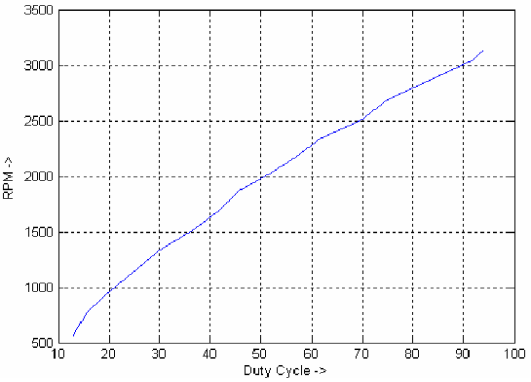

Fig. 9. Actual graph for Duty Cycle vs RPM (Reverse Direction)

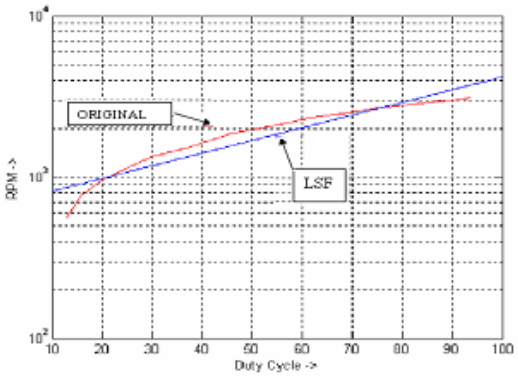

Fig. 10. Least Square Fit graph for Duty Cycle vs RPM (Reverse Direction)

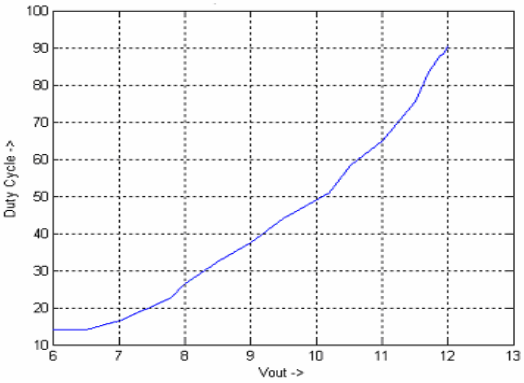

Fig. 11. Actual graph for V_{out} vs Duty Cycle

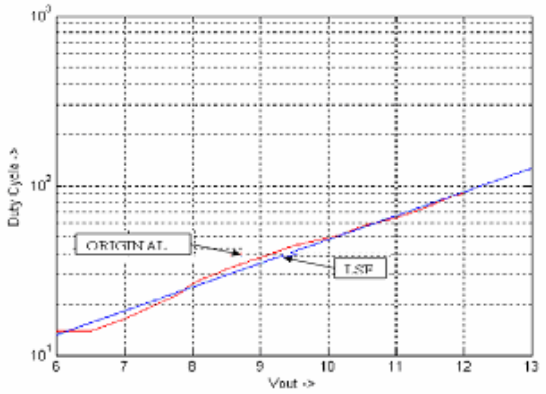

Fig. 12. Least Square Fit graph for V_{out} vs Duty Cycle

V. CONCLUSION

The main purpose of this experiment was to build DC motor speed controller that consumes less power and can perform more efficiently by using PWM technique. When considering a design for DC motor speed controller, a number of key elements have to be considered, such as a good understanding of the concept of modulation schemes and the electronic circuitry that goes into creating the scheme. These experimental circuits were designed for 12 volt DC motor or less.

The designs practically performed well in the laboratory. The Pulse Width Modulator along with the direction controller gave out good performance. The

hardware part of this experiment successfully controlled the speed of the motor. The opto-electronic sensor design for speed measurement was also good and gave better and clearer wave shape for measuring the RPM for a certain range. The software implementation will work really well if carried out with proper simulator and interfacing. Again, the design will work more efficiently, if we can use proper element for the project. As in some cases, it was very tough to find the appropriate IC for this experiment. The decade counter (CD4017), sometimes did not perform accordingly. As a result the direction control of the motor was not working as expected. If any other equivalent counter can be replaced with the current one, it can perform well. The duty cycle of the pulse width can not be measured in terms of high efficiency. If we can use better oscilloscope with high frequency response then the problem can be overcome. However, the designs can be implemented in practical systems with great patience and a lot of time. The values of the components can be decided upon by calibrating the design manually on trial and error basis. Once the values are fixed the designs will work really well and it can be used in various applications.

VI. ACKNOWLEDGEMENT

The authors acknowledge the contribution of Mr. Tanzil Rahman in making valuable suggestions in improving the contents of this paper and in the written English.

REFERENCES

[1] Lathi.B.P., "*Modern Digital and Analog Communications Systems*", 3rd ed., Oxford University press, 1998, PP-151-188.

[2] Z. Ghassemlooy, R. Saatchi, "Software Simulation techniques for Teaching Communication Systems," International Journal of Electrical Engineering Education, vol. 36, Issue 4, October 1999, pp. 287-297.

[3] MB. Sandler, "Digital-to-analogue conversion using pulse width modulation," Electronics & Communication Engineering Journal, vol. 5, Issue 5, November 1993, pp. 339-348.

[4] M. Ignat, G. Zarnescu, S. Soltan, V.Stoica, "Electromechanical .Microdrives for Robotics using piezoelectric Microactuators and Micromotors," SISOM, Bucharest, 2006, pp. 326.

[5] H. Sung-Rung, L. Shen-Iuan, "A 500-MHz - 1.25-GHz Fast- locking Pulsewidth Control Loop With Presettable Duty cycle," IEEE Journal of Solid-State Circuits, vol. 39, No. 3, March 2004, pp. 463-468.

[6] G. Jovanović, M. Stojčev, "Pulsewidth Control Loop as a Duty cycle Corrector, Serbian Journal of Electrical Engineering, Vol. 1, No.2, June 2004, pp 215 – 226.

[7] A Tahri , A Draou , M. Benghanem, "PWM Control techniques for Multilevel cascaded Inverter," Second international conference on Electrical and Electronic Engineering, ELECO2001, Bursa, Turkey, 7-11 November 2001.

[8] A Tahri , A Draou, "A Comparative Modelling Study of PWM control Techniques for Multilevel Cascaded Inverter," Leonardo Journal of Sciences, Issue 6, January-June 2005, pp. 42-58.

[9] Barr, Michael, "Closed-Loop Control," Embedded Systems Programming, August 2002 , pp.55-56.

[10] P. Li, U. Kruger, G. W. Irwin, "Identification of dynamic systems under closed-loop control**,"** International Journal of systems Science, vol. 37, Issue 3, February 2006, pp. 181-195.

Proceedings of 2009 12th International Conference on Computer and Information Technology (ICCIT 2009)
21-23 December, 2009, Dhaka, Bangladesh

Transmembrane Helix Prediction using Feed-Forward Neural Network

M. A. Mottalib, Md. Safiur Rahman Mahdi, A.B.M. Zunaid Haque,
S.M. Al Mamun, Hawlader Abdullah Al-Mamun
Dept. of Computer Science and Information Technology (CIT), Islamic University of Technology (IUT),
Board Bazar, Gazipur-1704, Bangladesh
mottalib@iut-dhaka.edu, mahdi05@iut-dhaka.edu, nashid@iut-dhaka.edu,
sharif05@iut-dhaka.edu, hamamun@iut-dhaka.edu

Abstract

Neural network is one of the successful methods for protein secondary structure prediction. Day to day this technology is modified, improved, even other methods also combined with it to get better result. In this paper we trained feed-forward neural network with transmembrane protein for helix prediction. Using Java Object Oriented Neural Engine (JOONE) our achieved accuracy is 71%. This paper is expected to benefit researchers in proteomics by presenting a summary of developments of neural network in this area.

Keywords: α-helix, bioinformatics, feed-forward neural network, transmembrane protein.

I. INTRODUCTION

Protein structure prediction is the foundation of protein structural biology. Proteins are macromolecules made up from 20 different L-α-amino acids which fold into a particular three-dimensional structure that is distinctive to each protein. This three-dimensional structure is in charge for the function of a protein. The ultimate goal is to understand the function of the protein. So, it is essential to understand the protein structure. Biochemistry refers four distinct aspects of a protein's structure: Primary structure, Secondary structure, Tertiary structure and Quaternary structure. Protein Secondary Structure Prediction (PSSP) means to predict α-helix, β-strand and coils from the amino acid sequence of a protein. A transmembrane protein is a membrane protein that spans from the internal to the external surface of the biological membrane. It comprises over 25% of proteins in complete genomes and plays key roles in diabetes, hypertension, cancer, and many other common diseases. It is essential as it performs communication between cells, communications between organelles and cytosol, ion transport, transport of nutrients.

Over the last 20 years, a huge number of works have been done for predicting secondary structure. A lot of strategies and methods have been used and most of them are probabilistic approach. The statistical methods were the very first method used on known protein structures to predict the protein secondary structure. Chou and Fasman, Garnier averaged the probabilities using small window in 1978 [1], [2]. Kabsch & Sander first defined the 3 categories of protein structure α-helix, β-strand and "other" in 1983 by the DSSP Program [3]. The first attempt of using neural networks in protein secondary structure prediction was done by Qian and Sejnowski at 1988. Later Kneller at 1990 [4] and Stolorz at 1992 [5] used the neural networks in various ways to predict the protein secondary structure. Zhang at 1992 [6] and Maclin and Shavlik at 1993 [7] used combination of neural networks and other methods in prediction. We found different levels of accuracy using varieties of methods. Using JOONE, for helix prediction we got 71% accuracy.

The rest of the paper is organized as follows. Section 2 describes the basic concept of neural network. Section 3 describes on a high level, the methods reviewed and followed by their comparison. Section 4 and 5 describes methodology and result respectively. Finally, section 6 ends with a conclusion.

II. BASIC CONCEPT OF NEURAL NETWORK

The neural network technique is based on the study of biological nervous system. It is the study of building a computer model which is made of large number of simple, highly interconnected computational units (neurons) operates parallel. Each unit combines its input and according to some threshold value it generates output. Initially random connection strengths (weights) and thresholds (biases) are modified in repeated cycles by maximizing the accuracy of secondary structure assignment using the dataset of known protein structure. This is called the "training" phase. After this phase, the learned "knowledge" (which is actually derived weight and threshold value) is used in "test" phase to predict the unknown protein secondary structure. The network is composed of one input layer, one or more hidden layer and one output layer. Input layer encodes a moving window into amino acid sequence and central residue of the window is predicted. The computation is done in each input layer and output layer. The total input "Ei" to unit "i" is,

$$E_i = \sum_j W_{ij} S_j + b_i \quad (1)$$

Where "b_i" is the bias of the unit and the output of each unit "i" is generated by:

$$S_i = F(E_i) = \frac{1}{1+e^{-E_i}} \quad (2)$$

978-1-4244-6283-4/09/$26.00 ©2009 IEEE

After calculating each time the error is predicted using the function

$$E = \sum_{c}\sum_{j}(O_{J,C} - D_{J,C})^2 \quad (3)$$

until the error is reduced to some satisfactory value. The basic neural network model is given below:

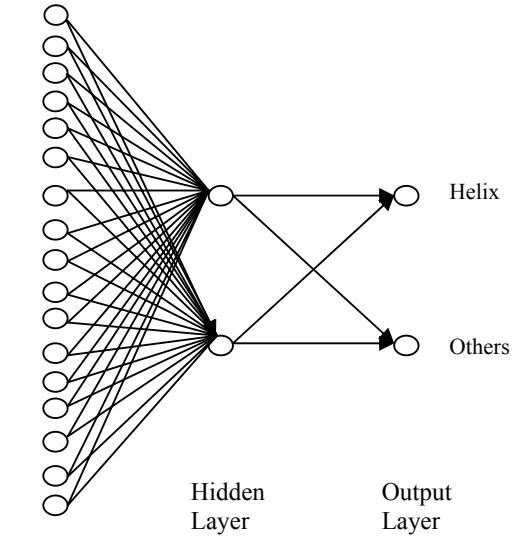

Fig. 1. Basic neural network

III. REVIEW OF PREVIOUS METHODS

Qian and Sejnowski were enormous in introducing a complete new era in protein secondary structure prediction. They used neural networks method which had more accuracy than other previous methods. They gained the accuracy of 64.3%. Qian et al. [8] and Holley et al. [9] worked based on the work of "Kabsch and Sander" [3]. Their work was also quite similar. But Holley et al. gained 63% accuracy which was 1.3% less than Qian et al. In [8] and [9] "supervised learning method" were used which was developed by Rosenblaft (1959) [10] and Widrow and Hoff (1960) [11]. Both [8] and [9] used "Feed forward neural network" and the "Back propagation learning algorithm". Qian et al. took the window size 13 which means the contiguous sequence of 13 amino acids where Holley et al. used the window size of 17. Both of them used 21 inputs. According to [8] the predicted best success rate regarding the number of hidden units is 40. But [9] got their peak success rate in prediction phase taking hidden layer size 2. Though taking more hidden units gave more accuracy to them in training phase but they were poor at test phase. Qian et al. used 3 output positions in the output layer for helix, sheet and coil determination where Holley et al. used only 2 units in output layer. Qian et al. used 106 proteins where subsets of them were used for testing and others were used for training. Other side Holley et al. used 62 proteins. For training first 48 proteins (83158 residues) were used and last 14 proteins (2441 residues) were used as test set. Qian et al. used "artificial structures" before using the real protein database. They measured it with first order artificial structures (no hidden layer) and also second order artificial structures (hidden layers present). They showed effect of noise in data and also effects of irrelevant weights [8]. Holley et al. did not use any artificial structure. They did one additional observation. They excluded the outputs that fall into a range centered near threshold 0.37. By this way they got significant improvement. By taking the strongest 31% of the database the prediction accuracy raise to 79%.They also did physicochemical encoding, means they characterized the amino acids for 48 proteins according to hydrophobicity, charge and backbone flexibility. Hence the accuracy gained for test set of 14 proteins is 61.1%.When they took 20 selected proteins whose structures with resolution better than 2.8 °A , crystallographic R factor less than or equal to 0.25 and sequence homology less than 50%. This case predictive accuracy was 63% and 34% of their strongest prediction was 76% accurate.

A. Over Fitting Problem

Though Qian et al. was more successful until they publish their work, but they had some problem like "over fitting". The problem occurred due to huge number of weight value needed to be deducted.

Rost and Sander, 1993 [12] tried to improve the system proposed by [8]. They used two methods to stop over fitting problem:

- Early stopping which means training stops when the training error is below some threshold.
- And also plotting different inputs in different networks and making average of the outcomes.

The success of [12] in use of alignment, they feed the multiple alignments to the network in profile manner. For every position of amino acid frequency vector is fed to network. The database in [12] used was 150 representative protein chain of known structure. Their database had not more than 30% similarity where, Zhang [6] used database of 49% homologous and Qian et al. used 46% homologous protein. According to Rost et al. the 130 chain is divided into 7 partitions (which is called 7-fold cross validation) and they are calculated separately and making average of their accuracy. Cross validation is important because accuracy is mostly dependent on which set is chosen as test set. Thus they achieved 69.7% of the three states prediction accuracy.

B. Multiple Sequence Alignment

Rost et al. mentioned that with appropriate cutoffs applied in a multiple sequence alignment, all structurally similar proteins can be grouped into a family and approximate structure of the family can be predicted. They

used the known protein structure to make the family in training phase. The family profile of amino acid frequencies at each alignment position was fed into network and they got the prediction accuracy 6% more.

C. Balance Training

The distribution of secondary structure types in globular protein is uneven. Approximately there was 32% α-helix, 21% β-strand and 47% loop in the database. So, prediction of loop was easy. So, Rost et al. tried to train the network in equal proportion and they got better result. Later, they used of 2 level network and got benefit from it. Though Qian et al. also used 2 level network but there was no improvement.

D. Jury of Networks

It is completely new idea by "Rost and Sander". Jury of networks predict by simple majority vote of a set of 12 different networks. Using this they got 2% improvement in overall accuracy. This was an effect of noise reduction which mitigated the bad effects of incomplete optimization. They had the overall accuracy 69.7% which is better than previous methods [8], [9], [6]. They used five prediction methods. The result is shown in Fig 2.

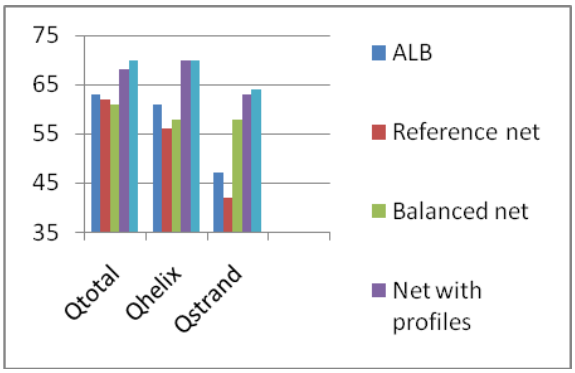

Fig. 2. Testing five secondary-structure prediction methods on the same set of proteins reveals the contribution of different devices to the improvement of accuracy [12].

For completely new protein, 72% of the observed helical and 68% of strand residues was predicted correctly [12] and the overall accuracy was 70.3%. Their method had some limitations too. The result is very poor with non-homologous protein and it is not applicable for membrane, non globular or non-water soluble proteins. They did their method of sequence profiles and neural networks at 1993. Soren et al. used a method, using structural neural network and multiple sequence alignments at 1996 [13]. First, they used "single structured network" and got the accuracy 66.3%. After that, they applied multiple sequence alignment and the accuracy become 71.3%. They used the database of 126 non-homologous globular proteins and 72% residue of the database gave 82% of prediction accuracy [13]. They got the accuracy of 66-67% in single sequence prediction which was 3-4% better than "fully connected network" method. After completing the whole system the result become 71.3% which was quite identical to Rost et al.

E. Genetic-Neural System

Recently a Hybrid Genetic-Neural System has been introduced by Armano et al. in 2005 [14]. They made a system MASSP3 (Multi agent Secondary Structure Prediction with Post-processing) which does the overall processing. They used "Feed forward ANN" layer that performs a structure-to-structure prediction. Armano et al. [14] used the same database as [15] where the training set contains 1180 sequence obtained for PDB database. Their proteins were more than 25% homologous. In their test set there were 126 non-redundant protein and they used the moving window of size 15. Several Experiments were performed by them:

E.1. Optimization of Genetic Experts

They used 600 experts which were randomly generated by guards [14]. They used BLAST-based encoding to get the input. Their hidden layer contained 10-25 neurons and they used back-propagation algorithm. They also filtered inputs by guards. The accuracy they got is 69.1%.

E.2. Input Encoding

The population was evolved using covering, single point crossover and mutation operations. The GA performed 60 epochs and the final population contained 550 experts. They filtered the population by removing those who did not match more than 0.1% of the overall inputs used for training. The result was obtained 71.8% accurate.

E.3. Expert's Specialization Technique

In this technique, the training was done over whole database for first 5 epochs. In the next epochs only inputs selected by guard were feed. This way the accuracy is raised to 73.2%.

E.4. Post-Processing Technique

The most successful one and Armano et al, emphasized most on this. It had a single MLP with moving window of 21 amino acids. They used Low pass Gaussian filter ($\sigma = 0.5$) to encode the output of Multiple experts. The improved accuracy is raised to 76.1%. The improvement is shown in table I.

Table I Results on the rs126 test set in accordance with the training strategies and encoding techniques that have been experimented [14]

Experiment	Accuracy
Random population	69.1
Generally-selected population	71.8
Improved experts' specialization technique (global + local)	73.2
Using PSI-BLAST profiles	74.7
Using post-processing	76.1

IV. METHODOLOGY

In this section, we describe the test set and the results we obtained for the prediction of the transmembrane helix using feed-forward network. For experimenting we have used a component based neural network framework built in Java named Java Object Oriented Neural Engine (JOONE).

A. Data Set

For the protein data we used transmembrane protein from the PDB (Protein Data Bank) data sets. We have classified the protein according to their structure, their size and their hydrophobicity. If the particular residue is helix then we have given 1 as the output value, otherwise 0. Table II shows the classification.

Table II Amino acid classification

Criteria	Amino Acids	Value
Electrically charged Side chain	Arg, His, Lys, Asp, Glu	0;0
polar but uncharged side chains	Ser, Thr, Asn, Gln, Tyr	0;1
Special cases	Cys, Gly, Pro	1;0
with hydrophobic side chains	Ala, Ile, Leu, Met, Phe, Trp, Val	1;1

B. Training with JOONE

We have trained 20 transmembrane proteins with JOONE. We have taken 2 nodes in input layers, 3 nodes in hidden layers, 1 node in output layer, learning rate 0.9, momentum 0.1, and epochs 10000. Table III shows the parameters used in the simulation and Fig 3 shows the network.

Table III Parameters used in experiments

Parameter	Value
Training pattern	4980
Epochs	10000
Learning rate	0.9
Momentum	0.1

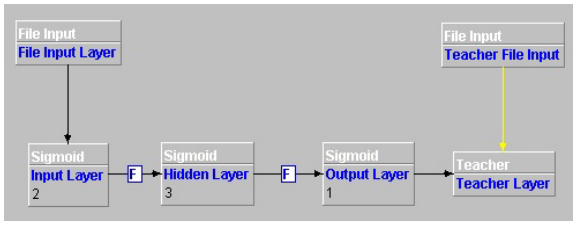

Fig. 3. Feed-forward network used in JOONE.

V. RESULT and DISCUSSION

We have tested the network with 1R2N, 1MGY, 1JV6, 1S8J and other similar tansmembrane proteins. In total, there are 1456 residues of helix and the network predicts 1048 of them including 186 false positive. So the accuracy is 71%. Accuracy varies with the number of nodes in input layer and sequence similarity of training proteins. Fig 4 shows the learning curve.

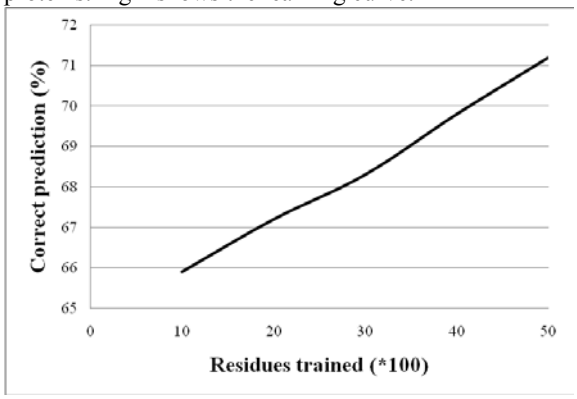

Fig. 4. Learning curve for feed-forward network. The percentage of correct predicted helix is plotted as a function of the number of amino acids presented during training.

VI. CONCLUSION

In this paper, we worked with only helix prediction. Here, we used the feed-forward network architecture. Future experiment can be done which includes helix and sheet for a complete secondary structure prediction. Still many challenges remain, requiring the development of alternate strategies to complement/improve existing techniques.

REFERENCES

[1] P. Y. Chou and G. D. Fasman, "Prediction of the secondary structure of proteins from their amino acid sequence," *Advanced Enzymol*, 1978, pp. 47, 45-148.

[2] J. Garnier, D. J. Osguthorpe, and B. Robson, "Analysis of the accuracy and implications of simple methods for predicting the secondary structure of globular proteins". *Journal of Molecular Biology*, 1978, 120:97-120.

[3] W. Kabsch and C. Sander, "Dictionary of protein secondary structure: pattern recognition of

hydrogen-bonded and geometrical features." *Biopolymers*, 1983a, pp. 2577 - 2637.

[4] D. Kneller, F. Cohen, and R. Langridge, "Improvements in protein secondary structure prediction by an enhanced neural network," *Journal of Molecular Biology*, 1990.

[5] P. Stolorz, A. lapedes, and Y. Xia, "Predicting protein secondary structure using neural net and statistical methods," *Journal of Molecular Biology*, 1992.

[6] X. Zhang, J. Mesirov, and D. Waltz, "Hybrid system for protein secondary structure prediction," *Journal of Molecular Biology*, 1992.

[7] R. Maclin and J. Shavlik, "Using knowledge based neural networks to improve algorithms: Refining the chou-fasman algorithm for protein folding," *Journal of Molecular Biology*, 1993.

[8] N. Qian and T. J. Sejnowski, "Predicting the secondary structure of globular proteins using neural network models," *Journal of Molecular Biology*, 1988.

[9] H. L. Holley and M. Karplus, "Protein secondary structure prediction with a neural network," Proc. Natl. Acad. Sci.USA, 1989.

[10] F. Rosenblatt, "Mechanization of thought processes," *Journal of Molecular Biology*, vol. 1, 1959.

[11] R. M. Widrow and M. E. Hoff, "In institute of radio engineers, western electronic show and convention," Convention Record, part 4, pp. 96–104, 1960.

[12] B. Rost and C. Sander, "Improved prediction of protein secondary structure by use of sequence profiles and neural networks," in National Academy of Sciences of the United States of America, 1993a.

[13] S. kamaric Riis and A. Krogh, "Improving prediction of protein secondary structure using structured neural networks and multiple sequence alignments," *Journal of Computational Biology*, 1996.

[14] G. Armano, G. Mancosu, L. Milanesi, A. Orro, M. Saba, and E. Vargiu, "A hybrid genetic-neural system for predicting protein secondary structure," BMC Bioinformatics, 2005.

[15] G. Pollastri, D. Przybylski, B. Rost, and P. Baldi, "Improving the prediction of protein secondary structure in three and eight classes using neural networks and profiles," *Proteins*, 2002.

Proceedings of 2009 12th International Conference on Computer and Information Technology (ICCIT 2009)
21-23 December, 2009, Dhaka, Bangladesh

An Adoption-Diffusion Model for RFID Applications in Bangladesh

M A Hossain and M Quaddus
Graduate School of Business, Curtin University of Technology
78 Murray Street, Perth, WA 6000, Australia
mohammed.quaddus@gsb.curtin.edu.au

Abstract

Radio Frequency Identification (RFID) technology is at its early stage of adoption in Bangladesh with a few business applications and pilot studies. It is expected that the next stage will be the organizational adoption and diffusion in more applications inspired by business cases. Eventually, the adoption will drive this technology into 'extended use' stage provided that the adopters and users are 'satisfied'. At this moment the RFID initiative is discrete in Bangladesh and do not have any long-term strategy leading into implementation-to-diffusion process. Without having a clear strategy to achieve large scale diffusion discrete RFID adoption may not inspire the process in reaching the full potential of RFID. This study, therefore, investigates the factors influencing the adoption diffusion of RFID and its extended use process; and then proposes a conceptual framework. The framework is an objective integration of innovation-diffusion theory and expectation-confirmation theory, with some logical modifications. It posits that while adoption of RFID is important but the long-term viability of RFID and its ultimate success depends on its continued and extended use, which is judged against 'satisfaction' and 'performance' derived from RFID. The implications of the framework in the context of Bangladesh are discussed.

Keywords: RFID, adoption, diffusion, extended use, Bangladesh

I. INTRODUCTION

Radio Frequency Identification (RFID) is one of the most effective enabling technologies which identifies an object automatically and uniquely and keep the desired data which can later be retrieved as information. Because of its enormous capabilities RFID has drawn the attention of the innovation architects and experts in recent years. Now-a-days, RFID technology is used extensively from supply chain management to animal tracking to Olympic Games [37]. Primarily and most significantly, the revolution of RFID technology started with the mandate from Wal-Mart and Department of Defense (DoD) to their suppliers. Eventually this pressure was intensified with supermarket giants Tesco, and Metro, and markets like Japan, European Union for livestock products. Therefore to save the local businesses, meat and livestock market as an example, many counties including Australia, Canada, and Uruguay im- ng systems.

978-1-4244-6283-4/09/$26.00 ©2009 IEEE

However, though the applications and deploying-organizations are different in nature but the basic objective is quite similar: tracking and tracing the object in real-time and additionally get as much data as required; quickly and authentically.

Though RFID technology existed since 1939, it has matured during the 1980s and early 1990s [34] and is still considered as an "innovation" [4] or "world's oldest new technology" because of its continuous exploration in newer applications. However, research on the behavioral aspect of RFID adoption diffusion is scarce except the study by Hossain and Prybutok [15] where consumer acceptance of RFID using students as subjects was investigated. In the context of Bangladesh, business enterprises do not have any RFID adoption diffusion model to follow and gain confidence in implementing this technology effectively. This article thus addresses and attempts to close this gap. Equipped with a background theory of adoption and diffusion of innovation this article develops a conceptual framework to examine and identify the factors affecting the adoption-diffusion and extended use of RFID which would answer the following research questions:

1. What are the factors that influence the adoption and diffusion of RFID technology in Bangladesh?
2. What are the factors that influence the continued and extended use of RFID?

II. CURRENT STATUS AND POTENTIAL APPLICATION OF RFID ADOPTION IN BANGLADESH

Bangladesh is a country of possibilities and planning to be 'digital Bangladesh' [1]. Unfortunately, despite the extreme potential of RFID applications in many areas, it is far beyond to be adopted and diffused extensively in Bangladesh. The reasons are multifold: insufficient government concern and support, scarcity of business cases and entrepreneurs, lack of strong science and technology-base and business champions. However, some start-up RFID hardware and software providers initiated the process [35]. The early adopters are Apollo Hospital and Bangladesh Army. Here we briefly review some of RFID and related applications in Bangladesh.

E-Passports: International Civil Aviation Organization has mandated that by 2014 all 190 member countries [18] must complete issuing electronic passports (e-

passports), embedded with RFID chips. At least 75 countries already have introduced the e-passports while others are on their way. However, Bangladesh is migrating to Machine Readable Passports (MRP) to comply with the minimal mandatory specification, which must need to be in action by April 2010. Bangladesh allocated BDT 283 crores [32] and already has issued 3.8 million MRPs until 2008. However, strategically it would be wiser to start the e-passports project straightaway instead of going via MRPs.

National ID Cards: One of the biggest challenges in Bangladesh is to identify a person uniquely from its 153 million citizens [7]. To this end, in 2007 Bangladesh Election Commission took a project and allocated BDT 547 crores [41] for voter registration and have already registered more than 80 million citizens using biometric face and fingerprint technology [11]. The voter registration process is believed to provide data for other national policies such as national ID card, and birth and death registration process. However, this project could be made better if an RFID chip were attached with the voter ID so that it would additionally serve as a driver's license, travel document to allied countries and as a card for public facilities like public transport, electronic toll payment, utility bill payment, tax return, access control, medical record and so on. Currently, Bangladesh Army has planned to employ RFID technology to track soldiers and visitors entering its Dhaka Cantonment and a prototype has been demonstrated for such a system [2]. Similar type of system can be installed for sensitive places including Secretariats, Courts, ports and concerts to trace-back any terrorist activities.

Healthcare Industry: To reduce the human errors hospitals all around the world started using wristbands, embedded with RFID chips, for identifying patients automatically and providing necessary surgical procedures and medication to the patients [5]. There is a huge potential of RFID technology in Bangladesh for its more than 1683 hospitals [40]. Apollo Hospital is, however, one of the early adopters in Bangladesh which implemented RFID technology to track employees' attendance and have plans to apply it in payrolls [2]. It is expected that Apollo will be the first hospital in Bangladesh that will use RFID for patient care and hopefully other hospitals will be inspired by Apollo's initiative.

Supply Chain: Garments sector's contribution to the Bangladesh's export earnings is around 74 percent [30]. It could gain more importers' confidence if the pallets or containers had RFID tags so that the products could be tracked in real-time. However, RFID has been tested in garment items in Bangladesh with an order from Germany [10]. Though the pilot test was for optimizing the most appropriate position of the tag, the application can be made throughout the supply chain, in future.

Other applications: In Bangladesh, as the mobile communication infrastructure is more prevalent than fixed-line infrastructure RFID does have a huge potential to be applied for mobile (electronic) payment where the customers need to carry just a card (Smart Wallet) and go to the nearest RFID booth to make the payment. RFID can be a good solution to spot unauthorized vehicle with fake registration plate. A system-architecture has been proposed recently to track the unauthorized vehicles in Bangladesh [14]. Other potential applications will be materials tracking in manufacturing industry [22], car rental system [16], public and private transportation system [20], vehicle parking [28], container depot [23], toll collection, library, automobile immobilizer and traffic controlling system. These types of automated asset management system hopefully will contribute in reducing corruptions in Bangladesh and provide more accountability through RFID based access control systems.

Above paragraphs highlight some current and potential applications of RFID in Bangladesh. However, as pointed out earlier, enterprises/corporations/government bodies in Bangladesh need to understand various factors which may enhance the adoption, diffusion and extended use of RFID. We propose a conceptual framework to this end which is based on several theoretical lenses.

III. THEORETICAL BACKGROUND

While initial acceptance and adoption of an innovation is important in realizing innovation success, long-term viability of an innovation and its ultimate success depends on its *continued* use rather than *first-time* use [3]. Even though adoption is a prerequisite for usage, factors that affect adoption may have the opposite effect on decisions for continued use of the innovation [38]. In literature no model explains the initial adoption and further diffusion and extended use behavior in a single frame. The present study, therefore, combines the 'innovation-diffusion theory' (IDT) and 'expectation-confirmation theory' (ECT), which is further refined using theoretical and empirical findings from prior literature, in developing a theoretically grounded, comprehensive framework to investigate the antecedents of the behavioral intention in RFID use.

A. Innovation-Diffusion Theory (IDT): An "innovation is the adoption of a change which is new to an organization and to the relevant environment" [19, p. 467]. Diffusion is "the process by which an innovation is communicated through certain channels over time among the members of a social system" [31, p. 5]. Therefore RFID can certainly be explained by IDT.

IDT proposes that potential adopters of an innovation must gain some knowledge about the innovation, then be persuaded of its value, decide to adopt and implement it, and confirm the decision to adopt the innovation [31]. But for pursuing the maximum benefits, mere-

ly adoption of RFID is not sufficient rather it is necessary to institutionalize this technology into routine operations and practices and extend its use to different applications, where possible and/or suitable and/or profitable [31], [33]. The continued and extended use behavior is different from and possibly more important than its initial adoption because many RFID adopters are initially driven by mandatory pressure and then later choose different level of uses depending on their internal judgments. IDT is silent explaining how the adopters go to the next stage of diffusion and to further 'innovative' application of the innovation. Moreover, IDT is primarily based on individual-level adoption decisions [9] but RFID adoption needs to be examined from government and organizational perspectives because it involves many national policies and requires modification of organizational structures and operations.

B. Expectation-Confirmation Theory: Expectation Confirmation Theory (ECT) is widely used in the consumer behavior literature to study consumer satisfaction and post-purchase behavior. The post-purchase behavior is somewhat related to the continued and extended use characteristics of an innovation. The process by which consumers reach repurchase intentions in an ECT framework is as follows [25, p. 462]. First, buyers form initial expectation of a specific product or service prior to purchase. Second, consumption reveals a perceived quality level which is influenced by expectations. Third, they determine the extent to which their expectation is confirmed. Fourth, they form a satisfaction based on their confirmation level and expectation. Finally, satisfied consumers form a repurchase intention, while dissatisfied users discontinue its subsequent use.

In ECT, *expectation* acts as the frame-of-reference to measure *confirmation* and *satisfaction*. ECT, however, does not explain the basis of expectations and ignores the driving forces behind adopting a product/service or an innovation. It ignores the mandatory introduction of a product/service rather is based on voluntary decisions. In a mandatory system the *expectations* are shaped and biased by the imposing authority and therefore is not an independent variable as proposed in ECT.

IV. CONCEPTUAL FRAMEWORK

Building on Rogers's IDT (1995) and Oliver's ECT (1980), this study suggests a conceptual framework of factors and variables that will enhance adoption, diffusion and extended use of RFID. The conceptual framework is shown in Fig. 1. Basically this framework suggests that some external factors contribute to the knowledge about RFID and subsequently its adoption. Expectation about RFID grows in parallel with the knowledge creation. This expectation is the baseline to confirm the innovation which affects the satisfaction about the innovation. Finally the satisfied adopters diffuse the innovation and apply it for extended use while the dissatisfied adopters may either reject or use it for limited operations(s). Thus the framework is presented in two parts: *External factors →Knowledge →Adoption and Implementation;* and *Expectations →Confirmation → Satisfaction→ Continued and Extended use.* We propose to use this conceptual framework to study the variables that influence the adoption, diffusion and extended use of RFID in the context of Bangladesh. Fig. 1 depicts the complete model while Table I presents the important variables with their type and a brief explanation.

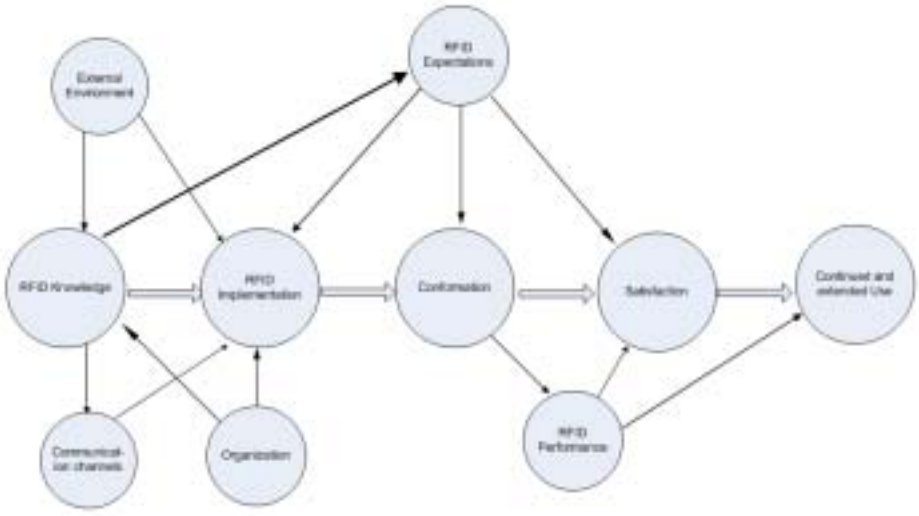

Fig. 1: Proposed Framework of RFID Adoption, Diffusion and Extended Use

Table I: Important Variables of RFID Adoption-Diffusion and Extended Use Framework

Variables related to	Variable type	Brief explanation
RFID Knowledge	Independent	RFID knowledge explains the degree of knowledge in the field of RFID that an adopter has acquired from theory and practice. Basic, technical and technological RFID knowledge is important for RFID adoption-diffusion. The degree of acquiring RFID knowledge depends on the influence of the external environment, communication channels and organization characteristics. RFID knowledge is expected to contribute forming 'RFID expectations' and also offers the implementation decisions.
External Environment	Independent	External environment is the 'global' controls where organizations operate and is beyond organizations' control. Organizations acquire RFID knowledge and RFID implementation decisions because of *government* policies [17], [21] and *market* control factors [12], [17].
Communication Channels	Independent	RFID facts and factors are transmitted though communication channels in different ways including magazine, newspaper, TV/radio programs (mass media channels) or though casual chats or meeting, seminar, workshop. These channels contribute the adopters in gaining RFID knowledge and taking implementation decisions.
Organization	Independent	Many studies found that the characteristics of organizations, such as *location, industry type, organizational readiness* and *organizational networks* are significant determinants of innovation adoption [17], [38] and thus expected to RFID adoption as well.
RFID Implementation	Mediating	RFID implementation process consists of 'RFID implementation decision' and 'actual implementation'. RFID implementation decision, sometimes, can be mandated by the external environment while the actual implementation is influenced by *RFID knowledge*, *expectations*, *organization*'s decision and *communication channels* [42] as the depth of implementation is decided based on organization's own judgment.
RFID Expectations	Independent	RFID expectations are the perceived characteristics of RFID that influence RFID implementation decisions and act as the basis in determining *confirmation* and *satisfaction*. IDT empirical researches found that *compatibility*, *complexity* and *relative advantage* [29] are consistently used attributes of innovations and are also considered to be appropriate for RFID. Some other expectations are also relevant for RFID adoption-diffusion such as *profitability*, *cost* [29], *risk* and *uncertainty*.
Confirmation	Mediating	Confirmation is the evaluation of *actual experience* with *expectations*. Confirmation results when the perceived performance matches the standards, whereas disconfirmation results from a mismatch. Studies found confirmation as one of the key variables affecting consumer satisfaction [8], [13].
Performance	Independent	Performance is the "manner of functioning or operating" which is viewed from general, technical, and financial contexts. Studies [27, for example] found that performance has a direct effect on satisfaction. Therefore, this study posits that *performance* affects the *satisfaction* about RFID.
Satisfaction	Mediating	ECT holds that consumers' intention to repurchase a product or continued use is determined primarily by their satisfaction [25], [26]. This study posits that the satisfaction is judged by the *confirmation*, *expectations* and *performance* of RFID.
Continued and Extended Use	Dependent	Based on users' satisfaction level, satisfied adopters may reject the RFID use (provided that the application is not mandatory by law and/or if it a business requirement they may decide not to do that business) or they might decide to diffuse it in current application only or to decide to go for extended use of RFID in other applications [3], [25], [26].

V. FUTURE DIRECTIONS AND CONCLUSIONS

Though most of the companies in Bangladesh are small-to- medium scale enterprises and are apprehensive of the high cost of deployment associated with RFID applications, and the unavailability of proper infrastructure; RFID vendors and adopters should sense a huge opportunity where the early adopters may hope for a quick return on investment.

This paper reviews some current and prospective applications of RFID in the context of Bangladesh. It then proposes a conceptual framework to study the variables which will enhance the adoption, diffusion and extended use of RFID. This paper will thus give the practitioners new insights at the operational level as well assist with strategic decisions about effective diffusion policies and RFID investments in Bangladesh.

The framework like presented in this paper has not been well explored in the literature. Future studies could test the entire framework as a research model. Parts of the framework could also be extracted and investigated in detail. The model, including both of its main constructs and sub-constructs can be taken and/or fine-tuned to do a comprehensive survey by the researchers. Organizations that are embarking on RFID adoption can use the constructs and factors of the study and do an internal audit to find out how they fare in terms of RFID implementation with respect to these constructs and factors. The proposed model also provides guidelines to RFID adoption-diffusion practitioners and consultants.

REFERENCES

1.Azad, A. A. (2009). Bangladesh is looking towards digital era. The Brunei Times. Brunei.

2. Bacheldor, B. (2008). "RFID takes root in Bangladesh" Retrieved 14/07/2009, 2009, from http://www.rfidjournal.com/article/articleview/3852/1/1/.

3. Bhattacherjee, A. (2001). "Understanding information systems continuance: an expectation-confirmation model" MIS Quarterly **25**(3): 351-370.

4. Chan, S. I. , S. Y. Hung, et al. (2008). "The determinants of RFID adoption in the logistics industry - a supply chain management perspective," The Communications of the Association for Information Systems **23**(12): 197-218.

5. Chen, C. C., J. Wu, Y. S. Su, S. C. Yang (2008). "Key drivers for the continued use of RFID technology in the emergency room" Management Research News **31**(4): 273-288.

6. Churchill, G. A. and C. Surprenant (1982). "An investigation into the determinants of customer satisfaction" Journal of Marketing Research **19**(4): 491-504.

7. CIA (2009). "The World Fact book" 2009, from https://www.cia.gov/library/publications/the-world-factbook/print/bg.html.

8. Deighton, J. (1984). "The interaction of advertising and evidence" Journal of Consumer Research **11**: 763-770.

9. Eveland, J. D. and L. G. Tornatzky (1990). The process of technological innovation. The Development of Technology, Lexington, MA: Lexington Books.

10. Freitag, M., E. Morales, et al. (2004). RFID technology enables autonomous logistic processes. 42-44.

11. Government-Technology (2008). "Bangladesh voter registration project using biometrics to detect and prevent duplicate registrations" Retrieved 14/07/2009, 2009, from http://www.govtech.com/gt/570230?topic=117691.

12. Grover, V. (1993). "An empirically derived model for the adoption of customer-based interorganizational systems" Decision Sciences **24**(3): 603-640.

13. Hoch, S. J. and Y. W. Ha (1986). "Consumer learning: advertising and the ambiguity of product experience" Journal of Consumer Research **13**: 221-233.

14. Hossain, M. F., M. K. Sohel, et al. (2009). Designing and implementing RFID technology for vehicle tracking in Bangladesh. National Conference on Communication and Information Security, Dhaka, Bangladesh.

15. Hossain, M. M. and V. R. Prybutok (2008). "Consumer acceptance of RFID technology: an exploratory study" IEEE Transactions on Engineering Management **55**(2): 316-328.

16. Huang, K. and S. Tang (2008). RFID applications strategy and deployment in bike renting system; 10th International Conference on Advanced Communication Technology.

17. Iacovou, C. L., I. Benbasat, et al. (1995). "Electronic data interchange and small organizations: adoption and Impact of Technology" MIS Quarterly **19**(4): 465-485.

18. ICAO (2009). "International Civil Aviation Organization (ICAO)." from http://www.icao.int/cgi/statesDB4.pl?en.

19. Knight, KE (1967). "A descriptive model of the intra-firm innovation process" The Journal of Business **40**(4): 478-496.

20. Kovavisaruch, L. and P. Suntharasaj (2007). Converging technology in society: opportunity for

Radio Frequency Identification (RFID) in Thailand's transportation system. Portland International Center for Management of Engineering and Technology.

21. Kuan, K. and P. Chau (2001). "A perception-based model of EDI adoption in small businesses using technology-organizational-environmental framework" Information and Management **38**(8): 507-521.
22. Min, Z., L. Wenfeng, et al. (2007). A RFID-based material tracking information system. IEEE International Conference on Automation and Logistics**:** 2922-2926.
23. Ngai, E. W. T., T. C. E. Cheng, S. Au and Kee-hung Lai (2007). "Mobile commerce integrated with RFID technology in a container depot" Decision Support Systems **43**(1): 62-76.
24. Niederman, F., R. G. Mathieu, et al. (2007). "Examining RFID applications in supply chain management" Communications of the ACM **50**(7): 92-101.
25. Oliver, R. L. (1980). "A Cognitive model for the antecedents and consequences of satisfaction decisions" Journal of Marketing Research **17**: 460-469.
26. Oliver, R. L. (1993). "Cognitive, affective, and attribute bases of the satisfaction response" Journal of Consumer Research **20**(3): 418-430.
27. Oliver, R. L. and W. S. DeSarbo (1988). "Response determinants in satisfaction judgments" Journal of Consumer Research **14**(4): 495-507.
28. Pala, Z. and N. Inanc (2007). "Smart parking applications using RFID technology" RFID Eurasia: 1-3.
29. Premkumar, G. and M. Roberts (1999). "Adoption of new information technologies in rural small businesses" Omega International Journal of Management Science **27**(4): 467-484.
30. Quddus, M. and S. Rashid "Garment exports from Bangladesh: an update and evaluation" available at *www.aedsb.org/JBS1art3.doc*
31. Rogers, E. M. (1995). Diffusion of Innovation, Free Press, New York.
32. Sabir, I. (2009). E-passports for Bangladesh: some thoughts. The Independent. Dhaka.
33. Saga, V. L. and R. W. Zmud (1993). The nature and determinants of IT acceptance, routinization, and infusion. IFIP TC8 Working Conference on Diffusion, Transfer and Implementation of Information Technology, Elsevier Science Inc. New York, NY, USA
34. Shepard, S. (2005). RFID: Radio Frequency Identification. NY, McGraw Hill.
35. Source-Security (2009). "RFID companies in Bangladesh" 2009, from http://www.sourcesecurity.com/companies/search-results/company-search/pa.rfid,c.bangladesh.html.
36. Sullivan, L. (2004). "RFID technology could be used to build a national livestock-tracking system", from http://www.informationweek.com/news/management/showArticle.jhtml?articleID=17300330.
37. Susanzheng (2007). "Beijing Olympic Games prompts RFID development in China" 2009, from http://www.networkworld.com/community/node/18988.
38. Tornatzky, L. G. and K. J. Klein (1982). "Innovation characteristics and innovation adoption-implementation: a meta-analysis of findings" IEEE Transactions on Engineering Management **29**(1).
39. Tse, D. K. and P. C. Wilton (1988). "Models of consumer satisfaction: an extension" Journal of Marketing Research **25**(2): 204-212.
40. Unknown (2007). Statistical pocket book Bangladesh - 2007. Bangladesh Bureau of Statistics.
41. Unknown (2009). Electoral roll with photograph Project, Bangladesh Election Commission.
42. Wu, N. C., M. A. Nystrom, et al. (2006). "Challenges to global RFID adoption" Technovation **26**: 1317-1323.
43. Zhu, K., K. Kraemer, et al. (2003). "Electronic business adoption by European firms: A cross-country assessment of the facilitators and inhibitors." European Journal of Information Systems **12**: 251–268.
44. Zmud, R. W. (1983). "The effectiveness of external information channels in facilitating innovation within software development groups". MIS Quarterly **7**(2): 43-58.

Proceedings of 2009 12th International Conference on Computer and Information Technology (ICCIT 2009)
21-23 December, 2009, Dhaka, Bangladesh

Central Base-Station Controlled Density Aware Clustering Protocol for Wireless Sensor Networks

Mst.Jannatul Ferdous, Jannatul Ferdous, Tanay Dey
Khulna University of Engineering and Technology
shumi_31@yahoo.com, lips_cse@yahoo.com, dtanay_2004@yahoo.com

Abstract

As wireless sensor networks are equipped with sensor nodes which have a limited energy and sensing capabilities, a good routing protocol must be designed to make the network energy efficient. In this paper, we propose a centralized routing protocol called Central Base Station Controlled Density Aware Clustering Protocol (CBCDACP) where the base station centrally performs the cluster formation task. In this protocol, an optimum set of cluster heads are selected by using a new cluster head selection algorithm focusing on both the density of the sensor nodes and the minimum distances among the cluster head and its neighbor nodes. The performance of CBCDACP is then compared with some prevalent clustering-based schemes such as Low Energy Adaptive Clustering Hierarchy (LEACH), Centralized LEACH (LEACH-C). Simulation results show that CBCDACP can improve system life time and energy efficiency in terms of different simulation performance metrics over its comparatives.

Keywords: Wireless Sensor Networks, setup phase, sensor density, density factor, cost function, steady-state phase.

I. INTRODUCTION

A wireless sensor network (WSN) is a wireless network consisting of spatially distributed autonomous devices using sensors to cooperatively monitor physical or environmental conditions, such as temperature, sound, vibration, pressure, motion pollutants, at different locations. Wireless sensor networks consist of hundreds to thousands of low-power multi functioning sensor nodes, operating in an unattended environment with limited computational sensing capabilities. The many randomly sited sensor nodes are used to gather meaningful information in the inaccessible area. Because of the two key resources**:** communication bandwidth and energy are more limited than in a tethered network environment, the design of Wireless Sensor Networks is a paramount challenge. In wireless sensor networks, the sensor nodes are equipped with small, often irreplaceable, batteries with limited power capacity [1]. The sensor nodes sense data and then send to the control center or the central base station from where the end user can access this data. For the transmission of different amount of data the nodes lose a certain amount of energy and since the nodes are energy constrained, so energy efficiency is the main issue in the design of wireless sensor networks.

In this paper, we propose a clustering-based routing protocol called Centralized Base-station Controlled Density Aware Clustering Protocol (CBCDACP) where base station performs the most energy intensive task of cluster formation. The nodes having higher Density Factor (DF) are selected as cluster head so that the energy consumption is minimized as well as network lifetime is maximized.

The remaining part of the paper is organized as follows: related work is briefly discussed in Section II. In Section III, we discuss the network and radio models. Section IV describes CBCDACP routing protocol in detail. In Section V, we simulate the proposed protocol by using NS-2 simulator and compare its performance with other prevalent ones. Finally, we present our conclusion in Section VI.

II. RELATED WORK

Since both device and battery technologies have only recently matured to the point where microsensor nodes are feasible, this is fairly new field of study. Researchers have begun discussing not only the uses and challenges facing sensor networks but have also been developing preliminary ideas as to how these networks should function as well as the appropriate low-energy architecture for the sensor nodes themselves [2].

Recently, there have been working on some application specific power aware routing protocols for wireless sensor networks. In minimum-transmission-energy protocol (MTE), nodes route data destined ultimately for the base station through intermediate nodes. The intermediate nodes are chosen such that the transmission energy is minimized. In Static-Clustering protocol first clusters are formed and remain unchanged for the entire system. The static clustering protocol is identical to LEACH except the clusters are chosen a-priori and fixed. As the cluster heads are fixed, so the network life time is low as the cluster heads die after a few rounds.

To alleviate this deficiency, an application specific routing protocol LEACH (Low-Energy Adaptive Clustering Hierarchy) [2] is developed. LEACH forms clusters by using a distributed algorithm, where nodes make autonomous decisions without any centralized intervention. In LEACH, distributed cluster formation can be done without knowing the exact location of any of

978-1-4244-6283-4/09/$26.00 ©2009 IEEE

the nodes in the network. Cluster heads are selected depending on a probability so that optimum set of cluster cannot be found.

In order to produce a better cluster by dispersing the cluster head nodes throughout the network a central control algorithm called LEACH-C is developed. Unlike the LEACH, LEACH-C utilizes the central base station for the formation of cluster heads. During set-up phase of LEACH-C, each node sends information about its current location and energy level to the BS (base station). BS computes the optimal cluster head sets based on this information using the simulated annealing algorithm [3]. For determining the optimal cluster heads, the simulated annealing algorithm calculates cost based only on the distance among the nodes in the network. So it does not determine the optimal cluster head set for a round.

III. NETWORK AND RADIO MODELS

A. The Network Model and Architecture

In CBCDACP, it was assumed that the base station is a high energy node with a large amount of energy supply. So to do the most energy intensive task base station (BS) was utilized in this protocol. In CBCDACP, a sensor network model was considered like [1] with the following properties:

- The base-station is fixed and located far away from the sensor nodes.
- The sensor nodes are energy constrained with a uniform initial energy allocation.
- The nodes are equipped with power control capabilities to vary their transmitted power.
- Each node in sensor network senses the data at a fixed rate and always has data to send to the base station.
- All sensor nodes are immobile.

B. The Radio Model

A typical sensor node consists of four major components which are a data processor unit, a micro-sensor, a radio communication subsystem that consists of transmitter or receiver electronics, antennae and an amplifier and a power supply.

As shown in the figure 1 the sensor nodes are equipped with these components [1]. Although energy is dissipated in data processor unit, microsensor and radio communication subsystem but here we only considered the energy dissipation in radio communication subsystem as the main objective of this paper was to maximize the network lifetime by developing an energy efficient network layer protocol.

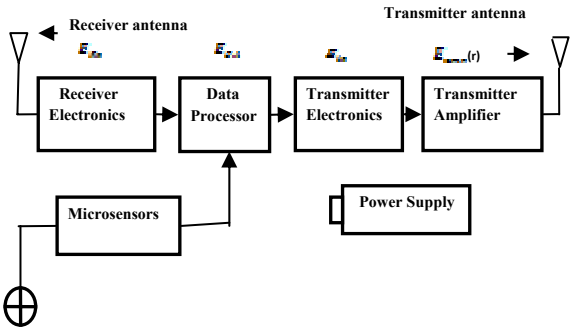

Figure 1: Radio Energy Dissipation Model

In this radio model, the energy consumed throughout the entire sensor network can be described as the energy consumption for data transmission E_{tx}. So the energy dissipation for transmitting data from a node to another node

$$E_{tx} = E_{amplify} + E_{processing} \quad (1)$$

Like [2], here we considered both the free-space model (d^2 power loss) and multi-path model (d^4 power loss).The free-space model was used for the communication between the cluster-head and the member nodes. According to the models the energy dissipation for transmitting *L*-bit message over a distance *D* is

$$E_{amplify}(L,D)=L\varepsilon_{fs}D^2 \quad : D< d_0 \quad (2)$$

$$E_{amplify}(L,D)=L\varepsilon_{mp}D^4 \quad :D\geq d_0 \quad (3)$$

Where, ε_{fs}=10pJ/bit/m^2 , ε_{mp}= 0.0013pJ/bit/m^4 and the threshold distance d_0=86.2 m.

In free space model, the transmission energy consumed is proportional to the square of the communication distance between the two communicating nodes (2). And for the communication between the cluster head and the base station multipath fading model (3) is used [4].So the total energy consumed in every round in the entire sensor network can be expressed by the following equation**:**

$$E_{total}= \sum_{i=1}^{N} E_{chead}(i) + \sum_{i=1}^{N_{total}-N_{chead}} E_{tx}(i) + N_{total}E_{sense} \quad (4)$$

Where E_{total} is the total energy consumed in each round, $E_{chead}(i)$ is the energy dissipated for data aggregation and data transmission to the base station of the i^{th} cluster head, E_{sense} is the energy dissipated for sensing data of a sensor node, N_{total} is the total number sensor nodes and N_{chead} is the number of cluster head at each round.

IV. PROPOSED CBCDACP PROTOCOL ARCHITECTURE

In CBCDACP, the clusters are formed using the central control algorithm by dispersing the cluster head nodes throughout the network. The advantage of using the centralized clustering algorithm is that the BS forms the cluster which is the most energy intensive task, so that the energy dissipation of the sensor nodes decreases and network lifetime increases. Here in each round all sensor nodes send their current location and energy level to the base station and the base station forms the clusters for the network by taking enhanced and effective processing of the current information of whole network. The operation of CBCDACP is divided into rounds. Each round begins with set-up phase when the clusters are formed, followed by a steady-state phase when the data are transferred from the nodes to the central base station through their respective cluster-heads. In CBCDACP, the BS ensures that the energy load is evenly distributed among all the nodes by determining good clusters. It also minimizes the amount of energy needed for the non-cluster head nodes to transmit their data to the cluster-head by minimizing the total sum of squared distances between the non-cluster head nodes and the cluster-head nodes and also considering the density factor of each cluster head.

A. The Setup Phase

1. *Sensor Density and Neighbor Determination*

The cluster head candidates were selected from the set of alive nodes whose energy was higher than the average energy. For cluster head selection, nodes were chosen from the candidate nodes depending on which had higher sensor density. A node will have higher density if it has more neighbor nodes at closest distance than others. For calculating a neighbor candidate node for any alive node *X*, it follows the following equation:

$$Neighbor(X) = \min\ (dist(1) + dist(2) + .. + dist(P)) \quad (5)$$

Where, 1, 2…P = set of candidate nodes

$dist(i)$ = Absolute distance between X and i.

If $Neighbor(X) = dist(i)$ so node *X* will be the neighbor of node *i* .And the no. of neighbor node will increase 1.

Let us consider a scenario in Figure 2 which shows a simple topology of the sensor network.

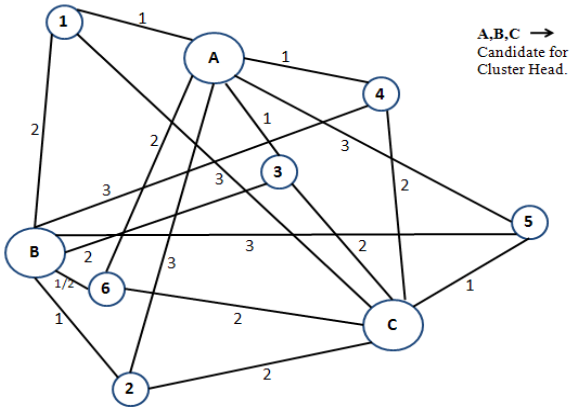

Figure 2: A sample Network Topology. The weight of every edge denotes the distance among the connecting Nodes.

A, B and C are three candidate nodes for cluster head selection. In LEACH-C cluster head is selected randomly, so it may be *A* or *B* or *C*. So the neighbor nodes for cluster formation may be or may not be in the minimum distance of the selected cluster head. But we selected cluster heads depending upon the higher density of the neighbor nodes in their minimum distances. Let, Distance between node 1 and *A* is 1m, Distance between node 1 and *B* is 2m, Distance between node 1 and *C* is 3m and so on.

To determine the neighbor node for node *A, B* and *C* the square distance is calculated between the candidate nodes and the non candidate nodes. If (x1, y1) be the coordinate of node 1, (xa, ya) for node *A* then the mathematical equation for distance calculation will be

$$dist(A,1) = (xa - x1)^2 + (ya - y1)^2 \quad (6)$$

According to this equation distance of node 1 from node *A* is 1, distance of node *B* is 2 and for node *C* it is 3. As node 1 is in minimum distance with node *A* comparing with other nodes, so it will belong to node *A*. This same mathematical equation is applicable for all other non candidate nodes to determine the closest node for *A, B*, and *C*. As shown in Figure 3 the neighbor node set for Candidate node *A*= {1, 3, 4}, Candidate node *B*= {2, 6}, Candidate node *C*= {5}.

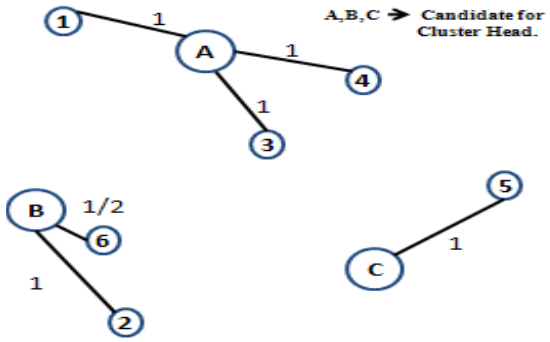

Figure 3: The nodes having smallest distance will be the neighbor of that candidate node.

Since *A* has higher node density than *B* and *C*. So that it may be perfect as a cluster head in cluster head selection process. (N.B: If a node has the same distance with more than one candidate node then its neighborhood will be determined depending on the current energy of the candidate nodes)

2. *Cost Function Calculation*

In LEACH-C, Simulated Annealing algorithm [3] is used to select the cluster heads. Here the group of candidate nodes selected for the last state to be the cluster-heads, is defined by *S* and the group of candidate nodes selected for the current state to be the cluster-heads, is defined by *S′*. The cost function of the set *S* is defined as *f(S)* and the cost function of *S′* is defined as *f(S′)*. If the value of *f(S)* is smaller than *f(S′)* then the probability for a node with smaller cost *f(S)* to become a cluster head gets bigger. The cost function *f(S)* in LEACH-C is defined by the equation (7).

$$f(S)=\sum_{i=1}^{N}\min\ (dist^2(i,s)),\text{where}(s\in S) \qquad (7)$$

Here *N* is the number of sensor node and *dist (i,s)* is the distance between node *i* and node *s*. So here the relation between the cost function and the communication distance is given as

$$Cost\ function \propto Communication\ distance(CD) \qquad (8)$$

So if the communication distance between cluster-head and the non cluster-head increases then the overall cost will increase and vise-versa. On the other hand, according to equation (2) if the communication distance (d^2) is minimized then the energy consumed for signal amplification ($E_{amplify}$) be minimized and thus the transmission energy (E_{tx}) will be minimized and so that the total energy consumed (E_{total}) in each round in the entire sensor network will be minimized according to equation (4). As E_{elec} is a nearly constant value depending on the processing byte length, the energy consumed in data signal amplification can be expressed as (2). So,

$$Total\ energy\ dissipation \propto Communication\ distance(CD) \qquad (9)$$

In our proposed protocol CBCDACP, we improved the equation of cost function by introducing another factor that was the Density Factor (DF). In cluster head selection process, we considered here that a candidate node which had more neighbor than others had more probability to become a cluster head than others. For each candidate node, neighbor nodes are selected according to equation (5). So as the distance between candidate node and neighbor nodes was minimized, the overall transmission energy was minimized. The relation of cost function and the density factor can be shown as

$$Cost\ function \propto \frac{1}{Density\ Factor(DF)} \qquad (10)$$

Here if the density of the candidate node is maximum then the cost function will be minimum and vice versa. So that by using equation (8) and equation (10) the relation of cost function can be written as

$$Cost\ function \propto \frac{CD}{DF} \qquad (11)$$

Finally in CBCDACP, we used the following cost function to select a set of cluster heads

$$f(S) = \frac{\sum_{i=1}^{N}\min\ (dist^2(i,s)for\ \ each\ s\in S))}{\sum_s DF} \qquad (12)$$

Where $dist^2(i,s)$= Square distance between i and s.

3. *Cluster Head Selection*

In CBCDACP, an optimum set of cluster heads were selected by the centralized clustering algorithm in central base station. For a round, cost function was calculated for large number of times and then finally we found the optimal set of cluster heads.

In our proposed protocol it is likely to acquire optimum set of cluster heads than other existing protocol, because here we had considered both the density of each candidate nodes and the distance among nodes from candidate nodes for cost function calculation. Each time the cost function was determined for each set of candidate nodes which was used for calculating the probability P_d for cluster head set selection which can be shown as

$$P_d = \begin{cases} e^{-(f(s')-f(s))/\alpha_d} & f(s)\geq f(s) \\ 1 & f(s') < f(s) \end{cases} \qquad (13)$$

Where, $\alpha_d = 1000\,e^{d/20}$

In a word, according to our proposed algorithm the nodes which have energy above the average energy will be the cluster head if they have more neighbor nodes

(sensor density) in their minimum distance than the others. So that the communication distance between the communicating nodes will be minimum that is the cost will be minimum and thus the energy dissipation E_{tx} will be minimized according to equation (4).So the total energy E_{total} consumed in a round will be decreased. So in compendium, it will increase the life time of the sensor network.

4. Cluster Head Selection Algorithm

In our proposed protocol cluster heads are selected depending upon the density function and minimum square distance among the communicating nodes. The density of each candidate node was selected by the following algorithm:

1. Let, XN_i and YN_idenote the X and Y coordinate of i^{th} node. XC_j and YC_j be the X,Y coordinate of j^{th} node of the currently selected as the cluster heads.
2. Initially min = 1000000
3. Repeat steps 4 to 8 for each alive node, N_i
4. Repeat steps 5 to 6 for each candidate node C_j,
5. Calculate maximum distance *D* between (XN_i, YN_i) and (XC_j, YC_j)
6. if $D < min$ then $min = D$ and W = C_j
7. So N_i will become the neighbor of *W*.
Update Neighborof[W] = Neighborof[W] + 1, for candidate node W
8. Update min=1000000

Then the cost function was calculated using equation (12) and finally by comparing the cost values the final optimum set of cluster heads were selected.

B. The Steady State Phase

After the selection of cluster heads the base station broadcasts a message containing IDs of cluster heads for the round to every sensor node in the network. When a node receives the message, it elects itself as a cluster head if its ID is included in the cluster head ID list. If not, the node determines its cluster and TDMA slot for transmitting data to its cluster head. At steady-state phase, CBCDACP performs a procedure identical to that of LEACH [2].

V. PERFORMANCE SIMULATIONS

A. Simulation Framework

1. Simulation Environment: In order to analyze the performance of the proposed protocol, we use NS-2 simulator [5] because it is simple and powerful. We use the network simulator package ns-allinone-2.27 with a mit wireless sensor package [6]. The simulation parameters are shown in Table 1.

Table 1: Simulation Parameters

Parameter	Value
Simulation Area(x,y)	100×100 to1000×1000m^2
Node's Initial Energy	2 joule
Simulation Time	3600 seconds
Base Station Location	(50,175)
Number of Nodes	100
Desired no. of Cluster	5
Round Time	20 seconds

2. *Performance Metrics [7]:* To compare the performance of the proposed protocol with the prevalent ones, we considered the following metrics:

a. ***Number of nodes alive****:* It is an important metric in the simulation of a sensor network. The performance of a network depends on the lifetime of its nodes. If the lifetime of the nodes is higher then the network life time increases and also transmits more data to the base station.

b. ***Amount of energy dissipation:*** The lifetime of a node and the amount of data being transmitted by the node depend on the energy level of the node. If the required energy to transmit data to the base station is very low for a node then lifetime of a node automatically increases and also the performance of the network increases.

c. ***Amount of data received:*** This metric determines how many data messages are received at the base station from the network. If the amount of data received is enough as we expect then we say that the network performance is well.

d. ***Network lifetime:*** This determines how long the network will send data to the base station. So higher network lifetime will incur great network performance.

B. Simulation Results and Analysis:

It is known that the network lifetime depends on how long the sensor nodes remain alive in a network. When the time duration of nodes' die is long, the network lifetime is also long. Figure 4 shows the simulation curve of different protocol like CBCDACP, LEACH-C, and LEACH. It shows the number of nodes alive with respect to network life time in a 100×100m^2

network area. The curve

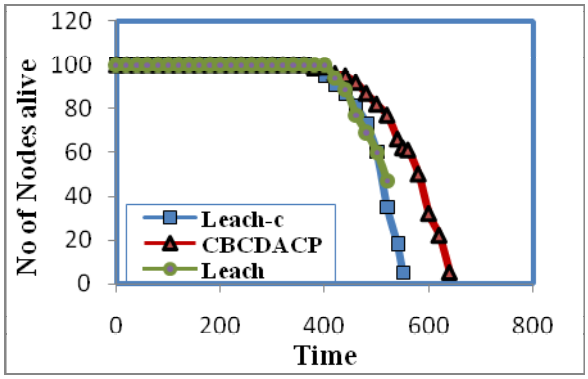

Figure 4: No of nodes alive with respect to network life time.

shows that as our protocol selects the energy effective node as the cluster head in each round so the lifetime of the nodes of CBCDACP is longer than LEACH-C and LEACH. On the other hand in LEACH and LEACH-C, the selected cluster head die quickly and thus the network lifetime in not longer. So the node dying rate in our proposed protocol CBCDACP is much less than other ones.

If the required energy to transmit data to the base station is very low for a node then lifetime of a node automatically increases and also the performance of the network enhances. In Figure 5 the amount of energy dissipation with respect to time in $100\times100 m^2$ is illustrated.

The curve shows that as in our protocol the clusters are formed efficiently and the energy efficient cluster heads are selected so that less energy is dissipated with respect to time than LEACH and LEACH-C.

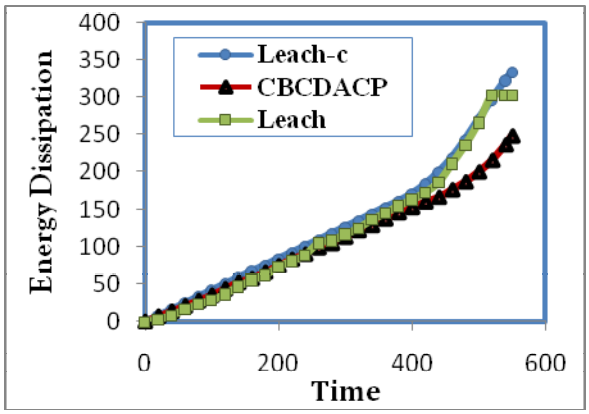

Figure 5: Amount of Energy Dissipation with respect to Time.

In Figure 6, the curve shows that the amount of data received at the base station with respect to network life time in a $700\times700 m^2$ network area for the protocols CBCDACP, LEACH-C and LEACH. If the rate of node die can be minimized then the network lifetime is increased and vice versa. Since from figure 6, it is evident that the node die rate in our protocol is less than the other comparatives, so all nodes can send more data in total network lifetime. So from the graph it is vivid that in our protocol the base station received more data than other ones.

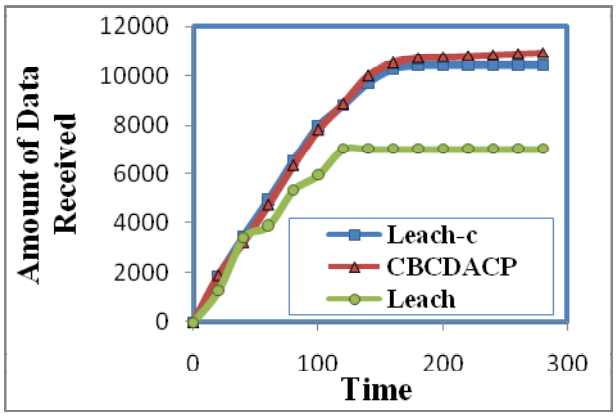

Figure 6: Amount of Data Received with respect to time

In Figure 7, we varied the network area from $100\times100 m^2$ to $1000\times1000 m^2$ in our simulation and obtained the network lifetime of LEACH, LEACH-C and our proposed one. From figure 5, as the node dying rate in case of protocol is less, so over different network area it should preserve high network life time. So in figure 7, CBCDACP reveals higher network life time over different network areas than LEACH and LEACH-C.

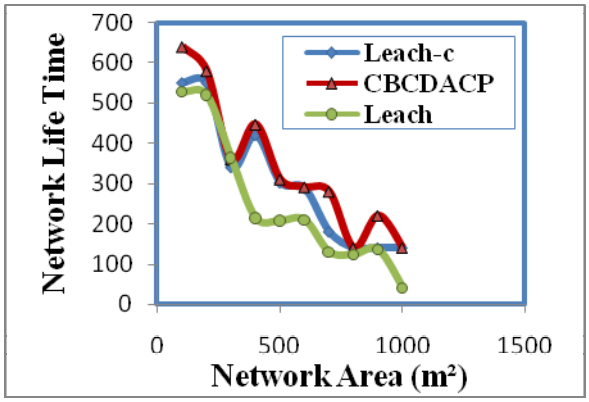

Figure 7: Network Life Time with respect to Network area.

VI. CONCLUSIONS

In this paper, we devise a new protocol for cluster head selection where the base station performs this most energy intensive task. In our proposed protocol for cluster head selection we consider the density factor of

each candidate node and the minimum squared distance between the cluster head and the neighbor node. By considering the minimum squared distance and the density factor of each candidate node a cost function is determined and by comparing the cost function, an optimum set of clusters are formed. In performance simulations, we have compared our protocol with prevalent protocols LEACH and LEACH-C. After analyzing, it shows that our proposed technique enhances the system performance in different performance metrics.

While proposed CBCDACP protocol appears to be a promising protocol, there are some areas for improvements to make the protocol more widely applicable. In the current implementation of CBCDACP, we use Simulated Annealing algorithm for cluster formations which is an approximation algorithm and very slow for problem with large search spaces. Again, it does not always provide the best optimal solution. As a future work direction it is possible to get better performance in sensor networks if a high performance approximation algorithm can be established instead of Simulated Annealing algorithm. So the proposed CBCDACP will be more effective in wireless sensor networks.

REFERENCES

[1] Siva D.Muruganathan, Daniel C.F.Ma,Rolly I.Bhasin, and Abraham O. Fapojuwo, "A Centralized Energy-Efficient Routing Protocol for Wireless Sensor Network", *Communications Magazine, IEEE In Communications Magazine, IEEE*, Vol. 43, No. 3, pp. S8-13, 2005.

[2] Wendi B. Heinzelman, Anantha P. Chandrakasan, and Hari Balakrishnan, "An Application-Specific Protocol Architecture for Wireless Microsensor Networks"*IEEE Transaction on Wireless Communications*, vol. 1, No. 4, pp. 660-670, October 2002.

[3] Tadahika Murata and Hisao Ishibuchi "Performance Evaluation of Genetic Algorithms for Flowshop Scheduling Problems", *Proc.1st IEEE conf. Evolutionary Computation,* vol.2, pp.812-817,June1994.

[4] Eui-Hyun JUNG, Sung-Ho LEE,Jae-Won CHOI and Yong-Jin PARK, "A Cluster Head Selection Algorithm Adopting Sensing-Awareness and Sensor Density for Wireless Sensor Networks", *IEICE Transaction COMMUN*, Vol.E90-B, No.9, pp. 2472-2480, September 2007.

[5] The network simulator-2 [Online]. Available: http://www.isi.edu/nsnam/ns/

[6] MIT package and pdf files – NS by Example.pdf and Ns_doc.pdf for wireless sensor networks." The MIT uAMPS Package Version 1.0 ", August 7, 2000 [Online]. Available: http://www.ece.rochester.edu/research/wcng/code/leach

[7] Solaiman ali, Tanay Dey, and Rahul Biswas, "ALEACH: Advanced LEACH routing protocol for wireless microsensor networks " *Proc. IEEE International Conference on Electrical and Computer Engineering (ICECE 2008)*, pp 909-914, Dhaka, Bangladesh, December 20-22, 2008.

Proceedings of 2009 12th International Conference on Computer and Information Technology (ICCIT 2009)
21-23 December, 2009, Dhaka, Bangladesh

A Study on Distributed Diffusion and its Variants

Nazia Perwaiz, Muhammad Younas Javed
Dept. of CE, E&ME College, National University of Sciences & Technology, Rawalpindi, Pakistan
nazia.nust@gmail.com, myjaved@ceme.edu.pk

Abstract

Energy awareness is an essential design issue in wireless sensor networks (WSN). The routing techniques of WSN are classified into three main categories Data-Centric, hierarchical and location-based. Data-Centric technologies perform in-network aggregation of data to yield energy-efficient dissemination; Sensor Protocols for Information via Negotiation (SPIN) and Directed Diffusion (DD) are basic Data-Centric routing protocols. This paper presents a survey on Data-Centric routing and specifically focuses on the Directed Diffusion and its variants (dissemination and aggregation variants) and the protocols that follow the similar concept like Directed Diffusion.

Keywords: directed diffusion, variants, sensor network

I. INTRODUCTION

Wireless Sensor Networks (WSNs) comprises of thousands of inexpensive wireless nodes, with sensing, computation, and communications capabilities, deployed closely to observe a phenomenon.

The energy efficiency is one of the key concerns in WSN. The main objective of routing and data dissemination protocols for WSN is to minimize the energy consumptions so as to minimize the nodes failure, hence, maximizing the lifetime of the network. The routing techniques in WSN are classified into three categories *Data-Centric, hierarchical and location-based.* In Data-Centric routing, querying an attribute of the phenomenon is used rather than querying an individual node and in-network aggregation of data is used to yield energy-efficient dissemination. In hierarchical-based routing, higher energy nodes are used to process and send the information while low energy nodes perform the sensing. In location-based routing, sensor nodes' positions are used to route data in the network.

This paper considers solely Data-Centric routing and specifically it focuses its sub-class Directed Diffusion [1][3], its variants and protocols following the similar concept like DD [5][8][9][10][11][12][13], variants are compared with original version of DD. Our objective is to provide deep understanding of the Data-Centric routing protocols.

II. RELATED WORK

The communication protocols in WSNs are surveyed in [1]. A study of the network layer, data routing, and design issues of routing protocols is described in [8]. Our paper differs from previous work as it focuses solely on the Data-Centric routing in WSN and the sub-class Directed Diffusion and its variants are explored further.

The rest of this paper is organized as follows. In Section 3, an introduction to Data-Centric routing, SPIN [6] and DD [3] is given. Section 4 comprises of DD variants and their classification. A comparison of DD variants is given in the conclusion section 5.

III. DATA-CENTRIC ROUTING

In Data-Centric routing, the sink node sends queries to certain regions and waits for data from the sensors located in the selected regions, attribute-based naming is used to specify the properties of data. No global identifier is assigned to each sensor node and data is usually transmitted from every sensor node within the deployment region with significant redundancy, Since it is very inefficient in terms of energy consumption, the routing protocols that will be able to select a set of sensor nodes and utilize data aggregation during the relaying of data have been considered (Data-Centric). Data-Centric routing has proven to be a good scheme for minimizing communication overhead and energy consumption by using in-network aggregation.

SPIN [6] is the first Data-Centric protocol, which considers data negotiation between nodes, Directed diffusion [3] was designed to eliminate redundant data and save energy. Many other protocols have been proposed either based on Directed Diffusion or following a similar concept.

A. SENSOR PROTOCOLS FOR INFORMATION VIA NEGOTIATION (SPIN)

Sensor Protocols for Information via Negotiation (SPIN) are a family of protocols that use data negotiation and resource adaptive algorithms for efficient information distribution (lacking in flooding & gossiping).

In SPIN, the data is named using meta-data. Before transmission, meta-data are exchanged among sensors via a data advertisement mechanism. SPIN's meta-data negotiation solves the classic problems of flooding such as redundant information passing, overlapping of sensing areas and resource blindness thus, achieving a lot of energy efficiency. SPIN is a 3-stage protocol, three types of messages defined in SPIN to exchange data between nodes. ADV: to allow a sensor to advertise a particular meta-data. REQ: to request the specific data. DATA: These are actual data messages with a metadata header.

The protocol starts when a SPIN node obtains new data for transmission. It advertises its new data by broadcasting an ADV message containing meta-data. If a neighbor is interested in the data, it sends a REQ message for the DATA and the DATA is sent to this neighbor node. The neighbor sensor node

978-1-4244-6283-4/09/$26.00 ©2009 IEEE

then repeats this process with its neighbors. As a result, the entire sensor area will receive a copy of the data. These protocols make use of the property that nodes in close proximity have similar data, and hence there is a need to only distribute the data that other nodes do not posses.

SPIN reduces energy dissipation by 3.5 factors than flooding and meta-data negotiation almost half the redundant data. However, SPIN's data advertisement mechanism cannot guarantee the delivery of data i.e. if the nodes that are interested in the data are far away from the source node and the nodes between source and destination are not interested in that data, such data will not be delivered to the destination at all. The SPIN family of protocols is made up of four protocols SPIN-PP, SPIN-EC, SPIN-BC and SPIN-RL

SPIN was found to perform better in smaller size networks because of its efficiency and high latency properties. The use of SPIN in large scale networks could potentially exhaust system resources in a much faster pace.

B. DIRECTED DIFFUSION (DD)

Another Data-Centric protocol, *Directed Diffusion* [1][3] has been developed after SPIN and has become a breakthrough in Data-Centric routing. Directed diffusion finds routes from multiple sources to a single destination that allows in-network consolidation of redundant data (Aggregation).

Data Dissemination: Directed Diffusion consists of three phases: a) Interest propagation, b) Initial gradients setup, and c) Data delivery reinforced path. In first phase, to create a query, an *interes*t (tracking task) is defined by the sink node using a list of *attribute-value pairs*. The interest is propagated from neighbor-to-neighbor towards sensor nodes in the specified region. Each sensor node that receives an interest remembers which neighbor or neighbors sent it an interest. In second phase to each such neighbor, it sets up a *gradient*. Upon sensing an event matching a sink's interest, the sensor generates a data packet and sends it to the sink via the neighbors for which it has a gradient. A node that receives this message checks if it has received the identical message before, if an identical data item exists in the cache, the node drops the message. If this data item does not exist in its cache, the node determines the matching interest, and resends the data along the gradient towards the neighbor. This process is repeated by each node receiving the data packet. The data packets are called *exploratory packets*, since they are sent to the sink along multiple paths. Eventually, in the last phase, the sink *reinforces* the path from which for example it received the first exploratory data packet. This means that only one path is selected from the sink to the packet source and this is the route that will be used by the sensor to delivery data to the sink. Finally, if a node on this preferred path fails, sensor nodes can attempt to *locally repair* the failed path.

In-network Data Aggregation: Application-specific, in-network processing is another key feature of diffusion; in-network aggregation can reduce data transferred across the network, and thereby conserve energy. Data from different sources is *opportunistically* aggregated**;** in opportunistic approach the most preferred neighbor is a neighbor which has delivered samples with the lowest delay (shortest path). Whenever similar data happens to meet at a branching node in the tree, the copies of similar data are replaced by a single message. Such aggregation points tend to be close to the sink because shortest path flows from different sources to the same sink intersect downstream. Energy-wise, opportunistic aggregation on a low-latency tree is not optimal because data may not be aggregated (or reduced) near the sources (rather near the sink).

To maintain good quality routes, flooding interests and exploratory data is periodically used. On one side, this periodic refreshing of gradients ensures that all sensors are updated with the events that interest to the sink. On the other side, periodic flooding imposes a non-negligible overhead for maintaining the routes.

IV. DIRECTED DIFFUSION VARIANTS

Directed diffusion variants are described with respect to the different *data dissemination algorithms* [15] and *data aggregation techniques* [1]. Some variants use DD concept with some additional improvements in some aspect. The following chart describes the classification of variants of DD.

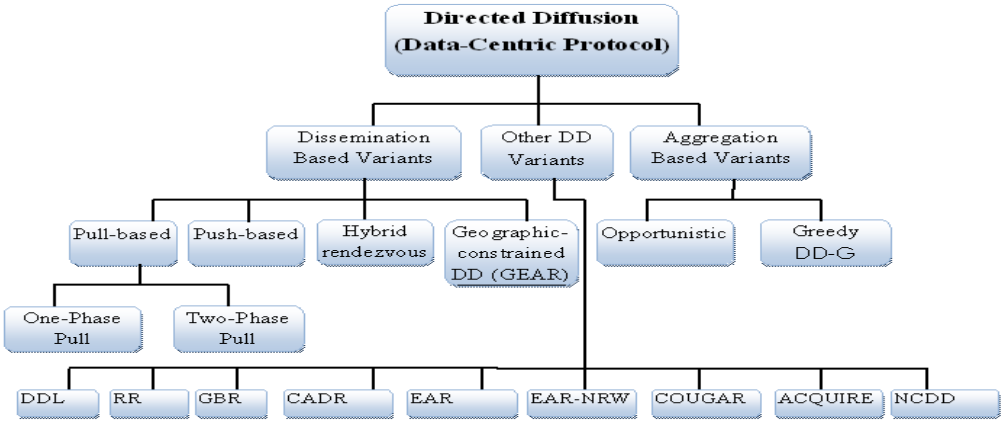

Fig1. Classification of the Variants of Directed Diffusion

A. DATA DISSEMINATION VARIANTS

A.1 Pull Based Diffusion

Pull based diffusion [15] has further two classes (two phase and one phase).

a. *Two-phase Pull Diffusion:* Simple directed diffusion is also called two-phase pull diffusion [Explained in Section 3.2][3]. Where sink seeks out data sources using interest, and then sources search to find the best possible path back to sink. Interests must be flooded throughout the network to find any data sources resulting in extra high overhead for maintaining the routes. Two-phase pull works well for applications having small number of sinks and not suitable for large number of sinks being used, because all sensors actively send interests and maintain gradients to all other sensors even though nothing is detected. In two-phase pull, data sinks are active, sending out interests, while sources are passive until interests arrive.

b. *One-phase pull diffusion*: Unlike two-phase pull, one-phase pull sends data only on the preferred gradient. The preferred gradient is determined by the neighbor who was the first to send the matching interest, thus suggesting the lowest latency path. Thus one-phase pull does not require reinforcement messages; the lowest latency path is implicitly reinforced. One-phase pull has two disadvantages compared to two-phase pull. First, it assumes symmetric communication between nodes since the data path) is determined by lowest latency in the interest path (sink-to-source). Second, one-phase pull requires interest messages to carry a flow-id.

A.2 Push-Based Diffusion*:*

Push [15] is not a good approach for applications with many sources continuously generating data. Push is designed for the case when there are many active sinks (listening for data), but relatively few nodes actually generating data occasionally. *Push* floods exploratory data messages only. Sinks become passive, with interest information kept local to the sink node. Sources become active; exploratory data is sent throughout the network without interest-created gradients. When exploratory data arrives at a sink a reinforcement message is generated and it recursively passes back to the source creating a reinforced gradient, and non-exploratory data follows only these reinforced gradients. A benefit of push diffusion compared to two-phase pull is that it has only one case where information is sent throughout the network (exploratory data) rather than two (interests and exploratory data).

A.3 Geographically Constrained Diffusion with GEAR:

GEAR (Geographic and Energy-Aware Routing) [13] extends diffusion when node locations and geographic queries are present. GEAR replaces network-wide communication with geographically constrained communication. Queries (interests) are sent towards that region using greedy geographic routing, flooding occurs only when interests reach the region rather than sent throughout the whole network. Exploratory data is sent only on gradients set up by interests, so the limited dissemination of interests also reduces the cost of exploratory data. GEAR provides a first example of application-specific diffusion. It optimizes diffusion for applications and networks that have geographically scoped queries. GEAR-extended versions of both push and pull diffusion in order to meet some energy constraints.

A.4 Hybrid Rendezvous Diffusion:

In Hybrid Rendezvous Diffusion, the sources and sinks both send information about interest or presence of data to the rendezvous point (RP) and if both are present a path is created. The challenge with such hybrid approaches is the location of the rendezvous point. However, when there is no pre-determined extraction point, nodes must still agree on a rendezvous scheme. Concentration of all traffic through a single node faces bandwidth limitations and will disproportionately consume energy at nodes near the extraction point. The best-case performance of hybrid rendezvous protocols is where the RP is located directly between the source and sink.

B. DATA AGGREGATION VARIANTS

In-network data aggregation [1] can reduce data transferred across the network, and thereby conserve energy.

B.1 Using Opportunistic Aggregation:

The initially defined directed diffusion uses opportunistic aggregation to aggregate similar data from different sources in order to reduce number of transmission and to save more energy of the nodes. Opportunistic aggregation uses *Shortest Paths Tree (SPT)* in this data aggregation scheme, each source sends its information to the sink along the shortest path between the two, and overlapping paths are combined to form the aggregation tree.

B.2 Using Greedy Aggregation: Directed Diffusion-Greedy (DDG)

Improvement of Directed Diffusion that exploits data aggregation is called Directed Diffusion Greedy (DD-G).

As energy-wise, opportunistic aggregation on a low-latency tree is not optimal *Greedy* aggregation is used to eliminate this problem. This approach uses greedy incremental tree (GIT). To construct a greedy incremental tree, a shortest path is established for only the first source to the sink whereas each of the other sources is incrementally connected at the closest point on the existing tree, making it possible to aggregate redundant data close to where such data have been generated.

Although the two data aggregation variants of directed diffusion are roughly equivalent at low-density networks, the greedy directed diffusion can achieve significant energy savings at higher densities.

C. OTHER VARIANTS OF DIRECTED DIFFUSION

Directed diffusion has some *other variants* that use directed diffusion scheme with some additional factors that improve DD functionality in some aspect.

C.1 Directed Diffusion-Light (DD-L)

Directed Diffusion Light [8] is a variant of Directed Diffusion protocol, it results in significant savings in terms of exchanged control messages and energy consumption hence increasing network lifetime. DD-L is based on the idea to first generate a sparse *logical topology* by means of simple, local rules, and then run Directed Diffusion over such topology. In contrast to DD high overhead due to the flooding (of interests and exploratory data), a low overhead, localized and distributed mechanism is defined for the construction of a *"virtual topology"* on top of the network topology which is considerably sparser. When Directed Diffusion is run on the obtained virtual topology it is called Direct Diffusion Light.

The sparse logical topology maintains the global connectivity properties of the original network topology. DD-L improves DD performance without affecting its robustness. DD-L also out performs DD-G in terms of all the relevant metrics of interests to Data-Centric routing.

C.2 Rumor Routing (RR)

Rumor routing [10] is a variation of directed diffusion and is specifically used for the applications where geographic routing is not possible. This scheme is basically used to lower the cost of interest-flooding for directed diffusion. The approach is to flood the events if the number of events is small and the number of queries is large. The basic idea is to create paths leading to each event. When a query is generated it can be sent on a random walk until it finds the event path. As soon as it discovers the event path (created by *agents*-long lived packets, TTL limited, generated by nodes on detection of an event) it can be routed directly to the event. If the path cannot be found, the application can try re-submitting the query. Whenever an agent crosses a path leading to an unseen event, it adapts the path that leads to both (or multiple) events. The agents optimize the paths in the network. Rumor routing performs well only when the number of events is small. For a large number of events, the cost of maintaining agents and event-tables in each node becomes high. Rumor routing cannot guarantee the delivery of data and the performance of the protocol heavily depends upon the topology of the network.

C.3 Gradient-Based Routing (GBR)

Gradient-based routing [12] is a variant of the directed diffusion. The basic idea in GBR is to remember the number of hops when the interest is diffused through the whole network. This way each node can discover the minimum number of hops to the sink, which is called *height of the node.* The difference between a node's height and that of its neighbor is considered the *gradient on that link*. A packet is forwarded on a link with the largest gradient. The *data aggregation* and *traffic spreading* is used along with GBR to balance the traffic uniformly over the network.

For data aggregation, when multiple paths pass through a node, relay node that may combine data according to a certain function. For data spreading three different techniques have been used, i.e. *Stochastic Scheme*: Randomly choose from the two or more next hops with the same gradients, *Energy-based scheme*: When a node's energy drops below a certain threshold, it increases its height and *Stream-based scheme*: The idea is to divert new streams away from nodes that are currently part of the path of other streams. The main objective of these data spreading schemes is to achieve an even distribution of the traffic throughout the whole network, increasing the network lifetime. GBR outperforms Directed Diffusion in terms of total communication energy.

C.4 Constrained anisotropic diffusion routing (CADR)

Constrained anisotropic diffusion routing (CADR) [16] is a variant of Directed Diffusion. The major difference from Directed Diffusion is the consideration of information gain in addition to the communication cost. The basic idea is to query sensors and route data in a network in order to maximize the information gain, while minimizing the latency and bandwidth (by activating only the sensors that are close to a particular event and dynamically adjusting data routes) In CADR, each node evaluates an information/cost and routes the data. In CADR, the querying nodes use IDSQ (information-driven sensor querying) mechanism to determine which node can provide most useful information by using estimation theory. Since CADR diffuses queries by using a set of information criteria to select which sensors to get the data, it is more energy efficient than Directed Diffusion where queries are diffused in an isotropic fashion, reaching nearest neighbors first.

C.5 Energy- Aware Routing (EAR)

Energy-aware routing protocol [17] is a destination initiated reactive protocol. The basic idea of EAR is that it maintains a set of paths instead of enforcing one optimal path. These paths are maintained and chosen by means of a certain probability which depends on how low the energy consumption of each path can be achieved. By having paths chosen at different times, the energy of any single path will not deplete quickly. The protocol EAR assumes that each node includes the location and types of the nodes. The protocol initiates a connection through localized flooding, which is used to discover all routes between source/destination pair and their costs. The high-cost paths are discarded and a forwarding table is built by choosing neighboring nodes cost. These forwarding tables are used to send data to the destination with a probability that is inversely proportional to the node cost. Localized flooding is performed by the destination node to keep the paths alive. EAR provides improvement on DD in energy saving and network lifetime. However, EAR requires gathering the location information and setting up the addressing mechanism for the nodes, which complicate route setup over DD.

C.6 Energy-Aware Routing Algorithm with Node Relay Willingness (EAR-NRW)

An energy-aware routing scheme with the node relay willingness [18], (a reactive and destination-initiated routing protocol) considers routing with sufficient energy reserves and through the light-loaded nodes (contention is minimized).

The data aggregation process is performed during information gathering, i.e. only one of the sensor nodes in the interest area is selected as the source node called aggregator. The sink node initiates by flooding the interest in the source node direction. Each intermediate sensor node calculates node relay willingness of the neighboring node and forwards the interest only to the neighbors which are closer to the source node than itself until the source node receives the interest packets from its neighboring nodes. During data packet transmission, the source node transmits the data packet to the neighbor in the forwarding table. Each intermediate node repeats the same until the data packet reaches the sink node.

Using energy sufficient reserves and routing packets through the light-loaded sensor nodes is energy-conserving, having longer network lifetime, and received much more data packets by the sink node than that of the routing algorithm considering the energy reserves only (EAR).

C.7 COUGAR

COUGAR [9] is a Data-Centric protocol that views the network as a huge distributed database system. Its main objectives are to use the declarative queries in order to abstract query processing from the network layer functions and utilization of in-network data aggregation to save energy.

In COUGAR a loosely-coupled distributed architecture is proposed to support its objectives. To enable declarative querying of sensor networks an additional network-layer independent *query layer* is created that lies between the network and application layers and for in-network aggregation. In COUGAR sensor nodes select a leader node (query optimizer) to perform aggregation and transmit the data to the gateway. In-network computation ability ensures energy-efficiency especially when the number of sensors generating and sending data to the leader is huge.

COUGAR drawbacks include extra overhead to sensor nodes due to additional query layer. Further in-network data computation from several nodes will require synchronization and the leader nodes should be dynamically maintained to prevent them from failure.

C.8 Active Query Forwarding In Sensor Networks (ACQUIRE)

ACQUIRE [12] follows directed diffusion concept with an extra ability to resolve one shot, complex queries by allowing many nodes to send responses.

The principle behind the ACQUIRE is to inject an active query packet into the network as this active query progresses through the network it gets progressively resolved into smaller components until it is completely solved and is returned back to the querying node as a completed response. When the query is forwarded by the sink and each node receiving the query, tries to respond partially by using its pre-cached information and forward it to another sensor. If the pre-cached information is not up-to-date, the nodes gather information from its neighbors within a look-ahead of *d* hops. Once the query is being resolved completely, it is sent back through either the reverse or shortest-path to the sink. In ACQUIRE the querying nodes uses IDSQ mechanism to determine which node can provide most useful information by using estimation theory and the next node to forward the query is either picked randomly or the selection is based on maximum potential of query satisfaction.

C.9 Nodes' Credit based Directed Diffusion (NCDD)

Nodes' Credit based Directed Diffusion [19] is based on nodes' credit for more energy efficient and reliable routing than DD and has the ability of traffic load distribution. Along with the knowledge required for DD it additionally consider energy level, traffic load and neighbor ability to aggregate data for making decisions about data transmission. The knowledge is enhanced based on credit of nodes. Computation of nodes' credit is done by using five factors; at each node i.e. the number of successful or unsuccessful transmission, the residual energy in candidate node's battery, the traffic load at each node, the distance of candidate node to destination (sink) and the number of sources that can cover by each node (for better in-network aggregation)

Each node computes its credit based on these factors. In NCDD, there is an additional field in the exploratory data that identifies nodes credit. Since each node has computed the credit, it utilizes exploratory message to inform its neighbor about its own credit, When the sink receives the exploratory data, it will respond with the reinforcement message, since each node has recorded its neighbor's credit, selects higher credit between them. So the sink will select the best path according to this credit to the source. Once a source receives the reinforcement message, it sends out the actual data.

Upon three metrics system lifetime, reliability of path and load distribution NCDD outperforms the DD.

V. CONCLUSION

In this paper we have focused the subclass of Data-Centric protocols, the Directed Diffusion. All protocols including DD and variants have a common objective to make efforts to save energy and to extend lifetime of the sensor network without compromising data delivery. Viewing *disseminating classification* we conclude that one-phase pull works well for applications with many sources, and push for applications with many sinks and pull and push extensions with GEAR outperforms the original versions both. Rendezvous also outperform pull and push variants. Viewing *aggregation variant*, greedy aggregation is more energy efficient than opportunistic one. Comparing rest of variants we conclude that

DD-L outperforms DD and DDG in energy saving, reliability and maximizing network lifetime. Rumor routing performs well over DD only when the number of events is small but not suitable for large number of events due to cost of event tables maintenance. GBR also outperforms DD in terms of total communication energy. CADR is more energy efficient than DD if queries are diffused in isotropic fashion. EAR provides improvement on DD in energy saving and network lifetime but it complicate route setup over DD. EAR-NRW is more energy efficient and more data packets are received by the sink than EAR. In-network computation ability of COUGAR makes it very energy efficient when a lot of sources generate and send data to sink. ACQUIRE outperforms DD in resolving complex queries efficiently. NCDD shows improvement over DD in terms of system life time, reliability and load distribution. This study has provided an insight of Distributed Diffusion and its variants in detail.

REFERENCES

[1] Bhaskar Krishnamachari, Deborah Estrin, and Stephen Wicker. "The impact of data aggregation in wireless sensor networks" In *Proceedings of the IEEE International Workshop on Distributed Event-Based Systems (DEBS)*, pages 575–578, Vienna, Austria, July 2002. IEEE.

[2] B. Krishnamachari, D. Estrin, S. Wicker, "Modeling Data-Centric routing in wireless sensor networks," in the *Proceedings of IEEE INFOCOM,* New York, NY, June 2002.

[3] C. Intanagonwiwat, R. Govindan, and D. Estrin. "Directed diffusion: A scalable and robust communication paradigm for sensor networks." In *Proceedings of the International Conference on Mobile Computing and Networks (MOBICOM)*, Boston, Massachusetts, August 2000.

[4] C. Intanagonwiwat, D. Estrin, R. Govindan, and J. Heidemann. "Impact of network density on data aggregation in wireless sensor networks" In *Proceedings of International Conference on Distributed Computing Systems (ICDCS)*, Vienna, Austria, July 2002.

[5] W. Heinzelman, J. Kulik, and H. Balakrishnan, "Adaptive protocols for information dissemination in wireless sensor networks," Proc. 5th ACM/IEEE Mobicom Conference (MobiCom '99), Seattle, WA, August, 1999. pp. 174-85.

[6] J. Kulik, W. R. Heinzelman, and H. Balakrishnan, "Negotiation-based protocols for disseminating information in wireless sensor networks," Wireless Networks, Volume: 8, pp. 169-185, 2002.

[7] Jamal N. Al-Karaki and Ahmed E. Kamal, "Routing techniques in wireless sensor networks: A Survey", IEEE Wireless Communications December 2004.

[8] Alessia Marcucci *et al. "*Directed Diffusion Light: Low overhead data dissemination in wireless sensor networks"

[9] Y. Yao and J. Gehrke, "The cougar approach to in-network query processing in sensor networks," in *SIGMOD Record,* September 2002.

[10] D. Braginsky and D. Estrin, "Rumor routing algorithm for sensor networks," in the *Proceeding of the First Workshop on Sensor Networks and Applications (WSNA),* Atlanta, GA, October 2002.

[11] C. Schurgers and M.B. Srivastava, "Energy efficient routing in wireless sensor networks," in the *MILCOM Proceedings on Communications for Network-Centric Operations: Creating the Information Force,* McLean, VA, 2001.

[12] N. Sadagopan et al., "The ACQUIRE mechanism for efficient querying in sensor networks," in the *Proceedings of the First International Workshop on Sensor Network Protocol and Applications, Anchorage, Alaska, May 2003.*

[13] Y. Yu, D. Estrin, and R. Govindan, "Geographical and Energy-Aware Routing: A recursive data dissemination protocol for wireless sensor networks," *UCLA Computer Science Department Technical Report, UCLA-CSD TR-01-0023*, May 2001.

[14] A.A. Ahmed, H. Shi and Y. Shang,"A survey on network protocols for wireless sensor networks", Information Technology: Research and Education (ITRE 2003), Aug. 2003

[15] B. Krishnamachari and J. Heidemann,"Application-specific modeling of information routing in wireless sensor networks", IEEE International Performance, Computing and Communications Conference (IPCCC 2004)

[16] M. Chu, H. Haussecker, and F. Zhao, "Scalable information-driven sensor querying and routing for ad hoc heterogeneous sensor networks," *The International Journal of High Performance Computing Applications*, Vol. 16, No. 3, August 2002.

[17] R. Shah and J. Rabaey, "Energy aware routing for low energy Ad Hoc sensor networks", in the *Proceedings of the IEEE Wireless Communications and Networking Conference (WCNC),* Orlando, FL, March 2002.

[18] Yoshitsugu Obashi and Huifang Chen, " An energy-aware routing scheme with node relay willingness in wireless sensor networks" International Journal of Innovative Computing, Information and Control Volume 3, Number 3, June 2007

[19] Farnaz Dargahi, Amir Masoud Rahmani, Sam Jabehdari, "Nodes' Credit based Directed Diffusion for wireless sensor networks" International Journal of Grid and Distributed Computing, 2007

Proceedings of 2009 12th International Conference on Computer and Information Technology (ICCIT 2009)
21-23 December, 2009, Dhaka, Bangladesh

Fair Slots Assignment Mechanisms of IEEE 802.11 Networks for Multiple Access Points

G. G. Md. Nawaz Ali, Rashma Shahin, Nushrika Mowna
Department of CSE, Khulna University of Engineering & Technology, Khulna – 9203, Bangladesh
taposh_kuet20@yahoo.com, rashma_shahin@yahoo.com, mowna_tammy@yahoo.com

Abstract

This paper is a research work to find out an efficient algorithm for slots assignments of multiple access points (APs) of IEEE 802.11 wireless LANs in a framework for seeking an approach which balances between quality of services (QoS) and fairness while achieving maximum network throughput. The explosive growth of wireless systems coupled with the extensive use of laptop and palmtop computers indicate bright future for wireless networks both as standalone systems and as part of large networking infrastructure. IEEE 802.11 wireless LAN has been improving in terms of data rates, radio services, security etc. ever since. Now-a-days WLAN is an essential part for providing both real time and non-real time services to a massive mobile users. But there are still lacking for WLAN to provide both QoS guarantee and fairness which makes it inappropriate for real time applications such as voice and video services. We analyze for a new framework which based on centralized coordination of APs, is a complementary to the emerging 802.11e standard for QoS and guarantee to overcome the hidden node and overlapping cell problems. We simulate three algorithms for slots assignment of multiple APs during contention-free period (CFP) of IEEE 802.11 point coordination function (PCF) medium access control (MAC) mode for ensuring the QoS, inter-AP fairness with maximizing the network throughput.

Keywords: Fairness, Quality of Service (QoS), Point Coordination Function (PCF), Distribution Coordination Function (DCF), Access Points (APs), Wireless LAN (WLAN), disk location, frequency etc.

I. INTRODUCTION

There have been many changes and enhancements in the radio resources to be used for Wi-Fi (Wireless Fidelity, the industrial term for WLAN). New mechanisms for security and improving quality of the network have been researched. But still there are many more remaining challenges ahead in this area of concern and many serious shortcomings of Wi-Fi must be overcome [1]. Some of these shortcomings include the inability to provide quality of service (QoS) guarantee, and the lack of fairness makes it inappropriate for real-time (RT) services such as voice and video conferencing. The IEEE 802.11 MAC standard defines two operation modes – the distribution coordination function (DCF) and the point coordination function (PCF). The DCF mode exhibits both short and long term unfairness [3], [6]. Numerous schemes have been researched up to now to overcome the shortcomings in this mode [3]. These papers show that the schemes are capable of providing fair service and support RT applications only when the network load is low and the stations are in the transmission range of each other. The PCF was designed for RT applications but the paper showing it [4] only consider networks with a single access point and assumes that all users are in the range of the access points. But when multiple access points are used, this property does not sustain and transmission collision occurs which we call as the "hidden node problem". It also leads to the "overlapping cell problem". Some recent works have addressed these problems [5] but they do not guarantee either fairness or QoS in the network [1].

In papers [1], [2] have been introduced a managed Wi-Fi (MiFi) system that ensures a fair service to the mobile users and provides the required QoS for the RT users. It also overcomes the hidden node and overlapping cell problems in multiple-APs WLAN networks. Our research work, based on the proposed MiFi framework, we have derived and simulated algorithms in different aspects for multiple APs and frequencies considering either disk location known or unknown and finally compare the simulated result to find the efficient one in varying condition.

II. LIMITATIONS OF PRESENT WI-FI SYSTEM

Present Wi-Fi system has been suffering from the following problems for providing real-time services:

A. Fairness and QoS limitations of Wi-Fi

Fairness is the ability of a network to provide the same level of service to all its users, while Quality of Service (QoS) is the ability of providing a service with some level of assurance for data delivery. This assurance is usually given in terms of guaranteed bandwidth, delay bounds and jitter, which are essential for RT applications like voice. Providing QoS assurance and fairness are two related problems, and a system that cannot provide a certain degree of fair service to its users, i.e., minimal allocated bandwidth, cannot provide QoS guarantees [2].

DCF employs a Carrier Sense Multiple Access/Collision Avoidance (CSMA/CA) scheme for channel access. In this mode the users compete for their opportunity to transmit data in a contention period.

978-1-4244-6283-4/09/$26.00 ©2009 IEEE

The second operation mode is the Point Coordination Function (PCF) that was designed to support real-time (RT) traffic. Here, a network access-point (AP) periodically initiates contention free periods (CFPs) in which, it polls its associated stations. The "connection-oriented" behavior of the PCF mode allows the network to provide bandwidth and delay guarantees that are necessary to support real-time applications [1]. So, in other sense, the PCF mode can ensure the QoS in the current Wi-Fi system.

B. The hidden node and overlapping cell problem

Although it has been shown that PCF mode can ensure QoS in Wi-Fi systems, it is only considered for networks with a single access point (AP). However, this property is not sustained in networks with multiple access-points that have overlapping transmission ranges or cells. In such networks transmission collisions may occur during a CFP as a result of the "hidden node" and "overlapping cell problems".

Hidden nodes in a wireless network refer to nodes that are out of range of other nodes or a collection of nodes. Let assume a physical star topology with an access point with many nodes surrounding it in a circular fashion: Each node is within communication range of the AP, but the nodes cannot communicate with each other, as they do not have a physical connection to each other. In a wireless network, it is likely that the node at the far edge of the access point's range, which is known as **r1**, can see the access point, but it is unlikely that the same node can see a node on the opposite end of the access point's range, **r2**. These nodes are known as hidden. The problem is when nodes **r1** and **r2** start to send packets simultaneously to the access point. Since node **r1** and **r2** cannot sense the carrier, Carrier sense multiple access with collision avoidance (CSMA/CA) does not work. To overcome this problem, handshaking is implemented in conjunction with the CSMA/CA scheme. IEEE 802.11 uses 802.11 RTS/CTS acknowledgment and handshake packets to partly overcome the hidden node problem. RTS/CTS is not a complete solution and may decrease throughput even further.

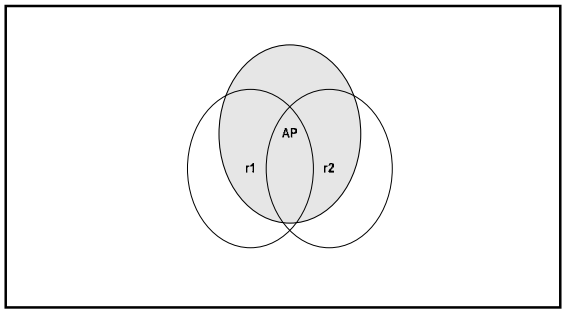

Fig. 1. Hidden node problem

The overlapping cell problem refers to the issue of interference during transmissions in a CFP due to the transmissions in adjacent cells. And it is a special case of a more subtle hidden node problem. The 802.11 standard or regular Wi-Fi systems address this problem by using both physical and virtual sensing mechanisms. However, these mechanisms provide only partial solution to these problems.

The hidden node problem causes a significant reduction in the system throughput and prevents the APs from providing fair service to their users even during their CFPs. In this case, appropriate synchronization of the CFPs is not sufficient, since the hidden node may be a mobile user operating in DCF mode that has not received the beacon message at the beginning of a CFP.

C. Balancing between fairness and throughput

The main goal of our research work is to delivering fair service to the non-stationary user and gaining QoS with maximum overall network throughput.

In the sense, usually a system provides a fair service if every user experiences the same network usage and has the same flow as any other user. This notion of fairness assumes that all users are identical and have the same requirements. However, in this system, RT users with very strict QoS requirements for latency and bandwidth co-exist with NRT users that would only like to maximize their average throughput. Thus, the notion of fairness is to ensure that users of a single type experience the same network usage and the network resources are proportionally allocated among the users of the two types. Moreover, the experienced service level should be independent of the distance between the users and their associated APs. In other words, we require spatial fairness. To achieve the fairness goals we need to consider both inter-AP and intra-AP fairness. An AP provides intra-AP fairness by balancing between resource allocation to its NRT and RT-users according to a given fairness criteria. For instance, a plausible fairness criterion may require that the success probability of a RT-session request be proportional to the efficient bandwidth given to each NRT-user. In addition, inter-AP fairness is obtained when the efficient bandwidth of an AP is directly proportional to the total number of users associated with it [1].

So we need a new system that would maintain a balance between fairness and throughput.

III. PROPOSED FRAMEWORK OF MiFi SYSTEM

The proposed MiFi system [1], [2] contain a network operation center (NOC) that coordinates the APs. For management purpose, the internal clocks of the NOC and the APs are required to be synchronized to a certain degree of accuracy. However, for ease of presentation we assume that the clock gap between any pair of APs is negligible. On-board each AP, special software is used to control its behavior for providing QoS and

fairness to the attached users and for communicating with the NOC. However, the system does not require any modification of the IEEE 802.11 standard or the software of the mobile users. It is only assumed that mobile users are able to convey, via request messages, the type of session they wish to initiate, which can be either a RT or a NRT session.

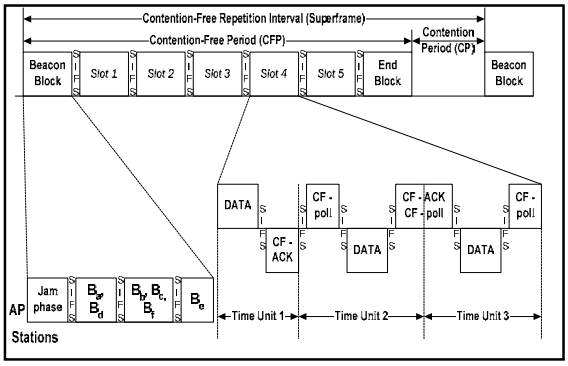

Fig. 2. A superframe of the proposed MiFi system with 5 slots [1], [2]

In MiFi system, network of single AP is extended to networks with multiple APs. This challenging goal cannot be obtained easily, mainly due to the overlapping cell and the hidden node problems. For achieving this goal, the system imitates the behavior of a single AP. The time is partitioned into repeated periods or superframes. Each superframe has a fix length *D* and it contains a Contention Free Period (CFP) followed by a Contention Period (CP). The CFP is used for data transmission of both RT and NRT sessions, for obtaining inter-AP fairness and QoS support, while the CP is used for serving the AP nearby users and as a signaling channel for initiating new sessions and sending management messages. The proportion of time allocated to each period is determined by the system needs to balance between fairness and network throughput. The CFP starts with a beacon block (BB) in which all the APs transmit 'almost' at the same time beacon messages for initiating a CFP in their vicinity. It ends with an end block (EB) in which all the APs send CF-end messages approximately at the same time to end their CFPs. This is illustrated in Fig. 2. During the CFP, the APs poll their associated users according to their polling-lists, and only stations that are polled are allowed to transmit [1], [2].

Overlapping cell problem is solved by the MiFi system which is achieved as follows. CFP is divided into slots, each of size at least Δ time units, for a specified parameter Δ. The slots are efficiently allocated by the NOC to the APs such that no two APs whose transmissions may interfere get the same slot. Every AP is allowed to poll its users only during its allocated slots. Moreover, it is ensured that transmissions in a slot terminate by the end of the slot, thus avoiding collisions with transmissions in the following slots. Here NOC only determines the slot assignments and synchronizes the APs. Each AP manages its own admission control mechanism for accepting new RT-sessions and determines its own order for polling its users. MiFi, CFP partitioning into slots and the polling mechanism is described in Fig. 2 [1].

IV. INTERFERENCE GRAPH

Generally, two APs may interfere, if a message exchanged by one AP, prevent a proper message decoding in the surrounding of the others. We do research how to remove the overlapping cell problem by allocating disjoint sets of slots to interfering APs. An interference graph represents this interference relationship. An example of an interference graph is depicted in Fig. 3 which shows the position of the APs in the graph as well as the individual requirement of an AP. The density of the interfering graph determines the system achievable throughput. The number of slots which is allocated to each AP is inversely proportional to its degree in the graph.

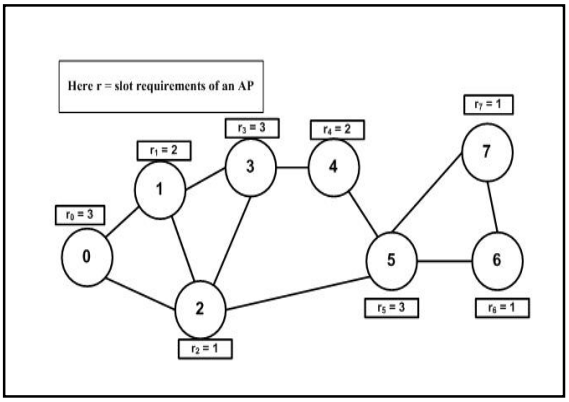

Fig. 3. Interference graph showing requirements of each AP

V. SLOTS ASSIGNMENT MECHANISMS

As described above, all the APs share a common CFP that is partitioned into slots, each of size at least Δ time units. Slots are assigned to APs such that no two interfering APs get scheduled in the same slot. Thus, the goal of the slot assignment mechanism is to maximize the network throughput while ensuring inter-AP fairness.

There can be different algorithms to assign slots to the APs keeping in mind that the APs do not interfere. In this research we have simulated 3 different algorithms and analyzed their performances. Algorithm 1 based on known location of APs whereas Algorithm 2 and 3 for varying locations with singe and multiple frequencies respectively.

A. Slots assignment algorithm with known disk location *(Algorithm 1)*

In this algorithm we assume that the locations of our APs also known as disk locations are known.

So, there is no need of ordering the APs for slot distribution. Slots distribution start from the reverse order of the APs list, where the list is created according to their non-decreasing X co-ordinate. According to the individual requirement of an AP slots are distributed so that no interfering APs get the same slot. Fig. 4 depicts the flow chart of this procedure.

In this mechanism AP's requirement reflects its weight because weight proportional to inverse of communication bit-rate and it inversely proportional to required time period. So weight is proportional to requirement of slot.

According to the requirements of the interference graph in Fig. 3, how slot is distributed revealed in Fig. 5. Here for 8 APs in the graph, algorithm 1 finds the optimal solution where minimum required number of slots is 6. Slots are distributed according to the order of 7, 6, 5, 4, 3, 2, 1 and 0, reverse of non-decreasing X co-ordinate of APs. AP 7, 6, and 5 requirements are 1, 1 and 3 respectively. Hence the set of assigned slots of them are {1}, {2} and {3, 4, 5} so that no 2 neighbors get the same slot. APs 4, 3, 2, 1 and 0 got slots in the same way.

B. Slots assignment with unknown disk locations and single frequency (*Algorithm 2)*

Algorithm 1, can't handle the unknown disk location. That's why we implement second algorithm which is slot assignment with unknown disk location and single frequency.

In this algorithm we order the unknown disk location with respect to total requirement. Total requirement means summation of own requirement and adjacency nodes' own requirement. Then node of minimum total requirement is found out from the total requirement of all nodes and this node will be the start node. Then own requirement of the start node is subtracted from its adjacency nodes of total requirement. Then again check the min total requirement for finding the second start node and continue the same process. This process is shown in Fig. 6. Considering interference graph of Fig. 3, algorithm 2 finds out the ordering of the APs is as 6, 7, 0, 1, 3, 2, 4 and 5. Slot distribution start from the reverse order of the list where 1st slot distributed node is 5 and the last one is 6. Like algorithm 1, algorithm 2 also needs minimum 6 slots for distribution among the 8 APs. Fig. 7 exhibits the details about that.

C. Slots assignment for unknown disk locations and multiple frequencies (*Algorithm 3)*

For algorithm 3, we calculate the order of the APs in the similar way of the algorithm 2. But here, we have another parameter that is frequency with the slot for slot assignment to the APs.

We also apply some rules to appropriately simulate this algorithm. We select the start node from the ordering list to the reverse order. As here frequency is another parameter so to distribute slots, we first consider what would be the efficient frequency for that AP then the required slots. There must be difference among the adjacent APs either in the frequency level or slots level to avoid interference. Mechanism of algorithm 3 is shown in Fig. 8. Considering interference graph of Fig. 3, Fig. 9 and 10 reveal what would be frequencies and slots set of the APs in the network while allocating number of frequencies 2 and 3 respectively. In the both figure, order of list of APs for frequency and slots distribution is same as used in algorithm 2. Although Fig. 9 and 10 use 2 and 3 frequency respectively, there is no significant able difference in efficiency for slots assignment. Here both require minimum 3 different slots and only difference is in the slot sets of node 1 and 6 where node 1 and 6 slot sets for Fig. 9 are {2, 3} and {2} and that for Fig. 10 are {1, 2} and {1}. This is true for the small interfering graph and number of nodes is low. But as number of nodes and their interconnecting edges increase, efficiency for using varying number of frequencies varied.

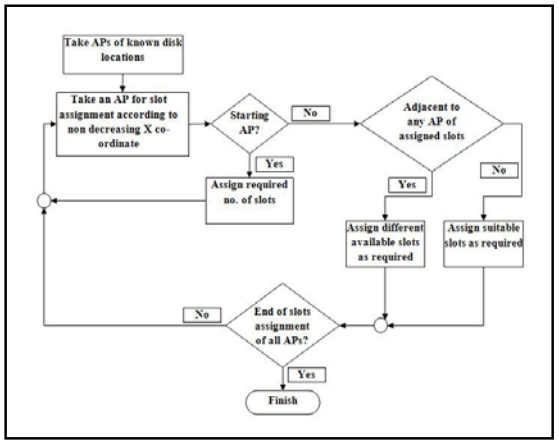

Fig. 4. Flowchart of Algorithm 1

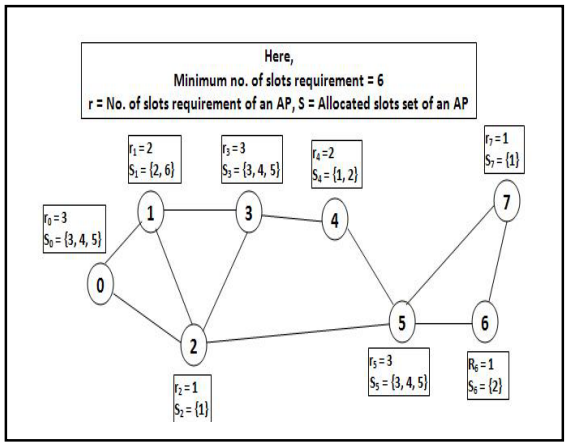

Fig. 5. Slots distribution using Algorithm 1

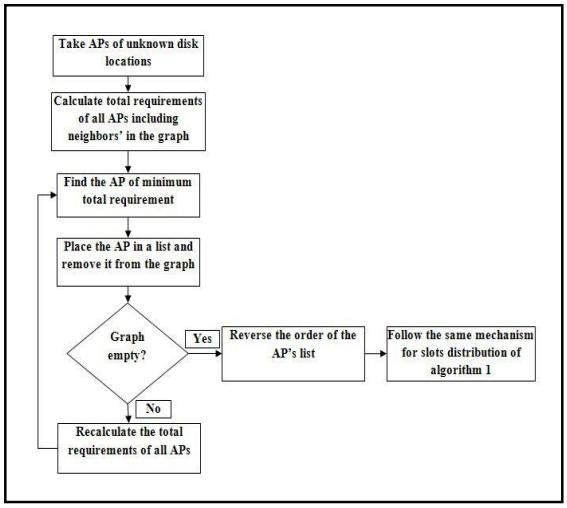

Fig. 6. Flowchart of Algorithm 2

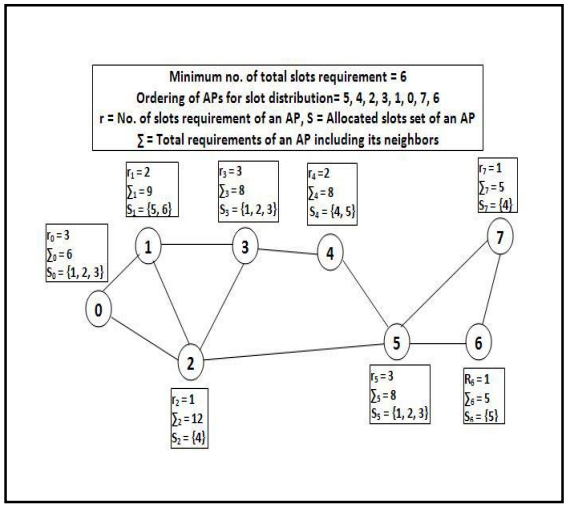

Fig. 7. Slots distribution using Algorithm 2

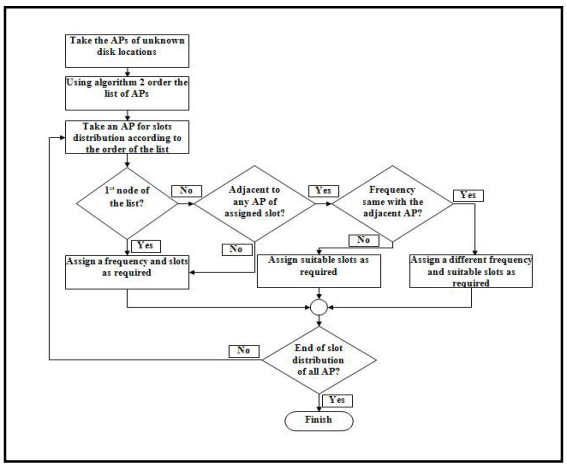

Fig. 8. Flowchart of Algorithm 3

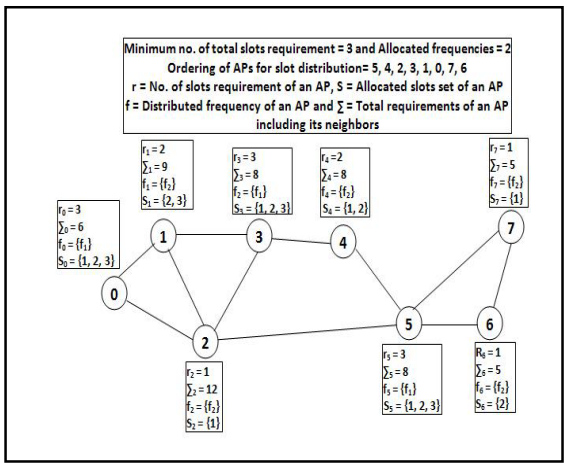

Fig. 9. Slots distribution using Algorithm 3 considering no. of frequencies 2

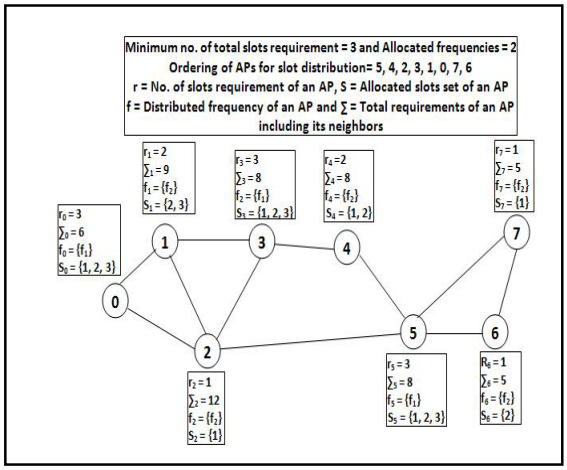

Fig. 10. Slots distribution using Algorithm 3 considering no. of frequencies 3

VI. PERFORMANCE ANALYSIS OF THE ALGORITMS

Algorithm 1 is a trivial solution for slot distribution of APs in comparison with algorithm 2 and 3 because it can only work for APs of known disk locations, hence it is limited solution. On the other hand, although algorithm 2 and 3 both work for APs of unknown disk locations but the later one is more efficient than the former because of its multiple frequencies handling ability. In Fig. 11 and 12, here performance is compared between algorithm 2 and 3 varying the size of interference graph. Fig. 11 shows the comparative figure of how required slots varied between 2 algorithms when no. of nodes (APs) varied. On the other hand Fig. 12 depict how no. of slots changes with the changes of no. of interconnecting edges of the interference graph. In both cases algorithm 3 is efficient than 2. If we consider that the slot no. is fixed and maximum requirement in the interference graph is variable, then it also found from Fig. 13 that algorithm 3 is more flexible and stable for the maximum requirement than algorithm 2.

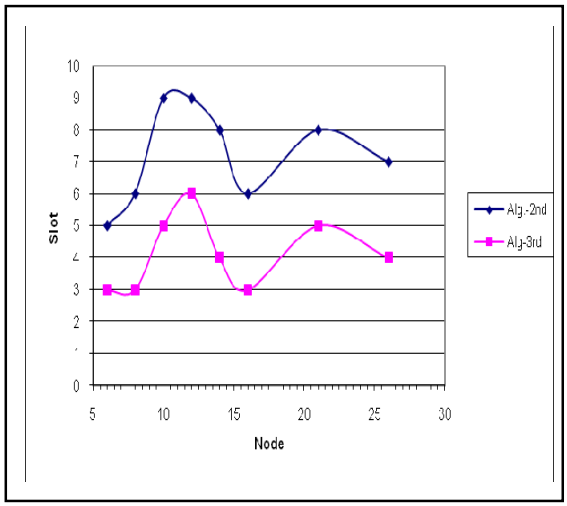

Fig. 11. Total no. of nodes vs. required slots

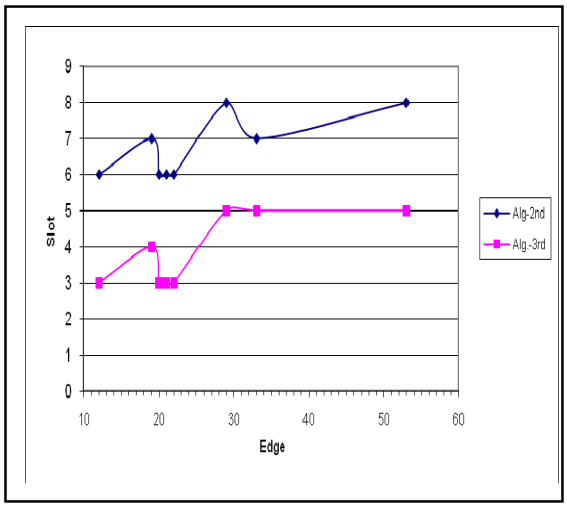

Fig. 12. Total no. of edges vs. required slots

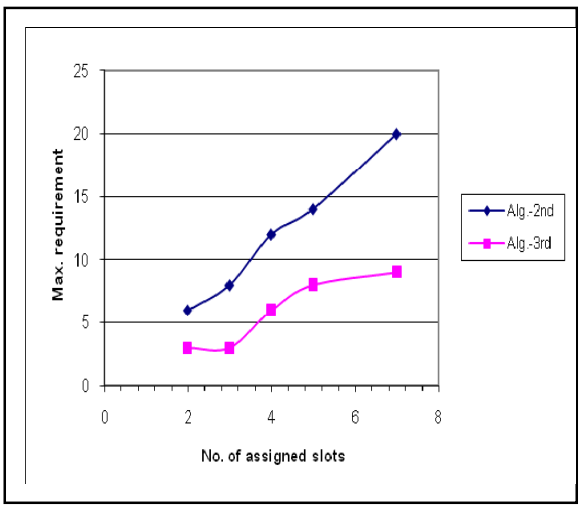

Fig. 13. Total no. of assigned slots vs. maximum requirements

VII. CONCLUSION

The MiFi [1] system reproduces the behavior of a single AP for handling multiple AP. The framework of this system, partition time into repeated periods or superframes where each superframe contains a fixed duration and a contention free period (CFP) and a contention period (CP). Moreover the CFP is divided into slots which are suitable for both RT and NRT data handling. We devise the slot handling mechanisms for considering the various situations and after analyze their performance, we find that algorithm 1 is recommended to use if the locations of APs are known but if the locations are unknown and there is an opportunity for using multiple frequencies then algorithm 3 is the best choice for slots distribution among the APs in an interference graph.

REFERENCES

[1] Y. Bejerano and R. S. Bhatia, "MiFi: A framework for fairness and QoS assurance in current IEEE 802.11 networks with multiple access points," in Proc. IEEE/ACM transactions of networking, vol. 14, No. 4, Aug. 2006.

[2] Y. Bejerano and R. S. Bhatia, "MiFi: A framework for fairness and QoS assurance in current IEEE 802.11 networks with multiple access points," in proc. IEEE INFOCOM' 04, 2004, pp. 1229-1240.

[3] T. Nandagopal, T-E. Kim, X. Gao, and V. Bharghavan, "Achieving MAC layer fairness in wireless packet networks", In proc. MobiCom, Aug. 2000, pp. 87-98.

[4] A. Kopsel and A. Wolisz, "Voice transmission in an IEEE 802.11 WLAN based access network", In proc. Workshop on Wireless Mobile Multimedia (WoWMoM), 2001, pp. 23-32.

[5] S. Mangold, "Coexistence of overlapping basic service sets", In Proc. Mobile Venue'02, 2002, pp. 131-135.

[6] C. E. Koksal, H. Kassab, and H. Balakrishnan, "An analysis of short-term fairness in wireless media access protocols (poster)", Int. Conf. Measurement and Modeling of Computer Systems, Jun. 2000.

Proceedings of 2009 12th International Conference on Computer and Information Technology (ICCIT 2009)
21-23 December, 2009, Dhaka, Bangladesh

Three Algorithms for Learning Artificial Neural Network: A Comparison for Induction Motor Flux Estimation

Md. Abdur Rafiq, Naruttam Kumar Roy, B. C. Ghosh
Department of Electrical & Electronic Engineering
Khulna University of Engineering & Technology (KUET), Khulna-9203, Bangladesh
mdabdurrafiq2003@yahoo.com, nkroy@yahoo.com, bcg@eee.kuet.ac.bd

Abstract

This paper presents a comparative study of three algorithms for learning artificial neural network. As neural estimator, back-propagation (BP) algorithm, uncorrelated real time recurrent learning (URTRL) algorithm and correlated real time recurrent learning (CRTRL) algorithm are used in the present work to learn the artificial neural network (ANN). The approach proposed here is based on the flux estimation of high performance induction motor drives. Simulation of the drive system was carried out to study the performance of the motor drive. It is observed that the proposed CRTRL algorithm based methodology provides better performance than the BP and URTRL algorithm based technique. The proposed method can be used for accurate measurement of the rotor flux.

Keywords: Back-propagation (BP), Correlated real time recurrent learning (CRTRL), Induction motor, Recurrent neural network, Rotor flux, Uncorrelated real time recurrent learning (URTRL).

I. INTRODUCTION

Artificial neural network (ANN) belongs to the area of artificial intelligence (AI). Basically, ANN is embedding human intelligence in a machine so that a machine can think intelligently like a human being. Recently, AI is widely used for machine control. Accurate flux estimation is an important task in implementing high-performance induction motor drives [1]–[6]. There are, in general, two methods for flux estimation: one is based on measured motor currents, and the other is based on measured voltages [1], [3], [6]. In the sense of parameters sensitivity, voltage measurement based method is suitable in which the motor flux can be obtained by integrating its back electromotive force (emf).

However, implementation of an integrator for motor flux estimation is not easy task. A pure integrator has dc drift and initial value problems [4], [6]. A dc component in measured motor back emf is inevitable in practice. This dc component, no matter how small it is, can finally drive the pure integrator into saturation. When a sinusoidal signal is applied to the integrator, a cosine wave is expected at its output. This is true only when the input sine wave is applied at its positive or negative peak. Otherwise, a constant dc offset will appear at the output. This offset, representing constant dc flux in the motor, which does not exist during motor normal operation. The dc offset can also be generated when there is a rapid change in the input signal. A common solution to these problems is to replace the pure integrator with a first-order low-pass (LP) filter. Obviously, the LP filter will produce errors in magnitude and phase angle, especially when the motor runs at a frequency lower than the filter cut-off frequency. Therefore, motor drives using LP filters as a flux estimator usually have a limited speed range, typically 1: 10 (6–60 Hz) [1]. Three modified integrators using new algorithms [7] are developed to solve the above mentioned problems. But the performances of these integrators tend to fail in low frequencies, since all of them are practically low-pass filters in which the pole is selected to be very close to zero. Another methodology called adaptive integration methodology [8] shows how to use a linear neural network, an ADALINE [9], for the integration of a signal to eliminate the dc component thus having a pure integrator unaffected by the dc drift and the initial conditions. This integrator uses two neural filters, each of which operates with two basic processes forming a feedback loop. But this methodology doesn't show accurate estimation of flux.

To solve the above mentioned problems, in this paper three methodologies are presented. These are BP, URTRL and proposed CRTRL based estimator. The performances of these methodologies are studied, verified and compared through simulation. By the comparative study, it is shown that the CRTRL algorithm based estimator presents better performances than the BP and URTRL algorithm based methodology.

II. ANN BASED FLUX ESTIMATOR

The identification and control of dynamical systems using neural networks have been widely studied in recent years. In adaptive neural integration the flux linkage is obtained from back emf by an integration method accomplished by a programmable cascaded low-pass filter (PCLPF) implemented by a hybrid neural network consisting of a recurrent neural network (RNN) and a feed-forward artificial neural network (FFANN) [11]-[13]. A common approach to realize an artificial-neural-network (ANN)-based dynamical system is to incorporate tapped delay lines to applied inputs, measured outputs, or the delayed feedback of a static feed forward

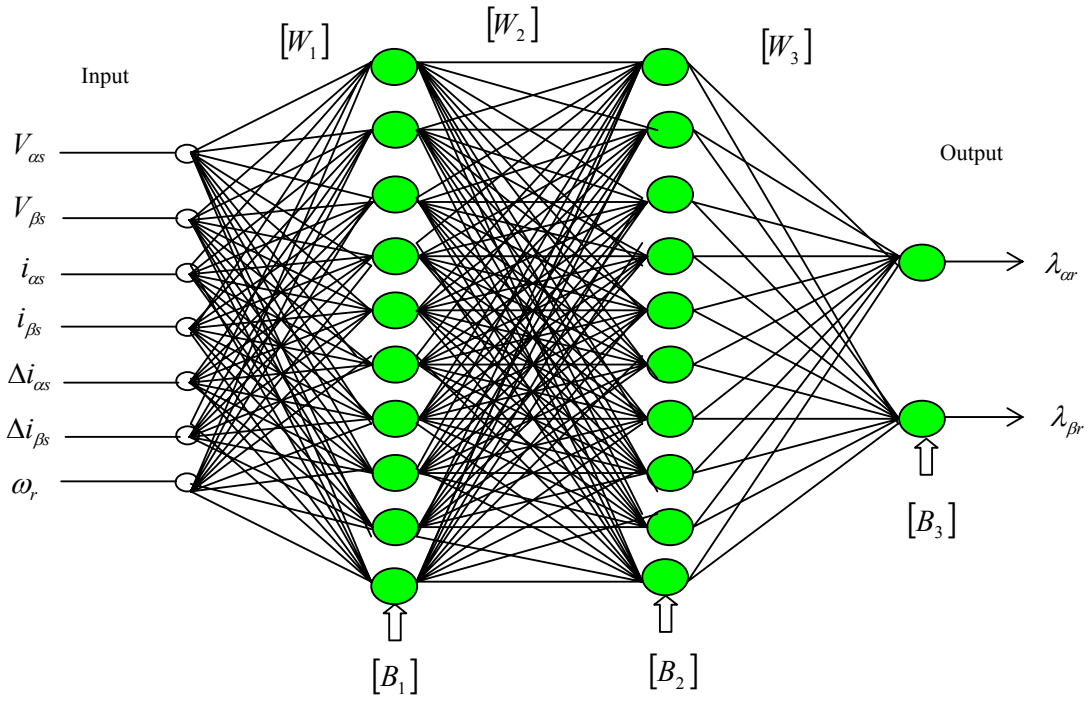

Fig. 1. Stationary α- and β-axis rotor flux synthesis by BP algorithm.

neural network [14]. The BP, URTRL and CRTRL algorithm for learning a neural network is given below.

A. BACK-PROPAGATION ALGORITHM FOR NEURAL NETWORK

The error signal at the output of neuron *j* at iteration *n* (i.e. presentation of the *n*th training example) is defined by [15]

$$e_j(n) = d_j(n) - y_j(n) \tag{1}$$

where, neuron *j* is an output node, .d_j (n) is desired output and y_j (n) is actual output.

The instantaneous value of total error energy can be written as per definition

$$\varepsilon(n) = \frac{1}{2}\sum_{j \in c} e_j^2(n) \tag{2}$$

where, the set *C* includes all the neurons in the output layer of the network. Let *N* denotes the total number of patterns contained in the training set. The *average squared error energy*, is obtained by summing $\varepsilon(n)$ over all n and then normalizing with respect to the set size *N* as shown by

$$\varepsilon_{av} = \frac{1}{N}\sum_{n=1}^{N} \varepsilon(n) \tag{3}$$

For a given training set, ε_{av} represents the cost function as a measure of learning performance. The objective of learning process is to adjust the free parameters of the network to minimize ε_{av}

Again, the induced local field $v_j(n)$ produced at the input of the activation function associated with neuron *j* is therefore

$$v_j(n) = \sum_{i=0}^{m} w_{ji}(n)\, y_i(n) \tag{4}$$

where, *m* is the total number of inputs (excluding bias) applied to the neuron *j*. The synaptic weight w_{j0} equals the bias b_j applied to the neuron *j*. Hence the functional signal appearing at the output of neuron *j* at iteration *n* is

$$y_j(n) = \varphi_j(v_j(n)) \tag{5}$$

The backpropagation algorithm applies a correction $\Delta w_{ji}(n)$ to the synaptic weight $w_{ji}(n)$, which is proportional to the partial derivative $\partial\varepsilon(n) / \partial w_{ji}(n)$. According to the chain rule of calculus we may express the gradient as

$$\frac{\partial\varepsilon(n)}{\partial w_{ji}(n)} = \frac{\partial\varepsilon(n)}{\partial e_j(n)}\frac{\partial e_j(n)}{\partial y_j(n)}\frac{\partial y_j(n)}{\partial v_j(n)}\frac{\partial v_j(n)}{\partial w_{ji}(n)}$$
$$= -e_j(n)\varphi_j'(v_j(n))y_i(n) \tag{6}$$

The left term represents a *sensitivity factor*.

The correction is defined by the *delta rule*:

$$\Delta w_{ji}(n) = -\eta\frac{\partial\varepsilon(n)}{\partial w_{ji}(n)} \tag{7}$$

where, η is the learning rate parameter of the back-propagation algorithm. The minus sign indicates *gradient descent* in weight space. Accordingly, the use of equation (6) in (7) yields

$$\Delta w_{ji}(n) = -\eta \delta_j(n) y_i(n) \tag{8}$$

where, the local gradient $\delta_j(n)$ is defined by

$$\delta_j(n) = -\eta \frac{\partial \varepsilon(n)}{\partial v_j(n)}$$

$$= -\frac{\partial \varepsilon(n)}{\partial e_j(n)} \frac{\partial e_j(n)}{\partial y_j(n)} \frac{\partial y_j(n)}{\partial v_j(n)} \tag{9}$$

$$= e_j(n) \varphi_j'(v_j(n)) \tag{10}$$

The local gradient points to required changes in synaptic weights. According to equation (9) the local gradient $\delta_j(n)$ for output neuron *j* is equal to the product of the corresponding error signal $e_j(n)$ for that neuron and derivative $\varphi_j'(v_j(n))$ of the associated activation function. Rotor flux synthesis by BP algorithm is shown in Fig. 1.

B. REAL TIME RECURRENT LEARNING (RTRL) ALGORITHM FOR THE RNN

In mathematical terms, the dynamical behavior of any noise free system can be described by the following pair of non-linear equations [15]:

$$x(n+1) = \varphi(W_a x(n) + W_b u(n)) \tag{11}$$

$$Y(n) = Cx(n) \tag{12}$$

where, $x(n)$ is the q-by-1 non-linear state matrix, $u(n)$ is the m-by-1 input matrix, $Y(n)$ is the p-by-1 corresponding output matrix, W_a is the q-by-q matrix, W_b is the q-by-(m+1) matrix and C is the p-by-q matrix.

The process equation (11) is reproduced here in the following expanded form:

$$x(n+1) = \begin{bmatrix} \varphi(w_1^T \xi(n)) \\ . \\ . \\ \varphi(w_j^T \xi(n)) \\ . \\ . \\ \varphi(w_q^T \xi(n)) \end{bmatrix} \tag{13}$$

It is assumed that all the neurons have a common activation function $\varphi(.)$. The (q+m+1)-by-1 vector w_j is the synaptic weight vector of neuron j in the recurrent network, that is:

$$w_j = \begin{bmatrix} w_{a,j} \\ w_{b,j} \end{bmatrix}, \text{j=1,2…..,q} \tag{14}$$

where $w_{a,j}$ and $w_{b,j}$ are the jth columns of the transposed weight matrices W_a^T and W_b^T respectively. The (q+m+1)-by-1 vector

$$\xi(n) = \begin{bmatrix} x(n) \\ u(n) \end{bmatrix} \tag{15}$$

The first element of $u(n)$ is +1 and, in a corresponding way, the first element of $w_{b,j}$ is equal to the bias b_j applied to neuron j.

The q-by- (q+m+1) partial derivative matrix of the state vector *x(n)* with respect to the weight vector w_j :

$$\Lambda_j(n) = \frac{\partial x(n)}{\partial w_j(n-1)} \quad \text{, j=1,2,….,q} \tag{16}$$

$U_j(n)$ is a *q*-by-(*q* +m + 1) matrix whose rows are all zero, except for the jth row that is equal to the transpose of vector $\xi^T(n)$:

$$U_j(k) = \begin{bmatrix} 0^T \\ \xi^T(n) \\ 0^T \end{bmatrix} \leftarrow jthrow \quad j = 1,2,...q \tag{17}$$

$\varphi(n)$ is a *q-by-q* diagonal matrix whose kth diagonal element is the partial derivative of the activation function with respect to its argument, evaluated at $w_j^T \xi(n)$:

$$\varphi(n) = diag \ [\varphi'(W_1^T \xi(n)), \varphi'(W_2^T \xi(n)), ... \\ .....\varphi'(W_q^T \xi(n))] \tag{18}$$

With these definitions, the following recursive equation Λ_j for the neuron j can be obtained by differentiating (13) with respect to w_j and using the chain rule of calculus:

$$\Lambda_j(n+1) = \varphi(n)[W_a(n)\Lambda_j(n) + U_j(n)] \tag{19}$$

where, j=1,2,….,q

The objective of the learning process is to minimize a cost function obtained by the instantaneous sum of squared errors at time *k*, which is defined in terms of *e(n)* by

$$\zeta(n) = \frac{1}{2} e^T(n) e(n) \tag{20}$$

where, the *p*-by-1 error vector *e(n)* is defined by using the measurement equation :

$$e(n) = \tilde{y}(n) - y(n) \tag{21}$$

where, $\tilde{y}(n)$ denotes the desired output vector.

The adjustment for the weight vector of the jth neuron, ΔW_j, is:

$$\Delta W_j = -\eta \frac{\partial \zeta(n)}{\partial W_i(n)} = \eta C \Lambda_i(n) e(n) \tag{22}$$

where, J=1,2,3,……,q

Two types of learning algorithms are found to work accurately for rotor flux estimation:

(a) Output Uncorrelated Real Time Recurrent learning (URTRL)
(b) Output Correlated Real Time Recurrent learning (CRTRL)

B.1 URTRL ALGORITHM FOR THE RNN

Rotor flux synthesis by URTRL algorithm is shown in Fig. 2. Here the rotor fluxes are uncorrelated and decoupled. The voltage and current components along α- and β- axes, the change in currents along α- and β- axes, the speed of the motor and bias are used as input variables in each case. Here α- and β- axes rotor fluxes are found from Fig. 2 (a) and Fig. 2 (b) respectively. There is no correlation between the outputs.

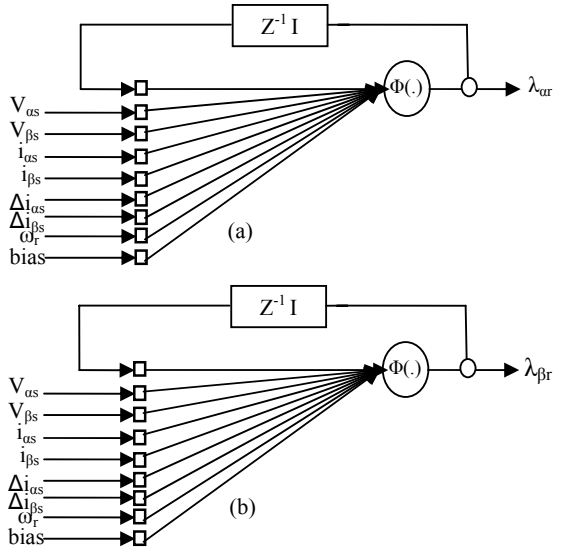

Fig. 2. (a) Stationary α- axis and (b) β- axis rotor flux synthesis by URTRL algorithm.

B.2 CRTRL ALGORITHM FOR THE RNN

The network design for this case is similar to URTRL with the outputs correlated and feed back. The networks for the rotor axis fluxes are indicated in Fig. 3. The same input variables are used here. The trained network consists of input and output layer. There is zero hidden layer. The outputs are α- and β- axes rotor fluxes. Here the feedback value of output is used in each case.

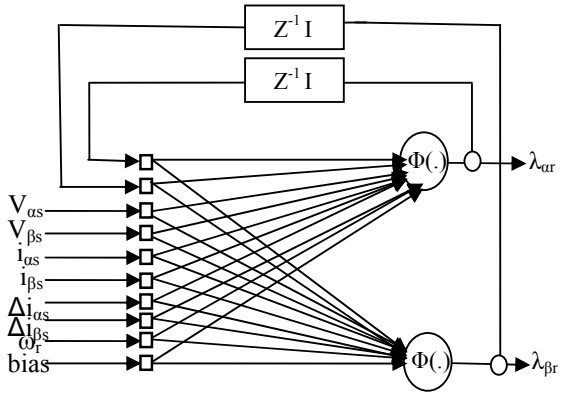

Fig. 3. Stationary α- and β- axes rotor flux synthesis by proposed CRTRL algorithm.

III. SIMULATION RESULTS

For induction motor simulation, the fifth order nonlinear state space model is represented in the stationary reference frame ($\alpha - \beta$) as follows:

$$v_{\alpha s} = (R_s + L_\sigma p) i_{\alpha s} + (L_m / L_r) p \lambda_{\alpha r} \tag{23}$$

$$v_{\beta s} = (R_s + L_\sigma p) i_{\beta s} + (L_m / L_r) p \lambda_{\beta r} \tag{24}$$

$$0 = -(L_m / \tau_r) i_{\alpha s} + \{(1/\tau_r) + p\} \lambda_{\alpha r} + \omega_r \lambda_{\beta r} \tag{25}$$

$$0 = -(L_m / \tau_r) i_{\beta s} - \omega_r \lambda_{\alpha r} + \{(1/\tau_r) + p\} \lambda_{\beta r} \tag{26}$$

$$T_{em} = Jp\omega_m + B\omega_m + T_L \tag{27}$$

where, $v_{\alpha s}$, $v_{\beta s}$: α-and β-axis stator voltage components; $i_{\alpha s}$, $i_{\beta s}$: α-and β-axis stator current components; $i_{\alpha r}$, $i_{\beta r}$: α-and β-axis rotor current components, T_{em}: develop electromagnetic torque of the induction motor.

Here,

$$\lambda_{\alpha r} = L_r i_{\alpha r} + L_m i_{\alpha s} \tag{28}$$

$$\lambda_{\beta r} = L_r i_{\beta r} + L_m i_{\beta s} \tag{29}$$

$$L_\sigma = L_s - (L_m^2 / L_r) \tag{30}$$

$$\tau_r = L_r / R_r \tag{31}$$

Equation (27) can be rewritten in terms of state variables with P_p-pole pairs as:

$$T_{em} = P_p (i_{\alpha r} [L_m i_{\beta s} + L_r i_{\beta r}] - i_{\beta r} [L_m i_{\alpha s} + L_r i_{\alpha r}]) \tag{32}$$

Simulation studies have been conducted in order to establish the functionality of the proposed estimation scheme. The simulated induction motor is 3-phase, 220 V, 1 hp. The model parameters for this motor are $P_p = 2$, $R_s = 1.798$ ohm, $R_r = 0.825$ ohm,

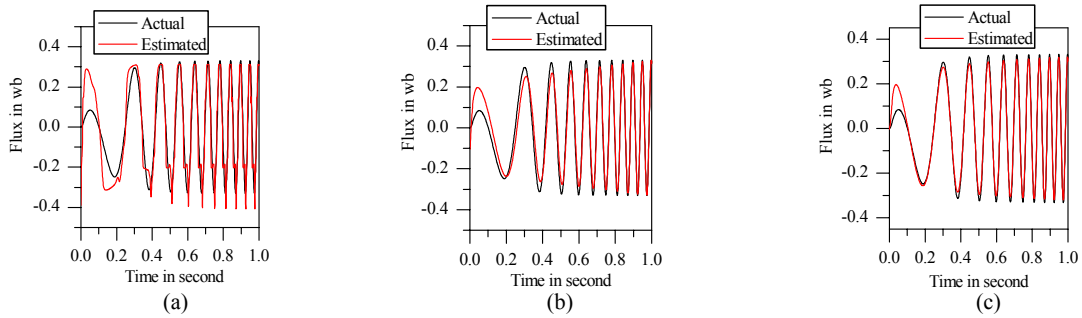

Fig. 4 α -axis rotor flux estimation using (a) Back-propagation, (b) URTRL, and (c) CRTRL algorithm.

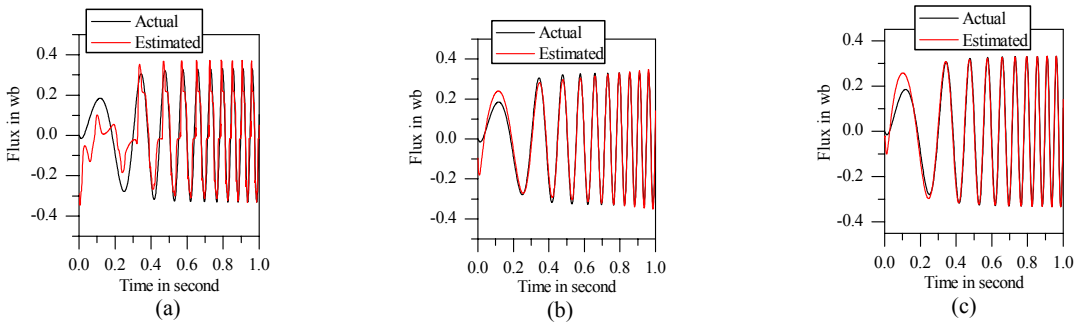

Fig. 5. β -axis rotor flux estimation using (a) Back-propagation, (b) URTRL, and (c) CRTRL algorithm.

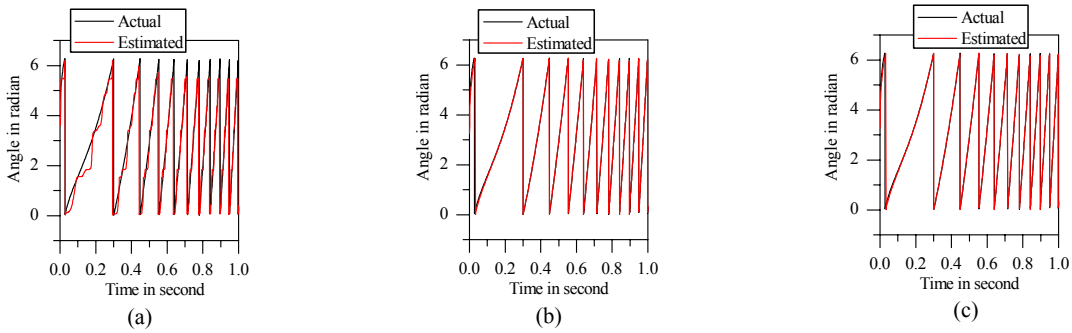

Fig. 6 Rotor flux angle estimation using (a) Back-propagation, (b) URTRL, and (c) CRTRL algorithm.

$L_s = L_r = 0.08323$ henry, and $L_m = 0.07613$ henry. The motor- load inertia and friction coefficient have been chosen to be $J = 0.095$ Nmsec^2 and $B = 0.0005$ Nm-sec/rad, respectively. After estimating the $\lambda_{\alpha r}$ and $\lambda_{\beta r}$, the rotor flux angle can be calculated as:

$$\theta = arctg \frac{\lambda_{\beta r}}{\lambda_{\alpha r}} \tag{33}$$

This angle θ leads to the decoupling between the magnetizing and torque producing current components. For BP algorithm the trained network consists of a three layer neural network with seven input nodes connected to ten sigmoid neurons (7-10-10-2). For BP, URTRL and CRTRL algorithm learning rate α is 0.00001, pseudo temperature μ_1 is 1.25, activation function is $f(x) = 1 - 2/e^{2x\mu_1}$ and the decision delay is 1. Both URTRL and proposed CRTRL have no hidden layer whereas the back propagation algorithm required two hidden layers for estimation of rotor flux. This section presents simulation results of the field orientation controlled induction motor concerning the proposed ANN estimators. In the simulated tests, for comparison purpose, the real flux has been obtained by the voltage flux model described in (23)-(26). The performance of the proposed CRTRL based estimator has been compared with the BP and URTRL methodology.

Fig. 4 (a), (b), and (c) show α -axis rotor actual and estimated flux for BP, URTRL and CRTRL algorithm respectively. At the starting period, the motor is in transient state and it gives oscillating and more non-linear nature in the actual flux. Fig. 5 (a), (b), and (c) show β -axis rotor actual and estimated flux for BP, URTRL and CRTRL algorithm respectively. Flux angle estimated from equation (33) is shown in Fig. 6 (a), (b), and (c). These figures illustrates that CRTRL based estimator works better than BP & URTRL methodology for both rotor flux and rotor flux angle estimation.

The comparison of mean square error is shown in Fig. 7, where the error is 0.0004 for Back- propagation and 0.00015 for URTRL and 0.00009 for CRTRL estimator. From the comparison graphs, it is clear that CRTRL estimator is superior to that of BP estimator as it uses feedback values for its training. Moreover, CRTRL training is faster than Back-propagation for its simple constitution such as it doesn't need any hidden node. For the benefit of less timing effect CRTRL based flux estimator is easier for real time implementation. Moreover, as outputs are correlated in CRTRL it gives better performance than URTRL estimator.

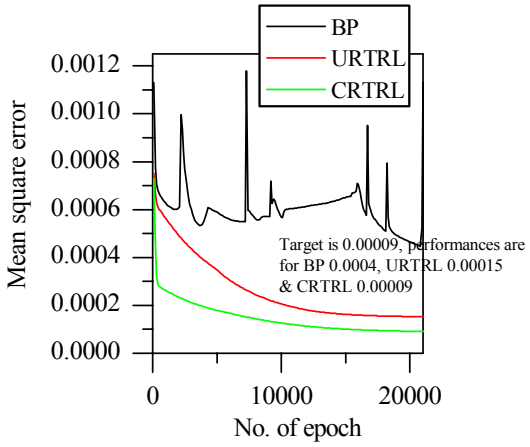

Fig. 7. Mean square error comparison of Back-propagation, URTRL, and CRTRL algorithm.

IV. CONCLUSION

In this paper, performances of three types of artificial neural network based flux estimator are described, investigated and compared. It has been observed that the back-propagation ANN has complex structure and fails to estimate the flux components at low speeds. The proposed CRTRL algorithm based estimator uses a very simple Recurrent Neural Network and it is therefore easier to implement than fixed notch filters in DSP based control systems. It is also observed that the proposed flux estimator is capable to estimate flux accurately than BP and URTRL estimator. During the design of the CRTRL based neural estimator, the results related to the training and validation tests seem to indicate that the proposed neural network estimator is rather satisfactory. A high performance response of the system indicates the effectiveness of the proposed CRTRL algorithm based flux estimator.

REFERENCES

[1] W. A. Hill, R. A. Turton, R. J. Dungan, and C. L. Schwalm, "A vector controlled cycloconverter drive for an icebreaker," *IEEE Transactions on Industry Applications*, Vol. 23, No. 6, 1987, pp. 1036–1042.

[2] Y.Yusof, A.H.M. Yatim, "Simulation and modeling of stator flux estimator for induction motor using artificial neural network technique," *Proceedings of Power Engineering Conference (PECON- 2003)*, Dec.15-16, 2003, pp. 11-15.

[3] I. Takahashi, T. Noguchi, "A new quick response and high efficiency control strategy of an induction motor," *IEEE Transactions on Industry Applications*, Vol. 22, No. 5, 1986, pp. 820–827.

[4] R. Wu, G. R. Slemon, "A permanent magnet motor drive without a shaft sensor," *IEEE Transactions on Industry Applications*, Vol. 27, No. 5, 1991, pp. 1005–1011.

[5] X. Xu, R. Doncker, and D. W. Novotny, "A stator flux oriented induction machine drive," *in IEEE PESC Conf. Rec.*, 1988, pp. 870–876.

[6] H. Tajima, Y. Hori, "Speed sensorless field oriented control of the induction machine," *in IEEE IAS Conf. Rec.*, 1991, pp. 385–391.

[7] J. Hu, B.Wu, "New integration algorithms for estimating motor flux over a wide speed range," *IEEE Transactions on Power Electronics*, Vol. 13, Sept. 1998, pp. 969–977.

[8] M. Cirrincione, M. Pucci, G. Cirrincione, and Gérard-André Capolino, "A new adaptive integration methodology for estimating flux in induction machine drives," *IEEE Transactions on Power Electronics*, Vol. 19, Jan. 2004, pp. 25- 34.

[9] B. Widrow, S. D. Stearn, *Adaptive Signal Processing*, Englewood Cliffs, NJ: Prentice-Hall, 1985.

[10] Bashudeb Chandra Ghosh, *Parameter adaptive vector controller for CSI-fed induction motor drive and generalized approaches for simulation of CSI-IM system,* Ph.D. Dissertation, Department of Electrical Engineering, IIT, Kharagpur, July 1992.

[11] L. E. B. de Silva, B. K. Bose, and J. O. P. Pinto, "Recurrent-neural network- based implementation of a programmable cascaded low-pass filter used in stator flux synthesis of vector-controlled induction motor drive," *IEEE Transactions on Industrial Electronics*, Vol. 46, June 1999, pp. 662–665.

[12] J. O. P. Pinto, B. K. Bose, and L. E. B. de Silva, "A stator-flux-oriented vector-controlled induction motor drive with space- vector PWM and flux-vector synthesis by neural network," *IEEE Transactions on Industry Applications*, Vol. 37, Sept./Oct. 2001, pp. 1308–1318.

[13] B. K. Bose, N. R. Patel, "A sensorless stator flux oriented vector controlled induction motor drive with neuro-fuzzy based performance enhancement," *in Proc. IEEE IAS'97* (Ind. Applicat. Soc. Annu. Meeting), Oct. 5–9, 1997.

[14] K. S. Narendra, K. Parthasarathy, "Identification and control of dynamic systems using neural networks," *IEEE Transactions on Neural Networks*, Vol. 1, Jan. 1990, pp. 4–27.

[15] S. Haykin, *Neural Networks: A Comprehensive Foundation*, 2nd Ed., Upper Saddle River, NJ: Prentice Hall, 1999, pp. 756-759.

Proceedings of 2009 12th International Conference on Computer and Information Technology (ICCIT 2009)
21-23 December, 2009, Dhaka, Bangladesh

Content Clustering of Computer Mediated Courseware Using Data Mining Technique

Golam Md. Muradul Bashir, Abu Sayed Md. Latiful Hoque†
CCE Dept., Patuakhali Science and Technology University, Patuakhali, Bangladesh
†CSE Dept., Bangladesh University of Engineering and Technology, Dhaka, Bangladesh
murad98csekuet@yahoo.com, asmlatifulhoque@cse.buet.ac.bd

Abstract

Computer Mediated Courseware (CMC) has been developed so far for individual courses considering single or multiple text books. A group of courseware can be developed by using multiple text books and in this case, it is a requirement to cluster the contents of different books to form a generalized clustered content. No work has been found to develop this generalized clustered content. We have proposed a methodology based on data mining techniques to construct a hierarchical general structure of a group of courseware combining the individual structure of a set of books. The clustering will help the courseware developer to dynamically allocate contents to develop different courses using a group of books. We have applied this methodology for different level of courses on database. The methodology is generalized and can be applied to any other courses.

Keywords: Clustering, Courseware, Proximity, Synonym.

I. INTRODUCTION

Computer Mediated Courseware (CMC) is educational computer software whose primary purpose is teaching or self-learning [1]. Computer Mediated Courseware (CMC) have been developed for different level of education e.g., distance learning [2-4], Engineering Education [5] and others [6,7,8] focusing on lecture video, audio or slide representation. Existing CMC for engineering education mainly guided by teacher centric and non-interactive. It is difficult to achieve the total coverage of the courseware. The effectiveness of a courseware depends on the organization of the courseware covering the total spectrum of the course.

Computer Mediated Courseware (CMC) has been developed so far for individual courses considering single or multiple text books. A group of courseware can be developed by using multiple text books and in this case, it is a requirement to cluster the contents of different books to form a generalized clustered content.

The basic element of a courseware is the topic that covers an atomic course item. An atomic item means that the item describes an idea or a theory or a rule that cannot be further decomposed. Multiple topics form a section/sub-section. A set of sections that elaborates similar things forms a chapter. A courseware consists of a number of chapters. In general a courseware is developed based on several text books written by different authors. Different text book organizes topics in different ways. A courseware based on different text book should have a general hierarchy of chapters→sections→subsection→topics such that it covers all the topics covered by different texts. It is a difficult job to develop this generalized hierarchy covering all the topics. Courseware so far has been developed based on a single text book and just referring the URL of other books or name and author names of books. This paper describes a generalized methodology of clustering the courseware topics to form the generalized hierarchy of a courseware. We have used similarity based clustering technique to form the higher level clusters of the content of a courseware based on multiple text books. We have considered three text books on Database Management System (DBMS), the core course on Computer Science and Engineering for the implementation of this clustering of contents. Section II describes the literature survey on courseware development methodology. Section III describes the structure of CMC. Section IV illustrates general structure of group courseware. Section V explains transformation of book tree into relational representation. Section VI elaborates the clustering procedure. Section VII is the result and discussion. Section VIII is the conclusion.

II. LITERATURE SURVEY

The mystification surrounding the term 'online course' arises because it is used indiscriminately to apply to nearly any course which makes even a passing use of the Internet, as well as to those where every aspect of the course is only accessible electronically [2]. John Bourne et al. [5] have discussed the Sloan Consortium's quest for quality, scale and breadth in online learning, the impact on both continuing education of graduate engineers as well as degree-seeking engineering students, and the future of engineering colleges and schools as worldwide providers of engineering education. The National Teaching and Learning Database (NTLD) project in Australia has been designed to provide access to learning materials [6]. Wade et al. [7] proposes an automated, third party WWW based evaluation service which focuses on usability issues of WWW based courseware and which can be used by any WWW course instructor/Student. This paper researches the design, development and trialing of a WWW based evaluation service for WWW courseware. The paper concludes with an assessment of the benefit of using such an evaluation service to improve WWW based courseware. Hoic-Bozic et al. [8] present the result of the questionnaire about the effectiveness and quality of

the courseware and the level of student acceptance of courseware as a teaching resource. Galvao et al. [9] present research that provides an analysis of various courseware features that are available on the Internet, in order to develop a new model that is based on some of the technologies, such as computers and telecommunications, within a constructivist context. Also, learning skills models and the main components of such courseware, so as to improve the resources available to the information society and enhance knowledge, are presented and discussed in [9]. How individual differences on cognitive styles, prior knowledge and gender influence the navigation pattern are elaborated by Somyurek et al. [10]. A methodology with conventional multimedia learning products involving the creation of interactive CDs is outlined by Barker et al. [11].

III. STRUCTURE OF CMC

We have considered a book as a tree structure where book title is the root of the tree. The first level children of the tree are the chapters of the book. The second level of the tree is the sections of the chapters. The third level is the sub-sections and the fourth level is the set of keywords that represents the sections or subsections. A courseware in general is based on multiple text books. Each text book has a unique tree structure. The tree structure for 'Database System Concept' by Korth et el. [12] is shown in Figure 1.

In the structures, the first level child node contains the chapter's title. Each chapter consists of a number of sections or subsections. So the second level nodes contain several titles of sections. Similarly the third level nodes contain a subsection title. The leaf nodes contain the keywords identifying the text of the sections or subsection. In our representation, each subsection is represented by a unique path from root to keyword sets of the subsection. From Figure1 we observe that each text book has a hierarchical organization.

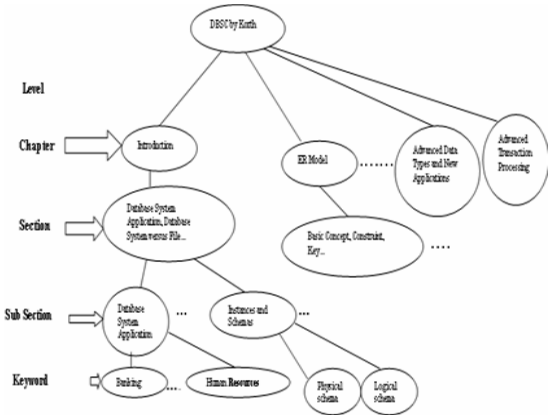

Figure 1: Tree structure for the book 'Database System Concept' by Korth et el.

If a courseware based on *n* books, it has *n* different hierarchical tree structures. We have to develop a common structure that covers all the topics of different books. It requires a dynamic merging or splitting of the structure. The general structure (Figure 2) independent of any book of the courseware can be formed by applying content clustering approach. Or a book structure can be considered as a standalone and a mapping can be found by applying the same approach.

IV. GENERAL STRUCTURE OF GROUP COURSEWARE

We have considered a group of courses together and hence the root of the generalized tree (Figure 2) is the CMC group id. The reasons to consider a group courses are:

i) Multiple courses are usually developed based on similar multiple text books. As for example, Database Basic Course, Database Advanced Course, Distributed Database Course are based on similar text books like 'Database System Concept' by Korth et al. [12], 'Database management systems' by Ramakrishnan et al. [13] and 'Database Systems' by Davies et al. [14].

ii) Multiple text books are clustered together to help unified development of multiple similar courses.

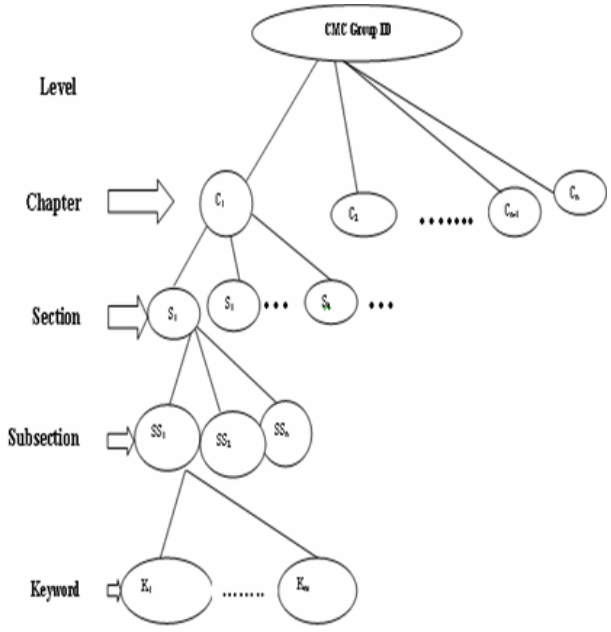

Figure 2: General structure of group courseware

Now we can model the group CMC as follows:

$$\text{Book} = \{\text{chapters}_1, \text{chapters}_2 \ldots | \text{ any chapter}_i \cap \text{chapter}_j = \varphi\}$$

$$\text{Chapters} = \{\text{section}_1, \text{section}_2 \ldots | \text{ any section}_i \cap \text{section}_j = \varphi\}$$

$$\text{Sections} = \{\text{Subsection}_1, \text{Subsection}_2 \ldots | \text{ any Subsection}_i \cap \text{Subsection}_j = \varphi\}$$

$$\text{Group Courseware} = \text{Book}_1 \cup \text{Book}_2 \cup \ldots\ldots\ldots\ldots \cup \text{Book}_p$$

$= \{C_1, C_2, C_3 \ldots\ldots\ldots\ldots C_n\}$

Each C_i is a cluster (equivalent to a chapter of a book) that is formed by applying clustering algorithm described in the following chapters.

In the generalized tree, an atomic content is represented by CMC Group id$\rightarrow C_1 \rightarrow S_1 \rightarrow SS_1 \rightarrow \{K_1, K_2 \ldots\ldots\ldots, K_m\}$.

Now we can give a formal definition of our problem of clustering group courseware:

i)A group courseware consists of one or many books.

ii)Each book can be represented by a unique tree.

iii)All the books trees can be merged to form generalized tree structure.

Input:

B: Set of books for group of courses;

n: number of books in the group.

Output:

GT: Generalized tree covering B;

Algorithm GT Formation () {

For (i=1, i++, i<=n) {

Construct BT (B_i) for each book B_i;

GT= **Merge** All BT ();

Figure 3: Algorithm GT (Generalized tree) Formation.

Figure 3 represents the clustering of group courseware content by merging all individual book trees of a group courseware. The merging is done by transforming all the book trees into a relational representation as described in the following section.

V. TRANSFORMATION OF BOOK TREE INTO RELATIONAL REPRESENTATION

To manage courseware tree we have represented each path of the tree as a tuple in the tabular representation. As for example, the path (DBSC by Korth)→Introduction→(Overview,……)→(Database System Application)→(banking, airlines,…..) represents the first tuple in the Table 1 for the book 'Database System Concept' by Korth et al. [12]. The schema relation is book-scheme (Book Title, Chapter Title, Section Title, Subsection Title, Topic keyword). For each subsection we have inserted one tuple in the relational representation. We have considered 'tuple id' as primary key which is useful for any kind of query.

Table 1: Table representation from the book 'Database System Concept' by Korth et al.

Tuple ID	Book Title	Chap Title	Section Title	Subsection Title	Topic Keyword
1	DBSC by Korth	Introduction	Overview, Historical Perspective,……	Database System Application	banking, airlines, universities,…
2	DBSC by Korth	Introduction	Overview, Historical Perspective,……	Database Systems versus File System	redundancy, inconsistency, access, ……
3	DBSC by Korth	Introduction	Overview, Historical Perspective,……	……..	…….
18	DBSC by Korth	ER Model	Overview of Database Design, Entities Attributes And Entity Sets,…….	Entity Set	Entity, Entity Set, Attribute, ……
19	DBSC by Korth	ER Model	Overview of Database Design, Entities Attributes And Entity Sets,…….	……..	…….

VI. CLUSTERING PROCEDURE

A. SELECTION OF KEYWORDS

Initially, we have considered the title text of the sections and subsection of a chapter to represent that chapter of the book. Considering only the topic keyword is not sufficient to represent a chapter, the proximity of the words has been considered as well. As for example, the individual consideration of 'database' and 'system' may mean different things than that of considering 'Database Management System'. A chapter is first identified by title of the chapter and then the keywords of the section/ sub-section headings considering the proximity. After that, we have considered a few keywords to represent the section/ sub-section and topics within subsections. Firstly we have removed all stop words which are included with different level title for unification. As for example 'Entity Relation Model' is defined as a chapter by one author whereas 'The Entity Relation Model' by another. Moreover we have converted all plural words to singular using grammatical rules and removed all hyphen or other characters which included in titles for matching.

Secondly we have set two books as reference clustering books and another book is used for mapping from the reference book. For this purpose, we have compared subsections keyword of target book with different level keywords of other reference books. As for example if a subsection be {A,B,C} keywords set of target book and {A,B,D}, {A,B,S}, {A,W,E,V} and {A,Q,S,W} be keywords set of different level of reference books then we have compared {A,B,C} with each level of reference books to find out matched keywords set for each level . To find out matched keywords set with {A,B,D} we have found the keyword set {A,B} in first iteration. In second iteration we have found {A,B,AB}. Then final matched keywords set has been {A,B,AB} for chapter keyword. We have reduced C related all combinations. As a result comparisons have reduced effectively.

We have considered synonym table for matching. e.g., 'overview' is subsection keyword of target book and 'introduction' is chapter keyword of reference book by Korth et al [12]. In real fact introduction and overview are same thing. By synonym table we have found that these two are same. This similarity consideration has

affected our result positively. We have considered weight for indicating relevance of a subsection with the chapter of reference book. The more the weight, the more is the relevance. We have given highest relevance when a subsection of target book matches exactly with the chapter keyword of reference book. Because this matching has indicated proximity. We have reduced this relevance with top down approach of tree manner. That means when same keyword matches with down level keyword like section, subsection or topic keyword then it will be given less relevance.

When a matching keyword /set of keywords in full have not been matched with different levels of reference book then we have matched different combinations of the keyword. In those cases we have not considered proximity. Here also we have given different relevance value for different levels. Total relevance for a subsection of the target book with the chapter of reference book has been summed. By sorting and taking the highest relevance, we have found the chapter of reference book which is more relevant to the target subsection. In this way we have found the total relevance table for reference books of Korth et al. [12] (case 1) and Davies et al. [14] (case2).

B. CLUSTERING ALGORITHM

We have applied following data mining clustering algorithm to form the required number of clusters as per requirement of the courseware.

```
Algorithm SS_Clustering (ch_keyword, s_keyword, ss_keyword, t_keyword, ref_subsection)
// ch_keyword, s_keyword, ss_keyword, t_keyword, are different level to represent a particular
// chapter of target books. Sourcekeyword is another keyword representing Subsection keyword
//of reference book, weight is a global variable, rs1 represents record sets of reference book and
//rs2 represents record sets of target books
While rs1.EOF = False{
Sourcekeyword= Call RemoveStopWord (ref_subsection)
Weight=0;
rs2.MoveFirst
While rs2.EOF = False{
        // Measure with proximity
        Ch_Stop_Free = Call RemoveStopWord (ch_ keyword)
        Chap_MatchedKeySets = Call MatchingCount (Ch_Stop_Free, sourcekeyword)
        If (Ch_Stop_Free = Chap_MatchedKeySets) {
        Calculate weight for Chap_MatchedKeySets
        Weight= weight* proximity
        S_Stop_Free =Call RemoveStopWord (s_ keyword)
        S_MatchedKeySets = Call MatchingCount (S_Stop_Free, sourcekeyword)
        If (S_Stop_Free = S_MatchedKeySets) {
        Calculate weight for S_MatchedKeySets
        Weight= weight* proximity
        SS_Stop_Free =Call RemoveStopWord (ss_ keyword)
        SS_MatchedKeySets = Call MatchingCount (SS_Stop_Free, sourcekeyword)
        If (SS_Stop_Free =SS_MatchedKeySets) {
        Calculate weight for Chap_MatchedKeySets
        Weight= weight* proximity
        T_Stop_Free =Call RemoveStopWord (t_ keyword)
        T_MatchedKeySets = Call MatchingCount (T_Stop_Free, sourcekeyword)
        If (T_Stop_Free = T_MatchedKeySets) {
        Calculate weight for T_MatchedKeySets
Weight= weight* proximity
        // Measure without proximity
    If (Count (Chap_Count)>1 and (Ch_Stop_Free <> Chap_Count)) or
    (Count (S_Count)>1 and (S_Stop_Free <> S_Count)) or
    (Count (SS_Count)>1 and (SS_Stop_Free <> SS_Count)) or
    (Count (T_Count)>1 and (T_Stop_Free <> T_Count)) {
            Calculate weight for different combinations of Chap_Count
    Calculate weight for different combinations of S_Count
    Calculate weight for different combinations of SS_Count
    Calculate weight for different combinations of T_Count
  rs2.MoveNext
rs1.MoveNext
    MatchingCount (Target_keyowrd, sourcekeyword){
            tmpcountKey = Split(Target_keyowrd, ",")
                    For i = 0 To n
If InStr(Target_keyowrd, tmpcountKey(i)){
tmpstrin = tmpstrin & tmpcountKey(i)
    Match= tmpstrin}
    RemoveStopWords (keyword){
            Replace all stop words like a, an, the, and, or, etc. from the keyword
```

Figure 4: Algorithm for Subsection Clustering.

VII. RESULT AND DISCUSSION

We have experimented our system with Pentium IV processor, 512 MB memory with 1.8 GHz Speed. We have considered the database group of courseware based on three text books namely 1) 'Database System Concepts' by Korth et al. [12], 2) 'Database Management Systems' by Ramakrisnan et al. [13] and 3) 'Database Systems' by Davies et al. [14]. The number of chapters, sections and subsections for the above three books are shown in Table 2.

Table 2: Book Information in Detail

Book Name	Authors Name	No. of Chapters	No. of Sections	No. of Subsections
Database System Concepts	Silberschatz, Korth, Sudarshan	24	120	458
Database Management Systems	Raghu Ramakrishnan, Johannes Gehrke	28	141	373
Database Systems	Paul Beynon-Davies	43	172	382

We have considered 'Database System Concepts' by Korth et al. [12] and 'Database Systems' by Davies et al. [14] as reference books and 'Database Management Systems' by Ramakrisnan et al.[13] as target book. We have clustered 373 subsections of Ramakrishnan with both reference books. Sample clustering results are shown in Table 3 taking the highest relevance for the book of Korth et al .

Table 3: Sample Clustering Result with Book of Korth et al.

Chapter name of reference book (Korth et al.)	Relevance	Subsection title of target book	Chapter name of target book
introduction	10000017	overview	introduction
introduction	17010001.711	history perspective	introduction
introduction	228.624	file system versus database management system	introduction
integrity and security	20000.014	advantages of database management system	introduction
relational model	520000065.013	relational model	introduction
relational model	0	outlier	outlier
……	……	……	……
relational model	10000.024	expressions and strings in the select command *(False positive)*	sql: queries, programming, triggers *(False positive)*

Table 3 comes from taking the highest relevance with total coverage of book by Korth et al. [12] using 24 chapters, 120 sections, 458 subsections and all topics keyword.

We have also taken results for different no. of chapters for both cases (1 and 2). When we have clustered all subsections of target book with one chapter of reference book then we have found most of the subsections have come into false positive chapter of reference book. In that case we have also found no. of outliers is highest. An outlier is an observation that is numerically distant from the rest of the data. With the addition of more chapters of reference book we have found true positive increases exponentially and outlier decreases rapidly. A database tuple predicted to be in a specific class and is actually in it is defined as true positive. . A database tuple predicted to be in a specific class but is not actually in it is defined as false positive. Here true positive means a subsection of reference book is properly mapped to a chapter of target book by clustering relevance. On the other hand, false positive means a subsection of reference book is not properly mapped to a chapter of target book by clustering relevance as it should be. An outlier is an observation that is numerically distant from the rest of the data. A database may contain data objects that do not comply with the general behavior or model of the data. These data objects are outliers. Here a subsection of the reference book which has no relevance value with the any chapter of the target book is considered as outlier.

When we have taken 24 chapters of the reference book by Korth et al. [12] (case 1) we have found highest no. of true positive and lowest no. of false positive, outlier. Again for reference book by Davies et al. [14] we have found highest no. of true positive and lowest no. of false positive, outlier when have been taken 43 chapters in clustering (case 2). The main reason of increasing true positive with more chapters is matching coverage spectrum increasing. Those subsections which have no relevance value by matching are considered as outlier because target subsections of lowest relevance also may indicate true positive. Analyzing result we have got interesting character of true positive, false positive and outlier. Initially for less number of chapters false positive and outlier remains higher whereas true positive lower for both reference books (case 1 & 2). This nature reverses with the increase of chapters. The Figure 5 and Figure 6 show it clearly.

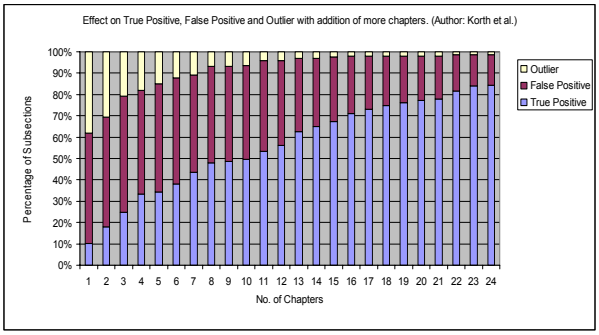

Figure 5: Effect on True Positive, False Positive and Outlier with addition of more chapters. (Author: Korth et al.)

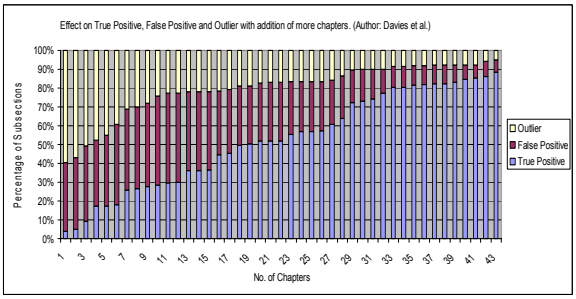

Figure 6: Effect on True Positive, False Positive and Outlier with addition of more chapters. (Author: Davies et al.)

For both books we have to check false positive manually due to different organization, structure and style of books by different authors. Repetition is another reason for false positive. Homonym and synonym are also other problems for clustering. We have solved synonym problem effectively by using synonym table. We have also reduced the effect of homonym using correspondence of keyword set. Some false positives and outlier we have to handle manually due to these reasons. In this way we can take all books as target books and can be clustered to a single reference book. As a result a general structure that covers all topics of different books will be developed.

Though we have found some false positives in our result by domain expert but those are less than 15%. A

very few number of outlier has occurred with both reference books when have been taken all chapters. For outlier indication we have not needed manual reckoning. More than 85% of true positive have occurred when we have taken total spectrum of the reference books.

VIII. CONCLUSION

Courseware so far has been developed for individual courses considering single book as a text and other books as reference. It is a necessity to cluster the contents of different books to form a generalized clustered content which is absent in the existing Computer Mediated Courseware. In this paper, a methodology has been proposed to construct a hierarchical general structure considering a group of courseware based on a set of text books. In that case we have combined the individual structure of the set of books.

We have considered each book as a unique tree structure. Each text book has a hierarchical organization. We have transformed the trees into relational representation. Each unique path of the tree from root to leaves represents a tuple in that representation. By dynamic merging or splitting of the structure we have developed a general structure that covers all the topics of different books.

For clustering purpose we have considered proximity as well as synonym. We have considered one book as reference and the other as target. Each subsection of target book has given a cumulative weight in accordance with matching with reference book for relevance. The more the weight, the more is the relevance. Similarity based clustering algorithm has been applied to find out the relevance. We have found clustering result for both reference books taking the chapter which consists of highest relevance.

Result shows that very few numbers of subsections were found as outlier. We have assigned them to different chapters manually. We have verified our result by domain expert and found some false positive that were handled manually. The precision of our clustering algorithm has been found about 85%. We have used the word precision to indicate the number of true positive occurrences. If we could apply full text retrieval system, it would improve the performance sacrificing the computational time. This could be a future work.

REFERENCES

[1] en.wikipedia.org/wiki/Courseware

[2] Mason, R., Models of online courses. ALN Magazine, 2, 2 (1998).

[3] http://www.cciencia.ufrj.br/educnet/eduead.htm

[4] http://www.uvex.edu/disted/definition.html

[5] Bourne, J., Harris, D. and Mayadas, F., "Online engineering education: learning anywhere, anytime" JALN, Vol. 9, Issue-1, March, 2005.

[6] Koppi, A. J., Chaloupka, M. J. and Llewellyn, R., "Computer mediated courseware development and the academic culture", In Proceedings of World Conference on Educational Telecommunications, Washington, June 19-24, 1999.

[7] Wade, V. P. and Lyng, M., "An automated evaluation service for educational courseware", In Proceedings of World Conference on the WWW and Internet, San Antonio, TX, October 30-November 04, 2000.

[8] Hoic-Bozic, N., Ledic, J.and Mezak, J., "Evaluating the use of World Wide Web courseware in student teachers' education: a case from Croatia ", In Proceedings of Society for Information Technology & Teacher Education International Conference, San Diego, California, February 8-12, 2000.

[9] Galvao, J. R. and Barreto, A. M., "What is courseware? A comparative analysis", Vol. 4, Issue-2, World Transaction on Engineering and Technology Education, 2005.

[10] Somyurek, S., Guyer, T. and Atasoy, B., "The effects of individual differences on learner's navigation in a courseware", Vol. 7, Issue-2, The Turkish Online Journal of Educational Technology – TOJET, April, 2008.

[11] Barker, P. and Giller, S., "Models and methodologies for multimedia courseware production", In Proceedings of World Conference on Educational Multimedia, Hypermedia & Telecommunications, Denver, Colorado, June 24-29, 2002.

[12] Silberschatz, A., Korth, H. and Sudarshan, S., "Database System Concepts", ISBN: 9780071244763, AUG-05

[13] Ramakrishnan, R. and Gehrke, J., " Database management systems", 3RD Edition, ISBN : 10-0072465352, Jul 2007

[14] Beynon, P. and Davies, "Database Systems", 3RD Edition, ISBN: 1–4039–1601–2, 2004

Proceedings of 2009 12th International Conference on Computer and Information Technology (ICCIT 2009)
21-23 December, 2009, Dhaka, Bangladesh

Hybrid Real-Coded Quantum Evolutionary Algorithm Based on Particle Swarm Theory

Md. Amjad Hossain, Md. Kowsar hossain, M.M.A. Hashem
Dept. of Computer Science and Engineering,
Khulna University of Engineering and Technology,
Khulna,Bangladesh
amjad_kuet@yahoo.com, auvikuet@yahoo.com, mma_hashem@hotmail.com

Abstract

This paper proposes a Hybrid Real-coded Quantum Evolutionary Algorithm (HRCQEA) for optimizing complex functions on the basis of the concept of quantum computing such as qubits and superposition of states and Particle Swarm Optimization (PSO). It combines PSO with Real-coded Quantum Evolutionary Algorithm (RCQEA) to improve the performance of RCQEA. The main idea of HRCQEA is to embed the evolutionary equation of PSO in the evolutionary operator of RCQEA. In HRCQEA, each triploid chromosome represents a particle and the position of the particle is updated using Complementary Double Mutation Operator (CDMO) and Quantum Rotation Gate (QRG), which can make the balance between exploration and exploitation. Discrete Crossover (DC) is employed to expand the search space and Hill-climbing selection (HCS) helps to accelerate the convergence speed. Simulation results of four benchmark complex functions with high dimensions show that HRCQEA performs better than other algorithms in terms of ability to discover of global optimum.

Keywords: Hybrid Algorithm, Evolutionary Algorithm, Particle Swarm Algorithm, Quantum Evolutionary Algorithm.

I. INTRODUCTION

To optimize complex functions of high dimensions, evolutionary algorithm known as quantum evolutionary algorithm (QEA) is proposed which is characterized on the basis of the concept and the principles of quantum computing such as qubits and superposition of states [1, 2, 3, 4]. It has observed that QEA traps into local optima during solving multi-peaks complex optimization functions [5-6].

Particle swarm optimization (PSO) is a population based stochastic optimization technique based on swarm intelligence. PSO shares many similarities with QEA. However, unlike QEA, PSO has no evolution operators such as crossover and mutation. In PSO, the potential solutions, called particles, fly through the problem space by following the current optimum particles. PSO is easy to implement than QEA and there are few parameters to adjust and it has faster convergence speed [7-8].

To optimize the complex function effectively and efficiently real-coded quantum evolutionary algorithm (RCQEA) was proposed in [9]. In RCQEA, real-coded triploid chromosome is used to keep the diversity of the solution. Using the advantages of PSO and RCQEA, this paper proposes a Hybrid Real-coded Quantum Evolutionary Algorithm (HRCQEA).

The paper is organized as follows. Section II describes some recent evolutionary techniques such as QEA, PSO and RCQEA. In Section III, the mechanism and procedure of proposed HRCQEA is explained. Section IV analyzes the experimental result of HRCQEA based on four benchmark complex functions. Section V concludes the paper.

II. RECENT EVOLUTIONARY TECHNIQUES

A. Quantum Evolutionary Algorithm

QEA uses qubit chromosomes to represent the solutions. The quantum chromosome is defined as:

$$\begin{bmatrix} \alpha_1 & | & \alpha_2 & | & \dots \alpha_m \\ \beta_1 & | & \beta_2 & | & \dots \beta_m \end{bmatrix} \quad (1)$$

where α_i and β_i are the probability amplitudes of i^{th} qubit and they satisfy the condition $|\alpha_i|^2 + |\beta_i|^2 = 1$, $i = 1, 2, 3 \ldots .m$. $|\alpha_i|^2$ and $|\beta_i|^2$ gives the probability that the qubit will be found in '0' state and 1' state respectively. The probability amplitudes of a qubit are updated by Q-gate which is a variation operator of QEA. After applying Q-gate, the qubit should satisfy the normalization condition $|\alpha'|^2 + \beta'|^2 = 1$. The following Q-gate is used as rotation gate:

$$U(\Delta\theta_i) = \begin{bmatrix} \cos(\Delta\theta_i) & -\sin(\Delta\theta_i) \\ \sin(\Delta\theta_i) & \cos(\Delta\theta_i) \end{bmatrix} \quad (2)$$

where $\Delta\theta_i$, $i = 1, 2, 3 \ldots$, m, is the rotation angle of a qubit towards the "0" state or "1" state depending on its sign [4].

B. Real-coded Quantum Evolutionary Algorithm

In RCQEA, a real-coded triploid chromosome is represented as

$$\begin{pmatrix} x_1 \cdots x_i \cdots x_n \\ \alpha_1 \cdots \alpha_i \cdots \alpha_n \\ \beta_1 \cdots \beta_i \cdots \beta_n \end{pmatrix} \quad (3)$$

where $(x_i\, \alpha_i\, \beta_i)^T$, $i = 1, 2 \ldots . n$ is the i^{th} allele of real-coded triploid chromosome, x_i is the real variable, a pair of probability amplitudes of one qubit is $(\alpha_i, \beta_i)^T$ which must satisfy the normalization condition $|\alpha_i|^2 + |\beta_i|^2 = 1$.

978-1-4244-6283-4/09/$26.00 ©2009 IEEE

Here, n is the length of real-coded triploid chromosome. RCQEA maintains a population of triploid chromosomes. The individuals are updated using CDMO and QRG. A real variable is randomly selected and updated using CDMO. A pair of probability amplitudes is updated using Quantum Rotation Gate (QRG) defined in (2). $\Delta\theta_i$ is calculated as follows:

$$\Delta\theta_i = \mathbf{sgn}\,(\alpha_i\beta_i)\theta_0 \exp\left(\frac{|\beta_i|}{|\alpha_i| + \gamma}\right) \quad (4)$$

where θ_0 is the initial rotation angle, γ is the scale parameter, θ_0 and γ control the value of the rotation angle together and have an effect on the speed of convergence, the sign **sgn** (.) determines the direction of the rotation angle and further guarantees the search direction of convergence to a global optimum [9].

C. Particle Swarm Algorithm

In PSO, each single solution is a "particle" in the search space. All of particles have fitness values which are evaluated by the fitness function to be optimized and have velocities which direct the flying of the particles. The trajectory of each particle in the search space is adjusted by dynamically altering the velocity of each particle, according to its own flying experience and the flying experience of the other particles in the search space.

The position vector and the velocity vector of the i^{th} particle in the D dimensional search space can be represented as $X_i = (X_{i1}, X_{i2}, \ldots, X_{iD})$ and $V_i = (V_{i1}, V_{i2}, \ldots, V_{iD})$,respectively. The best previous location that (the position giving the best fitness value) a particle has achieved is called *pBest*. The *pBest* of the i^{th} particle is represented as $P_i = (p_{i1}, p_{i2}, \ldots, p_{iD})$. The best position discovered by the whole population is represented as $P_g = (P_{g1}, P_{g2}, \ldots, P_{gD})$.Then the new velocities and the position of the particle for the next fitness evaluation can be calculated using following two equations in which above two best values are used [11]:

$$V_{id} = V_{id} + C_1 r_1 (P_{id} - X_{id}) + C_2 r_2 (P_{gd} - X_{id}) \quad (5)$$

$$X_{id} = X_{id} + V_{id} \quad (6)$$

where C_1 and C_2 are acceleration coefficients and r_1 and r_2 are two separately generated uniformly distributed random numbers in the range [0, 1].

III. PROPOSED HYBRID REAL-CODED QUANTUM EVOLUTIONARY ALGORITHM

A. Mechanism of the Proposed Algorithm

Let, S be the search space and $f : F \rightarrow R^n$ an objective function and $g_i : S \rightarrow R^n$, $i = 1, 2, \cdots, q$ set of functions (called constraints). The global optimization problem is then given as the task

Minimize $f(\mathbf{x})$, such that $g_i(\boldsymbol{x}) < 0$

$$\boldsymbol{x} = (x_1, \ldots, x_i, \ldots, x_n) \in S \quad (7)$$

where the subset F is called the feasible region in S, $\boldsymbol{x} \in R^n$ defines the n dimensional search space and each x_i is bounded within $[x_{i,min}, x_{i,max}]$, where $i=1,2,3,\ldots, n$. HRCQEA is proposed to optimize the complex functions and to accelerate the convergence speed. Fig. 1 describes the mechanism of HRCQEA, where p_u^t and p_v^t are real-coded triploid chromosomes, u ≠ v, u, v = 1, …, N and they define u^{th} and v^{th} particle in the particle swarm. Here, each individual in the population is considered as a particle of the swarm. b_u^t is the previous state with the best performance of the u^{th} individual. b_g^t is the global best solution which is the state with best performance so far in the neighborhood. In HRCQEA, particle swarm finds the global optimum solution based on the following four main points: Real-coded triploid chromosome, Mutation operator (CDMO and QRG which use the basic equation of PSO for calculation of $\boldsymbol{\theta}$), Discrete Crossover (DC) and "Hill climbing" selection (HCS).

A.1 Representation: Each particle or individual in HRCQEA is defined by the real-coded triploid chromosome (3), where n is the length of the real-coded triploid chromosome i.e., the dimensions of function optimized, the vector $\boldsymbol{x} = (x_1, \cdots, x_i, \cdots, x_n)$ represents the position of a particle that is a solution of optimization problem.

A.2 Mutation Operator: In single-gene mutation, only one gene is mutated which is selected from the individual chosen to mutate, but all the others gene are fixed. This mutation operator is used to update the population in each of iterations. It has been proved that single-gene mutation is superior to all-gene mutation in term of search efficiency [10]. One allele is selected randomly and CDMO is used to update real variable of that allele. QRG is used to update the pair of probability amplitudes of qubits of the individual selected to mutate where rotation angle is calculated using evolutionary equation of PSO. This updating of amplitudes is not limited to single gene.

Consider that HRCQEA maintains a population or a particle swarm of real-coded triploid chromosomes $P^t = \{p_1^t, \cdots, p_j^t, \cdots, p_N^t\}$ at generation t, where N is the size of population and $\{f_1^t, \cdots, f_j^t, \cdots, f_N^t\}$ describe the corresponding fitness values of individuals. p_j^t is an particle or individual defined as (3) and f_j^t is the fitness value of p_j^t. For convenient representation, let $k = \alpha, \beta$. If k is set to α, then "Fine search" is performed and if k is set to β, then "Coarse search" is implemented. From all alleles of p_j^t choose the i^{th} allele $(x_{j,i}^t \; \alpha_{j,i}^t \; \beta_{j,i}^t)^T$ randomly and update real variable, $x_{j,i}^t$, by Gaussian mutation, which is described as

$$x_{j,i}^{t+1,k} = x_{j,i}^t + (x_{i,max} - x_{i,min})\, N(0, (\sigma_{j,i}^{t,k})^2) \quad (8)$$

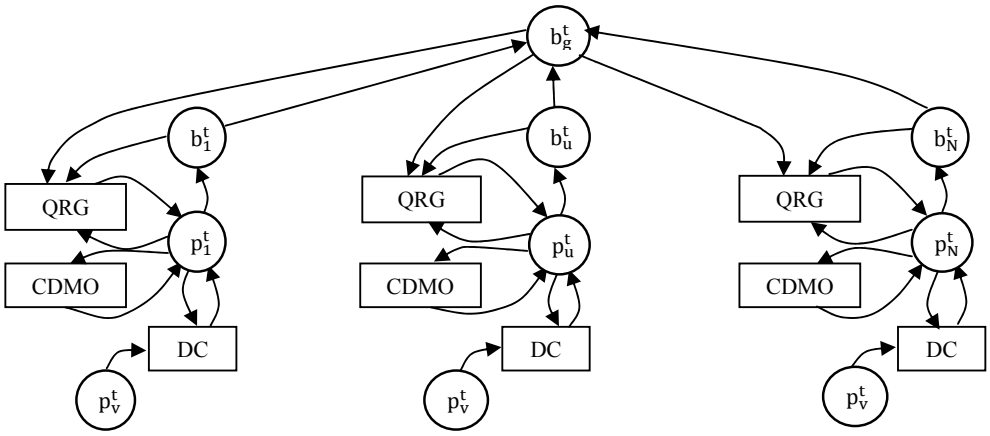

Fig. 1. Overall Structure of HRCQEA

where $N(0,(\sigma_{j,i}^{t,k})^2)$ denotes the Gaussian distribution of mean 0 and variance $(\sigma_{j,i}^{t,k})^2$. The variance can be defined as

$$(\sigma_{j,i}^{t,k})^2 = \begin{cases} |\alpha_{j,i}^t|^2, & k = \alpha \\ |\beta_{j,i}^t|^2 /5, & k = \beta \end{cases} \tag{9}$$

So in "Fine search", the variance is $|\alpha_{j,i}^t|^2$ and in "Coarse search", $|\beta_{j,i}^t|^2 /5$ is considered. It should be noted that the new real variable $x_{j,i}^{t+1,k}$ would exceed the limit of $x_{j,i}^t$ whether the value of $(\sigma_{j,i}^{t,k})^2$ is larger or the value of $x_{j,i}^t$ is close to the bound. To avoid making infeasible solution, new real variable $x_{j,i}^{t+1,k}$ is clipped as follows

$$x_{j,i}^{t+1,k} = \begin{cases} 2x_{i,max} - x_{j,i}^{t+1,k}, & x_{j,i}^{t+1,k} > x_{i,max} \\ 2x_{i,min} - x_{j,i}^{t+1,k}, & x_{j,i}^{t+1,k} < x_{i,min} \end{cases} \tag{10}$$

Equation (10) has to be performed repeatedly until $x_{j,i}^{t+1,k}$ lies in the feasible solution space.

If the new feasible solution $(x_{j,1}^t,\cdots,x_{j,i}^{t+1,k},\cdots,x_{j,n}^t)$ which is derived from (8), (9) and (10), is better than the old feasible solution $(x_{j,1}^t,\cdots,x_{j,i}^t,\cdots,x_{j,n}^t)$, we call that the valid evolution is carried out, otherwise the invalid evolution is done. When the valid evolution occurs, the probability amplitudes $(\alpha_{j,i}^t\ \beta_{j,i}^t)^T$ are fixed, that is $\alpha_{j,i}^{t+1} = \alpha_{j,i}^t$, $\beta_{j,i}^{t+1} = \beta_{j,i}^t$. On the contrary, once the invalid evaluation does the probability amplitudes $(\alpha_{j,i}^t\ \beta_{j,i}^t)^T$ are updated by QRG as follows [9]:

$$\begin{pmatrix} \alpha_{j,i}^{t+1} \\ \beta_{j,i}^{t+1} \end{pmatrix} = \begin{pmatrix} \cos(\Delta\theta_{j,i}^t) & -\sin(\Delta\theta_{j,i}^t) \\ \sin(\Delta\theta_{j,i}^t) & \cos(\Delta\theta_{j,i}^t) \end{pmatrix} \begin{pmatrix} \alpha_{j,i}^t \\ \beta_{j,i}^t \end{pmatrix} \tag{11}$$

Here $\Delta\theta_{j,i}^t$ is the rotation angle and it is defined by the basic equation of the PSO as follows

$$\Delta\theta_{j,i}^t = C_1 (x_{j,i}^{b,t} - x_{j,i}^t) + C_2(x_{g,i}^t - x_{j,i}^t) \tag{12}$$

where C_1 and C_2 are called the learning factor, $x_{j,i}^t$ is the i^{th} real variable of the p_j^t. $(x_{j,1}^{b,t},\cdots,x_{j,i}^{b,t},\cdots,x_{j,n}^{b,t})$ is the best position of the j^{th} particle p_j^t which is stored in b_j^t. In the (12), $x_{j,i}^{b,t}$ is the i^{th} real variable of b_j^t. $x_{g,i}^t$ is the i^{th} real variable of the best performance so far in the neighborhood that is global best performance b_g^t whose position vector is $(x_{g,1}^t,\cdots,x_{g,i}^t,\cdots,x_{g,n}^t)$.

when the i^{th} allele of p_j^t occurs continuously invalid evolution, a new approach will be used to update $\alpha_{j,i}^t$ and $\beta_{j,i}^t$ at larger scale apart from equation (11) and (12) so as to accelerate the convergence speed and achieve the aim of adaptive controlling the evolutionary process of algorithms by the evolutionary status of algorithms. Assume that c_i is used to store the number of invalid evaluation occurred by i^{th} allele. In every operation of either "Fine search" or "Coarse search", if invalid evolution is occurred then real variable of i^{th} allele will be hold, and the number of the continuously invalid evolution c_i for that allele will increase 1. On the contrary, if valid evolution is occurred, real variable of the allele appointed will be replaced, and c_i will be cleared.

Depending on the value of c_i, $i = 1, 2, \cdots n$, alleles are selected from p_j^t to update pair of probability amplitudes of these alleles. If c_i for i^{th} allele of p_j^t is 0, then

probability amplitudes $\alpha_{j,i}^t$and $\beta_{j,i}^t$ are not changed. If the value of c_i is less than equal to a specified value λ then equation (11) and (12) are used to update $\alpha_{j,i}^t$and $\beta_{j,i}^t$, otherwise following equation is used update them:

$$\begin{cases} \alpha_{j,i}^{t+1} = \alpha_{j,i}^{t+1}/(fix(\mathrm{c_i}/5) + 1) \\ \beta_{j,i}^{t+1} = \sqrt{1-(\alpha_{j,i}^{t+1})^2} \end{cases} \quad (13)$$

where fix(.) is a round function. From the above process, the allele $(x_{j,i}^t\ \alpha_{j,i}^t\ \beta_{j,i}^t)^T$ of p_j^t is updated. Meaningfully, from (11) and (12) and (13), it can be seen that with the increase of generation *t,* the value of $|\alpha_{j,i}^t|$ will decrease gradually and then the variance of (8), determined by (9), will reduce slowly. So, "Fine search" in the neighborhood of current solution is carried out. In reverse, the value of $|\beta_{j,i}^t|$will increase gradually and then the variance will enhance slowly. So, "Coarse search" in the whole solution space is realized. By "Fine search" in local search space and "Coarse search" in global search space, HRCQEA can treat the balance between exploration and exploitation, which is the origin of CDMO. Given the number of "Fine search" and "Coarse search" for every individual in population is m_1 and m_2 respectively and usually $m_1 > m_2$.

A.3 ***Discrete Crossover (DC):*** DC is performed after a fixed number of generations that is after a defined interval τ. In HRCQEA, DC is performed m times for each individual .The process of DC can be explained as follows: First, for the individual, p_u^t , u =1,⋯,N, select randomly another individual p_v^t , v =1,⋯, N , where u ≠ v. Let p_u^t and p_v^t are considered as parents. Then, every corresponding allele of them is exchanged with a 0.5 probability, and two new individuals, p_k^t, $k = 1, 2$, are formed. The above process can be described as

$$(x_{k,i}^t\ \alpha_{k,i}^t\ \beta_{k,i}^t)^T = \begin{cases} (x_{u,i}^t\ \alpha_{u,i}^t\ \beta_{u,i}^t)^T, & r < 0.5 \\ (x_{v,i}^t\ \alpha_{v,i}^t\ \beta_{v,i}^t)^T, & r \geq 0.5 \end{cases} \quad (14)$$

Where$(x_{u,i}^t\ \alpha_{u,i}^t\ \beta_{u,i}^t)^T$,$(x_{v,i}^t\ \alpha_{v,i}^t\ \beta_{v,i}^t)^T$ and$(x_{k,i}^t\ \alpha_{k,i}^t\ \beta_{k,i}^t)^T$ is the i^{th} allele of p_u^t, p_v^t and p_k^t, respectively, and r denotes a random number which is uniformly distributed in [0, 1]. In HRCQEA, DC would play important role on preventing the individual in the early generations from being trapped in the local optima by expanding search space [9].

A.4 ***"Hill-climbing" Selection (HCS):*** In HRCQEA, only if the offspring, which is formed from either mutation operator or DC, are superior to the parents, the parents are substituted for the offspring, otherwise the parents are saved. The above process is called "Hill-climbing" selection [9].

B. Procedure HRCQEA

Begin

t←0

Initialize parameters and population P^t

Evaluate P^t

Store best population B^t and global best b_g^t

while (not termination condition)do

Begin

Update P^t using CDMO and QRG

Evaluate P^t

if (crossover condition) **then**

Begin

Use Discrete Crossover (DC) to expand search space

end

Store best population B^t and global best b_g^t

t←t+1

End

End

Here, $B^t = \{b_1^t,\cdots,b_j^t,\cdots,b_N^t\}$ is the suboptimum best solutions.

IV. PERFORMANCE EVALUATION AND RESULTS ANALYSIS

A. Test Functions

To test the performance of HRCQEA, four benchmark functions are used as test functions [3].

F1: Sphere Function

$$\min f(x) = \sum_{i=1}^{D} x_i^2 \quad (15)$$

where -100 ≤ x_i ≤ 100 and D=30. The global minimum value is 0.0 at x = (0, 0….0).

F2: Rastrigin Function

$$\min f(x) = 10D + \sum_{i=1}^{D}(x_i^2\text{-}10\cos(2\pi x_i)) \quad (16)$$

where -5.12 ≤ x_i ≤ 5.12 and D=30. The global minimum value is 0.0 at x = (0, 0….0).

F3: Ackley Function

$$\min f(x) = -20\exp\left(-0.2\sqrt{\frac{1}{D}\sum_{i=1}^{D} x_i^2}\right) - \exp\left(\frac{1}{D}\sum_{i=1}^{D}\cos(2\pi x_i)\right) + 20 + e \quad (17)$$

where -32 ≤ x_i ≤ 32 and D=30.The global minimum value is 0.0 at x = (0, 0….0).

F4: Schwefel Function

$$\min f(x) = 418.9829D - \sum_{i=1}^{D} x_i \sin(\sqrt{|x_i|}) \quad (18)$$

where -500 ≤ x_i ≤ 500 and D=30.The global minimum value is 0.0 at x = (420.9687, 420.9687, …, 420.9687).

Table I Experimental results of four algorithms on F1~F4

Functions	Algorithm	Best fitness	Worst fitness	Mean fitness	Standard deviation (σ)
F1	QEA	2.21135	11.3576	5.28049	1.90678
	PSEQEA	0.009812	0.052016	0.025308	0.00954
	RCQEA	2.14e-16	3.69e-15	1.01e-15	6.82e-16
	HRCQEA	1.48e-85	2.44e-53	4.88e-55	3.4e-54
F2	QEA	48.5618	82.5023	67.9872	7.51928
	PSEQEA	33.0593	70.8951	47.8201	8.87899
	RCQEA	5.68e-14	3.97e-13	1.84e-13	7.75e-14
	HRCQEA	0	1.13e-13	1.59e-14	2.82e-14
F3	QEA	3.8292	8.0274	6.2414	0.975563
	PSEQEA	0.435038	2.50622	1.66972	0.570039
	RCQEA	2.08e-7	3.31e-7	2.48e-7	2.75e-8
	HRCQEA	1.71e-7	1.71e-7	1.71e-7	4.18e-15
F4	QEA	1785.71	3001.56	2381.23	280.418
	PSEQEA	80.1407	3954.99	735.387	567.67
	RCQEA	0.000381	236.877	35.5319	59.8204
	HRCQEA	0.00038	0.00038	0.00038	5.31e-8

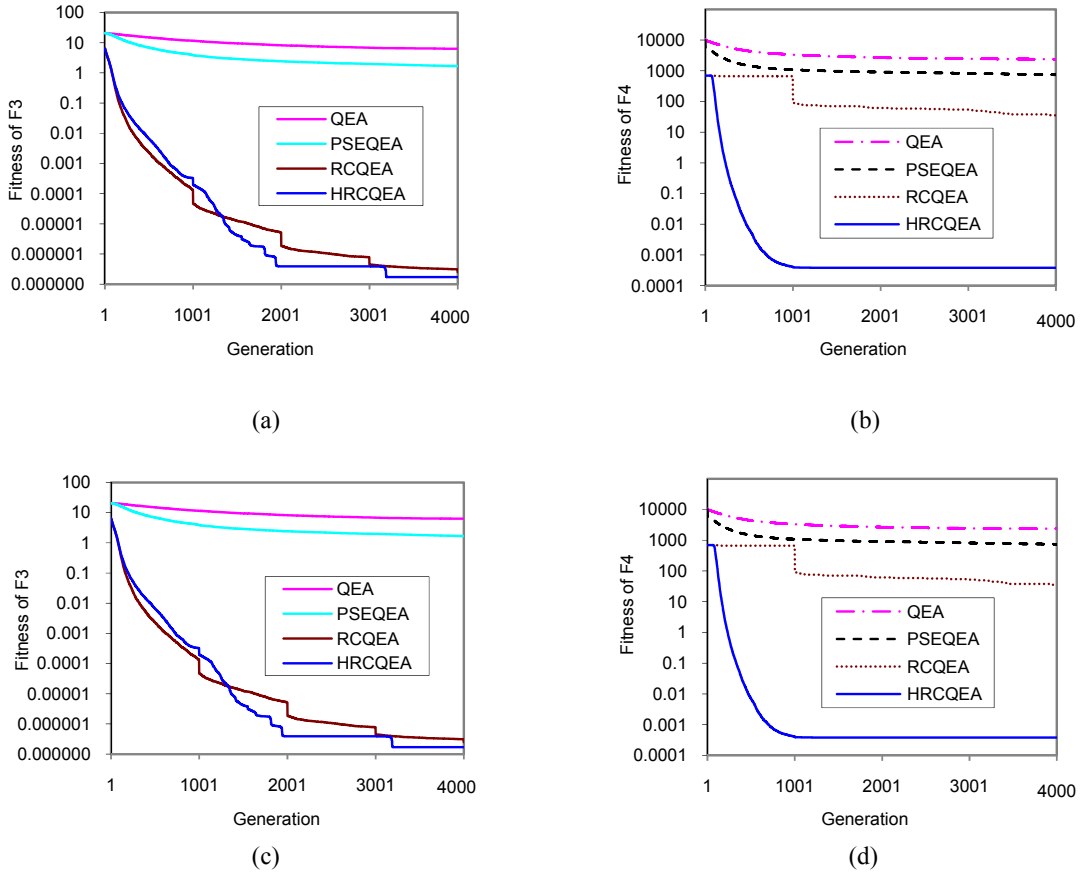

Fig. 2. Performance comparison of four algorithms on F1~F4

B. Results and Comparison on F1~F4:

For performance comparison, above four functions was solved by HRCQEA, QEA [4], RCQEA [9], and PSEQEA [11]. The maximum number of generation 4000, population size 10 and 50 run times was used for all of four algorithms. For generalization, number of "Fine search" and "Coarse search" for RCQEA and HRCQEA are defined in terms of dimension of the function optimized as follows:

$$m_1 = 1.5 * D \text{ and } m_2 = 0.5 * D \quad (19)$$

1) **QEA:** Number of qubits used for F1, F2, F3, and F4 are set to 18, 24, 26 and 30 (per variable), respectively.

2) **PSEQEA:** Number of qubits in PSEQEA is same as QEA. The value of c_1 and c_2 is set to 0.02π.

3) **RCQEA:** The period of discrete crossover τ=1000, number of continuous discrete crossover m=10, initial rotation angle $\theta_0 = 0.1\pi$, and scale parameter $\gamma = 5$.

4) **HRCQEA:** The value of τ and m is same as RCQEA. The value of learning factors $c_1 = c_2 = 5\pi$ and $\lambda = 1$.

Table I shows the experimental results of four algorithms with the dimensions D=30. It is seen that HRCQEA has meaningfully better performance than all others algorithms. Fig. 2. (a), (b), (c), and (d) show the progress of mean best fitness found by four algorithms with generations 4000 for functions F1, F2, F3 and F4 respectively. It should be noted that HRCQEA performs better than that of QEA, PSEQEA and RCQEA for all test functions.

V. CONCLUSION

In this paper, a hybrid algorithm named HRCQEA is proposed. The main idea of HRCQEA is to embed the evolutionary equation of PSO in RCQEA. The evolutionary equation of PSO makes full use of the information of the swarm and has more profound intelligent background. Using the evolutionary operation of PSO, HRCQEA can adjust the θ more reasonably. Thus the HRCQEA can find the optimum faster. Some complex optimization problems are used to test the performance of the new algorithm. The simulation results show that HRCQEA performs better than other algorithms in terms of global search capacity and convergence speed.

REFERENCES

[1] Narayannan A, Moore M, "Quantum-inspired genetic algorithms", *Proc. of IEEE int. Conference on Evolutionary Computation, Nagoya, IEEE Press,* pp.61-66, 1996.

[2] Han K H, Kim J H, "Genetic quantum algorithm and its application to combinatorial optimization problems", *Proc. of IEEE Congress on Evolutionary Computation*, vol.7, pp. 1354-1360, 2000.

[3] Han K H, Kim J H, "Quantum-Inspired Evolutionary Algorithms with a New Termination Criterion, H_ϵ gate, and Two-phase scheme", *IEEE Transactions on Evolutionary Computation,*vol.8, no.2, pp.156-169, 2004.

[4] Han K H, Kim J H, "Quantum-inspired evolutionary algorithm for a class of combinatorial optimization", *IEEE Transactions on Evolutionary Computation*, vol.6, no.6, pp. 580-593, 2002.

[5] Zhang G X, Jin W D, and Hu l Z, "Quantum evolutionary algorithm for multiobjective optimization problems", *Proc. of IEEE International Symposium on Intelligent control, Houston, Tesas: IEEE, Press,* vol.10, pp.703-708, 2003.

[6] Ying Li, Yanning Zhang, and Rongcuan Zhao etc, "The immune quantum-inspired Evolutionary algorithm", *proc. of IEEE int. Conference on systems, Man, Cybernetics*, pp.3301-3305, 2004

[7] J. Kennedy, R. Eberhart, "Particle swarm optimization", *Proc. of IEEE Int. Conf. Neural Networks*, pp. 1942–1948, 1995.

[8] M. Clerc, "The swarm and the queen: Toward a deterministic and adaptive particle swarm optimization", *Proc. IEEE Int. Congr. Evolutionary Computation*, vol. 3,p. 1957, 1999.

[9] Rui Zhang, Hui Gao, "Real –coded quantum evolutionary algorithm for complex function with high dimension", *Proc. of IEEE International Conference on Mechatronics and Automation,* pp. 2974-2979, August 5 - 8, 2007.

[10] Wang X Z,Yu S Y, "Improved evolution strategies for high-dimensional optimization," *Control Theory & Applications,* vol.23, no.1, pp.148-151, 2006.

[11] Yang Yu, Yafei Tian, and Zhifeng Yin," Hybrid Quantum Evolutionary Algorithms Based on Particle Swarm Theory", *proc. of IEEE International Conference on Industrial Electronics and Applications*, pp. 1-7 May 24-26, 2006.

Proceedings of 2009 12th International Conference on Computer and Information Technology (ICCIT 2009)
21-23 December, 2009, Dhaka, Bangladesh

Performance Analysis of a Novel Fuzzy Logic and MTPA Based Speed Control for IPMSM Drive with variable d- and *q*-axis Inductances

Md. Selim Hossain and Md. Jahangir Hossain
Department of Electrical and Electronic Engineering, RUET, Rajshahi-6204, Bangladesh
selim_hossain@yahoo.com

Abstract

This paper presents a novel speed control scheme of an Interior Permanent Magnet Synchronous Motor (IPMSM) using Fuzzy logic controller considering variable direct and quadrature axis inductances. The Fuzzy logic controller (FLC) has been designed on the basis of indirect vector control scheme of the IPMSM drive. The complete vector control scheme of the IPMSM drive incorporating the FLC is simulated for a IPMSM using Matlab/Simulink. The performances of the proposed FLC based IPMSM drive are investigated and compared to those obtained from the maximum torque per ampere (MTPA) based drive at various dynamic operating conditions, such as, certain change in command speed, step change in load, etc. The comparative results show that the FLC is more robust and, hence, found to be a suitable replacement of the MTPA control for the high performance industrial drive applications.

Keywords: Fuzzy Logic Controller, Interior Permanent Magnet Synchronous Motor, MTPA contol, High performance drive with variable direct axis and quadrature axis inductances and indirect vector control.

I. INTRODUCTION

The synchronous motor is offering serious challenge to the induction motor in the variable speed application domain .The main advantage of synchronous motors over the induction motors is their intrinsic ability to eliminate rotor I^2R slip power loss and to supply the reactive current. However, the wire-wound excited synchronous motors have some inherent disadvantages, such as, the requirement of extra power supply, slip rings and brush-gears at the rotor to provide field excitation. With the advent of high-energy permanent magnets like samarium cobalt, neodymium-boron-iron, etc., the drive technology has entered into a new era of brushless PM motor drives.
The main advantageous feature associated with these kinds of motors is that the magnetization is provided from a permanent magnet rotor. With brushless PM motors, it is possible to achieve motor performances that can surpass the conventional dc, induction, wire-wound excited synchronous motors. With respect to power density, high torque to inertia ratio and efficiency, brushless PM motors are superior to the conventional ac motors. Hence, depending on the application, there are many instances where brushless PM motors are preferable. Recently IPMSM is being used in high performance drives applications due to some desirable features, such as, high torque-current ratio, high power to weight ratio, low noise, highly efficient and robust operation [1]. The brushless IPMSM drive system involving the vector control scheme not only decouples the torque and flux [2] which ensures faster response but also makes the control task easy. The speed controller used in the brushless IPMSM drive system also plays an important role in meeting the other criteria of high performance drive. The motor control issues are traditionally handled by MTPA based . However, the maximum torque per ampere based system are very sensitive to parameter variations, load disturbances, etc. Thus, the controller parameters have to be continually adapted. The problem can be solved by several adaptive control techniques, such as model reference adaptive control (MRAC), Sliding-mode control (SMC), variable structure control (VSC), the mathematical model of an IPMSM drive can and self tuning PI controllers, etc. The design of all of the above controllers depends on the exact system mathematical model. However, is often difficult to develop an accurate system mathematical model due to unknown load variation, unknown and unavoidable parameter variations due to saturation, temperature variation, and system disturbances. In order to overcome the above problems, recently, the Fuzzy logic controller is being used for motor control purpose [3]-[8]. The mathematical tool for the FLC is the Fuzzy set theory introduced by Zadeh [9]. As compared to the MTPA, and their adaptive versions, the FLC has some advantages such as: 1) it does not need any exact system mathematical model; 2) it can handled nonlinearity of arbitrary complexity; 3) it is based on the linguistic rules with an IF-THEN general structure, which is the basis of human logic. However, the application of FLC has faced some disadvantages during hardware and software implementation due to its high computational burden. The earlier reported works for Fuzzy logic applications in motor drives are mainly based on at low speed operating conditions. Also they assume direct and quadrature axis inductances are fixed. But actually they are variable in nature [10]. There are several sources of variations in direct and quadrature axis inductances in PM machines: rotor inherent saliency, saturation based saliency (yoke, teeth) [11], rotor stator teeth harmonics [12], lamination direction based saliency [13], eddy current based saliency [14], rotor eccentricity based saliency. This paper investigates the successful applications of the FLC for normal speed control of IPMSM drives considering variable direct and quadrature axis inductances. The

978-1-4244-6283-4/09/$26.00 ©2009 IEEE

complete vector control scheme of IPMSM drive incorporating the FLC has been successfully simulated using Matlab Simulink [15]. The performance of the proposed drive has also been compared with those obtained from the MTPA control at different operating conditions. It is found that the proposed FLC is insensitive to temperature changes, inertia variations and load torque disturbances. This novel FLC could be a suitable replacement for the conventional MTPA control for high performance drive systems.

II. IPMSM DYNAMICS

The mathematical model of an IPMSM drive can be described by the following equations in a synchronously rotating rotor d-q reference frame for assumed sinusoidal stator excitation as

$$\begin{bmatrix} v_d \\ v_q \end{bmatrix} = \begin{bmatrix} R+pL_d & -P\omega_r L_q \\ P\omega_r L_d & R+pL_q \end{bmatrix} \begin{bmatrix} i_d \\ i_q \end{bmatrix} + \begin{bmatrix} 0 \\ P\omega_r \lambda_M \end{bmatrix} \quad (1)$$

$$T_e = T_L + J_m p\omega_r + B_m \omega_r \quad (2)$$

$$T_e = \frac{3P}{2}(\lambda_M i_q + (L_d - L_q) i_d i_q) \quad (3)$$

Where
V_d, V_q = d -q axis stator voltages;
L_d , L_q = d-q axis stator inductance;
I_q , I_d = d-q axis stator currents;
R= stator resistance per phase;
λ_M= constant flux linkage due to rotor permanent magnet;
ω_r = angular rotor speed;
θ_g = rotor position in electrical degrees;
P = number of poles of the motor;
T_e = developed torque;
T_L = load torque
B_m =Friction coefficient of the motor;
J_m = moment of inertia constant of the motor load;

$$L_d(\theta) = \frac{3L_{ao}}{2} + L_{a\sigma o} - (L_{a\sigma ts} - L_{a\sigma ys})\cos 2\theta - L_g - \frac{L_{a\sigma ys}}{2} \quad (4)$$

$$L_q(\theta) = \frac{3L_{ao}}{2} + L_{a\sigma o} - (L_{a\sigma ts} - L_{a\sigma ys})\cos 2\theta - \frac{L_{a\sigma ts}}{2} \quad (5)$$

After some manipulation the following equations are obtained for the direct and quadrature axis inductance:

$$L_d(\theta) = 0.0424 - 0.0159\cos 2\theta \quad (6)$$

$$L_q(\theta) = 0.0826 - 0.00917\cos 2\theta \quad (7)$$

From Equation (1-7) the following relationship is obtained,

$$V_q = [R + p(0.0826 - 0.00917\cos 2\theta)]\, i_q + P\omega_r (0.0424 - 0.0159\cos 2\theta)\, i_d + P\omega_r \lambda_M \quad (8)$$

$$V_d = [R + p(0.0424 - 0.0159\cos 2\theta)]\, i_d - P\omega_r (0.0826 - 0.00917\cos 2\theta)\, i_q \quad (9)$$

The key equations used for the flux weakening control of IPMSM.

$$i_d = -0.000119\,\omega_r^2 - 0.080316\,\omega_r + 10.5269 \quad (10)$$

$$i_q = -0.260375 i_d^2 - 0.244651 i_d + 3.4422727 \quad (11)$$

Block diagram in Fig.2 shows the control scheme of the motor drive. Using equation(10), the command d-axis current i_d^* is computed first, subsequently reference q-axis current i_q^* is calculated using equation (11). The command torque is obtained from a MTPA and fuzzy type speed controller. An estimated torque is calculated using (5), (10) and (11) and compared with the command torque.

III. DESIGN OF FLC FOR IPMSM

The followings are the member ship function for design of FLC.

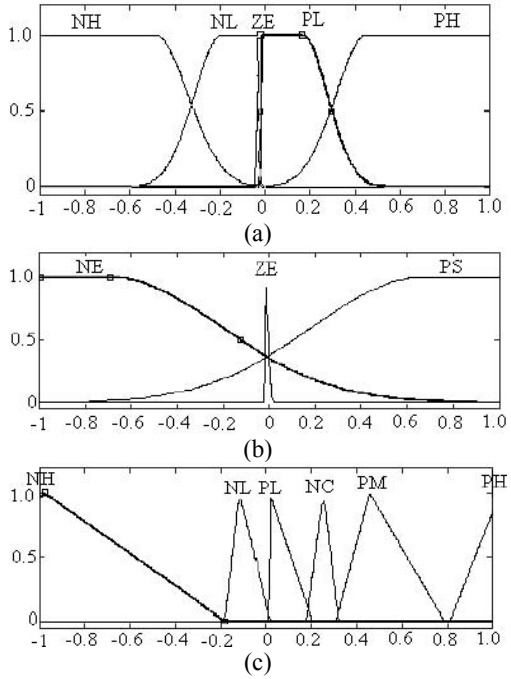

Fig.1. Membership Function for: (a) speed error Δω, (b) change of speed error Δe, (c) q-axis command current i_q.

The next step is to choose the scaling factors Kw, band k_T for fuzzification and obtaining the actual output of the command current. These scaling factors play a vital role for the FLC. The factors $K_\omega$and K are chosen that the normalized values of speed error and the change of speed error $\Delta\omega_r$ and Δe, respectively remain within the limit =1. The factor K is chosen that one can get the rated current for the rated conditions .In this paper, the constants are taken as next step is to choose the membership function of Δω, Δe and iq*, which form the important task of the FLC. The membership functions used for the input and output fuzzy sets are shown in Fig .1. The combined Gaussian functions are used as membership functions for all the fuzzy sets except the fuzzy set ZE (zero) of the

input vectors and fuzzy sets of the output vectors.

a) Gaussian function

$$f(k_T, a, c) = e^{\frac{-(x-a)^2}{xc^2}}$$

b) Triangular function

$$f(k_T, a, b, c) = \begin{bmatrix} \theta_r & x <= a \\ \frac{x-a}{b-a^2} & a <= x <= b \\ \frac{c-x}{c-b^2} & b <= x <= c \\ \theta_r & x => c \end{bmatrix}$$

The rules used for the proposed FLC algorithms are as follows:

(i) if Δωis PH (Positive High), i_q is PH (Positive High).
(ii) if Δωis PL (Positive Low), i_q is PM (Positive Medium).
(iii) if $\Delta\omega_r$ is ZE (Zero) and Δeis PS (Positive Small) i_q is PL (Positive Low).
(iv) if $\Delta\omega_r$ is ZE (Zero) and Δeis not PS (Positive Small) i_q is NC (No change). (v) if Δωis NL (Negative Low), i_q is NL (Negative Low).
(vi) if Δωis NH (Negative high), i_q is NH (Negative high).

Based on the above rules the fuzzy rule base matrix is show in table I. For the present works, Man dent type fuzzy inference is used. The values of the constants, membership functions, fuzzy sets for the input output variables and the rules used in this paper are selected by trial and error to obtain the optimum drive performance.

TABLE I. FUZZY RULE FROM MATRIX

$\Delta\omega r$ / Δe	NH	NL	ZE	PL	PH
NE	NH	NL	NC	PM	PH
ZE	NH	NL	NC	PM	PH
PS	NH	NL	PL	PM	PH

As long as the command torque is greater than the estimated torque, (9) and (10) are used to compute the three phase reference currents with the vector rotator. If the command torque is less than estimated torque, reference q-axis current is calculated using the command torque rather than the estmated torque. The speed error is processed by the fuzzy controller to generate the torque-producing current component command $i_q^*(n)$. The hysteresis current controller compares the reference three phase currents with actual currents and generates base signals for the transistorized inverter.

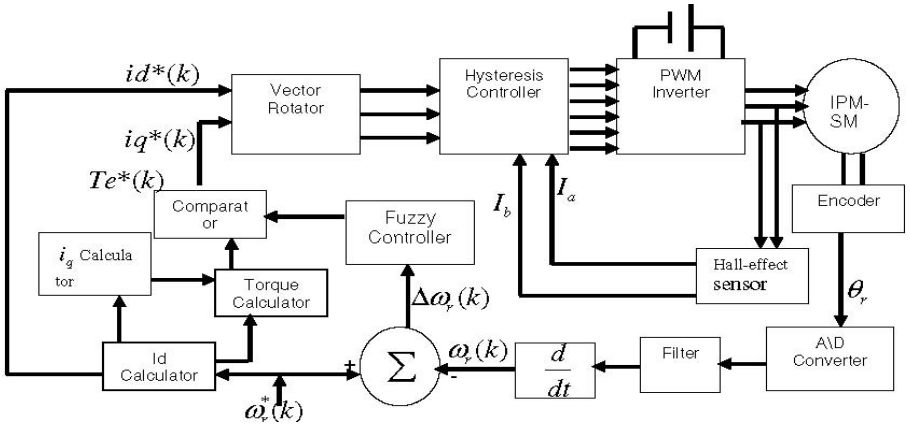

Fig.2. Block Diagram of FLC in Flux Weakening speed control of IPMSM Drive.

IV. RESULTS AND DISCUSSION

The performance of FLC based flux weakening control based IPMSM drive has been evaluated by computer simulation. The speed and current responses are observed under different operating conditions, such as, various command speeds, sudden application of load, step change in command speed and at different loading conditions. Some of the sample results are presented in this section. Figures 3.1 and 3.2 show the simulated starting performance of the drive with MTPA and FLC-based drive systems respectively for flux weakening control based IPMSM drive system with reference speed of 220 rad/sec at a load of 2 N-m. Although the MTPA control is give an optimum response, the fuzzy controller yielded better performances in terms of faster response time without any overshoot and lower starting current. Figures 3.3 (a) and (b) show speed responses of the drive system using MTPA and FLC, respectively with a step change in the reference speed. It is evident from Fig. 3.3 (b) that the proposed FLC based drive system can follow the command speed without any overshoot and steady state error. Thus, the FLC-based drive system is not affected by the sudden change of command speed. So, a good

tracking has been achieved for the FLC, whereas the MTPA control based drive system is affected with sudden change in command speed.

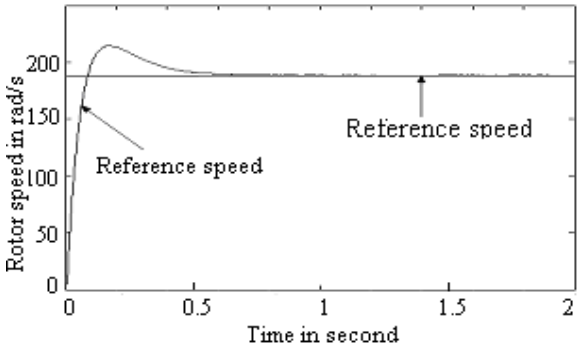

Fig. 3.1 (a) Simulated speed of IPMSM drive for flux weakening control with reference speed 220 rad/sec using MTPA.

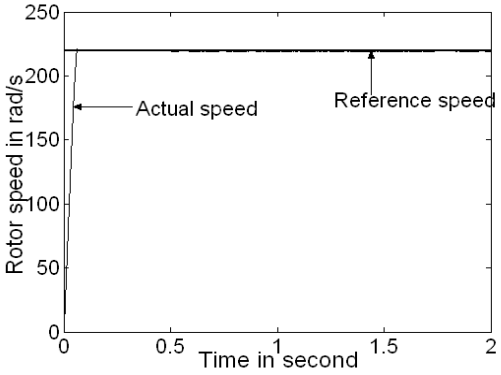

Fig. 3.1 (b) Simulated speed of IPMSM drive for flux weakening control with reference speed 220 rad/sec using FLC

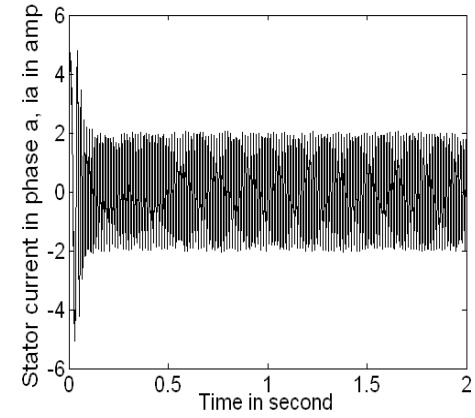

Fig. 3.2 (a)) Simulated current of IPMSM drive for flux weakening control with reference speed 220 rad/sec using MTPA.

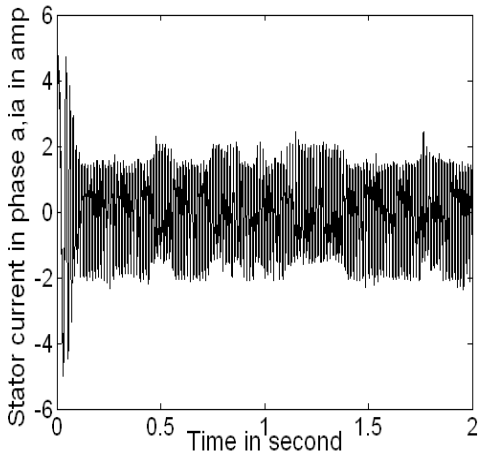

Fig. 3.2 (b) Simulated current of IPMSM drive for flux weakening control with reference speed 220 rad/sec using FLC.

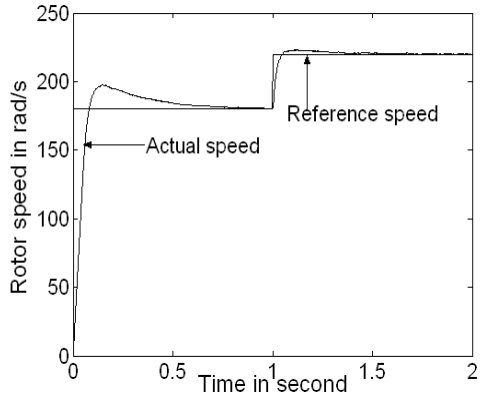

Fig. 3.3 (a) Simulated speed of IPMSM drive for flux weakening control with step change of reference speed using MTPA

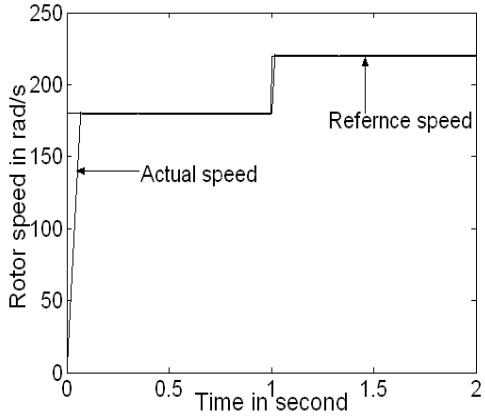

Fig. 3.3 (b) Simulated speed of IPMSM drive for flux weakening control with step change of reference speed using FLC .

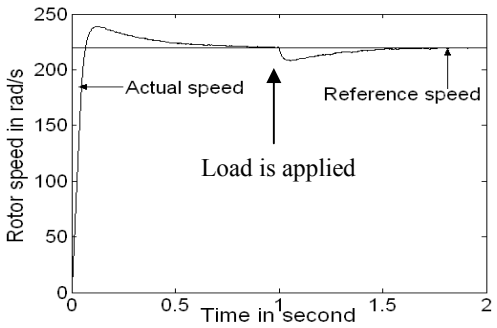

Fig. 3.4 (a) Simulated speed of IPMSM drive for flux weakening control with step change of load torque using MTPA.

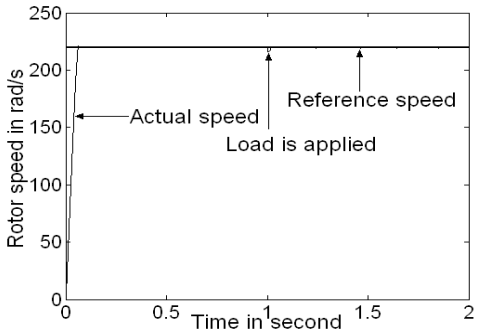

Fig. 3.4 (b) Simulated speed of IPMSM drive for flux weakening control with step change of load torque using FLC.

Figures 3.4 (a) and (b) show speed responses of the drive system using MTPA and FLC, respectively with a sudden change in loading torque. The motor was started with no load and this value was increased to 2 N-m after two seconds causing a drop in motor speed. The MTPA took less than 0.5 second and fuzzy logic controller negligible time to respond to this increase in torque and return the motor to the speed set point. Figures 3.5 (a) and (b) show simulated current response respectively for MTPA and Fuzzy logic controller negligible time to respond to this increase in torque and return the motor to the speed set point.

Figures 3.5 (a) and (b) show simulated current response respectively for MTPA and fuzzy controller based IPMSM drive system with sudden application of a load of 2 N-m.

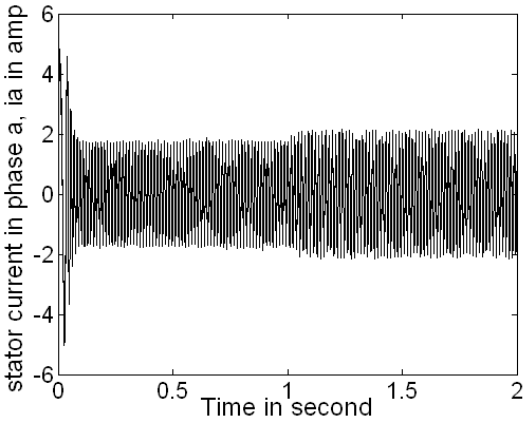

Fig. 3.5 (a) Simulated current of IPMSM drive for flux weakening control with step change of load torque using MTPA.

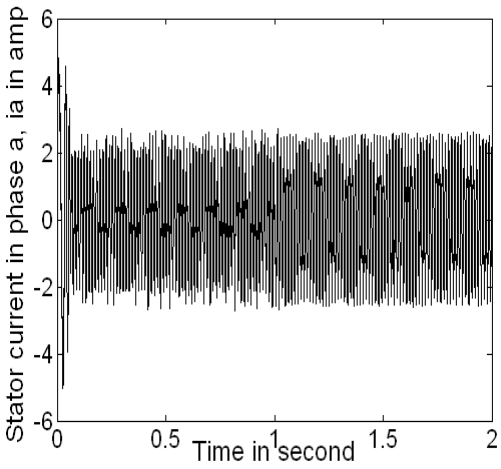

Fig. 3.5 (b) Simulated current of IPMSM drive for flux weakening control with step change of load torque using FLC.

V. CONCLUSIONS

In this work, a new approach for fuzzy logic based algorithm of flux weakening method has been applied for the speed control of IPMSM drive above the base speed with the consideration of variable d- and q axis inductances. Relatively simpler expressions of d- and q-axis currents have been derived and incorporated in the IPMSM drive system.

Simplified fuzzy controller for the IPMSM has also been designed with variable inductances and implemented through simulation. The IPMSM drive system is efficient enough to operate in no load and loading condition. Derived equation of voltage limited ellipse may dictate a new approach of flux weakening method for an optimum value of stator current, which will provide better performance in terms of efficiency. From the obtained results, it is obvious that the FLC based IPMSM drive has been found superior to the MTPA based system.

APPENDIX

Interior permanent Magnet Synchronous Motor Data
Type = Interior type PM motor
Rated power = 1 hp
Input line to line voltage = 208V
Rated frequency = 60 HZ
Number of Poles = 4
q- Axis inductance $L_q = 0.0795$H
d- Axis inductance $L_d = 0.0424$H

Stator resistance per phase $R_s = 1.5\Omega$
Inertia constant J =0.003 Kg.m^2
Damping constant B =0.00008 (N-m)/rad/sec
Magnet flux linkage $\lambda_M = 0.314$ volts/rad/sec.

REFERENCES

[1] R. Krishnan, "Selection criteria for servo motor drives", *IEEE Trans. Ind. Applicat.,* Vol. IA-23, pp. 270-275, Mar/April, 1987.

[2] S. Morimoto, Y. Takeda and T. Hirasa, "Current phase control methods for permanent magnet synchronous motors", *IEEE Trans, on Power Electr.,*Vol. 5, No. 2, 1990, pp. 133-139.

[3] I. Miki, N. Nagai, S. Nishiyama and T. Yamada, "Vector control of induction motor with fuzzy PIcontroller", in IEEE IAS Annu. Rec., 1992,pp.464-471.

[4] Y. Tang and L. Xu,"Fuzzy Logic Application for Intelligent Control of a Variable Speed Drive ", IEEE Trans. on Energy Conversion, vol. 9, pp. 679-685, Dec.1994.

[5] E. Cerruto, A. Consoli, A. Raciti and A. Testa, "Fuzzy Adaptive Vector Control of Induction Motor Drives", IEEE Trans. on Power Electron., vol. 12, pp.1028-1039, Nov. 1997.

[6] C.H. Won, S. Kim and B.K. Bose,"Robust Position control of induction motor using fuzzy logic control", in IEEE IAS Conf. Rec., Houston, TX, 1992, pp. 472-481.

[7] M.N. Uddin and M.A. Rahman, "Fuzzy Logic based Speed control of an IPM Synchronous motor drive", J. Advanced Comput. Intel., Vol. 4, no. 3, pp.212-219,2000.

[8] Mohammad Abdul Mannan, Toshiaki Murata, Junji Tamura and Takeshi Tsuchiya, "Indirect Field Oriented Control for high performance Induction motor drives using space vector modulation with consideration of core loss", in proc. PESC, 03, Acapulco, Mexico, pp.1449-1454, june,2003.

[9] L.A. Zadeh, "Fuzzy sets", inform. control, vol.8, pp. 338-353, 1965.

[10] Sigurd Ovrebo, Prof. Roy Nilsen, Prof. Robert Nilssen, "Saliency Modeling in Radial Flux Permanent Magnet Synchronous Machines", NORPIE 2004, Trondheim, Norway.

[11] M. Schroedl; "*Sensorless Control of A.C. Machines",* Ph.D. thesis, Wien, 1992.

[12] M.W. Degner; "*Flux, Position, and Velocity Estimation in AC Machines Using carrier signal injection"*, Ph.D. Dissertation, Dep. Of Mechanical Engineering, University of Wisconsin - Madison 1998.

[13] T Wolbank, J Machl "*Anisotropy in Induction Machine Lamination and its Influence on Mechanical Sensorless Control and Conditioning Monitoring*" EPE Toulouse 2003-10-22.

[14] M. Leksell, L. Harnefors, H.P. Nee; "*Machine Design Considerations for Sensorless Control of PM Motors"*, Proceedings International Conference on Electrical Machines, Istanbul, September 1998.

[15] Matlab, Simulink User Guide, The Math Works Inc., 1997.

[16] M.S. Hossain, M.J. Hossain, M.S. Anowar and M.A. Hoque " Fuzzy Logic based speed control of IPMSM drive" ICCIT-2007

Proceedings of 2009 12th International Conference on Computer and Information Technology (ICCIT 2009)
21-23 December, 2009, Dhaka, Bangladesh

Performance Evaluation of a Mobile Cellular Network with two Hop Ad-Hoc Relaying

Nusrat Sultana†, M. A. Jobayer Bin Bakkre†, Md. Imdadul Islam‡, and M. R. Amin†
†Department of Electronics and Communications Engineering, East West University, 43 Mohakhali, Dhaka 1212, Bangladesh
‡Department of Computer Science and Engineering, Jahangirnagar University, Savar, Dhaka 1342, Bangladesh
lethe7.29@gmail.com, jobayer@ewubd.edu, imdad@juniv.edu, ramin@ewubd.edu

Abstract

In a mobile cellular network, both new originating calls and handoff calls can be dropped at any time in the midst of a conversation when a user enters in a dead spot. Because of this, there is always some discrepancy between traffic originated by the mobile station (MS) and that of received by the base station (BS). A probability model is used in this paper to evaluate this discrepancy considering geometry of the service area and probability density function of user distribution. Blocking probability experienced by the BS is found less than that of evaluated from the offered traffic of user end, which is the central idea of this paper. Furthermore, the same traffic model is applied to an ad- hoc two hop relay mobile cellular system for performance evaluation.

Keywords: Ad-hoc relaying, performance evaluation, new originating call, handoff call, and wireless mobile communication.

I. INTRODUCTION

In mobile communication systems [1], in any type of access technique, the mobile station (MS) and the base station (BS) are connected by wireless link. When an MS initiates a call, the radio signal strength must be above threshold level otherwise the request will be ignored by the BS. Sometimes, the MS enters in a shadow zone of a cell and originates a call then it fails to receive acknowledgement from the BS and the call is not served and that arrival of the call is not experienced by the switching center; same is true for handoff cases. The BS watches over the signal strength of the MS. If the signal strength of a new entering MS falls below the threshold level then the BS initiates handover process. But if the MS coming from surrounding cell falls in a dead spot at the new cell before transferring its call to a new BS, it will also not be considered by the switching station. A solution of solving this dead spot problem is to apply an ad-hoc relay network to the cellular system. In an ad-hoc network [2], a terminal itself has a capability for relaying and routing, so that a network is dynamically formed by terminals only [3]. When an MS in a dead spot tries to issue a new call with the help of ad-hoc network relaying [4], it can still establish the connection with the base station by seeking a relay station. In Fig.1, we show a schematic diagram of a two hop relay ad-hoc network. We can see that there is a dead spot present inside the coverage area of a single BS, and all MSs are distributed inside the coverage area randomly. Some MSs, which are outside the dead spot, can communicate directly with the BS [5]. However, the MSs, which are inside the dead spot, can communicate with the BS indirectly via relay stations (RS) [1] using their ad-hoc air interface. The relay station has to be in a position outside the coverage area of dead spots but inside the relaying zone of the MS which is in the dead spot [1]. Tanaka et. al. [3] have already proposed a model based on this idea. They have proposed a method of theoretical calculation of the degree of improvement of communication traffic by means of two hop relaying [6]. They have also shown by simulation that multi hop relaying [7] does not give significantly greater performance improvement than that by two hop relaying.

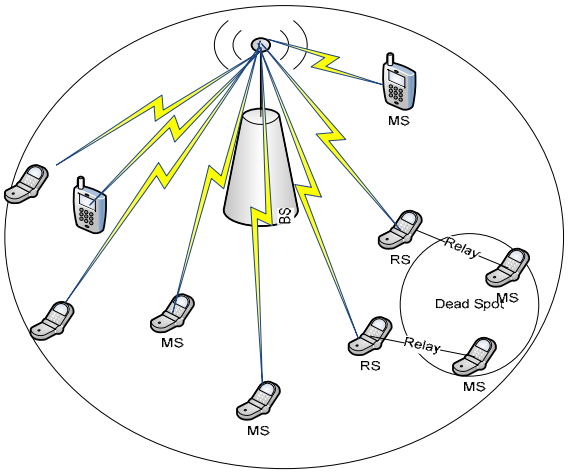

Fig. 1. Two-hop mobile cellular network.

Tanaka et. al. [3] have only considered new originating calls and ignored the handoff case which is a very important factor for a cellular system because there is major possibility that a handoff call may also enter in a dead spot at any time. In our present paper, we are giving more importance on handoff calls. If we apply the concept of ad-hoc [8] relaying here then it is possible to prevent the call drop. Definitely, the terminal which is in the middle of a conversation should

get more importance that the terminal that is originating a new call. In this paper, we have differentiated the offered traffic of a conventional cellular system into two parts, i.e., handoff calls and new originating calls. We have drawn a two-dimensional (2D) Markov chain [9], and based on the mathematical analysis of this chain, we proposed a solution of the dead spot problem.

The plan of the paper is as follows. In Section II, we have described our mathematical model. Section III focuses the results and findings of the work. Finally, the conclusion is drawn in Section IV.

II. TRAFFIC MODEL

We assume that when an MS is not in a dead spot and is able to directly communicate with the base station then the arrival rate of the call made by the terminal is λ_c [10]. If this arrival rate is used, the blocking rate of the conventional cellular system without ad-hoc relaying can be calculated by taking into account of the effect of the dead spot [3].

Now, let us assume that a call is generated from a terminal located within the cell and not in the dead spot. The distance between the terminal and the base station is expressed by a random variable *Y*. The two events are as follows:

Event A: $0 \le Y \le r_2$.

Event B: This terminal does not fall in a base station dead spot.

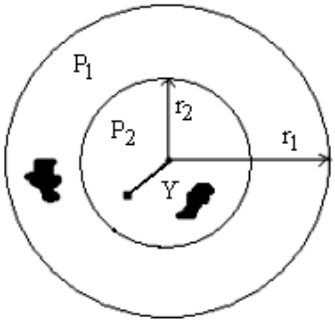

Fig. 2. Arrival of handoff calls.

The probability that a terminal located in the circle of radius r_2 and not in the dead spot is denoted as $P(B/A) = P_2$. Similarly, the probability that a terminal located in the circle with radius r_1 and not in the dead spot is denoted as $P(B/\overline{A}) = P_1$. Since these terminals are considered to be distributed uniformly within the cell, the probability that a terminal is not in a dead spot is then

$$P_B(r_1, r_2) = P(B/A)P(A) + P(B/\overline{A})P(\overline{A}) = P_2 \frac{{r_2}^2}{{r_1}^2} + P_1\left(1 - \frac{{r_2}^2}{{r_1}^2}\right). \quad (1)$$

Let us consider that the mobile stations from the surrounding cells enter the cell under consideration, in the range $r_1 - r_4$ of the cell shown in Fig. 3. Handoff users will remain at distance $r_4 \le Y < r_1$ from the center of the cell. In this case, two new events have to be considered here.

Event M: A handoff call will remain in $r_4 \le Y < r_1$.

Event N: MS is not in a dead spot.

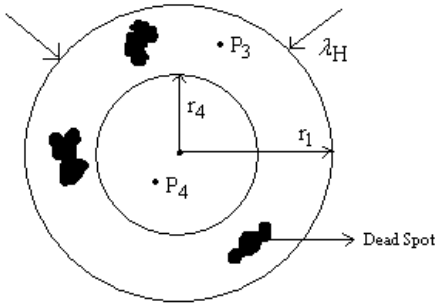

Fig. 3. A terminal located within the cell and not in a dead spot.

Now the probability that a handoff call is inside the region $(r_4 \le Y < r_1)$ and not in a dead spot is $P_3 = P(N \mid M)$ and the probability that a call is not in the dead spot and outside the region $(r_4 \le Y < r_1)$ is $P_4 = P(N \mid \overline{M})$. Since these terminals are considered to be distributed within the cell, we have the probability that a handoff terminal is not in a dead spot is then

$$P_N(r_1, r_4) = P(N \mid M)\,P(M) + P\left(N \mid \overline{M}\right)P\left(\overline{M}\right) = P_3\left(1 - \frac{r_4^2}{r_1^2}\right) + P_4\frac{r_4^2}{r_1^2}. \quad (2)$$

Let us assume that the parameter λ_H is representing the arrival rate of the handoff calls that can communicate directly with the base station and λ_O is representing the arrival rate of those calls which are originated inside the cell. Thus,

$$\lambda_H = \lambda_{HT} P_N(r_1, r_4) = \lambda_{HT}\left[P_3\left(1 - \frac{r_4^2}{r_1^2}\right) + P_4\frac{r_4^2}{r_1^2}\right], \quad (3)$$

and

$$\lambda_O = \lambda_{OT} P_B(r_1, r_2)$$
$$= \lambda_{OT}\left[P_2\left(\frac{r_2^2}{r_1^2}\right) + P_1\left(1-\frac{r_2^2}{r_1^2}\right)\right]. \quad (4)$$

The average holding time for handoff calls and newly originating calls inside the cell is t_{hO} and t_{hH} respectively, where $t_{hO} = 1/\mu_O$, $t_{hH} = 1/\mu_H$, $A_O = \lambda_O t_{hO}$, $A_H = \lambda_H t_{hH}$. The quantities μ_O, μ_H, A_O, and A_H respectively the service rate of the new originating calls, service rate of the handoff calls, offered traffic of new originating calls and offered traffic of the handoff calls respectively.

In mobile telecommunication systems, an improved method is introduced here for calculating the blocking rate of an ad-hoc relay system. We consider a two hop relay counting method. We assume that the parameter λ_1 is the arrival rate of those calls which are communicating directly with the base station and λ_2 is the arrival rate of those calls which need relaying and thus the total arrival rate is $\lambda_c = \lambda_1 + \lambda_2$. Considering relays, a new event, event *C*, is introduced here in addition to events A, B, M and N.

Event C: In this event, a terminal can communicate with the base station by relaying. Terminals can enter a base station dead spot independently and the dead spots could be anywhere inside the cell. So, a terminal exists in a base station dead spot and can relay a communication to the base station; this can be represented by a new event $\left(\overline{B} \cap C\right)$. The arrival rate of those calls which require two channels is

$$\lambda_2 = \lambda_c(1-P_2)P(C \mid A)\left(1-r_2^2/r_1^2\right) + \lambda_c(1-P_1)P(C \mid \overline{A})\left(r_2^2/r_1^2\right), \quad (5)$$

where

$$P\left(C \mid \overline{A}\right) = \int_{r_2}^{r_1} q(y)\, f\left(y \mid r_2 < Y \le r_1\right) dy,$$

$$P(C \mid A) = \int_0^{r_2} q(y) f\left(y \mid 0 < Y \le r_2\right) dy,$$

and

$$q(y) = 1 - e^{-P_d P_1 \lambda_s S_1}\ e^{-P_d P_2 \lambda_s S_2}.$$

A. Proposed Two Hop Network Model

We divide the arrival rate of a conventional cellular system into two types that is, handoff calls and new originating calls. Furthermore, we divide each of handoff calls and new originating calls into two parts: one channel required case and two channel required case. But in case of channel occupancy, the concept is, however, total sharing.

Based on the differentiation of one channel and two channel required cases, we have designed a 2D Markov chain where one dimension is representing the blocking of one channel required case and the other dimension is representing the blocking of two channel required case. In teletraffic engineering, probability of occupancy of all channels is called the blocking probability [3]. The total arrival rate of a conventional cellular system is

$$\lambda = \lambda_{1N} + \lambda_{1H} + \lambda_{2N} + \lambda_{2H},$$

where λ_{1N}, λ_{1H}, λ_{2N} and λ_{2H} are respectively the arrival rate of new originating calls which require one channel, arrival rate of handoff calls which require one channel, arrival rate of new originating calls which require two channels and the arrival rate of handoff calls which require two channels. According to our proposed model, we first design a simple Markov chain only for four channels, that is $m = 4$. After setting up the equations of the state transition probabilities for one channel and two channel required cases from the Markov chain shown in Fig. 4, we derive the generalized formulas for the blocking probabilities β_1 and β_2 of the above two cases.

The total arrival rate of calls which require one channel is $\lambda_1 = \lambda_{1N} + \lambda_{1H}$, and the arrival rate of calls which require two channels is $\lambda_2 = \lambda_{2N} + \lambda_{2H}$. We ignore the arrival rate of new originating calls that require two channels to avoid complicacy of drawing Markov chain that is, we assume $\lambda_{2N} = 0$ and so that, $\lambda_2 = \lambda_{2H}$. The sum of probabilities of the complete occupied states for one channel required case is $\beta_1 = P_{02} + P_{21} + P_{40}$ and for two channel required cases is $\beta_2 = P_{02} + P_{11} + P_{21} + P_{30} + P_{40}$.

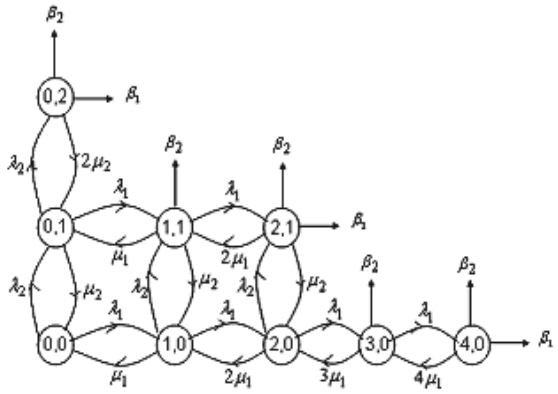

Fig. 4. Two dimensional Markov chain.

The blocking probabilities β_1 and β_2 for one-channel and two-channel required cases are obtained as

$$\beta_1 = P_{0,m/2} + \sum_{k=1}^{m/2} P_{2k,\frac{m}{2}-k}, \quad (6)$$

and

$$\beta_2 = P_{0,m/2} + \sum_{K=1}^{m/2}\left(P_{2k-1,\frac{m}{2}-k} + P_{2k,\frac{m}{2}-k} \right), \qquad (7)$$

where $P_{x,y} = \left(a_1^x / x!\right)\left(a_2^y / y!\right)P_{oo}$ and m represents the number of channels. By utilizing the normalization condition, i.e., by setting the sum of the probabilities equals unity, we obtain

$$P_{00} = \left(\sum_{y=0}^{m/2} \sum_{x=0}^{m-2y} \frac{a_1^x}{x!}\frac{a_2^y}{y!} \right)^{-1}. \qquad (8)$$

B. Comparison Between Blocking of Traffic Experienced by Base Station and Offered Traffic from User End

If we consider the offered traffic from user end, then the arrival rate and offered traffic of handoff and originating calls can be obtained as

$$\lambda_H(r_1, r_4) = \lambda_{HT} P_N(r_1, r_4),$$
$$\lambda_O(r_1, r_2) = \lambda_{OT} P_B(r_1, r_2),$$
$$\alpha_H(r_1, r_4) = \lambda_H(r_1, r_4)\, t_{hH},$$
$$\alpha_O(r_1, r_2) = \lambda_O(r_1, r_2)\, t_{hO}.$$

By considering offered traffic same as that of the user end, the arrival rate and offered traffic of handoff and new originating calls are given by $\lambda_H(r_1, r_4) = \lambda_{HT}$ and $\lambda_O(r_1, r_2) = \lambda_{OT}$.

Therefore, the Blocking probability is

$$\beta_1(m) = \beta_2(m) = \sum_{x=0}^{m}\left(\frac{\alpha_H(r_1, r_4)^x}{x!} \right)\left(\frac{\alpha_O(r_1, r_2)^{m-x}}{(m-x)!} \right) \times \left[\sum_{x=0}^{m}\sum_{y=0}^{m-x}\left(\frac{\alpha_H(r_1, r_4)^x}{x!} \right)\left(\frac{\alpha_O(r_1, r_2)^y}{y!} \right) \right]^{-1}. \qquad (9)$$

C. Comparison Between Blocking Probabilities of One Channel and Two Channel Required Cases with Respect to (i) Number of Channels, (ii) Offered Traffic, and (iii) Arrival Rate

The equation we use for the comparison between blocking probability [3] with respect to number of channels for one channel and two channel required cases according to generalized formula are as follows. The blocking for one channel required case is

$$\beta_1(m) = P_{0,\frac{m}{2},m} + \sum_{k=1}^{m/2} P_{2k,\frac{m}{2}-k,m}, \qquad (10)$$

and the blocking probability for two channel required case is

$$\beta_2(m) = P_{0,\frac{m}{2},m} + \sum_{K=1}^{m/2}\left(P_{2k-1,\frac{m}{2}-k,m} + P_{2k,\frac{m}{2}-k,m} \right), \qquad (11)$$

where

$$P_{x,y,m} = \frac{(\alpha_1/\mu_1)^x}{x!}\frac{\alpha_2{}^y}{y!} \times \left[\sum_{y=0}^{m/2}\sum_{x=0}^{m-2\cdot y} \frac{(\alpha_1/\mu_1)^x}{x!}\frac{\alpha_2{}^y}{y!} \right]^{-1}. \qquad (12)$$

III. RESULT AND DISCUSSIONS

It is desired that when a call originates, it reaches the base station or when a handoff call arrives, it can also communicate with the base station. But in real life situation, a certain amount of call becomes blocked because of dead spots. If the concept of ad-hoc relaying [11] is applied then it is possible to reduce the probability of blocking. We have studied this scenario here by varying different parameters. It has been found for every case that the blocking for two channel required case is higher compared to the one channel required case because the two channel required case occupies two channels for a single call establishment. We have taken typical values of all required parameters for our present analysis.

In this section, a comparison is made between blocking of 'offered traffic from user end' case and that of 'received traffic of base station side' case. Let us designate them as case-1 and case-2 respectively. For numerical appreciation of our results as described earlier, we have plotted in Fig. 5, the blocking probability with respect to channel number for both case-1 and case-2. Figure 5 shows that the blocking probability of case-1 and case-2 where both are decreasing with the increase of the number of channels. The rate of decrement of case-1 is more prominent than that of case-2. The reason is that, in case-2, a large number of calls do not reach the base station because of different types of obstacles.

We have plotted in Figs. 6 and 7, the blocking probability with respect to offered traffic and arrival rate respectively for both one channel and two channel required cases. Figure 6 shows the variation of the blocking probability with respect to the offered traffic for both one channel and two channel required cases. In both cases, blocking probability increases gradually with the increase of the offered traffic. It is seen from this figure that, in one channel required case, blocking increases slowly but in two channel required case, blocking increases very sharply and the rate is very high because the case of two channel required case occupies two channels to establish a call or to maintain a call. It is to be mentioned here that to improve the situation for probability of no channel available, which is a very important quantity for performance evaluation of a wireless mobile communication system, delay of data end user has been introduced in this work instead of delay of voice end user as the voice traffic is impatient traffic (customer retry until getting free channel) should have higher priority than the data traffic. It has been

found that by applying a small delay to the data end user, the probability of no channel available can be drastically reduced.

We have in this analysis incorporated different arrival rates of the voice and data traffic but same service termination rate.

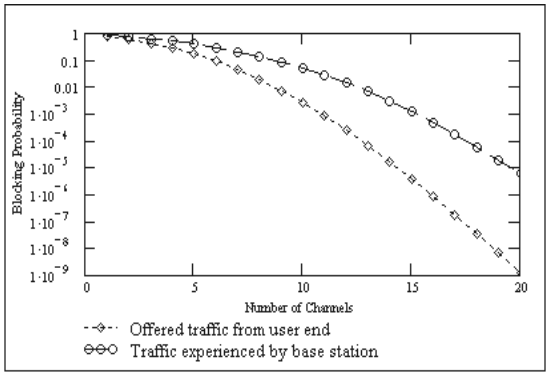

Fig. 5. Comparison between blocking probability of case-1 and case-2.

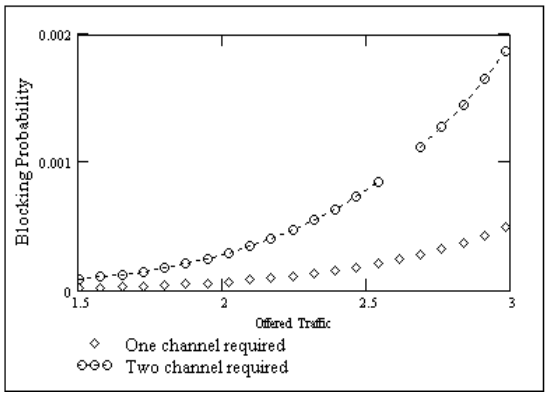

Fig. 6. Comparison between blocking probability with respect to offered traffic for one channel and two channel required cases (m=12).

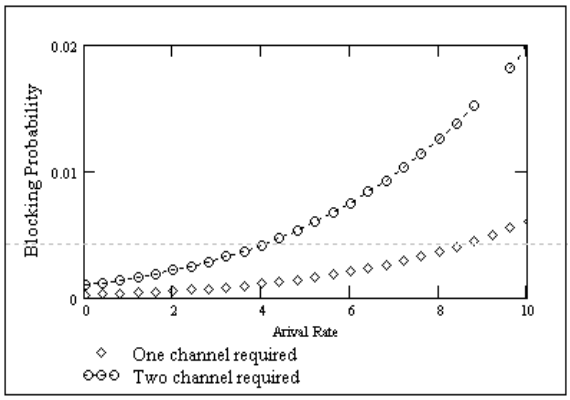

Fig. 7. Variation of blocking probability with respect to arrival rate for one channel and two channel required cases.

Figure 7 shows the variation of blocking probability with respect to the arrival rate for one channel and two channel required cases. Here, we also observe that with the increase of arrival rate, blocking probability increases and the same scenario is observed in this figure as in Fig. 6.

VII. CONCLUSION

A new architecture of cellular system using two hop relaying under the environment of dead spots is introduced in this paper. By dividing the total traffic into one channel and two channel required cases, that is, calls which can communicate directly with the base station and calls which need relaying, we have designed a 2D Markov chain, a method for theoretically calculating the traffic characteristics of a cellular system. The ad-hoc relay concept has been applied along the dimension representing two channel required case, to resolve the dead spot problem, a cause of deterioration of the performance of cellular system. By analyzing the communication traffic characteristics of traditional cellular system it has been found that not all calls initiated by the users reach the base station because of dead spots. This is the case where by applying ad-hoc relaying, we have found that the performance can be improved in a substantial amount. Also by analyzing the blocking for one channel and two channel required cases, it has been found that the blocking for two channel required case is much higher compared to the one channel required case. For simplicity, in this work, it has been considered that the mobile stations around the dead spots are stationary but in practical cases these all stations are not stationary, some are moving. To avoid complicacy, we have not considered here those new originating calls which require two channels. These limitations can be important consideration for further development of the work.

REFERENCES

[1] Wei-Feng Lu and Meng Wu, "Analysis of Communication Traffic Characteristics of Two-hop-realy Cellular System in the Dead Spot," 8th ACIS International Conference on Software Engineering, Artificial Intelligence, Networking and Parallel/Distributed Computing, IEEE Computer Society, 2007.

[2] Lin Chen, Chang-jun Jiang, Yu Fang, Fei Liu "*Performance evaluation of Ad Hoc networks based on SPN*", Proceedings on the International Conference on Wireless Communications, Networking and Mobile Computing, vol. 2, pp. 816-819, Sept. 2005.

[3] A. Tanaka, K. Nakano, M. Sengoku, and S. Shinoda, "Analysis of Communication Traffic Characteristics of a Cellular System with Ad-Hoc

Networking," Electron. and Commun. in Japan, Part 1, vol. 86, no. 11, Nov. 2003.

[4] Wei-feng Lu, Meng Wu, "*Performance Evaluation of Two-hop-relay WCDM Cellular Systems*", IEEE International Conf. on WiCom, pp. 722-726, 21-25 Sept. 2007.

[5] Jingyuan Sun, "Uplink Capacity Enhancement In Two-Hop cellular Networks With Limited Mobile Relays," 15th IEEE workshop on Local & Metropolitan Area Networks, pp. 134-138, June 2007.

[6] H. Wei, R. Gitlin, "Two-hop-relay architecture for next-generation WWAN/WLAN integration," IEEE Wireless Commun., vol. 11, no.2, pp.24-30, April 2004.

[7] Jiandong Li, Zygmunt J. Haas, and Min Sheng, "Capacity Evaluation of Multi-Channel Multi-Hop Ad Hoc Networks," IEEE International Conf. on Personal Wireless Communications, pp. 211-214, Dec. 2002.

[8] Anthony Lo, Jinglong Zhou and Ignas Niemegeers, "Multi-hop Cellular Networks: Integrated IEEE 802.11 Ad hoc and Universal Mobile Telecommunications System (UMTS) Networks," Proceedings of the 2nd European Research Consortium for Informatics and Mathematics (ERCIM) Workshop on eMobility, Tampere, Finland, 2008.

[9] Md Imdadul Islam, Liton Jude Rozario, "Telecommunication Traffic and Network Planning," published by Christian communications center, Protibeshi prokashani, Dhaka, June 2008.

[10] Tracy Camp, Jeff Boleng, Vanessa Davies, "A Survey of Mobility Models for Ad-Hoc Network Research," Wireless Communications and Mobile Computing (WCMC): Special Issue on Mobile Ad Hoc Networking: Research, Trends and Applications, vol. 2, no. 5, pp. 483-502, Sept. 2002.

[11] Sung-Ju Lee, William Su, Julian Hsu, Mario Gerla, and Rajive Bagrodia, "A Performance Comparison Study of Ad Hoc Wireless Multicast Protocols," Nineteenth Annual Joint Conference of the IEEE Computer and Communications Societies. Proceedings IEEE, vol. 2, pp. 565-574, Aug. 2006.

Proceedings of 2009 12th International Conference on Computer and Information Technology (ICCIT 2009)
21-23 December, 2009, Dhaka, Bangladesh

Adaptive Array Antenna System in Cancellation of Jammer and Noise of Wireless Link

Md. Imdadul Islam†, Md. Golam Gaus‡, Avijeet Das‡, Mushlah Uddin Sarkar‡, and M. R. Amin‡
†Department of Computer Science and Engineering, Jahangirnagar University, Bangladesh
‡Department of Electronics and Communications Engineering, East West University, Bangladesh
imdad@juniv.edu, shiplu_sarkar@hotmail.com, ramin@ewubd.edu

Abstract

Single element antennas have very little capability of variation of antenna gain pattern. For a desired directivity, shape of beam and steer able beam, array antenna is widely used in wireless network. Relative magnitude of feed currents, relative phases or separation between antenna elements, geometrical configuration of array are responsible for the overall radiation pattern. The weighting factor of each antenna element is governed by an adaptive algorithm based on input signal and desired signal to achieve dynamic shaping of antenna beam. In this paper, both single and multiple elements adaptive array antenna system is used to tune the gain in such a way that the gain is enhanced in the direction of desired signal and reduced in the direction of interference or jamming signals.

Keywords: Adaptive beamforming, auto-correlation, cross-correlation vector, jammer, radiation pattern, reference and primary omni.

I. INTRODUCTION

The present era can be considered to be the era of wireless communication systems. But wireless channel experiences different types of fading, deteriorates the quality of received signal [1], [2]. To enhance the performance of a wireless channel, multiple independent antennas are arrayed. In array antenna systems, several antennas are connected and arranged in a regular structure (linear, planer, circular) to form a single antenna. Antenna array produces radiation pattern, actually the combination of pattern of single elemental antenna. There are five factors which control the overall pattern of array antenna. They are: the geometrical configuration of the overall array (linear, circular, rectangular, spherical, etc.), the relative displacement between the elements, the excitation amplitude of the individual elements, the excitation phase of the individual elements, and finally, the relative pattern of the individual elements, as summarized in [3]-[5].

The desired signal is often contaminated by unwanted signal can be recovered using bandpass filter. Conventional filters often can not solve the situation, because the nature of input signal remains unknown. An adaptive filter can change its characteristic dynamically accord ing to the change in input signal. It is an FIR (Finite Impulse Response) or IIR (Infinite Impulse Response) filter with adjustable coefficients and an adaptive algorithm; where the output is feedback to the algorithm to update the filter coefficients [6]-[8]. Adaptive beamforming is a special technique by which we can transmit or receive signal from any desired direction while denying the signal of same frequency from other directions. Adaptive beamformer adjust the weighting factor of antenna elements analyzing the relative phase and amplitude of wave incident on the elements of the array. Final achievement is like: antenna gain is enhanced in the direction of arrival of desired signal and reduced in the direction of interference [9]-[11].

Organization of the paper is as follows. Section II discusses about the adaptive beamforming, sidelobe cancellation with both single reference antenna and multiple reference antennas. Section III deals with the results of previous sections and finally section IV concludes the entire analysis.

II. ADAPTIVEBEAMFORMING

In adaptive beam forming technique, a primary and a reference antenna element are connected in the fashion of adaptive noise cancellation. Here both antenna elements receive signal and interference from all the directions in case of omni directional antenna but there is a small phase shift between received signals of two antennas. The primary antenna will receive the desired signal with some interference and noise of the receiving device. Output of the adaptive filter will provide an estimated value of interference and noise. Hence the difference between these two signals will provide the desired signal [12].

In Fig. 1, we observe that there is the receiver noise present at the outputs of the two omnis. The omnis are separated by a distance *L*. A single signal is incident at an angle of θ_0. The signal component at the primary omni is [13], [14]

$$Primary\ signal = c\cos k\omega_0$$

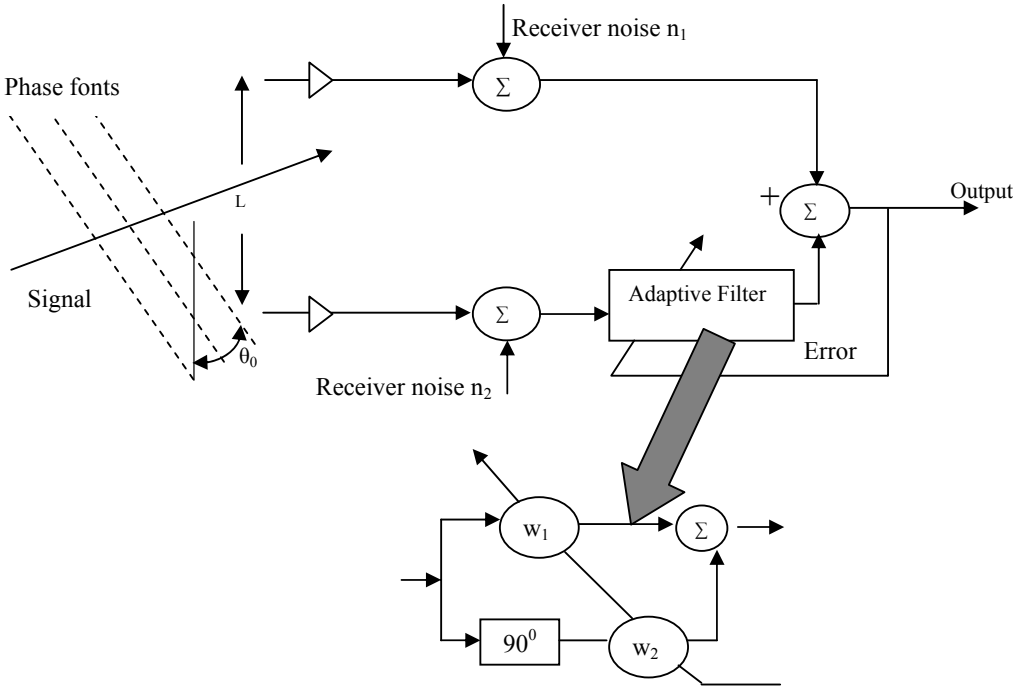

Fig. 1. Side lobe canceller with single incident signal.

For path difference, $L\sin\theta_0$, the change in phase is, $\delta_0 = (2\pi/\lambda)L\sin\theta_0$. Let the primary signal be $c\cos k\omega_0$, and the reference signal be $c\cos(k\omega_0+\delta_0)$.

The autocorrelation vector of reference signal is

$$\mathbf{R}_{\mathrm{r}} = E\left[\mathbf{X}_{\mathrm{k}}\mathbf{X}_{\mathrm{k}}^{\mathrm{T}}\right],$$

where

$$\mathbf{X}_{\mathrm{k}} = \begin{bmatrix} c\cos(k\omega_0+\delta_0) \\ c\sin(k\omega_0+\delta_0) \end{bmatrix}.$$

Thus, the matrix $\mathbf{R}_{\mathrm{r}}$ can be simplified to

$$\mathbf{R}_{\mathrm{r}} = \begin{bmatrix} \sigma_r^2 & 0 \\ 0 & \sigma_r^2 \end{bmatrix}, \quad (1)$$

where $\sigma_r^2 = c^2/2$ is the power of the reference signal. If the power of jamming signal is σ_j^2 then its auto correlation vector,

$$\mathbf{R}_{\mathbf{j}} = \begin{bmatrix} \sigma_j^2 & 0 \\ 0 & \sigma_j^2 \end{bmatrix}. \quad (2)$$

If the power of the noise is σ_n^2, then its autocorrelation vector is

$$\mathbf{R}_{\mathbf{n}} = \begin{bmatrix} \sigma_n^2 & 0 \\ 0 & \sigma_n^2 \end{bmatrix}. \quad (3)$$

The combined autocorrelation vector is then written as

$$\mathbf{R} = \begin{bmatrix} \sigma_r^2+\sigma_j^2+\sigma_n^2 & 0 \\ 0 & \sigma_r^2+\sigma_j^2+\sigma_n^2 \end{bmatrix}. \quad (4)$$

The cross-correlation vector of reference signal,

$$\mathbf{P}_{\mathbf{r}} = E[d_k X_k]$$

$$= E\left\{c\cos k\omega_0 \begin{bmatrix} c\cos(k\omega_0+\delta_0) \\ c\sin(k\omega_0+\delta_0) \end{bmatrix}\right\}$$

$$= \begin{bmatrix} \sigma_r^2\cos\delta_0 \\ \sigma_r^2\sin\delta_0 \end{bmatrix}. \quad (5)$$

The cross correlation of the jamming signal is

$$\mathbf{P}_{\mathbf{j}} = E[d_k X_k] = E\left\{c\cos k\omega_0 \begin{bmatrix} c\cos(k\omega_0+0) \\ c\sin(k\omega_0+0) \end{bmatrix}\right\}$$

$$= E\begin{bmatrix} c^2/2 \\ 0 \end{bmatrix} = \begin{bmatrix} \sigma_j^2 \\ 0 \end{bmatrix}. \quad (6)$$

If the noise is uncorrelated with d_k then its cross-correlation vector is

$$\mathbf{P_n} = \begin{bmatrix} 0 & 0 \\ 0 & 0 \end{bmatrix}. \quad (7)$$

Thus the combined cross-correlation vector can be written as

$$\mathbf{P} = \begin{bmatrix} \sigma_r^2 \cos\delta_0 + \sigma_j^2 \\ \sigma_r^2 \sin\delta_0 \end{bmatrix}. \quad (8)$$

From Winner filter theory, the optimum weighting vector is

$$\mathbf{W} = \mathbf{R}^{-1}\mathbf{P} = \begin{bmatrix} \dfrac{\sigma_r^2 \cos\delta_0 + \sigma_j^2}{\sigma_r^2 + \sigma_j^2 + \sigma_n^2} \\ \dfrac{\sigma_r^2 \sin\delta_0}{\sigma_r^2 + \sigma_j^2 + \sigma_n^2} \end{bmatrix}. \quad (9)$$

Therefore, the output signal is

$$\begin{aligned} \varepsilon &= d_k - \{c\cos(k\omega_0 + \delta_0) + W_2 c\sin(k\omega_0 + \delta_0)\} \\ &= (\cos k\omega_0)\{c - cW_1\cos\delta_0 - W_2\sin\delta_0\} + \\ &\quad (\sin k\omega_0)\{cW_1\sin\delta_0 - W_2\cos\delta_0\}. \end{aligned} \quad (10)$$

Let,

$1 - W_1\cos\delta_0 - W_2\sin\delta_0 = A\cos\alpha$

and

$$W_1\sin\delta_0 - W_2\cos\delta_0 = A\sin\alpha\,.$$

Thus,

$$\varepsilon = cA\cos(k\omega_0 - \alpha)\,,$$

where

$$\begin{aligned} A^2 &= (1 - W_1\cos\delta_0 - W_2\sin\delta_0)^2 + (W_1\sin\delta_0 - W_2\cos\delta_0)^2 \\ &= 1 + W_1^2 + W_2^2 - 2(W_1\cos\delta_0 + W_2\sin\delta_0)\,, \end{aligned} \quad (11)$$

which is known as array power gain. In some practical situation, multiple jammers can be present. To combat the situation, it is necessary to have more than one reference omni. Considering two spatially separated reference omnis, the primary signal is $c\cos k\omega_0$, the signal of reference-1 is $c\cos[(k + \delta_{10})\omega_0]$ and that of reference-2 is $c\cos[(k + \delta_{20})\omega_0]$.

The change in phases are $\delta'_{10} = kL_1\sin\theta_0$, $\delta_{10} = \delta'/\omega$, $\delta'_{20} = kL_2\sin\theta_0$, and $\delta_{20} = \delta'_2/\omega$, where $k = 2\pi/\lambda$ and θ_0 is the direction of arrival of signal.

The desired signal is

$$d_k = c\cos k\omega_0 + n_1 + j_1 + j_2\,. \quad (12)$$

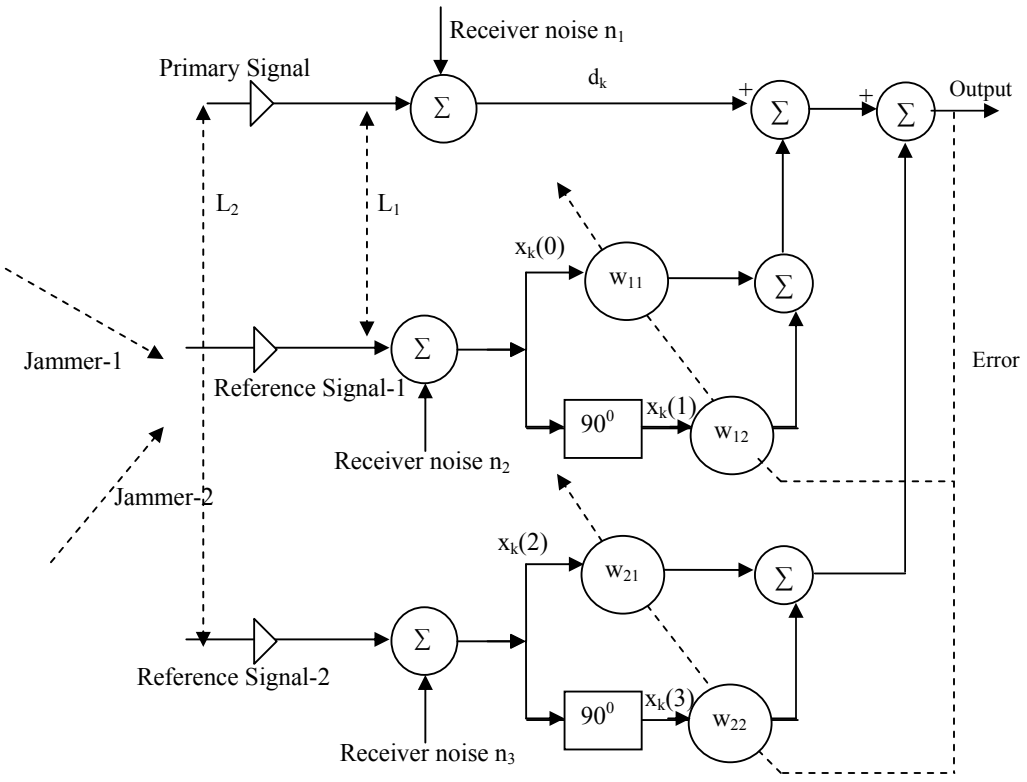

Fig. 2. Side lobe canceller with two incident signals.

The cross correlation vector is

$$\mathbf{P} = E\begin{bmatrix} d_k x_{k(0)} \\ d_k x_{k(1)} \\ d_k x_{k(2)} \\ d_k x_{k(3)} \end{bmatrix}. \quad (13)$$

Here,

$$x_{k(0)} = c\cos[(k+\delta_{10})\omega_0] + n_2 + j_1 + j_2,$$

$$x_{k(1)} = c\sin[(k+\delta_{10})\omega_0] + n_2' + j_1' + j_2',$$

$$x_{K(2)} = c\cos[(k+\delta_{20})\omega_0] + n_3 + j_1 + j_2,$$

$$x_{K(3)} = c\sin[(k+\delta_{20})\omega_0] + n_3' + j_1' + j_2'.$$

Therefore,

$$\mathbf{P} = \begin{bmatrix} \sigma_S^2\cos(\delta_{10}\omega_0) + \sigma_{J1}^2 + \sigma_{J2}^2 \\ \sigma_S^2\sin(\delta_{10}\omega_0) \\ \sigma_S^2\cos(\delta_{20}\omega_0) + \sigma_{J1}^2 + \sigma_{J2}^2 \\ \sigma_S^2\sin(\delta_{20}\omega_0) \end{bmatrix}, \quad (14)$$

where $\sigma_S^2 = c^2/2$. The autocorrelation matrix is

$$\mathbf{R} = E\left[\mathbf{X}_k \mathbf{X}_k^T\right] = \begin{bmatrix} a & 0 & b & c \\ 0 & a & d & b \\ e & d & a & c \\ c & f & 0 & a \end{bmatrix}, \quad (15)$$

where

$$a = \sigma_S^2 + \sigma_n^2 + \sigma_{j1}^2 + \sigma_{j2}^2,$$

$$b = (c^2/2)\cos(\delta_{10} - \delta_{20})\omega_0 + \sigma_{j1}^2 + \sigma_{j2}^2,$$

$$c = (c^2/2)\sin(\delta_{20} - \delta_{10})\omega_0,$$

$$d = (c^2/2)\sin(\delta_{10} - \delta_{20})\omega,$$

$$e = (c^2/2)\cos(\delta_{20} - \delta_{10})\omega_0 + \sigma_{j1}^2 + \sigma_{j2}^2,$$

$$f = (c^2/2)\cos(\delta_{20} - \delta_{10})\omega_0.$$

The optimum weighting factor can be determined from the Winner filter theory. Therefore, the output signal is

$$\begin{aligned} &= \cos k\omega_0 - w_{11}(\cos k\omega_0 \cos\delta_1\omega_0 - \sin k\omega_0 \sin\delta_1\omega_0) \\ &\quad - w_{12}(\sin k\omega_0 \cos\delta_1\omega_0 + \cos k\omega_0 \sin\delta_1\omega_0) \\ &\quad - w_{21}(\cos k\omega_0 \cos\delta_2\omega_0 - \sin k\omega_0 \sin\delta_2\omega_0) \\ &\quad - w_{22}(\sin k\omega_0 \cos\delta_2\omega_0 + \cos k\omega_0 \sin\delta_2\omega_0) \\ &= A\cos(k\omega_0 - \alpha). \end{aligned}$$

Therefore, the array gain is

$$A^2 = (1 - w_{11}\cos\delta_1\omega_0 - w_{12}\sin\delta_1\omega_0 - w_{21}\cos\delta_2\omega_0 - w_{22}\sin\delta_2\omega_0)^2 + (w_{11}\sin\delta_1\omega_0 - w_{12}\cos\delta_1\omega_0 + w_{21}\sin\delta_2\omega_0 - w_{22}\cos\delta_2\omega_0)^2. \quad (16)$$

The array gain in generalized form can be written as

$$A(\theta) = \sqrt{a+b}, \quad (17)$$

where

$$a = \left[1 - \sum_{i=0}^{m}\left[W_{i1}\cos(\beta L_1\sin\theta) + W_{i2}\sin(\beta L_1\sin\theta)\right]\right]^2,$$

and

$$b = \left[1 - \sum_{i=0}^{m}\left[W_{i1}\sin(\beta L_1\sin\theta) - W_{i2}\cos(\beta L_1\sin\theta)\right]\right]^2,$$

m is the number of elements of the beamformer, β is the phase constant, L_i is the separation of elements of beamformer and $W_{i,j}$ is the waiting factor; i= 0, 1, 2...,m; j=1 and 2.

III. RESULTS

Radiation pattern of a single reference adaptive beam former is shown in Fig. 3. Impact of weighting factors on direction of nulls are visualized from the Figs. 3(a)-3(d). When $w_1 \approx 1$ and $w_2 \approx 0$, then nulls form along 0° and 180^0. Similarly, for $w_1 \approx w_2$, nulls are along 15° and 165°; for $w_1 \approx 0$ and $w_2 \approx 1$, nulls form along 30° and 150°.

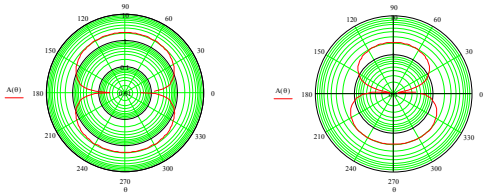

(a) w_1= 0.96 and w_2=0.003 (b) w_1=0.99 and w_2=0.5

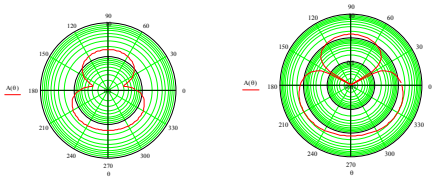

(c) w_1=0.5 and w_2=0.5 (d) w_1=0.0005 and w_2=0.99

Fig. 3. Radiation Pattern of single reference antenna system.

Only two nulls are found from single reference antenna case. Let us now consider the case of two reference an-

tennas of Fig. 2. Radiation pattern of two reference adaptive beamforming is shown in Fig. 4. When $w_{11} = -0.48, w_{12} = -0.87, w_{21} = 1.7, w_{22} = 1$, the null forms along $30°$, $150°$, $60°$ and $120°$ shown in Fig. 4(a). When $w_{11} \approx w_{12} \approx w_{21} \approx -w_{22}$, the nulls form only along $0°$ and $180°$. But if $w_{11} = 0.25$, $w_{12} = 0.5$, $w_{21} = -0.15$, $w_{22} = -0.5$, the nulls form along $225°$ and $315°$ shown in Fig. 4 (b).

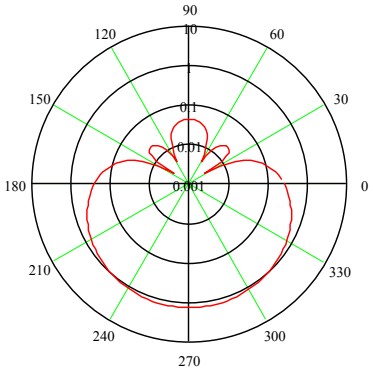

(a) (w_{11}= -0.48, w_{12}= -0.87, w_{21}=1.7, w_{22}=1)

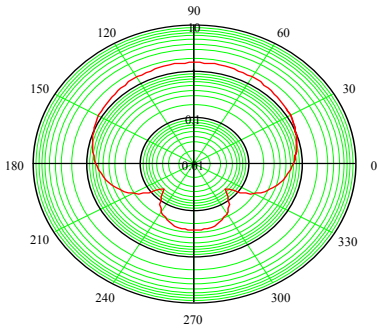

(b) (w_{11}=0.25, w_{12}=0.5, w_{21}= -0.15, w_{22}= -0.5)

Fig. 4. Radiation Pattern of two reference antenna system.

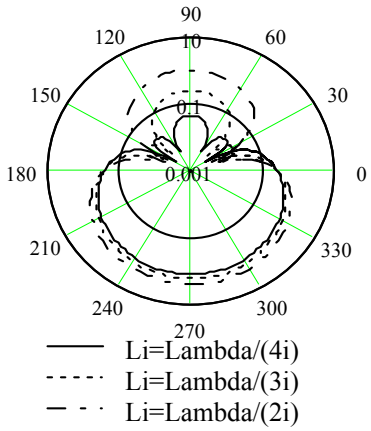

(a)

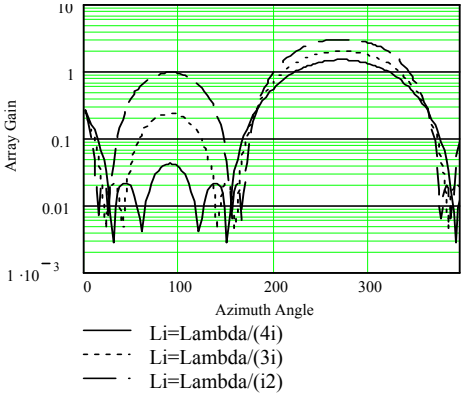

(b)

Fig. 5. The variation of antenna gain on Azimuth plane in polar and rectangular coordinate (two adaptive element beam former).

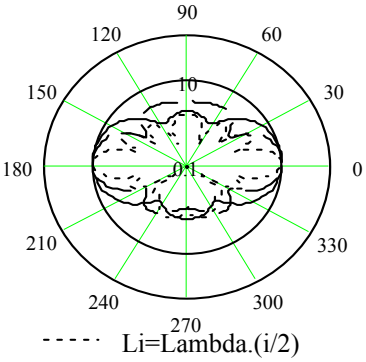

(a)

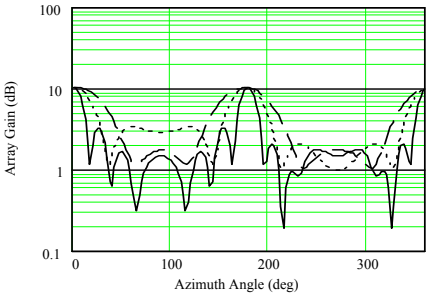

(b)

Fig. 6. The variation of antenna gain on Azimuth plane in polar and rectangular coordinate (seven adaptive element beam former).

Array gain of two element adaptive beamformer is plotted in Figs. 5(a) and 5(b) varying distance between primary and reference elements for $\lambda = 2$, $\beta = 2\pi / \lambda$, $L_i = \lambda / 4 \cdot i$, $w_{11} = -0.48$, $w_{12} = -0.87$,

$w_{21} = 1.7$, $w_{22} = 1$. It is visualized that, position of maxima remains fixed but the direction and number of jammer, i.e. the minima changes with changing the distance L_i (between primary signals and reference signals).

Finally array gain of seven element adaptive beamformer is plotted in Figs. 6(a) and 6(b) varying distance between primary and reference elements for $\lambda = 2$, $\beta = 2\pi/\lambda$, $L_i = \lambda/4 \cdot i$, $w_{11} = 0.099$, $w_{12} = -1.255$, $w_{21} = -0.266$, $w_{22} = -1.518$, $w_{31} = 0.182$, $w_{32} = -1.610$, $w_{41} = 0$, $w_{42} = -1.233$, $w_{51} = 0.182$, $w_{52} = -1.610$, $w_{61} = -0.266$, $w_{62} = -1.519$, $w_{71} = 0.099$, $w_{72} = -1.255$. It is visualized that, position of the maxima and minima and their number change with the distance L_i. In a time varying wireless channels weighting vector of the beamformer has to be adjusted using different adaptive algorithm to achieve desired signal to noise ratio (SNR) at receiving end.

IV. CONCLUSION

In this paper, multiple elements array antenna is used to control jamming signals from several directions whereas the single element antenna does the same job for two directions. The adaptive array tunes the antenna gain in such a way that the system can decrease the antenna gain on the direction of jammers and increase the gain in the direction of arrival of required signal. Increasing of antenna element will give the better performance but at the expense of mathematical complexity. Basic Wiener filter theory is applied in this research work; whereas incorporation of least mean square (LMS), recursive least square (RLS) and Kalman algorithm can also be used to observe the performance of the system.

REFERENCES

[1] S. Haykin and Michael Moher, 'Modern Wireless Communications' LPE, Pearson Education, 2005

[2] Harri Holma and Antti Toskala, 'WCDMA for UMTS,' John Wiley & Sons, 2000, pp. 31-33, pp.171-175

[3] L.C. Godara, 'Applications of antenna arrays to mobile communication, part I: Performance improvement, feasibility and system considerations,' *Proceedings of the IEEE,* vol. 85, no.7, pp. 1031-1063, July 1997

[4] C. A. Balanis, 'Antenna Theory: Analysis and Design,' 2nd ed., Wiley, New York, 1997

[5] John D. Kraus and R. J. Marhefka, 'Antennas: For All Applications,' 3rd ed., McGraw-Hill, 2001

[6] L.C. Godara, 'Application of antenna arrays to mobile communication, part II: Beamforming and direction of arrival consideration,' *Proceedings of the IEEE,* vol. 85, no.8, pp. 1195-1245, Aug. 1997

[7] Ghavami, M. and R. Kohno, Recursive Fan Filters for Broadband Partially Adaptive Antenna", IEEE Trans. Communications, pp. 185-188, Feb. 2000.

[8] Emmanuel C. Ifeachor and Barrie W. Jervis, 'Digital Signal Processing: A Practical Approach,' 2nd ed., PEARSON Education, 2004

[9] S. Haykin and T. Kailath, "Adaptive Filter Theory", 4th ed., Pearson Education, 2005.

[10] T. Do-Hong and P. Russer, "Analysis of wideband direction-of arrival estimation for closely-spaced sources in the presence of array model errors," *IEEE Microwave Wireless Components Letter.,* vol. 13, pp. 1–3, Aug. 2003

[11] S. Nowf Al Haque, M. Ariful Alam, Md. Imdadul Islam and M. R. Amin, 'Radiation pattern and beamwidth control of linear and rectangular array antenna system,' *East West University Journal,* vol. 1, pp. 119-128, 2007.

[12] M. R. A. Khandaker, Md. Imdadul Islam and M. R. Amin, 'Adaptive beamforming of linear array antenna system with provision of sidelobe cancellation,' *Proceedings of the 10th Conf. ICCIT, Dec. 27-29, Dhaka, Bangladesh,* 2007.

[13] Bernard Widrow and Samuel D. Stearns, 'Adaptive signal processing,' LPE, Pearson Education, 2005

[14] Ghavami, M. and R. Kohno, "Rectangular Arrays for Uniform Wideband Beamforming with Adjustable Structure."*Proceedings of the 3rd International Symposium on Wireless Personal Multimedia Communications,* pp. 12-15, November, 2000, Thailand

Proceedings of 12th International Conference on Computer and Information Technology (ICCIT 2009)
21-23 December, 2009, Dhaka, Bangladesh

Analysis and Design of Individual Tax Return Systems in Bangladesh

M.A. Hossain, A.A. Khan, S. Majumdar, R. Ahmed

Dept. of CSE/BUET, Dhaka, Bangladesh

dipuash@gmail.com,arif_cse_04019@yahoo.com,alok049@gmail.com,reaz@cse.buet.ac.bd

Abstract

Proper analysis and good design are essential for the successful implementation of any computer aided system. The sensitivity of the Tax return system amplifies the significance of analysis and design by many fold. Developed countries have achieved high tax return rates by introducing simple, Internet-based, computer-aided Tax return systems.

Valuable insights can be gained by analyzing the tax re- turn systems of the developed countries, which can serve as a base for designing an effective tax return system for an underdeveloped country. In this work we analyze the relative merits and demerits of individual tax return systems in United Kingdom (UK), Canada and Bangladesh. Based on this analysis we propose a design for automating individual tax return system for the National Board of Revenue, Bangladesh.

Keywords: Automated tax return, System analysis and design, Evaluation criteria

I. Introduction

The People's Republic of Bangladesh achieved political independence in 1971. Even after 38 years of independence, 15% of her national expense (as per the annual budget for fiscal year 2009) is supplemented with foreign aid. But Bangladesh's total tax revenue as a percentage of gross domestic product (GDP) is lowest (8.5%) among the seven South Asian countries; where Maldives earns highest (20.5%) and Bhutan is next to Bangladesh with 10.7%. This clearly indicates that Bangladesh Government can make more tax income than it is earning now. If they can Bangladesh will be no more an economically dependent country. To increase the Tax income of Bangladesh Government we have to facilitate the entire tax return system. Our main motivation is to design and propose a user-friendly, efficient and modern tax return system for individual tax returns.

In this work, we analyze and compare the tax return sys- tem of Bangladesh against that of two developed countries. Based on our analysis we propose a newly coined tax return system for Bangladesh. The motivation behind investigating the Tax systems in two developed countries are as follows:

1. To discern the good qualities of those systems that encourage the rate of individual tax return.
2. To infer a concise and modern individual tax return system for Bangladesh.

In this work, we have chosen two countries from two different continents: Canada from North America and UK from Europe.

In this work, our main focus is to develop a automated tax return system for Bangladesh. The number of cell phone users is very high in Bangladesh. Hence, we also focus on developing a mobile-based tax return mechanism.

II. Evaluation Criteria

In order to ensure a unified comparison, we have selected a set of evaluation criteria as outlined in this section.

A. Simplicity of Use

Filling a tax return form is not a straight forward task. It deals with sensitive financial information, complex calculations and legal interpretations. So simplicity of use is a prominent criteria of a good tax input form.

Simple Language Tax return form is used by people of different classes ranging from highly educated to ill educated. So the language of the form must be unambiguous, lucid and free of jargons as far as possible. Each field header should clearly indicate the required information in the field. It should be noted that the simplification process should not make the form unnecessarily lengthy.

Automation of Calculation A simple input system will capture only necessary (simple) data. Compound data should be calculated or derived in a manual process (for paper-based return) or automatically (for online return) without bothering the user.

Simple Layout of the Form The appearance of the forms should be designed in such a way that will encourage the user to fill it in. Some key factors for simple form layout includes: (a) spacing, (b) alignment, (c) indentation, (d) No. of lines per page, (e) appropriate highlighting using colors, bold face font etc.

B. Flow of Information

Sequencing the fields Information that are most easily answerable should get priority in ordering fields.

978-1-4244-6283-4/09/$26.00 ©2009 IEEE

Positioning of the Fields The data to be entered should be designed top-to-bottom and left-to-right.

Numbering the Fields Each field of the form should be given a number so that any reference to a field can be interpreted unambiguously.

Separation of Details For simplicity only the root entries will be placed in the main form and the details should be arranged in separate sub-forms.

C. Feedback

Some important criteria of a good feedback mechanism includes:

Frequently Asked Question(FAQ) FAQs should be selected in a scientific way that incorporates the interests of a wide variety of people. It should be updated continuously.

User Guide the user guide should contain following information:

1. Clear explanation of the field with example and different categories (mentioned in Categorical Return System).
2. Possible exceptions and clarification.
3. Warning on possible errors that may occur.

D. Categorical Return System

Tax law divides the tax payers into different categories based on their income or profit. For a sound tax law, these categories are mutually disjoint. This categorization should also be reflected on the tax return form so that a user of one category can skip those steps which are not applicable for him/her.

E. Multilingual Support

The tax return forms and user guides should be available in both state language and a second language of the relevant country.

F. Facilitating Tax Return Review

The tax return form should include some information to help the review process. There should be provision for identifying the members of the same family.

Business or job specification (Location, Rank, Organization) should be given in the form.

III. Study of the Tax Return Systems

A. Tax System in Bangladesh

The individual tax return forms and user guide for Bangladesh are available in [NBR-a 2009] and [NBR-b 2009].

A.1 Simplicity of Use

Simplicity of the individual tax return system in Bangladesh can be described by the following criteria:

Simple Language: The language of the tax return form is not simple enough. It uses difficult words in cases where easy to understand words can be used.

Automation of Calculation: There is no automated tax calculation system in Bangladesh. So a user has to perform all the complex tax calculations manually.

Simple Layout of the Form: The tax form looks simple. The form is well spaced, aligned properly and the pages are not heavily loaded with information. The words are in big font and easily readable. But there is some shortcoming such that in " Statement of Assets and Lia- bilities" portion. Though the text and the amount column are aligned but there should be line drawn to separate them.

A.2 Flow of Information

Flow of information can be described by the following criteria:

Sequencing the Fields The fields are properly sequenced. The most important field is placed before the less impor- tant ones.

Positioning the Fields The standard of positioning the fields from top-to-bottom and left-to-right is maintained in the forms. For example the first page of "IT-11GA form (entry 6 and 7)" maintains this convention.

Numbering the fields: The fields are not properly numbered in the tax form. The subtotal entries in the schedules should have the same number as the root entries in the form. Whereas the Schedules have completely separate numbering keeping no relation with the main form. Moreover "Salary Income" schedule (Schedule 1) has no numbering at all.

Separation of Details: Though Salary income, Income from house property, Tax rebate fields have detail in Schedule 1, Schedule 2 and Schedule 3, respectively; some other fields are worthy of having detail schedules.

A.3 Feedback

The feedback mechanism can be described by following criteria:

Frequently Asked Question (FAQ) The guide answers some frequently asked questions. Moreover there exists a lot of other questions frequently raised by the taxpayers which are not answered here.

User Guide The User Guide is very helpful with detail examples. The guide demonstrates calculation on almost each entry as well as complete tax return form of some professionals as examples. But the language is a bit pedantic which can be made much more simple and easier to understand. Some rules are also not clearly demonstrated.

A.4 Categorical Return System

Tax payers are divided into different categories according to their salary income but these category divisions are not stated even in the form and though stated in the guide, it is not

lucid everywhere. Such as "Tax Leviable on total Income" calculation has to be performed category wise.

A.5 Multilingual Support

There are tax return forms in both English and Bengali language but the guide is only available in Bengali.

A.6 Facilitating Tax Return Review

The TIN number of one's spouse is asked (if his/her spouse is an assessee), thus facilitating the review process of the return to trap any inconsistency in the given Statement. The form should also ask the TIN number of the other family members, business or job specification (location, rank, organization) to detect any inconsistency with the people of same category.

A.7 Workflow

The individual tax return process in Bangladesh can be presented as follows (see Figure 2).

Figure 2: Present workflow of tax return system in Bangladesh

1. Tax Payer collects the necessary tax return forms and guide from NBR office or download it from NBR website.
2. Employer Organization supplies the Tax Payer documents regarding Tax Paid at Source, Salary Breakdown, Pension Plan, etc., along with his/her salary that aids him to determine his/her tax.
3. Tax payer submits his/her tax return in paper form. NBR acknowledges receiving the return by giving a Tax Return receipt.
4. NBR sends Occasional Audits to organizations to check any anomaly.

B. Tax Return System in UK

The individual tax return forms and user guide for UK are available in [UK-a 2009] and [UK-b 2009].

B.1 Simplicity of Use

UK tax return system is very lucid and easy for the taxpayers. The simplicity of UK tax return system can be described by following criteria:

Simple Language Tax return forms use simple language and describe issues that may be critical for a taxpayer. Examples are provided for the complex issues.

Automation of Calculation In tax return form simple data is listed first and then the compound data. For paper- based tax return, compound data are calculated using a well-directed process from the simple data elements. For online tax return, compound data are auto-calculated.

Simple Layout of the Form In tax return form different parts of tax return is placed in different sections. All the necessary data are placed and calculated in different sections based on their relevance and the main form references these sections as needed. Data inputs are mainly taken in boxed format and alignment of the box is so well directed that a tax payer may not be misguided.

B.2 Flow of information

Flow of information in the UK tax return system can be described as follows:

Sequencing the Fields Every field in the tax return form is well sequenced and a user don't have to look beyond the present field for filling the field. Most priority field and fields that will be referenced later are placed in the reference order.

Numbering the Fields All the fields are numbered and a section based system is adopted. Each section has an integer number and the fields in its subsection is numbered in a hierarchical order of this integer number.

Positioning the Fields Fields are positioned on sequential way. Flow of necessary data can easily be identified by the field position within the form.

Separation of Details For detailed calculation of a field involving many subfields is placed in a separate form, called schedule.

B.3 Feedback

The feedback mechanisms of UK tax return system are described below:

Frequently Asked Question (FAQ) The UK tax return system has separate FAQ section in the user guide. Separate FAQ pages are available for online users. Moreover, the on- line tax system provides facility for submission of tax related questions to a tax expert.

User Guide UK tax return guide has step-by-step instructions to help a user to fill the tax return form. The notes in the guide are numbered to match the boxes of tax return form. For filling supplementary pages and schedules necessary instructions are also provided in the guide.

B.4 Categorical Return System

UK tax return system supports categorical return for different classes of occupation. Different schedules are made for different

occupation categories of the taxpayers and there is no bulk overhead for a user to see the pages that is not relevant for him/her. The schedule names are also self-explanatory.

B.5 Multilingual Support

UK tax return system supports no multilingual facility. There is no option for choosing the language and the forms are available only in English.

B.6 Facilitating Tax Return Review

UK tax return system collects information about the family members of a taxpayer and calculate tax by balancing tax return of all members in a family. They do not support location based tax return but organization based tax return is supported.

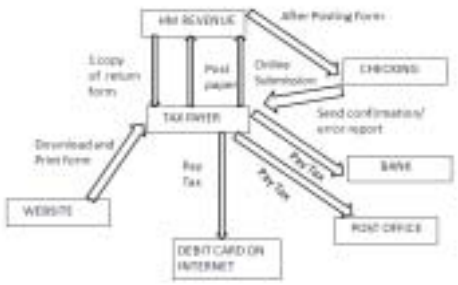

Figure 3: Workflow of Tax Return System in UK

B.7 Workflow

The conceptual workflow of individual tax return system UK is depicted in Figure 3 and described below:

1. HM Revenue sends a tax return package to the taxpayers. Optionally a taxpayer can download it from the website.
2. When one has completed his/her tax return, HM Revenue processes it by using filled figures to work out how much one owe and how much they owe to one. If any mistake is detected, HM Revenue points it out and re- quests the involved person to correct it.
3. One copy of the total tax calculation will be send to the person for further satisfaction. Then they will send a tax statement to tell him how to pay any due amount.
4. A taxpayer can pay his/her tax to bank, post office or online by debit card. Finally, enquiries are made to justify the information that was provided by the taxpayer.

C. Tax Return System In Canada

The individual tax return forms and user guide for Canada are available online at [CRA-a 2009] and [CRA-b 2009].

C.1 Simplicity of Use

Canada tax return forms and user guide are simple. But there is a scope of making it more user friendly as discussed below.

Simple Language The language of the forms is simple, short and easy to understand. Every complex topic is explained in the user guide with proper reference. In the user guide these topics are explained in details but in lucid language.

Automation of Calculation There are many offline and on- line software to prepare tax return in Canada. In both online and offline form, fillable schedules and payslips are provided. It is not required for a user to fill in those information which can be calculated automatically. Fields that are present multiple times in different forms are entered once and filled au- tomatically in other places. For example, Schedules are au- tomatically filled from the data given in the payslips.

Simple Layout of the Form The appearance of the forms are not that much impressive. It looks little bit clumsy, complicated. The good thing is that the entries are easily distinguishable from other texts. Entries are properly high- lighted.

C.2 Flow of Information

Sequencing the fields Fields are well-sequenced and free of any forward referencing where some fields require information from other forms.

Numbering of the Fields Each entry is given a 3 digit unique number.1st digit denotes the form number.

Positioning of the Fields Field layout is top to bottom and alternative ways are placed column wise.

Separation of Details Detail information are obtained and detail calculations are performed in separate schedule and forms.

C.3 Feedback

Frequently Asked Question (FAQ) Website of CRA answers frequently asked questions, moreover there are online interactive help, telephone help and tax clinic.

User Guide User guide is well written containing explanations of each entry and calculations exemplified. Clear directions are there to determine ones applicable category.

C.4 Categorical Return System

Different types of categories are demonstrated clearly to explain which entry is applicable for whom.

C.5 Multilingual Support

Everything is available both in French and English.

.

C.6 Facilitating Tax Return Review

Everyone has to enter SIN (Social insurance number) of his/her spouse in the main form.

C.7 Workflow

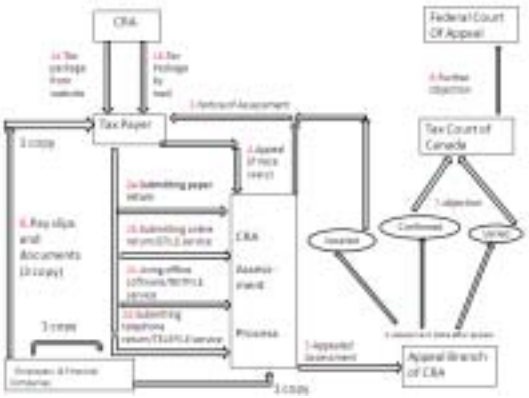

Figure 4: Workflow of Tax Return System in Canada

The conceptual workflow of individual tax return system Canada is depicted in Figure 4 and described below:

1. a) CRA sends a "tax package" to potential tax pay- ers. The "tax package" includes guides, forms, leaflets, booklets and all other publication needed to file one's tax return by mail. b) Alternatively, a user can down- load these from the Internet.

2. A taxpayer can file his return by various ways: a) Sub- mitting the hard copy sent to him by mail. b) EFILE service provider may complete and file one's return on- line. c) NETFILE service provides the flexibility to file one's return using offline software. d) TELEFILE ser- vice enables submitting return over telephone through toll free telephone number.

3. Taxpayers assess their tax liability by filing a return with the CRA by the required filing deadline. CRA will then assess the return based on the return filed and on information it has obtained from financial institutes, correcting it for obvious errors. Then it will send a "Notice of Assessment" to the taxpayer.

4. A taxpayer who disagrees with CRA's assessment of a particular return may appeal for reassessment.

5. The objection is then reviewed by the appeals branch of CRA.

6. An appealed assessment may either be confirmed, va- cated or varied by the CRA.

7. If the assessment is confirmed or varied, the taxpayer may appeal the decision to the Tax Court of Canada. If there is further objection, one can go to the Federal Court of Appeal.

IV. A Comparative Study

Table 1: A comparison of Individual Tax Return System in Bangladesh, UK and Canada

Criteria	Bangladesh	UK	Canada
Simplicity of Use	Language of the form is not easy to un- derstand, no directions for complex calcu- lations, layout is simple.	Complex sentences are avoided, step-by-step direction for complex cal- culations, well formatted layout.	Language of the form is short and simple. Well-directed forms and auto- mated software. Forms are little bit clumsy.
Flow of In- formation	No proper sequence of numbering, uncontrolled positioning of fields.	Proper hi- erarchical numbering, perfect posi- tioning of the fields.	Simple, well sequenced and flat numbering. Details are well- separated from summary.
Feedback	Insufficient FAQ sec- tion in the user guide and the user guide contains inadequate descriptions of the fields.	FAQ is avail- able and user guide gives step-by-step direction to fill the form.	Detailed FAQ and helpdesk in various forms are available and user guide has elaboration of each entry.
Categorical Return System	Described in the guide but no provision in return form.	Different schedules are available for different cat- egories of tax payer.	Different cate- gorical entries are integrated in one tax package.
Multilingual Support	Bengali and partially English.	English only.	English and French.
Facilitating Tax Re- turn Review	No inherent cross checking mechanism.	Cross checking information is collected along with the re- turn.	Cross checking information is collected along with the return.

V. Proposed Tax System for NBR

A. Workflow

To improve the tax return system in Bangladesh we have designed a workflow as depicted in Figure 5:

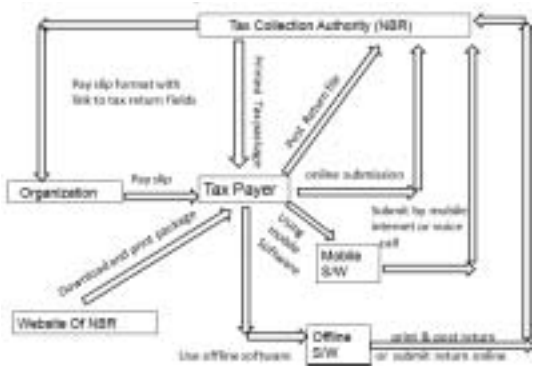

Figure 5: Proposed Workflow for Tax Return System In Bangladesh

1. NBR will send "tax package" to potential tax payers. payers may also download it from the NBR website.

NBR will also set standard formats for pay slips and different types of transactions and will send those formats to concern bodies.

2. Taxpayers will get pay slips from the other party of any transaction he takes part on which tax is applicable.
3. A taxpayer will submit his/her return file in any of the following ways a) via mail. b) online on NBR's website. c) Offline software can be used d) Mobile software can be introduced to submit return tax by mobile Phone.
4. Tax payer can pay his/her due tax in any of these ways: a) In cash/cheque or by any other regular payment system. b) Using e-banking system. c) Payment through mobile, in which case the mobile phone operator will provide a server for balance transfer from user to NBR account.

B. Schedules

Based on our study of the tax return system of Canada and UK, we have redesigned some of the existing schedules and have created some new schedules. In this section we focus one of them.

For different income categories of tax return in Bangladesh. A portion of the redesigned schedule is given below. As can be seen from Figure 6, the calculation of "Tax Leviable on Total Income" can be done as follows. A taxpayer has to first identify the category to which he/she falls among the five available categories depicted in five columns. Then he/she has to follow the steps to calculate applicable tax on total income. The proposed schedule makes the tax calculation easier in following ways:

• He/she can easily determine the category.

• User do not need to partition the income into different slabs and apply different tax rates on them. It is incorporated as a fixed amount (line F).

• Calculation of the percentiles are done (line D).

Figure 6: Schedule for Salary Income

C. Consistency Check

NBR should make a detail consistency check on the submitted returns of the taxpayers. By asking some more information than current form and utilizing those efficiently, NBR can implement a smart consistency checking mechanism. Consistency checking can be performed on different types of information such as: Professional income, Business Income, Assets and liabilities, Salary Income.

Different data items that should be asked in each category and the use of each data item is presented in Table 2

Table 2: Comparison table for checking inputs

Comparison Type	Data for Comparability Check	Data for Inconsistency Check
Professional Income Comparison	Academic/ Professional degree Organization Name Rank Practice Location	Professional Income
Business Income Comparison	Business Type Business Location Business Parameters	Business Income
Assets and Liabilities Comparison	Declaration of Shared Properties, Identity of Shareholders (TIN No)	Statement of Asset and Liabilities, Distribution of Shares
Salary Income Comparison	Name of the organization Rank Job Location	Salary Income

D. Automation

Based on the aforementioned analysis we have designed offline software and online portal that can be used by the taxpayers to file their tax return. For the web portal we have used APS.NET framework.

VI. Conclusion

After studying the tax system of Bangladesh we have got a feeling that the system itself is rather intimidating for even an educated taxpayer. Moreover there are many loopholes that can be exploited to evade tax returns. Our study of Canada and UK tax return system reveals that those systems are much more encouraging and user-friendly for the citizens. It is indisputable that there exist many scopes of development of the tax collection framework of Bangladesh. We believe that re- forming and automating the whole tax return system should get topmost priority among the other steps to increase revenue income of the new, envisioned Digital Bangladesh.

References

CRA-a, 2009. Official website of Canada revenue agency. online at: http://www.cra.gc.ca/.

CRA-b, 2009. Canada revenue agency general income tax and benefit guide-2007 available at: http://www.cra.c.ca/forms/.

NBR-a, 2009. Website of national revenue board, Bangladesh online at: http://www.nbr-bd.org/.

NBR-b, 2009. National revenue board, Bangladesh guide- lines to fill up the return form for individual tax payer available at http://www.nbr-bd.org/publication.html.

UK-a, 2009. Official website of HM revenue and customs. online at: http://www.hmrc.gov.uk/.

UK-b, 2009. HM revenue and customs, UK tax return guide available at: http://www.hmrc.gov.uk/.

Proceedings of 2009 12th International Conference on Computer and Information Technology (ICCIT 2009)
21-23 December, 2009, Dhaka, Bangladesh

Bangla Keyboard Layout Design Using Frequency and Association Among Bangla Characters *(Not Presented)*

Krishna Chnadra Bhadra, Chowdhury Mofizur Rahman
Dept. of Computer Science and Engineering, United International University, Dhaka, Bangladesh
krishna_bhadra@yahoo.com, cmr@uiu.ac.bd

Abstract

In this paper, we present a new design of a scientific and efficient Bangla keyboard for convenient typing. The design methodology takes into account frequency of Bangla characters, association among the characters after analyzing 17640 Bangla words from a Bangla dictionary, distribution of workloads on the fingers and strength and ease of movement among the fingers. We describe the ergonomic criterion we have used to evaluate and compare keyboards. This criterion is in terms of the distribution of the typing efforts among the ten fingers as well as increase in typing speed, ease of learning, accessibility of commonly used keys and various other factors. Measured against this criterion, our keyboard performs better than the 10 traditional keyboard layouts available in the market.

Keywords: monograph, digraph, trigraph, association rule, data mining, hand switching, support, confidence, frequent itemsets.

I. INTRODUCTION

Text entry is recognized as one of the most frequent human computer interaction. For that reason the keyboard remains the most popular text input device for computer application. The layout of the various characters on a keyboard has profound impact on the efficiency of a typist. If frequently occurring characters are not easily accessible, the rate of typing will go down. An ill-designed keyboard might place an excessively high load on the weaker fingers of the hand, leading to typing fatigue (even musculoskeletal injuries in the long term). One of the biggest problems is that we are not getting optimum speed in Bangla typing due to absence of standard Bangla Key board layout. But there is no scientific Bangla keyboard layout at present and very few research works have been done in this field. There are more than 10 keyboard layouts available in market, but a few are in use. Although Bangladesh Computer Council has developed a standard keyboard layout but it is not very popular. Hence it is important while designing a keyboard that a significant amount of thought be devoted to determine the most optimal arrangement of characters.

For English and other European language keyboards, considerable research has gone into finding an appropriate arrangement of characters. The standard keyboard is the QWERTY keyboard that everyone is familiar with. Also there is the Dvorak keyboard which was proposed in the 1920's and 30's by August Dvorak and William Dealey. This keyboard was a result of significant ergonomic research and is known to outperform the standard QWERTY keyboard on many factors (home row usage, for example).

There is a Bangla keyboard [8] using association rule which was proposed in 2004 by Hijbul Alam et. al. where only a subset of features were considered to design the keyboard layout. In this paper we have tried to design a Bangla keyboard layout considering frequency and association among Bangla characters by using the association rule of data mining as well as considering the Bangla Grammar consonant rules of alpo- pran and moha-pran combination. In addition distribution of workloads on the fingers and strength and ease of movement among the fingers also have been considered in our design. We have used the Bangla dictionary from Bangla Academy titled "Shahaj Bangla Obidhan" and we have used the association rule mining technique to extract the association between Bangla letters. The aims of keyboard design are:

- Easy to learn and easy to use
- To increase typing speed.
- To be more scientific and efficient than traditional keyboard layout available in the market.
- To make the design international standard like English and acceptable to all users.
- To find a keyboard arrangement that is better than the current traditional Bangla keyboard in terms of typing convenience and efficiency with equal hands' load and maximum hand switching.

II. ASSOCIATION RULE MINING

Association rule mining finds interesting association or correlation relationships, frequent patterns, causal structures among a large set of transaction databases, relational databases, and other information repositories. The discovery of interesting association relationships among huge amounts of transaction records can help in many decision-making processes. The application of association rule are Basket data analysis, cross-marketing, catalog design, loss-leader analysis, clustering, classification etc. Let $\mathbf{J} = \{i_1, i_2, \ldots, i_m\}$ be a set of items and $\mathbf{D} =$

978-1-4244-6283-4/09/$26.00 ©2009 IEEE

Set of database transactions where each transaction T is a set of items such that T ⊆J. **A, B** = Set of items. A transaction T is said to contain A if and only if A ⊆T. An association rule is an implication of the form A ⊆B, where A ⊆J, B ⊆J, and A ⊆B = ⊆The rule A ⊆B holds in the transaction set D with support *S*, where *S* is the percentage of transaction in D that contain A ⊆B, i.e., Support (A ⊆B) = P (A ⊆B). The rule A ⊆B has confidence *C* in the transaction set D if *C* is the percentage of transaction in D containing A that also contain B, i.e., confidence (A ⊆B) = P (B□A) = [support count(A ⊆B) / support count(A)][1,2,5]. Threshold values for minimum support and confidence are usually given to mine only interesting association rules.

The Apriori Algorithm is an influential algorithm for mining frequent itemsets and association rules from transaction databases. The Apriori Algorithm iteratively finds the frequent itemsets with cardinality from 1 to k (k-itemset) and uses these frequent itemsets to generate association rules. Apriori algorithm uses a *Level-wise* search, where *k-itemsets* (An itemset that contains *k* items is a *k-itemset*) are used to explore (*k*+1)-itemsets. At first the set of frequent 1-itemset is found. This set is denoted L1. L1 is used to find L2, the set of frequent 2-itemsets, which is used to fine L3, and so on, until no more frequent *k*-itemsets can be found. From the found frequent itemsets, association rules satisfying minimum support and confidence thresholds are extracted. In our keyboard design we have used Apriori Algorithm to find out association among Bangla characters.

III. HISTORY OF KEYBOARD LAYOUT

I. English Keyboard

For English keyboards, there are two types one is "QWERTY" and other is "DVORAK".

A. QWERTY:

- Today's computer keyboard layout is called "QWERTY" keyboard layout because the first six key on the top row of letters spell "QWERTY".
- QWERTY keyboard was designed in the 1860s by Christopher Sholes for mechanical typewriter and was actually designed so that successive keystrokes would alternate between sides of the keyboard so as to avoid jams [3].

B. DVORAK:

- It was designated as an alternate standard keyboard layout by the American National Standards Institute (ANSI) in 1930
- Dr. August Dvorak patented the keyboard layout in 1936
- The Dvorak layout was designed to address the problem of inefficiency and fatigue which characterized the "QWERTY" keyboard layout [4].

II. Bangla Keyboard

A. Munir keyboard Layout: In 1987 an engineer named Mainul Islam deserved the claim of this success but the original keyboard layout is taken from Bangla Typewriter layout which is designed by Shahid Munir Chowdhury. This key Board uses Numeric key pads also for Bangla character.

B. Bijoy Layout: In 1988 Mustafa Jabar of Anando Computers developed this keyboard. It is most widely used keyboard Layout in Bangladesh.

C. Microsoft key board Layout: This layout is used in India. Microsoft included Bangla support in Window XP service pack 2 by including Indica script and including a Bangla keyboard layout for Bangla typing. This layout has some shortcut of complex letters/combinations (Yuktakkhors). But this is not used in Bangladesh.

D. Bangladesh National Keyboard Layout: Bangladesh Computer Council designed a National Key Board layout through a private IT firm "Information Engineer and Consultant BD Ltd". This is same as Bijoy keyboard except two characters change position.

E. Few Key board Layout from research works:

E.1. Md. Hanif Seddique[7] Keyboard Layout: They have proposed three key board layout based on character frequency ,digraph and trigraph. They claim layout 3 is computer generated: maximum hand switching and balancing left and right load.

E.2. Md. Hijbul Alam[8] Keyboard Layout: They have proposed a keyboard layout based on Association rule of Data Mining which they claim Optimal bangle keyboard layout

E.3. Md. Abdus Sattar[9] Keyboard Layout: They have proposed a keyboard layout based on character and fingering frequency.

IV. PROPOSED WORKING PROCEDURE

To find frequency and association among bangle characters we need to collect a corpus of Bangla words. For that reason we selecte a Bangla dictionary from Bangla Academy titled "Shahaj Bangla Obidhan" and from it we take 17640 words. Then for converting character into numbers we assigned each character a unique code number which is shown in Table I.

Table I Bangla characters with assigned codes

21	22	23	24	25	26	27	28	29	30	31	32
A	B	C	D	E	S	G	H	I	J	K	L
65	**66**	**67**	**68**	**69**	**70**	**71**	**72**	**73**	**74**	**75**	**76**
33	34	35	36	37	38	39	40	41	42	43	44
M	N	O	P	Q	R	S	T	U	V	W	X
77	**78**	**79**	**80**	**81**	**82**	**83**	**84**	**85**	**86**	**87**	**88**
45	46	47	48	49	50	51	52	53	54	55	56
Y	Z	_	`	a	B	c	d	e	f	g	h
89	**90**	**95**	**96**	**97**	**98**	**99**	**100**	**101**	**102**	**103**	**104**
57	58	59	60	61	62	63	64	65	66	67	68
i	j	k	l	m	N	o	p	q	r	s	t
105	**106**	**107**	**108**	**109**	**110**	**111**	**112**	**113**	**114**	**115**	**116**
69	70	71	72	73	74	75	76	77	78	79	80
	v	w	x					‡	‰	Š	¨
117	**118**	**119**	**120**	**121**	**126**	**132**	**169**	**135**	**137**	**138**	**168**
81	82										
170	**20**										

By using minimum support count .001 (17 % with respect to 17640) in Apriori algorithm implementation [6] we find the frequent 1 itemsets in Table II. To design our layout we use up to 5 frequent itemsets. Table III, IV and V show some of the frequent 2, 3 and 4 itemsets and corresponding association among the characters .Table VI shows frequent 5 characters and association among them.

Table II Frequent 1 Itemsets

Code of char.	Char	Occur-rences	Code of char.	Char	Occurrences
70	v	11063	45	Y	977
71	w	6049	32	L	665
50	b	4965	63	o	660
46	Z	4506	69		602
31	K	4257	24	D	533
77	‡	4243	47	_	528
57	i	4187	52	d	510
53	e	4014	22	B	459
55	g	3748	74		446
61	m	3441	37	Q	416
58	j	3230	56	h	410
51	c	2879	35	O	406
73		2642	43	W	387
48	R	2534	67	s	368
21	A	2127	75		357
59	k	1754	34	N	308
33	M	1754	42	V	285
38	R	1716	40	T	258
72	x	1662	29	I	213
62	n	1566	79	Š	204
65	q	1419	27	G	195
36	P	1388	66	r	181
41	U	1290	78	‰	158
76		1286	39	S	138
81		1283	68	t	70
80	¨	1228	82		54
60	I	1183	44	X	51
54	f	1125	64	p	21
49	a	1061			

Table III Frequent 2 Itemsets and corresponding associations using character codes

Char 1		char 2	Confidence	Occurrences
31	==>	46	0.248532	1058
46	==>	31	0.234798	1058
31	==>	50	0.214705	914
31	==>	71	0.382664	1629
71	==>	31	0.269301	1629
31	==>	70	0.638243	2717
70	==>	31	0.245593	2717
46	==>	50	0.263205	1186

Table IV Frequent 3 Itemsets and corresponding associations using character codes

Char 1	Char 2		Char 3	Confidence	Occurrences
31	50	==>	46	0.21663	198
31	46	==>	71	0.516068	546
31	71	==>	46	0.335175	546
46	71	==>	31	0.264663	546
31	46	==>	70	0.612476	648
31	70	==>	46	0.238498	648
46	70	==>	31	0.244436	648
31	50	==>	71	0.449672	411
31	71	==>	50	0.252302	411

Table V Frequent 4 Itemsets and corresponding associations using character codes

Char 1	Char 2	Char 3		Char 4	Confidences	Occurrences
31	46	50	==>	71	0.5	99
31	50	71	==>	46	0.240876	99
31	46	50	==>	70	0.681818	135
31	46	70	==>	50	0.208333	135
31	50	70	==>	46	0.213608	135
31	71	70	==>	46	0.311292	306
46	71	70	==>	31	0.289225	306
31	71	70	==>	50	0.278739	274
50	71	70	==>	31	0.253001	274
46	71	70	==>	50	0.273157	289

Table VI Frequent 5 characters and corresponding associations showing individual characters

Char1	Char 2	Char 3	Char 4		Char 5	Confidence	Occurrences
i	‡	K	b	==>	৷	0.884615	46
j	‡	K	b	==>	৷	0.882353	45
j	‡	K	Z	==>	৷	0.843137	43
m	g	Z	b	==>	৷	0.807692	42
m	e	Z	b	==>	৷	0.724138	42
j	‡	K	॥	==>	৷	0.693333	52
I	K	॥	৷	==>	Z	0.37931	44
	Z	॥	৷	==>	b	0.361702	51
`	Z	॥	৷	==>	e	0.347107	42
`	b	॥	৷	==>	e	0.338462	66
m	Z	॥	৷	==>	K	0.336134	80
	Z	॥	৷	==>	c	0.326241	46
c	i	॥	৷	==>	Z	0.318182	56
m	b	॥	৷	==>	Z	0.312169	59
e	‡	৷	৷	==>	Z	0.309524	52
A	Z	৷	৷	==>	b	0.304878	50
i	Z	৷	৷	==>	K	0.304167	73
m	b	৷	৷	==>	e	0.301587	57
g	Z	৷	৷	==>	b	0.300885	68
i	b	৷	৷	==>	K	0.299595	74
`	e	b	৷	==>	‡	0.29927	41
c	b	॥	৷	==>	Z	0.298507	40
m	g	Z	৷	==>	b	0.295775	42
‡	K	॥	৷	==>	j	0.295455	52
A	Z	b	৷	==>	g	0.294964	41
c	K	॥	৷	==>	Z	0.291391	44
e	Z	॥	৷	==>	K	0.288321	79

To design an optimal Bangla key board layout following things were kept in mind.

- It is more difficult to type entire word with one hand. Typing is split more equally between hands.
- For maximum speed and efficiency, the most common letter/character should be in the home row where the fingers rest and least common letters should be on the bottom row which is the hardest to reach
- Minimal use should be made of the ring and little finger. Little finger is least dexterous especially when pressing keys outside home row
- The key board should contain only primary characters, with the help of primary key all composite characters can be formed.
- Most frequent and associated characters are in normal state and less frequent ones are in shift state for faster and efficient typing.
- Keyboard should be easy to learn and easy to use [10] . Characters should be arranged in such a way so that it can be easily remembered
- Keyboard should be complete ; all characters and symbol should be typeable[10]

I. Issues of designing Bangla Keyboard :

As there are 62 primary/basic characters we can not accommodate all primary characters in 26 keys. We have to use normal state, shift stare and AltGr state. The term AltGr state comes from “Alter Graphic”. The behavior of the AltGr key is always identical to pressing Control + Alt key simultaneously.

A. In Bangla there are many joined characters/ yuktakkhor. So it is not possible to design a Bangla keyboard that contains all the joined characters. Since each

joined character is made up of two or more primary/basic character it is possible to make a link between these two or more characters with the help of a character. This character is known as link character. In my proposed layout "G" is set as the link character because position of G is in the middle of the keyboard which is easily reachable by operator fingers.

- In Bangla consonants there is a division according to pronunciations, i.e., Alpo pran-Maha pran. (K-L, M-N, P-Q, R-S, U-V, W-X, Z-_, `-a, c-d, e-f, o-p). It is already used in Bijoy and BCC keyboard. We keep Alpo pran in normal state and Maha pran in shift state ; in general Maha pran characters are less frequent.
- After placing the character on to a key we try to put the characters adjacent or in shift state whose pronunciations are similar and are less frequent.
- While placing the characters we try to avoid using high frequent characters under little finger because it is harder to use in top or bottom row
- Highly frequent/associate characters will be in the same row or in adjacent positions

B. Let us first consider Table 1 (1 itemset) which contains primary/basic Bangla characters with their occurrences in all words. In this work we consider occurrences of 1itemsets as frequency of characters

C. From Table 1 we take 25 high frequency characters and put them on the 25 keys by following the above mentioned general principles. For home row consider the first 8 characters from Table 1 , their arrangement will be (left side of G: †, e , ৷ , ∨ , and right side of G : b , Z , K , i) for better hand switching, load balancing and utilization of home row advantage. Then remaining characters will be in top row and bottom row.

D. From Table 7 considering only 6th column characters we try to put all the highly associated characters, i.e, (colunm1-4 characters) in the following order by observing the following two principles:

- Only highly frequent and associated two or more characters will be adjacent and two or more characters having less association cannot change the position of high frequent /associated characters
- It two or more character are highly associated but one of the characters has lower frequency then it will be in shift position or in a bottom row.

II. Order of character position

A. If the characters are in home row then highly frequent/associated characters correspond to it will be

left or right in the same row (home row)

top row

bottom row

B. If the characters are in top row then highly frequent/associated characters correspond to it will be

left or right in the same row (top row)

home row

bottom row

C. If the characters are in bottom row then highly frequent/associated characters correspond to it will be

left or right in the same row (bottom row)

home row

top row

II. Some other issues

The numeric characters will be kept same as English keyboard. '|' will be on the shift G, in Bangla literature | is used for stop of a sentence.

'$' will be on the position of $.

"r" will be on the position of full stop (.) which is used in English literature for stop a sentence but in Bangla | is used for stop of a sentence which is already placed. Our keyboard layout is shown in the following figures 1

Fig 1a: Normal State / Position

Fig 1b: Shift State / Position

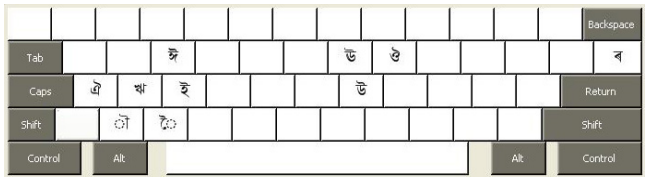

Fig 1c: AltGr Sate/ Position

V. COMPARISON WITH OTHER LAYOUTS

Munir layout is originally taken from the Bangla typewriter layout and was designed by Shahid Munir Chowdhury and later in 1987 an engineer named Manirul Islam converted it to a computer layout. Its main drawback is the use of four rows (Numeric keys) for Bangla typing. It is very hard for the operators to type specially characters which are in numeric row and it reduces typing speed.

In Bijoy layout we find more frequent characters are in the bottom row (i,b, m,g) and some frequent characters are in shift state (j, k, A). There are less frequent characters which are in home row (, ,, ,). This layout cannot utilize the home row advantage as a result typing speed of Bijoy keyboard is slow.

Microsoft layout also uses four rows (i.e., numeric keys) for typing. Frequent characters are in bottom row (g,b,e, j,m). Less frequent character are in home row (, P,U). It is very hard for the operators to type specially characters which are in numeric row and it cannot use home row advantage. Bangladesh National Keyboard layout is a minor alternation of Bijoy keyboard layout.

Seddiqui [7] Layout 3 they placed high frequency characters under little and ring finger in home row. No key allocated for four bangle character .If we want to type those character we need three key strokes. This will increase complexity and reduce typing speed. They don't present calculation procedure for hand switching.

Hijbul[8] layout where only a subset of features were considered to design the keyboard layout. high frequency characters under little and ring finger in home row.

Md. Abdus Satter[9] . To determine fingering frequency they didn't show any scientific (biological) evidence rather only depends on computer operator. As a result few home row key get low sequence number and few top row key those are under index key get low sequence number. They start from right side to find sequence number. Don't say any thing is this sequence number is applicable for left hand side people.

In our proposed layout

1. Most frequent characters are in home row and are in normal state, it increases the typing speed.
2. Characters are placed by considering the Bangla Grammar consonant rules of alpo-pran and mohapran combination.
3. Characters are placed according to their association, it also increases typing speed.
4. It is very easy to learn, easy remember and use
5. Proposed layout is optimal in the sense that it does not over look the operators' comfort.

VI. CONCLUSION

The proposed keyboard layout is developed which contain 62 primary/basic characters and all composite characters/ yuktaakhar are formed using one or more primary / basic characters. Like a standard English keyboard proposed layout use three row for character assignment. It can reduce typing time and increase speed. In designing this proposed layout we have used character frequency and association between characters. As a result more frequent and associated character is in close proximity and it will increase typing speed and efficiency. The proposed layout is designed based on Bangla phonetics. So layout is optimal on considering all the complexities of Bangla language which will hopefully help the user to speedup Bangla text processing.

REFERENCES

[1] Jiawei Han and Micheline Kamber, 2001. -*Data Mining: Concepts and Techniques*, Morgan Kaufmann Publisher: CA, 2001.

[2] R. Agrawal, Mannila, H; Srikant, R; Toivonan, H; Verkamo, A, -"Fast discovery of Association Rules", Advances in knowledge discovery and data mining, 1996.

[3] Qwerty and Dvorak keyboards - http://www.powertyping.com/dvorak/keyboard.html

[4] Dvorak Simplified Keyboard Wikipedia - http://en.wikipedia.org/wiki/Dvorak_Simplified_Keyboard

[5] S. M. Kamruzzaman and Chowdhury Mofizur Rahman - "Text Categorization using Association Rule and Naïve Bayes Classifier" *Asian Journal of Information Technology*, Vol 3, Number 9, pp-685-693, 2004.

[6] APRIORI implementation of Ferenc Bodon , version (2.4.9) March 2005 -http://www.cs.bme.hu/~bodon/en/apriori/

[7] Md. Hanif Seddiqui, Mohammad Mahadi Hassan,Md. Sazzad Hossain, Md. Nurul Islam -"An optimalKeyboard Layout"-ICCIT2002, EWU Dhaka, 2002.

[8] Md. Hijbul Alam, Abdul Kadar Muhammad Masum, Mohammad Mahadi Hassan and S M Kamruzzaman, - "Optimal Bangla Keyboard Layout using Association Rule of Data Mining," ICCIT2004, Dhaka ,2004.

[9] Md. Abdus Sattar, Al-Mukaddim Khan Pathan "DEVELOPMENT OF AN OPTIMAL BANGLA KEYBOARD LAYOUT BASED ON CHARACTER AND FINGERING FREQUENCY " - National Conference on Computer Processing of Bangla, 2004, Independent University, Bangladesh

[10] Gihan V Dias , G Balachandran " Keyboards for Indic Languages"

The 12th Annual Internationalisation and Localisation Conference organised by the Localisation Research Centre (LRC) XII, September 2007

Proceedings of 2009 12th International Conference on Computer and Information Technology (ICCIT 2009)
21-23 December, 2009, Dhaka, Bangladesh

Detection of various Denial of Service and Distributed Denial of Service Attacks using RNN Ensemble

A. B. M. Alim Al Islam, Tishna Sabrina
Department of Computer Science & Engineering, Bangladesh University of Engineering and Technology, Dhaka, Bangladesh
Department of Electrical and Electronics Engineering, Bangladesh University of Engineering and Technology, Dhaka, Bangladesh
alim_razi@cse.buet.ac.bd, tishna32@yahoo.com

Abstract

Denial-of-Service (DoS) and Distributed Denial-of-Service (DDoS) are widely known security attacks which attempt to make computer resources unavailable to its intended users. In this paper, I discuss some well known DoS and DDoS attacks. Experience shows that in the detection of these attacks human brain is more perfect than mathematical computation. Therefore, I propose a technique to incorporate the representative of human brain, Recurrent Neural Networks (RNN), to identify these attacks.

Keywords: - Denial-of-Service, Distributed-Denial-of-Service, IP spoofing, Flood attack, Zombie, RNN ensemble.

I. INTRODUCTION

With the advancement of the computer networks, security threats are becoming one of the major problems that hinder the enhancement of electronic services. Network security attacks appear in different forms and modes. One of the widely known attacks is Denial-of-Service (DoS).

DoS attacks consume the resources of a remote host or network that would otherwise be used for serving legitimate users. There are two principal methods of DoS. In the first method, attacker exploits existing software flaws to cause remote servers to crash or substantially degrade in performance. Most of the attacks in this method can be prevented by either upgrading faulty software or filtering particular packet sequences. In the second method, attacker overwhelms the victim's CPU, memory, or network resources by sending large numbers of spurious requests.

The most updated version of Denial-of-Service is the Distributed-Denial-of-Service (DDoS). It uses the power of the network components to increase the threats by distributing the attacking duties among some slave machines.

Because there is no simple way to distinguish the *good* requests from the *bad*, it can be extremely difficult to defend against these attacks. Therefore, the most difficult part to avoid these threats is to correctly identify them. In this paper, I propose an artificial intelligence based approach to correctly identify these attacks after brief discussion on them.

In the next section, I discuss some of the related works. In the following two sections, I describe and classify DoS and DDoS respectively. Then I propose a detection technique for them. Finally, I conclude the paper with shedding some lights on future works.

II. RELATED WORKS

A number of research works have already been conducted on DoS and DDoS along with their detection mechanism. In [1], trends in the deployment, use, and impact of DoS attack technology based on intruder activity and attack tools are analyzed. In [2], different forms of DoS attacks are discussed. It also quantitatively analyzes the impact of DoS on internet. In [3], DoS attacks are classified based on header content, ramp-up behavior, and techniques based on spectral analysis. In [4], a network-based denial of service attack called SYN flooding is analyzed for IP (Internet Protocol) based networks. In [5], the taxonomies of DDoS attacks, related software, and available countermeasures are described. In [6], a distributed approach to defend against DDoS attacks by coordination across the Internet is proposed. In [7], a behavior-based anomaly detection method is proposed to detect network anomalies by comparing the current network traffic against a baseline distribution. In [8], a method for detection of DDoS attacks is proposed based on a statistical pre-processor and an unsupervised artificial neural net.

III. DENIAL-OF-SERVICE (DoS)

Based on volume of packets and number of attackers DoS attacks can be broadly classified into two types [3] -*software exploits* and *flooding attacks*. Figure 1 shows the classification.

Flooding attacks can be further classified into single-source and multi-sources attacks based on the number of attackers. Software Exploits utilizes specific software bugs in the target operating system or applications and can potentially disable the victim machine with a single or a few packets. A well-

978-1-4244-6283-4/09/$26.00 ©2009 IEEE

known example is the *ping of death*, which causes the operating system to crash by sending a single large ICMP echo packet. Such attacks can only be prevented by diligently applying software updates.

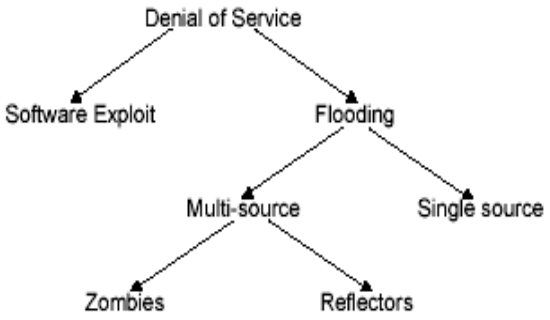

Figure 1: Classification of DoS.

Flooding attacks are the result of one or more attackers sending incessant streams of packets aimed at overwhelming link bandwidth or computing resources at the victim. Based on the location of the observation point, flooding attacks are classified as single-source attacks when a single zombie is observed to flood the victim and as multi-sources when multiple zombies are observed to flood the victim. In both cases, we may misclassify sources if our observation point misses any or some zombies. Another type of multi-sources attack is the *reflector* attack. Such attacks are used to hide the identity of the attacker and/or to amplify an attack. A reflector is any host that responds to requests, such as web servers or ftp servers that respond to TCP SYN requests with a SYN-ACK reply, or hosts that respond to ICMP echo requests with ICMP echo replies. Servers may be used as reflectors by spoofing the victim's IP address in the source field of the request, tricking the reflector into directing its response to the victim.

A. IP Spoofing

It is very common method to hide the own identification by the attacker. In IP Spoofing, the attackers take-off the source IP address field in each transmitted packet to conceal the location of the attacking host. Consequently, the packets appear to the victim to be arriving from one or more third parties rather the original attacker. Spoofing can also be used to *reflect* an attack through an innocent third party. For direct Denial-of-Service attacks, most programs select different source addresses, for each packet sent. When a spoofed packet arrives at the victim, the victim usually sends what it believes to be an appropriate response to the faked IP address.

If the attacker selects the source addresses on the fly, the victim's responses will be distributed with equal probability across the entire IP address space. This approach is called *backscatter* [2]. In Figure 2, the attacker sends a series of SYN packets towards the victim V, using a series of random spoofed source addresses named B, C, and D. After receiving these packets the victim responds by sending SYN/ACKs to each of spoofed hosts.

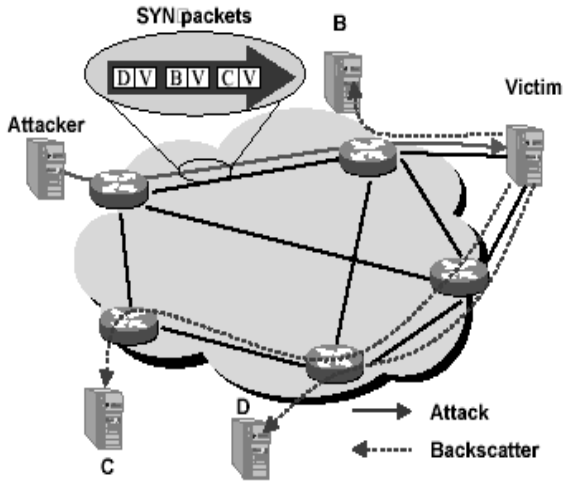

Figure 2: Backscatter

B. The SYN Flooding Attack

One of the most common DoS attacks is the SYN Flooding Attack [4]. This attack exploits the vulnerable feature of TCP protocol. TCP implementations are designed with a small limit on the maximum number of half-open connections per port that are possible at any given time. In Figure 3, an attacker 'A' initiates a SYN flooding attack by sending many connection requests with spoofed source addresses to the victim machine 'D'. As a result 'D' allocates resources. When the limit of half-open connections is reached, all successive connection establishment attempts are refused, whether they are legitimate or not. Here, neither outgoing connection attempts nor connections that are already established are affected by this attack.

This condition exists until either the timer expires, or some connections are completed or reset. If the timer expires for a particular half-open connection, the host will reset the connection and release all resources allocated for it.

On the other hand, if a spoofed SYN packet contains the source address of a reachable IP host 'S', that host (S) will receive the second message of the three-way handshake generated by 'D'. As 'S' is not expecting a SYN+ACK, it will eventually send a RST packet to 'D', and consequently cause 'D' to reset the connection. It is therefore in the interest of an attacker to forge source addresses that do not belong to hosts that are reachable from the victim 'D'.

If the attacker wants the denial of service condition to last longer than the timeout period, he needs to continuously keep requesting the victim for new connections. The amount of CPU and network bandwidth required by an attacker for a sustained attack is negligible.

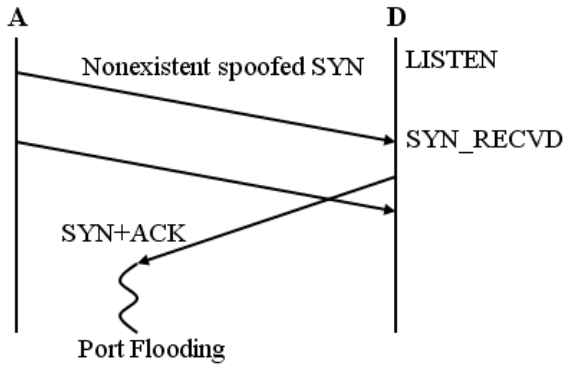

Figure 3: A system under attack

Typical SYN flooding attacks can vary several parameters –

- The number of SYN packets per source address sent in a batch (=*batch-size*),
- The delay between successive batches (=*delay*), and
- The mode of source address allocation (=*mode*).

Along with the variation of these parameters, attacker chooses different source addresses to spoof its own identity. There are three possible modes of source address allocation [4].

- In single address mode, the attacker takes as a parameter a single spoofed IP address that is used as the source address for all SYN packets. In the absence of any defense, this mode of attack is as successful as the other modes.
- In short list mode, the attacker can generate a small group of addresses to use them as source addresses to generate SYN packets.
- In no list mode, the attacker can create a different, randomly generated source IP address for each consecutive batch of SYN packets.

IV. DISTRIBUTED DENIAL-OF-SERVICE (DDoS)

It is obvious that the power of multiple attackers must be greater than the power of only one attacker. Moreover, it will be harder to detect multiple attackers than only one attacker. Therefore, the recent motivation for the attacker is to distribute the attacking power among some nodes rather confined it only to own. In distributed attack, an attacker compromises a set of Internet hosts (using manual or semi-automated methods) and installs a small attack daemon on each, producing a group of *zombie* hosts. This daemon typically contains both the code for sourcing a variety of attacks and some basic communications infrastructure to allow remote control. Using variants of this basic architecture an attacker can focus a coordinated attack from thousands of zombies towards a single victim.

There are wide varieties of DDoS attack techniques. Figure 4 shows the classification of DDoS. There are two main classes of DDoS attacks [5]: *bandwidth depletion* and *resource depletion* attacks.

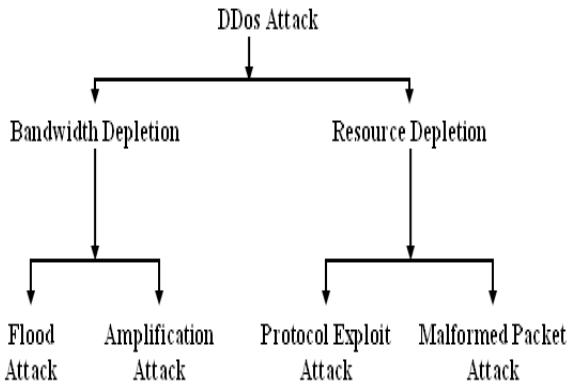

Figure 4: Classification of DDoS attacks

In bandwidth depletion attack, the attacker floods the victim network with unwanted traffic that prevents legitimate traffic from reaching the (primary) victim system. There are two main classes of DDoS bandwidth depletion attacks – flood attack and amplification attack. In flood attack, all zombies send large volumes of traffic to a victim system, to congest the victim system's bandwidth. In amplification attack, either the attacker or the zombies broadcast messages with spoofed IP address. In the response of this message, all systems in the subnet replies to the victim system. This method amplifies malicious traffic that reduces the victim system's bandwidth. For this type of DDoS attack, the attacker can send the broadcast message directly, or the attacker can use some agents to send the broadcast message to increase the volume of attacking traffic. Figure 5 shows this attack.

In resource depletion attack, attacker ties up the resources of a victim system. This type of attack targets a server or process on the victim system making it unable to process legitimate requests for service. There are two types of DDoS resource depletion attack - protocol exploit attacks and malformed packet attacks. Protocol exploit attacks utilize the vulnerable portions of a protocol. In malformed packet attack, attacker instructs the zombies to send incorrectly formed IP packets to the victim system in order to crash the victim system. There are two types of malformed packet attacks. In an IP address attack, the packet contains the same

source and destination IP addresses. This can confuse the operating system of the victim system and cause the victim system to crash. In an IP packet options attack, a malformed packet may randomize the optional fields within an IP packet and set all quality of service bits to one so that the victim system must use additional processing time to analyze the traffic. If this attack is multiplied using enough agents, it can shut down the processing ability of the victim system.

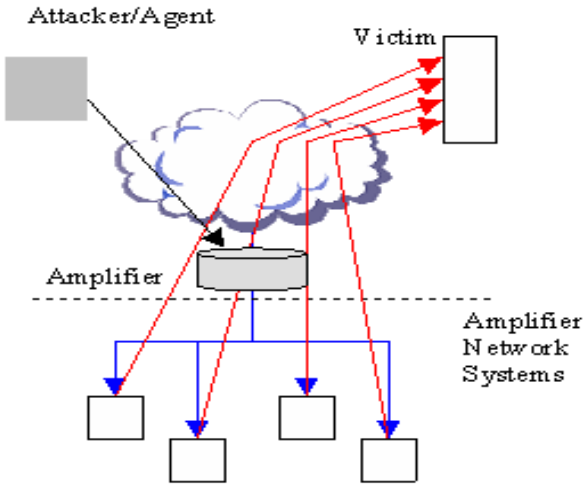

Figure 5: Amplification Attack

V. DETECTION MECHANISM

There are several features of DoS and DDoS attacks that hamper their successful detection and defense [6]:

- DoS and DDoS attacks generate a large volume flow to overwhelm the target host. The detection and defense of them should ideally be near the source of the attack. However, it is very difficult to identify the source of an attack as it generally uses IP spoofing.
- The volume of packets from only one source can be low enough to properly classify *good* and *bad* requests. Thus, a detection system based on only one site will have either high positive or high negative rates.
- DoS and DDoS traffic generated by available tools often has some identifying characteristics, making the detection based on statistics analysis possible. However, given the inherently busty nature of Internet, detecting those attacks is error prone.

Different types of detection mechanisms have already been proposed, such as entropy based detection [7], statistical and UNN based detection [8] etc.

According to the suggestions mentioned above, I propose a detection mechanism for these attacks in two points of connectivity –

1. Detection at Client Side
2. Detection at Intermediate Nodes

A. *Detection at Client Side*

There should be some steps of observation in the client side to detect the DOS and DDOS attack to enhance the system performance.

1. Obviously when a station is being affected, the number of rejected requests will increase;
2. The entropy of its resource usage will also be changed.

But increase in number of requests rejected and change in the resource usage entropy will not make it certain that the station is in under attack, i.e. it may be a side effect of a required request or operation. A human brain can best understand this situation. However, it is not possible to interface a human brain with a device. Therefore, the requirement of the involvement of artificial brain arises.

The *human brain* is a recurrent neural network (RNN) [9] or feedback neural network: a network of neurons with feedback connections. However, continuous use of RNN will degrade system performance. Therefore, we need to make a decision – "*when to activate it?*"

When both the resource entropy and the number of request rejected per time slot crosses a certain threshold the derived RNN ensemble will be fed with the respective features and the output will be a posteriori probability that will distinguish between good and bad requests. The reason for using the ensemble is that, the behavior of different types of DoS and DDoS can differ from each other. Each RNN in the ensemble will be responsible for different types of behavior. Therefore, with various RNN the degree of both accuracy and diversity will increase. The considered features for RNN will be –

1. Resource Usage parameters and
2. # of requests rejected in some previous time slots

Here, the resource usage parameters will be–

1. CPU Usage,
2. Physical Memory Usage, and
3. NIC Usage.

Figure 6 shows the corresponding algorithm.
Different states of this algorithm are as follows –

1. *Normal State:* In this sate, normal operations are going on in accordance with the checking of the number of requests rejected. When the number of requests rejected goes above a certain threshold, the resource usage entropy is compared against a certain threshold. If the value

is above the threshold, the suspected state will start.

2. *Suspected State:* Here, the possibility of attack arises as the bad effects are already being observed. So, now the RNN ensemble will be made activated. Here, the RNN ensembles are in operation. The output will be a posteriori probability. This probability is compared against some ranges. For being in highest range, it is obvious that, the attack is going on. So, the anti-attack actions state will be invoked. For, availability in the next range the alarm state will be invoked. Otherwise it is clear that, it is a side effect of some normal operation. So, it will return to the normal state.
3. *Anti Attack Action State:* Here, the corresponding measures to bring to an end of the obvious attack are taken.
4. *Alarm State:* In this state, system does not get any clear indication either of an attack or of a normal operation. Therefore, administrator will be notified to observe the proceeding of this crucial state. He will be solely responsible for the corresponding decision-making.

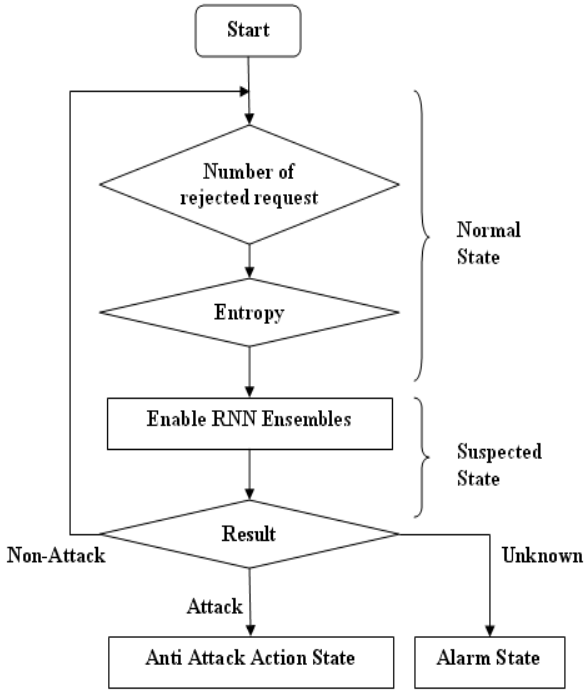

Figure 6: Algorithm for DoS and DDoS attack detection

The RNN ensembles can be obtained by constructive algorithms. One good approach related to this is to deploy CNNE [10].

B. Detection at Intermediate Nodes

We have to synthesize the features of a flow to detect an ongoing attack in an intermediate node. We should do it with the help of RNN. When the output posteriori probability crosses a certain threshold, an alarm should be generated and for obvious situation (crossing a higher threshold) the corresponding flow should be discarded. The flow should be considered here with the basis of the header info (such as timestamp).

The considerable features are –

1. N_{ICMP}: the percent of *ICMP* packets.
2. N_{UDP}: the percent of *UDP* packets.
3. N_{TCP}: the percent of *TCP* packets.
4. N_{TCPSYN}: the percent of *SYN* packets in *TCP* packets.
5. $N_{TCPSYNACK}$: the percent of *SYN+ACK* packets in *TCP* Packets.
6. N_{TCPACK}: the percent of *ACK* packets in *TCP* packets.
7. $Avg_{Packet\_Header\_Sizes}$: the average of packet header sizes.
8. $Avg_{Packet\_Data\_Sizes}$: the average of packet data sizes.

VI. CONCLUSION AND FUTURE WORK

Detection of DoS and DDoS is very complicated as they provide false data to IDS. The task of IDS is to distinguish their false data to identify the attack. This classification can best be done with the help of RNN. In this paper, I only consider the detection procedure. The output of the detection is posteriori probability. Actions should be done on the basis of the range of that probability. The applicability of the required actions for different ranges of probability is left as our future work.

REFERENCES

[1] K. J. Houle, G. M. Weaver, "Trends in Denial of Service Attack Technology", Security News Portal – SNPortal, 2001.

[2] Moore, Geoffrey M. Voelker and S. Savage, "Inferring Internet Denial-of-Service Activity", Proceedings of the 2001 USENIX Security Symposium, Washington D.C., August 2001.

[3] Hussain, J. Heidemann, C. Papadopoulos, "A Framework for Classifying Denial of Service Attacks", ACM SIGCOMM Conference, pp. 99-110. Karlsruhe, Germany, ACM. August, 2003.

[4] C. L. Schuba, I. V. Krsul, M. G. Kuhn, E. H. Spafford, A. Sundaram, D. Zamboni, "Analysis of a Denial of Service Attack on TCP", IEEE Symposium on Security and Privacy, pages 208--223. IEEE Computer Society Press, May 1997.

[5] S. Specht, R. Lee, "Taxonomies of Distributed Denial of Service Networks, Attacks, Tools, and Countermeasures", Technical Report CE-L2003-03, May 16, 2003.

[6] G. Zhang and M. Parashar, “Cooperative Defence against DDoS Attacks”, Journal of Research and Practice in Information Technology (JRPIT), Volume 38, Number 1, 2006.
[7] Y. Gu, A. McCallum, D. Towsley, “Detecting Anomalies in Network Traffic Using Maximum Entropy Estimation”, Internet Measurement Conference, 2005.
[8] R. Jalili, F. Imani-Mehr, M. Amini, H. R. Shahriari, “Detection of Distributed Denial of Service Attacks Using Statistical Pre-Processor and Unsupervised Neural Networks”, First Information Security Practice and Experience Conference (ISPEC 2005) Singapore, April 11-14, 2005.
[9] L. K. Hansen, P. Salamon, “Neural Network Ensembles”, IEEE Transaction on Pattern Analysis and Machine Intelligence, vol. 12, October 1990.
[10] M. M. Islam, X. Yao, K. Murase, “A Constructive Algorithm for Training Cooperative Neural Network Ensembles”, *IEEE Transactions on Neural Networks*, 14(4):820-834, July 2003.

Proceedings of 2009 12th International Conference on Computer and Information Technology (ICCIT 2009)
21-23 December, 2009, Dhaka, Bangladesh

Constructing SURF Visual-Words for Pornographic Images Detection

Yizhi Liu, Hongtao Xie†
Lab of Knowledge Processing and Networked Manufacture, Hunan University of Science and Technology, Xiangtan, Hunan Province, China
†Institute of Computing Technology, Chinese Academy of Sciences, Beijing, China
liuyizhi@ict.ac.cn, xiehongtao@ict.ac.cn

Abstract

Pornographic images detection is necessary for us to filter out objectionable information on the Internet. Bag-of-visual-words (BoVW) based pornographic images detection is promising because it can compensate the defect of the traditional approach. However, there are many choices to construct visual-words which are crucial to the tradeoff between the speed and the performance. We propose a novel method of constructing SURF (speeded up robust features) visual-words in skin regions and combining it with color moments. The results show that the performance of SURF visual-words is better than that of SIFT (scale-invariant feature transform) visual-words and our method is more effective to detect pornographic images than many existing methods.

Keywords: pornographic images detection, visual-words, SURF, SIFT, color moments.

I. INTRODUCTION

To prevent people from objectionable information while surfing on the Internet, many researchers and software developers have been focusing on pornographic images detection. One of the most difficult challenges is the tradeoff between the speed and the performance.

The traditional approach is mainly based on the global low-level visual contents. Global features are computed to capture the overall characteristics of an image. Especially, skin-color is proved to be fast-computing and powerful to pornographic images detection. However, the traditional approach is not the best choice for two reasons. Firstly, the "semantic gap" [1] exists between low-level visual features and the richness of human semantics. For instance, skin-color is not determinant but heuristic to detect pornographic images. Secondly, global features are often too rigid to represent an image and fail to identify important visual characteristics due to oversensitive to location [2].

Bag-of-visual-words (BoVW) based pornographic images detection is a promising approach owing to their simplicity and good performance. Its goal is to capture the local patterns of pornographic behavior, such as exposing pornographic parts, and showing pornographic poses. These patterns are decisive to judge accurately whether images are pornographic or not. SIFT (scale-invariant feature transform) visual-words have been performed to classify and rate pornographic images. However, the complexity of full affine-invariant features often has a negative impact on their robustness and does not pay off, unless really large viewpoint change are to be expected [3].

To detect pornographic images rapidly and accurately, we propose a novel method of constructing SURF (speeded up robust features) visual-words in skin regions and combining it with color moments. Thus, most of the SURF visual-words represent the local patterns of pornographic parts or poses. Moreover, SURF is a fast and excellent interest point detection-description scheme which outperforms the current state-of-the-art, both in speed and accuracy [4].

The paper is organized as follows. Section 2 describes related work. Section 3 presents the illustration of our method. Finally, section 4 shows the experiments and section 5 concludes the paper.

II. RELATED WORK

The traditional approach of content-based pornographic images detection is mainly based on the global low-level visual contents (such as shape, color, and texture). Shapes and colors are explored to be the criteria to judge whether images are pornographic or not. Textures are explored to reduce the false positive rate of skin-color detection because skin is smooth. Some previous works are illustrated as follows.

Forsyth et al. [5] constructed a human figure grouper after detecting skin regions, but consuming too much time and low detection accuracy are the two shortcomings. WIPE system [6] were explored to eliminates pornographic images by using a combination of an icon filter, a graph-photo detector, a color histogram filter, a texture filter, and a wavelet-based shape matching algorithm. Jones and Rehg [7] developed a statistical color model for detecting skin regions. Zeng et al. [8] implemented the image guarder system to detect pornographic images by different kinds of global features. AIRS [9] employs the MPEG-7 visual descriptors to identify and rate pornographic images. Kuan and Hsieh [10] used image retrieval technique and visual features are extracted from skin regions. Zheng et al. [11] used an edge-based Zernike moment method to detect harmful symbol objects. Rowley et al. adopted 27 visual features for Google to filter adult-content images, including

simple shape (lines), color, texture and face etc. [12].
However, it is difficult to detect accurately the images whose background colors are similar to skin-color. And it is challenging to identify images in the presence of occlusion, background clutter, pose and lighting changes.
BoVW has been applied to filter pornographic images as local features often correspond with more meaningful image components. Deselaers et al. [13] combine it with color histogram to classify images into different categories of pornographic content. Wang et al. [14] explore an algorithm to get 1,017 words from about 2,000 visual-words to detect pornographic images. Both of them use DoG (difference of Gaussian) detector and SIFT descriptor. Nevertheless, SURF is a fast and excellent interest point detection-description scheme which outperforms the current state-of-the-art, both in speed and accuracy [4].

III. OUR METHOD

For body text, please use a 10-point Times Roman font, or other Roman font with serifs, as close as possible in appearance to Times Roman in which these guidelines have been set. The goal is to have a 10-point text, as you see here. Please use sans-serif or non-proportional fonts only for special purposes, such as distinguishing source code text. If Times New Roman is not available, try the font named Computer Modern Roman. On a Macintosh, use the font named Times. Right margins should be justified, not ragged.
To reduce the noises of background, SURF visual-words is constructed in skin regions of annotated images. Thus, most of the SURF visual-words represent the local patterns of pornographic parts or poses. Furthermore, we use "product fusion" to combine color moments and SURF visual-words features to improve the performance.

A. Regions of Interest

We choose 500 typical pornographic images and use a kind of static threshold skin-color models to remove the background of the images and then to obtain the region of interest (ROI). Garcia and Tziritas [15] have shown that skin-like pixels are more correlated with C_r and C_b components than Y component. Therefore, the input image is transformed from the RGB color model to the YC_bC_r color space. A pixel is considered to be skin-like if its C_r and C_b components meet the following constraints:

$$C_r = \max\{-2(C_b+24), -(C_b+17), -4(C_b+32), 2.5(C_b+\theta_1), \theta_3, 0.5(\theta_4 - C_b)\};$$

and

$$C_r = \min\{(220 - C_b)/6, 4(\theta_2 - C_b)/3\}.$$

There are two constraints for θ_1, θ_2, θ_3, and θ_4:

- if $Y > 128$, then:

$$\theta_1 = -2 + (256 - Y)/16;$$
$$\theta_2 = 20 - (256 - Y)/16;$$
$$\theta_3 = 6;$$
$$\theta_4 = -8.$$

- otherwise:

$$\theta_1 = 6;$$
$$\theta_2 = 12;$$
$$\theta_3 = 2 + Y/32;$$
$$\theta_4 = -16 + Y/16.$$

We obtain 554,998 keypoints from ROIs, only 44.5 percent of the total keypoints without background removal.

B. References Visual Features

Besides the variety of keypoint detectors and descriptors, vocabulary size and weighting scheme are crucial to the speed and the performances of the BoVW method. Using a large vocabulary increases the cost associated with clustering keypoints, computing visual-words features, and running supervised classifiers. Adopting the binary scheme always produces top or close-to-top performance [16].
To create a small vocabulary, we choose the sizes between 200 and 300. We adopt the K-means algorithm based on DBSCAN to create adaptively visual-words after extracting 128-dimension of SURF features from each keypoint. After binary SURF visual-words, LIBSVM with RBF kernel is used because SVM (supported vector machine) has been proven to be the most powerful classifier in this domain.
To integrate the advantage of global features and then to improve the performance, we use "product fusion" to combine color moments and SURF visual-words features to improve the performance.

IV. EXPERIMENTS

We do all these experiments in the visual studio 2003 environment with the machine of 1.86 GHz Duo CPU and 2GB memory. We estimate our method with ROC (receiver operating characteristic) curve according to the definition from Wikipedia. A ROC space is defined by false positive rate (FPR) and true positive rate (TPR) as x and y axes respectively.

A. Our dataset and baseline

In this section, we provide more details about our datasets. We collect 90,000 images in all, more than 40,000 images from Internet and about 50,000 images from Corel Gallery. We divide them into two parts in which 50,000 labeled images for training and 40,000 unlabeled images for testing. The training set is made up of 10,000 pornographic images and 40,000 benign images. The testing set contains 10,000 pornographic images and 30,000 benign images. There are 10,000 benign images containing body parts (such as faces, hands, feet, trunks,

etc.) in both sets. Therefore, the rate of positive training samples to negative training samples equals to four for SVM training in all my experiments.

There is no common database in this field. Therefore, it is necessary to build a baseline. We take the performance of color histogram concatenated with edge histogram (i.e. CH+EH) as our baseline, which is one of the most typical traditional methods.

B. SURF Visual-Words Features

We adopt the K-means algorithm based on DBSCAN to create 209 and 284 SURF visual-words from 554,998 keypoints in ROIs of 500 annotated images. And the binary weighting method (BW) is applied to quantize visual words features. To show the good performance of our method, 265 and 340 SIFT visual-words are mined from 576,079 keypoints in 350 annotated images by the same clustering algorithm and the same weighting scheme (ROC curves shown in Figure 1).

In Figure 1, SURF-BW(209) represents the method of pornographic images detection on our dataset by using 209 SURF visual-words and binary weighting scheme in the BoVW method, and SIFT-BW(340) represents the method by using 340 SIFT visual-words and binary weighting scheme, and so on. The ROC curves of SURF visual-words are shown by the red lines with some triangles; the blue lines with some dots are the ROC curves of SIFT visual-words. The yellow one is the ROC curve of our baseline.

According to the observation of Figure 1, we can draw two conclusions: (1) The performances of SURF or SIFT visual-words are better than CH+EH. (2) The performances of SURF visual-words is better than those of SIFT. For example, the performance of SURF-BW(209) is better than that of SIFT-BW(265) and the performance of SURF-BW(284) is better than that of SIFT-BW(340). The vocabulary size in our method is about 1/4 of Wang et al. [14].

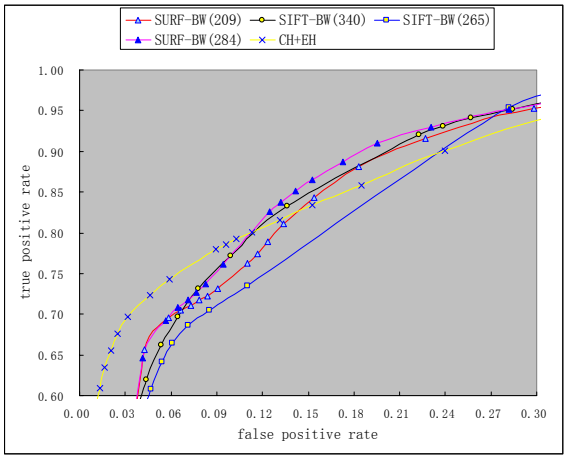

Fig. 1. Performances of visual-words

C. Fusion with Color Moments

Color moments (CM) provide a measurement for color similarity between images. In CM, we calculate the first 3 moments of 3 channels in Lab color space over 5×5 grid partitions, and aggregate the features into a 225-dimension feature vector.

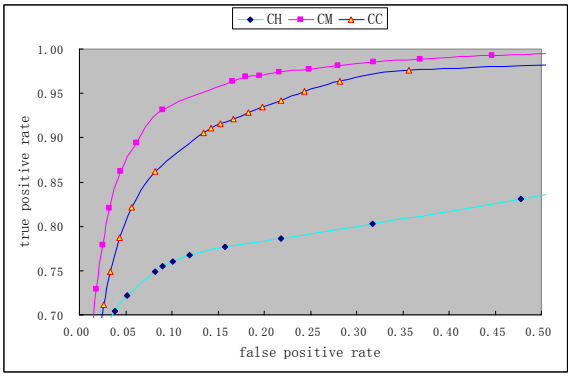

Fig. 2. Performances of global color features

We can observe by Figure 2 (the red line is the ROC curve of CM) that the performance of CM is better than those of CH and color correlogram (CC).

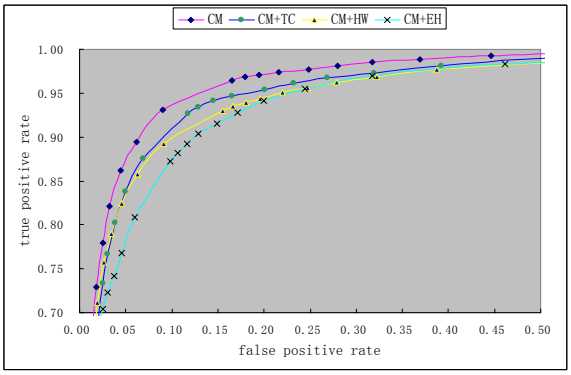

Fig. 3. Concatenations of CM and global texture features

From Figure 3, we can come conclusion that the performance of CM is better than those of "early fusion" with EH, texture co-occurrence (TC), and Haar wavelet (HW). In Figure 3, the ROC curves of CM, CM+TC, CM+HW, and CM+EH are shown in red, green, yellow, and cyan respectively.

Table I Comparisons of different methods

Methods	FPR(%)	TPR(%)
Forsyth & Fleck [5]	11.3	79.3
WIPE [6]	9.0	96.0
Jones & Rehg [7]	8.5	80.0
Zeng et al. [8]	5.0	76.5
AIRS [9]	23.0	99.3
Kuan & Hsieh [10]	9.5	90.8
Zheng et al. [11]	15.3	89.2
Rowley et al. [12]	35.0	90.0
Wang et al. [14]	18.8	91.1
Our method	**22.0%**	**98.9**

To integrate the advantage of global features and then to improve the performance, we use "product fusion" to combine color moments and SURF visual-words features. As shown in Table I and Figure 4, our method is more effective to detect pornographic images than many

existing methods introduced in section 2, except the method of [6] and [9]. Our method is only used to detect images instead of graph or photo, but the graph-photo detector in WIPE [6] achieves 100% sensitivity and nearly 100% specificity. The performance of our method is very approximate to that of AIRS which adopt three kinds of MPEG-7 visual descriptors.

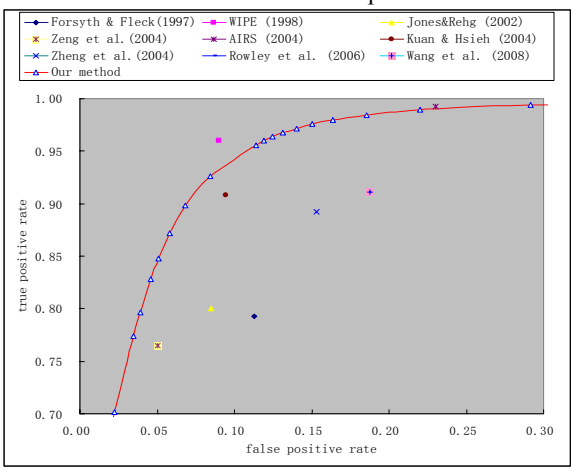

Fig. 4. The performance of our method

V. CONCLUSIONS

Bag-of-visual-words (BoVW) based pornographic images detection is a promising approach because the local patterns of pornographic behavior can be captured. Moreover, the variety of keypoint detectors and descriptors are crucial to the speed and the performances of the BoVW method. Considering that SURF is the most excellent interest point detection-description scheme both in speed and accuracy, we propose a novel method to construct SURF (speeded up robust features) visual-words in skin regions of annotated images for pornographic images detection. Therefore, most of the SURF visual-words represent the local patterns of pornographic parts or poses. To integrate the advantage of global color features, we use "product fusion" to combine color moments and SURF visual-words features and the results show that our method is more effective to detect pornographic images than many existing methods.

VI. ACKNOWLEDGEMENT

This work was supported by Hunan Project on Science and Technology in China (B10718).

REFERENCES

[1] A. Smeulders, M. Worring, A. Gupta, et al., "Content-based image retrieval at the end of the early years," *IEEE Transactions on Pattern Analysis and Machine Intelligence*, vol. 22, Dec. 2000, pp. 1349-1380.

[2] R. Datta, D. Joshi, J. Li, et al., "Image retrieval: ideas, influences, and trends of the new age," *ACM Computing Surveys*, vol. 40, April 2008, Article 5.

[3] D. Lowe, "Distinctive image features from scale-invariant keypoints, cascade filtering approach," *International Journal of Computer Vision*, vol. 60, Feb. 2004, pp. 91-110.

[4] H. Bay, T. Tuytelaars, L. V. Gool, "SURF: speeded up robust features," 9th *European Conference on Computer Vision*, Graz, Australia, 2006, pp. 404-417.

[5] M. M. Fleck, D. A. Forsyth, C. Bregler, "Finding naked people," 4th *European Conference on Computer Vision*, Cambridge, UK, 1996, pp. 593-602.

[6] J. Z. Wang, J. Li, G. Wiederhold, et al., "System for screening objectionable images," *Computation Communication*, vol. 21, 1998, pp. 1355-1360.

[7] M. J. Jones, J. M. Rehg, "Statistical color models with application to skin detection," *International Journal of Computer Vision*, vol. 46, Jan. 2002, pp. 81–96.

[8] W. Zeng, W. Gao, T. Zhang, et al., "Image guarder: an intelligent detector for adult," 6th *Asian Conference of Computer Vision*, Jeju Island, Korea, 2004, pp. 198-203.

[9] S. J. Yoo, "Intelligent multimedia information retrieval for identifying and rating adult images," 8th *International Conference on Knowledge-Based Intelligent Information & Engineering Systems*, Willington, New Zealand, 2004, pp. 164–170.

[10] Y. H. Kuan, C. H. Hsieh, "Content-based pornography image detection," *International Conference on Imaging Science, System and Technology*, Las Vegas, USA, 2004.

[11] Q. F. Zheng, W. Zeng, W. Gao, et al., "Shape-based adult images detection," *3th International Conference on Image and Graphics*, Hong Kong, China, 2004, pp. 150-153.

[12] H. A. Rowley, J. Yushi, and Shumeet Baluja, "Large scale image-based adult-content filtering," *1st International Conference on Computer Vision Theory and Applications*, 2006, pp. 290-296.

[13] Y. S. Wang, Y. N. Li, W. Gao, "Detecting pornographic images with visual words," *Transactions of Beijing Institute of Technology*, vol. 28, May 2008, pp. 410-413.

[14] T. Deselaers, L. Pimenidis, H. Ney, "Bag-of-visual-words models for adult image classification and filtering," 19th *International Conference on Pattern Recognition*, Tampa, USA, 2008, pp. 1-4.

[15] C. Garcia, G. Tziritas, "Face detection using quantized skin color regions merging and wavelet packet analysis," *IEEE Transactions on Multimedia*, vol.1, 1999, pp. 264-277.

[16] J. Yang, Y. G. Jiang, A. G. Hauptmann, et al., "Evaluating bag-of-visual-words representations in scene classification," *9th ACM SIGMM International Workshop on Multimedia Information Retrieval*, University of Augsburg, Germany, 2007, pp. 197-206.

Proceedings of 2009 12th International Conference on Computer and Information Technology (ICCIT 2009)
21-23 December, 2009, Dhaka, Bangladesh

Optimized Entity Attribute Value Model: A Search Efficient Representation of High Dimensional and Sparse Data

(Not Presented)

Razan Paul, Abu Sayed Md. Latiful Hoque
Department of Computer Science and Engineering,
Bangladesh University of Engineering and Technology, Dhaka 1000, Bangladesh
razanpaul@yahoo.com, asmlatifulhoque@cse.buet.ac.bd

Abstract

Entity Attribute Value (EAV) is the widely used solution to represent high dimensional and sparse data, but EAV is not search efficient for knowledge extraction. In this paper, we have proposed a search efficient data model: Optimized Entity Attribute Value (OEAV) for physical representation of high dimensional and sparse data as an alternative of widely used EAV. We have implemented both EAV and OEAV models in a data warehousing environment and performed different relational and warehouse queries on both the models. The experimental results show that OEAV is dramatically search efficient and occupy less storage space compared to EAV.

Keywords: EAV, OEAV, Open Schema, Sparse Data

I. INTRODUCTION

In various domains, integrating Large-scale heterogeneous data is important for knowledge discovery. Once this knowledge is discovered, the results of such analysis can be used to define new guidelines. We require an open schema data model to support dynamic schema change, sparse data, and high dimensional data. In open schema data models, logical model of data is stored as data rather than as schema, so changes to the logical model can be made without changing the schema. In open schema data model, schema is kept as data. EAV [1] is the widely used open schema data model to handle these challenges of data representation. However, EAV suffers from higher storage requirement and not search efficient. In this paper, we have proposed a search efficient open schema data model: OEAV. This model is storage efficient as well compared to existing EAV model.

Section 2 describes the related work. The overview of EAV, the details organizational structure and analysis of OEAV are given in section 3. A data transformation is required to adopt the existing data suitable for data warehouse representation for knowledge extraction. The transformation is elaborated in section 4. Analytical details of performance of the proposed models are given in section 5. Section 6 offers the result and discussion. Section 7 is the conclusion.

II. RELATED WORK

EAV gives us extreme flexibility in data representation but it is not search efficient as it keeps attribute name as data in attribute column and has no tracking of how data are stored. To handle the high dimensionality and sparseness of medical data, in [2] authors have used EAV, but EAV is not a search efficient data model for knowledge discovery. To handle data sparseness and schema change of phenotype data, the EAV model has been used for phenotype data management in [3]. Use of EAV for medical observation data is also found in [4], [5], [6], [7] as medical observation data are sparse, high dimensional and need frequent schema change. The Entity-Relationship Model is proposed in [8]. Storage and querying of high dimensional sparsely populated data is proposed in [9], but this model does not keep the data in search efficient way. Agarwal et al. in [10] propose several methods for the efficient computation of multidimensional aggregates. In [11] authors propose data cube as a relational aggregation operator generalizing group-by, crosstab, and subtotals.

III. OPEN SCHEMA DATA MODELS

A. Entity-Attribute-Value Model (EAV)

EAV is an open schema data model, which is suitable for high dimensional and sparse data like medical data. In EAV, every fact is conceptually stored in a table, with three sets of columns: entity, an attribute, and a value for that attribute. In this design, one row actually stores a single fact. It eliminates sparse data to reduce database size and allows changing set of attributes. Moreover, EAV can represent high dimensional data, which cannot be modeled by relational model because existing RDBMS only support a limited number of columns. EAV gives us extreme flexibility but it is not search efficient as it keeps attribute name as data in attribute column and has no tracking of how data are stored.

B. Optimized Entity Attribute Value (OEAV)

To remove the search inefficiency problem of EAV whilst preserving its efficiency of representing high dimensional and sparse data, we have developed a search efficient open schema data model OEAV. This model keeps data in a search efficient way.

This approach is a read-optimized representation whe-

reas the EAV approach is write-optimized. Most of the data warehouse systems write once and read many times, so the proposed approach can serve the practical requirement of data warehouse. Figure 1 shows the step by step approach of transformation of an EAV data representation to an equivalent OEAV data representation. In step 1, this model constructs an attribute dictionary where there is an integer code for each attribute.

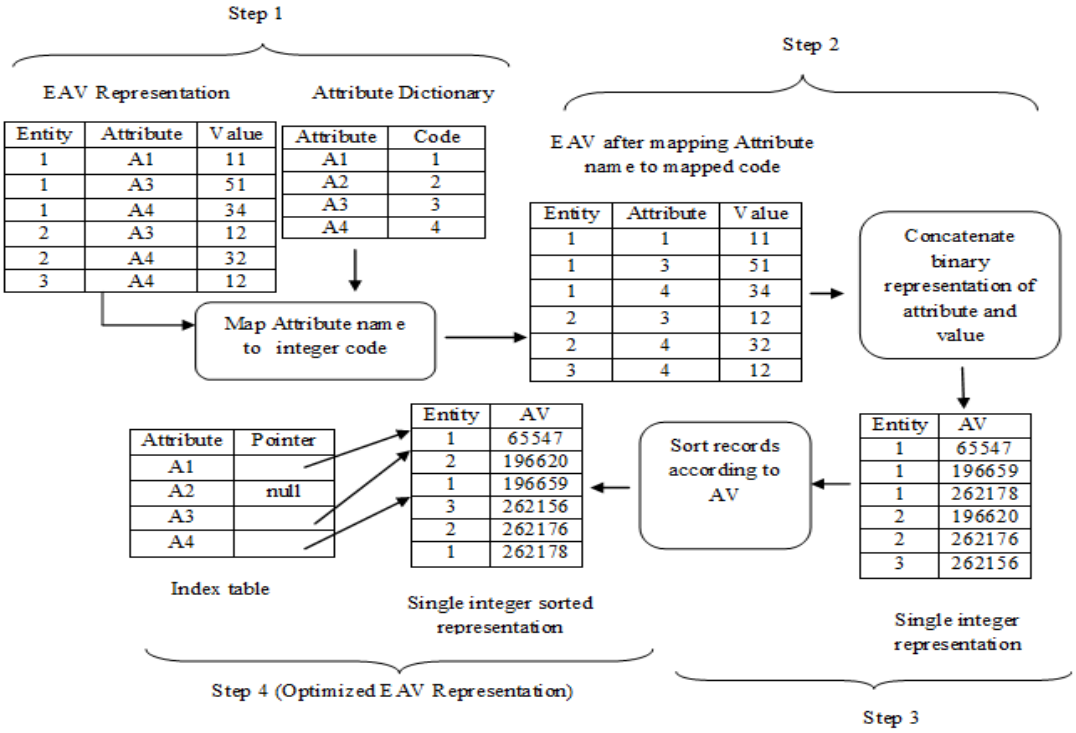

Fig. 1. Transformation of EAV model to Optimized EAV (OEAV) model.

Attribute name of each fact is mapped to an integer code using the attribute dictionary. All types of values are treated as integer using a data transformation as discussed in the following section. In step2, a compact single integer Attribute Value (AV) is created by concatenating binary representation of attribute code and value. In OEAV, every fact is conceptually stored in a table with two columns: the entity and the AV. It maps attribute code and value to p bit and q bit integer and concatenate them to n bit integer AV. For example, an attribute value pair (A3, 51), the code of attribute A3 is 3, will be converted in the following ways: (A3, 51) → (3, 51) → (0000000000000011, 0000000000110011) → 00000000000000110000000000110011 = 196659.

In step 3, the records of optimized EAV are stored as sorted order of AV field. As data are stored in sorted order of AV and the first p bits of AV are for attribute code, the records of an attribute in OEAV table remains consecutively. In step 4, an index structure, which is a part of OEAV representation, is created to contain the starting record number (Pointer) of each attribute in OEAV table. This makes the data partitioned attribute wise, which is expected by most analytical program. In sorted AV field, the values of an attribute also remain in sorted order and binary search can be applied on it. This model constructs a modified B+ tree index on entity field of OEAV to make entity wise search efficient. Here each leaf of the modified B+ tree keeps the block address of attribute values for each entity. These Search efficiencies of OEAV are absent in conventional EAV representation.

IV. DATA TRANSFORMATION USING DOMAIN DICTIONARY AND RULE BASE

For knowledge discovery, the data have to be transformed into a suitable transaction format to discover knowledge. We address the problem of mapping data to items using domain dictionary and rule base. The data are type of categorical, continuous numerical data, Boolean, interval, percentage, fraction and ratio. Domain expert have the knowledge how to map ranges of numerical data for each attribute to a series of items. For example, there are certain conventions to consider a person is young, adult, or elder with respect to age. A set of rules is created for each continuous numerical attribute using the knowledge of domain experts. A rule engine is used to map continuous numerical data to items using these developed rules.

Data, for which domain expert knowledge is not applicable, we have used domain dictionary approach to

transform these data to numerical forms. Here the mapping process as shown in Figure 2 for medical data is divided in two phases. Phase 1: a rule base is constructed based on the knowledge of domain experts and dictionaries are constructed for attributes where domain expert knowledge is not applicable, Phase 2: attribute values are mapped to integer values using the corresponding rule base and the dictionaries.

V. STORAGE ANALYSIS OF EAV & OEAV

Let b be the total number of blocks of observation table and k is the total number of attributes of observation table.

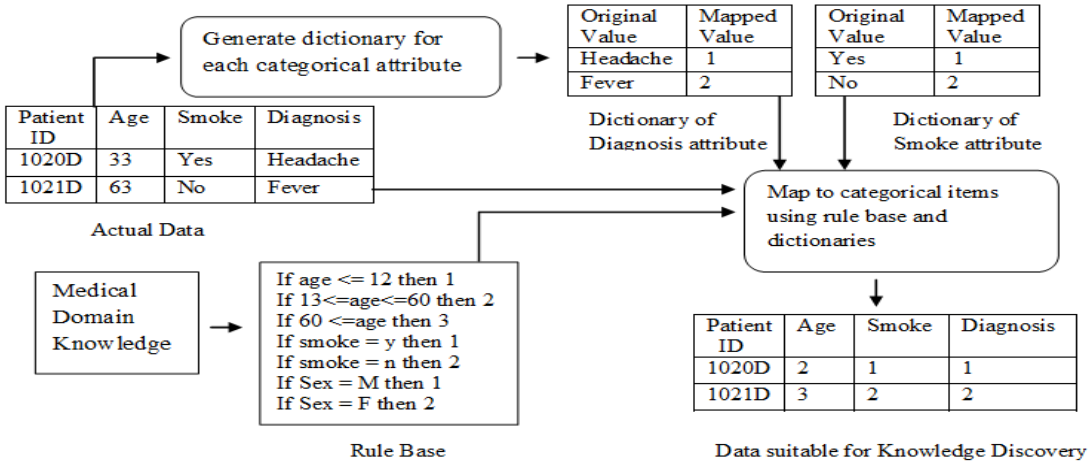

Fig. 2. Data Transformation of Medical Data.

A. Analysis of Storage Capacity of EAV

Let n = total number of facts, $_1$ average length of attribute names, $g =$ average length of values. In EAV, 32 bits (4 bytes) is required to represent entity. Size of each fact in EAV is $(4+q+g)$ bytes. Hence, the total size to hold all facts is $S = n \times (4+q+g)$ bytes.

B. Space Complexity of Medical domain dictionaries and Rule Base

Let $C_i =$ cardinality of ith attribute where domain expert knowledge is not applicable, $L_i =$ average length of ith attribute name, P = number of categorical attributes. Codes of attributes are not stored explicitly and the index of attribute is the code. Domain dictionary storage of ith attribute is $C_i \times L_i$ bytes. Total domain dictionaries storage (S_D) is $\sum_{i=1}^{p} (C_i \times L_i)$ bytes. If the size of rule base storage is R, the dictionary and rule base storage (S_{DR}) is $\sum_{i=1}^{p} (C_i \times L_i) + R$ bytes.

C. Analysis of Storage Capacity of OEAV

Let $p =$ number of attributes, $q =$ average length of attribute names. Total storage of attribute dictionary is $p \times q$ bytes. Let $S =$ size of each block address in byte. Total storage of index table is $p \times q + p \times S$ bytes. In OEAV, 32 bits are required to represent entity and 16 bits are required for attribute and value individually. 64 bits = 8 bytes = size of each fact in OEAV. Let n = total number of facts, m = total number of facts in a block, w = word size (bytes). Total number of blocks is $\lceil n/m \rceil$. The number of words per fact is $\lceil 64/w \rceil$. For block i where $1 \le i \le \lceil n/m \rceil$, the number of words per block is $\lceil (m \times \lceil 64/w \rceil) \rceil$ and the size of the block is $w(\lceil (m \times \lceil 64/w \rceil) \rceil)$. Hence the size to hold all facts is $S = \lceil n/m \rceil \times w \times (\lceil (m \times \lceil 64/w \rceil) \rceil)$. In OEAV, total size to hold all facts = storage for facts + storage for domain dictionaries and rule base + storage for attribute dictionary + storage for index table + storage for modified B+ tree

$$= \lceil n/m \rceil \times w \times (\lceil (m \times \lceil 64/w \rceil) \rceil) + \sum_{i=1}^{p} (C_i \times L_i) + R + (p \times q) + (p \times q + p \times S) + B$$

bytes.

VI. RESULTS AND DISCUSSION

The experiments were done using PC with core 2 duo processor with a clock rate of 1.8 GHz and 3GB of main memory. The operating system was Microsoft Vista and implementation language was c#. We have designed a data generator that generates all categories of random data: ratio, interval, decimal, integer, percentage etc. This data set is generated with 5000 attributes and 5-10 attributes per transaction on average. We have used highly skewed attributes in all performance evaluations to measure the performance improvement of our proposed open schema data models in worst case. For all performance measurement except storage performance, we have used 1 million transactions.

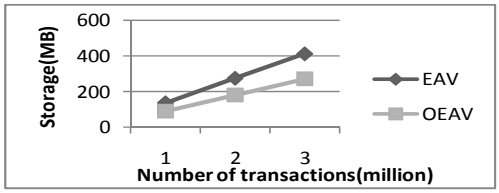

Fig. 3. Storage performance.

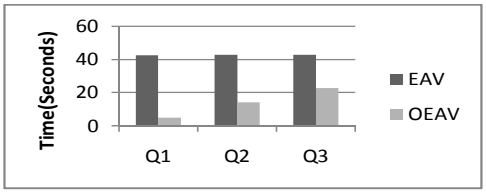

Fig. 4. Time comparison of projection operations.

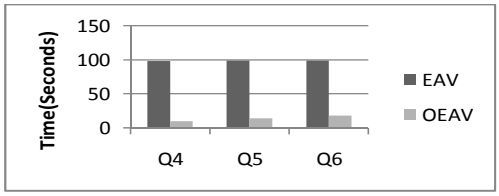

Fig. 5. Time comparison of select queries.

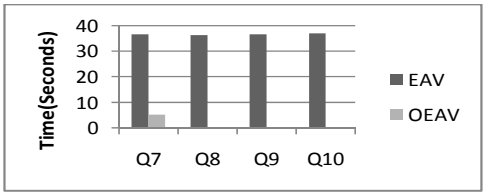

Fig. 6. Time comparison of aggregate operations.

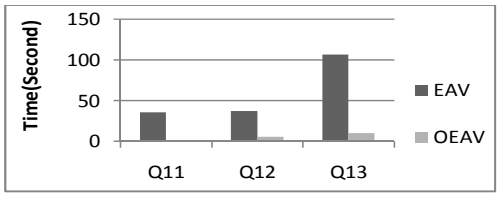

Fig. 7. Time comparison of statistical operations.

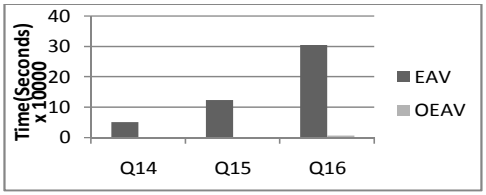

Fig. 8. Time comparison of CUBE operations.

Q1: Select A_i from observation;
Q2: Select A_i , A_j ,A_k from observation.
Q3: Select A_i, A_j, A_k, A_l, A_m from observation.
Q4: Select * from observation where A_i='XXX'.
Q5: Select * from observation where A_i='XXX' AND A_j='YYY'.
Q6: Select * from observation where A_i='XXX' AND A_j='YYY' AND A_k='ZZZ'.
Q7: Select AVG (A_i) from observation.
Q8: Select Max (A_i) from observation.
Q9: Select Min (A_i) from observation.
Q10: Select Count (A_i) from observation.
Q11: Select Median (A_i) from observation.
Q12: Select Mode (A_i) from observation.
Q13: Select Standard Deviation (A_i) from observation.
Q14: Select A_i, A_j, Max (Am) from observation CUBE-BY (A_i, A_j)
Q15: Select A_i, A_j, A_K, Max (A_m) from observation CUBE-BY (A_i, A_j, A_k)
Q16: Select A_i, A_j, A_K, A_m, Max (A_n) from observation CUBE-BY (Ai, A_j, A_k, A_m)

A. Storage Performance

Figure 3 shows the storage space required by EAV and OEAV. The EAV occupies significantly higher amount of storage than OEAV. This is due to the data redundancy of EAV models.

B. Time Comparison of Projection Operations

Figure 4 shows the performance of projection operations on various combinations of attributes. Almost same time is needed with different number of attributes in EAV, as it has to scan all the blocks whatever the number of attributes. In OEAV, it can be observed that the time requirement is proportional to the number of attributes projected. This is because that the query needs to scan more number of blocks as the number of attributes increases.

C. Time Comparison of Select Queries

Figure 5 shows the performance of multiple predicates select queries on various combinations of attributes. Figure 5 shows almost same time is taken with different number of attributes in EAV as it has to scans all the blocks twice whatever the number of attributes in predicate. The graph shows how time is varied in OEAV with different number of attributes as it scans number of attribute partitions proportional to number of attributes in select quires. This experiment shows EAV has taken much higher time compared to OEAV. It is because it has no tracking of how data are stored, so it has to scans all the blocks once to select entities and has to scan all the blocks one more time to retrieve the attribute values for the selected entities. OEAV has taken the lower time as it does not need to read unused attributes to select entities and can retrieve attribute values of these entity without reading any unused attribute value using entity indexing .

D. Time Comparison of Aggregate Operations

Aggregate operations compute a single value by taking a collection of values as input. Figure 6 shows the performance of various aggregate operations on a single attribute. Time is not varied significantly from one aggregate operation to another as different aggregate operations need same number of data block access for most of the cases. Figure 6 shows EAV has taken much higher time than OEAV as it has to scan all the blocks to compute each operation. OEAV has taken negligible time for max, min, count operations on a single attribute as to find max and min it has to scan only 1 block and count result is computed from its index table. For average operation on an attribute, it has taken considerable time, as it has to scan all the blocks of that attribute.

E. Time Comparison of Statistical Operations

Figure 7 shows the performance of various statistical operations on a single attribute. Time is varied significantly from one statistical operation to another as different statistical operations need different sorts of processing. This experiment shows EAV has taken much higher time compared to OEAV. It is because it has no tracking of how data are stored, so it has to scan all the blocks to compute each operation. We can see from this figure OEAV has taken negligible time for median operation as it has to scan 1 or 2 blocks for this operation. For mode and standard deviation, it has to scan all data blocks of the attribute for which particular operation is executing once, twice respectively.

F. Time Comparison of CUBE Operations

The CUBE operation is the n-dimensional generalization of group-by operator. The cube operator unifies several common and popular concepts: aggregates, group by, roll-ups and drill-downs and, cross tabs. Here no pre-computation is done for aggregates at various levels and on various combinations of attributes. Figure 8 shows the performance of CUBE operations on various combinations of attributes. It can be observed that the number of attributes in cube operations leads to the time taken as CUBE operation computes group-bys corresponding to all possible combinations of CUBE attributes. The experiment results show that EAV has taken much higher time compared to OEAV as it does not partition data attribute wise and it has no entity index.

VII. CONCLUSION

EAV is a widely used solution to model data which are sparse, high dimensional and need frequently schema change, but EAV is not a search efficient data model for knowledge discovery. In this paper, we have proposed a search efficient open schema data models OEAV to model high dimensional and sparse data as an alternative of EAV. We have implemented both EAV and OEAV models in a data warehousing environment and performed different relational and warehouse queries on both the models. We have achieved a query performance faster in the range of 15 to 70 compared to existing EAV model. These efficiencies arise due to binary data representation in OEAV where as string representation is used in EAV model. The experiment results show our proposed open schema data model is dramatically efficient in knowledge discovery operation and occupy less storage compared to widely used EAV model.

REFERENCES

[1] W. W. Stead, E. W. Hammond and J. M. Straube, "A chartless record—Is it adequate?," *Journal of Medical Systems*, vol. 7, no. 2, pp. 103-109, 1983.

[2] E. J. Thomas, T. W. Jeffrey and C. D. Joel, "A healthcare data model based on the HL7 reference information model," *IBM Systems Journal*, vol. 46, no. 1, pp. 5 - 18, 2007.

[3] J. Li, M. Li, H. Deng, P. Duffy and H. Deng, "PhD: a web database application for phenotype data management," *Oxford Bioinformatics*, vol. 21, no. 16, pp. 3443-3444, 2005.

[4] J. Anhøj, "Generic design of web-based clinical databases," *Journal of Medical Internet Research*, vol. 5, no. 4, p. 27, 2003.

[5] C. Brandt, A. Deshpande and C. Lu, "TrialDB: A web-based clinical study data management system AMIA 2003 Open Source Expo," in *Proceedings of the American Medical Informatics Association Annual Symposium*, Washington, 2003, p. 794.

[6] P. M. Nadkarni et al., "Managing attribute—value clinical trials data using the ACT/DB client—server database system," *The Journal of the American Medical Informatics Association*, vol. 5, no. 2, p. 139–151, 1998.

[7] P. Nadkarni. Yale University School of Medicine. [Online]. http://**ycmi**.med.yale.edu/nadkarni/Introduction%20to%2

0EAV%20systems.htm

[8] C. P. Peter, "The entity-relationship model—toward a unified view of data," *ACM Transactions on Database Systems*, vol. 1, no. 1, pp. 9 - 36, 1976.

[9] A. S. M. L. Hoque, "Storage and querying of high dimensional sparsely populated data in compressed representation," *Lecture Notes on Computer Science*, vol. 2510, pp. 418 - 425, 2002.

[10] S. Agarwal et al., "On the computation of multidimensional aggregates," in *Proceedings of the 22th International Conference on Very Large Data Bases*, 1996, pp. 506-521.

[11] G. Jim, C. Surajit and B. ADAM, "Data cube: a relational aggregation operator generalizing group-by, cross-tab and sub-totals," *Data Mining and Knowledge Discovery*, vol. 1, no. 1, p. 29–53, 1997.

Proceedings of 2009 12th International Conference on Computer and Information Technology (ICCIT 2009)
21-23 December, 2009, Dhaka, Bangladesh

Symmetric Tori Connected Torus Network

Faiz Al Faisal and M.M. Hafizur Rahman

Dept. of CSE, KUET, Khulna- 9203, Bangladesh
dipu_7009@yahoo.com, hafiz90305@gmail.com

Abstract

*A **S**ymmetric **T**ori connected **T**orus Network (**STTN**) is a 2D-torus network of multiple basic modules, in which the basic modules are 2D-torus networks that are hierarchically interconnected for higher-level networks. In this paper, we present the architecture of the STTN, addressing of node, routing of message, and evaluate the static network performance of STTN, TTN, TESH, mesh, and torus networks. It is shown that the STTN possesses several attractive features, including constant degree, small diameter, low cost, small average distance, moderate bisection width, and high fault tolerant performance than that of other conventional and hierarchical interconnection networks.*

Keywords: STTN, Node Degree, Diameter, Cost, Average Distance, Bisection Width, and Arc Connectivity.

I. INTRODUCTION

Sequential computer steadily increases their speed to meet the computation demand, and it has already been reached saturated. Thus, the only way to meet the increasing demand of computation power to solve the grand challenge problems is to use parallel computers. Massively Parallel Computer (MPC) systems with thousands of nodes have been commercially available and efforts have been made to build MPC systems with millions of nodes. In such computers, with millions of nodes, the large diameter of conventional topologies is completely infeasible. Hierarchical interconnection networks (HIN) [1] are a cost-effective way to interconnect a large number of nodes. A variety of hypercube-based HIN have been proposed [2-5], but for MPC systems, the number of physical links becomes prohibitively large. To alleviate this problem, several k-ary n-cube based HIN have been proposed. However, the performance of these networks does not yield any obvious choice of an interconnection network for MPC. No one is clear winner in all aspect of network design.

A Tori connected mESH (TESH) network [6,7] is an HIN aiming for large-scale 3D MPC systems, consisting of multiple basic modules (BMs) which are 2D-mesh networks. The BMs are hierarchically interconnected by a 2D-torus to build higher level networks. The restricted use of physical links between BMs in the higher level networks and within the BMs reduces the dynamic communication performance of this network [8]. It has already been shown that a torus network has better dynamic communication performance than a mesh network [9]. We have replaced the 2D-mesh of a TESH network by a 2D-torus network, and the modified HIN is called **T**ori-connected **T**orus **N**etwork (**TTN**) [10]. It is seen that TTN is suitable for a few tens of thousands of node [11]. For millions of nodes, TTN does not give better performance. The assignment of free links of BM for higher level interconnection is asymmetric in the TTN. We assign the free links in a symmetric order for higher level interconnection. This new interconnection network is called **S**ymmetric **T**ori connected **T**orus **N**etwork (**STTN**). It provides scalability up to a million of nodes with less cost.

In this paper, we address the architectures of the STTN and evaluate its static network performance. The static network performance will be evaluated in terms of node degree, network diameter, cost, average distance, bisection width, and arc connectivity. The main objective is generalized study of static network performance for the STTN.

The remainder of the paper is organized as follows. In Section **II**, we briefly describe the basic architecture of the STTN. Addressing of nodes of the STTN and the routing of messages are discussed in Section **III** and Section **IV**, respectively. The static network performance of the STTN is discussed in Section **V**. Finally, in Section **VI**, we conclude this paper.

II. INTERCONNECTION OF THE STTN

The **S**ymmetric **T**ori connected **T**orus **N**etwork (**STTN**) is a hierarchical interconnection network consisting of multiple basic modules (BM) that are hierarchically interconnected to form a higher level network. A ($2^m \times 2^m$) BM consists of a 2D-torus network of 2^{2m} processing elements (PE) having 2^m rows and 2^m columns, where m is a positive integer. Considering m=2, a BM of size (4×4) is depicted in Fig. 1(a). Each BM has 2^{m+2} free ports at the contours for higher level interconnection. All ports of the interior nodes are used for intra-BM connections. All free ports of the exterior nodes, either one or two, are used for inter-BM connections to form higher level networks. In this paper, BM refers to a Level-1 network.

Successive higher level networks are built by recursively interconnecting (2^{2m}) immediate lower level subnetworks in a ($2^m \times 2^m$) 2D-torus network. As portrayed in Fig. 1(b), considering (m = 2) a Level-2 STTN can be formed by interconnecting $2^{2\times2} = 16$ BMs. Similarly, a Level-3 network can be formed by interconnecting 16 Level-2 subnetwork and so on. Each

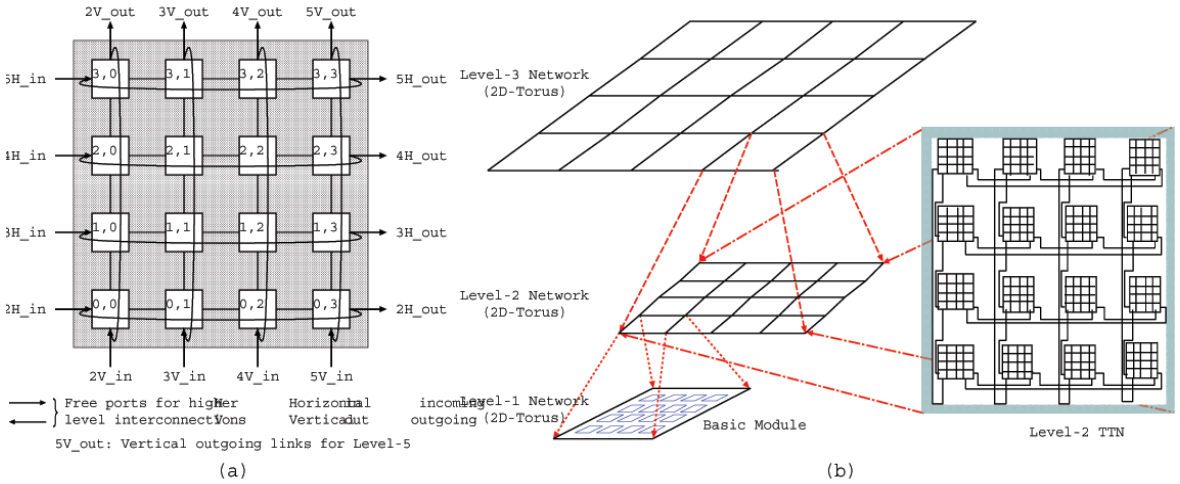

Fig. 1. Interconnection of a STTN (a) Basic module (b) Higher level network

BM is connected to its logically adjacent BMs. To avoid clutter, the wraparound links of the BMs are not shown. It is useful to note that for each higher level interconnection, a BM uses $4 \times (2^q) = 2^{q+2}$ of its free links, $2(2^q)$ free links for vertical interconnections and $2(2^q)$ free links for horizontal interconnections. Here, $q \in \{0, 1,\ldots, m\}$, is the inter-level connectivity. $q = 0$ leads to minimal inter-level connectivity, while $q = m$ leads to maximum inter-level connectivity. As shown in Figure 1(a), for example, the (4×4) BM has $2^{2+2} = 16$ free ports. If we chose $q = 0$, then $4(2^0) = 4$ of the free ports and their associated links are used for each higher level interconnection, 2 for horizontal and 2 for vertical interconnection. Among these 2 links, one is used for incoming link and another one for used for outgoing link, i.e., a single links is used for vertical_in, vertical_out, horizontal_in, and horizontal_out.

A STTN (m,L,q) is constructed using $2^m \times 2^m$ BMs, has L levels of hierarchy with inter-level connectivity q. In principle, m could be any positive integer value. However, if $m = 1$, then the network degenerates to a hypercube network. Hypercube is not a suitable network, because its node degree increases along with the increase of network size. If $m = 2$, then it is considered the most interesting case, because it has better granularity than the large BMs. If $m \geq 3$, the granularity of the family of networks is coarse. If $m = 3$, then the size of the BM becomes (8 × 8) with 64 nodes. Correspondingly, the Level-2 network would have 64 BMs. In this case, the total number of nodes in a Level-2 network is $N=2^{2\times3\times2} = 4096$ nodes, and Level-3 network would have 262144 nodes. Clearly, the granularity of the family of networks is rather coarse. In the rest of this paper we consider $m = 2$, therefore, we focus on a class of STTN (2, L, q) networks.

The highest level network which can be built from $(2^m \times 2^m)$ BM is $L_{max} = 2^{m-q}+1$. With $q = 0$ and $m = 2$, $L_{max} = 5$, Level-5 is the highest possible level. The total number of nodes in a STTN having $2^m \times 2^m$ BMs is $N=2^{2mL}$. Using maximum level of hierarchy, $L_{max} = 2^{m-q}+1$, the maximum number of nodes which can be interconnected by a STTN (m, L, q) is $N = 2^{2m\,(2m-q+1)}$. For the case of (4 × 4) BM with $q = 0$, a network consists of 1 million nodes.

The question may arise, whether we need massively parallel computers with thousands of nodes or millions of nodes. The answer is 'yes'. Solving the most challenging problems in many areas of science and engineering, such as defense (maintaining national security), aerospace (space exploration and shuttle operation), disaster management (recovering from natural disaster), and weather forecasting (predicting and tracking severe weather), requires teraflop performance for more than a thousand hours at a time. This is why, in the near future, we will need computer systems capable of computing at the tens of petaflops level or even exaflops level. To achieve this level of performance, we need MPC system with thousands or millions of nodes.

III. ADDRESSING OF NODES

Base-4 numbers are used for convenience of address representation. As seen in Figure 1(a), nodes in the BM are addressed by two digits, the first representing the row index and the next representing the column index. More generally, in a Level-L STTN, the node address is represented by:

$$\begin{aligned} A &= A^L A^{L-1} A^{L-2} \ldots \ldots \ldots A^2 A^1 \\ &= a_{n-1}\, a_{n-2}\, a_{n-3} \ldots \ldots .. a_2\, a_1\, a_0 \\ &= a_{2L-1}\, a_{2L-2}\, a_{2L-3}\, a_{2L-4} \ldots \ldots .. a_3\, a_2\, a_1\, a_0 \\ &= (a_{2L-1}\, a_{2L-2})\, (a_{2L-3}\, a_{2L-4}) \ldots \ldots (a_3\, a_2)(a_1\, a_0) \qquad (1) \end{aligned}$$

Here, the total number of digits is $n = 2L$, where L is the level number. A^L is the address of level L and left $(a_{2L-1}a_{2L-2})$ is the co-ordinate position of Level-(L-1) for Level-L network. Pairs of digits run from group number 1 for Level-1, i.e., the BM, to group number L for the L-th level. Specifically, l-th group $(a_{2L-1}a_{2L-2})$ indicates the location of a Level-(l-1) subnetwork within the l-th group to which the node belongs; $1 \leq l \leq L$. In a two-level network the address becomes $A = (a_4\, a_3)\, (a_1$

a_0). The first pair of digits (a_4 a_3) identifies the BM to which the node belongs, and the last pair of digits (a_1 a_0) identifies the node within that BM.

The assignment of inter-level ports for the higher level networks has been done quite carefully so as to minimize the higher level traffic through the BM. The address of a node n^1 encompasses in BM_1 is represented as $n^1 = (a^1_{2L-1}a^1_{2L-2} \ldots\ldots\ldots\ldots a^1_3a^1_2a^1_1a^1_0)$. The address of a node n^2 encompasses in BM_2 is represented as $n^2 = (a^2_{2L-1}a^2_{2L-2} \ldots\ldots\ldots\ldots a^2_3a^2_2a^2_1a^2_0)$. The node n^1 in BM_1 and n^2 in BM_2 are connected by a link if the following condition is satisfied.

$$\exists i\{a_i^1 = (a_i^2 \pm 1) mod\ 2^m \wedge \forall_j (j \neq i \rightarrow a_j^1 = a_j^2)\} \quad \text{where } i, j \geq 2 \qquad (2)$$

IV. ROUTING ALGORITHM FOR STTN

Routing of messages in the STTN is performed from top to bottom as in TTN [10]. That is, it is first done at the highest level network; then, after the packet reaches its highest level sub-destination, routing continues within the subnetwork to the next lower level sub-destination. This process is repeated until the packet arrives at its final destination. When a packet is generated at a source node, the node checks its destination. If the packet's destination is the current BM, the routing is performed within the BM only. If the packet is addressed to another BM, the source node sends the packet to the outlet node which connects the BM to the level at which the routing is performed.

```
Routing TTN(s,d);
source node address: s_{2L-1}, s_{2L-2}, s_{2L-3}, ..., s_1, s_0
destination node address: d_{2L-1}, d_{2L-2}, d_{2L-3}, ..., d_1, d_0
tag: t_{2L-1}, t_{2L-2}, t_{2L-3}, ..., t_1, t_0
  for i = 2L - 1 : 2
    if {(d_i - s_i + 2^m) mod 2^m} <= 2^m/2 then routedir = positive;
        t_i = {(d_i - s_i + 2^m) mod 2^m};
    else routedir = negative;
        t_i = {2^m - (d_i - s_i + 2^m) mod 2^m}; endif;
    g = get_group_number(s, d, routedir);
    while (t_i ≠ 0) do
      if (i mod 2) = 0, then
          outlet_node_x = outlet_x(g, ⌊i/2 + 1⌋, H, routedir);
          outlet_node_y = outlet_y(g, ⌊i/2 + 1⌋, H, routedir); endif;
      if (i mod 2) = 1, then
          outlet_node_x = outlet_x(g, ⌊i/2 + 1⌋, V, routedir);
          outlet_node_y = outlet_y(g, ⌊i/2 + 1⌋, V, routedir); endif;
       BM_Routing(outlet_node_x, outlet_node_y)
       if (routedir = positive), move packet to next BM; endif;
       if (routedir = negative), move packet to previous BM; endif;
       if (t_i > 0), t_i = t_i - 1; endif;
       if (t_i < 0), t_i = t_i + 1; endif;
     endwhile;
  endfor;
    BM_Routing(t_y, t_x)
end
BM_Routing (t_1, t_0);
BM_tag t_1, t_0 = receiving node address (r_1, r_0) - destination (d_1, d_0)
  for i = 1 : 0
    if (t_i > 0 and t_i ≤ 2^{m-1}) or (t_i < 0 and t_i = -(2^m - 1)), movedir = posi
    if (t_i > 0 and t_i = (2^m - 1)) or (t_i < 0 and t_i ≥ -2^{m-1}), movedir = nega
    if (movedir = positive and t_i > 0), distance = t_i; endif;
    if (movedir = positive and t_i < 0), distance = 2^m + t_i; endif;
    if (movedir = negative and t_i < 0), distance = t_i; endif;
    if (movedir = negative and t_i > 0), distance = -2^m + t_i; endif;
 endfor
  while(t_1 ≠ 0 or distance_1 ≠ 0) do
    if (movedir = positive), move packet to +y node; distance_1 = distance_1
    if (movedir = negative), move packet to -y node; distance_1 = distance_1
  endwhile;
```

Fig. 2. Routing algorithm of the STTN

Due to simplicity and fast routing, we have considered the dimension order routing algorithm for the STTN. At each level, vertical routing is performed first. Once the packet reaches the correct row, then horizontal routing is performed. Routing in the STTN is strictly defined by the source node address and the destination node address. Let a source node address be s = (s_{2L-1}, s_{2L-2}), (s_{2L-3}, s_{2L-4}), ... , (s_3, s_2), (s_1, s_0), a destination node address be d = (d_{2L-1}, d_{2L-2}), (d_{2L-3}, d_{2L-4}), ... ,(d_3, d_2),(d_1, d_0), and a routing tag be t = (t_{2L-1}, t_{2L-2}), (t_{2L-3}, t_{2L-4}), ... , (t_1, t_0), where t_i=d_i-s_i. Figure 2 shows the routing algorithm for the STTN. The function *get_group_number* gets a group number. Arguments of this function are s, d, and routing direction. Each free-link is labeled as (g,l,d,δ), where $2 \leq l \leq L$ is the level, d ∈ {V,H} is the dimension, and δ ∈ {+,-} is the direction. The functions outlet_x and outlet_y results the outlet node of the BM for higher level.

V. STATIC NETWORK PERFORMANCE

Although the actual performance of a network depends on many technological and implementation issues, several topological properties and performance metrics can be used to evaluate and compare different network topologies in a technology-independent manner. Most of these properties are derived from the graph model of the network topology. In this section, we discuss some performance metrics that characterize the cost and performance of an interconnection network. For the performance evaluation, we have considered mesh, torus, TESH network, TTN, and proposed STTN.

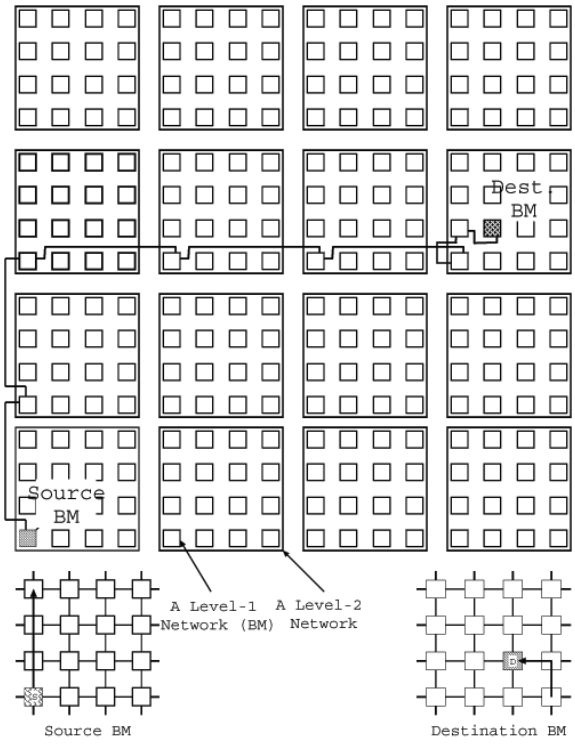

Fig. 3. An example of routing algorithm of the STTN

A. NODE DEGREE

The *node degree* is defined as the maximum number of physical links emanating from a node. Since each exterior node of the BM has six links, the degree of the STTN is 6, and it is independent of network size. Constant degree networks are easy to expand, and the network interface cost of a node remains unchanged with increasing network size. The I/O interface cost of a particular node is proportional to its degree. It is shown in Table 1 that the degree of the STTN exactly equal to that of TTN and is higher than that of mesh, torus, and TESH networks.

B. DIAMETER

The *diameter* of a network is the maximum inter-node distance, i.e., the maximum number of links that must be traversed to send a message to any node along the shortest path. As a definition, the distance between adjacent nodes is unity. Diameter is the maximum distance among all distinct pairs of nodes along the shortest path. The diameter is commonly used to describe and compare the static network performance of the network's topology. Networks with small diameters are preferable. The smaller the diameter of a network, the shorter the time to send a message from one node to the node that is farthest away from it. The diameter of the STTN with q=0 is calculated using the following equations:

$$D_{STTN(m,L,0)} = D_{BM(s)} + \max \sum_{i=L}^{2} \left(D_{BM}^{level-move} + D_i \right) + D_{BM(d)}. \quad (3)$$

$D_{BM(s)}$ = 4 is the maximum number of hops from the source to the highest level outgoing node. $D_{BM}^{\text{level - move}}$ is the number of hops for the immediate lower level outgoing node. D_i is the number of hops in the Level-i routing. D_i =7 for Level-2 and Level-3 routing. D_i =13 for Level-4 and Level-5 routing, because forward and backward nodes are separated by one node-distance. $D_{BM(d)}$ = 4 is the maximum number of hops from the incoming nodes of destination BM to the destination. $D_{BM(s)}$ and $D_{BM(d)}$ are the diameter of a $(2^m \times 2^m)$ torus network.

We have evaluated the diameter of the STTN, TTN, and TESH network by simulation and mesh and torus network by their static formula and the result is plotted in Fig. 4. Clearly, the STTN has a much smaller diameter than TESH, torus, and mesh networks. And it is slightly higher than that of TTN. However, it is shown that the difference is diminishing with the increase of number of nodes.

C. COST

Inter-node distance, message traffic density, and fault-tolerance are dependent on the diameter and the node degree. The product (diameter × node degree) is a good criterion for measuring the relationship between cost and performance of a multiprocessor system [3]. An interconnection network with a large diameter has a very low message passing bandwidth, and a network with a high node degree is very expensive. In addition, a network should be easily scalable; there should be no changes in the basic node configuration as we increase the number of nodes. The cost of different networks is plotted in Fig. 5, and it is shown that the cost of STTN is far lower than that of mesh and torus networks, and slightly higher than that of TTN and TESH networks.

D. AVERAGE DISTANCE

The *average distance* is the mean distance between all distinct pairs of nodes in a network. A small average distance results small communication latency, especially for distance-sensitive routing, such as store and forward. But it is also crucial for distance-insensitive routing, such as wormhole routing, since short distances imply the use of fewer links and buffers, and therefore less communication contention. We have evaluated the average distances for STTN, TTN, and TESH network by simulation and mesh and torus networks by their corresponding formulae and the result is plotted in Fig. 6. It is shown that the average distance of the STN is remarkably lower than that of TESH network, and far lower than that of mesh and torus networks. With large number of nodes, i.e., 2^{20} = 1 million nodes, the average distance of the STTN is lower than that of its rival TTN. Although the dynamic communication performance of a program on a multicomputer depends on the actual times taken for data transfer, a smaller average distance and diameter of an interconnection network yields a smaller communication latency of that network.

E. BISECTION WIDTH

The *Bisection Width (BW)*of a network is defined as the minimum number of links that must be removed to partition the network into two equal halves. Many problems can be solved in parallel using *binary divide-and-conquer*: split the input data set into two halves, and solve them recursively on both halves of the interconnection network in parallel, then merge the results from both halves into the final result. Small bisection width implies low bandwidth between the two halves, and it can slow down the final merging phase. On the other hand, a large bisection width is undesirable for the VLSI design of the interconnection network, since it implies a lot of *extra chip wires*, such as in hypercube [6]. The bisection width of the STTN(m, L, q) is given by:

$$BW_{STTN(m,\ L,\ q)} = 2^m \times 2^{\{2m(L-1)-1\}} \times 2 = 2^{m(2L-3)+1} \quad (4)$$

It is calculated by counting the number of links that need to be removed to partition the highest level (Level-L) torus network. We have calculated the average distance of STTN, TTN, TESH, mesh, and torus networks by their respective static formula and it is here

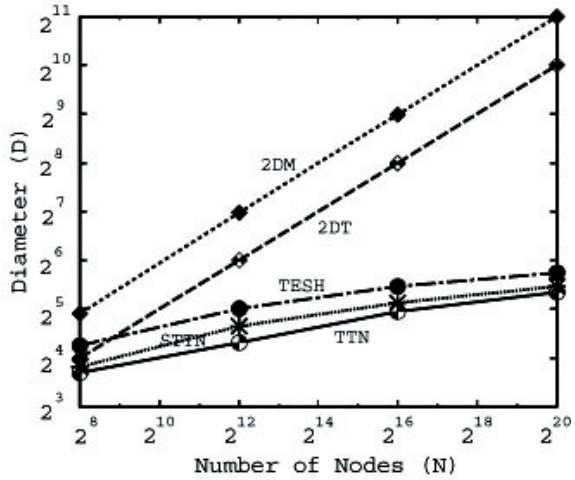

Fig. 4. Diameter of networks as a function of No. of nodes (N).

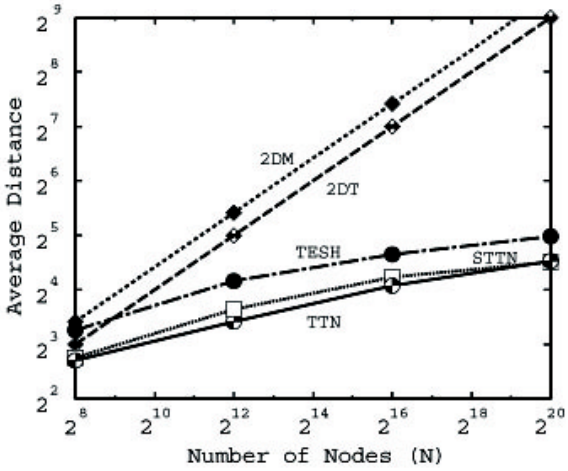

Fig. 6. Average distance of networks as a function of No. of nodes (N)

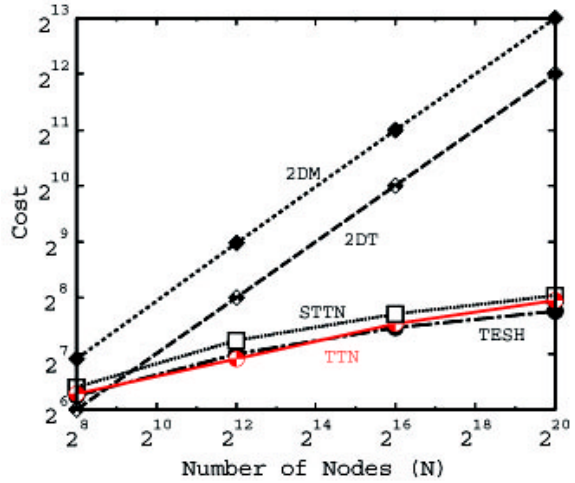

Fig. 5. Cost of networks as a function of No. of nodes (N).

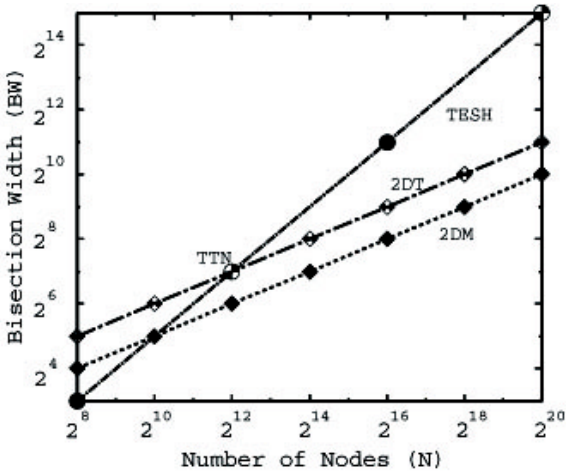

Fig. 7. Bisection Width of networks as a function of No. of nodes (N)

plotted in Fig. 7. It is shown that the bisection width of the STTN is exactly equal to that of the TTN and TESH network. And after 4096 node, it is higher than that of conventional mesh and torus networks.

F. ARC CONNECTIVITY

Arc Connectivity measures the robustness of a network. It is a measure of the multiplicity of paths between processors. Arc connectivity is the minimum number of links that must be removed in order to break the network into two disjoint parts. High arc connectivity improves performance during normal operation by avoiding link congestion, and also improves fault tolerance. The ratio between arc connectivity and the degree of a node gives a measure of static fault tolerance performance. A network is maximally fault-tolerant if its connectivity is equal to the degree of that network. The arc connectivity of various networks is shown in Table 1. Clearly, the arc connectivity of the STTN is exactly equal to that of TTN and torus network and higher than that of the mesh and TESH networks. However, the arc connectivity of the torus network is exactly equal to its degree. Thus, torus is more fault tolerant than all the networks. STTN is exactly equal fault tolerant to that of TTN and more fault tolerant than mesh and TESH networks.

Table 1. Comparison of degree and arc connectivity for various networks

	2DM	2DT	TESH	TTN	STTN
Degree	4	4	4	6	6
Arc Connectivity	2	4	2	4	4

The operating speed of a network is limited by the

corresponding physical length of links. With 2D-planar implementation, the maximum lengths of Level-2 and Level-3 STTN are 12 and 48, respectively. These are the wrap-around links of the higher level interconnection. The BM of STTN is a 2D-torus network. Thus, we need some more medium length links whose length is 2^m-1. The main demerit of STTN is that we need some medium and high length links. However, this cost yields better performance. To overcome this problem, we have kept in mind as future work, the replacement of the electronic links by optical links, i.e., to study the architecture and performance of opto-electronic-STTN or hybrid-STTN.

VI. CONCLUSION

A new hierarchical interconnection network, called **S**ymmetric **T**ori connected **T**orus **N**etwork (**STTN**), is proposed for the high performance MPC systems. The architecture of the STTN, addressing of nodes, and routing of messages were discussed in detail. We have evaluated the static network performance of the STTN, as well as that of several other interconnection networks. From the static network performance, it has been shown that the STTN possesses several attractive features, including constant node degree, small diameter, low cost, small average distance, better bisection width, and better fault tolerant performance. The diameter and average distance of the STTN is lower than that of TTN, TESH, torus, and mesh networks for very large size network. STTN is equal fault tolerant to that of TTN and more fault tolerant than mesh and TESH networks. The STTN yields better static network performances with reasonable cost for a network consist of millions of nodes, which are indispensable for next generation high-performance MPC. Therefore, STTN would be a good choice of an interconnection network for millions of nodes.

This paper focused on the architectural structure and static network performance. Issues for future work include the following: (1) evaluation of dynamic communication performance using dimension order routing and (2) assessment of the performance improvement of the STTN with an adaptive routing algorithm.

ACKNOLEDGEMENT

The authors are grateful to the anonymous reviewers for their constructive comments which helped us greatly to improve the clarity of this paper.

REFERENCES

[1] Y.R. Potlapalli, "Trends in Interconnection Network Topologies: Hierarchical Networks", *Int'1. Conf. on Parallel Processing Workshop*, 1995, pp. 24–29.

[2] A. El-Amawy and S. Latifi, "Properties and Performance of folded Hypercube", *IEEE Trans on Parallel and Distributed Systems*, Vol. 2, no. 1, 1991, pp. 31–42.

[3] J.M. Kumar and L.M. Patnaik, "Extended Hypercube: A Hierarchical Interconnection Network of Hypercube", *IEEE Trans on Parallel and Distrib. Systems*, vol. 3, no. 1, 1992, pp. 45-57.

[4] N.F. Tzeng and S. Wei, "Enhanced Hypecube," *IEEE Trans. on Computers*, vol. 40, no. 3, 1991, pp. 284-294.

[5] S.G. Ziavars, "A Versatile Family of Reduced Hypercube Interconnection Network", *IEEE Trans on Parallel and Distributed Systems,* vol. 5, no. 11, 1994, pp. 1210-1220.

[6] V.K. Jain, T. Ghirmai, and S. Horiguchi, "TESH: A new hierarchical interconnection network for massively parallel computing", *IEICE Trans. on Inf. & Syst.*, vol. E80-D, no. 9, 1997, pp. 837-846.

[7] V.K. Jain and S. Horiguchi, "VLSI Considerations for TESH: A New Hierarchical Interconnection Network for 3-D Integration", *IEEE Trans on VLSI Systems*, Vol. 6, no. 3, 1998, pp. 346–353.

[8] Y. Miura, "Wormhole Routing for Hierarchical Interconnection Networks", *Ph.D. Dissertation*, School of Information Science, JAIST, 2002.

[9] W.J. Dally, "performance Analysis of *k*-ary *n*-cube Interconnection Networks", *IEEE Trans. on Computers,* vol. 39, no. 6, 1990, pp. 775-785.

[10] M.M. Hafizur Rahman, Y. Inoguchi, Y. Sato, and S. Horiguchi, "TTN: A High performance Hierarchical Interconnection Network for Massively Parallel Computers"*, IEICE Trans. on Inf. & Syst.,* vol. E92-D, no. 5, 2009, pp.1062-1078.

[11] M.M. Hafizur Rahman, Xiaohong Jiang, and Faiz Al Faisal, "A Cost Efficient Hierarchical Interconnection Network", *Submitted in the Journal of Parallel Computing*, Elsevier, Holland, 2009.

Proceedings of 2009 12th International Conference on Computer and Information Technology (ICCIT 2009)
21-23 December, 2009, Dhaka, Bangladesh

A Recommended Market Research Based Approach for Small Software Companies for Improving Systematic Reuse Capability in Delivering Customized Software Solutions

Kiriti Prasad Choudhury, M. Rokonuzzaman†
School of Engineering & Computer Science, Independent University, Bangladesh (IUB), Dhaka, Bangladesh and Beximco Pharmaceuticals Ltd, Dhaka, Bangladesh
†School of Engineering & Computer Science, Independent University, Bangladesh (IUB), Dhaka, Bangladesh.
kpmoni@yahoo.com, zaman.rokon@yahoo.com

Abstract

Small software companies can neither be typical software product company like Microsoft, nor afford to develop each customized application for individual customer from clean slate without taking into consideration of reuse. Systematic reuse is an opportunity of continued cost reduction and quality improvement in software delivery. Small software companies in Bangladesh and the rest of the world need to exploit this opportunity to deal with ever increasing competitive market forces. Systematic reuse largely depends on the scope of delivering customized software applications in the same market segment repeatedly to multiple customers. Understanding the market for defining the generic software application concept which will be customized for meeting individual customer's demand and expectation in a profitable manner is difficult. Thorough market analysis provides basic inputs for defining generic product concept for launching customized software application for delivering services targeting suitable market segments. Choosing an appropriate market research methodology is challenging within the context where the market forces for software application are rapidly changing. And a successful new service launch around customized application delivery by targeting an attractive market segment is thought by many to be the key to business growth and profitability. The problem of establishing a successful new business around a generic software product concept is not challenging because of shortage of ideas, but rather problems exist in proper analysis of the market, studying different market segments, targeting the attractive segment, minimizing development expenses, pricing product appropriately, adopting reuse capability for continued price reduction and quality improvement to deal with evolving market forces and marketing the new product. This paper, therefore, suggests the application of market research methodology to screen new software application ideas based on market analysis and shows how a software company can combine market research with new software product development to provide exciting customized software applications that better meet consumer requirements and make the company profitable. Both state-of-art-review and filed investigation have been performed to assess global as well as local practices of market research methodology in different industries including the software industry. Upon analysis of review outputs and field level investigation findings, a set of recommendations for practicing market research methodology for small software companies have been derived for improving systematic reuse based sustained capability improvement in delivering customized software applications in attractive market segments in an increasing profitable manner.

Keywords: Software reuse, Systematic reuse capability, Software market research, Product-Line approach, Domain-specific Engineering, Small software companies, and Customized applications.

I. INTRODUCTION

Small software companies need to have business vision and strategy. Creating a vision for the company is very important, a vision which is long lasting, ambitious, motivating and make the company profitable. In today's competitive software industry, it is difficult for small software companies to make business as they work under severe limitations: mainly lack of sufficient resources and lack of robust processes. They have temptation to start work without preparation. These companies have traditional attitudes to run for projects neither considering domain specialization nor reuse capabilities. These small companies are building a series of software applications, but not using the product-line approach. Huge engagement with different types of projects without defined process and adequate resources simply produce significant wastes. Project managers take shortcuts to accommodate project schedule and they are frustrated at the amount of repeated work and wasted effort that is occurring among these projects.

Systematic reuse is an important issue in software engineering for increasing productivity and improving quality significantly [3]. Still today, it is a research topic but already accepted as a source of huge benefits, when systematic and disciplined approach is introduced in the software engineering process.

Software product lines are rapidly emerging as a viable and important software development paradigm allowing companies to realize order-of-magnitude improvements in time to market, cost, productivity, quality, and other business drivers. Software product line engineering can also enable rapid market entry and flexible response, and provide a capability for mass customization. Suc-

978-1-4244-6283-4/09/$26.00 ©2009 IEEE

cessful adoption of software product line practice is a careful blend of technological, process, organizational, and business improvements [3].

Small Software companies need to select attractive market segment of certain application domain [10] to improve their reuse capability, and to reduce both defect and rework. Problem is to select the business area targeting lucrative market segment. They need to have adequate market information to select the product-line or services that create value but the perception of value is a subjective one, and what customers' value this year may be quite different from what they value next year. Analysis is required to determine present market demand and how the reusability can take place for reducing the cost of delivery to meet that evolving demand.

II. APPROACH AND METHODOLOGY

Market Analysis for software product is the process of analyzing the market for its current and future trends. It is required to identify market demand through market needs, satisfaction issues, analysis of rival products, their features, current and future market trends. This approach would help the software firms to identify attractive market segment. It will help to predict behavior and demand forecasts for software products. Small software companies can select domain after analyzing market data to establish reuse based software business. Reuse of software product means software component reuse, asset reuse, architecture/design reuse as well as requirements reuse.

To identify present market scenario, market demand and challenges, key informant interviews are performed with both business experts and IT professionals, who have years of experience in their respective fields. The interview responses are recorded by taking detailed notes for each of the questions. Immediately after each interview, time was taken to review the manually written notes and fill in any required details. The respondents included business experts, project mangers, software engineers, developers, software consultants and researchers in a variety of industries, including software firms, pharmaceuticals, distribution agents and other manufacturing companies. A comprehensive analysis is done to determine the present domestic software market in Bangladesh. Data are collected from internet sources, industry experts and surveys in this study.

Selecting a prospective domain will boost reuse opportunity. Reusability will reduce the overall engineering effort required to produce and deliver similar software systems. It will increase business opportunity by improving systematic reuse capability. After delivery of the first project, when it is required to build another software application for the same domain, developers can reuse previously developed work products to minimize total time of delivery, cost and overall effort.

III. SOFTWARE REUSE – A SIMPLE IDEA BUT COMPLEX IN PRACTICE

An established definition of software reuse is the process of creating software systems from predefined software components. It is based on a simple and well-known idea. The most common type of reuse is the reuse of source code, but other artifacts or intermediate work products produced during the software development process can also be reused. Reusable software items are called reusable assets. These assets may be software designs, requirements, test cases, architectures, models, design patterns, use cases business processes, code-components etc.

Potential benefits of software reuse include reduced effort to build software systems, reduced time-to-market, increased quality such as robustness and decreased effort used for maintaining software [2]. Benefit of reuse cannot be achieved at the first project. It is a long-term investment but it increases company's assets. In addition to development and operational benefits, reuse may support strategic opportunity to lead the market, or the flexibility to respond to competitive forces and changing market conditions.

Software reuse has quite significant benefits but this simple idea is quite complex in practice [6]. It is not enough to gather interesting pieces of software into a library and offer them to people to reuse. Components have to be carefully designed and carefully developed so that they are of high quality and work well together. They have to be documented well so that re-users can understand them properly. Components have to be carefully chosen so that this extra investment will be repaid by significant reuse. This strategy works best when reusing components between members of a product line or product family [6].

IV. WORK BREAKDOWN STRUCTURE (WBS) AND REUSE

The Work Breakdown Structure (WBS) defines the work scope of a project. To understand the detailed work of any project, Work Breakdown Structure (WBS) is the best way to break the project down into the major phases, deliverables, and work products that need to be built. These work products can then be broken down into components that are required to build through activities.

Systematic approach of project management through work breakdown structure (WBS) makes structuring and reuse of software assets easy. WBS increases traceability. It makes easier to develop similar type of projects in a same domain. An effective WBS clearly describes what the project team intends to acquire from the repository and how to reuse it productively.

Product line engineering is done by exploiting commonalities among similar systems that have some variable characteristics. Such a set of systems is called a product family. The underlying idea of this is to build a reuse

infrastructure. Here the products are assembled from generic reusable assets, making software development more a matter of instantiation and composition of pre-built assets (work products). Work break down structure needs to represent the different project tasks/processes [7], their deliverables/products and their sequence. Thus, it will be easier to find and modify reusable assets from the repository. Development and maintenance of the products can be centralized by maintaining the reusable assets.

V. DOMAIN ANALYSIS FOR THE REUSE IN SOFTWARE DEVELOPMENT

Domain analysis is a good practice to develop efficient component-based software system to maximize reuse of diverse software assets including code, minimize code duplication, and create enhanced software quality in a substantially reduced development timeframe. Feature Oriented Domain Analysis (FODA) is a domain analysis and engineering technique, which focuses on developing reusable assets [9]. Small software companies can concentrate on domain analysis to improve reuse capabilities significantly as it helps to build reusable elements' library, systematically construct and improve reusable elements, and decrease adaptation costs.

This document is presenting a sample analysis on domain specific software business. Here in Fig 1, an attempt is taken to determine whether the product will fit within the overall mission and strategy of developing profitable software business.

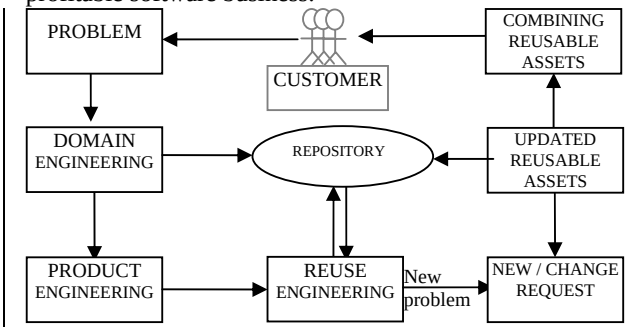

Fig 1: Systematic reuse for customized software solutions

Customer's satisfaction issues and the features they deserve from a new software product is analyzed to get envisioned product features. To elicit customers requirements, questions were asked to rate criteria: cost of new software product, how much new system can add value, beautification of software, user friendliness, matched with existing process, usage of new technology, reduce paper work, data sharing, reduce repeated work, faster performance, customized report availability, data security, access control, data accuracy and smooth operation.

VI. VALIDATING A MARKET ANALYSIS APPROACH TO SELECT A PROFITABLE DOMAIN

The world software industry and associated markets were estimated to be worth US$1300 in 2005 [11]. Facing present global financial crisis, the global software industry continued its progress. The market demands have significant changes, but demand for software products and services are increasing.

Market size of the total ICT industry in Bangladesh is estimated to be approximately BDT 1,100 crores (excluding the telecom sector). Of the total ICT market, production capacity of the local software industry is about BDT 170 crores (BASIS, 2006) but total demand for software in the local market is worth over BDT 300 crores and it is increasing day by day.

To enter in the market, here it is required to analyze the data taken earlier regarding market size, growth rate, segment and target customers. Before entering in the market, porters five force model can be verified, this is given below in Fig. 2

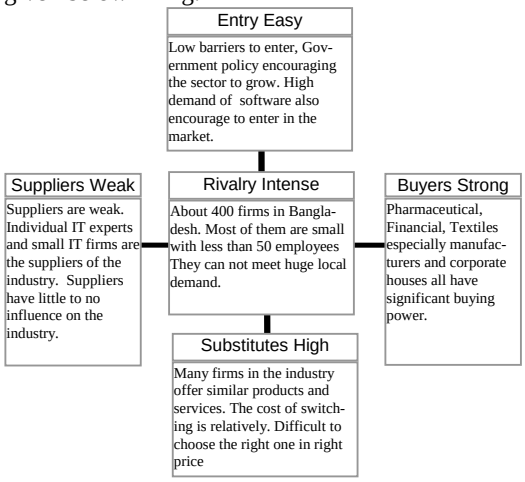

Fig 2: Porter's five forces in the software industry of Bangladesh

A large number of firms in the industry offer similar software products and services. Identified Bangladeshi software companies' competitive advantages are: low labor cost, high programmer productivity, widespread knowledge of English, the availability of a wide range of hardware platforms, existence of experienced software professionals and existence of experienced domain experts. Software is a knowledge based industry and only input required by the industry is the human effort. Computer Science and related schools are supplier to the industry. Suppliers have little bargaining power but bargaining power of customers in this industry is high because customers can find alternative sellers easily. Rivalry in the software industry is intense. There is no clear market leader with all the characteristics of a perfectly competitive market with a large number of firms and intense competition. Even though demand for customized software is growing rapidly, competition con-

tinues to be fierce as more firms enter the market. Products and services of competitors are so weakly differentiated that customers incur low costs in switching from one brand to another resulting in increased competition among firms [4].

It is found that entry of this market is easy. Software company's competitive advantages are strongly positive, suppliers are weak, and buyers are strong. In order to get the product based scenario, questions were asked earlier and after getting the answers from these questionnaires: Is it possible to select product to be lunched and proposed product's key performance indicators will be decided? While screening product idea, surveyed data are analyzed. This study is performed on a number of industries like garments, consumer product and pharmaceuticals industries; marketing experts of those industries are interviewed. After quantitatively analyzing their answers and feedback, essential features are identified and primary requirements are captured.

Price is not the main issue while purchasing a new product. Customers are aware of the features of proposed product and how much value the new product can add. Customers will not hesitate to pay if they are benefited from the purchased product. After conducting a market research on this segment, the following business sectors are found and can be deployed: For Product Distribution System, Table I show the prospective market size in the next 3 years in Bangladesh:

Table I PDS market size

SN	Industry	Number of Prospective Customers
1	Pharmaceuticals manufacturers	120
2	FMCG manufacturers	30
3	Plastic items manufacturers	12
4	Paper stationary manufacturers:	10
5	Lather goods manufacturers	12
6	FMCG Importers in Bangladesh	15
7	Foods manufacturers	18
Total		217

Analysis of market shares for Product Distribution System (PDS) reveals that here are approximately 8% companies using their in-house developed solution, 5% of these companies are presently using this software product purchased from abroad, 4% of them are using product which is taken locally and approximately 6% companies are not interested to purchase a product right now.

During concept development, study has been made interviewing industry experts and brainstorming regarding the proposed Product Distribution System. Here a sample product concept is given below:

A manufacturing company manufactures products and delivers these products to the customers. Many times, the place of manufacturing and the place where the consumers require the products is very far away form each other. Some of the major aspects of physical distribution are: Route Plan, Transportation Management, Ensure Distribution, Warehousing and Inventory Management. The problem lies with Inventory and Warehousing.

The final product needs to be developed in several modules with various level of access control and reports which can be seen by management or concerned person from anywhere, anytime. Product Concept is discussed with industry experts and it can be tested properly. All the expected features are listed and concept of operation document is developed.

Likely selling price is estimated based upon competition and customer feedback. Then it is decided that small company should pay less than a giant. PDS's price will depend on number of distribution channels and number of sales forces in a particular company. It is found that there are companies with less than 50 sales and distribution employees whereas here in Bangladesh, there are companies with above 2000 sales and distribution employees. So, estimation is that price can be varied from 200K BDT to 5000K BDT.

Estimated sales volume is calculated based on size of the market; for first three years target customers are 217 companies. Table II and Table III show the estimated sales value and business opportunity (price in thousand BDT):

Table II Estimated sales value

Product Base	No.	Qty. Req.	Pice	Total Price
Central Office (Central System required)	1	1	100	100
Distribution chanels (each depot require their customize service available)	10	10	25	250
Sales and distribution forces (Each Sales/Distribution person requires software on their PDA/Mobile)	400	400	1	400
Average cost for PDS				750K

TABLE III Investment and revenue projection

Year	Expected Customers	Expected Revenue	Expenditure				Income / Expense
			Office Rent	Salary & Allowances	Other Investments	Total	
1	0	0	50 X 12 = 600	10 X 50 X 12 =6000	2000	8,600	(8,600)
2	60	60 X 750 = 45,000	75 X 12 = 900	20 X 50 X 12 =12,000	3000	12,900	32,100
3	157	157 X 750 = 117,750	100 X 12 = 1200	30 X 50 X 12 =18,000	4000	23,200	94,550

After 2nd year breakeven calculation (thousand BDT):
Two (2) years total expense: (8,600 + 12,900) = 21,500
Two (2) years revenue: (0+ 45,000) = 45,000
After Two (2) years accumulated Income /Expense:
Revenue – Expense = 45,000 - 21,500 = 23,500
Estimate profitability and breakeven point: Sources of expenditures are Office Rent, Utilities & Maintenance, Hardware, Equipments & Internet, Salary & Allowances, Marketing & Consultation Services, Data & Map acquisitions, Advertising and Promotions for Branding, Training & Skill set build up, Certifications etc.
Investment and Revenue Projection: Here analysis is done for investment requirement and revenue generation for next 3 years (thousand BDT) which is showed in Tab III. After analyzing investment and revenue projection [Tab III], it is found that PDS system can be a profitable business area for small software companies.

VII. IMPROVING SYSTEMATIC REUSE CAPABILITY

Small Software companies can improve their reuse capability significantly by taking the advantage of market research approach for delivering customized software solutions profitably. Market research helps identify opportunities and will minimize risk. Right product selection will be easy through market research and it is the key to get success in reuse based software business.
Domain analysis is a systematic approach to identify common and similar features. Generally, component reuse is often domain-specific [8]. So domain specific engineering is required to improve component based reusability and it can be a good opportunity to get success using this methodology. In product engineering phase, work products must be defined properly. A proper WBS is a must. Then it is required to select reusable items and design them considering present and future perspective. But selecting and developing reusable asset is more difficult than delivering non-reusable one time product. Reuse-specific processes and repository should be added [1]. Project team should concentrate not only on code reuse [14] but also reuse of designs, requirements, test cases, architectures, models, design patterns, use cases business processes etc. The market is competitive and the domain is complex, so strong leadership and empowerment of skilled architects and developers required to develop effective reusable artifact [12]. Reusable items must be developed and stored in a way thus it can be easily identified and easily readable, updateable and pluggable.

VIII. BENEFITS OF MARKET RESEARCH AND DOMAIN SPECIFIC REUSE STRATEGY

This study is an attempt to define a customize methodology to establish product-line approach for small software companies to improve systematic reuse capability. Different companies may have different type of distribution processes. Here the product PDS may need to be customized for different industries; and this product-line approach will increase reusability and profitability. Systematic reuse is an opportunity of continued cost reduction and quality improvement in software delivery. System engineer can understand requirements easily. It will be easy to discretize the project and estimate the WBS properly. All work -products will be ready and minimum effort is required to make simple changes. It can be actionable by a limited number of people and can be deliverable within the scope of the project. Small software companies should consider systematic development of reusable components and can reuse these components as building blocks to create new systems. Improved systematic reuse capability can help to retrofit from existing product to create a new product; can cut development time and costs. Thus it will increase software development productivity, and improve software system interoperability. As a whole systematic reuse produce better quality software and provide a powerful competitive advantage and it is shown in Fig. 3.

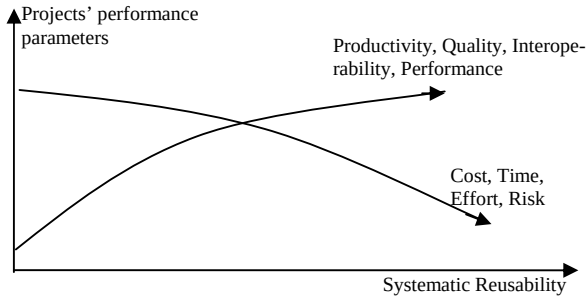

Fig 3 Benefit of systematic reusability

A defined process will help to develop a proper work breakdown structure (WBS) and improve the reusability

capacity of the firms. It will improve job division and job specialization as well as create clear and unambiguous interfaces. Through systematic reuse, value addition capacity will be high and it will force to reduce cost of delivery.

Potential benefits of systematic reuse include a reduction in development effort and cost, faster time-to market, and decreased maintenance effort. Reuse benefit measures to what extent expected benefits have materialized after the adoption of software reuse.

A marginal return from reuse in different stages of software development is showed in Fig 4:

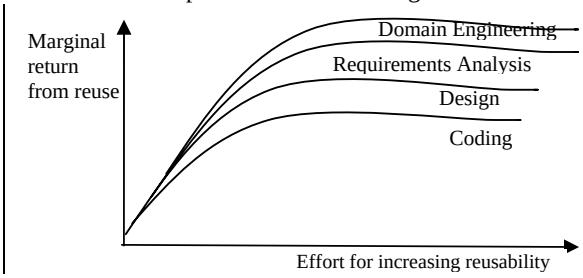

Fig 4 Marginal returns from reuse

A frequent claim is that reuse reduces the number of errors in the final product. Previously used components have already been tested. So, if an application is built from such components, the likelihood of failure is lower than in the case of building software from new untested components [13]. So Improved systematic reusability can reduce cost, time, effort, and risk; and can increase productivity, quality, interoperability and performance.

IX. SUMMARY & CONCLUSION

This study concentrated on market research approach with domain-specific engineering (DsE) methodology, which defines a methodology for the disciplined engineering of a family of similar products and reuse these work products to reduce the cost of delivery with improved quality in a predictable timeframe. This study is basically a combination of mass customizable product-line approach in a systematic reuse-driven cost reduction strategy. To establish this approach in a small company, top management commitment [5] is required. Proper market segmentation or domain analysis involves adequate resources to select prospective similar projects in a common architecture. Reuse education and training should be provided for staffs. A formal process should be established to ensure optimum reusability. But reuse capability can not be built in a day. Small companies should improve their reuse capability continuously. According to the business goal, companies should target their concentration area or market segment. After fixing a product-line approach, companies can define processes, project management methodologies, practices and work products and improve reuse capability, reduce rework and prevent defect. To assure continuous growth and improvement, small software companies can pursue systematic reuse strategy through domain-specific engineering and mass customizable product-line approach.

REFERENCES

[1] M. Morisio, M. Ezran, and C. Tully, "Success and Failure Factors in Software Reuse," IEEE Trans. Software Eng., vol. 28, no. 4, pp. 340-357, 2002.

[2] Mohagheghi P, Conradi R, Killi OM, and Schwarz H, "An Empirical Study of Software Reuse vs. Defect-Density and Stability," 26th International Conference on Software Engineering (ICSE'04).H. Poor, *An Introduction to Signal Detection and Estimation*. New York: Springer-Verlag, 1985.

[3] Software Engineering Institute - Software Product Lines; http://www.sei.cmu.edu/productlines/

[4] Syed Munir Khasru, "An Overview of the Software Industry in Bangladesh; The Cost and Management," Vol. 34 No. 6, November-December, 2006, p. 31-39

[5] T. Menzies and J. S. Di Stefano, "More Success and Failure Factors in Software Reuse", IEEE Trans. Software Eng, vol. 29, no. 5 2003.

[6] Martin L. Griss, "Systematic Software Reuse: Architecture, Process and Organization are Crucial", Fusion Newsletter, Oct 1996

[7] Joachim Bayer, Theresa Lehner, Dirk Muthig, "Product Line Engineering and Software Project Management", D. Research Report. 2006.

[8] Dr. David C. Rine, Dr. Nader Nada, "Software Reuse Manufacturing Reference Model: Development and Validation", Fairfax, VA: Survey, School of Information Technology and Engineering, George Mason University, 1998.

[9] David, M.Weiss, "Commonality Analysis: A Systematic Process For Defining Families", Lucent Technologies Bell Laboratories. 1997.

[10] Ferre, X., Vegas, S.: "An Evaluation of Domain Analysis Methods.", Proc. of 4th Int. Workshop on Evaluation of Modeling Methods in Systems Analysis and Design (EMMSAD'99), Heidelberg, Germany, 14-15 June, 1999

[11] McManus, John and Floyd, David (2005) "The global software industry". Management Services, 49 (2). pp. 26-31.

[12] Douglas C. Schmidt, "Why Software Reuse has Failed and How to Make It Work for You.", C++ Report magazine, January 1999.

[13] Marcus A. Rothenberger, Kevin J. Dooley, Uday R. Kulkarni, and Nader Nada, "Strategies for Software Reuse: A Principal Component Analysis for Reuse Practices", IEEE Trans. Software Eng, vol. 29, no 30, 2003.

[14] J. Parsons and C. Saunders, "Cognitive heuristics in software engineering applying and extending anchoring and adjustment to artifact reuse", IEEE Trans. Software Eng, vol. 30, no 12, 2004

Proceedings of 2009 12th International Conference on Computer and Information Technology (ICCIT 2009)
21-23 December, 2009, Dhaka, Bangladesh

Predictive Power of the Daily Bangladeshi Exchange Rate Series based on Markov Model, Neuro Fuzzy Model and Conditional Heteroskedastic Model

Shipra Banik, Mohammed Anwer and A.F.M. Khodadad Khan
School of Engineering and Computer Science, Independent University, Bangladesh, Dhaka, Bangladesh
banik@secs.iub.edu.bd, manwer@secs.iub.edu.bd , khoda@secs.iub.edu.bd

Abstract

Forecasting exchange rate is very important for many international agents e.g. investors, money managers, investment banks, funds makers and others. We forecasted the daily Bangladeshi exchange rate series for the period of January 1992 to March 2009 using popular non-linear forecasting models, namely Markov switching autoregressive model, fuzzy extension of artificial neural network model (ANFIS) and generalized autoregressive conditional heteroscedastic model. Our target is to investigate whether selected models can serve as useful forecasting models to find volatile and non-linear behaviors of the considered series. By most commonly used statistical measures: mean absolute percentage error, root mean square error and coefficient of determination, we found that ANFIS is a superior predictor than other two selected predictors. We believe findings of this paper will be helpful to make a wide range of policies for multinational companies who are involved with various international business activities.

Keywords: Artificial neural network models, forecasting, fuzzy logic, heteroscedasticity, Markov model, non-linearity, time series model.

I. INTRODUCTION

Exchange rate is the value of domestic currency against foreign currency, which often moves drastically because of demand and supply sides in the foreign exchange market. This generally affects multinational companies' (e.g. investors, money managers, investment banks, hedge funds and others) profit when companies involve various international business activities. For example, these types of companies have a variety of foreign-currency denominated payables, receivables, credit purchases, credit sales and others. All of these expose multinational companies to exchange rate risks and push companies to hedge against potential losses. Thus, understanding and forecasting exchange rate movements are important to a wide range of decision problems for these companies. A large amount of research ([1-6] and others) has been published in recent times and is continuing to find an optimal (or nearly optimal) prediction model for the exchange rate series. Many forecasting research ([2,7-9] and others) have shown that the behavior of exchange rate series cannot be modeled solely by linear time series models (e.g. regression model, AR(p) model, ARIMA(p,q) and others) because exchange rate nature is mostly complex (non-linear) and volatile. Therefore, developing a model for forecasting requires an iterative process of knowledge discovery, system improvement through data mining as well as trial and error experimentation. To overcome this problem, in recent years ([2,4,6,9,11] and others), we have noticed an increasing interest in modeling data as nonlinear models. This is due to the realization that these studies have revealed significant non-linear behaviors in time series data.

Various nonlinear models have been considered as alternatives to the widely used linear models. These are: (i) artificial intelligence (AI) models, including artificial neural network (ANN) model, fuzzy logic model, genetic algorithm model, hybridization of ANN and fuzzy system model (known as adaptive neuro fuzzy inference system (ANFIS)), (ii) Markov switching (MS) model, (iii) conditional heteroskedastic (CH) models and others. There is a growing interest in using AI models [1, 3-6, 8-9], MS model [2,10-11,15] and CH models [12-14] to forecast exchange rate series. The reason for this rising popularity is that these models pay particular attention to non-linearities and learning processes both of which can help to improve predictions for complex variables. For our study, we have used various models (e.g. MS model, AI model and CH model) to predict Bangladeshi exchange rates (BEXR) series in order to see whether selected models can help to raise predictive power. By analyzing applied models validity and precision, our plan is to find which model is the best to predict BEXR series.

The MS model is one of the most popular nonlinear time series model in literature, which involves

978-1-4244-6283-4/09/$26.00 ©2009 IEEE

multiple structures that can characterize time series behaviors in different regimes. By permitting switching between these structures, this model is able to capture more complex dynamic patterns. A novel feature of this model is that the switching mechanism is controlled by an unobservable state variable that follows a first-order Markov chain. In particular, the Markovian property regulates that the current value of the state variable depends on its immediate past value. As such, a structure may prevail for a random period of time and it will be replaced by another structure when a switching takes place. The most common AI model e.g. fuzzy extension of ANN, namely ANFIS is particularly useful for future predictions for variables, which is subject to non-linearities. Although ANN based models have been found to perform better compared to conventional statistical models, the main drawback of ANN models is their prediction capabilities deteriorate over a short period of time especially when data are very much chaotic. ANFIS has been proposed by many authors ([4-5, 8-9] and many others) to overcome this drawback and develop a reliable prediction of time series data. Thus, we have chosen ANFIS as an AI model to predict BEXR values.

The most successful CH models are the autoregressive conditional heteroskedasticity (ARCH) model introduced by Engle [13] and the generalized ARCH (known as GARCH) model extended by Bollerslev [14]. Engle won the Nobel Prize in 2003 for his contribution of modeling volatility in the financial time series. These models success stems from their ability to capture time-varying volatility and volatility clustering stylized facts of time series data. A time series is said to have ARCH or GARCH effect, the series is known as heteroskedastic (i.e. it's variance vary with time) otherwise homoskedastic. These types of models are widely used in empirical economics and finance. In this paper, we will investigate whether the selected models are useful tools to describe the behavior of BEXR series more efficiently. To our knowledge, forecasting daily BEXR series under the powerful nonlinear models yet not considered in literature. We have considered this project in this paper, thus we believe findings of the paper will be useful for those who are interested to make wise policies about the complex variable BEXR. The paper is organized as follows. Section 2 describes about the data set with numerical properties. The theoretical framework of considered models is reviewed in section 3. Section 4 contains experimental designs and results of the developed models. We end with some concluding remarks and some future research plans in final section.

II. DATA

The data under investigation are the daily BEXR series, over the period of January 1992 to March 2009 for a total of 6300 observations. The exchange rates are the local currency (TK) against the US dollar, collected from the site of http://ia.ita.doc.gov/exchange/bangladesh.txt. The training and testing data sets are shown in Fig. 1 and for understanding of changes, return series is depicted in Fig .2. To understand behaviors of the BEXR variable, summary statistics are reported in Table I. It is noticed that the minimum and maximun rates are 35.88 TK and 70.62 TK respectively. Mean rate is found to be 52.61 TK and SD rate is found to be 10.93 TK, which means that all times BEXR was not observed 52.61 TK (expected range: 41.68 TK to 63.54 TK). Skewed and kurtosis measures indicate that exchange rate patterns do not follow the normal distribution. More clearly, skewness (Sk) 0.15 indicates us most of days exchange rates are observed below 52.61 TK. Kurtosis 1.62 tells us exchange rates are spread in a wider fashion than the normal distribution, which means that fewer BEXR cluster near to 52.61 TK and more BEXR populate the extremes either far above or far below 52.61 TK as compared to the normal curve.

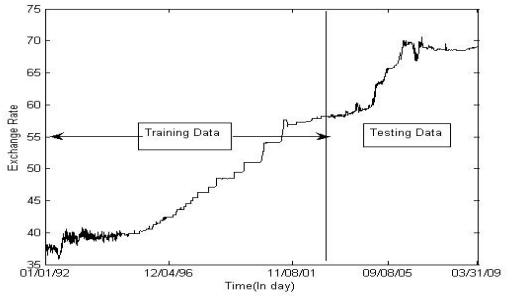

Fig. 1. Rates Bangladeshi taka

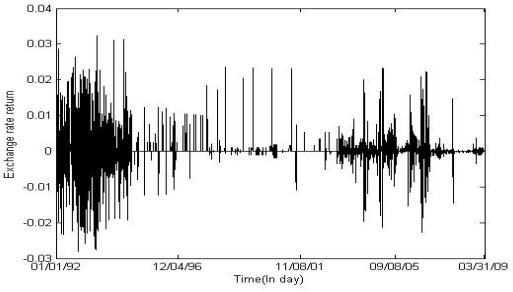

Fig. 2. The return series of BEXR

III. FORCASTING MODELS USED TO PREDICT DAILY BEXR SERIES

A. MS Model

In real world, changes in regime happen quite suddenly. For example, exchange rate appears to follow long swings. It means that rate drifts upward for a considerable period of time and then switches to a long period with downward drift. To model this dramatic change, a more practical and realistic model is the Markov switching autoregressive (MS_AR) model, developed by Hamilton [15]. This is a mixed model developed based on AR time series model and Markov model principles, which assume that regimes switching are exogenous (unknown) and there is a fixed probability for each regime changes. To understand the model clearly, consider the daily BEXR series at time t and S_t is an unobservable discrete state variable that takes values of 1 (appreciation period- an increase in the value of domestic currency relative to foreign currency) or 2 (depreciation period- a decrease in the value of domestic currency relative to foreign currency). The MS_AR model with two possible states is defined as follows:

$$BEXR_t = \alpha_{S_t} X_t + e_t, \quad S_t \in \{1,2\}, \; t = 1,2,\ldots,n$$

$$e_t \sim N(0, \sigma^2_{S_t})$$

where X_t includes an intercept (denoted by μ_i, i =1,2) and lags of the dependent variable $BEXR_t$, α_{S_t} are the parameters of lags of dependent variable $BEXR_t$ (details see section IV) and a random variable e_t with a state dependent variance $\sigma^2_{S_t}$. The changes in states are rules by transition probabilities, which is governed by a first order Markov process as follows:

$$P(S_t = 1 \mid S_{t-1} = 1) = p_{11}, P(S_t = 1 \mid S_{t-1} = 2) = p_{12},$$

$$P(S_t = 2 \mid S_{t-1} = 1) = p_{21}, P(S_t = 2 \mid S_{t-1} = 2) = p_{22}$$

with $p_{11}+p_{21}=1$ and $p_{12}+p_{22}=1$,

where p_{ij} (i=1,2 and j=1,2) are the transition probabilities for switching from one state to other state. The advantage of these transition probabilities is that they allow the series to tell the nature and incidence of significant changes. As S_t is unobserved, the parameter vector (say) $\theta = (\alpha_{S_t}, \sigma_1, \sigma_2, p_{11}, p_{12}, p_{21}, p_{22})$ is estimated by maximum likelihood method using EM algorithm developed by Hamilton [15]. Here fitted BEXR series will be calculated by the probability of S_t=1or 2 based on the observed BEXR series.

Table I Descriptive statistics of BEXR

Statistical Measures	n	Min	Max	Mean	SD	Sk	Kurtosis
	6300	35.88	70.62	52.61	10.93	0.15	1.62

B. ANFIS Model

Based on the fuzzy logic, Jang [8] introduced this model in computing literature, which is a combination of two intelligence systems: (i) neural network (NN) system and (ii) fuzzy inference system (FIS), where NN learning algorithm is used to determine parameters of FIS. NNs are non-linear statistical data modeling tools, which can capture and model any input-output relationships. FIS is the process of formulating the mapping from a given input to an output using the fuzzy logic. The process of FIS involves: i) membership functions (mfs) (ii) fuzzy logic operators and (iii) if-then-rules, where the above mapping provides a basis from which decisions can be made or patterns can be discerned. The structure of ANFIS has 5 layers: (i) 1 input layer (ii) 3 hidden layers that represents mfs and fuzzy rules and (iii) 1 output layer. The learning algorithm of ANFIS is a hybrid algorithm, which combines the gradient descent (GD) method and the least square estimation (LSE) for an effective search of parameters. ANFIS uses a two pass of learning algorithm to reduce error: (i) forward pass and (ii) backward pass. The hidden layer is computed by the GD method of the feedback structure and the final output is estimated by the LSE method (details, see [8-9]).

C. CH Model

As mentioned before, ARCH and GARCH are the most commonly used CH models to model financial time series data those exhibit time varying volatility clustering. To understand an ARCH model clearly, consider an AR(1) model:

$BEXR_t$ = Constant + $BEXR_{t-1}$+ e_t, t =1, 2, …, n

Suppose error term $e_t=\varepsilon_t\sigma_t$, where $\sigma_t = \beta_0 + \sum_{i=1}^{q} \beta_i e^2_{t-i}$ with $\beta_0 > 0$ and $\beta_i \geq 0$ (i = 1, 2, …, q) and $\varepsilon_t \sim N(0,1)$, known as ARCH process of order q.

In 1986, Bollerslev [14] improved the ARCH models by inventing the GARCH model, where the current volatility depends not only on the past errors, but also on the past volatilities. To understand it clearly, consider an AR(1) model:

$BEXR_t$ = Constant + $BEXR_{t-1}$+ e_t, t =1, 2, …, n

Suppose $e_t=\varepsilon_t\sigma_t$, where

$\sigma_t = \beta_0 + \sum_{i=1}^{q} \beta_i e^2_{t-i} + \sum_{j=1}^{p} \gamma_j \sigma_{t-j}$ with $\beta_0 > 0$, $\beta_i \geq 0$ (i =1, 2, …, q), $\gamma_j \geq 0$ (j = 1, 2, ..., p) and $\varepsilon_t \sim N(0,1)$, known as an GARCH process of orders p and q.

We have chosen GARCH as a CH model instead of ARCH because of ability of GARCH to deal with more variations than ARCH.

IV. RESULTS AND DISCUSSION

The first 4000 observations (63%) for daily BEXR series are used as the training period and the rest as the testing period (see Fig. 1). All computational works were carried out using the programming code of MATLAB (version 7.0).

A. Results

A.1 MS_AR Model

We begin by calculating the Bayesian Information Criteria (BIC) (other information criterions e.g. AIC, SIC and others can also be used) to find the number of lags to be used in the AR process for BEXR series. We found that the number of lags to be used is 4 for BEXR series. Based on this information, a MS with AR(4) model is considered and all parameters are estimated using the maximum likelihood method, which are reported in Tables IIA-IIC. These parameters estimates are used to predict daily BEXR series.

A.2 ANFIS Model

A trial and error approach is used to design the topology of ANFIS. Initially, a number of networks are trained and the error gradient was observed. Training algorithm is used to update the mfs parameters of FIS, is a hybrid rule. As a result, a decreased training error throughout the learning process is obtained. The performance of the network is evaluated by decreasing or increasing the number of inputs and the premise rules. Best performance is obtained by a network consists of: 4 inputs with 2 mfs (type Gaussian-shaped) with each input, 8 if-then fuzzy rules were learned, total parameters (44) = premise parameters (12) + consequent parameters (32), where premise parameters is calculated by # of inputs × # of mfs × # of parameters of Gaussian distribution and consequent parameters is calculated by # of mfs × # of parameters of Gaussian distribution × # of fuzzy rules. The training data was used with the MATLAB command Genfis1 in order to create a FIS (see Fig. 3 for mfs for first, second, third and fourth inputs respectively). Thus, the following ANFIS forecasting model was selected to predict daily BEXR values:

Table IIA Parameters estimates for the MS_AR(4) model for state 1

Parameters estimates	μ_1	σ_1	α_{11}	α_{12}	α_{13}	α_{14}
	0.0004 (0.0001)	0.0063 (0.0001)	-0.2062 (0.0269)	-0.1419 (0.0291)	-0.1462 (0.0296)	-0.1576 (0.0347)

Note: Standard errors are in parenthesis

Table IIB Parameters estimates for the MS_AR(4) model for state 2

Parameters estimates	μ_2	σ_2	α_{21}	α_{22}	α_{23}	α_{24}
	0.0005 (0.008)	0.0118 (0.0003)	0.1143 (0.0274)	-0.0800 (0.0402)	0.0029 (0.0610)	0.0029 (0.0610)

Note: Standard errors are in parenthesis

Table IIC Transition probability matrix

$$\begin{bmatrix} p_{11} & p_{12} \\ p_{21} & p_{22} \end{bmatrix} = \begin{bmatrix} 0.66 & 0.14 \\ 0.34 & 0.86 \end{bmatrix}$$

$$P_{5\text{th day\_BEXR}} = f(\text{Ist day\_BEXR}, \text{2nd day\_BEXR}, \text{3rd day\_BEXR}, \text{4th day\_BEXR})$$

A.3 GARCH Model

Higher order GARCH is seldom used. After having gone through pre and post analyses (using ACF, PACF, ARCH test and likelihood ratio test (estimation results are available upon request)), it was estimated that it would be good to try GARCH(2,1) model. The MATLAB output for GARCH (2,1) model is reported in Table III. Thus, the GARCH(2,1) model was used to predict BEXR series.

B. Discussion of Results

Forecasting performances are evaluated against three widely used statistical metrics, namely, Mean absolute percentage error (MAPE) =

$$\frac{1}{n}\sum_{i=1}^{n}\left|\frac{\text{Actural BEXR}_t - \text{Predicted BEXR}_t}{\text{Actural BEXR}_t}\right|$$

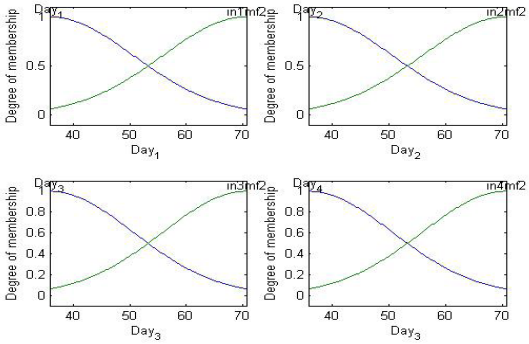

Fig. 3. Membership functions for first, second, third and fourth inputs

Root mean square error (RMSE) = $\sqrt{\frac{1}{n}\sum_{i=1}^{n}(\text{Actural BEXR}_t - \text{Predicted BEXR}_t)^2}$ and Coefficient of determination $R^2 = 1-(ESS/TSS)$, where ESS is the sum of squares of differences between actual and predicted BEXR rates and TSS is the sum of squares of actual BEXR rates. MAPE/RMSE are used to measure the accuracy of prediction through representing the degree of scatter. R^2 is a coefficient of determination measure of the accuracy of prediction of the trained network models. Smaller values of MAPE and RMSE metrics indicate higher day accuracy in forecasting. Higher R^2 values indicate better prediction. After a model is built using the training data, BEXR rate is forecasted over the test data. To compare forecasted and actual exchange rates, prediction performance is measured in terms of considered statistical metrics MAPE, RMSE and R^2 over the training and testing data. Fig. 4a to Fig. 6b presents the training and testing performance metrics graphically. In order to see how well our considered models fitted to the actual data, Fig. 7 was added, which shows the one-ahead predicted BEXR values over our considered data periods. From figures 4a, 5a and 6a, it is clear that ANFIS forecasting model is better in terms of all metrics (MAPE, RMSE and R^2), followed by the GARCH forecasting model, then the MS_AR model. In our experiment, this is consistently observed in case of testing data also (see Fig. 4b, Fig. 5b and Fig. 6b).

Table III The GARCH(2,1) model estimation results

Number of Model Parameters Estimated: 5

Parameter	Value	Standard Error	T-Statistic
Constant	1.5079e-005	1.073e-005	1.4053
β_0	2.3335e-007	2.7331e-009	85.380
β_1	0.16597	0.00366540	45.281
γ_1	0.42427	0.00072366	86.282
γ_2	0.40976	0.00120770	39.298

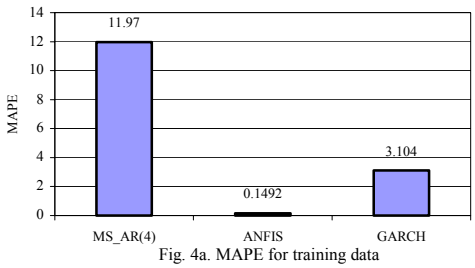

Fig. 4a. MAPE for training data

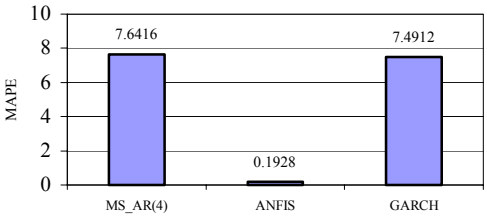

Fig. 4b. MAPE for testing data

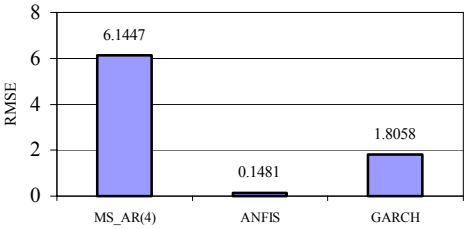

Fig. 5a. RMSE for training data

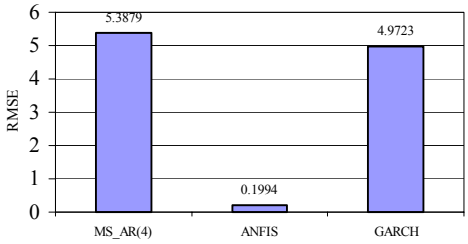

Fig. 5b. RMSE for testing data

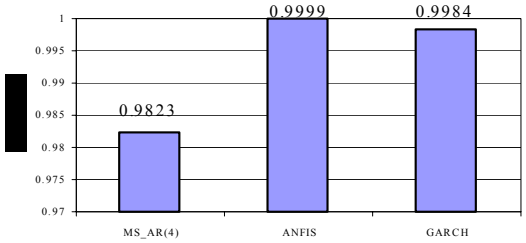

Fig. 6a. R-Square values for training data

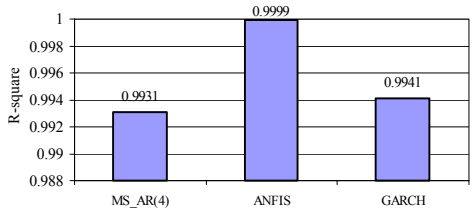

Fig. 6b. R-square values for testing data

Thus, our findings indicate us the ANFIS forecasting model is more suitable for BEXR series modeling than others. The daily actual and forecasted BEXR series for all considered models for the time period January 1992 to March 2009 are shown in Fig .7. From this figure, one can again easily imagine the superiority of the ANFIS

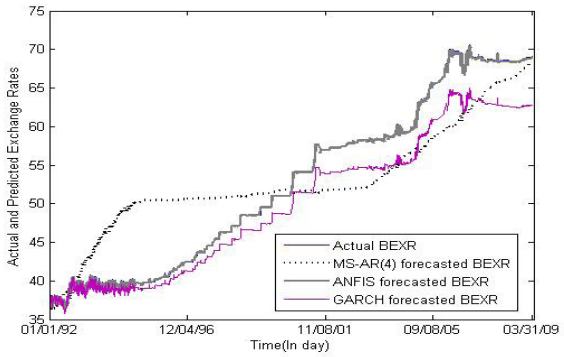

Fig. 7. Actual and predicted BEXR rates for 3 forecasting models

forecasting model over GARCH and MS_AR forecasting models.

V. CONCLUSION

In this paper, we investigated three popular forecasting models (MS_AR model, ANFIS model and GARCH model) to predict BEXR series. By nature, exchange rate is volatile and non-linear. Literature suggests that the above- mentioned popular models pay particular attention to non-linearities, which helps to improve complex data predictions. We used daily BEXR series for the period from January 1992 to March 2009. The forecasting performances of selected models are measured by commonly used measures MAPE, RMSE and R^2. Our findings suggest that the ANFIS forecasting model can forecast the daily BEXR series closely as compare to other two selected forecasting models, followed by GARCH. We believe our findings will be useful to researchers who are planning to make wise decisions with this complex variable. Our next step is to improve forecasting results using other forecasting models such as fuzzy extension of genetic algorithm model, MS-GARCH model etc.

REFERENCES

[1] G. Zhang, and M.Y. Hu, "Neural network forecasting of the British pound/US dollar exchange rate", *International Journal of Management Science*, 26, 1998, pp.495-506.

[2] M.T. Ismail, and Z. Isa, "Modeling exchange rates using regime switching models", *Sains Malaysiana*, 35, 2006, pp.55-62.

[3] C.M. Kuan, and T. Liu, "Forecasting exchange rates using feed forward and recurrent neural networks", *Journal of Applied Econometrics*, 10, 1995, pp.347-364.

[4] V. Kodogiannis, and A. Lolis, "Forecasting financial time series using neural network and fuzzy system-based techniques", *Neural Computing & Applications*, 11, 2002, pp.90-102.

[5] F. Lisi, and R.A. Schiavo, "A comparison between neural networks and chaotic models for exchange rate prediction", *Computational Statistics & Data Analysis*, 30, 1999, pp.87-102.

[6] W.C.H. Ping-Feng, Pai, L. Chih-Shen, and C.T. Chen, "A hybrid support vector machine regression for exchange rate prediction", *Information and Management Sciences*, 17, 2006, pp.19-32.

[7] H.H.Tae, and E. Steurer, "Exchange rate forecasting: Neural networks vs. linear models using monthly and weekly data", *Neurocomputing*, 10, 1995, pp.323-339.

[8] J.S.R. Jang, "ANFIS: Adaptive-network-based fuzzy inference systems", *IEEE Transactions on Systems, Man, and Cybernetics*, 1993, pp.665-685.

[9] S. Banik, F.H. Chanchary, K. Khan, R.A. Rouf, and M. Anwer, "Neural network and genetic algorithm approaches for forecasting Bangladeshi monsoon rainfall", *Proceedings of 11th ICCIT*, 2008, pp.735-740.

[10] C. Engel, and J.D.Hamilton, "Long swings in the dollar: Are they in the data and do markets know it?", *American Economic Review*, 80, 1990, pp.689-713.

[11] M. Dueker, and C.J. Neely, "Can Markov switching models predict excess foreign exchange returns?" *Journal of Banking and Finance*, 31, 2007, pp.279-296.

[12] R. Baillie, and T. Bollerslev, "Intra-day and inter-market volatility in foreign exchange rates", *Review of Economic Studies*, 58, 1991, pp.565-585.

[13] R.F. Engle, "Autoregressive conditional heteroscedasticity with estimates of the variance of UK inflation", *Econometrica*, 50, 1982,pp.987-1008.

[14] T. Bollerslev, "Generalized autoregressive conditional heteroskedasticity", *Journal of Econometrics*, 31, 1986, pp.307-327.

[15] J.D. Hamilton, "A new approach to the economic analysis of non-stationary time series and the business cycle", *Econometrica*, 57, 1989, pp.357-384.

Proceedings of 2009 12th International Conference on Computer and Information Technology (ICCIT 2009)
21-23 December, 2009, Dhaka, Bangladesh

An Extendible Data Structure for Handling Large Multidimensional Data Sets

K. M. Azharul Hasan†, Kamrul Islam†, Mojahidul Islam†, Tatsuo Tsuji‡

† Computer Science and Engineering Department, Khulna University of Engineering and Technology, Khulna 9203, Bangladesh

‡Department of Information Science, University of Fukui, Japan

azhasan@cse.kuet.ac.bd, polash_2k4@yahoo.com, shahin047@yahoo.com, tsuji@pear.fuis.fukui-u.ac.jp

Abstract

Multidimensional array is widely used in large number of scientific research and engineering applications for handling large multidimensional data. There exist many data structures to represent multidimensional data. But most of these data structures are static (such as traditional multidimensional array) and can not handle the dynamic extension or reduction of the array. The Traditional Multidimensional Array (TMA) is efficient in terms of accessing the elements of the array by random computing the addressing function but TMA is not extendible during run time. In this paper we propose a new scheme, Karnaugh Representation of Extendible Array (KEA), to represent the multidimensional data. The main idea of this scheme is to represent n dimensional array by a set of two dimensional extendible arrays. The scheme can be extended in any direction during run time. To evaluate our proposed scheme, we implement and compare with the existing systems for different operations with the Traditional Multidimensional Array (TMA), and Traditional Extendible Array (TEA). Our experimental result shows that the KEA scheme outperforms TMA and TEA.

Keywords: Multidimensional Array, Karnaugh Map, Extendible Multidimensional Array, Range Query, Time and storage cost.

I. INTRODUCTION

Large multidimensional arrays are widely used in scientific, statistical and engineering applications. Arrays are among the best understood and most widely used data structures. Few classes of data structures are as well understood or as widely used as arrays. Conventional schemes for storing multidimensional arrays do not support dynamic extension of an array and hence addition of a new column value is impossible if the size of the dimension overflows. But to be able to acquire the benefit of the fast random accessing capability inherent in the multidimensional array, contiguous storage should be allocated for all of the array elements. One striking deficiency in current techniques for handling arrays is the poor handling of flexibility and extendibility of arrays [1]. In this paper, a new scheme for implementing extendible array is presented. There are many existing array systems to represent multidimensional data such as Traditional Multidimensional Array (TMA) [2][3], Extended Karnaugh Map Representation (EKMR) [2][3], Traditional Extendible multidimensional Array (TEA) [4][5]. TMA is a good storage for storing multidimensional data set. One serious drawback of TMA is that it is not dynamically extendible [1]. To insert a new column value in the TMA total reorganization of the array is necessary which causes huge cost. Extended Karnaugh Map Representation (EKMR) represents *n* dimensional data by a set of two dimensional arrays [2]. But EKMR is not dynamically extendible. Traditional Extendible Array (TEA) has the property of extendibility and represents *n* dimensional data using *n* dimensional array [4][5]. An extendible array can extend in any direction without reallocating the data already stored. Such advantages make it possible to employ the TEA in wide area of applications like relational database [6], Data warehousing [1], Scientific and Statistical databases [7] and parallel and distributed database implementation [8].

In this paper, we propose a new scheme called Karnaugh Representation of Extendible multidimensional Array(KEA) for multidimensional array representation. The main idea of our proposed KEA is to represent multidimensional array by a set of two dimensional extendible arrays. This extension can be done in any direction in any time. Hence, efficient algorithms can easily be designed to represent multidimensional data set based on the KEA scheme. To evaluate our proposed scheme we have implemented and compared the result with TMA and TEA. The experimental result shows that KEA outperforms the TMA and TEA.

II. REVIEW OF EXISTING ARRAY SYSTEMS

Before presenting our proposed Karnaugh representation of Extendible multidimensional Array (KEA), we describe the TMA [2][6], EKMR [2][3], and TEA [4][5] schemes.

A. Traditional Multidimensional Array (TMA)

Traditional Multidimensional Array (TMA) is a representation scheme for multidimensional data which represent *n* dimensional data by *n* dimensional array. The TMA represent *n* dimensional data by an array cell in an *n* dimensional array. The key to the structure of arrays resides in the familiar coordinate system, which pictures an n-dimensional array as being imbedded in

the positive orthant of n-dimensional space, with array positions lay on the lattice points. An illustration of 3 dimensional TMA of dimension length 3×4×5 is given in Fig. 1.

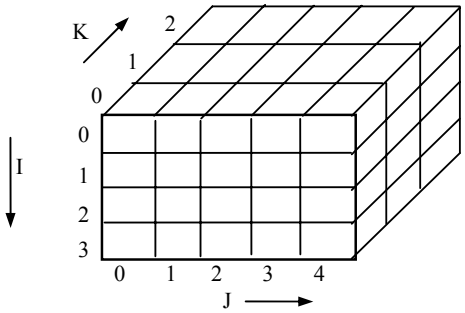

Fig. 1: A three dimensional TMA of size 3×4×5.

In the TMA scheme, a three dimensional array of size 3 × 4 ×5 can be viewed as three 4×5 two-dimensional arrays [1]. An element $(i_n,i_{n-1},\ldots i_1)$ in an n dimensional TMA of size $[s_n,s_{n-1},\ldots s_1]$ is allocated on memory using an addressing function [5]:

$f(i_n,i_{n-1},\ldots i_1)=s_1\ s_2\ldots\ s_{n-1}i_n + s_1\ s_2\ldots s_{n-2}i_{n-1} + s_1\ s_2\ldots\ s_{n-3}i_{n-2} +\ldots+ s_1i_2 +i_1$

Here $(s_1\ s_2\ldots.s_{n-1},\ s_1\ s_{2\ldots}\ s_{n-2},\ s_1\ s_{2\ldots}\ s_{n-3},\ldots,s_1)$ is called *coefficient vector.*

B. Extended Karnaugh Map Representation (EKMR)

A basic array representation scheme named Extended Karnaugh Map Representation (EKMR) is proposed in [2][3]. In this scheme, an n-dimensional array is represented by a set of 2 dimensional arrays. Fig. 2 shows an example of the EKMR system for dimension 3, i.e. EKMR(3).The idea of the EKMR scheme is based on the Karnaugh map (K-map). Consider a 3 input K-map and its corresponding EKMR(3) in Figure 2. The analogy between the EKMR(3) and the 3-input Karnaugh map is that the index variables i, j, and k correspond to the variables X, Y, and Z, respectively. Here, index variable i is used to indicate the row direction and the index variable j is used to indicate the column direction. The basic difference between TMA(3) and the EKMR(3) is the placement of elements along the direction indexed by k. The relative position makes the fundamental difference when using EKMR as array representations.

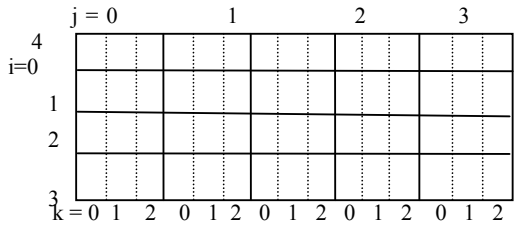

Fig. 2: An EKMR(3)

C. Traditional Extendible Array (TEA)

Conventional schemes for storing arrays do not support easy dynamic extension of an array. The Traditional Extendible Array (TEA) is another representation of multidimensional array. It has the property that the indices of the respective dimensions can be arbitrarily extended without reorganizing previously allocated elements. It is devised schemes [9] for multi dimensional storing arrays, which are readily extendible in all directions. An extendible array, however, does not store an individual array; rather, it is storing an array and all its potential extensions. Following is a short description of TEA [4]

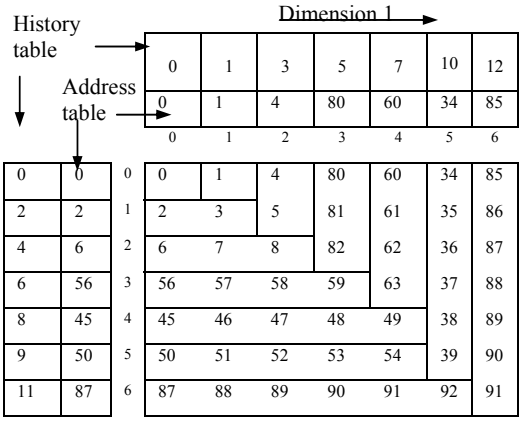

Fig. 3 : A two dimensional Traditional Extendible Array realization.

Extendible arrays are combination of subarrays. If the array is n dimensional then the subarray is n-1 dimensional. It has three types of auxiliary tables namely history table, coefficient table and address table. For each dimension these tables exist. Address table contains the first address of the subarray, history table contains the construction history of the subarrays. Coefficient table contains the coefficient of the n-1 dimensional subarrays. The coefficient vector is n-2 dimensional. In Fig. 3 the coefficient table is void because the array is 2 dimensional and the coefficient vector is zero. The extendible array can be extended in any dimension only by the cost of these three auxiliary tables.

Consider the element $<6, 2>$ in Fig.3. Compare $H_1[6]$ =12 and $H_2[2]$ = 4. Since $H_1[6] > H_2[2]$, it can be proved that the element $<6,2>$ has created as a result of extending 1st dimension and hence the element exist in the subarray having history value *12*. The offset of the element in the subarray is *2*. The corresponding first address is 95, which is stored in $L_1[6]$. Thus the element stored at the address *95+2=97*. The superiority of this scheme in element accessing speed and memory utilization is shown in [4] comparing with other schemes such as hashing [9].

III. AN IMPLEMENTATION SCHEME FOR EXTENDIBLE MULTIDIMENSIONAL ARRAY

The idea of KEA is based on Karnaugh Map(K-map). The K-map technique is used for minimizing Boolean expressions usually aided by mapping values for all possible combinations. Fig. 4 shows 3 input (Fig. 4(a)) and 4 input (Fig. 4(b)) K-map as a two dimensional array to represent possible 2^3 and 2^4 combinations respectively. In Figure 4(b) the variables w, x represents the row and the variables y, z represents the column to indicate the two dimensional array as 4 dimensional array. The array representation of K-map for 3 input and 4 input Boolean variable is shown Figure 5(a) and 5(b) respectively.

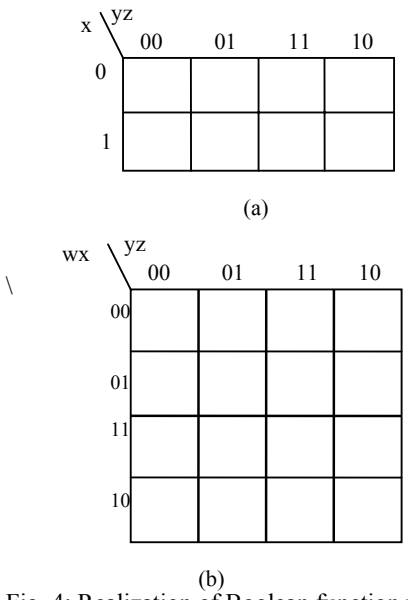

Fig. 4: Realization of Boolean function using K-map

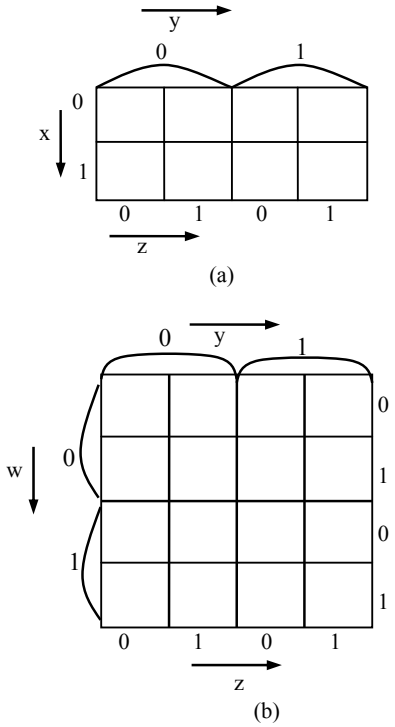

Figure 5: Realization of Boolean function using K-map

If the size of the array A is $[d_1\ d_2\ \ldots d_{n-1}\ d_n]$ and the extension dimension is i, then for extending A along i direction, subarray size can be calculated from the length of other $(n-1)$ dimensions. The size of subarray for extension along dimension i like this:

$$\textit{sub-array size}(i) = \prod_{j=1}^{n} d_j \quad j \neq i.$$

A Karnaugh representation of Extendible Array (KEA) has a history counter and three auxiliary tables, history table, address table and coefficient table. The history table stores the extension. history and the address table stores the first address of the extended subarray. The scheme is explained in the following using Fig. 6 and Fig. 7. Fig.6(a) illustrates the initial setup of the scheme. All address tables contain first address of starting coefficient value and the history counter is zero. And also the history tables contain one entry of 0. When an extension along d_4 direction is done as in Fig. 6(b), then the history counter is increased by 1. The value of history counter is stored in the history table of dimension d_4. The subarray size is calculated and the value of first address is stored in the address table of d_4 direction.

Subarray size = $d_1 \times d_2 \times d_{4=} 1 \times 1 \times 1 = 1$
History counter $= 1$
Dimension sizes: $d_1=1, d_2=1, d_3=2, d_4=1$

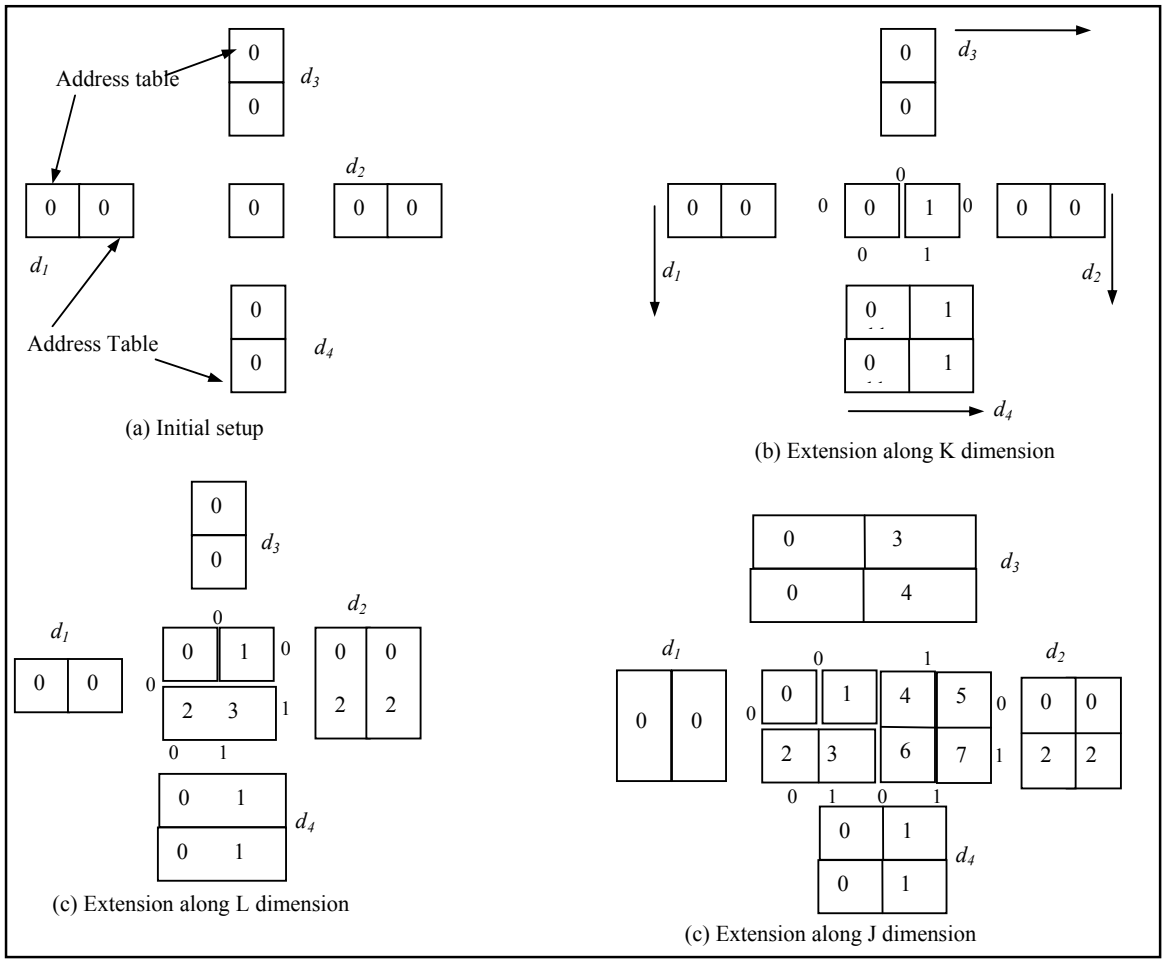

Fig. 6: The KEA scheme for extending in different dimension

Fig. 6(c) shows an extension along d_2 direction. Here the history counter again increased by 1 and this is stored in history table for dimension d_2. The number of values in the subarray is calculated using the formula and the first address for this subarray is stored in the address table for dimension d_2.

In Fig. 6(d) an extension along direction d_3 is done. So, as a result of extension history counter becomes 3 and sub-array size 4. Here, history table memorize a value of 3 in dimension d_3 and address table contain the first address of the extended subarray and it is 4. Fig. 7 shows the resulting KEA scheme after extending in the direction d_1 and d_2 consecutively

IV. PERFORMANCE RESULTS

To measure the performance of KEA we compare it with the TMA and TEA in terms of construction and retrieval cost. The experimental data are created. automatically and stored in the array in secondary storage.

A. Construction Cost

The construction cost is the cost that is needed for initializing the data structure and constructing the scheme. The construction cost is described by two parameters: memory requirement and construction time. The auxiliary tables of TEA and KEA are small and stored in main memory. And thus the storage cost for the auxiliary tables are ignored.

The memory requirement is explained with specific length of dimension along all dimensions. The construction memory needed for all schemes are shown in Fig. 8 for length of dimension *30* to *100* in all directions. As the length of dimension is same for all the schemes the array size is also the same and hence the memory requirements will be the same. If the length of different dimension is known for all schemes then storage requirement can be calculated as follows

Size of memory = $(\prod d_i) \times \lambda$ for i=1 to n

Where d_i=length of dimension i

λ = *Size of one cell in the array*

The second parameter is the construction time needed for constructing scheme with specific length in all

direction. The construction time needed are shown in Fig. 9 for all schemes for dimension length *30* to *100* in all direction.

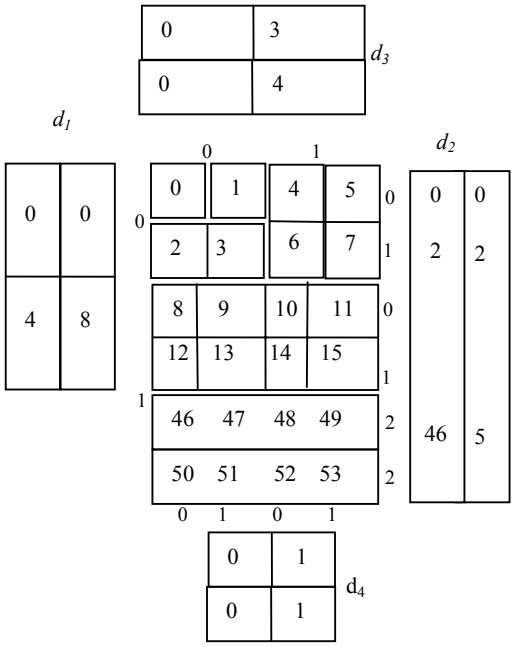

Fig. 7: The KEA scheme for extending in different dimension

The construction time shows that for small size array the time requirement is similar but for large size array the KEA and TEA scheme takes less time than TMA. This is because TMA needs more time to allocate storage when the storage size is large. On the other hand the KEA and TEA takes the size of subarrays which is smaller than that of TMA. The KEA outperforms the TEA because the subarrays are n-1 dimensional for TEA where as the subarrays are 2 dimensional for KEA as the KEA scheme is a set of two dimensional extendible arrays.

B. Retrieval Cost

For retrieval cost we have taken a partially specified query. A partially specified query [10] has a predicate of the form *column* $name_k$ *between* $value_j$ *and* $value_m$ *(* $k=1…n$, *and* $j, m \leq d_k$ *)*. The partially specified query cost is the time to access a block of data. The block is defined by defining the range value in all dimensions.

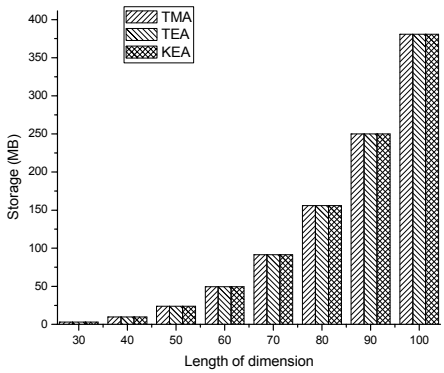

Fig. 8: Comparison among TMA, TEA and KEA for Storage Requirement.

The number of data in the defined block can be calculated as follows

$$\text{No of data in block} = \prod_{i=1}^{n} (ud_i - ld_i + 1)$$

where,

ud_i =upper limit of index along dimension *i*

ld_i =lower limit of index along dimension *i*

The retrieval cost depends on two things. One is the block size i.e. how many data have to be accessed and the other one is number of consecutive address for accessing data. If the block size is large then more time needed to query and to retrieve. If the number of consecutive address is more then less time is need to retrieve data. Fig.10 shows the experimental result for partially specified query for length of dimension 60 to 110. From the Fig. 10 it is seen that for small length of dimension KEA takes more time to search and retrieving data because here the number of consecutive address is less than the others.

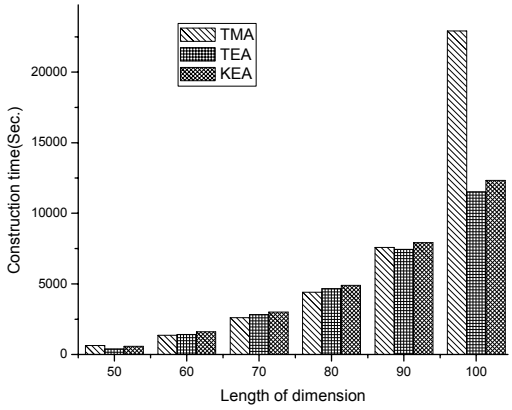

Fig. 9: Comparison among TMA, TEA and KEA for construction Time.

The KEA shows better performance than that of TEA and TMA. The array cells are organized in one stream in TMA hence the candidate records can be easily found from the addressing function but for TEA and KEA the candidate records are organized in different streams. As the subarrays are *n-1* dimensional for TEA and 2 dimensional for KEA. Hence it is necessary to calculate the addressing function for *n-1* dimensional for TEA to locate the candidate records in the array. But for KEA the calculation is simple. Hence KEA outperforms TEA. As the TEA needs to calculate an addressing function of dimension n although all the records are organized in one stream.

Finally it can be concluded that the proposed KEA scheme outperforms the TEA and TMA scheme in terms of retrieval performance.

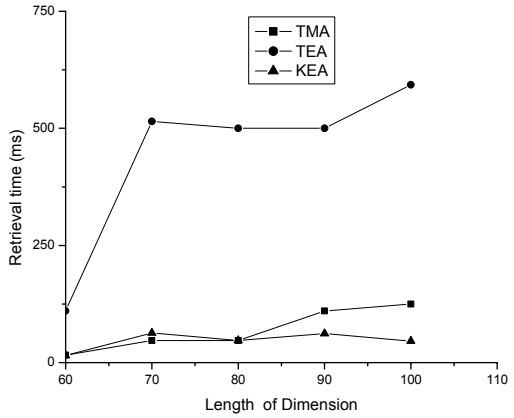

Fig. 10: Comparison among TMA, TEA and KEA in terms of Partially specified query time

V. CONCLUSION

In this paper, we have proposed a new scheme, Karnaugh Representation of Extendible Array(KEA), for multidimensional array representation. The main idea of KEA scheme is to represent multidimensional array by a set of two dimensional extendible arrays. We measure the performance of KEA with TMA, and TEA. From the experimental result we see that, construction time of KEA is greater because we need to perform some additional calculation to convert four dimensional data to two dimensional data. The retrieval cost of KEA is less than TMA, and TEA because the subarrays are 2 dimensional in KEA and also we found the facility to access consecutive address greater than that of others. So, from the experimental result we can say that the overall performance of KEA is better than that of TMA, and TEA. Throughout the paper we have used the number dimension is 4 we are developing for n dimension generalization of KEA scheme. The generalization will straight forward of having each dimension contains set of four dimensional KEA. In the future, our proposed scheme can also be extended to design an efficient method for inserting or deleting subarray at the middle of the data structure. One more important future direction is that, the scheme can be used in parallel platform. Because most of the operations described here is independent to each other. Hence it will be very efficient to apply this scheme in parallel environment.

REFERENCES

[1] K.M. Azharul Hasan, Tatsue Tsuji, Ken Higuchi, "An efficient implementation for MOLAP basic data structure and its evaluation", *DASFAA 2007, LNCS 4443, pp. 288-299, 2007.*

[2] Chun-Yuan Lin, Jen-Shiuh Liu, Yeh-Ching Chung,"Efficient Representation Scheme for Multidimensional Array Operations," *IEEE Transactions on Computers, Vol. 51, No. 3, pp. 327-354, March 2002.*

[3] Chun-Yuan Lin, Yeh-Ching Chung,Jen-Shiuh Liu, "Efficient Data Compression Methods for Multidimensional Sparse Array Operations Based on the EKMR Scheme," *IEEE Transactions on Computers, Vol. 52, No. 12, pp. 1640-1646, December 2003.*

[4] Otoo E. J and T. H. Merrett, "A storage scheme for extendible arrays". *Computing, Vol.31, pp.1-9, 1983.*

[5] A.L.Rosenberg, "Allocating Storage for Extendible Arrays". *JACM,Vol.21, 652-670, 1974.*

[6] K. M. Azharul Hasan, M. Kuroda, N. Azuma, T. Tsuji, K. Higuchi, "An Extendible Array Based Implementation of Relational Tables for Multidimensional Databases", Proc. of DaWak, pp 233-242, 2005.

[7] D. Rotem and J. L. Zhao, "Extendible Arrays for Statistical Databases and OLAP Applications", Proc. of SSDBM'96, pp.108-117, 1996.

[8] K. M. Azharul Hasan, Tatsuo Tsuji, and Ken Higuchi, "A Parallel Implementation Scheme of Relational Tables Based on Multidimensional Extendible Array", *International Journal of Data warehousing and Mining*, 2(4), pp.66-85, 2006.

[9] A. L. Rosenberg and L. J. Stockmeyer, "Hashing schemes for extendible arrays", JACM, Vol.24, pp.199-221, 1977.

[10] E. Bertino and W. Kim, "Indexing techniques for queries on nested objects", IEEE Transactions on Knowledge and Data Engineering, Vol 1. No. 2, June 1989.

Proceedings of 2009 12th International Conference on Computer and Information Technology (ICCIT 2009)
21-23 December, 2009, Dhaka, Bangladesh

Performance study and simulation analysis of CSMA and IEEE 802.11 in Wireless Sensor Networks and limitations of IEEE 802.11

Shaiful Alam Chowdhury, Mohamamd Tauhidul Islam†, Fariha Tasmin Jaigirdar‡, Md. Rokan Uddin Faruqui‡, Shahid Al Noor‡
Department of computer Science, Stamford University Bangladesh, Dhaka, Bangladesh
†Department of Computer Science, American International University-Bangladesh, Dhaka, Bangladesh
‡Department of Computer Science and Engineering, Bangladesh University of Engineering and Technology, Dhaka, Bangladesh
‡Department of Computer Science and Engineering, University of Chittagong, Chittagong, Bangladesh
‡Department of Computer Science, Stamford University Bangladesh, Dhaka, Bangladesh
msacbd@yahoo.com, tauhid@aiub.edu, farihajaigirdar@yahoo.com, rufaruqui@gmail.com, shaahid_noor@yahoo.com

Abstract

Since its birth wireless communication became an indispensible part of the modern society. One major area that has a gigantic impact on the performance of wireless sensor networks (WSNs) is the Medium Access Control (MAC) layer. Many random access protocols exist in wireless sensor networks. Some of these protocols include Carrier Sense Multiple Access (CSMA), Multiple Access with Collision Avoidance (MACA), Multiple Access with Collision Avoidance for wireless (MACAW) and IEEE 802.11. All the protocols mentioned above except CSMA use Request To Send/Clear To Send (RTS/CTS) packets to avoid collisions (hidden terminal problem) which was a great problem for CSMA and that is the reason CSMA is almost obsolete for wireless communications. But after using RTS/CTS packets the protocols have to encounter some extra problems such as, energy consumption and end-to-end delay. The objective of this paper is to show the pros and cons of using RTS/CTS packets by comparing CSMA (does not use RTS/CTS) and IEEE 802.11 (uses RTS/CTS packets). We also portray that under some specific scenario the IEEE 802.11 is outperformed by CSMA which is also the novelty and contribution of this research work. This observation suggests that a lot of works have to be done to consider IEEE 802.11 an approximate perfect MAC layer protocol for WSNs.

Keywords: CSMA, IEEE 802.11, MAC layer protocols, RTS/CTS.

I. INTRODUCTION

The ongoing progress in miniaturization, power-efficient wireless communication, micro sensor and microprocessor hardware, small-scale energy supplies in conjunction with the significant progress in distributed signal processing, ad hoc networks protocols and distributive computing have made Wireless Sensor Networks (WSNs) a novel technological vision [1][2]. As the Internet has revolutionized our life through the exchanges of diversified information readily among a large number of users, WSNs may very well, be equally significant by providing information regarding the physical phenomena of interest and ultimately being able to detect and control them or enable us to construct more exact models of physical worlds.

A Wireless Sensor Network (WSN) is a wireless network consisting of spatially distributed autonomous gadgets using sensors to cooperatively monitor the physical or environmental conditions, such as temperature, sound, vibration, pressure, motion or pollutants, at different locations [3][4]. The evolution of wireless sensor networks was originally motivated by military applications such as battlefield surveillance [5]. However, wireless sensor networks are now used in many civilian application areas, including environment and habitat monitoring, healthcare applications, home automation, vehicle detection and flare stack monitoring [3][6].

Besides one or more sensors, each node in a sensor network is typically equipped with a radio transceiver or other wireless communication device, a small microcontroller, and an energy source, usually a battery. The size of a single sensor node can vary from shoebox-sized nodes down to devices the size of grain of dust although functioning specks of genuine microscopic dimensions are yet to be designed [3]. The key features of a sensor node are its limitations in energy, transmission power, memory and computing power. So, the MAC layer protocols should be aware of the fact that, the memory of the nodes should not overflow and energy consumption at the nodes is minimized.

II. RELATED WORKS

MAC stands for Media Access Control. A MAC layer protocol is the protocol that controls access to the physical transmission medium on a network. It tries to ensure that no two nodes are interfering with each other's transmissions and deals with any possible interference.

After the evaluation of diversified problems in Wireless Sensor Networks we can say that a perfect MAC layer protocol must have at least some properties to cope with the situations such as, handle hidden terminals, minimize energy consumption, successfully handle memory overflow problem and allow exposed terminals to talk.

In CSMA (Carrier Sense Multiple Access) a node willing to transmit first checks to see whether the transmission medium is free to transmit, if it is not the case then it waits for the medium to be free and then transmit at the next available time slot otherwise it starts transmitting right away [7]. The CSMA protocol has been used in a number of packet-radio networks [8][9]. Although they are trivial in nature and can achieve acceptable throughput under certain situations, they suffer from the well-known "hidden terminal" and "exposed terminal" problem in multi-hop wireless sensor networks, which significantly deteriorates their performance [10][7].

IEEE 802.11 adopted the technique of using RTS (Request to Send)/CTS (Clear to Send) to eliminate the "hidden terminal" problem. In most of the situations this technique works fine but under certain circumstances the IEEE 802.11 fails to solve this "hidden terminal" problem which is shown in Figure 1.

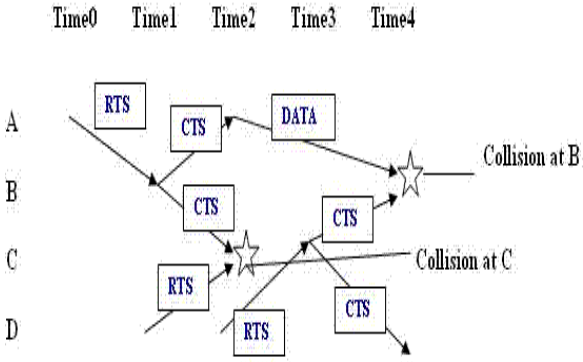

Figure-1: Hidden terminal problem after using RTS/CTS control packets

The scenario in Figure-1 can be portrayed as; A wants to send data packet to B. So A sends RTS to B. Upon receiving the RTS, B sends CTS to A and C. At the same time D sends RTS to C for transmitting data packet. The CTS and RTS packets collide at C. After receiving CTS from B, A transmits data to B and D resends RTS to C. On this occasion C sends CTS to B and D. The data and CTS packets collide at B.

From the above mentioned sequence of events we find that the "hidden terminal" problem is not fully solved using the IEEE 802.11. The use of RTS/CTS control packets and ACK partially solves the hidden node problem but the exposed node problem remains unaddressed like CSMA [11]. Until a saturation point is reached as the offered load increases the number of successfully received packets also increases whereas, after the saturation point the number of successfully received packets is reduced rapidly because of the limited memory of the nodes [12].

We already mentioned that the MAC layer protocols have great impact on the performance of wireless sensor networks. So a lot of works have been done for the improvement of MAC layer protocols. An important work described in [13], is current random access MAC protocols for ad hoc networks support reliable unicast but not reliable broadcast. So in this paper, they proposed a random access MAC protocol, Broadcast Support Multiple Access (BSMA), which improves broadcast reliability in ad hoc networks. In the paper [14] performance analysis between CSMA/CA that is carrier sense multiple access with collision avoidance and IEEE 802.11 is done which is closely related to our work. As the exposed node problem is not solved in IEEE 802.11, a solution for that problem is described in [11]. In the paper [15] a very important work has been done where they found the strength and weakness of different MAC layer protocols which will help to select a specific protocol for a specific work. Though RTS/CTS technique is responsible for some extra problems, as it plays a vital role for MAC layer protocols numerous works have been done to minimize the problems associated with using the RTS/CTS.

III. PERFORMANCE COMPARISON USING GLOMOSIM-2.03

To find out where it is not efficient to use IEEE 802.11 we evaluated and compared the performance of CSMA and IEEE 802.11 by setting the parameters to different values (for fewer number of nodes to higher number of nodes with fewer number of packets to higher number of packets). The performance metrics that we used for comparison are; percentage of packet loss, end-to-end delay, average throughput in the destination node and energy consumption.

We adopted for Global Mobile Information System Simulator (GloMoSim) for the simulation purpose because it is a widely accepted and scalable simulation environment for large wireless networks. GloMoSim uses a parallel discrete-event simulation capability provided by Parsec [14]. Here simulation time is set to 500 minutes and the Terrain dimension is set to 150 by 150 for 50 nodes. Then the dimension is changed for 100, 150, 200, 250 and 300 nodes. Node placement is uniform which means that based on the number of nodes in the simulation; the physical terrain is divided into a number of cells. Within each cell, a node is placed randomly. The default value of RADIO-TX-POWER was 15.0 and RADIO-RX-THRESHOLD was -81.0 but these are changed to 9.0 and -71.0 to set the transmis-

sion range of the nodes to approximately 100 meters. Five fixed sources are used to send data to node number 99 (destination for all the sources) when the number of nodes is 100. The destination is changed to node number 199 when the number of nodes in the network is 200 and similar changes for other number of nodes in the network. That is sources are always fixed but the only destination node is the last node (in number) in the network. So as the number of nodes in the network is changed the destination node is also changed.

To analyze, we collected the results from glomo.stat file and modified the code of GloMoSim developed by Parsec to get the result in an excel file. The graphs derived from the statistics found in glomo.stat file are given below:

A. Percentage of packet loss for 500 packets and 5000 packets

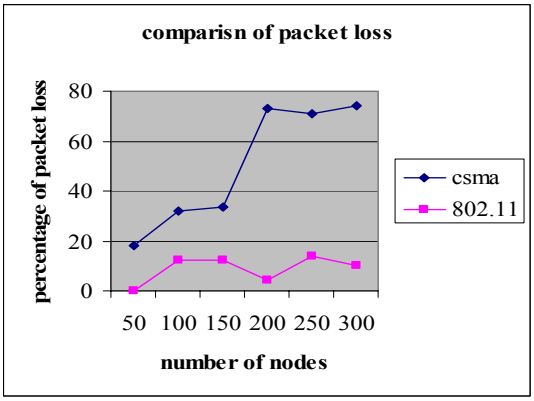

Figure-2(a): Percentage of packet loss for CSMA and IEEE 802.11 (500 packets)

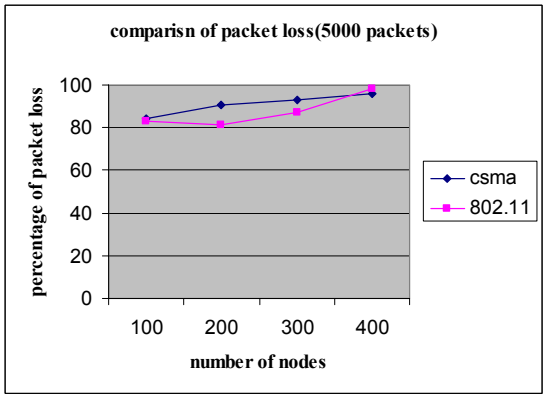

Figure-2(b): Percentage of packet loss for CSMA and IEEE 802.11(5000 packets)

From Figure 2(a), for CSMA the percentage of packet loss increased from 20% to near 80% with the number of nodes increased from 50 to 200. But after that the percentage of packet loss was almost constant. From Figure-2(b), when the number of packets was 5000 then for CSMA the percentage of packet loss was 84% to near about 96%.

For IEEE 802.11 and for 500 packets from Figure-2(a), we see that the percentage of packet loss is very low. For 50 nodes the percentage of packet loss is approximately zero. It remains below 20% for the number of nodes from 50 to 300 which is very good. But from Figure-2(b), for IEEE 802.11 and 5000 packets we see that the percentage of packet loss is very high. It started from above 80% for 100 nodes and it went to approximately 98% for 400 nodes. It is significant to note that, although IEEE 802.11 uses the RTS/CTS control packets to solve the hidden terminal problem and also uses acknowledgement for packet loss, packet loss remains a great problem in a high traffic network for IEEE 802.11. In our simulation we observed memory overflows at the nodes in high traffic network for IEEE 802.11. So for overflow problem there is no great difference between CSMA and IEEE 802.11 in case of reliability for a congested network.

B. Average End-to-End delay for 500 packets and 5000 packets

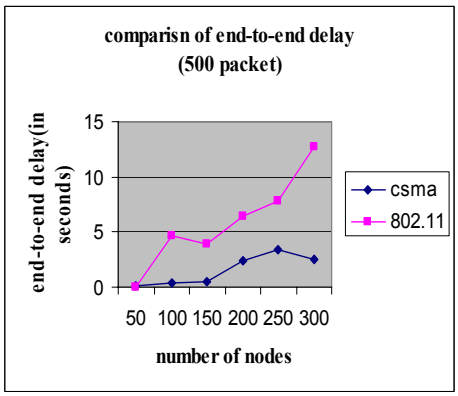

Figure-3(a): Average End-to-end delay for CSMA and IEEE 802.11(500 packets)

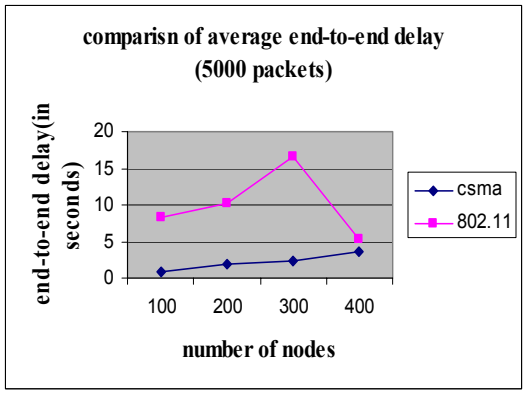

Figure-3(b): Average End-to-end delay for CSMA and IEEE 802.11(5000 packets)

From Figure-3(a) we find that, for CSMA the average end-to-end delay for 500 packets remains between 0 to 4 seconds which is very good. From Figure-3(b) we observe that, for 5000 packets the average end-to-end delay remains between 0 to 4 seconds. But from Figure-3(a) we see that, for IEEE 802.11 the average end-to-end delay for 500 packets is clearly in increasing order and from 0 to near about 13 seconds. From Figure-3(b), we also observe that the average end-to-end delay went high for IEEE 802.11 up to approximately 17 seconds when packet number was 5000 for 100 nodes to 300 nodes. But the surprising matter is that it falls down to 5 seconds for 400 nodes. The reason is that for 400 nodes most of the packets were lost due to the overflow problem.

The average end-to-end delay for IEEE 802.11 is generally more than CSMA because of the extra RTS/CTS control packets and as it tries to solve the hidden terminal problem by restricting a node to access the medium when one of its neighbors is transmitting. So in case of end-to-end delay CSMA is better than IEEE 802.11 most of the times.

C. Throughput for 500 packets and 5000 packets

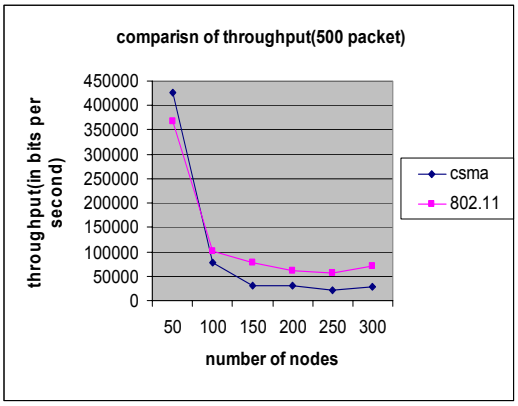

Figure-4(a): Throughput for CSMA and IEEE 802.11(500 packets)

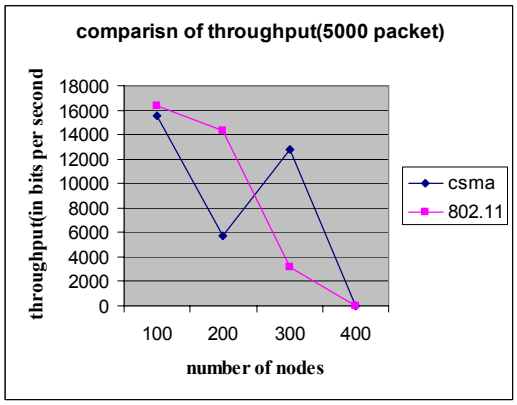

Figure-4(b): Throughput for CSMA and IEEE 802.11 (5000 packets)

From Figure-4(a), for CSMA and for 500 packets we observe that the throughput is above 400000 bits per second when the number of nodes is 50. But for 100 nodes it falls down to approximately 75000 bits per second and when the number of nodes is between 150 and 300 the throughput always remains approximately 25000 bits per second.

From Figure-4(b), for CSMA and for 5000 packets when the number of nodes is 100 the throughput is approximately 16000 bits per second but when the number of nodes is 200 it falls down drastically and it rises again at 300 nodes and again falls down to approximately 5 bits per second.

We observe from Figure-4(a) that, for IEEE 802.11 and 500 packets the throughput is above 350000 bits per second when the number of nodes is 50. But it falls down to 100000 bits per second when the number of nodes is 100 and it remains between 100000 and 50000 bits per second as the number of nodes goes to 300.

But from Figure-4(b), for IEEE 802.11 and 5000 packets the throughput is unpredictable like CSMA in the same situation. So from our simulation we find that for high traffic network it is really unpredictable to decide which protocol is better in terms of throughput. As mentioned earlier only the average throughput in the destination node is considered for this research work.

D. Energy Consumption for 500 packets and 5000 packets

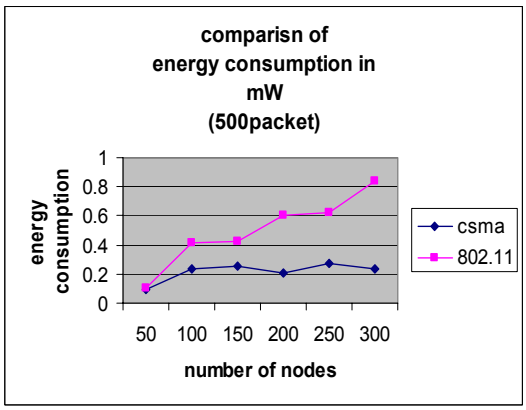

Figure-5(a): Energy consumption for CSMA and IEEE 802.11(5000 packets)

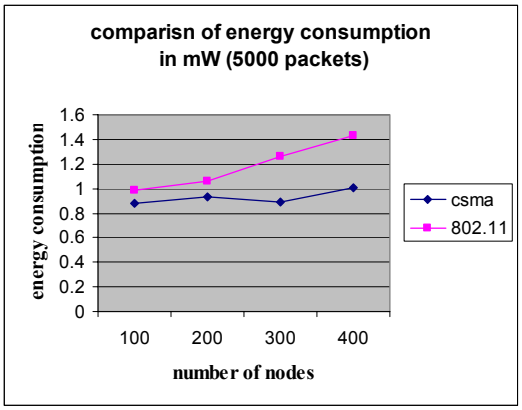

Figure-5(b): Energy consumption for CSMA and IEEE 802.11(500 Packets)

From Figure 5(a) and 5(b) we see that, IEEE 802.11 always consumed more energy than CSMA because of extra RTS/CTS control packets and possible retransmission. Whether a node is used in any data transfer process or not it has to consume some energy to remain alive in the network. Our calculation used the energy consumed by only those nodes that were in the best path from source to destination excluding the energy consumed by the nodes to stay alive in the network. As the wireless sensor network is sensitive to the energy consumed by the sensors, in terms of energy consumption IEEE 802.11 is outperformed by CSMA.

IV. CONCLUSION AND FUTURE WORKS

In this paper we find a lot of limitations for IEEE 802.11 as compared to CSMA though IEEE 802.11 is the standard MAC layer protocol. As IEEE 802.11 uses extra RTS/CTS control packets to solve "hidden terminal" problem it needs more energy and more time to transmit data than CSMA. Also it is not always better than CSMA in case of throughput. The only case when it is better than CSMA is in terms of percentage of packet loss for low traffic networks. But for high traffic networks it performs the same as CSMA for the memory overflow of the nodes or sensors.

It would be really tempting to solve the exposed terminal problem and the partially solved hidden terminal problem in IEEE 802.11. More analysis on the overflow problem could be performed to increase the average throughput and decrease the packet loss. Comparing the performance of CSMA and IEEE 802.11 with all the routing protocols to determine which routing protocol is best with which MAC layer protocol (CSMA and IEEE 802.11) in specific situations could be a potentially fruitful research area.

REFERENCES

[1] D. Estrin, R. Govindan, J. Heidemann and S.Kumar "Next Century Challenges: Scalable Coordination in Sensor Networks," *Proc. of Mobocom'99*, Seattle, Pages 263-270, August 1999.

[2] H. Karl and A. Willig. "A short survey of wireless sensor networks." TKN *Technical Report TKN-03-018,* Technical University Berlin, October 2003.

[3] K. Romer and F. Mattern,. "The Design Space of Wireless Sensor Networks". *IEEE Wireless Communications*.11(6):54-61, December 2004.

[4] T. Haenselmann (2006-04-05), "*Sensornetwork*". GFDL Wireless Sensor network textbook, retrieved on 2006-08-29.

[5] Th. Arampatzis, J. Lygeros and S. Manesis, "A Survey of Applications of Wireless Sensors and Wireless Sensor Networks", *Mediterranean Conference on Control and Automation Limassol*, Page 719-724, June 27-29, 2005.

[6] S. Hadim and N. Mohamed , " Middleware Challenges and Approaches for Wireless Sensor Networks". *IEEE Distributed Systems Online*, 7(3), March 2006.

[7] "A Comprehensible GloMoSim Tutorial", compilation by Jorge Nuevo, *INRS - Universite du Que bec*, March 4, 2004.

[8] L. Kleinrock and F. Tobagi, "Packet Switching in Radio Channels: Part I--Carrier Sense Multiple-Access Modes and Their Throughput-Delay Characteristics", *IEEE Transactions on Communications*, 23(12):1400-1416, December 1975.

[9] R. L. Brewster and A. M**.** Glass, "Throughput Analysis of Non-Persistent and Slotted Non-Persistent CSMA/CA Protocols," *4th International Conference on Land Mobile Radio*, pp. 231-6, 1987.

[10] L. Kleinrock and F.Tobagi, "Packet switching in radio channels: Part II - the hidden terminal problem in carrier sense multipleaccess modes and the busy-tone solution", *IEEE Transactions on Communications,* 23(12): 1417-1433,1975.

[11] D. Shukla, L. Chandran-Wadia and S. Iyer, "Mitigating the Exposed Node Problem in IEEE 802.11 Ad Hoc Networks", *12th international conference on Computer Communications and Network*, Pages 157-162, 2003.

[12] J. Liu, D. M. Nicol, L. F. Perrone and M. Liljenstam, "Towards High Performance Modeling Of The 802.11 Wireless Protocol", *Proceedings of the 2001 Winter Simulation Conference*, Pages 1315-1320, 2001.

[13] K. Tang and M. Gerla, "Random Access MAC

for Efficient Broadcast Support in Ad Hoc Networks**",** *Wireless Communications and Networking Conference,* volume-1, Page 454-459, 2000.

[14] T. Ho, K. Cben. "Performance Analysis of IEEE 802.11, CSMA/CA Medium Access Control Protocol*", 7th IEEE international Symposium on Personal, Indoor and Mobile Radio Communications*, Volume-1, pages 407-411, 1996.

[15] I. Demirkol, C. Ersoy, and F. Alagöz, "MAC Protocols for Wireless Sensor Networks: A Survey", *Communications Magazines IEEE,* 44(4):115-121, 2006.

Proceedings of 2009 12th International Conference on Computer and Information Technology (ICCIT 2009)
21-23 December, 2009, Dhaka, Bangladesh

Performance Analysis of DS-CDMA under Perfect and Imperfect Power Control

Md. Mahbub Hossain, Md. Abdul Awal, Dipankar Roy, Md. Asraful Islam, Md. Anwar Hossain
Electronics and Communication Engineering Discipline; Khulna University, Khulna -9208, Bangladesh
mahbub.eceku@yahoo.com, awalece04@yahoo.com

Abstract

CDMA refers to multiple access method in which the individual terminals uses spread spectrum techniques and occupy the entire spectrum whenever they transmit. This feature makes CDMA different from FDMA and TDMA. In the wireless communication, the Signal to Interference Ratio (SIR) and Bit Error Rate (BER) are the predominant parameter that characterizes the system performance. This paper presented here Standard Gaussian Approximation (SGA) methods presented in the international literature concerning the computation of the SIR and the BER in DS-CDMA systems under perfect and imperfect power control over fading and non-fading channel. The content and conclusions of this paper have driven to take many important decisions by varying different DS-CDMA communication parameters such as processing gain, number of interfering cells, multipath components etc. using SGA techniques. As SGA is analytically developed and is very computationally efficient solution for the system performance estimate in terms of SIR and BER, it helps us to avoid the tedious and cost-inefficient simulations.

Keywords: BER, CDMA, DS-CDMA, SGA, SIR.

I. INTRODUCTION

Code Division Multiple Access (CDMA) is a well-known radio communication technique to allow multiple users to share the same spectrum simultaneously. In CDMA, users are multiplexed by distinct codes rather than by orthogonal frequency bands or by orthogonal time slots [1]. Direct-Sequence (DS) CDMA is the most popular of CDMA techniques. The DS-CDMA transmitter multiplies each user's signal by a distinct code waveform. The detector receives a signal composed of the sum of all users' signals, which overlap in time and frequency. In a conventional DS-CDMA system, a particular user's signal is detected by correlating the entire received signal with that user's code waveform. Multiple Access Interference (MAI) is a factor which limits the capacity and performance of DS-CDMA systems. MAI refers to the interference between direct- sequence users. This interference is the result of the random time offsets between signals, which make it impossible to design code waveforms to be completely orthogonal. While the MAI caused by any one user is generally small, as the number of interferers or their power increases, MAI becomes substantial. Therefore, any analysis of performance of a CDMA system has to take into account the amount of multiple-access interference and its effects on the parameters that measure the performance, in particular the signal-to-interference and noise ratio at the receiver and the related bit error probability on the information bit stream. This paper is to analyze a set of solutions proposed in several works for the problem of the statistical description of the MAI in the up-link (users-to-base station link) of a DS-CDMA cellular system. The goal of our analysis is to highlight the benefits and limitations yielded by the use of those solutions, essentially by comparing them in different working conditions. It is worth to notice henceforth that the most popular approach is the Gaussian Approximation method and its variants.

II. CONCEPTS OF DS-CDMA

CDMA is a branch of multiple access radio communication processes in which multiple users have access to the same system, using the same frequency. This is accomplished by means of an m -bit PN generator, which provides $2^m - 1$ different code. Out of these codes, only m codes, known as orthogonal codes are derived and assigned to m users. The function of the PN code is to spread the traffic data the entire transmission band while uniquely identifying each user. Because the spreading is accomplished by direct application of a PN sequence, the overall process is described as direct sequence code division multiple access of DS-CDMA [2].

A. DS Spectrum Spreading Techniques

From the definition of DS-CDMA it is necessary to know the spreading and despreading techniques.DS spectrum spreading is accomplished by means of a two input exclusive OR gate where A is low speed NRZ data and B is a high speed PN sequence. In Boolean expression this is given by

$$C = A\overline{B} + \overline{A}B$$

B. DS Spectrum Despreading Techniques

DS spectrum despreading is a process of data recovery from the composite spread-spectrum signal. This is accomplished by means of another exclusive OR gate, where the composite data C is applied to one input and an identical PN sequence is applied to second input. The output "Y" is a decomposed signal, PN sequence (the B signal) is identical for both spreading and despreading; otherwise, the desired signal will never be recovered as shown in Figure1

978-1-4244-6283-4/09/$26.00 ©2009 IEEE

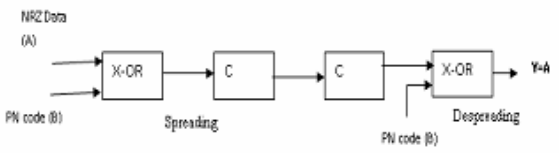

Fig 1. A block diagram to illustrate spectrum spreading and despreading .

C. Reverse Link DS-CDMA (MS to BTS)

As an illustration, representing a conceptual model of a reverse link DS-CDMA system, providing access to K mobile users: MS1, MS2… MSK, using the same carrier frequency fc. Each mobile is assigned a unique PN code: PN1, PN2… PNK, where PN1 is assigned to MS1, PN2 to MS2 and so on. The base station to identify each piece of traffic uniquely by means of array of MOD2 adders, biased with the respective PN codes. Each MOD2 adder then despread one of the K signals, which is desired traffic.

D. Forward Link DS-CDMA (BTS to MS)

The incoming traffic from a link is spread by means of an array of MOD2 adders, biased with the respective PN codes (PN-1, PN-2, ……, PN-k). Each spread-spectrum signal is then modulated, unconverted and finally transmitted. These signals are received by all the mobiles in the service area and MOD2 added by the respective PN code to recover the desired traffic.

III. DS-CDMA MODEL

A. System Model

We consider up-link (mobiles to base station) of a single cell asynchronous DS-CDMA System that supports Ku active users.Each of them transmits a signal in the form described by [4]

$$s\ (t-\tau_{\prime k})=\sqrt{2P_k}b_k(t-\tau_{\prime k})a_k(t-\tau_{\prime})\cos(\omega_c t+\theta_k) \quad \ldots\ldots. (1)$$

where $b_k(t)$ is the data signal, a_k (t) is the spectral-spreading signal, P_k is the power of transmitted signal, ω_c is the carrier frequency, τ'_k is the time delay that accounts for the lack of synchronism between the transmitters, and θ_k is the phase angle of the Ku carrier. The Ku user's data signal is a sequence of unit amplitude rectangular pulse of duration Tb, talking values from {-1, +1}, with equal probability. This sequence can be expressed as

$$b_k(t)=\sum_{j=-\infty}^{\infty} b_j^k\, pT_b(t-jT_b) \quad \ldots\ldots\ldots\ldots . (2)$$

where $PT_b=1$,for $0\le t\le T_b$ and $PT_b=0$, otherwise.

The spreading signal $a_k(t)$ can be expressed as

$$\alpha_k(t)=\sum_{i=-\infty}^{\infty} a_i^k \psi(t-jT_b) \quad \ldots\ldots\ldots\ldots\ldots (3)$$

where ψ (t) is a chip waveform that is time-limited to [0,T_c] and normalized to have T_c , where $\int_0^{T_c} \psi^2(t)dt = T_c$ is the chip period , and a_i^k is the i^{th} chip value of k_u users; this chip value can be either -1 or +1. There are G_p chips per bit and thus $G_p = \frac{Tb}{Tc}$ is the process gain for user k. We assume that the desired user is k = 0 and all other users contribute to MAI.

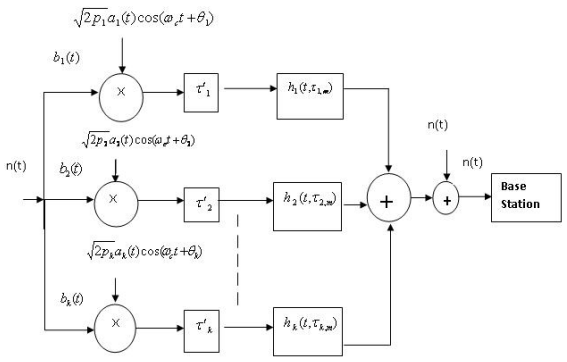

Fig 2: DS-CDMA System Model.

B. Channel Model

The K-th source signal is transmitted through a channel $h_k(t)$ which can be represented by means of three fundamental models [1].Additive White Gaussian Noise (AWGN) channel, which simply adds a white random process n(t) to the delayed transmitted signal. Flat fading channel, which introduces a random path gain multiplicative factor, generally modeled with Rayleigh distribution. Frequency-selective fading channel, which generates the multipath phenomenon, that is a number of replicas of the source signal characterized by their own delays, phase rotations and Rayleigh distributed amplitudes.

IV. NEAR- FAR EFFECT AND NEED OF POWER CONTROL

When power control is not implemented, all mobiles transmit their signal with the same power without taking into consideration the fading and the distance from the base station, in this case mobiles close to the base station will cause a high level of interference to the mobiles that are far away from the base station, this problem is known as the near-far effect [1]. Near-far problem is generated for conventional receiver without any resistance to it. It degrades performance, reduces capacity and causes dropped calls [2].

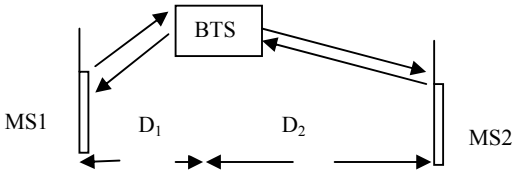

Fig3. Near-Far Effect

If the mobilesMS1 and MS2 are permitted to transmit the same power from two different distances, D_1 and D_2, the received signal strength Intensity (RSSI) at the base station will be [2]

$$\frac{RSSI_1}{RSSI_2} = \left(\frac{D_2}{D_1}\right)^{\gamma} \quad \ldots\ldots\ldots\ldots\ldots\ldots (4)$$

Where γ is the path loss exponent (propagation environment).

When $D_1 \neq D_2$, then received signal will be different for different mobiles depending on the propagation environment and the respective distances. For example D_2= $5D_1$ and γ = 4(typical dense urban area), $RSSI_1$ from MS1 will be 1024 times (30dB) stronger than $RSSI_2$ from MS2 (using equation 4) and the base station receiver will unable to recover $RSSI_2$. For this reason, power control is necessary. It is used with direct sequence CDMA techniques over radio channels to combat various fading effects. The basic control mechanism can be open loop, closed loop, or a combination of both.

V. TECHNIQUES OF ANALYSIS

A. Standard Gaussian Approximation (SGA)

The signal from the MS arrive at the BTS at a random time .The random process produced by this physical phenomena are often such that Gaussian model is appropriate. Moreover, the Gaussian model that describes these phenomena is usually confirmed by experiments. Thus for a large number of physical random process, the Gaussian model is appropriate and can be expressed mathematically and make the Gaussian process very important tools in Wireless communication system [3]. For this reason Gaussian Approximation is used to determine the Signal-to-Interference Ratio (SIR) and the Bit Error Rate (BER) for a CDMA communications system is based on the argument that the bit decision statistic Z_0 may be modeled as a Gaussian random variable. It can be described by [1]:

$$Z_0(m) = D_0(m) + I + v \quad \ldots\ldots\ldots (5)$$

Where D_0 is the useful information component and represents a deterministic variable given the transmitted bit, while the MAI and thermal noise components, I and V, are independent zero-mean Gaussian random variables. Thus, defining $\xi = I + v$, Z_0 is a Gaussian random variable with mean D_0 and a variance which is equal to the variance of ξ (σ_{ξ}^2) .

The SIR and BER equations under perfect and imperfect power control over fading and non-fading channel using SGA techniques are used in many international Literatures [1].These are given bellow.

A.1. Channels without Fading

A.1.1. Perfect Power Control

In typical mobile radio environments, communication links are interference-limited and not noise limited. For the interference-limited case the thermal noise term can be neglected. Ideally, in non-interference limited case with perfect power control, the average SIR and the average BER can be approximated by [1]:

$$SIR = \frac{0.5}{\frac{K_u - 1}{3G_p} + \frac{N_0}{2T_b P_0}} \quad \ldots\ldots\ldots\ldots (6)$$

$$BER = Q\sqrt{\frac{1}{\frac{K_u - 1}{3G_p} + \frac{N_0}{2T_b P_0}}} \quad \ldots\ldots\ldots (7)$$

Where G_p is the process gain, N_o is the thermal noise power spectral density, T_b is bit duration and K_u is the number of user. The function $Q(.)$ is called Q function. In the interference-limited case, the average SIR and the average BER can be approximated by [1]:

$$SIR = \frac{3G_p}{2(K_u - 1)} \quad \ldots\ldots\ldots\ldots\ldots (8)$$

$$BER = Q\sqrt{\frac{3G_p}{K_u - 1}} \quad \ldots\ldots\ldots\ldots (9)$$

A.1.2. Imperfect Power Control

When the power control is imperfect, the received amplitude A_k of the k-th user can be modeled as random variable with uniform distribution around the nominal value of the received power level A_k. In absence of fading and interfering cells with imperfect power control the average SIR and the average BER can be simplified as [1]:

$$SIR_{IM} = \frac{1}{\frac{N_0}{2E_b} + \frac{K_u - 1}{3G_p}\left(1 + \frac{V^2}{3A_0^2}\right)} \quad \ldots\ldots\ldots (10)$$

$$BER_{IM} = Q\sqrt{SIR_{IM}} \quad \ldots\ldots\ldots\ldots\ldots (11)$$

Where E_b/N_o is called the signal-to-noise ratio.

A.2. Channels with Fading

A.2.1. Perfect Power Control

If we consider a frequency non-selective fading channel, the path gain component can be modeled as a Rayleigh distribution. This is practical case. So the number of interfering cell, Nc and number of multipath, M in the signal propagation are expected. With perfect power control, the average SIR and the average BER in the fading channel can be written as [1]:

$$SIR_M = \frac{2\sigma_2}{2\frac{N_0}{E_b} + \frac{2\sigma_2}{3G_p}[(1+\frac{N_c}{5})MK_u - 1]} \quad \text{..... (12)}$$

$$BER_M = \frac{1}{2}\left(1 - \frac{1}{\sqrt{1+\frac{N_0}{2E_b\sigma_2} + \frac{2}{3G_p}[(1+\frac{N_c}{5})MK_u - 1]}}\right) \quad \text{.....(13)}$$

Where σ^2 is the variance of the Rayleigh random variable modeling in the fading process.

If a RAKE receiver is used, all the uncorrelated multi-path components contribute to the useful signal. So, with perfect power control, the SIR and the BER can be derived as

$$SIR = \frac{x}{2\frac{N_0}{E_b} + \frac{2\sigma_2}{3G_p}[(1+\frac{N_c}{5})MK_u - 1]} \quad \text{...(14)}$$

$$BER = Q\left(\sqrt{\frac{x}{2\frac{N_0}{E_b} + \frac{2\sigma_2}{3G_p}[(1+\frac{N_c}{5})MK_u - 1]}}\right) \quad \text{...(15)}$$

Where $x = \sum_{m1}^{M} \alpha_{m1 \cdot i}^2$ and $\alpha_{m1 \cdot i}^2$ is a particular distribution.

A.2.2. Imperfect Power Control

In the case of conventional correlation-type receiver, the average SIR and the average BER are given by [1]

$$SIR_{IM} = \frac{2\sigma_2}{2\frac{N_0}{E_b} + \frac{2\sigma_2}{3G_p}(1+\frac{V_2}{3A_0^2})[(1+\frac{N_c}{5})MK_u - 1]} \quad \text{.....(16)}$$

$$BER_{IM} = \frac{1}{2}\left[1 - \frac{1}{\sqrt{1+\frac{N_0}{2E_b\sigma_2} + \frac{2}{3G_p}(1+\frac{V_2}{3A_0^2})[(1+\frac{N_c}{5})MK_u - 1]}}\right] \quad \text{... (17)}$$

Where V is the maximum variation range of the received signal with respect to the mean value A_0.

In RAKE receiver, the SIR and the BER are given by

$$SIR_{IRM/X} = \frac{x}{\frac{N_0}{2E_b} + \frac{2\sigma_2}{3G_p}(1+\frac{V_2}{3A_0^2})[(1+\frac{N_c}{5})MK_u - 1]} \quad \text{...(18)}$$

$$BER_{IRM|x} = Q\left(\sqrt{\frac{x}{\frac{N_0}{2E_b} + \frac{2}{3G_p}(1+\frac{V_2}{3A_0^2})[(1+\frac{N_c}{5})MK_u - 1]}}\right) \quad \text{...(19)}$$

VI. RESULT AND DISCUSSION

A. Simulation

A set of numerical tests using MATLAB obtained through the implementation of the equations are presented here. We consider different scenarios: the cases of a channel with or without fading and the cases of perfect or imperfect power control. The received power of the desired signal is normalized to 1. The Signal-to-Noise Ratio Eb/No =10 dB and the processing gain Gp and K=V/Ao is chosen arbitrarily.

A.1. For Non-fading channel

In the following figures the BER and SIR are plotted by using the equation (6) to equation (11) for ideal non-fading. We can observe that the BER becomes significantly lower Increasing Gp which is our main expectation whereas SIR gradually increased as increasing Gp. Figure 5 also compare perfect and imperfect power control using Gp = 64 and 256.

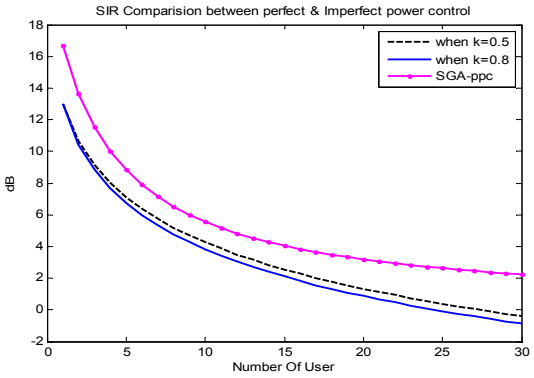

Fig4. SIR Comparison between perfect and imperfect power control for SGA Approximation over a non–fading channel

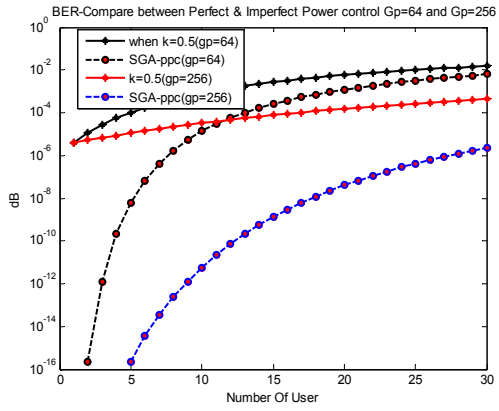

Fig5.BER Comparison between perfect and imperfect power control for SGA Approximation a non- fading channel

A.2. For fading channel

This section analyzes the behavior of the system when the fading is modeled as a Rayleigh random variable with variance σ^2 .

A.2.1 Perfect power control

In the following Figures the BER and SIR are plotted by using the equation (12) to equation (15) for non ideal fading channel with perfect power control. In this analysis $\sigma^2 = 1$ .We observed the effect of BER and SIR increasing the number of interfering cell (Nc) and also for different multipath components (M). BER and SIR performance degrades when we increased the number of interfering cell and also for different multipath components and increases for G_p.

we implemented different scenarios for conventional correlation receiver and RAKE receiver (using equation 12,13,14,15) with M=4 and $\sigma^2 = 1$ .It can be observed that using a RAKE receiver the performance of the system is better than a conventional correlation receiver They also degrade their performance with respect to perfect power control.

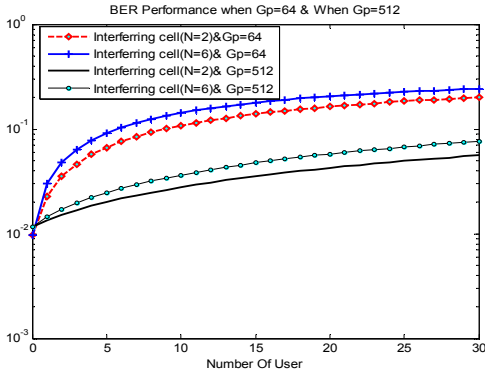

Fig6.BER Performance when Gp=64 and Gp=512

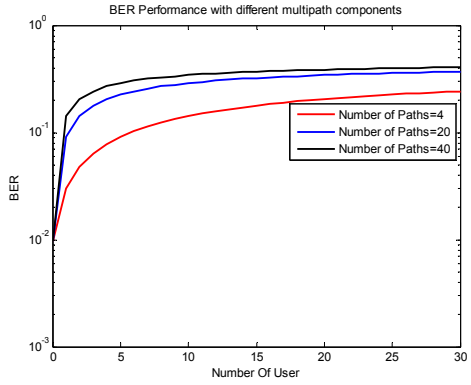

Fig7. BER Performance with different multipath components (M=4, 20, 40)

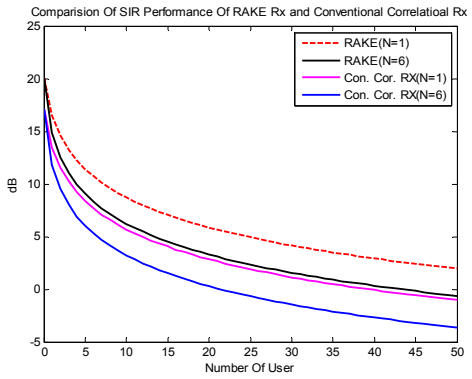

Fig8.SIR Comparison of Conventional Correlation Receiver and RAKE Receiver

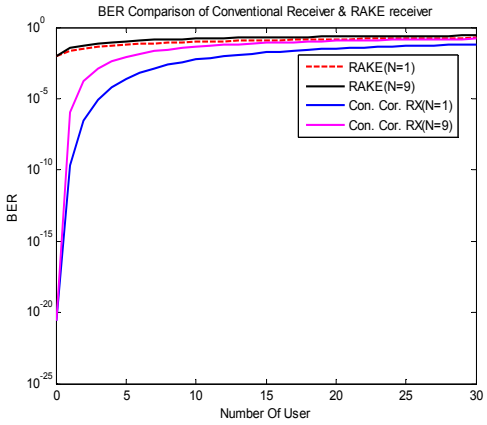

Fig9. BER Comparison of conventional Correlation Receiver and RAKE Receiver

A.2.2 Imperfect power Control

In the analysis of a system over fading channel with imperfect power control, we consider the SGA approximation through the equations (16) and (17) for a conventional correlation receiver, equations (18) and (19) for a RAKE receiver. In both cases we consider the interference of multipath and users of other cells with M=4and $\sigma^2 = 1$.

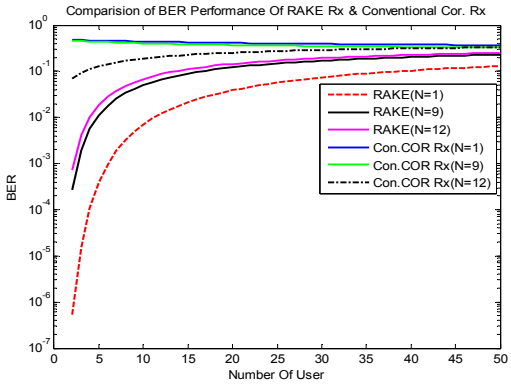

Fig10. BER Comparison of RAKE and Conventional correlation receiver.

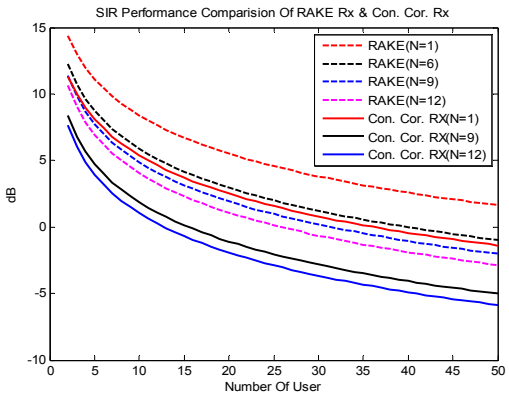

Fig11. SIR Comparison of RAKE and Conventional correlation receiver

B. Results

We used SGA techniques to determine SIR and BER over fading and non-fading channel under perfect and imperfect power control by varying different parameters such as process gain (Gp), K, number of interfering cell (Nc), number of path in propagation (M). Fig4 and Fig5 for non-fading channel.Fig4 shows the performance of SIR, when k=0.5,0.8 and SGA-PPC. Their performance decreased when the number of user increased. Another fact is that, SGA-PPC performed better than imperfect power control. The Fig5 shows the BER performance. By increasing Gp we get better performance. But to increase Gp, the system needs more instruments, amplifiers etc that means increases complexity.

Fig6 to Fig11 for fading channel.Fig6 and Fig7 evaluates BER performance by varying Nc and M respectively. When the value of M and Nc lower then the system perform better. In rural areas interference and multi-path is lower than urban areas. So, from these figures we can take decision that, only in urban area we need to increase Gp to get same result by decreased value of Gp in rural area. Fig 8 and Fig 9 indicates that, the performance of RAKE receiver is better than Conventional Correlation receiver. Performance degrades when increasing Nc.

Fig10 and Fig11 for imperfect power in non-fading channel.We get better BER and SIR performance lowering Nc. Besides RAKE receiver performed 10times better in perfect power control.

Here, we experimented a lot of important factors which help us to take many significant decisions such as handover, data recover capacity etc .SIR and BER performance increases with increasing processing gain (Gp) whereas performance decreases with increasing M and Nc

VII. CONCLUSION

This paper focused the attention on the standard Gaussian Approximation (SGA) for reverse link performance analysis. Different types of scenarios were driven with respect to perfect and imperfect power control over a fading and a non fading channel. Here the SIR and BER were evaluated. The paper evaluated SIR and BER as function of number of users. Here different parameters are used as a variable such as the number of multipath parameters, the number of interfering cell and processing gain.

SIR and BER are compared for different cases. These scenarios help us to take many decisions such as dynamic channel assignment, handoff, power control etc which is very important for wireless communication.

Several improvements have been proposed for the standard method (IGA, SEIGA), that slightly better behave in case of reduced number of interferers and/or imperfect power control. These can be left as future works. Although the Gaussian hypothesis could appear a strained operation for some situations (for real situations),it seems however the unique practical, very flexible and very computationally efficient method that has been provided in order to give an estimate of the interference effects in DS-CDMA system.

REFERENCES

[1] Emanuela Falletti, Francesca Vipiana Renato Locigno, “On SIR and BER Approximatons on DS-CDMA System”

[2] Saleh Faruque , “Cellular Mobile Systems Engineering” – New Edition, Chapter 4, Artech House Publishers, Doston London.

[3] Simon Haykin, “Digital Communications” Eight Edition, Wiley India (Pv) Lt

[4] Seedahmed S. Mahmoud, Zahir M. Hussain, Peter O’Shea,“ BER Performance of DS-CDMA System Over a Frequency Selective Multipath Rayleigh Fading Channel”

Proceedings of 2009 12th International Conference on Computer and Information Technology (ICCIT 2009)
21-23 December, 2009, Dhaka, Bangladesh

Minimized Reversible Synthesis of Non-Reversible Quinary Logic Function

Mozammel H. A. Khan, Raqibul Hasan
Department of Computer Science and Engineering, East West University, 43 Mohakhali C/A, Dhaka 1212, Bangladesh
mhakhan@ewubd.edu, raqib_cse@yahoo.com

Abstract

Reversible multiple-valued logic circuit has several advantages over reversible binary logic circuit. In this paper, we propose a method of minimization of Galois field sum of products (GFSOP) expression for non-reversible quinary logic function. We also propose a method of reversible realization of quinary GFSOP expression as cascade of quinary reversible gates. Experimental results show that a significant minimization can be achieved using the proposed minimization method.

Keywords: Galois field expansion, GFSOP expression, GFSOP minimization, GFSOP synthesis, quinary logic, reversible logic

I. INTRODUCTION

According to Bennett's theorem [1], a binary logic circuit theoretically does not dissipate heat if it is built using reversible gates. Bennett's theorem suggests that every future binary technology will have to use some kind of reversible gates in order to reduce heat dissipation. This is also true for multiple-valued logics, which by themselves demonstrate several potential advantages over binary technology.

Reversible synthesis of ternary [2] - [11] and quaternary [12] - [16] logic functions has made a significant advancement. These synthesis methods can be divided into three broad areas of approaches. Papers [3] and [7] deal with circuit synthesis using technology primitive reversible/quantum Muthukrishnan-Stroud (M-S) gates [17]. This approach produces circuit with low cost but the design methods are generally very difficult to use for functions with many input variables. The papers [2], [5], [6], [8] - [11], [13] - [15] deal with circuit synthesis using macro-level gates those are realizable on the top of technology primitive gates. This approach is relatively easier, but the produced circuit is of higher cost. This approach is also relatively difficult to use for functions with many input variables. The third approach is synthesizing circuits as Galois field sum of products (GFSOP) circuits [4], [12], [16]. The advantage of this approach is that any function with many input variables can be represented as GFSOP expression [4], [16] and the GFSOP expression can be easily implemented as cascade of reversible/quantum gates [4], [12]. This approach uses multiple-input Toffoli gate for GFSOP realization. The most remarkable drawback of this approach was that macro-level Toffoli gate realization on the top of primitive gates requires a large number of ancilla input constants, which makes the synthesized circuit having a very large number of ancilla input constants. Recently, ancilla input free realization of Toffoli gate on the top of 1×1 and M-S gates is reported in [18]. This new development allows GFSOP based synthesis very promising for functions of many input variables. This approach has two distinct jobs, one is representing the function as minimized GFSOP expression and the other is realizing the GFSOP expression as cascade of reversible gates. Good methods for GFSOP based reversible synthesis of ternary [4] and quaternary [12], [16] logic functions are already reported. We have introduced the preliminary idea of GFSOP based synthesis of quinary logic function in [19], but no method for GFSOP minimization for quinary function is discussed there. In this paper, we present a method for GFSOP minimization of quinary logic function using the Galois field expansions from [19]. In addition, we present a method of realization of GFSOP expression using cascade of quinary reversible gates. Thus, the proposed method synthesizes a non-reversible quinary logic function into a reversible circuit. We experiment with 17 functions and the experimental results show a significant improvement over canonical GFSOP expression.

II. GF(5) ARITHMETIC

Galois field 5 or GF(5) is a set G = {0, 1, 2, 3, 4} with two binary operations - addition (denoted by +) and multiplication (denoted by · or juxtaposition) as defined in Table I. Readers can see that GF(5) operations are integer mod 5 operations. GF(5) addition and multiplication are commutative and multiplication is distributive over addition. In this paper, unless otherwise specified, addition (+) and multiplication (·) operations represent GF(5) operations.

Table I GF(5) addition and multiplication.

+	0	1	2	3	4
0	0	1	2	3	4
1	1	2	3	4	0
2	2	3	4	0	1
3	3	4	0	1	2
4	4	0	1	2	3

·	0	1	2	3	4
0	0	0	0	0	0
1	0	1	2	3	4
2	0	2	4	1	3
3	0	3	1	4	2
4	0	4	3	2	1

978-1-4244-6283-4/09/$26.00 ©2009 IEEE

III. QUINARY GFSOP EXPRESSION

For expressing a quinary logic function as GFSOP expression, we will use two types of quinary literals – 1-reduced Post literals (1-RPLs) and reversible literals as defined below:

Definition 1. A 1-reduced Post literal (1-RPL) represents a mapping form a variable x to a transformed value x^i, $x^i : \{0, 1, 2, 3, 4\} \rightarrow \{0, 1\}$, such that

$$(\forall i \in \{0,1,2,3,4\})\ x^i = \begin{cases} 1 & \text{if } x = i \\ 0 & \text{otherwise} \end{cases}.$$

Definition 2. A reversible literal represents a bijective mapping from a variable x to a transformed value $x^{<q>}$, $x^{<q>} : \{0, 1, 2, 3, 4\} \rightarrow \{0, 1, 2, 3, 4\}$, where $<q>$ is a string from the alphabet {+, /, 0, 1, 2, 3, 4}. There are 5! = 120 quinary reversible literals, which will be represented using the symbols discussed below. Let us assume that $a, b, c, d, e \in \{0, 1, 2, 3, 4\}$ and $a \neq b \neq c \neq d \neq e$.

(i) Literal $x^{+a} = x + a$. There are five such literals.

(ii) Literal $x^{<q>} = x^{abcde}$ represents a cyclic change of the value of the variable x, i.e., a becomes b, b becomes c, c becomes d, d becomes e, and e becomes a. If the length of the string $<q>$ is less than five, then the missing values remain unchanged. There are 80 such literals.

(iii) Literal $x^{<p/q>} = x^{ab/cde}$ represents a cyclic change of the value of the variable x in two segments, i.e., a becomes b and b becomes a; c becomes d, d becomes e, and e becomes c. If the sum of the lengths of the two substrings is four, the missing value remains unchanged. There are 35 such literals.

Readers should note that the length of the superscript for 1-RPLs is one and that of the reversible literals is two to six.

GFSOP expression is defined using the following definitions.

Definition 3. Product of 1-RPLs and reversible literals are known as Galois field product (GFP). For example, $x^1y^{23}z^{01/234}$ is a GFP.

Definition 4. Sum of GFPs is known as GFSOP expression. For example, $x^1y^{23}z^{01/234} + y^3z^{234}$ is a GFSOP expression.

Definition 5. If a GFSOP expression contains only 1-RPLs and each GFP contains all variables, then we call that expression a canonical GFSOP expression. For example, $x^1y^3z^0 + x^3y^3z^2$ is a canonical GFSOP expression.

IV. QUINARY GALOIS FIELD EXPANSIONS

In this paper, we will use 114 Galois field expansions (GFEs) from our preliminary paper [19] for minimization of GFSOP expression.

Definition 6. The cofactors of an n-variable quinary logic function f_k where $k \in \{0, 1, 2, 3, 4\}$, with respect to the variable x_i are defined as $f_k = f(x_1, \ldots, x_{i-1}, k, x_{i+1}, \ldots, x_n)$. For example, $f_2 = f(x_1, \ldots, x_{i-1}, 2, x_{i+1}, \ldots, x_n)$.

Definition 7. A composite cofactor is the sum of more than one cofactors such as $f_i + f_j$, where $0 \leq i < j \leq 4$, and is represented as f_{ij}. For example, $f_{02} = f_0 + f_2$.

The fundamental quinary GFE is given in the following theorem from [19].

Theorem 1. Any n-variable quinary logic function f can be expanded with respect to the variable x using the GFE:

$$f = x^0f_0 + x^1f_1 + x^2f_2 + x^3f_3 + x^4f_4 \quad \text{(GFE1)}$$

GFE1 is the fundamental expansion using 1-RPLs and, if applied on all variables, the resultant expression will be a canonical GFSOP expression. Based on this GFE1, other 113 GFEs using 1-RPLs and reversible literals are developed in [19]. For space constraint, we show only GFE87 and GFE105 here from [19].

$$f = x^0f_{03} + x^1f_1 + x^2f_{24} + x^{+1}x^{+3}x^{0341}f_3 + xx^{+2}x^{0231}f_4 \text{(GFE87)}$$

$$f = x^0f_0 + xx^{+1}x^{+2}f_1 + x^2f_{12} + x^3f_{34} + xx^{0132}x^{0341}f_4 \text{ (GFE105)}$$

Application of GFEs on variables of a quinary logic function produces a non-canonical GFSOP expression that leads to minimization of GFSOP expression.

V. MINIMIZATION OF GFSOP EXPRESSION

The size of the minimized GFSOP expression depends on both variable ordering and GFE selection for the variables for application of GFEs. Here we propose a heuristic algorithm for simultaneous variable ordering and GFE selection with the view to maximize the number of zeros in the transformed vector. The n-variable completely specified quinary logic function f is represented by its output vector as an array with indices 0 to $5^n - 1$, where the indices correspond to the input values. For the proposed heuristic algorithm, we consider groups of 5^{n-i} length for $i = 1, 2, \ldots, n$ starting from the group boundary index $j5^{n-i}$ for $j = 0, 1, \ldots, (5^i - 1)$. For example, if $n = 2$ and $i = 1$, then the group length is 5 and the groups start from indices 0, 5, 10, 15, and 20, respectively. If such a group contains all 0s, then the cofactors resulting from that group will all be 0. We will designate such a group of 5^{n-i} 0s by Z_i.

The following heuristic algorithm simultaneously determines variable ordering and GFEs for variables:

1. For all n variables, find expansions for the GFEs 1 to 114. For each expansion compute Z_1 to Z_n.
2. Select the variable and GFE corresponding to the highest Z_1. In case of a tie, break it using Z_2 to Z_n. This selection will produce maximum number of 0s in the transformed vector. If the tie can not be resolved using Z_1 to Z_n, break it arbitrarily.
3. For the next transformation, repeat steps 1 and 2 for the remaining $(n - 1)$ variables. Repeat this process until all the variables are exhausted.
4. For multi-output function, repeat steps 1 to 3 for all output functions separately. Then, identify the common GFPs.

We illustrate the heuristic algorithm using a two-variable example function

$F(A, B) = [00104\ 00203\ 02302\ 12342\ 43213]^T$ (1)

expressed as output column vector, where the vector entry is the output value and the index of the vector entry is the input combination. The algorithm identifies variable A as the first variable and the corresponding GFE is GFE105. After application of GFE105 on the variable A of the vector of (1), the transformed vector is

$[00104\ 00203\ 02000\ 00000\ 43213]^T$ (2)

The only remaining variable is B and the algorithm identifies GFE87 as the best GFE for this variable. After application of GFE87 on the variable B of the vector of (2), the final transformed vector is

$[00004\ 00003\ 02000\ 00000\ 03013]^T$ (3)

Minimized GFSOP expression is written from the final transformed vector of (3). The first non-zero element of the final vector is 4, whose index is 4 and the input combination is $AB = 04$. As the value of the variable A is 0, we take the product corresponding to the 0th location of GFE105 (corresponding to the cofactor f_0), which is A^0. As the value of the variable B is 4, we take the product corresponding to the 4th location of GFE87 (corresponding to the cofactor f_4), which is $BB^{+2}B^{0231}$. Then these two products are multiplied with the constant 4 resulting into the product $4A^0BB^{+2}B^{0231}$. The constant 4 can be eliminated by multiplying it with any reversible literal of the product term. For example $4B = B^{14/23}$. Therefore, the product $4A^0BB^{+2}B^{0231}$ can be rewritten as $A^0B^{14/23}B^{+2}B^{0231}$. Similarly, determining products for all non-zero elements and then summing them up, we find the minimized GFSOP expression from (3) as follows:

$$F(A, B) = A^0B^{14/23}B^{+2}B^{0231} + A^{1342}A^{+1}A^{+2}BB^{+2}B^{0231} + 2A^2B^1 + A^{1342}A^{0132}A^{0341}B^1 + AA^{0132}A^{0341}B^{+1}B^{+3}B^{0341} + A^{1342}A^{0132}A^{0341}BB^{+2}B^{0231} \quad (4)$$

The GFSOP expression of (4) is a minimized GFSOP expression having only six product terms. If we would represent the same function as canonical GFSOP expression, it would need 17 product terms.

VI. REVERSIBLE GATES

Any 1×1 reversible operation can theoretically be realized using reversible technologies. For example, any d-valued ($d > 2$) 1×1 reversible operation can be realized using liquid ion-trap technology [17] as 1×1 gate. Thus, 120 quinary reversible literals discussed in Definition 2 can be realized using 1×1 gates. We will represent an 1×1 gate using the symbol of Fig. 1, where A^z is the output of the gate after reversible operation z is applied on the input A.

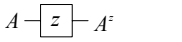

Fig. 1. Symbol of quinary 1×1 gate.

Muthukrishnan and Stroud [17] proposed a liquid ion-trap realizable 2×2 d-valued ($d > 2$) controlled quantum (which is reversible in nature) gate family, where a reversible operation is applied on the controlled input when the value of the controlling input is $d - 1$. We will refer to this family of gates as Muthukrishnan-Stroud (M-S) gate family. The symbol of quinary M-S gate is shown in Fig. 2.

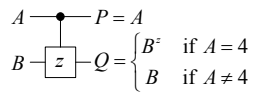

Fig. 2. Symbol of quinary M-S gate family.

We propose here a method of realization of quinary 1-RPLs using 1×1 and M-S gates as shown in Fig. 3. The 1×1 gate $+(4 - i)$ generates the required controlling value of x. The 1×1 gate $+(1 + i)$ restores the value of the input A, since $+(4 - i) + (1 + i) = 0$. The value of $i = 0$, 1, 2, 3, 4 will realize 1-RPLs A^0, A^1, A^2, A^3, A^4, respectively.

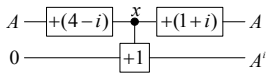

Fig. 3. Realization of quinary 1-RPLs.

The symbol of quinary Feynman gate is shown in Fig. 4. Feynman gate is a macro-level gate and can be realized on the top of 1×1 and M-S gates without using any ancilla input [18]. The symbol of 3-input quinary Toffoli gate is shown in Fig. 5. Toffoli gate may have three or more inputs. If the inputs of an n-input Toffoli gate are $(A_1, A_2, \ldots, A_{n-1}, A_n)$, then the outputs are $(A_1, A_2, \ldots, A_{n-1}, A_n + A_1A_2\ldots A_{n-1})$. Toffoli gate is a macro-level gate and can be realized on the top of 1×1 and M-S gates without ancilla input [18]. Readers can easily see that the Feynman gate can be considered as a two-input Toffoli gate.

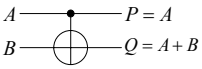

Fig. 4. Symbol of quinary Feynman gate.

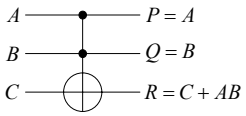

Fig. 5. Symbol of quinary 3-input Toffoli gate.

VII. REALIZATION OF GFSOP EXPRESSION

A quinary GFSOP expression is realized as a cascade of 1×1, M-S, Feynman, and n-input Toffoli gates. The product terms are generated and summed with other product terms using Toffoli gates. For realization of literals, necessary copies of the concerned input is made using Feynman gate. To reduce the number of additional copies of the input, we generate the literals along the same copy of the input. To reduce the number of 1×1 gate, we use a literal as many times as possible before changing it to another literal. For this purpose, we develop literal and product ordering techniques as briefly discussed below:

1. Determine the literal counts for each variable in the given GFSOP expression. Order the literals for each variable in the decreasing order of count. Break the tie arbitrarily. Rearrange the literals in the given GFSOP expression using the order. This

rearrangement of the literals will make the most frequent literal appears first in the product term.

2. Determine the score for each product term of the given GFSOP expression as sum of its literal counts. Order the product terms in the decreasing order of scores. Break the tie using decreasing number of matches with the preceding product term. Rewrite the GFSOP expression according to the decreasing order of the product terms. This sort of rearrangement of the literals and the product terms will ensure that most frequent literals appear in consecutive product terms and the literals can be realized once and used for generating the concerned product terms. This will help reduce number of 1×1 gates needed to generate the literals.

Because of space constraint, the above literal and product ordering technique is not illustrated with example. However, application of the above technique on the GFSOP expression of (4) results into the rewritten GFSOP expression as follows:

$$F(A, B) = A^{1342}A^{0132}A^{0341}B^{+2}B^{0231}B + A^{1342}A^{+1}A^{+2}B^{+2}B^{0231}B + A^{1342}A^{0132}A^{0341}B^{1} + A^{0132}A^{0341}AB^{+1}B^{+3}B^{0341} + A^{0}B^{+2}B^{0231}B^{14/23} + 2A^{2}B^{1} \quad (5)$$

We develop a method for GFSOP synthesis using cascade of reversible gates as briefly discussed below:

1. Count the maximum number of reversible literals of each variable appearing in any product term of the GFSOP expression. If these numbers are more than one, then create additional copies of the variables using Feynman gate. If any variable has 1-RPLs in the GFSOP expression, then add an input constant 0 line with that variable. If some constants cannot be eliminated from the GFSOP expression, then add a constant input line.
2. A reversible literal is generated by changing the previous literal to the desired literal by using an 1×1 gate. The 1-RPLs are generated along the constant 0 line as in Fig. 3. Though the 1-RPLs are generated along the same constant 0 line, depending on the value of the input variable, only one 1-RPL will be generated along the line.
3. The literals of the first product term are generated and then multiplied and summed with the 0 input constant by a Toffoli gate. The literals of the second product term that are not already available are generated and all the literals are multiplied and summed with the previous product term with another Toffoli gate. In this way we complete the circuit. This technique ensure that the literal that is used more than once is tried to be generated once and used in concerned product terms generations. This will eventually reduce the number of 1×1 gates needed. Generating the literals along the same line, rather than using different copy of the variable, will reduce the width of the circuit.

For space constraint, the above method of GFSOP synthesis is not illustrated with example. However, the realization of the GFSOP expression of (5) using the above synthesis technique is shown in Fig. 6.

VIII. EXPERIMENTAL RESULTS

We implement the GFSOP minimization algorithm using C language on a PC. We experiment with the following functions:

prod*n*: input $x_0, x_1, \ldots, x_{n-1}$; output $y = (x_0x_1\ldots x_{n-1}) \bmod 5$. [Output is the GF(5) product of n input variables.]

sum*n*: input $x_0, x_1, \ldots, x_{n-1}$; output $y = (x_0 + x_1 + \ldots + x_{n-1}) \bmod 5$. [Output is the GF(5) sum of n input variables.]

***n*cy*r*:** input $x_0, x_1, \ldots, x_{n-1}$; output $y = \left[\sum_{i=0}^{n-1} + \left(\prod_{j=0}^{r-1} x_{(i+j) \bmod n}\right)\right] \bmod 5$. [A quinary GFSOP function of n input variables, where the products consist of r input variables in cyclic order. For example, 3cy2 is $y(a, b, c) = (ab + bc + ca) \bmod 5$.]

sqsum*n*: input $x_0, x_1, \ldots, x_{n-1}$; output

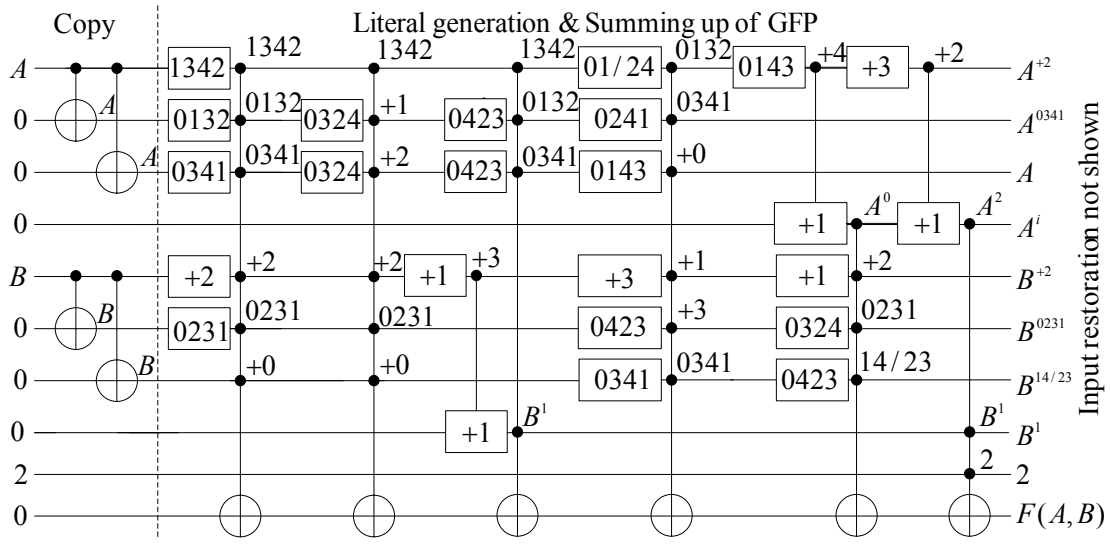

Fig. 6. Realization of quinary GFSOP expression of (5).

$y = \left(x_0^2 + x_1^2 + \cdots + x_{n-1}^2\right) \bmod 5$. [Output is the GF(5) sum of squares of n input variables.]

avg*n*: input $x_0, x_1, \ldots, x_{n-1}$; output $y = \text{int}[(x_0 + x_1 + \ldots + x_{n-1})/n] \bmod 5$. [Output is the integer part of the average of n input variables expressed as mod 5 value.]

a2bcc: input a, b, c; output $y = (a^2 + bc + c) \bmod 5$. [An arbitrary quinary function.]

qhadd: input a, b; output $c = \text{int}[(a + b)/5]$, $s = (a + b) \bmod 5$. [Quinary half-adder]

qfadd: input a, b, c; output (carry out) $c_o = \begin{cases} \text{int}[(a+b+c)/5] & \text{if } c_i \le 1 \\ \text{don't care} & \text{if } c_i > 1 \end{cases}$, (sum) $s = \begin{cases} (a+b+c) \bmod 5 & \text{if } c_i \le 1 \\ \text{don't care} & \text{if } c_i > 1 \end{cases}$. [Quinary full-adder]

mul2: input a, b; output $c = \text{int}[ab/5]$, $m = ab \bmod 5$. [2-digit quinary multiplier.]

mul3: input a, b, c; output $c = \text{int}[abc/5]$, $m = abc \bmod 5$. [An arbitrary quinary function.]

The proposed GFSOP minimization algorithm works with only completely specified quinary logic function. That is why, in our experiment, we have replaced the don't care outputs of incompletely specified function by 0s. The experimental results are shown in Table II. In the table "Func" is the function name as defined above, "# of in" is the number of input variables, "# of out" is the number of outputs, "# of cano prod" is the number of products in the canonical GFSOP expression, "# of mini prod" is the number of products in the minimized GFSOP expression, and "% of minimization" is the percentage of minimization with respect to canonical GFSOP expression. The experimental results show that a significant minimization over canonical GFSOP expression is achieved for the functions **prod2**, **prod3**, **prod4**, **a2bcc**, **mul2**, and **mul3**. Minimizations of other functions are also quite satisfactory.

IX. CONCLUSION AND FURTHER WORK

Multiple-valued logic functions can be very easily represented as GFSOP expression [4], [16] and the GFSOP expression can be realized as cascade of reversible gates [4], [12]. This approach uses multiple-input Toffoli gates for the cascade. Previously, multiple-valued Toffoli gate realization required many ancilla constant making the realized GFSOP circuit very wide. Ancilla free realization of Toffoli gate [18] makes this GFSOP based synthesis more promising than the earlier. GFSOP based synthesis of ternary [4] and quaternary [12], [16] logic functions are already reported. In this paper, we show the technique for minimization of quinary logic function as GFSOP expression. For this purpose, we use 114 Galois field expansions (GFEs) from our preliminary paper [19]. Then, we show method for realization of GFSOP expression as cascade of reversible gates. We synthesize GFSOP expression as a cascade of 1×1, M-S, Feynman, and n-input Toffoli gates. To reduce the number of gates in the realization, we develop literal ordering and product ordering techniques. We also develop a technique of synthesizing GFSOP expression using reversible gates so that the width of the synthesized circuit and the total number of gates required are as minimum as possible.

We experiment with 17 functions of two to four input variables and one to two outputs. Experimental results show a significant minimization of six functions. Minimizations of other functions are also quite good. We are doing new experiments with functions having more than four input variables to see the performance of the proposed minimization technique.

Table II. Experimental results.

Func	**# of in**	**# of out**	**# of cano prod**	**# of mini prod**	**% of minimization**
prod2	2	1	16	4	75.00
prod3	3	1	64	8	87.50
prod4	4	1	256	130	49.22
sum2	2	1	20	17	15.00
sum3	3	1	100	97	3.00
sum4	4	1	500	457	8.60
3cy2	3	1	68	59	13.24
sqsum2	2	1	16	12	25.00
sqsum3	3	1	90	78	13.33
sqsum4	4	1	480	413	13.96
avg2	2	1	22	17	22.73
avg3	3	1	115	95	17.39
a2bcc	3	1	100	60	40.00
qhadd	2	2	27	23	14.81
qfadd	3	2	58	54	6.89
mul2	2	2	20	9	55.00
mul3	3	2	90	46	48.89

The proposed GFSOP synthesis method implicitly converts a non-reversible function into a reversible function for synthesis using reversible gates.

We are working for developing more quinary GFEs. We expect that proposed minimization method with additional quinary GFEs (old 114 and more new) will produce more interesting minimization results.

The proposed GFSOP minimization method works with completely specified functions. Further attempt may be taken to develop GFSOP minimization method for incompletely specified functions, though the problem is very difficult to handle.

REFERENCES

[1] C.H. Bennett, "Logical reversibility of computation," *IBM Journal of Research and Development*, vol. 17, 1973, pp. 525-532.

[2] E. Curtis and M. Perkowski, "A transformation

based algorithm for ternary reversible logic synthesis using universally controlled ternary gates," *Proceedings of International Workshop on Logic and Synthesis (IWLS 2004)*, Tamecula, California, USA, 2-4 June 2004.

[3] N. Denler, B. Yen, M. Perkowski, and P. Kerntopf, "Synthesis of reversible circuits from a subset of Muthukrishnan-Stroud quantum multi-valued gates," *Proceedings of International Workshop on Logic and Synthesis (IWLS 2004)*, Tamecula, California, USA, 2-4 June 2004.

[4] M.H.A. Khan, M.A. Perkowski, M. R. Khan, and P. Kerntopf, "Ternary GFSOP minimization using Kronecker decision diagrams and their synthesis with quantum cascades," *Journal of Multiple-Valued Logic and Soft Computing*, vol. 11, 2005, pp. 567-602.

[5] D.M. Miller, D. Maslove, and G.W. Dueck, "Synthesis of quantum multiple-valued circuits," *Journal of Multiple-Valued Logic and Soft Computing*, vol. 12, no. 5-6, 2006.

[6] M. Perkowski, A. Al-Rabadi, and P. Kerntopf, "Multiple-valued quantum logic synthesis," *Proceedings of 2002 International Symposium on New Paradigm VLSI Computing*, Sendai, Japan, 12-14 December 2002, pp. 41-47.

[7] B. Yen, P. Tomson, and M. Perkowski, "Sum of non-disjoint cubes covering generation for multi-valued systems of base 2, for use in Muthukrishnan-Stroud quantum realizable gates: an extension of the EXOR covering problem," *Proceedings of International Workshop on Logic and Synthesis (IWLS 2005)*.

[8] M.H.A. Khan and M.A. Perkowski, "Quantum ternary parallel adder/subtractor with partially-look-ahead carry," *Journal of System Architecture*, vol. 53, no. 7, 2007, pp. 453-464.

[9] M.H.A. Khan and M.A. Perkowski, "Quantum realization of ternary encoder and decoder," *Proceedings of 7th International Symposium on Representations and Methodology of Future Computing Technologies (RM 2005)*, Tokyo, Japan, 5-6 September 2005.

[10] M.H.A. Khan, "Design of reversible/quantum ternary multiplexer and demultiplexer," *Engineering Letters*, vol. 13, no. 2, 2006, pp. 65-69.

[11] M.H.A. Khan, "Design of reversible/quantum ternary comparator circuits," *Engineering Letters*, vol. 16, no. 2, pp. 178-184.

[12] M.H.A. Khan and M.A. Perkowski, "GF(4) based synthesis of quaternary reversible/quantum logic circuits," *Journal of Multiple-Valued Logic and Soft Computing*, vol. 13, 2007, pp. 583-603.

[13] M.H.A. Khan, "Reversible realization of quaternary decoder, multiplexer, and demultiplexer circuits," *Engineering Letters*, vol. 15, no. 2, 2007, pp. 203-207.

[14] M.H.A. Khan, "A recursive method for synthesizing quantum/reversible quaternary parallel adder/subtractor with look-ahead carry," *Journal of Systems Architecture*, vol. 54, no. 12, 2008, pp. 1113-1121.

[15] M.H.A. Khan, "Synthesis of quaternary reversible/quantum comparators," *Journal of Systems Architecture*, vol. 54, no. 10, 2008, pp. 977-982.

[16] M.H.A. Khan, N.K. Siddika, and M.A. Perkowski, "Minimization of quaternary Galois field sum of products expression for multi-output quaternary logic function using quaternary Galois field decision diagram," *Proceedings of 38th International Symposium on Multiple-Valued Logic (ISMVL 2008)*, Dallas, TX, USA, 22-24 May 2008, pp. 125-130.

[17] A. Muthukrishnan and C.R. Stroud Jr., "Multivalued logic gates for quantum computation," *Physical Review A*. vol. 62, 2000, 052309/1-8.

[18] M.H.A. Khan, "Quantum realization of multiple-valued Feynman and Toffoli gates without ancilla input," *Proceedings of 39th International Symposium on Multiple-Valued Logic (ISMVL 2009)*, Naha, Okinawa, Japan, 21-23 May 2009, pp. 103-108.

[19] M.H.A. Khan, "Reversible synthesis of quinary logic function," *18th International Workshop on Post-Binary ULSI Systems (ULSIWS2009)*, Naha, Okinawa, Japan 20 May 2009.

Proceedings of 2009 12th International Conference on Computer and Information Technology (ICCIT 2009)
21-23 December, 2009, Dhaka, Bangladesh

Capacity Enhancement of Limited User Traffic of Mobile Cellular Networks Using DOVE Technique

Md. Omar Faruq†, Md. Arifur Rahman†, Md. Imdadul Islam‡, and M. R. Amin†

†Department of Electronics and Communications Engineering, East West University, 43 Mohakhali, Dhaka 1212, Bangladesh
‡Department of Computer Science and Engineering, Jahangirnagar University, Savar, Dhaka 1342, Bangladesh
imdad@juniv.edu, ramin@ewubd.edu

Abstract

In this paper, a simple scheme is presented to improve the performance of mobile cellular networks by using delay of voice end user (DOVE) to the new originating calls over handoff calls in a two-dimensional (2D) traffic model for finite number of users. Expressions for probability of forced termination of handoff calls and the blocking probability of new originating calls have been derived. From this study, it has been found that the probability of forced termination of handoff calls is significantly reduced due to the incorporation of the delay of voice end user compared to the case when no such delay of voice end user is used in the system.

Keywords: Limited user traffic, DOVE, new originated calls, handoff calls, blocking probability.

I. INTRODUCTION

In wired or wireless communications, performance of a network is measured in terms of grade of service (GoS) or call blocking probability. From a handoff perspective, it is important that a free channel be available in a new cell whenever handoff occurs, so that undisrupted service is continued. It is well known that a handoff call being dropped is more disastrous than a new originated call being unsuccessful due to blocking. Therefore, it is much more important to provide a higher priority to an existing call that can be continued through the handoff process compared to the new originating calls.

One of the established strategies is to use guard channels or priority reservation scheme [1]-[3]. The use of guard channels is one of the easiest way of ensuring a certain GoS and is widely accepted and implemented. This technique of having a fixed number of channels in each cell, reserved exclusively for handoff requests. These extra channels reduce the negative effect caused by dropping a call in progress, thus providing the overall GoS of the network. However, the drawback for using reserved channels for handoff calls is that the channels that are reserved may be unoccupied for a long duration and the service provider may loose huge revenue. Another strategy employed is the queuing to improve the GoS [4], [5]. Some schemes propose the insertion of a queue to deal with new originating calls, given the less restrictive delay constraint of this type of calls in comparison with handoff calls. Some studies also propose for queuing the handoff calls, in an attempt to reduce the call dropping probability. Mixed schemes with guard channels and buffering techniques have also been proposed [6]-[9].

Oliver and Joan [10] have recently proposed a variable reservation scheme for mobile cellular networks, based on prioritization of handoff calls over new originating calls. They have shown that a noticeable improvement in blocking and call dropping probabilities have been achieved using adaptive channel reservation mechanism. However, such improvement is achieved at the expanse of signaling protocol overhead.

Voice calls are assigned preemptive priority over data calls [11]. These schemes, however, do not differentiate handoff calls from new originating calls, thus the strict requirement of handoff dropping probability cannot be met. A preemptive handoff scheme is proposed by Li et al. [12], where handoff voice calls have the right to preempt data calls. Since handoff voice calls and new originating calls use the same set of channels, voice handoff dropping probability is still high when there are too many new originating voice calls. A dual trunk reservation with queuing scheme has been studied by Wu et al. [13], in which two thresholds are used, one to reserve bandwidth for handoff voice calls and the other for managing the data traffic.

Recently, two handoff schemes with and without preemptive priority procedures were proposed by Zeng and Agrawal [14], where both real time and non-real time handoff requests are allowed to be queued. These schemes are based on the complete sharing strategy with an objective of maximizing channel utilization. However, since the different types of traffic share the same set of channels, QoS of one type of traffic is affected by the other. Consequently, QoS of each service cannot be easily controlled [3]. In addition, these schemes reserve guard channels for handoff calls in order to minimize handoff dropping probability [15]. The limitation of the guard channel schemes, as has been discussed earlier, is that some of reserved channels for handoff requests may be idle when new calls are blocked if handoff requests are not very often.

In this present study, a very simple scheme is proposed to improve the performance of mobile cellular networks by adopting some delay to the last user of the new originating calls over the handoff calls. A two-dimensional (2D) traffic model is studied here for the

978-1-4244-6283-4/09/$26.00 ©2009 IEEE

delay of voice end user (DOVE) on the performance evaluation [16], particularly the probability of forced termination of the handoff calls and the blocking probability of the new originating calls [17]. It has been found in this study that the probability of forced termination of handoff calls is drastically reduced.

The paper is organized as follows. Section II describes in short the analytical model. In this section, expressions for the probability of forced termination of handoff calls and the blocking probability of new originating calls are derived. Results and discussions are given in Section III and finally Section IV concludes the paper.

II. THE TRAFFIC MODEL

For simplicity, a mobile cellular system with homogeneous cells and a fixed number of channels which are permanently allocated to each cell is considered. In such a system, attention is focused on a single cell; let this cell be called as the reference cell. Newly generated calls in the reference cell are called originating calls. When a moving real time service (voice call, called handoff call) user holding a channel approaches from a neighboring cell, a handoff request is generated in the reference cell.

The Engset loss formula applies to telephony situations where the number of customers is small relative to the number of available circuits. Such situations include: an exchange in a small rural community, PABX, or a lucrative satellite service to a small number of customers. Let the call holding times be independent identically distributed (iid) and exponentially distributed with mean $1/\mu$ and the time until an idle source attempts to make a call is also exponential with mean $1/\lambda$, where μ and λ are respectively the average service termination rate and the average arrival rate. Let the number of customers (sources of traffic) be *N*, the number of circuits be *m*.

The proposed model here is developed by using the DOVE in the system for the performance improvement of mobile cellular networks. No channel reservation for the handoff calls is assumed in the system. In this scheme, the handoff calls are given priority and will be served without delay and the new originating call of the end user is given a delay of $d = 1/\delta$. In this situation all assumptions are equally applicable to all cells in the system. The resulting 2D Markov chain in this case is shown in Fig. 1. Here, in this Fig. 1, only the probability states for new originating calls are shown in the column but as it is a 2D model there are also probability states for handoff calls along a row, which are not shown in Fig. 1.

After solving the node equations of 2D Markov chain of Fig. 1, the stationary probability distributions are obtained as

$$P_{x,y} = \binom{N}{x}\binom{N}{y} a_H^x \, a_O^y \, P_{0,0} \,, \qquad (1)$$

where $0 \le y \le m-x-1, 0 \le x \le m$ and $a_H = \lambda_H / \mu_H$ and $a_O = \lambda_O / \mu_O$.

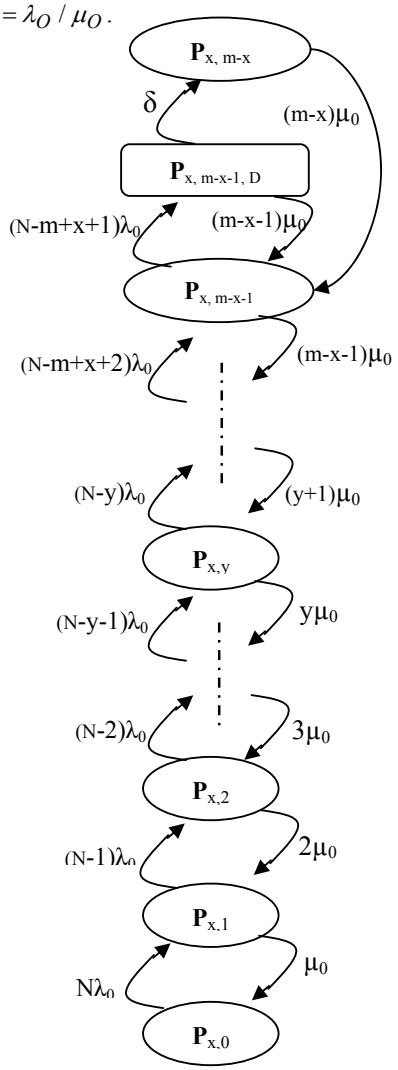

Fig. 1. 2D Erlang model for limited user traffic of originating call showing the vertical direction at x position in the horizontal direction.

After some mathematical manipulations, the expression for the probability state $P_{x,D}$ becomes

$$P_{x,D} = \left(\frac{N-m+x+1}{\delta+(m-x-1)\mu_O}\right)\lambda_O \times \binom{N}{x}\binom{N}{m-x-1} a_H{}^X a_O{}^{m-x-1} P_{0,0}. \qquad (2)$$

And expression for $P_{x,m-x}$ is obtained as

$$P_{x,m-x} = \left(\frac{\delta}{\delta+(m-x-1)\mu_O}\right) \times \binom{N}{x}\binom{N}{m-x} a_H{}^X a_O{}^{m-x} P_{0,0}. \qquad (3)$$

After normalization, that is, setting the sum of the probabilities of all the possible stationary states to unity, we obtain

$$P_{0,0} = (A+B)^{-1}, \tag{4}$$

where

$$A = \sum_{x=0}^{m} \sum_{y=0}^{m-x-1} \binom{N}{x}\binom{N}{y} a_H^x a_O^y ,$$

and

$$B = \sum_{x=0}^{m} \left(\frac{\delta + (m-x)\mu_O}{\delta + (m-x-1)\mu_O} \right) \binom{N}{x}\binom{N}{m-x} a_H^x a_O^{m-x} .$$

The probability of forced termination is

$$P_{FT} = \sum_{x=0}^{m} \left(\frac{\delta}{\delta + (m-x-1)\mu_O} \right) \binom{N}{x}\binom{N}{m-x} a_H^x a_O^{m-x} P_{0,0} , \tag{5}$$

and the blocking probability is obtained as

$$P_B = \sum_{x=0}^{m} \left(\frac{\delta + (m-x)\mu_O}{\delta + (m-x-1)\mu_O} \right) \binom{N}{x}\binom{N}{m-x} a_H^x a_O^{m-x} P_{0,0} . \tag{6}$$

III. RESULTS AND DISCUSSION

To obtain a better numerical appreciation of the results, we assume the following parameters for a cell of a mobile cellular system: number of users in a cell, N = 150, number of channels in the cell, m = 15 and 20, arrival rate of new originating calls, $\lambda_O = 0.02 - 0.04 / \min$, termination rate of new originating calls, $\mu_O = 1.2 - 1.6 / \min$, arrival rate of handoff calls, $\lambda_H = 0.015 - 0.03 / \min$, termination rate of handoff calls, $\mu_H = 1.4 - 1.8 / \min$, delay of voice end user, d = 0.1, 0.2, 0.5 and 1.0 min.

The probability of forced termination of the handoff calls, P_{FT} from Eq. (5) and the blocking probability P_B from Eq. (6) are plotted against the offered traffic of new originating calls and handoff calls in Figs. 2 – 5. In Fig. 2, the probability of forced termination for the handoff calls is drawn against the offered traffic of handoff calls in the 2D Erlang traffic model for the DOVE (where, last end user of voice originating calls is delayed). Here 15 channels are considered. It is observed from the Fig. 2 that the probability of forced termination in the case of DOVE is drastically reduced as the offered traffic of handoff calls increases beyond $a_H = 0.016$ Erls compared to the case when there is no delay to the voice end user is considered. From Fig. 3, it is noticed that the blocking probability of handoff calls for DOVE is almost same for the usual Erlang model. It is observed from Fig. 4 that the probability of forced termination in the case of DOVE is drastically reduced as the offered traffic of handoff calls increases beyond $a_H = 0.016$ Erls compared to the case when there is no delay to the voice end user is considered. Here the number of channels is kept same as that in Fig. 2, but the delay is extended to 1.0 min. We see, time extension over 0.5 min gives slow decrease to the probability of forced termination.

It has been seen (though not shown in figure) that the blocking probability of handoff calls is also almost same as the usual Erlang model. We do not see any further change in curves for time extension to 1.0 min. Fig. 5, shows the variation of the probability of forced termination with respect to the offered traffic of the handoff calls. It is observed from Fig. 5 that the probability of forced termination in the case of DOVE falls significantly with the offered traffic of handoff calls in comparison with the usual Erlang model with no delay to the voice end user. Here the number of channels is taken as 20.

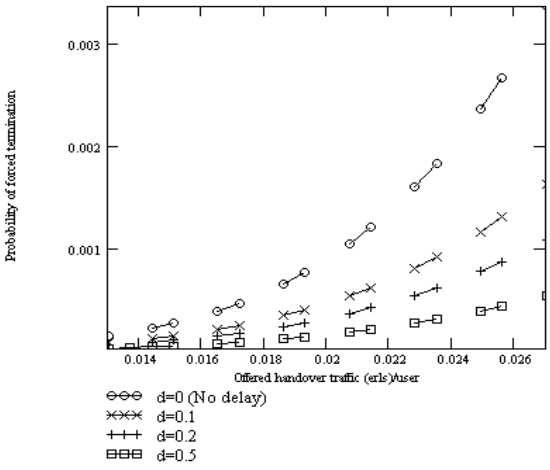

Fig. 2. Variation of the probability of forced termination of handoff calls against offered traffic of handoff calls (m=15, N=150, $\mu_O = 1.5$, $\mu_H = 1.4$, d=0 min, d=0.1 min, d=0.2 min, d=0.5 min).

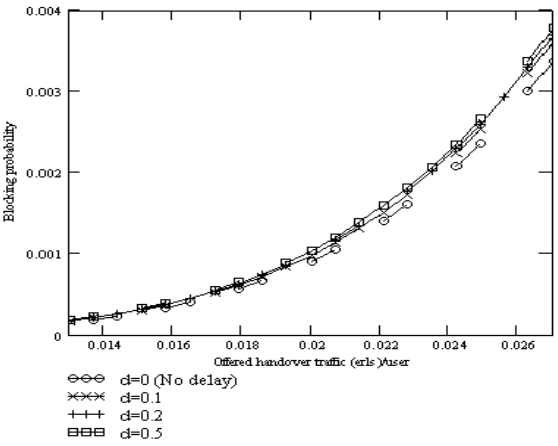

Fig. 3. Variation of the blocking probability of new originating calls against offered traffic of handoff calls (m=15, N=150, $\mu_O = 1.5$, $\mu_H = 1.4$, d=0 min, d=0.1 min, d=0.2 min, d=0.5 min).

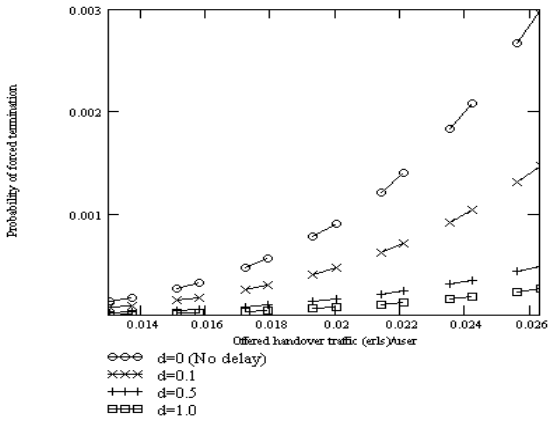

Fig. 4. Variation of the probability of forced termination of handoff calls against offered traffic of handoff calls (m=15, N=150, $\mu_O = 1.5$, $\mu_H = 1.4$, d=0 min, d=0.1 min, d=0.5 min, d=1.0 min).

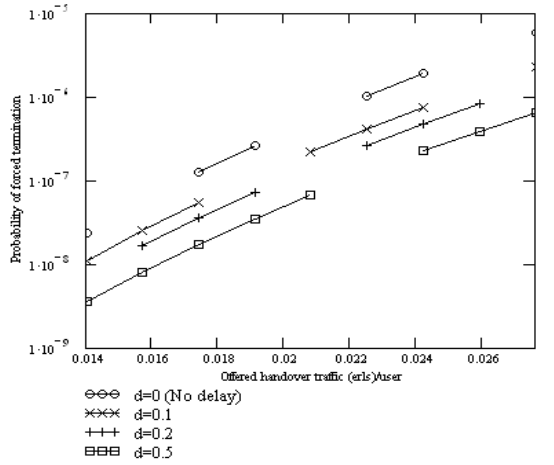

Fig. 5. Variation of the probability of forced termination of handoff calls against offered traffic of handoff calls (m=20, N=150, $\mu_O = 1.3$, $\mu_H = 1.6$, d=0 min, d=0.1 min, d=0.2 min, d=0.5 min).

It is observed from Fig. 2, 4 and 5 for the probability of forced termination that a drastic improvement of performance in the case of DOVE occurs compared to the case of no delay to the voice end user. This is the new finding of the present study for finite users. Thus by introducing a very small delay to the voice end user, the model provides a tremendous performance improvement over the existing channel reservation scheme.

It should be mentioned here that the blocking probability of new originating calls is somewhat increased (negligibly) (Fig. 3) when we include DOVE for the new originating calls in the system. From the user`s point of view, as to handle a handoff request is more important than the blocking of new originating calls, this negligible increase in the blocking probability has no effect on the Erlang capacity for the users of the new originating calls.

IV. CONCLUSION

A new scheme of reducing the probability of forced termination of handoff calls is presented in this study in a limited user traffic model. The effects of delay of voice end user of new originating calls have been studied using a 2D traffic model for DOVE, with delay to the last end user of the new originating calls. It has been found from the study that the probability of forced termination of handoff calls is reduced drastically compared to the case when no delay to the voice end user is used in the system. The obtained results are also compared with the Erlang model for no delay used exclusively to handle handoff calls. It has been found in the case of DOVE that the model works much better than the existing method of channel reservation scheme for handoff calls. It is stressed that the concept of DOVE discussed in this study can easily be implemented in mobile cellular networks to improve the GoS without any resource constraint.

REFERENCES

[1] Y.B. Lin and I. Chlamtac, "Wireless and Mobile Network Architecture", 1st Edn., John Wiley and Sons, New York, ISBN: 978-0471394921, 2000.

[2] R. Ramjee, R. Nagarajan, and D. Towsley, "On optimal call admission control in cellular networks", INFOCOM 96. Fifteenth Annual Joint Conference of the IEEE Computer Societies. Networking the Next Generation. Proceedings IEEE, March 24-28, San Francisco, CA, USA., pp. 43-50, 1996.

[3] J. Wang, Z. Qing-An, and P. Dharma Agrawal, "Performance analysis of a preemptive and priority reservation handoff scheme for integrated service-based wireless mobile networks", IEEE Trans. Mobile Comput., vol. 2, pp. 65-75, Jan-March 2003.

[4] S. Tekinay and B. Jabbari, "A measurement-based prioritization scheme for handovers in mobile cellular networks", IEEE J. Select. Areas Commun., vol. 10, no. 8, pp. 1343-1350, Oct. 1992.

[5] D. Hong and S.S. Rappaport, "Traffic model and performance analysis for cellular mobile radio telephone systems with prioritized and non-prioritized handoff procedures", IEEE Trans. Veh. Technol., vol. 35, no. 3, pp. 77-92, Aug. 1986.

[6] R. Guerin, "Queuing-blocking system with two arrival streams and guard channels", IEEE Trans. Commun., vol. 36, no. 2, pp. 153-163, Feb. 1998.

[7] Q.A. Zeng, K. Mukumoto, and A. Fukuda, "Performance analysis of mobile cellular radio system with priority reservation handoff procedures", Proc. IEEE Veh. Technol. Conf., vol. 3, pp. 1829-1833, 1994.

[8] S.S. Rappaport, "The multiple-cell handoff problem in high capacity communications system", IEEE Trans. Veh. Technol., vol. 40, no. 3, pp. 546-557, Aug. 1991.

[9] C. Purzynski and S.S. Rappaport, “Multiple call handoff problem with queued handoffs and mixed platform types”, Inst. Elect. Eng. Proc. I, vol. 142, pp. 31-39, Feb. 1995.

[10] M. Oliver and B. Joan, “Performance evaluation of variable reservation policies for hand-off prioritization in mobile networks”, IEEE INFOCOM, vol. 1, pp. 1187-1194, 1999.

[11] F.N. Pavlidou, “Two-dimensional traffic models for cellular mobile systems”, IEEE Trans. Commun., vol. 42, no. 2-4, pp. 1505-1511, Feb.-April 1994.

[12] B. Li, Q.A. Zeng, K. Mukumoto, and A. Fukuda, “A preemptive priority handoff scheme in integrated voice and data cellular mobile systems”, Proc. Int. Conf. Commun. Technol., vol. 1, pp. 67-71, 1998.

[13] H. Wu, L. Li, B. Li and L. Yin, “On handoff performance for an integrated voice/data cellular system”, Proc. 13th IEEE Int. Symp. Personal, Indoor, Mobile Radio Commun., vol. 5, pp. 2180-2184, 2002.

[14] Q.A. Zeng and D.P. Agrawal, “Modeling and efficient handling of handoffs in integrated wireless mobile networks”, IEEE Trans. Veh. Technol., vol. 51, no. 6, pp. 1469-1478, Nov. 2002.

[15] B. Epstein and M. Schwartz, “Reservation strategies for multimedia traffic in a wireless environment”, Proc. IEEE Veh. Technol. Conf., vol. 1, pp. 165-169, 1995.

[16] M. Mahdavi, R.M. Edwards, and S.R. Cvetkovic, “Policy for enhancement of traffic in TDMA hybrid switched integrated voice/data cellular mobile communications systems”, IEEE Commun. Lett., vol. 5, no. 6, pp. 242-244, June 2001.

[17] M. R Amin and Md. I. Islam, “Evaluation of Delay of Voice End User in Cellular Mobile Networks with 2D Traffic System”, Research Journal of Information Technology vol. 1, no. 2, pp. 57-69, Feb. 2009.

Proceedings of 2009 12th International Conference on Computer and Information Technology (ICCIT 2009)
21-23 December, 2009, Dhaka, Bangladesh

Realization of Systolic Array using Ternary Reversible Gates

Naushin Nower and Ahsan Raja Chowdhury
Department of Computer Science and Engineering, Faculty of Engineering and Technology,
University of Dhaka, Dhaka-1000, Bangladesh
naushin64@yahoo.com, farhan717@cse.univdhaka.edu

Abstract

Multi valued logic synthesis is a very promising and affluent research area at present because of allowing designers to build much more efficient computers than the existing classical ones. Ternary logic synthesis research has got impetus in the recent years. Many existing literature are mainly perceptive to the realization of efficient ternary reversible processors. This research is based on the design of a reversible systolic array, which is one of the best examples of parallel processing, using micro level ternary Toffoli gate. General architecture of the ternary reversible systolic array multiplier is shown along with example. Lower bound for the garbage outputs produced in the proposed design and the quantum cost of the entire circuit is calculated here to prove the compactness of the design.

Keywords: Garbage Output, Reversible Gate, Systolic Array, Ternary Logic, Quantum Cost.

I. INTRODUCTION

In digital design, energy loss plays a significant role. Energy dissipation is associated to non-identity of switches and materials. It has been proved that, irreversible logic computation generate $kT*ln2$ heat for every bit that is lost (where k is the Boltzmann's constant and T is the temperature) [1, 2]. Though for a room temperature T, the amount of dissipating heat is minuscule (i.e. $2.9*10^{-21}$ joules) but not irrelevant. The design that doesn't resulting information loss called reversible. Reversible logic is emerging as a flourishing area of research having its applications in different sectors such as quantum computing, nanotechnology, and optical computing etc. Again systems that perform some operations in a reversible fashion can dissipate less energy and might prove competitive today.

Reversible are circuits (gates) in which the number of inputs is equal to the number of outputs and there is a one-to-one mapping between vectors of inputs and outputs; thus the vector of input states can always be re-constructed from the vector of output states [2]. More formally, a **reversible** logic gate is a k-input, k-output (denoted $k*k$) device that maps each possible input pattern into a unique output pattern [2]. This fact also applicable for multiple-valued logic, which demonstrates several potential advantages over binary technology. Quantum technology is inherently reversible and is one of the most potential technologies for future computing systems [3].

Ternary logic synthesis research provides a new-fangled era at present. Syntheses on ternary quantum logic using basic 2-qutrit controlled gates are presented on [4, 5]. The major sub-circuit needed for ternary logic has already been proposed in many literatures. Practically important ternary circuits like adder, subtractor, encoder, decoder, multiplexer, demultiplexer, comparators has already been proposed and currently been revising in many literatures. Realization of ternary reversible/quantum adder/subtractor is given in [5]. Synthesis of ternary reversible/quantum encoder and decoder is given in [6]. Realization of ternary reversible/quantum multiplexer/demultiplexer is given in [7]. In this paper, we present a design of reversible/quantum realization of ternary systolic array which is first proposed in literature. The design is based on Toffoli gates and 2-qutrit Muthukrishnan-Stroud (M-S) gates [8].

The rest of the paper is organized as follows: Section II provides the necessary background on reversible logic along with the examples of some popular reversible gates. Section III provides the design technique for Reversible Ternary Systolic Array. Evaluation of the proposed design is presented in Section IV. The paper concludes in Chapter V. Some important references are listed in Section VI.

II. BASIC DEFINITION & LITERATURE REVIEW

In this section introduces some basic terms and definitions used in this paper and some outcome of previous researchers.

A. TERNARY QUANTUM LOGIC

A ternary, three-valued or trivalent, logic is the simplest introduction of multivalued logic which is also referred to as 3VL. To define ternary logic let $A = \{0, 1, 2\}$. A ternary logic circuit f with n input variables, $A_1, \ldots, A_n$, and n output variables, $P_1, \ldots, P_n$, is denoted by $f : A^n \longrightarrow A^n$, where $(A_1, \ldots, A_n) \in A^n$ is the input vector and $(P_1, \ldots, P_n) \rightarrow A^n$ is the output vector. There are $3n$ different assignments for the input vectors. A ternary logic circuit f is reversible if it is a one-to-one and onto function (bijection). A ternary reversible logic circuit with n inputs and n outputs is also called an n-qudit ternary reversible gate.

In ternary quantum logic system the unit of memory (information) is a qutrit (quantum ternary digit). Ternary logic values of *0, 1*, and *2* are represented by a set of distinguishable different states of an object that

978-1-4244-6283-4/09/$26.00 ©2009 IEEE

represent the qutrit. After encoding these distinguishable quantities into ternary constants, qutrit states are represented by $|0\rangle, |1\rangle and\ |2\rangle$ respectively, and are called the computational basis states [5].

B. TERNARY GALOIS FIELD LOGIC

Ternary Galois Field (TGF) consists of the set of elements $T = \{0, 1, 2\}$ and two basic binary operations– ***addition*** (denoted by +) and ***multiplication*** (denoted by **.** or absence of any operator) as defined in Table I. GF3 addition and multiplication are closed, i.e., for $x, y \in T$, $x + y \in T$ and $xy \in T$. GF3 addition and multiplication are also commutative and associative, i.e., $x + y = y + x$ and $xy = yx$ (commutative), and $x + (y + z) = (y + z) + x = z + x + y$ and $x(yz) = (xy)z$ (associative). GF3 multiplication is distributive over addition, i.e. $x(y + z) = xy + xz$

Table I Ternary Galois Field (GF3) operations

+	0	1	2
0	0	1	2
1	1	2	0
2	2	0	1

•	0	1	2
0	0	0	0
1	0	1	2
2	0	2	1

C. TERNARY MUTHUKRISHNAN-STROUD GATE

Muthukrishnan and Stroud proposed a family of 2-qudit (quantum digit) *d*-valued gates, which applies a 1-qudit unitary transform on the second qudit conditional on the first qudit being (*d* – 1). The ternary M-S gate is a controlled gate [8] where the input *A* is the controlling input and the input *B* is the controlled input. The output *P* is equal to the input *A*. The output *Q* is the *Z* transform of the controlled input *B* if the controlling input *A* = 2, *Q* is equal to *B* otherwise. The ternary M-S gates can be realized using liquid ion trap quantum technology as an elementary gate [8]. Therefore, we assign these gates a cost of 1.

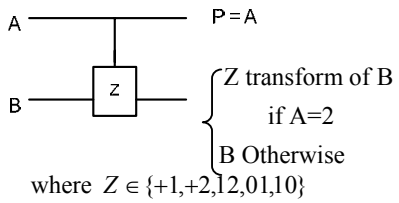

Fig. 1. Symbol of M-S gate

D. QUANTUM COST

Calculating Quantum cost of reversible circuit is a significant one. Every reversible gate can be calculated in terms of quantum cost and hence the reversible circuits can be measured in terms of quantum cost. Reducing the quantum cost from reversible circuit is always a challenging one and works are still going on in this area. In this paper we will show the quantum equivalent diagram of reversible gate that will be used to calculate the final quantum cost of proposed reversible ternary Systolic Array.

E. TERNARY TOFFOLI GATE

Ternary Toffoli gate is shown in Fig. 2(a), where its' corresponding MS implementation is shown in Fig. 2(b). If the two controlling input values are 2, then Z transform is applied on controlled input otherwise controlled input is passed unchanged. That is the outputs of the gate are $P = A$, $Q = B$, and $R = Z$ transform of C if $A = 2\ \hat{}\ B = 2$, where $Z \in \{+1,+2,12,01,10\}$; $C = Q$ otherwise.

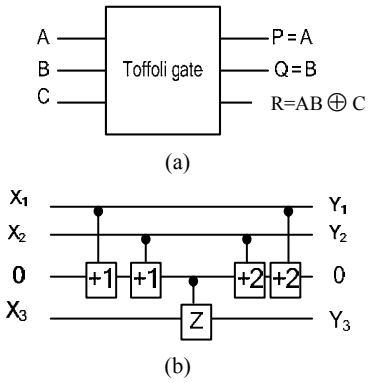

Fig. 2. 3-Qutrit ternary Toffoli gate: (a) Toffoli gate with I/O mapping (b) realization using M-S gates

Realization of this gate using M–S gates is shown in Fig. 2(b), where a constant input 0 is changed to 2 by using two +1 transforms controlled from the two controlling inputs *A* and *B*, and then the resultant constant 2 is used to control the input *C* [6]. The right most two gates are the inverse gates of the left most two gates used to restore the constant input 0. The quantum cost of this realization is 5.

F. GARBAGE OUTPUT

Every gate output that is not used as input to other gate or as a primary output is called garbage. The unutilized outputs from a gate are called "garbage". Heavy price is paid off for every garbage output. Suppose we want to find the Ex-OR between two variables in reversible computation, then the circuit will looks like Fig. 3. One extra output should be produced to make the circuit reversible and that unwanted output (*P=A,* marked as *) is known as garbage.

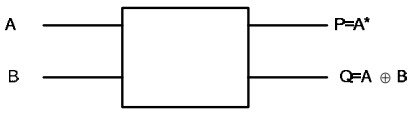

Fig. 3. The garbage output A*

III. REALIZATION OF TERNARY SYSTOLIC ARRAY: THE PROPOSED DESIGN

Systolic array [9] is a specialized form of parallel computing. A systolic array formed by interconnecting a set of identical data-processing cells in a uniform manner is a combination of an algorithm and a circuit that implements it, and is closely related conceptually to arithmetic pipeline. In a systolic array, data words flow from external memory in a rhythmic fashion, passing through many cells before the results emerge from the array's boundary cell and return to external memory. The external memory connected to the systolic array's boundary cell stores both input data and results. Upon receiving data words, each cell performs same operation and transmits the intermediate results and data words to adjacent cells synchronously. The underlying principle of systolic array is used to achieve massive parallelism with a minimum communication overhead. The basic functional unit of a systolic array is cell which act as an autonomous processor. Cells (processors) compute data and store it independently of each other. The Fig. 4 demonstrates the elementary cell structure. The distinguish features of reversible systolic array have been discussed in many literature. The authors of the paper [10] have been illustrated the composition of fuzzy relations and describe a systolic array structure to compute that fuzzy relations on binary logic.

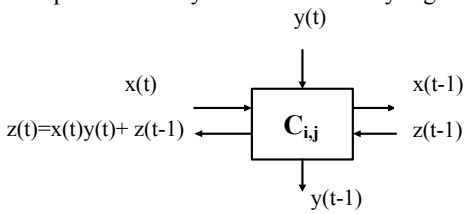

Fig. 4. Systolic array cell structure

But this paper provides a realization of ternary systolic array using M-S gate which is not introduced in any other literature in precedent.

In this paper each cell is intended to perform as a ternary systolic array operation. The function of proposed ternary systolic array processor is to execute the multiplication in pipeline fashion, which is represented by following equations:

$$z(t) = z(t-1) + x(t).y(t)$$

$$x(t) = (x_{n-1}, x_{n-2}, \ldots\ldots x_0)$$

$$y(t) = (y_{n-1}, y_{n-2}, \ldots\ldots y_0)$$

where, x is the multiplicand with n trits, y is the multiplier with n trits.

Ternary form of this equation becomes:

$$z(t) = (((a(t) * b(t)) \bmod 3 + z(t-1)) \bmod 3$$

or

$$z(t) = (z(t-1) + a(t) * b(t)) \bmod 3$$

First one is used for generating ternary performance of systolic array. From the first equation the subsequent Table II is generated.

Table II Truth Table for Ternary Systolic Array

a	b	(a*b) mod 3	z(t-1)	z(t)
0	0	0	0	0
0	0	0	1	1
0	0	0	2	2
0	1	0	0	0
0	1	0	1	1
0	1	0	2	2
0	2	0	0	0
0	2	0	1	1
0	2	0	2	2
1	0	0	0	0
1	0	0	1	1
1	0	0	2	2
1	1	1	0	1
1	1	1	1	2
1	1	1	2	0
1	2	2	0	2
1	2	2	1	0
1	2	2	2	1
2	0	0	0	0
2	0	0	1	1
2	0	0	2	2
2	1	2	0	2
2	1	2	1	0
2	1	2	2	1
2	2	1	0	1
2	2	1	1	2
2	2	1	2	0

where *z (t) = ((a*b) mod3 +z (t-1)) mod3*

By observing the truth table closely, we find that we can formulate Ternary Toffoli Gate as a single cell of the proposed Reversible Ternary Systolic Array. For clarity, truth table for Ternary Toffoli Gate in shown in Table III. After designing the cell, the full architecture can be realized using the same method of any conventional systolic array.

Table III Truth Table for Ternary Toffoli Gate

C\AB	00	01	02	10	11	12	20	21	22
0	0	0	0	0	1	2	0	2	1
1	1	1	1	1	2	0	1	0	2
2	2	2	2	2	0	1	2	1	0

Consider an example of *2×2* matrix multiplication.

$$\mathbf{X} = \begin{vmatrix} \mathbf{1}\,(x_{11}) & \mathbf{2}\,(x_{12}) \\ & \end{vmatrix} \quad \mathbf{Y} = \begin{vmatrix} \mathbf{1}\,(y_{11}) & \mathbf{1}\,(y_{12}) \\ & \end{vmatrix}$$

2 (x_{21}) **1** (x_{22}) **0** (y_{21}) **2** (y_{22})

So, their resultant product is

$$\mathbf{Z} = \begin{vmatrix} \mathbf{1}\,(z_{11}) & \mathbf{2}\,(z_{12}) \\ \mathbf{2}\,(z_{21}) & \mathbf{1}(z_{22}) \end{vmatrix}$$

where $z_{11} = x_{11} \times y_{12} + x_{12} \times y_{22}$

$z_{12} = x_{11} \times y_{12} + x_{12} \times y_{22}$

And z_{21} and z_{22} is calculated by the same way.

IV. EVALUATION OF THE PROPOSED DESIGN

In this section, we will evaluate the proposed design with a Theorem and Lemma, along with examples.

Theorem 4.1 Let, the dimension of two matrices to perform systolic array are $n \times m$ and $m \times r$. If T_{GB} is the total number of garbage output generated to the realized systolic array then

$$T_{GB} >= (2n-1)\times(2n+2r-1)+ (p-(2n-1))\times(2n+2r-2)$$

where, p =total number of needed cycle.

Proof: To multiply 2 matrixes with dimension $n \times m$ and $m \times r$, we need a systolic array with $n \times (2r-1)$ cells.

Let p (the number of needed cycle) $= n \times (2r-1) - 2$

Q denotes the total output = $n \times r$

T_{GB} denote the total number of garbage output generated by the systolic array.

If we consider a systolic array, we can observe that we get garbage output from three sides of a systolic structure. The side boundaries can denote by

G_L = left boundary = n

G_B = below/down/bottom boundary = $2r-1$

G_R = right boundary = n

The upper side of a systolic array is only restricted for to provide inputs.

Now consider the 1st cycle of a systolic array. In the case of 1st cycle the number of garbage output $=(n+2r-1+n)$. From the observation we see that up to $(2n-1)_{th}$ cycle the total garbage produced = $(2n-1) \times (n+2r-1+n)$. Apart from first $(2n-1)_{th}$ cycle the number of garbage output produced by the other cycle = $(p-(2n-1))\times(n+2r-1+n-1)$.

So total number of garbage output produced by the systolic array

$$T_{GB} >= (2n-1)\times(n+2r-1+n) + (p-(2n-1))\times(n+2r-1+n-1)$$

$$T_{GB} >= (2n-1)\times(2n+2r-1) + (p-(2n-1))\times(2n+2r-2)$$

Example 4.1: Consider an example of *2× 2* matrix multiplication. Initial state of the corresponding architecture is shown in Fig. 5. In this case the number of garbage output produced by 1st cycle is $(n+2r-1+n) = (2\times(2\times2-1)+2 = 2+3+2 = 7$

Up to (2n-1) cycle the garbage output is 7. That is for 2×2 matrix multiplication up to 3 cycles the produced garbage is 7. From the Fig. 6 we see that the $x_{11} \times y_{11}$ is produced at 2nd cycle and it appear as an output at 4th cycle (as in Fig. 8). Output of the 2nd cycle is shown in Fig. 7.

So up to 3rd cycle we get total 7 garbage output. After *(p-(2n-1))* that is, from the 4th cycle we get output from each of the left side boundary cell alternatively. From the 4th cycle to pth cycle the garbage output will be (*n + 2r – 1 + n – 1)* = 6.

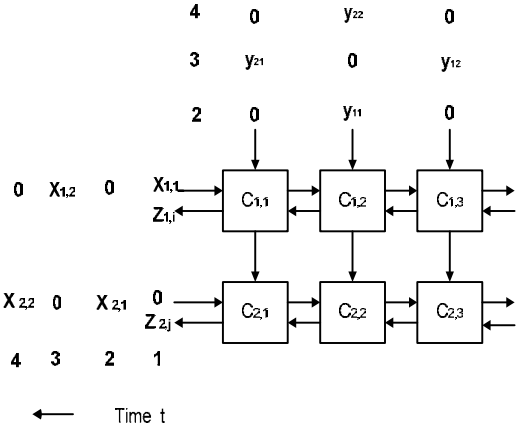

Fig. 5. Systolic array for 2×2 matrix multiplication

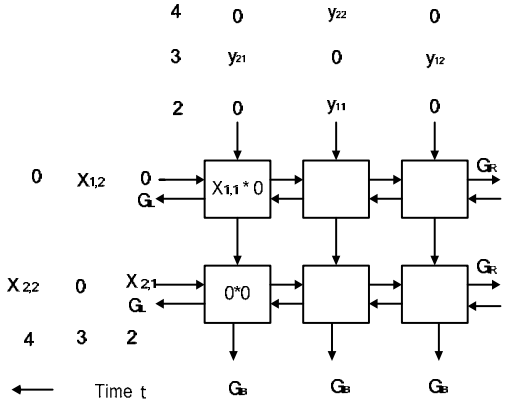

Fig. 6. The garbage output produced at 1st cycle

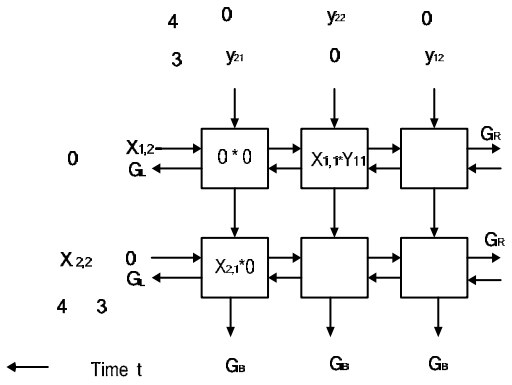

Fig. 7. The garbage output produced at 2nd cycle

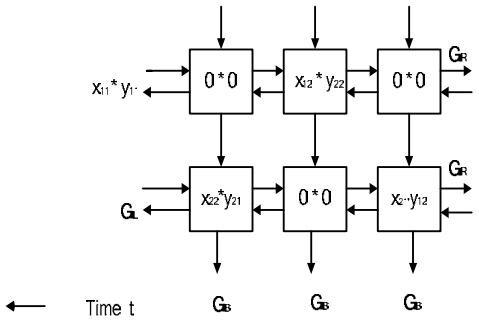

Fig. 8. First output ($x_{11} \times y_{11}$) produced at 4th cycle

Lemma 4.1: The quantum cost of a systolic array, using each cell as a Toffoli gate is 5 × C, where, C is the number of cell used in a systolic array.

Proof: As we know each quantum gate operates by manipulating qubits and and quantum cost is associated with qubits [3]. The proposed systolic array is implemented by using 3 qurit ternary Toffoli gate as a cell. The quantum cost of the used cell realization is 5. So if the number of cell required in a systolic array is C then the total quantum cost of the proposed realization is 5 ×C. □

V. CONCLUSION

In this paper, we present the realization of ternary reversible systolic array. We have developed the proposed architecture with the aid of Toffoli gate. Lower bound for Garbage output is developed very significantly to evaluate the proposed design. We haved proposed the first Ternary Systolic Array in [11], but this paper presents a procedural and step by step presentation of the idea.

VI. ACKNOWLEDGEMENT

Author expresses their gratitude and thanks to Dr. Suraiya Pervin, Chairperson and Professor, Department of Computer Science and Engineering, University of Dhaka, Bangladesh, for her cooperation throughout the work.

REFERENCES

[1] C. H. Bennett, "Logical Reversibility of Computation", *IBM J. Research and Development*, 31(1), pp.16-23, January 1988.

[2] R. Landauer, "Irreversibility and Heat Generation in the Computational Process", *IBM journal of Reseach and Development*, pp.183-191, 1961.

[3] Nielsen and I. Chuang, "Quantum Computation and Quantum Information", *Cambridge University Press*, 2000.

[4] D. M. Miller, G. W. Dueck, and D. Maslov, "A Synthesis Method for Reversible Logic", *Proc. 34th Int. Symposium On Multiple–Valued Logic*, Toronto, Canada, 19-22 May 2004, pp.74-80.

[5] M. H. K. Azad, M. A. Perkowski, "Quantum ternary parallel adder/subtractor with partially-look-ahead carry", *7th Int. Symposium on Representations and Methodology of Future Computing Technologies (RM2005)*, Tokyo, Japan, 5 - 6 September 2005.

[6] M. H. A. Khan, M. A. Perkowski, "Quantum Realization of Ternary Encoder and Decoder", *7th International Symposium on Representations and Methodology of Future Computing Technologies (RM2005)*, Tokyo, Japan 5-6 September 2005.

[7] M. H. A Khan, "Design of Reversible/ Quantum Ternary Multiplexer and Demultiplexer" *Engineering Letters*, vol. 13 no. 2, 2006, pp. 65-69.

[8] A. Muthukrishnan, C. R. Stround, Jr, "Multivalued logic gates for quantum computation", *Phys. Rev. A*, 62(5), 052309/1-8, 2000.

[9] N. Petkov: Systolic Parallel Processing: *North Holland Publishing* Co, 1992.

[10] H.M.H. Babu, A.A. Ali, and A.R. Chowdhury. "Realization of Digital Fuzzy Operations Using Multi-Valued Fredkin Gates", *CDES 2006*, Nevada, USA, pp. 101-106.

[11] N. Nower and A. R. Chowdhury, "On the Realization of Reversible Ternary Systolic Array", Silver Jubilee Conference on Communications and VLSI Design Vellore Institute of Technology (VIT), Vellore, India, Oct 8-10, 2009, pp. 490-491.

Proceedings of 2009 12th International Conference on Computer and Information Technology (ICCIT 2009)
21-23 December, 2009, Dhaka, Bangladesh

A New Hashing and Caching Approach for Reducing Call Delivery Cost and Location Server's Load in Wireless Mobile Networks

Md. Mohsin Ali, Md. Amjad Hossain, Md. Kowsar Hossain, G. M. Mashrur-E-Elahi, Md. Asadul Islam
Department of Computer Science and Engineering (CSE)
Khulna University of Engineering & Technology (KUET), Khulna – 9203, Bangladesh
mohsin_kuet_cse@yahoo.com, amjad_kuet@yahoo.com, auvikuet@yahoo.com, ranju2k4cse_kuet@yahoo.com, asad_kuet@yahoo.com

Abstract

This paper proposes a new approach for reducing average call delivery cost and location server's load of wireless mobile networks. It uses caches whose up-to-date information is responsible for dropping these costs and these caches are updated not only during call arrival moment from the calling Mobile Hosts (MHs) but also during call receiving moment to those MHs. To achieve load balancing among replicated Home Location Registers (HLRs), hashing technique is also used and this load is also affected by up-to-date cache information. The analytical model and experimental results show that our proposed method prepares the cache with up-to-date information more frequently with the increase of average call arrival rate as well as average call receiving rate. This increases probability of finding MH's location as well as hit ratio of the cache. As a result, both the average call delivery cost and load on a particular HLR are minimized considerably than all other previous approaches.

Keywords: Call arrival and receiving rate, call delivery cost, hashing and caching, Home Location Register (HLR), load balancing, Visitor Location Resister (VLR).

I. INTRODUCTION

Location management is concerned with the issues of tracking and finding MH in order to roaming in the network coverage area. To maintain the MHs' locations, two types of location databases like HLR and Visitor Location Register (VLR) are commonly used in all wireless communications systems like basic IS-41 [1] and GSM [2]. These databases are organized in two levels of data hierarchy. In basic scheme of wireless mobile networks, network coverage is divided into cells. Each cell has a Base Transceiver Station (BTS) to which MH of the cell communicate through a wireless link. Each BTS is connected to a Mobile Switching Center (MSC) through a wired network. To facilitate the tracking of a moving MH, the wireless network is partitioned into many Registration Areas (RAs). Each RA includes tens or hundreds of cells. Each RA has a VLR servicing it and a VLR is designed to monitor only one RA. The HLR is the centralized database which contains the records of all users' services in addition to location information for an entire network. The VLRs (distributed databases) download data from HLR concerning current users within the VLR's specific service areas. Two basic operations in location management are location update and call delivery. Location update is performed whenever an MH crosses the RA boundaries. Call delivery is the process of determining the serving VLR and the cell location of the called MH. It has been shown that average location update cost and call delivery cost can be reduced by caching and hashing [3], [4].

This paper proposes a new approach to improve the overall network performance in terms of average call delivery cost and individual location servers load by considering both the call arrival and receiving rate at the calling MH to update its cache information.

The paper is organized as follows: Section II provides an overview of the related recent research work. Our proposed scheme is described in section III. Section IV gives the analytical model and comparison among different methods based on some experimental results. We provide a concluding remark in section V.

II. RELATED WORK

There has been considerable amount of work done on location management to improve the overall performance of the wireless mobile networks [5], [7], [8]. The main issues of location management are to reduce the average call delivery cost and location update cost. To reduce these costs, the location of MH can be cached at its caller site where the majority of calls originate [5]. Recently, the distributed database architecture based on hierarchical organization is used for locating MH rather than using centralized database architecture [6].

A number of replicated centralized databases, each of which is known as HLR, can be maintained to reduce the load on the database. To achieve the load balancing among the replicated HLRs, a protocol is proposed in [9]. Location updates and queries are multi-casted to subsets of location servers. These subsets vary with time and depends on the location of MH's querying of MSC and load on the server. At least one common database can exist at each pair of subsets. Hashing technique is used for the construction of the subsets. In [4], a

978-1-4244-6283-4/09/$26.00 ©2009 IEEE

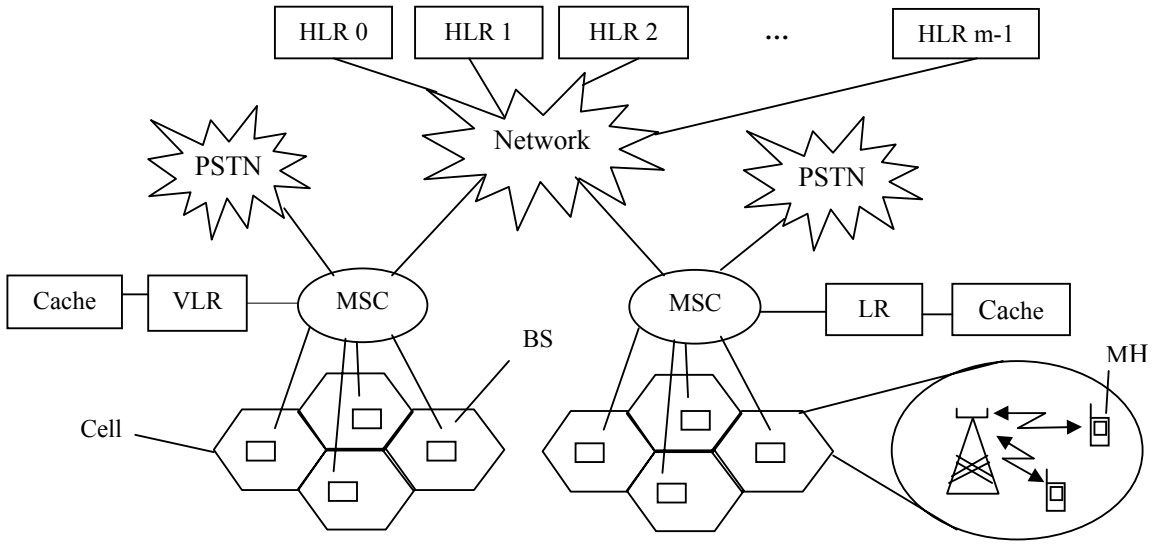

Fig. 1. Overall architecture of the wireless mobile networks with hashing and caching.

hashing and caching scheme on location management is proposed to reduce average call delivery cost where only call arrival rate is used to cache the MHs location. Only one location server is chosen by using the hashing technique which simplifies the load balancing protocol and reduces the database operation. Fig. 1 shows the architecture of the wireless mobile networks which uses caches to store the location of MHs and hashing function for load balancing among replicated HLRs.

III. PROPOSED APPROACH

In our proposed approach, a set of location servers are used which are identical in nature. Hashing function is used to select one of these servers dynamically. Every MH, location server, and VLR has specific Mobile Host Identifier (MHID), Server Identifier (SERVERID), and VLR Identifier (VLRID), respectively. Assume, there are m location servers (0 to $m-1$) in the system. We use the function SERVERID = f (MHID, VLRID, m) = (MHID + VLRID) mod m to find the specific location server among m servers which contains the MH's location identified as MHID.

The location information is also cached at VLR to reduce average call delivery cost and server's load. The cached location information of an MH is updated not only during call arrival moment from the calling MH but also during call receiving moment to that calling MH. At first, every call at VLR is checked to identify whether it is arrival call, receiving call, or handoff. Then, the cache is checked for MHs' location information during call arrival time as well as during call receiving time. If that information is available in the cache during call receiving time and up-to-date, then the cache remains unchanged. Otherwise, the location information in the cache is obsolete or unavailable. In this case, cache is updated by extracting calling MH's location information from signaling message or by saving the information in the cache. During call arrival time, if that location information is found in the cache, then it is also checked to see whether it is up-to-date or not. The call is established in case of cache's up-to-date information. If location information is obsolete or absent in the cache, then it is collected from the location server selected by means of hashing function and updated or saved it to the cache. In case of handoff, MH's new location information is updated in one of the new location servers among m by applying hashing function. Then, this information is multi-casted to remaining $m-1$ location servers by the selected server. The flow chart in Fig. 2 describes our proposed approach.

IV. ANALYTICAL MODEL AND EXPERIMENTAL RESULTS

We know that the database access cost and signaling cost mainly depend on the database query delay and signal transmission delay. We mainly focused on the call delivery cost because the location update cost remains almost the same as basic IS-41 scheme [1] and as hashing and caching scheme [4] if we use lazy caching. In IS-41 scheme, total three queries are required to make a call. The first query is at calling VLR (D_v), the second at HLR (D_h), and the third at called VLR (D_v). So, the total database access cost is $2D_v + D_h$ [4]. Fig. 3 shows that total signaling cost depends on the following things

1. Two messages exchange between calling VLR and HLR ($2C_h$),
2. Two messages exchange between HLR and called VLR ($2C_h$), and
3. One Message exchanges between calling VLR and called VLR (C_v).

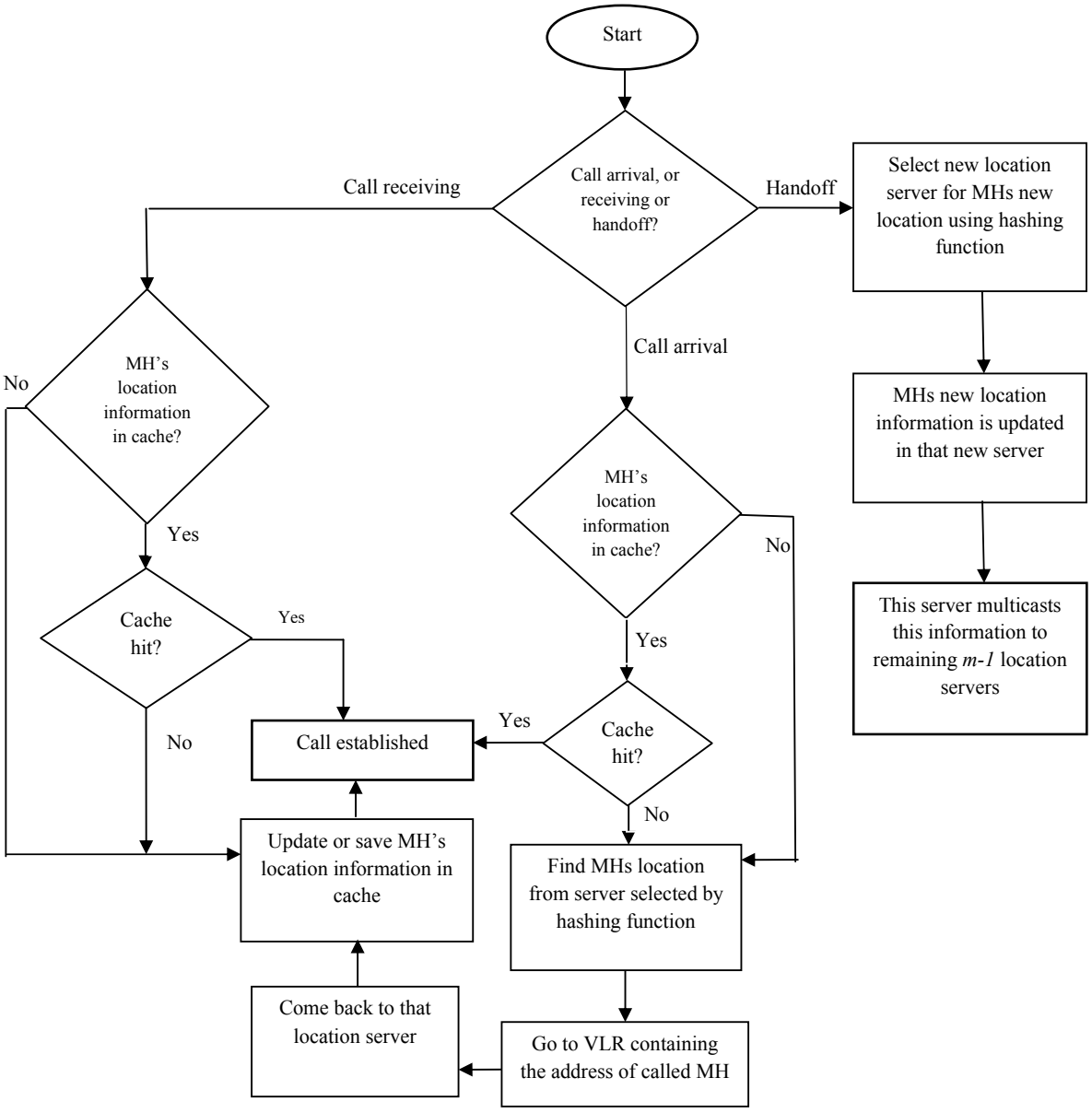

Fig. 2. Flow chart of the proposed method.

So, the total signaling cost is $4C_h + C_v$. As a result, the average call delivery cost of basic IS-41 scheme is $C_b = 4C_h + C_v + 2D_v + D_h$ [4].

In hashing and caching scheme [4], location information is stored in the cache at the moment of call arrival. If it is in the cache, then cache hit may occur and at that time total cost depends on the cost of one query access in the cache and one message exchanges between calling VLR and called VLR (C_v). Otherwise, cache miss occurs means the information is obsolete. At that time, the total cost depends on the cost of one query access in the cache, one message exchanges between calling VLR and called VLR (C_v), the total cost of basic IS-41 scheme (C_b) and an update cost in the cache. The location information may not exists in the cache and then the total cost depends on the cost of one query access in the cache, the total cost of basic IS-41 scheme (C_b), and an update cost in the cache. Query access and update cost of the cache is considered negligible. Consider C_c as average call delivery cost of hashing and caching scheme, C_{ch} as average call delivery cost if the location information is in the cache, p as cache hit ratio, and q as probability that the location information is in the cache. So, C_c is defined as follows [4].

$$C_c = q * C_{ch} + (1 - q) * C_b \quad (1)$$

Where,

$$C_{ch} = p * C_v + (1 - p) * (C_v + C_b) \quad (2)$$

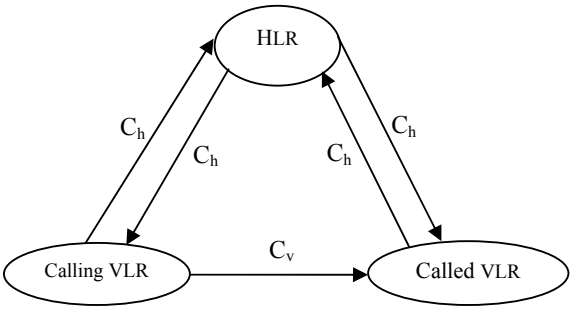

Fig. 3. The basic signaling process of the wireless mobile networks.

Assume, the call arrivals to MHs and MHs' mobility follow the Poisson distribution. The mean call arrival rate is λ and the mean mobility rate is μ_m. *LCMR* is the Local Call to Mobility Ratio. According to [4], p is defined as follows

$$p = \frac{\lambda}{(\lambda+\mu_m)} \tag{3}$$

According to [8], $LCMR = \frac{\lambda}{\mu_m}$. So, (3) is written as follows

$$p = \frac{LCMR}{1+LCMR} \tag{4}$$

From (3), it is shown that in hashing and caching scheme, p depends only on λ and μ_m, but in our proposed scheme, p depends not only on λ and μ_m, but also on the mean call receiving rate, λ_r. So, it can be defined as follows

$$p = \frac{\lambda*(\lambda_r+1)}{\{\lambda*(\lambda_r+1)+\mu_m\}} \tag{5}$$

If $\lambda_r = \lambda$, then (5) becomes

$$p = \frac{\lambda^2+\lambda}{(\lambda^2+\lambda+\mu_m)} \tag{6}$$

If we consider λ_{max} as maximum call arrival rate, then q in hashing and caching scheme depends only on λ and λ_{max}. So, it can be defined as follows

$$q = \frac{\lambda}{\lambda_{max}} \tag{7}$$

Consider, $\lambda_{r_{max}}$ as maximum call receiving rate. In our proposed scheme, q depends on λ, λ_r, λ_{max}, and $\lambda_{r_{max}}$. So, for this scheme, it can be defined as follows

$$q = \frac{\lambda}{\lambda_{max}} + \left(1 - \frac{\lambda}{\lambda_{max}}\right) * \frac{\lambda_r}{\lambda_{r_{max}}} \tag{8}$$

If $\lambda_r = \lambda$ and $\lambda_{r_{max}} = \lambda_{max}$, then (8) becomes

$$q = \frac{2\lambda}{\lambda_{max}} - \frac{\lambda^2}{{\lambda_{max}}^2} \tag{9}$$

Fig. 4 shows different average call delivery cost, obtained by varying average call arrival or receiving rate for three different values of $\frac{D_h}{C_v}$. It depicts that with increasing average call arrival or receiving rate, average call delivery cost of basic IS-41 scheme remains constant, because it does not depend on average call arrival or receiving rate relating to cache. But, this cost for both hashing and caching and proposed scheme is smaller for each of the three values of $\frac{D_h}{C_v}$ since caches are used to find out MH's location to deliver call instead of finding out it in the location server with more penalties. However, for proposed method, this cost decreases significantly than that of the remaining methods with respect to λ. Because, we use not only call arrival rate but also call receiving rate for cache update considering both of them as equal. So, the cache is updated more frequently than hashing and caching scheme. As a result, cache hit ratio increases and the average call delivery cost decreases.

The load performance of location server is measured by throughput of location servers. For basic IS-41 scheme, the HLR is the only location server. For measuring the load performance of this scheme, we define X as throughput and μ as HLR query rate (service rate). This scheme is modeled as an *M/M/1* queuing system. The call arrival times of this system are independent and exponentially distributed with parameter λ. Service times are also exponentially distributed with parameter μ. A single server is used in this system. So, the system throughput is equal to λ.

For hashing and caching scheme, we assume that there are m location servers. MSC sends requests to $server_i$, where $i = 1,2,\cdots, m$. We define x_c as the throughput of one location server, λ_s as call arrival rate at $server_i$, μ_s as one of the location server's service rate, and p_{r_i} as the probability of querying to $server_i$. We assume that the query service rate of one location server is $\mu_s = \mu$. The server is selected uniformly using basic hashing method. So, p_{r_i} is defined as $\frac{1}{m}$. Thus, λ_s is defined as follows [4]

$$\lambda_s = \lambda * p_{r_i} * (1 - q) \tag{10}$$

Now, (10) becomes

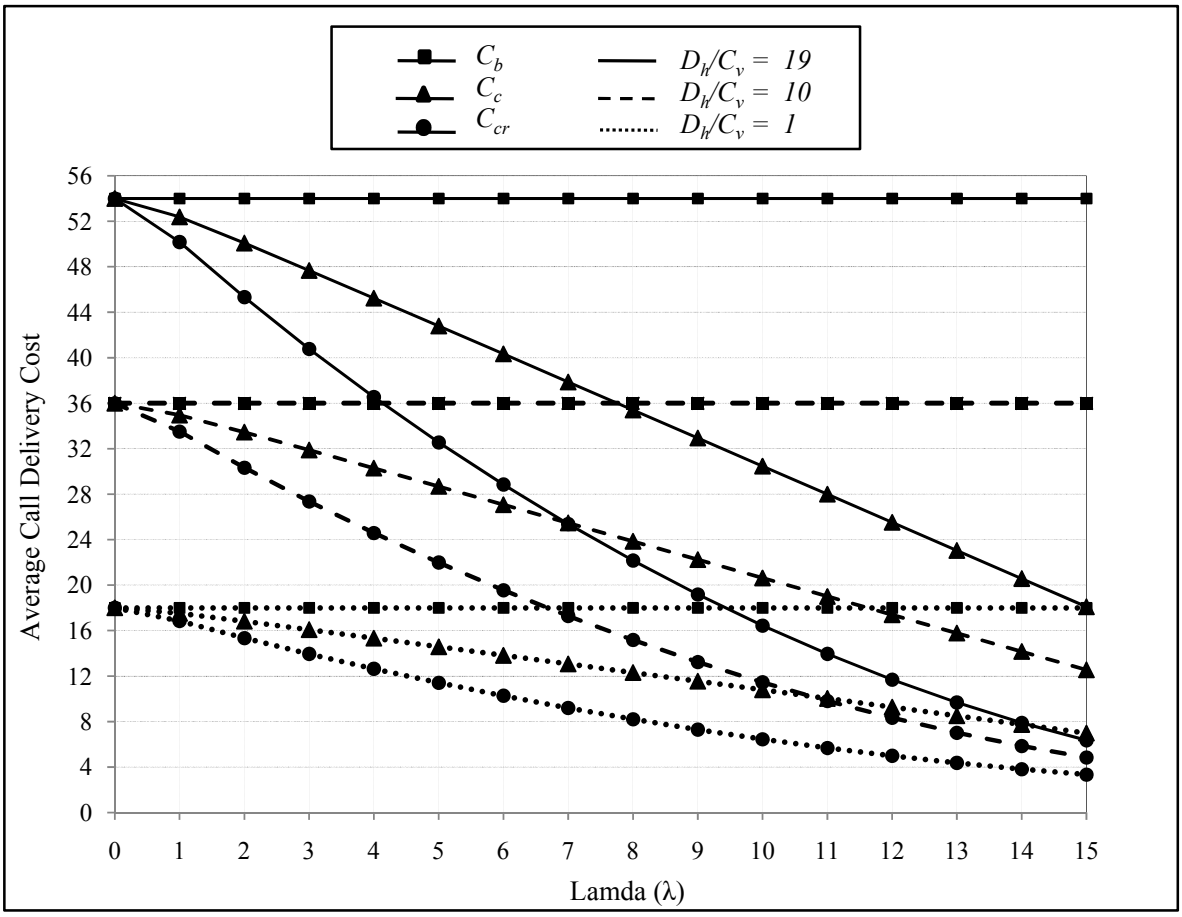

Fig. 4. Performance comparison of basic IS-41, hashing and caching and proposed schemes based on average call delivery cost.

$$\lambda_s = \lambda * \frac{1-q}{m} \quad (11)$$

Where, (*1-q*) is the probability that the location information is not in the cache. As there are *m* servers, we can model the system as *m* number of *M/M/1* queues. Now, the throughput of location $server_i$ is as follows [4]

$$x_c = \lambda_s = \lambda * \frac{1-q}{m} \quad (12)$$

In our proposed scheme, we have considered both call arrival and receiving rate for cache update. So, x_c will be the same as (12); but, q of this equation will be defined by (8) instead of (7).

Fig. 5 shows different server loads obtained with respect to average call arrival or receiving rate for three different values of *m*. It shows that with increasing average call arrival or receiving rate, the server load increases linearly in basic IS-41 scheme. This is because, there is only one location server to serve this scheme, no caching is used and all the calls are delivered by searching in the single server. On the other hand, the server load of hashing and caching and proposed scheme initially increases until a particular value of λ and then decreases with the increase of call arrival as well as call receiving rate for any value of *m*. Because, there are *m* location servers to serve these two schemes and there are caches to find out MH's location instead of directly searching in the location servers. Moreover, in proposed scheme, server load decreases more than the remaining schemes because it updates the cache more frequently during both call arrival and call receiving moment at calling MH instead of only during call arrival moment at that MH like hashing and caching scheme. But, larger values of *m* similarly make the server load of these two schemes smaller.

V. CONCLUSION

In this paper, we propose a new approach to improve the overall performance of the wireless mobile networks in terms of average call delivery cost and location server's load. We show that hit ratio of the cache used for storing MHs location information increases as we consider both call arrival rate and call receiving rate for updating cache information. A hashing function is used for load balancing among location servers and this load depends on the up-to-date cache information. The analytical model and experimental results show that with the improvement of hit ratio, the probability of

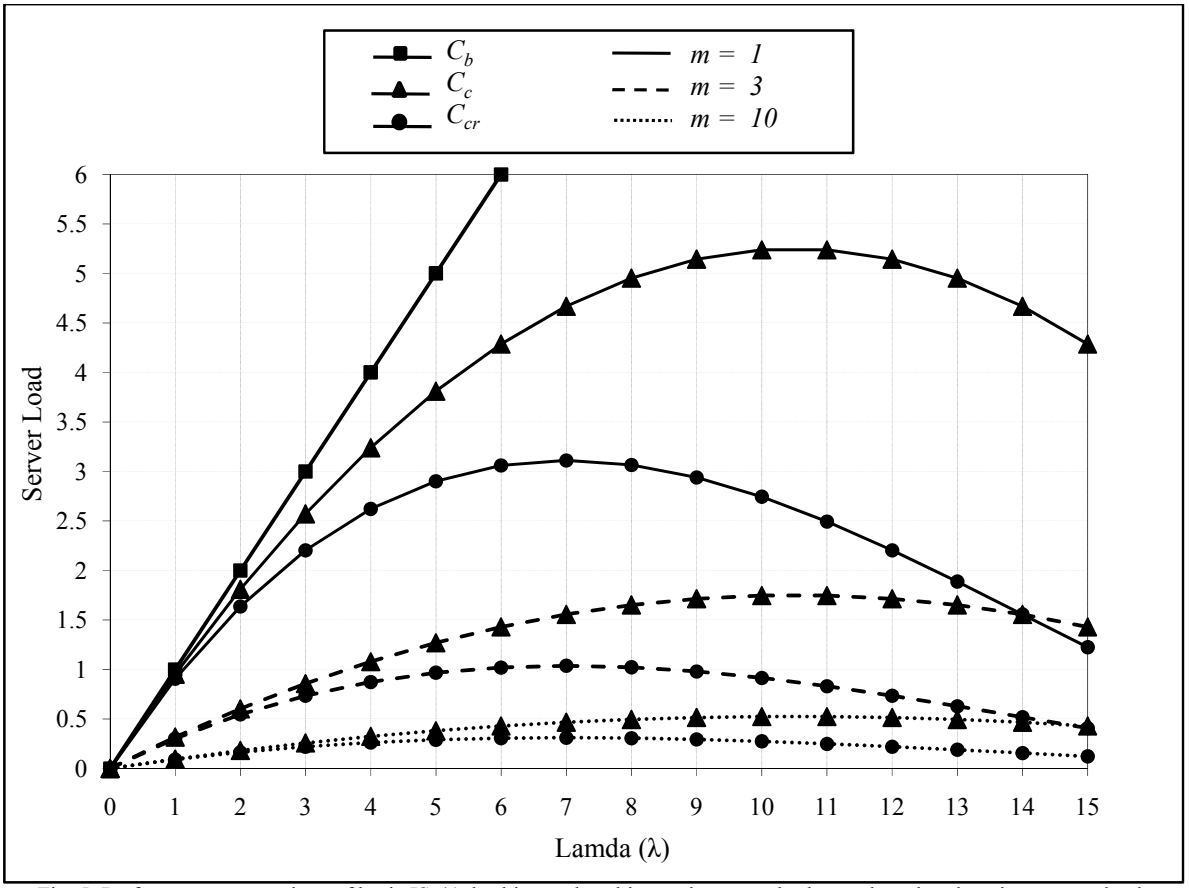

Fig. 5. Performance comparison of basic IS-41, hashing and caching and proposed schemes based on location servers load.

finding MHs location in cache also increases and thus average call delivery cost and location servers load are reduced significantly compared to all other previous methods.

We are currently working with more appropriate hashing function for selecting one of the location servers with low congestion and minimized load.

REFERENCES

[1] EIA/TIA. "Cellular radio-telecommunications intersystem operations," Tech. Rep. IS-41 Revision B, EIA/TIA, December 1991.

[2] M. Mouly and M.B. Pautet, "The GSM system for mobile communications," 49 rue Louise Bruneau, Palaiseau, France, Telecom Publishing, January 1992.

[3] Chang Woo Pyo, Jie Li, Hisao Kameda, and Xiaohua Jia, "Dynamic Location Management with Caching in Hierarchical Databases for Mobile Networks," *DNIS 2002, LNCS 2544*, *Springer-Verlag,* vol. 2544, pp. 253–267, Berlin/Heidelberg, December 2002.

[4] Weiping He and Athman Bouguettaya, "Using Hashing and Caching for Location Management in Wireless Mobile Systems," *MDM 2003, LNCS 2574, Springer-Verlag*, vol. 2574, pp. 335–339, Berlin/Heidelberg, January 2003.

[5] I. Akyildiz, J. McNair, J. Ho, H. Uzunalioglu, and W. Wang, "Mobility management in next-generation wireless systems," *In Proceedings of the IEEE*, vol. 87, no. 8, pp. 1347–1384, August 1999.

[6] Y. Bejerano and I. Cidon, "An efficient mobility management strategy for personal communication systems," *In The Fourth Annual ACM/IEEE International Conference on Mobile Computing and Networking*, ACM Publishers, pp. 215-222, Dallas, Texas, United States, October 1998.

[7] A. Bouguettaya, "On the construction of mobile database management systems," *In The Australian Workshop on Mobile Computing & Databases & Applications*, Melbourne, Australia, February 1996.

[8] E. Pitoura and G. Samaras, "Data Management for Mobile Computing," vol. 10, Kluwer Academic Publishers, 1998.

[9] R. Prakash and M. Singhal, "Dynamic hashing + quorum = efficient location management for mobile computing systems," *In Proceedings of the Sixteenth Annual ACM Symposium on Principles of Distributed Computing*, ACM Press Publisher, pp. 291, August 1997.

Proceedings of 2009 12th International Conference on Computer and Information Technology (ICCIT 2009)
21-23 December, 2009, Dhaka, Bangladesh

An Efficient Protocol for Ensuring 24x7 Availability in P2P Networks *(Not Presented)*

Farhadur Rahman, Habibur Rahman, Reaz Ahmed
Department of Computer Science and Engineering, Bangladesh University of Engineering and Technology, Dhaka, Bangladesh
farhadur@yahoo.com, tuhincse028@yahoo.com, reaz@cse.buet.ac.bd

Abstract

One of the challenges in peer-to-peer (P2P) systems is to support distributed group based resource management for increased resource availability. Replication increases resource availability, but ensuring uninterrupted 24X7 availability of resource requires intelligent replication strategy utilizing the knowledge of connectivity pattern of participating peers. In this paper we present a intelligent replication and indexing mechanism for ensuring 24X7 resource availability by maintaining minimal number of replications. We have adopted and tailored the original Chord protocol in a two level hierarchy, where peers are organized into groups based on interest to increase the lookup efficiency. We will also present simulation results showing the effectiveness of the proposed mechanism in improving 24x7 resource availability.

Keywords: P2P, Availability, Interest-based P2P grouping, Modified Chord.

I. INTRODUCTION

The File-sharing is the most popular among the different applications of P2P networks. There exists many successfully deployed P2P file sharing systems such as Napster[4], Gnutella[2], KaZaA[3] and FastTrack[1]. These systems utilize extensive replication of resources to improve availability but they do not provide any optimal mechanism that will ensure 24X7 resource availability with minimal replication.

Chord is a distributed lookup protocol for P2P network designed by MIT in 2001 [16]. Chord has three distinguished character from other P2P routing protocols, which are simplicity, correctness and provable performance. These features attract many researchers to study and enhance the model in various aspects in order to get better performance.

In this paper we present an improved Chord model introducing a grouping mechanism, in which we organize the nodes into small groups according to its interest. Moreover this interest based groups are suitably arranged such that 24x7 availability can be ensured. We have designed a scalable resource management architecture for distributed systems which is a group based virtual hierarchical architecture. Peer in are classified into groups. Members within the same group share similar interest. Super peers are used to build the original chord ring in which normal peers will publish their information. Super peer can also publish their data into some other peers in the Chord ring.

Interest based grouping improves the search efficiency by organizing the similar-interest members within a small network radius and reduces the system maintenance cost by restricting most of the updates inside group. Group-based architecture can facilitate collaboration and make it easy for us to analyze the general group activity model.

II. AVAILABILITY MEASUREMENT

Measuring availability in P2P network is not a straight forward task. There exists mainly two schools of thoughts for measuring availability: time-based availability [6] [14], and presence-based availability.

$$availability = \frac{MTTF}{MTTF + MTTR}$$

Here, MTTF is the mean-time-to-failure and MTTR is the mean-time-to-recovery. In other words, it is the proportion of time a system works correctly to the total time of usage. Presence-based availability measurement [10], on the other hand, measures availability of peers based on the presence of individual peers. In [10] the authors have compared time-based and presence-based measurement metrics and their implication on assessment of availability in P2P networks.

In this work we have adopted the time-based measurement model of availability as it is more suitable for measuring document availability in P2P networks..

III. SYSTEM STRUCTURE

Before forwarding to the main architecture, we introduce the definitions which will be used throughout this paper-

- **outerChordRing:** Nodes of this Chord ring are arranged by hashing its interest. Chord uses SHA-1 for hash which is used in cryptography. We also used SHA-1 hash mechanism, which takes a variable length byte string as argument and produces a 160-bit random identifier. This identifier is used to organize the OuterChordRing**.**
- **innerChordRing:** Every node in the OuterChordRing has an innerChordRing unless it is the only node with a given interest. The nodes of the innerChordRing are arranged by hashing their ip address using SHA-1**.**

978-1-4244-6283-4/09/$26.00 ©2009 IEEE

- **outerSuccessor(n):** This function gives the successor of **n** in the outerChordRing by hashing the interest of **n**.
- **innerSuccessor(n):** This function gives the successor of **n** in the innerChordRing by hashing the ID of **n.**
- **Superpeer:** Superpeers are used to construct the Chord rings inner and outer. They are used because they have the long-term availability and better stability.
- **Normalpeer:** Nodes which will not be available for a long time and stability is not satisfactory will participate as regular or normalpeers. These peers will use the outerChordRing and the innerChordRing to publish their documents. They will not participate in constructing the Chord rings.
- **Gatewaynode:** Each node in the outerChordRing can work as a gateway node between an innerChordRing and the outerChordRing. These nodes have two routing tables, innerRouting table and outerRouting table, as they are part of both inner and outer Chord rings.
- **Nodelist:** Each node in the innerChord ring has a nodelist. Nodelist consists of information of NormalPeer and SuperPeer which hashes into that particular innerNode

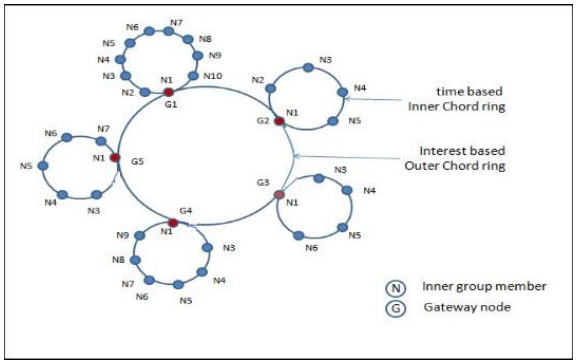

Fig.1. Original Chord Ring.

The overall system architecture of the proposed system is presented in Fig. 1. Communication inside groups and among groups both rely on Chord protocol. outerChordRing is used to facilitate the collaboration among different groups. .innerChordRing is used to facilitate inner group resource-management. For the gateway nodes it has two kinds of routing table. Inner routing table is a collection of specific neighbor inside the group and outer routing table is a collection of specific neighbors selected from different group. According to the Chord protocol, Gateway nodes maintain both routing table. A gateway node maintains a successor list for its outerChordRing. A inner node also maintains innerSuccessorList for the inner Chord ring. Data structure for the gateway node and inner node is given in Fig. 2 and Fig 3, respectively.

IV. NODE JOIN

When a new peer wants to join the indexing system as a Superpeer, it finds the gateway node in the

<<GatewayNode>>
groupID
nodeID
innerSuccessorLIst
outerSeccessorList
innerFingerTable
outerFingerTable

Fig. 2: Gateway Node

<<InnerNode>>
groupID
nodeID
innerSuccesssorList
innerFingerTable

Fig. 3: Inner Node

outerChordRing by hashing its own interest. This gateway node is called the outerSucccessor of the new node. If there exits now outerChordRing peer with the same interest as the new peer, then the new node creates a new group and places joins the outerChordRing. Eventually, this newly joined peer becomes the gateway node as more peers join the network with the same interest. On the other hand, if the new peer finds an outerChordRing node, say M, with the same interest then it joins the innerChordRing connected to M by hashing its own ip address. The pseudo code for the join algorithm is presented Algorithm 1.

Algorithm 1 Join(Node newNode, Node ringNode)

1: Input: ringNode: a node in the Chord ring known by the new node.
2: ringNode finds a outerSucc in the OuterChordRing based on the interest of the newNode.
3: **if** outerSucc has different interest than newNode **then**
4: newNode creates a new group in the OuterChordRing.
5: newNode.gateWayNode = TRUE.
6: newNode.innerSuccessor = NULL.
7: newNode.inne Predecessor = NULL.
8: newNode.outerSuccessor = outerSucc.
9: newNode.innerPredecessor = outerSucc.outerPredecessor.
10: **else**
11: outerSuccessor searches for innerSucc in it's InnerChordRing
12: newNodejoins in the InnerChordRing.
13: newNode.gateWayNode = FALSE.
14: newNode.innerSuccessor = innerSucc.
15: newNode.innerPredecessor = innerSuc .innerPredecessor
16: newNode.outerSuccessor = NULL.
17: newNode.outerPredecessor = NULL.
18: **end if**
19: **if** newNode is gateWayNode then
20: newNode creates it's innerRoutingTable.
21: newNode creates it's outerRoutingTable.
22: **else**
23: newNode creates it's innerRoutingTable.
24: **end if**

V. NODE DEPARTURES AND FAILURE

When an innerNode leaves gracefully, it gives its information to innerSuccessor and informs its innerPredecessor about the departure so the innerPredecessor can link to the departing node's innerSuccessor. When a gateway node leaves, it gives its information to the innerSuccessor and the innerSuccessor becomes the new gateway node for that node.

When a node (say n) fails, nodes whose finger tables include n, must find n's successor. In addition, the failure of n must not be allowed to disrupt queries that are in progress as the system is re-stabilizing. Every innerNode maintains a innerSuccessorList. If an innerNode notices that its successor has failed, it looks up on its innerSuccessorList and replaces the innerSuccessor with first alive node. As time passes, stabilize procedure will correct finger table entries and innerSuccessorList entries pointing to the failed node. On the other hand, each gateway node maintains a outerSuccessorList which contains the innerNodes of its outerSuccessor. If any gateway node finds that its outerSuccessor is not alive then, it replaces its outerSuccessor.

VI. PERFORMANCE ANALYSIS

Let there be G nodes in the OuterChordRing and g nodes in average in an InnerChordRing. When a new node joins, first it needs to find an appropriate node in the OuterChordRing and then an appropriate position in InnerChordRing is selected. The total cost of this look up is O(log G + log g). The second part is to update the finger tables for both itself and others. Each inner node has to maintain only one finger table also known as innerFingerTable. Updating cost of this innerFingerTable is O(log g). Gateway node has two finger table innerFingerTable, outerFingerTable. Updating cost of these two finger tables is O(j*log G) +O(k*log g), where j and k are the expected number of entries in the finger table entries in outerFingerTable and innerFingerTable, respectively.

VII. PUBLISHING PEER

Both normalPeer and superPeer will publish themselves in the Chord ring so that their uptime distribution can be known by other peers. When a peer wants to publish itself, it will first select interest and time duration of its alive time. Then a gateway node in the outerChordring is selected by hashing the interest of that normal peer. The gateway node will then select a innerNode in the innerChordRing by hashing alive time of the peer. That innerNode will contain the information like ip address, uptime distribution of that peer in its nodelist. The uptime publishing mechanism has been depicted by an example in Fig 4.

VIII. PUBLISHING DOCUMENTS

When a peer wants to publish a document it will first select a node in the Chord ring which is already known to that peer. The selected node then hashes documents interest to find a gateway node in outerChordRing. The gateway node then selects a certain time and hashes that duration to find innerNode. After that the innerNode selects the normal peers from its nodeList and replicates this document in those peers. This process is continued until 24x7 availability is ensured. The pseudo code for document publishing algorithm is presented in Algorithm-2.

Algorithm 2 PublishDocument (Node ringNode, Document document)

1: Input: ringNode : an node in the Chord ring known by the new node.
2: ringNode finds a gatewayNode in the OuterChordRing based on the subject of the document.
3: **repeat**
    4: gatewayNode selects a innerNode from the innerChordRing by hashing a random time
    5: innerNode select a node from its nodeList
    6: innerNode replicate the document to the selected Node
7: **until** 24X7 hour availability of the document is ensured

IX. EXPERIMENTAL EVALUATION

In this section we analyze some performance characteristics of our proposed system. In the following experiments we investigate the behavior of the system in the following circumstance:

- First we find the impact of network size on expected availability of documents in the system.
- Then we highlight the effect of the number of different interest groups in the system on availability.
- Finally we find the effect of normalPeer failure and superPeerfialuer on availability.

A. Expected availability vs Network size

Here, peers published themselves to store their information in the Chord ring. After that we calculate the expected availability for variable number of normalPeers. To calculate expected availability, we first publish 100 documents in the Chord ring. Then, we execute query to retrieve the document at random time. In this case, we assume that no node will fail in the meantime. Here number of SuperPeer is 1000 and number of interest is 50.

ity remains almost constant despite of the increase in the number of interest-based groups within the network. This indicates

peer	interest	Time to live
a	G2	10 -11
b	G2	11-12
c	G2	11-12
d	G2	7-8
e	G2	8-9
f	G2	9 -10
g	G2	7-8
h	G2	9-10

Super Peer	Nodelist
N1	d,g
N2	e
N3	f,h
N4	a
N5	b,c

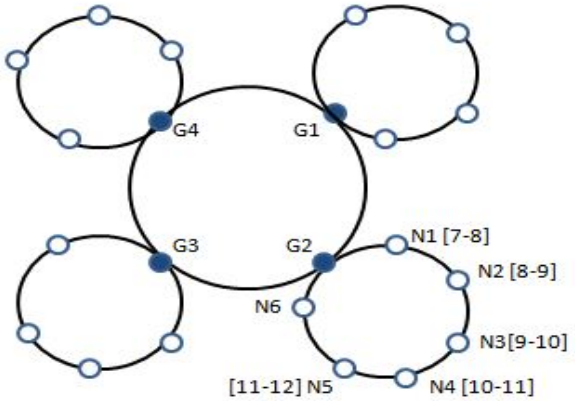

Fig. 4. Publish peer inside the Chord ring

that for large networks, having more than 40,000 peers, there will enough peer in each of the interest group to support the 24X7 coverage of a document. Here number of SuperPeer and number of Normal Peer is 1000 and 35k respectively.

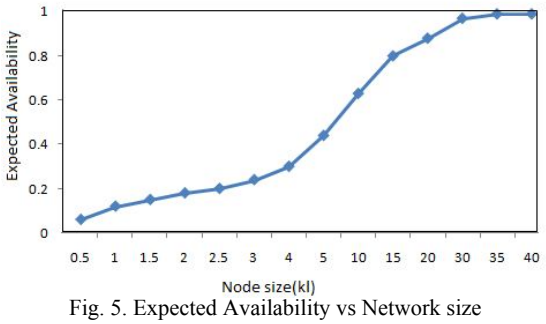

Fig. 5. Expected Availability vs Network size

B. Expected availability vs Number of Interest

In this experiment, we varied the number of interests in the system to determine the change in the expected availability. For each level of interest, 40000 peers published themselves to store their information

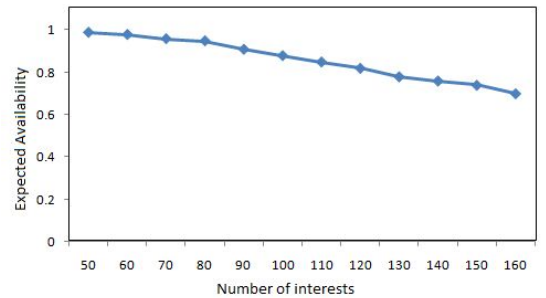

in the Chord Ring. As illustrated in Fig.6, document availabil-

C. Availability vs Node failure

In Here, 40000 peers published their own uptime distribution to the System. To calculate availability in this setup, we first published 100 documents in the Chord ring. Then we increase the percentage of node failure and executed query to retrieve documents at random time. The percentage of documents retrieved successfully gives us the obtained availability.

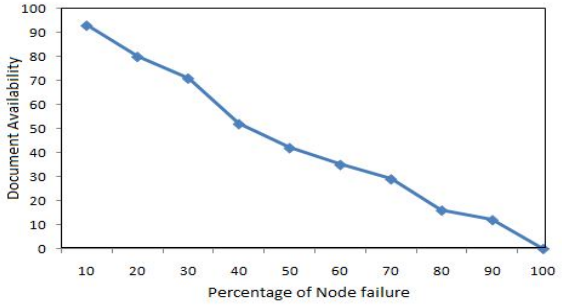

Fig. 7. Obtained availability vs Node failure

It can be seen from Fig 7. that the document availability remains above 0.8 even up to 70% peer failure. This high level of availability is achieved only because of the time-based replication strategy adopted by the proposed architecture.

D. Availability vs Indexing node failures

Here, we increased the failure percentage of indexing nodes and then we execute the retrieval query for 100 documents at a

random time to determine the change in obtained availability.

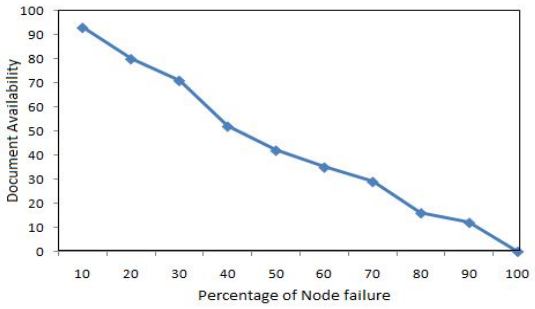

Fig. 8. Availability vs Indexing node failures.

It can be seen from Fig. 8, that the failure rate of indexing peers affects availability significantly. Unlike failure of regular Peers (as explained in Fig. 7), failure of super Peers holds linear relationship with availability.

.

X. RELATED WORK

Many research activities, including [10] [13] [11] [12], have focused on improving document availability in P2P environment in presence of high population dynamism.

In [13], a time-related replication has been proposed for P2P storage networks. In this work, the authors have proposed a replication strategy based on session time of the peer holding the primary replica of a resource. Secondary sparse replicas are used to provide redundancy and to fill any time gap between consecutive sessions two primary replica peer. The replication strategies proposed in [5] and [7] uses on demand replication of an object whenever the number of replica falls below a given threshold. In those works different strategies have been proposed to minimize the volume of replication traffic. A number of approaches, including [10] [15] [17], focus on minimizing replica update traffic in P2P networks.

In [9], the authors proposed an improved Chord model in which nodes are organized into groups and with this strategy they also shown how shared files can be transmitted simultaneously. In [18], the authors proposed another group based distributed architecture where it organizes the nodes inside groups by Chord [16] protocol but it defines new communication protocol for nodes among different groups and removes server/super peer for group management. In [12], another group structured peer-to-peer network is proposed and they show that this protocol is highly capable and powerful even in the dynamic nature of P2P networks.

Interest sensitive distributed systems [8] [9] [11], are lately getting much attention in P2P networks. Group organization and management are key issues in these systems. It sounds better to group members with similar interest together and do group organization respectively. Currently centralized or hierarchical approach has been widely used. For distributed resource management and ensuring 24x7 availability, this paper uses interest based grouping and replication of documents. Group based management ensures the look-up efficiency and availability is ensured by finding suitable nodes to replicate the documents. Initial number of indexing node is 1000

XI. CONCLUSION

In our group based Chord system we strive to ensure 24x7 availability by replicating documents based on uptime distribution. The original Chord employs compact protocols and has provable correctness and performance, the proposed extension on Chord takes the advantages of the original Chord protocol and at the same time enhances the look-up efficiency. Our theoretical analysis, simulations and experimental results confirm that expected availability of the documents remains stable for large networks with moderate level of dynamism.

REFERENCES

[1] The FastTrack Peer-to-Peer technology, http://www.fasttrack.nu/.

[2] The Gnutella website, http://www.gnutella.com.

[3] The KaZaA website, http://www.kazaa.com/.

[4] The Napster website, http://www.napster.com/.

[5] R. Bhagwan, Y.-C. Cheng K. Tati, S. Savage, and G. M.Voelker. Total recall: System support for automated availability management. In Proc. of the 1st ACM/USENIX Symposium on Networked Systems Design and Implementation (NSDI), San Francisco, CA, March 2004.

[6] R. Bhagwan, S. Savage, and G. Voelker. Understanding availability. In Proc. of the 2nd International Workshop on Peer-to-peer Systems, Berkeley, CA, December 2002.

[7] B. G. Chun, F. Dabaek, A. Haeberlen, E. Sit, H. Weath-erspoon,M. F. Kaashoek, J. Kubiatowicz, and R. Morris. Effcient replica maintenance for distributed storage systems. In Proce. of the 3rd Symposium on Networked Systems Design and Implementation(NSDI), May 2006.

[8] E. Cohen, A. Fiat, and H. Kaplan. Associative search in Peer-to-Peer networks: Harnessing latent semantics. In Proc. Of INFOCOMM, 2003.

[9] Yu Dan, Chen XinMeng, and Chang YunLei. An improved p2p model based on chord. Proceedings of the Sixth Internation Conferece on Paralled and Distribute Computing Applicationsand Technologies, 2005.

[10] Richard J. Dunn, John Zahorjan, Steven D. Gribble, and-Henry M. Levy. Presence-based availability and p2p systems.Peer-to-Peer Computing, IEEE International Conference on,0:209–216, 2005.

[11] O. B. Karimi, S. Yousefi, M. Fathy, and M. Mazoochi. Availability in peer to peer management networks. In Proc. Of APNOMS and LNCS, volume 5297, page 552555. Springer-Verlag Berlin Heidelberg, 2008.

[12] Sarder Kashif Ashraf Khan and Laurissa N Tokarchuk. Interest-based self organization in group-structured p2p

networks. Con-sumer Communications and Networking Conference, 2009.CCNC 2009. 6th IEEE, 2, 2009.
[13] K. Kim. Time-related replication for p2p storage system. In Proc. of International Conference on Networking, 2008.
[14] S. Saroiu, P. K. Gummadi, and S. D. Gribble. A measurement study of peer-to-peer file sharing systems. In Proc. of Multimedia Computing and Networking,, San Jose, CA, January 2002.
[15] E. Sit, A. Haeberlen, F. Dabek, B. G. Chun, H. Weatherspoon, R. Morris, M. F. Kaashoek, , and J. Kubiatowicz. Proactive replication for data durability. In Proc. of IPTPS, February 2006.
[16] Ion Stoica, Robert Morris, David Karger, M. Frans Kaashoek, and Hari Balakrishnan. Chord: A scalable peer-to-peer lookup service for internet applications. pages 149–160, 2001.
[17] J. Tian, Z. Yang, and Y. Dai. A data placement scheme with time-related model for p2p storages. In Proc. of P2P, September 2007.
[18] Rong Zhang, Koji Zettsu, Yutaka Kidawara, and Yashushi kiyoki. Decentralize architecure for resource management of group-based distributed systems. Frontiers of Computer Science in China, 2, 2008.

Proceedings of 2009 12th International Conference on Computer and Information Technology (ICCIT 2009)
21-23 December, 2009, Dhaka, Bangladesh

Using an Old Technique in a New Technology — A Novel Method for Defining the Scope of ISs in BPM Projects

Morteza Alaeddini, Ahmad A. Kardan†
Department of Computer Engineering and Information Technology, Amirkabir University of Technology, Tehran, Iran
† Advanced e-Learning Technologies Group, Amirkabir University of Technology, Tehran, Iran.
m.alaeddini@aut.ac.ir, aakardan@aut.ac.ir

Abstract

Nowadays, using business process management (BPM) systems is so prevalent through the world, so that deploying information systems (IS) based on this technology has become one of the application development methods in the new age of software engineering. Due to acquisition and using this technology in many organizations without awareness or program, that is the main reason which would fail this type of projects, we are looking for an efficient method in order to grain information systems, based on organization's business processes for the sake of defining the scope of their related software development projects, in the shortest time and with the lowest cost. We have started our scientific researches on this field in a few projects with the nature of information technology (IT) planning and gained noteworthy results that one of them is described in this paper as a case study. This new method will be used as the first step in defining project portfolios according to BPM approach, and in some actions like enterprise architecture (EA) or IT/IS planning.

Keywords: Business Process Management (BPM), Information System (IS), Value Chain, Clustering, Affinity Analysis.

I. INTRODUCTION

In recent years, businesses have been faced with more challenges raised from fast changing environments, which quickly have changed from centralized and closed situation to distributed and open one. Consequently, business processes displaying more complexity because of interactions between their internal components and interactions of the processes with the environment. Thereupon, organizations should pay more attention to support the management of their own business processes to make themselves adaptable with the new complex environments.

Business process management (BPM) is a new approach rooted in management science concepts and commonly considered to be the development of business applications that directly follow the execution logic of the underlying business processes, while traditional approaches pay more attention to software engineering aspects [1] to model and manage the processes and use workflow technology as a predefined logical procedure of activities.

From the managerial viewpoint, BPM can be seen as a set of methodologies, techniques, and tools for analysis and improvement of business processes [1], [2] that organizational leaders recognize it today as an essential element in organizational performance. Also, from a technological viewpoint, BPM supports these processes by using methods, techniques, and software to design, enact, control, and analyze [1] operational processes.

The main purpose of this paper is to present a method so that to define the scope and boundary of the organization's required information systems to manage their business processes that helps its senior managers not only prioritize the implementation and deployment of their various processes, but also make a certain estimation of expenditure and volume of IS development activities, and providing an infrastructure for outsourcing some services like designing and implementation of various processes to specialized consultants in each business domain.

This paper begins by surveying different definitions of BPM explained by thinkers and leader corporations in this arena and specifying our intention of this concept. This survey includes a brief history of BPM, its concepts and phases, and software development lifecycle for deploying a BPM system in an organization. After the theoretical foundation is established, attention turns to application of the "value chain" model and the "process orientation" approach as major tools and techniques for determining the scope of projects in each organization that want to develop its information systems based on BPM. Furthermore, an actual case and its gained results are explained at the end of this paper.

II. RESEARCH BACKGROUND

A. Different Attitudes on BPM

The background of using BPM term in meaning of business process management dates back to the early years of the 21st century, although it can be traced from the so-called researches in the 1990s [3], [4], [5], [6]. Usage of this term has been so prevalent in management, system engineering, and software engineering texts in recent years. Entrance of different consultation and software companies into the BPM market in the recent years and various interpretations that each company uses about the concept of BPM, has caused misunderstanding about the exact definition of this concept

which shows that, no two corporations or analysts with the same definition of BPM can be found [7].

Validation of this literature shows that BPM term includes a wide range of definitions, from a structured method of understanding, documenting, modeling, analyzing, simulating, executing and continuously changing end-to-end business processes and all relevant resources in relation to an organization's ability to add value to the business [8], [9], [10], [11], to a set of features and tools for modeling, analyzing, executing and controlling the organization's workflow and integrating its application systems [7], [12], [13], [14].

From the history of management, in the time of "process-based management", some methods and approaches like the business process reengineering (BPR), 6-Sigma, total quality management (TQM) and lean thinking have been introduced based on business process concepts and gradually spread. All of these methods have emphasized on the review and reform of business processes in organizations to achieve their strategic goals and success in the competition arena. In past years, BPR methods have helped organizations to achieve IT-enabled radical changes. With a review of the literature, it is deducted that while use of the term BPR may have diminished today, BPR itself has continued to evolve as one approach within the broad umbrella of BPM [9], [10].

Efforts for more aligning IT development methods with business development goals and methods, especially with regard to the concepts of business processes continuous improvement cycle also has caused creation of a new viewpoint on application systems development [7], [15]. In this point of view, which BPM is presented as a method for application systems development, efforts are trying to adapt the standards of application systems development with business processes execution and improvement standards.

Furthermore, from a technology viewpoint, software components like process modeling tools, workflow engines, business rule tools and engines, process analysis and assessment tools, software integration solutions and tools, and content and document management tools that today are assembled and presented as BPMSs, were existed separately already and exist now too [12]. These tools present a new solution to solve an old problem: controlling, supervising, improving and supporting business processes in response to the requirements of recent age [16] when existing enterprises are expanding from local organizations to international distributed companies where business processes dynamically form temporary alliances, joining their business in order to share their costs, skills and resources in supporting certain activities [17].

Recently, BPMSs have a grown and distinctive market through the world and can change the concept of software architecture singularly or by influencing the enterprise applications [7]. From this viewpoint BPM is the convergence of workflow, enterprise application integration (EAI), and unstructured or ad-hoc processes that would be seen as a software technology. BPM is currently revolutionizing businesses by providing an enterprise infrastructure [13] that manages and automates both human and system related processes.

As found in above scrip, there is no unique idea about the concept of BPM between companies and professionals in this domain. Totally, by researching in literature it can be understood that nowadays BPM term is using in four different meaning and each meaning is a viewpoint on it:

- BPM as a management approach;
- BPM as an application system development method;
- BPM as a software technology; and
- BPM as a type of enterprise application integration.

The focused concept of BPM in this research includes two major viewpoints: "BPM as an application system development method" and "BPM as a software technology".

B. Enterprise Information System Development based on BPM Approach

In traditional methods of developing ISs, development path was a linear path from user requirements gathering to a software production that finally could be delivered to end users by traversing a technical development path (based on software engineering processes). However, many efforts have been done to collaborate with users in the software development process up to now but the nature of traditional methods of application systems development restricts the possibility of users' effective collaboration [7] and above all, changing software along with continuous changes of business requirements is so difficult.

Since over 15 years ago there has been a shift from "data-aware" information systems to "process-aware" information systems [18]. To support business processes, an enterprise information system (EIS) needs to be aware of these processes and their organizational context. In new methods of application system development by using BPMS tools, development and execution phases will be done in a cycle [12], [19] which is very similar to the process improvement cycle.

In the first step of this method of IS development, the organization should acquire a suitable technical infrastructure to implement and deploy its own processes which a BPMS with a proper efficiency is the most important sector of this. Then four phases design, execution, monitoring and improvement will initiate after defining prior business domains by qualified consultants' helps.

With this method, the main unit of application systems in an organization will be a "business process" and classification of these processes under different ISs, will be merely for the sake of application portfolio management. Thus, two major changes are happened in the

viewpoint of IS development into its traditional approach that consists:

- Changing in apportion of ISs in the form of process classification instead of function classification, and
- Separating an organization's IS development phases to two phases: "providing a BPMS infrastructure" and "system development using provided BPMS" [15]

By using the BPM infrastructure, the IS development phase will be showed off. A critical issue in using an input–output construct is defining the "system boundaries". The boundaries of a system are where elements of the system interact with elements outside the system. Everything outside this boundary is considered the "system environment". The system environment can be described as those external factors of the system that will influence the system over the period of measurement [20]. Identification of each system's boundaries for developing it internally or by qualified consultants will be the first step of software development project portfolio management and will be one of the necessities in a successful implementation of a BPM project.

III. RESEARCH TOOLS AND MODELS

To define IS boundaries in implementation of a BPM project, two categories should be noticed: "value chain" and "process orientation" [21]. The value chain model, in fact, considers activities that create, deliver and support the organization's products or services. Michael Porter has partitioned these activities into two major groups: "primary activities" and "support activities" [22]. Furthermore, process orientation is the way to organize the activities of the enterprise. Process orientation is based on a critical analysis of Taylorism as a concept to organize works. This approach uses functional breakdown of complex work to small granularities [21], so that these work units of small granularity should be especially done by personnel or identified roles in organization.

A. Value Chain

Fig. 1 shows value chain model presented by Michael Porter. As shown in Fig. 1, primary activities are those directly are related to the value creation in products or services, whereas support activities include processes that enforce existence and perpetuity of initial activities in the organization [23].

The aim of these activities is delivery of a level of value to customers that supports cost of them and presents a benefit margin to the organization. The primary value chain activities are:

- Inbound Logistics: the receiving and warehousing of raw materials and their distribution to manufacturing as they are required.
- Operations: the processes of transforming inputs into finished products and services.
- Outbound Logistics: the warehousing and distribution of finished goods.
- Marketing and Sales: the identification of customer needs and the generation of sales.
- Service: the support of customers after the products and services are sold to them.

These primary activities are supported by:

- The infrastructure of the firm: organizational structure, control systems, company culture, etc.
- Human resource management: employee recruiting, hiring, training, development, and compensation.
- Technology development: technologies to support value-creating activities.
- Procurement: purchasing inputs such as materials, supplies, and equipment.

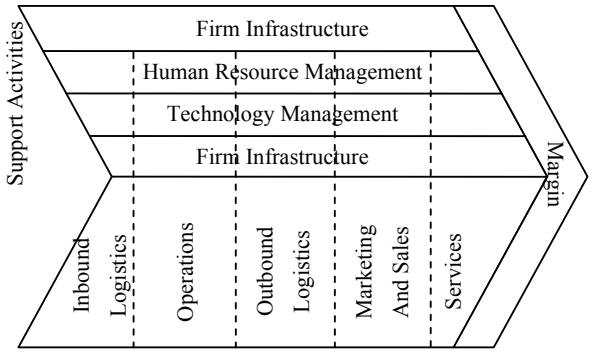

Fig. 1. Internal structure of value chain.

The value chain as a well-known approach in business administration is used to organize the work that a company conducts to achieve its business goals. The organization can achieve its own process hierarchy in its different levels by breaking down a coarsegrained function into finer-grained functions that is called functional decomposition. Functional decomposition is an important concept to capture and manage complexity in the organization [21]. Based on it and, whereas BPMSs have process-based nature, this hypothesis that we can use the value chain model as a strong tool for defining different IS boundaries in a BPM project was fortified. Speedup in planning and better recognition of systems scopes are most important reasons which mainly impact on this hypothesis.

B. Process Orientation

Furthermore, as a response to increasing competition and more demanding customers, various authors have suggested [24] companies to put less emphasis on hierarchical and functional structures, but instead focus and improve on entire chains of business operations, ranging often from customer to customer. In the 1993 the process orientation identified as an essential ingredient for successful process redesign and reengineering efforts within organizations [25], [26]. It must be noticed

that the lack of process orientation is an inhibitor to successful BPMS implementation in organizations [24].

In the 1990 being among the early propagators of this concept, the process orientation explicitly articulated as a beneficial management practice [27]. Furthermore, various authors have referred to organizations that adopted this view as "the horizontal organization", "the process-centered organization", "the process enterprise" or "process focused organizations" [24]. At an organizational level, process orientation has led to the characterization of the operations of an enterprise using business processes [21]. These business processes universally have similar stakeholders and there is an interwoven relationship between them.

IV. RESEARCH METHODOLOGY

Using the organization's value chain is the unique method, which we offer to define the scope of ISs in a BPM project. By using this approach, each part of organization's value chain will be reputed as an information system to develop by a BPMS infrastructure. Evidently, each IS will be consisted of two main parts: processes and data subjects (entities) related to each other.

Our research consisted of two phases:

(1) method with a simple checklist to characterize that how this method can support operational requirements; and

(2) A subsequent case study validation of the affinity analysis to predict implementation success.

Therefore, to evaluate the compliance of operational and informational requirements of the IS scope definition with this method, it has been compared with distinguished variables of process orientation (operational requirement) and affinity analysis between data subjects (informational requirement) that are illustrated as follows.

The respective instruments of checklist and case study will be elaborated in the remainder of this paper. As it will become clear, the feedback group of four organizations, where we have applied this method also played an important role in the validation and augmentation of the instruments, in this way adding an important practical dimension to findings from literature. These mentioned organizations consist of Charmahal Bakhtiari Electrical Power Distribution Company (CBEPDC: www.chb-edc.ir), Razi Vaccine & Serum Research Institute (RVSRI: www.rvsri.com), Ministry of Welfare and Social Security of Iran (MWSS: www2.refah.gov.ir), and Mapna Group (MAPNA: www.mapna.com).

A. Satisfying Operational Requirements

Process orientation content in an organization depends on multiple factors introduced in Table I. Furthermore, this table shows how our proposed method can support these factors. As shown in Table I, this method can satisfy all of requirements of process orientation.

The conceptual model underlying the process orientation checklist is based on the process orientation definition by Davenport [26]: "A process orientation to business involves elements of structure, focus, measurement, ownership and customers." The five primary elements, i.e. structure, focus, measurement, ownership, and customer are thought to formatively construct process orientation and for each of them, Table I contains its various aspects and suitable variables to make these aspects measurable.

Table I. Checklist of process orientation

Elements [24]	**Distinguished variables [24]**	**Satisfying with proposed method**
Structure	Organizational structure	Parts of value chain; BPMS features in defining roles
Focus	Use of process language	Modeling/execution language in BPMS
	Level of process documentation	BPMS features in process modeling
	Utilization of process documentation	BPMS features in process execution
	Information systems architecture	BPMS architecture and infrastructure
Measurement	Level of process performance measurement	BPMS features in process monitoring
Ownership	Existence of process managers	BPMS features in defining roles Parts of value chain
Customer	Understanding of customer requirements	

As seen in Table I, all elements and their variables of process orientation can be complied with our proposed method where different parts of a BPMS cannot respond to them. Therefore, it can be claimed that implementing a BPM project based on this method to plan different ISs and by using a BPMS as an infrastructure can be done.

B. Satisfying Informational Requirements

Several methodologies of ISs planning and software development like as business systems planning (BSP) methodology – presented by IBM corp. [28] – and information engineering (IE) methodology – innovated by Martin in 1980s – have proposed using CRUD matrix for defining the scope of ISs. Rows of this matrix comprise organization's processes and its columns are data subjects related to these processes. Each cell of this matrix will be empty (without any relationship) or filled by C (Create), R (Retrieve), U (Update) or D (Delete) according to relationship between its related process and data subject. Shuffling of rows and columns to align all

the entries with the "C" word along the north-west, south-east diagonal by diagonalizing and affinity analyzing, the scope and boundaries of ISs will be defined. These activities have introduced in appendix 1.

Using the structure of value chain to define the scope of organization's ISs, it will be seen that because of the whole previously mentioned reasons about the value chain and process orientation, nearly all the cells with the "C" word will be placed on main diagonal, if CRUD matrix be prepared. In addition, because of most relationships between data subjects and processes which are placed in each domain, higher value of affinity can be seen between data subjects in that domain and therefore, each domain (each part of value chain) can be enumerated as one of Martin's clusters. The realm of extracted ISs based on our proposed method that described in this paper can be confirmed in a way by this result.

V. CASE STUDY

For better understanding, the case that is implemented in the project of "Preparing IT Master Plan for CBEPDC" by Golsoft Co. (www.golsoft.com) is discussed. A major phase of this project was designing the company's target architecture in the business, data & information, application, and infrastructure layers. Based on the company's business traits, using BPM approach in IS development was proposed in target infrastructure layer. In this project, we identified 112 data subjects in the target data & information layer and recognized 141 processes in the target business layer.

A. Case Description

After defining the company's idealistic processes and data subjects, referenced to the company's policy about using BPMS infrastructure for IS development, we were looking for a way which helps us to define the scope of company's ISs at least possible time. Meanwhile we had to have more attention to the company's business processes because BPM approach was chosen to develop the company's ISs and correct classification of implementable processes in each system for the awareness of company's functional requirements by consultants was so important.

Herein, defining the scope of ISs by using prevalent methodologies like Martin's clustering algorithm was loosed because of two reasons: firstly, in this type of methodologies, more focus is on interdependencies between data subjects than coherence of processes and for this reason often the identified scope of ISs is not adapted to the organization's process domains. Secondly, using these methods need to a huge time and especial expertise because of their complex calculations.

B. Solution Finding

Point to above problems, so many studies we concluded that the best way to determine the scope of CBEPDC's ISs is to use process domains, which are in the company's value chain. These business domains were recognized in the business architecture layer of the baseline phase. Furthermore, target situation of this architectural aspect was designed based on the company's value chain and these business domains. They could support the whole of the company's business scope and also the processes of each domain had sufficient coherence because of functional decomposition described above.

By using this method, all of 141 desirable company's processes and 112 data subjects constituted totally 12 ISs adapted to 12 process domains in the company's value chain. Some of these ISs are being developed now and the others are tendering to choose qualified implementers.

When we ran Martin's algorithms, similar results were gained. The scope of proposed ISs that are defined based on described method in this paper has been compared with results of affinity analysis and Martin's clustering algorithm in below lines. By using our method, data subjects of each IS are identified according to value "C" in cells aligned to processes of that IS in the CRUD matrix provided by Microsoft Excel and in less than an hour. Whereas it took a week when we used Microsoft Excel and Microsoft SQL Server to implement the Martin's affinity analysis and his clustering algorithms for identifying all data subjects related to each IS. Albeit using some tools like IEW (Information Engineering Workbench by KnowledgeWare Inc.) or IEF (Information Engineering Facility by Texas Instruments Information Engineering) can considerably reduce this time, it should be reminder that using these tools needs to both of expending some cost to acquire and preparing all models in them and based on IE methodology that nowadays its use is seldom.

C. Result Analysis

We found that firstly, the number of ISs defined by both methods was equal and secondly, there were only 13 inconsistencies between results of Martin's affinity analysis and our proposed method that is 11.6 percent of the whole entities. The maximum value of this inconsistency was 33.3 percent (See Fig. 2).

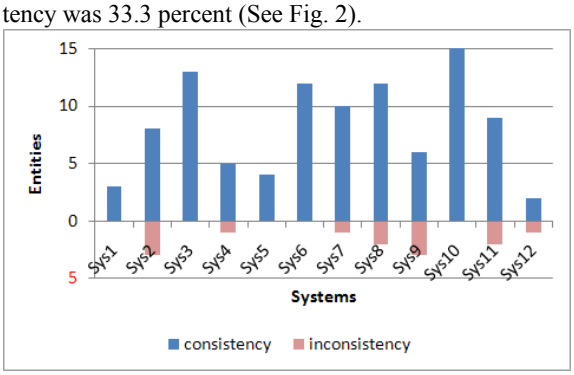

Fig. 2. Comparison of inconsistencies in defining the scope of ISs based on proposed method and Martin's

After examining the reasons for this conflict, it was clear that inconsistencies are seen in some entities,

which are informational contact points between two different systems. Only since the number of processes interacted with an entity in an IS may be more than the number of processes in its comprised IS, this entity has been shifted to another IS in Martin's method.

Since Martin believes that analyst's viewpoint is preferred to results of this algorithm [29] and changes and modifications done by him are more favored than results of clustering and affinity analysis, we can say that this percentage of inconsistency is referred to analyst's viewpoint and profess that gaining these results confirms our proposed method.

As said above, competencies of using this method in the mentioned project of CBEPDC include below:

- Saving time (time less than an hour in comparison with at least a week in similar projects);
- Not requiring any tools to support complex calculations for the Martin's method; and
- More adaptation between the scope of defined ISs and the company's business domains.

VI. CONCLUSION

As said foregoing, the model in mind that at present has been dominant in organizations' management recommends continuous and gradual improvement of processes instead of suddenly reforming them. Sometimes this model is phrased as business process management (BPM) that is prolonged of the business process reengineering (BPR) discussions. Acquiring BPM technology is a competitive advantage for each organization. In addition by using BPM, the organization can focus on other its competitive advantages like deliverable customer services and improve its key processes. This technology has not a long old in the IT world market and motion to it is partly new. This issue is clear that the lack of a distinct framework for acquisition and applying this technology in organizations is a great and important subject.

In this paper, a novel method has been presented to define and determine the scope of ISs in organizations based on the Porter's value chain for the sake of developing on a BPMS platform. This is the first step of defining the target architecture of the organization's application layer and planning its information systems. After defining boundaries of the organization's ISs, it will be possible to create the projects' portfolio for developing these ISs and prioritize them by gap analysis and using planning techniques.

After the experience in CBEPDC, this study did in other mentioned organizations to determine the scope of their ISs, based on insights from literature augmented with our experience in this field. Process orientation is increasingly recognized in theory and practice as a significant factor affecting the ease and success of implementing a BPMS, and we could realize it by using the value chain model with acquiring a suitable BPMS. Four case studies were used to validate the method, as presented one of them here.

Importance of this unique method is discussable from several aspects. First, it has a new glance to some old concepts like the value chain and process orientation, and because of natural adaption with these concepts; it can assure more compliance of the scope of organization's ISs with its business processes and be pursued by more coherence of each system's processes. Second aspect is related to reducing the time of defining the scope of systems and thereupon time of planning and decision making due to this scoping. Moreover, needing no complex calculation and loose of requiring supportive tools for these calculations is third advantage point of this method in comparing with previous methods. Results of applying this method in several projects that we allude to one of them are its demonstratives.

The method has been offered in this paper can be strongly adviser of future researches to present an insight methodology or framework for acquiring and applying BPM technology. This methodology/framework has to join preceding technical aspects with managerial issues and discussions related to the organization's maturity for acceptance and establishment of BPM, required phases and activities for deployment, working teams' structures, and the style of interaction between them in similar projects. It is noteworthy that the place of such a framework that we also in the near decide to practice it is empty or so inconspicuous in existing researches until now, and it is one of the research priorities under this topic.

VII. APPENDIX 1: A SHORT REVIEW ON MARTIN'S AFFINITY ANALYSIS METHOD AND CLUSTERING ALGORITHM

In Martin's opinion, the organization's processes have a natural and internal affinity with together because each process use information created by another process [29]. Furthermore, he has proposed a technique called "affinity analysis" for evaluating this affinity between data subjects. The affinity of entity E_i to entity E_j will define as [29]:

$$\frac{a(E_i, E_j)}{a(E_i)} \tag{1}$$

where $a(E_i)$ is no. of processes interacted with entity E_i and $a(E_i, E_j)$ is no. of processes interacted with both entities E_i and E_j.

In addition, to define and determine the scope of different ISs and separate them from each other, Martin has proposed clustering technique. This algorithm can be summarized as below:

- Constructing a matrix of affinity values,

- Sorting the entity pairs from highest to lowest affinity value,
- Forming the nuclei of clusters based on entity pairs with the highest affinity, and
- Assigning other entities to clusters with this condition: When each entity E_k wants to add to a cluster containing entities E_i, E_{i+1}, … and E_n, value of following division should be maximized in remained affinity values in affinity matrix [29]:

$$\frac{\sum_{j=i}^{n} \frac{a(E_k, E_j)}{a(E_k)} \times a(E_j)}{\sum_{j=i}^{n} a(E_j)} \quad (2)$$

After the formation of clusters, each of them can be seen as a business area [29] and its development can be planned as an information system. It should be noted that Martin believes that analyst's viewpoint prior to this algorithm, which changes and modifications done by him are preferred to results of clustering and affinity analysis [29].

VIII. ACKNOWLEDGEMENT

The authors would like to express appreciation to the CEO and CIO of Charmahal Bakhtiari Electrical Power Distribution Company and other three organizations for their time and support for this study. The authors would also like to thank Mr. Reza Karami, CEO of Golsoft Co., and Mrs. Mona Rashidi Rad for their feedback and related help throughout this work.

REFERENCES

[1] M. Wang and H. Wang, "From process logic to business logic—A cognitive approach to business process management," *Information & Management*, vol. 43, p. 179–193, 2006.

[2] K. Vergidis, C.J. Turner, and A. Tiwari, "Business process perspectives: Theoretical developments vs. real-world practice," *Int. J. Production Economics*, vol. 114, p. 91–104, 2008.

[3] F. Leymann and D. Roller, "Business Process Management With FlowMark," in *39th IEEE Computer Society International Conference*, California, 1994, pp. 230–234.

[4] J. K. Bombardier, "Product Defect Reduction through the Use of Business Process Management," in *1992 IEEUSEMI Advanced Semiconductor Manufacturing Conference*, 1992, pp. 43–48.

[5] J. Boardman, "Corporate intranets and business process management: a challenge for systems engineering," *Computing & Control Engineering Journal*, pp. 245– 256, Dec 1997.

[6] D. J. Elzinga, T. Horak, C. Y. Lee, and C. Bruner, "Business Process Management: Survey and Methodology," *IEEE Transactions on Engineering Management*, vol. 42, no. 2, pp. 119–128, May 1995.

[7] R. Karami, "Business Process Management (BPM) Solutions," Golsoft Co., Tehran, Technology Analysis Collection, GEADeF Architecture Framework Documents GEADeF.WP.TA.BPM, 2007.

[8] S. Chong, "Business process management for SMEs: an exploratory study of implementation factors for the Australian wine industry," *Journal of Information Systems and Small Business*, vol. 1, no. 1-2, pp. 41–58, 2007.

[9] M. H. Fagan, "Exploring city, county and state egovernment initiatives: an East Texas perspective," *Business Process Management*, vol. 12, no. 1, pp. 101–112, 2006.

[10] P. Puah and N. Tang, "Business Process Management, a Consolidation of BPR and TQM," in *The 2000 IEEE International Conference on Management of Innovation and Technology (ICMIT 2000)*, 2000, pp. 110–115.

[11] G. S. Tian and L. Quan, "An Improved Framework of Business Process Management System Which Integrating the Strategy Management," in *15th International Conference on Management Science & Engineering*, Long Beach, USA, 2008, pp. 256–261.

[12] M. Weske, W. M. P. Aalst, and H. M. W. Verbeek, "Advances in business process management," *Data & Knowledge Engineering*, vol. 50, pp. 1–8, 2004.

[13] C. Prior, "Workflow and Process Management," Maestro BPE Pty Ltd., Australia, Technical report 2006.

[14] M. A. A. Pantazi and N. B. Georgopoulos, "Investigating the impact of business-processcompetent information systems (ISs) on business performance," *Managing Service Quality*, vol. 16, no. 4, pp. 421–434, 2006.

[15] K. Vergidis, C.J. Turner, and A. Tiwari, "Business process perspectives: Theoretical developments vs. real-world practice," *Int. J. Production Economics*, vol. 114, pp. 91–104, 2008.

[16] M. Wang and H. Wang, "From process logic to business logic—A cognitive approach to business process management," *Information & Management*, vol. 43, p. 179–193, 2006.

[17] J. Y. Kuo, "A document-driven agent-based approach for business processes," *Information and Software Technology*, vol. 46, p. 373–382, 2004.

[18] W. M. P. Aalst, B. Benatallah, F. Casati, F. Curbera, and E. Verbeek, "Business process management: Where business processes and web services meet," *Data & Knowledge Engineering*, vol. 61, pp. 1–5, 2007.

[19] C. Moore and C. Teubner, "Making Sense Of The Business Process Management Landscape," Forrester Inc., Forrester Research May 23, 2006.

[20] R. Bullock and R. Deckro, "Foundations for system measurement," *Measurement*, vol. 39, no. 8, p. 701–709, 2006.

[21] M. Weske, Business Process Management: Concepts, Languages, Architectures, 1st ed.: Springer, 2007.
[22] M. E. Porter and V. E. Millar, "How information gives you competitive advantage," *Harvard Business Review*, pp. 149–160, July-August 1985.
[23] K. E. Pearlson, Managing and Using Information Systems: A Strategic Approach. USA: John Wiley &Sons, 2004.
[24] H. A. Reijers, "Implementing BPM systems: the role of process orientation," *Business Process Management*, vol. 12, no. 4, pp. 389–409, 2006.
[25] M. Hammer and J. Champy, *Reengineering the Corporation: A Manifesto for Business*. New York: Harper Collins, 1993.
[26] T. H. Davenport, Process Innovation: Reengineering Work through Information Technology. Boston: Harvard Business School Press, 1993.
[27] T. H. Davenport and J. Short, "The new industrial engineering: information technology and business process redesign," *Sloan Management Review*, vol. 31, no. 4, pp. 11–27, 1990.
[28] IBM Corporation, *Business Systems Planning: Information Systems Planning Guide*, 4th ed. Atlanta, USA: IBM Corporation, 1984.
[29] J. Martin, Information Engineering - Book II: Planning and Analysis.: Prentice-Hall Inc., 1989.

Proceedings of 2009 12th International Conference on Computer and Information Technology (ICCIT 2009)
21-23 December, 2009, Dhaka, Bangladesh

Collision Minimization in IEEE 802.11e Using Fine-Tuned Contention Window Mechanism *(Not Presented)*

Shah Ahsanuzzaman Md. Tariq, Khalada Perveen[†], Quazi Delwar Hossain[‡], Md. Akbar Hossain[‡]
Department of Information Engineering and Computer Science, University of Trento, Trento, Italy
[†] Department of EEE, Stamford University, Bangladesh
[‡]Department of EEE, Chittagong University of Engineering and Technology, Bangladesh
ahsanuzzaman.tariq@gmail.com, khalada.perveen@gmail.com, quazi@cuet.ac.bd, akbar002426@gmail.com

Abstract

The IEEE 802.11e draft has been introduced to provide QoS to the real time applications in wireless network. The new MAC protocol mainly defines HCF (Hybrid Coordination Function) and EDCF (Enhanced Distributed Coordination Function). EDCF is a contention based channel access scheme and is a part of HCF for infrastructure network. In this paper, we proposed to enhance the EDCF performance with the fine tuning of the minimum contention window along with the randomized AIFSN (Arbitration Interframe Space Number) value that depends on the traffic load. The main purpose of our paper is to reduce collision in the WLAN that is caused due to small contention window.

Keywords: AIFSN, contention window, collision, IEEE 802.11e, EDCF.

I. INTRODUCTION

IEEE 802.11 is the widely accepted protocol in the wireless communications. It has become a standard technology that provides efficient internet access to almost every user. Today, Real time multimedia applications have become the most demanding applications on wireless channels which require Quality of Service (QoS) [2]. But, providing this Quality of data traffic over network is a challenge for IEEE 802.11 protocol. Hence, an enhanced version IEEE 802.11e was introduced which enable service differentiation and support QoS requirements. 802.11e uses EDCA for service differentiation and providing QoS.

The work is organized as follows: Section II provides brief introduction to the IEEE 802.11e protocol. Section III introduces the collision mechanism. Section IV describes the proposed algorithm and Section V concludes the paper with future work.

II. IEEE802.11E

A. OVERVIEW

IEEE 802.11e is the enhanced version of the IEEE 802.11 MAC that is dedicated to provide Quality of Service. It supports QoS by the service differentiation and prioritization mechanism. Different data traffic has different priority based on the QoS requirements. Basically, applications are divided into four Access Categories (AC) [2], [9]. Every frame with a specific priority of data traffic is then assigned to one of these access categories. For each AC, service differentiation is defined by utilizing a different set of contention parameters to get the medium access.

B. HCF AND EDCF

HCF is the centralized coordination function that combines the features of Distributed medium access like DCF (Distributed coordination function) and centrally controlled medium access like PCF (Point coordination function) with improved QoS techniques. HCF defines two types of access mechanisms, The distributed contention-based channel access mechanism is called EDCA (Enhanced Distributed Channel Access) and the centrally controlled contention free access mechanism is called HCCA (HCF Controlled Channel Access) [3], [5], [10].

The EDCA scheme uses Carrier Sense Multiple Access with Collision Avoidance (CSMA/CA) and slotted Binary Exponential Back-off (BEB) mechanism as the basic access method. The EDCA defines multiple ACs with AC-specific Contention Window (CW) sizes, Arbitration Interframe Space (AIFS) values, and Transmit Opportunity (TXOP) limits to support MAC-level QoS and prioritization [1].

Every station has four independent EDCAFs, one for each AC. AC's range from 0 – best effort (AC_0), 1-background (AC_1), 2 – video (AC_2) and 3 – voice (AC_3). AC with highest priority has the shorter CW so that the highest priority traffic can be transmitted before the lower ones. The CW is determined from the range of CWmin [AC] and Cowman [AC] which is computed for different values of ACs. Also, different Interframe space (IFS) is introduced according to ACs. Transmission begins if the channel is sensed idle in EDCF, otherwise the stations executes a back-off procedure after waiting a period of AIFS [AC]. The back-off time is drawn from the interval [1, CW [AC]+1]. Each AC within a single station behaves like a virtual station that can independently start transmission if the channel is idle. AIFSN refers to length of the AIFS [2].

C. TIMING RELATIONSHIP FOR EDCA

Fig. 1 shows the timing operations in 802.11e EDCA. To achieve differentiation, instead of using fixed DIFS (Distributed Interframe Space) (as in 802.11 DCF), EDCA assigns higher priority ACs with smaller CWmin, CWmax, and AIFS to influence the successful

978-1-4244-6283-4/09/$26.00 ©2009 IEEE

transmission probability (statistically) in favor of high-priority ACs [7]. The AC with the smallest AIFS has the highest priority, and a station needs to defer for its corresponding AIFS interval. The smaller the parameter values (such as AIFS, CWmin and CWmax) the greater the probability of gaining access to the medium [2]. Individual virtual station contends for access to the medium and independently starts its back-off procedure after detecting the channel being idle for at least an AIFS period. The back-off procedure of each AC is the same as that of DCF.

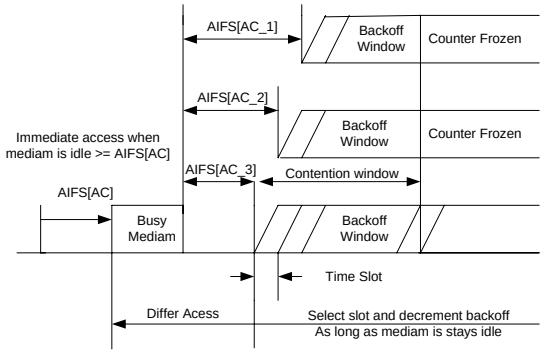

Fig. 1. EDCA timing operation

IEEE 802.11e EDCA defines an time interval in which a particular station can initiate transmissions called transmission opportunity limit (TXOPlimit) [7]. During this period, stations are allowed to transmit multiple data frames from the same access categories (ACs) continuously within the time limit defined by TXOPlimit. In 802.11e EDCA the higher priority ACs have a longer TXOPlimit, while lower priority ACs have a shorter TXOPlimit. Priority differentiation used by EDCA ensures better service to high priority class while offering a minimum service for low priority traffic. This mechanism improves the quality of service of real-time traffic.

Table I CW and AIFSN for different ACs.

AC	CWmin[AC]	CWmax[AC]	AIFSN
0	CWmin	CWmax	7
1	CWmin	CWmax	3
2	(CWmin+1)/2-1	CWmin	2
3	(CWmin+1)/4-1	(CWmin+1)/2-1	2

The preferred values of each access categories (ACs) access mechanism parameters that the standard recommends are shown [2] in Table 1 where CWmin= 31 and CWmax=1023.

The performance obtained is not being optimal since EDCA parameters cannot be adapted according to the network conditions [9]. Minimization of different access categories traffic impacts during transmission which occurred by high traffic load could be challenges.

III. COLLISION

Higher priority ACs has small contention window that is the reason they suffer from higher collisions. Two types of collision can be experienced.

A. INTERNAL COLLISION

Every AC in the single station can act as a virtual station and transmit whenever channel is idle. When more than one EDCAF in the same station count their back-off timers to zero and try to transmit at the same time, it leads to a situation referred to as internal collision or virtual collision. In such situation, the access to the medium is granted to the EDCAF for the highest priority AC among the colliding EDCAFs, and the lower priority colliding EDCAF doubles its Contention Window and back-off, similar to an external collision.

B. EXTERNAL COLLISION

An external collision occurs if back-off timers of the EDCAFs at two or more stations reach zero at the same time and win access to the medium. After the external collision the colliding EDCAFs double their Contention Windows as original standard and choose new back-off values, and the rest of the EDCAFs retain their paused back-off timers.

IV. COLLISION MINIMIZATION

Collision will minimize with proper adjustment of CW according to access categories. Adjustment mechanism for contention window and AIFSN should be finely tuned when collision rate and traffic load is high. Dynamically adjusting the contention window minimizes the internal and external collision of IEEE 802.11e [3].

A. PROPOSED ALGORITHM FOR CONTENTION WINDOW ADJUSTMENT

We proposed a collision minimization process which is not being simulated but logically it should minimize the overall collision. The minimization process is designed according to both contention window and AIFSN scheme. We focused on collision reduction and appropriate service differentiation according to collision rate (CR), Traffic load (TL), AIFSN which indicates fine tuning of contention window (FTCW). We propose the mechanism as the following behavior:

f^{i}_{CR} : Collision Rate in i^{th} station at a interval

f^{i}_{CRTh} : Collision Rate threshold, minimum collision that does not dramatically changes overall collision

CW^{i}_{new} : New contention window in i^{th} station

$CW^{i}_{new}[AC_H]$: New contention window for higher priority level (AC_3 and AC_2) in i^{th} station

$CW^{i}_{new}[AC_L]$: New contention window for lower priority level (AC_0 and AC_1) in i^{th} station.

AIFS range : $AIFSN^{i}_{\max}[AC_{H,L}]$ equal to 7 and $AIFSN^{i}_{\min}[AC_{H,L}]$ equal to 1.

PF_{new} : New Persistence factor value depends on CR and TL.

TL_{TH} : Threshold Trafic load: Approximate parameter that depends on the collision rate and number of stations.

if (Collision occurs and $f^{i}_{CR} > f^{i}_{CRTh}$ then

$CW^{i}_{new}[AC_H] = CW^{i}_{max}[AC\_VI]$

$CW^{i}_{new}[AC_L] = PF_{new} . (CW^{i}_{old}[AC_L] + 1) - 1$

if $TL > TL_{TH}$ then

$AIFSN^{i}_{new}[AC_{H,L}] = AIFSN^{i}_{\max}[AC_{H,L}]$

else

$AIFSN^{i}_{new}[AC_{H,L}] = AIFSN^{i}_{\min}[AC_{H,L}]$

endif

else

CW^{i}_{new} , $AIFSN^{i}[AC_{H,L}]$ and CW^{i}_{max} are set to be default values.

endif

B. DISCUSSION

The simulation of this proposed algorithm is out of the scope but we tried to approximate the size of contention window without simulation. The collision rate is equal to the ratio between number of collisions and number of data sent in an interval q. When collision occurs and CR is larger than the threshold (the threshold should be set according to previous experimental value), then the new contention window of AC_H will be set to the maximum CW size of the AC_2. This mechanism depends upon CR and set the CW of AC_L according to the value of new persistence factor and old CW size. The new PF parameter will change according to CR and TL but its minimum value is two. Also, we include the AIFS mechanism, when the TL is larger than the threshold; the new AIFSN will be set to the max (AIFSN) and vice versa. If no collision or CR is acceptable or less than threshold then both the CW and AIFSN mechanism value should be set as default.

V. CONCLUSION AND FUTURE WORK

AC_3 has more virtual collision due to small CW and small AIFS. Here, we focused on the CW size so that it will increase according to Traffic load and collision rate. In this paper we proposed a CW adjustment mechanism named the fine tuned contention window (FTCW), this will minimize the internal and external collision among different access categories. Due to a fixed CW size of AC_H when collision occurs and larger than the CR threshold, this will satisfy logically that CW of AC_H will be high and collision of AC_H will be minimized. Also, we include the threshold (Traffic load) based AIFSN value which will add an advantage over higher traffic of $AC_{H,L}$. This logically satisfies that the overall collision should be reduced. In future it can be simulated by using any of the network simulation software (GloMoSim, OPNET, ns2).

REFERENCES

[1] IEEE Standard 802.11: Wireless LAN medium access control(MAC) and physical layer (PHY) specifications: Medium access control (MAC) Quality of services (QoS) enhancements, IEEE 802.11e Std.

[2] D.Gu and J.Zhang, “Qos Enhancement in IEEE 802.11 Wireless Local Area Networks”, *IEEE Communication Magazine*, vol 41, issue 6. pp.120-124, June 2003.

[3] D-J. Deng and R-S. Chang. “A priority scheme for IEEE 802.11 DCF access method”. *IEICE Transactions on Communications*, E82-B(1), January 1999.

[4] Romdhani, L., Ni, Q., and Turletti, T.,“Adaptive EDCF: Enhanced Service Differentiation for IEEE 802.11 Wireless Ad-Hoc Networks”, in the Proceedings of the *IEEE WCNC’03*.

[5] L. Gannoune, “A Comparative Study of Dynamic Adaptation Algorithms for Enhanced Service Differentiation in IEEE 802.11 Wireless Ad Hoc Networks,” in *AICT-ICIW ’06*: Proceedings of the Advanced Int’l Conference on Telecommunications and Int’l Conference on Internet and Web Applications and Services, Guadeloupe, French Carribean, February2006.

[6] S. E. Housseini and H. Alnuweiri, “Adaptive Contention-Window MAC Algorithms for QoS-Enabled Wireless LANs,” in *International Conference on Wireless Networks, Communications, and Mobile Computing*.

[7] D.He, C.Q.Shen, "Simulation Study if IEEE 802.11e EDCF", *Proc.IEEE VTC-Spring 2003*, Jeju, Korea, May 2003

[8] S. Mangold et al, "IEEE 802.11e Wireless LAN for Quality of Service", *Proc. European Wireless*, Florence, Italy, Feb 2002

[9] D. Grilo and M. Nunes. "Performance evaluation of IEEE 802.11E", *Proc IEEE PIMRC*, pp. 511–517, 2002.

[10] "Amendment 7: Medium Access Control (MAC) Quality of Service (QoS) Enhancements" IEEE P802.11e, October 2004.

Proceedings of 2009 12th International Conference on Computer and Information Technology (ICCIT 2009)
21-23 December, 2009, Dhaka, Bangladesh

Variable Rate Steganography in Gray Scale Digital Images Using Neighborhood Pixel Information

Moazzam Hossain, Sadia Al Haque, Farhana Sharmin
Department of Computer Science & Engineering, International Islamic University Chittagong, Bangladesh
mhmilon@yahoo.com, sah_40760@yahoo.com, farhana_iiuc@yahoo.com

Abstract

In order to improve the security by providing the stego image with imperceptible quality, three different steganographic methods for gray level images are presented in this paper. Four Neighbors, Diagonal Neighbors and Eight Neighbors methods are employed in our scheme. These methods utilize a pixel's dependency on its neighborhood and psycho visual redundancy to ascertain the smooth areas and edged areas in the image. In smooth areas we embed three bits of secret information. In the edged areas, variable rate bits are embedded. From the experimental results it is seen that the proposed methods achieve a much higher visual quality as indicated by the high Peak Signal-to-Noise Ratio (PSNR) in spite of hiding a larger number of secret bits in the image. In addition, to embed this large amount of secret information, at most only half of the total number of pixels in an image is used. Moreover, extraction of the secret information is independent of original cover image.

Keywords*:* Steganography, Four Neighbors, Diagonal Neighbors, Eight Neighbors, Peak Signal-to-Noise Ratio.

I. INTRODUCTION

The advent of Internet along with progress made by digital technology gave the world of communication a new dimension. Exchange of digital documents, images, audio and even video via Internet is fast, cheap and simple. This ease of communication brought along with it, problems of security. Digital media are easy to intercept, forge, tamper, copy and distribute illegally. Thus, issues dealing with digital data security and copyright protection are receiving growing attention. Steganography is one such means of achieving security by hiding the data to be communicated within a more innocuous data.

The main goal of Steganography is higher capacity and security of the confidential message. A typical steganographic system consists of a cover media into which the secret message is embedded. The resultant is called the stego media [1].

So far, many steganographic methods have been proposed [2],[3],[4],[5],[6]. The most common of these is replacing *least significant bits* (LSB) of the pixels with the secret message. The basic drawback of this method is that all pixels cannot endure same amount of change and hence distortions are more visible. To obtain better visual quality of the stego-image obtained by simple LSB, Chan and Cheng [2] proposed the *optimal pixel adjustment process* (OPAP). OPAP is applied on the stego image such that the resulting pixel value is much closer to the original value. Both these methods are non-adaptive. Wu and Tsai [3] have proposed an adaptive method based on inter pixel relationship where the number of secret bits to be embedded is variable. This method greatly enhanced the stego image quality.

In this paper, we proposed three efficient steganographic methods that utilize the neighborhood information to estimate the amount of data to be embedded into an input pixel of cover image without producing perceptible distortions. The neighborhood relationship decides the smooth and edged areas of an image. Small amount of secret information is embedded into the smooth areas whereas a large amount is embedded into the edged areas. This is based on psycho visual redundancy in gray scale digital images that edged areas can tolerate greater distortion compared to smooth areas. In our schemes we embed a fixed three bits of information in smooth areas. A variable number of bits are embedded into the edged areas. Though more than half of the total number of pixels of an image is exempted from hiding secret information, where methods discussed in [3] and [8] use almost all the pixels of an image for the same amount of hiding capacity, a significantly higher hiding capacity has been achieved.

II. PROPOSED METHODS

Our proposed methods take advantage of psycho visual redundancy and the dependency of a pixel on its surrounding neighbors. The correlation between a pixel and its neighbors decides whether it is located in smooth area or in edged area.

A. Four Neighbors Method

This method takes into consideration the upper, lower, left and right neighbors of a pixel. The cover image is scanned in a raster scan order considering every second pixel from left to right starting from the second row till the $(N-1)^{th}$ row.

In Fig. 1, the white pixels (*Used* pixels) represent the pixels into which bits are embedded. The black pixels are *Unused*, that is, they do not contribute to the embedding process. The striped pixels remain unchanged. *Unchanged* pixels are the neighborhood pixels. These are not used for embedding data bits but are used for calculation. Thus they differ from *Unused* pixel which serve no purpose (embedding or calculative). To explain further, reference is made to

Fig. 1, in our 'Four Neighbors Method', *Unchanged* pixels are the four neighbors to the *Used* pixel. The number of bits to be hidden in the *Used* pixel is calculated based on these *Unchanged* pixel. The remaining black pixels are unused, that is they do not contribute to the embedding process.

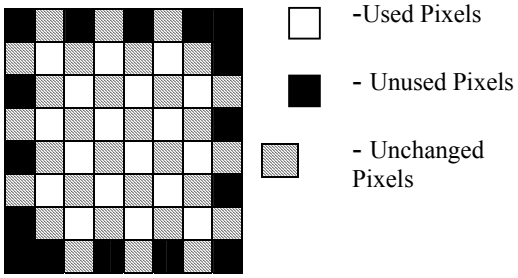

Fig. 1. Scanning the cover image for Four Neighbors Method

The secret information is a text file. The file is converted into binary prior to the embedding process.
The difference value d_i that indicates the smooth or edged region is calculated using the following equation:

$$d_i = (p_{upper} + p_{lower} + p_{left} + p_{right}) /4 - p_i \qquad (1)$$

A small value of d_i indicates that the 3x3 region is smooth. When the magnitude of d_i lies between 0-7, the region is considered to be smooth. Only 3 bits of secret data is embedded into pixels that fall in a smooth region. A larger value of d_i implies that our pixel is in an edged or edged region. Variable rate of secret bits to embed, n, is calculated by

$$n = floor(log_2 |d_i|) \qquad (2)$$

n bits of bit stream is extracted from the secret data and converted into its decimal equivalent, say b, and added to lower bound 2^n, to produce new difference value d_i'. d_i' also lies in the same range $[2^n, 2^{n+1} - 1]$ as d_i.

$$d_i' = \begin{cases} 2^n + b, & d_i \text{ is positive} \\ -(2^n + b), & \text{otherwise} \end{cases} \qquad (3)$$

Sometimes, the new value of pixel p_i may fall off the boundary of the range [0,255]. In those cases, the falling off boundary condition for the embedding process is verified as in [7]. If a pixel satisfies the condition then it is not used for embedding. Two cases for deciding whether a pixel is in a falling of boundary condition are:
Case 1: if $d_i >= 8$ and $((p_{upper} + p_{lower} + p_{left} + p_{right})/4) < 2^{n+1} - 1)$ then $p_i' = p_i$.

Case 2: if $d_i < 8$ and $((p_{upper} + p_{lower} + p_{left} + p_{right})/4 + 2^{n+1}) > 256$ then the corresponding stego pixel is the same as the original value.

The corresponding pixel value of the stego image p_i' is then calculated as

$$p_i' = (p_{upper} + p_{lower} + p_{left} + p_{right}) /4 - d_i' \qquad (4)$$

Extraction is the reverse of the embedding. The difference value d_i^* is calculated for every white pixel using equation (1). Based on d_i^* the secret information b is obtained.

$$b = \begin{cases} d_i^* - 2^n, & d_i^* \text{ is positive} \\ -(2^n + d_i^*), & \text{otherwise} \end{cases} \qquad (5)$$

b is converted into its binary representation which consists of n bits. The falling off boundary condition is also considered to decide whether the pixel contains secret information or not.

B. Diagonal Neighbors Method

This method determines the smooth and edged areas in the cover image based on a pixels relationship with its diagonal neighbors.

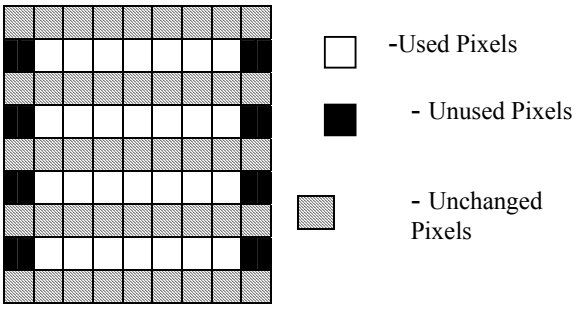

Fig. 2. Scanning the cover image for Diagonal Neighbors Method.

The embedding and extraction steps are similar to the Four Neighbors Method. However, the difference value d_i is given as

$$d_i = (p_{upper\text{-}left} + p_{upper\text{-}right} + p_{lower\text{-}left} + p_{lower\text{-}right}) /4 - p_i \qquad (6)$$

As in the previous method, three bits of secret information are embedded into the smooth areas and n bits are embedded into the edged areas. Fall off boundary conditions are modified for diagonal neighbors such that a pixel is used for embedding or exempted based on the average of diagonal neighbors.

C. Eight Neighbors Method

As the name implies, this method makes use all the eight neighbors of a pixel in a 3x3 region. Hence the smooth and edged areas are much more accurate than the previous two methods. This method results in a stego image with imperceptible quality.

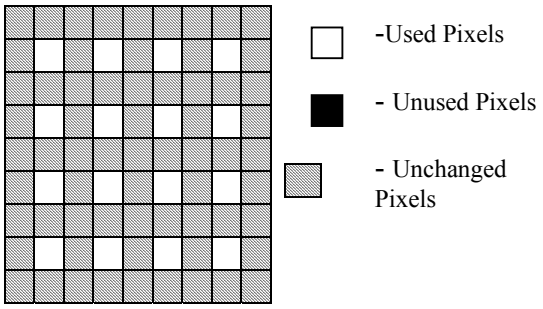

Fig. 3. Scanning the cover image for Eight Neighbors Method.

The value of d_i is given by the following equation

$$d_i = (p_{upper} + p_{lower} + p_{left} + p_{right} + p_{upper\text{-}left} + p_{upper\text{-}right} + p_{lower\text{-}left} + p_{lower\text{-}right}) /8 - p_i \quad (7)$$

The remaining steps for embedding are the same as the previous two methods. The fall off boundary condition takes all eight neighbors into consideration. The extraction steps are the same as discussed in the first method except that eight neighbor pixel values are used.

III. EXPERIMENTAL RESULTS AND DISCUSSIONS

In this section, we present the experiments carried out to justify our proposal and discuss the corresponding experimental results along with the future extension of our proposal.

A. Experimental Results

Some standard 512 X 512 gray scale images are used as the cover image. A secret message is created to be hidden in the images. We have used the Peak Signal-to-Noise Ratio (PSNR) to measure the quality of the stego images. PSNR is a statistical measurement used for digital image/ video quality assessment. Larger PSNR indicates better quality of the image or in other terms lower distortion. An image of high quality raises no curiosity to the observer when compared to images wherein a large portion is heavily distorted. And the human eye is keen in looking for problems and problematic areas. The larger the PSNR value the smaller the possibility of visual attack by human eye [8].

In Fig. 4, four of the standard gray scale images, named Lena and Baboon, Peppers, Tank, have been shown. These four images can exhibit us how the amount of smooth regions and edged regions in an image influences the embedding capacity and PSNR.

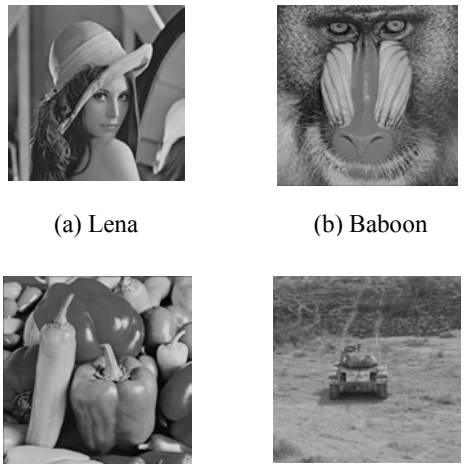

(a) Lena (b) Baboon

(c) Peppers (d) Tank

Fig. 4. Original cover images

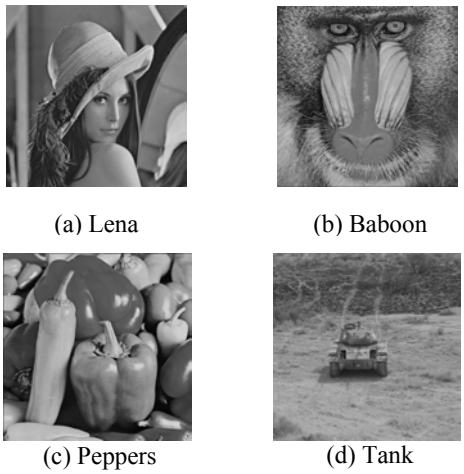

(a) Lena (b) Baboon

(c) Peppers (d) Tank

Fig. 5. Stego images resulted from Four Neighbors Method

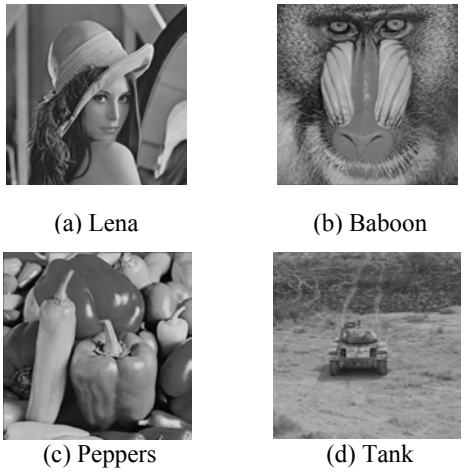

(a) Lena (b) Baboon

(c) Peppers (d) Tank

Fig. 6. Stego images resulted from Diagonal Neighbors Method

(a) Lena

(b) Baboon

(c) Peppers

(d) Tank

Fig. 7. Stego images resulted from Eight Neighbors Method

It is seen from Fig. 5, Fig. 6 and Fig. 7 that, the distortions take place in the stego images due to embedding a large amount of secret message using Four Neighbors Method, Diagonal Neighbors Method and Eight Neighbors Method are unrevealed to human eye. In addition, the image Baboon is comparatively more edged than the image Lena because it contains more edge areas where the gray scale variation is very frequent. Thus it has a greater embedding capacity than that of the image Lena.

The data displayed in Table I, Table II and Table III have the same opinion about what discussed in the previous paragraph.

Moreover, the proposed methods use less than half of the total number of pixels in an image where methods discussed in [3] and [8] use almost all the pixels of an image for the same amount of hiding capacity. For instance, Four Neighbors Method uses only 130048 pixels of the image Lena to hide 392208 secret bits. And in case of the image Baboon, the number of pixels used to embed 435223 secret bits is 129488. It can be added that, the total number of pixels in a 512x512 gray scale image is 262144.

Table I The experimental results for the proposed Four Neighbors Method.

Images	Maximum Capacity (in bits)	PSNR (in dB)	RMSE
Lena	392208	41.1468	2.2346
Baboon	435223	36.5154	3.8086
Peppers	393891	41.0315	2.2610
Tank	395415	40.8102	2.3260

Table II The experimental results for the proposed Diagonal Neighbors Method.

Images	Maximum Capacity (in bits)	PSNR (in dB)	RMSE
Lena	395680	40.6504	2.3660
Baboon	443165	35.0725	4.4970
Peppers	397382	40.1429	2.3878
Tank	405760	39.4487	2.6978

Table III The experimental results for the proposed Eight Neighbors Method

Images	Maximum Capacity (in bits)	PSNR (in dB)	RMSE
Lena	196968	43.9590	1.6165
Baboon	220575	38.8280	2.9184
Peppers	197868	43.5124	1.6629
Tank	199771	43.2939	1.7258

B. Comparison

After getting the experimental results of our proposed schemes for different images, we have compared the results with some of the literatures we have reviewed.

Na-I Wu's method [8] also used a range table like Wu-Tsai's method [3] except that the range table has been modified. Here, the range table has been divided into two levels: Lower level (0 to 15) and Higher level (16 to 255). Basically Na-I Wu increased the message capacity by hiding more data in the lower level. For higher level he used Wu-Tsai's scheme. In Na-I Wu's method, secret data have been hidden in the smooth areas and edged areas by LSB substitution method and PVD method respectively.

Like Wu-Tsai's method, Na-I Wu's method also has the shortcoming that while the receiver extracts secret messages; the original range table must be present. The problem is removed by our proposed methods, as our proposed methods do not use any range table.

Table IV Comparison results between Na-I Wu's method and proposed Four Neighbor Scheme.

Cover Images	Capacity (in bits)	PSNR (in dB) in Na-I Wu's method	PSNR (in dB) inOur Method
Lena	392208	34.3962	41.1468
Baboon	435223	30.4130	36.5154
Peppers	393891	33.7496	41.0315
Tank	395415	33.7779	40.8102

Table V Comparison results between Na-I Wu's method and proposed Diagonal Neighbor Scheme.

Cover Images	Capacity (in bits)	PSNR (in dB) in Na-I Wu's method	PSNR (in dB) inOur Method
Lena	395680	33.1248	40.6504
Baboon	443165	29.5465	35.0725
Peppers	397382	32.4844	40.1429
Tank	405760	32.5494	39.4487

Table VI Comparison results between Na-I Wu's method and proposed Eight Neighbor Scheme.

Cover Images	Capacity (in bits)	PSNR (in dB) in Na-I Wu's method	PSNR (in dB) inOur Method
Lena	196968	36.4887	43.9590
Baboon	220575	32.4793	38.8280
Peppers	197868	35.1155	43.5124
Tank	199771	35.7348	43.2939

Wu-Tsai's method fabricates a range table with n contiguous ranges. The n contiguous ranges, say R_i, where i = 1,2,…,n. The range table ranges from 0 to 255. While hiding secret information, the amount of data to hide is depended on the range table. The smaller R_i stands for smooth area and hiding less secret data. And larger R_i stands for edged area and hiding more secret data. While extracting secret information, the range table is needed. So, the receiver has to have the range table or the sender has to send the range table to the receiver, which is a risky task.

In our method, we did not use any range table to hide. Secret information can be extracted from the stego image directly; even the original image is not needed. Another point is that, Wu-Tsai's method modifies more pixels (almost all of the pixels in an image) of an image in hiding information for the same capacity while our proposed schemes modify a smaller number of pixels (less than half of the total number of pixels in an image).

C. Discussions

All three proposed methods implemented the adaptive method of steganography, that is, the amount of secret bits to hide is variable. Thus the quality of stego images is progressively improved.

The first method is Four Neighbors Method, which can hide a large number of secret bits in digital images and can maintain a very good PSNR. The second method, Diagonal Neighbors Method, can hide more bits than Four Neighbors Method. However this is accomplished by sacrificing the PSNR. The PSNR values are slightly less than in Four Neighbors Method, but are still good. In Diagonal Neighbors Method, the maximum capacity for the same image is much more than in the Four Neighbors Method. The reason is that, pixels are more related to its four neighbors, difference is not so larger and thus they are closed. The difference between the pixel and its diagonal neighbors is slightly larger and so it can hide more bits. The third method that we proposed for Steganography is Eight Neighbors Method, where a large number of pixels remain unchanged, but hiding a considerable amount of secret data.

Our secret information can first be encrypted and then embedded. In this way we provide an extra layer of security to our systems.

Combining LSB method [2] with our proposed scheme may lead to increased data hiding capacity. This is because our proposed schemes leave almost half of the total number of pixels in an image unused (i.e. these pixels are used neither for embedding nor for calculation), These Unused pixels can be used for embedding. LSB substitution may be used as the method for embedding bits of secret information into the unused pixels.

Introducing flags for detection of any kind of manipulation such as change of a bit due to transmission errors or intruders or image processing operations such as cropping and rotation, can help detect whether the stego image contains the exact information or not. This flag may be a bit in the unused pixels or can be included in the image header.

IV. CONCLUSIONS

We have proposed three novel and efficient steganographic methods to embed secret information into images without producing perceptible distortions. The methods do not require referencing the original image when extracting the embedded data from a stego-image. The method utilizes the neighborhood information to estimate the amount of data that can be embedded into an input pixel of cover image. The pixels in edge areas may embed more data than those in non-edge areas.

Our experimental results have shown that the proposed method provides an efficient way for embedding large amount of data into cover images without making noticeable distortions. Moreover, the proposed methods use less than half of the total number of pixels in an image where methods discussed in [3] and [8] use almost all the pixels of an image for the same amount of hiding capacity.

REFERENCES

[1] D. Sellars, *An Introduction to Steganography*, http://www.totse.com/en/privacy/encryption/163947.html, Accessed on 13th January 2009.

[2] C. K. Chan, L. M. Cheng, *Hiding data in images by simple LSB substitution*, Pattern Recognition Letters, vol. 37, pp. 469-474, 2004.

[3] D. C. Wu, W. H. Tsai, *A Steganographic method for images using pixel value differencing*, Pattern Recognition Letters, vol. 24, pp. 1613-1626, 2003.

[4] N. Provos, P. Honeyman, *Hide & Seek-An introduction to Steganography*, http://niels.xtdnet.nl/papers/practical.pdf. Accessed on 17th March 2009.

[5] J.M. Buchanan, *Creating a robust form of Steganography*, http://etd.wfu.edu/theses/available/etd05092004110852/unrestricted/Buchanan_STEM04.pdf, Accessed on 11th December 2008.

[6] T. Morkel, J.H.P. Eloff, M.S. Olivier, *An overview of image steganography*, http://mo.co.za/open/stegoverview.pdf, Accessed on 13th January 2009.

[7] C. C. Chang, H. W. Tseng, *A Stegangraphic Method for Digital Images Using Side Match*, Pattern Recognition Letters, vol. 25, pp. 1431-1437, 2004.

[8] Na-I Wu, *A Study on Data Hiding for Gray-Level and Binary Images*, http://ethesys.lib.cyut.edu.tw/ETD-db/ETD-search/getfile?URN=etd-0707104-144705&filename=etd-0707104-144705.pdf. Accessed on 25th March 2009.

Proceedings of 2009 12th International Conference on Computer and Information Technology (ICCIT 2009)
21-23 December, 2009, Dhaka, Bangladesh

Extracting Unique Patterns from Human Actions

H. M. Imran Hassan, Md.Fahad Hasan, Md. Fazle Elahi Khan, Md. Shahjahan
EEE, Khulna University of Engineering & Technology, Khulna, Bangladesh
KUET, Khulna, Bangladesh
iimran_eee@yahoo.com, razib_03092@yahoo.com, mdjahan8@yahoo.com

Abstract

Human walks, runs, dances and left behind interesting information on their actions. This paper presents how chaotic dynamics help to interpret and classify human actions. The trajectories of two legs are extracted during a motion such as walk. These trajectories of foot points are collected from an artificial human video arrangement. Each dimension of trajectory represents a time series. The phase space for each time series is reconstructed using appropriate time delay and dimension. The plot exhibited a characteristic trajectory representing the regularity of the time series. Analysis of time series obtained in human with three different motions revealed that the trajectory behaves in such a way that the time series is governed with a deterministic rule. Unique patterns are observed for a particular motion. This can be revealed from the phase space and self organizing map (SOM) network. The motions (walk, run, and jump) can be categorized in terms of different shape of phase space and output of the SOM network. The results are validated with correlation dimension. These representations are very useful in classifying the human motions.

Keywords: Human action, classification, chaos, phase space, correlation dimension.

I. INTRODUCTION

Human action (HA) interpretation is an important and challenging topic in computer vision, with many important applications including video surveillance, automated cinematography, human computer interaction and entertainment. A challenging issue in this field originates from the diversity of information which describes an action. For any kind of human action main movable body part is human head, two hands, and two legs. So it is seen that for movement of various pattern and different speed human action differ. Hence we take the trajectory of five body points as the experimental data. The aim of this paper is to represent the interpretation of the dynamical system generating the human actions directly from the experimental data.

The type of the mapping function determines whether it is a linear [1], non-linear [2] or chaotic dynamical system [3]. The complexities of the different actions are calculated using correlation dimension (CD). The phenomenon that appears random but is regulated under a deterministic rule is called deterministic chaos. Chaos has been found in real biological organs and artificial systems such as brain neuron activity [4] and artificial neural network [5]. Chaotic variation is even found in rain fall and other weather parameters. The analysis of chaotic dynamics recently has attracted much attention to study the regularity and complexity of a nonlinear system. This is an art rather than engineering. The regularity in HA during any moving condition is found in real and artificial human motion. This paper presents the results of convergence of unique patterns of human motions.

II. Experimental studies

This section describes the three types of motion of artificial human, and the collection of the data during walking, running, and dancing. A total of fifteen time series from three motion and five body points are collected from the artificial video arrangement.

The state of the system evolves in accordance with a deterministic evolution function and the path traced by the systems states as they evolve over time is referred to as a trajectory or orbit. In our present work five body joints corresponding to two hands, two feet, and head are taken as the reference joints. To make the presentation scale and translation invariant, trajectories of the first five joints are normalized with respect to the belly point. Hence, for any given action we use five trajectories to represent the action as shown in Fig. 1. These trajectories are used to extract invariant features of the constructed phase space that represent the underlying dynamical system. The time series belongs to five body points exhibit chaotic phenomena. These time series are collected from the artificial arrangement. The normalized trajectory of a point a is represented as

$$X^a = [x_1^a, x_2^a, x_3^a \cdots\cdots\cdots\cdots x_t^a] \quad (1)$$

where $X \epsilon R^k$, with k = 3 for the motion capture data. Finally, we have $k \times N_{RP}$ scalar time series for each action, where N_{RP} is the number of the reference points. Since we have five reference points, N_{RP} is five.

978-1-4244-6283-4/09/$26.00 ©2009 IEEE

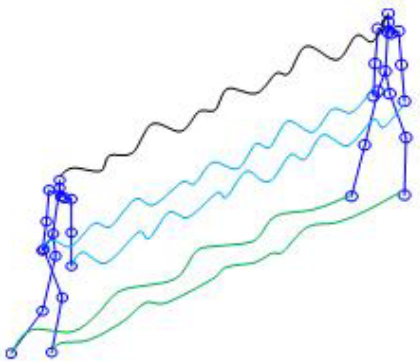

Fig. 1. A sample set of 3-dimensional trajectories of walking action. Trajectories from five landmarks (two hands, two feet and the head) on human body are used as input to our method from the motion capture data set. The time series are collected from the arrangement.

III. Analysis

To interpret human action experimental analysis is carried on 3D motion capture dataset collected from FutureLight [6]. It contains actions of run, walk, sit, dance, and jump. Walk, run, jump are taken in this study. For every action, trajectories of five body points are extracted. Trajectory of each body point is a three dimensional data. Each dimension is considered as single time series. Hence five body points for three motions - walk, run and jump. A total of 15 time series are collected. For the convenience of the experiment, we only took the time series for the foot for walk, run and jump.

A time series data will show chaotic behavior if it has two property, first is nonlinearity and second regularity. The human motion has these properties. When applying chaos theory to a given a problem, the goal often is to extract information required to identify and classify strange attractors of the dynamical system from the experimental data. Chaos is one of the ways to study nonlinear phenomena. Chaos theory provides a way of determining the description of a dynamical system from a time series data. The procedure can be broken down into a few relatively easy steps. These are: find a suitable embedding of the data, verify the existence of deterministic structure, compute dynamical, topological and metric invariants of the periodic orbits, and finally we use the invariants for the identification purposes. In this paper we use reconstructed phase space and SOM network to extract the unique patterns. Appropriate embedding delay and dimension are necessary to compute to reconstruct phase space as described below.

IV. Reconstruction of phase space

Embedding is a mapping from one dimensional space to a d-dimensional space. For estimating embedding delay and dimension, we use the mutual information and the Cao's Method [7]. The embedding delay and dimension are found to be 5 and 7 respectively.

Finally phase spaces for different motions are reconstructed using these computed time delay and embedding dimension. The required delay and dimension estimation processes are described above. After estimating the values of τ and m we can construct d-dimensional phase space from a time series as.

$$X = \begin{pmatrix} x_0^a & x_\tau^a & \cdot & \cdot & x_{(m-1)\tau}^a \\ x_1^a & x_{1+\tau}^a & \cdot & \cdot & x_{1+(m-1)\tau}^a \\ x_2^a & x_{2+\tau}^a & \cdot & \cdot & x_{2+(m-1)\tau}^a \\ \cdot & \cdot & \cdot & \cdot & \cdot \end{pmatrix} \quad (2)$$

Each component of the d-dimensional vector is separated by an interval τ and each row of the above matrix is now a point in the d- dimensional constructed phase space. The same process is done for all time series.

The Fig. 2 exhibits the reconstructed phase space for the walk motion. The top and bottom figures are for right foot and left foot respectively. They are functionally similar. There is a nice positive correlation between them. They are unique in their shape.

Similarly, Fig. 3 exhibits the phase spaces for the Run motion. Interestingly they are similar but different from that of the walk motion. Similarly, Fig. 4 exhibits the phase spaces for the Jump motion. In this case the figures are also similar in shape but there is a difference from other two motions-walk and run. Because the jump motion starts to jump using the entire body and have a zigzag shape. The interesting finding is that they are different for three motions – walk, run and jump, although they have marginal correlation among them. These phase spaces are 3D representations. The shape for walk motion for left and right foots are slightly different, since the time series are taken from opposite side.

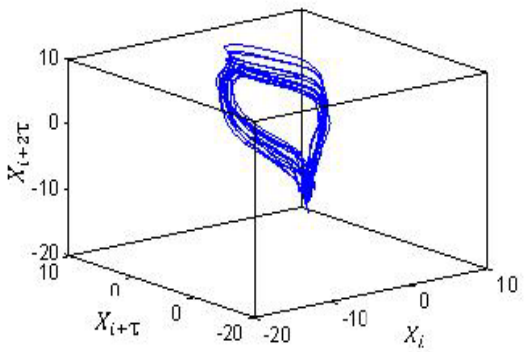

(a)

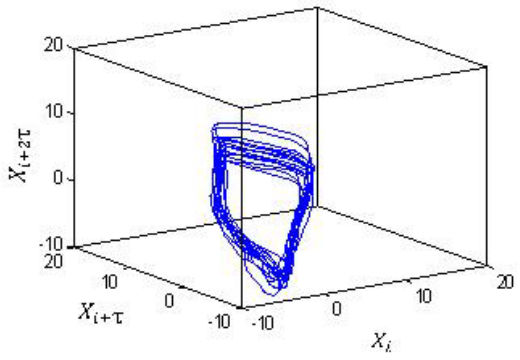

(b)

Fig. 2. Reconstructed phase spaces for right (a) and left (b) foots in *Walk* motion.

Similarly, the 3D view of run motion for right and left foots are slightly different since each time series is taken from their corresponding foot side.

These shapes are very useful to classify the human motions. Since underlying classes or categories are not known in advance, we have to apply any unsupervised algorithm. We apply the time series to a self organizing map (SOM) neural network to classify them and to understand a clear distinction between the human motions.

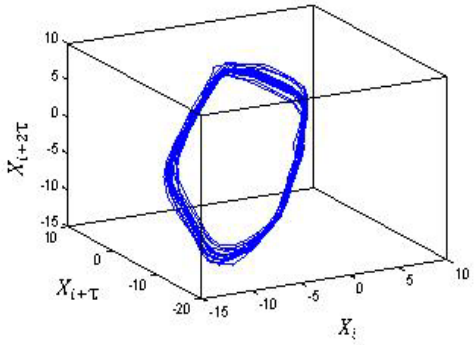

(a)

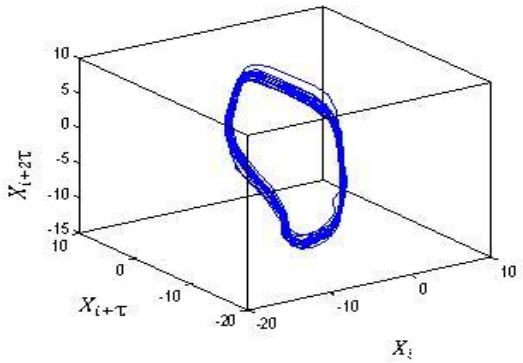

(b)

Fig. 3: Reconstructed phase spaces for right foot (a) and left foot (b) for *Run* motion.

The MATLAB tool for SOM was used to classify them. The output is nothing but a two dimensional view of the input space. The output of the SOM network represents the unique pattern for a particular motion. We have only shown the convergence of weight vectors in a SOM network

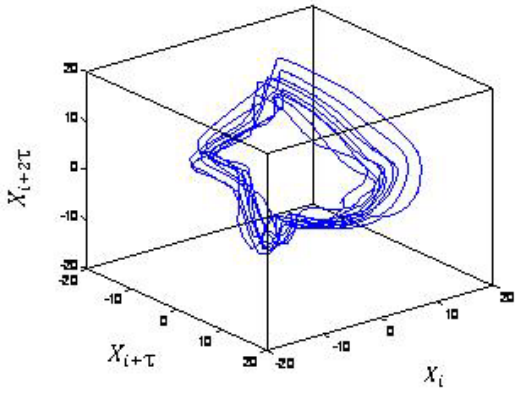

(a)

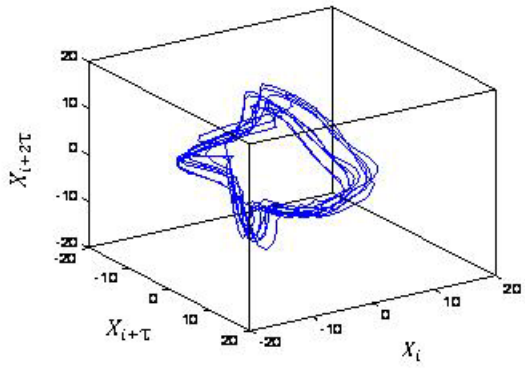

(b)

Fig. 4: Reconstructed phase spaces for right foot (a) and left foot (b) for *Jump* motion.

The convergence of weight vectors results the unique pattern for a particular motion. This reveals that the walk, run and jump have the different underlying dynamics which help to recognize the motion perfectly.

Figures 5, 6 & 7 represent the convergence of weight vectors for walk, run and jump respectively. It is clear from the Fig. 5 that the converged weight vectors are unique for both foots although there are some differences between left and right foots in walk motion.

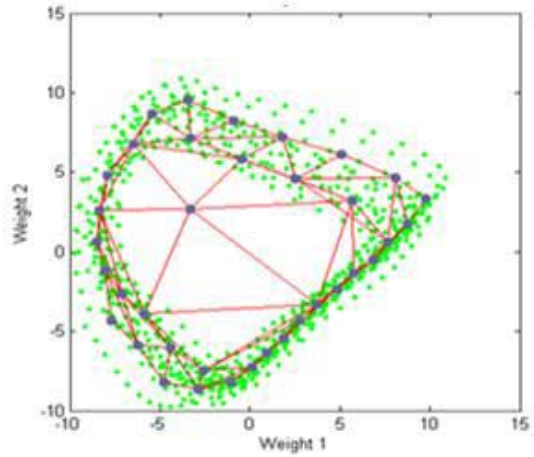

(a)

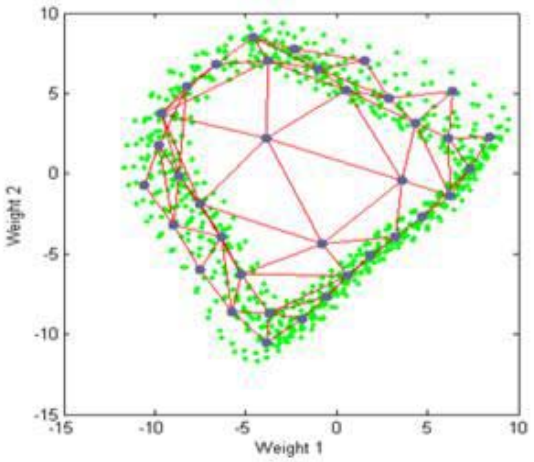

(b)

Fig. 5: Convergence of weight vectors of a SOM neural network for *Walk* motion. Top figure is for right foot(a) and bottom for left foot(b).

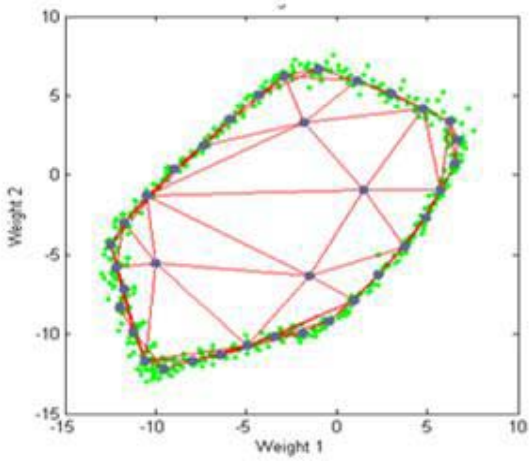

(a)

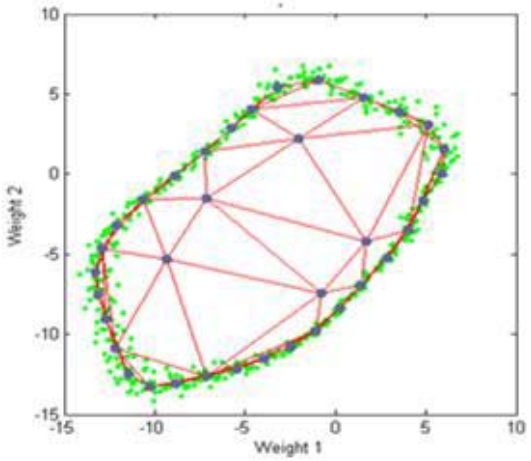

(b)

Fig. 6. Convergence of weight vectors of a SOM neural network for *Run* motion. Top figure is for right foot(a) and bottom for left foot(b).

Similarly, Fig. 6 represents the converged weight vectors of SOM network. Here we observe the same similarity between the left and right foots for run motion.
Figure 7 exhibits the converged weight vectors for jump motion. They are similar in their final shape. This indicates that the underlying dynamics of jump motion are unique for both foots for jump motion. In all cases we have used the MATLAB program to find the SOM weight vectors.

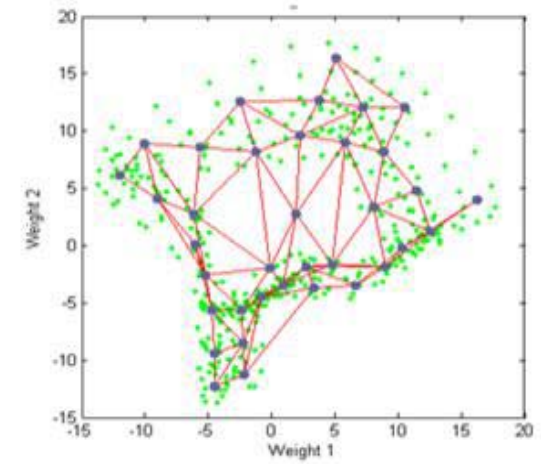

(a)

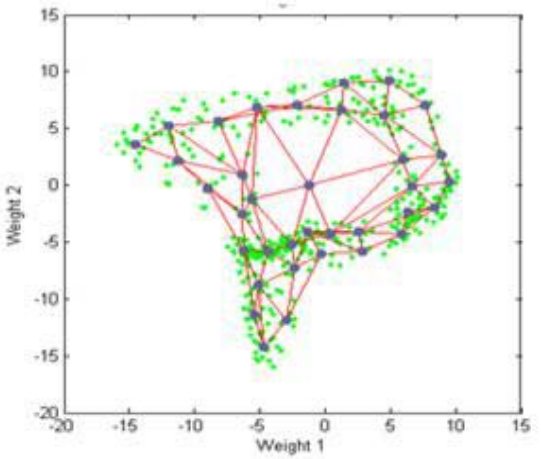

(b)

Fig. 7. Convergence of weight vectors of a SOM neural network for *Jump* motion. Top figure is for right foot (a) and bottom for left foot(b).

V. Correlation dimension

The correlation dimension (CD) [8] is a measure of the dimensionality of the space occupied by a set of random points, often referred to as a type of fractal dimension. This is computed with correlation integral. For the simplicity sake we ignore the computation of correlation integral. For clear understanding we just give a brief overview of it.

The correlation integral is a metric invariant, which characterizes the metric structure of the attractor by quantifying the density of points in the phase space. It achieves this through a normalized count of pair of points lying within a radius *r*. Formally correlation integral C(r) is defined as

$$C(r) = 2/N(N-1)\sum_{i=1}^{N}\sum_{j=i+1}^{N}\Theta(r-\left\|x_i - x_j\right\|) \quad (2)$$

where Θ is the Heaviside function. Note that, x_i in this case refers to a point in the phase space i.e. it corresponds to *i*th row vector of X. In our experiments, we computed C(r) for a fixed value of r and used it as a feature vector.

Correlation dimension measures the change in the density of phase space with respect to the neighborhood radius r. In this study, the correlation integral C(r) of one-dimensional time series is calculated according to sphere counting method proposed by Grassberger and Procaccia [20]. In order to estimate the correlation dimension m, we estimate the slope of the linear relation between log(C(r)) and log(r). The first step is to choose the scaling region; we do this by looking at plots of the log(C(r)) against log(r). The scaling region is chosen to be the values of r for which the linear relationship between log(C(r)) and log(r) appears to hold. We estimate the slope of the linear relationship using the least squares estimator. Here for walking, running and jumping actions, correlation dimension were computed. We just report the CD computed from correlation integral in Table 1.

We can see that the CDs are 2.8 and 2.7 for right and left foot for walk motion. They are approximately the same. This reveals that they have uniqueness in their time histories. Similarly, we can conclude that other two motions run and jump have unique CDs with different values such as 2.3 & 2.5 for run and 3.5 & 3.4 for jump. One of the interesting points here is that the values of CD for jump motion is higher than other two motions. This is reasonable because the jump motion is more complex than the other two. Another interesting but not surprising point is that the CDs for run motion are 2.3 and 2.5 as shown in the table which are a bit smaller than walk. This is reasonable since the run motion is more regular and uniform than walk motion.

We have observed another interesting point which was not explored yet. Off course this is an empirical observation – not hard and fast rule for other chaotic system. That is whether or not there is a vector relation among the motions. We must be careful to make an argument on the issue. Should we find out jump from the walk and run motions?

The approximation observation was that the vector sum of the values of CDs of walk and run gives the values of CD for jump. We have found for both right and left foot the jump is approximately 3.62, where as originally they are 3.5 and 3.4. We can understand that the angle between the values of CDs of walk and run is not 90^o but less than 90^o. From the trigonometric relation we found out the values of angle between walk and run was 86^o and 81.5^o respectively for right and left foot. However this is an approximation – not a theory. From the above discussion it is evident that the jump is the function of walk and run. This is reasonable since jump has relation with them. The higher CD indicates higher

complexity of the underlying time series. Therefore, jump motion has the most complex dynamics.

Table I: Correlation dimension

Motion	*Right foot*	*Left foot*
Walk	2.8	2.7
Run	2.3	2.5
Jump	3.5	3.4

VI. Conclusions

Extraction of human actions is of great importance in computer vision and criminal identification. This paper presents the results of the uniqueness of human action using phase space, self organizing map and correlation dimension. Firstly, phase spaces of three motions such as walk, run and jump are computed with proper delay and dimension. Secondly, we apply those time series to a SOM network in order to view the representation of the category clearly. Thirdly, CDs for those motions are computed to see the complexity of the underlying motions. We have found that the underlying patterns of human motions such as walk, run and jump are unique in their shape and dynamics. Finally, we observe an interesting point that they are related with approximately a trigonometric relation where jump motion is extracted from other two motions. However, this is an empirical study.

One can easily speculate that walk and run motions are inherently merged in jump motion. We have studied the dynamics of foot only for walk, run and jump. It will be interesting to study the cases for head, hand as well.

REFERENCES

[1] Bissacco, A. Chiuso, A. Yi Ma Soatto, S. "Recognition of Human Gaits", Proceedings of IEEE Conference on Computer Vision and Pattern Recognition, vol. 2, pp. 52-57, 2001.

[2] L. Ralaivola and F. d'Alché-Buc, "Dynamical Modeling with Kernels for Nonlinear Time Series Prediction", Neural Information Processing System, MIT press, 2004.

[3] B. North et. al., "Learning and classification of complex dynamics," IEEE trans. Pattern Analysis and Machine Intelligence, 22(9), 2000.

[4] Babloyantz, A., Salazar, J. M., & Nicolis, C. (1985). "Evidence of chaotic dynamics of brain activity during sleep cycle". Physics Letters A, 111, 152–156.

[5] Aihara, K., Takabe, T., & Toyota, M. "Chaotic neural networks." Physics Letters A, 144(6), 333–340, 1990.

[6] FutureLight, R&D division of Santa MonicaStudios. *http://www.urgpurg.com/temp/noroff/mocap/Cstudio/Motions/MoCap/BVH/SantaMonicaStudios/About.txt*

[7] Eli Shechtman , Michal Irani, "Space-Time Behavior Based Correlation," Proceedings of the 2005 IEEE Computer Society, Conference on Computer Vision and Pattern Recognition , vol. 1, pp. 405-412, June 2005.

[8] M. Perc, "The Dynamics of Human Gait," European Journal of Physics, vol. 26, pp. 525-534, 2005.

Proceedings of 2009 12th International Conference on Computer and Information Technology (ICCIT 2009)
21-23 December, 2009, Dhaka, Bangladesh

A Currency Recognition System Using Negatively Correlated Neural Network Ensemble

Kalyan kumar debnath, Jayanta kumar ahdikary, Md. Shahjahan
Department of EEE, Khulna University of Engineering & technology, Khulna-9203, Bangladesh
kalyan_2004@yahoo.com, jayanta109@gmail.com, mdjahan8@yahoo.com

Abstract

This paper represents a currency recognition system using ensemble neural network (ENN). The individual neural networks (NN) in an ENN are trained via negative correlation learning. The object of using negative correlation learning (NCL) is to expertise the individuals in an ensemble on different parts or portion of input patterns. The available currencies in the market consist of new, old and noisy ones. It is often difficult for machine to recognize these currencies; therefore we propose a system that uses ENN to identify them. We performed our experiment for seven different types of TAKA (Bangladeshi currency) they are 2, 5, 10, 20, 50, 100 and 500 TAKA. The image of different types note is converted in gray scale and compressed in our desired range. Each pixel of the compressed image is given as an input to the network. This system is able to recognize highly noisy or old image of TAKA. Ensemble network is very useful for the classification of different types of currency. It reduces the chances of misclassification than a single network and ensemble network with independent training. In experimental results we have shown this. We also find good result for similar pattern available in market.

Keywords: Neural network ensemble, Diversity, Negative correlation learning, Image processing, Currency recognition.

I. INTRODUCTION

Artificial neural networks (ANN) have been applied in various application domains for solving real world problems such as, feature extraction from complex data sets, direct and parallel implementation of matching and search algorithm, forecasting and prediction in a rapidly changing environment, recognition and image processing applications etc. The currency recognition is one of the important application domains of ANN.

A reliable currency recognition system is important for the automation in different sectors for a country such as vending machine, rail way ticket counter, banking system, shopping mall, currency exchange service etc. The paper currency recognition is important for a number of reasons. a) They become old frequently than coins; b) The possibility of joining broken currency is higher than that of coin currency; c) Coin currency is limited to smaller range.

Various methodologies have been proposed for the recognition of paper currency in different countries. Most of these use a single multilayer feed-forward NN for the recognition [1]-[5]. The features are first extracted from the image then it applied to network for training. These uses edge detection technique for feature extraction [1] and it reduces the network size. For new notes feature extraction from edge detection is easy. But for the noisy notes it is very difficult. Furthermore the currency recognition system should be highly reliable. If a network makes a false classification it will be impractical. So a single network is not reliable enough. Therefore we proposed ENN [6] to solve this problem. The negative correlation learning was to produce different individual NN in the ensemble, so that entire ensemble learns the input pattern completely.

In our proposed system we use the ENN for currency recognition. NCL was used for the training of the network [7]. The use of NCL is to produce the diversity among the individual networks in ensemble. The final decision of the network is taken from voting among the individual NN. In voting each network gives a vote for a certain class and it is done by the winning neuron of that network. Our experimental result is very much good for the recognition of noisy images and found almost negligible misclassification for different testing input.

This paper organized as follows. Section 2 describes the NCL algorithm of ENN. Image preprocessing is described in sect. 3. The network structure is in sect. 4. Results & discussion are in sect. 5 & finally we conclude the paper in sect. 6.

II. NEGATIVE CORRELATION LEARNING

ENN [6] is a learning paradigm where a collection of finite number of neural networks is trained for the same task. The input vectors are applied simultaneously in all the ensembles. The negative correlation learning is to produce the diversity among the individual networks using a penalty term. The NCL can be found elsewhere [7] and a brief of it is given below.

Assume a training set **S** of size **N**.

$S = \{(x(1), d(1), x(2), d(2)), \ldots\ldots\ldots (x(N), d(N))\}$

Where x is the input vector and d is the desired output. Consider estimating d by forming an ensemble whose output $F(n)$ is the average in the component NN output $F_i(n)$

$$F(n) = \frac{1}{M}\sum_{i=1}^{M} F_i(n) \quad (1)$$

Where M and n refer to the number of NN in ensemble and training pattern, respectively. The error function E_i of the network i in NCL is given by the following (2).

$$E_i = \frac{1}{N}\sum_{n=1}^{N} E_i(n) \quad (2)$$

$$= \frac{1}{N}\sum_{n=1}^{N}\frac{1}{2}(F_i(n) - d(n))^2 + \frac{1}{N}\sum_{n=1}^{N}\lambda p_i(n) \quad (3)$$

Where $E_i(n)$ is the value of the error function of the network i for the n^{th} training pattern. The first term of (3) is the empirical risk function of the network i. In the second term, p_i is a correlation penalty function is given by (4).

$$P_{i(n)} = \big(F_i(n) - F(n)\big)\sum_{j\neq i}^{M}\big(F_j(n) - F(n)\big) \quad (4)$$

The partial derivative of $E_i(n)$ with respective to the output network i on the nth training pattern is

$$\frac{\partial E_i(n)}{\partial F_i(n)} = F_i(n) - d(n) + \lambda\frac{\partial P_i(n)}{\partial F_i(n)}$$
$$= F_i(n) - d(n) + \lambda\sum_{j\neq i}\big(F_j(n) - F(n)\big)$$
$$= F_j(n) - d(n) - \lambda(F_i(n) - F(n))$$
$$= (1-\lambda)(F_i(n) - d(n)) + \lambda(F(n) - d(n)) \quad (5)$$

The NCL is a simple extension to the standard BP (Back-propagation) algorithm [8]. In fact, the only modification that is needed is to calculate an extra term of the form $\lambda(F_i(n) - F(n))$ for the i^{th} network. During the training process, the entire ensemble interacts with each other through their penalty terms in the error functions. Each network i minimizes not only the difference between $F_i(n)$ and $d(n)$, but also the difference between $F(n)$ & $d(n)$. That is, negative correlation learning considers errors what all other networks have learned while training a network.

III. IMAGE PREPROCESSING

To give an image to the network we first need to preprocess it. In our proposed system we use the gray scale image. The RGB image Fig.1 (a), found from the scanner is converted in to gray scale (Black-White) image Fig.1 (b), [9]. To reduce the network size we compress the image gray scale image into 125×80 dimension Fig.1 (c). Each pixel of the compressed image is applied as an input to the network. The pixel values were kept in the range of 0-1.

(a) RGB image from scanner

(b) Gray scale image

(c) Compressed image of 125×80

Fig. 1. Image processing steps

IV. NETWORK STRUCTURE

We perform our experiment for seven types of TAKA (2, 5, 10, 20, 50, 100, and 500). To increase the accuracy of the NN ensemble we applied one new & another older or noisy TAKA for each different type. So our total input pattern is 28 as we want to train both side. We consider an ENN where every network is a 3 layer feed forward network. Each network contains 7 neurons in output layer, 70 hidden units & 10,000 (125*80=10000, according to compressed image) input units. Each neuron in output layer is responsible for a definite class of TAKA. Such as 1st neuron for 2 TAKA, 2nd neuron for 5 TAKA and so on. We performed our experiment for single network and an ensemble with 3, 4 & 5 individual networks. In input and hidden layer we have applied a bias unit. The output of bias unit is +1. The weights of hidden & output layer are first assigned randomly then the network is trained according to NCL [7]. We choose the value of λ (Strength of penalty term) and η (Learning rate) are 0.75 & 0.15 respectively. Sigmoid function was used as an activation function both in hidden & output layer.

The images are applied one after another. After the application of first image we apply the second image & update the weight of both hidden and output layer. But we need to conscious about the output for that particular image. Such as, when we apply the image of TAKA 2 the desired output of each network should be 1 0 0 0 0 0 0 (i.e. output of 1st neuron will be 1 and other will 0). For all the images of TAKA 2 the desired output should be same. Similarly for all images of TAKA 5 the desired output should be 0 1 0 0 0 0 0.

Input vector

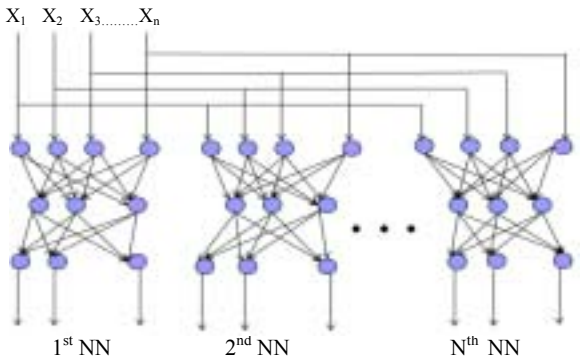

Fig. 2. Ensemble neural network

V. RESULTS & DISCUSSION

For training ENN we use NCL. The error is reduced to a desired range. The iteration vs. error curves are shown in Fig. 3, Fig. 4, Fig. 5 & Fig. 6 for single, three, four and five individual networks in the ensemble respectively.

After training we tested the network for unseen and noisy pattern. For applying an image to the network it must be preprocessed as we described in section 3. Voting method was used for making the final decision of ENN. In our work we tested network performance for noisy TAKA of different noise intensity. Here we add Gaussian noise with difference variances. A certain variance's noise is applied for 100 different times and tested. We have done this because the currencies are seen with different degree of noises. Both the single network and ENN were tested for the same image. In Table I, II, III & IV we have shown the classification results of single network and an ensemble with 3, 4 & 5 individual networks.

In Table I, we see that single network is able to recognize lower noisy note. But for higher noisy intensity the misclassification is higher. So the single network is not sufficient enough. However, here we reduced the misclassification by ENN. Consider the result of TAKA 20 of variance 0.05 (table IV), the network recognizes 87 times & misclassify 1 times. For 12 times the network cannot make any decision. But the single network (table I) recognized 66 times and misclassify 34 times for the same input.

In our experimental results we see that the recognition persentage of all class is not equal for higher noisy input patterns. This is because recognition percentage depends on the number of different features, size of currency, degree of noise added. In our experiment we compress all the currency images to a fixed dimension of 125×80 what ever their actual sizes are. To make the

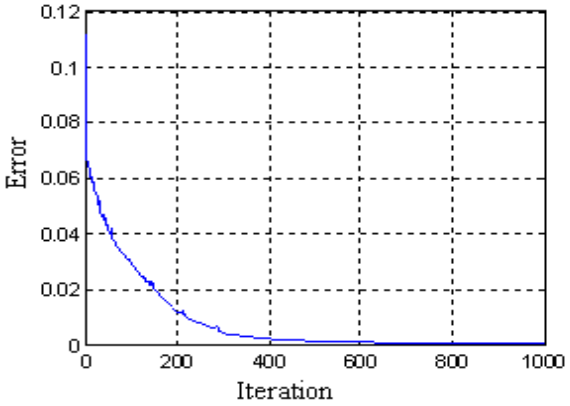

Fig. 3. Error curve for single Network

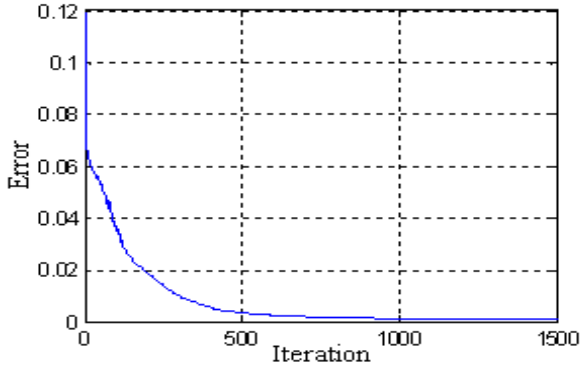

Fig. 4. Error curve of 3 NNs

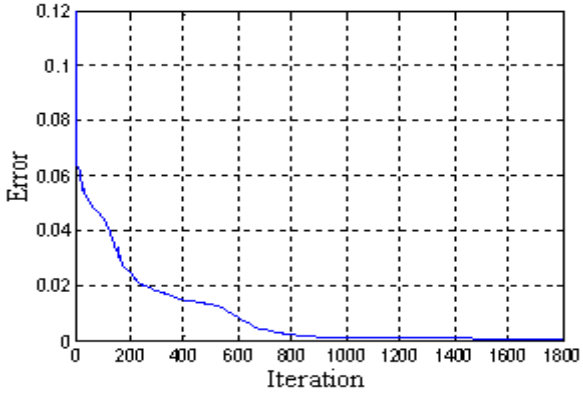

Fig. 5. Error curve of 4 NNs

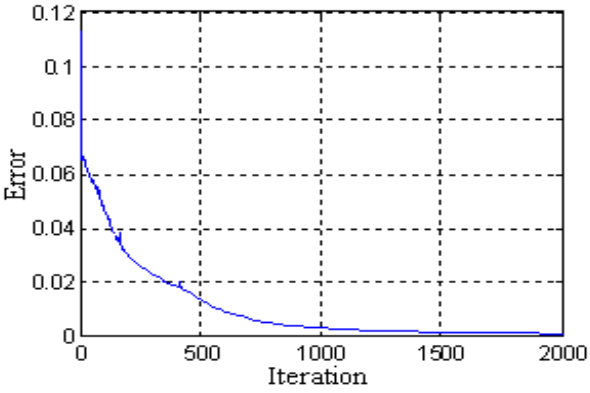

Fig. 6. Error curve of 5 NNs

network size constant one needs do this. Sometimes small image such as, 2 TAKA shows better performance than the other class. This is because the unique features in two TAKA are smaller in numbers than others. Moreover as we used NCL for training so sometimes an input pattern gets more expertized than other patterns. However, as a whole entire ensemble with NCL learns all patterns completely and differently. As a result the over all recognition percentage of NCL is much better than individual learning of ensemble. In table V we shown the classification result of unseen pattern which are collected from the market and banks (in Fig. 7.).

Table I Performance of single NN on matlab simulation for 100 runs.

Different variance's Noisy input		2 TAKA	5 TAKA	10 TAKA	20 TAKA	50 TAKA	100 TAKA	500 TAKA
0.00	% Recognized	100%	100%	100%	100%	100%	100%	100%
	misclassification	0	0	0	0	0	0	0
0.01	% Recognized	100%	98%	97%	99%	97%	90%	90%
	misclassification	0	2	3	1	7	10	10
0.02	% Recognized	97%	89%	75%	79%	75%	84%	74%
	misclassification	3	11	25	21	25	16	26
0.03	% Recognized	93%	82%	73%	75%	68%	71%	68%
	misclassification	7	18	27	25	32	29	32
0.04	% Recognized	87%	77%	63%	69%	58%	68%	62%
	misclassification	13	23	37	31	42	32	38
0.05	% Recognized	82%	74%	63%	66%	59%	58%	62%
	misclassification	18	26	37	34	41	42	38

Table II Performance of 3 NN in the ensemble on matlab simulation 100 runs.

Different variance's Noisy input		2 TAKA	5 TAKA	10 TAKA	20 TAKA	50 TAKA	100 TAKA	500 TAKA
0.00	% Recognized	100%	100%	100%	100%	100%	100%	100%
	misclassification	0	0	0	0	0	0	0
0.01	% Recognized	100%	100%	100%	99%	99%	99%	99%
	misclassification	0	0	0	1	1	0	0
0.02	% Recognized	83%	97%	89%	93%	95%	90%	94%
	misclassification	1	0	3	1	0	1	1
0.03	% Recognized	70%	84%	82%	88%	82%	77%	88%
	misclassification	5	2	5	1	4	3	5
0.04	% Recognized	64%	76%	67%	86%	73%	68%	79%
	misclassification	6	6	7	4	7	8	4
0.05	% Recognized	51%	61%	61%	79%	59%	54%	65%
	misclassification	9	8	11	1	4	10	6

Table III Performance of 4 NN in the ensemble on matlab simulation 100 runs.

Different variance's Noisy input		2 TAKA	5 TAKA	10 TAKA	20 TAKA	50 TAKA	100 TAKA	500 TAKA
0.00	% Recognized	100%	100%	100%	100%	100%	100%	100%
	misclassification	0	0	0	0	0	0	0
0.01	% Recognized	100%	99%	98%	100%	99%	99%	98%
	misclassification	0	0	0	0	0	0	0
0.02	% Recognized	98%	88%	85%	96%	78%	86%	75%
	misclassification	0	0	0	0	0	0	0
0.03	% Recognized	90%	70%	74%	81%	66%	74%	53%
	misclassification	1	0	0	0	0	0	0
0.04	% Recognized	74%	70%	61%	74%	57%	62%	42%
	misclassification	1	0	0	0	0	0	1
0.05	% Recognized	56%	41%	45%	74%	39%	55%	33%
	misclassification	1	2	0	1	0	0	2

Table IV Performance of 5 NN in the ensemble on matlab simulation 100 runs.

Different variance's Noisy input		2 TAKA	5 TAKA	10 TAKA	20 TAKA	50 TAKA	100 TAKA	500 TAKA
0.00	% Recognized	100%	100%	100%	100%	100%	100%	100%
	misclassification	0	0	0	0	0	0	0
0.01	% Recognized	100%	100%	100%	100%	100%	99%	100%
	misclassification	0	0	0	0	0	0	0
0.02	% Recognized	100%	95%	100%	100%	98%	86%	100%
	misclassification	0	0	0	0	0	0	0
0.03	% Recognized	96%	87%	92%	98%	84%	74%	95%
	misclassification	0	1	0	0	1	0	0
0.04	% Recognized	95%	74%	84%	88%	80%	62%	80%
	misclassification	0	1	0	0	2	0	0
0.05	% Recognized	90%	52%	75%	87%	72%	55%	69%
	misclassification	0	2	0	1	1	0	0

Here we also see that misclassification is decreased as the number of network in ensemble is increased. We also tested these image for 5 network ensemble with individual learning. For both NCL & individual learning of ENN the misclassification is zero, but ENN with NCL recognized much.

Were performed all the experiments in a core 2 duo 2.4 GHz computer with 1GB of RAM. Programs were written in matlab R2008a version. The recognition time of different network is shown in Table VI.

Fig. 7. Unknown patterns (collected from market)
1-7 & 8-14 shows front and back side of TAKA (2, 5, 10, 20, 50, 100 & 500) respectively.

neural network ensemble for currency recognition. The recognition rate is better than single network.

Table V Classification result for unseen pattern shown in Fig. (7)

Ensemble	Recognized	Not Recognized	Misclassification
single network	6	0	8
3 networks	9	1	4
5 networks	14	0	0
5 networks (λ=0)	9	5	0

Table VI Recognition time

Number of network in ENN	Recognition time (second)
Single network	0.068853
3 network	0.121139
4 network	0.147763
5 network	0.175004

VI. CONCLUSION

In this paper we have represented a currency recognition system using negatively correlated ensemble neural network. Though we have performed our experiment for Bangladeshi currency but it is equally applicable in any paper currency recognition.

In our study we have proposed the ENN for currency recognition. The Ensemble network has better performance for recognition than single network. For training we used the negative correlation learning. In negative correlation the entire networks are negatively correlated through the strength of penalty term. The entire ensembles interact with each other and each network has specialized for a particular portion of input vector. So when we apply a noisy pattern the network will be able to recognize as a whole. We have found a nice recognition capability of negatively correlated

REFERENCES

[1] D. A. K. S. Gunaratna, N. D. Kodikara and H. L. Premaratne, "ANN Based Currency Recognition System using Compressed Gray Scale and Application for Sri Lankan Currency Notes", *Proceedings of world academy of science, engineering and technology,* vol. 35, Nov. 2008, ISSN 2070-3740, pp. 235-240.

[2] E. Zhang, B. Jiang, J. Duan and Z. Bian, "Research on paper currency recognition by neural networks" in Proc. *2nd International Conf. Machine Learning and Cybernetics*, Xi'an, 2003, pp2193-2196.

[3] S. Omatu, T. Fujinaka, T. Kosaka, H. Yanagimoto, and M. Yoshioka. "Italian lira classification by lvq". In Proc. *International Joint Conference on Neural Networks, IJCNN*, pp 2947-2951, 2001,

[4] F. Takeda and T. Nishikage, "Multiple kinds of paper currency recognition using neural Network and application for euro currency". In Proc. *IEEE International Joint Conference on Neural Networks*, 2000, pp 143-147.

[5] M. Gori, A. Frosini and P. Priami. "A neural network-based model for paper currency recognition and verification", *IEEE Trans. Neural Networks*, Nov.1996, pp1482-1490.

[6] L.K Hansel and P. Salamon, "Neural networks ensemble", IEEE Trans. Pattern Anal. Mach. Intell., vol.12, no.10, 1990, pp.993-1001.

[7] Yong Liu and Xin Yao "Ensemble Learning via Negative Correlation" Neural Networks Vol. 12, pp 1399-1404, 1999.

[8] Simon Haykin "*Neural Network- a Comprehensive Foundation*", second edition, 1995.

[9] Rafael C. Gonzalez, Richard E. Woods, Steven L. Eddins "*Digital image processing using Matlab*" . Printed in 2008.

Proceedings of 2009 12th International Conference on Computer and Information Technology (ICCIT 2009)
21-23 December, 2009, Dhaka, Bangladesh

A Reduced Complexity Message Passing Algorithm with Improved Performance for LDPC Decoding

Vikram Arkalgud Chandrasetty and Syed Mahfuzul Aziz
School of Electrical & Information Engineering, University of South Australia,
Mawson Lakes, SA 5095, Australia
vikramac@ieee.org, mahfuz.aziz@unisa.edu.au

Abstract

In this paper, a simplified message passing algorithm for decoding Low-Density Parity-Check (LDPC) codes is proposed with a view to reduce the implementation complexity. The algorithm is based on simple hard-decision decoding techniques while utilizing the advantages of soft channel information for improvement in decoder performance. The algorithm has been validated through simulation using LDPC code compliant with Wireless Local Area Network (WLAN –IEEE 802.11n) standard. The results show that the proposed algorithm can achieve significant improvement in bit error rate (BER) performance and average decoding iterations compared to fully hard-decision based decoding algorithms.

Keywords: Digital communication, Error correction coding, Low-Density Parity-Check, Iterative decoding.

I. INTRODUCTION

The Low-Density Parity-Check (LDPC) codes were first proposed by Gallager in 1962 [1]. They were not popular for a few decades after its introduction due to high implementation complexity. However, it gained its popularity after it was formally re-introduced by MacKay and Neal in 1997 [2]. It has been shown that LDPC codes, when optimally designed, have the capability to perform very close to Shannon Limit [3]. LDPC codes have several advantages over turbo codes, including reduced implementation complexity, better bit error rate (BER) performance at low signal to noise ratio (SNR) and the inherent code structure that supports high degree of parallelism [4]. Hence LDPC codes have become increasingly popular and have been adopted in latest generation high data rate applications such as WLAN, WiMax and Digital Video Broadcasting - Second Generation (DVB-S2) [5].

II. OVERVIEW OF LDPC DECODING

LDPC codes belong to a class of block codes [6]. As their name suggests, its parity-check matrix (H) consists of very small number of non-zero elements. The sparseness of H determines the decoding complexity and the minimum distance of the code. Apart from the requirement that the LDPC matrix be sparse, there is no other difference between the LDPC code and any other block code [7]. The LDPC matrix is described by various parameters. The code rate is defined by the number of rows to columns ratio of the H matrix. The number of non-zero entries in each of the rows and columns of H matrix is collectively known as *degree distribution*. An H matrix is said to be *regular* if the degree distribution of rows and columns are uniform, otherwise it is *Irregular*. The H matrix can be represented as a graph called *Tanner graph*. A cycle in the graph is a sequence of connected nodes, which start and end at the same node. The *girth* or the smallest cycle in the parity-check graph, significantly contributes to the performance of the iterative decoding algorithms [8, 9]. A regular (3, 6) parity-check matrix with 10-bit code length is shown in Fig. 1 (a) and the corresponding Tanner graph representation of the parity-check matrix is shown in Fig. 1 (b).

$$H = \begin{bmatrix} 1 & 0 & 0 & 0 & 1 & 1 & 1 & 0 & 1 & 1 \\ 0 & 1 & 1 & 0 & 0 & 1 & 0 & 1 & 1 & 1 \\ 1 & 0 & 1 & 1 & 1 & 0 & 0 & 0 & 1 & 1 \\ 0 & 1 & 1 & 1 & 1 & 0 & 1 & 1 & 0 & 0 \\ 1 & 1 & 0 & 1 & 0 & 1 & 1 & 1 & 0 & 0 \end{bmatrix}$$

(a) An LDPC matrix

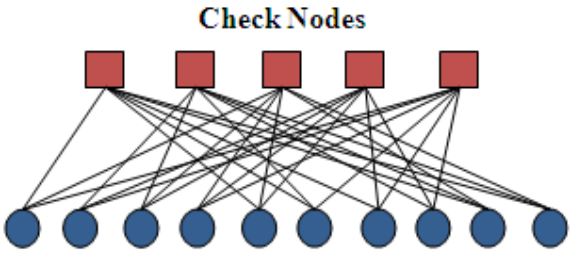

(b) Tanner graph representation of LDPC matrix

Fig. 1. A ½ rate (3, 6) 10-bit LDPC code

The decoding of LDPC code involves passing of messages between the nodes along the edges in the Tanner graph. This class of decoding algorithms is often called as *message passing algorithm*. Each of the nodes in the Tanner graph works in isolation with information available along the connected edges only. These decoding

978-1-4244-6283-4/09/$26.00 ©2009 IEEE

algorithms require passing of the messages between the nodes for a fixed number of times or till the result is achieved. Hence such algorithms are also known as *iterative algorithms* [9]. LDPC decoding algorithms generally operates by making either *hard-decision* or s*oft- decision* on the messages received from the noisy channel. In the former case, a binary hard-decision is made on the data received from the channel and then passed to the decoder, e.g. Bit-Flip Algorithm (BFA). But in case of soft-decision based algorithms, the input data to the decoder is the channel probabilities represented in logarithmic ratio which is also known as *log-likelihood ratio* (LLR). The messages passed between the nodes in the decoder are also soft messages, e.g. Belief Propagation based algorithms uses soft LLR input for decoding. It is known that the decoder using soft-decision methods perform better compared to that of the hard-decision, due to its ability to correct errors based on the bit probabilities [7].

The Sum-Product Algorithm (SPA) which is based on soft-decision decoding achieves best BER performance but with high complexity. Many modifications have been proposed to simplify the algorithm operations, but the implementation complexity of these algorithms is still high. Although the check node operation of SPA is simplified in the min-sum algorithm, it requires higher quantized messages to be passed between the nodes for decoding [10]. In [11], a simplified sum-product algorithm is proposed with a modification in check node operation. However, the implementation of the algorithm is still complex. In contrast, Bit-Flip algorithm which is based on hard-decision decoding has the least complexity but suffers from poor performance. A number of modifications have been proposed to improve the performance, but all these algorithms require complex operations that can achieve very little improvement in performance [12], [13]. In [14], an improved weighted bit-flip (WBF) algorithm is proposed. However, WBF algorithms require complex variable node operations and are still based on hard-decision decoding technique.

In this paper, a low complexity LDPC decoding is proposed to achieve a tradeoff between implementation complexity compared to fully soft-decision based algorithms (SPA) and decoding performance (such as BER and iterations) compared to fully hard-decision based algorithms (BFA). The algorithm is based on a simple hard-decision message passing technique to reduce the complexity. However, it uses the soft inputs and performs a distinct variable node operation to improve the decoding performance. With a slight increase in complexity of variable node operation, the proposed algorithm not only improves the BER performance, but also reduces the average iterations required for decoding.

The rest of the paper is organized as follows. In section III, a brief overview of LDPC decoding algorithms are presented. Section IV discusses about the proposed algorithm and its node operations. Section V provides performance simulation results of the proposed algorithm, followed by conclusion in Section VI.

III. LDPC DECODING ALGORITHMS

In this section, a highly complex Sum-Product algorithm that can achieve very good performance compared to a low complexity Bit-Flip algorithm that suffers from poor performance is presented.

A. Sum-Product Algorithm

The Sum-Product algorithm for LDPC decoding is a soft-decision message-passing algorithm that requires LLR (intrinsic message) for variable node operations to make decoding decisions. To begin with the decoding process, the LLRs are passed over to the variable nodes. The variable nodes (V) perform the 'sum' operations on the input LLRs, as in (1) and the computed messages (extrinsic) are passed along the connected edges to the check nodes (C) [10].

SPA Variable node operation:

$$V_i = LLR_n + \sum_{j \neq i} C_j \tag{1}$$

where, n = 1,2,….number of variable nodes
i, j = 1,2,….degree of variable node

The check nodes (C) perform the parity check operation and also computes the messages [10], that are to be passed to the respective variable nodes (V), as in (2). This process is repeated till the maximum iterations is reached or the parity check is satisfied.

SPA Check node operation:

$$C_k = 2 \tanh^{-1}\left(\prod_{k \neq l} \tanh \frac{V_l}{2} \right) \tag{2}$$

where, l, k = 1,2,….degree of check node

It can be noted that the SPA has non-linear function in the check node operation and also requires high precision extrinsic messages to be passed between the nodes. This represents high decoding complexity. However, the SPA can achieve very good decoding performance [10].

B. Bit-Flip Algorithm

The Bit-Flip algorithm is based on hard-decision message-passing technique. A binary hard-decision is done on the received channel data and then passed to the decoder. The messages passed between the check node and variable nodes are also single-bit hard-decision values. The variable node (V) sends the bit information to the connected check nodes (C) over the edges. The

check node performs a parity check operation on the bits received from variable node (Eq. 3) [12]. It sends back the message to the respective variable nodes with a suggestion of the expected bit value for the parity check to be satisfied.

BFA Check node operation:

$$C_k = V_1 \oplus V_2 \oplus ..... \oplus V_l \qquad \forall l \neq k \tag{3}$$

where, l, k = 1,2,….degree of check node

The variable node (V) receives a set of response or the suggested bit values from the check nodes (C). Based on the majority of the suggested bit values, the variable node flips the current bit (Eq. 4) [12] or retains the original value. This operation is repeated until the parity check is satisfied or maximum number of iterations is reached

BFA Variable node operation:

$$V_n = \begin{cases} 0 & If, majority(C_i) = 0 \\ 1 & If, majority(C_i) = 1 \\ V_n & Otherwise, \end{cases} \tag{4}$$

where, n = 1,2,….number of variable nodes
i = 1,2,….degree of variable node

Clearly the BFA has simple check node and variable node operations, thus making it a very low complexity decoding algorithm compared to the SPA presented above. But this advantage comes with a poor decoding performance [12].

IV. SIMPLIFIED MESSAGE PASSING ALGORITHM

It is well known that SPA can achieve good decoding performance [10] but with high implementation complexity and BFA has low implementation complexity but poor performance [12]. The main aim of the proposed Simplified Message Passing Algorithm (SMPA) is to achieve a tradeoff between the decoding performance and implementation complexity of the above two algorithms. The check node and variable node operations of the proposed SMPA are presented next.

A. Check Node Operation

The complexity of a message passing algorithm significantly depends on the quantization length of extrinsic messages and the check node operation. These aspects are particularly critical in case of hardware implementation of large LDPC codes. In order to reduce the complexity of SMPA, the check node consists of a simple parity check operation (Eq. 5) only, similar to BFA. However, the performance improvement of SMPA over BFA is achieved from a distinct variable node (V) operation.

SMPA Check node operation:

$$C_k = V_1 \oplus V_2 \oplus ..... \oplus V_l \qquad \forall l \neq k \tag{5}$$

where, l, k = 1,2,….degree of check node

B. Variable Node Operation

A fully hard-decision based decoding algorithm suffers from poor performance because of the hard-decision intrinsic and extrinsic messages used in the decoding process. In SMPA, the performance improvement is achieved by using soft LLR input for decoding, like any other soft-decision based algorithms. The variable node (V) performs 'sum' operation similar to SPA, but the difference is that SMPA requires original LLR value only at the beginning of the decoding cycle, as in (6). The updated new LLR value is used in subsequent iterations, as in (9). In the analysis of hard-decision based channels presented in [15] the variable node operates directly on the hard-decision bit received from the check nodes. In contrast, the proposed SMPA maps the bit suggestion from the check nodes (C) to an optimized integer constant called 'Weight' (±W), which is determined from simulations to achieve the best possible BER performance. It is either added to or subtracted from the current LLR value. For example, at a variable node if binary '0' is received from the check node, it is mapped to $+W$ and if its binary '1' it is mapped to $-W$, as in (7) and (8) respectively. After this operation, a hard-decision is performed on the updated LLR value and it is sent across to the respective check nodes for parity check, as in (10). The process is repeated until the parity check is satisfied or the maximum iteration is reached.

SMPA variable node operation:

Initial (at iteration 0): $V_n = LLR$ (6)

Subsequent iterations:

$$X_i = +W, \quad If \quad C_i = 0 \tag{7}$$

$$X_i = -W, \quad If \quad C_i = 1 \tag{8}$$

$$V_n = V_n + \sum X_i \tag{9}$$

$$V_i = sign(V_n - X_i) \tag{10}$$

['+' → '0' and '-'→'1']

where, n = 1,2,….number of variable nodes
i = 1,2,….degree of variable node
W = optimized integer constant obtained from

simulations

Note that in SMPA, the variable node performs addition operations and uses mapping logic, and check node performs simple XOR operation. Hence it can be implemented using simple hardware blocks, such as adders and Look-Up-Tables (LUT).

A comparison of check node and variable node structures for the SMPA, SPA and BFA is shown in Fig. 2.

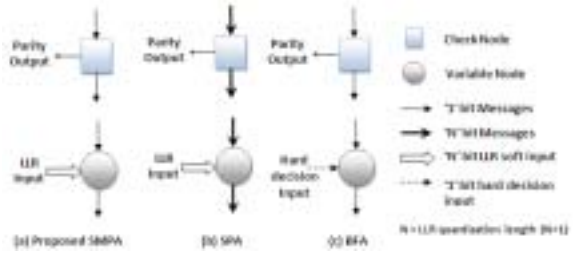

Fig. 2. Comparison of decoding node structures for SMPA, SPA and BFA

V. PERFORMANCE ANALYSIS

To evaluate the performance of the proposed algorithm, simulations were carried out for two different code lengths, 1000-bit and 648-bit. The latter is compliant with WLAN (IEEE 802.11n) standard [16]. A bit-true simulation model has been developed using the C programming language in MatLab environment. The LDPC codes were generated using Progressive Edge Growth (PEG) based algorithm [17] and the simulations were carried out assuming that the codewords were Binary Phase Shift Keying (BPSK) modulated and passed over an Additive White Gaussian Noise (AWGN) channel [18]. Simulations were done with different LLR precisions to study the effect on the decoding performance. The LDPC code parameters and specifications used in the performance simulations are as follows:

- *Code lengths* – 648-bit (WLAN) and 1000-bit
- ½ *rate* and (3, 6) *regular code*
- *LLR quantization for SMPA:* 3-bit, 4-bit (*Weight, W = 1*) and 5-bit (*Weight, W = 2*)
- *Maximum decoding iterations* – 10

The BER and frame error rate (FER) performance simulation results for the proposed SMPA are shown in Fig. 3 and Fig. 4 respectively. A comparison of BER and FER performances is provided in Table I. From the simulations, it can be observed that the error correction capability (BER and number of iterations) has improved in SMPA compared to BFA. This has been the consequence of using soft LLR inputs and a unique variable node operation. The BER improvement of using 3-bit LLR in SMPA compared to BFA is at least 0.8 dB at 10^{-5}. It is clear that the performance improves gradually as the LLR precision increases in the variable node operation. At a BER of 10^{-5}, a significant improvement of over 1.8 dB is achieved compared to BFA by using 4-bit LLR. However, little improvement in performance is achieved (0.1~0.2 dB at 10^{-5} BER) by using 5-bit LLRs over 4-bit. A similar behavior is observed in case of FER performance. The convergence rate of the algorithms is assessed by analyzing the average decoding iterations for each of the algorithms, as shown in Fig. 5. The average iteration results clearly indicate that the proposed SMPA (4-bit and 5-bit) has higher convergence rate and requires fewer iterations compared to BFA. The results also indicate that the average decoding iteration reduces as the LLR precision increases. Although the iteration count for SPA is much lower than SMPA, each of the iteration in SPA is likely to take significantly more time due to the highly complex operations at the variable and check nodes (see Eq. 1 and Eq. 2). In contrast, the proposed SMPA has much simpler node operations (see Eq. 5-10).

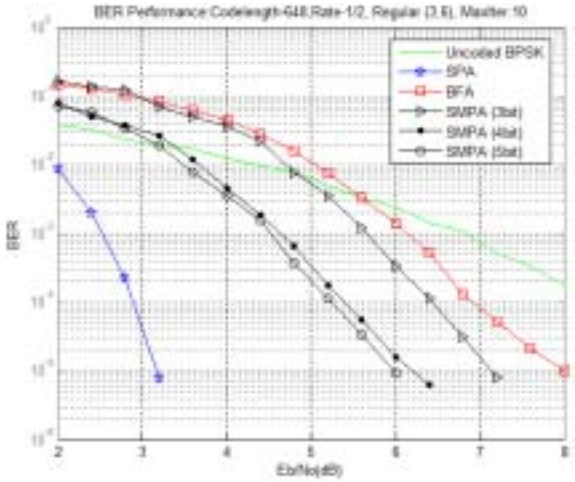

(a) 648-bit LDPC code

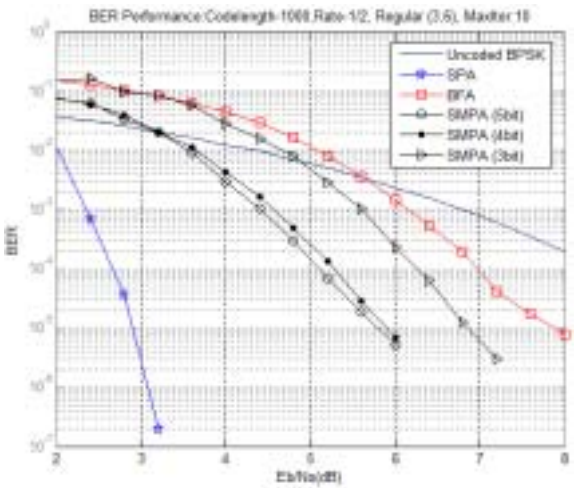

(b) 1000-bit LDPC code

Fig. 3. BER performances for the SMPA, SPA and BFA

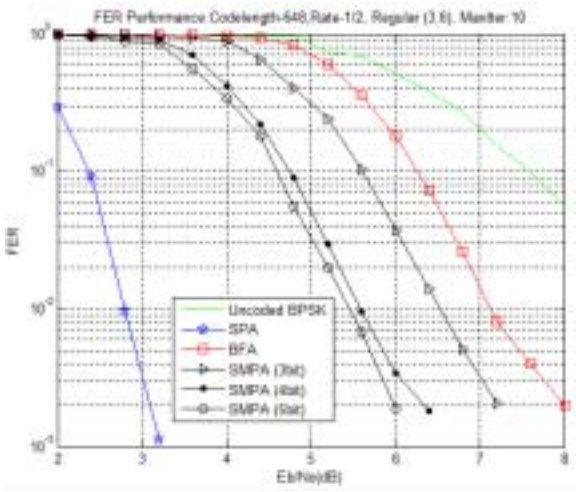

(a) 648-bit LDPC code

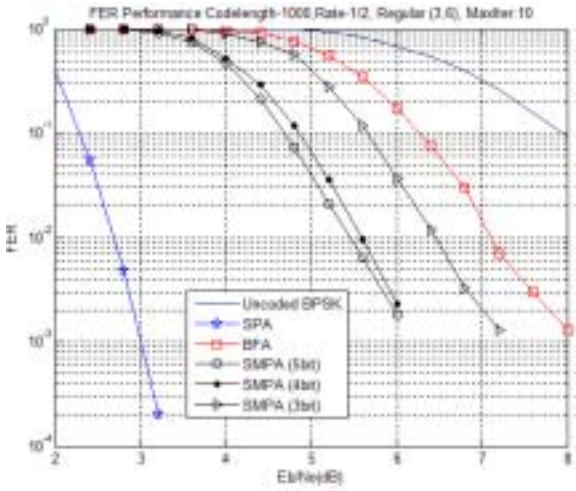

(b) 1000-bit LDPC code

Fig. 4. FER performances for the SMPA, SPA and BFA

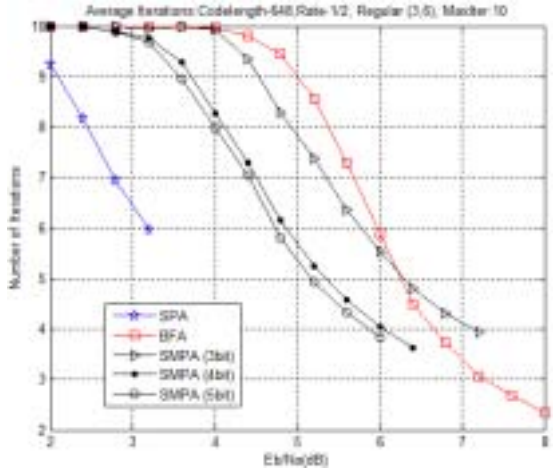

(a) 648-bit LDPC code

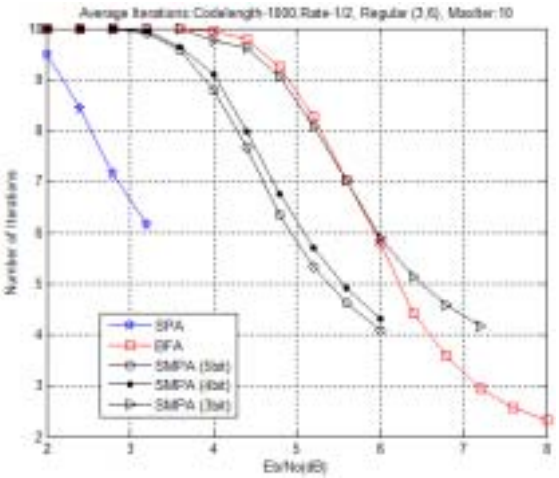

(b) 1000-bit LDPC code

Fig. 5. Average decoding iterations for the SMPA, SPA and BFA

Table I. Comparison of BER and FER performance of the algorithms

Algorithms		**648-bit (WLAN)**		**1000-bit**	
		BER	**FER**	**BER**	**FER**
SPA		10^{-5} 3.2 dB	10^{-2} 2.8 dB	10^{-5} 2.9 dB	10^{-2} 2.6 dB
BFA		10^{-5} 8 dB	10^{-2} 7.1 dB	10^{-5} 7.9 dB	10^{-2} 7.1 dB
SMPA	3-bit	10^{-5} 7.2 dB	10^{-2} 6.5 dB	10^{-5} 6.8 dB	10^{-2} 6.5 dB
	4-bit	10^{-5} 6.2 dB	10^{-2} 5.6 dB	10^{-5} 5.9 dB	10^{-2} 5.6 dB
	5-bit	10^{-5} 6.0 dB	10^{-2} 5.5 dB	10^{-5} 5.8 dB	10^{-2} 5.5 dB

VI. CONCLUSION

In this paper a simplified message passing algorithm has been proposed. The algorithm incorporates a novel approach to improve the overall performance of the decoder compared to fully hard-decision based decoding solutions. It uses soft-inputs for variable node operation along with hard-decision messages between the nodes. It has been shown that both the BER and FER performances are improved by combining higher LLR precisions with single-bit hard-decision message passing between the decoding nodes. It is also shown that the average decoding iterations are reduced compared to the fully hard-decision based decoding algorithms. The proposed algorithm significantly reduces computational complexity at the decoding nodes and will lead to much reduced hardware implementation overheads.

VII. ACKNOWLEDGEMENT

The authors wish to acknowledge Dr Mark Ho of the School of Electrical and Information Engineering, University of South Australia, for his advice on carrying out the performance simulations.

REFERENCES

[1] R. Gallager, *Low-density parity-check codes.* IRE Transactions on Information Theory, vol. 8, no.1, pp. 21-28, 1962.

[2] D.J.C. MacKay and R.M. Neal, *Near Shannon limit performance of low density parity check codes.* Electronics Letters, vol. 33, no.6, pp. 457-458, 1997.

[3] D.J.C. MacKay, *Good error-correcting codes based on very sparse matrices.* IEEE Transactions on Information Theory, vol. 45, no.2, pp. 399-431, 1999.

[4] G.L.L. Nicolas Fau (2008) *LDPC (Low Density Parity Check) - A Better Coding Scheme for Wireless PHY Layers* Design and Reuse Industry Article.

[5] Tetsuo Nozawa (2005) *LDPC Adopted for Use in Comms, Broadcasting, HDDs*. Nikkei Electronics Asia.

[6] D. Costello Jr, et al. *A comparison between LDPC block and convolutional codes*. in *Proceedings of the Information Theory and Applications Workshop*. 2006. San Diego, USA.

[7] S.J. Johnson, *Introducing Low-Density Parity-Check Codes*. 2006, University of Newcastle, Australia.

[8] B. Leiner, *LDPC Codes–a brief Tutorial*, in *Stud. ID.: 53418L April*. 2005.

[9] J.C. Moreira, *Essentials of error-control coding*, ed. P.G. Farrell. 2006, West Sussex, England: John Wiley & Sons.

[10] A. Anastasopoulos. *A comparison between the sum-product and the min-sum iterative detection algorithms based on density evolution*. in *IEEE Global Telecommunications Conference*. 2001.

[11] S. Papaharalabos and P.T. Mathiopoulos, *Simplified sum-product algorithm for decoding LDPC codes with optimal performance.* Electronics Letters, vol. 45, no.2, pp. 116-117, 2009.

[12] N. Miladinovic and M.P.C. Fossorier, *Improved bit-flipping decoding of low-density parity-check codes.* IEEE Transactions on Information Theory, vol. 51, no.4, pp. 1594-1606, 2005.

[13] T.M.N. Ngatched, F. Takawira, and M. Bossert, *An improved decoding algorithm for finite-geometry LDPC codes.* IEEE Transactions on Communications, vol. 57, no.2, pp. 302-306, 2009.

[14] Q. Dajun, et al. *A Modification to Weighted Bit-Flipping Decoding Algorithm for LDPC Codes Based on Reliability Adjustment*. in *IEEE International Conference on Communications*. 2008.

[15] G. Lechner, T. Pedersen, and G. Kramer. *EXIT Chart Analysis of Binary Message-Passing Decoders*. in *IEEE International Symposium on Information Theory*. 2007.

[16] *IEEE 802.11n Wireless LAN Medium Access Control MAC and Physical Layer PHY specifications*. 2006, IEEE 802.11n-D1.0.

[17] X.-Y. Hu. *Software to Construct PEG LDPC code*. 2008 [cited 2009 May]; Available from: http://www.inference.phy.cam.ac.uk/mackay/PEG_ECC.html.

[18] J.G. Proakis, *Digital communications*. 5th ed. ed, ed. M. Salehi. 2008, New York: McGraw-Hill, pp. 10-102.

Proceedings of 2009 12th International Conference on Computer and Information Technology (ICCIT 2009)
21-23 December, 2009, Dhaka, Bangladesh

An Intelligent SMS-Based Remote Water Metering System

Nusrat Sharmin Islam and Md. Wasi-ur-Rahman
Department of Compuper Science & Engineering,
Bangladesh University of Engineering & Technology, Dhaka-1000, Bangladesh
nusrat@cse.buet.ac.bd, wrrobin@cse.buet.ac.bd

Abstract

The Integrated Prepaid Water Meter System is a technology for prepaid billing of water along with sufficient monitoring of the water meter readings automatically from a remote place without any human intervention. This system promises fast and accurate billing of water as well as prevents any misuse of it. In this paper, a technique having adequate security support, for prepaid billing of water using Short Message Service (SMS) has been illustrated. Existing Global System for Mobile communications (GSM) networks have been used for sending and receiving SMS. A prototype of the system has been designed and developed for system exploration and experiment.

Keywords: SMS, GSM, Microcontroller, Database, Central server.

I. INTRODUCTION

The conventional billing system for water is that an assigned person visits each house and reads the meter readings manually. Then the collected meter readings are used for bill calculation. This manual process can become very time consuming and tiresome. It can cause human error and can open an opportunity for corruption done by the human meter readers as well as illegal users. Sometimes users disconnect the water supply line from the water meter and collect water directly from the supply line. Due to the absence of automatic monitoring system with the existing water meter, the water supply authority is unable to detect the illegal users and this leads to wastage and illegal use of water to a great extent. Thus the billing system can become in-accurate and inefficient.

The recent advances in the field of information technology have made the exchange of information fast, secured and accurate. The digital revolution caused rapid drop of cost of digital devices such as computers and telecommunication devices. Communication networks like the internet, GSM networks etc. are available in almost all the countries of the world. In the work presented here, a technique has been developed for prepaid billing of water. In this system, water is supplied to a house only when its corresponding meter is recharged with some credit. A remote server of the water supply authority reads the meter readings automatically using the existing GSM networks [2] for cellular phones and as soon as the credit of the meter expires, water supply is halted. The central server can also halt water supply if any kind of security breach is detected. The meters send the meter readings like remaining credits, amount of water used, security breach information etc. by SMS [2] to a central server. The central server then stores the information in database for analysis and starting and halting of water supply. The system is also equipped with a tank overflow indicator.

The SMS based data collection can be done very quickly and efficiently. As there is no human intervention in the entire process, there is no chance of human error and corruption. Also, unwanted weather conditions like heavy snow, rain, storm, etc. will not hamper on collecting data as long as the GSM networks are stable. By applying complex encryption algorithms on the data SMS, data security can be ensured. Though, the development cost of the SMS based remote meter will be higher than conventional meter, the water supplier will revenue more in the successive months because it will eliminate the possibility of corruption done by the customers and employees and it can be a prolific solution to stop wastage and illegal use of water. Moreover, it can eliminate the bill preparation and paying overhead.

The rest of the paper is organized as follows. Section II mentions some previous related works. Section III describes total system architecture with both hardware and software specifications. Section IV shows the experimental results obtained. Section V concludes the paper.

II. RELATED WORK

One approach of AMR (Automatic Meter Reading) is that the meter reader walks by or drives by the meter and, using a handheld device, reads monthly usage of water. This approach requires human involvement and it is tiresome and time consuming. More advanced AMR products have been developed commercially. Some of them used internet for data transmission. The MainsTalk [3] and Archnet [4] use Power Line Carrier (PLC) [1] technology to remove extra wiring for internet connection with the meter. But in this approach, the data on the line are available within a short range (approximately 300 meters). If data needs to be sent at a more distant place, the information must be collected in a data collector unit located within 300 meters which should be connected with the internet or any phone network. In our work, we have used a mobile set which is connected with the meter using serial port. The information in the meter is sent to a central server by SMS. Thus our approach does not need any extra data collector unit, no extra external wiring is necessary and data can be transmitted to any place at any time where the GSM network is available.

978-1-4244-6283-4/09/$26.00 ©2009 IEEE

III. SYSTEM ARCHITECTURE

The main purpose of this integrated prepaid water meter system is to provide a prepaid mechanism along with sufficient monitoring. The system consists of the following units:

1. Prepaid Unit
2. Main Server Unit (the Central Server)
3. User Unit

The Prepaid Unit connects the water supply line of the water supply authority to the user supply line. It controls the supply of water to the user line and measures water usage. The Prepaid Unit keeps information about how much water to be supplied. Depending on that information, the Prepaid Unit may disconnect the user line and gives no more supply of water to the house. So, Prepaid Unit should be recharged. That is why it needs to communicate with the Main Server Unit to receive recharge updates. It also transmits security alert signals to the Main Server Unit. The Main Server Unit updates all the Prepaid Units and also stores necessary user information. Using the User Unit, anyone can recharge his Prepaid Unit with the help of the Main Server Unit. The overall system is shown in Fig. 1.

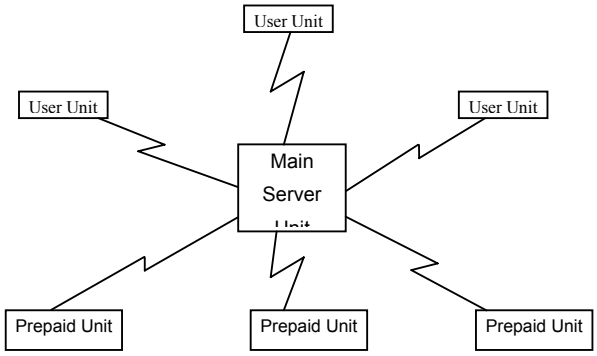

Fig. 1: A block diagram of the Prepaid Water Meter System

3.1 Prepaid unit

The Prepaid Unit is responsible for controlling water supply to the user and communicating with the Main Server Unit. It has a unique number (meter ID) assigned by the water supply authority. It consists of two parts:

(a) Control Unit

(b) Transceiver Unit

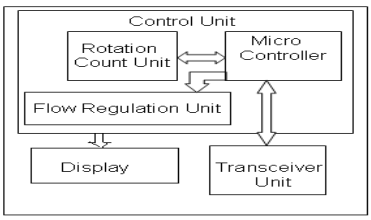

Fig. 2: A block diagram of the Prepaid Unit

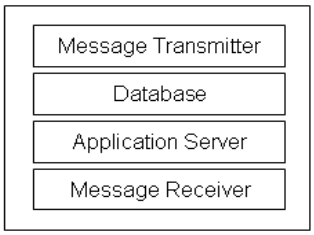

Fig. 3: A block diagram of the Main Server Unit

3.1.1 Control Unit

The control unit consists of a Rotation Count Unit, Flow Regulation Unit, Microcontroller Unit, a Display Unit, a Data Storage Unit, Real Time Clock (RTC), Relay Unit and a GSM modem as shown in Fig. 2. Each of the unit is described below.

3.1.1.1 Rotation Count Unit

The Rotation Count Unit consists of a turbine which measures the amount of water supplied to the house by converting water velocity to proportional electric signal.

3.1.1.2 Flow Regulation Unit

This unit stops passing water through the turbine when the user credit runs out, thus providing the prepaid paradigm. It starts water supply again as soon as the Prepaid Unit is recharged.

3.1.1.3 Tank Overflow Detector Unit

This unit stops passing water through the turbine when the user water tank fills up to a specific level, thus avoiding the overflow of the water tank. It starts water supply again as soon as the water in the tank goes below of that level. These two units control the water flow in the meter by using a sliding door.

3.1.1.4 Microcontroller Unit

An 8051 architecture microcontroller (AT89C55WD) is used as the Microcontroller Unit. The 8051 is an 8 bit RISC microcontroller originally developed by Intel in 1980. It is one of the most popular microcontrollers in the world for its high performance, rich instruction set (MCS-51®), and low cost. It has four 8 bit ports, total 32 I/O lines. Different peripherals of the meter are connected with its ports. It has 64KB of program memory and 256 byte of RAM.

3.1.1.5 Permanent Data Storage Unit

If power fail occurs, the content of the RAM must be stored in EEPROM so that when power is back, the meter can start from its last state. An I2C EEPROM (AT24C64) of 8KB size is used for this purpose. Also, different billing slabs containing rates for peak and off peak hour, meter ID etc. are stored here.

3.1.1.6 Real Time Clock (RTC)

An RTC is used to get the current date and time information.

3.1.2 Display Unit

A 16 x 2 character LCD (HD44780) is interfaced with the microcontroller port using 4 data wire mode. Different meter readings like remaining balance, amount of water used, date, time etc. are displayed here.

3.1.3 Transceiver Unit

The transceiver Unit works as a connector of Control Unit to the Main Server Unit. This unit is responsible for maintaining communication between the Control Unit and Central Server via SMS. Whenever it gets messages from the Main Server Unit to recharge the meter, it feeds the information to the Control Unit. Again, if in any case, the Main Server Unit needs to stop the water supply to a particular user, it can send message to the specific Transceiver Unit to do so. This unit consists of the following subunits:

3.1.3.1 GSM Modem

A GSM modem is interfaced with the microcontroller's serial port for sending and receiving SMS. Using FBUS protocol, the microcontroller sends different commands to the modem and receives data SMS frames from the GSM modem.

3.1.3.2 Temper Detection Unit

If any unauthorized person tries to disconnect the meter box from the supply line, the Temper Detection Unit will activate and the meter will not let any water to flow to the customer. The Temper Detection Unit detects such breach of security and informs the Transceiver Unit to send alert message to the Main Server Unit. An SMS is automatically sent to the Central Server reporting the temper. The Main Server Unit then sends a signal to the Flow Regulation Unit to stop water flow to that particular user.

3.2 Main Server unit

The Main Server Unit is basically a server with which all the User Units and Prepaid Units communicate. It receives the incoming messages from the User Units to recharge the Prepaid Units. It also stores necessary information of its users, the meter IDs, the usage history and other necessary data for further use. After necessary validation and verification, this unit communicates with the specific Prepaid Unit and transfers necessary data. For example, after receiving the message to recharge a user account, it updates the specific Prepaid Unit to be recharged by that particular amount. This unit also receives messages from the Prepaid Unit when its security is violated. The block diagram of the main server unit is shown in Fig. 3. The central server mainly consists of a GSM Hardware unit and several Server Software modules as shown in Fig. 4.

3.2.1 GSM Hardware Unit

It mainly consists of a *GSM Modem* which is used to send and receive SMS. To interface the modem with the server's serial (RS232) port, an *RS232 Module* is used in between them. This module converts the TTL logic levels compatible with the server's COM port.

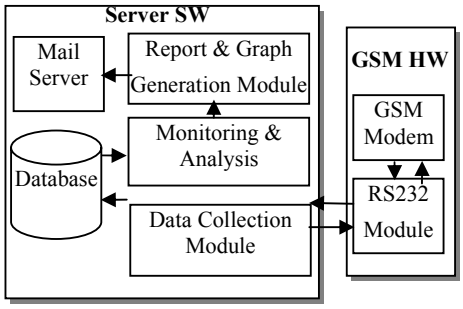

Fig. 4: Modules of the Central Server

3.2.2 Server Software

There are several techniques of building the Central Server [11]. Our proposed Central Server is built on Linux operating system with Java as the programming language. For database, ORACLE 10g is used. The *Data Collection Module* communicates with the GSM modem using FBUS protocol. When the server wants to collect information from a particular prepaid meter, it sends a *Request* SMS massage to the target meter and then waits for data from the GSM modem. After the prepaid meter receives the *Request* SMS massage, it makes a data frame consisting of the meter's information and sends it to the server by SMS. The server then gets the SMS data from the GSM modem and stores the information in the *Database.*

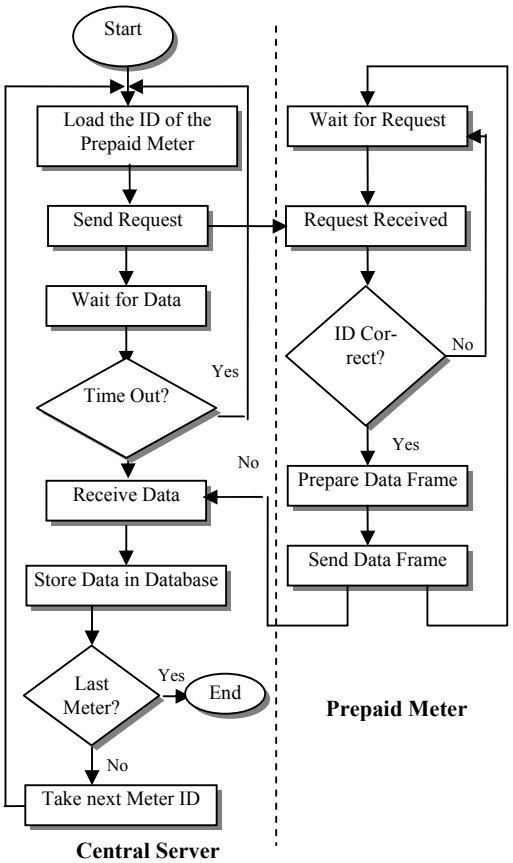

Fig. 5: Communication between the Central Server and the Prepaid Meter

Sometimes SMS messages are not delivered by the GSM network. We have developed the protocol such that if data SMS is not received after one minute, the server sends another request massage to the meter and waits for the data. In this way, the server makes total three attempts. If data SMS is not received in three attempts, the server shows network error massages. The overall communication flow chart of the *Data Collection Module* of the central server and the prepaid meter is shown in Fig. 5. The data collection can be done at any time or periodically such as hourly, daily, weekly or monthly basis. The *Monitoring & Analysis Module* gets data from the *Database* and calculates the overall water usage patterns of the meter. If any unexpected water usage pattern occurs, warning massages are generated and the server operator can send *Disconnection* SMS massage to the prepaid meter to disconnect the meter and thus stop the customer to consume further water. The *Report & Graph Generation Module* generates detailed report consisting of the current month bill, average water usage, unexpected behavior descriptions, water usage curve etc.

3.3 User unit

The water supplier will produce scratch-cards and distribute them to local shops. Customers will buy scratch-cards from

Fig. 6: Recharge Message Format

their nearby shop and then send a special SMS (Fig. 6) using their personal cellular phone to the Central Server consisting of the customer's meter ID and the scratch-card's secret pin number. When the Central Server receives the SMS, it checks the validity of the meter ID and the pin number from the database.

If the meter ID is valid and the pin number is also valid and still unused, then the server gets the customer meter's GSM modem call number from the database and sends an encrypted SMS to the customer's meter which contains the information of how much balance will be recharged in the meter. The meter receives the SMS, decodes it and recharges with the balance. Then it sends an acknowledgement SMS to the server indicating whether the balance is successfully recharged or not. After receiving the acknowledgement from the meter, the server then sends a report SMS to the customer's personal cellular phone mentioning the meter's current balance. The flow of this procedure is shown in Fig. 7.

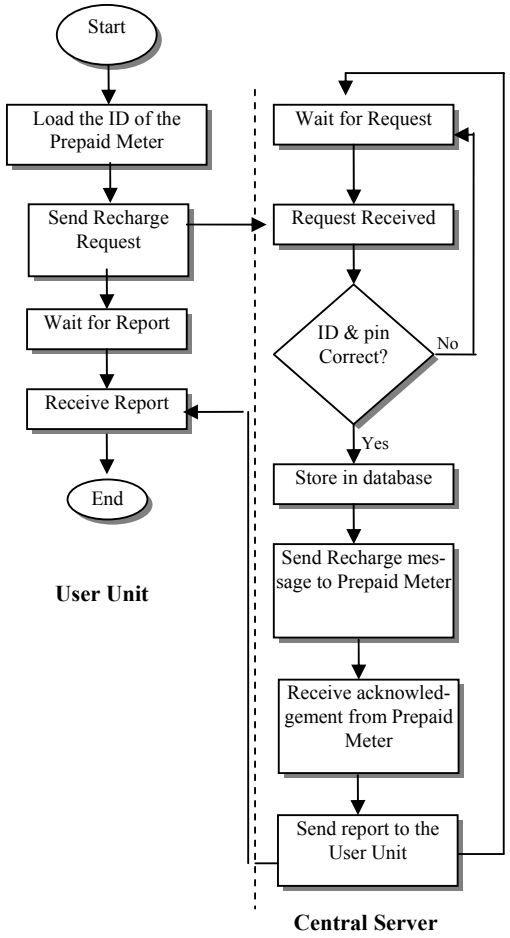

Fig. 7: Communication between the Central Server and the User unit

IV. EXPERIMENTS

An SMS based remote metering system prototype is developed and several experiments have been conducted. We developed two remote meters and one central server. The total time taken to get a data SMS from the remote meter to the central server is approximately 30 seconds. This time may vary a little bit depending upon the GSM network condition. In our experiment, for 95% cases, data SMS was received successfully by one attempt. For the remaining 5% cases, data SMS was received after second or third attempt. Fig. 8 shows a graph plot of consumed water in miliLitre (mL) unit of a consumer. The graph is generated by the central server based on the remotely received data.

Fig. 8: A Graph Plot Generated by the Central Server

V. CONCLUSION

In this paper, an SMS based integrated prepaid water meter system has been proposed. Different hardware and firmware unit of the prepaid meter is described. The central server's different modules and the communication protocol with the prepaid meters are also shown. Several experiments with two remote meters and one central server have been conducted. Our future work includes interfacing a General Packet Radio Service (GPRS) modem with the prepaid meter so that faster and continuous data can be received in the central server.

REFERENCES

[1] Archnet, "http://www.archnetco.com/", 2007.

[2] L. Cao, J. Tian and D. Zhang, "Networked Remote Meter Reading System based on Wireless Communication Technology", *proc. of* IEEE International Conference on Information Acquisition, China, August 2006.

[3] Embedtronics, "http://www.embedtronics.com", 2005.

[4] Energy Controls, "http://www.energycontrols.org", 2007.

[5] Gnokii, "http://www.gnokii.org/", 2006.

[6] Grameen Phone, "http://www.grameen-info.org", 2007.

[7] Q. Hao and Z. Song. "The Status and Development of the Intelligent Automatic Meter Reading System", *proc of* China Science and Technology Information, no.19, pp.72, October 2005.

[8] L. Hong and L. Ning. "Design and Implementation of Remote Intelligent Management System for City Energy Resources based on Wireless Network", Study of Computer Application, no. 12, pp. 237-239, 2004.

[9] S. W. Lee, C. S. Wu, W. M. S. Chiou and K. T. Wu. "Design of an Automatic Meter Reading System", *proc of* IEEE International Conference on Industrial Electronics, Control, and Instrumentation, vol. 1, pp. 631–636, 1996.

[10] Microcontrollers & Embedded System Designs, "http://www.ucdevelopers.page.tl/", 2007.

[11] H. Xiting and S. Zhonghong. "Design on the Software of Master Station of Automatic Meter-Reading System", Yan tai Normal University Journal (Natural Science), vol. 20, no.4, pp. 268-271, 2004.

[12] C. Yin-kang, L. Xiang-yang and X. Jing. "The Hardware Design of Concentrator for Wireless Intelligent Meter Reading System", Element and IC, no. 1, pp. 37-39, 2005.

[13] X. Zhaoyin and H. Shiyong, "Automatic Remote Meter Reading System using Bluetooth", Journal of Transducer Technology, vol. 23, no. 7, pp. 68-70, 2004.

Proceedings of 2009 12th International Conference on Computer and Information Technology (ICCIT 2009)
21-23 December, 2009, Dhaka, Bangladesh

Process Centric Work Breakdown Structure for Easing Software Project Management Challenges : Business Case Analysis Example

S. M. Saiful Islam, M. Rokonuzzaman†
School of Engineering & Computer Science ,Independent University, Bangladesh (IUB), Dhaka, Bangladesh and,
PyxisNet Ltd., Dhaka, Bangladesh
† School of Engineering & Computer Science, Independent University, Bangladesh (IUB), Dhaka, Bangladesh
shaikatdsbd@yahoo.com, zaman.rokon@yahoo.com

Abstract

Software Project management involves coordinating various aspects of a project in order to bring forth a positive result. There have been increasing challenges faced by Project Managers. The major challenges of project management include unrealistic deadlines, communication deficit, uncertain dependencies, failure to manage risk, not well-defined vision and goals, and invisibility of the final product. Meeting these challenges is very difficult and in many cases they are not met which eventually leads to the project failure. This situation is even worse where project dispersion is higher. Different studies reveal that an IT project is more likely to be unsuccessful than successful and 7 out of 10 IT projects fail in some respect. The process centric work breakdown structure (WBS) can play a very vital role in this regard to improve the situations significantly. Instead of hierarchical work breakdown structures as a tree, the process centric WBS takes whole software production process and splits whole process into smaller process units which take right set of inputs with the right set of standar, put right set of practices in place that eventualy produce the work products with expected standards and quality. This process centric work breakdown structure helps project Managers plan, estimate, monitor and control the project activities in greater accuracy and efficiency. In this article, Business Case Analysis phase of software projects has been taken as an example to demonstrate how process centric WBS can help for easing project management challenges.

Keywords: Work Breakdown Structure, Project Management Challenges, Process Centric Work Breakdown Structure, Work Products, and Easing Project Management Challenges.

I. INTRODUCTION

Software project management encompasses the knowledge, techniques, and tools necessary to manage the development of software products. Over the past five to ten years, there have been increasing challenges faced by Project Managers. The major challenges of software project management include estimation, planning and scheduling, progress monitoring, and control[1, 2, 4]. A number of studies were conducted by the different study groups around the globe which provide the failure statistics of software projects which is really alarming. The Robbins-Gioia Survey (2001) reveals that 51% of ERP implementation was unsuccessful. The Conference Board Survey (2001) finds that 40% of the projects failed to achieve their business case within one year of going live. On the success side, the average is only 16.2% for software projects that are completed on-time and on-budget. The OASIG Study (1995) indicates that 7 out of 10 IT projects "fail" in some respect [17, 18]. One of the major causes of Software project failure is high degree of estimation error. The estimation error significantly increases for distributed projects. Distributed software development is becoming more and more common as a development strategy. Even in high process maturity environments, dispersion significantly reduces development productivity and has effects on conformance of quality, and these negative effects of dispersion can be significantly mitigated through deployment of structured software engineering processes [19,24].

A work breakdown structure (WBS) in project management and systems engineering, is a tool used to define and group a project's discrete work elements (or tasks) in a way that helps organize and define the total work scope of the project [5,6,7]. The traditional tree form representation of WBS is not giving the complete visibility about the different production steps, their work products, the complete linkages and dependencies, the parallelism in the production steps, and the coordination and communication effort. Therefore, the traditional WBS cannot ease the complexity of project management. On the contrary, the process centric work breakdown structure can play a significant role to address these problems. The objectives of this article are:

1. To review and identify the major challenges of software project management.
2. To describe the concept of process centric work breakdown structure and describe its strength to address project management challenges.
3. Demonstrate the Business Case Analysis as an example of process centric work breakdown structure.

978-1-4244-6283-4/09/$26.00 ©2009 IEEE

II. PROBLEM STATEMENT

To achieve the major objectives of this article stated in the previous section, literature has been reviewed to investigate on the major challenges of software project management, software failure statistics and their underlying failure reasons, concept of WBS and its role to support estimation, monitoring, control, and risk management. Study has been conducted on a number of research papers and published resources. Literature review reveals that the process centric WBS practices can play a vital role to deal with these challenges. The underlying concept of process centric WBS is to discretize the production process to define work products up to the optimum level. This discretization will better enable the project manager to estimate, monitor, control and improve project activities to achieve desired goals.

A typical software project starts with the setting up of target business value and ends with the business value assessment during the implementation and uses of the product along the years. The Fig. 1 depicts the typical software production process expected to be coverd by project management activities. The achievable business value has to be determined in the very begining of the project. Otherwise there will be confusion whether business value has been met or not. The project has two main roles which are current and future - the current role of project is to complete the project in estimated time and money; and the future role of the project is to give the customer maximu return on investment (RoI). To demonstrate the concept of process centric WBS, the Business Case Analysis has been taken as example and explanation has been given so forth.

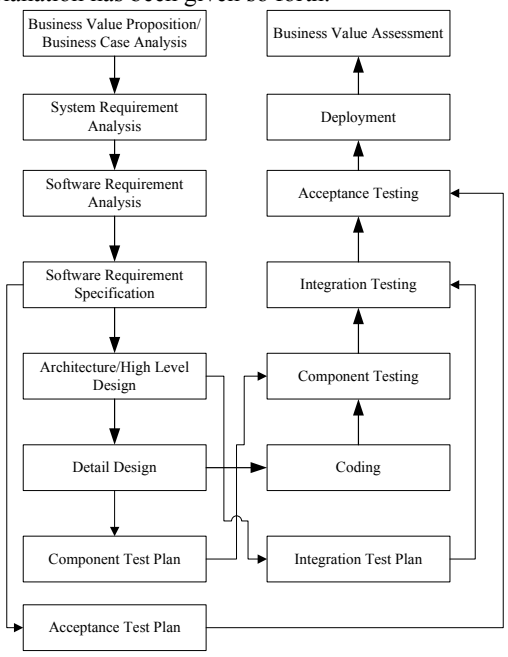

Fig. 1. Software production process

III. LITERATURE REVIEW

The Work Breakdown Structure (WBS) was initially developed by the U.S. defense establishment, and it is described in Military Standard [15] as "a product oriented family tree composed of hardware, software, services, data and facilities .... (it) displays and defines the product(s) to be developed and./or produced and relates the elements of work to be accomplished to each other and to the end product(s)". The CMMI also defines WBS as a product-oriented hierarchical structure [7,16]. A work breakdown structure, in project management and systems engineering, is a tool used to define and group a project's discrete work elements (or tasks) in a way that helps organize and define the total work scope of the project [3, 5, 6, 8, 9]. A well-organized, detailed WBS can assist key personnel in the effective allocation of resources, project budgeting, procurement management, scheduling, quality assurance, quality control, risk management, product delivery and service oriented management [10, 11, 12, 13]. But traditional work breakdown structure will not be able to define the total scope of the project accurately and specifically if it does not take production process into consideration. In tree structure work breakdown will simply consider the total work scope in linier way. But practically this doesn't happen. How much parallelism can be brought into production process, how many resource can be loaded and when, what could be the waiting time due to dependency should also be considered. The coordination and communication need has to be determined and estimated. Otherwise the main purpose of WBS will not be met.

The reason for using a WBS in projects is to help with assigning responsibilities, resource allocation, monitoring the project, and controlling the project. This also allows for better estimating of cost, risk, and time because one can work from the smaller tasks back up to the level of the entire project [13,14]. But practically this is also very difficult to be met in traditional work breakdown structure. In traditional work breakdown structure, it is not specified what would be inputs for a particular work package and from where one is getting those, what would be the outputs from that work package and who will be using those. That means dependencies and linkages are absent in traditional work breakdown structure which will significantly limit the success of project resource allocation, monitoring and controlling the project. Here, the communication and coordination aspect is completely missing.

One of the main reasons for Software Project failure is high degree of estimation error. Each project has high degree of uncertainty (variability) in software cost [20] which may risk the project very high. Many models such as COCOMO primarily use the number of source lines of code (SLOC) as the basis for effort estimation. An alternative metric for SLOC is function points (FPs), where the FP is the product of the number of function counts and the processing complexity adjustment

[22,25]. The COCOMO II model, which is the current version of COCOMO, uses 17 effort multipliers and five scale factors to estimate development effort based on project size [21,23]. But, in most of the cases these turn out insignificant and which eventually leads to high degree of estimation error. The basis for this estimation is traditional WBS where communication and coordination effort is absent or insignificant and consideration of uncertainty is insufficient.

IV. PROCESS CENTRIC WBS - BUSINESS CASE ANALYSIS EXAMPLE

The process centric work breakdown structure is different from the traditional tree structured work breakdown structure. Here, total production process is broken down into small process units. Each process unit takes a set of inputs with the right set of standards. A right set of practices has to be put in place; that will produce work products with expected standards. One output work product will be the input to one or multiple process units. Before going to be input to the other process units, the complainace of workproducts with appropriate standards is ensured so that it can't cause any harm such as entry of defects for the next outputs. All the process units are linked together which ultimately complete the production process. The Fig. 2 depicts a typical procss unit. To complete a process, a set of practices has to be performed. Quality of the produced work products has to be ensured after producing or before using as input to the other process unit through verification and validation.

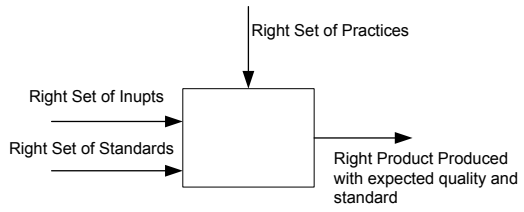

Fig. 2. WBS process unit

The Fig. 3 depicts the typical process centric work breakdown structure of Business case analysis. Here, only the main process units are considered. The review and verification of work products have been omitted to keep it simple. Each process unit or work package needs to perform some specific practices to produce the desired work product. Some standard and templates have to be put in place to produce the right quality of work products. Some measurement framework has also to be put in place so that effectiveness of the process and quality of the product can be assessed, controlled and improved.

Major pracatices need to perform to produce the desired work products includes the following:

- Briefly define business case for detail study
- Document the background, objectives and scope of the business case
- Identify the stakeholders & document their involvement requirement along with their expectations
- Formulate market research methodology to be applied for market study about the business case
- Prepare market research plan to conduct the market study
- Conduct key informant interview
- Conduct questionnaire survey
- Conduct focused group discussion
- Analyze the market data and prepare analysis report
- Identify and document functional capability of the current system
- Prepare process model - both current and proposed
- Take process performance measurement
- Indentify system component roles - current and proposed
- Validate system requirement through prototyping
- Document system requirement

Major work products produced during the execution of business case analyis are

- Business case description
- Background, objectives, scope description
- Stakeholders & their involvement list
- Market research methodology
- Market research plan
- Market analysis report
- Functional capability
- Process model
- System component roles
- System requirement

V. MATRICS OF PRACTICES AND WORKPRODUCTS: BUSINESS CASE ANALYSIS EXAMPLE

A metric is a quantifiable measurement of software product, process, or project that is observed, calculated, or predicted. Software measurement is the quantitative assessment of any aspect of a software engineering process, project, product, or context; it aims to enhance ones understanding and to help to control, predict, and improve what one produces and how s/he produces it. The driving force of measurement is dealing with the uncertainty, uncertainty about size, complexity, productivity, quality, ROI, readability, maintainability, reliability, etc. The metric is related with the purpose of the work products and the process unit that produced that work products. The objective of business case analysis metric is to see the effectiveness of the business case analysis processes and the quality of work products. The proposed Metrics for Business Case Analysis are shown in Table I against major work products. The Table II shows the data requirement for the major metrics. However, readability, clarity, complexity, effort variance and reusability can be used as a thumb rule.

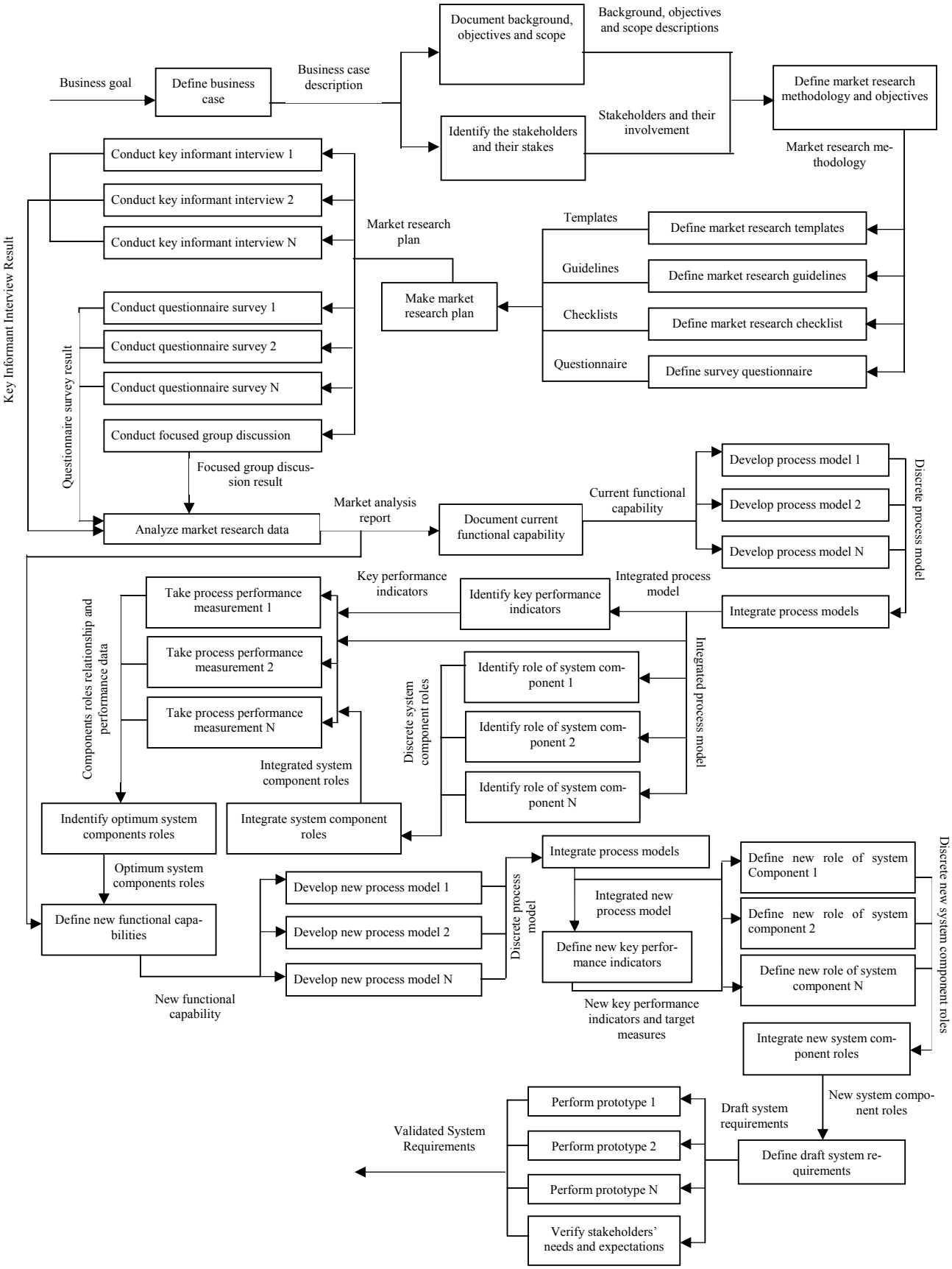

Fig. 3. Process centric WBS of business case analysis

Table I Business case analysis metrics

Work Product	Product Metric	Process Unit	Process Metric
Business case description	Clarity	Identify Stakeholders & their Involvement	Reusability, Manageability
Background, Objectives, Scope Description	Clarity, Completeness	Make Market Research Plan	Reusability, Flexibility, Manageability
Stakeholders & their involvement list	Clarity	Conduct Key Informant Interview	Clarity, Reusability, Rework
Market research methodology	Reusability	Conduct Questionnaire Survey	Manageability, Productivity
Market research plan	Complexity, Practicability, Reusability	Conduct Focused Group Discussion	Productivity, Quality
Market analysis report	Readability, Clarity, Completeness	Analyze Market Research Data	Productivity, Flexibility, Quality
Functional capability	Clarity, Completeness, Stability	Develop Process Model	Reusability, Flexibility, Complexity
Process model	Readability, Reusability, Complexity	Take Process Performance Measure	Quality, Productivity, Complexity
System component roles	Completeness	Define System Component Roles	Manageability, Productivity
System requirement	Readability, Completeness, Consistency	Perform Prototyping	Quality

Table II Data Requirement for metrics

Metric Name	Data Requirement	Measure
Clarity	Number of ambiguous or unclear statement. Number of sections/ pages.	No. of unclear statements per sections/pages
Completeness	Number of missing points, Number of sections/pages/documents.	No. of missing points per sections/pages/documents
Reusability	Number of reusable sections/ templates/ models/ concept/ documents. Number of reusable sections/ templates/ models/ concept/ documents.	% of reusable work products
Stability	Number of changed work products. Number of work products.	% of stable work products
Readability	Number of comments. Number of sections/pages.	No. of comments per sections/pages
Consistency	Number of inconsistency found. Number of work products.	No. of inconsistency per work product
Quality	Number of defects found. Number of sections/ pages/ work products.	Defect density
Productivity	Number of pages/documents/work products produced. Unit of Time Required/ Spent.	No. of pages/documents/work products per unit of Time

VI. BENEFITS OF PROCESS CENTRIC REPRESENTATION OF WBS

As stated earlier, the process centric work breakdown structure is different from the traditional tree structure work breakdown structure. In process centric work breakdown structure, total production process is broken down into small logical process units which take a set of inputs with the right set of standards and perform the appropriate set of practices to produce required work products with expected standards. This is the main strength of process centric WBS. The process centric WBS provides a great tool to the project manager to define estimates, monitor, control and improve the project activities from process perspective. Following are the benefits which can be achieved from process centric WBS:

1. Full production process split into small logical process units following 8/80 rules or like that. This ensures full process view at a glance at the planning stages.
2. Parallel process steps are clearly shown. Therefore, resource planning and resource loading will be efficient, less error prone, and easier.
3. A process unit takes quality inputs in compliance with applicable standards and performs specific practices in specified manner.

4. A process unit or work package's task is very clear; dependency and stakeholders' engagement are clearly defined. This ensures better estimation and scoping of the project.
5. Ensure efficient management of distributed projects as communication and coordination need and overhead is clearly understood.

All process units are dynamically reconfigurable. The project manager would be able to choose the required process units, standards, templates and products to adjust production process based on the diverse project forces.

VII. SUMMARY AND CONCLUSIONS

Project management is a capability that takes time to develop in a person or organization. Achieving success requires analyzing setbacks and failures in order to improve. Focusing on each project's challenges and learning from them will help to build a more capable and successful project management capability. The process centric WBS is a great tool to the project manager in this respect. The practicing of process centric WBS can ease project management in a great deal. The probability of making the project successful will increase dramatically. But, the main challenge is to optimally discretize the production process. Too much discretization will increase the visibility but will complicate communication and manageability. So, there is a need to make a balance. The measurement and review process cost time and money. Therefore, the measurement and review of process should also be optimum. The main focus should be on value creation from such process centric WBS representation and RoI of such value creation should be maximized by practicing optimum level of process decomposition.

REFERENCES

[1] J.E. Tomayko, H.K. Hallman, "Software Project Management." SEI Curriculum Module SEI-CM-21-1.0 July 1989. ftp://ftp.sei.cmu.edu/pub/ documents/misc/cms/ pdf/cm21.pdf

[2] P. W. Ford, "Top 10 Project Management Challenges." http://projectmanagementcourse. com/ project- challenges. html

[3] Project Management – Challenges. ITJobsCareer. http://www.itjobscareer.com/2007/05/project-management-challenges.html

[4] J. Amalraj, C. Hernani, K. Ladouceur, A. Verma, "Project Management: Challenges & Lessons Learned." http://www.beg.utexas.edu/energyecon/ ua_2007/ AB_ Project_Mgt_challenges.pdf

[5] Booz, Allen, Hamilton. "Earned Value Management Tutorial Module 2: Work Breakdown Structure", Office of Project Assessment, doe.gov. Accessed 01. Dec 2008.

[6] NASA (2001). NASA NPR 9501.2D. May 23, 2001.

[7] Work Breakdown Structure (WBS). http://www. hyperthot. com/pm_wbs.htm

[8] Electronic Industries Alliance Standard Systems Engineering Capability Model EIA-731.1

[9] Institute of Electrical and Electronics Engineers Standard for Application and Management of the Systems Engineering Process IEEE Std 1220-2005

[10] Work Breakdown Structure. http:// searchsoftware-quality .techtarget.com/sDefinition/ 0,,sid92 _gci1261335,00.htm

[11] Concept: Work Breakdown Structure. http://www. chambers.com.au/Sample_p/wbs_cncp.htm

[12] Mathis, M. "Work Breakdown Structure: Purpose, Process and Pitfalls." http://www.projectsmart. co.uk / work-breakdown-structure-purpose-process-pitfalls.html

[13] Project Management Work Breakdown Structure. http://www.online-project-management-training.com /work-breakdown-structure.html

[14] Create Work Breakdown Structure (WBS). Project Management Knowledge. http://www.project-management-knowledge.com/definitions/c/create-work-breakdown-structure-wbs/

[15] "Work Breakdown Structures for Defense Materiel Items - MIL-STD-8818", US Department of Defense, March 25.1993.

[16] Capability Maturity Model Integration (CMMISM), Version 1.l, Staged Representation, August 2002.

[17] Statistics over IT project failure rate. IT Cortex. http://www.it-cortex.com/Stat_Failure_Rate.htm

[18] Failure Causes Statistics. IT Cortex. http://www.it-cortex.com/Stat_Failure_Cause.htm

[19] N. Ramasubbu, R.K. Balan, "Globally Distributed Software Development Project Performance: An Empirical Analysis." http://www.cs. cmu. edu/ ~rajesh/ papers/ fse07.pdf

[20] B. Yang, H. Hu, and L. Jia, "A Study of Uncertainty in Software Cost and Its Impact on Optimal Software Release Time," IEEE TRANSACTIONS ON SOFTWARE ENGINEERING, VOL. 34, NO. 6, NOVEMBER/ DECEMBER 2008, pp. 813-825

[21] M. Agrawal, K. Chari, "Software Effort, Quality, and Cycle Time: A Study of CMM Level 5 Projects," IEEE TRANSACTIONS ON SOFTWARE ENGINEERING, VOL. 33, NO. 3, MARCH 2007, pp. 145-156

[22] M. Jørgensen, M. Shepperd. "A Systematic Review of Software Development Cost Estimation Studies," IEEE TRANSACTIONS ON SOFTWARE ENGINEERING, VOL. 33, NO. 1, JANUARY 2007, pp. 145-156

[23] M. Agrawal, K. Chari, " Software Effort, Quality, and Cycle Time: A Study of CMM Level 5 Projects", IEEE TRANSACTIONS ON SOFTWARE ENGINEERING, VOL. 33, NO. 1, JANUARY 2007, pp. 133-156

[24] R. Kommeren, P. Parviainen, "Philips experiences in global distributed software development", Empir Software Eng (2007) 12:647–660

[25] J.E. Matson, B.E. Barrett, and J.M. Mellichamp, "Software Development Cost Estimation Using Function Points," IEEE Trans. Software Eng., vol. 20, pp. 275-287, 1994.

Proceedings of 2009 12th International Conference on Computer and Information Technology (ICCIT 2009)
21-23 December, 2009, Dhaka, Bangladesh

A Logical Formal Model for Verification of Web Service Choreography

Zahra Madani, Naser Nematbakhsh†
Dept. of Computer Engineering, Islamic Azad University, Najafabad Branch, Isfahan, Iran
† Dept. of Computer Engineering, Isfahan University, Isfahan, Iran
zmadani@iaun.ac.ir, nemat@eng.ui.ac.ir

Abstract

Several methods and languages have been developed to describe computer system specifications and some of them have been deployed to validate and verify the functionality of the system. No one method is equally appropriate for all application domains. Service Oriented Architecture and using web services is a wide growing domain of applications in software engineering these days, so to achieve more goals and benefits in large business works, we need to compose the existing web services from different organizations. In this paper we discuss about web service composition mechanisms and related formal methods and verification issues. One of the solutions in highest level is to use Web Service Choreography Definition Language (WS-CDL) to design the composition of services. With regard to this, we need to get sure about the correctness of choreography behavior, before to employ it for developing and executing services collaboration. In this paper we present a method using first order logic notation based on the partial-order planning problems. This method can be used for interactive systems that all participants have a common understanding of interaction rules. This method will be able to model variable specification of the system. It is consist of three parts included precondition, action and effect, so has a simple structure to understand. In this method we can check the properties of the model for reachability of ideal and safe states. We show the method in a web service interaction case study and verify it in Prolog tool.

Keywords: Web Service Choreography, Verification, Rule-based Model.

I. INTRODUCTION

A choreography model describes a collaboration between a collection of services in order to achieve a common goal. It captures the interactions in which the participating services engage to achieve this goal and the dependencies between these interactions, including control-flow dependencies (e.g., a given interaction must occur before other one), data-flow dependencies, message correlations, time constraints, transactional dependencies, etc. A choreography does not describe any internal action that occurs within a participating service that does not directly result in an externally visible effect, such as an internal computation or data transformation. A choreography captures interactions from a global perspective, meaning that all participating services are treated equally. In other words, a choreography encompasses all the interactions between the participating services that are relevant with respect to the choreography's goal [10]. One of the requirements of WS-CDL is to provide a means for tools to validate conformance to choreography descriptions to ensure interoperability between web services. To enable design time or static validation and verification of choreographies to ensure correctness properties such as livelock, deadlock, leak freedom, safety and reachability, or to ensure that the runtime behavior of participants conforms to the choreography plan, WS-CDL must be based on or related to a formal language that provides these validation capabilities. Although WS-CDL appears to borrow terminology from pi-Calculus [6], the link to this or any other formalism is not clearly established [10]. Formal methods have deployed for various domain of software engineering and many verification tools have been developed and some of them is employed to verify choreography specifications.

Here the method that is used for describing choreography activities is based on partial-order planning problems and uses first-order logic predicates. The choreography is decomposed to several actions that have some execution order to achieve the goal of business.

This model can simply define every specification of WS-CDL and the existing rules by predicates. Then the predicates are written in Prolog tool and the reachability of partial goals for verification of choreography behavior is asked by questioner predicates.

Because of pre and post conditions in partial-order planning problems, all constraints, policies and obligations in choreography behavior can be modeled upon.

II. CHOREOGRAPHY SPECIFICATIONS

In this section the main specifications of a choreography that represent its behavior is selected and described[10], [11].

- Activities and ordering structures – For description of rules of actions to perform, choreography uses ordering structures containing sequence, parallel and choice.
- Interaction activity - An interaction is the basic building block of a choreography. It results in an exchange of information between participants and possible synchronization of their observable infor-

978-1-4244-6283-4/09/$26.00 ©2009 IEEE

mation changes using variables exchange and time-out record.

- ChannelType - A channel determines where and how the information be exchanged between participants.
- Variables – A variable is used to record the state of roles and the whole of system, so two kind of information exchange variables and state-capturing variables are considered.

III. FORMAL METHODS AND TOOLS

In recent years some formal methods and verification tools have been used for checking various properties of web service composition, orchestration and choreography. Here We describe the methods and specifications of choreography that have been used to verify its behavior. most methods have been used are Pi calculus, Process Algebra, Finite State Automata, Petri net, Reo, LTL and CTL and some other new methods. In [12] it provides rules to compose choreographies in sequence, parallel and choice. Also shows how to deal with dynamic channel passing. In the choreography interaction, Time-outs allow each party to fix the time for an action to occur, while alignments are synchronizations between two peer-to-peer parties, So in [3] timed automata model and UPPAAL tool is used to simulate and analyze the behavior of the system and checks safeness and liveness properties. Also in [7], it presents a set of transformation rules for construction of timed automata for choreography and scope including exception handler, finalizer blocks and fault and compensation handler. The main work of [8] is to model the interactions with recordings of state/channel variable changes that can occur as a result of performing an interaction. In [1] it provides the capability for verifying data-related properties such as availability of channel variables and reachability of states. It checks choreographies in SPIN. One important problem in the choreography is to ensure that each service in a composition can always get sufficient and correct channels for completing their collaborative work, so in [5] it propose a pair of formal languages that support channel passing on both global and local levels, together with their semantics and can check the deadlock freedom. In [9], it works on compositional construction of web services using the Reo coordination language and constraint automata. It investigate the possibility of representing the behaviour of web services using constraint automata as black-box components within Reo circuits. It describes the orchestration of web services by the product of corresponding constraint automata, and use Reo circuits for choreography of web services.

IV. RULE-BASED MODEL

To map the choreography to a logical formal rule-based model, a three parts structure must be developed witch is made of: initial state or initial facts, rules or action relations, goal state or goal test.

The three parts below are detailed:

- **Initial facts**, witch is contained of:
  - Channel specifications
  - Interaction specifications
  - Role specifications
  - Channel variables in each interaction
  - State variables in each role
  - Information variables in each role
- **Action relations**, witch is contained of:
  - Information exchange
  - Channel exchange (Channel Passing)
  - State variable changes
  - Information variable changes
- **Goal test**, witch is contained of:
  - Whether information is in the target?
  - How is routing of information?
  - Reachability of goals and partial goals

V. PARTIAL-ORDER PLANNING

This section shows that how the order of activities is modeled upon partial-order planning model. The relation and rules of activities order under pre and post conditions is shown by finite automata.

Three kinds of control flows are shown in figures 1-4:

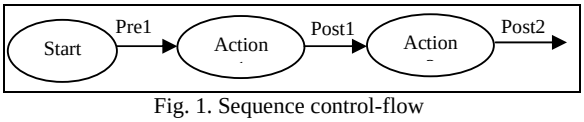

Fig. 1. Sequence control-flow

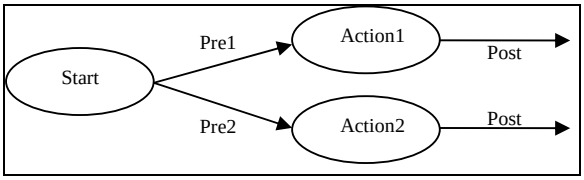

Fig. 2. Choice control-flow

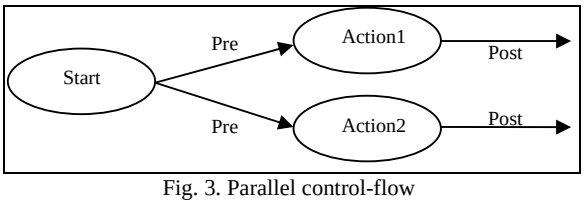

Fig. 3. Parallel control-flow

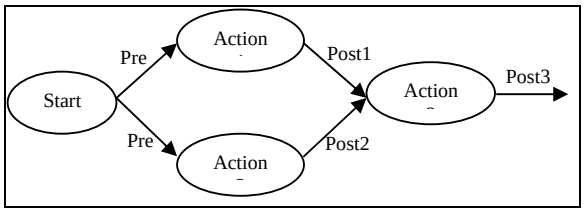

Fig. 4. Synchronized parallel control-flow

VI. THE PREDICATES FOR MODEL

In this section the translation of WS-CDL to predicates is described. It is consist of some predicates for representation of main specifications and some sentences that explain static rules of information exchange and is repeated in each choreography, and some sentences that explain order of data exchange by determination of pre and post conditions and shows behavior of choreography. You can see them below.

A. Specification Representation

```
<channelType name="NCName"
        usage="once"|"distinct"|"shared"?
        action="request-respond"|"request"|"respond"? >
  <passing channel="QName"
        action="request-respond"|"request"|"respond"?
        new="true"|"false"? />*
  <roleType typeRef="QName" behavior="NCName"? />
  <reference>
    <token name="QName"/>
  </reference>
  <identity usage="primary"|"alternate"|"derived"|"association">
    <token name="QName"/>+
  <identity>*
</channelType>
```

Fig. 5. ChannelType syntax

channelPassing(nCName, qName).

usage(nCName,"once ").

action(nCName," request").

refrence(nCName,party1).

identity(nCName,"primery","orderid").

action(qName,"request").

new(qName,"true").

```
<interaction name="NCName"
        channelVariable="QName"
        operation="NCName"
        align="true"|"false"?
        initiate="true"|"false"? >
  <participate relationshipType="QName"
        fromRoleTypeRef="QName" toRoleTypeRef="QName" />
  <exchange name="NCName"
        faultName="QName"?
        informationType="QName"?|channelType="QName"?
        action="request"|"respond" >
    <send variable="XPath-expression"?
        recordReference="list of NCName"?
        causeException="QName"? />
    <receive variable="XPath-expression"?
        recordReference="list of NCName"?
        causeException="QName"? />
  </exchange>*
  <timeout time-to-complete="XPath-expression"
        fromRoleTypeRecordRef="list of NCName"?
        toRoleTypeRecordRef="list of NCName"? />?
  <record name="NCName"
        when="before"|"after"|"timeout"
        causeException="QName"? >
    <source variable="XPath-expression"? | expression="XPath-expression"? />
    <target variable="XPath-expression" />
  </record>*
</interaction>
```

Fig. 6. Interaction syntax

toRole(nCName, qName1).

fromRole(nCName, qName2).

channelvariable(nCName, qName).

ttc(nCName, value).

align(nCName,value).

init(nCName,value).

B. Static Rules

1.The target role of an interaction will have the information, if the related exchange is successful and data is exchanged:

hasInfo(Role, Information):- exchange(Exchange, Interaction), action(Exchange, 'request'), toRole(Interaction, Role), data(Exchange, 'info', Information).

hasInfo(Role, Information):- exchange(Exchange, Interaction), action(Exchange, 'request-response'), toRole(Interaction, Role), data(Exchange, 'info', Information).

hasInfo(Role, Information):- exchange(Exchange, Interaction), action(Exchange, 'response'), fromRole(Interaction, Role), data(Exchange, 'info', Information).

2.The target role of an interaction will have the channel, if the related exchange is successful and data is exchanged:

hasChannel(Role ,Channel):- exchange(Exchange, Interaction), action(Exchange, 'request'), toRole(Interaction, Role), data(Exchange, 'channel', Channel).

hasChannel(Role, Information):- exchange(Exchange, Interaction), action(Exchange, 'request-response'), toRole(Interaction, Role), data(Exchange, 'channel',Information).

hasChannel(Role ,Channel):- exchange(Exchange, Interaction), action(Exchange, 'response'), fromRole(Interaction, Role), data(Exchange, 'channel', Channel).

3.The role determined in the interaction will have the channel variable of that interaction.

hasChannel(Role, Channel):- fromRole(Interaction, Role), channelVariable(Interaction, Channel).

4.The interaction will initiate, if the source and target role have the related channel:

initiate(Interaction, Channel):- fromRole(Interaction, RoleA), hasChannel(RoleA, Channel) , toRole(Interaction, RoleB), hasChannel(RoleB, Channel).

C. Dynamic Rules

All exchanges in the choreography is dependent to initiation of related interaction and existing information in the source role and checking value of some state variables:

exchange(exchange1, interaction1):- initiate(interaction1, channel1), hasInfo(role1, information1), value(variable1, role1, value1).

The data will be exchanged if the related exchange is successful and the time-to-complete constraint is satisfied:

data(exchange1, 'info', information1):- exchange(exchange, intraction1), ttc(interaction1, Value), Value<= t.

data(exchange1, 'channel', channel1):- exchange(exchange1, intraction1), ttc(interaction1, Value), Value<= t.

VII. CASE STUDY

In this section we present an example from W3C working draft[11], to describe modeling of exchanges and reasoning about reachability of partial states.

This example shows four roles: Buyer, Seller, CreditAgency and Shipper. The roles interact through channels. a BuyerRole - this role will be responsible for providing quote request, a SellerRole - this role will be responsible for providing quote responsing, a CreditAgencyRole - this role will be responsible for providing credit checking facilities, a ShippingRole - this role will be responsible for providing onward shipping of the good bought and shipping details which need to be delivered back to the BuyerRole.

In this example we use state transition numbering to save the transition route of the system in Prolog tool. Also we use the backtracking search using these predicates:

solve([1],[]).

solve(Gol,L):-
action(Golp,Y,Gol),solve(Golp,Lp),append(Lp,Y,L).

The representation of initial state, rules and goals are available in Appendix.

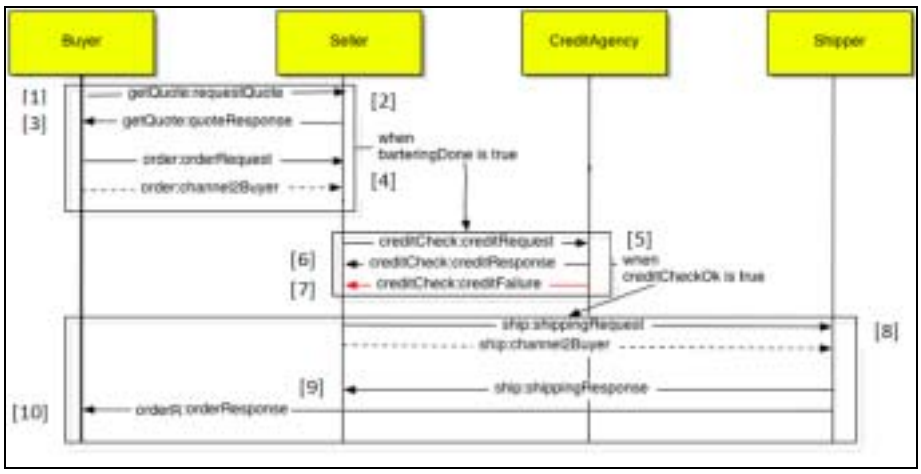

Fig. 7. Buyer-Seller choreography example

VIII. CONCLUSION

Here, we represented that how to transfer the choreography structure to the new model based on partial-order planning and write predicates upon. Using answers taken from asking reachability of partial goals,

we can detect points of problems in the description and improve it to reach suitable states. The problem may be occurred in situations like channel-absence, time-out and constraint-unsatisfiablity.

The model covers static and dynamic aspects of choreography like control flows, channel passing, time to complete and policy changes, so can be used for verification of various examples.

Further, we can generate more detailed rules to cover all attributes of choreography elements. And we can make a tool to generate predicates automatically from the text of WS-CDL.

IX. APPENDIX

- **Initial state**

As an example, some of facts are shown:

```
hasInfo(buyer,goodsList).

fromRole(getQuote,buyer).
toRole(getQuote,seller).
channelVariable(getQuote,b2sChannel).
…
fromRole(orderR,buyer).
toRole(orderR,shipper).
…
action(b2sChannel,'request').
hasChannel(seller,b2sChannel).
channelPassing(b2sChannel,shChannel).
…
action(requestQuote,'request').
…
action(passChS2Sh,'request').
…
```

- **Dynamic Rules**

As an example, some of data exchanges are shown:

```
exchange(requestQuote, getQuote):-
initiate(getQuote), hasInfo(buyer, goodsList),!.
data(requestQuote,'info', goodsList):-
exchange(requestQuote, getQuote).
action([1],[data(requestQuote,'info', goodsList)],[2]):-data(requestQuote,'info', goodsList).

exchange(quoteResponse, getQuote):-
initiate(getQuote), hasInfo(seller, goodsList),!.
data(quoteResponse,'info', quote):-
exchange(quoteResponse, getQuote).
action([2],[data(quoteResponse,'info', quote)],[3]):-data(quoteResponse,'info', quote).
…
exchange(shippingResponse, ship):-
initiate(ship), hasInfo(shipper, orderList),!.
data(shippingResponse,'info', orderOk):-
exchange(shippingResponse, ship).
action([8],[data(shippingResponse,'info', orderOk)],[9]):-data(shippingResponse,'info', orderOk).

exchange(orderResponse, orderR):-
initiate(orderR), hasInfo(shipper, orderList),hasChannel(shipper, shChannel),!.
data(orderResponse,'info', orderDeliver):-
exchange(orderResponse, orderR).
action([8],[data(orderResponse,'info', orderDeliver)],[10]):-data(orderResponse,'info', orderDeliver).

exchange(passChB2S, order):-
initiate(order), hasChannel(buyer, shChannel),!.
data(passChB2S,'channel', shChannel):-
exchange(passChB2S, order).

exchange(passChS2Sh, ship):-
initiate(ship), hasChannel(seller, shChannel),!.
data(passChS2Sh,'channel', shChannel):-exchange(passChS2Sh, ship).
```

- **Partial goals**

As an example, some of reachability questions are shown:

```
?-solve([1],L),write(L),write(nl),fail.
?-solve([2],L),write(L),write(nl),fail.
…
?-solve([8],L),write(L),write(nl),fail.
?-solve([9],L),write(L),write(nl),fail.
?-solve([10],L),write(L),write(nl),fail.
```

The final answers to achieve the partial goals can be seen here:

```
[]
 [data(requestQuote,info,goodsList)]
…
[data(requestQuote,info,goodsList),data(quoteResponse,info,quote),data(orderRequest,info,order),data(creditReque
```

st,info,orderPrice),data(creditResponse,info,checkOk),data(shippingRequest,info,orderList)]

[data(requestQuote,info,goodsList),data(quoteResponse,info,quote),data(orderRequest,info,order),data(creditRequest,info,orderPrice),data(creditResponse,info,checkOk),data(shippingRequest,info,orderList),data(shippingResponse,info,orderOk)]

[data(requestQuote,info,goodsList),data(quoteResponse,info,quote),data(orderRequest,info,order),data(creditRequest,info,orderPrice),data(creditResponse,info,checkOk),data(shippingRequest,info,orderList),data(orderResponse,info,orderDeliver)]

REFRENCES

[1] H. Yang, X. Zhao, C. Cai, and Z. Qiu, "Model-Checking of Web Services Choreography," in *Service-Oriented System Engineering, 2008. SOSE '08. IEEE International Symposium on* Jhongli, Taiwan, , 2008, pp. 79-84.

[2] P. Geguang, S. Jianqi, W. Zheng, J. Lu ,L. Jing, and H. Jifeng, "The Validation and Verification of WSCDL," in *Software Engineering Conference, 2007. APSEC 2007. 14th Asia-Pacific*, 2007, pp. 81-88

[3] E. C. Maria, M. Pardo, J. P. Juan, D. Gregorio, and V. Valentin, "Timed Automata for Web Services Verification," in *World Scientific and Engineering Academy and Society*, 2006.

[4] H. Yang, C. Cai, L. Peng, X. Zhao, and Z. Qiu, "Reasoning about Channel Passing in Choreography," in *Proceedings of the 2008 2nd IFIP/IEEE International Symposium on Theoret* Washington, DC, USA 2008, pp. 135-142.

[5] P. U. Chao Cai Hongli Yang Xiangpeng Zhao Zongyan Qiu LMAM & Dept. of Inf., Beijing;, "A Formal Model for Channel Passing in Web Service Composition," in *Services Computing, 2008. SCC '08. IEEE International Conference*. vol. 2, 2008, pp. 495-496.

[6] C. Chao and Q. Zongyan, "An Approach to Check Choreography with Channel Passing in WS-CDL," in *Web Services, 2008. ICWS '0*8 . *IEEE International Conference on* Beijing, China,, 2008, pp. 700-707.

[7] L. Sagara and B. D. Chaudhary, "A Model of Scope for Verification of Implementation of Choreography with Exception Handler Using UPPAAL," in *Mobile Ubiquitous Computing, Systems ,Services and Technologies, 2008. UBICOMM '08. The Second International Conference on* Valencia, Spain, , 2008, pp. 510-519.

[8] H. Foster, S. Uchitel, J. Magee, and J. Kramer, "Model-Based Analysis of Obligations in Web Service Choreography," in *Telecommunications, 2006. AICT-ICIW '06. International Conference on Internet and Web Applications and Services/Advanced International Conference on*, 2006, pp. 149- 149.

[9] M. Sun and A. Farhad, "Web services choreography and orchestration in Reo and constraint automata," in *Symposium on Applied Computing Proceedings of the 2007 ACM symposium on Applied computing*, Seoul, Korea, 2007, pp. 346 - 353.

[10] B. Alistair, D. Marlon, and O. Phillipa, "A Critical Overview of the Web Services Choreography Description Language (WS-CDL)," www.bptrends.com, 2005.

[11] Web Services Choreography Description Language: Primer - W3C Working Draft 19 June 2006. http://www.w3.org/TR/2006/WD-ws-cdl-10-primer-20060619/(accessed 2009).

[12] M. Carlo and S. Laura, "A Logical View of Choreography," *Coordination Models and Languages*, vol. 4038/2006, pp. 179-193, 2006.

Proceedings of 2009 12th International Conference on Computer and Information Technology (ICCIT 2009)
21-23 December, 2009, Dhaka, Bangladesh

Performance Analysis of Datagram Congestion Control Protocol (DCCP)

Iffat Sharmin Chowdhury, Jutheka Lahiry, Syed Faisal Hasan
Dept. of Computer Science and Engineering, University of Dhaka, Dhaka, Bangladesh
sharmin.iffat@gmail.com, juthekalahiry@yahoo.com, hasansf@gmail.com

Abstract

Applications like streaming audio, Internet telephony and multi-player online games prefer timeliness in packet delivery to reliability. TCP's reliability through packet retransmission and abrupt rate control features are unsuitable for these applications. As a result, these applications prefer UDP as the transport layer protocol. UDP does not have any congestion control mechanism which is vital for the overall stability of the Internet. For this reason, a new transport layer protocol Datagram Congestion Control Protocol (DCCP) has been introduced by the Internet Engineering Task Force (IETF). DCCP is suitable for these applications because of its exclusive characteristics. It can be useful for those applications which need a session and congestion control unlike UDP and do not need reliability or retransmission like TCP. However, since DCCP is a new protocol, its performance for these applications has to be analyzed thoroughly before it emerges as a de facto transport protocol for these applications. This paper describes the basic principle of DCCP, its congestion control mechanism and measures the performance of DCCP. The results show that DCCP provides better performance for those applications that suffers the tradeoff between delay and in-order delivery.

Keywords: CCID2, CCID3, congestion control, DCCP, IETF, streaming multimedia.

I. INTRODUCTION

Now-a-days, almost every website includes streaming multimedia applications. So, it is really essential to send audio video files in time. Generally, Internet uses Transmission Control Protocol (TCP) and User Datagram Protocol (UDP) for sending application data. TCP ensures ordered packet delivery and reliability. So, when a packet is lost, TCP retransmits it and all the following packets have to wait and TCP considers that network is congested. Then TCP sender reduces its sending rate and that rate may not meet the requirements of streaming multimedia. So, TCP is not suitable for streaming multimedia applications. On the other hand, if we use UDP for those applications, then it may be quite impossible to recover from congested network because UDP has no congestion control mechanism. For this reason, a new transport layer protocol, DCCP (Datagram Congestion Control Protocol), is proposed by IETF [1]. It is a message oriented transport layer protocol. It provides reliable connection setup, congestion control and feature negotiation. It is useful for those applications where timing constraints exists in delivery of data but does not require reliable ordered delivery. DCCP does not provide congestion control at the application layer. It has built in congestion control mechanism. Two congestion control mechanisms of DCCP are TCP-like (Congestion Control IDentifier 2) and TCP-friendly (Congestion Control IDentifier 3). This is useful for those applications where a steady rate of data transmission is required rather than reliable in order delivery of packets. Some experiments have been done to measure the performance of DCCP's congestion control mechanism [2]. Those experiments evaluate the performance of TCP, UDP, and DCCP. In this paper, the performance analysis of DCCP's two alternative congestion control mechanism is illustrated as DCCP is completely a new protocol. It is still under research whether DCCP can be used for real time applications practically. The objective of the work is to measure the performance of TCP and DCCP at various environments and to show whether the performance of DCCP is better or not. From the experiments given later, it can be ensured that there are no abrupt changes in bit rate of CCID 3. So, CCID 3 can be used for those applications that needs smooth rate.

This paper is organized as follows-

Section I introduces DCCP, section II depicts some related works, section illustrates background study, section III and section IV explain performance evaluation goal and testing consecutively, section V demonstrate contribution and future works and section VI includes acknowledgment.

II. RELATED WORKS

Floyd et al. [13] initially proposed and introduced the definition of TCP-friendly flows.

In an experimental study, Timothy Sohn and EimanZolfaghari [14] reported an initial implementation and experimentation of Datagram Control Protocol (DCP) and its equation-based congestion control mechanism to show its TCP-friendliness behaviors. Horia Vlad Balan, Lars Eggert, Saverio Niccolini and Marcus Brunner [15] evaluated the voice quality that Internet telephony calls achieve over prototype implementations of basic DCCP and several DCCP variants, under different network conditions and with different codecs. Saleem Bhatti, Martin Bateman and Dimitris Miras [16] com-

978-1-4244-6283-4/09/$26.00 ©2009 IEEE

pared the performance of DCCP CCID2 relative to TCP New Reno. They assessed overall throughput and fairness-how well these protocols might respond to each other when operating over the same end-to-end network path.

Unlike their work, we focus on the performance of CCID 2 and CCID 3 relative to TCP.

III. BACKGROUND STUDY

There are two very common transport layer protocols named TCP and UDP. Recently, a new transport layer protocol DCCP is invented to meet various dynamic changes of network bandwidth.

A. TCP CONGESTION CONTROL

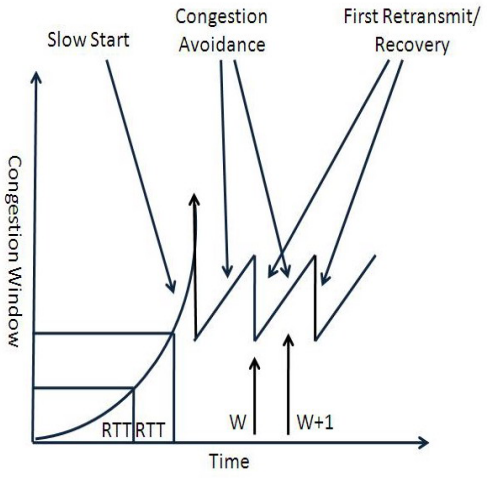

Fig. 1. TCP congestion control mechanism

Fig. 1 depicts that when a TCP connection begins, the value of congestion window (CongWin) is typically initialized to 1 MSS (RFC 3390), resulting an initial sending rate of roughly MSS/RTT. After every RTT, the sender increases its rate exponentially by doubling its value of CongWin. TCP congestion control algorithm behaves differently after a timeout event than after the receipt of triple duplicate ack. After a timeout event, CongWin is reduced to 1 MSS that is called Slow Start phase. Whereas after receiving triple duplicate acknowledgements, it only cuts it's CongWin in half and then grows linearly. The cancelling of the slow start phase after triple duplicate acknowledgements is called fast recovery.

B. DATAGRAM CONGESTION CONTROL PROTOCOL (DCCP)

Datagram Congestion Control Protocol (DCCP) is message and connection oriented transport layer protocol. It differs from UDP, in that, it includes congestion control mechanism and it differs from TCP, in that, it does not provide guaranteed reliability.

C. DATAGRAM CONGESTION CONTROL PROTOCOL (DCCP)

Datagram Congestion Control Protocol (DCCP) is message and connection oriented transport layer protocol. It differs from UDP, in that, it includes congestion control mechanism and it differs from TCP, in that, it does not provide reliability.

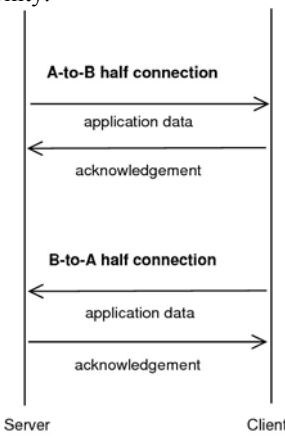

Fig. 2. DCCP's two half connections

C.1 THE DCCP CONNECTION

DCCP implements bidirectional connections between hosts. The connection is established between two hosts and any host can initiate the connection [3]. Data may passes from any host to another host which is depicted in Fig. 2. A DCCP connection consists of two unidirectional connections, called half-connection but this distinction is logical [4].

C.2 DCCP PACKET STRUCTURE

The DCCP header consists of 12 to 1020 bytes and the first part of the header is the same for all packet types. After the generic header, comes the additional fields which depend on types of packets and then comes variable length optional field of options. Application data follows the header and the packet structure [4] is depicted on Fig. 3.

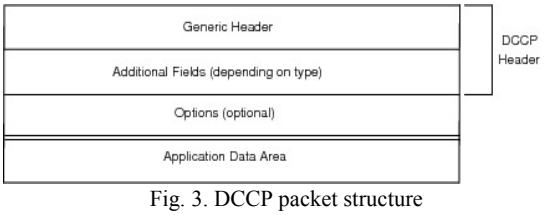

Fig. 3. DCCP packet structure

C.3 UNRELIABLE DATA TRANSFER

Each DCCP packet carries a sequence number so that losses can be detected and reported. But there is no retransmission of lost packets and hence DCCP is an unreliable protocol.

C.4 DCCP CONNECTION MANAGEMENT

DCCP server and client go through many states when establishing a connection between them. The steps are depicted at Fig. 4.

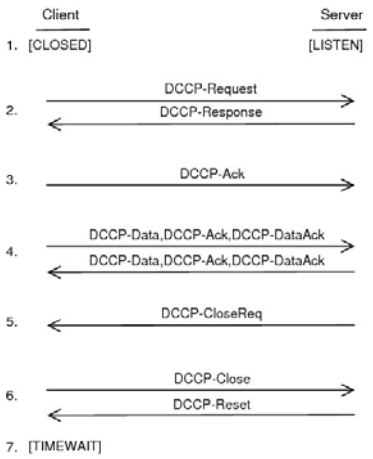

Fig. 4. DCCP's connection management

- Client is in closed state and server is in listening state.
- Client sends DCCP request, which specifies server and client ports, and server sends DCCP response to specific client, which means the willingness of server to exchange messages.
- Client sends DCCP acknowledgement to server to inform that DCCP response is received.
- Server and client then exchange DCCP-Data, DCCP-Ack and DCCP-DataAck packets, which includes piggybacked acknowledgement.
- Server sends DCCP-CloseReq to client for requesting to close the connection.
- Client acknowledges the request by sending DCCP-Close packet. Server then sends DCCPReset packet and clears its connection state.
- Client receives DCCP-Reset packet and holds the time wait state for two maximum segment lifetimes to allow on transit packets to clear the network.

D. DCCP CONGESTION CONTROL

DCCP implements congestion control and the user of the applications can make a choice of congestion control mechanisms. The two hosts agreed on the congestion control mechanism during the initiation of the connection. One byte congestion control identifier called CCID, defines the mechanisms. Among various Congestion Control IDentifier, CCID 2 and CCID 3 are well defined.

D.1 CCID 2

CCID 2 is TCP like congestion control mechanism. It is perfect for those applications which can adapt to the changes of congestion control window and which need as much bandwidth as possible in the network. CCID 2 uses TCP like congestion control mechanism [5]. There are some particular features of CCID2 connection-

- Duplicate acknowledgement indicates some loss of data packet.
- The sender has timeout option, which is handled like TCP's retransmission timeout. The sender calculates round trip time for a window at most once and uses TCP's algorithm for maintaining the round trip time.

After a congestion event occurs, CCID 2 reduces its congestion window (cwnd). Every congestion event consists of explicitly indicated that is ECN marked or via duplicate acknowledgements. For this case, cwnd is halved.

D.2 CCID 3

CCID 3 is TCP friendly rate control mechanism [6]. It provides TCP friendly rate by reducing the changeable characteristics of TCP or TCP like congestion control. The sender maintains its sending rate by observing the loss event send by the receiver and goes through a constant sending rate [7].
CCID 3 uses TCP friendly rate control mechanism for congestion control. The DCCP sender calculates its transmission rate based on the following equation-

$$T = \frac{s}{R\sqrt{\frac{2bp}{3}} + t_{RTO}(3\sqrt{\frac{3bp}{8}})p(1+32p^2)}$$

- T = transmission rate in bytes/second
- s = packet size in bytes
- R = round trip time in seconds
- b = number of packets acknowledged by a single TCP acknowledgement
- p = loss event rate
- tRTO = TCP retransmission time out value in seconds

This results a fair smooth transmission rate which is required for real time applications.

IV. PERFORMANCE EVALUATION GOAL

In this paper, we have compared the performance of

TCP and CCID2 and CCID3 of DCCP based on throughput. We have varied loss rate and delay. The performance is compared by sending fixed size packet because the audio/video streaming applications sent fixed size packets.

V. TESTING

For these experiments, we had to compile the Linux kernel [8] and we used some tools like-iperf [9], GnuPlot [10] and a network emulator [11]-Netem.

A. EXPERIMENTAL SETUP

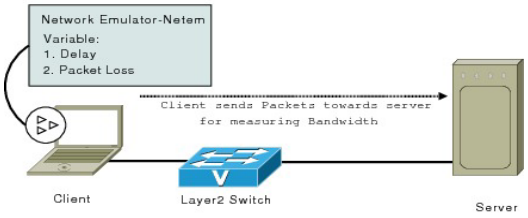

Fig. 5. Testbed Configuration

The setup of two machines is illustrated in Fig. 5. One machine acts as DCCP server and other machine acts as DCCP client. Client machine is used to emulate network changes. The server machine acts as a sink. These network conditions are applied on the interface of the client machine using Netem [12] functionality.

B. PERFORMANCE EVALUATION

We are going to show the results and to analyze whether our goal has been satisfied or not. We will also discuss the various behaviors of the transport layer protocols in different environment.

B.1 TIME VS BIT RATE

The transmission rate of TCP, CCID 2 and CCID 3 at time interval 1 second and total transmission time 10 seconds are shown in the following graph.

Fig. 6 shows the bit rate in Mbps to y-axis corresponding to the time in seconds to x-axis. The graph shows us that the bit rate of TCP and CCID 2 which is TCP like congestion control are high and the bit rate of CCID 3 which is TCP friendly rate control is low and a bit smooth.

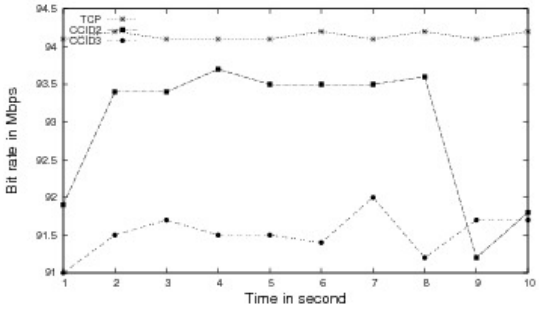

Fig. 6. Time vs Bit rate of TCP, CCID 2 and CCID 3

In the graph, we observe that at interval 1-2 and 8-9 to the time axis, in CCID 2, there are sudden changes in bit rate. But there is no abrupt change in CCID 3. As there is no loss of data between sender and receiver, there is no sharp rise and fall on TCP throughput. In our experimental setup, the link bandwidth was 100 Mbps, so TCP throughput can't exceed this range.

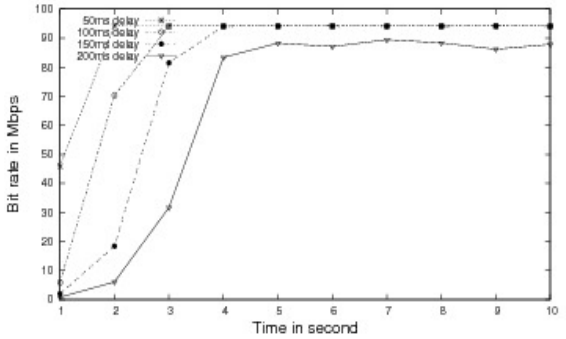

Fig. 7. Time vs Bit rate of TCP in varying delay

B.2 DELAY VARIANT

Fig. 7 shows TCP's behavior in varying delay. The X-axis shows the time in seconds and Y-axis shows the bit rate in Mbps. The graph shows the bit rate with delay 50ms, 100ms, 150ms and 200ms.

With low delay, TCP's transmission rate is very much high and it looks like a straight line. That means, there are no changes in bit rate as there was no congestion event or loss event in the environment at that moment. From Fig. 7, we see that with the increasing of delay, the bit rate decreases. With delay 200 ms, the bit rate is lower than with delay 150 ms.

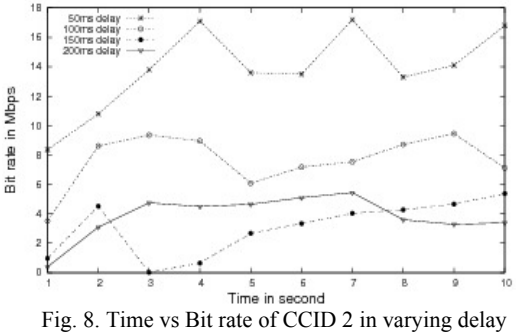

Fig. 8. Time vs Bit rate of CCID 2 in varying delay

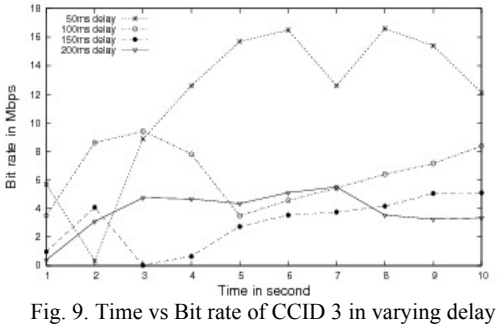

Fig. 9. Time vs Bit rate of CCID 3 in varying delay

Fig 8. and Fig. 9 shows CCID 2's and CCID 3's behavior in varying delay consecutively. Again the X-axis shows the time in seconds and Y-axis shows the bit rate in Mbps. The graphs show the bit rate at delay 50ms, 100ms, 150ms and 200ms. There is a subtle difference between the graph for TCP and the graphs for CCID 2 and CCID 3. CCID 2 and CCID 3's bit rate are very much low with delay 200ms.

B.3 LOSS VARIANT

Fig. 10 shows TCP's behavior in varying loss rate. The X-axis shows the time in seconds and Y-axis shows the bit rate in Mbps. The graph shows the throughput of TCP at loss rate 0%, 1%, 3%, 5%, 10% and 15%. When graph goes down, we can say, at that moment, a loss has

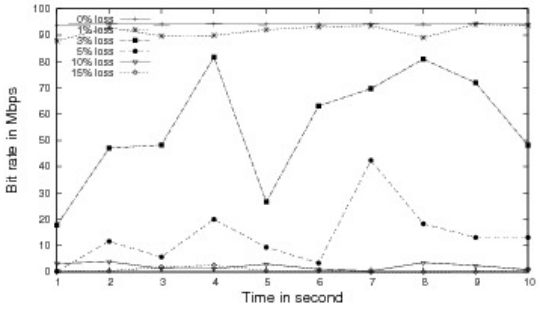

Fig. 10. Time vs Bit rate of TCP in varying loss rate

occurred and TCP sender reduces its transmission rate. When maximum loss occurs, sharpness can be seen on the graph.

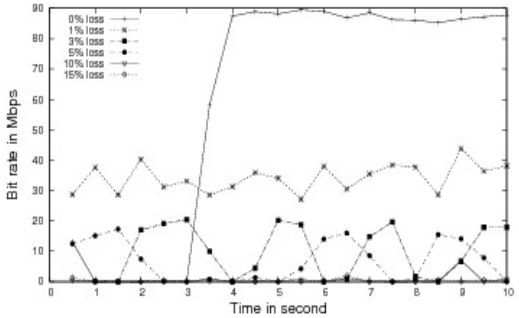

Fig. 11. Time vs Bit rate of CCID 2 in varying loss rate

Fig. 11 shows CCID 2's behavior in varying loss rate.

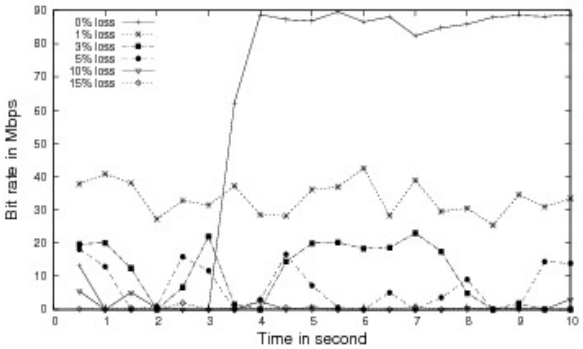

Fig. 12. Time vs Bit rate of CCID 3 in varying loss rate

Fig. 12 shows CCID 3's behavior in varying loss rate. Again the X-axis shows the time in seconds and Y-axis shows the bit rate in Mbps. The graph shows the bit rate at loss rate 0%, 1%, 3%, 5%, 10% and 15%. Sharp fall of the graph is less than the previous graph of TCP. But if we compare the graph for CCID 2 and CCID 3, we can see that CCID3 falls smoothly than CCID 2.

B.4 BEHAVIOR OF CCID 2 AND CCID 3

If we integrate the graph of CCID 2 and CCID 3, then we find the graph like Fig. 13.

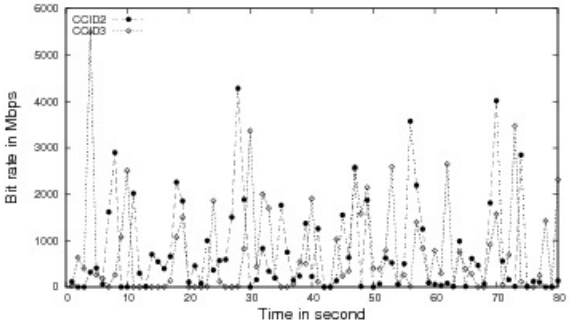

Fig. 13. Time vs Bit rate of CCID 2 and CCID 3 on 10% loss

The bit rate of the graph shows the characteristics of CCID 2 and CCID 3 with 10% loss. From this graph, we can see that the graph of CCID 2 is sharper than CCID 3 and CCID 3 goes smoothly.

The graphs which we have presented have been taken by emulating network. In the same environment and in the same network conditions, the bit rate may change and the graph behavior may change too. Even in some environment, CCID 2 changes smoothly than CCID 3. But most of the time, CCID 3 will be a bit smooth in bit rate than CCID 2. For these reasons, DCCP is till now experimental. To fix the characteristics of this protocol, many researches are going on DCCP.

VI. CONTRIBUTION AND FUTURE WORKS

In this paper, we have compared the protocol behavior of DCCP (Datagram Congestion Control Protocol) with mostly used protocol TCP. We have also compared the characteristics of Congestion Control Identifier 2 (CCID 2) and Congestion Control IDentifier 3 (CCID 3).

- From our experiments, we observe that with low delay, throughput of TCP is high and throughput of CCID 2 is close to TCP. Though the throughput of CCID 3 is not so good, its rate of changes is much smoother than CCID 2.
- From experimental graphs, we can ensure that there are no abrupt changes in bit rate of CCID 3. So, CCID 3 can be used for those applications that needs smooth rate.
- In varying loss rate, we found that TCP and CCID 2 take advantages of the available bandwidth in an environment. On the other hand,

CCID 3 does not use as much bandwidth as possible because it tries to minimize abrupt changes of bandwidth.

From all the experimental results it is clear that CCID 3 maintains a fair rate. It can be stated that CCID 3 can be a better choice for real time applications. DCCP can be used for those applications that suffer the trade-off between delay and in order delivery.

In future, we will further study, how to satisfy the dynamic requirements for multimedia applications. We will also try to transfer live audio/video files using congestion control mechanism CCID 3 and evaluate DCCP to long range wireless links. Finally, because DCCP is directed towards those applications which currently use UDP without any form of end-to-end congestion control, an area of interest would be to implement a layer of reliability on top of the DCCP layer.

VII. ACKNOWLEDGEMENT

I.S.C and J.L are grateful to chairperson, Professor Dr. Suraiya Pervin, Department of Computer science and Engineering, University of Dhaka, for her support and help and for giving us the opportunity to carry out the project work by providing us with the necessary resources and materials.

REFERENCES

[1] S. Floyd, M. Handley and E. Kohler. Problem statement for Datagram Congestion Control Protocol. IETF, RFC 4336, LA, USA, 2006.

[2] Stanimir Statev and Seferin Mirtchev. Experimental study of datagram congestion control protocol in varied network states. Technical report, Technical University of Sofia, Bulgaria, 2008.

[3] lwn.net-Linux info source http://lwn.net/Articles/149756/

[4] E. Kohler and M. Handly and S. Floyd. Datagram Congestion Control Protocol (DCCP). IETF, RFC 4330, LA, USA, 2006.

[5] S. Floyd and E. Kohler. Profile for Datagram Congestion Control Protocol (DCCP), Congestion Control ID 2: TCP-like Congestion Control. IETF, RFC 4330, LA, USA, 2006.

[6] Jitendra Padhye, Sally Floyd and Eddie Kohler. Profile for DCCP Congestion Control ID 3: TFRC Congestion Control. Internet Engineering Task Force, 2002

[7] S. Floyd, E. Kohler and J. Padhye. Profile for Datagram Congestion Control Protocol (DCCP), Congestion Control ID 3: TCP-Friendly Rate Control (TFRC). IETF, RFC 4342, LA, USA, 2006.

[8] the Linux kernel archives, http://www.kernel.org/

[9] Jon M.Dugan. Using Iperf. Lawrence Berkeley National Laboratory, NANOG 43, Brooklyn, NY, 2008

[10] gnuplot, http://www.duke.edu/hpgavin/gnuplot.htm

[11] wikipedia, http://en.wikipedia.org/wiki/Network emulation

[12] Ariane Keller and ETH Zurich. Packet Filtering and netem. tc manual, USA, 2006

[13] S. Floyd and K. Fall, Promoting the Use of End-to-End Congestion Control in the Internet, IEEE/ACM Transactions on Networking, August 1999.

[14] Timothy Sohn and Eiman Zolfaghari. Experimentation of the Datagram Control Protocol. California, USA, 2002.

[15] Horia Vlad Balan, Lars Eggert, Saverio Niccolini and Marcus Brunner, An Experimental Evaluation of Voice Quality over the Datagram Congestion Control Protocol, Appeared in INFOCOM 2007.26th IEEE International conference on computer communications. IEEE, Publication date:6-12 May 2007,on pages 2009-2017

[16] Saleem Bhatti and Martin Bateman and Dimitris Miras.A Comparative Performance Evaluation of DCCP. London, UK.

Proceedings of 2009 12th International Conference on Computer and Information Technology (ICCIT 2009)
21-23 December, 2009, Dhaka, Bangladesh

Performance Evaluation of Time Dependent Micro Macro Cellular Network Using MMPP Traffic

Mushlah Uddin Sarkar†, Md. Imdadul Islam‡, and M. R. Amin†
†Department of Electronics and Communications Engineering, East West University, Bangladesh
‡Department of Computer Science and Engineering, Jahangirnagar University, Bangladesh
shiplu_sarkar@hotmail.com, imdad@juniv.edu, ramin@ewubd.edu

Abstract

Two-dimensional (2D) and three-dimensional (3D) steady state Markov chains are widely used to analyze the traffic performance of communications networks. When the characteristics of the network changes with time, such steady state Markov chain is unable to determine different probability states. Markov Modulated Poisson Process (MMPP) is a special case of Markov Arrival Process (MAP) where arrival rate depends on probability states. In this paper, a traffic model of micro-macro cellular network of time dependent traffic load is modeled and its probability states are evaluated using MMPP varying load condition of the network under different parts of observation time.

Keywords: Counting Process, Kronecker sum, MAP, MMPP, Probability state and Sojourn time.

I. INTRODUCTION

To cope with ever increasing demand of offered traffic of users in a network, different strategies are taken to support overflow traffic. Micro-macro cellular system is the most popular technique to enhance the capacity of a mobile cellular network. In micro-macro cellular system several micro cells are overlaid by a big umbrella cell called macro cell. Initially, any offered traffic will search a channel of micro cell and incase of unavailability of that channel, call will be transferred to macro cell. Any call under macro cell will continuously monitor for a free channel of corresponding micro cell to make a take back. Offered traffic in a mobile cellular network varies depending on the time of the day. Since, call arrival rate depends on probability state at a certain time [1], [2], therefore, Markov modulated Poisson process (MMPP) is considered as a special case of Markov arrival process (MAP), is the best fit to analyze such traffic.

MAP is defined as a process $(N(t), J(t))_{t>>0}$ on the state space $\{(i,j); i \geq 0, 1 \leq j \leq m\}$; where $N(t)_{t>>0}$ is a counting process of "arrivals", indicated the number of arrivals in (0, t] and $J(t)_{t>>0}$ is a Markov process with a finite state space, $1 \leq j(t) \leq m$ of the underlying Markov chain. MAP is characterized with an infinitesimal generator matrix **Q** [3]-[5]:

$$\mathbf{Q}^* = \begin{bmatrix} \mathbf{C} & \mathbf{D} & 0 & 0 & \dots \\ 0 & \mathbf{C} & \mathbf{D} & 0 & \dots \\ 0 & 0 & \mathbf{C} & \mathbf{D} & \dots \\ \vdots & \vdots & \vdots & \vdots & \ddots \end{bmatrix}, \quad (1)$$

where both **C** and **D** are $m \times m$ matrices. The matrix **C** has negative diagonal elements and nonnegative off-diagonal elements where each element of **C** corresponds to state transition without arrival. The matrix **D** has nonnegative elements and each element correspond to transition with an arrival. The matrix **Q** is defined [6] as **Q=C+D.**

MMPP is a doubly stochastic process whose arrival rate is given by $\lambda[J(t)] \geq 0$ where $t \geq 0$, is an m-state irreducible Markov process. The arrival rate takes on only m values $\lambda_1, \lambda_2, \cdots\cdots, \lambda_m$ and equal to λ_j whenever the Markov process is in the state $j = 1,2,3, \cdots\cdots, m$. If the underlying Markov process has infinitesimal generator **Q** and **D**=diag$(\lambda_1, \lambda_2, \cdots\cdots, \lambda_m)$, then **C=Q-D**.

II. TRAFFIC MODEL

In this paper, we consider a micro-macro cellular system, expressed by a two state Markov chain, where states are indicated as i_m and i_M for micro cell and macro cell respectively. Here R different parts of a day or observation time are considered in drawing the Markov chain as in Fig. 1. The call arrival rate under Microcell during time slot i is λ_{im} and that of at macro cell is λ_{iM}. After a sojourn time at micro cell, the traffic of the network makes a transition from underload state (i_m) to overload state (i_M) with a rate λ_i'. Similarly, the transition rate from overload to underload state is μ_i'. The rate of transition from i-th to (i+1)-th time slot is $\sigma_{i,i+1}$. Therefore, the sojourn time of i-th time slot is $1/\sigma_{i,i+1}$ except for the R th and (R+1)-th time slot for which the sojourn time is $1/\sigma_{R,1}$ and $1/\sigma_{R+1,R+R}$ respectively [7]. The complete state transition chain for R different time slot of total observation time is shown in Fig. 1.

978-1-4244-6283-4/09/$26.00 ©2009 IEEE

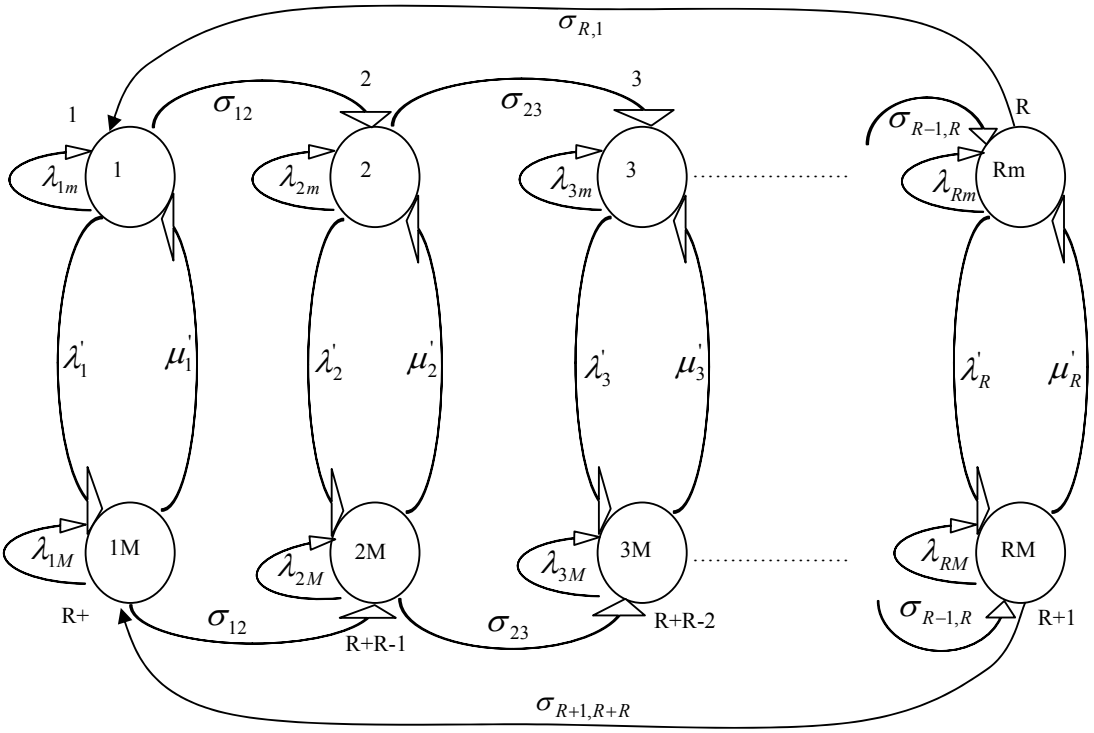

Fig. 1. State transition chain of micro macro cellular system taking R time slot over total observation time.

Let us determine **C** and **D** matrices of the Markov chain considering only two time slot of the entire observation time of Fig. 2. The matrices **C** and **D** are given as follows:

$$\mathbf{C}=\begin{bmatrix} -\lambda_{1m}-\sigma_{12}-\lambda_1' & \sigma_{12} & 0 & \lambda_1' \\ \sigma_{21} & -\lambda_{2m}-\sigma_{21}-\lambda_2' & \lambda_2' & 0 \\ 0 & \mu_2' & -\lambda_{2M}-\sigma_{34}-\mu_2' & \sigma_{34} \\ \mu_1' & 0 & \sigma_{43} & -\lambda_{1M}-\sigma_{43}-\mu_1' \end{bmatrix} \tag{2}$$

and

$$\mathbf{D}=\begin{bmatrix} \lambda_{1m} & 0 & 0 & 0 \\ 0 & \lambda_{2m} & 0 & 0 \\ 0 & 0 & \lambda_{2M} & 0 \\ 0 & 0 & 0 & \lambda_{1M} \end{bmatrix}. \tag{3}$$

The cumulative distribution function of the probability state is [8]

$$\mathbf{F(x)}=(\mathbf{I}-\exp(\mathbf{C}(x)))(-\mathbf{C})^{-1}\mathbf{D}; \tag{4}$$

where **I** is an identity matrix of same dimension.

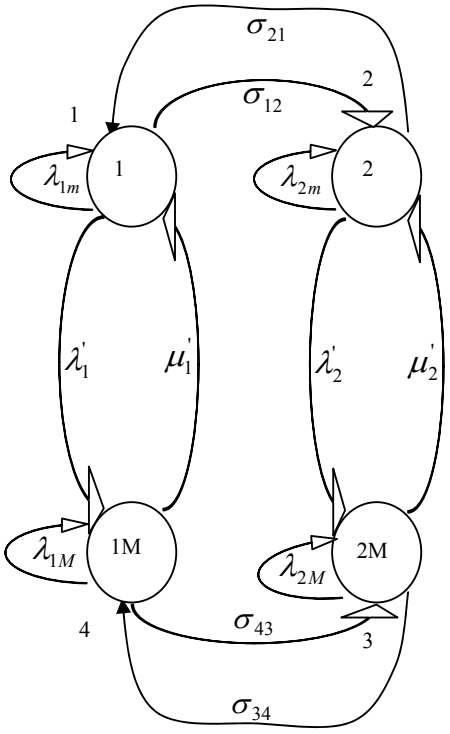

Fig. 2. State transition chain of the micro-macro cellular system considering two time slots over total observation time.

III. RESULTS

In this paper we have considered observation period of network traffic for 24 hours of a day and divided it into two time slots/duration. In duration one, traffic conditions of the network are chosen as

$$\lambda_{1m} > \lambda_{2m}, \lambda_{1M} > \lambda_{2M}; \sigma_{12} < \sigma_{21}; \lambda_1' < \mu_1'; \lambda_2' > \mu_2';$$
$$\sigma_{21} = \sigma_{34} \text{ and } \sigma_{12} = \sigma_{43}.$$

We take the following traffic parameters:

λ_{1m} =1.2, λ_{2m} =0.8, λ_{1M} =1.6, λ_{2M} =0.8, $\sigma_{12} = \sigma_{43}$ =0.

$\sigma_{21} = \sigma_{34}$ =0.8, λ_1' =0.6, λ_2' =0.4, μ_1' =0.4 and μ_2' =0.6.

The matrices **C** and **D** and steady state matrix **F** are found as

$$\mathbf{C} = \begin{bmatrix} -2.2 & 0.4 & 0 & 0.6 \\ 0.8 & -2.0 & 0.4 & 0 \\ 0 & 0.6 & -2.2 & 0.8 \\ 0.4 & 0 & 0.4 & -2.4 \end{bmatrix},$$

$$\mathbf{D} = \begin{bmatrix} 1.2 & 0 & 0 & 0 \\ 0 & 0.8 & 0 & 0 \\ 0 & 0 & 0.8 & 0 \\ 0 & 0 & 0 & 1.6 \end{bmatrix},$$

$$\mathbf{F} = \begin{bmatrix} 0.6298 & 0 & 0 & 0 \\ 0 & 0.4666 & 0 & 0 \\ 0 & 0 & 0.4184 & 0 \\ 0 & 0 & 0 & 0.7592 \end{bmatrix}.$$

Under this situation, the network is in overloaded condition in duration one and probability of staying in macro cell under that duration will be maximum. Similarly probability of staying in both micro- and macro- cells under duration two will be less then any state of duration one. Four probability states are plotted in Fig. 3, where P_{11} and P_{44} are the probabilities of staying in micro and macro cell under duration one and P_{22} and P_{33} are that of under duration two. The profile of four probability states support above traffic conditions.

In duration two, traffic conditions of the network are chosen like,

$$\lambda_{1m} < \lambda_{2m}, \ \lambda_{1M} < \lambda_{2M}; \ \sigma_{12} > \sigma_{21}; \ \lambda_1' > \mu_1';$$
$$\lambda_2' < \mu_2'; \sigma_{21} = \sigma_{34}; \sigma_{12} = \sigma_{43}.$$

Taking traffic parameters,

λ_{1m} =1.2, λ_{2m} =1.8, λ_{1M} =1.6, λ_{2M} =2.8, $\sigma_{12} = \sigma_{43}$ =1.4,

$\sigma_{21} = \sigma_{34}$ =0.8, λ_1' =0.4, λ_2' =0.8, μ_1' =0.6, μ_2' =0.2.

Corresponding matrices **C** and **D** and steady state matrix **F** are found as

$$\mathbf{C} = \begin{bmatrix} -3.0 & 1.4 & 0 & 0.4 \\ 0.8 & -3.4 & 0.8 & 0 \\ 0 & 0.2 & -3.8 & 0.8 \\ 0.6 & 0 & 1.4 & -3.6 \end{bmatrix},$$

$$\mathbf{D} = \begin{bmatrix} 1.2 & 0 & 0 & 0 \\ 0 & 1.8 & 0 & 0 \\ 0 & 0 & 2.8 & 0 \\ 0 & 0 & 0 & 1.6 \end{bmatrix},$$

$$\mathbf{F} = \begin{bmatrix} 0.4654 & 0 & 0 & 0 \\ 0 & 0.6093 & 0 & 0 \\ 0 & 0 & 0.8215 & 0 \\ 0 & 0 & 0 & 0.5011 \end{bmatrix}.$$

At this situation, the network is in overloaded condition in duration two and probability of staying in macro cell under that duration will be maximum. Similarly probability of staying in both micro- and macro- cells under duration one will be less then any state of duration two. The profile of four probability states of Fig. 4 supports above traffic conditions.

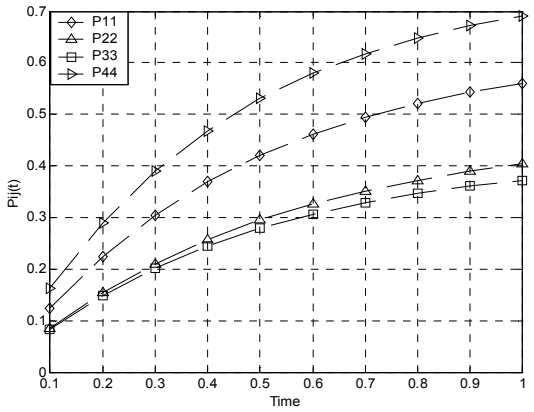

Fig. 3. Variation of probability of states with time when the network is overloaded in second observation time.

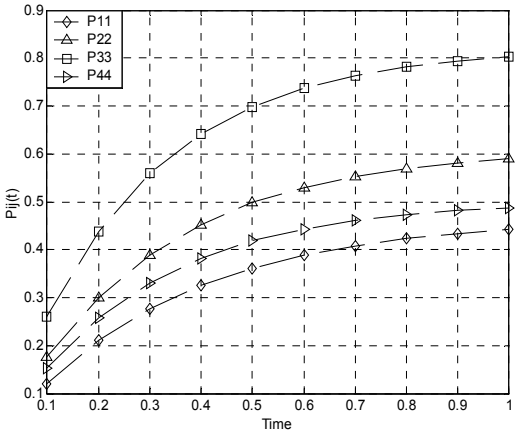

Fig. 4. Variation of probability of states with time when the network is overloaded in first observation time.

$$\mathbf{C} = \begin{bmatrix}
-5.2 & 1.4 & 0 & 0.4 & 0.4 & 0 & 0 & 0 & 0 & 0 & 0 & 0 & 0.6 & 0 & 0 & 0 \\
0.8 & -5.6 & 0.8 & 0 & 0 & 0.4 & 0 & 0 & 0 & 0 & 0 & 0 & 0 & 0.6 & 0 & 0 \\
0 & 0.2 & -6.0 & 0.8 & 0 & 0 & 0.4 & 0 & 0 & 0 & 0 & 0 & 0 & 0 & 0.6 & 0 \\
0.6 & 0 & 1.4 & -5.8 & 0 & 0 & 0 & 0.4 & 0 & 0 & 0 & 0 & 0 & 0 & 0 & 0.6 \\
0.8 & 0 & 0 & 0 & -5.0 & 1.4 & 0 & 0.4 & 0.4 & 0 & 0 & 0 & 0 & 0 & 0 & 0 \\
0 & 0.8 & 0 & 0 & 0.8 & -5.4 & 0.8 & 0 & 0 & 0.4 & 0 & 0 & 0 & 0 & 0 & 0 \\
0 & 0 & 0.8 & 0 & 0 & 0.2 & -5.8 & 0.8 & 0 & 0 & 0.4 & 0 & 0 & 0 & 0 & 0 \\
0 & 0 & 0 & 0.8 & 0.6 & 0 & 1.4 & -5.6 & 0 & 0 & 0 & 0.4 & 0 & 0 & 0 & 0 \\
0 & 0 & 0 & 0 & 0.6 & 0 & 0 & 0 & -5.2 & 1.4 & 0 & 0.4 & 0.8 & 0 & 0 & 0 \\
0 & 0 & 0 & 0 & 0 & 0.6 & 0 & 0 & 0.8 & -5.6 & 0.8 & 0 & 0 & 0.8 & 0 & 0 \\
0 & 0 & 0 & 0 & 0 & 0 & 0.6 & 0 & 0 & 0.2 & -6.0 & 0.8 & 0 & 0 & 0.8 & 0 \\
0 & 0 & 0 & 0 & 0 & 0 & 0 & 0.6 & 0.6 & 0 & 1.4 & -5.8 & 0 & 0 & 0 & 0.8 \\
0.4 & 0 & 0 & 0 & 0 & 0 & 0 & 0 & 0.4 & 0 & 0 & 0 & -5.4 & 1.4 & 0 & 0.4 \\
0 & 0.4 & 0 & 0 & 0 & 0 & 0 & 0 & 0 & 0.4 & 0 & 0 & 0.8 & -5.8 & 0.8 & 0 \\
0 & 0 & 0.4 & 0 & 0 & 0 & 0 & 0 & 0 & 0 & 0.4 & 0 & 0 & 0.2 & -6.2 & 0.8 \\
0 & 0 & 0 & 0.4 & 0 & 0 & 0 & 0 & 0 & 0 & 0 & 0.4 & 0.6 & 0 & 1.4 & -6.0
\end{bmatrix}$$

$$\mathbf{D} = \begin{bmatrix}
2.4 & 0 & 0 & 0 & 0 & 0 & 0 & 0 & 0 & 0 & 0 & 0 & 0 & 0 & 0 & 0 \\
0 & 3.0 & 0 & 0 & 0 & 0 & 0 & 0 & 0 & 0 & 0 & 0 & 0 & 0 & 0 & 0 \\
0 & 0 & 4.0 & 0 & 0 & 0 & 0 & 0 & 0 & 0 & 0 & 0 & 0 & 0 & 0 & 0 \\
0 & 0 & 0 & 2.8 & 0 & 0 & 0 & 0 & 0 & 0 & 0 & 0 & 0 & 0 & 0 & 0 \\
0 & 0 & 0 & 0 & 2.0 & 0 & 0 & 0 & 0 & 0 & 0 & 0 & 0 & 0 & 0 & 0 \\
0 & 0 & 0 & 0 & 0 & 2.6 & 0 & 0 & 0 & 0 & 0 & 0 & 0 & 0 & 0 & 0 \\
0 & 0 & 0 & 0 & 0 & 0 & 3.6 & 0 & 0 & 0 & 0 & 0 & 0 & 0 & 0 & 0 \\
0 & 0 & 0 & 0 & 0 & 0 & 0 & 2.4 & 0 & 0 & 0 & 0 & 0 & 0 & 0 & 0 \\
0 & 0 & 0 & 0 & 0 & 0 & 0 & 0 & 2.0 & 0 & 0 & 0 & 0 & 0 & 0 & 0 \\
0 & 0 & 0 & 0 & 0 & 0 & 0 & 0 & 0 & 2.6 & 0 & 0 & 0 & 0 & 0 & 0 \\
0 & 0 & 0 & 0 & 0 & 0 & 0 & 0 & 0 & 0 & 3.6 & 0 & 0 & 0 & 0 & 0 \\
0 & 0 & 0 & 0 & 0 & 0 & 0 & 0 & 0 & 0 & 0 & 2.4 & 0 & 0 & 0 & 0 \\
0 & 0 & 0 & 0 & 0 & 0 & 0 & 0 & 0 & 0 & 0 & 0 & 2.8 & 0 & 0 & 0 \\
0 & 0 & 0 & 0 & 0 & 0 & 0 & 0 & 0 & 0 & 0 & 0 & 0 & 3.4 & 0 & 0 \\
0 & 0 & 0 & 0 & 0 & 0 & 0 & 0 & 0 & 0 & 0 & 0 & 0 & 0 & 4.4 & 0 \\
0 & 0 & 0 & 0 & 0 & 0 & 0 & 0 & 0 & 0 & 0 & 0 & 0 & 0 & 0 & 3.2
\end{bmatrix}$$

If several networks under different service providers exist simultaneously in a common service area and each of them follows MMPP traffic then the combined traffic can be modeled by the superposition of individual traffic. In this case, matrices **C** and **D** will be the Kronecker sum [9]-[11] of individual matrices **C** and **D** derived as

$$\mathbf{C} = \mathbf{C_1} \oplus \mathbf{C_2} = \mathbf{C_1} \otimes \boldsymbol{I_m} + \boldsymbol{I_n} \otimes \mathbf{C_2}$$

and

$$\mathbf{D} = \mathbf{D_1} \oplus \mathbf{D_2} = \mathbf{D_1} \otimes \boldsymbol{I_m} + \boldsymbol{I_n} \otimes \mathbf{D_2}\,.$$

where $\boldsymbol{I_m}$ and $\boldsymbol{I_n}$ represent identity matrices with appropriate dimensions, which may be different for the different networks.

V. CONCLUSION

In this paper, only two probability states per time slot are considered for simplicity of analysis. The graphs of the result section support the theoretical approach of the paper, as mentioned earlier, which validates our analysis. This traffic model will be helpful for a network operator for management of traffic load of a network. Other intermediate states like delay of voice end user can be incorporated like MAP (n) for better results. The traffic model used in this paper can also be used for comparison of performance of different call admission schemes, for example, Dynamic Partition (DP), Guard Channel (GC), and Dual threshold Bandwidth Reservation (DTBR) schemes, etc.

REFERENCES

[1] Seok K. Hwang · Dongsoo S. Kim, *"Markov model of link connectivity in mobile ad hoc networks,"* Springer, Telecommun. Sys., vol. 34, no. 1-2, pp. 51–58, Feb. 2007.

[2] Sheldon M. Ross, *"Introduction to Probability Models"* 7th Edition, ISBN-81-7867-055-0, pp.216-225, Academic Press, A Harcourt Science and Technology Company, San Diego, USA, 2001.

[3] D. M. Lucantoni, K. S. Meier-Hellstern, and M. F. Neuts, *"A single-server queue with server vacations and a class of nonrenewal arrival processes,"* Advances in Applied Probability, vol. 22, no. 3, pp. 676–705, 1990.

[4] D. M. Lucantoni, *"New results for the single server queue with a batch Markovian arrival process,"* Stochastic Models, vol. 7, no. 1, pp. 1-46, 1991.

[5] M. F. Neuts, *"Structures Stochastic Matrices of M/G/1 type and their Applications,"* New York: Marcel Dekker, 1989.

[6] Sang H. Kang, Yong Han Kim, Dan K. Sung and Bong D. Choi, *"An application of Markovian Arrival Process (MAP) to modeling superposed ATM cell stream,"* IEEE Transaction on Communications, vol. 50, no.4, pp.633-642, April 2002.

[7] D. Niyato, E. Hossain, and A. S. Alfa, *"Performance analysis of multi-service wireless cellular networks with MMPP call arrival patterns,"* Global Telecommunications Conference, 2004. GLOBECOM apos; 04. IEEE, Volume 5, Issue, Page(s): 3078 – 3082, vol.5, 29 Nov– 3 Dec. 2004.

[8] M. F. Neuts, *"Models based on Markovian arrival process,"* IEICE Trans, Commun, vol. E75-B, pp. 1255-1265, Dec. 1992.

[9] Laub, A.J. *"Matrix Analysis for Scientists and Engineers",* Society for Industrial and Applied Mathematics (2005).

[10] Yujuan Bao, Ilker N. Bozkurt, Tu Grul Dayar, Xiaobai Sun, and Kishor S. Trivedi, *"DECOMPOSITIONAL ANALYSIS OF KRONECKER STRUCTURED MARKOV CHAINS,"* Electronic Transactions on Numerical Analysis, vol. 31, pp. 271-294, 2008.

[11] Guy L. Curry, Natarajan Gautam, *"CHARACTERIZING THE DEPARTURE PROCESS FROM A TWO SERVER MARKOVIAN QUEUE: A NON-RENEWAL APPROACH",* Proceedings of the 2008 Winter Simulation Conference, S. J. Mason, R. R. Hill, L. Mönch, O. Rose, T. Jefferson, J. W. Fowler Eds.

Proceedings of 2009 12th International Conference on Computer and Information Technology (ICCIT 2009)
21-23 December, 2009, Dhaka, Bangladesh

Logical Clock based Last Update Consistency model for Distributed Shared Memory

Rubaiyat Islam Rafat, Kazi Muheymin Sakib
Institute of Information Technology, University of Dhaka, Dhaka, Dhaka, Bangladesh
rafat.mit.806@gmail.com, sakib@univdhaka.edu

Abstract

Excessive locking and cumulative updates in Distributed Shared Memory (DSM) not only reduces the parallelism for block access but also causes a serious degradation in response time for a dense network. This paper proposes a new consistency model in DSM named Last Update Consistency (LUC) model, where the model uses logical clock counter to keep the DSM consistent. The logical clock always increases never decreases. So the increasing order of the logical clock value is used to provide the request to the DSM. In this model, multiple nodes can perform READ operations over the same block at a time. For WRITE operation over the same block, only the last modification will exist and the earlier WRITE operations will be treated as obsolete WRITE and should be discarded. The experimental and analytical analysis showed that the proposed model effectively reduces the unnecessary network traffic and cumulative block updates that exist in the Sequential Consistency Model and Release Consistency Model.

Keywords: Consistency Model, Distributed Shared Memory, Distributed System, Shared Memory, Timestamp Protocol.

I. INTRODUCTION

Increasing network density invokes the scalability issue for DSM. When large number of nodes exists in the distributed system, regular broadcast of block modification not only degrades the performance of DSM but also abuse the network traffic of the system. Cumulative block modification is another factor that degrades the performance of DSM and becomes a threat for the existing limited storage structure [1].

When a DSM model provides more concentration on sequential consistency, parallelism is reduced as a trade off. For maintaining consistency, one phase locking and two phases locking (SHARED and EXCLUSIVE) protocol [2] have been used by Release Consistency (RC) and Entry Consistency (EC) models. But both of these models are highly infected with cumulative modification of blocks updates. Although the ancient Sequential Consistency (SC) model is free from cumulative updates, it does not free from broadcasting block updates to the irrelevant nodes in the DSM [3].

If a DSM model uses different techniques for maintaining sequential consistency rather than locking mechanism, the higher response time issue in DSM might be minimized. Such a technique should be Timestamp Based Protocol. The proposed Last Update Consistency (LUC) model uses Timestamp based protocol or logical clock counter to maintain sequential consistency because Timestamp based protocol is easy to implement and always ensures sequential consistency.

If the view level of data is considered, we can see that the user always get the last updated view of the data, no matter how and who has modified the data. Under this phenomenon, the cumulative updates of data are useless for the view layer of the user. If we want to ensure view consistency [4] and optimize our storage structure, we need to clean up the cumulative updates and keep the last modified data in the DSM. The proposed LUC model ensures view consistency [5] by storing only the last updated data.

The experimental result shows that the bytes transferred and response time for both WRITE and initial WRITE (UPLOAD) operation for different models considerably differs from each other. RC model shows better performance in bytes transferred for UPLOAD operation, while scores worst on response time for WRITE operation. SC model scores well in response time for WRITE operation but stuck on bytes transferred for UPLOAD. On the other hand, the proposed LUC model performs better for both the cases compared to existing consistency models. In response time comparison, LUC model improves 24% (average) over SC model and 32.5% (average) over RC model. In network traffic comparison, LUC model improves 22% (average) over SC model and 44% (average) over RC model.

The rest of the paper is organized as follows; second section elaborates important and widely used consistency models for DSM and necessary Background study for developing LUC model. Third section describes the proposed model, how this model operates in DSM and underlying algorithms of LUC model. Forth section focuses on analytical information and comparative study between LUC model and other existing consistency models. Fifth section illustrates performance analysis of LUC model and other existing consistency models. The next section provides improvement discussion of LUC model for network traffic and response time factors and finally a summary of this paper and future scope of this model is discussed in the Conclusion section.

II. BACKGROUND AND RELATED WORK

This section elaborates important and widely used consistency models for DSM and related background study for developing LUC model. This section is divided into two sub sections namely, Related Works and Thomas Write Rule. First subsection focuses on the major contributions and research works regarding to DSM. Second subsection focuses on the major problem of Timestamp based protocol and how to overcome the problem using Thomas Write Rule.

A. Related Work

In the following sub section important research solutions for improving efficiency of the existing DSM system has been discussed.

Cristiana Amza in her paper describes Trademarks [6] DSM system that implements Lazy Release Consistency (LRC) model [7]. This model does not require the update propagation at release time. Although, the Lazy Release Consistency (LRC) model improves the Release Consistency (RC) model [8] by performing time selection and processor selection, the unnecessary update propagation is further postponed and stored until another processor has successfully executed an acquire phase.

Bershad, describes Midway [9], a DSM that introduces a new consistency Model - The Entry Consistency (EC) model [2] that tried to remove the propagation of useless updates in LRC by requiring the programmer to annotate association between ordinary data objects and synchronization data objects (e.g. locks). Although the useless updates are prohibited in this model, the cumulative updates still remain in this system.

L. Iftode et al. in their paper describe another new consistency model namely, The Scope Consistency (ScC) model [10]. This model is very similar to EC, except it can partially automate the association between ordinary data objects and synchronization data objects by introducing the concept of consistency scope. The major disadvantage of this technique is, scopes have to be explicitly annotated by the programmer for non-critical regions. If the annotation is not correct, ScC cannot guarantee Sequential Consistency for the program.

Object based DSM [11] is another type of DSM where a document is considered as an object. The Parent Class inherits the critical sections of the Child class, so false sharing and network traffic is reduced in such a system. LUC model is implemented on page based DSM not based on object based DSM.

Different consistency models emphasizes on different factors. SC model emphasizes more on sequential consistency but highly infected with increasing network traffic due to broadcasting updates. RC model emphasizes more on locking mechanism but highly infected with increasing network traffic and response time due to cumulative updates and excessive locking. LRC model emphasizes more on propagation of network traffic but highly infected with increasing volume of storage, uses for cumulative updates. EC model emphasizes more on removing unnecessary locking mechanism but highly infected with increasing volume of storage, uses for cumulative updates. ScC model emphasizes more on scope annotation but highly infected to guarantee sequential consistency, if the scope annotation is not correct. So, the users of DSM demand such a model that not only overcomes the above limitations of the existing models but also ensures high degree of parallelism. The proposed LUC model tries to overcome the limitations of the existing models. It ensures sequential consistency, reduces the network traffic and response time, free from cumulative updates and also ensures view consistency that increases the parallelism in DSM.

B. Thomas Write Rule

While implementing the Timestamp based protocol one major challenge was obsolete write operation. When a later node executes a write operation over the same block that was writing in previous by another node, the earlier node's write operation has been treated as an obsolete write because only the latest modification will exist in the system. To avoid such problem LUC model uses Thomas Write Rule provided by R.H. Thomas [12] for obsolete write operation.

$$\begin{bmatrix} T1 & T2 \\ R(A) & \\ & W(A) \\ & Com. \\ W(A) & \\ Com. & \end{bmatrix}$$

Fig. 1. A non conflicting serialize able transaction schedule

$$\begin{bmatrix} T1 & T2 \\ R(A) & \\ W(A) & \\ Com. & \\ & W(A) \\ & Com. \end{bmatrix}$$

Fig. 2. Equivalent non conflicting serialize able transaction schedule

Thomas Write Rule states that if Timestamp on a transaction *T* is *TS (T)* and Write Timestamp on an object *O* is *WTS (O)* and such a situation occurs that, *TS (T)* < *WTS (O)* then the current write action has been made obsolete by the most recent write of *O*, which follows the current write according to Timestamp ordering. If we consider a non-conflict serialize able transaction schedule *S* where *T1* and *T2* transactions can perform concurrently then Thomas Write Rule relies on the fact that *T1*'s write on object *A* is never seen by any transaction and postulates that the schedule in Figure-1 is equivalent to the schedule in Figure-2, where *T2* occurs strictly after *T1*, and that hence the write of *T1* can be ignored. This happens because the view level of data only gets the last modification of the data and all previous modification are ignored.

III. PROPOSED MODEL FOR CONSISTENCY IN DISTRIBUTED SHARED MEMORY

For developing LUC Model, a page based DSM system has been chosen like IVY [13]. The sequential consistency is maintained by the incremental order of Timestamp or logical clock counter that only increases and

never decreases. In this model, the DSM manager will maintain a LUC matrix for tracking the request and response of different nodes in DSM (Table 1). When a node wants to perform a READ or WRITE operation, the DSM manager will provide that node a logical counter value C_i. If the operation is a READ operation, the request type will be treated as Read Request (RRQ) (Table 1), if it is a WRITE operation, Write Request (WRQ) (Table 1). If a node found itself as a obsolete block writer, it will discard its modification over that block and sends an Urgent Update Request (UURQ) (Table 1) to the later block writer informing the node to send the updated block. After proper modification, the later node found that already an UURQ is waiting for updated block; it will replicate and migrate the updated block to the requester node and sends an Update Complete (UC) (Table 1) message to the LUC matrix.

Table I Last Update Consistency Matrix

Request	Counter	Node	Block	Operation
WRQ	1	P_1	A	Write
WRQ	2	P_3	A	Write
UURQ	3	P_1	A	Wait
UC	4	P_3	A	Update
RRQ	5	P_2	A	Read

Next when any other node wants to perform READ operation over the same block but does not contain the replicated copy of the block will search in the LUC matrix for the last updated block owner and replicate and migrate the block for READ. One of the main features of LUC Model is, only the last updated block will exist in the system and any obsolete write operations will be discarded according to Thomas write rule. This mechanism should relief us from the cumulative updates problem. Moreover, the logical clock counter not only ensures sequential consistency but also reduces memory and time consumption from two phase locking mechanism.

A. LUC Algorithm

Initially the LUC matrix remains empty and the counter initiates with 1 [Algorithm 1, line 1].The incoming operations on DSM are categorized into 3 categories namely, READ, WRITE and UPLOAD (Initial WRITE). If a READ operation occurs then READ algorithm performs. If a WRITE operation occurs then WRITE algorithm performs else the block is uploaded into DSM. Finally the counter is incremented with 1 [Algorithm 1, line 10].

Algorithm 1 LUC Algorithm

Require: $LUC_{matrix} = empty$

```
1:  C(n) ⇐ 1
2:  for all Operations do
3:    if READ then
4:      READ Algorithm
5:    else if WRITE then
6:      WRITE Algorithm
7:    else
8:      UploadBlock to DSM
9:    end if
10:   C(n) ⇐ C(n) + 1
11: end for
```

Fig. 3. Last Update Consistency Algorithm

B. READ Algorithm

First of all READ algorithm search the LUC matrix for any request type containing UC [Algorithm 2, line 2, 3].

Algorithm 2 READ Algorithm

```
1:  repeat
2:    BSearch(LUC_matrix)
3:  until RQ_type = UC
4:  if Found then
5:    if TS ≠ (n − 1) then
6:      repeat
7:        BSearch(LUC_matrix)
8:      until RQ_type = WRQ
9:      if Found then
10:       LUC_matrix ⇐ RQ_type(UURQ)
11:       break
12:     end if
13:   end if
14:   if Node = own then
15:     LUC_matrix ⇐ RQ_type(RRQ)
16:     StartRead
17:   else {Node = other}
18:     RMB
19:     LUC_matrix ⇐ RQ_type(RRQ)
20:     StartRead
21:   end if
22: else
23:   RMB from Initial Uploaded Node
24:   LUC_matrix ⇐ RQ_type(RRQ)
25:   StartRead
26: end if
```

Fig. 4. The READ Algorithm for LUC Matrix

If no record exists, the requested node replicate and migrate the block from the original uploaded node and inserts a record containing request type RRQ in the LUC matrix [Algorithm 2, line 23].If any record exists [Algorithm 2, line 4], the requested node search LUC matrix for any request type containing WRQ [Algorithm 2, line 8].If any record exists, that record indicates currently writing over the block. So, the requested node inserts an UURQ type request in the LUC matrix [Algorithm 2, line 10] and waits for updated block from the modifying node. Now if the last modified node is the requesting node itself, it starts READ operation and inserts a entry containing request type RRQ in the LUC matrix [Algorithm 2, line 14]. Otherwise, replicate and migrate the block from the last modified node and insert a record containing request type RRQ in the LUC matrix [Algorithm 2, line 18].

C. WRITE Algorithm

First of all, WRITE algorithm search the LUC matrix for any request type containing UC [Algorithm 3, line 2, 3].

```
Algorithm 3 WRITE Algorithm
 1: repeat
 2:    BSearch(LUC_matrix)
 3: until RQ_type = UC
 4: if Found then
 5:    if TS ≠ (n − 1) then
 6:       repeat
 7:          BSearch(LUC_matrix)
 8:       until RQ_type = WRQ
 9:       if Found then
10:          LUC_matrix ⇐ RQ_type(UURQ)
11:          break
12:       end if
13:    end if
14:    if Node = own then
15:       LUC_matrix ⇐ RQ_type(WRQ)
16:       StartWrite
17:    else {Node = other}
18:       RMB
19:       LUC_matrix ⇐ RQ_type(WRQ)
20:       StartWrite
21:    end if
22:    repeat
23:       BSearch(LUC_matrix)
24:    until RQ_type = UURQ
25:    if Found then
26:       C(n) ⇐ C(n) + 1
27:       RMB to the Requested Nodes
28:       LUC_matrix ⇐ RQ_type(UC)
29:    end if
30: else
31:    RMB from Initial Uploaded Node
32:    LUC_matrix ⇐ RQ_type(WRQ)
33:    StartWrite
34: end if
```

Fig. 5. The WRITE Algorithm for LUC Matrix

If no record exists, the requested node replicate and migrate the block for writing from the original uploaded node and inserts a record containing request type WRQ in the LUC matrix [Algorithm 3, line 30]. If any record exists in the matrix [Algorithm 3, line 4], the requested node looks for any request type containing WRQ [Algorithm 3, line 8]. If any record exists, that record indicates currently writing over the block. So, the requested node inserts an UURQ type request in the LUC matrix [Algorithm 3, line 10] and waits for updated block from the modifying node. Now if the last modified node is the requesting node itself, it starts WRITE operation and inserts a entry containing request type WRQ in the LUC matrix [Algorithm 3, line 14]. Otherwise, replicate and migrate the block from the last modified node and insert a record containing request type WRQ in the LUC matrix [Algorithm 3, line 18]. Now, WRITE algorithm search the LUC matrix again for any request type containing UURQ [Algorithm 3, line 23]. If any record exists, the current node replicates and migrate the block to the requested node submitting request type UURQ and inserts an entry for UC [Algorithm 3, line 30].

IV. ANALYTICAL ANALYSIS

It is difficult to provide a generic equation or a mathematical expression to measure the performance of any consistency model, but in general for measuring the network traffic or transferred block for any consistency model a general mathematical expression can be expressed as follows-

A. Sequential Consistency Model

For READ operation SC model transmits an ACK message (M) to all existing nodes (n) in DSM and transmits respective block size (B') for read in network traffic. For WRITE operation SC model transmits both ACK message (M) and respective block size (B) for write to all existing nodes (n) in DSM.

$$f_r(x) = \sum_{i=1}^{n-1} M_i + B' \tag{1}$$

$$f_w(x) = \sum_{i=1}^{n-1} M_i + \sum_{i=1}^{n} B_i \tag{2}$$

B. Release Consistency Model

For READ operation RC model transmits an ACK message (M) to all relevant nodes (n') in DSM and transmits respective block size (B') for read in network traffic. In addition if any cumulative updates exist (p) for any node then that also transmits. For WRITE operation RC model transmits ACK message (M) to all relevant nodes (n') in DSM and transmits respective block size (B) for write in DSM. In addition if any cumulative updates exist for any node then that also transmits.

$$f_r(x) = \sum_{i=1}^{n'-1} M_i + B' + \sum_{i=0}^{p} B_i \tag{3}$$

$$f_w(x) = \sum_{i=1}^{n'-1} M_i + \sum_{i=1}^{p} B_i \tag{4}$$

C. Last Update Consistency Model

For READ operation LUC model transmits a ACK message (M) to all relevant nodes (n') in DSM and transmits respective block size (B') for read in network traffic. For WRITE operation LUC model transmits ACK message (M) to all relevant nodes (n') in DSM and transmits respective block size (B) for write in DSM.

$$f_r(x) = \sum_{i=1}^{n'-1} M_i + B' + \sum_{i=0}^{p} B_i \tag{5}$$

$$f_w(x) = \sum_{i=1}^{n'-1} M_i + \sum_{i=1}^{p} B_i \tag{6}$$

In the above equations it is considered that the bytes transferred for write operation is considerably greater than the bytes transferred for read operation and bytes transferred for read operation is considerably greater than the bytes transferred to DSM manager for acknowledgment. Also the total number of nodes is considerably greater than the selective nodes of the network containing the same block.

V. EXPERIMENTAL PERFORMANCE ANALYSIS

For comparing the performance between two existing consistency models and the LUC model, two major factors have been chosen. They are Network Traffic and Response Time for accomplishment of the operations. Initially, Sequential Consistency (SC) model and Release Consistency (RC) model have been developed and then the proposed Last Update Consistency (LUC)

model has been developed. The Network Traffic Analysis and Response Time Analysis depend on different factors, like in Response Time Analysis the nature of the system (Homogenous/ Heterogeneous) affects more. So, Homogenous system has been used where all nodes have the same components.

A. System Environment Description

For experiment, 6 nodes had been used. Each node contained individual DSM manager for memory mapping. All nodes had identically similar processing power and memory. For developing the system a wired distributed network was chosen where all nodes were connected by bus topology.

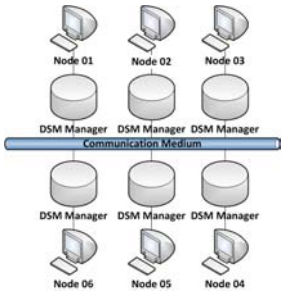

Fig. 6. System Architecture

A. Response Time Analysis

The graph shows that the RC model shows off worst performance compare to other models, because of its cumulative update nature. RC model's performance degradation is proportional to the network density. The graph also shows that the LUC model performs best in this experiment because of its optimized resource using strategy.

B. Network Traffic Analysis

The graph shows that the RC model shows off worst performance compare to other models, because of its cumulative update nature. RC model's performance degradation is proportional to the network density. The graph also shows that the LUC model performs best in this experiment because of its optimized resource using strategy.

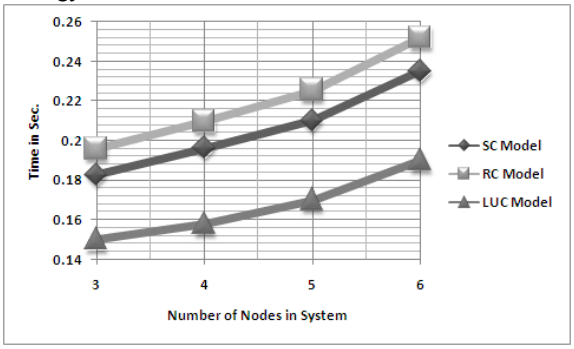

Fig. 7. Response Time Performance Analysis for WRITE Operation

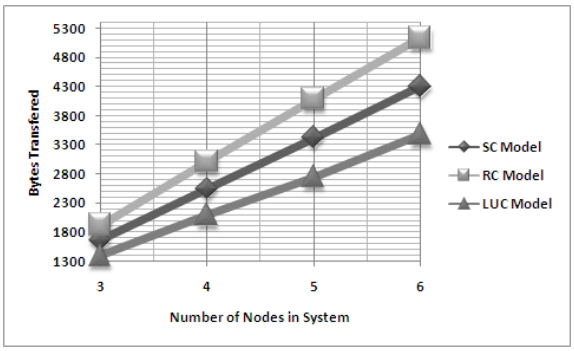

Fig. 8. Network Traffic Performance Analysis for WRITE Operation

B. Improvement Analysis

Firstly, the improvement of LUC model over SC model in Response Time shows an exponential curve having the incremental improvement of 21.73%, 24.11%, 24.82% and 25.11% with respect to scalability issue. The average improvement is 23.95%.

Secondly, the improvement of LUC model over RC model in Response Time shows an exponential curve having the incremental improvement of 30.47%, 32.59%, 33.35% and 33.68% with respect to scalability issue. The average improvement is 32.52%.

Thirdly, the improvement of LUC model over SC model in Network Traffic shows an exponential curve having the incremental improvement of 19.11%, 21.89%, 22.92% and 23.56% with respect to scalability issue. The average improvement is 21.87%.

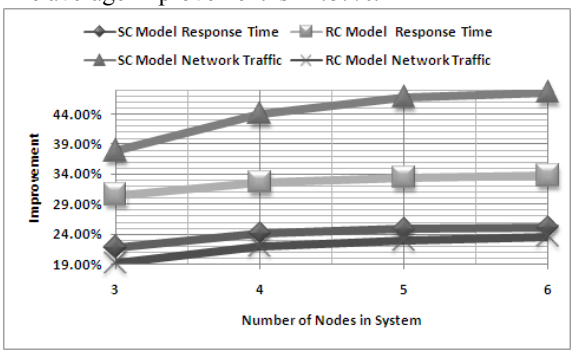

Fig. 9. Improvement of LUC Model over SC Model and RC Model on Network Traffic and Response Time

Finally, the improvement of LUC model over RC model in Network Traffic also shows an exponential curve having the incremental improvement of 37.79%, 44.01%, 46.77% and 47.56% with respect to scalability issue. The average improvement is 44.03%.

VI. DISCUSSION

In this section the improvement of LUC model over RC and SC model in different factors is being discussed.

Firstly, the improvement of LUC model over SC model in Response Time shows an average improvement of 23.95%. Secondly, the improvement of LUC model over RC model in Response Time shows an average

improvement of 32.52%. So, LUC model increases improvement of 8.57% over RC model than SC model. RC model decreases its performance in response time for excessive locking mechanism (both READ and WRITE) and cumulative update propagation. SC model is free from cumulative update propagation so it scores better than RC model. Thirdly, the improvement of LUC model over SC model in Network Traffic shows an average improvement of 21.87%. Finally, the improvement of LUC model over RC model in Network Traffic shows an average improvement of 44.03%. So, LUC model increases improvement of 22.16% over RC model than SC model. RC model decreases its performance in network traffic for cumulative update propagation. SC model is free from cumulative update propagation so it scores better than RC model. LUC model is infected neither cumulative updates nor excessive locking mechanism and shows the best result in both response time analysis and network traffic analysis.

VII. CONCLUSION

The major contribution of this paper over the concept DSM is to provide a new model that reduces the network traffic and response time while accessing DSM. The existing DSM systems use locking mechanisms for ensuring sequential consistency and do not ensure view consistency. LUC model has been developed on Logical Clock that reduces excessive locking mechanisms and ensures sequential consistency. Moreover, LUC model ensures view consistency by committing only the last modified data and discarding the obsolete write operations [12].

LUC model successfully shows its improvement over different aspects between two most popular existing consistency models namely SC model and RC model. LUC model improves 22% in Network Traffic over SC model and 44% in over RC model. On the other hand, LUC model improves 24% in Response Time over SC model and 32.5% in over RC model. Although the response time and bytes transferred has been mitigated by this model, the programmer's annotation and the code complexity of the LUC model increased highly. This is the trade off for LUC that the network traffic and response time has been optimized but the difficulty to implement and uses of local memory increases badly. For large scale distributed system Network Traffic and Response Time for receiving a service are major concerns rather how much local memory is used by the system. So for a large scale distributed system LUC model should be chosen over the existing consistency models.

In this proposed model, page based DSM is considered because it is simple and easy to implement. In Future we will implement LUC model for object based DSM [11] to reduce False Sharing and Network Traffic of the system.

REFERENCES

[1] John P Ryan, Brian A. Coghlan, "Distributed Shared Memory in a Grid Environment" *John Von Neumann Institute for Computing. NIC Series*, vol. 33, 2006, pp.129–136.

[2] B. N. Bershad, "Shared Memory Parallel Programming with Entry Consistency for Distributed Memory Multiprocessors" *CMU Technical Report, CMU-CS-91-170*, September 1991.

[3] Chengzheng Sun, Zhiyi Huang, Wanju lei, Saitar A., "Toward Transparent Selective Sequential Consistency in Distributed Shared Memory Systems", *Proc. 18th International Conference on Distributed Computing Systems*, 26-29 Issue, May 1998, pp.572–581.

[4] Z. Huang, C. Sun, M. Purvis, and S. Cranefield, "View-based Consistency and Its Implementation", *Proc. of the First IEEE/ACM Symposium on Cluster Computing and the Grid, IEEE Computer Society*, 2001, pp.74–81.

[5] C. Sun, Z. Huang, W.J. Lei, and A. Sattar, "Towards Transparent Selective Sequential Consistency in Distributed Shared Memory Systems", *Proc. of the 18th IEEE International Conference on Distributed Computing Systems*, Amsterdam, May 1998, pp.572–581.

[6] C. Amza, "Tread Marks: Shared memory computing on networks of workstations", *IEEE Computer*, vol.29 (2), February 1996, pp.18–28.

[7] P. Keleher, "Lazy Release Consistency for Distributed Shared Memory", Ph.D. Thesis, Dept. of Computer Science, Rice University, 1995.

[8] K. Gharachorloo, D. Lenoski, J. Laudon, "Memory consistency and event ordering in scalable shared memory multiprocessors", *Proc. of the 17th Annual International Symposium on Computer Architecture*, May 1990, pp.15–26.

[9] B. N. Bershad, "The Midway Distributed Shared Memory System", *Proc. of IEEE COMPCON Conference, 1993*, pp.528–537.

[10] L. Iftode, J. P. Singh and K. Li, "Scope Consistency: A Bridge between Release Consistency and Entry Consistency", *Proc. of the 8th Annual ACM Symposium on Parallel Algorithms and Architectures*, 1996, pp.277–287.

[11] Deo Prakash Vidyarthi, Kirti Rani, "Distributed Shared Memory for Object Allocation in DCS" *International Journal of Information Technology and Management*, 2006, pp.87–91.

[12] R. H. Thomas, "A Majority Consensus Approach to Concurrency Control", *ACM Transactions on Database Systems*, vol. 4, no. 2, 1979, pp.180–219.

[13] K. Li, P. Hudak, "Memory Coherence in Shared Virtual Memory Systems" *ACM Transaction on Computer Systems*, vol. 7, November 1989, pp.321–359.

Proceedings of 2009 12th International Conference on Computer and Information Technology (ICCIT 2009)
21-23 December, 2009, Dhaka, Bangladesh

Performance Evaluation of Heterogeneous Network for Next Generation Mobile

Abu Sayed Chowdhury, Mark Gregory
School of Electrical and Computer Engineering, RMIT University, Melbourne, Australia
s3191682@student.rmit.edu.au, mark.gregory@rmit.edu.au

Abstract

It is a universally stated design requirement that next generation mobile systems will be compatible and interoperable with IPv6 and with various access technologies such as 802.11x. The current growth of WLANs worldwide has yielded a demand to integrate with existing 3G mobile technologies. Interworking incorporates all of the best features of an individual network into a single integrated system thus providing ubiquitous data services with high data rates in WLAN hotspots. The attempt to build hybrid networks has been linked with many technical challenges such as seamless vertical handovers across WLAN/3G radio technologies, security, common authentication, unified accounting & billing, etc. This paper evaluates the performance of two 3G/WLAN integration schemes: Tight and Loose Coupling. Mobile IP is used as a mobility management scheme and EAP-AKA for common authentication.

Keywords: WLAN, 3G, Mobile IP, EAP-AKA, VOIP Codec.

I. INTRODUCTION

One of the goals for next generation mobile systems is to provide better access and integration with existing Internet Protocol (IP) based networks. Successful integration of the third–generation cellular network (3G) and wireless local area networks (WLAN 802.11x) would be a step along the path towards a next generation network. The 3G network aims to provide customers with a highly developed global service providing circuit switched or packet switched traffic; new mobile multimedia services (e.g. streaming/mobile TV, location base services, downloads, multi-user games) giving more flexibility for the operator to introduce new services to its portfolio and from the user point of view, more services and a variety of higher, on-demand data rates compared with the previous 2.5-2.75G mobile system. However existing 3G implementations have a moderate data rate and high-priced wide area deployment. WLAN on the other hand have been deployed in small areas or hotspots and are cost-effective, easy to deploy and provide high data rates in an unlicensed frequency band. WLAN was not designed for wide area deployment. In order to provide large varieties of services at high data rate in the hotspots and campus-wide areas, 3G service providers regard WLAN as a technology to compliment their 3G system. Thus, efficient authentication and a mobility management scheme are crucial to support a heterogeneous domain and a seamless handover scheme is needed to ensure the success of 3G/WLAN interworking. The concept of integrating two or more access networks to provide ubiquitous service to mobile users is not new. Considerable research has been completed focusing on interworking issues between WLAN and the Universal Mobile Telecommunication System (UMTS) networks including 3G mobile networks [1-5]. In heterogeneous network literature, a terminal with a double communication capability allows the user to switch connection from one radio access network to another without packet loss [6, 7]. Studies may be found on the performance of these hybrid WLAN/UMTS networks for various internet applications. For example, Song and Jamalipur [8] focus on the performance of a network selection algorithm rather than individual traffic sessions. The performance of a loose coupling architecture with regard to the continuity of real-time video traffic for UMTS connections was modelled by Salkintzis, et al. [9]. Kumudu and Abbas [10] have proposed an IP Multimedia Subsystem (IMS) based integration where the system presented can manage real time sessions with the use of the IMS as a unified session controller. In [4], Salkintzis proposed architectures that enable 3G subscribers to benefit from high throughput IP connectivity in strategic hotspot locations. Salkintzis also discussed authentication, authorisation, accounting (AAA) signaling for interworking 3G/WLAN rather than analysing performance. Finally, Abu-Amara, et al. [11] present the performance of loose coupling and open coupling with two mobility schemes. The results presented by Abu-Amara, et al. provided the motivation to analyse the performance of loose coupling and tight coupling with various internet applications. The paper is organized as follows: Section ii provides an overview of 3G/WLAN interworking; Section iii presents the mobile IP based interworking; Section iv presents the authenticate key agreement scheme for the integration of 3G/WLAN; Section v briefly describes the system being tested; Section vi describes the simulation strategy for the network design and Section vii provides a discussion of the simulation results. Finally, in Section viii conclusions are presented.

II. OVERVIEW OF 3G-WLAN INTERWORKING

UMTS/WLAN is currently being studied within the 3GPP [12]. Until now, WLAN is mainly operated as an extension of the 3GPP access network. A literature re-

978-1-4244-6283-4/09/$26.00 ©2009 IEEE

view highlighted four interworking architecture approaches: tight coupling, loose coupling, open coupling and very tight coupling.

A. Open Coupling

In an open coupling scheme WLAN and UMTS use their own separate access and transport networks and billing and user management occurs through different authentication mechanisms.

B. Loose Coupling

In a loose coupling scheme the use of a common authentication mechanism provides a link between the authentication, authorisation and accounting (AAA) server in the WLAN network and the Home Location Register (HLR) in the UMTS network. In other words, loose coupling provides the subscribers with access to the 3G based packet services without making any changes to the WLAN and UMTS protocols. The key element to support mobility management in this architecture is mobile IP [13]. However, there are other variants to this coupling, which may involve the user data traffic being routed to the UMTS Core Network (CN) [3, 4]. The data traffic is routed directly via an IP network which is an advantage of this method.

C. Tight Coupling

The tight coupling scheme integrates two networks at the CN level where a WLAN Access Point (AP) is connected as a Radio Network Controller (RNC) to the UMTS Service GPRS Support Node (SGSN) to support the handover between WLAN and UMTS networks. In other words, tight coupling makes two different radio access technologies work together with a single core network. The key functional element in the system is the handover between a WLAN and a UMTS network and this may be likened to the handover occurring between two individual wireless network cells. The tight coupling integration scheme includes the reuse of UMTS AAA mechanisms, usage of common subscriber databases and billing systems, and increased security features (since the UMTS security mechanisms are reused). Tight coupling provides for the possibility of continuous sessions as users move across the two networks, since the handoff in this case is very similar to an intra-UMTS handoff as the WLAN AP appears as another RNC to the SGSN node. An obvious benefit of this approach is that the UMTS mobility management techniques can be directly applied.

D. Very Tight Coupling

The very tight coupling approach is the same as that in the tight coupling scheme with the addition that the WLAN AP is connected to the RNC.

III. MOBILE IP BASED INTERWORKING

Mobile IP is one of the most popular network layer solutions for IP network mobility and it fulfils the requirement to maintain internet connectivity throughout user sessions. When integrating 3G and WLAN, mobile IP is employed to restructure the connections while a Mobile Station (MS) moves from one network to another, eg. from UMTS to WLAN. Outside of the UMTS network, the MS is identified by a Care of Address (COA) associated with its point of attachment to the UMTS network. Encapsulation and packet delivery is managed by a collocated foreign agent. In a loose coupling scheme network integration mobile IP is used to support mobility management.

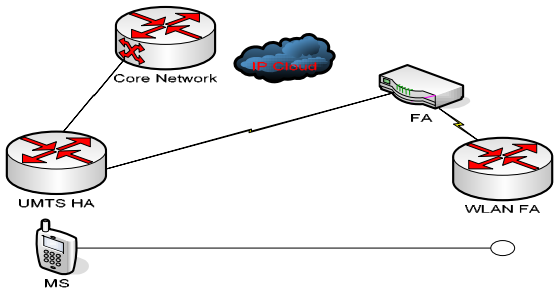

Fig. 1. Mobile IP showing session continuity with handover

IV. AUTHENTICATE KEY AGREEMENT

EAP-AKA was proposed by the 3GPP to provide access security for 3G/WLAN interworking [14]. It is based on the UMTS-AKA mechanism. In the EAP-AKA scheme the 3G home domain does not delegate the responsibility for authentication to the WLAN network. EAP-AKA was used for authentication of 3G/WLAN during the simulations presented in this paper. A successful EAP-AKA procedure is illustrated in Figure 2.

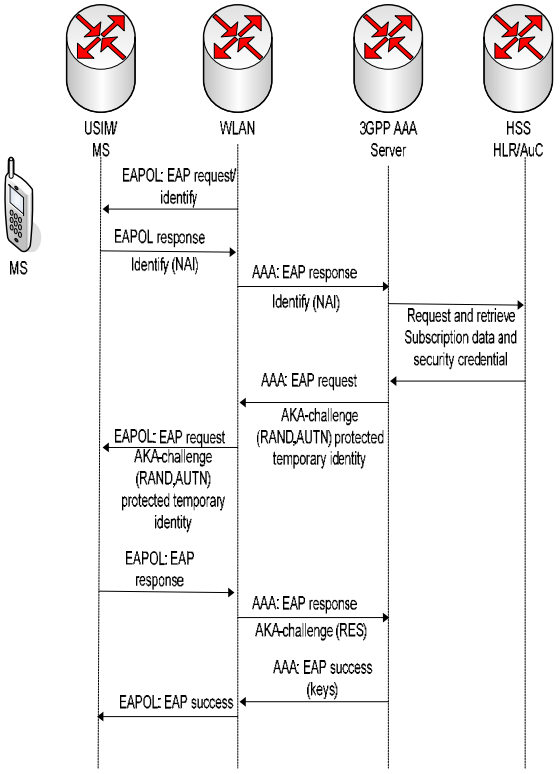

Fig. 2. EAP-AKA Procedure

V. VOIP CODEC

A codec (Coder/Decoder) converts analogue signals to a digital bit stream, and another identical codec is placed at the far end of the communication system to convert the digital bit stream back into an analogue signal. In a Voice over IP (VoIP) system, codecs are used to convert voice signals into digital data to be transmitted over the Internet or any IP based digital network supporting VoIP calls. Some codecs also support silence suppression, where silence is not encoded and transmitted. In Table 1 the codecs that were used in the simulation are identified.

Table I Simulation VoIP Codecs

Codec	Algorithm	Bit rate (Kbps)
ITU G.711	PCM (Pulse Code Modulation)	64
ITU G.729A	CS-ACELP (Conjugate Structure Algebraic-Code Excited Linear Prediction)	8
GSM FR	RPE-LTP (Regular Pulse Excitation Long-Term Prediction)	13

VI. SIMULATED NETWORK DESIGN ARCHITECTURE

This section describes the simulation model and the applications used to evaluate the performance of tight and loose coupling. In this research Opnet Modeler 15.0 [15] was used to simulate the hybrid UMTS and WLAN network. OPNET is a very flexible tool which provides drag and drop facilities for the communication devices like (routers, user equipments, and servers), interconnecting models (ATM link, fiber optics, both wired and wireless LAN and PPP links) and multiple protocols. However, Opnet doesn't provide some of the major components needed in the network such as AAA, HLR, 3GAAA, Mobile IP under UMTS model and the EAP-AKA protocol. All of the additional components have been developed during this research. Two network scenarios were developed and the first included a tight coupling scheme and the second included a loose coupling scheme.

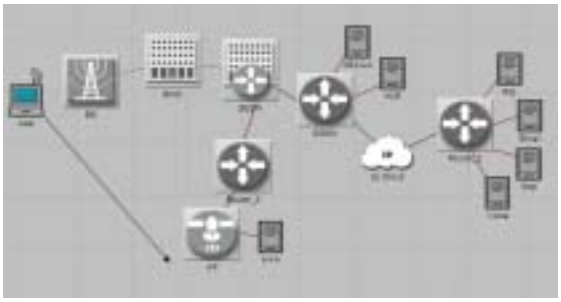

Fig. 3. Tight Coupling

A 3G model was combined with a 802.11g model to evaluate the network performance. In the tight coupling scheme a WLAN AP was connected through a router to a UMTS CN at the SGSN node while in the case of the loose coupling scheme the AP was connected through the router to an IP cloud. The service applications used in the simulation were added to the network design and the applications included ftp, http, email and VoIP. The network design for the two scenarios is shown in Figure 3 and Figure 4.

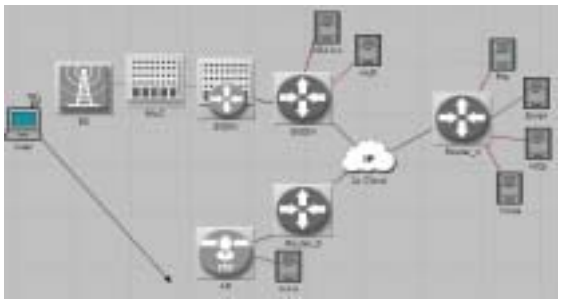

Fig. 4. Loose Coupling

VII. RESULT ANALYSIS

In this section the simulation results will be presented and discussed. Figure 5 shows the jitter for the three different VoIP codecs used for both coupling schemes. Jitter, the variation of packet or cell inter-arrival delay, is another factor which affects delay, especially during a handoff.

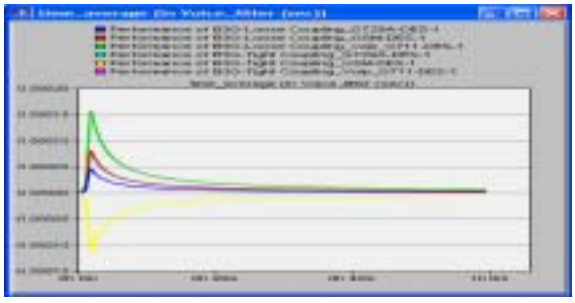

Fig. 5. Jitter for 3G/WLAN

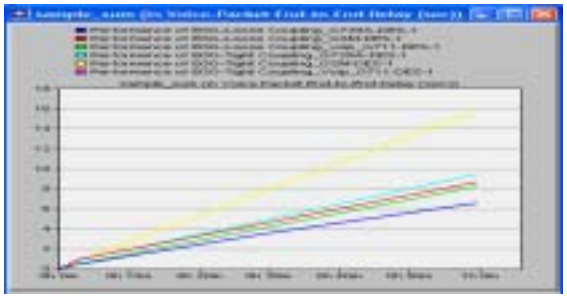

Fig. 6. End to End Delay for a VoIP application

Figure 6 shows the end to end delay for voice packets. From the result of Figure 5 and Figure 6, loose coupling with G729A give a better performance overall with less jitter and end to end delay. The simulation results for tight coupling with GSM included negative jitter. Negative jitter indicates that the time difference between the packets at the destination node was less than that at the source node. However, considering the end-to-end delay tight coupling with GSM was found to have greater delay when compared to loose coupling with G729A.

Figure 7, represents the ftp download and upload response time for both coupling schemes. To download files loose coupling had a lower response time though at the beginning of the simulation when traffic was reduced loose coupling was slower to get response when compared to tight coupling. However, as traffic increases the results showed that tight coupling was not as responsive as loose coupling. On the other hand, for uploading files the simulation results showed that tight coupling had a lower response time.

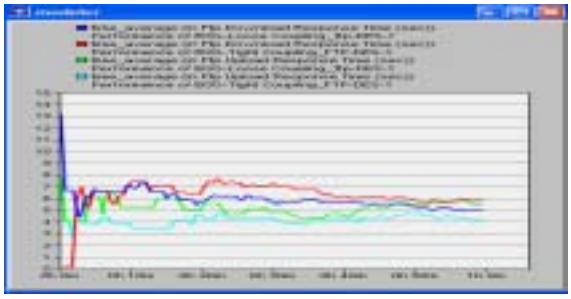

Fig. 7. FTP response time

In Figure 8, both coupling schemes provided roughly equal response times though at the beginning of the simulation when traffic was lower the loose coupling scheme provided a lower response time when compared to tight coupling. However, during the peak traffic as the simulation progressed the response time for both coupling schemes decreased. Regarding the http page response time as shown in Figure 9 tight coupling had a lower response time, though for an object the response time of loose coupling provided better performance.

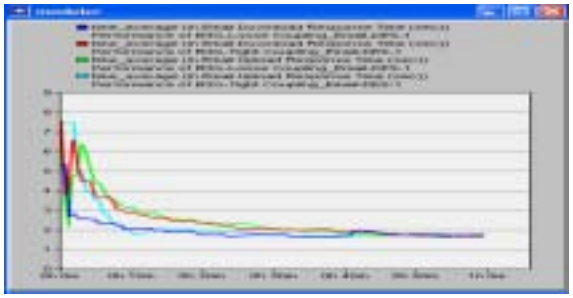

Fig. 8. Email response time

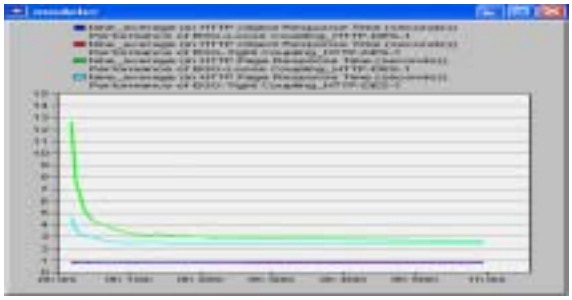

Fig. 9. HTTP response time

VIII. CONCLUSION AND FUTURE WORK

This research highlights that tight and loose coupling have advantages depending on the application. For VoIP loose coupling with the G729A codec provides lower jitter and end to end delay. Loose coupling was also found to provide a lower response time for a http page although when fetching http objects tight coupling provides a lower response time. Tight coupling provides a lower response time for ftp file uploads however to download ftp files loose coupling provides a lower response time. Tight and loose coupling were found to be comparable when downloading and uploading emails. To implement tight coupling changes to the protocols used in WLAN are necessary. Loose coupling may be implemented more readily and provides simplicity and efficiency for 3G/WLAN integration. Prospective research work may include how to reduce the http page and ftp file upload response time for loose coupling.

REFERENCES

[1] Shiao-Li Tsao; Chia-Ching Lin; "Design and evaluation of UMTS-WLAN interworking strategies", *Proceedings. VTC 2002-Fall*, IEEE 56th Volume 2, pp.777 - 781, Sept. 2002.

[2] Muhammad Jaseemuddin. "An Architecture for Integrating UMTS and 802.11 WLAN Networks", *8th IEEE ISCC*, p.716, 2003.

[3] Apostolis K. Salkintzis, "Interworking Techniques And Architectures For WLAN/3G Integration Toward 4G Mobile Data Networks," IEEE Wireless Communications, vol. 11, June 2004, pp. 50-61.

[4] A. Salkintzis, "WLAN/3G Interworking Architectures for Next Generation Hybrid Data Networks", IEEE International Conference on Communications 2004, Vol. 7, pp. 3984-3988.

[5] C. Liu and C. Zhou, "HCRAS: A novel hybrid interworking architecture between WLAN and UMTS cellular networks", IEEE Second Consumer Communications and Networking Conference, (CCNC), 2005, pp. 374-379. processing, 2005 Fifth International Conference page(s): 607-612.

[6] F. Siddiqui,S. Zeadally and S. Fowler, A Novel Architecture for Roaming between 3G and Wireless LANs, 1st International Conference on Multimedia Services Access Networks, MSAN'05, 2005.

[7] Abdul-Aziz Al Helali, Ashraf Mahmoud, Talal Al-Kharobi, Tarek Sheltami, "A Novel Dual-Mode User Equipment Design and Enhanced Gateway Selection Algorithm for B3G Networks" Parallel Processing - Workshops, 2008. ICPP-W '08, pp. 162-166, ISSN: 1530-2016, September 2008.

[8] Q. Song; A. Jamalipour, "Network Selection in an Integrated Wireless LAN and UMTS Environment Using Mathematical Modeling and Computing Techniques," IEEE Wireless Communications, Vol. 12, Issue 3, pp. 42- 48, 2005.

[9] A. Salkintzis, G. Dimitriadis, D. Skyrianoglou, N. Passas, N. Pavlidou, "Seamless Continuity of Real-Time Video Across UMTS and WLAN Networks: Challenges and Performance Evaluation," IEEE

Wireless Communications, Vol. 12, Issue 3, pp. 8-18, 2005.

[10] K. S. Munasinghe and A. Jamalipour, "Interworking of WLAN-UMTS Networks: An IMS-based Platform for Session Mobility," IEEE Communications, vol. 46, no. 9, pp. 184-191, 2008.

[11] Marwan Abu-Amara, Ashraf Mahmoud, Tarek Sheltami, Adel Al- Shahrani, Khalid Al-Otaibi, S.M.Rehman, and Taha Anwar, “Performance of UMTS/WLAN Integration at Hot-Spot Locations Using OPNET” IEEEGCC 2007, ID Code: 1463, June 2008.

[12] 3GPP, Technical Specification Group Services and System Aspects; 3GPP system to Wireless Local Area Network (WLAN) interworking; System description (Release 7), 3GPP TS 23.234 v7.4.0 Dec. 2006.

[13] V. Varma, S. Ramesh, K.D. Wong, M. Barton, G. Hayward and J. Friedhoffer. “Mobility Management in Integrated UMTS/WLAN Networks”, *IEEE ICC*, Anchorage, Alaska, USA, May 2003.

[14] Arkko, J. and Haverinen, H., “EAP-AKA Authentication”, <draft-arkko pppext-eap-aka- 12.txt>, June 2004.

[15] OPNET Modeler 15.0, http://www.opnet.com.

Proceedings of 2009 12th International Conference on Computer and Information Technology (ICCIT 2009)
21-23 December, 2009, Dhaka, Bangladesh

Performance Analysis of a MIMO-OFDM Wireless Link with STBC in the Presence of Fading and Timing Jitter

A. K. M. Nazrul Islam, S. P. Majumder†
Dept of EECE, Military Institute of Science and Technology (MIST),
Mirpur Cantonment, Dhaka-1216, Bangladesh
† Dept of EEE, Bangladesh University of Engineering and Technology (BUET),
Dhaka-1000, Bangladesh
nazrul_4620@yahoo.com, spmajumder@eee.buet.ac.bd

Abstract

The performance of a wireless communication system is analyzed considering multi-carrier OFDM with Multiple-Input-Multiple-Output (MIMO) wireless channel and Space-Time Block Coding (STBC). Bit Error Rate (BER) expression for MIMO-OFDM system without and with STBC is presented considering fading and timing jitter with QPSK, DPSK and DQPSK modulation schemes. The performance results are evaluated without and with rate ½ convolution coding with hard decision decoding. The results are presented in terms of BER, power penalty due to fading and coding gain due to error correction coding. It is noticed that there is significant power penalty due to fading and can be reduced by increasing the number of receiving antennas. Among the different modulation schemes QPSK is found to provide the best performance.

Keywords: Diversity, MIMO, OFDM, Rayleigh and Rician fading, STBC, and Timing jitter.

I. INTRODUCTION

Techniques to improve spectral efficiency and overcome various channel impairments such as signal fading and interference [1], [2] have made an enormous contribution to the growth of wireless communications. MIMO [3], [4] based communication system are capable of accomplishing these objectives. MIMO system take advantage of spatial diversity [1], [3] obtained through the spatially separated antennas in a dense multi-path scattering environment. Theoretical studies indicates that the capacity of MIMO systems grows linearly with the number of transmit antennas used. OFDM [2] is a promising multi-carrier modulation scheme that shows high spectral efficiency and robustness to frequency selective channels. In OFDM, a frequency selective channel is divided into a number of parallel frequency flat subchannels, thereby reducing the receiver complexity in signal processing of the system. The combination of MIMO and OFDM is a promising technique to achieve high bandwidth efficiency and system performances [5], [6]. STBC [3], [7], [8], and convolution codes [1] introduced to generalize the transmission scheme to an arbitrary number of transmit antennas and is able to achieve the full diversity promised by transmit and receive antennas. These codes retain the property of having a very simple maximum likelihood decoding algorithm based only on linear processing at the receiver.

The purpose of this paper is to analyze and evaluate the performance of the space–time block codes and convolution code with MIMO-OFDM in fading environment including timing jitter [12] with the application of different modulation schemes [9]-[13]. Then we provide analytical and simulation results confirming that the system achieves a significant performance gain at almost no processing expense.

II. SYSTEM MODEL OF MIMO-OFDM WITH STBC

The system model of a MIMO-OFDM with STBC considered for analysis is shown in fig. 1. The input serial data stream b[n] is formatted into the word size required for transmission by serial to parallel conversion. The data is then transmitted in parallel by assigning each data word to one carrier in the transmission. The data to be transmitted on each carrier is mapped into a format. The data is encoded by STBC to achieve coding and diversity gain [1], [3].

Cyclic Prefix (CP) is added at the transmitted symbol and removed at the receiver before the demodulation to avoid Inter Symbol Interference (ISI) and Inter Carrier Interference (ICI) [2]. The symbols are then converted back to a serial time waveform as the baseband signal for the OFDM transmission. OFDM modulation is computed on each set of symbols by Inverse Fast Fourier Transform (IFFT), on the input "signal" x_n. The Discrete Fourier Transform (DFT) computes the X_k from the x_n, while the Inverse Discrete Fourier Transform (IDFT) shows how to compute the x_n as a sum of sinusoidal components $X_k \exp(2\pi ikn/N)/N$ with frequency k / N cycles per sample. The diversity in transmission is achieved by multiple transmit antennas which helps to utilize the space diversity also. The channel is time-selective rayleigh/rician fading with AWGN.

The *receiver* does the reverse operation to the transmitter. The guard period is removed and the DFT of each symbol is then carried out to find the original transmitted spectrum and returns to N parallel streams. The-

978-1-4244-6283-4/09/$26.00 ©2009 IEEE

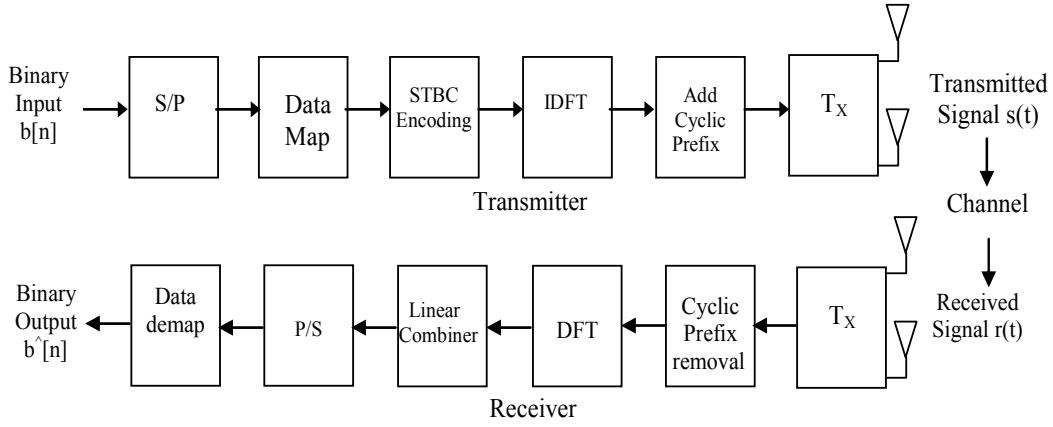

Fig. 1. System model of MIMO-OFDM with STBC

phase angle of each transmitted carrier is then evaluated and converted back to binary stream by demodulating the received phase. These streams are then recombined into a serial stream, $\hat{b}[n]$ which is an estimate of the original binary stream at the transmitter.

III. ANALYSIS OF MIMO-OFDM SYSTEM

Let, MIMO-OFDM system with P number of transmitting and N_R receiving antennas with Ns number of OFDM sub-carriers in time-selective rayleigh and rician fading channel is to map the binary input data to a modulation symbols {a(i)} that are assumed to have the following properties:

$$E[a(i)] = 0; \quad E[a(i)\, a^*(j)] = 1, \; i=j \qquad (1)$$
$$= 0, \; i \neq j$$

The input sequence {a(i)}, i=0, 1, 2 …….. (N_sP-1)} is serial-to-parallel converted into P sequences each of length N_s, as $a_p(k)= a(k+(p-1)N_s)$ where, p=1, 2……P and k=0, 1, 2……$(N_s -1)$ Each of the N_s sequences {$a_1(k)$ …….. $a_P(k)$}, k=0,1,2……..,$(N_s -1)$ is mapped to a matrix Ψ_k of size P×P by using a quasi orthogonal STBC with constellation rotation. For P=4, the 4×4 quasi orthogonal scheme is given as [10]:

$$\Psi_k = \begin{bmatrix} a_1(k) & -a_2^*(k) & e^{j\Phi}a_3(k) & -e^{-j\Phi}a_4^*(k) \\ a_2(k) & a_1^*(k) & e^{j\Phi}a_4(k) & e^{-j\Phi}a_3^*(k) \\ e^{j\Phi}a_3(k) & -e^{-j\Phi}a_4^*(k) & a_1(k) & -a_2^*(k) \\ e^{j\Phi}a_4(k) & e^{-j\Phi}a_3^*(k) & a_2(k) & a_1^*(k) \end{bmatrix} \qquad (2)$$

where, the rotation angle Φ depends on the signal constellation. Then we take the IDFT of Ψ_1, Ψ_2, …… Ψ_k in order to form the transmitted signal as:

$$S_m = \frac{1}{\sqrt{N_s}} \sum \Psi_k . e^{j(2\pi/Ns)mk}, \; m=0,1\ldots\ldots(Ns-1) \qquad (3)$$

S_m is a P×P matrix, which represents the transmitted signals on the m_{th} subcarrier. We define

$$\Psi=[\Psi_0^T, \ldots\ldots\ldots\ldots \Psi_{Ns-1}^T]^T, \; (N_sP \times P) \qquad (4)$$

$$S=[S_0^T, \ldots\ldots\ldots\ldots S_{Ns-1}^T]^T, \; (N_sP \times P) \qquad (5)$$

where, $(.)^T$ denotes transpose, then S can be written as:

$$S=(U \otimes I_p)^H \Psi \qquad (6)$$

Here, $(.)^H$ denotes complex conjugate transpose, $\otimes$ denotes kronecker product, I_p is the P×P identity matrix, and U is the $N_s \times N_s$ unitary discrete fourier transform matrix. In frequency-selective fading channels with L resolvable paths, there exists inter-block interference (IBI). To minimize this IBI, a cyclic prefix of length c_p ($c_p \geq L$) is added to each OFDM symbol. At the receiver, the cyclic prefix is discarded, leaving IBI-free, information-bearing signals. The model of the channel with L resolvable multipath components can be expressed as:

$$h(\tau) = \sum_{l=0}^{L-1} \rho_l \delta(\tau - \tau_l T_s) \qquad (7)$$

where, ρ_l is the zero-mean complex Gaussian random variable, and τ_l is the delay of the *l*th path normalized with respect to T_s. The delays τ_l is assumed to be uniformly distributed over the cyclic prefix c_p. The channel has an exponential power-delay profile $\theta(\tau_l) = e^{-\frac{\tau_l}{\tau_{rms}}}$, where τ_{rms} represents the rms delay spread, also normalized with respect to T_s. The P symbols in each column of Ψ_k are transmitted from the P transmit antennas simultaneously during every OFDM symbol period. Considering the channel matrix H the received signals is expressed in an $N_s \times P$ matrix as:

$$R=HS+V, \qquad (8)$$

where, $V=[v_0, \ldots\ldots v_{Ns-1}]^T$, $(N_s \times P)$ is the additive white gaussian noise (AWGN) matrix whose elements are independent and identically distributed. Hence,

$$E[vec(V).vec(V)^H] = \sigma^2 I_{NsP} \qquad (9)$$

where, σ^2 is the variance of the zero-mean noise samples when the transmitted symbol energy is normalized to unity. In the presence of time-selective fading, H is no longer a block-circulant matrix. Consequently, $G = UH(U \otimes I_P)^H$ is not a block diagonal matrix. This shows that time-selective fading causes ICI, which is represented by the off-diagonal blocks of G. The received signal R is processed by multiplying it with U, forming $N_s \times P$ matrix X as:

$$X=[x_0^T, \ldots\ldots\ldots x_{Ns-1}^T]^T = UR, \qquad (10)$$

Now from (8) we get

$$X=U(HS+V)=G\Psi+W \quad (11)$$

where, $x_k=[\,x_1(k), \ldots\ldots x_P(k)\,]^T$, $w_k=[\,w_1(k),\ldots w_P(k)\,]^T$ and $W=UV=[w_0, \ldots. w_{Ns-1}\,]^T(N_s\times P)$ (12)

$$x_k^T=g_{k,k}^T\Psi_k+\sum_{k'=0,k'\neq k}^{N_s-1} g_{k,k'}^T\Psi_{k'}+w_k^T,\ k=0,\ldots\ldots,N_s\text{-}1 \quad (13)$$

$$g_{k,k'}=[g_{k,k'}^{(1)},\ldots\ldots\ldots\ldots,g_{k,k'}^{(P)}]^T, k, k'=0,\ldots\ldots\ldots, N_s\text{-}1 \quad (14)$$

$g_{k,k'}$ is the $(k,k')^{th}$ block of G. The signal X is received in N_R receiving antennas. Diversity combiner at the receiver selects the best instantaneous signal of the P antennas. The received signal can be detected through differential or coherent scheme. SNIR for quasi-orthogonal MIMO-OFDM-STBC system with N_s OFDM sub carriers without timing error is given by (15) below. Where, f_D is the maximum Doppler frequency, $J_0(.)$ is the Bessel function of the first kind of zeroth order.

Let us denote the symbol energy by E_s, Guard Interval (GI) ratio δ and Rician parameter K. Symbol energy is twice the bit energy E_b for DQPSK and QPSK; and for DPSK it is equal to E_b. Timing Jitter causes the signal power to degrade by a factor of (1-ϵ) over a time slot and also causes interference, which is added as E_b ϵ. Here ϵ is the timing error normalized by symbol duration T_s i.e. (ϵ = Δ / T_s). The received bit energy E_b is the product of input bit energy E_{in} and the multiplicative fade α^2, $E_b = E_{in} \times \alpha^2$. To incorporate the jitter effect along with fading and AWGN, the equation of SNIR for DQPSK and QPSK is derived as (16). Equation (16) can be modified for DPSK modulation, replacing $2E_{in}$ by E_{in}.

$$SNIR=\frac{P\sum_{l=0}^{L-1}[[N_s+N_R\sum_{i=1}^{N_s-1}(N_s-i)J_0(2\pi if_DT_s)]]e^{-\frac{\tau_l}{\tau_{rms}}}}{P[\sum_{k'=1}^{N_s-1}\sum_{l=0}^{L-1}\{N_s+N_R\sum_{i=1}^{N_s-1}(N_s-i)J_0(2\pi if_DT_s)\cos(\frac{2\pi}{N_s}k'i)\}e^{-\frac{\tau_l}{\tau_{rms}}}]+\sigma^2} \quad (15)$$

$$SNIR(\varepsilon,\alpha)=\frac{P\sum_{l=0}^{L-1}[\{\frac{(2E_{in}\alpha^2)(1-\varepsilon)}{(K+1)(1+\delta)}\}[N_s+N_R\sum_{i=1}^{N_s-1}(N_s-i)J_0(2\pi if_DT_s)]]e^{-\frac{\tau_l}{\tau_{rms}}}}{P\{\frac{(2E_{in}\alpha^2)(1-\varepsilon)}{(K+1)(1+\delta)}\}[\sum_{k'=1}^{N_s-1}\sum_{l=0}^{L-1}\{N_s+N_R\sum_{i=1}^{N_s-1}(N_s-i)J_0(2\pi if_DT_s)\cos(\frac{2\pi}{N_s}k'i)\}e^{-\frac{\tau_l}{\tau_{rms}}}]+(\sigma^2+2E_{in}\alpha^2\varepsilon)} \quad (16)$$

IV. EXPRESSIONS OF BER

A. BER Analysis of Modulation Schemes

The expression of BER for DQPSK modulation in fading channel is evaluated as [9], [12].

$$Pe=\frac{\{1-J_0(2\pi f_DT_s)\}(\frac{SNIR}{2})+1}{2(\frac{SNIR}{2}+1)}\exp(-\frac{K.\frac{SNIR}{2}}{\frac{SNIR}{2}+1}) \quad (17)$$

To incorporate the jitter effect along with fading and AWGN, the expression for DQPSK is:

$$P(\varepsilon,\alpha)=\frac{\{1-J_0(2\pi f_DT_s)\}\{\frac{SNIR(\varepsilon,\alpha)}{2}\}+1}{2\{\frac{SNIR(\varepsilon,\alpha)}{2}+1\}}\exp\{-\frac{K.\frac{SNIR(\varepsilon,\alpha)}{2}}{\frac{SNIR(\varepsilon,\alpha)}{2}+1}\} \quad (18)$$

The unconditional BER for STBC and convolution coding can be calculated by averaging the conditional BER, over all possible values of α and ϵ by:

$$P_e=\int_{-\infty}^{\infty}\int_{-\infty}^{\infty}P_e(\alpha,\varepsilon)P(\alpha)P(\varepsilon)d(\alpha)d(\varepsilon) \quad (19)$$

The equation of BER of QPSK system in AWGN channel is found as:

$$Pe=0.5erfc\sqrt{E_b/N_0}=0.5erfc\sqrt{\text{SNIR}} \quad (20)$$

To find the BER performance of QPSK/OFDM system in presence of fading, jitter and AWGN the equation is:

$$Pe(\varepsilon,\alpha)=0.5erfc\sqrt{\text{SNIR}\ (\varepsilon,\alpha)} \quad (21)$$

The equation of BER for DPSK (DBPSK) system in AWGN channel is found as [11]

$$Pe=0.5\exp(-E_b/N_0)=0.5\exp(-SNIR) \quad (22)$$

BER performance of DPSK/OFDM system in presence of fading, jitter and AWGN can be obtained as:

$$Pe(\varepsilon,\alpha)=0.5\exp\{-SNIR(\varepsilon,\alpha)\} \quad (23)$$

B. BER Analysis with Coding

Channel coding is added to improve transmission performance. Soft decision is always a good solution to optimize the use of the correction capacity of a particular code. STBC and Convolution coding is chosen for the system to improve the transmission performance. An expression of the bit error probability P_e cannot be worked out exactly in the presence of channel coding, showing the need for a good upper bound. It is well known that using a rate R= K/N convolution coding and a Viterbi algorithm decoding, the bit error probability for an information symbol is bounded by:

$$P_e \le \frac{1}{K} \sum_{d=d_f}^{\infty} W(d) P(d) \quad (24)$$

where, P(d) is the probability for the decoding algorithm to choose a path at distance d from the correct path, d_f is the free distance of the encoder and W(d), a characteristic coefficient of the encoder, is defined as:

$$W(d) = \sum_{i=1}^{\infty} i a(d,i) \quad (25)$$

where, a(d, i) is the number of paths at distance d from the correct path and corresponding to i information symbols equal to '1'. In general, the a(d, i) are deduced from the transfer function of the encoder. Considering the uncoded BER to be P_{un} the value of $P(d)$ can be expressed as follows:

$$P(d) = \{4 P_{un} (1 - P_{un})\}^{d/2} \quad (26)$$

W(d) is obtained from the code weights table [10]
Substituting equation (15) in (17) and equation (16) in equation (18) we obtain the conditional BER of STBC-OFDM system for DQPSK and QPSK modulation. Similarly, the conditional BER of STBC-OFDM system for DPSK can also be calculated. The unconditional BER of STBC-OFDM is calculated averaging the conditional BER by equation (19) in the same approach for OFDM systems.

V. RESULTS AND DISCUSSIONS

Theoretical analysis on STBC-OFDM considering time-selective rayleigh and rician fading channel are presented in section III. SINR for quasi-orthogonal STBC-OFDM system has been derived for the BER performance of a STBC-OFDM wireless communication system in presence of fading, AWGN and timing jitter. We considered four transmit antennas, sixteen OFDM sub carriers, maximum Doppler frequency of 60 Hz and 1 Mbps data rate.

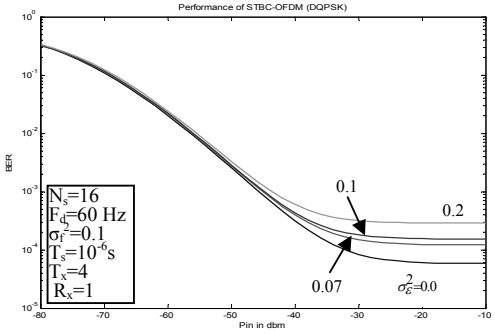

Fig. 2. BER vs. P_{in} (dBm) in presence of timing jitter for STBC-OFDM (DQPSK)

Fig. 2. shows the effect of timing jitter in a DQPSK OFDM system with one receiving antenna and fading variance of 0.1. It is revealed that, with the increase in jitter the BER performance degrades and BER floor earlier for higher values of jitter variance. At a jitter variance σ_ϵ^2 of 0.2, the BER floor occurs at about 10^{-3} compared to 10^{-4} for the case of without timing error. The BER degrades slightly upto -45 dBm and then after the BER degradation is noticeable.

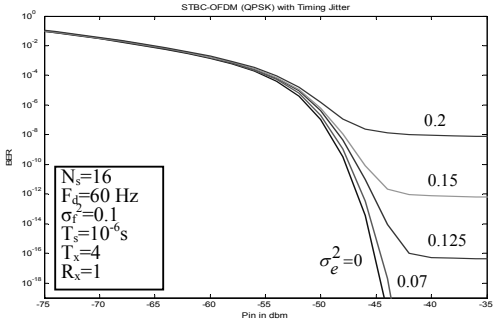

Fig. 3. BER vs. P_{in} (dBm) in presence of timing jitter for STBC-OFDM (QPSK)

Similar performances of the system employing QPSK and DPSK modulation are shown in fig. 3 and fig. 4 respectively. It is noticed that the jitter causes BER floor in both the cases and is more pronounced in QPSK and DPSK than in DQPSK. It is also noticed that the BER degrades slightly upto -45 dBm and then after the BER degradation is noticeable and increase with timing jitter. It is noticed that, the BER do not floor at jitter variances σ_ϵ^2 of 0.0 and 0.07, both in QPSK and DPSK. BER floor occurs approximately at about 10^{-17} for σ_ϵ^2=0.125, both for QPSK and DPSK but in case of QPSK it starts a bit earlier.

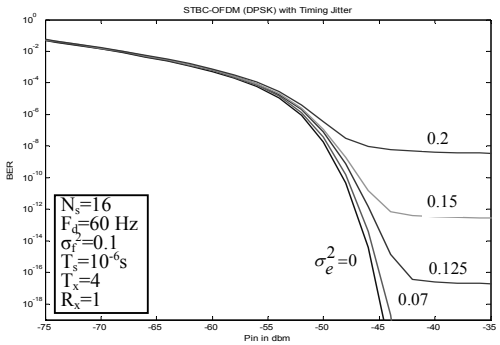

Fig. 4. BER vs. P_{in} (dBm) in Presence of Timing Jitter for STBC-OFDM (DPSK)

It is noticed that, at higher values of jitter, DPSK suffers more penalty than QPSK and the power penalty is almost same upto -45 dBm for lower values of jitter variance. The amounts of penalty in dB suffered by the systems due to timing jitter at BER=10^{-8} are shown in Table I.

Table I. Power penalty due to jitter at BER=10^{-8}

Type	BER=10^{-8}			
	σ_ϵ^2=0.07	σ_ϵ^2=0.125	σ_ϵ^2=0.15	σ_ϵ^2=0.2
QPSK	0.3	0.8	1.1	6
DPSK	0.3	0.8	1.2	9

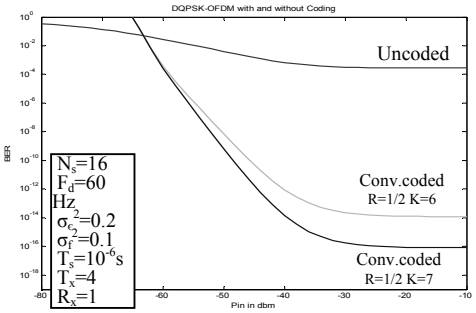

Fig. 5. BER vs. P_{in} (dBm) with and without Coding for DQPSK-OFDM

The systems performances with and without convolution coding in presence of jitter for DQPSK, QPSK and DPSK are shown in fig. 5, fig. 6 and fig. 7 respectively. Significant improvement of the BER performance is achieved by applying convolution coding. For convolution code of rate ½, the coding gain is 29 dBm for Constraint length K=6 and 30 dBm for K=7 at an uncoded BER of 10^{-9} with QPSK modulation..

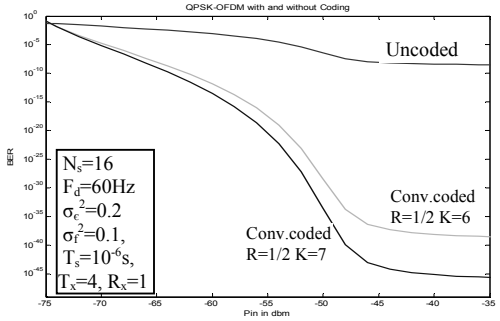

Fig. 6. BER vs. P_{in} (dBm) with and without Coding for QPSK-OFDM

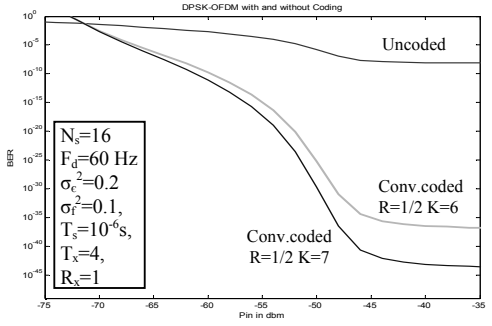

Fig. 7. BER vs. P_{in} (dBm) with and without Coding for DPSK-OFDM

It is also noticed that for higher amounts of input power, the coding gain is substantially higher in K=7 than in K=6

Table II. BER improvement with coding

Modulation	Pin (dBm)	Uncoded BER	Coded BER (R=1/2 K=6)	Coded BER (R=1/2 K=7)
QPSK	-40	10^{-9}	10^{-39}	10^{-46}
DPSK	-40	10^{-9}	10^{-37}	10^{-43}
DQPSK	-40	10^{-3}	10^{-13}	10^{-15}
DQPSK	-35	$10^{-3.5}$	10^{-13}	10^{-16}
DPSK	-35	10^{-9}	10^{-38}	10^{-42}
QPSK	-35	10^{-9}	10^{-39}	10^{-47}

Table II shows the BER improvement with coding than uncoding and best performance is achieved in case of QPSK modulation scheme.

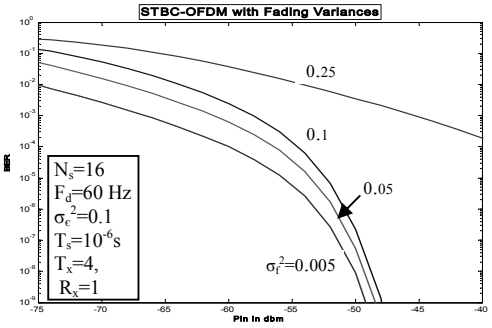

Fig. 8. BER vs. P_{in} (dBm) with Fading Variance for STBC-OFDM (QPSK)

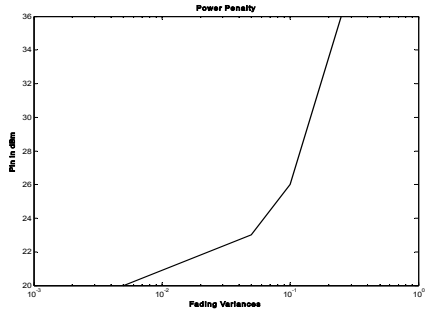

Fig. 9. Power Penalty curve for STBC-OFDM (QPSK)

The effect of fading variances on the BER performance (analytical) of QPSK OFDM system with one receiving antenna and four transmitting antennas are shown in fig. 8. The BER performances are degraded with the increase of fading variances. For a fixed jitter variance = 0.1, and at -60 dBm input power with fading variance σ_f^2 =0.005 the BER is 10^{-4}, σ_f^2 =0.05 the BER is 10^{-3} σ_f^2 =0.1 the BER is 10^{-2} and at σ_f^2 =0.25 the BER increases to 10^{-1}. Similar results are obtained in different dBm as shown in the plot. The Power penalty curve is shown in fig. 9.

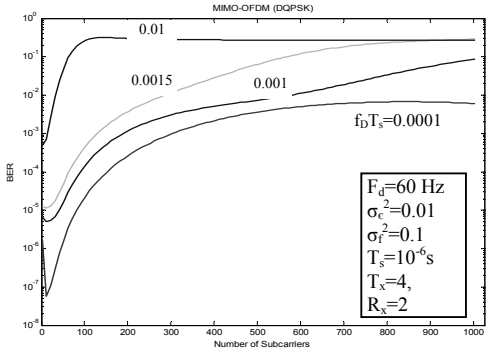

Fig. 10. BER vs. N_s (number of subcarriers) for MIMO-OFDM (DQPSK)

The plots of BER vs. number of subcarriers (Ns) for different values of Doppler frequency normalized by symbol period are plotted in fig. 10. The plot shows that, the BER increases with the increase in Doppler frequency. It is also revealed that with increase in N_s, the BER decreases to minimum and then increases for a particular value of Doppler frequency. The BER remains almost constant for $N_s \geq 100$ for F_dT_s=0.01 and at F_dT_s=0.0001 the BER performance is minimum where N_s=13. The increment of BER beyond N_s>300 is slow and the increment is almost constant at N_s>500.

VI. CONCLUSION

In this paper an analytical approach is presented to evaluate the bit error rate performance of a MIMO-OFDM wireless link with STBC considering the effects of fading and timing jitter. Convolution coding is employed as Forward error correction coding (FECC). The results show that the reliability of the wireless link can be improved significantly using MIMO-OFDM link with STBC system. Table II shows BER improvement with coding than uncoding and best performance that can be achieved in case of QPSK modulation. The future study can be initiated to evaluate the performance investigation of MIMO- STBC with Smart Antenna (SA).

VII. ACKNOWLEDGEMENT

The research presented in this paper has been carried out in Bangladesh University of Engineering and Technology (BUET), and Military Institute of Science and Technology (MIST) Dhaka, Bangladesh. The authors express their sincerest gratitude to BUET and MIST authority for supporting its publication.

REFERENCES

[1] Garg V. K. "Wireless Communication and Networking" Morgan Kaufmann publishers, San Fransisco, CA 94111-Printed on 2007, pp. 60-64, 150-175, 237, 300-310.

[2] Hanzo L., Munster M., Choi B. J. and Keller T. "OFDM and MC-CDMA for Broadband Multi-user Communications, WLANs and Broadcasting" Jhon Wiley & Sons Ltd, Reprinted March 2004, June 2004. Chapter 2 and pp. 112-114, 590-600.

[3] Vaucetic B. and Yuan J, "Space-Time Coding" John Wiley & Sons Ltd. ISBN 0-470-84757-3, Chapter 1, 2 and 3.

[4] Abdolee R. "Performance of MIMO Space-Time Coded System and Training Based Channel Estimation for MIMO-OFDM System" Universiti Teknology Malaysia -2006/2007 (http://eprints.utm.my/288/1/RezaAbdoleeMED2006TTT.pdf)

[5] WIKIPEDIA, the free Encyclopedia, and the websites based on MIMO-OFDM with STBC, Multiplexing and Multiple accesses, Diversity and different coding.

[6] Peng J. Y. and Chang D. C. "Thesis on Design and Implementation of a MIMO-OFDM System for WLANs"- College of Electrical Engineering and Computer Science, National Central University, Taoyuan, Taiwan 320, R.O.C, Republic of China, July 2005

[7] Tarokh V., Jafarkhani H., and Calderbank A. R., "Space–Time Block Coding from Orthogonal Designs," IEEE Transactions on Information Theory, July 1999.

[8] Kar A., Majumder S. P. "Performance Study of Space-Time Block Code for Wireless Communication" Department of EEE, BUET, Dhaka-1000, Bangladesh. "to be published".

[9] Alamouti S. M. "A Simple Transmitter Diversity Technique for Wireless Communications," IEEE Journal on Select Areas in Communications, vol. 16, no 8, pp. 1451-1458, Oct. 1998.

[10] Zhang Y. and Liu H. "Impact of Time-Selective Fading on the Performance of Quasi-Orthogonal Space-Time-Coded OFDM Systems" IEEE Transactions on communications, vol. 54 no. 2, pp. 251-260. February 2006.

[11] Sasamori F., Handa S. and Oshita S. "A Simple Method of BER Calculation in DPSK/OFDM Systems over Fading Channels" IEICE Transactions on fundamentals of electronics, communications and computer science. vol. E88-A(1) pp. 366-373, January 2005.

[12] Sasamori, F., Umeda, H., Handa, S., Maehara, F., Takahata, F., and Oshita, S., "Approximate Equation of Bit Error Rate in DQPSK/OFDM Systems over Fading Channels", European wireless 2002, pp 602-607, February 2002.

[13] Tomba, L., Krzymien, W. A., "A Model for the Analysis of Timing Jitter in OFDM Systems", IEEE International conference on communications (ICC 98), Vol-3, pp 1227-1231, 7-11 June 1998.

Proceedings of 2009 12th International Conference on Computer and Information Technology (ICCIT 2009)
21-23 December, 2009, Dhaka, Bangladesh

Offshore-Outsourced Software Development Risk Management Model

†Shareeful Islam, ‡Siv Hilde Houmb, †Daniel Mendez-Fernandez and Md. Mahbubul Alam Joarder
†Institut für Informatik, Technische Universität München, Germany
‡Connected Objects Laboratory, Telenor R&I Service Platforms, Norway
Institute of Information Technology, University of Dhaka, Bangladesh
islam@in.tum.de, siv-hilde.houmb@telenor.com, mendezfe@in.tum.de, joarder@univdhaka.edu

Abstract

Offshore-outsourced software development is gaining popularity because companies are continuously forced to reduce production costs while keeping sustainable competitive strength. However, this trend of software development increases projects' complexity and brings up risks to the overall project environment. Therefore, risks of offshore software development require to be managed as early as possible for a successful project. This paper considers a risk management model from a holistic perspective to manage offshore software development risk, integrated into early stages of development. The approach effectively identifies and specifies the goals of a project and the related risk factors. This is done at the basis of selected software development components within the running project. We show how to trace and control these risks already during early requirements engineering activities. The model at hand is implemented into an on-going offshore software development project to (1) identify goals and risk factors from the local context and finally (2) to determine its applicability of the approach in offshore software development projects from a vendor's perspective.

Keywords: Software development risk, goal modeling language, offshore outsourced software development, requirement engineering.

I. INTRODUCTION

Offshore-outsourced software development (O-OSD) has become a highly favored topic for companies aiming at cost savings while achieving final product delivery within estimated time schedules. Still, this type of development has several challenges due to its inherent nature. For instance, decreased degrees of communication, lack of knowledge about customers' business domains, disputes on legal issues [1, 6] may pose any potential risks to the project. A recent report [1] suggested that outsourcing magnifies existing risks and creates additional threats to the offshore projects. These risk factors are not only given by technical issues, but also by non-technical issues. There is in general an observable tendency to over-manage the technical issues and underestimate the non-technical ones. Consequently, O-OSD has to emphasize particular goals, such as an effective co-ordination of project works between offshore customers/users with local development teams, building trust, attain security besides generic software development goals like schedule, cost and quality.

This paper evaluates a goal-driven risk management model (GSRM) that is integrated into Requirement Engineering (RE) activities in order to manage risks of O-OSD. The approach explicitly defines the relations between the goals relating to project success from offshore environment and the risk factors that obstruct the goals respecting technical as well as non-technical development components. In addition, it defines the control actions that enable the satisfaction of the goals. Therefore, GSRM assesses and manages risk that relate to the challenges of the offshore context right from the beginning of a project. We claim that this integration contributes to a reduction of errors that arise from elicited user and / or detailed system requirements. This is in particular important to the offshore environment because our result showed that requirements errors are a common problem in offshore development projects [8, 12, 13].

We performed a field study within an on-going offshore software project in Bangladesh. The field study evaluates applicability of the model and compares the identified risk factors with our previously published survey results from the same local context [8] and with the other published risk factors [6, 14] of the offshore context. The study context is from a developing country where the offshore market in rapidly expanding by significantly increasing investments in the recent years [5].

The remainder of the work is as follows. We first give in Sect. 2 an overview on risk management approaches and related survey. In Sect. 3 we introduce the basic concepts of goal-based risk management and in Sect. 4 the O-OSD specific approach. It is evaluated in Sect. 4 before giving in Sect. 5 finally some concluding remarks.

The work is partly supported by the German Academic Exchange Service (DAAD), Germany and the Institute of Information Technology (IIT), University of Dhaka, Bangladesh.

II. RELATED WORK

There are several valuable contributions in the research area of software risk management, including models, process descriptions and techniques. Still, only few focus on the integration with RE. Boehm proposed a risk-driven spiral model in [4] including an iterative approach to manage risks in software project. Karolak proposed the Software Engineering Risk Management (SERIM) framework based on four interconnected risk trees including 81 risk factors, in turn, categorized by technology, cost and schedule [9]. Kontio proposed the Riskit methodology [10] by initially identifying stakeholder goals and risks that threaten the goals. Risks are analyzed and prioritized by deriving scenarios which is a non-trivial task when a scenario depends on more than one probabilistic element. A recent contribution that focuses on integrating risk management into RE is the one of Ansar et al [2]. It contributes by using Tropos a goal-driven approach to identity and manage risks that obstruct the goals within RE. Procaccino et al. [15] identifies seven early development factors and discusses how these contribute to the success or failure of a software project. Other directions of work empirically analyze risk factors. Iacovou et al. summarize for example in [6] the top ten risk factors for offshore-outsourced development projects. Aspray et al. consider in the ACM task force report [1] risks from both technical and non-technical issues. Tsuji et al. [14] propose questionnaires assessment schemes based on software, vendor, and project properties to quantify risks in offshore software outsourcing. The survey shows that vendor properties including communication and project management abilities affect more the result to development in comparison to software (technical) properties like requirement volatility.

However, our risk management model is goal-driven and extends the basic concepts of the KAOS approach. We focus on a holistic view of technical and non-technical issues.

III. GOAL & RISK FACTORS

We analyze early software development components and project success factors from the existence literature as a background foundation to develop the model. This lays the foundation for GSRM considering a holistic view from a both technical and a non-technical. We consider technical issues in software development as those aspects that directly relate to hardware and software while non-technical issues relate to human, managerial, organizational and environmental factors. Based on a literature survey, we categorized development components according to project constraints, development process, product, human and finally (internal & external) environment. These components are described through the essential elements that are required for software development. The elements may be described by single or by multiple factors. Therefore, elements and factors together represent the activities, the activities' results (the artefacts) and the general characteristics of the individual components. For instance, project planning and control is an element under the component project constraints that represents project schedule, budget, staffing and other project planning and management related issues. This hierarchy eases the identification of goals to be satisfied and risk factors that obstruct these goals like maintaining a realistic project schedule. Based on this hierarchical framework, we consider a conceptual view for the risk management model within GSRM, as shown by Fig. 1. Goals are derived from the development components by considering the factors relating to project success. Project stakeholders are responsible to these goals. Risk factors certainly obstruct these goals and support casual relationships to the risk event. Likelihood of risk events along with the risk impact supports to prioritize the risks. Finally, control actions are implemented to reduce the risk event and contribute for the goal satisfaction.

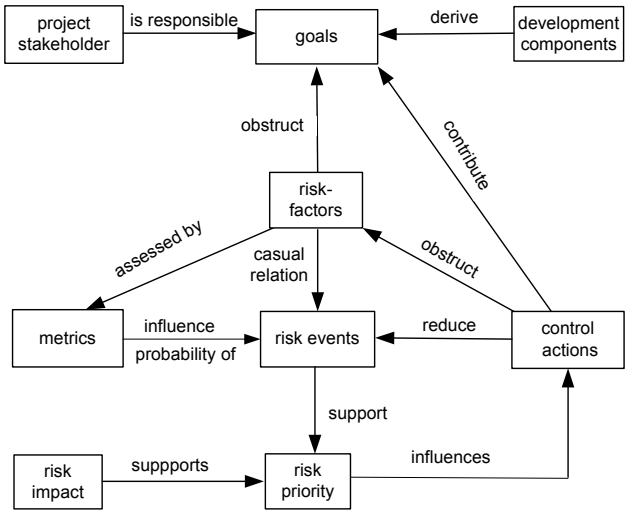

Fig. 1. Conceptual view for the risk management model

IV. O-OSD RISK MANAGEMENT MODEL

GSRM is based on existing goal modeling techniques to accommodate risk management activities. We extend the KAOS goal modeling approach [11] to support risk management activities and integrate it with RE respecting O-OSD. Goals in general provide an anchor to analyse the risks in software development. Therefore, risk management requires the identification, the analysis and the refinement of the goals and the risk factors that obstruct the goals [11]. KAOS defines an obstacle as an undesirable behavior against stakeholders' strategic interests [11]. GSRM adopts this concept of KAOS and defines software risks as obstacles that contribute

negatively to the fulfillment of specific goals. In GSRM we extend KAOS furthermore with risk assessment and treatment techniques as shown in [7]. This is done by using four layers of abstraction within the modeling structure of GSRM. Fig. 2 depicts the four different layers that are subsequently described.

Goal Layer. Goals are the objectives, constraints and expectations that have to be achieved by a software development project through the cooperation of system agents. These agents represent the development components and the project stakeholders. Therefore, the model initiates with the goals by following the development component, the elements and the factors hierarchy besides the project stakeholders' expectations. Goals can be stated at different levels of abstraction from higher level coarsely grained to lower level finely-grained goal assertions. This goal hierarchy enables developers to model all system agents, even though these often are somewhat fuzzy. GSRM follows informal temporal pattern as stated in KAOS [11] to represent each goal. The pattern structures an assertion into a prefix and a condition/property. For instance, a statement could be "reduce [erroneous requirement]", whereby the prefix "reduce" represents a goal that demands a reduction of defected requirement.

Risk Obstacle Layer. The risk obstacle layer encompasses the potential obstacles and specifies which goals they obstruct, i.e. incurred problems within the development environment. The layer allows the practitioner to directly link all types of obstacles to the goals. Same and similar risk obstacles can be relevant to more than one goal. This is important in order to consider effective treatment options. Risk factors that cross-cut several goals are in general more effective to counter since the treatment effect often then propagate also to goals that are not directly linked with the particular risk factor. In GSRM, we follow a set of questionnaires based on the early development components and brainstorming techniques to identify these risk obstacles. All identified obstacles are then analyzed further within the assessment layer.

Assessment Layer. The assessment layer mainly analyses the risk events that influence single or multiple risk factors. Each risk event is characterized by two properties: *likelihood* and *impact*. Likelihood specifies the rate of occurrences of a risk event and is modeled as a property of the risk event itself. The impact is a measure over the negative outcome of the risk event occurrence. All risk events and goal relationships are modeled by adding an obstruction link from the risk event to the specific goal that it obstructs, and in cases where several goals are affected, an obstruction link is established between the risk event and each of these goals. GSRM supports the use of risk metric values to identify the likelihood of the risk event by estimating the casual relationship of the related risk factors. GSRM uses for this purpose the Bayesian interpretation and in particular Bayes theorem to estimate the risk events based on their casual relationship with the risk factors. Risk events likelihood and impact in particular with high-highs, high-mediums and medium-mediums while ignoring low-lows give us certain beliefs about the dissatisfaction (DSAT) and the satisfaction (SAT) of the goal fulfillment. Finally, risks are prioritized based on their likelihood and impact.

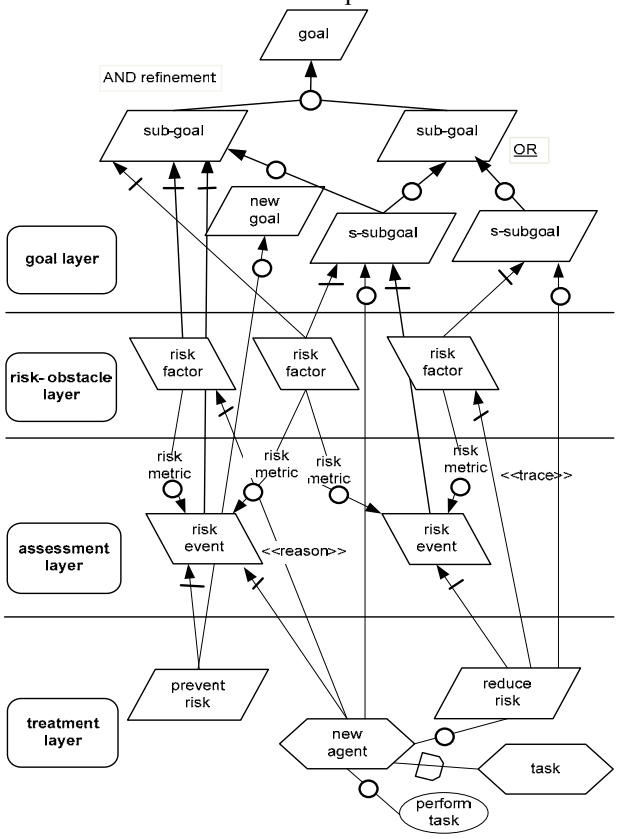

Fig. 2. GSRM framework

Treatment Layer. Once the goals, risk factors and risk events are identified and analyzed, it is crucial to identify and then implement suitable and cost effective countermeasures. Therefore, the aim of the treatment layer is to gain control of the risks as early as possible and preferable during RE activities by assigning appropriate countermeasures. To visualize the relationship between treatment, risk obstacle and goal, we establish a contribution link from chosen control actions to the goal by specifying the ability of the treatment to support the goal and by reducing the effect or likelihood of removing the associated risk factors. Additionally it is also necessary to analyze the cost-benefits before

implementing a suitable control action.

V. FIELD STUDY

We have conducted a field study to evaluate the model through an on-going software development project by a vendor company in Bangladesh. A customer that is located in Australia triggers the project. Due to space limitation we present a brief overview of the study and its results. We formulated two research questions and derived the study design according to these questions.

(**RQ1**) "*How valid are the identified risk factors*?"

We analyze the validity of the identified risk factors by comparing the identified risk factors from the field study with previously published ones [6, 8, 14]. Although the identified risk factors are suitable, the process can still be inefficient. For this reason we analyze in a second step the applicability of GRSM.

(**RQ2**) "*Is GSRM applicable to offshore software project*?"

We analyze the GSRM according to its applicability as part of structured interviews respecting particular advantages and limitations (lessons learned) in an active software development project.

A. Study Design

Our case study is conducted in two different phases. The first one addresses RQ 1, the second RQ 2.

We have performed the approach in collaboration with a Bangladeshi vendor, implementing the approach to an ongoing project. In the first phase, we conducted a brainstorming session to identify the goals of the early development components as expectation for the project to success besides obtaining background information of the company and the selected practitioners involved in the project. We provided a short tutorial for understanding the basic terminology and features of risk management in particular about GSRM. Finally we derived by following the approach the risk factors and evaluated them for their validity. In the second phase, a structured interview was conducted to the individual participants of the project in order to evaluate the applicability. The interview template contained 108 questions including 80 close questions and remaining open questions. The questionnaires were prepared by reviewing checklists, similar questionnaires format from literature and by considering the goals and sub-goals for the project's success. Each close question has three possible answers. Open questions obtain the information relating to the on-going project and existing practice of risk management throughout their projects and about GSRM. A total of nine interviewers participated in the second phase.

B. Results

The project concerns the development of a system to support the core business processes of a sales department. It contains two modules "account" and "reporting" with several features such as bar code readable sales system, inventory and purchase. The project size was nine man-months with a total duration of eleven months. The vendor only listed generic risks once in the overall development period mostly focusing on time and budget. No other risk factors such as human, environment, technology related issues are considered. As a preparation for applying GSRM, we start to identify the main goals from the project context. After approving the goals, participants were interviewed to identify the state of the development components, elements and factors so that risks relating to these components are identified.

B.1 Research Question 1

We have reviewed and agreed a set of goals with the project participants by following the development components, elements and factors concept of GSRM. The identified goals are rather high level but their refinements are not included in the paper due to confidentiality reason. Most of the goals require a prefix of different types such as maintain, attain, reduce and improve, depending on the nature of the goal. For instance:

- When a goal concerns maintenance, it implies that certain conditions of the development elements or factors should always be kept at the same level throughout the software development.
- When a goal concerns achievement it implies that certain conditions of the development elements or factors should be achieved beyond the current state.
- When a goal concerns reduction, it implies that a certain state of the elements or factors should be reduced, respectively minimized.
- When a goal concerns improvement, it implies that certain conditions, states of the elements or factors should be increased.

Some of the agreed high level goals under the development components are:

- Project constraints
  - Maintain [actual estimated budget]
  - Maintain [actual estimated schedule]
  - Reduce [project complexity]
- Process
  - Improve [development activities]
  - Improve [formal risk management practice]
- Product
  - Attain [clear business needs]
  - Reduce [error from requirements]
  - Improve [product quality]
- Human
  - Improve [competency of team members]

Improve [communication & coordination]
Improve [proper management direction & support]
Improve [customer/user involvement]

- Internal & external environment
  Improve [adequate development facilities]
  Maintain [implementation of policies & procedure]

We have identified major risk factors based on the responses to the interview. Interview questions mainly focus on the identification of the state of the development components that obstruct the goals. A total of thirty eight risk factors are identified that directly obstructs the goals while creating problems to the development. Table I shows the major risk obstacles that influence several risk event for the project such as erroneous requirements, budget and schedule over-runs, poor communication, incompetence practitioner, all having likelihood and impact between high and medium for the risk event.

Table I Major risk factors

Risk-obstacles
• Requirements faults: incorrect, unstable, incomplete and ambiguous/underspecified
• passive customer/user involvement
• lack of project specific domain knowledge of the software practitioners
• unstable organization structure
• hidden factors(variation of bank fee, strike, interrupt power and internet supple) for schedule & budget overruns
• incomplete requirement specification document
• ineffective RE process to elicit, analyze , validate, and document requirements
• employee absence
• inadequate support to handle change

Most of the identified risk factors of table I are from the product and human components and mainly influence the non-technical issues. In order to answer finally RQ1 we made a cross study of our finding with the published risk factors from our previously study [8] as well as with the other published risk factors from the offshore environment [6, 14]. This comparison shows similarities with our previously published risk factors in [8]. Several common risk factors from the local context are requirements faults, lack of domain knowledge, employee absence, hidden factors that influence for schedule or budget overruns, erroneous requirements and ineffective communication. We have noticed that some risk factors take influence on other risk factors as well as several risk events to occur. We treated these as important risk factors (see Tab. I) for the project that required evaluation and control actions as early as possible. Requirements problems are the most important ones from the local context. This is due to the passive involvement of the customer/ user, lack of practitioner project specific domain knowledge or ineffective RE process. An unstable organizational structure and incomplete requirement specifications are newly identified risk factors for this project context as an outcome of the study. In comparison to other published risk factors by Iacovou et al. [6], we observed both similarities and dissimilarities. For instance, inadequate user involvements, poor change control and lack of business know-how to by offshore team from Iacovou et al are also identified by our case study. But the participants confirmed that they faced no problems arising from the lack of top management commitment, cross-cultural and time-zone difference, technical knowledge difference, threats to the security of information resources, and project contract as stated in [6]. Requirements volatility is the top prioritized risk factor by our field study which shows not as much severe by Tsuji et al. in [14]. Therefore, our result regarding risk factors in offshore environment concludes that local environmental context certainly plays an important role for the success of offshore project. Technology differences between the vendor and the offshore client, differences in the time zone, cultural difference, security problems and finally disputes in contractual agreement are no longer important problems in the local context. This study also increases our confidence about the validity of the recorded result by comparing it with other published literature.

B.2 Research Question 2

Due to tight schedule pressure in the project we were not able to perform a comprehensive risk management approach under GSRM to the on-going project. In particular, this affected the probability estimation of the risk event occurrence. The participants were more interested to consider the control actions in order to mitigate risk factors rather than continuing detailed risk analysis through assessment layer. By analysing the participant's response to the open questions we observed that they are more concern about simple and straightforward techniques for software risk management. They remarked GSRM as quite straight forward goal – driven process for risk management. The underlying principles of GSRM are relatively easy to communicate in general to the software practitioners and in particular to the project manager and requirements engineers. The participants appreciate the combination of questionnaires and brainstorming sessions concerning the identification of risk obstacles. The effort of developing the risk artefacts such as detailed risk factors, goal-risk-treatment models and risk treatment plans require some extra resource with a minimum level of domain knowledge. This is especially important within tight time schedules. Based on our observation several lessons are learned from the study. In conclusion, they are:

- Risk management should be considered from early stages of development accompanying the software development activities.
- The identification and elaboration of goals certainly ease the risk management process as well as the communication with the project practitioners.
- Risk identification through questionnaires and brainstorming session allow including experiences along with checklists for systematically identifying software development risks.
- Many risk factors of offshore software development are influenced by local environmental context. Traditional offshore software risks, such as time difference, mismatch in technology or legal disputes are not always important to our context.
- An organization should have a repository for reusing risks across several projects. This is important, because project members are always under constant time pressure and without having explicit list of risk it is hard for them to spend sufficient time. Besides this aspect it is not economically reasonable to analyze risks from the beginning for each new project.

VI. CONCLUSIONS & FUTURE DIRECTION

Risk is a fuzzy concept term and it can mean different things to many people. Therefore, a systematic simplified approach is required to handle risk management in hectic on-going project environments. We believe that GSRM contributes within this context by structuring goals and risk factors and choosing suitable control actions. The identified goals and risk factors from our study and previous study result would be effective for developing the offshore market in Bangladesh.

However, we neither fully implemented the GSRM to the running project nor did we perform detailed elaboration of the goals. Therefore, a detailed analysis of GSRM in terms of its usefulness is not fully completed through the study. Still, we have learned some lessons. We plan to use the information gained from the field study to improve the GSRM in particular the tasks and methods used for the risk management activities. We also did not cover the cost/benefit analysis of the model during the evaluation since it is hard to quantitatively analyze costs and benefits within the risk management context. Hence, we are planning to conduct the field study to evaluate the model further in terms of its usefulness and feasibility regarding integration into RE.

REFERENCES

[1] Astray, W., Maydays, F., and Verdi, M.Y. Globalization and of shoring of Software: A Report of the ACM Job Migration Task Force. ACM, NY, 2006.

[2] Ansar, Y. and Georgina, P. Modeling Risk and Identifying Countermeasure in Organizations. In: Proceedings of the 1st International Workshop on Critical Information Infrastructures Security, pp. 55–66. Springer, Heidelberg, 2006.

[3] Boehm, B.W. Software Engineering Economics. Englewood Cliffs, N.J., 1981.

[4] Boehm, B.W. Software Risk Management: Principles and Practices, Piscataway: IEEE Software, v. 8, p. 32-41, Jan. 1991.

[5] Bangladesh Associate of Software & Information Services (BASIS), http://www.basis.org.bd.

[6] Iacovou, C. L. and Nakatsu, R. A Risk Profile of Offshore-outsourced development projects. Communication of ACM 51, June 2008.

[7] Islam, S. 2009. Software development risk management model: a goal driven approach. In Proceedings of the Doctoral Symposium for ESEC/FSE on Doctoral Symposium (Amsterdam, The Netherlands, 2009). ACM, New York, NY, 5-8. DOI=http://doi.acm.org/10.1145/1595782.1595785

[8] Islam, S. Joarder, M. A., Houmb, S.H. Goal and Risk Factors in Offshore Outsourced Software Development from Vendor's Viewpoint, pp. 347-352, In proceedings of the Fourth IEEE International Conference on Global Software Engineering, 2009, Ireland. http://dx.doi.org/10.1109/ICGSE.2009.54

[9] Karolak, D. Software Engineering Risk Management, IEEE Computer Society Press, Los Alamitos, CA, USA, 1996.

[10] Kontio, J. The Riskit Method for Software Risk Management. Version 1.00, Technical Report,CS-TR-3782 /UMIACS-TR-97-38, University of Maryland, Computer Science, College Park, USA, 1997.

[11] Lamsweerde, Van A. Requirements Engineering: From System Goals to UML Models to Software Specifications, Wiley, January 2009.

[12] Linberg, R., Software Developer Perceptions about Software Project Failure: A Case Study, the Journal of Systems and Software, Vol. 49, Issue 2/3, 1999.

[13] McConnell, S. Rapid Development. Microsoft Press, 1996.

[14] Tsuji, H., Sakurai, A., Yoshida, K., Tiwana, A. and Bush, A. Questionnaire-Based Risk Assessment Scheme for Japanese Offshore Software Outsourcing, B. Meyer and M. Joseph (Eds.): SEAFOOD 2007, LNCS 4716, pp. 114–127, 2007.

[15] Procaccino, J. D, and Verner, J. M. Case Study: Factors for Early prediction of software development success; Information and Software Technology; Vol. 44, 2002.

Proceedings of 2009 12th International Conference on Computer and Information Technology (ICCIT 2009)
21-23 December, 2009, Dhaka, Bangladesh

A QoS Aware Route Selection Mechanism Using Analytic Hierarchy Process for Mobile Ad Hoc Network

Abu Hamed Mohammad Misbah Uddin†, Mohammad Iftekhar Monir‡, Shahid Md. Asif Iqbal‡
† The Royal Institute of Technology, Sweden
‡Dept. of Computer Science & Engineering, Premier University, Chittagong, Bangladesh
cseminhaj@yahoo.com, monir1175@yahoo.com, asifcsep@yahoo.com

Abstract

To truly realize potential of MANET, multimedia services must be provisioned with a minimum level of QoS. To meet the QoS requirement of such services, many attributes need to be considered. To keep the routing process lightweight, standard QoS aware routing protocol in MANET works with one or two such parameters. In this paper, we have proposed an on-demand source routing protocol for MANET that works with six important QoS attributes by varying priority for different category of traffic flow. We have reflected this variation by incorporating Analytic Hierarchy Process in the proposal.

Keywords: AHP, MANET, QoS, Traffic Categorization, Weight.

I. INTRODUCTION

Mobile Ad Hoc Network has gained importance as a recognized field of research due to its decentralized, dynamic and self configuring nature. In its early stage, much of the efforts have been placed in providing solution for the best effort services. However, since the last decade, it has been observed that multimedia services have been a major catalyst for mass recognition of a technology. In failing to guarantee such services through typical best effort design, use of MANET in the real world has been limited. Therefore focus has been shifted towards the provision of better defined QoS in this field.

QoS routing plays a major role in QoS provisioning as it tries to find the best route to serve application's QoS requirement. Some QoS routing protocol works as an integral part of session admission control whereas some tries to improve overall performance through particular metrics. Majority of proposed QoS routing for MANET has included throughput and delay as routing parameter. However, many other metrics are also important to quantify QoS. But working with more attributes is difficult and therefore, researchers have avoided working with more than two attributes to design QoS routing [1]. Analytic Hierarchy Process is a powerful and flexible decision making tool to set priorities when both qualitative and quantitative aspects of a decision are considered. When complex multi-criteria based decision making problem needs to be solved, AHP is a very good choice as it simplifies by reducing complex decisions to a series of one-on-one comparisons and then synthesizing the results [2]. Keeping that in mind, we have devised an on demand source routing protocol for MANET which will use six important QoS attributes to find out the best route by the help of Analytic Hierarchy Process.

Remainder of the paper is designed as follows. In section II we discuss the theoretical background for our proposal. Section III gives an overview of related research works in the field. Section IV presents the proposed mechanism. Finally, section V summarizes our work by discussing the achievement, limitation and future work of the proposal.

II. THEORETICAL REVIEW

A. QoS Parameters and Traffic Categorization

The ITU has defined five important QoS Parameters for IP transport: Transfer Delay, Delay Variation, Loss Ratio, Error Ratio, and Throughput [3]. Here, Loss Ratio and Error Ratio can also be described in terms of Reliability. Other than these, some more parameter can be regarded in case of wireless ad hoc network, whether mobile or stationary. As every mobile node acts as intermediate router, load and power condition of these nodes should also be considered [4]. Therefore, when QoS aware routing is concerned above mentioned parameters should be taken into concern.

Some wireless technologies have defined service classes and related QoS parameters. ITU has defined six service classes (class 0-5) with recommended values of the QoS parameters given in [3]. Enhanced Distribution Coordination Function (EDCF) has introduced prioritize four access categories, designated 3, 2, 0, 1 from highest to lowest priority for IEEE 802.11 in [5]. These four access categories are not allocated to any particular type of traffic but allocation that is often use is: voice, video, best effort and background. QoS categorization in 802.16 is provided by means of four alternate scheduling services: Unsolicited Grant, Real Time Polling, Non Real Time Polling and Best Effort [6]. UMTS specifies four service classes: Conversational, Streaming, Interactive and Background [7]. As there is no specified traffic categorization for Ad Hoc Wireless network, one of these categorizations can be utilized in modified form, if QoS provisioning is in concern.

978-1-4244-6283-4/09/$26.00 ©2009 IEEE

B. AHP

The Analytic Hierarchy Process (AHP) is a structured solution process to work with complex decisions of dealing multiple criteria to choose one of the multiple options. It is used globally in a wide variety of decision situations, in fields such as government, technology, business, industry, healthcare, and education.

AHP first decompose decision problem into a hierarchy of more easily understandable sub-problems, which are evaluated independently. The elements of the hierarchy can relate to any aspect of the decision problem—tangible or intangible, carefully measured or roughly estimated, well- or poorly-understood —anything at all that applies to the decision at hand.

Once the hierarchy is built, the decision makers systematically evaluate its various elements by comparing them to one another at a time. In making the comparisons, the decision makers can use concrete data about the elements, or they can use their judgments about the elements' relative meaning and importance. The AHP converts these evaluations to numerical values that can be processed and compared over the entire range of the problem. A numerical weight or priority is derived for each element of the hierarchy, allowing diverse and often incommensurable elements to be compared to one another in a rational and consistent way. In the final step of the process, numerical priorities are calculated for each of the decision alternatives. These numbers represent the alternatives' relative ability to achieve the decision goal, so they allow a straightforward consideration of the various courses of action [2].

III. RELATED WORKS

There have been regular efforts in designing QoS aware routing protocols. As supporting more than one QoS constraint make the QoS routing problem NP-complete [8], majority of the routing protocols have focused on providing QoS based on one or two metrics, mostly throughput and delay. In [9], the authors have designed a QoS-aware routing protocol through the use of the approximate bandwidth estimation by using two (admission control and feedback) bandwidth estimation methods. Zhu and Corson, has developed an end to end bandwidth based QoS routing protocol for mobile ad hoc networks employing TDMA [10]. Similarly, MACA/PR [11] provides guaranteed bandwidth support via reservation for real time traffic. On the other hand, Application Aware QoS Routing [12] works with both transmission delay and session throughput requirement to assure throughput, bounded delay and jitter. ODCR [13] uses delay to find out the best route with bounded delay.

Other QoS parameter based routing solution is also evident. DSARP [14] has used load condition (buffer fullness) to provide bounded delay and jitter. GAMAN [15] uses node traversal delay and reliability to achieve robust QoS routing solution. MRPC [16], a power aware routing protocol uses Min Max formulation to select the path that has the largest packet capacity by using residual battery power and the link error rates.

IV. PROPOSED SCHEME

A. Process Overview

Our proposed system contains three important blocks: Flow Classifier, Routing Information Base (RIB) and AHP Engine. Flow classifier assigns access class to the traffic flows according to their nature through some defined process. Routing Information Base runs an on demand source routing protocol similar to DSR protocol and gathers values of QoS attributes for different route throughout the process. AHP pre- computes the weight distribution of the QoS parameters and stores them. The engine also accumulates the values of QoS attributes of different routes from RIB. Finally, it performs calculation using the weight and the value of QoS parameters according to AHP process to generate routing metric. Each unit is explained in the following sections.

B. Flow Classifier

Importance of the QoS attributes varies for different traffic flow. To reflect the appropriate importance of attributes while calculating metric for QoS routing protocol, common user traffic needs to be divided into multiple classes so that attribute priority are easily attached to them. As there is no strongly defined allocation strategy to common user applications to different classes defined in EDCF, following categorization (adapted from UMTS QoS classification [7]) is used in the design.

Table I: Traffic flow category

Category 3	Voice/Video Telephony
Category 2	Streaming, Audio/Video on demand
Category 0	Web browsing, Database access, Re-
Category 1	Email, File Download

Flow classifier uses category defined in table I to assign a class to a flow by one the following mechanism: IP ToS, 802.1p, DSCP [17].

C. RIB & The Routing Process

The RIB runs an on-demand source routing protocol similar to DSR [18]. According to the design, route request is generated by the source and route is selected by the destination. The route discovery process works as follows. When a node wants to send data to another node but it does not have the route to reach the destination, the source node broadcasts a route request packet directed towards the destination. When an intermediate node receives the broadcast it adds itself as well its current values of QoS attributes.

As discussed in the literary review, common parameters that attributes to the QoS of a traffic flow in MANET are: Throughput, Delay, Jitter, Reliability (defined by

Packet Loss and Bit Error Rate), Load and Battery power. These QoS metrics can be classified as additive, concave or multiplicative metrics based on their mathematical properties [19]. Additive metrics are defined as $\sum L_i(m)$, over path P, where L_i (m) is the value of the metric m over link L_i and L_i P. The value of concave metric $C_m$is defined as the minimum value of that metric over a path, C_m = min(L_i (m)). Finally, multiplicative metric Mm is calculated by taking the product of the values along a path, $M_m=\prod L_i$ (m). Thus, delay is an additive metric, as it is cumulative over the whole path and throughput is a concave metric. Therefore, these six metrics are calculated for each link over a route according to its nature and placed in route request packet.

When the destination receives the route request packet(s), it replies the best route to the source. Upon receiving the packet, RIB in destination node stores each route along with its QoS values for the six parameters. To compute the best route, the destination node uses QoS attribute values only. While sending route request, source node sets category of the traffic flow for which the route is intended. This is used by the RIB in the destination node, as it informs AHP engine to perform calculation according to the category.

D. AHP ENGINE

The AHP engine collects the discovered routes along with their QoS values from the RIB. It is also informed about the flow class for which the route is intended. From the class definition, AHP uses the appropriate precomputed priority weight and multiplies these weights with perceived QoS values through a process defined in Analytic Hierarchy Process. Outcome of the calculation is the relative preference of the routes. Using relative preference value, destination node identifies the best route and sends route reply accordingly. AHP process is defined as follows.

In the first step, the problem is organized into a three level hierarchy as figure 2. The key objective here is to select the best route suited to QoS requirement of the traffic flow. Therefore route selection is placed at the root of the tree.

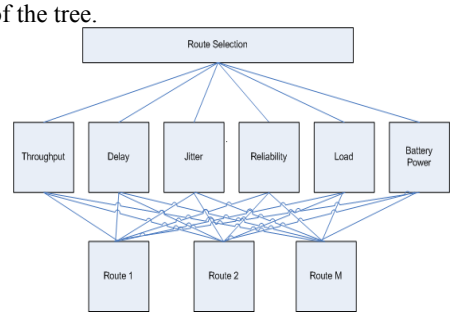

Fig. 1. AHP 3 Tier Hierarchy

Factors contributing to the objective are shown in the tier 2 and alternatives or route options are mentioned in tier 3 of the hierarchy.

Usually the AHP method consist four steps: 1) Create the input values by pair-wise comparisons of decision elements, 2) Estimate the relative weights of the decision elements, 3) Check for consistency, 4) Combine the relative weights to determine the ranking of the different decision alternatives. While designing solution for MANET, one has to keep in mind that the protocol should be as lightweight as possible. That's why we have used a variant of AHP process explained in [20]. This mechanism reduces the processing by eliminating step 3 and simplifying step 2.

The next step is creating judgments on the parameters' importance, made in pairs, aij, relating the importance of parameter i to that of parameter j. A theoretically justified fundamental scale according to [2], is used to represent the intensities between each attribute. Usually the scale consists of nine levels but to make it easier, we use more restricted scale with three levels mentioned in the following table. Reason behind this simpler scale is that we have categorized the value and requirement of the attributes in three levels: high, medium and low.

Table II: Intensity of Importance Scale

Intensity of Impor-	Definition
1	Equally Important
3	Moderately More Important
5	Strongly More Important

At first, keeping the objective of route selection in focus, QoS attributes are pair-wise compared. A square matrix of order n, A = [a_{ij}], is created using the comparisons where, $a_{ij}>0$, indicating the importance of parameter i relative to parameter j as show in equation (1).

$$A = \begin{pmatrix} a11 & a12 & a13 & \dots & a1j \\ a21 & a22 & a23 & \dots & a2j \\ \dots & \dots & \dots & \dots & \dots \\ ai1 & ai2 & ai3 & \dots & aij \end{pmatrix} \quad \dots\dots\dots\dots\dots (1)$$

Obviously, a_{ij} = 1, when i=j, while $a_{ij} = 1/a_{ji}$; which reflects the reciprocal importance of parameter j relative to parameter i. Then we are going to determine the weight distribution of the parameters using the comparison matrix mentioned in equation (1), in which w_i is the weight of parameter i in the weight vector w = [w_1, w_2, w_3, …. , w_n] for n attributes. This vector can by found by the equation (2) based on [2], given as follows:

$$w_i = \sum_{j=1}^{n} a_{ij} / \sum_{i=1}^{n} \sum_{j=1}^{n} a_{ij} \quad \dots\dots\dots\dots (2)$$

Where, a_{ij} is the $(i,j)^{th}$ entry of the comparison matrix A.

Thus, we find w_{ij}, column matrix, where i = 1 to n, for a particular flow class j. Aligning column matrices, w_{i1}, w_{i2}, w_{i3} … to column 1, 2, 3 … and so on, we form another matrix B = [b_{ij}] of order n X m, where, where n is the number of parameter and m is the number categories.

We perform another set of pair-wise comparison but this time for the routes and build a set of comparison square matrix for all QoS attributes, C = [C_{ij}] of order p, where p is the number of routes. Using the mechanism

given in equation (2), we construct R_{ij}; where, R_{ij} is route weight distribution of route i for parameter j. We represent R_{ij} in matrix $D = [D_{ij}]_{p \times n}$, where p is the number of routes and n is the number of parameter. Finally, we perform matrix multiplication within D x B = $[E]_{p \times m}$. This is the solution matrix. Highest value of each column represents the best route for a particular category of flow traffic.

E. Case Study

To demonstrate how AHP engine works we will use an example ad hoc network scenario. The topology of the scenario is given below (figure 2). S wants to send VoIP traffic to D and it is discovering route for D. In this topology, S can reach to D, using one of the three routes (Route 1: H-I-J-K, Route 2: A-B-C, Route 3: E-F-G). Following section demonstrates how AHP calculates the matrix.

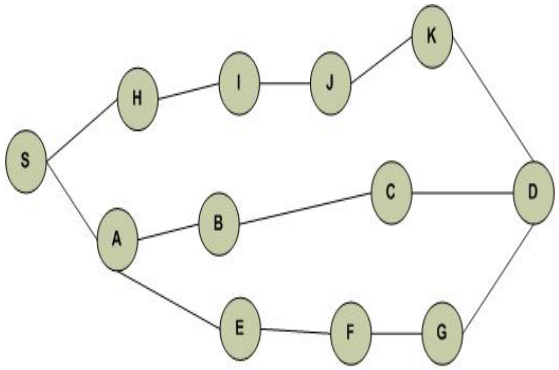

Fig. 2. Ad Hoc Network topology

Using the stringency of common application with their QoS requirement adapted from [21], following matrixes are pre-computed to all nodes which shows the pair wise weight distribution of the QoS attributes for different categories. Although almost all of the QoS attribute requirement varies for different access class traffic but requirement of load and battery power level is uniform for all categories. That's why we have placed uniform intensity of importance of those two attributes throughout the matrices. We have used following notation for simpler usage: Throughput = T, Delay = D, Jitter =J, Reliability = R, Load = L, Battery Power = B.

Table III: Factor comparison category 3

Cat 3	T	D	J	R	L	B	Row Sum	Score
T	1	3/5	3/5	3	1	1	7.2	0.132
D	5/3	1	1	5	5/3	5/3	15.33	0.28
J	5/3	1	1	5	5/3	5/3	15.33	0.28
R	1/3	1/5	1/5	1	1/3	1/3	2.4	0.044
L	1	3/5	3/5	3	1	1	7.2	0.132
B	1	3/5	3/5	3	1	1	7.2	0.132
Total							54.66	1

Table IV: Factor comparison category 2

Cat 2	T	D	J	R	R	B	Row Sum	Score
T	1	5	1	5	5/3	5/3	15.33	0.28
D	1/5	1	1/5	1	1/3	1/3	3.07	0.05
J	1	5	1/5	5	5/3	5/3	15.33	0.28
R	1/5	1	1/5	1	1/3	1/3	3.07	0.05
L	3/5	3	3/5	3	1	1	9.2	0.17
B	3/5	3	3/5	3	1	1	9.2	0.17
Total							55.2	1

Table V: Factor comparison category 0

Cat 0	T	D	J	R	L	B	Row Sum	Score
T	1	1	3	3/5	1	1	7.6	0.17
D	1	1	3	3/5	1	1	7.6	0.17
J	1/3	1/3	1	1/5	1/3	1/3	2.53	0.05
R	5/3	5/3	5	1	5/3	5/3	12.67	0.27
L	1	1	3	3/5	1	1	7.6	0.17
B	1	1	3	3/5	1	1	7.6	0.17
Total							45.6	1

Table VI: Factor comparison category 1

Cat 1	T	D	J	R	L	B	Row Sum	Score
T	1	1	1	1/5	1/3	1/3	3.87	0.07
D	1	1	1	1/5	1/3	1/3	3.87	0.07
J	1	1	1	1/5	1/3	1/3	3.87	0.07
R	5	5	5	1	5/3	5/3	19.33	0.37
L	3	3	3	3/5	1	1	11.6	0.21
B	3	3	3	3/5	1	1	11.6	0.21
Total							54.14	1

Now, different routes are pair wise compared for each QoS attributes. Before forming this pair wise comparisons we need to obtain the values for the QoS attributes and order them according to the intensity of importance. To do that we use two threshold values: $\alpha 1$ and $\alpha 2$, where $\alpha 1 > \alpha 2 > 0$. If perceived value of a QoS attribute is beyond $\alpha 1$ then its intensity level is considered high. On the other hand, if the value lies between $\alpha 1$ and $\alpha 2$ then intensity level is medium. Otherwise, intensity is considered low. We will assume that from a set of perceived values of the attributes in the network, following table is formed:

Table VII: Ranking for other categories

Parameter	Route 1	Route 2	Route 3
Throughput	High	Medium	Medium
Delay	Medium	Low	High
Jitter	Medium	Low	High
Reliability	High	Medium	High
Load	Medium	High	Low
Battery Power	Medium	High	Low

Following matrices shows the pair wise comparison and

priority rating of the each route for each of the parameters based on the information in table VIII.

Table VIII: Pair wise comparison for Throughput

Throughput	Route 1	Route 2	Route 3	Row Sum	Score
Route 1	1	5/3	5/3	4.33	0.44
Route 2	3/5	1	1	2.6	0.27
Route 3	3/5	1	1	2.6	0.27
Total				9.53	1

Similarly, pair-wise weight distribution of all the routes for other attributes are calculated and following matrix is formed.

Table IX: Priority rating of options against all factors

	Throu-ghput	Delay	Jitter	Reli-ability	Load	Battery Power
Route 1	0.44	0.33	0.33	0.39	0.33	0.33
Route 2	0.27	0.56	0.56	0.22	0.11	0.11
Route 3	0.27	0.11	0.11	0.39	0.56	0.56

The last step is to establish the overall ranking among the alternatives by combining the priority matrices – weight distribution of criteria and weight distribution of options. The outcome from this product is the overall ranking for the options in achieving the goal. Following matrix multiplication will determine the overall ranking of the routes for VoIP traffic flow. As VoIP traffic falls into category 3, weight distribution of routes are multiplied with the weight distribution of attributes for category 3. Product from the above combination results the final overall ranking shown in table XI, with Route 2 coming out as the most favorable alternatives for category 3.

Table 10: Combined Matrix

Thro-ugput	Del-ay	Jitt-er	Reli-ability	Lo-ad	Batt-ery Power		Cat 3
0.44	0.33	0.33	0.39	0.33	0.33		0.132
0.27	0.56	0.56	0.22	0.11	0.11	*	0.28
0.27	0.11	0.11	0.39	0.56	0.56		0.28
							0.044
							0.132
							0.132

Table XI: Ranking of routes for category 3

Route	Category 3
Route 1	0.34716
Route 2	0.38796
Route 3	0.26224

Table XII shows the ranking of the routes if other categories of traffic are considered. Here, Route 1 is the most favorable route in category 2, Route 3 is the most favorable for category 0 and Route 1is the most favorable for category 1. The destination node will send a route reply to the source accordingly.

Table XII: Ranking for other categories

Category 2	Category 0	Category 1
0.3638	0.3649	0.3599
0.3088	0.2659	0.2249
0.3218	0.3658	0.4138

V. CONCLUSION

Current trend in research in the field of QoS routing in MANET shows that that, researchers are putting a great emphasis on the session admission (QoS route finding) capability of their protocol, which is admittedly very important. Conforming to that, we present a QoS aware route selection mechanism for mobile ad hoc network. In order to make a more accurate route selection for best QoS support we select the most important QoS attributes from different aspects. AHP is used to calculate the integral value of multiple parameters and make the route selection decision in which the human aspect is involved to determine the importance between different criteria. As the calculations are neither numerous nor complicated, a use for real time route selection is possible. It can be expanded for additional criteria and attributes. So, this scheme significantly advances the system flexibility and extensibility, and provides more accurate and effective route selection at any time.

However, session completion is also as important as session admission from a user perspective. This is because the perceived QoS is better when some sessions are blocked but none are dropped in mid session. In this proposal we have not explained any QoS assurance procedure. We will look into the aspect of session completion in future research. Furthermore, we will also look into fast local QoS route-repairing schemes require to improve QoS session completion rates and protocols' robustness against mobility. Finally, experimental result from simulated environment will reflect the strength of our proposal. We are going to provide outcomes of simulated experiments in the upcoming works.

REFERENCES

[1] Hanzo-II, L.; Tafazolli, R**.,"**A SURVEY OF QOS ROUTING SOLUTIONS FOR MOBILE AD HOC NETWORKS", Communications Surveys & Tutorials, IEEE Volume 9, Issue 2, Page(s):50 – 70, Second Quarter 2007.

[2] Saaty, Thomas L. "How to make decision: The Analytic Hierarchy Process", European Journal of Operational Research, Vol. 48, pp 9-26, 1990.

[3] ITU-T Y.1540 AMD 1: Internet protocol data communication service – IP packet transfer and availability performance parameters Amendment 1.

[4] Prasant Mohapatra, Jian Li, and Chao Gui, "QoS in Mobile Ad hoc Networks," Special Issue on QoS in Next-Generation Wireless Multimedia Communications Systems *in IEEE Wireless Communications Magazine*, June 2003.

[5] Daqing Gu Jinyun Zhang, "QoS enhancement in IEEE 802.11 wireless local area networks", Communications Magazine, IEEE, Volume: 41, Issue: 6, page(s): 120- 124, June 2003.

[6] IEEE 802.16-2004, "IEEE Standard for Local and Metropolitan Area Networks – Part 16: Air Interface for Fixed Broadband Wireless Access Systems", October 2004.

[7] UMTS: Quality of Service, http://www.umtsworld.com/technology/qos.htm, Last accessed on 29th July, 2009

[8] S. Chen," Routing Support for Providing Guaranteed End-to-End Quality-of-Service", PhD thesis, University of IL at Urbana-Champaign, 1999.

[9] Lei Chen, Wendi B. Heinzelman, "QoS-Aware Routing Based on Bandwidth Estimation for Mobile Ad Hoc Networks", Selected Areas in Communications, IEEE Journal on Volume 23, Issue 3, Page(s): 561 – 572, March 2005.

[10] Chenxi Zhu, M. Scott Corson, "QoS routing for mobile ad hoc networks", Infocom 2002, Available at:http://www.ieeeinfocom.org/2002/papers/121.pdf, Last accessed on: 29 July, 1009.

[11] Lin, C.R. Gerla, M, "Asynchronous Multimedia Multihop Wireless Networks", INFOCOM '97. Sixteenth annual Joint Conference of the IEEE Computer and Communications Societies. Proceedings IEEE Vol: 1, page(s): 118-125, Apr1997.

[12] M. Wang and G.-S. Kuo, "An application-aware QoS routing scheme with improved stability for multimedia applications in mobile ad hoc networks," in Proc. IEEE Vehicular Technology Conf., pp. 1901–1905, Sep. 2005.

[13] B. Zhang and H. T. Mouftah, .QoS routing for wireless ad hoc networks: problems, algorithms and protocols, *IEEE Communication Magazine*, vol. 43, pp. 110.117, Oct. 2005.

[14] M. Sheng, J. Li, and Y. Shi, "Routing protocol with QoS guarantees for ad-hoc network", Electronics Letters, volume 39, pp. 143.145, Jan. 2003.

[15] L. Barolli, A. Koyama, and N. Shiratori, "A QoS routing method for ad-hoc networks based on genetic algorithm", In Proceedings of 14th International Workshop. Database and Expert Systems Applications, pp. 175. 179, Sep. 2003.

[16] A. Misra and S. Banerjee, "MRPC: Maximizing network lifetime for reliable routing in wireless environments", In Proceedings of IEEE Wireless Communications and Networking Conference., March 2002.

[17] WLAN Quality of Service, Available at: http://www.cisco.com/en/US/docs/solutions/Enterprise/Mobility/vowlan/41dg/vowlan_ch2.html, Last accessed on 29th July, 2009.

[18] D. Johnson, Y. Hu, D. Maltz, "RFC 4728: The Dynamic Source Routing Protocol (DSR) for Mobile Ad Hoc Networks for IPv4", February 2007

[19] T. B. Reddy, I. Karthigeyan, B. Manoj, and C. S. R. Murthy, "Quality of service provisioning in ad hoc wireless networks: a survey of issues and solutions." available online: http://www.sciencedirect.com, Last accessed on 29th July, 2009.

[20] Dr S. Tom Foster, Dr. Gerald LaCava, "The Analytical Hierarchy Process: A step by step approach", Available at: https://acc.dau.mil/GetAttachment.aspx?id=5479&pname=file&aid=18722&lang=en-US, Last accessed on 29th July, 2009.

[21] Andrew S. Tanenbaum, "Quality of Service: Requirements", Computer Network, Chapter 5, page: 397, Fourth Edition, Prentice Hall, October 2002.

Proceedings of 2009 12th International Conference on Computer and Information Technology (ICCIT 2009)
21-23 December, 2009, Dhaka, Bangladesh

Palmprint based Verification System Robust to Rotation, Scale and Occlusion

Badrinath G S and Phalguni Gupta
Dept. of Computer Science and Engineering, Indian Institute of Technology Kanpur, India
badri@cse.iitk.ac.in, pg@cse.iitk.ac.in

Abstract

This paper proposes an efficient palmprint based verification system which is robust to rotation, scale and occlusion. Images are obtained using a flat bed scanner. Scale Invariant Feature Transform (SIFT) operator is used to extract features from the palmprint. Nearest neighbor ratio method is used to determine the similarity between extracted features of live and enrolled palmprints and to make matching decision. The proposed system has been tested using three databases-IITK database having 549 hand images, CASIA database with 5239 hand images and PolyU database of size 7752. Accuracy of the proposed system is found to be 99.97% with FAR of 0.06% in case of IITK database, while for CASIA and PolyU database is more than 99%. Further the robustness of the system with respect to scale rotation and occlusion has been studied.

I. INTRODUCTION

Palmprint is a region between wrist and fingers and has features like principle lines, minutiae points, ridges, wrinkles and texture that can be used for its representation [1]. Unlike other biometrics systems, palmprint meets the requirement for designing an efficient biometrics system. Some of these requirements that are available in palmprint are (i) relatively stable and unique features (ii) easy and non intrusive way of data collection (iii) minimum cooperation requirement from users (iv) use of minimum cost (i.e. low resolution) used scanners (v) maximum accuracy. Thus systems based on hand features are highly acceptable to users [2]. Furthermore, palmprint also serves as reliable biometric features because the print patterns are not same even in monozygotic twins [3].

However, despite of its significant features limited work has been reported on palmprint based identification/verification. Efforts have been made to build a palmprint based system using structural features of palmprint like line features [4], crease points [5], local binary pattern histgrams [6] and datum points [7]. There exist systems based on statistical features of palmprint using Karhunen-Lowe transforms [8], Discrete Cosine Transforms [9], Independent Component Analysis, Fourier transforms [10], Wavelet transforms [11], [12], Linear Discriminant Analysis (LDA) [13], Gabor filter [2], Neural networks [14], [4], hand gometry [14] and statistical signature [12]. There are multimodal biometric sytems fusing palmprint features with these of other traits like fingerprint [8], hand geometry [14], and face [15] to improve the accuracy. However, to the best of authors knowledge there is no system reported in literature which is robust to scale or rotation or occlusion. Palmprint based system has many unattended but critical problems. Some of them are enlisted below:

- The device used for acquiring hand image should be constraint free, so that physically challenged or injured people can provide biometric sample for registration or verification
- The system may use scanner with different spatial resolution for acquiring image during verification. System should be able to verify the user.
- Due to misalignment of CCD [2] and pegs holding rest, the palmprint image obtained may be rotated. The system should be able to handle such a situation.
- The user may not be able to expose complete palmprint for verification. The system should be able to verify the user with partial palmprint.
- The system should perform satisfactorily, independent to input device used for acquiring hand images.

Furthermore, it should be highly accurate and be available at reasonable price.

This paper uses Scale Invariant Feature Transform (SIFT) [16] to extract features from palmprint which can be used for personal verification. The extracted features of live and enrolled palmprint are matched using nearest neighbour ratio matching [17]. The proposed system also handles some of the above said problems.

II. SCALE INVARIANT FEATURE TRANSFORM

The Scale Invariant Feature Transform (SIFT) has been used in machine vision applications and object detection [18], [19], [20], [21]. It has been designed to extract stable features which are highly distinctive and invariant to affine transformations. Features are efficiently detected through stage filtering in scale space. Feature vectors are formed by means of local patterns around key-points from scale space decomposed image. Following are the major stages of computation used to generate set of SIFT features:

- Scale-space extrema detection: It is the first stage of computation searches over all scales and image locations. It is implemented efficiently by using a

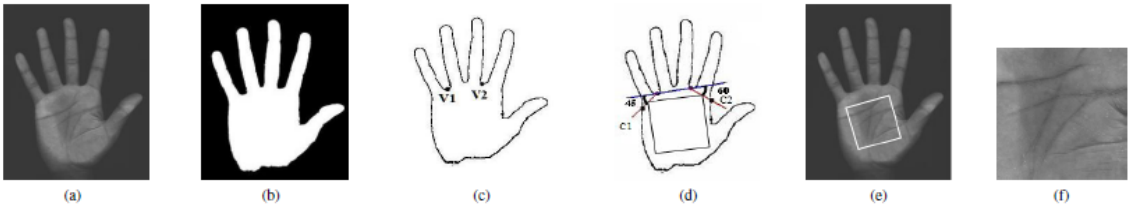

Fig. 1: (a) Scanned Image. (b) Binarized Image. (c) Hand Contour and reference points. (d) Relevant points and palmprint. (e) Palmprint in gray scale hand image (f) Extracted palmprint.

Difference-of- Gaussian function to identify potential interest points that are invariant to scale.

- Key-point localization: At each candidate location, a detailed model is fitted to determine location and scale. Key-points are selected based on measures of their stability.
- Orientation assignment: Consistent orientation is assigned to the key-point based on the local image properties. Hence it makes the key-point descriptor rotation invariant.
- Key-point descriptor: Feature vector of 128 values is computed for the local image region at key-point.

III. PROPOSED SYSTEM

The process starts with acquiring the input image of hand using low cost scanner. In the palmprint extraction module the acquired hand images are pre-processed and palmprint is extracted. Palmprint features are extracted using SIFT in feature extraction module. Extracted features of live palmprint and enrolled palmprint in the database are matched using nearest neighbor ratio method. Matching decision is done based on number of matching points. The detailed description of steps involved in the proposed system is given as follows.

A. IMAGE ACQUISITION

Hand image from users are obtained using a flat bed scanner at resolution of 200 dots per inch, and 256 gray level. Sample hand image in gray level obtained using flat bed scanner is shown in Fig. 1a. The scanner used to obtain hand image is constraint (pegs) free.

B. PRE-PROCESSING AND PALMPRINT EXTRACTION

In this section palmprint is extracted from the acquired hand image. Since hand image and background are contrasting in color, global thresholding can be applied to obtain the binarized hand image (shown in Fig. 1b). The contour of the hand image is obtained using contour tracing algorithm [22] on binarized hand image. Two valley points ($V1$ - $V2$) between fingers are detected on the contour of the hand image as shown in Fig. 1c.

Square area as shown in Fig 1d with two of its adjacent corners coinciding with mid-points of line segments ($V1$ - $C1$) and ($V2$ - $C2$) is considered as palmprint. The line segments (V 1 - $C1$) and ($V2$ - $C2$) are inclined at an angle of 45^0 and 60^0 to line joining ($V1$ - $V2$) respectively. The palmprint region in hand image is shown in Fig. 1e. Extracted palmprint is shown in Fig. 1f.

C. FEATURE EXTRACTION AND MATCHING

SIFT [16] is used to extract the features which provides good discriminating ability. SIFT has been designed to extract highly distinctive and invariant features from images. Thus extracted feature from palmprint image can be matched correctly with high probability against feature from a large palmprint database. The SIFT extracted features are found to be invariant to scaling, translation and rotation of the image [16]. The detected SIFT key-points for a palmprint image are shown in Fig. 3. The extracted features are live and enrolled palmprint are matched for similarity using nearest neighbour ratio matching [17].

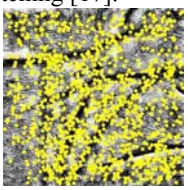

Fig. 3: SIFT key-points for palmprint

The matching key-points between two palmprint images are shown in Fig. 4.

Fig. 4: Matching key-points for enrolled and live palmprints.

IV. EXPERIMENTAL RESULTS

The proposed system is tested on three database: The Indian Institute of Technology Kanpur (IITK) database, The Hong Kong Polytechnic University (PolyU) [24] database and The Chinese Academy of Sciences Institute of Automation (CASIA) [23].

A. DATASETS

1) *IITK database* contains 549 hand images from

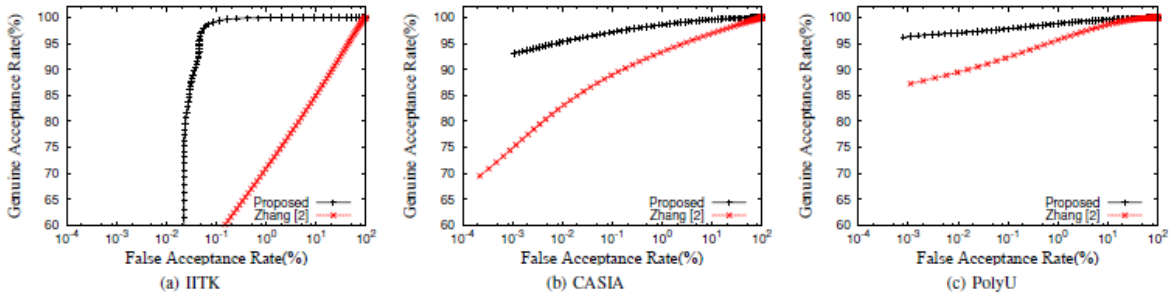

Fig. 5: ROC curves of proposed system and Zhang [2]

150 users corresponding to 183 different. Three hand images have been collected per palm using flat bed scanner at 200 dpi spatial resolution, and 256 gray levels. One image per palm is considered for training and remaining two images are used for the testing.

2) *CASIA database* consists of 5,239 hand images captured from 301 subjects corresponding to 602 palms. For each subject, around 8 images from left hand and 8 images from right hand are collected using CMOS and 256 gray-level. Two images per palm are considered for training and remaining six images are used for the testing.

3) *PolyU database* consists of 7,752 grayscale images from 193 users corresponding to 386 different palms. Around 17 images per palm are collected in two sessions using CCD [2] at spatial resolution of 75 dots per inch, and 256 gray levels. Six images per palm are considered for training and remaining ten images are used for the testing.

The performance of the proposed system is compared with the best known proposed system in [2]. The Receiver Operating Characteristics Curves (ROC) of both the systems for IITK, CASIA and PolyU are shown in Fig. 5. It can be observed from Fig 5 that the proposed system performs better than [2] for all the datasets. The accuracy (abbreviated as Acc) of the systems are computed as follows:

$$Accuracy = \frac{\max}{Mth}\left(100 - \frac{FAR + FRR}{2}\right)$$

where *MTh* is the threshold for matching palmprints.

The EER and accuracy along with FAR and FRR for both the systems on all three datasets is shown in Table I. From results in Fig. 5 and Table I, it can be said that the proposed system performs satisfactorily and outperforms the best known system in [2]. Since the proposed system performs satisfactorily for hand images of IITK, CASIA and PolyU which have acquired images using flat bed scanner, CMOS and CCD. Hence, the proposed system is robust to input device used to acquire hand images.

V. ROBUST TO ROTATION

The proposed system extracts palmprint features using SIFT descriptors of key-points. The SIFT key-point descriptors are relative to dominant orientation to the key-point. Hence the key-point descriptors remains same independent to orientation of palmprint image. So the proposed system is robust to rotation of palmprint image.

In order to investigate the robustness of the system for rotation the palmprint images in the testing set are rotated to 0^0, 5^0, 10^0, 20^0, 45^0, and 90^0 using bicubic interpolation. Matching points between the enrolled and rotated palmprint images are shown in Fig. 6. The ROC curves of the system for different angles of testing images are shown in Fig. 7a, Fig. 7b and Fig 7c for IITK, CASIA and PolyU databases respectively. The EER and accuracy along FAR and FRR of the system for different angles of testing images for is shown in Table II. It can be observed from Table II and Fig. 7, that the accuracy of the system is approximately same independent to orientation of the testing image. Hence it can be inferred that the proposed system is highly robust to rotation.

VI. ROBUST TO SCALE

Since the palmprint features extracted using SIFT are invariant to scale of the image [16], the system is robust to scale (spatial resolution). In order to investigate the robustness of proposed system to scale, palmprint images of the testing set are downscaled to ($0.9W \times 0.9H$), ($0.8W \times 0.8H$), ($0.7W \times 0.7H$), ($0.6\text{W} \times 0.6H$), ($0.5W \times 0.5H$), ($0.4W \times 0.4H$), ($0.3W \times 0.3H$) and ($0.2W \times 0.2H$) using bicubic interpolation, where W and H are width and height of the image respectively. Matching points between the downscaled live palmprint and enrolled palmprint images are shown in Fig. 7. ROC

TABLE I: Performance of the Proposed System and Zhang [2]

	IITK				CASIA				PolyU			
	Acc	FAR	FRR	EER	Acc	FAR	FRR	EER	Acc	FAR	FRR	EER
Proposed	**99.97**	**0.051**	**0.014**	**0.059**	**98.98**	**0.550**	**1.479**	**0.814**	**99.03**	**0.328**	**1.603**	**0.842**
Zhang [2]	85.90	11.08	17.10	15.13	96.44	2.30	4.80	10.0	98.56	0.44	0.83	3.760

TABLE II: Performance for Different Rotations

	IITK		CASIA		PolyU	
Angle	Acc (%)	EER (%)	Acc (%)	EER (%)	Acc (%)	EER (%)
0^0	99.97	0.059	98.98	0.814	99.03	0.842
5^0	99.97	0.044	98.82	1.016	99.26	0.585
10^0	99.97	0.044	98.55	1.310	99.25	0.588
20^0	99.91	0.142	98.76	1.270	99.42	0.545
45^0	**99.96**	**0.067**	**98.80**	**1.184**	**99.29**	**0.515**
90^0	99.96	0.059	98.89	1.194	99.04	0.845
180^0	99.96	0.067	98.93	1.148	99.08	0.842

curves obtained for different scales are shown in Fig. 8a, Fig. 8b and Fig 8c for IITK, CASIA and PolyU databases respectively. The EER and accuracy along with FAR and FRR of the system for different scales of the testing set images of three datasets is shown in Table III. It has been observed that the accuracy of the system dropped below 80% for testing set image size downscaled below 0.5W × 0.5H. It has been also observed that there is no matching point when testing set images are downscaled below $0.2W \times 0.2H$. However, from the results in Table III, it can be said that the system is robust to scale.

TABLE III: Performance for Different Scales

	IITK		CASIA		PolyU	
(W×H)	Acc (%)	EER (%)	Acc (%)	EER (%)	Acc (%)	EER (%)
1.0	99.97	0.058	98.98	0.814	99.03	0.842
0.9	99.93	0.127	98.74	1.143	98.93	0.830
0.8	99.70	0.485	98.86	1.028	98.61	1.113
0.7	98.95	1.189	98.37	1.786	98.01	1.568
0.6	99.25	1.136	98.13	1.419	96.89	3.275
0.5	**98.72**	**1.241**	**96.81**	**3.056**	**94.98**	**4.982**
0.4	97.39	2.549	93.71	6.531	88.90	10.11
0.3	94.67	4.904	79.78	20.34	77.73	20.86
0.2	78.32	23.30	56.32	44.47	57.40	42.66

TABLE IV: Performance for Different Occlusion Sizes

	IITK		CASIA		PolyU	
(W×H)	Acc (%)	EER (%)	Acc (%)	EER (%)	Acc (%)	EER (%)
0.0	99.97	0.059	98.98	0.814	99.03	0.842
0.1	99.96	0.059	98.88	1.192	99.07	0.847
0.2	99.88	0.179	98.86	1.307	99.11	0.897
0.3	99.75	0.373	98.70	1.452	98.98	0.966
0.4	99.55	0.698	97.86	1.732	98.75	1.155
0.5	98.98	1.151	97.01	2.389	97.78	1.798
0.6	**98.30**	**1.652**	**95.45**	**4.563**	**94.35**	**5.479**
0.7	96.70	2.833	90.82	8.944	86.25	13.32
0.8	92.00	6.967	79.18	18.47	72.91	27.46
0.9	72.23	27.95	56.73	42.11	56.07	42.10

VII. ROBUST TO OCCLUSION

The proposed systems extracts palmprint features using SIFT, which describes palmprint with local region around key-points. Hence the key-point descriptors are independent to the area of occlusion and matching can be performed between SIFT key-points of non-occluded regions of live and enrolled palmprint images. So, the proposed system can be used in the place where user can expose partial palmprint region to the scanner. In order to investigate robustness of the the proposed system for occlusion, ($0.9W \times 0.9H$), ($0.8W \times 0.8H$), ($0.7W \times 0.7H$), (0.6W × 0.6H), ($0.5W \times 0.5H$), ($0.4W \times 0.4H$), ($0.3W \times 0.3H$) and ($0.2W \times 0.2H$) of the palmprint images in the testing set are occluded. The matching key-points between enrolled and different sizes of occluded palmprint image is shown in Fig. 9. The ROC curves obtained for different sizes of occlusion is shown in Fig. 10a, Fig. 10b and Fig 10c for IITK, CASIA and PolyU databases respectively. The EER and accuracy along with FAR and FRR for different sizes of occlusion on testing set are shown in Table IV. From the results in Table IV it can be observed that the system for occlusion $0.6W \times 0.6H$ performs with accuracy more than 98% with FAR of 1.4% in case of IITK database. Further the robustness for PolyU and CASIA is more than 94.5%, which implies that the proposed system is robust to occlusion.

VIII. CONCLUSIONS

In this paper development of robust palmprint based verification system is described. It uses hand images obtained from low cost flat bed scanner. SIFT features are used to extract the features of the palmprint. The live and enrolled palmprint SIFT features are matched using nearest neighborhood ratio method. The system is tested using IITK database of 549 hand images, CASIA database of 5239 hand images and PolyU databases of 7752 hand images, which are acquired using flat bed scanner, CCD and CMOS respectively. The accuracy of the system is more than 98.50% along with FAR and FAR less than 0.6% and 1.6% respectively at original sizes. Proposed system outperforms the best known system in [2]. Performance of the proposed system for all three datasets which are acquired using flat bed scanner (IITK), CCD (PolyU) and CMOS (CASIA) shows that the system is robust to input device used to acquire hand images. It is also robust to scale, rotation and occlusion. The accuracy of the system is more than 94% for downscaled testing set images upto $0.5W \times 0.5H$, while it performs with accuracy more than 98% for any angle of rotation, and performs with accuracy 94% for occlusion size of $0.6W \times 0.6H$. Thus the proposed system which is robust (a) to translation and

orientation of placement of hand on scanner, (b) to scale of palmprint, (c) to rotation of palmprint, (d) to occlusion of palmprint, (e) to device used to obtain hand images along with its performance, speed and use of pegs free low cost scanner can be considered for human verification.

REFERENCES

[1] W. Shu and D. Zhang, "Automated personal identification by palmprint," Optical Engineering, vol. 37, no. 8, pp. 2359–2362, 1998.

[2] D. Zhang, A. W. Kong, J. You, and M. Wong, "Online palmprint identification," IEEE Transactions on Pattern Analysis and Machine Intelligence, vol. 25, pp. 1041–1050, September 2003.

[3] T. Connie, A. Teoh, M. Ong, and D. Ngo, "An automated palmprint recognition system," Image and Vision Computing, vol. 23, pp. 501–515, May 2005.

[4] C. Han, H. Cheng, C. Lin, and K. Fan, "Personal authentication using palm-print features," Pattern Recognition, vol. 36, pp. 371–381, February 2003.

[5] J. Chen, C. Zhang, and G. Rong, "Palmprint recognition using crease," in International Conference on Information Processing, pp. 234–237, 2001.

[6] X. Wang, H. Gong, H. Zhang, B. Li, and Z. Zhuang, "Palmprint identification using boosting local binary pattern," in Intl. Confrence on Pattern Recognition, pp. 503–506, 2006.

[7] D. Zhang and W. Shu, "Two novel characteristics in palmprint verification: datum point invariance and line feature matching," Pattern Recognition, vol. 32, pp. 691–702, April 1999.

[8] S. Ribaric and I. Fratric, "A biometric identification system based on eigenpalm and eigenfingerfeatures," IEEE Transactions on Pattern Analysis and Machine Intelligence, vol. 27, pp. 1698–1709, November 2005.

[9] X. Jing and D. Zhang, "A face and palmprint recognition approach based on discriminant dct feature extraction," Systems, Man, and Cybernetics-B, vol. 34, pp. 2405–2415, December 2004.

[10] L. Wenxin, D. Zhang, and X. Zhuoqun, "Palmprint identification by fourier transform," International Journal of Pattern Recognition and Artificial Intelligence, vol. 16, pp. 417–432, September 2002.

[11] G. Badrinath and P. Gupta, "An efficeint multi-algorithm fusion system based on palmpring for personnel identification," in Intl. Conf. On Advanced Computing, pp. 759–764, 2007.

[12] L. Zhang and D. Zhang, "Characterization of palmprints by wavelet signatures via directional context modeling," Systems, Man, and Cybernetics, vol. 34, pp. 1335–1347, June 2004.

[13] X. Wu, D. Zhang, and W. K., "Fisherpalms based palmprint recognition," Pattern Recognition Letters, vol. 24, pp. 2829–2938, 2003.

[14] A. Kumar and D. Zhang, "Personal recognition using hand shape and texture," IEEE Transactions on Image Processing, vol. 15, pp. 2454–2461, August 2006.

[15] R. Rowe, U. Uludag, M. Demirkus, S. Parthasaradhi, and A. Jain, "A multispectral whole-hand biometric authentication system," Proc. of Biometrics Symposium Biometric Consortium Conference, pp. 1–6, September 2007.

[16] D. Lowe, "Distinctive image features from scale-invariant keypoints," International Journal of Computer Vision, vol. 60, pp. 91–110, November 2004.

[17] K. Mikolajczyk and C. Schmid, "A performance evaluation of local descriptors," Pattern Analysis and Machine Intelligence, vol. 27, pp. 1615–1630, October 2005.

[18] D. Lowe, "Local feature view clustering for 3d object recognition," in Computer Vision and Pattern Recognition, pp. I:682–688, 2001.

[19] D. Lowe, "Object recognition from local scale-invariant features," in Internation Confrence in Conputer Vision, pp. 1150–1157, 1999.

[20] M. Bicego, A. Lagorio, E. Grosso, and M. Tistarelli, "On the use of sift features for face authentication," in Computer Vision and Pattern Recognition Workshop, pp. 35–41, 2006.

[21] P. Chakravarty, "Vision-based indoor localization of a motorized wheelchair," 2005.

[22] T. Pavlidis, Algorithms for Graphics and Image Processing. Computer Science Press, 1982.

[23] "The casia palmprint database." http://www.cbsr.ia.ac.cn/.

[24] "The polyu palmprint database." http://www.comp.polyu.edu.hk/ biometrics.

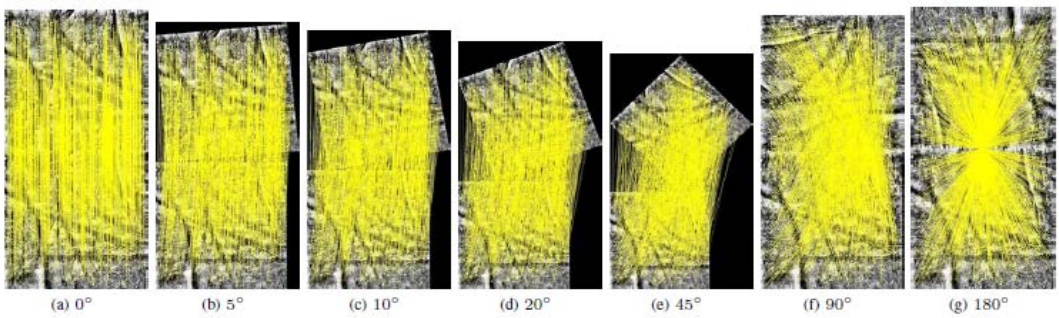

Fig. 12: Matching Points between Enrolled and Rotated Live Palmprint.

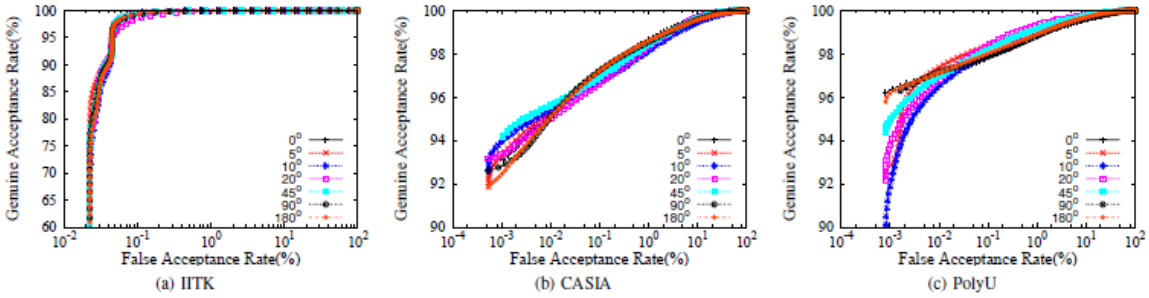

(a) IITK (b) CASIA (c) PolyU

Fig. 6: ROC Curves of the Proposed System for Different Rotations

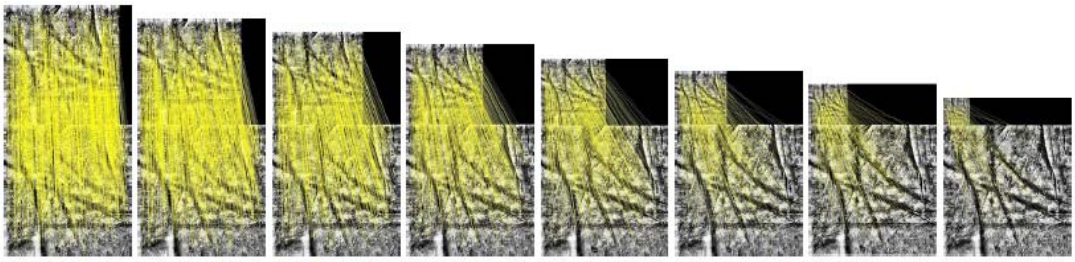

(a) $0.9W \times 0.9H$ (b) $0.8W \times 0.8H$ (c) $0.7W \times 0.7H$ (d) $0.6W \times 0.6H$ (e) $0.5W \times 0.5H$ (f) $0.4W \times 0.4H$ (g) $0.3W \times 0.3H$ (h) $0.2W \times 0.2H$

Fig. 7: Matching Points between Enrolled and Downscaled Live Palmprint

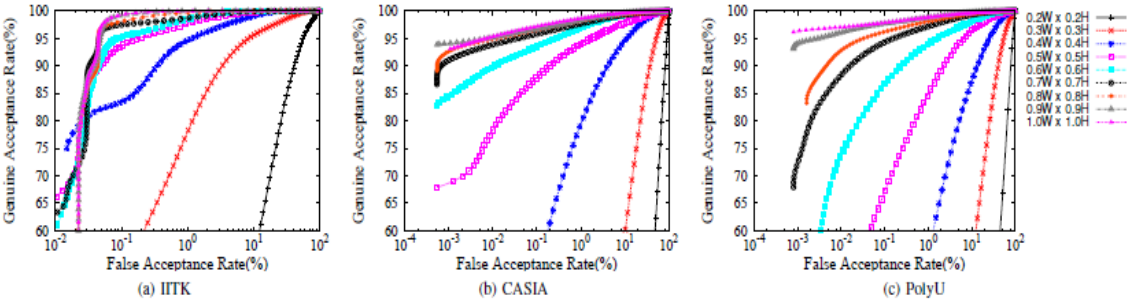

(a) IITK (b) CASIA (c) PolyU

Fig. 8: ROC Curves of Proposed System for Different Scales

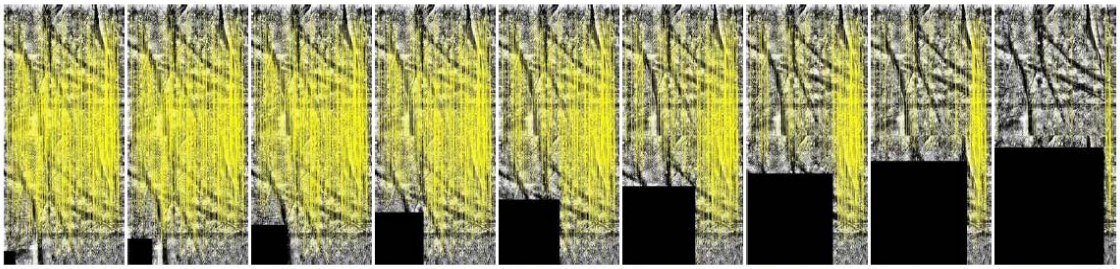

(a) $0.1W \times 0.1H$ (b) $0.2W \times 0.2H$ (c) $0.3W \times 0.3H$ (d) $0.4W \times 0.4H$ (e) $0.5W \times 0.5H$ (f) $0.6W \times 0.6H$ (g) $0.7W \times 0.7H$ (h) $0.8W \times 0.8H$ (i) $0.9W \times 0.9H$

Fig. 9: Matching Points between Enrolled and Partially Occluded Live Palmprint.

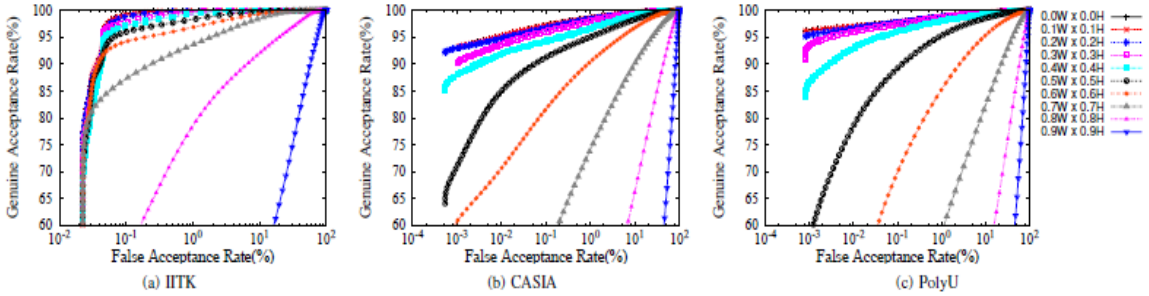

(a) IITK (b) CASIA (c) PolyU

Fig. 10: ROC Curves of Proposed System for Different Sizes of Occlusion

Proceedings of 2009 12th International Conference on Computer and Information Technology (ICCIT 2009)
21-23 December, 2009, Dhaka, Bangladesh

Process Centric Work Breakdown Structure of Software Coding for Improving Accuracy of Estimation, Resource Loading and Progress Monitoring of Code Development

A.K.M Zahidul Quaium, Ahmed Latif Shahriar, M. Rokonuzzaman
School of Engineering & Computer Science, Independent University, Bangladesh (IUB), Dhaka, Bangladesh
zahidulqu@gmail.com, alshahriar@gmail.com, zaman.rokon@yahoo.com

Abstract

This study introduces process centric Work Breakdown Structure (WBS) for managing challenges for coding phase of software development cycle. The approach represents WBS as a process centric view to understand the inter relationships and dependencies between activities. Suggested WBS reduces complexities and gaps of the project plan and its execution by early simulation of diverse coding activities through process centric view. It is believed that such process centric approach instead of tree form representation of WBS will improve the visibility of coding process during planning stage for increasing the accuracy of estimation, resource loading, and progress monitoring.

Keywords: Estimation, Estimation accuracy, software coding, Manpower loading, SW-CMMI, Work breakdown structure, Process centric WBS, and Work product.

I. INTRODUCTION

A. Some statistics of software projects' successes and failures

It appears that the history of software project management is dominated by failure statistics. Standish group's research shows 31.1% projects will be cancelled before they ever get completed. 52.7% of projects will cost over 189% of their original estimation. Another survey says 7 out of 10 projects fail in some respect. On the other hand, 16.2% projects are completed on-time and on-budget; in large companies it is 9% [1].

B. Likely reasons for failures and success

It has been reported that reasons of project failure are poor project planning, poor estimation, lack of risk assessment etc. Lack of proper distribution of tasks among the team members may lead the project to failure. Sometimes project also fails due to week business case, lack of support and involvement of top managements, weak definitions of requirements at project planning stage, use of unproven technology, and failure of meeting the commitments of the vendors. Lack of user involvement, lack of resources, lack of IT management or executive support, change in client's business, and inadequate measurements may cause the project to be failed as well. On the other hand, effective project planning helps the project to be succeeded; reduced cost estimation error, effective measurement technique, and controlled tracking lead the project to success.

C. Defining the concept of process centric software production

The concept describes the whole production cycle as an integration of processes consisting of different discrete tasks to be executed in certain sequence. Every process unit is shown ordered and linked to other processes units with input or entry and output or exit criteria. Parallelism of process is another feature of the concept. The approach emphasizes on logic and preventing unstructured work. Process centric approach emphasizes on process performance. Approach helps improve manageability to deliver higher quality and productivity through early visualization of production activities along with their interdependencies. Process centric software production is not limited to any particular model as waterfall or agile. It fits to any conventional model.

D. Defining the current concept of work breakdown structure (WBS)

Work Breakdown Structure (WBS) [2] is a project management tool that captures all the work of the project. It is a tree formatted graphical project management tool [3] that discrete tasks in organized way into different work groups at different levels and also shows effort required to achieve an objective in its subdivision [4]. WBS also defines the scope of the project and helps to prepare project schedule. WBS also provides frameworks for project estimation. It represents the end objective, dividing in terms of size, duration, tasks, and subtasks step by step. WBS is also used to identify and track work packages and deliverables [5]. In Fig. 1, a basic structure of WBS is shown.

978-1-4244-6283-4/09/$26.00 ©2009 IEEE

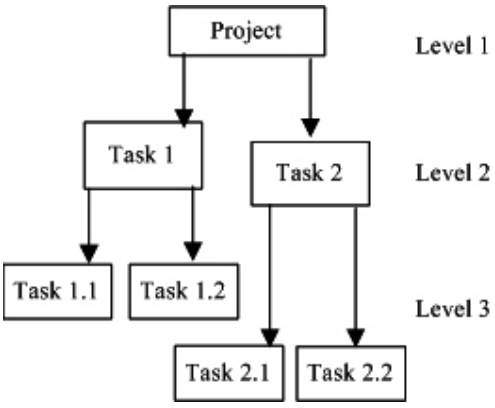

Fig. 1. Basic Structure of WBS

E. Role of WBS in resource estimation, scheduling, progress monitoring, detecting deviations, and taking control actions

Work breakdown structure (WBS) provides a framework of planning, estimating and controlling the project. The WBS is organized around the primary products of the project instead of the work needed to produce the planned actions. As the planned outcomes are destinations of the project, they form a relatively stable set of categories in which the costs of the planned actions needed to achieve them can be collected. A well-designed WBS makes it easy to assign each project activity to only one node of the WBS [3]. In addition to its function in cost accounting, the WBS also helps map requirements from one level of system specification to another, for example a requirements cross reference matrix mapping functional requirements to high level or low level design documents. In planning a project, it is normal to find oneself temporarily overwhelmed and confused, when one begins to take hold of the details and scope of even a modest sized project. This results from one person trying to understand the details of work that will be performed by a number of people over a period of time. The way to get beyond being overwhelmed and confused is to break the project into pieces, organize the pieces in a logical way using a WBS, and then get help from the rest of project [6].

F. Similarities and differences between existing WBS concept and process centric production process

Both existing WBS and Process centric [7] WBS have graphical representation of development activities as project planning tools. Process centric WBS representation emphasizes representation of dependency, links and parallelism of tasks where existing tree structured WBS concept emphasizes on hierarchical representation [8]. Tree form representation of WBS is not able to represent parallelism and interrelation among tasks clearly [9].

G. Concept of process centric WBS representation taking inputs from SW-CMMI

In CMMI Process area 'Integrated Project Management', it is described to establish objective entry and exit criteria to authorize the initial and completion of the task described in the WBS [9]. Process centric WBS inherits the concept of entry and exit criteria. But SW-CMMI [10] got limitation guiding WBS in areas of reducing estimation error, improving manpower loading and adopting parallelism of activities. It has also no guidance to simulate the project assumptions with respect to interfaces between tasks, their interdependencies and scope of parallel execution in the early stage of the project [11].

H. Benefits of process centric representation of WBS in improving project management capability

Main benefit of process centric [12] representation is the ability to model and simulate the WBS at the planning stage taking into consideration of entry and exit criteria of every task, scope of parallel execution of multiple tasks and interdependence between tasks. Such representation of WBS increases the visibility of execution level project at the planning stage and reduces the gap between model of production process used in planning stage [13] and the process which is executed during the development phase. As a result, there are reasons to believe that estimation error will go down, manpower loading error will fall and ability to monitor progress during the production stage will improve [14], [15].

II. PROCESS CENTRIC WBS FOR CODING

Process centric WBS for software coding is described graphically represented in Fig. 2, Fig. 3, and Fig. 4. The each node of WBS is considered as process that got one or more activities. Each node is connected to each other indicating activity sequences and dependencies. There are also Input and output criteria against process nodes in the WBS representation. It should be noted that Fig. 2, Fig. 3, and Fig. 4 are continuation of same WBS.

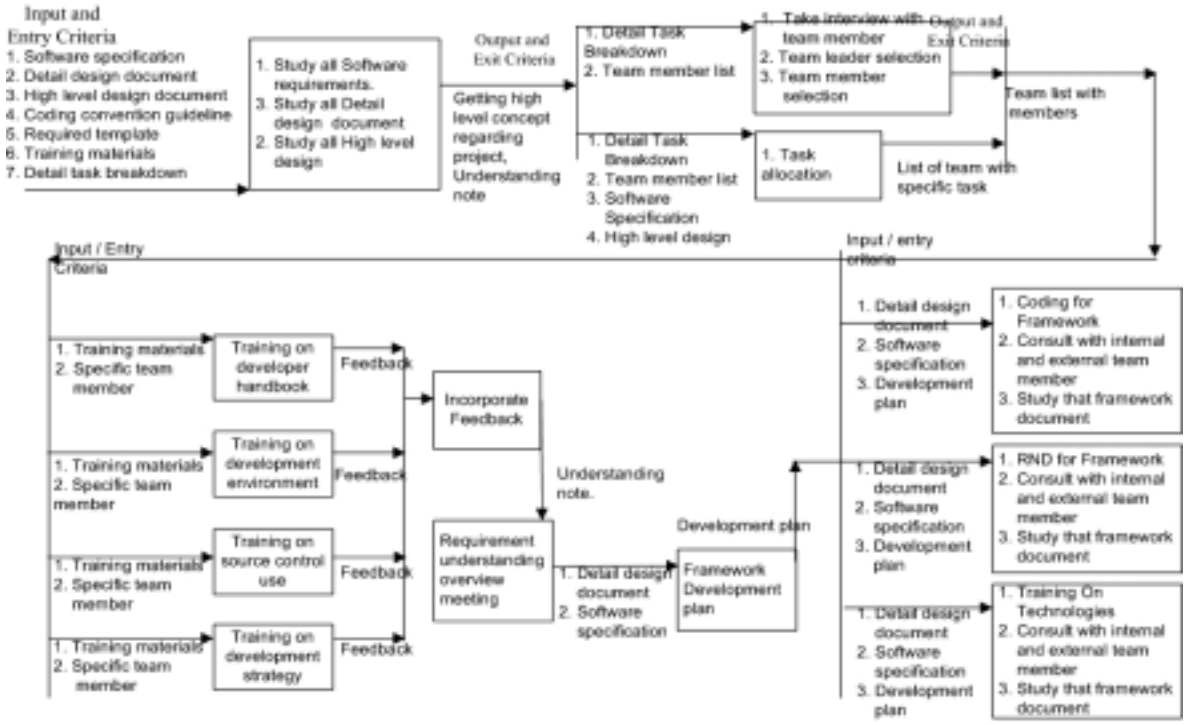

Fig. 2. Step1 Of process centric WBS of software coding phase

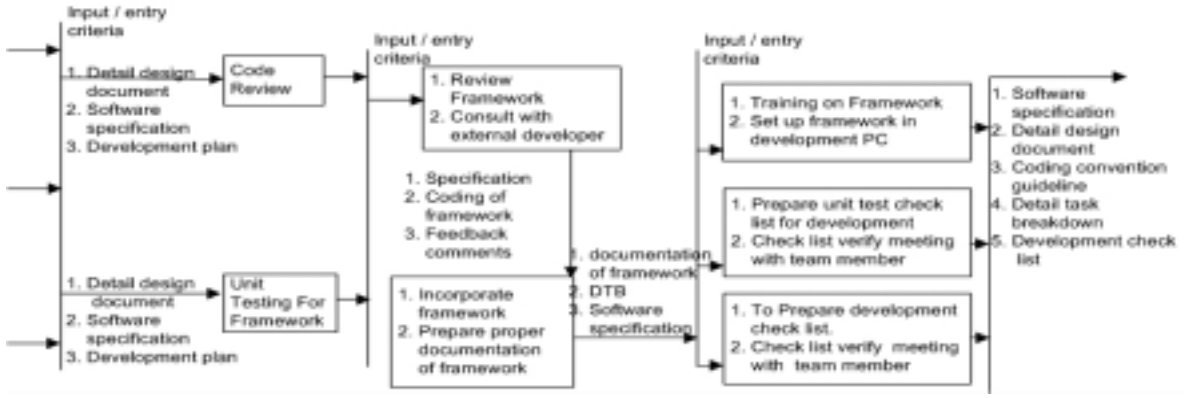

Fig. 3. Step2 Of process centric WBS of software coding phase

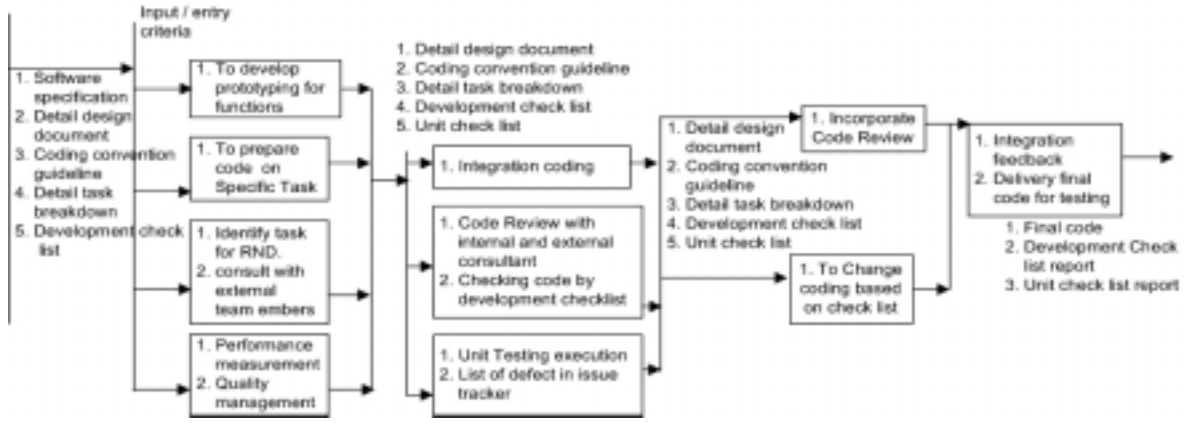

Fig. 4. Step3 Of process centric WBS of software coding phase

A. Practices and sub-practices for stepwise reduction of complexities

In a table, against each practice, sub-practices and work product are listed. Such table should help to reduce the complexities at project planning stage. Table I contains sample practices, sub-practices and work products for software coding.

Table I Sample of sub-practices and work products against practices for coding

No.	Practice	Sub-practices	Work product
01	1. Study all Software requirements. 2. Study all Detail design document 3. Study all High level design	1. To study all software requirements. 2. To study all detail design documents 3. To study all high level design documents 4. To study all coding convention guideline 5. To understand all required template 6. To understand all detail task breakdown	1. Requirement Understand ion report.
02	1. Take interview with team member 2. Team leader selection 3. Team member selection	1. To take interview with existing team members for involving with new teams 2. Identify how many team leaders are needed to develop. 3. Select team leaders for developing. 4. To select each team for developing and also for other task	1. Numbers of team define. 2. Team selection criteria for final selection
03	1. Task allocation	1. Task allocation to each team 2. Task dissuasion within team	1. Task assigned report.

B. Leaf level sub-practices should follow certain rules for maximum and minimum grain size of each task

Maximum and minimum grain should be determined following certain rule against leaf level sub-practices. Table II contains sample value against leaf level sub-practices.

Table II Leaf level sub-practices with grain size

No.	Sub-practices	Maximum grain size	Minimum grain size
01	To study all software requirements.	15	12
02	To study all detail design documents	6	4
03	To study all high level design documents	6	4
04	To study all coding convention guideline	2	1
05	To understand all required template	3	2
06	To understand all detail task breakdown	10	7
07	To take interview with existing team members for involving with new teams	3	2
08	Identify how many team leaders are needed to develop.	3	2
09	Select team leaders for developing.	2	1
11	To select each team for developing and also for other task	3	2
12	Task allocation to each team	6	4

C. Sequence of flow of execution of practices

In coding phase follow sequence of practices is required to be executed as shown in Fig. 5.

D. Standard templates for work products

Templates for work products of each practice should be prepared to ease the work. A sample template for work product 'Unit test check lists' is shown at Table III.

E. Measurements requirement of each practice and work products

Measurement is the one of the main challenge of software project management. In coding phases management should consider to measure the coding work products based on following attributes:

Table III Template for Unit test check lists

Independent System Limited.						
Document Title:	Unit test check list					
Product Title:	Health Care Automation					
Product ID:	01					
Version:	01.01					
Creation Date:	July 3, 2009					
Issued By:	<Owner Name>					
Practice	Prepare development checklist and unit test checklist					
Priority	High – H	Medium – M	Low – L	Can wait – C		
Issue Type	New Issue-N	Bug-B	Enhancement-E			
Status Types	Unassigned – U	Assigned – A	Progress-P			
	Solve – S	Re-solve-N	Close – C			

No	STR ID	Module ID	Description	Priority Type	Issue Type	Status Types	Created Date	Assigned Date
01	DTS-01			H	N	U		
02	DTS-02			M	N	N		
03	DTS-03			L	N	P		

Time & effort – it is one of the main challenges of a project manager. If manager can split-out all the tasks of the projects and measure time & effort each and every individual single task, he can easily calculate total time & effort the project.

Quality of code block – every coding block must comply with organizational or project coding standard.

Resource assumption – To know actual resource capability and employee turnover is also a challenge of project management, as a result accurate skill matrix is very much needed to measures resources.

Complexity of coding – complexity can be a major factor if product is innovative. In such situation, innovation functions should be identified and their complexities should be measured.

Process centric representation of WBS defines different work products to be produced in the coding process. Establishment of definitions of work products at the planning stage enables stakeholders to determine the measurement need to assess the quality of work products that will be produced by different activities of the coding process during the development phase.

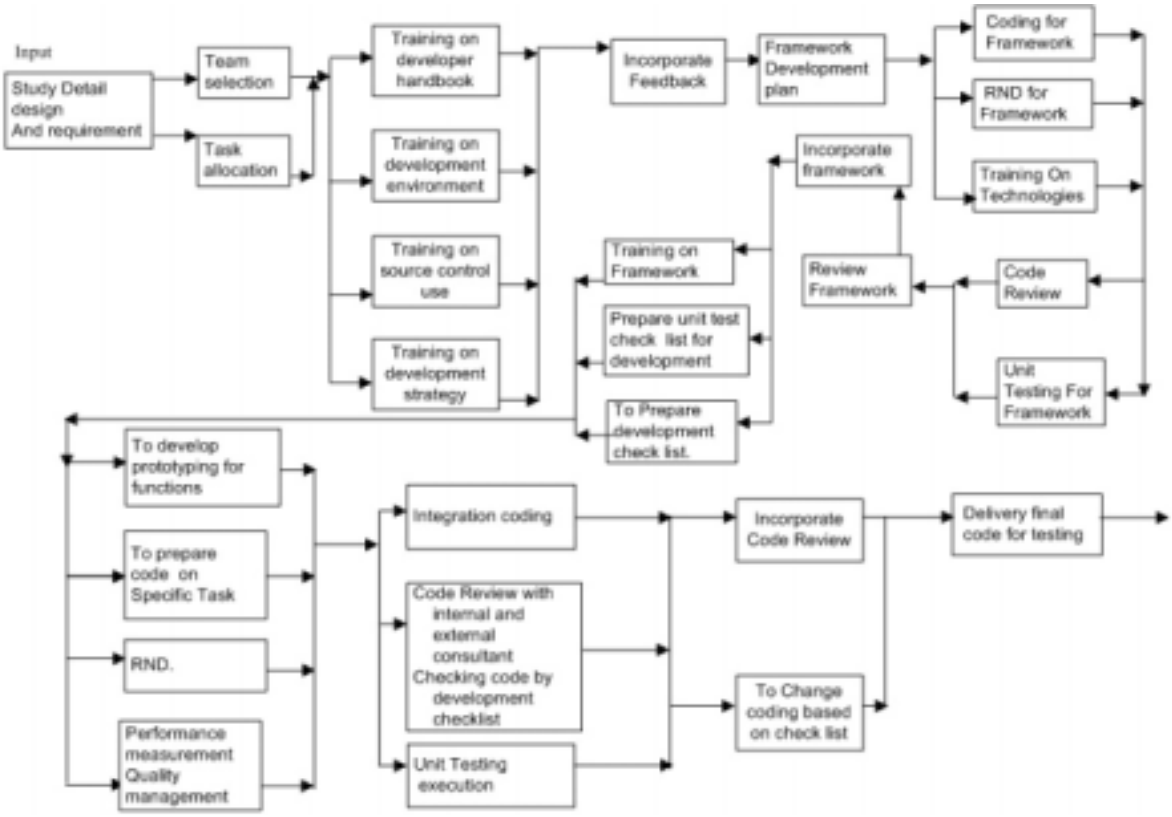

Fig. 5. Sequence of flow of execution of practices

F. Stakeholders of practices and proposed communication management process with these stakeholders

In coding phase, coders need to frequently contact with stakeholders for better understanding of the inputs and outputs. Process centric representation of WBS establishes the visibility of diverse communication need among stakeholders at the planning stage. It should be noted that communication and coordination cost has been increasing at very high rate due to increase of project size and geographical distribution of project team [6]. Typical communications with these stakeholders are summarized below:

Project manager – every developer needs to frequently contact with project manager for better understanding of project's requirement. Communication should be formal and informal.

Team leader – in every project, coding phase is depended on team leader, actually team environment is based on team leader so team leader and software coder's relation is very much important. Communication should be formal and informal.

Chief technical officer – in general, application coders don't need to frequently contact CTO; whenever a coder need to contact then communication must be formal.

Quality assurance manager – Quality assurance manager also works very closely with application coders. Sometime QA manager cannot imagine before developing any unit of the project then QA manager

needs to contact with coders and sometime coders need to talk to QA manager for improving better quality. Communication should be informal or formal.

Testing manager – sometime application coders need to talk to testing manager for understanding and clarifying the actual output of the product.

III. SUMMARY AND CONCLUSION

Process centric WBS of coding helps project manager to estimate more accurately for coding phase. It helps to figure out the tasks that can be done in parallel; it visualizes dependency between tasks improving scheduling capability. Thus it helps to figure out manpower loading more accurately and helps to form the teams more effectively for coding phase. Process centric view should help the project manager to simulate the plan for coding phase at very early stage. Overall, it should help the project plan with reduced gap between planning and execution. The limitation of the proposed model is about feedback of the industry yet to be taken and it has not been applied in any real-life project yet. In future, the enhancement of the proposed approach can be made by verifying the model with the opinion of industry practitioners and implementing it in several projects.

REFERENCES

[1] Statistics over IT Failure Rate, http://www.it-cortex.com/Stat_Failure_Rate.htm

[2] Work Breakdown Structure, WBS Chart, Project Management WBS, http://glossary. tenrox. com/Work-Breakdown-Structure.htm

[3] Work breakdown structure - Wikipedia, the free encyclopedia, http://en.wikipedia.org/ wiki/Work_ breakdown_structure

[4] WBS Concept, http://www.chambers. com.au/ Sample_p/wbs_cncp.htm

[5] Work Breakdown Structure - Pmpedia, http://pmpedia.com/wiki/index.php?title= Work_Breakdown_Structure

[6] R. Kommeren, P. Parviainen, "Philips experiences in global distributed software development", Journal of Emperical Software Engineering, Vo. 12, 2007, pp. 647-660.

[7] An Intorduction to Process, http://www2.computer.org/portal/web/seonline/process

[8] The lowest levels of a WBS represent discrete deliverable items & performance measured, http:// www.chambers.com.au/Sample_p/ wbs_ cncp.htm

[9] Osellus - Software Process Solutions - Business Drivers for Process-Centric Outsourcing,

http://www.osellus.com/services/outsourcing/business_ drivers_for_process-centric_outsourcing.html

[10] M. Agrawal, K. Chari, "Software Effort, Quality, and Cycle Time: A Study of CMM Level 5 Projects," IEEE Transactions in Software Engineering, vol. 33, no. 3, March 2007, pp. 145-156

[11] Capability Maturity Model Integration (CMMISM), Version 1.l, Staged Representation, August 2002.

[12] D. Draheim, L. Pekacki, "Process-Centric Analytical Processing of Version Control Data", http://www.pekacki. de/publications/ processingVersionControl.pdf

[13] J. Amalraj, C. Hernani, K. Ladouceur, A. Verma, "Project Management: Challenges & Lessons Learned." http://www.beg. utexas.edu/ energyecon/ ua_2007/ AB_ Project_ Mgt_ challenges.pdf

[14] J.E. Tomayko, H.K. Hallman, "Software Project Management." SEI Curriculum Module SEI-CM-21-1.0 July 1989. ftp://ftp.sei.cmu. edu/pub/ documents/misc/cms/ pdf/cm21.pdf

[15] http://www.projectsmart.co.uk/project-management-time-estimates-and-planning.html

Proceedings of 2009 12th International Conference on Computer and Information Technology (ICCIT 2009)
21-23 December, 2009, Dhaka, Bangladesh

A Compact Loop Type Antenna for Millimeter Band Applications

Kheya Banerjee, Abu Md. Numan-Al-Mobin and Khaled Mahbub Morshed
Department of ECE, KUET, Khulna, Bangladesh
kheya2006@yahoo.co.in, nmobin27@yahoo.com, kmm_ece@yahoo.com

Abstract

A millimeter band microstrip patch antenna was developed to achieve a bandwidth of 2GHz from 58.995GHz to 60.995GHz with linear polarization capability. In this paper the key configuration of the antenna consists of two loops having an opening at opposite side. The bandwidth of the antenna is enhanced by taking the advantage of this double loop arrangement and the mutual coupling between the inner and outer loops. In this paper, properties of the proposed two loop antenna are investigated in the frequency range from 58.995 GHz to 60.995 GHz which is efficient for satellite millimeter band applications.

Keywords: Broadband antenna, compact microstrip antenna, millimeter band applications, satellite applications, UC-PBG structure.

I. INTRODUCTION

Extremely high frequency is the highest radio frequency band EHF. It runs the range of frequencies from 30 to 300 GHz, above which electromagnetic radiation is considered to be low [1]. It is also referred to as terahertz radiation. This band has a wavelength of ten to one millimetre, giving it the name millimeter band or millimetre wave, sometimes abbreviated MMW or mmW. Compared to lower bands, terrestrial radio signals in this band are extremely prone to atmospheric attenuation, making them of very little use over long distances. Even over relatively short distances, rain fade is a serious problem, caused when absorption by rain reduces signal strength. In climates other than deserts absorption due to humidity also has an impact on propagation. While this absorption limits potential communications range, it also allows for smaller frequency reuse distances than lower frequencies. The small wavelength allows modest size antennas to have a small beam width, further increasing frequency reuse potential [2].

International passenger transportation by air, rail, automobile or sea transport is growing daily. One of the major tasks of the customs service is examination of passengers and their luggage for detection of foreign objects and prohibited substances. At customs luggage control, methods of both direct examination and automated examination equipment are widely used. However, current technical means do not go beyond applications of different types of metal detectors, which guarantee detection of hidden metal objects (weapons) on the human body, but cannot detect nonmetal objects, such as explosive and narcotic substances, or weapons made from ceramic materials. Due to their low absorption in fabric materials, millimeter band electromagnetic waves can serve for the customs service as an additional source of remotely obtained information concerning any relevant discontinuities located on a human body under clothes, and the dimensions and types of such discontinuities. These peculiarities could essentially reduce the number of persons subjected to additional personal control and, as a result, essentially raise efficiency of customs examination as a whole. Based on reception of a person's own heat radiation, the method of passive radiometric supervision is expected to have the best prospects, as it is not connected with generation in public places of additional high intensity electromagnetic fields, which may have negative effects on both inspected people and customs staff [3].

In this paper, properties of the proposed two loop antenna are examined in the frequency range from 58.995 GHz to 60.995 GHz. Specifically the ability of the antenna to detect unauthorized subjects in a small range is investigated. As the general simulated parameters of an antenna are not below the satisfactory range, this antenna is said to be optimized in this frequency range.

II. ANTENNA CONFIGURATION

The schematic configuration of the proposed antenna is shown in Fig. 1. The total size of the antenna is 3.4mm×3.4mm. The dimension of the inner loop is 2mm×2mm. Both the loops contain an opening with length of 0.8mm but at the opposite side. The gap between the two rings is 0.4mm. The source is connected with the antenna by two transmission lines which are 2mm and 4mm in length. The characteristic impedance for both the transmission lines is 50Ω. The proposed antenna is embedded upon a perfect ground substrate. This configuration is called the Coupled Split Square Ring (SSR) and suggested by Pendry and Smith [4][5]. The proposed SSR in constructing left-handed materials can be made resonant at wavelength much larger than the diameter of the rings [6]. The prescribed antenna is simulated with NEC.

978-1-4244-6283-4/09/$26.00 ©2009 IEEE

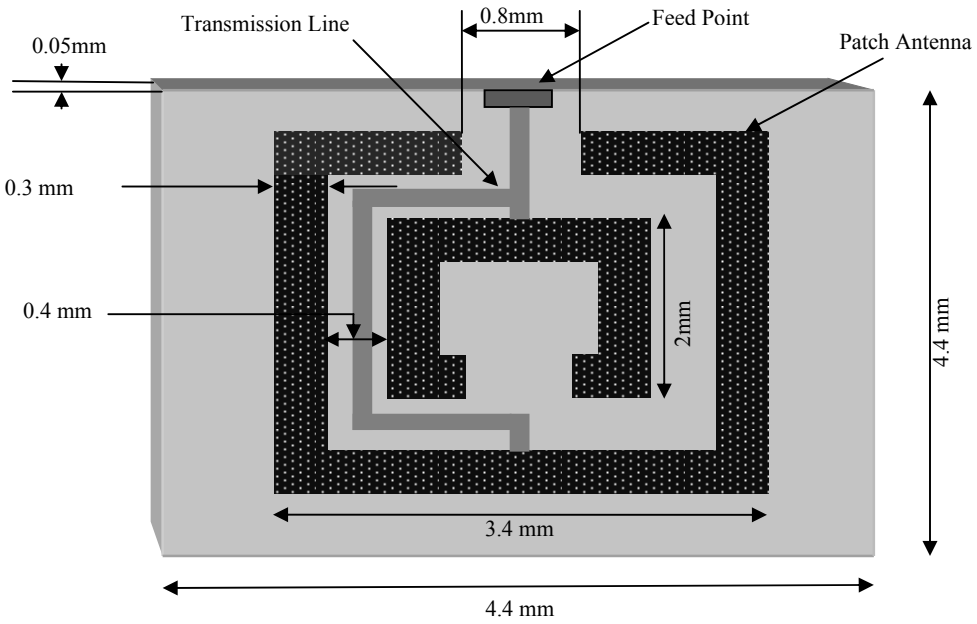

Fig. 1. Antenna configuration.

III. RESULT ANALYSIS

As the antenna is designed for millimeter band application, the simulated figures should show good results at the shorter distances so that the detection of unauthorized objects becomes easier. From the results of the prescribed antenna we can see that the antenna is suited well for the proposed applications.

The input parameters of the prescribed antenna at resonant frequency are given in Table I:

Table I Input parameters of compact loop type antenna

Input Parameters		Values	
Name	**Unit**	**Real**	**Imaginary**
Voltage	Volts	5	0
Current	Amps	0.176237	0.00692201
Impedance	Ohms	28.3271	-1.11259
Admittance	Mhos	0.0352475	0.0013844
Power	Watts	0.440593	

The different kind of radiation patterns of the prescribed antenna is shown below. All the gains are taken on vertical plane. As seen from Fig 2, the pattern of the horizontal, vertical and total gain is quite the same. The most significant property of the radiation pattern is it's directivity, which is unidirectional. For this property, it can be used efficiently for hidden object detection.

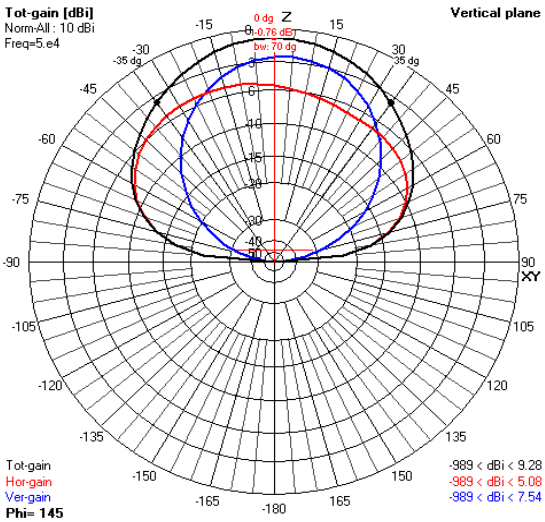

Fig. 2. Radiation pattern of the antenna.

The 2D plot of Fig. 2. is shown in Fig. 3.

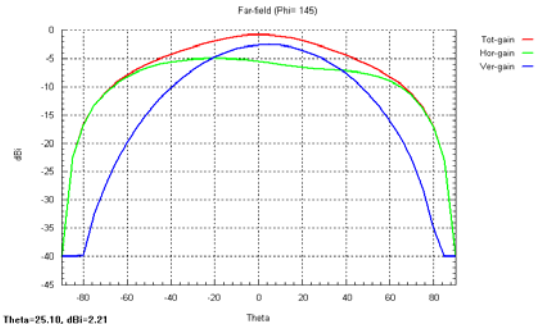

Fig. 3. 2D plot of the radiation pattern.

The most significant property of an antenna is it's SWR. In Fig. 4. the SWR of the prescribed antenna is shown. As seen from the figure, the SWR is slowly decreasing from 50.995GHz but at the resonant frequency 59.995 GHz, it has decreased sharply and achieved a value of 1.76 which is quite satisfactory.

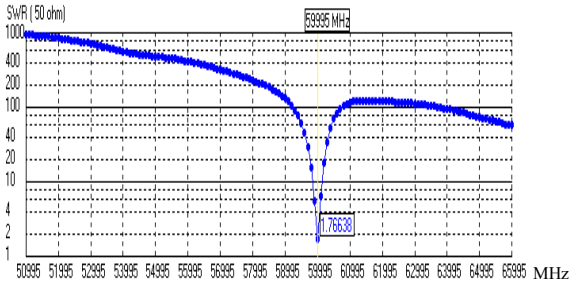

Fig. 4. Standing Wave Ratio (SWR) of the antenna.

Another significant property is the return loss or reflection coefficient. The required value of the return loss for an efficient antenna is -10dB. From Fig. 5., it is clearly shown that the value of the return loss is -11.149dB at the resonant frequency. So in terms of return loss, the antenna is also acceptable.

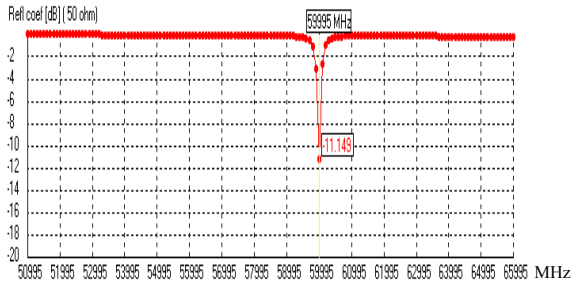

Fig. 5. Reflection coefficient of the antenna.

To be efficient, an antenna must have a gain which is more than unity. As seen from Fig. 6., the gain of the prescribed antenna is 10.02 at the resonance frequency. This value provides a suitable efficiency for the antenna.

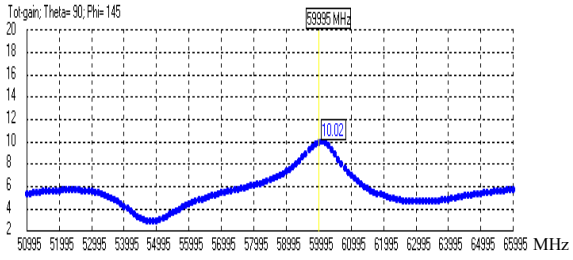

Fig 6. Total gain of the antenna.

The front to back ratio and front to rear ratio is shown in Fig. 7. Although the curve is fluctuating frequently, there is a significant change near the resonant frequency.

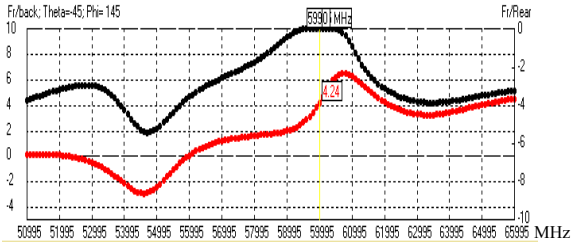

Fig. 7. Front to back ratio of the antenna.

Fig. 8. shows the resistance and reactance and Fig. 9. shows the impedance and phase change of the prescribed antenna with respect to frequency. Both the figures shows very sharp change at and near the resonant frequency. The values of resistance, reactance, impedance and phase at this frequency are also acceptable.

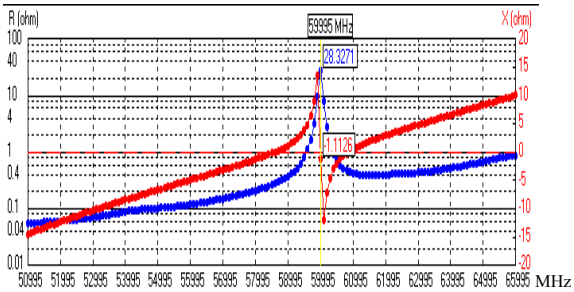

Fig. 8. Resistance and reactance of the antenna.

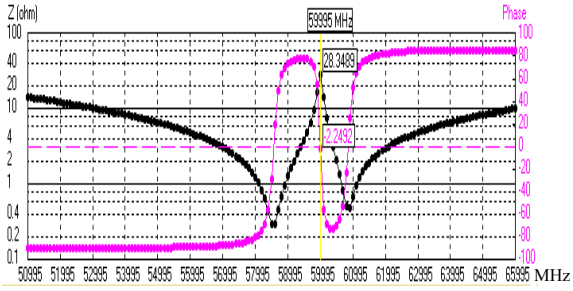

Fig 9. Impedance and phase of the antenna.

From the above results, it is clear that the prescribed antenna shows some significant changes near the resonant frequency i.e. 59.995GHz. By examining all the figures, we observe that the change in the characteristic of the antenna has started from 58.995 GHz and ends at 60.995 GHz. So, we can say that the bandwidth of the antenna is about 2 GHz. To show that the power in this antenna is used efficiently, the power budget is given in Table II.

Table II Power budget for compact loop type antenna

Power Budget	
Parameters	**Values**
Input power	0.44059 Watts
Radiated power	0.44059 Watts
Structure loss	0 Watts
Network loss	2.5813E-14 Watts
Efficiency	100%

IV. CONCLUSION

A compact two loop microstrip antenna is presented for satellite millimeter band applications. The proposed antenna has a compact dimension of 3.4mm×3.4mm and has obtained the broad bandwidth of 2 GHz by adjusting the mutual coupling between the two loops. The required parameters for the design of the proposed antenna are optimized at the frequency of 59.995 GHz. Maximum gain at the resonant frequency is achieved 10.02 dBi which is the noteworthy result for this antenna.

REFERENCES

[1] Tri T. Ha, 'Digital Satellite Communications' Second Edition McGraw-Hill Publishing Company.

[2] www.wikipedia.com.

[3] S.A Shilo, V.A Komyak, Yu.N Muskin and V.A.Berezhnoy,' MM-band radiometric system for contraband detection applications,' *The Fourth International Kharkov Symposium on Physics and Engineering of Millimeter and Sub-Millimeter Waves*, 2001 Volume 1, Issue , 2001 Page(s):463 - 465 vol.1.

[4] J.B Pendry, A.J. Holden, D.J. Robins, W.J. Stewart; 'Magnetism from Conductors and Enhanced Nonlinear Phenomena' *Microwave Theory and Techniques, IEEE Transactions on*, Volume: 47 Issue: 11, Nov. 1999 Page 2075-2084.

[5] R. A. Shelby, D. R. Smith, S. C. Nemat-Nasser and S. Schultz, 'Microwave Transmission Through a Two Dimensional, Isotropic, Left-handed Metamaterial'. *Applied Physics Letters*, Vol 78, Number 4, Jan. 2001. Page: 489-491.

[6] Y. Hao and C.G. Parini, 'A novel Embedded UC-PBG Structure for Microstrip Antennas' , *IEEE Trans. Antennas Propagation,* vol 51, no 1, pp. 121-125, Jan 2003.

Proceedings of 2009 12th International Conference on Computer and Information Technology (ICCIT 2009)
21-23 December, 2009, Dhaka, Bangladesh

Can Information Retrieval Techniques Meet Automatic Assessment Challenges?

Md Maruf Hasan
School of Technology, Shinawatra University, Thailand
maruf@siu.ac.th

Abstract

In Information Retrieval (IR), the similarity scores between a query and a set of documents are calculated, and the relevant documents are ranked based on their similarity scores. IR systems often consider queries as short documents containing only a few words in calculating document similarity score. In Computer Aided Assessment (CAA) of narrative answers, when model answers are available, the similarity score between Students' Answers and the respective Model Answer may be a good quality-indicator. With such an analogy in mind, we applied basic IR techniques in the context of automatic assessment and discussed our findings.

In this paper, we explain the development of a web-based automatic assessment system that incorporates 5 different text analysis techniques for automatic assessment of narrative answers using vector space framework. We apply Uni-gram, Bi-gram, TF.IDF, Keyphrase Extraction, and Keyphrase with Synonym Resolution before representing model answers and students' answers as document vectors; and then we compute document similarity scores. The experimental results based on 30 narrative questions with 30 model answers, and 300 student's answers (from 10 students) show that the correlation of automatic assessment with human assessment is higher when advanced text processing techniques such as Keyphrase Extraction and Synonym Resolution are applied.

Keywords: Computer Aided Instruction, Information Retrieval, Intelligent Text Analysis, and Natural Language Processing.

I. INTRODUCTION

With the advent of WWW and ubiquitous access to huge amount of information, research in Information Retrieval (IR) gained new momentum in the recent years. Several new techniques and tools are developed to aid the IR tasks. In the context of IR, the similarity scores between a query and a set of documents are calculated, and the relevant documents are retrieved and ranked based on their similarity scores. IR systems often consider queries as *short* documents containing only a few words. Similarity scores between documents are the indicators of *relevance*. In Computer Aided Assessment (CAA) of *narrative* answers, when model answers are available, the similarity score between the Students' Answers (SA) and respective Model Answer (MA) may be a good indicator of *quality*. With such an analogy in mind, we applied basic IR and text analysis techniques in the context of automatic assessment and discussed our findings. In this paper, we explain the development of a web-based automatic assessment system that incorporates 5 different text analysis techniques for automatic assessment of narrative answers using a vector space representation.

Online education is gaining widespread interest mainly because of the flexibility it offers in terms of scheduling, effective teaching time usage and learning pace. Therefore, assessment of students' understanding in the online environment is becoming a major concern. Many researchers are paying attention to how to improve the online assessment system and which techniques should be adopted in an online assessment system. Most online assessment systems resort to just True/False, Multiple Choice, and Fill-in-the-Blank type questions due to their simplicity. However, it is a general opinion in the field that such objective tests *without* narrative questions is not sufficient in fully evaluating the knowledge of a learner. Assessment of non-narrative answers is straight forward. However, the proposed online assessment system aims to integrate assessment of objective questions and narrative questions *together* to assess comprehensive knowledge and understanding of the learners.

Automatic assessment of *narrative* answers is a field that has attracted attentions to online education community in the recent years. Several systems have been developed under academic and commercial initiatives using statistical, Natural Language Processing (NLP), and Information Extraction (IE) techniques. Some researchers also used clustering, semantic networks and other hybrid approaches [1]. In our research, we experimented with 5 different text analysis techniques for automatic assessment of narrative answers using the *vector space* framework. We use Uni-gram, Bi-gram, TF.IDF, Keyphrase Extraction, and Keyphrase Extraction along with Synonym Resolution [2][3][4] to represent model answers and student's answers as vectors; and then similarities between the model answer and the students' answer are computed by using cosine similarity [5].

The Web-based online assessment system integrates the assessment of both objective and narrative answers. The system is easy to use and modular in design - new assessment modules can be added easily and existing ones can be revised as necessary. The system allows teachers to set test papers manually, or automatically (according to specific criteria from a question-bank); and students to take the test online. The automatic assessment may be performed instantly using any or all of the proposed text

978-1-4244-6283-4/09/$26.00 ©2009 IEEE

analysis techniques. The automatic scores may also be validated and finalized by the teacher.

II. BRIEF OVERVIEW THE ONLINE ASSESSMENT SYSTEM

We focused on developing a Web-based online assessment system that is modular and easy-to-use for both teachers and students. The system is developed using ASP.NET and Microsoft SQL Server. Some key features of the system are explained in this section. The overall system design is summarized in Fig. 1.

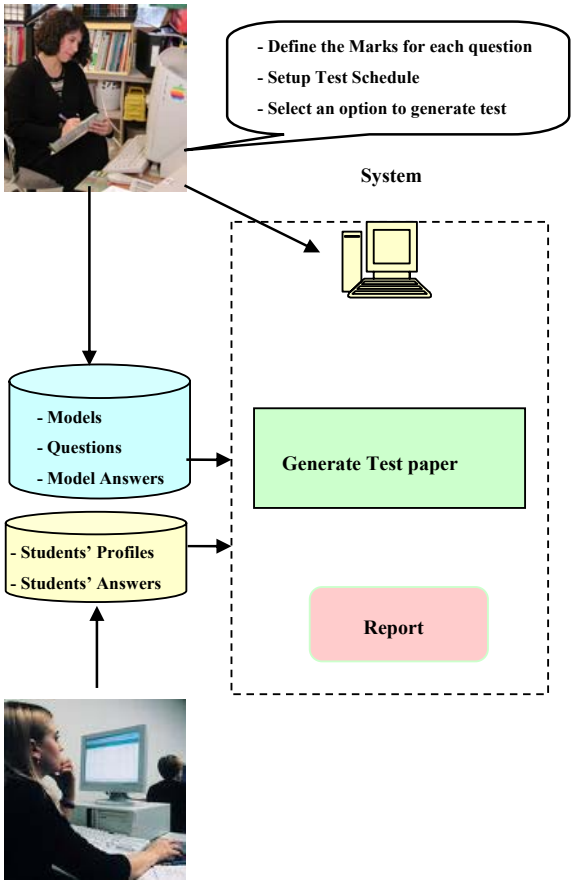

Fig. 1. Overview of the Online Assessment System

Teacher: The teacher interacts with the system by entering questions along with their model answers. The teacher can also set the test paper, exam schedule and define the full marks for each question. For the assessment of narrative answers, the teacher may choose one or more text analysis techniques. In our system, we incorporated 5 different text analysis modules which will be discussed later. For certain approaches (such as Keyphrase Extraction), the teacher also needs to train a model automatically using available machine learning algorithms.

Student: The students have to authenticate and register themselves to take the test by giving their personal details. Upon registration and authentication, they need to choose from the available courses to get the relevant test paper and answer each question from the test online. The student sessions end with submission of their answers.

System: The system stores several crucial information in the backend database, which include students' information, course information, set of questions associated with each course, customized tests composed by the teachers (manually and automatically). Automatic selection of test question from the so-called question-bank can be random or filtered by some criteria (such as level of difficulty).

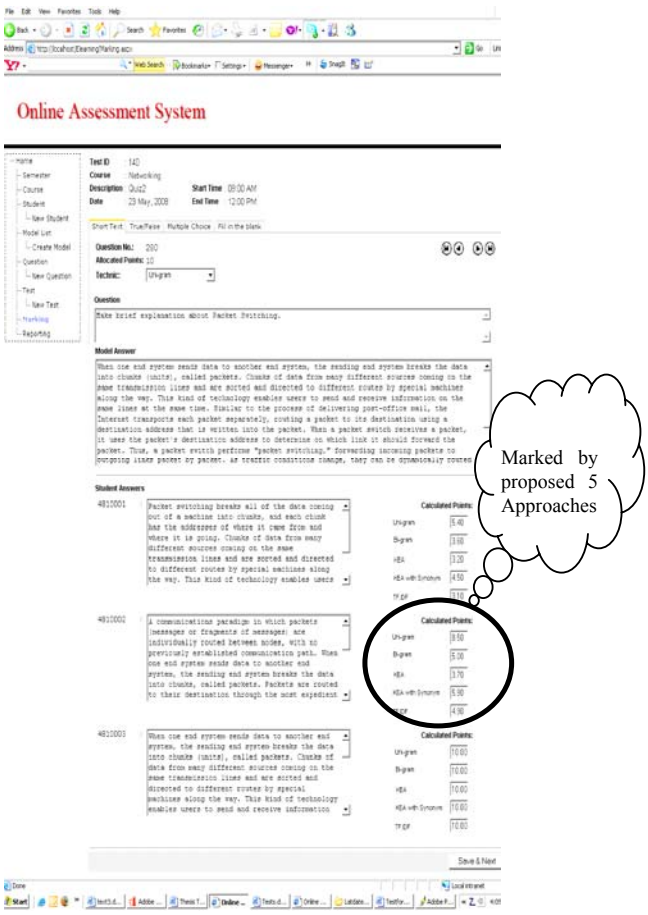

Fig. 2. Similarity Scores of Student's Answers (SAs) calculated for all 5 Proposed Techniques

Based on the assessment techniques chosen, the system makes comparison between Students' Answers (SA) and the respective Model Answers (MA); and calculates the cosine similarity score. Fig. 2 shows the similarity scores of a narrative question using all 5 proposed techniques.

The online system also generates report for each test-taker which includes the test ID, name of the course, description of test, exam time, and exam date including students' information and score for that test as validated

by the teacher. The snapshot of such a report is shown in Fig. 3. Nevertheless, the system archives historical data (e.g., students' answers along with given scores), which may be further analyzed to augment the quality of automatic assessment.

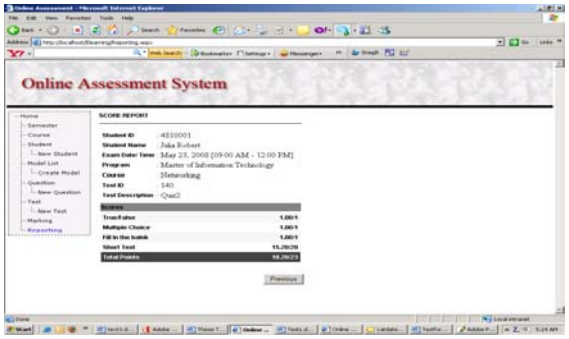

Fig. 3. Student's Grade Report Generated by the System

III. TEXT ANALYSIS AND IR TECHNIQUES

In this research, we experimented with 5 different text analysis and IR techniques for automatic assessment of narrative answers using vector space framework. We use Uni-gram, Bi-gram, TF.IDF, Keyphrase Extraction, and Keyphrase Extraction along with Synonym Resolution to represent both model answers and student's answers as vectors; and then similarities between the model answer and the students' answer are computed by using cosine similarity. For each approach, some pre-processing was necessary (cf. Fig. 4).

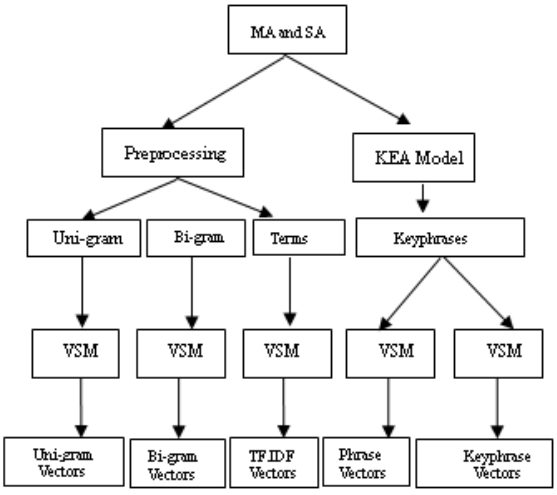

Fig. 4. Processing Steps of the Proposed Techniques

- For the *Uni-gram* approach, we remove stop-words first. After stemming, we compute single word (Uni-gram) frequency to prepare MA and SA vectors.
- For the *Bi-gram* approach, we count bi-gram frequency from MA and SA after stop-words and stemming.
- For the *TF.IDF* approach, we also perform stop-word removal and stemming; and compute term-frequency (TF) and inverse document frequency (IDF) to prepare MA and SA vectors.
- For the last two approaches – *Keyphrase Extraction* and *Keyphrase with Synonym*, we use the Keyphrase Extraction Tool (KEA) [2] to train a Keyphrase Extraction Model to be used to extract Keyphrases from MAs and SAs.
- Additionally, for the *Keyphrase with Synonym*, we also use a thesaurus for synonym resolution.

A. Document Pre-Processing

The major preprocessing steps include tokenization, stop-word removal [6] and stemming [7]. For our experiment setup, document pre-processing has to be performed before applying Uni-gram, Bi-gram and TF.IDF based approaches. Preprocessing was not necessary for KEA based approaches since KEA has stemmer and stop-word removal built-in. For Uni-gram and Bi-gram approaches, we refer to word-based n-gram approach [8].

B. TF.IDF Weights

The TF.IDF weight is a weight often used in information retrieval and text mining in term weighting. The TF.IDF weight weighs each word in the text document according to how unique it is [9]. The similarity score between the query and the documents in a document collection shows how *relevant* a document is for that particular query. IDF tends to weigh *rare terms* highly. In the context of automatic assessment, where model answer is modeled as a query against a set of Students Answers (SAs), apparently TF/IDF weights (unlike TF.IDF) appear to be more appropriate (*common terms* should get more attention in an optimistic assumption where majority of students would be using similar terminologies to answer narrative question). However, in our experiments, we noticed that TF/IDF weights did not perform as assumed. Therefore, we used TF.IDF weights instead in calculating term weights. The similarity score between a the model answer and a student answer is supposedly indicating the *quality* of the students answer.

In our experiment, the term frequency (TF) and inverse document frequency (IDF) weights are calculated using the following formula:

Term Frequency (TF):

$$TF_{i,j} = \frac{f_{i,j}}{\max_j f_{i,j}} \qquad (1)$$

where $f_{i,j}$ = frequency of term i in collection j. Collection consists of 11 documents (1 MA and 10 SAs).

Inverse Document Frequency (IDF):

$$IDF_t = \log(1 + \frac{N}{n_t}) \qquad (2)$$

where N = 11 documents consisting of 1 MA and 10 SAs

n_t = the number of documents in 11 answers that contain term, t.

C. Keyphrase Extraction Algorithm (KEA)

KEA [2] is a keyphrase extraction tool based on supervised machine learning techniques [4][10]. For the fourth and fifth approach in this experiment, we use KEA to extract keyphrases from MA and SA and make comparison between them.

KEA's extraction algorithm has *two* stages:

1. **Training:** In the training phase, KEA creates a keyphrase extraction model for identifying keyphrases, using training documents. We use 50 documents from *computer network* domain to train KEA. Manual keyphrases were available for these documents.
2. **Extraction:** In the extraction phase, using the trained model, we extract keyphrases from the students' answers and model answers.

Fig. 5 shows the KEA's training and extraction process in detail. KEA uses supervise learning mechanism and relies on candidate keyphrase.

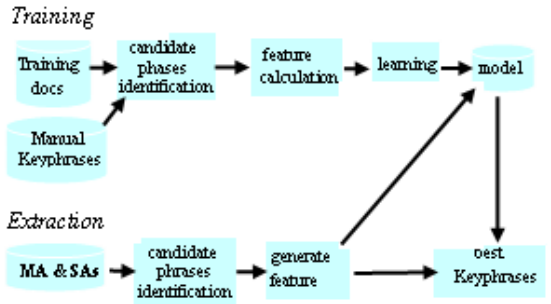

Fig. 5. Training and Extraction Processes in KEA

Candidate Keyphrase:

1. Candidate phrases are limited to a certain maximum length (usually three words).
2. Candidate phrases cannot be proper names (i.e. single words that only appear with an initial capital).
3. Candidate phrases cannot begin or end with a stop-word.

KEA's features:

For each candidate phrase, KEA computes 4 feature values:

1. *TF.IDF* is a measure describing the specificity of a term for this document under consideration, compared to all other documents in the corpus. Candidate phrases that have high TF.IDF value are more likely to be keyphrases.
2. *First occurrence* is computed as the percentage of the document preceding the first occurrence of the term in the document. Terms that tend to appear at the start or at the end of a document are more likely to be keyphrases.
3. *Length of a phrase* is the number of its component words. Two-word phrases are usually preferred by human indexers.
4. *Node degree* of a candidate phrase is the number of phrases in the candidate set that is semantically related to this phrase.

In summary, KEA uses high level linguistic features and supervised learning with or without a thesaurus. Maximum numbers of keyphrase to be extracted can also be specified in KEA.

D. The Vector Space Framework

The Vector Space Model (VSM) [5] is a flexible representation framework for documents (as well as queries in the context of IR) to be represented as vector of terms. Terms could be single word, bi-gram and keyphrase etc. Term vectors may contain Boolean term-weights (1 and 0 to represent presence or absence of a term) as well as complex weighting schemes (such as TF.IDF). The Boolean weighting scheme is not suitable for partial matching. Therefore, we used frequency and other weighting scheme as appropriate [9].

In our experiment, the similarity between MA and SA vectors is measured using cosine similarity as follows:

$$sim(SA_i, MA) = \frac{SA_i \cdot MA}{|SA_i||MA|} = \frac{\sum_j w_{i,j} \; X \; w_{MA,j}}{\sqrt{\sum_j w^2_{i,j}} \sqrt{\sum_j w^2_{MA,j}}} \qquad (3)$$

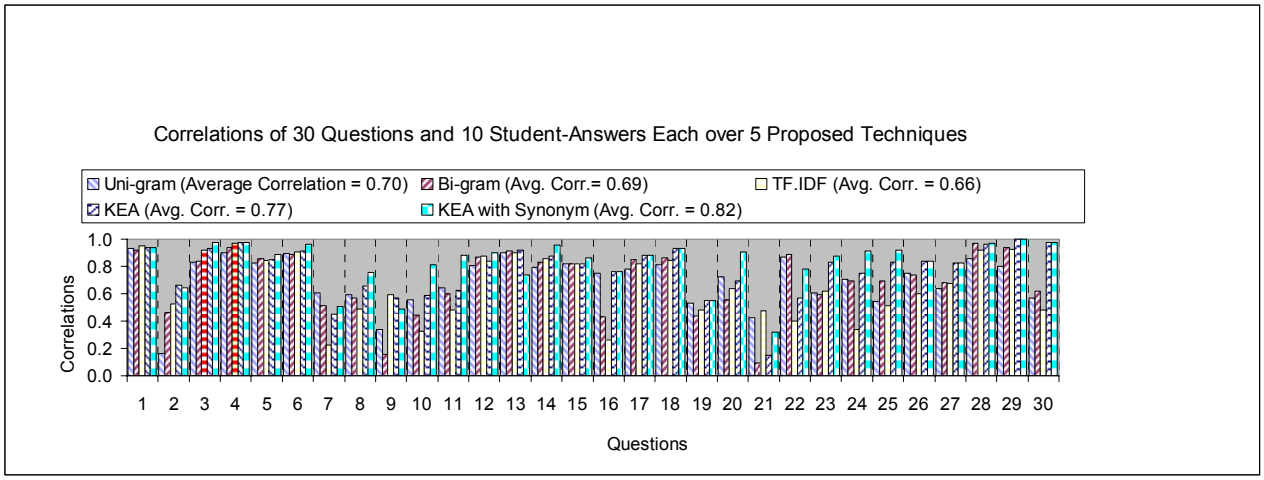

Fig. 6. Correlation of Proposed 5 Approaches with Human Judgment for 30 Questions Answered by 10 Students

IV. EXPERIMENTS AND EVALUATIONS

In our experiment, we used 30 narrative questions with 30 model answers (MA). A group of 10 students attempted all 30 questions and therefore student's answer set (SA) consists of a total of 300 documents. For the first three approaches (i.e., Uni-gram, Bi-gram and TF.IDF), we preprocessed both MAs and SAs and represent them as respective MA and SA vectors. Similarity score is then computed using cosine measure.

For the last two approaches (i.e., KEA and KEA with Synonym), we trained a KEA keyphrase extraction model using a set of 50 domain-specific documents with manually annotated keyphrases. Keyphrase vectors for MA and SA are computed with or without synonym resolutions. As before, we measure cosine similarity between SA vectors with the relevant MA vector.

For each 300 student's answer, human assessments were available. The correlation between human assessment and automatic assessments using all five approaches are calculated using Pearson Correlation Coefficient as follows:

$$Correlation(x,y) = \frac{Covariance(x,y)}{standardDev(x) \times standardDev(y)} \quad (4)$$

The correlations between human and automatic assessment for 30 questions using all 5 automatic assessment approaches are presented in Fig. 6.

As shown in Fig. 6, the highest average correlation is achieved with KEA with synonym resolution. This is due to the fact that KEA uses high-level features and synonym resolution that captures differences in term usage. The correlation value for Uni-gram is relatively high. However, in a VSM representation (i.e., a *bag-of-word* representation), Uni-gram based assessment may be vulnerable to abuse.

Although it is not directly comparable, for reference purpose, we presented a table showing the correlation values of other existing systems [11] and those of ours in Table 1.

Table I Correlations of existing systems along with our proposed approaches

System	Technique	Correlation	Language
AEA	LSA, PLSA or LDA	0.75	English
Apex Assessor	LSA	0.59	French
Automark	IE	0.59	English
IEMS	Pattern Matching	0.80	English
Jess	Pattern Matching	0.71	Japanese
MarKLt	NLP, Pattern matching and statistics	0.75	English
PEG	Linguistic features	0.87	English
SEAR	N/A	0.45	English
Atenea	Statistical, NLP and LSA	0.56	English
Uni-gram	*N-gram word*	**0.70**	*English*
Bi-gram	*N-gram word*	**0.69**	*English*
TF.IDF	*TF.IDF weight*	**0.66**	*English*
KEA	*Keyphrase Extraction*	**0.77**	*English*
KEA with Synonym	*Keyphrase+ Synonym*	**0.82**	*English*

The average correlations of our approaches are listed in the bottom 5 rows of Table 1 (also, cf. Fig. 6). The average correlations for all 5 approaches are significant.

The proposed approaches are rather straight-forward. Therefore, it is worthy to investigate them further using further refinements in the context of automatic assessment. In our implementation of the online assessment system, each technique is implemented as a separate module that is easy to revise. Moreover, it is also easy to add new assessment modules.

V. CONCLUSIONS AND FUTURE WORK

We have experimented with a set of 30 narrative questions and 300 students' answers using 5 different approaches. The average correlations between human assessment and automatic assessments for each approach are comparable with existing systems. We observe that KEA with Synonym Resolution yields the highest correlation. For automatic assessment it is necessary to integrate high-level linguistic features. Similar observations are also prevalent in Information Retrieval tasks. The advances in natural language processing will certainly have implications in modeling Information Retrieval as well as Computer Aided Assessment of narrative answers.

The online assessment system outlined here is based on a modular design. Therefore, the existing approaches can be further augmented or amended easily. Any new approach can also be integrated with ease. Moreover, the online assessment system allows us to easily archive *historical data* (students' answers along with human validated grades). We also wish to employ supervised machine learning techniques on such historical datasets to develop *adaptive* and *interactive* assessment algorithms. The idea behind *relevance feedback* employed in some IR systems is to take advantage of human relevance judgments in reformulating the query for better retrieval results. In the context of CAA, such feedback mechanisms are easy to incorporate.

It should be noted that automatic assessment is so far not a substitute of humans with computers, but an aid to help the teachers to cut down their time or to cross-check their own assessment which may be prone to inadvertent human errors or omissions. We wish to refine our algorithms to incorporate some high-level linguistic features using state-of-the-art natural language processing techniques [12][13].

VI. ACKNOWLEDGEMENT

The author would like to thank his graduate student, Ohmar Thwin for her assistance in experiments and system implementation as part of her M.Sc. dissertation.

REFERENCES

[1] D. P'erez, O. Postolache, E. Alfonseca, D. Cristea and P. Rodriguez, "About the effects of using Anaphora Resolution in assessing free-text student answers," In *Proceedings of Recent Advances in Natural Language Processing Conf.* (Borovets, Bulgaria, 2005, pp. 380-386)

[2] Keyphrase Extraction Algorithm (KEA) [Online] Available: http://www.nzdl.org/KEA/

[3] E. Frank, G.W. Paynter, I.H. Witten, C. Gutwin and C.G. Nevill-Manning, "Domain-specific keyphrase extraction," In *Proceedings of the Sixteenth International Joint Conference on Artificial Intelligence*. (California: Morgan Kaufmann, 1999, pp. 668-673)

[4] I.H. Witten, G.W. Paynter, E. Frank, C. Gutwin and C.G. Nevill-Manning. "KEA: Practical Automatic Keyphrase Extraction," In *Processing of the Fourth ACM Conference on Digital Libraries. ACM Press,* (Berkeley, CA, USA, 1999, pp. 254-255).

[5] G. Salton, A. Wong and C. S. Yang, "A Vector Space Model for Automatic Indexing, Communications," the ACM, vol. 18, no. 11, pp. 613-620, 1975.

[6] M. Jarmasz and S. Szpakowicz,, "Roget's thesaurus and semantic similarity" In *Processing of the International Conference on Recent Advances in Natural Language Processing*, (Borovets, Bulgaria, 2003, pp. 212–219).

[7] Porter Stemming [Online] Available: http://www.comp.lancs.ac.uk/computing/research/stemming/general/porter.htm

[8] N-gram Models. [Online] Available: http://en.wikipedia.org/wiki/N-gram/

[9] Y. Zhang, L. Gong, and Y. Wang. "An improved TF-IDF approach for text classification," Network *& Information Center, School of Electronic & Information Technology, Shanghai Jiaotong University,* (Shanghai, China, 2004, pp. 49-50).

[10] Weka Machine Learning Suite [Online] Available: http://weka.sourceforge.net/

[11] D. Pérez , E. Alfonseca and P. Rodriguez, "About the effects of combining Latent Semantic Analysis with natural language processing techniques for free-text assessment", Revista Signos, Vol. 38(59), pp. 325-343.

[12] L.S. Larkey, "Automatic Essay Grading Using Text Categorization Techniques," In *Proceedings of the 21st Annual International ACM SIGIR Conference on Research and Development in Information Retrieval*, Melbourne, Australia, 1998, pp. 90–95.

[13] C.P. Rosé, A. Roque, D. Bhembe, and K. VanLehn, "A hybrid text classification approach for analysis of student essays," In *HLT-NAACL Workshop on Building Educational Applications Using Natural Language Processing*. (Edmonton, Canada, 2003, pp. 68–75).

Proceedings of 2009 12th International Conference on Computer and Information Technology (ICCIT 2009)
21-23 December, 2009, Dhaka, Bangladesh

An Audible Bangla Text-Entry Method in Mobile Phones with Intelligent Keypad

Md. Enamul Hoque Prince, Gahangir Hossain†, Ali Akbar Dewan, Pijush Debnath
Dept. of Computer Science & Engineering,
Chittagong University of Engineering & Technology (CUET), Bangladesh
† Dept. of Electrical and Computer Engineering, University of Memphis, Memphis, TN, USA

Abstract

Communication through mobile device is the most effective and fastest way that becomes a part of our daily life nowadays. Particularly, Short Message Service (SMS), is one of the most popular and relatively cheaper application of cell phone. In Bangladesh, there has been an enormous growth of mobile users and in this context, it is quite reasonable that people like to send SMS with their own language. Taking these challenges, a few initiatives were taken to introduce Bangla text in Mobile phones, more specifically, in messaging. But unfortunately, Bangla SMS is not popular yet in our country due to the presence of large number of characters and complex script. In fact, it is very much difficult to map Bangla characters efficiently on a mobile with 12 keys only. That's why, it motivated us to design an intelligent mobile keypad layout, which significantly reduces the number of keystrokes than existing methods, and remove difficulties of entering text. We eliminate traditional multi-tapping on a single button and introduce two key press technique, by arranging characters in two-dimensional matrix. Using this keypad the system becomes faster, reliable and flexible. Predictive text input method is also added in the system for further speeding up messaging. Moreover, our text-entry system ensures accessibility to visual impaired people by avoiding disambiguation caused by multi-tapping and introducing audio feedback for inserting each Bangla characters, which is not supported by existing systems. Finally, after analyzing the result on different sample SMS data, we showed that, our proposed keypad with the predictive input system reduces the number of key presses than the common Bangla keypad by 60.34%.

Keywords: A Mobile Keypad, Text Entry, Bangla SMS, Predictive Text Input, Visual Impaired.

I. INTRODUCTION

Nowadays, the mobile phone is an essential communication device for many people in Bangladesh. Though its main purpose is making calls, a number of other uses are also getting increasing popularity. Like many other countries, short Message Service (SMS) is now used frequently by the mass population of Bangladesh [1]. This growth is related to the fact that, SMS is cheaper and more importantly, it neither disturbs the receiver nor requires an immediate answer.

Although the number of mobile phone users are increasing surprisingly in both rural and urban area, very few of them are able to use all the features, as the interface of mobile phones is mostly in English. A few mobile phone operators have successfully introduced SMS in Bangla, however, not so much evidences have found in achieving popularity. Still people in Bangladesh are generally sending SMS in Bangla using English alphabet. The main challenge of Bangla SMS is that, it is very difficult to map a large number of characters using a standard mobile keypad. To address this problem, in this paper, an efficient mobile keypad is proposed with predictive text input facility, so that the number of key presses can be reduced significantly. Moreover, a considerable number of people in our country are visually impaired. They cannot participate in SMS, contributing to frustration and social exclusion. To enable them in writing SMS voice feedback support is included in the system. On the other hand, people with little literacy can use this software to write Bangla SMS with the help of voice feedback, which can ultimately become a very significant step for appealing mass people in mobile computing environment. They may use several SMS based services like mobile Banking, bill pay, quizzes, advertisements, news, etc. where mobile devices can become input devices accessible from remote area.

The rest of the paper is organized as follows: Section II focused on Background and present state of the problem, in Section III we explain our proposed system, Section IV provides experimental results and analysis and finally, Section V concludes the paper.

II. BACKGROUND

In the last few yeas, the mobile device's memory and processing power increased exponentially, however, input and output capability is still much more limited. The problem is severe for Bangla language, because it is really a challenging task to map 50 alphabets, modified vowels, consonants, and joint characters with only 12 keys on a mobile. To address this problem, a number of text-entry methods in mobile devices have proposed. Moreover, A few mobile operators have released their Bangla SMS software.

978-1-4244-6283-4/09/$26.00 ©2009 IEEE

A. Existing Bangla Keypad

Common Bangla layout: This keypad is based on alphabet ordering which is currently used by some mobile phone manufacturers (Figure 1). It is quite simple layout but requires excessive keystrokes for inserting a single character. For example, to enter the Bangla word 'সিএসই', this keypad needs 19 [*+3+5+8+3] keystrokes [2].

1 Punctuation key	2 ক খ গ ঘ ঙ ১	3 চ ছ জ ঝ ঞ ২
4 ট ঠ ড ঢ ণ ৩	5 ত থ দ ধ ন ৪	6 প ফ ব ভ ম ৫
7 য র ও ল শ ষ স ৬	8 হ ড় ঢ় য় ৎ ঃ ঁ ৭	9 অ ই ঈ উ ঊ ঋ এ ঐ ও ঔ ৮
* া ি ী ু ূ ৃ ে ৈ ো ৌ ্	0 special symbol	# joint character

Figure 1: Generalize keypad layout

Bangla keypad based on phonetics: Bangla phonetic keypad for mobile employs the idea of mapping the Bangla characters under the similar sounding to equivalent English characters [2]. A simple calculation depicts that each English character has to be assigned to at least two Bangla characters. To overcome this problem, it has taken two adjacent Bangla characters (with a few exceptions) as a cluster (Figure 2). However, the keypad design suffers from the problem of excessive key pressing, especially for the short vowels which are the used very frequently.

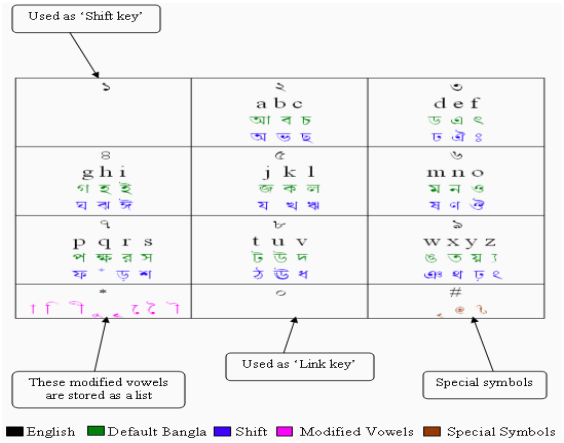

Figure 2: Mobile keypad based on Phonetic [2]

Ergonomic keypad: This keypad layout tries to minimize the finger movement by placing the characters in such a way that most frequent characters are appeared in the most comfortable zone [3]. The keypad is divided into three zones: (a) most comfortable zone, (b) medium comfortable zone and (c) least comfortable zone. The most comfortable zone consist off 1, 2, 4, 5, 7 and * keys. The medium comfortable keys are 3, 6 and 8 .The least comfortable keys are 9, 0 and #. However, in the paper it was assumed that the keypad would be used by right-handed people. But many people use the keypad using left hand or even by both hands. In such cases it may not have a very significant effect.

Frequency based two-layer multitap input method: In this method, characters are ordered in such a way that the most frequent letter appears with one keystroke, the next frequent letter in second keystroke and so on [4]. But since the mappings of characters are changing frequently user may feel it very uncomfortable to find out a particular character.

A few mobile operators have released their Bangla SMS software but have not achieved sufficient popularity yet. The major problems associated with most of the existing systems are, needs of excessive key pressing, difficulties in memorizing character mapping and lack of comprehensiveness. AKTEL, a mobile phone operator in Bangladesh implemented a Multitap input method in Bangla for text-entry. It is a One-Layer Multitap (OLM) [4] method. In this method, all the Bangla scripts and symbols are kept in one layer. To use Bangla SMS, one will need to install "AKTEL Mayer Bhasha" [4, 7] software in one's handset. SMS can be sent to any other, who has the software installed in his/her mobile. But it is overwhelmed with the key pressing. For example, to insert the letter 'ঽ', it needs 12 keystrokes. Grameen-Phone Ltd. introduced Bangla SMS named "Amar Bhasha" [4, 8] by two-dimensional matrix arrangements of the alphabets; they reduced key presses significantly but some extra key presses are needed for entering joint characters and it does not provide predictive text input. Citycell [4, 9] introduced Bangla SMS using English alphabet called Romanization. The customer will write the text in English with Bangla format and in return, he will receive in Bangla. Actually it is a picture message. Pictures are 72*14 or 72* 28 pixel. But only 25 characters are allowed to use for a single message.

B. Predictive Text Input Method

Predictive input technologies use language knowledge to predict what text the user is going to enter. Letter anticipators predict the next letter based on the prefix entered by the user. Hybrid systems combine the letter anticipators and the word completers. T9 (Text on 9 keys) is the most widely used predictive system on mobile phones [5]. There was an attempt in Bangla also [6] where user can finish a word according to the suggested word(s) generated by the system that starts with the prefix characters. However, this system may need unnecessary key pressing to choose less frequent words that are appearing at the bottom.

C. Text-Entry System for Visual Impaired

Existing text-entry systems cannot be used by blind users since these are strongly rely on visual feedback for their correct operation. On the other hand there are some Braille devices which are large, heavy and

cumbersome to use in mobile context. With the enormous growth of mobile phones and applications it is urgent to provide for blind individuals the ability to operate such kind of devices. Recently, in English a few works have done successfully to develop text entry system in mobiles compatible for blind people. "BloNo" is a mobile text entry interface for the visual impaired based on a vowel navigation based text-entry method and speech synthesis feedback [10]. Besides text-entry based applications, BloNo provides the necessary feedback to navigate through menus and access applications. But in Bangla no such attempt has taken yet.

III. SYSTEM ARCHITECTURE

A. The Proposed Keypad Layout

The prime objective of our proposed keypad is to minimize keystrokes needed for inserting text as much as possible. Moreover, it is also necessary avoid multi-tapping on a single key. More importantly, keypad layout is also needed to be user friendly and easy to memorize. To ensure these criteria, we employ the idea of using two key technique applied on the two dimensional matrix with the alphabets i.e., to enter a letter user selects corresponding the row and column from the matrix. Thus, maximum two key presses needed for entering Bangla characters. Our proposed keypad design is shown in Figure 4. Whenever a key is pressed, the system decides which row is selected (shown on the key no.) and shows all the letters along with their column number at the bottom of the user interface. Then the next key press required is to select the column (shown as prefix before the character) and thus the character [row][column] is displayed. However, if a certain time is elapsed after the row is selected first column of that row i.e., character [row][1] is automatically selected for ensuring further reduction of key presses. For instance, according to the matrices arrangement in Figure 3 (denoted by solid line) enter the character 'ফ', user need to choose row 5 and column 2. However, to enter 'ট' it requires only pressing key 3. In the keypad, 1,2,3,4,5,6,7 are used for entering consonants. In the key 8,9,* are used for entering modified vowels, modified consonants and a few special symbols (ং ঃu ,etc).

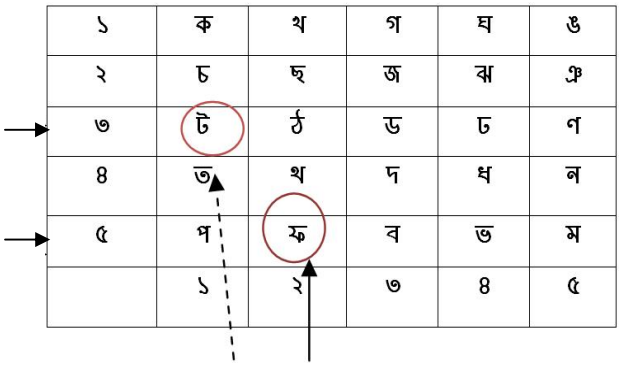

Figure 3: Two key technique using Two Dimensional Matrix (showing a portion of the matrix)

Shift Key: In Key 8 we used for modified vowels by default, because in messaging Bangla modified vowels are used much frequently than vowels. To change it in vowel character mode one needs to press '0' two times consecutively. But single press of '0' is used for entering space. According to Unicode rules these modified vowels should used after entering any consonant.

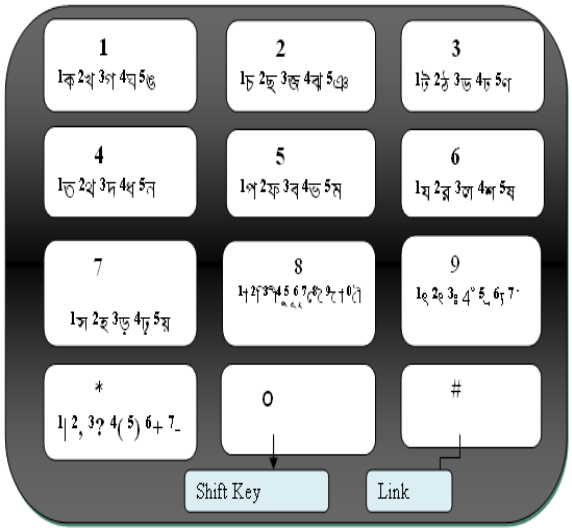

Figure 4: Proposed system keypad (Each key denotes row, each prefix before any character denote corresponding column)

Link Key: '#' is used for entering the ligature (Juktakhhor) as well as link key for entering numeric character. For a single press it get ready for working as ligature and for the next key press it is used for entering numeric characters. After pressing the '#' key it will serves as link key. Then the next need to character that associated with the previous regular will be pressed.

B. Text Entry Method

To accomplish our goals, a new text-entry method is developed. The flowchart of the method is shown in Figure 5.

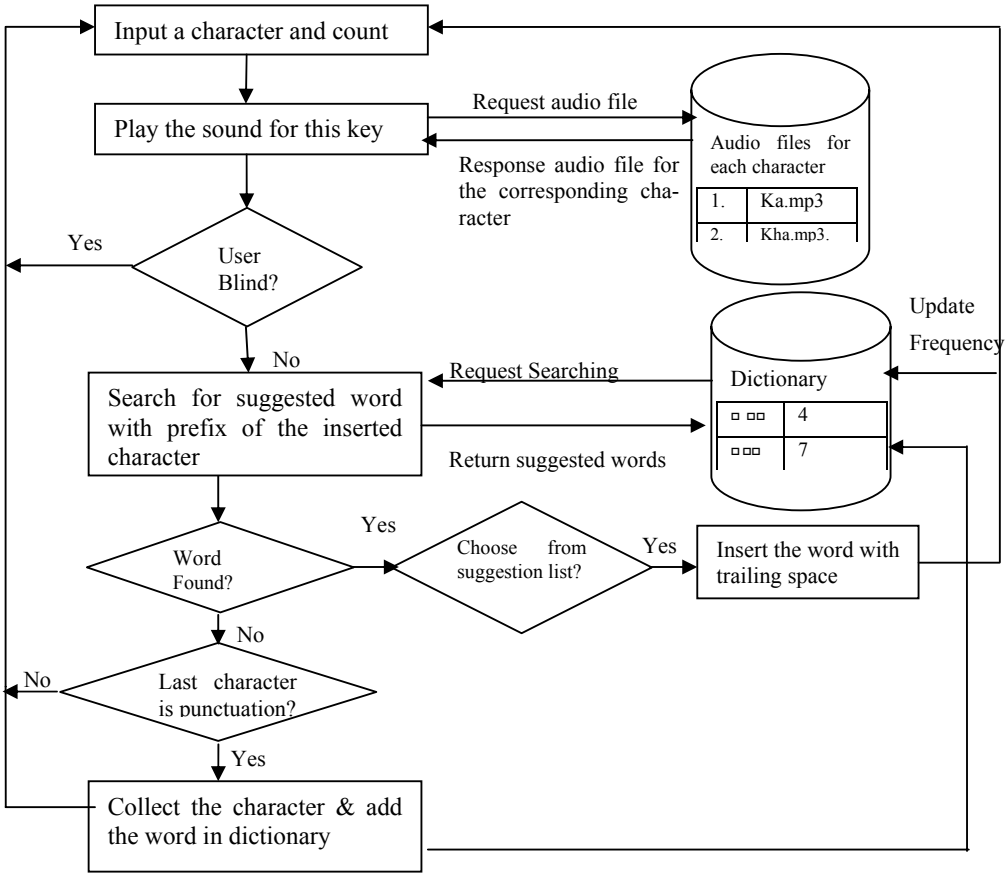

Figure 5: Complete flowchart of text entry method

According to the flowchart after selecting a character using appropriate key it is shown on the screen and the corresponding audio file is played for the visual impaired person. However, for visually capable people the predictive text-entry system searches on the dictionary according to leading character(s). If word(s) found with prefix of inserted characters, display the suggested list. User can scroll the words and choose the word to insert it. If the users select the word from the list, the word will insert with trailing space.

B. 1 Predictive Text Input

Our predictive text input system allows user to choose from a list of possible words starting with the inserted prefix. Moreover, it also automatically updates the frequency of words in the dictionary according to the user's message and later uses it to generate the priority of the suggested words. At the initializing stage, a Dictionary that contains a list of words along with their frequency is created from a collection of Bangla SMS. But since word frequencies may vary from user to user, we propagate the intensification of the predictive input system by increasing the frequency accordingly, as user composes more messages. After inserting any punctuation symbols, we assume that a new word has appeared and the word is added in the dictionary if it is not existed.

Algorithm for Predictive Input:

1. Initialize the dictionary D with words extracted from collected SMS along with their frequency.
2. FOR each input of character
3. IF the character is punctuation mark indicating the end of a word THEN
4. IF the word not exists in D THEN add it to D and set its frequency to 1.
5. ELSE increase the frequency of the word in D by 1.
6. ELSE Generate a list of all word(s) starting with the prefix input characters and
8. Sorted the words according to the decreasing order of frequency.
9. Allow the user to choose from the suggestion word list.
10. IF user selects any word from suggestion list THEN
11. Append the word in the text
12. Increase the frequency of the word in D by 1.
13. END FOR

B. 2 Audible System

It is easy to understand that, when audio file is played, user receives voice feedback before accepting

any letter, therefore reducing entry mistakes. This is the most important issue for blind people as they totally rely on audio feedback, performing the text entry task successfully and increasing the motivation to improve the writing skills. To play the audio we collect the utterance of all the characters as .MP3 format audio file. There are 61 .mp3 file representing audio for all the vowels, consonant and numbers. The audio files have the size between 4 Kb to 7Kb, so that, they can be loaded very quickly and audio feedback can be provided instantly. When a key is pressed, the system searches on the resource directory for the corresponding audio file. Then it plays the audio file of the corresponding character and renders the character.

IV. EXPERIMENTS AND ANALYSIS

A. Experimental Setup

In completing our research work we use Java 2 Micro Edition (J2ME) [11-13] programming language. For implementing audible input we use J2ME MMAPI [14] (Mobile Media API) and WMA (Wireless Messaging API) [14] for wireless messaging. In the predictive input system, we use J2ME RecordManagement [13] for storing words and their frequency. We develop our system with latest graphical interface design tool for J2ME named LightWeight User Interface Toolkit (LWUIT) [15] and Unicode was used for representing characters instead of pictures. We tested our software on Nokia – 3110c which is a S-40 series java supported hand set with MIDP 2.0.

B. The User Interface

At the startup of the software we use four options to choose. These are "Write message" allies "বার্তা লিখ", "Inbox" allies "বার্তা পড়", "Help" allies "সাহায্য" and "Exit" as "বের হও". So, choosing the "write message" option user enters on new interface where user can write message, send message, add new words.

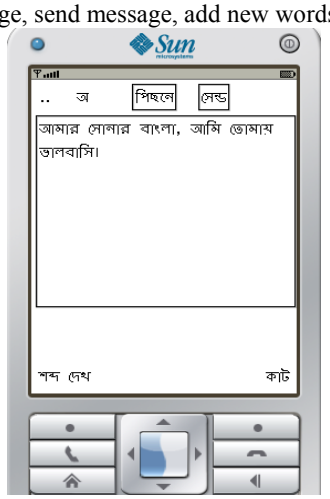

Figure 6: Writing interface of the Software

At the top of the screen, a label is denoting users typing mode. 'অ' represents the normal mode i.e., it is the default setting for operating the software. 'ঌ' mode represent is the shift mode is used for entering ligature (Figure 6). The keypad act as a numeric keypad in "১" mode. In this mode, it needs only single press to enter a digit. In figure 7 we see that a list of word is suggested after user press the character '© য'. User either can scroll the word from the list or can press the index no of the word to append it in the text. For example pressing '6' will implies selection of যদি.

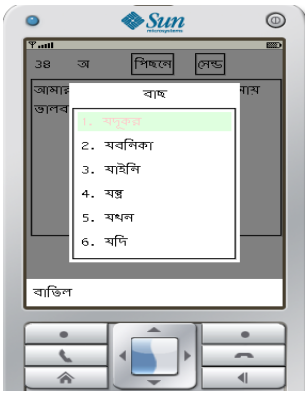

Figure 7: Predictive input interface

C. Experimental Result

Tests were made after collecting about 100 messages from various persons to ensure the nature of data to be more heterogeneous. Then we calculate the number of keystrokes needed for entering those messages according to the proposed method and other previous methods. In Table 1, we show a portion of the comparison of key presses for entering words, between our proposed text entry process and conventional process. Figure 8 compares keystrokes needed in several methods for some sample messages, where message length ranges from 8 to 20.

Table 1: Comparison of key presses required for several words between proposed system and existing systems

Sl No	Word	Generalized keypad	Phonetic keypad	Proposed keypad	Proposed keypad (with predictive)
1.	আমি	10	4	6	4
2.	আজ	5	2	4	4
3.	আসব	10	7	5	4
4.	না	7	3	4	4
5.	তোমরা	12	14	7	6
6.	কখন	8	7	5	4
7.	যাবে	12	11	7	5
8.	কেমন	12	11	7	5
9.	আছ	4	5	4	4
10.	পড়া	5	6	5	3
....	....	....	....	....	....

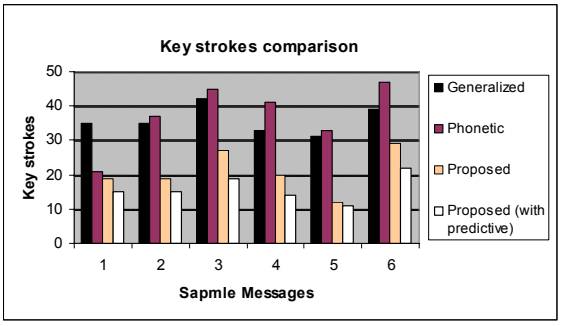

Figure 8: Keystrokes comparison among several methods for 6 sample messages

Figure 9 depicts the performance comparison on the basis of average key presses per word. Among them Phonetic input method requires larger number of keystrokes than others. Our proposed keypad with predictive input system reduces 60.34% and 70.82% key strokes than generalized keypad and Phonetic keypad respectively. It is apparent from Figure 9 that, our proposed keypad layout with predictive input is much more feasible way of entering text in mobile devices.

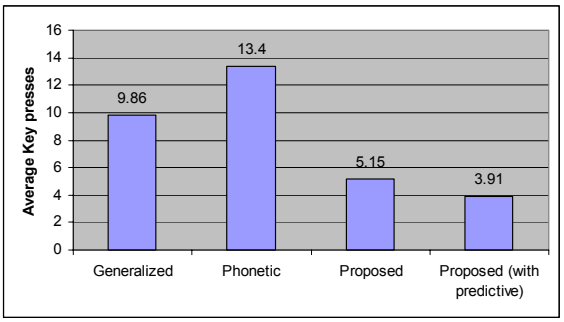

Figure 9: Comparison of average keystrokes per word

In order to test the accessibility of visually impaired people, five users were first instructed about the text entry method in details. Then they were requested to write down a few sentences. All the users were able to write the message with reasonable time delay (around two words per minute) and error rate (7.24%) was fairly acceptable. In general, all the users were more or less satisfied with the messaging system and gradually improved their performance.

V. CONCLUSION

The experimental results show that the number of keystrokes reduced considerably using the proposed keypad layout and outperforms generalized and phonetic keypad. Moreover, when predictive input system is added, messaging becomes even faster. The idea of audio feedback system is highly significant in terms of providing accessibility to not only visually impaired individuals but also the less literate people. We believe that, this comprehensive text-entry system can considerably improve the human computer interaction in enormous growth of mobile computing environment in the context of Digital Bangladesh.

There may be some possible improvements that can be applied to our system. As future work, we will try to combine transileration facility in our text-entry system. Moreover, there is no option to read the SMS by a visual impaired user at the receiving end. Introduction of a speech synthesizer for end user mobile phone is our another future plan.

REFERENCES

[1] GSMA's Hubbing Programme to Streamline Global Delivery of SMS Message, GSM Association Press release (12th October, 2006), [Online]http://www.gsmworld.com/newsroom/press-releases/2093.htm

[2] Al-Mukadin Khan, Salimur Rashid, A.K.M. Najmul Islam and Abdullah Azfar, "Design of an Interactive Bangla Mobile Keypad Based on Phonetics", International Conference on Computer and Information Technology" (ICCIT '05), pp. 658-660, 2004.

[3] Muhammad Raisul Alam, Md. Masum, Shafiul Hasan Md Tareq and Mostafa Wasiuddin Numan "Design of an Interactive Bangla Mobile Keypad Based on Ergonomics", 10th International Conference on Computer and Information Technology, (ICCIT 2008), Khulna, Bangladesh.

[4] M. M. Morshed, Y. K. Thu and Y. Urano, "Frequency Based Two-Layer Multitap Bangla Input Method for Mobile Phones," 10th International Conference on Computer and Information Technology, (ICCIT 2007), pp. 1-7, Dec. 2007.

[5] T9: How it works: (January 20, 2005) [Online] http://www.t9.com/

[6] Md. Kamrul Hasan Bhuiyan, Ahsan Murshed, Md. Golam Rabiul Alam, Md. Emdad Hossain, "Bangla Predictive Text Input Technique for Cell Phone" Proceeding of International Conference on Computer and Information Technology (ICCIT 2005).

[7] Aktel Bangla SMS. http://www.aktel.com/

[8] GrapmeenPhone Ltd. Bangla SMS http://www.grameenphone.com/

[9] CITYCELL SMS. http://www.citycell.com/

[10] Paulo Lagoa, Pedro Santana, Tiago Guerrerio, Daniel Goncalves and Joaquim Jorge, "BloNo: A New Mobile Text-Entry Interface for the Visually Impaired", IICCII 2007, pp. 908-917, 2007.

[11] James Keogh "J2ME: The Complete Reference", Tata McGraw-Hill Edition 2003.

[12] Singli and Jonathan Knudsen "Beginning J2ME: From Novice to Professional", Apress- Third Edition.

[13] Developers Guide "LightWeight UI Toolkit" [Online] https://lwuit.dev.java.net/

Proceedings of 2009 12th International Conference on Computer and Information Technology (ICCIT 2009)
21-23 December, 2009, Dhaka, Bangladesh

A New Word Separation Algorithm for Continuous Bangla Speech Recognition

Nipa Chowdhury, Md. Abdus Sattar†
Dept. of CSE, Dhaka University of Engineering & Technology (DUET), Gazipur, Bangladesh
†Dept. of CSE, Bangladesh University of Engineering & Technology (BUET), Bangladesh
nipa83@yahoo.com, masattar@cse.buet.ac.bd

Abstract

Word separation algorithm is needed to separate words from continuous speech for improving performance of Speech Recognition. Studies show that existing techniques suffer from separating words into disjoint sub-words and then we present a new word separation algorithm to overcome this problem. Prosody has great impact on Bangla speech and the algorithm is developed by considering prosodic feature with energy. At first continuous Bangla speech signals are fed into the system and the word separation algorithm separate speech into isolate words. Performance of the proposed algorithm is compared to the existing algorithms and result shows that 98% word boundaries are correctly detected.

Keywords: Pitch, Stress, Word Separation, Continuous Bangla Speech.

I. INTRODUCTION

In the age of information technology Human-Computer Interaction (HCI) has gained importance. Speech is the primary mode of communication among human being and people expect to exchange natural dialect with computer due to recent development of speech technology.

Speech recognition is the process of extracting necessary information from input speech signal to make correct decision and applied in automation of operator assisted services, dictation, interactive voice response, medical transcription, data entry, pronunciation in Computer aided Language Learning etc.

Speech recognition can be classified as speaker dependent or independent, Isolated or Continuous and can be for large vocabulary or small vocabulary. An isolated speech recognition system requires that a speaker offer clear signature between words whereas continuous speech consists of continuous utterance. Isolated speech recognition is much easier than continuous speech recognition because start and end point determination of a word is easier because of clear pause or silence.

In this paper we investigate problems of existing algorithms to separate words from continuous bangla speech and then propose a new method for word detection in continuous bangla speech by using prosodic feature. Result shows that not all prosodic parameters convey useful information for word separation and performance of the proposed word separation algorithm, in terms of accuracy is higher than other existing algorithms.

II. RELATED WORKS

Although Bangla is one of the highest spoken language in the world (ranking 5th) and almost 8% of total population in the world speaks in Bangla, works on Bangla speech recognition is not satisfactory [1]. By using Reflector coefficient, autocorrelations as speech feature and Euclidian distance for taking decision, recognition of vowel [2] was done with 80% efficiency. 66% recognition accuracy was obtained for Bengali phoneme recognition [3] where rms value used as feature and ANN as classifier. In [4] experiment was carried out for a database consisting of 30 different Bangla words. A word separation algorithm had been developed for Continuous speech Recognition [5] by comparing noise energy and zero crossing with speech and for 13 words. Among them 1 word is not separated and it requires huge memory, training time.

Crucial point is that continuous speech does not offer any clear signature like pause, silence between words. In CSR word boundary detection is important otherwise task of speech recognizer is more complicated. Because a new word may begin at any time and require huge search space [6]. But if words can be correctly detected than strategy of isolated speech recognition can be applied for continuous speech recognition.

Existing word separation algorithm [5] was employed to separate words from continuous Bangla speech by comparing noise's energy and zero crossing rates to speech. We implement the existing algorithm and performance is shown below. In Figure 1 at first section input speech 'Artho noi somman chai' is shown and in second section speech is segmented using existing

algorithm. This shows that 'Artho' is not separated correctly ('Ar,tho).

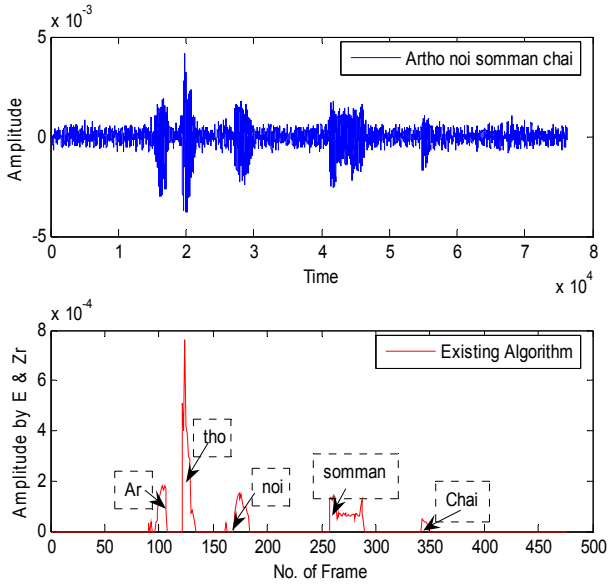

Fig 1: Separation of the word 'koto bastota amader' using existing methods.

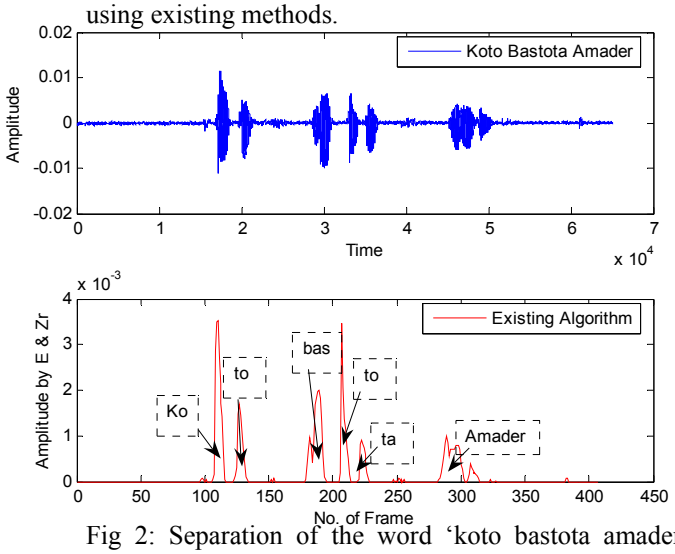

Fig 2: Separation of the word 'koto bastota amader' using existing methods.

Figure 2 shows that 'koto' is separated incorrectly (ko, to), Bastota as (Bas,to,ta). So silence may exist within a word. Considering only word length with energy & zero crossing rates do not give good result.

III. OUR APPROACH

Bangla is a bound stress language unlike English [6,9]. It gives prominence on word that is high on initial word and become low at end of the sentences. So, our idea is if this prominence can be detected then words can be separated. To achieve this at first Speech pattern is detected by comparing speech's energy to noise energy and then stress information are find out. Stress consists of pitch, intensity, duration [7]. Pitch means dominant frequency, intensity means power and duration means time duration. To find fundamental frequency of speech autocorrelation methods is used. By using above stress information a Word Separation algorithm is developed.

IV. DETAILS OF EXPERIMENT

Conversion of analog speech signal into digital is the first step of speech signal processing. For this reason speech signal is digitized with sampling frequency 11025Hz and sampling size is 16 bit per sample. Human speech production is dynamic and nonstationary. But within a short period of time (20-40ms) its behavior is quasi stationary. Speech is framed of 40 ms length with 20ms overlapping. Then windowing is performed to remove unnatural discontinuities in the speech signal. Hamming window is used in this experiment.

Speech is easily affected by noise. Noise removal of speech is the most challenging because noise nature is random. For this reason energy from first 100ms speech data considered as noise energy and threshold value ($E_{noiseth}$) is set. Now energy for other speech frame, E_{sth} is calculated according to the following formula.

$$E_{sn} = \sum_{m=1}^{N} s_m^2$$

Now if energy of speech frame, E_{sn} is greater than $E_{noiseth}$ then speech exist and next it consider for stress analysis so consecutive frames are tagged as candidate word. Other frames are considered as noise.

A. Stress information

Stress consists of pitch, intensity and duration. Intensity can be derived by using

$$p = \frac{1}{T}\sum_{i=1}^{k} s^2(i)$$

Duration is simple time duration of candidate word. Pitch is the most useful information for word separation of Bangla speech. But the general problem of fundamental frequency or pitch estimation is to take a portion of signal and to find dominant frequency of repetition. Because fundamental frequency of the periodic signal may be changing over the time and not all signals are periodic. Signals that are periodic with interval T are also periodic with interval 2T, 3T etc, so we need to find the smallest periodic interval or highest fundamental frequency.

Different methods have been used for pitch detection like Zero Crossing, LPC based, Autocorrelation,

Cepstrum, Harmonic structure etc. Out of them autocorrelation methods is still one of the most robust and reliable pitch detectors. The autocorrelation computation is made directly on the waveform and fairly straight forward [10]. Autocorrelation function finds the similarity between the signal and shifted version of itself.

$$y(n) = \sum_{m=1}^{N} s(m)s(m-\alpha)$$

This finds peaks in fundamental frequency and multiple of fundamental frequencies if the speech signal is harmonic. Actually as the shift value α begins to reach the fundamental period of the signal, the autocorrelation between the shifted signal and original signal begin to increase and rapidly approaches to peak at the fundamental period. But length of frame is important for autocorrelation [10]. So we have to select frame size as long enough to contain at least one period and detect peak clearly. Hence we use short time autocorrelation function with frame size 40ms which exactly matched to our speech frame length.

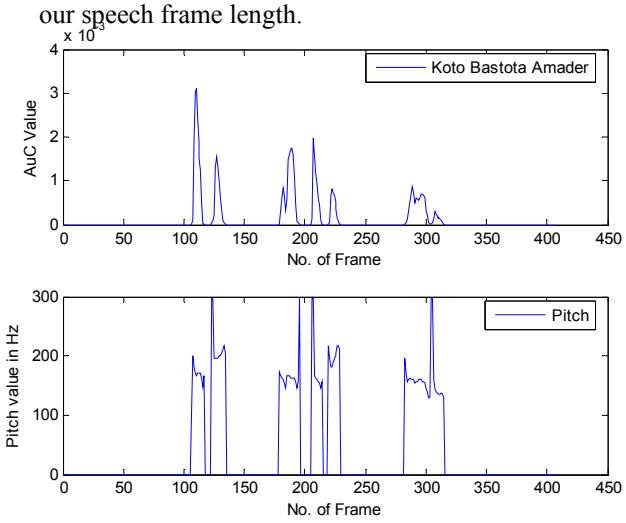

Fig 3: Shows frequency of speech 'koto bastota amader' by autocorrelation method

In Figure 3 resultant value of autocorrelation and frequency that derived by autocorrelation is shown. Fundamental frequency of male voice is 85-155Hz and female voice is 165-255 Hz. So we estimate fundamental frequency in between 60-300Hz. By using this pitch information we merge candidate words into one word. If pitch information of consecutive candidate words are high within certain gap then those candidate word form a single word.

V. RESULTS AND DISCUSSIONS

Speech signal are recorded in room environment using microphone. Sampling frequency of 11025Hz and sampling size bits per sample and mono channel is set. Total 270 sentences are uttered by speaker. Last 135 sentences are the repetition of first 135 sentences but word position is varied. For example, in first 135, if a sentence forms like this 'Tomar amar bangladesh' then in second 135(136-270), it forms like 'Bangladesh tomar amar'. This is done to verify that our algorithm is error prone to specific position of word or not. So total 270 sentences with 1755 words forms our database. After separation of words from speech each word is saved in a wave file to take decisions. Word Separation of several speeches is shown using existing algorithm in Table 1 and new algorithm in Table 2.

Table 1: Separation of word using existing algorithms

Sentences	Candidate Word	Separation Result
Koto bastota Amader	Ko	W
	To	W
	Bas	W
	to	W
	Ta	W
	Amader	C
Artho noi somman chai	Ar	W
	tho	W
	noi	C
	Somman	C
	Chai	C
Pakhi sob kore rob	Pa	W
	khi	W
	sob	C
	Kore	C
	Rob	C

Here W stands for Wrong and C for Correct

Table 2: Separation of words using new algorithms

Sentences	Candidate Word	Pitch	Change Boundary	Separation Result
Koto bastota Amader	Ko	165	Yes	C
	to	218		
	bas	169	Yes	C
	to	188		
	ta	201		
	amader	160	No	C
Artho noi somman chai	Ar	180	Yes	C
	tho	226		
	noi	155	No	C
	somman	173	No	C
	chai	149	No	C
Pakhi sob kore	Pa	163	Yes	C
	Khi	197		
	Sob	174	No	C

rob	kore	178	No	C
	Rob	145	No	C

Experimental result shows that our proposed algorithm that uses stress information with energy performs excellent compare to existing algorithm. Other stress information like intensity and duration does not contain useful information for word separation of Bangla speech. We implement existing algorithm [5] and result is given in Table 3. Result shows that 598 words are not separated by existing algorithm and the number is 28 by our new algorithm. Performance is improved by 8% when database in [5] is used, while it increased by 32% for our new database that consists of 1755 words. Success rate is also higher than the previous rate of 81% reported in [6].

Table 3: Comparison of proposed algorithm vs. existing algorithm [5].

Database	Algorithm	Correct Separation	Wrong separation	Performance
Existing[5]	Existing[5]	12	1	92%
Existing[5]	New	13	0	100%
New	Existing[5]	1157	598	66%
New	New	1727	28	98%

Here existing database consist of 13 words and new database consist of 1755 words.

VI. CONCLUSIONS

Prosodic feature has great importance on Language and its behavior vary from Language to Language (English [7], Hungarian, Finnish [8], Bengali [6, 9] etc). English is said to 'stress-timed', as opposed Bangla is said to be bound stress. Stress in Bangla is high at initially and become low at the end of speech. We try to correlating this stress information with word. Result shows that energy and pitch information is important parameter for word separation. We use energy, zero crossing rate and pitch to separate words and get same results. Further study can be conducting to build a large vocabulary continuous speech recognizer for separated words.

REFERENCES

[1] M. A. Mottalib, "A Review on Computer based Bangla Processing", *Proc. of the National Conf. on Comp. processing of Bangla (NCCPB),* Independent University, Dhaka Bangladesh,27 February,2004,pp.72-81.

[2] A. H. M. R. Karim, M. S. Rahman and M. Z. Iqbal, "Recognition of Spoken Letters in Bangla", *Proc. of the 5th Int. Conf. on Comp. and Info. Tech.(ICCIT),* East West University, Dhaka, Bangladesh, 27-28 December, 2002, pp. 213-216.

[3] M. R. Hassan, B. Nath and M. A. Bhuiyan," Bangla phoneme recognition- A New Approach.", *Proc. of the 6th Int. Conf. on Comp. and Info. Tech. (ICCIT),* Jahangirnagor University, Dhaka, Bangladesh, 19-21 December 2003, pp. 365-369

[4] M. R.Islam, A. S. M.Sohail, M. W. H. Sadid and M. A. Mottalib, "Bangla Speech Recognition using three layer Back-propagation neural network", *Proc. of National Conf. on Comp. processing of Bangla,(NCCPB),*Independent University, Dhaka Bangladesh,27 February, 2004 , pp.44-48.

[5] K. J. Rahman, M. A. Hossain, D. Das, A. Z. M. T. Islam and Dr. M. G. Ali, "Continuous Bangla Speech Recognition System", *Proc. of the 6th Int. Conf. on Comp. and Info. Tech. (ICCIT),* Jahangirnagor University, Dhaka, Bangladesh, 19-21 December 2003, pp. 303-307.

[6] S. K. D. Mandal, A. K. Datta, B. Gupta, "Word Boundary Detection of Continuous Speech Signal for Standard Colloquial Bengali (SCB) Using Supra segmental Features", *The Int. Symposium on Frontiers of Research on Speech and Music (FRSM),*IIT, Kanpur, India.15-16 February,2003.

[7] K. Imoto, M. Dantsujiy, T. Kawahara," Modeling of the Perception of English Sentences Stress for Computer-Assisted Language Learning", *6th Int. Conf. on Spoken Language Processing (ICSLP),* Beijing, China, 16-20 October, 2000, Vol-3,pp 175-178.

[8] K. Vicsi and G. Szaszák, "Automatic Segmentation of Continuous Speech on Word Level based on Supra-segmental features", *Int. Journal of Speech Tech.*,Netherlands, ,December, 2005,Vol-8, pp 363-370.

[9] www.en.wikipedia.org/wiki/Bangla_language

[10] L. R. Rabiner, "On the use of Autocorrelation Analysis for pitch detection", *IEEE Transactions on Acoustics, Speech and Signal Processing*, February 1977, Vol.ASSP-25, No-1.

Proceedings of 2009 12th International Conference on Computer and Information Technology (ICCIT 2009)
21-23 December, 2009, Dhaka, Bangladesh

Moving Object Tracking - A Parametric Edge Tracking Approach

Mahbub Murshed, M. Ali Akber Dewan†, and Oksam Chae‡
Department of Computer Engineering, Kyung Hee University, Suwon, South Korea
† Dept. of CSE, Chittagong University of Engineering and Technology, Chittagong, Bangladesh
‡ Department of Computer Engineering, Kyung Hee University, Suwon, South Korea
mmurshed@gmail.com, dewankhu@gmail.com, oschae@khu.ac.kr

Abstract

In this paper, an edge based tracking algorithm is proposed. Our algorithm makes efficient use of edge-segment on the Canny edge map by utilizing the edge structure in the moving object region. Curvature-based features are used for moving edge registration. We use the maximum curvature correspondences between two edge segments then the 2D affine transformation computes their movement by solving a system of linear equations. The registration error is then minimized. A Kalman Filter is used to track each individual edge segments. Segments are clustered using a k-mean algorithm. Finally, a group motion tracker is used for tracking moving object from each cluster. Experiments show that our edge-segment based tracking algorithm can track moving objects efficiently under varying illumination conditions.

Keywords: Affine Transformation, Curvature Point, Edge Segment based Moving Object Tracking, Kalman Filter, K-means Clustering.

I. INTRODUCTION

Moving object segregation and tracking is of important research interest for widespread applications in diverse disciplines. Tracking the events of potential interest from a large volume of image data is essential, since human observers may easily be distracted from this task. A survey on object tracking can be found in [1]. Image information lies mostly on the edges of different regions [2]. Extraction of edge from an image significantly reduces the amount of data and filters out useless information, while preserving the important structural properties in an image [3]. In dynamic environment, edge-based methods show more robustness as compared to pixel intensity-based methods as edge-based features are less sensitive to illumination variation than intensity features [4]. Moreover, edge information is less sensitive to noises and is more consistent than the pixel values in the video sequence. However, traditional edge pixel-based moving object detection methods do not represent edge information using any data structure and thus they need to visit all the image location [5] [6]. These methods treat each edge point independently which is not convenient for matching and tracking. It is also difficult to handle dynamic background where foreground can temporarily act like background for an arbitrary period.

In our method, edges are extracted from video frames and are represented as segments using an efficiently designed edge class using the method proposed by [2]. This representation helps to obtain the geometric information of edge in the case of edge matching and shape retrieval; and creates effective means to incorporate knowledge into edge segment during background modeling and motion tracking. We use edge curvature points as our salient features for object tracking. Since edge Curvatures is invariant to transformation; gives us good estimate to motion parameters for successive frames while using least squares approach. Additionally, this motion information is used by Kalman filtering for edge fitting. Finally, a clustered group motion tracker helps tracking moving objects in a simple but more reliable and robust way.

II.OBJECT TRACKING APPROACHES

Based on feature selection, object tracking algorithms can be categorized into three groups, namely point tracking, kernel tracking and silhouette tracking. In point tracking, object is represented by a set of points, the centroid [7] or by a set of points [8]. Objects in every frame are represented by points, and their locations are estimated based on the previous object state and position. Kalman filter [9] [10] is widely used in the vision society for point based feature tracking in sequence image. Particle filter [11] is robust for non-linear systems, but needs a large number of samples which makes it computationally expensive. Particle filter also suffers from the particle impoverishment problem [12]. Point trackers are suitable for tracking very small objects. Multiple points tracking is challenging due to the problem to distinguish multiple objects, and its background. Kernel based object tracking is usually represented with rectangular or elliptical shape of kernel [13]. Here, color histograms, mean color of a predefined shape kernel are used as features. Change in illumination and non-uniform texture and assigning arbitrary weight makes the approach less suitable. Contour or silhouette tracking represents the boundary of object [14]. Object boundary usually shows sharp changes in image intensities. Edge detectors bring out these changes.

978-1-4244-6283-4/09/$26.00 ©2009 IEEE

Edges are less sensitive to illumination changes compared to color or texture. Boundary tracking algorithms usually use edges as the representative feature. However, due to the motion of a moving object, different parts of the object undergo different movement even in the case of rigid body. In the existing edge pixel based methods, it is not possible to apply different amount of transformation for different parts of edge pixels at the same time. As a result, it cannot achieve accurate matching of all parts of the object model in subsequent frames.

III. EDGE SEGMENT BASED MOVING OBJECT TRACKING

Tracking problem is to reliably recognize the moving regions within frame correspond to same moving object over time. To do so, we have used Julius et al. [2] method for moving edge detection. Here, moving edges are extracted from video and represents as segments using an efficiently designed edge class. There, authors first model the background edges with a very good initial reference sequences. Reference edges are updated to adapt with the change in background scene which takes care of dynamic background. The matching method between corresponding segment of input edge and reference edge can tolerate fluctuation of camera focus or calibration error. Segment-based representation using edge class helps to access edge pixels fast as we do not need to access all the pixels in the image. Detection and update can be performed by using edge list, without accessing input frame. This representation helps to incorporate a fast, efficient and flexible edge tracking algorithm. From the remaining part of this paper we use the notation 'edge segment' for 'moving edge segment' in order to simplifying our notation.

A. Edge Curvature Points Registration

A common problem in computer vision is the registration of feature point sets [15]. Especially when a cluster of point samples from one frame of an object is matched with another cluster in another frame. The task of registration is to place the data into a optimum location by estimating the transformations of the object between the two frames. The parameter vector of the object's motion is estimated based on minimizing the sum-of-squared differences between the reference feature points in the reference frame and the observed feature points in the tracking sequence frame. This becomes challenging because correspondences between the point sets are not known before-hand. The selection of invariant features that can be reliably computed is a key component to such registration approaches. Curvatures are local features that are invariant to all affine transformations. Past research on range data has shown that surfaces may be classified by observing the signs of their mean and Gaussian curvatures [16]. Thus, if curvatures could be reliably and consistently calculated, they would be ideal for feature-based registration. The computation of curvature of a surface requires the estimation of the second derivative of the surface. For a plane curve given parametrically as c(u) = (x(u), y(u)), the curvature is

$$\kappa = \frac{|x'y'' - x''y'|}{(x'^2 + y'^2)^{3/2}} \quad (1)$$

Where

$x' = dx/du,\ x'' = d^2x/du^2,\ y' = dy/du,\ and\ \ y'' = d^2y/du^2$

We selected curvature points [17] (local maximum curvature) as salient features of an edge. We combine the advantage of transformation invariant curvature points along with edge features which maintain structural information. We will term 'selected high curvature points' as simply 'curvature points' for the remaining sections to further simplify our explanation.

B. Point Matching by Curvature

Given a sequence of N_T image frames I^{t-1}, t = 2, 3, …, N_T, we estimated the motion of all curvature points from one list $EL^{(t-1)}$ extracted from I^{t-1} to another list $EL^{(t)}$. For each curvature point on the edge list $EL^{(t-1)}$, p^{th} segment, q^{th} curvature point $\kappa_{p,q}$ with location coordinate (x', y') on frame $I^{(t-1)}$, we define a window of size W×W over $EL^{(t)}$ centered at $(x, y) = (x', y')$. Now for all curvatures $\kappa_{i,j}$ on the edge list $EL^{(t)}$ we take the best *n* curvature values within the W × W window as the candidate points from $EL^{(t)}$ that minimizes the following error equation:

$$E = \| \kappa_{p,q} - \kappa_{i,j} \| \quad (2)$$

Now among this *n* candidate curvature points we select one curvature point that is closest to the corresponding curvature location.

$$\kappa^c_{i,j} = \underset{\kappa_{(i,j)}}{\operatorname{argmin}} \| location(\kappa_{(i,j)}) - location(\kappa'_{(p,q)}) \| \quad (3)$$

In Eq. (3), the *location* ($\kappa_{i,j}$) operator gives the (x,y) location of j^{th} curvature on the i^{th} segment in $EL^{(t)}$ of frame $I^{(t)}$ where as *location* ($\kappa'_{p,q}$) operator gives the (x', y') location of q^{th} curvature on the p^{th} segment in $EL^{(t-1)}$ of frame $I^{(t-1)}$.

C. Edge Orientation Using Least Square Linear Method

Affine transformations are well known in computer vision for recognizing objects. It has been shown that a 2-D affine transformation is equivalent to a 3-D rigid motion of the object followed by orthographic projection and scaling [18]. Given the point correspondences between the two views, the affine transformation which relates the two views can be computed by solving a system of linear equations using a least-squares approach.

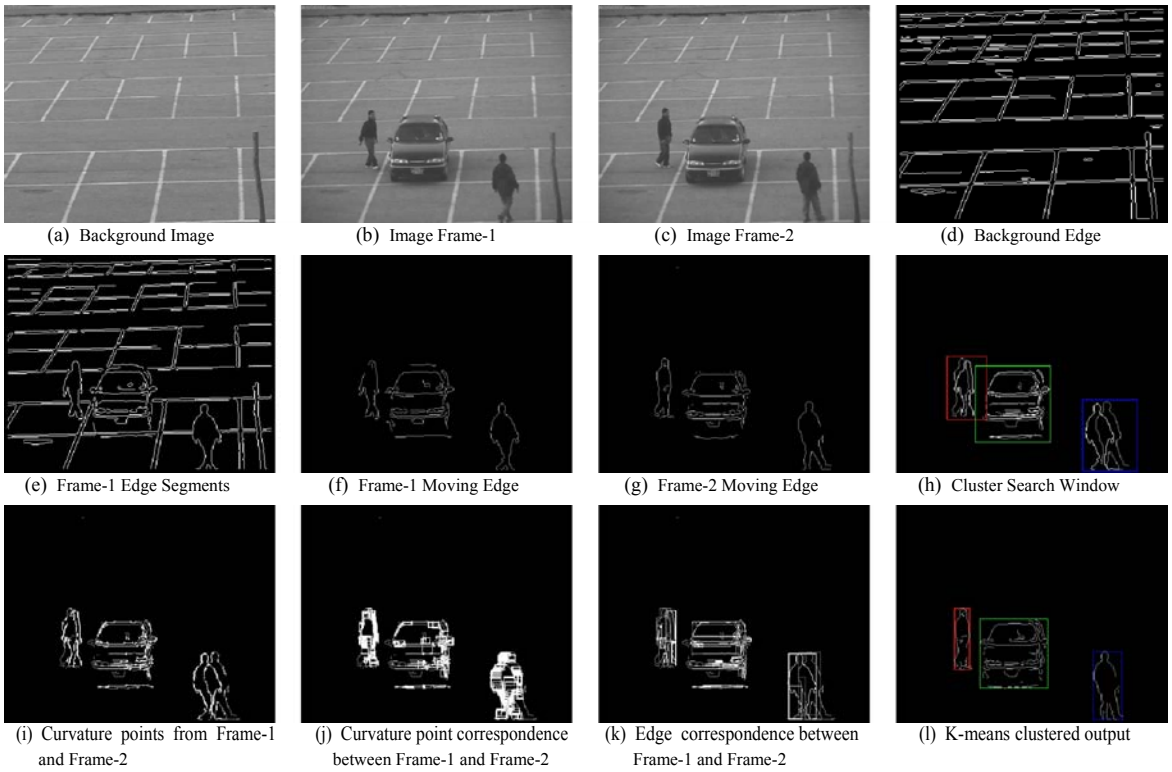

Fig. 1. Extraction of moving edge segments using the proposed approach (a) Background Image (b) Image Frame-1 (c) Image Frame-2 (d) Background Edge Segments (e) Edge segments from Frame-1 (f) Moving Edge segments from Frame-1 (g) Moving Edge Segments from Frame-2 (h) Cluster Search Window (i) Curvature points from Frame-1 and Frame-2 (j) Curvature point correspondence between Frame-1 and Frame-2 (k) Edge correspondence between Frame-1 and Frame-2 and (l) K-means clustered output.

In this paper, we propose an alternative approach for refining the output of the affine transformation parameters based on Kalman predictor. The idea is to feed the already computed parameters using the least squares method to the Kalman predictor for the successive frames and take the output of the Kalman predictor as the transformation parameters. The main reasons which motivated us in using Kalman predictor to solve this problem is that, it is interesting to think of this problem as a learning problem. There have also been proposed several other approaches [18] [19] which treat similar problems as learning problems. For computing edge segment orientation, Let us assume that each edge is represented by list of curvature points $(\kappa_1, \kappa_2, ..., \kappa_n)$. Point $\kappa(x, y)$ can move to point $\kappa'(x', y')$, then the coordinates of κ' can be expressed in terms of the coordinates of κ, through an affine transformation, as follows:

$$\kappa' = A \times \kappa + b \tag{4}$$

An affine transformation that handles translation, rotation, scale, and shear in 2D space can be described by 6 parameters. Rewriting Eq.(4), in terms of the image point coordinates, we have:

$$x' = a_{11}x + a_{12}y + b_1 \tag{5}$$

$$y' = a_{21}x + a_{22}y + b_2 \tag{6}$$

The above Eq.(5), (6), imply that given two different orientation of an edge segment or object, one known and one unknown, the points coordinate of the unknown view can be represented by a linear combination of the corresponding points coordinate in the known view. For a known view ϕ and an unknown affine transformed view ϕ' of the same edge segment, with point correspondences between them an affine transformation [18] can bring ϕ into alignment with ϕ'. Eq.(7) and Eq.(8) show this transformation.

$$\phi\begin{bmatrix} A \\ b \end{bmatrix} = \phi' \tag{7}$$

$$\begin{bmatrix} x_1 & y_1 & 1 \\ x_2 & y_2 & 1 \\ \vdots & \vdots & \vdots \\ x_n & y_n & 1 \end{bmatrix} \begin{bmatrix} a_{11} & a_{21} \\ a_{12} & a_{22} \\ b_1 & b_2 \end{bmatrix} = \begin{bmatrix} x'_1 & y'_1 \\ x'_2 & y'_2 \\ \vdots & \vdots \\ x'_n & y'_n \end{bmatrix} \tag{8}$$

In our algorithm, curvature point correspondence is done for those edge segments where number of curvture points over that segment is more than 3. This condition is mandatory sine we are using 6 parametric model.

Eq.(8) can be written as AX = B; A solution to the problem can be written as Eq.(9).

$$X = (A^T A)^{-1} A^T B \tag{9}$$

D. Design of Kalman Filter for edge segment tracking

The edge tracking algorithm consists of two stages. In the first stage, we use least squares approach as in Section III-B. We then apply Kalman filtering [10] to predict every edge segments location in the next frame. Since a Kalman filter only needs information from the previous state, we can update filter for each frame and predict for the next frame. Now, for a number of frames, if a corresponding segment match is not found, we keep the segment to be tracked by lowering its weight value. This type of activity helps us to track segments even if segments are missing due to noise or due to objects occlusion.

Let, $x_i^{(t)}$ be state vector, for the edge segment i from frame $I^{(t)}$. $w_i^{(t)}$ be process noise and $v_i^{(t)}$ represents measurement noise; White, Gaussian, mean=0. Process noise covariance matrix Q, measurement noise covariance matrix R which is Uncorrelated with $w_i^{(t)}$. $K_i^{(t)}$ is the Kalman gain. Covariance of prediction error $P_i^{(t)}$, Measurements $z_i^{(t)}$ and Edge segment location $loc_i^{(t)}$.

The following equations are used for the predictor:

The prediction phase:

$$\begin{aligned} \hat{x}_i^{(t)-} &= A\hat{x}_i^{(t-1)} + w_i^{(t-1)} \\ z_i^{(t-1)} &= loc_i^{(t-1)} + v_i^{(t-1)} \end{aligned} \tag{10}$$

The update phase:

$$\begin{aligned} S_i^{(t-1)} &= P_i^{(t-1)} + R \\ K_i^{(t-1)} &= AP_i^{(t-1)} S^{(t-1)-1}_i \\ P_i^{(t)} &= AP_i^{(t-1)} A^T + Q - AP_i^{(t-1)} S^{(t-1)-1}_i P_i^{(t-1)} A^T \\ \hat{x}_i^{(t)} &= A\hat{x}_i^{(t-1)-} + K_i^{(t-1)}(z_i^{(t)} - A\hat{x}_i^{(t-1)-}) \end{aligned} \tag{11}$$

The estimated motion information of Kalman predictor helps limiting search space which increase accuracy as well as speed. For details about Kalman filtering, please see [9].

E. Edge Segment Clustering

We cluster segments based on edge segment connectivity while giving emphasis on relative edge distance. Initially, we group clusters based on k-means clustering [20] algorithm for the first two frames. To cluster segments, each edge segment is enclosed within a rectangular boundary and the midpoint of this boundary is used as the edge representative in the computation of the K-centroids for the K-clusters. The algorithm aims to minimize the following objective function in Eq.(12).

$$J = \sum_{k=1}^{K} \sum_{i=i}^{n} \| p_i - C_k \|^2 \tag{12}$$

Where $\| p_i - C_k \|^2$ is the distance between the midpoint of the rectangular edge segment boundary to the k^{th} cluster center (C_k) and n is the total number of moving edge segments present in that frame. Afterward we start with this initial clusters and then start tracking clusters in the subsequent frames. Here we divide / merge clusters based on edge availability / connectivity and edge locational information in that frame. Once cluster is formed, we store cluster information, i.e. member edge segments along with their motion parameters also group average (cluster) motion parameters.

F. The Proposed Cluster Tracking Algorithm

Let $EL^{(t)}$ and $EL^{(t-1)}$ be the Edge segment list extracted from the first two frames $I^{(t)}$ and $I^{(t-1)}$, here t is time index. $N^{(t)}$, and $N^{(t-1)}$ be the total edge segments in $EL^{(t)}$ and $EL^{(t-1)}$ respectively. ω_k be the k^{th} extracted edge cluster. ϕ_i be the i^{th} edge segment from $EL^{(t)}$, ϕ'_p be the p^{th} edge segment from $EL^{(t-1)}$. $\kappa_{i,j}$ be the curvature in edge list $EL^{(t)}$ on the i^{th} segment and j^{th} curvature point. $\kappa'_{p,q}$ be the curvature in edge list $EL^{(t-1)}$ on the p^{th} segment and q^{th} curvature point. $\kappa^c_{i,j}$ be the curvature in edge list $EL^{(t)}$ that finds a close match with curvature $\kappa'_{p,q}$. $N^{(t),i}$, $N^{(t-1),p}$ be the number of high curvatures on segment i from $EL^{(t)}$ and segment p from $EL^{(t-1)}$. $N_w^{(t)}$ be total number of clusters computed at frame $I^{(t)}$. Also let $MASK$ be the window of size $W \times W$. Curvature difference threshold τ_k, curvature location distance threshold $\tau_{distance}$ distance and edge frame history threshold τ_{edge}. Also let *location*() operator gives pixel position in the 2D space. Now for the first two frames moving edge segments are tracked using Algorithm 1. For the following frames moving object cluster is tracked by Algorithm 2. Here let $N^{(t)}_{\omega,k}$ be the total number of edge segments in cluster ω_k, $\Phi_{k,i}$ be the i^{th} segment in cluster k, C_k be the cluster center of ω_k, also let $KMASK$ be a small window which is placed towards the movement direction for every edge segment. Fig.1 represents some steps in our proposed method.

IV. RESULTS AND DISCUSSION

We have tested our method on several video sequences and it was able to track almost all of the moving objects in the sequences. For every frame pair, edges were matched using corresponding high curvature points-

Algorithm1. Moving Edge Tracking for first two frame

Compute $EL^{(t)}$ *from* $I^{(t)}$
Compute $EL^{(t_i-1)}$ *from* $I^{(t_i-1)}$
$\omega_k \Leftarrow NULL$
for p := 1 to N^{t-1} **do**
  for q := 1 to $N^{(t-1),p}$ **do**
    if $N^{(t-1),p} > 3$ **then**
      if $\exists \kappa_{i,j} \in EL^{(t)} : inside\ MASK$
      & $\| \kappa_{i,j} - \kappa'_{p,q} \| \leq \tau_k$ **then**
        $\kappa^c_{i,j} := \kappa_{i,j}$
      end if
    end if
  end for
  if *count*($\kappa^c_{i,j}$) > 1 **then**
  $\kappa^c_{i,j} = \underset{\kappa_{(i,j)}}{\operatorname{argmin}} \| location(\kappa_{(i,j)}) - location(\kappa'_{(p,q)}) \|$
  end if
  if $\forall j : \kappa^c_{i,j} : count(\phi_{(i)}) > 3$ **then**
   Add $\phi'_{(i)}$ *to cluster* $\omega_k = \underset{k}{\operatorname{argmin}}\ distance(\phi'_{(i)}, C_k)$
    If $N^{(t)}_{\omega} = 0$ *or* $distance(\phi'_{(i)}, C_k) > \tau_{(distance)}$ **then**
     Add $\phi'_{(i)}$ *to new cluster* ω_{new}
     Update C_{new}
     Use $\kappa'_{p,q}$ & *corresponding* $\kappa_{i,j}$ *for matching*
     Update Kalman predictor
    end if
    else
     Reduce Weight (ϕ_p)
     Add $\phi_{(p)}$ *to* ω_k *where* $Weight(\phi_{(p)}) \leq \tau_{edge}$
    end if
end for

where curvature threshold difference was allowed τ_k = 0.001. For the first two frame the search window size was $W \times W$ = 30×30, i.e we have allowed a maximum 30 edge pixel distance between two consecutive frames for registration. We have maintained edge segment appearance history for the last 20 frames by using weight value in the edge list structure. Finally, while clustering edge segments, we merged two clusters when the cluster boundary overlapped. An example of our tracking system is given in Fig. 2.

In the example, The tracking outcome along with cluster labeling is shown. Two moving objects labeled 3(Man) and 4(Car) are shown in frame 198. In fig.2 (b) a new moving object (Minibus) came into the scene and it is labeled with 5. We also see that the object labeled 4(Car) stopped moving. Thus 4(car) becomes a background object at frame 261. Furthermore, in fig.2(f), the two moving objects comes too close to each other, therefore, respective moving clusters were merged and yields a new cluster labeled 7(Minibus and Man). Finally, Frame 290 describes, the labeling of new cluster.

Algorithm2. Moving Object Cluster Tracking

if $N^{(t)}_{\omega} = 0$ **then**
  Call Algorithm 1.
  else
  Compute $EL^{(t)}$ *from* $I^{(t)}$
  for k := 1 to $N^{(t)}_{\omega}$ **do**
    $\forall i\ \Phi_{k,i}$, *compute predicted cluster motion*
    for i := 1 to $N^{(t)}_{\omega,k}$ **do**
      Register curvatures form $\Phi_{k,i}$ *and* ϕ_i *and use KMASK as search window*
      if $\Phi_{k,i}$ *matched with* ϕ_i **then**
        Remove $\Phi_{k,i}$ *from* ω_k & *Add* ϕ_i *to* ω_k
        else
        if $Weight(\Phi_{k,i}) > \tau_{edge}$ **then**
          Reduce Weight($\Phi_{k,i}$)
        else
          Remove $\Phi_{k,i}$
          if $N^{(t)}_{\omega,k} = 0$ **then**
            Delete cluster ω_k
          end if
        end if
      end if
      if $Boundary(\omega_k) \cap Boundary(\omega_{k'}) \neq \varnothing$ **then**
        Merge(ω_k , $\omega_{k'}$)
      end if
      Upate C_k
    end for
  end for
end if

V. CONCLUSION

The strength of our approach lies in the ability to track edge segments in successive frames. As we know, the shape and size of a edge segment changes from frame to frame. Our system successfully handles edge instability problem by using weighted edge segments. Once, edge segment is not shown, we keep the parent edge segment reducing it's weight. Thus we keep edge history which can solve the problem of edge instability or occlusion. Curvature point correspondence is another challenging issue since same curvature values might be found in several places within the search window. We take all available point correspondence pair. Here if we have at least 50 percent correct point correspondence our Kalman tracker will give us optimum transformation parameters after some initial frames. For clustering, our method uses K-means clustering where we can add new clusters based on edge location, again clusters close to each other can be merged together to form a new one. One limitation in out tracking algorithm is that we have incorporated locational information and edge continuity only for clustering. So, if two different object of different speed or motion direction intersect each other,

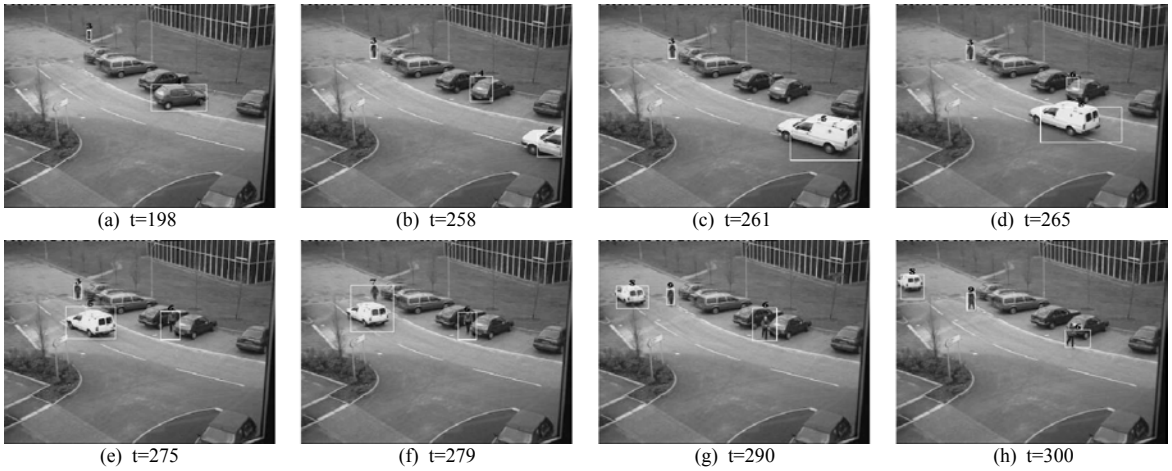

(a) t=198 (b) t=258 (c) t=261 (d) t=265

(e) t=275 (f) t=279 (g) t=290 (h) t=300

Fig. 2. (a)-(h) Output of the proposed edge segment based tracker . (a) Frame no. 198, where two moving objects are labeled as 3(Man) and 4(Car) (b) Frame no. 258, Moving object 4(car) becoming background object as it's edges are non moving from this point onwards. (c) Frame no. 261, Moving object 4(Car) disappears completely. (d) Frame no. 265, discovery of a new moving object 6(Man). (e) Three moving objects 3(Man), 5(Minibus) and 6(Man) tracking. (f) Two clusters 3 and 5 are merged together to form a new cluster 7. (g) and (h) Tracking of the three moving objects 6(Man), 8(Minibus), and 9(Man).

our algorithm will merge the two clusters and start tracking as a single cluster. In our future work, we will use model to refine these clusters and extract important movements from the scene. We will incorporate movement information into the cluster along with object's color or texture, this will help tracking different overlapping clusters more robustly and efficiently.

REFERENCES

[1] A. Yilmaz, O. Javed, and M. Shah, "Object tracking: A survey," ACM Comput. Surv., vol. 38, no. 4, p. 13, 2006.

[2] M. J. Hossain, M. A. A. Dewan, and O. Chae, "Moving Object Detection for Real Time Video Surveillance: An Edge Based Approach," IEICE Trans Commun, vol. E90-B, no. 12, pp. 3654–3664, 2007.

[3] M. Yokoyama and T. Poggio, "A contour-based moving object detection and tracking," in Visual Surveillance and Performance Evaluation of Tracking and Surveillance, 2005. 2nd Joint IEEE International Work-shop on, Oct. 2005, pp. 271–276.

[4] P. L. Rosin, "Edges: Saliency measures and automatic thresholding," in Machine Vision and Application, 1995, pp. 139–159.

[5] C. Kim and J.-N. Hwang, "Fast and automatic video object segmentation and tracking for content-based applications," IEEE Trans. Circuits Syst. Video Techn., vol. 12, no. 2, pp. 122–129, 2002.

[6] A. D. Sappa and F. Dornaika, "An edge-based approach to motion detection," in International Conference on Computational Science, 2006, pp. 563–570.

[7] D. Serby, E. Koller-Meier, and L. V. Gool, "Probabilistic object tracking using multiple features," Pattern Recognition, International Conference on, vol. 2, pp. 184–187, 2004.

[8] D. Comaniciu, V. Ramesh, P. Meer, S. Member, and S. Member, "Kernel-based object tracking," IEEE Transactions on Pattern Analysis and Machine Intelligence, vol. 25, pp. 564–577, 2003.

[9] G. Welch and G. Bishop, "An introduction to the kalman filter," Chapel Hill, NC, USA, Tech. Rep., 1995.

[10] R. E. Kalman, "A new approach to linear filtering and prediction 7 problems," Transactions of the ASME - Journal of Basic Engineering, no. 82 (Series D), pp. 35–45, 1960.

[11] S. Arulampalam, S. Maskell, N. Gordon, and T. Clapp, "A tutorial on particle filters for on-line non-linear/non-gaussian bayesian tracking," IEEE Transactions on Signal Processing, vol. 50, pp. 174–188, 2001.

[12] U. Orguner and F. Gustafsson, "Risk-sensitive particle filters for mitigat-ing sample impoverishment," IEEE Transactions on Signal Processing, vol. 56, no. 10, Oct. 2008.

[13] P. Fieguth and D. Terzopoulos, "Color-based tracking of heads and other mobile objects at video frame rates," in in Proc. IEEE Conf. on Computer Vision and Pattern Recognition, 1997, pp. 21–27.

[14] A. Baumberg and D. Hogg, "An efficient method for contour tracking using active shape models," in In Proceeding of the Workshop on Motion of Nonrigid and Articulated Objects. IEEE Computer Society, 1994, pp. 194–199.

[15] A. W. Fitzgibbon, "Robust registration of 2d and 3d point sets," Image and Vision Computing, vol. 21, no. 13-14, pp. 1145 – 1153, 2003, british Machine Vision Computing 2001.

[16] F. Quek, R. Jain, and T. E. Weymouth, "An abstraction-based approach to 3-d pose determination from range images," IEEE Trans. Pattern Anal. Mach. Intell., vol. 15, no. 7, pp. 722–736, 1993.

[17] D. J. Williams and M. Shah, "A fast algorithm for active contours and curvature estimation," CVGIP: Image Understanding, vol. 55, no. 1, pp. 14–26, January 1992.

[18] G. Bebis, M. Georgiopoulos, N. D. V. Lobo, M. Shah, and D. G. Bebis, "Learning affine transformations," Pattern Recognition, vol. 32, pp. 1783–1799, 1999.

[19] T. Poggio and S. Edelman, "A network that learns to recognize three-dimensional objects," Nature, vol. 343, pp. 263–266, 1990.

[20] S. S. Khan and A. Ahmad, "Cluster center initialization algorithm for k-means clustering," Pattern Recogn. Lett., vol. 25, no. 11, pp. 1293–1302, 2004.

Proceedings of 2009 12th International Conference on Computer and Information Technology (ICCIT 2009)
21-23 December, 2009, Dhaka, Bangladesh

Diphone Preparation for Bangla Text to Speech Synthesis

Muhammad Masud Rashid, Md. Akter Hussain, M. Shahidur Rahman
Shahjalal University of Science and Technology, Sylhet
masudcoder@yahoo.com, akter.1985@yahoo.com, rahmanms@sust.edu

Abstract

This paper presents methodologies involved in diphone preparation for Bangla text to speech synthesis. A concatenation based synthesis system comprises basically two modules- one is natural language processing and other is digital signal processing (DSP). Natural language processing implies converting text to its pronounceable text, called text normalization and the diphone selection method based on the normalized text is called Grapheme to Phoneme (G2P) conversion. We developed a speech synthesizer for Bangla using diphone based concatenative approach. Diphone preparation, labeling and selection techniques are described in this paper.

Keywords: diphone, grapheme-to-phoneme, speech synthesis, text normalization.

I. INTRODUCTION

Creation of synthetic voice from text is usually referred with the general term text-to-speech (TTS), though it requires a wide range and variety of procedures. Voice technology applications have created a growing demand for multi-lingual, multi-voice, multi-style speech synthesis system. There are many techniques available for speech synthesis like formant synthesis, concatenative synthesis, articulacy synthesis etc [1, 2]. The formant synthesis uses fundamental frequency, voicing, noise levels instead of human speech samples to create a synthetic waveform of speech and the concatenative synthesis uses segments of recorded human speech. Concatenative synthesis has subtypes like unit selection and diphone synthesis where both have advantages and weaknesses. Unit selection stores speech unit like phone, half-phone, diphone, word etc and index them. At runtime best chain of units are determined by the selection algorithm. It requires large size database to store units and as the optimal search and/or selection algorithms used are not 100% reliable, both high and low quality synthesis is produced. Diphone synthesis uses a minimal speech storage that contains all diphones (two adjacent half-phones, cut in the middle, joined into one unit) of a language, applies little DSP and uses an easy to implement selection algorithm. Huge works have already been done on TTS systems for many European languages [1, 2, 3]. However, for Bangla languages, speech synthesis is yet to attain the level for direct large-scale applications. As per our knowledge, two complete systems have been reported. C-DAC, Kolkata has developed a Bangla TTS system named Bangla Vaani [4]. Very recently, CRBLP of BRAC University has released another Bangla TTS, Katha, [5] which is built under the Festival framework [6, 7] using unit selection. Recently, we have developed a TTS in Bangla based on diphone concatenation. With diphone concatenation, less memory is needed, but the sample collecting and labeling procedures are more difficult. In this paper, we have described the procedures of diphone preparation and diphone labeling. As seen in the simplified block diagram of a TTS system in Fig. 1, the contribution of this paper is involved with the second stage- Grapheme to Phoneme/Diphone selection. Diphone prepared in the proposed way have been demonstrated to produce intelligible and much natural sounding speech.

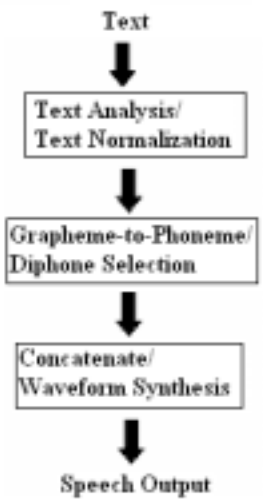

Fig.1: Block diagram of a diphone based TTS system.

II. DIPHONE IN BANGLA AND ITS CLASSIFICATION

Diphone is usually used to refer sound transition from middle of one phone/ letter to middle of another phone/letter. For example, diphones of a Bangla word 'অনুভূতি' (Onuvuti) are shown in Fig. 2.

```
   o   n   u   v   u   t   i    ----- letters
|-----|-----|-----|-----|-----|-----|-----|-----|
  o  on  nu  uv  vu  ut  ti   i  ----- diphones
```

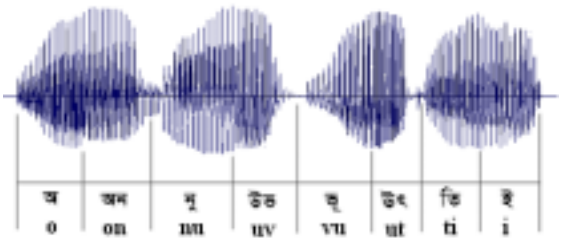

Fig. 2: Diphones in the waveform of word 'অনুভূতি' (Onuvuti)

Diphones can be categorized as:

- vowel-consonant (vc): ইক (ik), উজ (uj) etc
- consonant-vowel (cv): জা (ja), ক (ko) etc
- vowel-vowel (vv): আই (ai), ইউ (iu) etc
- vowel-'য় (vy): অয় (oy), আয় (ay) etc
- vowel-'য়-vowel (vyv): ইয়া (iya), উয়অ (uyo) etc
- consonant-consonant (cc): ন্দ (nd), স্ক (sk) etc
- fade-in vowel/consonant ({v,{c): {অ({o), {ভ({v) etc
- fade-out vowel/consonant (v},c}): অ}(o}), ভ}(v}) etc.

Here, fade-in (silence-to-phone) / fade-out (phone-to-silence) represents terminal letter. In the word আশা, for example,

আশা = '{আ' (fade-in 'আ') + 'আশ' + 'শা' + 'আ}' (fade-out 'আ'),

Starting 'আ' denoted with '{' and the ending 'আ' denoted with '}' implies fade-in and fade-out respectively.

III. CONSONANT-CONSONANT (CC) TYPE DIPHONES

Some 'cc' type diphones are simply silence. If the first consonant is nasal (ন, ণ, ম, ঙ, ং), lateral (ল), trill (র), flapped (ড়, ঢ়), fricative (শ, ষ, স) or affricate then diphone is meaningful. Otherwise if the first consonant is plosive (ক, চ, ট, ত, প, খ, ছ, ঠ, থ, ফ, গ, জ, ড, দ, ব, ঘ, ঝ, ঢ, ধ, ভ) then it can be treated as silence. Here are some examples: ক্ত (kt), দ্ন (dn), প্ন (pn), ত্ন (tn), জ্গ (jg), প্স (ps) etc. Silence length is approximately 100-200 milliseconds.

If the silence is shorter (less then 100 millisecond), 'VCCV' type sound is pronounced as 'VCV'. For example, the word টাক্কা (takka) will be pronounced as টাকা (taka). This is illustrated in Fig. 3 with the aid of signal waveform.

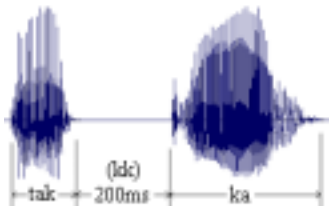

Fig. 3(a): Word টাক্কা (takka) (200 ms silence)

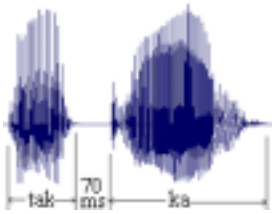

Fig. 3(b): Word টাকা (taka) (70 ms silence)

IV. DIPHONE PREPARATION

A. Basic Issues

In diphone preparation, there are some issues that should be addressed for naturalness of the synthesized speech. These are amplitude mismatch, phase mismatch, pitch mismatch, and duration of diphone. The process of corpus recording can play signification role in addressing those issues. We maintained the following conditions during corpus recording.

- Constant speed of utterance
- Utterance at constant pitch
- Similar duration of the vowel sound
- Utterance at uniform amplitude and not to give unnecessary stress to any portion of the utterance

A professional speaker is thus important for corpus recording. In our case, we trained a speaker with knowledge of phonology [8] skilled in accurate pronunciation. Speech corpus is recorded in an apparently noiseless environment. Speech signal is sampled at 44100 Hz as mono sound. After the recording process is complete, diphone is prepared using a powerful signal processing application capable of noise reduction, amplitude and pitch modifications. The epoch synchronous technique [9] is used to overcome phase mismatch.

B. Quick Corpus

A Quick Corpus shown in Table 1 has been used to prepare the diphones required for a typical speech synthesizer containing 'cv', 'vc', 'vv', 'vy', 'vyv', '{p', 'p}' type diphones.

Table 1: Quick Corpus

‘vc’ and ‘cv’ type diphone:	ধধ ধাধ ধিধ ধুধ ধেধ ধোধ ধ্যাধ	স্ক স্খ স্ট স্ত স্থ স্ন স্প স্ফ স্ম
কক কাক কিক কুক কেক কোক ক্যাক	নন নান নিন নুন নেন নোন ন্যান	ক্র খ্র গ্র ঘ্র চ্র ছ্র জ্র ঝ্র ট্র ঠ্র ড্র ঢ্র প্র ত্র থ্র দ্র ধ্র ন্র প্র ফ্র ব্র ভ্র ম্র য্র ল্র শ্র/ষ্র/স্র হ্র
খখ খাখ খিখ খুখ খেখ খোখ খ্যাখ	পপ পাপ পিপ পুপ পেপ পোপ প্যাপ	ক্ল গ্ল ঙ্ক্ল জ্ঞ ত্ত্ব ত্ম ত্ল দ্দ্ব দ্ম দ্ল হ্ণ ক্ষ স্ক্র স্খ্র স্ট্র স্ত্র স্থ্র স্প্র স্ফ্র স্ক্র স্ম্র
গগ গাগ গিগ গুগ গেগ গোগ গ্যাগ	ফফ ফাফ ফিফ ফুফ ফেফ ফোফ ফ্যাফ	
ঘঘ ঘাঘ ঘিঘ ঘুঘ ঘেঘ ঘোঘ ঘ্যাঘ	বব বাব বিব বুব বেব বোব ব্যাব	
চচ চাচ চিচ চুচ চেচ চোচ চ্যাচ	ভভ ভাভ ভিভ ভুভ ভেভ ভোভ ভ্যাভ	
ছছ ছাছ ছিছ ছুছ ছেছ ছোছ ছ্যাছ	মম মাম মিম মুম মেম মোম ম্যাম	
জজ জাজ জিজ জুজ জেজ জোজ জ্যাজ	যয যায যিয যুয যেয যোয য্যায	
ঝঝ ঝাঝ ঝিঝ ঝুঝ ঝেঝ ঝোঝ ঝ্যাঝ	রর রার রির রুর রের রোর র‍্যার	
টট টাট টিট টুট টেট টোট ট্যাট	লল লাল লিল লুল লেল লোল ল্যাল	
ঠঠ ঠাঠ ঠিঠ ঠুঠ ঠেঠ ঠোঠ ঠ্যাঠ	শশ শাশ শিশ শুশ শেশ শোশ শ্যাশ	
ডড ডাড ডিড ডুড ড ডেড ডোড ড্যাড	সস সাস সিস সুস সেস সোস স্যাস	
ঢঢ ঢাঢ ঢিঢ ঢুঢ ঢেঢ ঢোঢ ঢ্যাঢ	হহ হাহ হিহ হুহ হেহ হোহ হ্যাহ	
ততত তাত তিত তুত তেত তোত ত্যাত	ড়ড় ড়াড় ড়িড় ড়ুড় ড়েড় ড়োড় ড়্যাড়	
থখ থাখ থিখ থুখ থেখ থোখ থ্যাখ	কং কাং কিং কুং কেং কোং	
দদ দাদ দিদ দুদ দেদ দোদ দ্যাদ		

Dipthongs:	এ্যাই - ক্যাই	আয়অ - কায়ন	উয়ে - কুয়েন	**Consonant**:
অই - কই	এ্যাউ - ক্যাউ	আয়া - কায়াল	উয়ো - কুয়োন	ক খ গ ঘ ঙ
অউ - কউ	এ্যাও - দ্যাও	আয়ি - কায়িফ	এয়অ - কেয়ন	চ ছ জ ঝ ঞ
অও - কও	অয় - কয়	আয়ু - কায়ুন	এয়া - কেয়াল	ট ঠ ড ঢ ণ
আই - যাই	আয় - যায়	আয়ে - কায়েন	এয়ি - কেয়িফ	ত থ দ ধ ন
আউ - দাউ	ইয় - মিয়	আয়ো - কায়োন	এয়ু - কেয়ুন	প ফ ব ভ ম
আও - খাও	উয় - কুয়	ইয়অ - কিয়ন	এয়ে - কেয়েন	য র ল শ ষ স হ ড় ঢ় য়
ইই - দিই	এয় - দেয়	ইয়া - কিয়াল	এয়ো - কেয়োন	
ইউ - মিউ	ওয় - শোয়	ইয়ি - কিয়িফ	ওয়অ - কোয়ন	**Vowels** - অ আ ই উ এ ও ঔ এ্যা
ইও - নিও	এ্যায় - ন্যায়, ব্যয়	ইয়ু - কিয়ুন	ওয়া - কোয়াল	
উই - মুই	অয়অ - কয়ন	ইয়ে - কিয়েন	ওয়ি - কোয়িফ	
উও - কুও	অয়া - কয়াল	ইয়ো - কিয়োন	ওয়ু - কোয়ুন	
এই - যেই	অয়ি - কয়িফ	উয়অ - কুয়ন	ওয়ে - কোয়েন	
এউ - কেউ	অয়ু - কয়ুন	উয়া - কুয়াল	ওয়ো - কোয়োন	
এও - নেও	অয়ে - কয়েন	উয়ি - কুয়িফ		
ওই - বোই	অয়ো - কয়োন	উয়ু - কুয়ুন		
ওউ - বোউ				
ওও - শোও				

C. Diphone Labeling System

Efficient access of the diphone-files are important for a speech synthesizer to be useful in real-time. We use Unicode (Hexadecimal) value [10] of a letter to label diphones. Before labeling, short forms of vowels are converted to corresponding long forms (e.g. ‘া’ is converted to ‘আ’).

For example, the diphone ‘কা’ is converted to ‘কআ’.

The Unicode value of ‘ক’ and ‘আ’ are 0x995 and 0x986, respectively. Thus, we label the diphone file as **995986.wav**.

Some other labeling examples are given below.

vowel-consonant (vc):

ইক = 987995 (ই = 987, ক = 995)

consonant-vowel (cv):

জা(জআ) = 99c986 (জ = 99c, আ = 986)

vowel - vowel (vv):

ইউ = 987989 (ই = 987, উ = 989)

vowel - 'য়' (vy):

অয় = 9939df (অ = 993, য় = 9df)

vowel - 'য়' - vowel (vyv):

ইয়া = 9879df 986 (ই=987, য়=9df, আ=986)

consonant - consonant (cc):

ন্দ = 9a89a6 (ন = 9a8, দ = 9a6)

fade-in vowel/consonant ({v, {c):

{অ = 7b985 ({ = 7b, অ = 985)

fade-out vowel/consonant (v}, c}):

ভ} = 9ad7d (ভ = 9ad, } = 7d)

Special symbols:

Comma (,) = 0x2c and Dari (।) = 0x964.

V. DIPHONE SELECTION (GRAPHEME-TO-PHONEME CONVERSION) ALGORITHM

The algorithm of the diphone selection can be described as follows:

Repeat until the end of a Word

1. If it is the beginning of a word select diphone named "{+current letter".
2. If it is the end of a word select diphone named "previous letter +}".
3. If the current letter is য-ফলা then select diphone named "previous letter + য-ফলা".
4. If the previous letter is য-ফলা and it is not the last letter of a word then select diphone named "য-ফলা+current letter".
5. If the previous letter is য-ফলা and it is the last letter of a word then select diphone named "য-ফলা+}".
6. If it is a conjunct with র-ফলা or ল-ফলা then select diphone named "{+first of joint letter" and "র/ল+dependent vowel".
7. If it is 'য়' and is preceded by a consonant then select diphone named "previous letter+a" and "a + য় + next dependent vowel". If the preceding letter is not a consonant then select only "previous dependent letter + য় + next dependent vowel".
8. If it is a dependent vowel then select diphone named "previous letter + dependent vowel".
9. If it is not a dependent vowel and the previous letter is a consonant then select diphone named "previous letter+a" and "a+current letter".
10. Otherwise, select diphone named "previous letter + current letter"

Previous or current letter mentioned above can be a dependent vowel. Dependent vowels are actually short forms of the vowels like া, ি, ে etc. as mentioned earlier in Sec. 5, in diphone selection, dependent vowels are converted to actual vowels.

It should be mentioned that the word we used for grapheme-to-phoneme conversion is a result of Text-normalization process [11, 12, and 13] which gives the actual pronounceable format of a raw word.

Examples on diphone-selection for several words are presented below.

V: ও = '{ও' + 'ও}' (o o)

C: ক = '{ক' + 'কঅ' + 'অ}' (k ko o)

CV: মা = {ম্ + মা + আ} (m ma a)

VC: আট = {আ + আট + ট} (a + at + t)

VCV: আটা = {আ + আট + টা + আ} (a + at + ta + a)

CVC: ভুত = {ভ + ভউ + উত + ত} (v + vu + ut + t)

CCV: স্কা = {স + কা + আ} (s + ka + a)

VCC: আস্ত = {আ+আস+সত+তো+ও} (a+as+st+to+o)

VCCV:আস্থা = {আ+আস+সথ+থা+আ}(a +as+sth+tha+a)

CCCV: স্ত্রি = {স + {ত + র্‌ি + ই} (s + t + ri + i)

VCCC: অন্ত্র=অ + অন + ত} + রঅ + অ} (o+on+t+ro+o)

Examples on diphone-selection for sentence case are shown below.

'তা কী হয়' = {ত + তা + আক + কি + ইহ্ + হঅ + অয়

Actually, we do not stop when we speak. This is why every word-sound is mixed with that of the neighbor words. 'য়' is handled specially. Examples:

হয় = {হ + হঅ + অয়, মিয়া = {ম + মি + ইয়া + আ}

The effects of the symbols Comma (,) and Dari (।) are simulated by inserting 200 ms and 400 ms silence, respectively.

The whole process of diphone selection and labeling is depicted below in Fig. 4 for the word সৌভাগ্য.

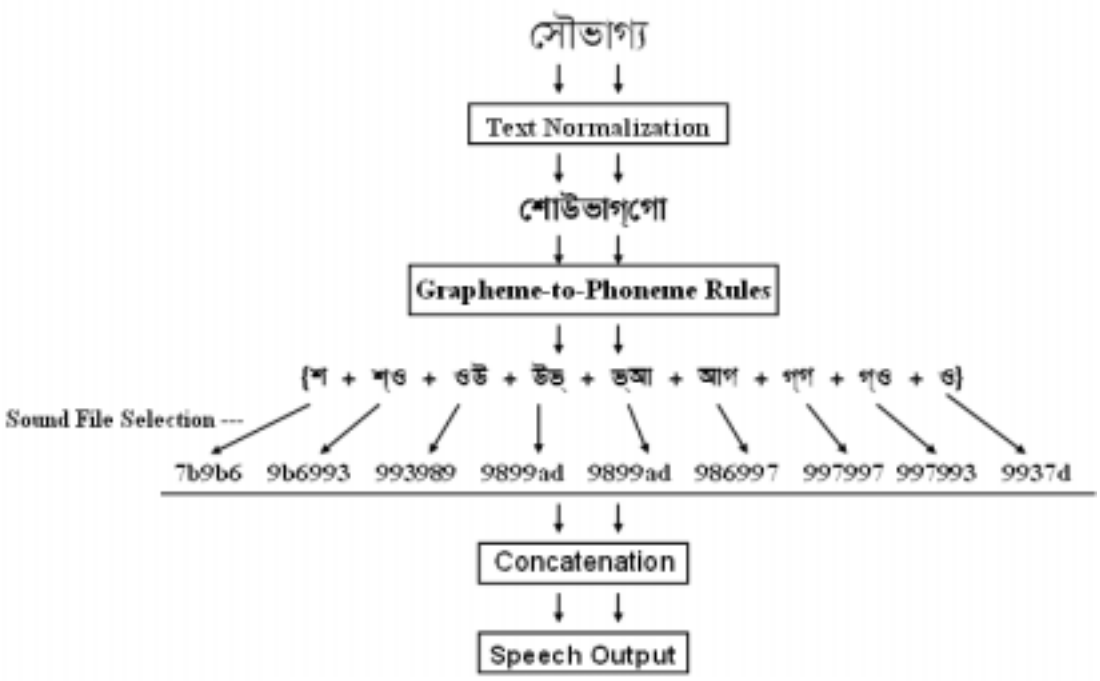

Fig. 4: Diphone selection and labeling process in TTS system

VI. CONCLUSION

Techniques for diphone preparation, labeling and selection have been described in this paper. The rules and algorithms proposed here are actually applicable on normalized text. The proposed methods have been applied to develop a typical speech synthesizer. The speech synthesizer has been demonstrated (before a big number of university students and teachers) to produce intelligible and much natural sounding speech. Research is going on to add more fine-tunings to further improve the synthesizer quality.

REFERENCES

[1] Thierry Dutoit, "An Introduction to Text-To-Speech Synthesis," Kluwer Academic Publishers, 1997.

[2] Speech Synthesis, http://en.wikipedia.org/wiki/Speech_synthesis

[3] M. Beutnagel, A. Conkie, J. Schroeter, Y. Stylianou, and A. Syrdal, "The AT&T next-gen TTS System," HTTP WWW Research AT&T Labs – Research, Available in: http://www.research.att.com/projects/tts

[4] C-DAC: Research & Development - Speech Research: www.kolkatacdac.in/html/texttospeech.htm

[5] Firoj Alam, Promila Kanti Nath and Mumit Khan, "Text To Speech for Bangla Language using Festival," Proc. of 1st International Conference on Digital Communications and Computer Applications (DCCA2007), Irbid, Jordan, 2007.

[6] Tanuja Sarkar, Venkatesh Keri, Santhosh Yuvaraj, Kishore Prahalad, "Building Bengali Voice Using Festival," Proc. of ICLSI 2005, Hyderabad, India, 2005.

[7] Building Synthetic Voices - http://www.festvox.org/bsv/

[8] Muhammad Abdul Hai, "Dhvani Vijnan O Bangla Dhvani-Tattwa," Mullick Brothers Publishers, 2000

[9] Mandal, Shyamal Kumar Das and Datta, Asoke Kumar, "Epoch synchronous non-overlap-add (ESNOLA) method-based concatenative speech synthesis system for Bangla," 6th ISCA Workshop on Speech Synthesis (SSW6), Bonn, August 22 − 24, 2007

[10] Unicode chart - http://unicode.org/charts/

[11] Noren Biswash, "Bangla Academy Bangla Uccharan Ovidan," Bangla Academy, January 2003

[12] Md. Hanif Seddiqui, Muhammad Anwarul Azim, Md. Shahidur Rahman, and M. Zafar Iqbal, "Algorithmic Approach to Synthesize Voice from Bengali Text," Proc. of ICCIT, Vol. 5, pp. 233-236, December, 2002.

[13] Firoj Alam, S.M. Murtoza Habib, Mumit Khan, "Text Normalization System for Bangla," Proc. of Conf. on Language and Technology, Lahore, 22-24 January, 2009

Proceedings of 2009 12th International Conference on Computer and Information Technology (ICCIT 2009)
21-23 December, 2009, Dhaka, Bangladesh

Textual Labeling of Segmented Structures in 2D CT Slice Views *(Not Presented)*

Muhammad Masud Tarek
Dept. of Computer Science and Engineering, Shah Jalal University of Science and Technology, Sylhet, Bangladesh
masudtarek@gmail.com

Abstract

The parallel processing of verbal elements like textual labels, annotations etc. with non-verbal i.e. visual elements, provides maximum integration of human mind. But it is a very challenging task to generate hand-made like illustration labels in automated system. The paper represents a noble approach for dynamic external labeling of segmented 2D computer tomography (CT) slices. Various efficient algorithms are approached to solve labeling problems in modular form. The system emphasizes on the readability and clarity of labels while generating dynamic group labels in real time for 2D slices using external labeling layout.

Keywords: External labels, medical data visualization.

I. INTRODUCTION

Images are considered as very powerful medium for communicating ideas. However to make an image more meaningful and informative, textual descriptions like labels, legends, captions etc. have become essential parts of images especially in educational and scientific documents. Labels are largely classified as internal and external labels. Internal labels are placed within the objects of a picture. On the other hand, external labels are placed into the empty spaces, outside of the objects. Both internal and external labels are used to describe or distinguish different graphical elements. In case of external labels, lines are drawn between labels and their corresponding referenced objects. As aesthetic is a very important factor, illustrators have to be very careful to maintain the visual balance while labeling a handmade illustration. Automated and interactive labeling systems are still a challenge. Poor placement of labels may have negative impact on understanding a visual system. Whether it is interactive or automated system, the main goal of labeling an illustration is to employ any of the layout conventions that are used by human illustrators, so that labels can be read comfortably and visual balance of the image is preserved.

For quantitative measurement, segmentation of computer tomography (CT) is needed by many image analysis procedures. A number of researches are going on to produce CT segmented images [12], [13]. Different segmentation masks are used to distinguish background and different structures. In real life application, doctors sometimes need verbal description of the segmented structures. Also medical students need textual contents along with the CT images for better understanding. Manual labeling would be a naïve way for this type of application as hundreds of labels might needed to be generated on the fly during analyzing CT images slice by slice. So here, a dynamic label placement system is developed which can generate external textual labels for segmented CT images. The system finds good placements of labels while viewing 2D slices with the consideration of different labeling aspects.

In section II, some related works are reviewed. Section III states the system architecture while section IV describes the developed dynamic labeling system. Section V provides some results with discussion. Finally, the paper concludes with some hints of future extension.

II. RELATED WORKS

Dynamic textual labeling for CT images is still largely unexplored. However, there are some interactive systems for 3D models that address some of the labeling problems. For example, *Zoom Illustrator* [15] uses dedicated part on the screen for text so that they do not overlap any image object. Also *Fish View Technique* [8] is used to show more textual information without overlapping other labels. *Talking Shadows* [4] and *Illustrative Shadows* [16] use object shadows for placing text information of the associated objects. But they hardly address any labeling layout problem.

A Virtual Reality application, *View Management* [3] dynamically places labels for objects. It considers most of the labeling problems such as internal or external labeling layout, empty space management, minimization of label overlapping etc. However, as it uses bounding box technique to determine the area of an object, thin long diagonal objects may wrongly occlude other small objects. Map labeling is a well studied field and many works are done for dynamic internal map labeling layout. However, it is found that global optimization (i.e. no overlapping of labels) is computationally N-P hard [6]. So, change of one label position effects the entire map labeling layout.

Few good algorithms are developed for 3D dynamic labeling. They consider major labeling layout problems such as label layouts (flash or radial, internal or external), placement of external labels in to empty space, minimization of line crossings, elimination of label overlapping etc. *Floating Labels* [10] uses some potential force fields to eliminate overlapping of labels. It also addresses frame coherency to minimize visual discontinuity. In [9], calmer parts of the animated 3D objects are determined where anchor points or internal labels can be put to achieve lesser flickers among frames. Ali et al. [1] employed different layout methods for external labeling of 3D illustrations. The system is greatly suitable for compact and convex 3D models with

978-1-4244-6283-4/09/$26.00 ©2009 IEEE

having enough empty spaces surrounding the object. These techniques can be adopted for 2D layered CT images with considerations. However, achieving all the aesthetic criteria of a labeling layout at a same time is very difficult as some criteria may conflict each other. Also most approaches trade-off between labeling quality and computational costs.

III. SYSTEM ARCHITECTURE

After reviewing related works and analyzing medical illustrations [17], [19] it is found that a good labeling system should consider the following aspects:

Readability: Labels and lines should have good background contrast. Font size, text shadow, background and foreground color can be adjusted by the users as needed.

Aestheticism: Placement of the labels should be such that there should not be any overlapped label. Also line crossings should be eliminated or reduced. Anchor points should be at salient positions of the structures.

Efficiency: Good, efficient algorithm should be used so that the system can be implemented for real time application.

Grouping: Same structure may be seen in different places. Some criteria should be utilized to group them together and thus minimizes number of labels.

Slice Coherency*:* Sizes, locations of structures may vary within different slices. So it is likely to vary the position of labels also, which may generate blinking effect. So measures should be taken to minimize this blinking effect.

The system architecture (Fig. 1) is designed to achieve the above mentioned global requirements. The input segmented image itself contains the identification text (labels) and other color-coded information for each object, while users can define various label properties such as text size, color, text-background color and transparency etc. in the *User Interface (UI)* module. In the *Image Processing* modules, available empty spaces (i.e. background) are calculated where labels can be put. Acceptable anchor points for each object are also calculated here. A textual label is connected to an anchor point by a line to indicate the corresponding object. In the label layout modules, initial placement of each label is determined. Here, there are several other modules for eliminating label overlapping, grouping and eliminating intersection of connected line segments and thus final placements of all the labels of a slice are determined. The last module stabilizes anchor points to reduce visual discontinuity between two adjacent slices.

IV. THE DYNAMIC LABELING SYSTEM

Modular approach is used to implement the dynamic labeling system. For better contrast between image and textual labels, each label is enclosed within a rectangular box. The size of the box depends on the text length and font size of the label. Users are able to change rectangle background color on the fly (Fig. 2). For aesthetic reason, these rectangle boxes are transparent, so that some parts of the graphical structures are visualized and thus minimizing visual clutter. *Alpha Blending* [14] is used for the transparency effect using the formula:

$$New\_Pixel\_Value = BG * (1- \alpha) + FG * (\alpha)$$

Where, BG=background, FG=foreground and $\alpha = 0$ to 1

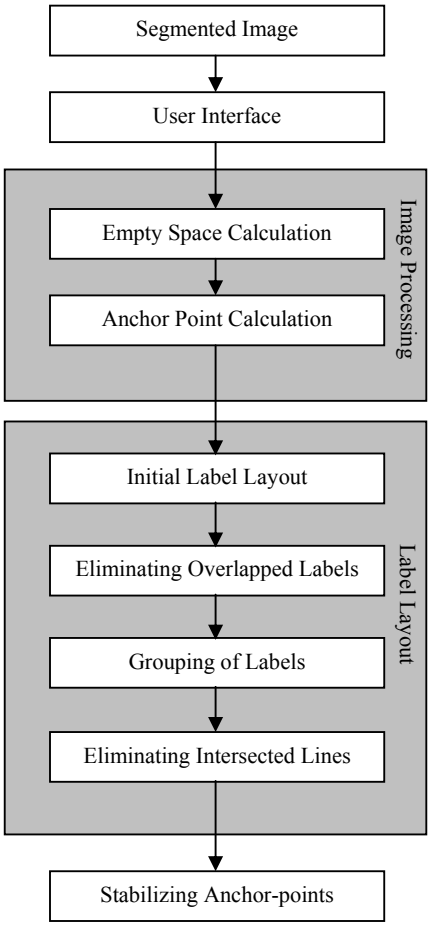

Fig. 1: System Architecture

For each slice, the generalized algorithm is:

1. Calculate background spaces which are available for putting labels
2. Identify each object uniquely
3. Calculate anchor point for each object
4. Determine initial label placement
5. Eliminate label overlapping by either
   a. moving overlapped labels up or down repetitively to a minimum distance, or
   b. using potential repulsive forces among labels and attractive forces between an anchor point and corresponding textual label of an object
6. Group same objects under a single textual label if those objects are within a threshold distance
7. Draw connection line from anchor points to their associated label

8. Eliminate connected line intersections
9. Stabilize anchor points of next slice if they are within a threshold value of current slice.

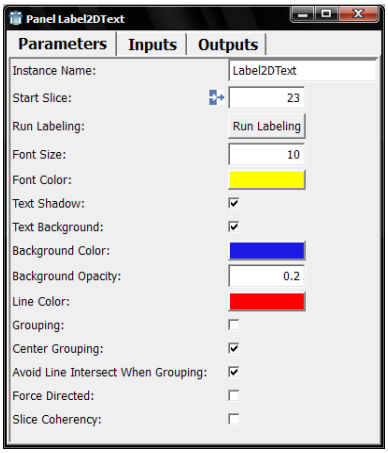

Fig. 2: User Interface

A. Uniquely Identifying an Object

In a segmented CT slice, objects are color-coded uniquely but same object (i.e. same color code) may appear in different places within a slice. For a successful labeling, each part has to be uniquely identified. Connected component labeling algorithm [5] may be used for that purpose. But if objects have many edges, a sheer amount of data in the equivalent table have to be managed which is extremely difficult. So here the system scans 8-neighbors of a pixel recursively to determine the area of an object. The algorithm is fast enough for a real time system as a flag variable is used to avoid additional scanning of a pixel.

B. Anchor Point Calculation

The point of the object up to which the line from a textual label is drawn is known as anchor point. As placement of a label depends upon anchor point position, a good calculation is much needed. For a fast output, any point of an object could be used as anchor point. But it would not be an aesthetic choice. In [15], some criteria are discussed that should be taken into account during anchor point computation. For example, the point should be valid i.e. part of the corresponding structure. To avoid overlapping and visual clutter, anchor points should not cluster together and of course, calculations should be fast enough for an interactive system. Most importantly, it should be a salient point, i.e. at the visually most dominant part of the object. Skeletonization [11] is a good approach to find a salient point but computationally very expensive $O(n^2)$. To meet most of the criteria, the system uses the most inner point of an object as the anchor point using distance transform mapping [18] with computational cost $O(n)$. To avoid real number calculation, Euclidean or city-block distance matrices are avoided. Instead, Pseudo-Euclidean method [2] is implemented which uses integer approximation. It would not give actual distance (which is not required for this system) but most inner point of an object can be determined efficiently.

C. Label Placement

For simplicity, the system uses flash left-right labeling layout. So, a label will be placed either left or right side of an object. Initially, after sorting all the anchor points of a slice, the system would try to place labels from top to bottom one by one. If the anchor point is at the left side of the slice, the system would try to find enough empty space at left side of the object for the label. If failed, it would place at the other side. Initially a label is placed at the same y-coordinate of the associated anchor point. If any two labels are overlapped, they would be moved up or down at a minimum distance. The value of the minimum distance can be chosen by user. Other already placed labels would be rechecked repeatedly to ensure no overlapping is happened (Fig. 3a).

The system can also use force directed method for the placement of labels. Fruchterman and Reingold introduced spring-embedding approach for graph drawing which considers two forces [7]. The attractive force attracts the connected vertices each other while the repulsive force causes all other vertices to repel each other. The same approach can be used for the external labels. Here a label is attracted by associated anchor point, whereas, labels have repulsive forces to each other. To avoid collapse of a label to its object, all the pixels of that object except anchor point have repulsive forces on the label. Also labels get repulsion from image boundary walls so that they will always be within the image area.

To employ the graph drawing method, labels are considered as zero length points. The attractive force between an anchor point and associated label can be given by,

$F_a(x) = x^2/k$ where, x is the distance between the anchor point and the label and k is tolerable distance between them. Typically the value of k is 30 to 50. Similarly, repulsion forces among labels can be calculated by,

$F_r(x) = -k^2/x$ where, x is the distance between two labels and k is the ideal distance between them.

All forces are summed up to calculate the displacement for a label (Fig. 3b). However a temperature t is used to control the displacement. At first the temperature is given high (1.0) and a cooling function is used to cool it in each iteration. Typical cooling rate is 0.95 to 0.90. During iteration minimum of temperature and normalized force value is used for a small displacement of the label. Typically, after 20 to 30 iteration a satisfactory label placement can be achieved (Algorithm 1).

D. Grouping

In a CT slice, same object (or structure) may appear more than once. Sometimes it is desirable to group those objects under one label. This would make the output image more readable. However, it may not always produce good result. Many objects under one label may cause visual clutter. So, for grouping of labels we must

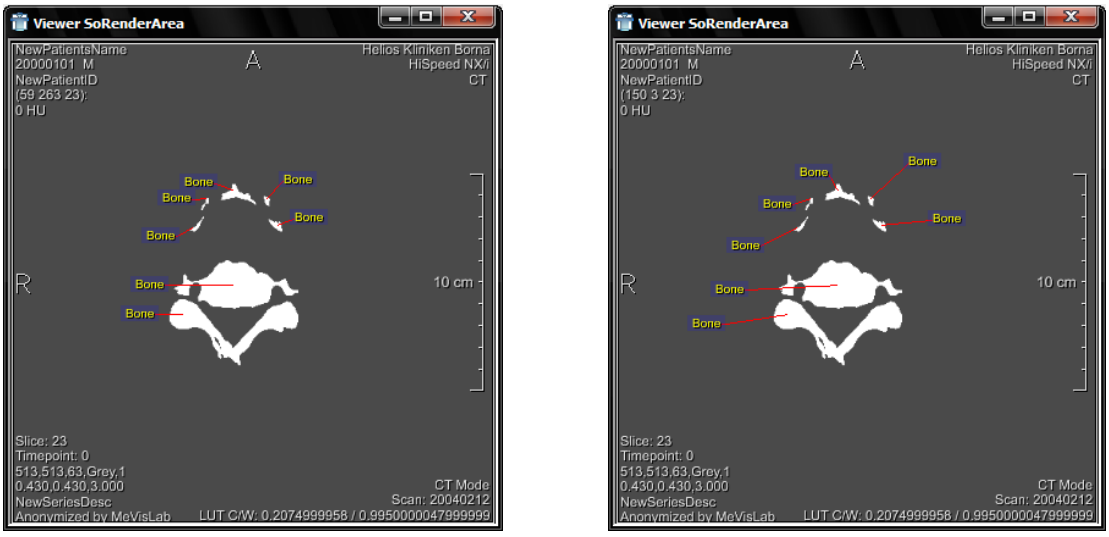

(a) (b)

Fig. 3: (a) Without force directed method labels are put closer, (b) Force directed approach puts labels more uniformly

Algorithm 1: Force directed method

```
L = list of labels
A = anchor points
W = boundary points of the slice
O = list of objects' border points

for iteration:=1 to max_iteration // typically, max_iteration=20 to 30
   for each L[i]
        TDisp[i]:=0
       // a label attracts its referenced anchor point
        Disp:=L[i]-A[i]
        TDisp[i]:= TDisp[i]- sign(Disp)* AForce(abs(Dis))

        for each L[j]
             if (i!=j)
                  // a label repulses other labels
                  Disp:=L[i]-L[j]
                  TDisp[i]:= TDisp[i]+ sign(Disp)* RForce(abs(Disp))
                  // a label repulses non-referenced anchor points
                  Disp:=L[i]-A[j]
                  TDisp[i]:= TDisp[i]+ sign(Disp)* RForce(abs(Disp))
             end if
        end for
        // a label repulses slice-border points
        for each W[j]
             Disp:=L[i]-W[j]
             TDisp[i]:= TDisp[i]+ sign(Disp)* RForce(abs(Disp))
        end for
        // a label repulses its object's border points
        for each O[i]
             Disp:=L[i]-O[i]
             TDisp[i]:= TDisp[i]+ sign(Disp)* RForce(abs(Disp))
        end for
        // calculate new label position with initially, Temperature=1
        EffectiveDisp:= sign(TDisp[i]) * min(norm(TDisp), Temp)
        L[i].pos:=L[i].pos + EffectiveDisp
       Temp=cool(Temp)
   end for
end for

function AForce(x){return  k^2/x;} // k=ideal distance
function RForce(x){return x^2/k;}// k=tolerable distance
function cool(temperature) {return temperature * coolingRate;}
//initially temperature=1.0, typical coolingRate=0.95
```

consider some criteria such as the number of maximal objects that can be grouped together, maximum distances among group objects etc. The real challenge is the good placement of label for a group of objects. One simple approach is to take the initial label position of the most upper object of the group. But it would not give a salient position. So the system uses more complex approach. Here, the centroid of the candidate anchor points is calculated. The initial label of the nearest anchor point of the centroid is served as the label of all group members. All other labels are deleted and connection lines are redrawn from the selected label to anchor points (Fig. 4).

E. Eliminating Line Intersections

Using elementary geometry knowledge, each pair of line segments are checked for any intersections. For non-group labels, if any intersection is found, label positions are swapped, thus eliminating line intersections. After swapping, corresponding segment is again rechecked with other lines. As number of labels within a slice is not much (usually less than 30), so the above mentioned method can be used in real time system without much difficulty. For grouped labels, if any intersection is occurred, it would be more complex to solve. In that case, the object which is responsible for line intersection is left out from the group.

F. Slice Coherency

The system generates labels dynamically according to objects' location, computed anchor points and available empty spaces. When users go through slices interactively, it is more desirable to have minimal change of label locations. Abrupt change of labels may generate flicker and users' attention may be destructed. If users go through slices very quickly, as new anchor points are

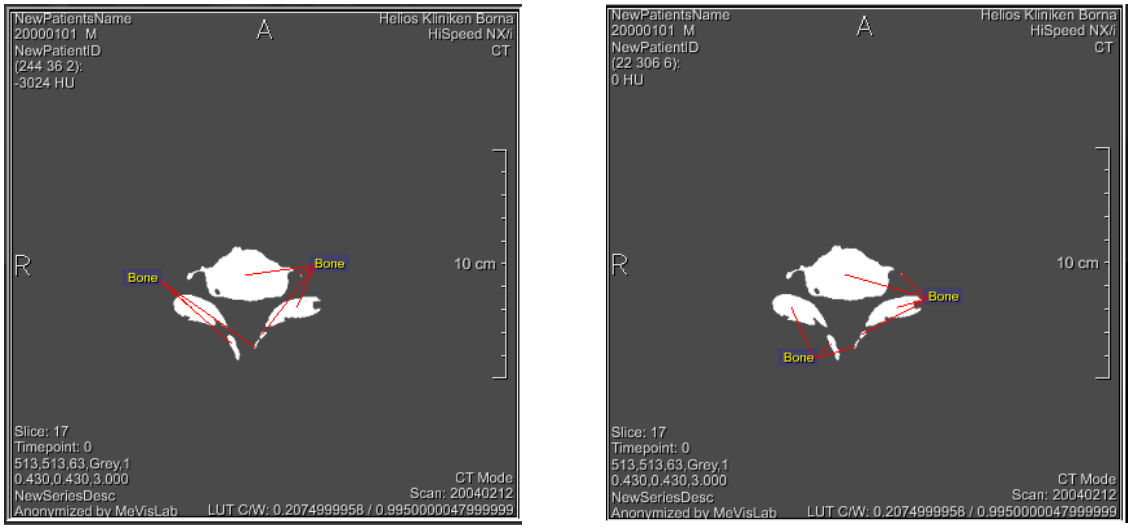

(a) (b)

Fig. 4: Grouping (a) without and (b) with considering the centroid of anchor points.

likely to generate in every slices due to change of object's size and location. As a result, blinking effect may produce. To reduce this effect, anchor points should not be changed as long as possible. However, this may cause non-salient anchor points for objects. The system remembers the anchor points of previous slice. After computing new anchor points for current slice, it compares them with previous positions. If positions are not changes for a certain thresh-hold value, previous positions are used. Label positions are unlikely to change much for unchanged anchor points. As a result, labels do not jump much (Fig. 5).

V. RESULTS AND DISCUSSION

The system is developed using *MeVisLab*, a medical data visualization tool based on *QT* framework and *Open Inventor* toolkits. The primary goal of the system is to generate external labels for CT slices which would help doctors and medical students to recognize different objects within the slices easily. So, for such system, perfect evolution should be empirical, i.e. users' feedback. Unfortunately as the system is still under developing phase, no real world user feedback is available. From the numerical point of view, four segmented CT images were used to generate labels with total 154 slices (Table 1). Among 1074 objects, all were labeled successfully. Because of attractive forces among objects and anchor points, it is seen that labels overlapped with objects (2.14%) are slightly more than while no force directed method is used (1.49%). Though, both figures are very low compare to number of total objects. There is only 0.1% line intersection which is a great result for readability and clarity. As, there are usually less than 30 objects per slice, current standard computers take less than 2 seconds to generate labels for a slice. Even force directed method takes insignificant time. So, system is very suitable for real time application.

VI. FUTURE WORK AND CONCLUSION

Generating textual labels dynamically for CT slices are very helpful for both doctors and medical students. As usual, there are always some scopes for future extensions of the work. The system currently only uses left-right flash layout. It can be extended for other labeling layouts like top-bottom, ring, radial etc. The system uses 2D texts for labeling. Using 3D texts in future more features like text zooming, rotating etc. can be added. Another good extension would be contextual grouping where objects with similar functionalities can be labeled together. Interactivity can be added so that users can choose which functional objects will be labeled.

No. of CT images = 4 Total slices =154 Total objects =1074 Failure to label = 0
With Non-grouping labeling No. of label overlap (no force)=12 No. of line Intersect (no force)=02 No. of label overlap (with force)=16 No. of line Intersect (with force)=03
With grouping labeling No. of line intersect=02 No. of label overlap each other=0 No. of label overlap with objects (no force)=16 (1.49%) No. of label overlap with objects (with force)=23 (2.14%)

Table 1: Summary of experimental results

VII. ACKNOWLEDGEMENT

The author thanks Prof. Bernhard Preim, Faculty of Informatics, OvG University of Magdeburg, Germany for lab facilities and input source images.

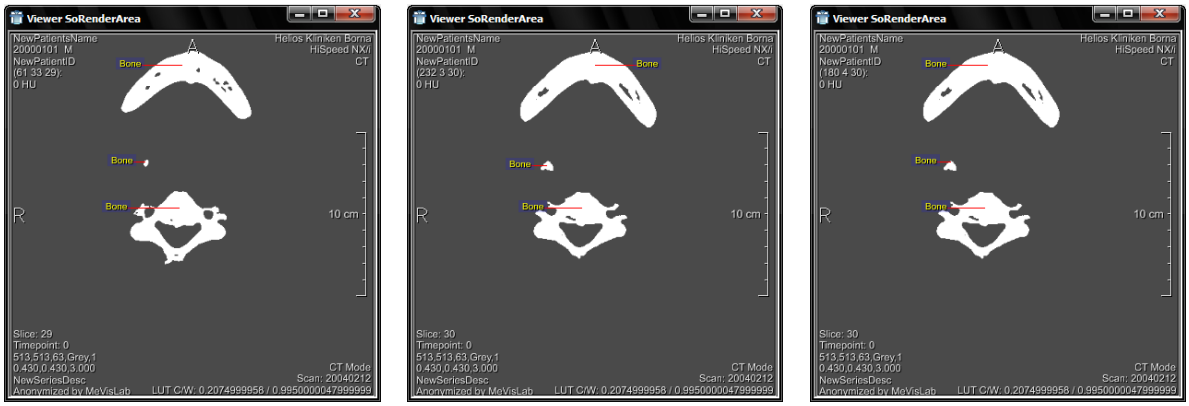

(a) (b) (c)

Fig. 5: With no slice coherency, slice 29 (a) and slice 30 (b) have different label positions, while, with anchor point stabilization approach, slice 29 (a) and slice 30 (c) have almost similar label positions thus minimizes blinking effects.

REFERENCES

[1] K. Ali, K. Hartmann, & T. Strothotte, "Label layout for interactive 3D illustrations" in *Journal of the WSCG*, 13:1–8, 2005.

[2] Carlo Arcelli and Gabriella Sanniti di Baja, "Finding local maxima in a pseudo-euclidean distance transform" in *Computer Vision, Graphics and Image Processing*, 43(3):361–367, 1988.

[3] B. Bell and S. Feiner, "Dynamic space management for user interfaces" in *Proceedings of Symposium on User Interface Software and Technology*, p 238–248, 2000.

[4] W. Chigona, H. Sonnet, F. Ritter, and T. Strothotte, "Shadows with a message" in *Smart Graphics: Third International Symposium on Smart Graphics* 2003, pp. 91–101. Springer Verlag, Berlin, 2003.

[5] M. B. Dillencourt, H. Samet, and M. Tamminen, "A general approach to connected-component labeling for arbitrary image representations" in *J. ACM* 39(2), pp. 253–280, 1992.

[6] M. Formann and F. Wagner. "A packing problem with applications to lettering of maps" in *ACM Symp. on Comp. Geometry*, volume 7, pages 281–288, 1991.

[7] T.M.J. Fruchterman and E.M. Reingold, "Graph drawing by force-directed placement" in *Software-Practice and Experience*, 21(11):1129– 1164, 1991.

[8] Furnas, G.W. "Generalized fisheye views", *Proc. ACM SIGCHI'86 Conference on Human Factors in Computing Systems*, Boston, April, pp. 16-23, 1986

[9] T. Götzelmann, K. Hartmann, and T. Strothotte "Annotation of animated 3D objects" in *Online Proc. 18th Simulation and Visualization Conference*, Magdeburg, Germany, March 2007

[10] K. Hartmann, K. Ali, and T. Strothotte, "Floating Labels: applying dynamic potential fields for label layout" in *Smart Graphics: 4th International Symposium (SG 2004)*, pp. 101–113, 2004.

[11] Ramesh Jain, Rangachar Kasturi, and Brian G. Schunck in *Machine Vision*, McGraw-Hill, Inc., 1995.

[12] S. Loncaric and D. Kovacevic, "A method for segmentation of CT head images" in *Proceedings of the 9th International Conference on Image Analysis and Processing*, pp.388-395, Fl., Italy, 1997

[13] Z. Majcenic and S. Loncaric "CT image labeling using simulated annealing algorithm" in *Proceedings of the IX European Signal Processing Conference*, Vol. 4, pp. 2513-2516, Island of Rhodos, Greece, 1998.

[14] Thomas Porter and Tom Duff, "Compositing digital images" in *Computer Graphics*, 18(3), July 1984, 253-259

[15] B. Preim, A. Raab, and Thomas Strothotte, "Coherent zooming of illustrations with 3D-graphics and text" in *Proceedings of Graphics Interface*, pages 105–113, 1997.

[16] F. Ritter, H. Sonnet, K. Hartmann, and Th. Strothotte, "Illustrative Shadows: integrating 3D and 2D information displays" in *International Conference on Intelligent User Interfaces*, pages 166–173, 2003.

[17] A. W. Rogers, *Textbook of Anatomy*, Churchill Livingstone, Edinburgh, 1992.

[18] A. Rosenfeld and J. Pfaltz, "Distance functions in digital pictures" in *Pattern Recognition*, vol 1, p33–61,1968.

[19] J. Sobotta, R. Putz, and R. Pabst, editors. Sobotta: *Atlas of Human Anatomy. Volume 2: Thorax, Abdomen*, Pelvis, Lower Limb. Williams & Wilkins, Baltimure, 12. English edition, 1997.

Proceedings of 2009 12th International Conference on Computer and Information Technology (ICCIT 2009)
21-23 December, 2009, Dhaka, Bangladesh

Personnel Selection Method Using Analytic Network Process (ANP) and Fuzzy Concept

Mohammed Ayub, Md. Jonaed Kabir, Md. Golam Rabiul Alam†
Department of Business Administration
† Department of Computer Science and Engineering, International Islamic University Chittagong, Bangladesh
ayubtly@yahoo.com, mjk_iiuc@yahoo.com, gra9710@yahoo.com

Abstract

Due to complex functionality of the organization, it requires the most competent and skilled personnel to challenge the global trends. To focus such personnel an integrated scientific selection procedure is a must. Analytic thinking approaches are the most suitable methods to address this problem of personnel selection. Analytic Hierarchy Process (AHP) is more suitable when the hierarchical levels are independent of each other and Analytic network Process (ANP) is used when there are factors, which are dependent of the other factors in the same hierarchical levels or other levels. The method proposed in this paper successfully models the ambiguity and imprecision associated with the pair wise comparison process and reduces the personal biasness. The model allows many qualitative and qualitative factors and provides the importance level of each criteria/sub-criteria so that the decision maker has the ability to determine which factors are to be given emphasize. All the members of the decision maker have the opportunity to express their judgments and hence participative decision-making is achieved.

Keywords: Analytic Network Process, Analytic Hierarchy Process, Human Resource Management, Supermatrix, Personnel Selection and Fuzzy.

I. INTRODUCTION

Decision-making is an essential part of almost all-human life. Decisions could be made based on the persistence of some personnel selector or a personnel selector's ability to persuade others to accept his or her ideas. Decisions chosen under such circumstances are defined as subjective judgment. Analytic thinking approaches break down the 'system' into clusters and subdividing these clusters into smaller ones, and so on hierarchically, large amounts of information are integrated into the structure of a problem and form a more complete picture of the whole system [7]. The main objective of this paper is to provide an approach to minimizing subjective judgments in the crucial procedures of personnel selection and provide a frame work for participative group decision making. The other objectives includes enhancing the potential of the ANP for dealing with imprecise and uncertain human comparison judgments by allowing fuzzy value, and the decision capability of the decision maker by structuring the complex problem into hierarchical structure with dependencies and feedback system.

II. LITERATURE REVIEW

Basic function of personnel selection operations is determining, among the candidates applying for specific jobs in the company, the ones having the necessary knowledge, skill, and ability in order to be able to perform the requirements of the job successfully [3]. In literature, there are various methods regarding personnel selection [1], [2], [7], [10]. An attempt is made to explore and review the most relevant papers including DAĞDEVİREN and YÜKSEL's "Personnel Selection Using Analytic Network Process"[4].

A. Personnel Selection Using ANP

The factors within the personnel selection model are determined in a general level, is not aimed at a specific sector or workplace. As it can be seen in Figure 1, the model developed consists of three phases.

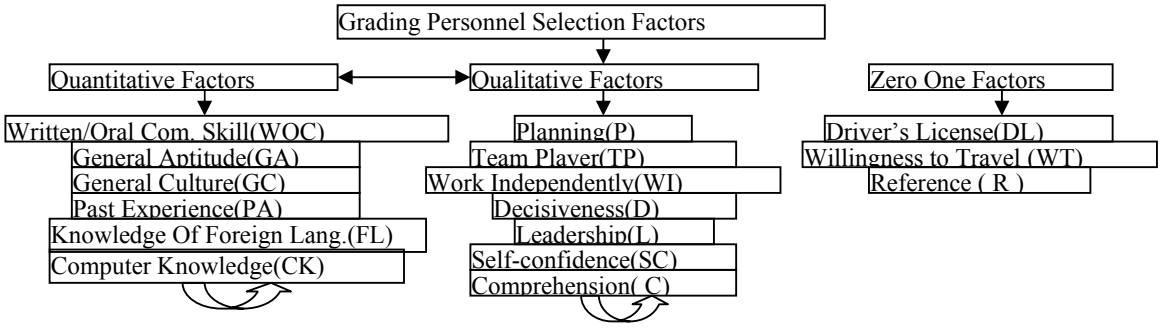

Fig.1 ANP Selection Model

In the first phase there is the goal, second phase consists of factor groups called qualitative, quantitative and 0-1factors; while in the third phase, within the model there are 6 quantitative, 7 qualitative, and 3 zero-one, i.e. a

978-1-4244-6283-4/09/$26.00 ©2009 IEEE

total of 16 factors. There are dependencies between qualitative and quantitative factor groups, and between sub factors belonging to these factor groups. Such interdependencies between factors are indicated with arrows on the figure. Zero-one factor group is independent from other factor groups; likewise, the factors of this group are independent from each other.

A.1 Building Pairwise Comparison Matrix and Determining Weights of the Factors

In this method, first, pairwise comparison decision matrices were created in order to determine weights of factors in the groups. Similarly, other factors are also evaluated with 19 pairwise comparison decision matrices. Point to be remembered is that the 0-1 factor group is seen independent. In the next stage, the method calculates the weights of factors belonging to zero-one factor group.

A.2 Super Matrix formation and Global Weights of Factors

Initial super matrix is formed by making use of priority vectors obtained from pair wise comparison decision matrices. In the next stage, quantitative and qualitative factor groups are assumed to have equal priorities, and the initial super matrix is weighted basing on this assumption. Limit super matrix is formed via raising the weighted super matrix to the power of an arbitrarily large number to obtain weight vectors for factors. Column 4 in Table I exhibits the weights of factors belonging to quantitative and qualitative factor groups. Global weights corresponding to the factors are calculated by multiplying weight values found via pairwise comparison matrix with weight values found through the limit supermatrix shown in column 4 of table I. For 0-1 factors the global weight is calculated by multiplying the priority of 0-1 factors with the weight found by pairwise comparison of the 0-1 factors.

In the method, the alternatives are not evaluated using pairwise comparison matrix. Rather it used certain measurement scales to evaluate the factors of a single alternative. Hence it did not provide the comparative rankings of alternatives at the same time. The measurement scale for quantitative factors are made using interval like $n1<X<n2$, where n1 and n2 are first and second boundary of the interval respectively, and X represents the factors of selection model. The measurement scales for qualitative factors are expressed using linguistic variable such as good, very good and poor etc. After the established the grade (interval), they assigned a scale value between 1 and 0 to each grade

Table I Weight vectors obtained from Limit Supermatrix [4]

Factor Group (1)	Weight (2)	Factors (3)	Weights of the factors (4)	Global Weights (5)	Result of Exam/ interview (6)	Scale Values (7)	Factor points (8)
Quantitative	0.889	WOC	0.030	0.026	72 points	0.8	0.020
and Qualitative Factor group		GA	0.080	0.072	85 points	0.9	0.064
		GC	0.058	0.051	70 points	0.7	0.035
		PA	0.254	0.225	5 years	0.5	0.112
		FL	0.047	0.043	65 points	0.7	0.030
		CK	0.032	0.028	83 points	0.9	0.025
		P	0.044	0.039	Good	0.8	0.031
		TP	0.064	0.056	Average	0.6	0.033
		WI	0.059	0.053	Good	0.8	0.042
		D	0.077	0.068	Good	0.8	0.054
		L	0.017	0.016	Average	0.6	0.009
		SC	0.095	0.084	Good	0.8	0.067
		C	0.143	0.128	Average	0.6	0.076
0-1 Factor	0.111	DL	0.239	0.027	Negative	0.0	0.000
		WT	0.623	0.069	Positive	1.0	0.069
		R	0.138	0.015	Positive	1.0	0.015
				1.000	Competency points		0.682

Factor points shown in column 8 of table I are calculated by multiplying global weights by scale values shown in column 7 of table I, and applicant's total grade is estimated by summing up the factor points. In this case, the applicant's competence score is 68.2%. In [4], the authors urged that in a personnel selection procedure wrong choices will be unavoidable if the factors do not define the job. The authors also suggested that their model might be incapable if the pairwise comparison matrix for the factors that cannot be formed with crisp values.

III. PROPOSED MODEL

A. Problem Structuring

Problem structuring is the first step of ANP. In order to identify the most important criteria and subcriteria for the post lecturer of a university, we conducted a survey of size 15 consisting of university professor and members of selection board. Questionnaire was designed by grouping the factors into 4 groups: Personnel Attributes, Skills Attributes, Education and Knowledge, and Experience & Other Attributes. A total of 13 subcriteria with respect to 4 criteria are recommended and the complete problem structure using these is shown in fig. 2. For determination of dependencies, we construct a zero-one matrix of criteria against criteria using the number one to signify dependence of one criterion on another, and zero otherwise. A criterion need not depend on itself. For each column of this matrix, construct a pairwise comparison matrix only for the dependent criteria, derive the priority vector, and augment it with zeros for the excluded criteria. If a column is all zeros, then assign a zero vector to represent the priorities. [5] The same procedure is followed for all subcriteria.

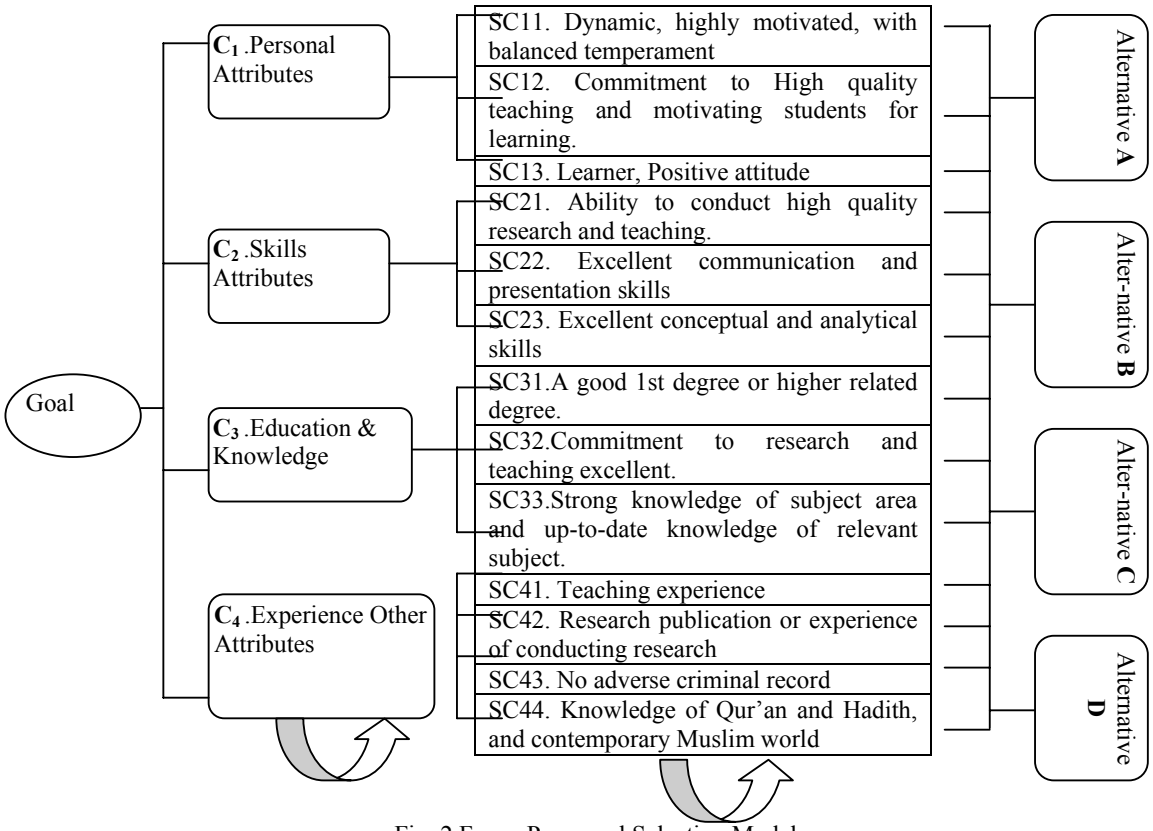

Fig. 2 Fuzzy Personnel Selection Model

B. Fuzzyfication, Aggregation of TFNs of Experts and Defuzzyfication

In this step, the triangular fuzzy numbers are established using the following rules shown in the table II. Fuzzyfication is the process of converting the crisp value obtained by questionnaire into triangular fuzzy values. This process is carried out for each expert opinion and these TFNs of different experts are aggregated using the procedures explained below.

Table II conversion Rules from crisp to fuzzy TFNs [6]

Crisp PCM Value	Fuzzy PCM Value	Crisp PCM Value	Fuzzy PCM Value
1	(1,1,1) if diagonal;	5	(3,5,7)
1	(1,1,3) otherwise	6	(4,6,8)
2	(1,2,3)	7	(5,7,9)
3	(1,3,5)	8	(6,8,10)
4	(2,4,6)	9	(7,9,11)

Saaty contended that the geometric mean accurately represents the consensus of experts and is the most widely used in practical applications. Here, geometric mean is used as the model for triangular fuzzy numbers [8]. Fuzzy set theory deals with the uncertainty due to imprecision and vagueness. A major contribution of fuzzy set theory was its capability of representing vague data. A fuzzy set is characterized by a membership function, which assigns to each object a grade of membership ranging between zero and one [9]. Since each number in the pair-wise comparison matrix represents the subjective opinion of decision makers and is an ambiguous concept, fuzzy numbers work best to consolidate fragmented expert opinions. A TFN is denoted simply as (L, M, U). The parameters L, M and U, respectively, denote the smallest possible value, the most promising value and the largest possible value that describe a fuzzy event as shows in formulae (1)-(4). Here we also use l, m and u for representing the same.

The triangular fuzzy numbers $\widetilde{U}_{ij}$ are established as follows:

$$\widetilde{U}_{ij} = \left(L_{ij}, M_{ij}, U_{ij}\right) \ldots \quad \ldots \quad \ldots (1)$$

where $L_{ij} \le M_{ij} \le U_{ij}$ and $L_{ij}, M_{ij}, U_{ij} \varepsilon \left[\frac{1}{11}, 11\right]$

$$L_{ij} = \min(a_{ijk}) \ldots \quad \ldots \quad \ldots (2)$$

$$M_{ij} = \left(\prod_{k=1}^{n} a_{ijk}\right)^{1/n} \ldots \quad \ldots \quad \ldots (3) \text{ and}$$

$$U_{ij} = \max(a_{ijk}) \ldots \quad \ldots \quad \ldots (4)$$

Where a_{ijk} represents a judgment of expert k for the relative importance of two criteria Ci-Cj .

In the previous step we convert the different opinions of the experts into triangular fuzzy numbers using the various mathematical formulas. Now, in this step we establish FPCM for each criterion and all the fuzzy values are defuzzyfied using the formula given in (5).

$$a = (l + 2m + u)4 \ldots \quad \ldots \quad \ldots (5)$$

This procedure is applied for all pairwise comparison matrices in all tables.

C. Pairwise Comparison Matrix and Calculation of Priority Vectors

Pairwise comparison is made using the judgment scale [8] shown in the following table III. If one criteria or subcriteria is strong importance than the other with respect to a control criteria then from the table we represent this with 5. If activity i has one of the nonzero numbers (1-9) assigned to it when compared with activity j, then j has the reciprocal value when compared with i . The question asks for pairwise comparison is that "which one is more important/dependent than other given a control criteria".

Table III Judgment Scale

1	Equal		
2	Weak or slight	6	Strong plus
3	Moderate	7	Very strong
4	Moderate plus	8	Very, very strong
5	Strong	9	Extreme

Table IV Expert opinions for criteria with respect to goal

	Personal attributes (C1)	Skill attributes (C2)	Education & Knowledge (C3)	Experience & Other (C4)
Personal attributes (C1)	(1, 1, 1)	(1/7,1/5,1/3)	(1/8,1/6,1/4)	(1/5,1/3,1)
	(1, 1, 1)	(1/7,1/5,1/3)	(1/6,1/4,1/2)	(1/4,1/2,1)
	(1, 1, 1)	(1/8,1/6,1/4)	(1/9,1/7,1/5)	(1 ,1,3)
	(1, 1, 1)	(1,1,3)	(1/5,1/3,1)	(1/4,1/2,1)
Skill attributes(C2)	(0, 0 ,0)	(1, 1, 1)	(1/7,1/5,1/3)	(1/7,1/5,1/3
	(0, 0 ,0)	(1, 1, 1)	(1,2,4)	(1/5,1/3,1)
	(0, 0 ,0)	(1, 1, 1)	(1/6,1/4 ,1/2)	(1/8,1/6,1/4
	(0, 0 ,0)	(1, 1, 1)	(1/3,1,1)	(1,2 ,4)
Education & Knowledge (C3)	(0, 0 ,0)	(0, 0 ,0)	(1, 1, 1)	(3 ,5,7)
	(0, 0 ,0)	(0, 0 ,0)	(1, 1, 1)	(1 ,2 ,4)
	(0, 0 ,0)	(0, 0 ,0)	(1, 1, 1)	(1/9,1/7,1/5)
	(0, 0 ,0)	(0, 0 ,0)	(1, 1, 1)	(1,1,3)
Experience & Other (C4)	(0, 0 ,0)	(0, 0 ,0)	(0, 0 ,0)	(1, 1, 1)
	(0, 0 ,0)	(0, 0 ,0)	(0, 0 ,0)	(1, 1, 1)
	(0, 0 ,0)	(0, 0 ,0)	(0, 0 ,0)	(1, 1, 1)
	(0, 0 ,0)	(0, 0 ,0)	(0, 0 ,0)	(1, 1, 1)

The table IV shows the pairwise judgments of Criteria with respect to goal. For a single table entry there are four rows which represent the opinion of four experts and three columns which represent the three values l, m and u. That is every expert expresses their judgment in three levels that are represented in the table as columns. This procedure is implied for all entries of the all tables. The results of FANP are shown from table V through 7. Realizing that it would be very time consuming to do all these manually, Matlab software is used to program all these operations. The weight vectors are calculated using pairwise comparison matrix using the following algorithm. This algorithm is applied for all w22, w32, w33 and w43.

Algorithm:

1. Every expert opinion is converted into triangular fuzzy numbers using the rules given in table II then each TFN aggregated using equation (1) to (4).
2. The aggregated TFN are defuzzyfied using equation (5)
3. Find the column sum of each column of the PCM.
4. Divide every row entry of that column with the sum obtained in step 3.
5. Again each row is summed and finds the mean which is the weight vector

Table V: TFN for Criteria with respect to goal using FANP

	C1L	C1M	C1U	C2L	C2M	C2U	C3L	C3M	C3U	C4L	C4M	C4U
Personel	1	1	1	0.1250	0.2857	3	0.1111	0.2111	1	0.2000	0.5373	3
Skill	0	0	0	1	1	1	0.1429	0.5623	4	0.1250	0.3861	4
Edu & Knowledge	0	0	0	0	0	0	1	1	1	0.1111	1.0933	7
Experience & Other	0	0	0	0	0	0	0	0	0	1	1	1

Table VI FANP Defuzzified result for criteria with respect to goal

	Personel	Skill	Edu & Knowledge	Experience & Other
Personel	1	0.9241	0.3833	1.0686
Skill	0	1	1.3169	1.2243
Edu & Knowledge	0	0	1	2.3244
Experience & Other	0	0	0	1

Complete PCM for criteria with respect to goal is obtained by getting the reciprocal of defuzzified matrix obtained in table VI. This an established fact that in pairwise comparison matrix if the upper/lower triangular matrix is obtained the remaining one can be found by reciprocating the other. Complete PCM together with weight vector is shown in the table VII.

Table VII: Complete PCM and weight vectors of Criteria with respect to goal for FANP (W21)

	Personel	Skill	Edu & Knowl...	Experience ...	Weight Vector
Personel	1	0.9241	0.3833	1.0686	0.1886
Skill	1.0821	1	1.3169	1.2243	0.2792
Edu & Knowledge	2.6089	0.7594	1	2.3244	0.3535
Experience & Other	0.9358	0.8168	0.4302	1	0.1788

D. Supermatrices

The generalized form of super matrix is shown in table VIII.

Table VIII Generalized Form of Super Matrix

	Goal	Criteria	Subcriteria	Alternatives
Goal	0	0	0	0
Criteria	w_{21}	w_{22}	0	0
Subcriteria	0	w_{32}	w_{33}	0
Alternatives	0	0	W_{43}	I

Where w21 is weight of criteria with respect to goal, w22 is weight of criteria with respect to criteria, w32 is weight of subcriteria with respect to criteria, w33 is weight of subcriteria with respect to subcriteria and w43 is weight of alternatives with respect to subcriteria. The initial super matrices are shown following table IX. As

mention before the super matrices are the weight of different criteria, subcriteria and alternatives placed in systematic manner. As it is too big to show it is given in two parts.

Table IX (a) Partial View of Initial super matrix for FANP (Part-I)

	G	C1	C2	C3	C4	SC11	SC12	SC13	SC21	SC22	SC23
G	0	0	0	0	0	0	0	0	0	0	0
C1	0.1885	0.308	0.1458	0.2006	0.1525	0	0	0	0	0	0
.....	.....	.....	.....	.....	.....	.....	.....	.....	.....	.....	.....	.....
C4	0.1788	0.0976	0.0973	0.0833	0.1168	0	0	0	0	0	0
SC11	0	0.4662	0	0	0	0	0.1273	0.129	0	0	0
.....	.....	.....	.....	.....	.....	.....	.....	.....	.....	.....	.....	.....
SC44	0	0	0	0	0.1384	0.0836	0	0.0631	0.081	0	0
A	0	0	0	0	0	0.1297	0.135	0.1018	0.1624	0.2594	0.1135
.....	.....	.....	.....	.....	.....	.....	.....	.....	.....	.....	.....	.....
D	0	0	0	0	0	0.5226	0.5401	0.5393	0.2886	0.3357	0.5945

Table IX (b) Partial View of Initial supermatrix for FANP (Part-II)

	SC31	SC32	SC33	SC41	SC42	SC43	SC44	A	B	C	D
G	0	0	0	0	0	0	0	0	0	0	0
C1	0	0	0	0	0	0	0	0	0	0	0
.....	.....	.....	.....	.....	.....	.....	.....	.....	.....	.....	.....	.....
SC11	0	0.1036	0.1033	0	0.098	0	0.1548	0	0	0	0
.....	.....	.....	.....	.....	.....	.....	.....	.....	.....	.....	.....	.....
SC43	0	0	0	0	0	0	0.1356	0	0	0	0
SC44	0	0	0	0	0	0	0	0	0	0	0
A	0.1331	0.1544	0.1587	0.3338	0.1062	0.25	0.378	1	0	0	0
D	0.5567	0.3194	0.4548	0.1115	0.3606	0.25	0.3067	0	0	0	1

The initial supermatrix is not stochastic and is made stochastic using relevant technique. Again to obtain the final priority vectors of criteria, subcriteria and alternatives the weighted super matrix is raised a large power. At one stage all the entries except the rows of Alternatives become zero. The final ranking is shown in the table X.

Table X The final ranking of alternatives in FANP

	G	C1	C	C3	C4	SC11	SC12	SC13	SC21	SC22	SC23	SC31	SC32	SC33	SC41	SC42	SC43	SC44
A	0.1700	0.1577	0.1752	0.1618	0.1911	0.1511	0.1512	0.1361	0.1652	0.2242	0.1412	0.1524	0.1597	0.1627	0.2476	0.1340	0.2082	0.2688
B	0.3184	0.2971	0.3311	0.3125	0.3328	0.2797	0.2862	0.2659	0.3778	0.3272	0.2688	0.2741	0.3852	0.3039	0.3921	0.3640	0.2822	0.2398
C	0.1058	0.1034	0.1044	0.1048	0.1124	0.0992	0.0989	0.1209	0.1119	0.0954	0.0962	0.1027	0.1040	0.1119	0.0967	0.1183	0.1761	0.1235
D	0.4056	0.4417	0.3891	0.4208	0.3635	0.4700	0.4637	0.4771	0.3451	0.3531	0.4938	0.4707	0.3510	0.4215	0.2637	0.3837	0.3335	0.3679

IV. ANALYSIS AND COMPARISON

The results of the proposed model are compared with AHP and Crisp ANP with respect to lecturer selection problem. Here the alternatives mean the applicants applied for the post. The points of alternative with respect to subcriteria for the AHP models are shown in table XI(a). In AHP, total result is the summation of the points of subcriteria. So in AHP it does not actually represent the points of alternatives for subcriteria. The reason is that in AHP there is no concept of stochastic i.e. making column sum to 1. In ANP, the points in the respective column represent the actual rankings of alternatives with respect to that column. But for the final ranking we must only consider the rankings only with respect to goal.

Table XI(a) Points of Alternatives with respect to different subcriteria using AHP

	SC11	SC12	SC13	SC21	SC22	SC23	SC31	SC32	SC33	SC41	SC42	SC43	SC44	AHP Result
A	0.0022	0.0058	0.0010	0.0063	0.0134	0.0040	0.0141	0.0089	0.0120	0.0301	0.0077	0.0128	0.0215	0.1397
B	0.0053	0.0126	0.0024	0.0252	0.0234	0.0097	0.0263	0.0307	0.0302	0.0465	0.0298	0.0128	0.0121	0.2670
C	0.0033	0.0058	0.0016	0.0093	0.0095	0.0068	0.0221	0.0089	0.0168	0.0093	0.0142	0.0128	0.0135	0.1340
D	0.0160	0.0360	0.0073	0.0270	0.0397	0.0329	0.0955	0.0338	0.0698	0.0107	0.0471	0.0128	0.0306	0.4592

Table XI(b) Points of Alternatives with respect to different subcriteria using CANP

	G	C1	C	C3	C4	SC11	SC12	SC13	SC21	SC22	SC23	SC31	SC32	SC33	SC41	SC42	SC43	SC44
A	0.1280	0.1151	0.1254	0.1152	0.1482	0.1019	0.1126	0.1054	0.1134	0.1551	0.1004	0.1068	0.1148	0.1064	0.2114	0.0971	0.1881	0.2050
B	0.2820	0.2644	0.2886	0.2759	0.2902	0.2337	0.2595	0.2364	0.3351	0.2979	0.2430	0.2366	0.3405	0.2714	0.3864	0.2974	0.2691	0.2116
C	0.1280	0.1216	0.1245	0.1267	0.1337	0.1267	0.1098	0.1285	0.1320	0.1137	0.1256	0.1316	0.1175	0.1269	0.1085	0.1347	0.1871	0.1577
D	0.4616	0.4986	0.4612	0.4819	0.4277	0.5377	0.5181	0.5298	0.4195	0.4332	0.5310	0.5250	0.4271	0.4954	0.2937	0.4707	0.3556	0.4257

From the table X it can be observed that Alternative B has more points in SC21, SC32 and SC41 than alternative D. It can also be noticed from the table that all the alternatives have the distinct points almost in all subcriteria. No close competency is observed in all alternatives. Again if CANP is considered, from the table XI(b) it can be seen that Alternative B has higher point than D only in SC41. And also close competency is seen between alternative A and C. From all these observation it can be said that the result provide by FANP is more realistic and robust. The pure advantage of ANP over AHP is that the decision maker can have the opportunity to evaluate the applicants with respect to each criteria and subcriteria.

Table XII: Comparison of the result of the FANP model with AHP and CANP

	AHP result	AHP Ranking	CANP result	CANP Ranking	FANP result	FANP Ranking
Alternative A	0.1397	III	0.1280	III	0.1700	III
Alternative B	0.2670	II	0.2820	II	0.3184	II
Alternative C	0.1340	IV	0.1280	III	0.1058	IV
Alternative D	0.4592	I	0.4616	I	0.4057	I

From the table XII, it is seen that when the FANP is used the alternative D has the first rank with 0.4057 points and Alternative C has the fourth rank with 0.1058. When CANP is used Alternative D has the first rank with 0.4616 and both Alternative A and C has the same ranking of third. In AHP the same ranking with different points are obtained as of FANP. It can be said from the observation that in both AHP and CANP, the competency points of all alternatives are much closed. More precisely if the points are rounded up to three decimal places the result is almost the same. But in FANP method each alternative has distinct competency score which leaves no confusion for decision maker to take the final decision. From that point it can be urged that Fuzzy Analytic Network Process (FANP) provides the clear and distinct result in personnel decision making. Moreover, it is interesting to see that FANP converge at the lower power than CANP. That is when FANP is used the limit super matrix is obtained at 15th power of weighted super matrix and when CANP is used the limit super matrix is reached at 17th power of weighted super matrix.

V. CONCLUSION

The network model proposed in this paper (FANP) maps the complex selection problem into hierarchical dependence and feedback, and the involvement of fuzzy concept adequately resolve the inherent uncertainty and imprecision associated with the mapping of a decision maker's perception to exact numbers. All the members of the decision maker have participative decision making and hence reduce personnel biasness. Finally, we recommend that administrators or decision makers can use this model to select any other personnel with little modification of the model. The proposed method will be also enhanced by undergoing a survey for identifying the criteria and sub criteria using Delphi method. Besides, the analysis of BOCR (Benefit, Opportunity, Cost & Risk) will also enhance the robustness of the model.

REFERENCES

[1] Thomas L. Saaty, "Fundamentals Of The Analytic Network Process", ISAHP 1999, Japan, August 12-14,

[2] Thomas L. Saaty,"The Analytic Hierarchy and Analytic Network Measurement Processes: Applications to Decisions under Risk", European Journal Of Pure And Applied Mathematics Vol.1, No. 1, 2008, p122.

[3] Kaynak T., "Human Resources Management", Nobel Yayınevi, Đstanbul. (2002),

[4] Metin DAĞDEVĐREN and Đhsan YÜKSEL, "Personnel Selection Using Analytic Network Process", Đstanbul Ticaret Üniversitesi Fen Bilimleri Dergisi Yıl: 6 Sayı:11 Bahar 2007/1 s. 99-118.

[5] Thomas L. Saaty and Luis G. Vargas, "Decision Making With The Analytic Network Process", p-17

[6] Lee Hua Jie, Mak Chee Meng, Chin Wen Cheong, "Web Based Fuzzy Multicriteria Decision Making Tool", International Journal of The Computer, the Internet and Management Vol. 14.No.2 ,2006, pp 1-14.

[7] Saaty. T.L., "Decision Making for Leaders: The Analytic Hierarchy Process for Decisions in a Complex World", RWS Publications, Pittsburgh. 2001b.

[8] Thomas L. SAATY, "Decision Making – The Analytic Hierarchy and Network Processes (AHP/ANP)", Journal Of Systems Science And Systems Engineering, Vol. 13, No. 1,pp1-34 March, 2004.

[9] ZADEH, L.A., "Making Computers Think Like People", IEEE Spectrum, 8, pp. 26-32,1984.

[10] Pita, "Analytic Thinking Approach: an Application in Assessment and Measurement of Strategic Information Systems Planning", 19th Australasian Conference on Information Systems, 3-5 Dec 2008, Christchurch.

Proceedings of 2009 12th International Conference on Computer and Information Technology (ICCIT 2009)
21-23 December, 2009, Dhaka, Bangladesh

Proposed Domain Name System (DNS) for Improved E-Government Services of Bangladesh

Md. Monirul Islam
Department of Computer Science and Engineering
International Islamic University Chittagong
monirliton@yahoo.com

Abstract

In recent time Bangladesh government has given lot of attention to the electronic government (e-government) to fulfill the vision of digital Bangladesh. This paper focused specifically on whether Bangladesh e-government domain names comply with the standard of other countries Domain Name or not. I have also proposed a standard domain name system for all government web sites so that the citizens and others will able to locate the site easily and will get better, secure e-government services. The consequences of this issue together with how to address it are discussed in this paper. The results of this study will provide Bangladesh government a clear concept of the current situation of e-government websites' domain names which should be helpful to the evaluation of e-government websites in Bangladesh.

Keywords: E-government, DNS, URL, website, Digital Bangladesh

I. INTRODUCTION

E-Government has been defined as "the use of information and communication technologies, and particularly the internet, as a tool to achieve better government."[1]. Better government means to deliver public services and process internal works in government in a much more convenient, customer oriented, cost-effective, and better way [2]. Heeks [3] has described e-Government as "the use of information and communication technologies (ICTs) to improve the activities of public sector organizations." More broadly, e-Government refers to "the government's applications of information technology to enhance access to, and delivery of, public services to citizens and other government agency" [2].

It is expected that the introduction of e-government in Bangladesh will foster the administrative reform by transforming government functions, streamlining procedures, and enhancing administrative transparency. The aim of implementation of e-government in Bangladesh is to bring about a more efficient and effective government, which can gradually reduce the administrative cost and at the same time provide better services to Bangladesh citizens. There is a genuine risk that the existing Bangladesh e-government websites will continue to use the noncompliance domain names and those being about to go online will also have non-compliance domain names. Experience from other countries show that this will make the general publics more and more confused on how they can simply judge whether a website is a genuine e-government website. Because there are both a lack of trust and an increased need for trust on the Internet, this feeling of confusion will lead to severe distrust of e-government websites and result in less and less use of e-government websites. In this case, the investments and efforts exerted by Bangladesh government is good for nothing.

The main objective of this study is to evaluate the domain names of the Bangladesh e-government websites posted on the official Government Online portal http://www.bangladesh.gov.bd.

II. LITERATURE REVIEW

A. DNS

According to the Internet Corporation for Assigned Names and Numbers (ICANN), the Internet's domain-name system (DNS) allows users to refer to web sites and other resources using easier-to-remember domain names (such as "www.yahoo.com") rather than the all-numeric IP addresses (such as "69.0.100.123") assigned to each computer on the Internet. A domain name is thus a series of character strings (called "labels") separated by dots [4]. The DNS forms a treelike hierarchy. The right-most label in a domain name is referred to as its Top Level Domain" (TLD). Each TLD includes many second-level domains; each second-level domain can include a number of third-level domains, and so on. On the Web, the domain name is part of the Uniform Resource Locator (URL) such as: [URL] = http://www.bangladesh.gov.bd/index.php

Table 1: URL

3rd Level Domain	2nd Level Domain	Top Level Domain	Web page
Bangladesh	gov	bd	index.php

index.php is file name it is not part of the domain name. TLDs with two letters such as .bd, .my, jp etc. have been established for most of the countries and are referred to as country-code (TLDs) or (ccTLDs)[5]. The ccTLD assigned to Bangladesh is ".bd" [6].

DNS can be used in full name, abbreviation acronym, key word etc. The summary of advantages and disadvantages of each of type of DNS are as follows [7]:

Table 2: Types, advantages and disadvantages of DNS

Type	Example	Advantage	Disadvantage	Recommendation
Full Name	bangladeshbureauofstatistics.gov.bd.	An exact match to the function	Likely to contain several words	Only use if the full name is short and easily remembered.
Abbreviation	bdbureaustats.gov.bd	Short.	May not be meaningful to users	Only use if the abbreviation is well-known to users.
Acronym	bbs.gov.bd	Easy to read and type.	May not be meaningful to users.	Only use if the acronym is well-known by users
Key Word	statistics.gov.bd	Short. Easy to read and remember	May be too generic, and misleading	Suitable but have to careful about the nature of information.

B. Standard DNS for Government

Many countries like Australia, China, USA have set out the Government Domain Name Standard to regulate the government domain names. For example China[8] has set the following standard for domain names:

1) government domain names must end with gov.cn

2) The basic standard for the domain names of province level governments is: www.abbreviation of the geographical name of province level government.gov.cn

3) The basic standard for the domain names of prefecture level governments (cities, leagues, autonomous prefectures) is: www. full name of the geographical name of prefecture level government.gov.cn

4) The basic standard for the domain names of county/district level governments is: www.abbreviation of the geographical name of province level government + full name of the geographical names of county/district level government.gov.cn

C. Study of DNS of Other Nation

There were similar study have been conducted to measure the DNS of Chinese local government. The objective of the study was to advice government to use the standard DNS for province level as prescribed by the China government. This study found that China local governments are using diverse domain names and around 4000 of the examined domain names do not comply with the Standard set by the government of China. In addition, this study found that there is virtually no improvement on the domain name issue across year 2005 and 2006[9].

III. METHODOLOGY

To make a study on domain names of Bangladesh e-government websites are difficult because how to judge the compliance and what rules or regulations have been used as reference since we do not have any standard yet. Based on the DNS of other countries I have proposed a standard and made a comparative study.

a. If a domain name ends with ".gov.bd" and uses abbreviation in its third-level domain, it will be judged as 'Compliance'.

b. If a domain name ends with ".gov.bd" but does not use abbreviation in its third-level domain, it will be judged as 'Partial Compliance'.

c. If a domain name does not end with ".gov.bd", it will be judged as 'Non Compliance'.

IV. PROPOSED DNS

The diversity of Bangladesh government domain names exposes the government websites to a great danger of being counterfeited. Because government websites are now using all kinds of domains such as ".com", ".net", org, country code of other country and even IP address. Based on the above discussion I proposed the following DNS for Bangladesh e-government:

1) Top level of the government domain names must use the country code " *.bd"*

2) Second level of the government domain names must use "*.gov."*

3) Acronym must use in 3rd level domain, if there any duplicate then go for abbreviation.

Example for Bangladesh Railway: www.br.gov.bd not www.railway.gov.bd

4) It must only include letters a-z, numbers 0-9 and hyphen (-). No other characters, such as $, @, %, _, are allowed.

5) To strengthen the local e-government services all district must use a 2 characters code.

V. RESULTS

The domain names were collected in July 2009. The different domain names of government related websites was collected only from the official Government Online portal (http://www.bangladesh.gov.bd)[10]. The result was analyzed in aggregate as well as different categories to show a clear picture.

A. Aggregate Result

There are about 239 different domain names of government related websites were found on the official Government Online portal and following table shows the summary of the different DNS:

Table 3: Aggregate Results of DNS

Category	Frequency	Percent	Cumulative %
Compliance	142	59	59
Partially Compliance	37	16	75
Non Compliance	60	25	100

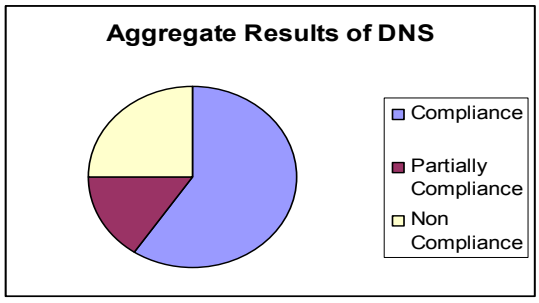

Chart 1: Aggregate result of DNS in Pie Chart

An analysis of the results showed that about 59% of the 239 different domain name of government related web sites are fully comply with the proposed standard, 16% of them partially comply with the standard, and 25% does not comply wih the standard.

B. Ministries

There are 35 domain names of different ministries were found on the official Government Online portal (http://www.bangladesh.gov.bd) and following table shows the summary of the acronym of the different ministries and the 3rd level domain name have been chosen:

Table 4: Acronym and Used 3rd Level Domain of Different Ministries

Acronym of Ministries	3rd Level DNS used	Acronym Ministries	3rd Level DNS used
MOA	moa	MOEF	moef
MOC	mincom	MOEWOE	moewoe
MOC	moc	MOF	mof
MOCA	moca	MOFA	mofa
MOCAT	mocat	MOFDM	mofdm
MOCHTA	mochta	MOFL	mofl
MOD	mod	MOHA	mha
MOE	moedu	MOHFW	mohfw
MOE	moestab	MOHPW	mohpw
MOI	Moi	MORA	mora
MOI	Moind	MOS	mos
MOL	Minland	MOSICT	mosict
MOLE	Mole	MOSW	msw
MOLGRDC	Not Found	MOTJ	motj
MOLJPA	Minlaw	MOWCA	mowca
MOLWA	Mlwa	MOWR	mowr
MOPT	Mopt	MOYS	moysports
MORA	Mora	PMO	pmo

An analysis of the results showed that about 71% of the 35 domain names of different ministries are fully comply with the proposed standard and 29% of them partially comply with the standard. Unfortunately LGRD ministries web site was not found but it is mentionalble that all DNS ends with gov.bd so that none of the DNS is under the non compliance category.

Table 5: Results of Ministries

Category	Frequency	Percent	Cumulative %
Compliance	25	71	71
Partially Compliance	10	29	100
Non Compliance	0	0	0

C. Deputy Commissioner's Offices

There are only 15 Deputy Commissioner's offices out of 64 were found in the official web portal these are as follows: Dhaka, Gazipur, Habiganj, Jessore, Joypurhat, Lalmonirhat, Moulvibazar, Magura, Pirojpur, Sylhet, Thakurgaon, Bandarban, Jhalakhati, Lakshmipur, Khagrachari. One good thing is all the DNS are under a same fashion. So we can consider this as a standard format. Acronym of Deputy Commissioner (DC) with the full geographical name of the district. gov.bd. Example http://www.dcdhaka.gov.bd/.

In USA, they have the standard abbreviation of all 50 states like NY for New York; some other country also has the same for all the provinces. I have suggested 2 character names for all 64 districts that we can use to build up website to strengthen local government.

D. Embassy/High Commission

There are only 20 different domain names of Bangladesh embassy/High Commission websites were found on the official Government Online portal (http://www.bangladesh.gov.bd) under the ministry of foreign affairs. The DNS are as follows:

Table 6: DNS of Embassy of Bangladesh

DNS
http://www.bangladoot-canberra.org/
http://www.bangladeshembassy.be/
http://www.bdhc.org/
http://www.bangladeshembassy.de/
http://www.bhcdelhi.org/
http://www.bangladesh-highcomkl.com/
http://www.bdembjp.com/
http://www.bangladeshembassyinitaly.com/
http://www.bangladeshembassy.ru/en/
http://www.bangladeshembassy.nl/
http://www.bdhcpk.org/
http://www.bangladeshembassy.org.sa/
http://www.bcgjeddah.com/
http://www.bangladesh.org.sg/cms/
http://www.bangladoot.se/
http://www.bhclondon.org.uk/
http://www.bangladoot.org/
http://www.un.int/bangladesh/
http://www.bdcgny.org/
http://www.bangladeshconsulatela.com/

An analysis of the results showed that 0% of the 20 domain name of different Bangladesh embassy/high commisions are fully comply with the proposed standard i.e none of them end with gov.bd, even none of them use a standard name in its 3rd level, so 100% does not comply wih the standard. Only 5 out of 20 used bangladeshembassy in its 3rd level domain no other conclusion can made from the above result.

Table 7: Results of Embassy/High Commissions of Bangladesh

Category	Frequency	Percent	Cumulative %
Compliance	0	0	0
Partially Compliance	0	0	0
Non Compliance	20	100	100

E. Other Government Divisions

There are 168 domain names of different government related websites were found on the official Government Online portal (http://www.bangladesh.gov.bd). The domain names were collected in July 2009 and following table shows the summary of the different DNS:

Table 8: Results of Other Government Divisions

Category	Frequency	Percent	Cumulative %
Compliance	102	61	61
Partially Compliance	27	16	77
Non Compliance	39	23	100

An analysis of the results showed that about 61% of the 168 domain names of different government websites are fully comply with the proposed standard, 16% of them partially comply with the standard, and 23% does not comply wih the standard.

VI. DISCUSSIONS

This study found that Bangladesh governments are using diverse domain names and about 25% of the examined domain names do not comply with the standard. The diversity of Bangladesh government domain names exposes the government websites to a great danger of being counterfeited. Because government websites are now using all kinds of domains such as ".com", ".net", country code of other country and even IP addresses. Anyone can easily deceive the general publics to believe that their websites are genuine government websites. Once this happens, it must seriously affect the general publics trust in government websites and thus impair the development and implementation of e-government in Bangladesh.

For example, a person can register the domain name "www.mofa.com" and claim it represents the official government website of Ministry of Foreign Affairs. Or, can use any IP address to deceive the general publics. However, if all the government websites have used ".gov.bd" domain names, this will help the general publics to form the concept that only ".gov.bd" websites are official government websites and thus greatly reduce the possibility of being deceived by the unauthorized people.

Moreover, the diversity of Bangladesh government domain names makes it difficult for the general publics to find government websites. This will definitely affect people's willingness to use e-government websites if they cannot find them easily.

The results suggest that in order to standardize the domain names in Bangladesh, firstly, the Standard needs to make it clear the meaning of the "abbreviation" for the domain names of Bangladesh governments because using the acronyms of geographical names cannot eliminate the possible duplicates among names. For example, the acronyms of the Ministry of Education and Ministry of Establishment all are "MOE". This might be the reason that none of them used the domain name "www.moe.gov.bd". As a solution, government need to prescribed codes for all related names.

VII. RECOMMENDATIONS

A. Recommended DNS for District Level

It is necessary to create website for district level to provide the information and government services to all the citizens. Precribed code based on acronym must set for every district. Since the sites have not build yet so I have proposed the following 2charactername for every district so that people will not confused and the e-commerce or e-government security will be ensured for local government. For example the domain name for Bagerhat district will be www.bh.lgrd..gov.bd

Table 9: Proposed Short Name for Districts

District Name	Abbreviation	District Name	Abbreviation
Bagerhat	BH	Madaripur	MP
Bandarban	BB	Magura	MA
Barguna	BG	Manikganj	MG
Barisal	BS	Meherpur	ME
Barnmanbaria	BA	Moulavibazar	MB
Bhola	BH	Munshiganj	MU
Bogra	BO	Mymensingh	MY
Chandpur	CP	Naogaon	NN
Chittagong	CG	Narayangan	NG
Chuadanga	CD	Narsingdi	NS
Comilla	CO	Natore	NA
Cox's Bazar	CB	Nawabgonj	NW
Dhaka	DH	Netrokona	NE
Dinajpur	DP	Nilphamari	NP
Faridpur	FP	Noakhali	NK
Feni	FE	Norail	NO
Gaibandha	GB	Pabna	PA
Gazipur	GP	Panchagarh	PG
Gopalganj	GG	Patuakhali	PK
Habiganj	HG	Pirojpur	PP
Jaipurhat	JH	Rajbari	RB
Jamalpur	JP	Rajshahi	RS
Jessore	JE	Rangamati	RM
Jhalakathi	JK	Rangpur	RP
Jhinaidah	JD	Satkhira	SK
Khagrachari	KC	Shariyatpur	SP
Khulna	KH	Sherpur	SH
Kishoreganj	KI	Sirajgonj	SI
Kurigram	KG	Sunamganj	SU
Kushtia	KU	Sylhet	SY
Lakshmipur	LP	Tangail	TA
Lalmonirhat	LH	Thakurgaon	TH

B. Recommended DNS for Emabassy/High Commission

There are two standard we can find from different countries, and can choose any one of them. Geographical name of the city use in 4th level domain dot bdembassy dot gov.bd. Example http://newdelhi.bdsembassy.gov.bd/. Or, we can use the DNS of Ministry of Foreign Affairs: mofa/ embassy/name of the city. Example: www.mofa.gov.bd/embassy/islamabad

VIII. CONCLUSION

E-government is a necessity for good and corruption free nation. To provide e-government services to the citizens and others it is very important to give a standard DNS so that people can trust and easily locate the site to get the services. This paper studies the DNS of e-government in Bangladesh. It clearly demonstrates the necessity to standardize the government domain names in Bangladesh. It is high time to correct the existing domain names and follow a standard in future. The domain issue to a large extent reflects an important issue in the course of e-government development in Bangladesh, that is, the Bangladesh government officials may overlook the concept that e-government in every aspect should be a way to provide better services to general publics but not just merely a web presence of government. A seemingly small issue may have serious consequences when being ignored, for example, the domain issue discussed in this study.

In summarizing the above discussions, Government of Bangladesh needs to make a proper policy on e-government domain name. In order to achieve this, it is very important for Bangladesh government to assess the implementation, operation, and performance of e-government in Bangladesh and take necessary actions based on the results of these assessments. The lack of a proper domain name policy leads to confusion, lack of trust in the users, higher transaction costs and, ultimately, poor interaction between the users and administrations.

REFERENCES

[1] OECD, *OECD e-Government Studies: The e-Government Imperative*, OECD Publications, France, 2003.

[2] Song, H. J., *Building E-Government through Reform*, Governance Research Series 2, Ewha Womans University Press, Seoul, Korea, 2004.

[3] Heeks, R., *e-Government for Development*, Institute for Development Policy and Management, University of Manchester, UK, 2008.

[4] ICANN. Top-Level Domains (gTLDs). Available at: http://www.icann.org/tlds/

[5] IANA. Root-Zone Who is Information: Index by TLD Code. Available at: http://www.iana.org/cctld/cctldwhois.htm

[6] Country Code Top Level Domain, List of ccTLD, http://en.wikipedia.org/wiki/Country_code_top-level_domain

[7] Consider how best to present your information or service in a domain name format. Available at: http://www.domainname.gov.au/Eligibility_and_Allocation_Policy

[8] Govonline.cn (n.d.). China Government Domain Name Regulations. Available at: http://www.govonline.cn/frontmanger/yuming/yuming_rule.jsp

[9] Y. Shi, "Improving E-Government Services Should Start with Domain Names: A Longitudinal Study of Chinese E-Government Domain Names", Available at: http://ieeexplore.ieee.org/stamp/stamp.jsp?tp=&arnumber=4383938

[10] National Web Portal of Bangladesh, Available at: www.bangladesh.gov.bd/

Proceedings of 2009 12th International Conference on Computer and Information Technology (ICCIT 2009)
21-23 December, 2009, Dhaka, Bangladesh

Development of a Novel Quaternary Algebra with the Design of Some Useful Logic Blocks

Ifat Jahangir*, Dihan Md. Nuruddin Hasan†, Shajid Islam‡, Nahian Alam Siddique†, Md. Mehedi Hasan‡

† Dept. of Electrical and Electronic Engineering, Bangladesh University of Engineering and Technology, Dhaka-1000, Bangladesh

‡ Dept. of Electrical, Electronics and Communication Engineering, Military Institute of Science and Technology, Mirpur Cantonment, Dhaka-1216, Bangladesh

ifat00@gmail.com

Abstract

A completely new scheme for quaternary logic is proposed. Instead of conventional Fuzzy logic or Galois Field theory, the logic system is based on the extension of Boolean algebra. The logic is capable of handling both quaternary and coupled-binary inputs, where binary operands are coupled in pairs to form quaternary entities. All necessary operators are defined and several theorems and properties are derived to develop a way of expressing arbitrary truth tables with sum-of-product functions. To demonstrate the functionality of this novel logic scheme, some useful logic blocks such as decoder, multiplexer, and half-adder are designed.

Keywords: Decoder, half-adder, multiplexer, quaternary algebra, quaternary logic.

I. INTRODUCTION

Binary logic has been serving as the basis for all digital systems for a very long time. Boolean algebra is used to describe and design such systems. This is based on set theory and it provides simplest possible way of implementing a digital system. However, due to the rapid advancement of VLSI technology and the invention of novel electron devices like Carbon Nanotube Transistor, FinFET, G4-FET, Silicon Nanowire FET, etc., it is now possible to couple several binary inputs to form a multi-valued input for faster processing. Since multi-valued system comes with the advantage of containing more information in a single digit than that of binary system, it can be adopted as the basis of future computers and other digital devices. Many researchers have been working on multi-valued logic scheme for a long time and several schemes on ternary and quaternary logic have already been proposed. For example, some researchers have adopted the Fuzzy logic-based MIN and MAX functions as building blocks of multi-valued system [1] due to their relative simplicity in circuit design. Some other works are based on Galois Field theory [2]. The drawbacks of such systems are that they do not utilize the designs of the wide variety of existing binary logic devices and they are sometimes very difficult to implement for multi-input circuits. Since multi-valued logic circuits are more complex in nature than binary logic circuits, it is often difficult to design a large system from the scratch. Besides, these schemes are not suitable for coupled-binary inputs. That is why a new logic scheme is required to overcome these problems.

Although multi-valued logic scheme can be a solution for the demand of increasing data storage capability and faster computing [3],[4], limitations imposed by VLSI technology restrain the usage of too many levels in logic systems. Thus quaternary logic seems to be a perfect choice in this regard.

In this paper, we have defined the basic operators of our proposed quaternary logic system. The system has evolved from and closely related to binary logic system. We have derived several theorems and properties to facilitate the development of a fully functional algebra. We have formulated a method for finding the sum-of-product (SOP) expression of an arbitrary function. Finally we have shown the design of some very important logic blocks such as decoder, multiplexer and half adder.

II. THE NOVEL QUATERNARY LOGIC

The quaternary logic we are proposing here consists of quaternary states or variables and operators. The quaternary states are 0 (absolute low), 1 (medium low), 2 (medium high) and 3 (absolute high), which can also be represented as 2-bit binary equivalents 00, 01, 10 and 11. If the bits of the binary equivalent interchange their positions and still the quaternary state remains unchanged, then it is said to have binary symmetry; otherwise it is asymmetric. Thus 0, 3 are symmetrical and 1, 2 are asymmetrical. When expressed as a number, a single quaternary digit is called a qudit.

The basic quaternary operators are defined as bitwise binary operators working on the binary equivalents and they are obtained from Boolean algebra. These are or, and, basic inverter or basic not and xor. The word basic is used before the ordinary inverter to differentiate it from other special inverters that will be discussed later. Also there are some compound basic operators like basic nand, basic nor and basic xnor.

Here we propose some special operators to facilitate the development of quaternary algebra. They are all single-input operators and very useful in designing complex logic circuits. These special operators are:

(a) Outward inverter or full inverter

(b) Inward inverter or half inverter

(c) Binary bitswap

978-1-4244-6283-4/09/$26.00 ©2009 IEEE

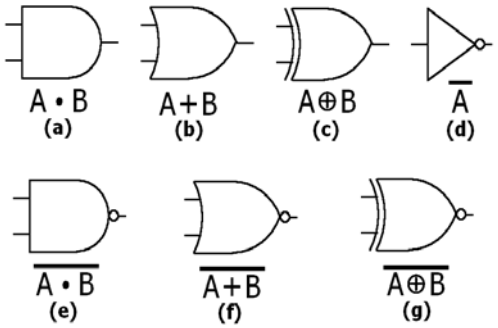

Fig. 1. Circuit symbols for the basic quaternary operators; (a) and, (b) or, (c) xor, (d) basic not, (e) basic nand, (f) basic nor, (g) basic xnor .

The outward inverter inverts the input just like the basic inverter, but after that it changes the asymmetrical values to nearest symmetrical values. That means the outward inverter will invert 0, 1 into 3 and 2, 3 into 0. Thus, for outward inverter, no matter whether the input is symmetrical or not, the output is always symmetrical i.e. 0 or 3.

The operator is named as outward or full inverter because it pushes the output of a basic inverter to the nearest marginal value of the domain of quaternary number which is 0 or 3. It can also be named as symmetrical inverter.

The inward inverter inverts the input just like the basic inverter, but after that it changes the symmetrical values to nearest asymmetrical values. That means the outward inverter will invert 0, 1 into 2 and 2, 3 into 1. Thus, for outward inverter, no matter whether the input is symmetrical or not, the output is always asymmetrical i.e. 1 or 2.

This operator is called inward or half inverter since the output is never a marginal value of quaternary domain. Instead the range of the output spans half of the total range of the quaternary domain. It can also be named as asymmetrical inverter.

The binary bitswap swaps the two bits of the binary-equivalent of the quaternary operand. It leaves the symmetrical numbers unchanged but inverts (basic inversion) the asymmetrical numbers. That is why it is classified as a special inverter-like operator.

Like basic inverter, bitswap operator and special inverters can be cascaded with other operators to form compound operators such as inward nand, outward nor, bitswap xor, etc. Circuit symbols for special operators and their compound derivatives are shown in Fig. 2.

The bitswap operator distinguishes between the symmetrical and asymmetrical inputs, so it can be used to identify a symmetrical input.

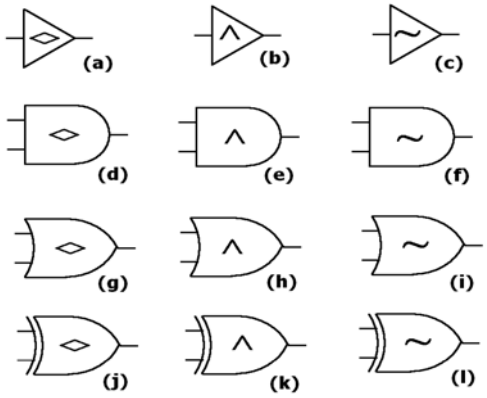

Fig. 2. Circuit symbols for the special quaternary operators and their derivatives: (a) Inward inverter; (b) Outward inverter; (c) Binary bitswap; (d) Inward nand; (e) Outward nand; (f) Bitswap and; (g) Inward nor; (h) Outward nor; (i) Bitswap or; (j) Inward xnor; (k) Outward xnor; (l) Bitswap xor.

Circuit symbols for special operators and their compound derivatives are shown in Fig. 2. The mathematical definitions of the special operators are given below:

$$\text{Inward Inverter, } a' = \begin{cases} \overline{a}.2 & ; a < 2 \\ \overline{a} + 1 & ; a > 1 \end{cases} \quad (1)$$

$$\text{Outward Inverter, } \hat{a} = \begin{cases} \overline{a} + 3 & ; a < 2 \\ \overline{a}.0 & ; a > 1 \end{cases} \quad (2)$$

$$\text{Binary Bitswap, } \tilde{a} = \begin{cases} \overline{a} & ; a \text{ asymmetric} \\ a & ; a \text{ symmetric} \end{cases} \quad (3)$$

The special operators are necessary for designing logic circuits. Among them, binary bitswap is the most important one. It is used to define equality operator, which gives the sum of product (SOP) expression of a quaternary function. The equality operator is written as a^b which means "compare a with b". It is defined as

$$a^b = b^a = \begin{cases} \overline{a}.a & ; a \neq b \\ \overline{a} + a & ; a = b \end{cases} = \begin{cases} 0 & ; a \neq b \\ 3 & ; a = b \end{cases} \quad (4)$$

Table I Basic Quaternary Multi-input Operators

A	B	AND	OR	XOR	BASIC NAND	BASIC NOR	BASIC XNOR
0	0	0	0	0	3	3	3
0	1	0	1	1	3	2	2
0	2	0	2	2	3	1	1
0	3	0	3	3	3	0	0
1	1	1	1	0	2	2	3
1	2	0	3	3	3	0	0
1	3	1	3	2	2	0	1
2	2	2	2	0	1	1	3
2	3	2	3	1	1	0	2
3	3	3	3	0	0	0	3

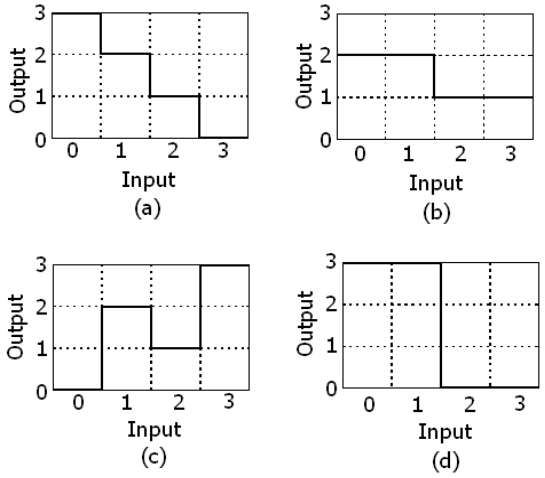

Fig. 3. Transfer functions of the quaternary inverters and inverter-like operators: (a) Basic Inverter; (b) Inward or Half Inverter; (c) Binary Bitswap; (d) Outward or Full Inverter.

The basic inverter and binary bitswap can be decomposed into outward and inward inverters using the following expressions:

$$\overline{a} = \begin{cases} \hat{a} \ ; \ a \text{ symmetric} \\ a' \ ; \ a \text{ asymmetric} \end{cases} = \begin{cases} \hat{a} \ ; \ a = 0, 3 \\ a' \ ; \ a = 1, 2 \end{cases} \quad (5)$$

$$\tilde{a} = \begin{cases} a \ ; \ a \text{ symmetric} \\ a' \ ; \ a \text{ asymmetric} \end{cases} = \begin{cases} a \ ; \ a = 0, 3 \\ a' \ ; \ a = 1, 2 \end{cases} \quad (6)$$

Since inward and outward inverters can be made of simple CMOS circuits using multi-threshold technology [5], these expressions are useful to construct basic inverter and binary bitswap operator using such simpler circuits. It is anticipated that in near future, using novel devices like FinFET, G4-FET or SiNW-FET, it might be possible to implement basic inverter and binary bitswap without using their decomposed versions.

III. ELEMENTARY QUATERNARY ALGEBRA

The proposed quaternary logic scheme has its own algebra just like Boolean algebra in binary logic. Since basic operators are actually bitwise binary operators, the properties and axioms of Boolean algebra are applicable for basic quaternary operators. These include commutativity, associativity, distributivity, etc.

Apart from the basic properties, the special operators have many other important properties of their own. These properties are indispensable in designing quaternary logic circuits. Some of these properties are as follows:

$$\overline{\overline{a}} = a, \quad \tilde{\tilde{a}} = a, \quad a'' \neq a, \quad \hat{\hat{a}} \neq a \quad (7)$$

$$\tilde{a'} = \begin{cases} a + 1 \ ; \ a < 2 \\ a.2 \ ; \ a > 1 \end{cases} \quad (8)$$

$$\tilde{a} + a = \begin{cases} 3 \ ; \ a \neq 0 \\ 0 \ ; \ a = 0 \end{cases} \quad (9)$$

$$\tilde{a}.a = \begin{cases} 3 \ ; \ a = 3 \\ 0 \ ; \ a \neq 3 \end{cases} \quad (10)$$

$$\tilde{a} \oplus a = \begin{cases} 3 \ ; \ a \text{ asymmetric} \\ 0 \ ; \ a \text{ symmetric} \end{cases} \quad (11)$$

$$a'.\hat{a} = \begin{cases} 0 \ ; \ a > 1 \\ 2 \ ; \ a < 2 \end{cases} \quad (12)$$

$$a' + \hat{a} = \begin{cases} 1 \ ; \ a > 1 \\ 3 \ ; \ a < 2 \end{cases} \quad (13)$$

A. DE MORGAN'S THEOREM IN FULL INVERTER

The modified version of De Morgan's theorem holds true for outward inverter:

$$(a \hat{+} b) = \hat{a}.\hat{b} \text{ and } (\hat{a.b}) = \hat{a} + \hat{b} \quad (14)$$

The following three cases need to be considered for the verification of this statement.

1. $a > 1, b < 2$
2. $a > 1, b > 1$
3. $a < 2, b < 2$

If $x > 1$, $\hat{x} = 0$ and if $x < 2$, $\hat{x} = 3$

1. $a > 1$, $b < 2$; so $a + b > 1$ and $a.b < 2$

From definition $\hat{a}=0$, $\hat{b}=3$ and $(a \hat{+} b)=0, (\hat{a.b})=3$

$\therefore (a \hat{+} b) = \hat{a}.\hat{b}$ and $(\hat{a.b}) = \hat{a} + \hat{b}$

2. $a > 1$, $b > 1$; so $a + b > 1$ and $a.b > 1$

Now $\hat{a} = \hat{b} = 0$ and $(a \hat{+} b) = (\hat{a.b}) = 0$

$\therefore (a \hat{+} b) = \hat{a}.\hat{b}$ and $(\hat{a.b}) = \hat{a} + \hat{b}$

3. $a < 2$, $b < 2$; so $a + b < 2$ and $a.b < 2$

Therefore $\hat{a} = \hat{b} = 3$ and $(a \hat{+} b) = (\hat{a.b}) = 3$

$\therefore (a \hat{+} b) = \hat{a}.\hat{b}$ and $(\hat{a.b}) = \hat{a} + \hat{b}$

Thus the modified form of De Morgan's theorem holds true for outward inverter.

B. DE MORGAN'S THEOREM IN HALF INVERTER

De Morgan's theorem does not hold true for inward inverter. Actually, the distribution of inward inverter over basic operators can not be expressed through a simple relation. Therefore

$$\left.\begin{array}{l} (a + b)' \neq a'.b' \text{ and } (a'.b') \neq a' + b' \\ (a + b)' \neq a' + b' \text{ and } (a'.b') \neq a'.b' \end{array}\right\} \quad (15)$$

To verify the validity of this statement the following three cases need to be considered.

1. $a > 1, b < 2$
2. $a > 1, b > 1$
3. $a < 2, b < 2$

If $x > 1$, $x' = 1$ and if $x < 2$, $x' = 2$

1. $a > 1$ and $b < 2$, so $a + b > 1$ and $a.b < 2$

$\therefore a' = 1, b' = 2, (a + b)' = 1$ and $(a.b)' = 2$

Clearly $(a + b)' \neq a'.b' \neq a' + b'$ and

$(a.b)' \neq a' + b' \neq a'.b'$

2. $a > 1,\ b > 1$; so $a' = b' = 1$

From definition $(a+b)' = (a.b)' = 1$

$\therefore (a + b)' = a'.b'$ and $(a.b)' = a' + b'$

3. $a < 2,\ b < 2$; so $a' = b' = 2$

From definition $(a+b)' = (a.b)' = 2$

$\therefore (a + b)' = a'.b'$ and $(a.b)' = a' + b'$

So when both operands are less than 2 or greater than 1, only then De Morgan's theorem can be extended for inward inverter. In general this is not valid for inward inverter.

C. DE MORGAN'S THEOREM IN BINARY BITSWAP

De Morgan's theorem does not hold true for binary bitswap, the actual relation is:

$$(a \tilde{+} b) = \tilde{a} + \tilde{b} \quad \text{and} \quad (a \tilde{.} b) = \tilde{a}.\tilde{b} \qquad (16)$$

To verify the validity of this statement the following three cases need to be considered.

1. a = symmetric , b = asymmetric
2. both a and b are symmetric
3. both a and b are asymmetric

Binary Bitswap, $\tilde{x} = \begin{cases} \overline{x} & ; \ x \text{ asymmetric} \\ x & ; \ x \text{ symmetric} \end{cases}$

1. From the definition of symmetry, $\tilde{a} = a,\ \tilde{b} = \overline{b}$

$\therefore a \tilde{+} b = \begin{cases} a & ; a = 3 \\ \overline{b} & ; a = 0 \end{cases}$; $a \tilde{.} b = \begin{cases} \overline{b} & ; a = 3 \\ 0 & ; a = 0 \end{cases}$

Now $\tilde{a}.\tilde{b} = a.\overline{b} = \begin{cases} \overline{b} & ; a = 3 \\ 0 & ; a = 0 \end{cases}$

Again $\tilde{a} + \tilde{b} = a + \overline{b} = \begin{cases} a & ; a = 3 \\ \overline{b} & ; a = 0 \end{cases}$

$\therefore a \tilde{+} b = \tilde{a} + \tilde{b}$ and $a \tilde{.} b = \tilde{a}.\tilde{b}$

2. Since both operands are symmetric, $\tilde{a} = a,\ \tilde{b} = b$

Now $a \tilde{+} b = a + b$; $a \tilde{.} b = a.b$

$\therefore a \tilde{+} b = \tilde{a} + \tilde{b}$ and $a \tilde{.} b = \tilde{a}.\tilde{b}$

3. Both operands are asymmetric, so $\tilde{a} = \overline{a},\ \tilde{b} = \overline{b}$

If $a = b$, $a \tilde{+} b = a + b$ and $a \tilde{.} b = a.b$

Again if $a \neq b$, it is obvious that $b = \overline{a}$

Here both $a + b$ and $a.b$ are symmetric.

$\therefore a \tilde{+} b = \tilde{a} + \tilde{b}$ and $a \tilde{.} b = \tilde{a}.\tilde{b}$

Thus considering all three cases it is obvious that the correct relations regarding the distributivity of bitswap over AND and OR gates are

$$a \tilde{+} b = \tilde{a} + \tilde{b} \quad \text{and} \quad a \tilde{.} b = \tilde{a}.\tilde{b}$$

D. PROPERTIES OF SPECIAL OPERATORS

The special quaternary operators have some special properties. These properties are useful when the special operators are cascaded with other single input operators (unary operators i.e. inverters) and compound basic operators like xor. It is observed that bitswap operator has a very interesting property; it can be distributed over any basic operator, not only just and, or operators. The last property listed below shows this where bitswap is found to be distributed over xor.

(i) The order of basic inversion and outward inversion can be interchanged. The basic inversion of a followed by the outward inversion can be written as

$$\hat{\overline{a}} = (\hat{3-a}) = \begin{cases} 3; & a > 1 \\ 0; & a < 2 \end{cases}$$

Similarly the outward inversion of a followed by the basic inversion can be written as

$$\overline{\hat{a}} = (3-\hat{a}) = \begin{cases} 0; & a < 2 \\ 3; & a > 1 \end{cases}$$

Therefore we can write $\hat{\overline{a}} = \overline{\hat{a}}$ (17)

(ii) The order of inward inversion and outward inversion can not be interchanged. The inward inversion of a followed by the outward inversion can be written as

$$(\hat{a'}) = \begin{cases} (\hat{\overline{a}.2}) \ ; a < 2 \\ (\hat{\overline{a}+1}) \ ; a > 1 \end{cases} = \begin{cases} 0 \ ; a < 2 \\ 3 \ ; a > 1 \end{cases}$$

Similarly the outward inversion of a followed by the inner inversion can be expressed as follows

$$(\hat{a})' = \begin{cases} (\overline{a} + 3)' \ ; & a < 2 \\ (\overline{a}.0)' \ ; & a > 1 \end{cases} = \begin{cases} 1 \ ; & a < 2 \\ 2 \ ; & a > 1 \end{cases}$$

From above we can write $(\hat{a'}) \neq (\hat{a})'$ (18)

(iii) The order of basic inversion and inward inversion can be interchanged. To prove this we can write the basic inversion of a followed by inward inversion as below

$$(\overline{a})' = (3-a)' = \begin{cases} 2 ; & a > 1 \\ 1 ; & a < 2 \end{cases}$$

Similarly the inward inversion of a followed by basic inversion can be expressed as

$$(\overline{a'}) = \begin{cases} (\overline{\overline{a}.2}) \ ; a<2 \\ (\overline{\overline{a}+1}) \ ; a>1 \end{cases} = \begin{cases} 1 \ ; a < 2 \\ 2 \ ; a > 1 \end{cases}$$

Therefore we can write $(\overline{a})' = (\overline{a'})$ (19)

(iv) The order of bitswap and basic inversion can be interchanged. We can write the bitswap of a followed by basic inversion as

$$\overline{\tilde{a}} = \begin{cases} \overline{\overline{a}} \ ; \ a \text{ asymmetric} \\ \overline{a} \ ; \ a \text{ symmetric} \end{cases} = \begin{cases} a \ ; \ a \text{ asymmetric} \\ \overline{a} \ ; \ a \text{ symmetric} \end{cases}$$

Similarly the opposite operation can be shown as

$$\tilde{\overline{a}} = \begin{cases} \overline{a} \ ; \ a \text{ symmetric} \\ \overline{\overline{a}} \ ; \ a \text{ asymmetric} \end{cases} = \begin{cases} \overline{a} \ ; \ a \text{ symmetric} \\ a \ ; \ a \text{ asymmetric} \end{cases}$$

So we can write $\overline{\tilde{a}} = \tilde{\overline{a}}$ (20)

(v) The order of outward inversion and bitswap can

not be interchanged. The property can be proved considering the symmetry of qudits. We can write

$$\tilde{\hat{a}} = \begin{cases} \hat{a} \; ; \; a \text{ symmetric} \\ \hat{a} \; ; \; a \text{ asymmetric} \end{cases} ; \quad \hat{\tilde{a}} = \begin{cases} \hat{\tilde{a}} \; ; \; a \text{ asymmetric} \\ \hat{a} \; ; \; a \text{ symmetric} \end{cases}$$

So it is obvious that $\tilde{\hat{a}} \neq \hat{\tilde{a}}$ (21)

(vi) The order of bitswap and inward inversion can not be altered. One direct consequence of (19) is

$$(\tilde{a'}) = \begin{cases} (\overline{a'}); \; a \text{ symmetric} \\ (\overline{a'}); \; a \text{ asymmetric} \end{cases} = a''$$

Again the interchange of both the operators reveals that,

$$(\tilde{a})' = \begin{cases} (\overline{a})' \; ; \; a \text{ asymmetric} \\ a' \; ; \; a \text{ symmetric} \end{cases} = \begin{cases} a'' \; ; \; a \text{ asymmetric} \\ a' \; ; \; a \text{ symmetric} \end{cases}$$

These expressions imply that $(\tilde{a'}) \neq (\tilde{a})'$ (22)

(vii) The distribution of bitswap operator over quaternary xor gate can be obtained from (20) as shown below

$$\tilde{a} \oplus \tilde{b} = \left(\tilde{a}.\overline{\tilde{b}} + \tilde{b}.\overline{\tilde{a}}\right) = \left(\tilde{a}.\tilde{\overline{b}} + \tilde{b}.\tilde{\overline{a}}\right) = (\tilde{a.\overline{b}}) + (\tilde{b.\overline{a}})$$

Similarly, distribution of bitswap operator implies,

$$(\tilde{a \oplus b}) = \left(a.\overline{b} \; \tilde{} + b.\overline{a}\right) = (\tilde{a.\overline{b}}) + (\tilde{b.\overline{a}})$$

Thus, we find that, $\tilde{a} \oplus \tilde{b} = (\tilde{a \oplus b})$ (23)

E. THE EQUALITY OPERATOR

The equality operator compares two values and returns 3 if they are identical and 0 if they are different. The circuit can be built in several ways. Three such ways are shown in Fig. 4.

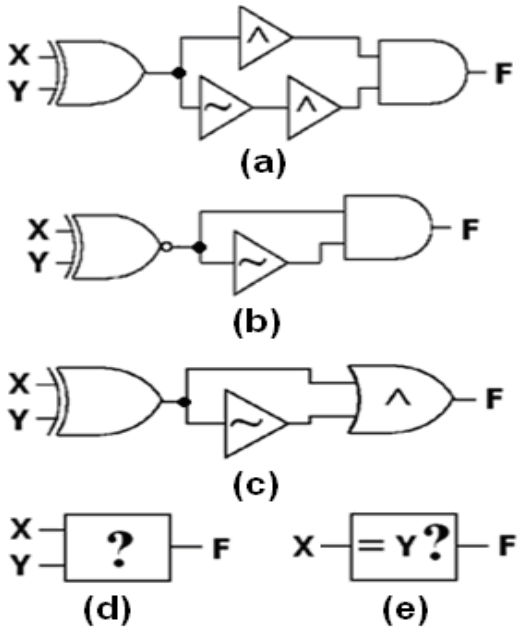

Fig. 4. (a) - (c) Quaternary equality operator, (d) circuit symbol for equality operator, (e) compact circuit symbol for equality operator.

The SOP expression of a function has several minterms; but unlike binary minterms, they correspond to functional values among 1, 2 and 3. So we can use equality blocks to compare the inputs with minterm components and then having the results fed to an and gate along with the functional value. For many cases we need to minimize the SOP expression for optimization. Different logic schemes offer different forms of SOP expressions [6], but minimization is necessary for optimum design of a system. As an example of minimization according to our proposed algebra, here we present the quaternary Galois Field addition operator in terms of our logic scheme. Here "+" denotes the output of GF4 addition operation.

Table II Quaternary Galois Field Addition (GF4+)

A	B	+	A	B	+	A	B	+	A	B	+
0	0	0	1	0	1	2	0	2	3	0	3
0	1	1	1	1	0	2	1	3	3	1	2
0	2	2	1	2	3	2	2	0	3	2	1
0	3	3	1	3	2	2	3	1	3	3	0

The minimization is done as follows:

$$\begin{aligned} F_{add}(a,b) = {} & a^0.b^0.0 + a^0.b^1.1 + a^0.b^2.2 + a^0.b^3.3 \\ & + a^1.b^0.1 + a^1.b^1.0 + a^1.b^2.3 + a^1.b^3.2 \\ & + a^2.b^0.2 + a^2.b^1.3 + a^2.b^2.0 + a^2.b^3.1 \\ & + a^3.b^0.3 + a^3.b^1.2 + a^3.b^2.1 + a^3.b^3.0 \\ = {} & a^0.b + a^1.(b.2 + \overline{b}.1) + a^2.(b.1 + \overline{b}.2) + a^3.\overline{b} \\ \therefore \; & F_{add}(a,b) = a.\overline{b} + \overline{a}.b = a \oplus b \end{aligned} \quad (24)$$

IV. DESIGN OF SOME QUATERNARY CIRCUITS

Our proposed quaternary operators can be used to design many important and frequently used logic circuits. Here we present the designs of quaternary decoder, multiplexer and half adder along with their truth tables.

A. QUATERNARY DECODER AND MULTIPLEXER

The truth tables of quaternary 4-to-1 multiplexer and 1-to-4 decoder are shown in Table III. Here $L_0 - L_3$ are decoder outputs, F is multiplexer output, $D_0 - D_3$ are multiplexer inputs. Selector is common for both devices.

Table III Quaternary Decoder and Multiplexer

Selector	L_0	L_1	L_2	L_3	F
0	3	0	0	0	D_0
1	0	3	0	0	D_1
2	0	0	3	0	D_2
3	0	0	0	3	D_3

The quaternary decoder can be designed using equality operator, and this decoder can be used to form multiplexer. This is shown in Fig. 5.

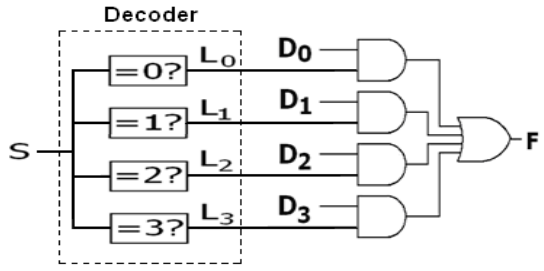

Fig. 5. A quaternary 4-to-1 multiplexer using a 1-to-4 decoder. The dotted rectangle shows the decoder.

B. QUATERNARY HALF-ADDER

It is possible to build quaternary half-adder using the basics we have already developed. The truth table of single-digit quaternary addition is shown Table IV. Here S is sum and C is carry.

Table IV Quaternary Half-adder

X	Y	S	C	X	Y	S	C	X	Y	S	C	X	Y	S	C
0	0	0	0	1	0	1	0	2	0	2	0	3	0	3	0
0	1	1	0	1	1	2	0	2	1	3	0	3	1	0	1
0	2	2	0	1	2	3	0	2	2	0	1	3	2	1	1
0	3	3	0	1	3	0	1	2	3	1	1	3	3	2	1

The quaternary half-adder circuit is designed using SOP simplification techniques as described earlier. The circuit is shown in Fig. 6.

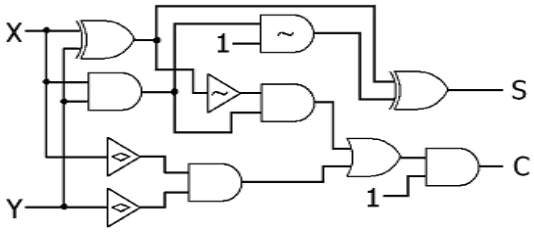

Fig. 6. Quaternary half-adder circuit.

V. CONCLUSION

In this paper we have proposed a new quaternary logic system. A set of operators are defined; some of which are closely related to Boolean operators, others are chosen for special purposes. Many properties of these operators are presented here and a functional quaternary algebra is developed. This new quaternary system is capable of handling ordinary quaternary inputs as well as coupled-binary inputs. We have also formulated a method for expressing an arbitrary function in SOP form. Using the proposed logic system, we have designed some very useful logic blocks such as decoder, multiplexer and half-adder. These designs are simpler than many other alternative designs present in the literature [7]. The logic blocks shown in this work can be implemented using novel electronic and photonic technologies such as double pass transistor logic [8], all-optical quaternary technology [9], etc. In [10], we have shown more details on the design of combinational logic blocks based on this scheme.

REFERENCES

[1] Inaba, M.; Tanno, K.; Ishizuka, O.; "Realization of NMAX and NMIN functions with multi-valued voltage comparators", Proceedings, 31st IEEE International Symposium on Multiple-Valued Logic (ISMVL), pp.27 - 32 , 22-24 May, 2001.

[2] Khan, M. H. A.; "Quantum Realization of Quaternary Feynman and Toffoli Gates", Proceedings, 4th International Conference on Electrical and Computer Engineering (ICECE), pages: 157 – 160, 19-21 December 2006.

[3] http://www.ternarylogic.com

[4] Hurst, S. L; "Multiple-Valued Logic – Its Status and Its Future", Computers, IEEE Transactions on Vol. C-33, Issue: 12, pp.1160-1179, Dec. 1984.

[5] Cunha, R.; Boudinov, H.; Carro, L.; "Quaternary Look-up Tables Using Voltage-Mode CMOS Logic Design", Proceedings, 37th IEEE International Symposium on Multiple-Valued Logic (ISMVL), pp.56 - 56 , 13-16 May, 2007.

[6] Khan, M. H. A.; Perkowski, M. A.; Kerntopf, P.; "Multi-Output Galois Field Sum of Products Synthesis with New Quantum Cascades", Proceedings, 33rd IEEE International Symposium on Multiple-Valued Logic (ISMVL), pp.146 - 153 , 16-19 May, 2003.

[7] Khan, M. M. M.; Biswas, A. K.; Chowdhury, S.; Tanzid, M.; Mohsin, K. M.; Hasan, M.; Khan, A. I.; "Quantum realization of some quaternary circuits", Proceedings, TENCON 2008, IEEE Region 10 Conference, 19-21 Nov. 2008.

[8] Park, S. J.; Yoon, B. H.; Yoon, K. S.; Kim, H. S.; "Design of quaternary logic gate using double pass-transistor logic with neuron MOS down literal circuit", Proceedings, 34th IEEE International Symposium on Multiple-Valued Logic (ISMVL), pp.198 - 203 , 19-22 May, 2004.

[9] Chattopadhyay, T.; Roy, J. N.; "Polarization-encoded all-optical quaternary multiplexer and demultiplexer – A proposal", Optik - International Journal for Light and Electron Optics, In Press, Corrected Proof, 11 June 2008.

[10] Jahangir, I.; Hasan, D. M. N.; Reza, M. S.; "Design of Some Quaternary Combinational Logic Blocks Using a New Logic System", Proceedings, TENCON 2009, IEEE Region 10 Conference, 23-26 Nov. 2009, to be published.

Proceedings of 2009 12th International Conference on Computer and Information Technology (ICCIT 2009)
21-23 December, 2009, Dhaka, Bangladesh

Design of Quaternary Sequential Circuits Using a Newly Proposed Quaternary Algebra

Ifat Jahangir*, Dihan Md. Nuruddin Hasan†, Nahian Alam Siddique†, Shajid Islam‡, Md. Mehedi Hasan‡

† Dept. of Electrical and Electronic Engineering, Bangladesh University of Engineering and Technology, Dhaka-1000, Bangladesh

‡ Dept. of Electrical, Electronics and Communication Engineering, Military Institute of Science and Technology, Mirpur Cantonment, Dhaka-1216, Bangladesh

ifat00@gmail.com

Abstract

Using a novel quaternary algebra, several sequential circuits are designed. The quaternary logic scheme used here is obtained by extending Boolean algebra into quaternary domain. A set of operators capable of handling both coupled-binary and ordinary inputs are used to design the sequential circuit elements such as latches, flip-flops, registers and counters. Sufficient conditions for stable operation of the sequential blocks are derived mathematically and demonstrated graphically using simulated timing diagrams.

Keywords: Counters, flip-flops, latches, registers, quaternary sequential circuits.

I. INTRODUCTION

At the beginning of modern electronics, almost all the devices were analog. With the development of electronic devices, digital circuits have gradually replaced analog circuits in many cases. In the fields of communication and computation, digital technology is mostly dominant because it performs better in preventing noise contamination, reliable storage and processing of data and so on. For many years digital system has been represented by binary numbers 0 and 1. Boolean algebra is used as the backbone of binary logic and hence it governs the design of all digital circuits. With the development of multi-gate and gate-all-around devices like G4-FET, Silicon Nanowire FET, Carbon Nanotube FET, FinFET, etc., it is now possible to implement circuits for more complicated logic systems [1]. These novel devices can be used more effectively if we move beyond binary logic. Some multi-valued logic systems such as ternary and quaternary logic schemes have been developed and they are being experimented for a long time [2]. These logic systems are often derived from Fuzzy logic or Galois field theory [3]. It is clear that a binary system can be converted into a quaternary system by coupling each pair of consecutive bits of a binary bit stream to form a quaternary bit stream. Then the binary system can be replaced by an equivalent quaternary system.

The quaternary system has several advantages over binary logic [4]. Since it requires half number of digits than equivalent binary data, it is good for storage. In quaternary system more information is contained in a single digit, so it requires less parallel circuits to process same amount of data than that needed in binary system. Newer devices offer flexible yet sophisticated design opportunities which can be utilized more efficiently and meaningfully if quaternary system is adopted.

In our recent works [5],[6], we proposed a novel quaternary logic close to Boolean algebra. It extends binary functions in quaternary, at the same time incorporates some new functions of its own. Extending Boolean algebra makes this logic system ideal for replacing binary logic as its logic blocks are compatible with their binary counterparts. In this work, we begin with a brief introduction to the elements of the new logic system and then we present the design of some important sequential logic blocks like latches, flip-flops, registers and counters.

II. QUATERNARY ALGEBRA

Quaternary states (0, 1, 2, 3) can be imagined as 2-bit binary equivalents 00, 01, 10, 11. They are named as absolute low, medium low, medium high and absolute high respectively. If the bits of the binary equivalent interchange their positions and still the quaternary state remains unchanged, then it is said to have binary symmetry; otherwise it is asymmetrical. Thus 0, 3 are symmetrical and 1, 2 are asymmetrical. When stated as a number, a single quaternary digit is called a qudit.

The basic quaternary operators are very similar to binary operators and they are obtained from Boolean algebra. They are or, and, basic inverter, xor, basic nand, basic nor, basic xnor (Fig. 1(a)-(g)). The word basic is used before the ordinary inverter to differentiate it from other special inverters.

The logic we have proposed in our other works contains some special operators to facilitate the development of quaternary algebra [5],[6]. These operators are useful in defining various logic blocks and expressing arbitrary functions in sum-of-product forms. The logic scheme is well-suited for both ordinary quaternary and coupled-binary inputs. The special operators are:

(a) Outward inverter or full inverter
(b) Inward inverter or half inverter
(c) Binary bitswap

The outward inverter (Fig. 1(l)) changes 0, 1 to 3 and 2, 3 to 0. The inward inverter (Fig. 1(h)) changes 0, 1 to 2 and 2, 3 to 1.

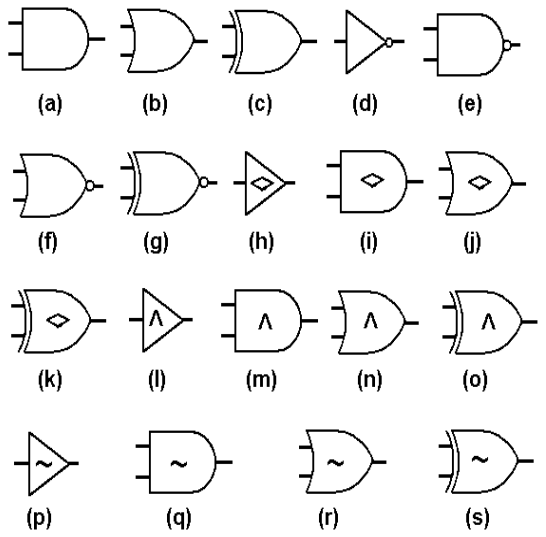

Fig. 1. Circuit symbols for the quaternary operators. (a) and; (b) or; (c) xor; (d) basic NOT; (e) basic nand; (f) basic nor, (g) basic xnor; (h) Inward Inverter; (i) Inward nand; (j) Inward nor; (k) Inward xnor; (l) Outward Inverter; (m) Outward nand; (n) Outward nor; (o) Outward xnor; (p) Binary Bitswap; (q) Bitswap and; (r) Bitswap or; (s) Bitswap xor.

The binary bitswap (Fig. 1(p)) swaps the two bits of the binary-equivalent of the quaternary operand. It leaves the symmetrical numbers unchanged but inverts (basic inversion) the asymmetrical numbers. That is why it is classified as a special inverter-like operator.

Among the special operators, binary bitswap is the most important one. It is used to define equality operator, which gives the sum of product (SOP) expression of a quaternary function. The equality operator is written as a^b which means "compare a with b". It is defined as

$$a^b = b^a = \begin{cases} \overline{a}.a & ; a \neq b \\ \overline{a} + a & ; a = b \end{cases} = \begin{cases} 0 & ; a \neq b \\ 3 & ; a = b \end{cases} \quad (1)$$

Table I Basic Quaternary Multi-input Operators

A	B	AND	OR	XOR	BASIC NAND	BASIC NOR	BASIC XNOR
0	0	0	0	0	3	3	3
0	1	0	1	1	3	2	2
0	2	0	2	2	3	1	1
0	3	0	3	3	3	0	0
1	1	1	1	0	2	2	3
1	2	0	3	3	3	0	0
1	3	1	3	2	2	0	1
2	2	2	2	0	1	1	3
2	3	2	3	1	1	0	2
3	3	3	3	0	0	0	3

Table II Quaternary Single-input Operators

A	BASIC NOT $\overline{A}$	INWARD NOT A'	OUTWARD NOT $\hat{A}$	BINARY BITSWAP $\tilde{A}$
0	3	2	3	0
1	2	2	3	2
2	1	1	0	1
3	0	1	0	3

Like binary Boolean algebra, the proposed quaternary logic scheme has its own algebra. Since it has evolved from Boolean algebra, the properties and axioms of Boolean algebra are applicable for basic quaternary operators. These include commutativity, associativity, distributivity, etc.

Apart from the basic properties, the special operators have many other important properties of their own [5]. These properties are indispensable in designing quaternary logic circuits. Some of these properties are as follows:

$$\overline{\overline{a}} = a, \quad \tilde{\tilde{a}} = a, \quad a'' \neq a, \quad \hat{\hat{a}} \neq a \quad (2)$$

$$\tilde{a'} = \begin{cases} a+1 & ; a < 2 \\ a.2 & ; a > 1 \end{cases} \quad (3)$$

$$\tilde{a} + a = \begin{cases} 3 & ; a \neq 0 \\ 0 & ; a = 0 \end{cases} \quad (4)$$

$$\tilde{a}.a = \begin{cases} 3 & ; a = 3 \\ 0 & ; a \neq 3 \end{cases} \quad (5)$$

$$\tilde{a} \oplus a = \begin{cases} 3 & ; a \text{ asymmetric} \\ 0 & ; a \text{ symmetric} \end{cases} \quad (6)$$

$$a'.\hat{a} = \begin{cases} 0 & ; a > 1 \\ 2 & ; a < 2 \end{cases} \quad (7)$$

$$a' + \hat{a} = \begin{cases} 1 & ; a > 1 \\ 3 & ; a < 2 \end{cases} \quad (8)$$

$$(a \hat{+} b) = \hat{a}.\hat{b} \text{ and } (\hat{a.b}) = \hat{a} + \hat{b} \quad (9)$$

$$(a \tilde{+} b) = \tilde{a} + \tilde{b} \text{ and } (\tilde{a.b}) = \tilde{a}.\tilde{b} \quad (10)$$

$$\left.\begin{array}{l} (a+b)' \neq a'.b', \ (a'.b') \neq a'+b' \\ (a+b)' \neq a'+b', \ (a'.b') \neq a'.b' \end{array}\right\} \quad (11)$$

$$\left.\begin{array}{l} \hat{\overline{a}} = \overline{\hat{a}}, \ (\hat{a'}) \neq (\hat{a})', \ (\overline{a})' = (\overline{a'}) \\ \overline{\tilde{a}} = \tilde{\overline{a}}, \ \tilde{\hat{a}} \neq \hat{\tilde{a}}, \ (\tilde{a'}) \neq (\tilde{a})' \end{array}\right\} \quad (12)$$

$$\tilde{a} \oplus \tilde{b} = (a \tilde{\oplus} b) \quad (13)$$

The equality operator mentioned in (1) is built using the properties given above. It compares two values and returns 3 if they are identical and 0 if they are different. The operation can be performed using following equations:

$$\left.\begin{array}{l} Z = X \oplus Y \\ F = \hat{Z}.\tilde{Z} \end{array}\right\} \quad (14)$$

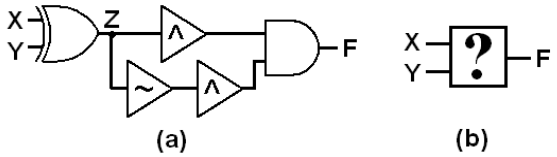

Fig. 2. (a) Quaternary equality operator using a binary bitswap and two outward inverters; (b) Circuit symbol for equality operator.

III. QUATERNARY SEQUENTIAL CIRCUITS

Sequential circuits are necessary when we aim to meet the requirement of memory operation. The basic challenges for an efficient sequential logic block are critical races, metastability and unwanted propagation delay [7]. The quaternary algebra we have developed can be used to develop combinational [6] and sequential circuits.

A. QUATERNARY LATCHES

Like binary latches, quaternary latches can be constructed. For example, a binary S-R latch can be made by using two nand or nor gates. We can do the same thing by using quaternary basic nand or nor gates. The latch has two outputs Q and Q' which should be complementary as is the case in binary latches. Besides, for all input combinations Q should either follow the state of S or remain unchanged, but it should not go to any other state. It should not oscillate between states at any situation. But for the quaternary S-R latches built with nand or nor gates, outputs deviate from such standard behavior.

The conditions for stable and glitch-free operation of S-R latch can be derived mathematically. The latch is said to be stable and glitch-free if the following two conditions are satisfied:

(i) The outputs follow any changes made to the inputs after some propagation delay regardless of the past and present states of the inputs. If the circuit exhibits undue delay in following particular input combinations or assumes some intermediate states before following the inputs, then it is referred to as a glitch.

(ii) The output states remain unchanged as long as the inputs are unchanged, it is called stable operation.

For nor-nor latch we can derive the conditions for proper operation by starting from arbitrary input and output combinations. Here we assume that the propagation delay due to each nor gate is identical and it remains constant for all possible input and output combinations.

Let us assume that at a time t_0 the outputs are $Q(t_0)$ and $Q'(t_0)$. These are initial conditions. Now we calculate the outputs for t_1 and t_2 , two arbitrary times following t_0. The inputs remain constant at these instances and they are $S(t_0) = S(t_1) = S(t_2) = S$ and $R(t_0) = R(t_1) = R(t_2) = R$. The outputs are obtained mathematically.

$$Q(t_1) = \overline{R(t_1) + Q'(t_0)} = \overline{R(t_1)} \cdot \overline{Q'(t_0)} = \overline{R} \cdot \overline{Q'(t_0)}$$

$$Q'(t_1) = \overline{S(t_1) + Q(t_0)} = \overline{S(t_1)} \cdot \overline{Q(t_0)} = \overline{S} \cdot \overline{Q(t_0)}$$

$$Q(t_2) = \overline{R} \cdot \overline{Q'(t_1)} = \overline{R} \cdot [S + Q(t_0)]$$

$$Q'(t_2) = \overline{S} \cdot \overline{Q(t_1)} = \overline{S} \cdot [R + Q'(t_0)]$$

For the desired performance as described earlier, the outputs and inputs are related by the following relations.

$$Q(t_1) = Q(t_2) = S \tag{15}$$

$$Q'(t_1) = Q'(t_2) = R \tag{16}$$

From (15) and (16), we can write

$$\overline{R} \cdot \overline{Q'(t_0)} = S \tag{17a}$$

$$\overline{R} \cdot [S + Q(t_0)] = S \tag{17b}$$

$$\overline{S} \cdot \overline{Q(t_0)} = R \tag{18a}$$

$$\overline{S} \cdot [R + Q'(t_0)] = R \tag{18b}$$

Since (17b) and (18b) relate the outputs with the inputs at t_2 , they are used to justify condition of stability. The condition for glitch-free operation is reflected in (17a) and (18a). Inverting (17b) we find that

$$R + \overline{S} \cdot \overline{Q(t_0)} = \overline{S}$$

Substituting R from (18a) we get

$$S = \overline{R} \tag{19}$$

Equations (17)-(19) are the required and sufficient conditions for stable and glitch-free operation of a nor-nor S-R latch.

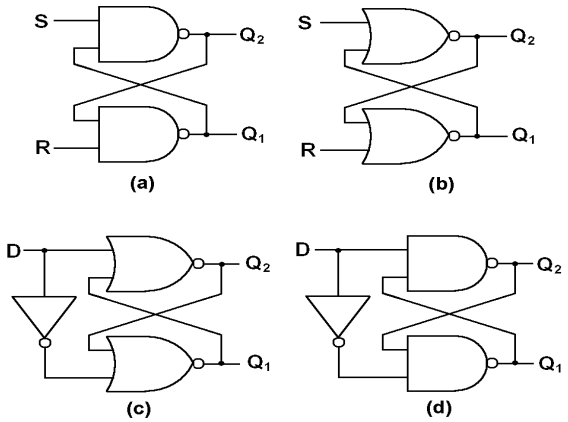

Fig. 3. (a) S-R latch with nand gates; (b) S-R latch with nor gates; (c) D latch with nor gates; (d) D latch with nand gates.

Although the derivation is done for nor-nor latch, similar analysis can be done for nand-nand latch.

From the equations mentioned above, it is obvious that the S-R latch cannot be used directly to develop sequential circuits. (19) asserts that the inputs must be complementary to each other. Hence it can be easily predicted that D latch is better than S-R latch where

$$S = D \quad \text{and} \quad R = \overline{D} \tag{20}$$

The input of a conventional D latch never violates (19), so the outputs are level sensitive and do not oscillate. But the conditions stated in (17), (18) or (29), (30) might be violated for certain input and output combinations. So the conventional D latch is not free from glitches also.

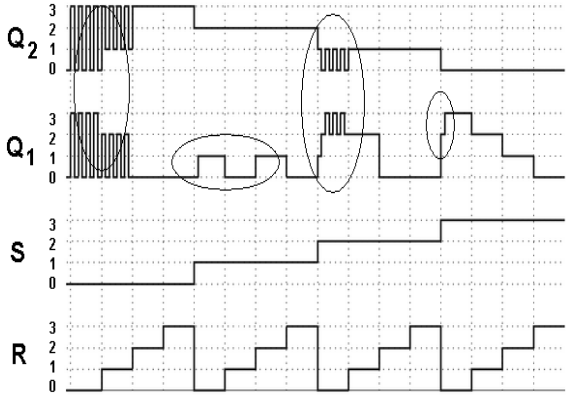

Fig. 4. Timing diagram of a S-R latch with nor gates. Gate propagation delays are neglected here to depict the glitches clearly. The marked regions show unstable outputs and a few glitches.

Because of these reasons, we have adopted a different technique to design a S-R or D latch that is free from stability problems and glitches. The modified S-R latch works on the following fundamental equations:

$$\left.\begin{aligned} X &= \overline{S}^{R} \\ Q &= S\,.\,X + Q\,.\,\overline{X} \end{aligned}\right\} \qquad (21)$$

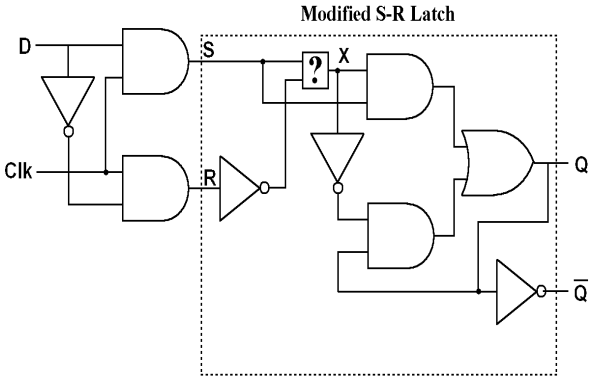

Fig. 5. Gated D latch. The dotted rectangle shows the modified S-R latch. The clock signal is coupled with the input signal via and gates. When clock signal is low, the inputs to the modified S-R latch will be low. Since these low inputs are non-complementary, the latch will hold its previous outputs.

Here X is high if S and R are complementary, otherwise it is low. Then X acts as the selector of a 2-to-1 multiplexer and chooses either S or Q to be passed to Q. The optional complementary output is not used anywhere in the latch operation and can be neglected.
The D latch alone is not a practical device since the output is always changing here as the input changes. The output cannot be latched as there is no way to make S and R non-complementary. So we use gated D latch which can be used to latch the output by using a clock signal. We are demonstrating active high devices so the output will be changed only when the clock signal is high.
The gated D latch is the building block of all sequential circuits in our proposed scheme. It is used to create master-slave flip-flops, registers and counters.

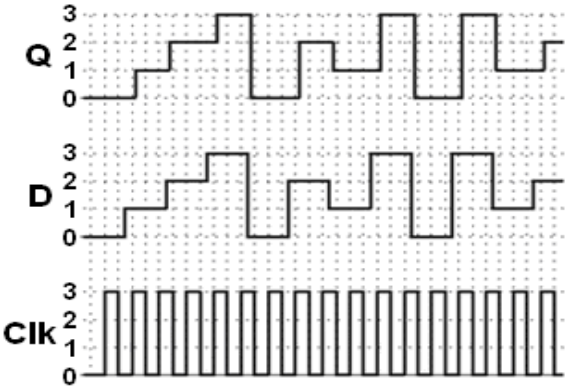

Fig. 6. Timing diagram of a level-sensitive gated D latch. The clock signal edges and data signal edges do not coincide. To simulate practical situation arbitrary propagation delay is included in the simulation.

B. MASTER-SLAVE FLIP-FLOPS

The quaternary master-slave flip-flop is similar to its binary counterpart; the binary gated D latch is replaced by its quaternary variant. Here two gated D latches are used with alternating clock signals. Altering the configuration of the clock inputs, a flip-flop can be either positive or negative edge-triggered.

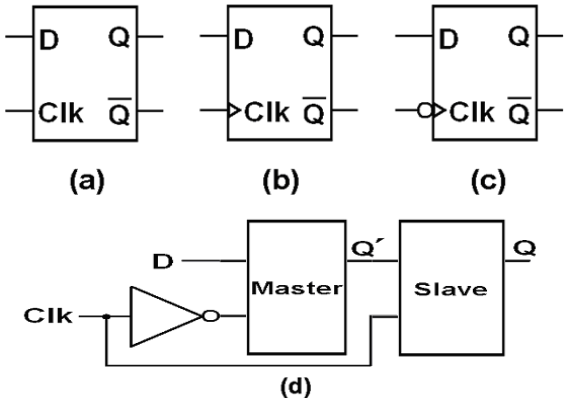

Fig. 7. Circuit symbols for (a) level-triggered gated D latch, (b) positive edge-triggered flip-flop, (c) negative edge-triggered flip-flop. (d) Circuit diagram of positive edge-triggered master-slave flip-flop.

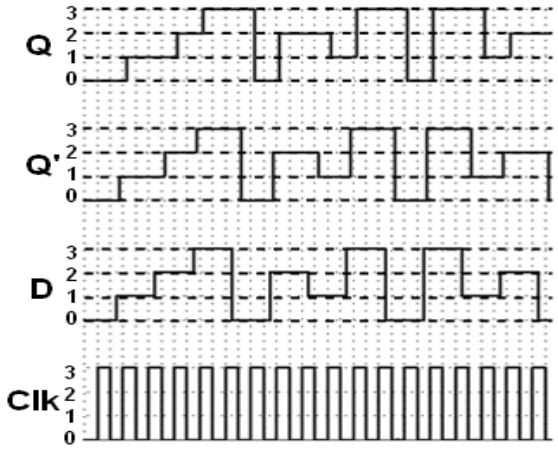

Fig. 8. Timing diagram of a positive edge-triggered master-slave flip-flop. Q' and Q are intermediate and final outputs of the flip-flop, respectively.

C. REGISTERS

Shift registers can be constructed using edge-triggered flip-flops. We are using positive edge-triggered flip-flops as an example. The quaternary shift register is similar to binary shift register, the binary logic blocks are simply replaced by quaternary blocks. Here we present a serial-in serial/parallel-out shift register (Fig. 9(a)), but it is possible to construct other kinds of registers also.

The serial/parallel-in registers have dual input flip-flops each with a selector to choose either serial or parallel input (Fig. 9(b)).

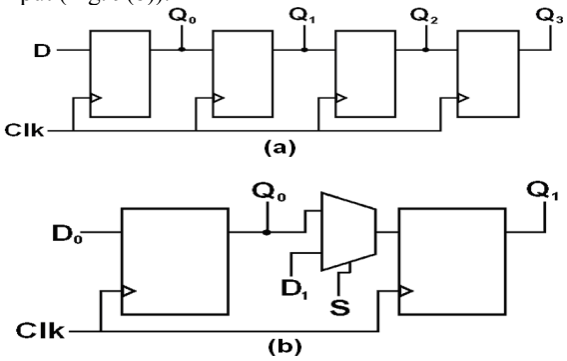

Fig. 9. (a) A quaternary 4-qudit serial-in serial/parallel-out shift register. (b) A quaternary 2-qudit register with serial/parallel input and serial/parallel output.

D. COUNTERS

We have observed that quaternary flip-flops and registers can be constructed like their binary counterparts. But in case of counters, there are significant differences. In quaternary logic the toggling of states does not solve the problem like binary counters as there are four states. So we use a half-adder here to change output states of flip-flops. No carry is needed from the adder.

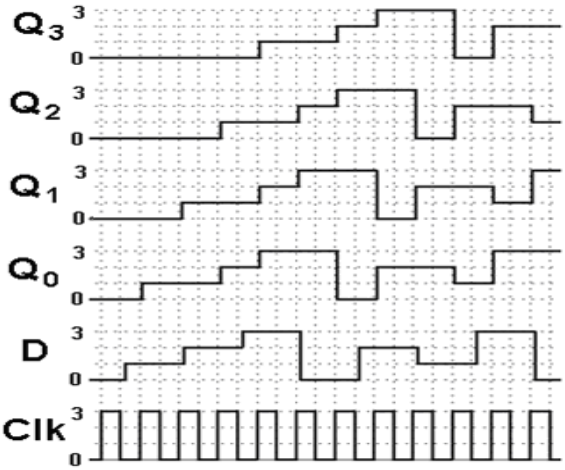

Fig. 10. Timing diagram of a 4-qudit positive edge-triggered serial-in shift register shown in Fig. 9(a).

Table III Quaternary Half Adder (Without Carry-out)

X	Y	S	X	Y	S	X	Y	S	X	Y	S
0	0	0	1	0	1	2	0	2	3	0	3
0	1	1	1	1	2	2	1	3	3	1	0
0	2	2	1	2	3	2	2	0	3	2	1
0	3	3	1	3	0	2	3	1	3	3	2

This truth table can be implemented using following circuit (Fig. 11).

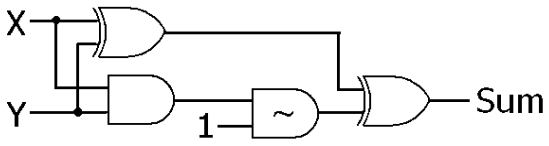

Fig. 11. Quaternary half-adder circuit (without carry-out).

At first we present the design of a up-counter. Here we are ignoring propagation delays and assuming zero initial conditions.

Let us take a 3-qudit counter, so $Q_0 = Q_1 = Q_2 = 0$. Now at every clock edge, Q_0 is increased up to 3 and then it returns to 0. The output of the second flip-flop is incremented when the first output is going from 3 to 0.

So the inputs of the flip-flops in n-qudit up-counter are determined by the following equations:

$$D_0 = Q_0 + 1 \quad (22a)$$

$$D_i = Q_i + (Q_{i-1})^3.1 \; ; \; i = 2, 3, \ldots.n-1 \quad (22b)$$

The down-counter can be designed in a similar manner. The inputs of the flip-flops in n-qudit down-counter are determined by the following equations:

$$D_0 = Q_0 + 3 \quad (23a)$$

$$D_i = Q_i + (Q_{i-1})^0.3 \; ; \; i = 2, 3, \ldots.n-1 \quad (23b)$$

Comparing (22) and (23), we can write generalized equations of a universal counter. This counter can be

used as both up-counter and down-counter. The general equations of the universal counter are

$D_0 = Q_0 + Y$ (24a)

$D_i = Q_i + (Q_{i-1})^X.Y$; i = 2, 3, ….n-1 (24b)

From (22) and (23), we can say that for an up-counter X = 3 and Y = 1. For a down-counter the values will be X = 0 and Y = 3. We can use 2-to-1 multiplexers to select X and Y for required counting operation.

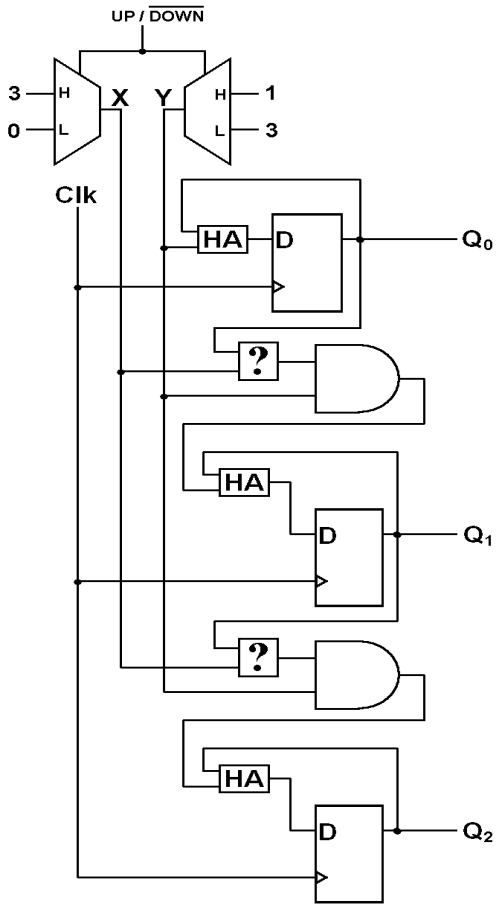

Fig. 12. The universal counter. If the selector of the multiplexers is set to 3, then the counter will work as an up-counter. If the selector input is 0, then the counter will be a down-counter.

IV. CONCLUSION

The quaternary sequential circuits presented here can be used in conjunction with combinational logic circuits to construct useful quaternary systems. The main challenge of implementing such systems is the physical limitation imposed by existing VLSI technology. It is obvious that conventional CMOS technology may not be proved effective in designing such logic blocks [8], so non-conventional and emerging technologies are required to be explored.

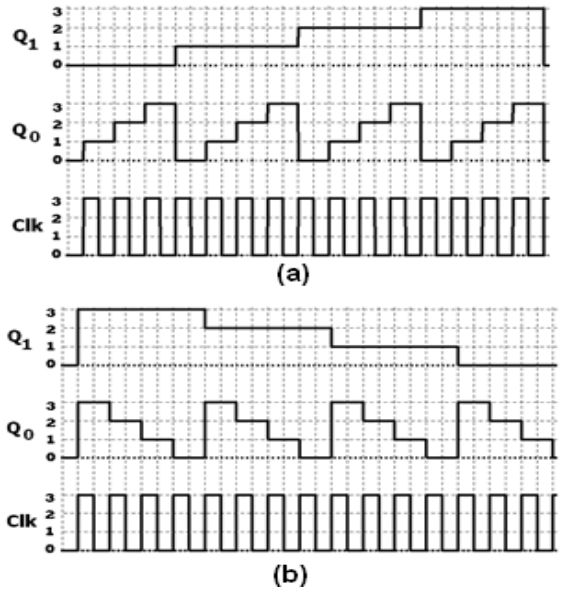

Fig. 13: Timing diagram of (a) 2-qudit up-counter; (b) 2-qudit down-counter.

REFERENCES

[1] Keshavarzian, A. P.; Navi, K.; "Optimum Quaternary Galois Field Circuit Design through Carbon Nano Tube Technology", Proceedings, International Conference on Advanced Computing and Communications (ADCOM), 2007. pp: 214 - 219, 18-21 Dec. 2007.

[2] Hurst, S. L; "Multiple-Valued Logic – Its Status and Its Future", Computers, IEEE Transactions on Vol. C-33, Issue: 12, pp.1160-1179, Dec. 1984.

[3] Khan, M. H. A.; "Quantum Realization of Quaternary Feynman and Toffoli Gates", Proceedings, 4th International Conference on Electrical and Computer Engineering (ICECE), pages: 157 – 160, 19-21 December 2006.

[4] http://www.ternarylogic.com

[5] Jahangir, I.; Hasan, D. M. N.; Islam, S.; Siddique, N. A.; Hasan, M. M.; "Development of a Novel Quaternary Algebra with the Design of some Useful Logic Blocks", Proceedings, ICCIT 2009, 12th International Conference on Computers and Information Technology, 21-23 Dec. 2009, to be published.

[6] Jahangir, I.; Hasan, D. M. N.; Reza, M. S.; "Design of Some Quaternary Combinational Logic Blocks Using a New Logic System", Proceedings, TENCON 2009, IEEE Region 10 Conference, 23-26 Nov. 2009, to be published.

[7] Unger, S. H., "Hazards, critical races, and metastability", Computers, IEEE Transactions on, Vol. 44, Issue 6, pp: 754 – 768, Jun 1995.

[8] Current, K.W. , "CMOS quaternary latch", 22 June 1989, IET Electronics Letters, Volume: 25, Issue: 13, page(s): 856-858.

Proceedings of 2009 12th International Conference on Computer and Information Technology (ICCIT 2009)
21-23 December, 2009, Dhaka, Bangladesh

Effectiveness of Selection and Maximal Ratio Combining Diversity Techniques on a DS-CDMA Wireless Communication System Impaired by Fading

Masuda Hossain, Md. Rubaiyat Hossain Mondal†
TM International, Dhaka, Bangladesh
† IICT, BUET, Dhaka, Bangladesh
hossain.masuda@yahoo.com, †rubaiyat97@iict.buet.ac.bd

Abstract

The effectiveness of different diversity combining techniques in improving the bit error rate (BER) performance of a direct- sequence code-division multiple-access (DS-CDMA) system is presented in this paper. The overall performance of a DS-CDMA system is degraded by multipath fading and additive white Gaussian noise (AWGN). To evaluate the degradation, the expression for the conditional BER, conditioned on a given level of fading is derived and then the unconditional BER is evaluated. This approach is also extended to estimate the BER performance of the system having multiple receiving antennas. The selection method and maximal ratio combining (MRC) method are employed as diversity combining schemes and it is found that both the schemes offer almost the same BER improvement. Moreover, convolutional channel coding is applied in the DS-CDMA system and it is noted to provide more enhancements in the system performance.

Keywords: Diversity Combining, convolutional coding, DS-CDMA, multipath fading, maximal ratio combining.

I. INTRODUCTION

In direct-sequence code division multiple access (DS-CDMA) system, the narrowband message is multiplied by a large bandwidth signal, which is called the spreading signal. The spreading signal is generated by convolving a pseudo-noise (PN) code with a chip waveform whose duration is much smaller than the symbol duration. By assigning different code sequences to each user, it is possible to allow many users to share the same channel and frequency simultaneously. However, like other wireless communication systems, the transmission quality is affected by thermal noise as well as multipath fading which can change the amplitude and phase of the received signal. Several reports present methods for deriving bit error rate (BER) of the DS-CDMA system under multipath channels [1-7]. The BER performance of DS-CDMA systems communicating over Additive White Gaussian Noise (AWGN) channels has been reported in [1], [2] whereas the analysis for multipath fading channels have been carried out in [3]-[7].

The advantaged of using spatial diversity through multiple antennas have been widely recognized in the field of DS-CDMA. The employment of multiple antennas has been reported in few recent works [8]-[10]. In addition, a novel high spectral efficiency transmission scheme is proposed for a multiple antenna CDMA system [11]. However, in these works the comparison of different diversity combining techniques are absent. Therefore, there is a need to find the effect of multipath fading, timing jitter and noise analytically on a DS-CDMA system with different diversity combining schemes.

In this paper, an analytical approach is developed to find the combined effect of multipath fading and AWGN on the BER of DS-CDMA systems. Both Doppler frequency shift and channel attenuation are regarded as parameters of wireless fading channels. The analysis is carried out for a perfect synchronized system as well as for a system with timing synchronization errors. To alleviate the fading impairment, we evaluate the system considering multiple receiving antennas with 'selection combining' and 'maximal ratio combining (MRC)' as two different diversity combining methods. Moreover, the performances of these two diversity techniques are also compared in terms of BER and power requirement. We also apply convolution coding to assess the effectiveness of coding in minimizing the channel effects.

This rest of the paper is organized as follows. Section II describes the model of the DS-CDMA scheme with multiple receiving antennas. In Section III, the theoretical analysis of SNR and BER of the proposed system is depicted in presence of channel fading. Section IV reveals the results of the analysis through numerical computations and finally, conclusions of the work are drawn in Section V.

II. SYSTEM MODEL

The model of the DS-CDMA system is described in Fig. 1. The model is expressed in an equivalent low-pass system. In the transmitter section, the information

978-1-4244-6283-4/09/$26.00 ©2009 IEEE

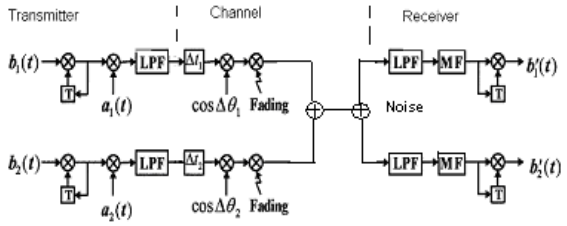

Fig. 1. DS-CDMA System Model

signal of each transmitting user with the form of binary sequence is made to carry out the differential coding and then the spreading. In addition, the signal is shaped by root cosine roll-off filter regarded as a low pass filter (LPF). In the channel block, the time delay and the phase offset are added to the signals, which are affected independently by fading. This is because the respective users access asynchronously to the system. The signals from all users are combined, and then respective users receive the combined signal added with AWGN.

In the receiving side the reverse operation to the transmitter takes place. The signal is received by multiple receiving antennas and the diversity combiner provides single improved signal from these received signals. In the demodulation block, the received signal is made to carry out the band limitation, the code matching by means of the matched filter (MF) and the differential detection. Finally, the desired information signal is demodulated.

III. THEORETICAL ANALYSIS

In wireless communication systems fading is caused by multipath reception of the signal. The receiving antennas receive a large number of reflected and scattered waves from transmitters. Because of wave cancellation effects, the instantaneous received power at the moving antenna becomes a random variable, dependent on the location of the antenna. All waves experience their own phase rotation and the resulting vector may significantly change in amplitude if individual components undergo different phase shifts. Considering such a DS-CDMA system with only Additive White Gaussian Noise (AWGN) and fading, the expression of signal-to-noise ratio (SNR) with perfect time synchronization can be expressed as [3], [4]:

$$\mathrm{SNR}=\frac{\frac{2E_b}{N_0}}{k+1} \tag{1}$$

where N_0 is the Gaussian noise, E_b is the bit energy and k is the Rician parameter of the fading channel. The bit error rate (BER) performance of DS-CDMA system considering DBPSK modulation, over multipath fading channels can be evaluated as [3]:

$$P_e=\frac{\left\{1-J_0(2\pi F_d T_s)\right\}\{\frac{SNR}{2}\}+1}{2\{\frac{SNR}{2}+1\}}\exp\{-\frac{k\frac{SNR}{2}}{\frac{SNR}{2}+1}\} \tag{2}$$

here F_d is the maximum Doppler frequency and T_s is the symbol duration. In any fading channel, the received signal energy is random depending on random fade whereas the noise energy remains unchanged. The energy received per bit (E_b) is a function of input bit energy E_{in} and the multiplicative fade α^2, i.e. $E_b = E_{in}\alpha^2$. This multiplicative fade is considered to be the attenuation of a fading channel. Therefore, it can be considered as an important parameter of the fading effect. So, with the inclusion of channel attenuation, the expression of SNR for a stand alone DS-CDMA system can be expressed as follows:

$$\mathrm{SNR}(\alpha)=\frac{\frac{2(E_{in}\alpha^2)}{N_0}}{k+1} \tag{3}$$

Considering both channel attenuation and Doppler frequency as fading parameters, the bit error rate (BER) performance for DS-CDMA system over multipath fading channels can be evaluated as:

$$P_e(\alpha)=\frac{\left\{1-J_0(2\pi F_d T_s)\right\}\{\frac{SNR(\alpha)}{2}\}+1}{2\{\frac{SNR(\alpha)}{2}+1\}}\exp\{-\frac{k\frac{SNR\,\alpha)}{2}}{\frac{SNR(\alpha)}{2}+1}\} \tag{4}$$

where $J_0(2\pi F_d T_s)$ is the time correlation function. Equation (4) represents the conditional bit error rate conditioned on a give value of channel attenuation α. To find the average bit error rate, the probability density function (pdf) of α must be determined.

In a Rayleigh fading channel α is Rayleigh distributed and therefore has an expression as of [11]:

$$\mathrm{p}(\alpha)=\frac{\alpha}{\sigma^2}\exp(-\frac{\alpha^2}{2\sigma^2}) \tag{5}$$

where σ is the Rayleigh parameter. Both the mean and variance of the Rayleigh density function are functions of σ. On the other hand, in Rician fading channels α is Rician distributed having the following pdf [11]:

$$\mathrm{p}(\alpha)=\frac{\alpha}{\sigma^2}\exp(\frac{-(\alpha^2+m^2)}{2\sigma^2})\ I_0(\frac{\alpha m}{\sigma^2}) \tag{6}$$

where I_o is the zeroth order Bessel function and m is a function of σ^2. The average BER (P_e) can be calculated by averaging the conditional BER $P_e(\alpha)$, over all possible values of α:

$$P_e = \int_{-\infty}^{\infty} P_e(\alpha)\ p(\alpha)\ d\alpha \tag{7}$$

With the existence of timing synchronization error, the signal power degrades by a factor of (1-ε) over a time slot. Here ϵ is the timing error normalized by symbol duration T_s i.e. ($\epsilon = \Delta / T_s$). This timing jitter causes interference too, which is neglected in the analysis. To incorporate the jitter effect along with fading and AWGN, the equation of SNR in (3) can be modified as follows:

$$\mathrm{SNR}(\varepsilon,\alpha) = \frac{\frac{2\{E_{in}(1-\varepsilon)\alpha^2\}}{N_0}}{k+1} \tag{8}$$

With timing synchronization error, the expression of average bit error rate in (7) will be extended as:

$$P_e = \int_{-\infty}^{\infty}\int_{-\infty}^{\infty} P_e(\varepsilon,\alpha)\ p(\varepsilon)\ p(\alpha)\ d\varepsilon\ d\alpha \tag{9}$$

Where $p(\varepsilon)$ represents the pdf of Gaussian distributed timing jitter/error with jitter variance σ_ε^2.

To improve the performance of the system multiple receiving antennas can be employed. The common diversity combining techniques are the selection combining, switched combining, equal gain combining and maximal ratio combing. With selection diversity, the receiver selects the antenna with the strongest received signal power and ignores observations from other antennas. As the expression of P_e in (7) is the average bit error probability without diversity, the average BER with selection diversity combining can be calculated as [12]:

$$P_{select}(A) = 2P_e(A) - P_e(A/2) \tag{10}$$

where A denotes the average SNR. This expression can be utilized to find the BER of the CDMA system with multiple receiving antennas.

On the other hand, in maximum ratio combining technique the received signals are weighted with respect to their SNR and then summed. That is, branches with strong signal are further amplified, while weak signals are attenuated. Considering n_r receiving antennas the effective SNR is modified as of [10]:

$$\mathrm{SNR}(u,\alpha) = \sum_{i=1}^{n_r} h_i^2\ \mathrm{SNR}(\alpha) \tag{11}$$

where $u = \sum_{i=1}^{n_r} h_i^2$ and h_i is the channel of the i^{th} antenna. Furthermore, n_r = 1, 2, 3, ……. represents the number of receiving antennas. The pdf of u is expressed as [10]:

$$\mathrm{pdf}(u) = \frac{1}{(n_r-1)!}\ u^{n_r-1}\ e^{-u} \tag{12}$$

The expression for the average BER of the system with maximal ratio combining can be expressed as:

$$P_{mrc} = \int_0^{\infty} P_e(u)\ pdf(u)\ d(u) \tag{13}$$

where $P_e(u)$ is the BER for a single receiving antenna conditioned on the value of u.

In addition to using multiple antennas, channel coding is added to improve the system performance. To optimize the use of the correction capacity of a particular code, soft decision is always a good solution. Thus, convolutional coding is applied to the DS-CDMA system. It is well known that using a convolutional coding and a Viterbi decoding algorithm, the bit error probability for an information symbol is bounded by the following expression:

$$P_{err} \le \frac{1}{K_1} \sum_{d=d_f}^{\infty} W(d)P(d) \tag{14}$$

where *P(d)* is the probability for the decoding algorithm to choose a path at distance d from the correct path in the decoding trellis, d_f is the free distance of the encoder and *W(d)* is a characteristic coefficient of the encoder obtained from code weights. Considering the uncoded BER to be P_{un} the value of *P(d)* can be expressed as follows:

$$P(d) = \{4\ P_{un}\ (1-P_{un})\}^{d/2} \tag{15}$$

By substituting (10) or (13) in the above expression the value of *P(d)* can be calculated.

IV. RESULTS AND DISCUSSION

In this section, the numerical results are derived from the analytical expressions. The bit error rate performance results are evaluated at a data rate of 1 Mbps with maximum Doppler frequency of 60 Hz in a multipath fading channel. Fig. 2 shows the effect of fading variance i.e. variance of channel attenuation α, on the BER performance of the DS-CDMA system. It is found that with increase in fading variance i.e. increase in channel gain; there is enhancement in system BER performance. We find that at fading variance σ_f^2 =0.2, the BER is 10^{-5} whereas at σ_f^2 =0.1, the BER increases to 10^{-4} at -10 dBm input power. Fig. 3 shows the plots of BER vs. P_{in} (dBm) for both Rayleigh and Rician fading channels. It is noticed that BER performance is better in Rician fading channel. This is because in Rician channel there exists one dominant line-of-sight path that is absent in Rayleigh channel.

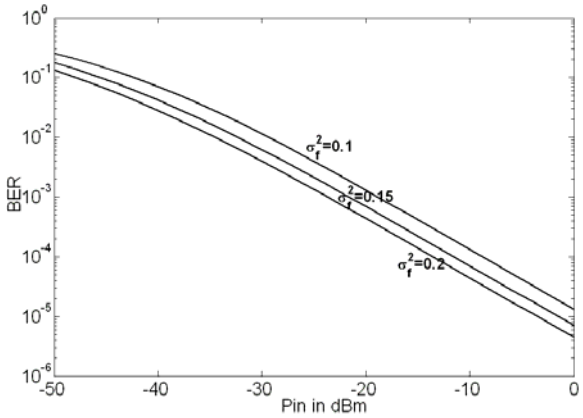

Fig. 2. Plots of BER vs. P_{in} (dBm) for different fading variance in a DS-CDMA system in Rayleigh fading channel (F_d=60 Hz, T_s=10^{-6}s)

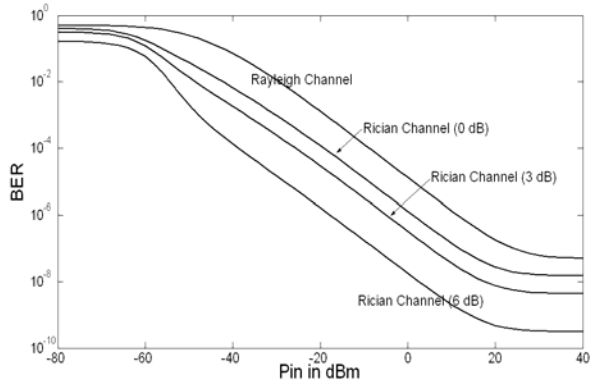

Fig. 3. Plots of BER vs. P_{in} (dBm) for Rayleigh and Rician channels for DS-CDMA (F_d=60 Hz, σ_f^2 =0.1, T_s=10^{-6}s)

From Fig. 3, it is also revealed that BER performance improves with increase in Rician factor. For example, at 0 dBm input power, the BER of a Rayleigh fading channel is slightly less than 10^{-4} whereas Rician channels have a BER in the order of 10^{-5}, 10^{-6} and 10^{-7} for K=0 dB, 3 dB and 6dB respectively. This result can be explained from the fact that higher Rician factor indicates more dominant line-of-sight path.

For a fixed fading variance of 0.1, the performance of the system is compared with and without timing error/ jitter. Fig. 4 shows the plots of BER vs. P_{in} (dBm) for a DS-CDMA system with different values of jitter. From Fig. 4, it is noticed that the BER slightly degrades with increase in jitter. Therefore, the timing jitter effect is negligible for the CDMA system.

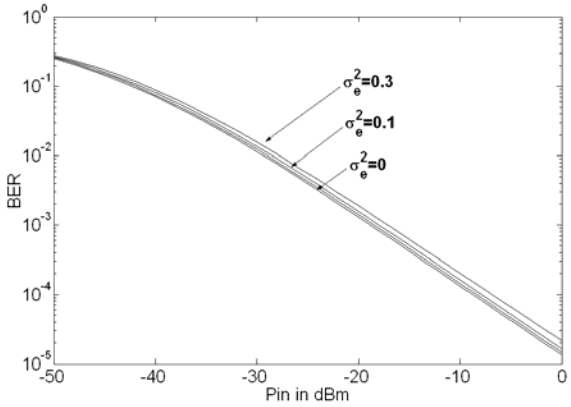

Fig. 4. Plots of BER vs. P_{in} (dBm) for different values of jitter variance for DS-CDMA (F_d=60 Hz, T_s=10^{-6}s) in Rayleigh fading channel

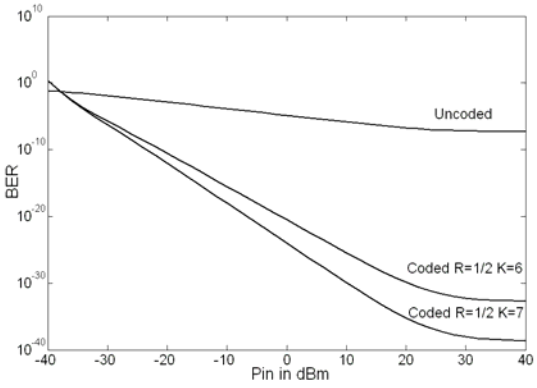

Fig. 5. Plots of BER vs. P_{in} (dBm) with and without coding for DS-CDMA systems in Rayleigh fading channel (F_d=60 Hz, T_s=10^{-6}s)

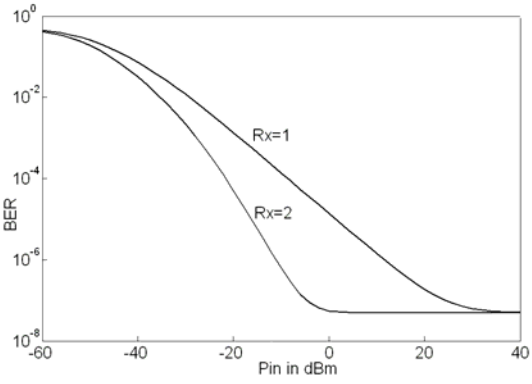

Fig. 6. Plots of BER vs. P_{in} (dBm) with single antenna and with multiple receiving antennas in Rayleigh fading channel (selection combining)

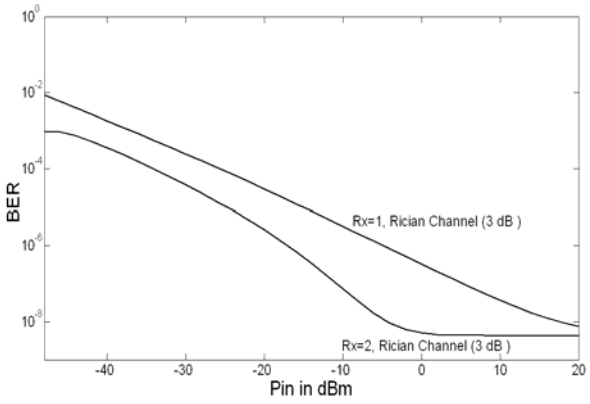

Fig. 7. Plots of BER vs. P_{in} (dBm) with single antenna and with multiple receiving antennas in Rician fading channel (selection combining)

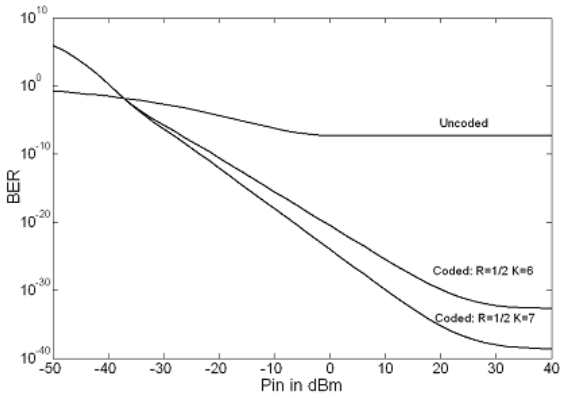

Fig. 8. Plots of BER vs. P_{in} (dBm) with and without coding for DS-CDMA systems with multilple receiving antennas in Rayleigh fading channel (selection combining)

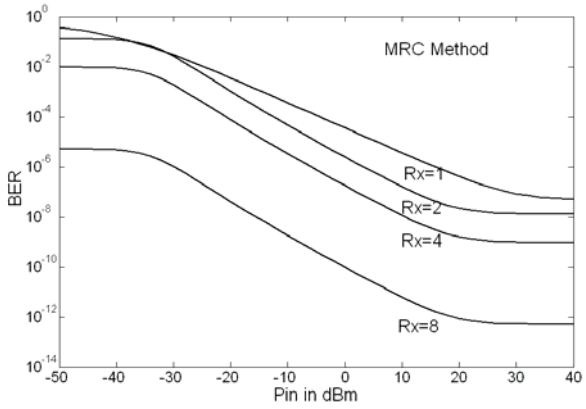

Fig. 9. Plots of BER vs. P_{in} (dBm) with single antenna and with multiple receiving antennas in Rayleigh fading channel (MRC combining)

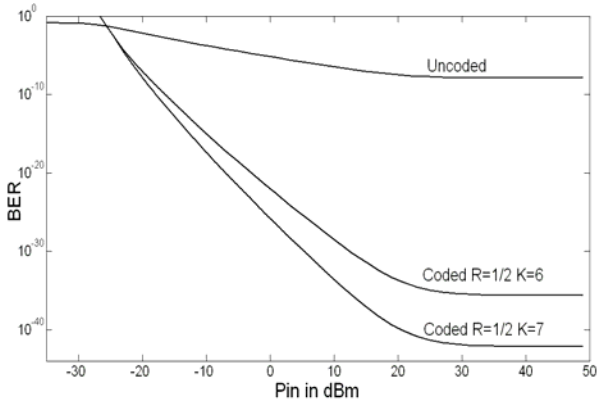

Fig. 10. Plots of BER vs. P_{in} (dBm) with and without coding for DS-CDMA systems with multilple receiving antennas in Rayleigh fading channel (MRC combining)

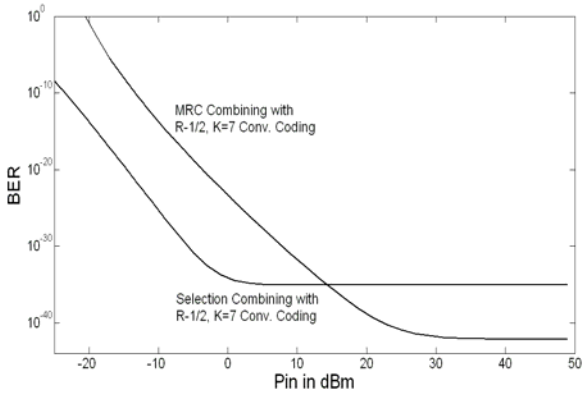

Fig. 11. Plots of BER vs. P_{in} (dBm) with selection combining and MRC combining

To improve the system performance of a stand alone CDMA system, channel coding can be applied. From Fig. 5, it is revealed that with the application of convolutional coding, the BER performance of the system improves significantly. At input power of 0 dBm, the BER is 10^{-5} for uncoded system whereas it decreases to 10^{-25} for convolutional coded system with constraint length K=7. Fig. 6 illustrates the performance comparison of DS-CDMA systems with and without receiver diversity in a Rayleigh fading channel. In this case selection diversity combining method is employed. The plots show that at -10 dBm input power, the BER reduces from 10^{-4} to 10^{-7} when selection diversity combining technique is used. The same graph is plotted for a Rician fading channel in Fig. 7. From this figure it is found that the performance in Rician channel with 3 dB Rician factor is slightly better than that of Rayleigh fading channel. At -5 dBm input power the BER reaches to 10^{-8} for selection combining of two receiving antennas.

Fig. 8 shows the plots of multiple-antenna (using selection combining) CDMA system with and without

convolutional coding in presence of fading. At uncoded BER of 10^{-7} and with convolutional code of rate ½, the coding gain is 24 dB for constraint length K=6 and 26 dB for K=7. It is also noticed that for higher amounts of input power, the coding gain is substantially higher in K=7 than in K=6.

The application of maximal ratio combining method is demonstrated in Fig. 9. From this figure, it is noted that with the increase in number of receiving antennas the BER performance is sharply enhanced. The BER of the system improves from 10^{-7} to 10^{-12} when the number of receiving antennas is increased from two to eight. At BER of 10^{-6}, the power gain is almost 15 dB for two number of receiving antennas whereas it is almost 50 dB for eight antennas. The effectiveness of convolutional coding with a system having two receiving antennas combined through MRC method is demonstrated in Fig. 10. The plots of uncoded and coded systems show almost similar characteristics as of the plots for selection combining method. From the plots of Fig. 10, it is noticed that to achieve a target BER of 10^{-9} the uncoded system requires 19 dBm power whereas a coded system with K=7 requires only -17 dBm power. Therefore, the coding gain over a system with MRC combining scheme is 36 dB at a BER of 10^{-9}. Fig. 11 depicts the performance comparison of a DS-CDMA scheme with selection combining and MRC combining. From Fig. 11, it is revealed that from -25 dBm to 15 dBm power the selection method outperforms MRC method in terms of BER. However, after 15 dBm power the MRC provides more BER improvement than the selection combining method. As the selection method shows better performance than MRC method at the BER of interest (10^{-9}), it is more acceptable in practical wireless communication systems. On the other hand, selection method already has the advantage of simpler and easier practical implementation. Therefore, the selection combining method is the best choice for a multiple-antenna DS-CDMA scheme.

V. CONCLUSION

We have analyzed the combined effects of multipath fading and AWGN on the BER performance of a CDMA system. In addition, the effect of timing jitter has been considered and is found to have less pronounced impact. For DS-CDMA with DBPSK modulation it is noted that with increase in channel attenuation the BER increases. We also observe that the BER of a CDMA system is much higher in Rayleigh fading channel than Rician channel. We compute the BER in Rician fading channels with different Rician parameters and numerical results show that the performance is improved with higher values of Rician parameter. We extend the analysis for a multiple antenna DS-CDMA system with selection method for combining multiple receiving antennas and find substantial improvement in the system performance. We then applied maximal ratio combining method instead of the selection method for diversity combining and found that both the schemes provide BER performance improvement. As the selection method has better BER performance, it can be more acceptable for mobile wireless DS-CDMA systems.

REFERENCES

[1] A. Mirbagheri and Y. C. Yoon, "Performance Analysis of a Linear MMSE Receiver for Bandlimited Random-CDMA Using Quadriphase Spreading over Multipath Channels," IEEE Trans. On Wireless Commun., vol. 3, no. 4, pp. 1053–1066, July 2004.

[2] Y. C. Yoon, "Quadriphase DS-CDMA with Pulse Shaping and the Accuracy of the Gaussian Approximation for Matched Filter Receiver Performance Analysis," IEEE Trans. On Wireless Commun., vol. 1, no. 4, pp. 761–768, October 2002.

[3] F. Sasamori and F.Takahata, "Theoretical and Approximate Derivation of Bit Error Rate in DS-CDMA Systems under Rician Fading Environment" IEICE Trans. Fundamentals, vol. E82-A , no.12, pp.2660-2668 , Dec.1999 .

[4] S. S. Mahmoud, Z. M. Hussain, and P. O'Shea, "Approximate Equation of Average Bit-Error Rate in DS-CDMA Systems Over Fading Channels", in Australian Telecommunications, Networks and Applications Conference (ATNAC), Melbourne, Australia, 8-10 December, 2003.

[5] J. Cheng and N. Beaulieu, "Accurate DS-CDMA Bit-Error Probability Calculation in Rayleigh Fading," IEEE Trans. On Wireless Commun., vol. 1, no. 1, pp. 3–15, January 2002.

[6] K. Sivanesan and N. C. Beaulieu, "Accurate BER Analysis of Bandlimited DS-CDMA System with EGC and SC Diversity over Nakagami Fading Channels," in IEEE Wireless Communications and Networking Conference, vol. 2, New Orleans, Louisiana, USA, 13-17 March 2005, pp. 956–960.

[7] Q. Shi and M. Latva-Aho, "Accurate Bit-Error Rate Evaluation for Synchronous MC-CDMA over Nakagami-m-Fading Channels Using Moment Generating Functions," IEEE Trans. On Wireless Commun., vol. 4, no. 2, pp. 422–433, March 2005.

[8] O. Shin and K. B. Lee, "Use of Multiple Antennas for DS/CDMA Code Acquisition", IEEE Trans. On wireless Communications, vol. 2, no. 3, May 2003.

[9] P. Nagvanshi, E. Masry and L. B. Milstein, "Performance of Multiple Antenna DS-CDMA UWB System With Noisy Channel Estimates and Narrow-Band Interference", IEEE Journal of Selected Topics in Signal Processing, vol. 1, no. 3, October 2007

[10] K.M. Ahmed, S. P. Majumder, "Performance analysis of a MIMO-OFDM wireless communication system with convolutional coding", in International conference on Electrical and Computer Engineering (ICECE), Dhaka, Bangladesh, 20-22 December, 2008.

[11] T. S. Rappaport, Wireless Communications: Principles & Practice, 2nd edition, Pearson Education Pte Ltd., pp. 210-214. 2002.

[12] K. Feher, Wireless Digital Communication (Modulation and Spread Spectrum Application). pp. 209-214, Prentice-Hall. 2005

Proceedings of 2009 12th International Conference on Computer and Information Technology (ICCIT 2009)
21-23 December, 2009, Dhaka, Bangladesh

Computer Vision-based Bangladeshi Sign Language Recognition System

Salma Begum, Md. Hasanuzzaman
Department of Computer Science & Engineering, University of Dhaka, Dhaka, Bangladesh
jennycsdu@yahoo.com, hzamancsdu@yahoo.com

Abstract

Sign language is a specific area of human gesture communication and a full-edged complex language that is used by various deaf communities. In Bangladesh, there are many deaf and dumb people. It becomes very difficult to communicate with them for the people who are unable to understand the Sign Language. In this case, an interpreter can help a lot. So it is desirable to make computer to understand the Bangladeshi sign language that can serve as an interpreter. In this paper, a Computer Vision-based Bangladeshi Sign Language Recognition System (BdSL) has been proposed. In this system, separate PCA (Principal Component Analysis) is used for Bengali Vowels and Bengali Numbers recognition. The system is tested for 6 Bengali Vowels (অ, আ, ই, উ, এ, ও) and 10 Bengali Numbers (০, ১, ২, ৩, ৪, ৫, ৬, ৭, ৮, ৯).

Keywords: American Sign Language, Bangladeshi Sign Language, Computer-Vision, Principal Component Analysis.

I. INTRODUCTION

Sign language is one form of communication for the hearing and speech impaired. Similar to spoken language, there is no universal sign language. Sign language is itself a separate language with its own grammar and rules. There are different sign languages all over the world such as American Sign Language (ASL), British Sign Language (BSL), French Sign Language, Danish Sign Language, Taiwan Sign Language, Australian Sign Language, etc. These all languages are developed independently [1]. In the same way, BdSL (Bangladeshi Sign Language) is structurally different with other countries sign languages. In Bangladesh, to represent Bengali and English alphabet two hands are used so to recognize Bangladeshi sign language is more complicated.

According to the manual of Bangladeshi Sign Language, there are approximately 5000 sets of gestures for alphabet, numbers and common words that are used by deaf and dumb people to communicate [2]. Some signs are expressed as static gestures while others incorporate some dynamic hand, face and body movements. For static gestures, the prominent sign is captured within a specific time frame. For dynamic gestures, a sequence of finger and hand positions needs to be identified and analyzed in order to recognize [3]-[4]. To interact with sign user the machine should recognize and learn sign characters and language. Automatic gesture and sign language recognition has been attracting computer vision researchers for a long time [5]. It offers enhancement of communication capabilities for the speech-impaired and deaf people. Automatic sign recognition has been investigated since around 1995 [6]. Researchers used a variety of techniques, such as Fuzzy logic [7], neural networks [6]-[8], PCA method [9], and Hidden Markov Models (HMMs) [10] to recognize hand gestures.

Unfortunately, in Bangladesh there is a tremendous lack of people who have an in-depth knowledge of sign language, which leads to the social isolation of the Deaf community. This has brought forth motivation for the development of this system capable of automatically interpreting Bangladeshi sign language. As seen in previous works, a reduced set vocabulary is very important for developing the basic recognition system. It would be too ambitious at this stage to attempt to recognize all 5,000 sets of BdSL gestures. Therefore, we develop a reduced set vocabulary of essential BdSL signs.

This paper consists of five sections. Section II describes proposed Bangladeshi sign language recognition system. Section III focuses on system description and implementation methods. Section IV presents Experimental Results and Discussions and section V concludes this paper.

II. PROPOSED BANGLADESHI SIGN LANGUAGE RECOGNITION SYSTEM

The proposed system uses PCA (Principal Component Analysis) based pattern matching method for 6-Bengali vowels and 10- Bengali numbers recognition. Fig **1** shows the proposed system architecture. Proposed system is composed of three modules: Preprocessing, Training and Recognition. In this system the image is captured using CCD camera, where 30 frames are captured per second. These images are passed through preprocessing module. This is the first step of this recognition system for both the training and test images. This system utilizes several morphological operation and skin color based segmentation approach in the preprocessing module.

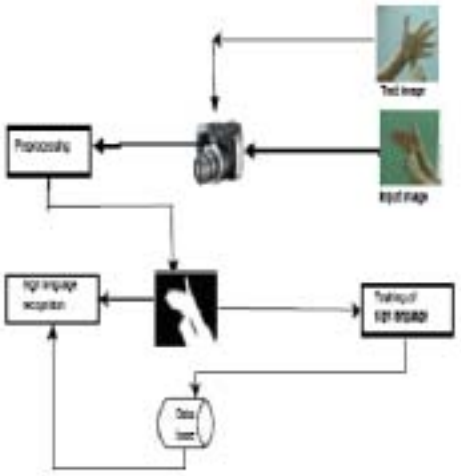

Fig. 1. Proposed System Architecture

III. SYSTEM DESCRIPTIONS AND IMPLEMENTATION

A. PREPROCESSING

To make the computation faster the image scaled to 0.40. After that, human skin color based segmentation approach is used. Results of these preprocessing steps are shown in Fig 2.

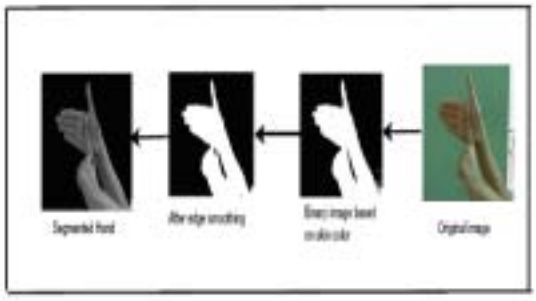

Fig. 2. Example Output of Preprocessing Method

The RGB images captured by the video camera are converted to HSV (Hue, Saturation and Value) color coordinate system [11]. Skin color region is determined by applying threshold values on Hue. If the Hue value satisfies a specific range (H_Low<H<H_High) then the value of the pixel color is white (1), otherwise it is black (0). Thus the original image is converted to binary image. Closing operation is performed for filling the gaps, smoothing their outer edges of binary images and Opening operation is for removing snowflakes [11]. The original color image is again converted to gray scale image using (1). The image is saved as a gray bmp image, where Gr_i is the gray level value of the i^{th} pixel of the gray image. R_i, G_i, B_i corresponds to intensity values of Red, Green and Blue of the i^{th} *pixel* in the color image. Finally, binary image is superimposed on the gray-level image and thus hand pose is segmented from the background.

$$Gr_i = \frac{R_i + G_i + B_i}{3}, i = 1,2,3,\ldots\ldots M \times N, \quad (1)$$

B. TRAINING ALGORITHM

In this system, Turk and Pentland's trick was used to get the eigenvectors of AA^T from the eigenvectors of $A^T A$ [12]. This algorithm includes the following operations:

Step 1:

Prepare training images $I_1\ (p \times q), I_2\ (p \times q) \ldots I_M\ (p \times q)$ where M is the total number of images.

Step 2:

Represent each images $I_i\ (p \times q)$ as a vector $T_i\ (pq \times 1)$

Step3:

Compute the average vector

$$\Psi = \frac{1}{M}\sum_{k=1}^{z} T_i \quad (2)$$

Step 4:

Subtract the mean from each of the training images

$$\phi_i = T_i - \Psi \quad (3)$$

Step5:

Form the matrix

$$A = [\phi_1, \phi_2, \ldots\ldots\ldots \phi_Z] \quad (4)$$

Step 6:

Compute the covariance matrix C

$$C = AA^T \quad (5)$$

Step 7:

Compute the eigenvectors v_i *and* eigenvalues u_i of C using Matlab function,

$$[v_i\, u_i,] = \text{eig}(c) \quad (6)$$

Step 8:

Sort the eigenvectors based on eigenvalues u_i *in* the ascending order.

Step 9

Select only K-eigenvectors of v_i *(*corresponding to the higher order of eigenvalues) to form PCA. These vectors define the eigenspace of hand images. Fig. 3(a). shows sample eigenhandimages.

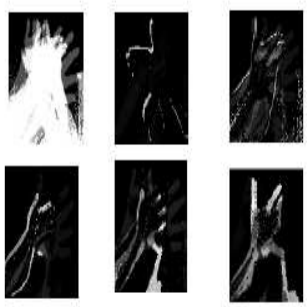

Fig. 3(a). Sample of eigenhand images

Step 10:

Project each training image onto the eigenspace and determine weight vector Ω_i.

$$w_l = v_k^T \phi_i \quad (7)$$

$$\Omega_i = [w_1, w_2, \ldots\ldots, w_k] \quad (8)$$

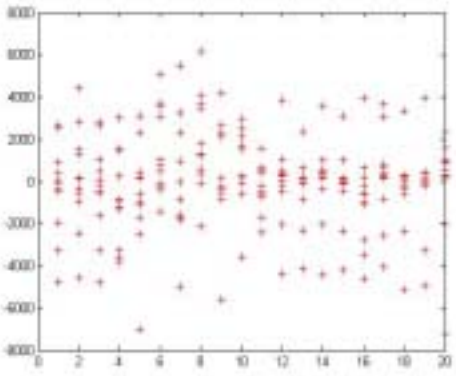

Fig. 3(b). Feature point distribution

Fig. 3(b). shows the feature point distribution for 20 training images of two Bengali vowels from two different persons (2x5x2) after projecting onto the eigenspace. In this case, 11 eigenvectors are selected to form PCA set or eigenspace.

C. RECOGNITION ALGORITHM

Step 1:

Read a test image $S(p \times q)$, segment and preprocess as like as training images. Thus make it as same size and type of training images.

Step 2:

Subtract the mean from the test image as (3).

Step 3:

Project the test image onto the eigenspaces and calculate a set of weight vectors Ω using (7) and (8).

Step 4:

Calculate minimum Euclidian distance using

$$e_r = \min \| \Omega - \Omega_i \| \quad (9)$$

Step 5:

If $e_r < T_h$ then the test image is recognized as image i from the training set where T_h is the predefined threshold T_h.

Table I summarizes the symbols that are used for describing training and recognition algorithm.

Table I List of Symbols Used in Training and Recognition Algorithm

$\Gamma_i (p \times q)$	Training Images
Ti	Vector that have the gray value of training Images
ψ	Mean image
ϕ_i	Keeps the result of subtraction from the original image to mean image
C	Covariance matrix
v_i	Eigenvectors of the training images
u_i	Eigenvalues of the training images
Ω_i	Weight vector
$S(p \times q)$	Test image
Ω	Weight vectors generated from test image
e_r	Minimum Euclidian distance
T_h	Predefined threshold value

IV. EXPERIMENTS, RESULTS AND DISCUSSIONS

A. EXPERIMENTAL SETUP

The goal of the system is to recognize the BdSL characters using PCA method. This system uses CCD camera for image acquisition that captures 30 image frames per second. The system uses an Intel Celeron 2.54 Hz PC with 1 GB RAM.

B. TRAINING IMAGE DATABASE

The system is trained to recognize 16 hand shapes (6 Bengali vowels and 10 Bengali numbers). Separate PCA is used for Bengali vowels and Bengali numbers. In case of Bengali vowels 5 images of each hand sign are captured from 8 different people for training. This resulted in 240 (8x6x5) training images for Bengali vowels. Again, 5 images of each hand sign for Bengali numbers are captured from 8 different persons for the training set. This resulted in 400 training images for Bengali numbers (8x10x5). For the test case, 10 images of each hand sign are captured from 8 different people where five are females and three are males. This re-

sulted in 480 (8 x6x10) test images for Bengali vowels. Again, 10 images of each hand sign of number are captured from 8 different people for Bengali numbers. This resulted in 800 (8x10x10) images for Bengali numbers. Fig. 4(a). and 4(b). show the sample training images of 6-Bengali vowels and 10- Bengali numbers.

Fig. 4(a). 6- Bengali vowels

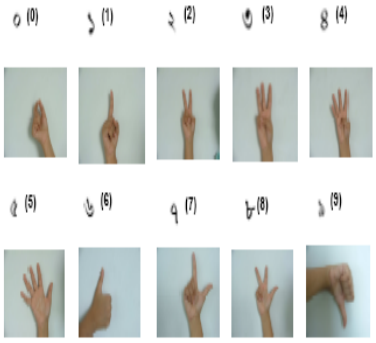

Fig. 4(b). 10- Bengali numbers

C. RESULTS OF BENGALI VOWELS RECOGNITION SYSTEM

This system can detect Bengali signs involving two hands, which is complex one. Table II shows the confusion matrix for the results of hand sign recognition for 6 Bengali vowels. In this table the first column represents the input image classes and other columns represent recognition results. The last column represents the hand signs that are recognized as unknown. For example, among 80 test hand signs for **অ,** 59 are correctly recognized, 17 are wrongly recognized and 4 are recognized as unknown. Table III presents precision rate and recall rate of vowel recognition system calculated from the confusion matrix as defined in Table II. The precision is defined by the ratio of the numbers of correct recognition to the total numbers of recognition for each hand signs. The recall rate is defined by the ratio of the numbers of correct hand sign identification to the total number of hand signs. Fig. 5. shows the graph of corresponding precision rate and recall rate.

Table II Confusion matrix for 6-Bengali vowels

Bengali Number	**অ**	**আ**	**ই**	**উ**	**এ**	**ও**	**Unknown**
অ (80)	59	4	1	5	3	4	4
আ (80)	1	49	0	15	5	10	0
ই (80)	4	0	63	11	0	2	0
উ (80)	0	7	0	41	11	21	0
এ (80)	2	2	0	11	54	11	0
ও (80)	0	14	0	7	2	5	0

Table III Precision rate and Recall rate for Bengali vowels

Bengali Vowels	**Precision rate(%)**	**Recall rate(%)**
অ	89	78
আ	64	61
ই	98	79
উ	46	51
এ	72	68
ও	54	71

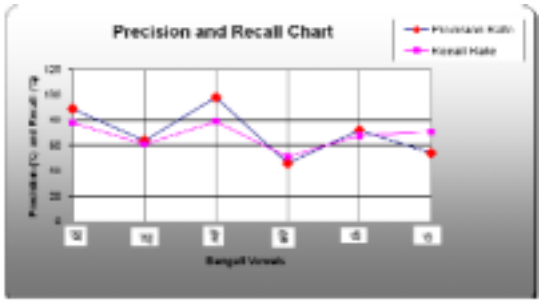

Fig. 5. Precision and Recall rate for Bengali vowels

D. RESULTS OF BENGALI NUMBERS RECOGNITION SYSTEM

This system can detect Bengali numbers from 0 to 9 involving one hand. Table IV shows the confusion matrix for the results of hand sign recognition for Bengali numbers. For example, among 80 test hand signs for **0,** 71 are correctly recognized and 9 are recognized as other numbers. Table IV presents precision rate and recall rate of this system calculated from the confusion

matrix as defined in Table II. Fig. 6. shows the graph of corresponding precision rate and recall rate.

Table IV Confusion matrix for Bengali numbers

Bengali Number	0	১	২	৩	৪	৫	৬	৭	৮	৯	Unknown
0 (80)	71	1	1	0	3	0	0	0	1	2	2
১ (80)	2	69	1	0	3	1	0	1	2	1	0
২ (80)	3	2	65	1	0	0	5	2	0	2	0
৩ (80)	3	0	0	60	4	2	3	0	5	2	1
৪ (80)	0	4	3	1	65	2	0	3	0	2	0
৫ (80)	3	2	3	2	0	64	0	0	2	4	0
৬ (80)	0	2	0	3	0	0	68	1	3	1	2
৭ (80)	3	0	0	0	3	2	1	69	1	1	0
৮ (80)	1	3	0	2	0	4	0	0	67	0	3
৯(80)	0	0	0	3	2	0	1	0	0	71	3

Table V Precision rate and Recall rate for Bengali numbers

Bengali Number	Precision rate(%)	Recall rate(%)
0	83	89
১	84	86
২	87	81
৩	83	75
৪	81	81
৫	83	80
৬	84	85
৭	87	86
৮	83	84
৯	82	89

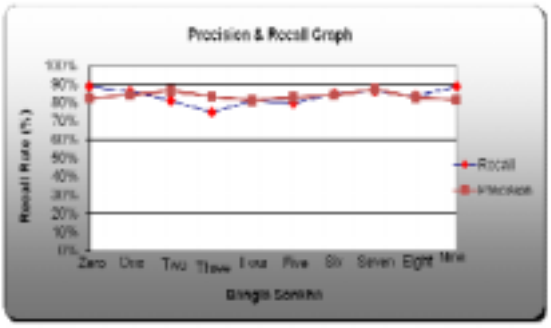

Fig. 6. Precision rate and Recall rate for Bengali numbers

V. CONCLUSION

This work makes major contribution in areas of Computer Vision Based Bangladeshi Sign Language Recognition. Most of the signs of other sign language that have been studied so far are based on the gesture of one hand and because of that those signs are easy to process and are comprehensible for a recognition system. But Bengali Sign Language uses both hand to represent a sign (except numbers) and for a recognition system this two wrist gestures becomes very difficult to be precisely recognized. From the experimental results, it can be concluded that recognition performance of the system is satisfactory instead of the complexity of the work. The ultimate goal of this paper is to further improve the proposed sign language recognition system using more improved pattern recognition algorithms and eliminate the limitations and use it successfully for Human to Machine Interface for disable people.

VI. ACKNOWLEDGEMENT

I would like to express my heartiest gratitude and thanks to my supervisor , Dr. Md. Hasanuzzaman ,Associate Professor, Department of Computer Science and Engineering , University of Dhaka for his time, advice, encouragement and critical reviews throughout my thesis. I would also thank to the Department of Computer Science and Engineering, University of Dhaka for providing valuable resources and materials. Finally, I would like to thank my parents, teachers and fellow-mates for their support and encouragement.

REFERENCES

[1] Padden Carol A. and Tom Humphries, *Deaf in america*, in Harvard University Press, 1988.

[2] Centre for Disability in Development (CDT), "Manual on Sign Supported Bangla," in *Computer Vision and Image Understanding*, 1-50, 2002.

[3] M Hasanuzzaman, T. Zhang, V. Ampornaramveth, and H. Ueno,"Gesture-based human-robot interaction using a knowledge-based software platform, "

in *International Journal of Industrial Robot*, Vol. 33, No. 1, pp. 37-49, 2006.

[4] Hasanuzzaman M. "Vision and Knowledge-Based Gesture Recognition for Human-Robot Interaction," *Ph.D. thesis*, NII, Tokyo, Japan, March 2006.

[5] V. I. Pavlovic, R. Sharma and T. S. Huang, "Visual Interpretation of Hand Gestures for Human-Computer Interaction: A Review," in *IEEE Transactions on Pattern Analysis and Machine Intelligence (PAMI)*, Vol. 19, No. 7, 1997, pp. 677-695.

[6] M.B. Waldron, and S. Kim, "Isolated ASL Sign Recognition System for Deaf Persons," in *IEEE Transactions on Rehabilitation Engineering*, Vol. 3, No. 3, 1995, pp. 261-271.

[7] Holden, E.-J., R. Owens, and G. Roy, "Adaptive fuzzy Expert System for Sign Recognition, " in *Proceedings of the International Conference on Signal and Image Processing (SIP'2000)*, Las Vegas, USA, 2000, pp. 141-146.

[8] Vamplew, P. and A. Adams, "Recognition of Sign Language Gestures using Neural Networks," in *Australian Journal of Intelligent Information Processing Systems*, Vol. 5, No. 2, 1998, pp. 94-102.

[9] H. Birk, T. B. Moeslund, and C. B. Madsen, "Real-time Recognition of Hand Alphabet Gesture Using Principal Component Analysis, " in *Proceeding of 10th Scandinavian Conference on Image Analysis*, Finland, 1997.

[10] Vogler, C. and D. Metaxas, "Adapting Hidden Markov Models for ASL Recognition by Using three-Dimensional Computer Vision Methods," in *Proceedings of the IEEE International Conference on Systems*, Man and Cybernetics SMC97, IEEE Computer Society: Orlando, Florida. 1997, pp. 156-161.

[11] Rafael C. Gonzalez and Richard E.Woods, *Digital Image Processing*, Pearson Education Pte. Ltd., India, 2003. [12]

[12] Turk M. and Pentland, "Eigenfaces for recognition," in *The Journal of Cognitive Neuroscience*, 3(1): 71-86., 1991.

Proceedings of 2009 12th International Conference on Computer and Information Technology (ICCIT 2009)
21-23 December, 2009, Dhaka, Bangladesh

Challenges in Building Trust in B2C E–Commerce and Proposal to Mitigate Them: Developing Countries Perspective

Subrata Kumar Dey, Mohammad Noor Nabi, Mohammed Anwer
School of Engineering & Computer Science, Independent University, Bangladesh
subrata@secs.iub.edu.bd, mnnabi@secs.iub.edu.bd, manwer@secs.iub.edu.bd

Abstract

In this technology mediated world, e–Commerce is becoming more and more powerful medium for doing business, globally. Existing security technologies are proven to protect online transaction and fund transfer. However, while transacting with global e–merchants, trustworthiness of secure fund transfer and delivery of products/services are affected, and they could not leverage the potential benefit of e–Commerce. In this paper, the authors firstly overview the current state-of-threat by surveying was people's perception about trust in e–Commerce in developing countries like Bangladesh and argue that the security requirements of e–Commerce service generally go beyond the more traditional requirements of network security. The result analysis shows that, challenges in building trust for Business-to-Consumer (B2C) e–Commerce venture (local/international) is the major concern. The authors propose an e–Commerce enabled model for secure electronic fund transfer, and discuss ways to mitigate challenges in building trust in B2C.

Keywords: e–Commerce, B2C, Secure Electronic Transaction, Trust, Local Trusted Third Party.

I. INTRODUCTION

In recent years, Internet has revolutionized e–commerce in developed countries. However, the full potential of e–Commerce will be achieved iff there exist trustworthiness and both consumers and merchants have confidence in trading electronically. The Internet and e–Business are complementary events linked with enhancement of web technology and internet security [1]. Depending on participants and scope, e–Commerce can be divided into business–to–business (B2B), business–to–consumer (B2C), consumer–to–consumer (C2C), government-to-constituent (G2C), etc. In a complete and mature economy; B2B, B2C and C2C e–Commerce may not be treated discriminately [2].

Currently there are enormous numbers of players in e–Commerce market. But there are restricted numbers of e–Commerce corporate-s which successfully have made businesses in the severely competitive market, such as Amazon.com and eBay [3]. Globally reputed e–Commerce ventures are secured by the existence of strong Public Key Infrastructure (PKI) and legal framework of their respective countries. Thus, for countries to prosper in e–Commerce, they need to establish Local PKI (LPKI) and develop other necessary infrastructure and legal framework.

Concerns over the security of the Internet, could not fully assure users about the safety of online trade and have a great impact on successful e–Commerce. Online transactions ultimately rely on security of the trading environment, and establishment of trust and cooperation between consumers and merchants. Trust is a concept of subject across and it is being studied in domains as social psychology, marketing, management, economics [4]. Trust is a dynamic program. Scholars in E–Commerce put out a concept of trust that is widely accepted. Their opinion is "trust is one will always act in the way that the other wants him to, no matter how high the risks are". Trust is a setup on the estimate of the other's behavior. So, trust is not a kind of behavior or choice but a dynamic process of a kind of causal psychology. This definition is also efficient to B2C e-commerce, except that the protocol of e–Commerce is electronic or concealed.

To investigate major challenges in building trust in B2C, a survey was conducted on Bangladeshi merchants, financiers and consumers for establishing trusted B2C e–Commerce. A model for secure electronic transaction is proposed involving LPKI and local trusted third party; which could be applied to facilitate trust in B2C.

The following section review relevant works and literature. Section III outlines challenges in building trust for B2C e–commerce initiatives. Section IV presents and discusses the results. Section V focuses on mitigating challenges in building trust in B2C e–Commerce and proposes ECE-set protocol. Finally, section VI draws some conclusions from the findings and outlines future work in this field.

II. LITERATURE REVIEW

The e–Commerce issues like the navigation style, the response time and the design of the interface are identified by Fiona and Davis [5]. The paper also discusses the trust requirements and provides suggestions to improve trust but these suggestions are all about the authenticity of the ecommerce sites and does not address many trust concerns identified in the survey. The article at e-future [6] discusses the back-end issues for the im-

978-1-4244-6283-4/09/$26.00 ©2009 IEEE

provement of e-commerce.

There are a few related studies in measuring customer satisfaction with e–Commerce systems as "Measuring e–Commerce Success: Applying the DeLone & McLean information systems success model" by DeLone & McLean [7], "Evaluating e–Commerce functionality with a focus on customer service" from Lightner [8]. Both studies are based on customer satisfaction as DeLone & McLean focuses on user satisfaction and Lightner on customer service. Molla & Licker have highlighted that existing works related to the user information satisfaction (UIS), and customer satisfaction (CS) as a measure for e–Commerce success were limited in scope and treatment to fully describe e–Commerce success and lacked comprehensiveness in capturing the full functionality of e–Commerce systems [9].

III. CHALLENGES IN BUILDING TRUST FOR B2C

A. Innovative Challenges

Coping with newer and newer innovations on technology adoption, product offerings, after-sales service, user-interface/navigation, knowledge/content management, supply-chain management, etc, is a prerequisite task for building trust and become a successful B2C venture. Some of the innovative challenges are [10]: a) Relative Advantage, b) Complexity, c) Compatibility, d) Trial-ability, e) Demonstrability, f) Visibility, g) Image, etc.

B. Consumer Personality Challenges

Various studies on human personality shows that [11], personality influence them greatly in decision making. Favorable decision making behaviors of consumer is a vital issue in building perceived trust on B2C venture .As defined by Littauer [12]; and discussed by Lumsden and MacKay [11], different personality traits affecting consumer trusts can be categorized as: a) Popular Sanguine, b) Perfect Melancholy, c) Powerful Choleric, and d) Peaceful Phlegmatic`.

These personality traits play different role to influence consumers differently in building perceived trust on B2C e–Commerce by means of: a) customer testimonials and feedback, b) professional website design, c) consistent (professional) graphic design, d) ease of navigation, e) branding, f) third party security seals, g) up-to-date technology and security measures, h) alternative channels of communication between consumers and the vendor, i) clearly stated policies and vendor information, etc.

D. Technical Challenges

1) Non–existence of Public Key Infrastructure for Local Currency Transaction — A PKI consists of client software, server software, hardware, requisite acts and legal framework, and necessary operational–procedures/protocols [13].

2) Inadequate Internet Speed and Other Infrastructure — In developing country like Bangladesh, most of the internet infrastructure is own by telecom industry (e.g. till today, all the ISPs in Bangladesh need to buy bandwidth from BTCL [14] and most of the Internet user are dial–up user and uses BTCL phone lines), which may not be too much willing to change to high bandwidth infrastructure like DSL, country–wide fiber network, or Wi–Fi implementation in large scale.

3) Inadequate Skilled Human Resources — In many organizations, human resources cost the biggest portion of their budget, and yet there remains lack in skilled and efficient personnel. The key knowledge areas of e–Commerce venture and corresponding skills needed by developers may include [15]: a) Technical skills, Human skills, and Organizational skills.

D. Social Challenges

1) *Traditional Purchase Habit and High Cost of Doing Business* — In a under developed and perhaps in many developing countries, less number of online transactions may increase the cost of doing business as compared to traditional commerce. However, if the e–Commerce ventures of developing countries can tap foreign markets and build trust among foreign consumers, the cost of business will come down and the merchants can be relieved from local peculiarity.

2) *Challenging Customer Relationship Management and Customer Retention* — CRM [16] is an interactive process to achieve optimum balance between corporate investments and satisfaction of customer needs, eventually maximizing the profit. Due to the lack of personal contact, CRM processes in e–Commerce, relies on web–based interaction of merchants with their consumers.

3) *Poor Penetration Rate of Internet Access* — A recent UN developing agency (UNCTAD) report [17] reveals that though there is a claim in narrowing of digital divide, in 2006 there was a six–fold gap in Internet penetration rates between developed and developing (including underdeveloped) countries.

4) *Distrust in Technology Due to Ignorance in Understanding Threats* — Some of these common Internet threats are phishing and pharming attacks, which attempt to dupe the user into divulging sensitive information such as credit card numbers, bank account details, passwords and the like.

4.1. Unaware of Phishing Attack — in computing, phishing is the criminally fraudulent process of attempting to acquire sensitive information such as usernames, passwords and credit card details, by masquerading as a trustworthy entity in an electronic communication.

4.2. Unaware of Pharming Attack — Pharming is a hacker's attack aiming to redirect a legitimate website's traffic to a bogus website. Pharming can be conducted

either by changing the hosts file on a victim's computer or by exploitation of a vulnerability in DNS server software.

4.3. Ignorance of Using Secure Websites — a secure web site uses encryption and authentication standards to protect the confidentiality of web transactions and many of the internet users are ignorant about this. Currently, the most commonly used protocol for web security is Secure Sockets Layer (SSL).

5) *Distrust due to Problems in Electronic Negotiation* — Electronic negotiation between participants allows cooperative and competitive sharing of information to determine a proper price. Recent research and practice has reveled that [18] most of the e–Negotiation options are for electronic auction; most auction sites support price negotiations only. While traditional negotiations typically include discussion of other attributes such as: a) delivery terms, b) payment conditions, c) insurance policy, etc.

6) *Security Breach* — Inadequate hardware protection of the network and usage of illegal/pirated software is a serious concern in developing countries. Consumers often go through sense of insecurity and refrain from using personal and financial information over the internet.

E. Non-Compliance to Legal Issues

Another important barrier in e–Commerce success is non–compliance to legal issues such as: a) violation of copyright act and cyber law, b) limited/no accountability of merchants, c) difficulties in Enforcing consumer's rights, d) resolving cross–country legal differences, etc.

IV. RESULTS AND ANALYSIS

In the survey, the authors intended to identify the current status of Bangladeshi e–Commerce and evaluate the trust–level of B2C consumers. In doing so, the survey is conducted in three phases: a) Surveying Bangladeshi e–Commerce websites to evaluate their status, b) Interviewing local citizen with experience to date with B2C e–Commerce shopping, and c) Interviewing Merchants handling local credit cards at POS (point–of–sale) counter, Merchants without POS terminals, Local Bank personnel and local citizen with POS(point–of–sale) shopping to discover their perception of trust in e–Commerce.

Trust parameters considered for questionnaire and interview were: a) Lack of technical Knowledge, b) Concern Over Security Issues, c) Lack of Human Resources, d) Lack of IT Infrastructure, e) Lack of Funding, f) Little Upper Management Support, g) Lack of Legal framework, and h) No Model e–Commerce Venture. The response values are converted into percentage.

The survey result in figure-2 shows that, merchants having PoS as well as without PoS considers lack of technical knowledge, concern over security, lack of human resources, as the major barriers of building trust. Merchants without PoS also has huge concern on lack of funding, lack of legal framework and no model B2C venture as trust barriers. Bank personnel identified lack of technical knowledge, lack of legal framework and no model B2C e–Commerce venture as significant trust barriers. Consumers using PoS have concern on all the trust factors considered for survey; especially on secured transaction, proper legal framework and absence of ideal local B2C ventures.

Fig.1. Survey result of Merchant's, Financier's and Consumer's (PoS) view on trust factors influencing B2C e–Commerce

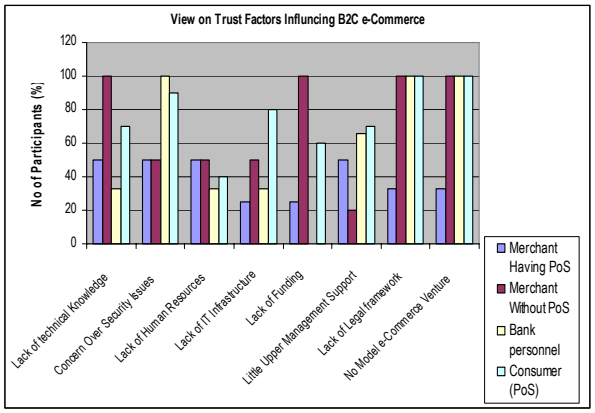

The objective of interviewing local citizen with experience to date with B2C e–Commerce shopping was to carry out an *initial* analysis of the B2C e–Commerce customers so that we might make some initial *trust situation which* later followed up with more extensive research. About 80% of respondents had previously made an online purchase. When asked about issues affecting online transaction respondent provided variety of answers as shown in figure 2.

Fig.2. Issues Affecting Online Transaction (discouraging factors)

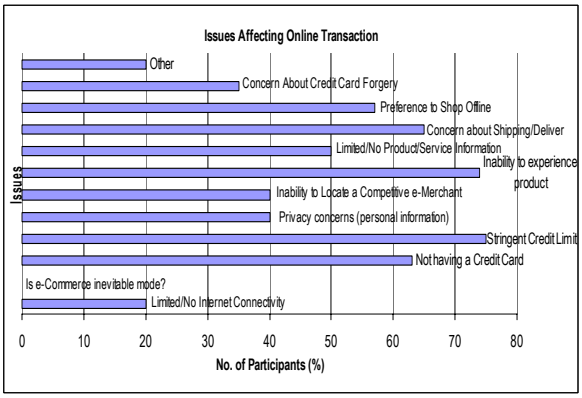

More than half of respondents identified that not having a credit card, stringent credit limit, inability to locate a competitive e-merchant, limited/no product/service information, concern about shipping/delivery, and preference to shop offline are affecting online transaction. In

developing countries credit availability affects online shopping. Other apprehensions raise issue of lack of trust in e-commerce.

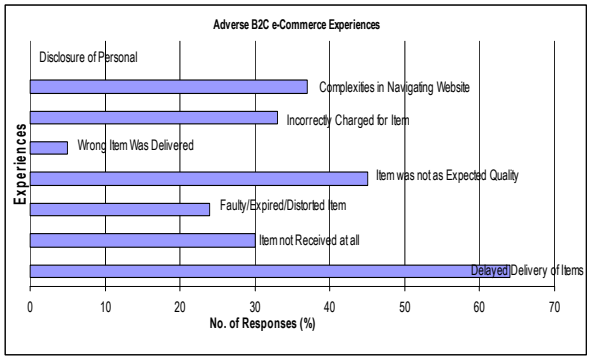

Fig.3. Adverse B2C e–Commerce Experience (discouraging experiences)

When asked to describe the adverse B2C e–Commerce Experience, respondents provided a variety of answers as shown in figure 3. Approximately one third of all respondents who had reported a bad experience with online shopping indicated that items was not delivered on time, not received at all, or quality was not as expected when they did arrive. These findings suggest that currently e–Commerce vendors are perhaps often not providing sufficiently reliable level of service to meet the expectations of their consumers, and this is leading to an adverse perception of the e–Commerce shopping experience amongst those consumers. Obviously, we cannot draw any statistically supported conclusions from the findings. However, the observations highlight lack of trust in e-Commerce.

V. MITIGATING CHALLENGES IN BUILDING TRUST IN B2C

A. Modeling of B2C Platform Ensuring Trust

To mitigate the challenges in building trust, a prospective B2C venture needs to address the trust factors (innovative, personality, technical and social challenges) discussed earlier. For this purpose, a B2C platform needs to be modeled before implementation of the venture, considering the following:

1) *Offering Appropriate Products/Services* — For a B2C e–Commerce venture, it is necessary to offer variety of products/service both in depth and breath. Among other factors, offering wide variety of products/services supported by proper supply chain management and appropriate pricing policy will lead to gain consumer trust and revisit of consumer.

2) *Ensuring Richness of Information* — To compare the intended product with similar/peer products in terms of features/quality/pricing, etc. Research shows that [19], enabling consumer with rich product information will enhance consumer's trust on the merchant.

3) *Ensuring User friendly Navigation & User Interface* — Capability of finding required information with ease is a vital trust issue. Hierarchical organization of data with customized user interfaces portraying the consumer's social, economic, ethnic preferences; is a key to build trust in e-Commerce. It is also advantageous to provide multi-lingual user interface.

4) *Ensuring Consumer Satisfaction by providing Perceived Quality* — Perceived consumer satisfaction can be obtained by ensuring: a) On time delivery with quality product with proper packaging and shipment method; b) Quick response to consumer queries; c) Visibility of contentious development of service quality, payment methods, delivery systems resulting to confidence building of consumer; d) Offering personalized product/service, etc.

5) *Adoption of B2C Business Model* — It is very much important for an e–Commerce venture to adopt a suitable business model keeping in mind: a) the social, economic and ethnic background of the consumer-base, b) business expansion plan, c) budget and cash flow for contentious technology investment for innovation, d) the anticipated market opportunities, e) legal issues of the territories of target consumers, etc.

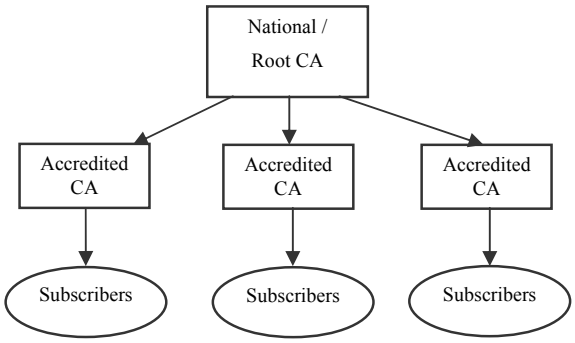

Fig.4. Model of LPKI formation

B. Building Sustainable Trust

As the product/service can't be verified like offline trading, it's not easy to build trust and confidence in consumer. However, it is more difficult to sustain the acquired trust and confidence. Some of the key strategic areas for maintaining sustainable trust are [20][21][22]: a) Ensuring Perceived Trust Adoption of Marketing & Advertising strategy, b) Adoption of appropriate e-CRM techniques, c) Adoption of Knowledge Management, d) Adoption of Supply Chain Management: Ensuring timely delivery of products/services, e) Providing Help Systems, etc.

C. Establishment of Local Public Key Infrastructure (LPKI)

1) *Existence of LPKI Enabling Authority and Administration* — Ministry of ICT will be the main authoritative organ of the government in implementing LPKI. However, to plan, implement and monitor LPKI infrastructure, an apex body need to be formed, which may be

called as National PKI Council (NPC). The model of LPKI is illustrated in Figure 4.

2) *Existence/Formation of LPKI enabling ICT Act* — The apex body, NPC will be liable in devising: a) Digital Signature Act, b) Certificate Authority Licensing Act (covering detailed pricing policy, technology standards, etc), c) Cyber Crime Act, d) e–Governance Act, e) e–Commerce Act, etc, and other necessary laws to create the legal framework of LPKI.

3) *Settlement on Technology Standards* — A working group/subcommittee may be formed for the settlement of technology standards for authentication, encryption, decryption, issuing digital signature, etc. the group will continuously monitor the global development of technology changes and recommend for necessary amendments to NPC.

4) *Establishment of Root/National Certificate Authority (RCA)* — A government organization under NPC will act as the Root/National Certificate Authority (RCA). The role of RCA will be to evaluate, accredit and license interested organizations to act as Accredited Certificate Authority (ACA), which in turn will issue digital certificates to its subscribers. ACAs can be classified into two broad categories such as: a) Government ACAs, and b) Commercial ACAs.

5) *Establishment of Accredited CA* — Interested and capable organizations are accredited and licensed by RCA to issue and manage digital signatures to various clients to take advantage of LPKI and secure electronic transactions. In a large developing country with high population, there may be several ACAs, whereas in a small developing country with limited population, one or couple of ACAs can be enough.

D. Proposal for Local Trusted Third Party (LTTP) for B2C e-Commerce

In association with credit card issuer bank and merchant's acquirer, the associated payment gateway can complete the fund transfer procedure. However, for ensuring trust in B2C, a model of Local Trusted Third Party is proposed. They can build sense of trust in consumer as well as merchant's by endorsing the e–Commerce venture. Apart from acting as a part of local payment gateway system, LTTP will guarantee the delivery of products/services as promised within stipulated date. LTTPs are local sector-specific non-profit organizations formed by Ministry of Commerce and various business chambers/associations.

E. Proposed e-Commerce Enabled SET Protocol

In this section, the working mechanism of Secure Electronic Transaction (SET) is described and discussed the proposed ECE–SET (E–Commerce Enabled SET) protocol accommodating LTTP

1) *Brief Description of SET* — Secure Electronic Transaction (SET) [23][24] is an open encryption and security specification design to protect credit card transactions on the Internet. SET is not itself a payment system, rather it is a set of security protocols and formats. SET provide a secure communications channel among all parties involved in a transaction.

2) *Participants of SET* — Participants of SET include: a) Cardholder, b) Merchant, c) Issuer, d) Acquirer, e) Payment gateway, and f) Certification authority (CA). Five sub–protocols of SET consist of: a) Cardholder registration, b) Merchant registration, c) Purchase request, d) Payment authorization, and e) Payment capture.

3) *Role of the Participants of SET*: The Role of Card Issuer — Issues credit card to the consumer; The Role of Acquirer Bank — Handle transaction details on behalf of the merchant; The Role of Accredited Certificate Authority — Issues certificates to credit card holder, merchant, acquirer, and other involved parties; The Role of Payment Gateway — facilitates the transfer of information between the website and the acquirer bank.

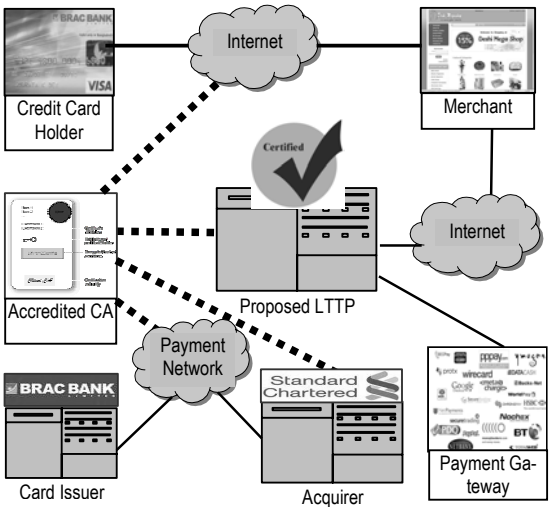

Fig.5. E-Commerce Enabled SET (Proposed)

4) *E–Commerce Enabled SET Protocol (ECE-SET)* — the proposed model for using credit card in online transaction is dependent on the EEC–SET protocol. Pictorial view of the protocol is depicted in Figure–5. The participants of ECE–SET includes: a) Cardholder, b) Merchant, c) Card issuer, d) Acquirer, e) RCA, f) ACA, g) LTTP, and h) Payment gateway. Before initiating a transaction; ACA issues certificates to i) card holder, ii) merchant, iii) card issuer, iv) acquirer, and v) LTTP.

LTTPs will accredit intending B2C merchants by issuing e-merchant certificates, which also will be encapsulated with merchant's digital certificate issued by a CA in the ECE-SET procedure. They will resolve disputes among merchants, consumers and other third parties like supply chain partners. LTTPs will periodically evaluate the trust parameters of B2C e-merchants and update their dynamic directory by revoking accreditation status for the defaulter e-merchants. The merchant's

and consumer's banks will verify concerned LTTP's dynamic directory for valid B2C transaction.

VI. CONCLUSIONS

The Internet has gone through revolutionary changes; and in developed countries, e–Commerce became a common norm of doing business. However, developing and underdeveloped countries are lagging behind in taping full benefit of growing e–Commerce; mainly due to: a) Non–existence of national level Public Key Infrastructure b) distrust about secured electronic transaction in local currency; c) various innovative, consumer's personality related, social and other technical challenges; d) non-compliance to legal issues. In this paper, the authors identified the basic challenges in establishing trust in B2C e-Commerce. The surveys suggest that currently e–Commerce vendors are not providing sufficiently reliable level of service to meet the expectations of their consumers, and this is leading to negative perception of the e–Commerce shopping experience.

Finally, the authors suggested ways to handle those challenges by proposing: a) a model for B2C platform; b) ECE–SET (secure electronic transaction with local trusted third party); c) discussing ways to sustain consumer trust in B2C; and d) highlighting on establishment of local PKI to create trust among consumers and merchants, alike. In future, the authors intend to work on some more identified issues such as: a) Accommodate Multiple and Cross–Currency Transactions, b) Convergence of m–Commerce and e–Commerce.

REFERENCES

[1] *Oreku, G.S., Jianzhong Li*, "Rethinking E–commerce Security"; International Conference on Intelligent Agents, Web Technologies and Internet Commerce, 2005.

[2] *Jianxin Shi, Yongxiang Wu*, "B2B, B2C and C2C: Should They be Treated Equally in China"; Canadian Conference on Electrical and Computer Engineering, 2006 (CCECE '06).

[3] Electronic Commerce Branch of Industry Canada, "Barriers to e-Business Adoption", viewed 28 Sep 2004, http://e-com. ic.gc.ca/epic/internet/inecic-ceac.nsf/en/gvOO 148e.html, 2003.

[4] *Pan Xia1, Ju Xiao-feng* "A Research on Development of Chinese B2C E-commerce Trust" 978-1-4244-4589-9/09/$25.00 ©2009 IEEE.

[5] Fiona Fui-Hoon Nah, Sid Davis, "Hci research issues in e-commerce",Journal of Electronic Commerce Research, VOL. 3, NO. 3, 2002.

[6] "Back-End Issues in E-Commerce", URL: http://www.e-future.ca/.

[7] W.H. DeLone, & E.R. McLean, "Measuring e-Commerce Success: Applying the DeLone & McLean Information Systems Success Model", International Journal ofElectronic Commerce, Vol.9, No. 1,p.31, 2004.

[8] N.J. Lightner, "Evaluating E-Commerce Functionality With A Focus On Customer Service", Communications ofthe ACM, Vol.47, No.10,pp.88-92, 2004.

[9] A. Molla, & P.S. Licker, "E-Commerce Systems Success: An Attempt To Extend And Respecify The Delone And Maclean Model Of Is Success", Journal ofElectronic Commerce Research, VOL. 2, NO. 4,pp.131-141, 2001.

[10] *Craig Van Slyke, France Belanger, Christie L. Comunale*, "Factors influencing the adoption of web-based shopping: the impact of trust", SIGMIS Database by ACM, Volume 35 Issue 2, June 2004.

[11] *Jo Lumsden, Lisa MacKay*, "How does personality affect trust in B2C e-commerce?", published in ACM 8th International Conference on Electronic commerce: The new e-commerce: innovations for conquering current barriers, obstacles and limitations to conducting successful business on the internet.

[12] *Littauer, F.*, "Personality Plus: How to Understand Others by Understanding Yourself", Grand Rapids, Michigan, USA: Fleming H. Revell Publishing, 2005, pp. 204.

[13] http://www.wikipedia.org.

[14] http://www.bttb.net.

[15] *Fred Niederman*, "Staffing and management of e–commerce programs and projects"; ACM SIGMIS CPR conference on Computer personnel research, 2005.

[16] *Susanne Glissmann, Lutz M. Kolbe, Nicholas C. Romano, Jr., Jerry Fjermestad,* "minitrack: Electronic Customer Relationship Management"; 41st Annual International Conference on System Sciences, Hawaii, 2008.

[17] http://www.breitbart.com/article.php?id=D8UL0AN03&show_article=1.

[18] *Cairo O.; Olarte J.G.; Rivera–Illingworth F.*; "A negotiation strategy for electronic trade using intelligent agents"; International Conference on Web Intelligence, 2003.

[19] *Lei-da Chen, Mark L. Gillenson, Daniel L. Sherrell*, "Consumer acceptance of virtual stores: a theoretical model and critical success factors for virtual stores", SIGMIS Database by ACM, Volume 35 Issue 2, June 2004.

[20] *Shan L. Pan, Jae-Nam Lee*, "Using e-CRM for a unified view of the customer", Communications of the ACM, Volume 46 Issue 4, April 2003.

[21] http://www.webtransitions.com/articles/ecommerce-marketing.asp.

[22] *Tian, Yuhong*, "Knowledge management mechanisms in e-commerce: A study of online retailing and auction sites", Publication: The Journal of Computer Information Systems; available at: http://www.allbusiness.com/technology/internet-technology/933686-1.html.

[23] Cryptography & Network Security: Principles & Practices (3rd Edition, 2003) – by William Stallings (Pearson Education).

[24] Network Security Essentials: Applications and Standards – by William Stallings (Pearson Education).

Proceedings of 2009 12th International Conference on Computer and Information Technology (ICCIT 2009)
21-23 December, 2009, Dhaka, Bangladesh

Numerical Analysis of Impedance Matched Inverted-L Antennas for Wi-Fi Operations

Khaled Mahbub Morshed, Debabrata Kumar Karmokar†, Abu Md. Numan-Al-Mobin
Department of Electronics & Communication Engineering, Khulna University of Engineering & Technology, Khulna, Bangladesh
†Department of Electrical & Electronic Engineering, Khulna University of Engineering & Technology, Khulna, Bangladesh
kmm_ece@yahoo.com, debeee_kuet@yahoo.com, nmobin27@yahoo.com

Abstract

This paper presents the numerical simulations of Inverted-L and stair inverted-L antennas capable of generating high gain with less than 1.5 dBi gain variation within the -10 dB return loss bandwidth for 5.5 GHz wireless-fidelity (Wi-Fi) operation with and without resistor-inductor-capacitor (RLC) impedance matching network. Moreover, the proposed antennas can provide bandwidth of 510 and 120 MHz respectively, making it easily cover the required bandwidths for Wi-Fi operation in the 5.5 GHz band. In application of matching network, the input impedance of the antennas well matched to the feeding cable, also improvement in return loss and voltage standing wave ratio (VSWR) is achieved.

Keywords: Inverted-L antenna, Matching network, Stair inverted-L antenna, Wi-Fi, Wireless local area network.

I. INTRODUCTION

Nowadays a Wi-Fi device is installed in many personal computers, video game consoles, smart phones, printers, and other peripherals, and virtually all laptop or palm-sized computers to provide flexible wireless communication to every user. Wi-Fi operates in the 2.4 GHz band (2.4 GHz–2.5 GHz) and 5 GHz band (5.15-5.35 GHz, 5.47-5.725 GHz and 5.725-5.875 GHz) [1]. To serve up the increasing demand and cover up the wide application area an antenna with high gain and matched with the feeding network is desired.

To realize the Wi-Fi operation where size, weight, cost, performance, ease of installation, flexible for mass production, and aerodynamic profile are constraints, low-profile antennas like microstrip and printed slot antennas are required [1-4]. To ensure the entire mentioned requirements inverted-L antenna is one of the good candidates if the impedance matching is provided, because in high frequency application inverted-L antenna has low input impedance than commonly required to match with the source. A coplanar waveguide (CPW)-fed slot antenna has input impedance of 50 Ω but the antenna gain is limited to 4 dBi [5]. On the other hand in planar-diversity folded dipole antenna, the antenna input impedance is matched by the 50 Ω microstrip feeding line where the antenna gain is of less than 6 dBi [6]. If the antenna input impedance is not matched with the feeding network then matching network can be used in between them. For the matching microstrip feeding line equivalent to RLC network for coaxial connector can be used so that the antenna gain and radiation of the antenna will not be hindered but the VSWR and return loss will improve in significance. For the RLC matching two techniques proposed one is parallel RLC resonator cell in series [10] and other one is coupling element based method [11]. For the antenna size reduction capacitive load can be used without degrading the antenna performance [7-9]. If the antenna is of compact size then matching is the key to enhance the performance parameters.

This paper addresses the numerical analysis of two proposed structures as inverted-L and modified inverted-L antenna named as stair inverted-L antenna to realize the 5.5 GHz Wi-Fi operation with RLC matching. The cost of FR4 substrate is higher than the RT/duroid 5880. For the lower cost, in numerical analysis we considered the RT/duroid 5880 substrate with permittivity of $\varepsilon_r = 2.2$ and substrate thickness of 1.27 mm. The analysis is performed numerically using method of moments in Numerical Electromagnetics Code (NEC).

II. ANTENNA CONFIGURATION

The design of antenna for Wi-Fi operation is started from the low profile printed T-shaped monopole antenna by considering the antenna has low gain [3]. We examined the possibility of increasing the gain by simplifying the structure of the antenna for 5.5 GHz Wi-Fi operation. Figure 1 and 2 shows the proposed structures of inverted-L and modified inverted-L antennas respectively for the 5.5 GHz Wi-Fi operation and the parameters with their length are listed in Table I for both antennas. The inverted-L antenna (ILA) is a short monopole with the addition of a horizontal segment of wire at the top. Moreover, when the stair type loaded strip is applied on the ILA then the modified antenna named as stair ILA. The major problem of ILA is the low input impedance [12]. If matching network is used in between the antenna and feeding network then the problem is solved. For this low pass RLC pi-filter is used in this analysis to solve the problem of mismatch.

The antennas are assumed to feed by a 50-Ω coaxial cable, with its central conductor connected to the

feeding point and its outer conductor connected to the ground plane. In the analysis the dimensions of the ground plane considered as 60 mm × 60 mm. Due to the small dimensions of the proposed antennas, it can be mounted in any type of portable devices to support the Wi-Fi operations.

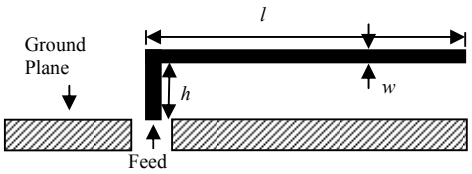

Fig. 1. Inverted-L antenna.

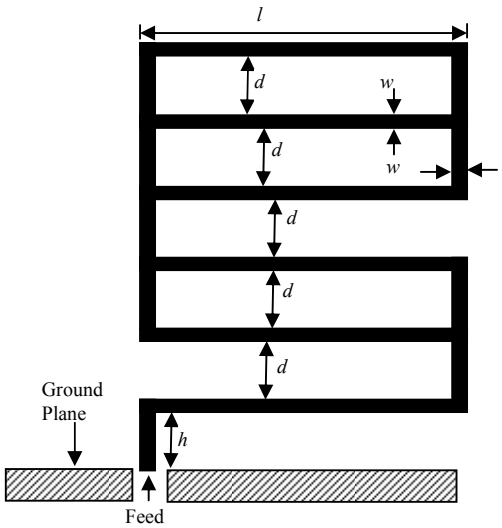

Fig. 2. Stair inverted-L antenna.

Table I Dimension of the proposed antennas

Antenna Name	Antenna Parameters	Length (mm)	Antenna Dimension
Inverted-L Antenna	*h*	8	08 × 35 mm^2
	l	35	
	w	3	
Stair Inverted-L Antenna	*h*	5	35 × 48 mm^2
	l	35	
	w	3	
	d	5	

III. SIMULATION RESULTS

Figure 3 shows the structure of the matching networks for ILA and stair ILA. Parameters of the matching network for the ILA and stair ILA are listed in Table II. The proposed antennas have the return loss appreciable than the commonly required return loss -10 dB level. Without matching the ILA has the VSWR 1.121 with return loss -24.9 dB and total gain of 5.62 dBi at 5.5 GHz with less than 1.5 dBi gain variation within the antenna bandwidth. But when the low pass Pi-filter is used as a matching network then the VSWR is 1.0098, return loss -66.171 dB and gain 5.62 dBi. These are shown in Figure 4, 5 and 6.

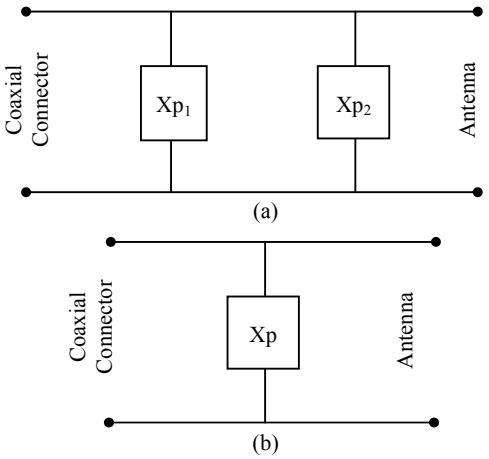

Fig. 3. Matching network for (a) inverted-L antenna (b) stair inverted-L antenna.

Table II Matching network parameters

Antenna name	Network Parameters	Value
Inverted-L antenna	Xp_1	0.12 pF
	Xp_2	0.13 pF
Stair inverted-L antenna	Xp	0.26 pF

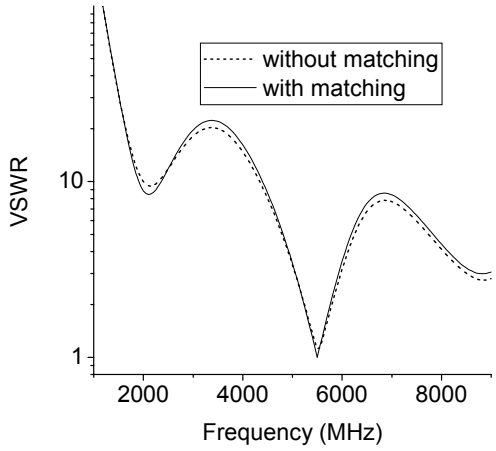

Fig. 4. VSWR of inverted-L antenna with frequency.

The simulation results shows that the antenna gain is unaffected by the matching network but the VSWR and return loss improves in significance. The -10 dB return loss bandwidth of the ILA under no matching is 530 MHz (5260 – 5790 MHz) which is much wider bandwidth for the 5.5 GHz Wi-Fi applications. Under

matching condition impedance bandwidth of the ILA is 510 MHz (5240 – 5750 MHz). Thus, due to the application of filter the antenna impedance bandwidth is decreased by 20 MHz but the gain variation within the impedance bandwidth remains the same.

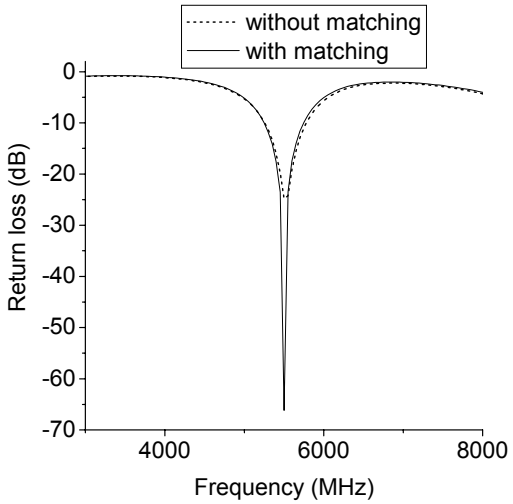

Fig. 5. Return loss of inverted-L antenna with frequency.

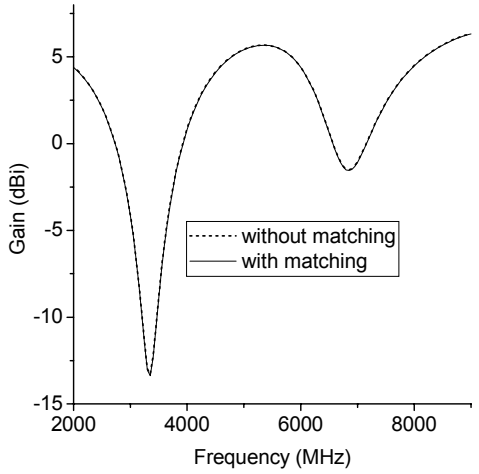

Fig. 6. Total gain of inverted-L antenna with frequency.

Figure 7 shows the radiation pattern of ILA in horizontal plane (XY plane) and vertical plane (XZ, YZ plane). Matching network has no effect on the radiation pattern of the antenna and the antenna has good radiation characteristics with acceptable gain in each plane. Figure 8 shows the input impedance variation of ILA with and without matching network. Without matching the antenna input impedance is 48.39 Ω, due to this input impedance there is a mismatch between the coaxial connector and the antenna. But the application of filter network helps to match the antenna with the coaxial connector. This matching network acts as an impedance matching device between the antenna and the coaxial connector. Using matching network input impedance of ILA changes to 50.0389 Ω.

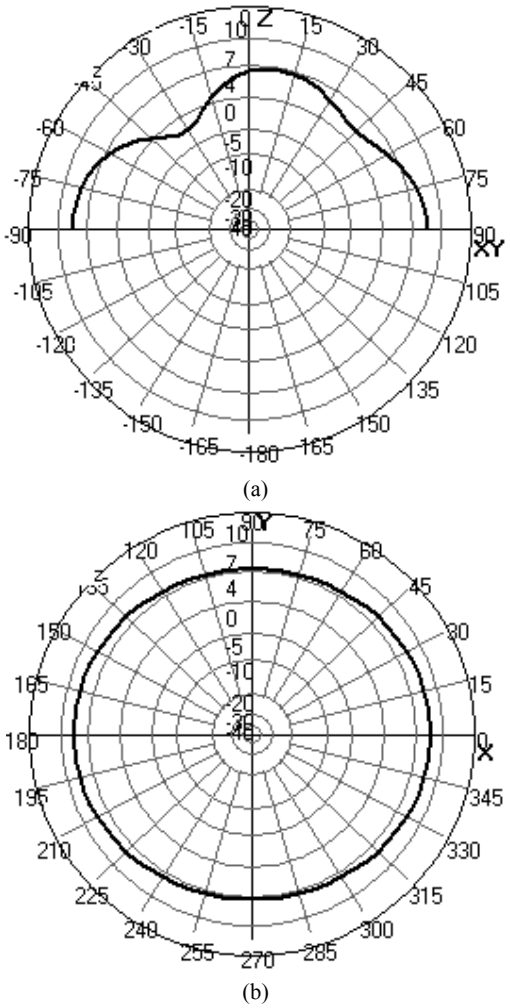

Fig. 7. Total gain pattern of inverted-L antenna at 5.5 GHz in (a) vertical plane and (b) horizontal plane.

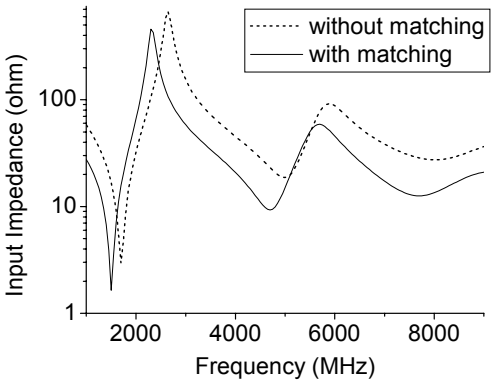

Fig. 8. Input impedance variation of inverted-L antenna.

The phase angle variation of ILA with and without matching network is shown in Figure 9. Due to the matching network the phase changes from 6.244^0 to

0.0344^0. This indicates the reactive components decreases and resistive component increases at the antenna input terminal. This makes the antenna more efficient in radiation of electromagnetic signal.

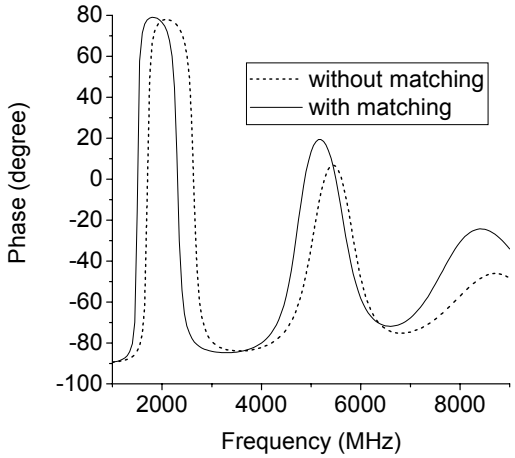

Fig. 9. Phase angle variation of inverted-L antenna with frequency.

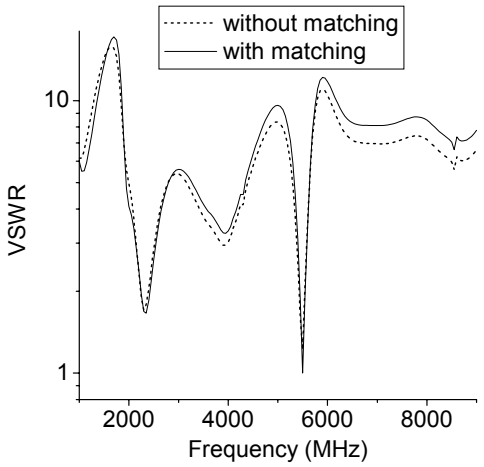

Fig. 10. Variation of VSWR of stair inverted-L antenna with frequency.

Figure 10 and 11 shows the VSWR and return loss variation with frequency of stair ILA under matching and non-matching condition. From the simulation, under matching condition the VSWR shifted from 1.222 to 1.00167 and return loss -20 dB to -61.555 dB. The impedance bandwidth of the stair ILA is 120 MHz (5420 – 5540 MHz) and with matching the bandwidth remains same. This antenna covers the 50% of the 5.5 GHz Wi-Fi operating band. The antenna bandwidth is decreased with the application of load to the ILA but the antenna bandwidth still has acceptable value. The gain variation within the -10 dB return loss bandwidth is less than 1.5 dBi, which means the antenna has stable gain within the antenna impedance bandwidth. This makes the antenna efficient for the required applications.

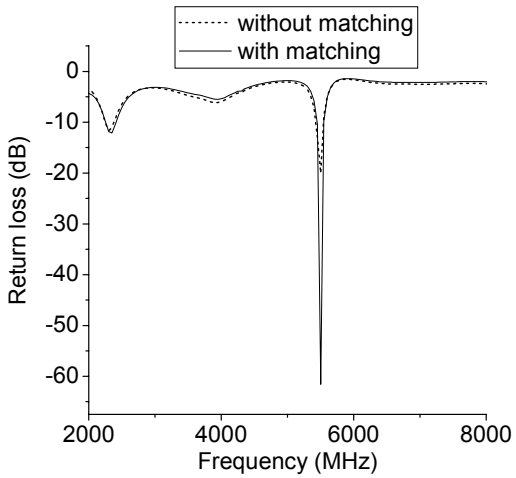

Fig. 11. Return loss variation of stair inverted-L antenna with frequency.

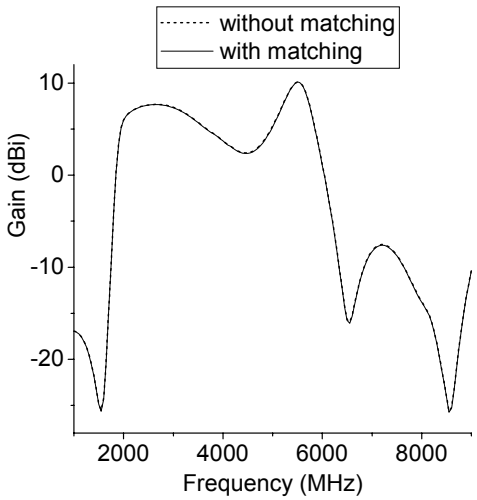

Fig. 12. Total gain variations of stair inverted-L antenna with frequency.

When suitable structured stair type high load is applied on the ILA it is possible to improve the gain of the antenna. Hence, stair ILA has much higher gain (10.12 dBi) than ILA (5.62 dBi). Though the geometry of stair ILA is slightly larger than ILA, in consideration of performance parameter the dimension of the antenna can be neglected. The gain variation of the antenna is shown is Figure 12. From this figure the antenna gain is unchanged under the application of matching network. Total gain patterns of the antenna in vertical plane (XZ, YZ plane) and horizontal plane (XY plane) at 5.5 GHz Wi-Fi operation are shown in Figure 13. From the pattern, the antenna has omnidirectional radiation in

horizontal plane and quite onmidirectional in vertical plane.

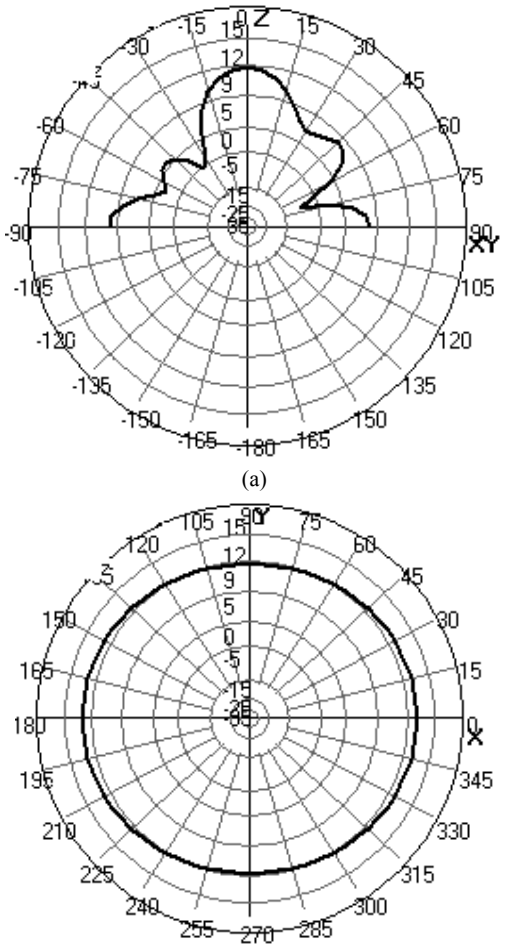

(a)

(b)

Fig. 13. Total gain pattern of stair ILA at 5.5 GHz in (a) vertical plane and (b) horizontal plane.

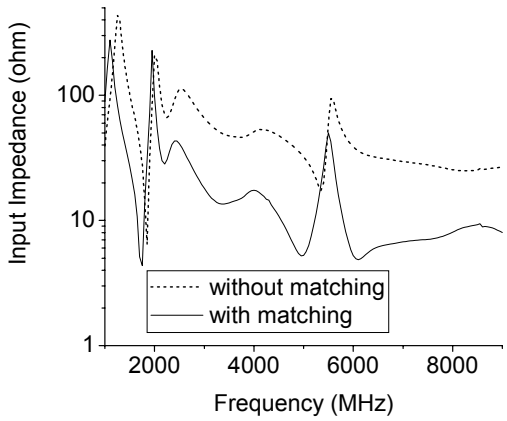

Fig. 14. Input impedance variation of stair ILA with frequency.

Figure 14 shows the stair ILA input impedance variation with frequency from 1000 MHz to 9000 MHz. Without matching network the antenna has input impedance of 59.84 Ω which causes reflection of waves. For well matching a low pass RLC pi-network is used. Under matching condition the antenna input impedance is 50.0836 Ω, this means the antenna is welly matched with the coaxial cable. Figure 15 shows the phase variation of stair ILA with and without matching network. The phase angle of stair ILA changes from 5.006^0 to 0.0004^0, hence the resistive component of the antenna input impedance increases more significantly than reactive components. Based on the numerical simulations, characteristics of the inverted-L antenna vary with the change of loaded strip.

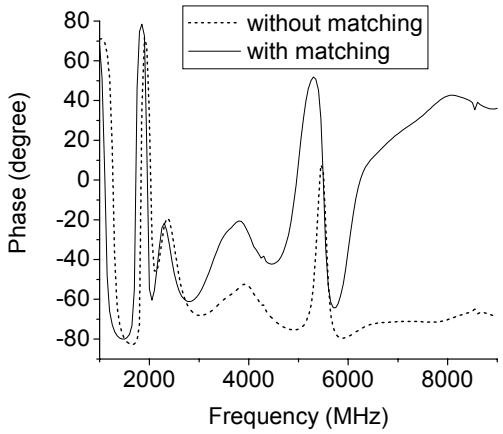

Fig. 15. Phase angle variation of stair ILA with frequency.

The T-shaped monopole antenna has the gain of 3.5 dBi and the gain of two-step tapered monopole antenna is 5.5 dBi at the Wi-Fi operating frequency [2-3], [5-6]. But the gain of the proposed inverted-L and stair inverted-L antennas is 5.62 and 10.12 dBi respectively with the gain variation of less than 1.5 dBi within the -10 dB return loss bandwidth for 5.5 GHz Wi-Fi frequency band. One of the apparent observations is that when suitable structured load is applied to the inverted-L antenna the gain is improved with the reasonable return loss and bandwidth.

IV. CONCLUSION

A simple structured inverted-L and stair inverted-L antennas for 5.5 GHz WLAN (Wi-Fi) operation have been proposed. Improvement in antenna input impedance is achieved when RLC matching network (pi-filter) between feeding and antenna is used. The impedance bandwidth of the ILA and stair ILA is larger than the required bandwidth for 5.5 GHz Wi-Fi operation. The simulated radiation patterns, return loss, gain and VSWR as of the proposed antennas are suitable for the 5.5 GHz WLAN (Wi-Fi) applications under the application of RLC matching network. Further improvement in the gain and radiation characteristics has been obtained from numerical

analysis while appropriate structured load is applied to the horizontal strip of inverted-L antenna.

We are currently working on increasing the gain of the antenna as possible at the same time reducing the size of the stair ILA using capacitive or inductive loading.

REFERENCES

[1] L. Pazin, N. Telzhensky, and Y. Leviatan, "Multiband Flat-Plate inverted-F antenna for Wi-Fi/WiMAX operation," *IEEE antennas and wireless propagation letters*, Vol. 7, 2008.

[2] R. Zaker, Ch. Ghobadi, and J. Nourinia, "A modified microstrip-fed two-step tapered monopole antennas for UWB and WLAN applications," *Electromagnetic research*, PIER 77, PP. 137-148, 2007.

[3] S. W. Su, K. L. Wong, and H. T. Chen, "Broadband low-profile printed T-shaped monopole antenna for 5-GHz WLAN operation," *Microwave and optical technology letters*, Vol. 42, No. 3, 2004.

[4] W. Ren, "Compact dual-band slot antennas for 2.4/5 GHz WLAN applications," *Electromagnetic research B*, Vol. 8, pp. 319-327, 2008.

[5] T. Shanmuganantham, K. Balamanikandan, and S. Raghavan, "A CPW-fed slot antenna for wideband applications," *Internationa journal of antennas and propagation*, Vol. 2008.

[6] G. Y. Lee, W. S. Chen, and K. L. Wong, "Planar diversity folded dipole antenna for 5 GHz WLAN operation," *Microwave and optical technology letters*, Vol. 39, No. 5, 2003.

[7] S. Schulteis, C. Waldschmidt, W. Sorgel, and W. Wiesbeck, "Design of a capacitively loaded inverted F antenna for wireless LAN applications," *Proc. International ITG conference on antennas, Berlin*, pp. 187-190, 2003.

[8] S. Schulteis, C. Waldschmidt, W. Sorgel, and W. Wiesbeck, "A small planar inverted F antenna with capacitive and inductive loading," *Proc. IEEE antennas and propagation society international symposium 2004*, Vol. 4, Issue 4, pp. 4148-4151, 2004.

[9] C. R. Rowell, and R. D. Murch, "A capacitively loaded PIFA for compact mobile telephone handsets," *IEEE transaction on antennas and propagation*, Vol. 45, Issue 5, pp. 837-842, 1997.

[10] I. Pele, A. Chousseaud, and S. Toutain, "Simultaneous modeling of impedance and radiation pattern antenna for UWB pulse modulation," *IEEE antennas and propagation society international symposium 2004*, Vol. 2, pp. 1871-1874, 2004.

[11] J. Villanen, and P. Vainikainen, "The design of optimum impedance matching networks for coupling element based antenna structures," *IEEE antennas and propagation society international symposium 2007*, pp. 3672-3675, 2007.

[12] D. A. Wunsch, "A closed from expression for the driving point impedance of the small inverted-L antenna," *IEEE transaction on antennas and propagation*, Vol. 44, No. 2, 1996.

Proceedings of 2009 12th International Conference on Computer and Information Technology (ICCIT 2009)
21-23 December, 2009, Dhaka, Bangladesh

Iris Recognition: A new approach for Iris segmentation

(Not Presented)

Md. Selim Al Mamun, Md. Hasanuzzaman
Department of Computer Science and Engineering University of Dhaka
mamun0013@yahoo.com, hzamancsdu@yahoo.com

Abstract

Iris recognition system provides automatic identification of an individual based on a unique feature of iris pattern possessed by the individual. Iris recognition is regarded as the most stable and accurate biometric identification system. An iris recognition system basically consists of four steps- segmentation, normalization, encoding and matching. This paper proposes a new approach for iris segmentation to develop an automated iris recognition system. This paper uses iris images from CASIA database (version 1.0) to verify the uniqueness of iris pattern and to evaluate the performance of the proposed system. The new approach is proved to be very successful and almost 90% images of dataset are segmented successfully. The iris recognition system resulted in False Reject Rates and False Accept Rates of 5.222 and 1.932 respectively.

Keywords: CASIA: The Chinese Academy of Sciences-Institute of Automation. FAR: False Accept Rate, FRR: False Reject Rate, EER: Equal Error Rate.

I. INTRODUCTION

A biometric system refers to the identification and verification of individuals based on certain physiological traits of a person. The commonly used biometric features include facial features, voice, fingerprint, handwriting, retina and the one presented in this paper, the iris. Iris method is a newly emergent technique in the world of biometric system. It is gaining lots of attention due to its accuracy, reliability and simplicity as compared to other biometric systems.

The iris is an externally visible, yet protected organ located behind the cornea. The features of iris include trabecular meshwork, crypts and the pigment spots that is moles and freckles and the color of the iris. These visible patterns are unique to all individuals and it has been found that the probability of finding two individuals with identical iris patterns is almost zero. Even the left and correlate with genetic determination right irises for a given person are different from each other [1].

Some prototype systems of iris recognitions had been proposed earlier, but it was not until the early nineties that Cambridge researcher John Daugman[2] practically implemented a working iris recognition system. It was the first implemented working automated iris recognition system. Besides Daugman system some other systems had been developed. The most notables are the systems of Wildes et al [3], Boles and Boashash [4], Lim et al [5] and Noh et al [6].

This paper consists of five sections. Section II describes Proposed Iris Recognition System, section III gives System description and implementation, section IV presents

978-1-4244-6283-4/09/$26.00 ©2009 IEEE d section V

II. PROPOSED IRIS RECOGNITION SYSTEM

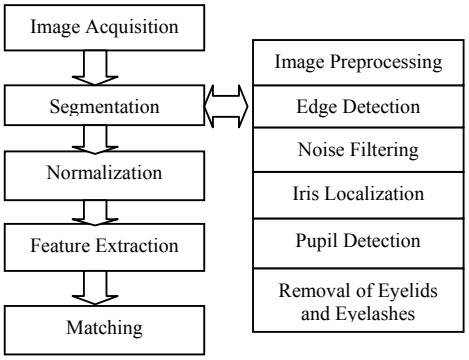

Fig. 1. Proposed System Architecture

Fig.1 shows the proposed system architecture. Proposed system is composed of five modules: (a) Image Acquisition: CASIA dataset, (b) Segmentation: locating the iris region in an eye image (c) Normalization: creating a dimensionally consistent representation of the iris region, (d) Feature Extraction: creating a template containing only the most discriminating features of the iris and (e) Matching : Matching a test template with the stored templates. The proposed segmentation approach includes image preprocessing, edge detection on the eye image, noise filtering, iris localization, pupil detection and removal of eyelids and eyelashes.

III. SYSTEM DESCRIPTION AND IMPLEMENTATION

A. IMAGE ACQUISITION

This step is one of the most important and deciding factors for obtaining a good result. A good and clear image eliminates the process of noise removal and also helps in avoiding errors in calculation. This paper uses CASIA iris image database (version 1.0). It contains 756 iris images from 108 subjects. All iris images are 8 bit gray-level JPEG files, collected under near infrared illumination and free from specular reflection.

B. IMAGE SEGMENTATION

B.1. IMAGE PREPROCESSING

To make the computation faster the image is scaled down to 0.40. The images of CASIA are already pre-processed for iris research and there is very little to clean up the image. The images are filtered using Gaussian smoothing filter, which blurs the image and reduces effects due to noise. The degree of smoothening is decided by the standard deviation and in this case it is chosen 2.0.

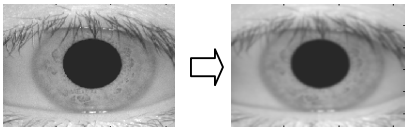

Fig. 2. Result of Preprocessing

B.2. EDGE DETECTION

This paper uses modified canny edge detection algorithm for detecting edges in the eye image. The modified edge detection algorithm involves three steps: finding the gradient, non-maximum suppression and the hysteresis thresholding. Kovesi's [7] algorithm is used for finding the gradients in the image. For iris area vertical gradient is weighted by 1.0 and horizontally by 0.0 and for pupil both vertical and horizontal gradients are weighted by 1.0 as Wildes[3] suggestion. This gradient image is used to find peaks using non-maximum suppression. A pixel *(x,y),* in the gradient image and given the orientation (x,y), the edge intersects two of its 8 connected neighbors. The point at (x,y) is a maximum if its value is not smaller than the values at the two intersection points. Here this paper uses original J. Canny's algorithm [8]. Any pixel having a value greater than a threshold T1 is presumed to be an edge pixel, any pixels that are connected to this edge pixel and that have a value greater than another threshold T2 are also selected as edge pixels.

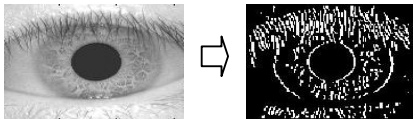

Fig. 3. Result of Edge Detection

B.3. NOISE FILTERING

A median filter is used in order to decrease the extraneous data found in the edge detection stage. This can reduce the pixels on the circle boundary but still successful localization of the boundary can be obtained even with the absence of few pixels. It does not make only the circle localization accurate but it is also computationally faster since the boundary pixels are lesser for calculation.

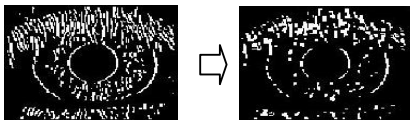

Fig. 4. Result of Noise Filtering

B.4. IRIS LOCALIZATION

To detect the outer circle in the iris/sclera boundary a modified Circular Hough Transformation algorithm is used. The range of radius values is set manually, the iris radius range from 90 to 150 pixels. For each edge point, circles with different radii are drawn and the points on the circles surrounding it at different radii are taken, and their weights are increased if they are also edge points. These weights are added to the accumulator array. When for all the edge points the circle points for different radius are considered, the maximum from the accumulator array is used to find the center of the circle and its radius.

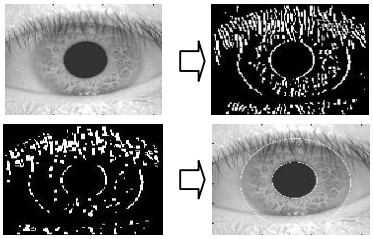

Fig. 5. Result of Iris Localization

B.5. PUPIL DETECTION

For pupil detection again circular Hough Transformation algorithm is applied. The radius range for pupil is 28 to 75 pixels. In order to make pupil detection process more efficient and accurate, the Hough transform for iris/pupil boundary is performed within the iris region, instead of the whole eye region, since the pupil is always within the iris region. After this process a circle is clearly present along the pupil boundary.

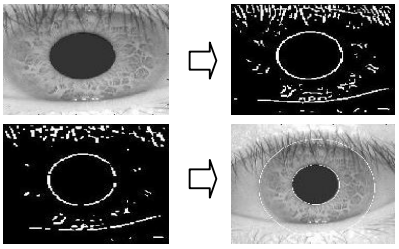

Fig. 6. Result of Pupil Detection

B.6 REMOVAL OF EYELIDS AND EYELASHES

To isolate eyelids from the rest of the image, a line to the upper and lower eyelids drawn using the linear Hough transforms. The lines are fitted exterior to the pupil region and interior to the iris region. The points upper and lower the lines are marked as NaN (Not a number). The eye lashes are very dark compared to the whole iris image. So it is easily removed using simple thresholding technique. Those pixels were marked as NaN. Fig. 10 shows the result.

C. NORMALIZATION

The next step is to normalize this part, to enable generation of the iris template and present them in a generalized way for comparisons. For this purpose, a technique based on Daugman's rubber sheet model is employed. The center of the pupil is considered as the reference point and a remapping formula is used to convert the points on the Cartesian scale to the polar scale.

$$r' = \sqrt{\alpha\beta} \pm \sqrt{\alpha\beta^2 - \alpha - r_1^2}$$

Where $\alpha = \sigma_x^2 + \sigma_y^2$ And $\beta = \cos\left(\pi - \tan^{-1}\left(\frac{\sigma_y}{\sigma_x}\right) - \theta\right)$

The displacement of the centre of the pupil relative to the centre of the iris is given by σ_x, σ_y and r' is the distance between the edge of the pupil and edge of the iris at an angle θ around the region, and r_1 is the radius of the iris.

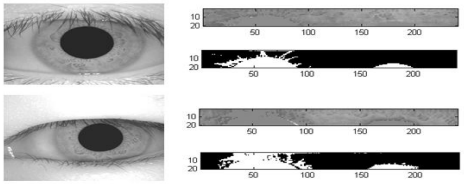

Fig. 8. Result of Normalization

D. FEATURE EXTRACTION

Encoding is done using the Gabor filter, by breaking up the 2D normalized pattern into a number of 1D wavelets, and then these signals are convolved with 1D Gabor wavelets. The output of filter is then phase quantized to four levels using the Daugman [2] method, with each filter producing two bits of data for each phasor. The iriscode is formed by assigning 2 bits for each pixel of the image. The bit is 1 or 0 depending on the sign + or – of the real and imaginary part respectively.

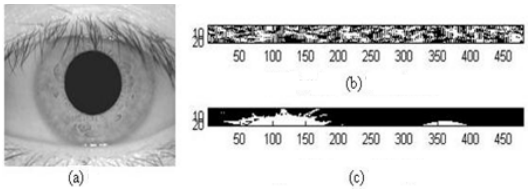

Fig. 9. Result of Feature Extraction : (a) Original image, (b) Template of the eye image and (c) Mask of the eye image

E. MATCHING

E.1. HAMMING DISTANCE

This paper uses modified Hamming distance for matching which also incorporates noise masking so that only significant bits are used in calculating the Hamming distance between two iris templates. The modified hamming distance algorithm that is used for matching is given below.

$$HD = \frac{1}{N - \sum_{k=1}^{N} Xn(OR)Yn_k} \sum_{j=1}^{N} X_j\,(XOR)Y_j\,(AND)\,Xn_j'\,(AND)\,Yn_j'$$

Where *Xj* and *Yj* are the two bit-wise templates to compare, Xn_j' and Yn_j' are corresponding noise masks for *Xj* and *Yj*, and *N* is the number of bits represented by each template.

E.2. ROTATION VARIATION ADAPTION

In order to account for rotational inconsistencies, when the Hamming distance of two templates is calculated, one template is shifted left. This bit-wise shifting in the horizontal direction corresponds to rotation of the original iris region by an angle given by the angular resolution used for iris detection.

IV. EXPERIMENTAL RESULTS AND DISCUSSIONS

In this chapter performance of the developed system is evaluated. Different types of tests are conducted to evaluate the accuracy of the system. These include decidability, False Accept Rate (FAR), False Reject Rate (FRR), Equal Error Rate and number of shifts to make the system rotation invariant.

A. EXPERIMENTAL SETUP

The proposed system is implemented using MATLAB 7.50. For statistical analysis a statistical tool 'R' is used. The system is implemented in Intel Core 2duo-2.13 GHz with 2GB RAM (DDR2, 800 bus). The system is tested using CASIA dataset where number of subject is 108 with 7 samples each.

B. RESULT OF SEGMENTATION

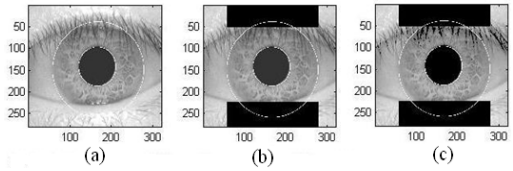

Fig. 10. Result of Segmentation: (a) Original Image, (b) After removing eyelids and (c) After removing eyelashes

The proposed segmentation approach is proved to be very successful. The new segmentation approach successfully segmented 681 out of 756 of eye images of CASIA (version 1.0) which corresponds to a success rate of around 90%.

There are some cases where segmentation of iris fails. The problem images had small intensity differences between the iris region and the pupil regions. This situation is shown in the following figures.

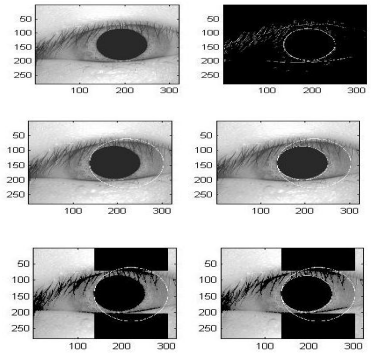

Fig. 11. Cases where segmentation fails

C. PERFORMANCE EVALUATION

The key issue in all pattern recognition problems is to find a unique separation point between intra-class and inter class variability. An individual can be reliably classified only if the variability among different instances of a given class is less than the variability between different classes. So a threshold value must be chosen so that a decision can be made as to whether two templates were created from the same individual or whether they were created from the different individuals. From figure 12 it is easily visible that the common region between intra-class and inter-class is very small which gives indication of good result.

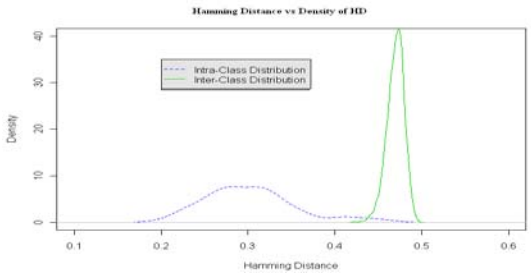

Fig. 12. Distribution of Hamming Distance (HD Vs Density)

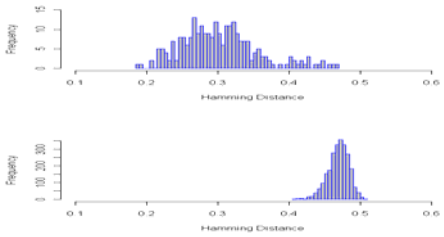

Fig. 13. Distribution of Hamming Distance(HD Vs Frequency)

C.1. DECIDABILITY

A popular metric for determining the threshold value for pattern recognition or identification is 'decidability'. It is evaluated from the mean and standard deviation of the intra-class and intra class distribution. The decidability is defined as

$$d' = \frac{|\mu_S - \mu_D|}{\sqrt{\frac{(\sigma_S^2 + \sigma_D^2)}{2}}}$$

The greater the decidability, the greater the variation between the intra-class and inter-class distributions which is the key to the iris recognition system. The decidability calculated from the result is given below. The values of decidability for each test are found near 5.0 or greater which is a good result.

C.2. FAR, FRR AND EER

$$\text{FAR} = \frac{\int_0^x p_{\text{inter-class difference}}(x)dx}{\int_0^1 p_{\text{inter-class difference}}(x)dx} \quad \text{and}$$

$$\text{FAR} = \frac{\int_0^x p_{\text{intra-class difference}}(x)dx}{\int_0^1 p_{\text{intra-class difference}}(x)dx}$$

False Accept Rate and False Reject Rate are related inverse proportionally. An important way to judge the system's FAR at 5 % of FRR.

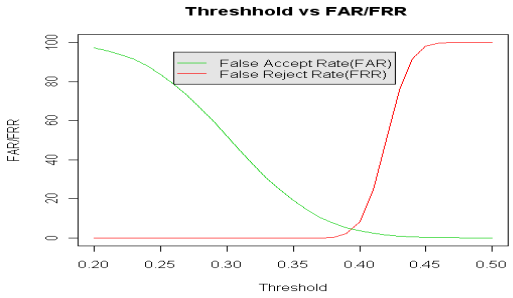

Fig. 14. Threshold Vs FAR and FRR

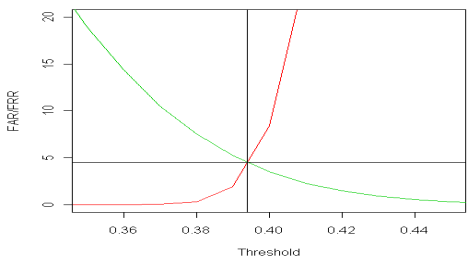

Fig. 15. Threshold Vs FAR and FRR(Closed look)

At threshold 0.39, the FAR is 1.932% and FRR is 5.222%, at 0.394 FAR = FRR and it is 4.8% = EER. Accuracy = 95.2%.

C.3 ROTATION VARIATION ADAPTION

Robust representation for iris pattern recognition must be invariant to changes in size, position and rotation. To compensate the rotation variant the templates of the iris images are shifted 8bits in both sides: left and right and then the hamming distance are taken.

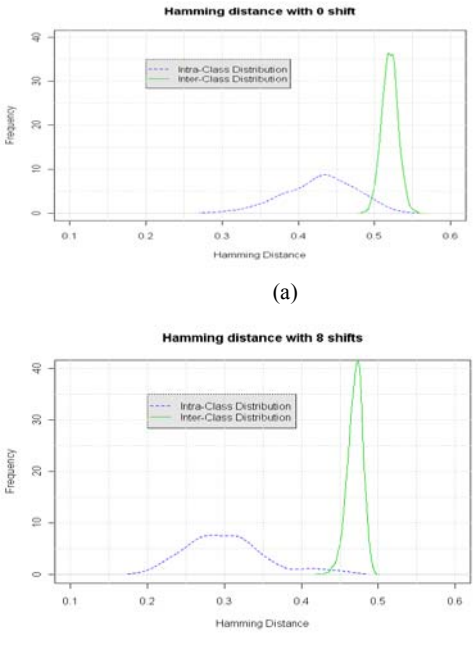

Fig. 16. Density of Intra-Class and Inter-Class Distribution with (a) 0 shift and (b) 8 shifts

Due to rotational inconsistencies a significant number of templates are not aligned and common area is large which means larger false rate. With 8 shifts values become much closer distributed around the mean and common area is decreased.

Without considering rotation variation, at threshold value 0.44, the FRR is found 5.397 % and FAR is 33.609 %. But considering the rotation variation at threshold value 0.39 the FRR is 5.222 % and FAR is 1.932 %.

V. CONCLUSION

This paper proposes a new segmentation approach including image preprocessing, edge detection, noise filtering, iris localization, pupil detection and removal of eyelids and eyelashes methods. Experimental result shows that segmentation accuracy is around 90% which is better than kovesi[7] where segmentation accuracy was 83% for the same dataset(CASIA). This paper also implements iris recognition system using this new segmentation approach and experimental result shows that FAR is 1.932% and FRR is 5.222 % which is satisfactory. There are still some issues that need to be considered. To make the system fully automated an iris acquisition camera should be included rather than having a fixed set of iris images from a database. The most of the time required for computation include performing the Hough transform, and calculating Hamming distance values. Speed of the system can be improved if these two methods are implemented using C.

REFERENCES

[1] El-Bakry, H.M, Human Iris Detection Using Fast Cooperative Modular Neural Nets, Neural Networks, Proceedings of International Joint Conference on IJCNN '01, vol.1, 2001, pp 577 –582.

[2] J. Daugman. How iris recognition works. Proceedings of 2002 International Conference on Image Processing, Vol. 1, 2002.

[3] R. Wildes, J. Asmuth, G. Green, S. Hsu, R. Kolczynski, J. Matey, S. McBride: A Machine-vision System for Iris Recognition. Machine Vision and Applications Vol. 9 (1996).

[4] W. Boles, B. Boashah: A Human Identification Technique Using Images of the Iris and Wavelet Transform. IEEE Transaction on Signal Processing Vol. 46 (1998).

[5] S. Lim, K. Lee, O. Byeon, T. Kim. Efficient iris recognition through improvement of feature vector and classifier. ETRI Journal, Vol. 23, No. 2, Korea, 2001.

[6] S. Noh, K. Pae, C. Lee, J. Kim. Multiresolution independent component analysis for iris identification. The 2002 International Technical Conference on Circuits/Systems, Computers and Communications, Phuket, Thailand, 2002.

[7] P. Kovesi. MATLAB Functions for Computer Vision and Image Analysis.Available at: http://www.cs.uwa.edu.au/~pk/Research/MatlabFns/index.html.

[8] Canny, J. A Computational Approach To Edge Detection, IEEE Trans. Pattern Analysis and Machine Intelligence, 8:679-714, 1986.

Proceedings of 2009 12th International Conference on Computer and Information Technology (ICCIT 2009)
21-23 December, 2009, Dhaka, Bangladesh

Performance Evaluation of Fast TCP and TCP Westwood+ for Multimedia Streaming in Wireless Environment

Sifatur Rahim, Syed Faisal Hasan
Department of Computer Science & Engineering, University of Dhaka, Bangladesh
sifaturrahim@gmail.com, hasansf@gmail.com.

Abstract

Although TCP is one of the key protocols of the Internet infrastructure, it is not optimized for either wireless environment or multimedia streaming applications. It fails to meet the service requirement of streaming applications because of its strict adherence to congestion control. Besides, non-congestion packet loss fools TCP to slow down its sending rate over wireless links. Fast TCP and TCP Westwood+ are two well known TCP variants which are supposed to resolve these problems. This paper analyzes the performance of TCP Westwood+ and Fast TCP for various issues in wireless network for multimedia streaming. Simulation results show that, Fast TCP shows better goodput, average throughput, and fairness index but TCP Westwood+ shows less jitter and better performance in presence of heavy reverse flows.

Keywords: Fast TCP, TCP Westwood+, Multimedia streaming, Wireless Network.

I. INTRODUCTION

During the last few years the Internet has experienced a boost up of multimedia applications and deployment of wireless access links. Today each netizen feels sheer thirst to remain in the flows of seamless communicating networks while moving between places. But transmission of multimedia contents over the Internet is a challenging task, especially when the access is through the wireless links.

The technique, whose affiliation has accelerated the demand of multimedia applications in the Internet enormously, is known as *Streaming*. Prior to its appearance, the only way of viewing a multimedia content was to hang around until the full download was completed. In compare to this time consuming approach a streaming client can start enjoying the earlier portion of a media file almost instantly while the later portion is being downloaded. One does not has to wait for the full download of a multimedia file before starting playback. This is the prime factor explaining why streaming has revolutionized in the way of distributing multimedia contents on the Web. Streaming differs remarkably from existing elastic applications as it is delay sensitive but tolerant to loss to a certain range. Like other applications, streaming must rely on such a transport protocol that suits itself the best. A significant fraction of commercial streaming traffic in the current Internet uses TCP. Real Media and Windows Media, the two dominant streaming media products, both support TCP streaming [1]. In 2004, it has been shown that, in case of live streaming the use of TCP sessions by Windows Media, Real Media and Quicktime are 88%, 51% and 44% respectively of all sessions [2].

Although these studies strongly recommend TCP for streaming applications, still there exist many problems. For example, TCP cannot remove jitter or guarantee any end-to-end delay etc. So, we see that although TCP performs very well for general applications it is not best suited for streaming applications. Moreover, TCP being optimized for wired network fails to perform well over wireless links. As a result, streaming over wireless networks has really become much more challenging (problem details are given in section IV). So, we conclude by saying that, current Internet is in crying need of such a transport protocol that is well suited for both streaming applications and wireless environment while being TCP friendly too.

The main contribution of this paper is the performance evaluation of two comparatively recent TCP variants, Fast TCP and TCP Westwood+ for streaming applications in wireless environment. The analysis demonstrates that, Fast TCP shows stunning performance for FTP applications in long delay and high bandwidth networks. On the other hand TCP Westwood+ performs remarkably well in case of lossy wireless links (discussed in section III). The well-known network simulator ns-2 [3] has been used to develop several simulation environments. Then necessary issues like throughput, jitter, fairness etc were analyzed to reveal the responsive nature of Fast TCP and TCP Westwood+.

The rest of this paper is organized as follows. Section II summarizes the related works. Section III contains background and existing approaches to remove TCP limitations in wireless networks. In section IV, we illustrate the problem in details. Section V contains the comparison of Fast TCP and TCP Westwood+ in different simulation environment for various issues. Finally, we conclude in section VI with our findings, comments and future works.

II. RELATED WORK

TCP Reno and TCP Vegas was compared and analyzed in [4], where TCP Vegas was shown to use network resources more efficiently, being fairer and having a better bandwidth estimation scheme than TCP Reno. In [5], the performance of TCP Westwood and TCP

Westwood+ was evaluated for file transfer applications where TCP Westwood+ was shown to have improved goodput and fairness with respect to TCP Reno which was shown to overestimate the available bandwidth. In 2004, TCP Westwood+, TCP Newreno and TCP Vegas were investigated for goodput, fairness and friendliness issues in [6] for file transfer applications in both simulation based and real life environments. Results showed that, Westwood+ TCP is friendly towards New Reno TCP and improves fairness in bandwidth allocation.

To the best of our knowledge, no comparison was done with Fast TCP and TCP Westwood+ for streaming applications in wireless networks.

III. BACKGROUND

There are many proposals in the literature describing how to optimize TCP performance in wireless networks. The inherent idea of these proposals is- TCP should reduce its transmission rate only in case of congestion, not for transmission errors. These optimizations can be broadly classified into four categories. The names of these categories are self explanatory. First, the *Link layer approach* which include Snoop [7], WTCP [8] and TULIP [9]. Second, the *Split connection approach* which include Indirect TCP (I-TCP) [10] and others. Third, the *Explicit notification approach* which include Explicit Loss Notification (ELN) [11] and others. Finally, the *End-to-end approach* which include TCP Westwood [12] and others.

A. Characteristics of Streaming Traffic

In a streaming server the streaming flow can be either a Constant Bit Rate (CBR) flow, or Variable Bit Rate (VBR) flow. In CBR, a multimedia content is encoded at a constant rate. It offers the advantage of limiting the data transfer rate of streaming to a fixed amount. Streaming of a MP3 file may be CBR flow of 96, 128, 192 or 256 Kbps [13]. Streaming of a video content can be a CBR flow of 384 KBps as known to be standard. For real time streaming CBR is a good choice in perspective of network bandwidth as it limits the maximum bandwidth. VBR encoding of a multimedia file tries to maintain the quality of data. The size of the file varies after the encoding process. VBR produces sudden increase of sending rate which is similar to spike. To benefit from VBR, the network must be able to accommodate bandwidth spikes, which is difficult to ensure.

B. TCP Westwood+

TCP Westwood+ [6] has derived from TCP Westwood [14]. TCP Westwood+ differs from TCP Westwood by employing a new bandwidth estimation algorithm that works more accurately in the presence of ACK compression event.

The Algorithm and End-to-end bandwidth estimation of TCP Westwood+ is discussed elaborately in [6].

C. FAST TCP

Fast TCP [16] stands for FAST AQM Scalable TCP, where AQM stands for Active Queue Management. Being delay based, it performs immensely well for high delay bandwidth product networks. The congestion control mechanism of FAST TCP has four functionally independent components - *Data control, Window control Burstiness control* and *Estimation* component [14]. FAST TCP uses queuing delay as the main measure of congestion in its window adjustment algorithm. It periodically updates the congestion window (*cwnd)* based on the average RTT as:

$$w \leftarrow \min\left\{2w, (1-\gamma)w + \gamma\left((baseRTT/RTT)w+\alpha\right)\right\}$$

Where γ is a constant between 0 and 1, *RTT* is the current average RTT, *baseRTT* is the minimum RTT observed so far, and α is a protocol parameter [14].

IV. THE PROBLEM

The main problem addressed in this paper consists of three sub problems. *First*, TCP, being the most widely deployed transport protocol, is not suitable for streaming applications. *Second*, it is hard to meet the service requirements of streaming in wireless networks. *Third*, TCP is not well suited for wireless networks. We discuss these problems in details in the following.

A. Challenges of Multimedia Streaming Over TCP

Here we illustrate the service requirements of streaming and judge TCP's behavior to address these requirements. *First*, Streaming requires a smooth transmission rate but TCP fails to continue the smoothness because of its AIMD (Additive Increase Multiplicative Decrease) approach after a congestion event. *Second*, the appearance of jitter problem (at the receiving end) is quite an undesired event for streaming. TCP cannot ensure to eliminate jitter problem. *Third*, TCP cannot ensure any fixed end to end packet delay for streaming applications. *Finally*, Streaming applications are loss tolerant. TCP ensures reliability of each packet and retransmission of these lost packets often becomes useless for the delay sensitive streaming applications.

B. Challenges of Streaming over wireless Links

To satisfy the requirements of streaming are really difficult in wireless networks. *First*, the data rate required for streaming applications is really hard to meet in wireless networks. The broadband wired network transmission links are characterized by high transmission rates (in the order of Gbps) and very low error rates (10^{-9} – 10^{-8}). On the other hand, wireless links have a much smaller transmission rate (Kbps-Mbps) and a much higher error rate (10^{-4} – 10^{-3}) [16]. *Second*, mobility of

wireless nodes adds a new event called hand-off, which is a major issue to consider. *Third*, factors related to wireless links like signal fading, interference etc. contribute to packet errors, latency, jitter which severely hampers the streaming applications.

C. Challenges of TCP over Wireless Links

TCP is a connection oriented transport protocol which provides a reliable byte stream to the application layer. TCP does not perform well in wireless environment. *First*, TCP segments may be lost due to poor radio conditions and low reliability of the link layer protocol. *Second*, due to a handover event in wireless networks a whole window of data in TCP may be lost. It may cause a timeout event which is actually unnecessary. *Third*, TCP may also misinterpret a sudden increase in the round trip time as data loss. As TCP considers all packet loss as congestion event, it is certainly false for wireless networks.

D. Difficulties for a straight forward solution and the logic behind the choice of Fast TCP and TCP Westwood+

We argue that, to develop a straight forward solution to all the challenges (described in section IV) is very hard. The fact is, finding the exact reason for packet loss in wireless network is still a research issue. So, different existing TCP variants make different assumptions to control their own *cwnd* and slow start threshold *(ssthresh)* and thus lose TCP friendliness. But, any solution that is not TCP friendly is not acceptable indeed.

Therefore, we propose to find the ultimate solution by reverse engineering method. That means, we would compare the some most appropriate TCP variants and observe how they meet the service requirement of streaming. Chosen TCP variant must possess some features - *first*, it should be end-to-end because this approach does not produce extra load in the intermediate nodes. *Second*, the TCP variants should be delay based. This is very important because retransmission of packets over wireless links is costly and often worthless for delay sensitive streaming applications.

Fast TCP is delay based, showing stunning performance over current TCP variants for file transmission in high delay bandwidth product networks. On the other hand, TCP Westwood+ shows remarkable performance in lossy wireless links. Both of them meet the criteria needed to address the problem and both are TCP friendly. So, these two seemed most attractive to us for analysis for streaming applications in wireless environment.

V. SIMULATIONS AND RESULT ANALYSIS

In this section we would study the performance of Fast TCP and TCP Westwood+ in terms of suitable issues. In our simulation environments, we used CBR 64, 128 and 384 for voice, mp3 and video streaming respectively. We have a short discussion on necessary issues for comparing these TCP variants in the following

A. Evaluation Criteria for Comparison in Simulation Environments

"End-to-end delay", "packet loss" and "jitter" are very important issues to compare. As streaming rate should be smooth we would compare with "total throughput" and "goodput". Goodput is computed by:

Goodput=(sent_data-retransmitted_data)/transfer_time

Finally, to investigate how fair these TCP variants are, we would compare the fairness index by calculating the well-known Jain Fairness index [16] for some number of flows. It is computed using the following equation: $\mathbf{J_{FI}} = (\sum_{i=1}^{M} b_i)^2 / (M \sum_{i=1}^{M} b_i^2)$, where b_i is the goodput for i^{th} connection and M is the number of total connections. The Jain Fairness Index belongs to the interval [0, 1].

B. Scenario-1: Comparison in Hand-off Event

Fig. 1, describes a hand-off event where the source is a wired node and the destination is a mobile node

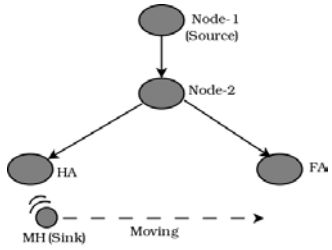

Fig 1. Simulation scenario-1

Table I Parameters of scenario-1

Parameter	Value
Bandwidth of wired links	1Mbps
Delay of wired links	100ms
CBR flow rate	64/128/384 Kbps
Speed of mobile node	5 m/s

moving from one base station to another. CBR flows of 64, 128 and 384 Kbps are transmitted from the source to destination. Here, we find out and compare throughput fluctuations, jitter and packet drops. The parameters of Fig. 1 are given in Table I.

Fig. 2 compares the total throughputs at different CBR flows. Here, Fast TCP shows better throughput.

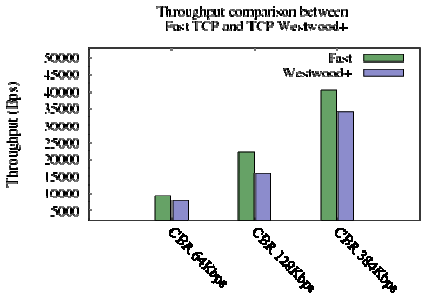

Fig 2. Comparison of total throughputs of Fast TCP and TCP Westwood+ at different CBR flows

Fig. 3 compares the total no. of packet drops at the CBR flows of 64, 128 and 384 Kbps respectively. Here, TCP Westwood+ performs better.

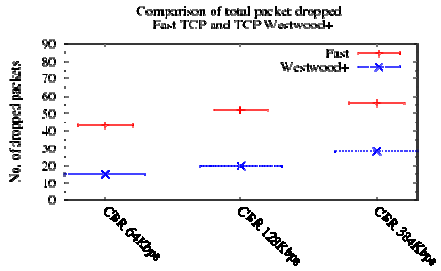

Fig 3. Comparison of total no. of packet drops between Fast TCP and TCP Westwood+ at different CBR flows

Fig. 4(a), 4(b), 4(c) compares for jitter for CBR

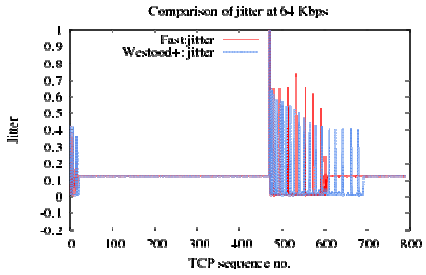

(a) 64 Kbps CBR flow

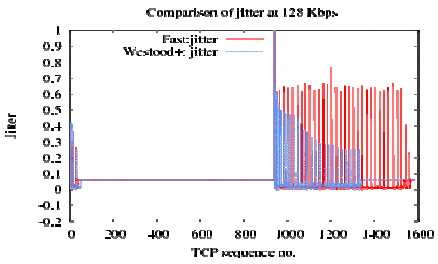

(b) 128 Kbps CBR flow

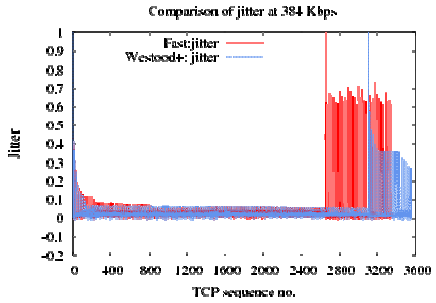

(c) 384 Kbps CBR flow

Fig. 4. Comparison of jitter of Fast TCP and TCP Westwood+ in (a), (b) and (c).

64/128/384 Kbps flows. Here, Fast TCP suffers more from jitter, especially in mp3 and video streaming.

C. Scenario-2: Incorporation of Reverse Flows

Fig. 5 illustrates another simulation scenario, where we measure the goodput, packet drop and delay of Fast

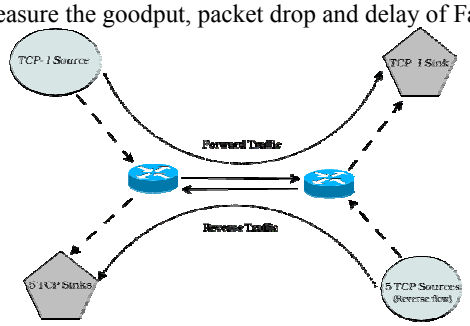

Fig 5. Simulation environment of scenario-2

TCP and TCP Westwood+ in presence of a considerable amount of reverse flows. Parameters are given in

Table II Parameters of scenario-2

Parameter	Value
Bandwidth of link between routers	1Mbps
Delay of wired link between routers	100ms
Queue size (all nodes)	50
Forward flow CBR rate	128/384 Kbps
Forward flow packet size	1000 Bytes

Table II.

In this scenario, some TCP connections on the backward path follow an ON-OFF-ON-OFF pattern in order to investigate the effect of reverse traffic. In particular, the reverse traffic is ON during the intervals [250-500]sec, and [750-1000]sec and is OFF during the intervals [0-250]sec and [500-750]sec. During their ON state, these TCP variants experience the ACK compression event.

Fig. 6(a) and 6(b) compares goodputs for Fast TCP and TCP Westwood+ for different fragmented times. We observe that, goodputs of Fast TCP and TCP Westwood+ are almost similar in 6(a). But for video streaming in 6(b), TCP Westwood+ performs slightly better.

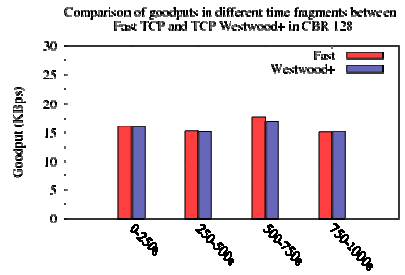

(a) 128 Kbps CBR flow

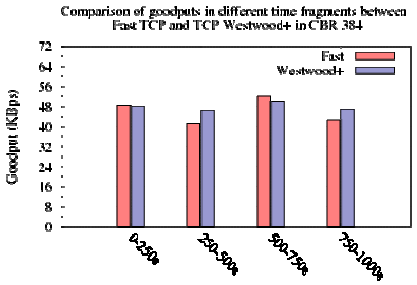

(b) 384 Kbps CBR flow

Fig 6. Comparison of goodputs of Fast TCP and TCP Westwood+ in (a) and (b).

Fig. 7(a) and 7(b) present delays at CBR 128 of Fast TCP and Westwood+. We observe that, Fast TCP has small packets with longer delays and TCP Westwood+ has comparatively large packets with short delays.

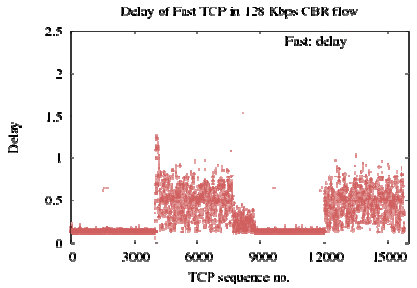

(a) Fast TCP

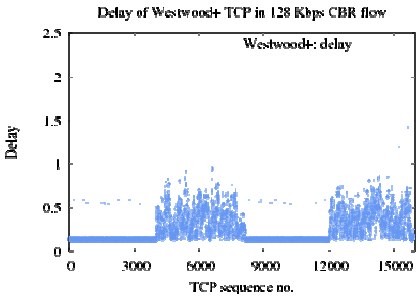

(b) TCP Westwood+

Fig 7. Comparison of packet delay of at CBR 128 Kbps flow (a) and (b)

Fig. 8(a) and 8(b) compare packet drops for Fast TCP and TCP Westwood+ for different fragmented times at the CBR flows of 128 and 384 Kbps respectively. We observe that, Fast TCP have smaller number of packet drops in compare to TCP Westwood+.

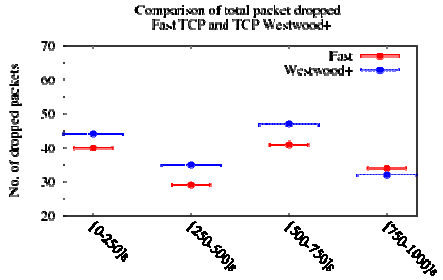

(a) 128 Kbps CBR flow

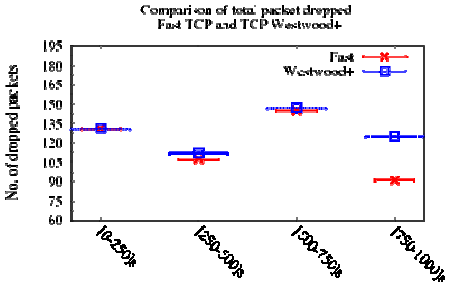

(b) 384 Kbps CBR flow

Fig 8. Comparison of packet drops of Fast TCP and TCP Westwood+ in (a) and (b)

D. Scenario-3: Comparison in the basis of Jain Fairness Index

In Fig. 9, we illustrate the simulation scenario-3, where multiple Fast TCP and TCP Westwood+ sources are competing for network bandwidth. Associated parameters are given in Table III.

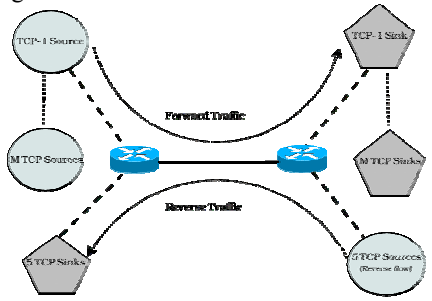

Fig 9. Simulation environment of scenario-3

Table III Parameters of scenario-3

Parameter	Value
Bandwidth of link between routers	10Mbps
Delay of wired link between routers	100ms
Queue size (all nodes)	50
Forward flow CBR rate	64/128 Kbps
Forward flow packet size	1000 Bytes

We calculate the total throughput of each flow and then calculate Jain Fairness Index in Fig 10(a) and 10(b).

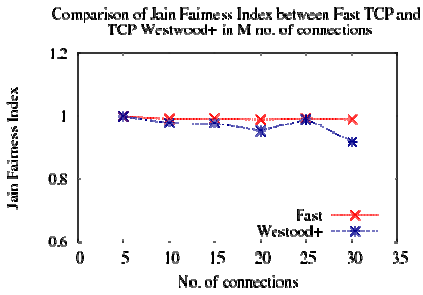

(a) At64Kbps

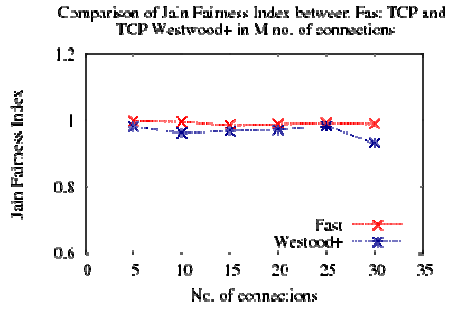

(b) At CBR 128 Kbps

Fig 10. Comparison of Jain Fairness Index for some Fast TCP and TCP Westwood+ connections (a), (b)

Here, Fast TCP shows to have better fairness index in compare to TCP Westwood+.

VI. FINDINGS FROM THE EXPERIMENTS AND CONCLUDING REMARKS

From the experiments above we observe that, Fast TCP gives better throughputs almost in all cases which is positive for streaming. Again, Fast TCP suffers more severely than TCP Westwood+ in case of jitter issue. So, TCP Westwood+ becomes a better choice at this point and it also performs better in presence of heavy reverse traffic. Fast TCP shows few packets with longer delays, where TCP Westwood+ has more packets with comparatively shorter delay. Besides, Fast TCP shows less packet drops in presence of reverse traffic. Finally, Fast TCP is observed to show better fairness index than TCP Westwood+ in case of both audio streaming.

So, we conclude that, neither Fast TCP nor Westwood+ TCP can be regarded as the best choice, but both exhibits positive features for streaming from which we may develop another TCP variant which would be best suited for streaming in wireless networks.

REFERENCES

[1] B. Wang, J. Kurose, P. Shenoy, and D. Towsley, "Multimedia streaming via TCP: An analytic performance study," 2008.

[2] K. Sripanidkulchai, B. Maggs, and H. Zhang, "An analysis of live streaming workloads on the Internet," in Proceedings of the 4th ACM SIGCOMM conference on Internet measurement. ACM New York, NY, USA, 2004, pp. 41–54.

[3] "Information on ns-2 network simulator (Version 2.33)" available at, http://www.isi.edu/nsnam/ns/

[4] J. Mo, R. La, V. Anantharam, and J. Walrand, "Analysis and comparison of TCP Reno and Vegas," in IEEE INFOCOM'99. Eighteenth Annual Joint Conference of IEEE Computer and Communications Societies. Proceedings, vol. 3, 1999.

[5] S. Mascolo, L. Grieco, R. Ferorelli, P. Camarda, and G. Piscitelli, "Performance evaluation of Westwood+ TCP congestion control," Performance Evaluation, vol. 55, no. 1-2, pp. 93–111, 2004.

[6] L. A. Grieco and S. Mascolo, "Performance evaluation and comparison of westwood+, new reno, and vegas tcp congestion control," SIGCOMM Comput. Commun. Rev., vol. 34, no. 2, pp. 25–38, April 2004.

[7] H. Balakrishnan, S. Seshan, and R. Katz, "Improving reliable transport and handoff performance in cellular wireless networks", Wireless Networks, vol. 1, no. 4, pp. 469–481, 1995.

[8] K. Ratnam and I. Matta, "WTCP: An efficient transmission control protocol for networks with wireless links," in Proceedings of Third IEEE Symposium on Computer and Communications (IEEE ISCC), 1998.

[9] C. Parsa and J. Garcia-Luna-Aceves, "Improving TCP performance over wireless networks at the link layer," Mobile Networks and Applications, vol. 5, no. 1, pp. 57–71, 2000.

[10] A. Bakre and B. Badrinath, "Implementation and performance evaluation of indirect TCP," IEEE Transactions on Computers, vol. 46, no. 3, pp. 260–278, 1997.

[11] H. Balakrishnan and R. Katz, "Explicit loss notification and wireless web performance," in Proceedings of the IEEE Globecom, Internet Mini-Conference, 1998.

[12] S. Mascolo, C. Casetti, M. Gerla, M. Y. Sanadidi, and R. Wang, "Tcp westwood: Bandwidth estimation for enhanced transport over wireless links," in MobiCom '01: Proceedings of the 7th annual international conference on Mobile computing and networking. New York, NY, USA: ACM Press, 2001, pp. 287–297.

[13] "Information about Constant Bit Rate (CBR) streaming of mp3 audio files" available at, http://www.mp3-tech.org/tests/gb/index.html, last accessed at 31th May, 2009.

[14] D. X. Wei, C. Jin, S. H. Low, and S. Hegde, "Fast TCP: motivation, architecture, algorithms, performance," in IEEE Infocom, 2004.

[15] S. K. Das and M. Chatterjee, "Challenges in wireless multimedia networks."

[16] R. Jain, The Art of Computer Systems Performance Analysis: techniques for experimental design, measurement, simulation, and modeling. Wiley, 1991.

Proceedings of 2009 12th International Conference on Computer and Information Technology (ICCIT 2009)
21-23 December, 2009, Dhaka, Bangladesh

Geometric Model for Minimizing Node Discovery Load in Network Simulators for Large Ad hoc Networks

Roksana Akter, M. Lutfar Rahman †
Department of Computer Science and Engineering, Southeast University, Dhaka, Bangladesh
† Department of Computer Science and Engineering, University of Dhaka, Dhaka, Bangladesh
jolly_csdu@yahoo.com, lrahman@univdhaka.edu

Abstract

The area of wireless ad hoc networking has been receiving increasing attention among researchers in recent years. NS2 is the most common simulator which is used to simulate wireless ad hoc networks. But, NS2 does not scale the simulation well, where there are a large number of nodes in a simulation area. In this paper a geometric approach is proposed targeting the optimization of the area that exists between the approximated area for processing and the area outside the coverage area of a transmitter. Thus, this proposed algorithm reduces the number of unaffected nodes (considering the transmission signal range), which are currently considered by the NS2 simulator for checking, whether the node resides inside the transmission area or not. The current version of NS2 uses a block based optimization but the algorithm, proposed here, reduces the coverage area of the blocks near the boundary of the transmission range, targeting the improvement of the performance of NS2 for the simulation of large ad hoc networks. These theoretic assumptions have been followed by extensive realistic test conditions for generating a set of sensible result-set for achieving the optimum from the proposed physical propagation model to facilitate NS2 with a faster simulation performance for larger wireless ad hoc mobile network. The proposed approach saves the coverage area from at least 12.5% upto 78.15% than in existing solution.

Keywords: MANET, Receiving Threshold (RT), Carrier-Sense Threshold (CST), Grid based node organization, List based node organization, Network Simulator NS2, Minimal Rectangle.

I. INTRODUCTION

Ongoing research into dynamic, self-organizing, multihop wireless networks, called mobile ad hoc networks (MANET), promises to improve the efficiency and coverage of wireless communication. Such networks have a variety of natural civil and military applications. However, the ability to scale such networks to large numbers of nodes remains an open research problem. For example, routing and transmitting packets efficiently over ad hoc networks become difficult as they grow in size. Progress in this area of research fundamentally depends on the capabilities of simulation tools and, more specifically, on the scalability of wireless network simulators. But the problem to obtain a result with reasonable runtime is a serious issue in the simulation of large mobile ad hoc scenarios (1000s or more mobile nodes, comprising approximately $1 - 10$ km^2 of area). In such a simulator the most computation-intensive part is the interference computation, since a system with N pairs of transmitters and receivers requires that $O(N^2)$ pair wise interactions are computed [5]. Naoumov and Gross used the limited interference computation (LIC) based algorithm [1] to improve the performance of NS2 simulator using grid based structure.

In this paper the basic Grid based node organization is modified using a geometric model to scale down the number of probable nodes that might receive the transmitted signal with the experimental results and comparative analysis to show that it is correct and efficient, the proposed model is capable of reducing the number of probable nodes in a significant amount, compared to the existing technique. The experiment is conducted for densely populated regions, as represented by the large geographic area and large number of nodes, network performance can be increased noticeably through the proposed algorithm based on the concept of minimal rectangular area selection.

In section II previous approaches to simulate large networks are discussed. Section III contains the overview of simulation coverage area and existing algorithms, section IV proposes a new approach to optimize simulation area for large network simulation followed by results and performance analysis in section V. Section VI gives the concluding remarks.

II. BACKGROUND STUDY

In a particular performance comparison study [3], the authors used NS2 simulator and the fact comes out that, DSR delivers 5-50% fewer packets than AODV depending on the traffic load. The authors have complained that NS2 is too slow to cover any larger scenario. In research [6], [2] on performance comparison of different ad hoc protocols on discrete issues, the simulation of larger network (with several hundreds to thousands of nodes) was not physically feasible even with the fastest Intel PC.

Perrone and Nicol [5] considered the computation of transmission power levels and the SNR (Signal to Noise Ratio). They showed that techniques devised for the simulation of systems of self-gravitating bodies (N-body problem) can be successfully applied to reduce the complexity of interference computations in simulations

978-1-4244-6283-4/09/$26.00 ©2009 IEEE

of wireless systems. Their research covered the area of cellular networking, where there is a base station. Naoumov and Gross [1] used the limited interference computation (LIC) based algorithm to improve the performance of NS2 simulator. They directly worked with the ad hoc network and basically proposed two modification of node organization (grid based and list based node organization). Though, their proposed algorithm for the grid based node organization can perform well enough for a several number of cases, but this sort of node organization does not produce suitable result while the CST induced radius is more than or about equal to half of the width of the simulation area.

In the proposed algorithm, the both of the grid and list based node organization are integrated to a unified node arrangement model where the node organization will reduce the time required for all cases and with all possible variations in CST value. We present simulation results and performance analysis supporting the proposed algorithm.

III. MODELING AND SIMULATION OVERVIEW

NS2 uses the simple Free Space Propagation Model to simulate MANET protocols. A modeling choice to define if a transmission can be detected by a tagged receiver is to define a receiving threshold (R_1) and a carrier-sense threshold (R_2) for every device [4]. For every simulated transmission, this requires evaluation, for each receiver, if the receiving power perceived for the ongoing transmission is sufficient for reception (i.e., greater than RT), if it is sufficient for detection and carrier sensing (i.e., greater than CST), or if it is simple interference.

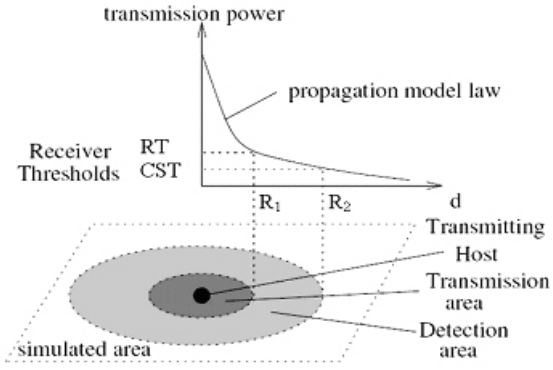

Fig. 1. Simulation area

The detection area of a wireless transmission device is the area where the signal propagates, and where it can be detected by a carrier sensing mechanism, without being necessarily decoded (i.e., CST ≤ Received Signal Power ≤ RT). Circular coverage areas can be defined for open-space propagation models, and centered on the transmitter position.

A. Grid-based Node Organization

The simulation area is divided into cells to form a grid, 3D array of pointers able to store, if necessary, all mobile nodes in the topography if they are all located in the same cell. This organization of the array allows each cell to know which mobile nodes are currently located in it and which not. Every time the position of a node is calculated in the grid to determine the cell a node belongs to. Also keep information to get list of nodes affected by the current transmission. First the radius is determined by CST and then selects those nodes that belong to the grid's cells covered by a circle with this radius. Subsequently, only nodes in these cells are involved in a computation, while the original NS2 considers all nodes on a channel.

B. List-based Node Organization

Another data structure that can be used to improve simulation performance is a double-linked list of mobile nodes, ordered by their X-coordinates. Here to keep track of nodes new members are added to the mobilenode, mobilenode *prevX, *nextX and a new static member xListHead. When a new node is created its constructor simply appends the node to the list. Once the coordinates are assigned, the list is sorted in ascending order based on the X-coordinate. Every time a node moves its position, the list is updated. This set is formed by the nodes in the list with X-coordinates from $X-R_2$ to $X+R_2$ that have their Y-coordinates in the range $Y-R_2$ to $Y+R_2$, where (X, Y) are the coordinates of the current (transmitting) node.

IV. ALGORITHM

The ultimate target of the proposed system is to reduce the number of nodes from the boundary region of the transmission coverage area. In this purpose, the minimal rectangular coverage area is introduced. This will consider only those nodes inside the minimal rectangular coverage area.

A. System Architecture

The entire simulation area is composed of cells of same size defined as a two dimensional area. Each node inside a cell is kept in a sorted list using bucket sort and in the sequence of Y and X co-ordinates. When a node moves around, the position of the node is matched with the current block and the node-list of the block/cell is sorted again.

When the transmitter transmits a signal, the system first detects all the blocks/cells those are intersected or covered by the circle or the sphere. For those cells, covered partially by the transmission region, the nodes within the minimal rectangular/cubical region are selected. As the node-list is already sorted, those nodes can be found easily.

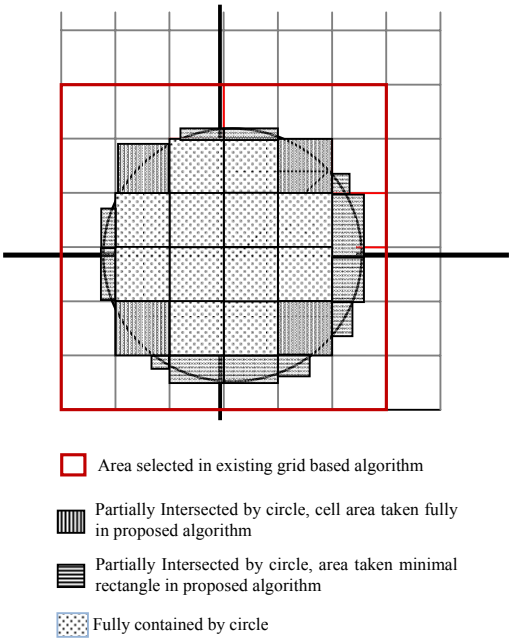

Fig. 2. Selected area in proposed algorithm

B. System Operation:

Every time any node tries to transmit a signal, the proposed system must actively supply the nodes that are going to be tested for the transmission. In this respect the system can be divided into three functional units:

- Block Initialization
- Node Selection
- Node Mapping

B.1. Block Initialization

When the simulation environment is setting up, the virtual cells should be created and the references/pointers of the nodes are mapped to the cells, in which it is situated considering its location value. Here is the Block Initialization Algorithm:

```
1.   MEASURE height, width OF transmission_area
2.   SET block_width := AVERAGE (R)
3.   SET num_of_blocks_per_row :=
                    CEILING (width / block_width)
4.   SET num_of_blocks_per_column :=
                      CEILING (height / block_width)
5.   SET blocks:=new rectan-
gle[num_of_blocks_per_column][ num_of_blocks_per_row]
6.   FOR ( j = 0 TO num_of_blocks_per_row )
7.   DO
8.     FOR ( i = 0 TO num_of_blocks_per_column )
9.       DO
10.           blocks[i][j].top_left = j * block_width;
              blocks[i][j].height = block_width;
              blocks[i][j].width = block_width
11.      END
12.    END
```

B.2. Node Selection

The node selection process assumes that all the nodes are already mapped to the corresponding cells. With this assumption, the proposed system first identifies the Super Set, then those cells are selected that has its maximum area inside the circle, name this Covered Set. Add all the nodes inside the Covered Set to the output list. There are still a few cells that are partially covered. Determining Minimal Rectangle for these partially covered cells include only those nodes that are inside the Maximal Rectangle of each partially covered cell.

Table 1: Geometric assumptions determining minimal rectangle

Case	Conditions	Intersecting Sides of Cell	Special Considerations (If any)
1	x +ve, $y \le Y_{node}+R/\sqrt{2}$	Top & Bottom or Left & Bottom	X_{max} = Intersection point of Bottom
2	x +ve, $y \ge Y_{node}+R/\sqrt{2}$	Left & Bottom or Left & Right	Y_{max} = Intersection point of Left
3	x -ve, $y \ge Y_{node}+R/\sqrt{2}$	Left & Right or Right & Bottom	Y_{max} = Intersection point of Right
4	x -ve, $y \le Y_{node}+R/\sqrt{2}$	Right & Bottom or Bottom & Top	X_{max} = Intersection point of Bottom
5	x -ve, $y \ge Y_{node} - R/\sqrt{2}$	Bottom & Top or Right & Top	X_{max} = Intersection point of Top
6	x -ve, $y \le Y_{node} - R/\sqrt{2}$	Right & Top or Right & Left	Y_{max} = Intersection point of Right
7	x +ve, $y \le Y_{node} - R/\sqrt{2}$	Right & Left or Left & Top	Y_{max} = Intersection point of Left
8	x +ve, $y \ge Y_{node} - R/\sqrt{2}$	Left & Top or Top & Bottom	X_{max} = Intersection point of Top

Determining Super Set: If any cell has any point within the region defined by [(X ± radius), (Y ± radius)], then the cell is included in the Super Set.

Determining Covered Set: If the distance of the center of the cell with the center of the circle is less than the length of the radius, then the cell will be included in the Covered Set.

Determining Minimal Rectangle: It is enough to find out the maximum value of X, or Y that constructs a rectangle with the nearest point of a cell. Determining the

minimal rectangle requires some simple geometric assumptions and calculations that are shown in table 1.
Suppose X and Y axes are drawn, considering the center of the circle (transmitter's position is the center) as origin. If the center of the cell creates an angle less than 45º with the center of the circle, it is clearly visible that, the circle intersects the bottom line with larger X coordinate value and if the block is not intersected at the top line, it is intersected at the left side.
If the angle is between 45º and 90º, the maximum value of Y is the intersection point with the left side of the cell. Assuming the center of the circle as the virtual origin and these X and Y axes as virtual axes, this 0º - 90º segment (first Quadrant) can be mirrored horizontally or vertically to devise the calculation for Minimal Rectangle. So, there could be 8 such cases.

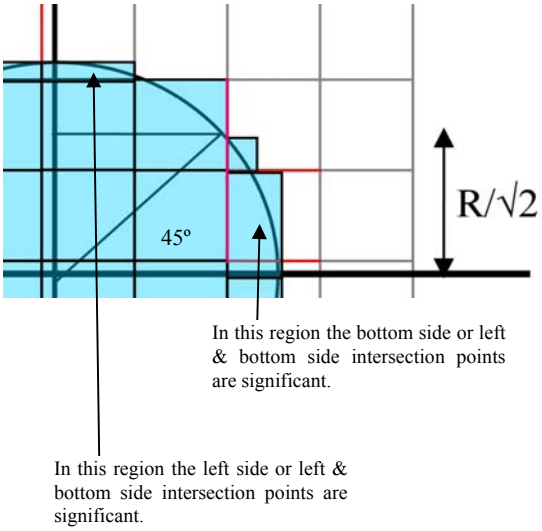

Fig. 3. Determining intersection points

The following algorithm decides which side of the partially covered rectangle is intersected by the circle:

```
IF x +ve AND y≤Ynode+R/√2
    THEN Xmax = Intersection point of Bottom
ELSE IF x +ve AND y≥Ynode+R/√2
    THEN Ymax = Intersection point of Left
ELSE IF x –ve AND y≥Ynode+R/√2
    THEN Ymax = Intersection point of Right
ELSE IF x –ve AND y<Ynode+R/√2
    THEN Xmax = Intersection point of Bottom
ELSE IF x –ve AND y>Ynode-R/√2
    THEN Xmax = Intersection point of Top
ELSE IF x –ve AND y<Ynode-R/√2
    THEN Ymax = Intersection point of Right
ELSE IF x +ve AND y<Ynode-R/√2
    THEN Ymax = Intersection point of Left
ELSE IF x +ve AND y>Ynode-R/√2
    THEN Xmax = Intersection point of Top
```

B.3. Node Mapping

Whenever a mobile node moves, its location is checked whether it has crossed the boundary of a cell and entered to the other cell. If the node has moved to another cell, the entry of its pointer is deleted from the old cell and added to the new cell. Node movement is managed through the following algorithm:

```
IF node IS IN old_block
    THEN BUCKET_SORT (old_node_list)
ELSE IF node IS IN new_block
        REMOVE node FROM old_node_list
        ADD node IN new_node_list
        BUCKET_SORT (new_node_list)
END IF
```

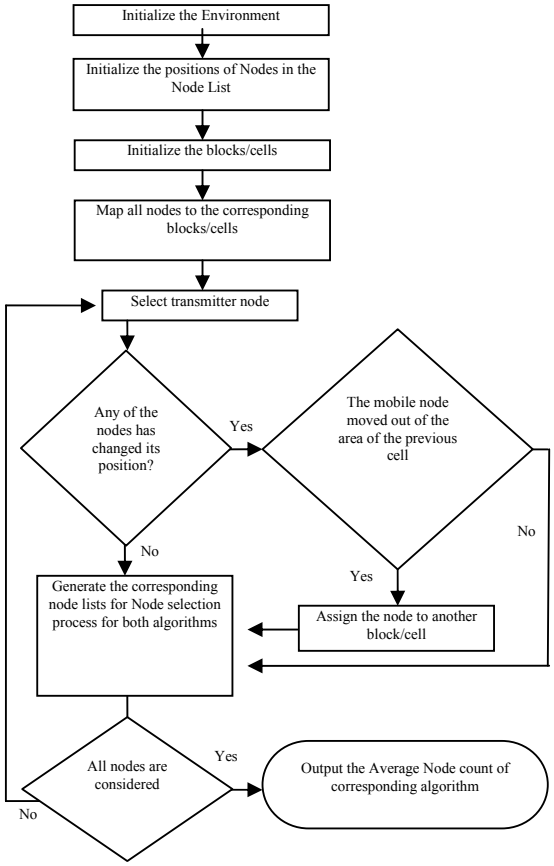

Fig. 4. Flow chart of the implemented system

V. RESULTS AND PERFORMANCE ANALYSIS

The simulation was conducted in both small-scale (100 nodes) and large-scale (1000-10000 nodes) networks satisfying different conditions (e.g. variation in number of nodes, size of the simulation area, size of the unit block). Random distribution of nodes inside the simulation area was ensured and all the test case results were aggregates of over hundred occurrences of simulation. The Simulation was done in a PC (Intel CoreTM 2 Duo processor at 2.00 GHz, 2 GB DDR2 RAM) using a custom simulator for both cases (existing Grid based Node

organization & our proposed algorithm). The implementation architecture is shown in figure 4.

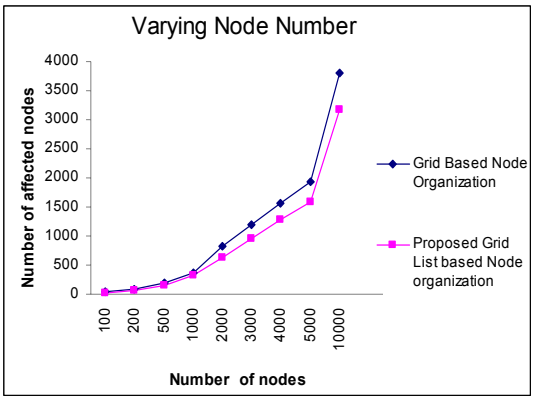

Fig. 5. Results with varied total number of nodes

Figure 5 shows the success rate of the affected nodes as a function of the total number of nodes for the fixed area (4000m X 5000m) with varying number of nodes using both of the existing and proposed algorithms.

Figure 6 shows the average number of affected nodes for the fixed block size and the total number of nodes 1000. Here results have been reported for small area, medium area and also for large area (10 km X 8 km).

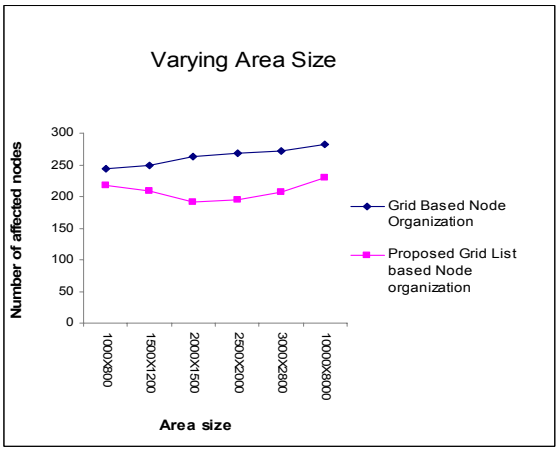

Fig. 6. Results with varied simulation area

Figure 7 illustrates the results with varied block size for the total number of nodes 1000 and area 2 km X 1 km.

The results showed the behavior of the proposed grid list based algorithm for faster simulation under different conditions, assuming random distribution of nodes in the simulation region as well as with varied number of nodes, area size and varying block size. From various results it is clear that when network area is heavily loaded with huge number of nodes this proposed algorithm gives much better result with reduced number of affected nodes.

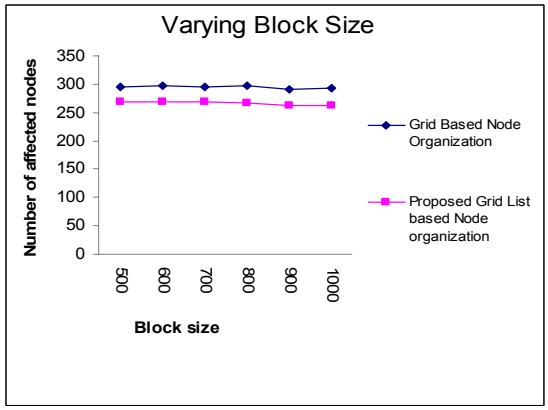

Fig. 7. Results with varied block size

From figure 8, it is clear that difference between selected nodes increases as the total number of nodes increases. This increment is not static, proportional to the increase of total number nodes. So this algorithm will show a great impact for large mobile ad hoc networks with large number of nodes. This is an important point for the proposed algorithm.

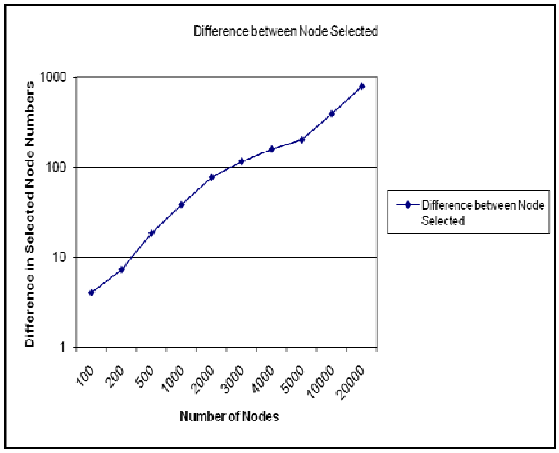

Fig. 8. Differences between two results with varied total number of nodes

In the existing Grid Based Node Organization, the total area of coverage for primary node filtering is between $(2R_2)^2$ and $(2(R_2 + l))^2$, where l is the length of one side of a cell/block. But in this proposed Node organization, the considered area is close to the area of the circle of the transmission area; i.e., almost $(3.14159 * R_2^2)$. So it is clear that minimal rectangle area is less than the existing grid based algorithm and here an approximate value 3.5 unit is subtracted from the previous area.

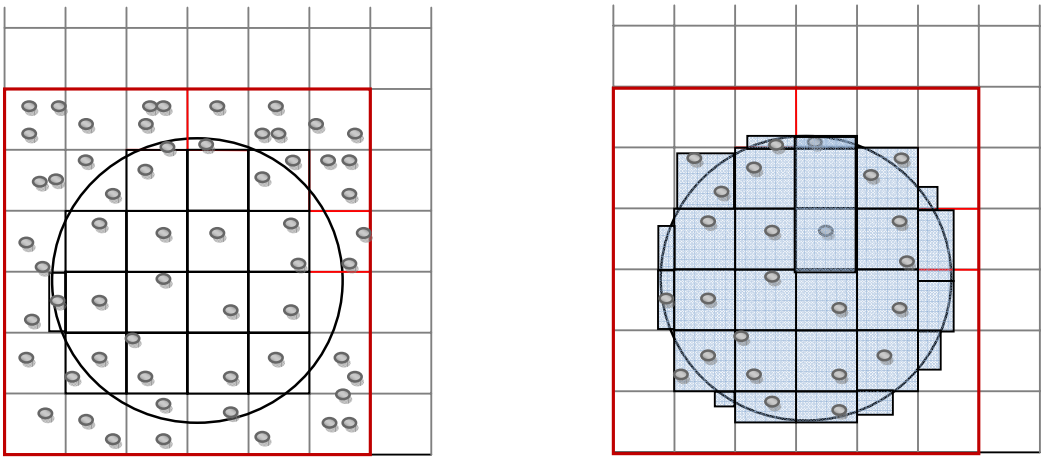

(a) (b)

Fig. 9. Visual illustration of coverage area (affected nodes) in (a) existing grid based algorithm (b) proposed algorithm

Thus, if the simulation environment contains evenly distributed nodes, and then there is an improvement of about:

Minimum: $((4-3.5)*R_2^2 / 4R_2^2) * 100\% = 0.125 * 100\% = 12.5\ \%$

Maximum: $((4(R_2+l)^2 - 3.5* R_2^2) / 4(R_2+l)^2) * 100\% = 78.15\ \%$ [assuming $l = R_2$]

So, the proposed approach to node organization saves the coverage area at least 12.5% upto 78.15% than in previous solution.

Figure 9 shows that the proposed grid list based algorithm, assuming random distribution of nodes in the simulation region, selects lower number of nodes than existing grid based algorithm. The proposed algorithm therefore reduces the area that exists outside of the transmission coverage area of a transmitter and reduces number of nodes that are unaffected by the transmitter.

VI. CONCLUSION AND FUTURE WORKS

The intended purpose of this work is reducing the number of considerable nodes for wireless signal transmission in a standard simulation environment for mobile ad hoc networks. The core concept behind this effort is to determine the minimal possible area under the transmission range in an efficient manner and find the affected nodes for further transmission. The reduced coverage area thus results in a reduced set of probable nodes for simulation. The theoretic proof and the implementation result show the decrease in the coverage area under consideration and at the same time the number of considerable nodes is reduced, comparatively in a better proportion. Reducing the number of considerable nodes reduces the execution time of the simulation of the entire network. For reducing the sorting overhead an on-demand sort strategy could be adopted, where the nodes of a cell would be sorted only if it is on the boundary of the transmission region and not already sorted.

REFERENCES

[1] Valeri Naoumov, Thomas Gross, “Simulation of large ad hoc networks”, MSWiM’03, San Diego, California, USA, September 19, 2003.

[2] A. Roksana, M. Lutfar Rahman, “Performance analysis of MANET routing protocols using NS2,” unpublished.

[3] S. Samyak, K. Amit, S. Mahesh, B. Girish, “Performance Evaluation of Ad Hoc Routing Protocols Using NS2 Simulation”, in Mobile and Pervasive Computing (CoMPC), 2008, p. 167-171.

[4] J. Banks. “Introduction to simulation”. In P. A. Farrington, H. B. Nembhard, D. T. Sturrock, and G.W. Evans, editors, Proceedings of the Winter Simulation Conference, 1999.

[5] L. Perrone and D. Nicol. “Using n-body algorithms for interference computation in wireless cellular simulations.” In MASCOTS 2000 Intl. Workshop Modeling, Analysis and Simulation of Computer and Telecommunication Systems, pages 49–56, 2000.

[6] S. Das, C. Perkins, and E. Royer. “Performance comparison of two on-demand routing protocols for ad hoc networks”. In INFOCOM’2000 (1), pages 3–12, 2000.

Proceedings of 2009 12th International Conference on Computer and Information Technology (ICCIT 2009)
21-23 December, 2009, Dhaka, Bangladesh

A Two-Layer Hierarchical Permission Based Mutual Exclusion Algorithm

Mohammad Ashiqur Rahman†, Md. Mostofa Akbar‡, Mohammad Shafiul Alam†
†Dept. of Computer Science and Engineering, Ahsanullah University of Science and Technology, Bangladesh
‡ Dept. of Computer Science and Engineering, Bangladesh University of Engineering and Technology, Bangladesh
ashiq_others@yahoo.com, mostofa@cse.buet.ac.bd, shuvo23@gmail.com

Abstract

Due to the growing application of peer-to-peer computing, the distributed applications are continuously spreading over extensive number of nodes. To cope with this large number of participants, various cluster based hierarchical solutions have been proposed. Cluster based algorithms are scalable by nature. Several of them are quorum based solutions. All of these solutions exploit the idea of coordinator/leader of cluster. Thus, fault tolerance of these algorithms is low. If any coordinator fails, election of new one is required. Here we propose a two-layer hierarchical cluster based solution where no coordinator is used. We simulate our proposed algorithm and show that it outperforms related ME algorithms.

Keywords: Cluster, Distributed Algorithm, Hierarchical, Mutual Exclusion, Permission, Quorum.

I. INTRODUCTION

In distributed systems, different processes run on different nodes of a network and they often need to access shared data and resources, or need to execute some common events. These processes should be consistent, and the access to these shared entities should be mutually exclusive. The portion of an event or application, where any shared component or common events are accessed, is the Critical Section (CS). Mutual Exclusion (ME) algorithms ensure the consistent execution of the CS. As the shared memory is absent in distributed systems, the solutions of the ME problem is not straightforward. Due to the enormous importance of ME and the difficulty of its solution, it is an active research area since last three decades. The classic algorithms for Mutual exclusion that have been proposed for fixed networks can be classified in two types: centralized and distributed approaches. In the centralized solutions, a node is designated as coordinator to deliver permission to the other nodes to access the CS, while in the distributed solutions the permission is obtained from consensus among all network nodes.

Distributed mutual exclusion algorithms are generally classified in two categories: token based and permission based [18]. Permission based mutual algorithms [4]–[7] impose that a requesting node must receive permissions from other nodes (a set of nodes or all other nodes) to access the CS. In the token-based mutual exclusion algorithms [1]–[3], a unique token is shared among the set of nodes. The node holding the token can enter the CS. The basic idea of token based algorithms is: a node must own the unique token before entering the CS. So, in the best case, no communication is necessary since the token may be available locally. Otherwise, a mechanism is needed to locate the token. In Raymond [1], a spanning tree of network for locating the token is used and it shows that the average number of messages exchanged in this protocol is $O(\log n)$. But if the node holding the token fails, expensive token regeneration protocols [17] must be executed. Nisho presented a highly resilient, though still complex, token based mutual exclusion algorithm [2]. Naimi proposed an algorithm [3] that takes $O(\log n)$ cost too.

Ricart and Agrawala proposed the first permission based algorithm [4] in 1981, which takes $2(n-1)$ messages for a node to get consensus. To access the CS a node sends request to all other $n-1$ nodes in the network and then waits for the replies from them. When it receives all the replies, it enters into the CS. A node sends reply against a request only if it is earliest than any other requests, otherwise it defers the request. As consensus from every node is required, this algorithm suffers due to high message cost and node and communication failures.

Concept of quorum improves the performance of permission-based algorithms to a great extent. In quorum based algorithms, to achieve mutually exclusive access of the CS, a node needs to have permissions from all of the nodes of a quorum. This kind of algorithms takes lower message cost and is resilient to node and communication failures. Message cost of these algorithms is proportional to the quorum size. Therefore these algorithms try to achieve the two goals: small quorum size with high degree of fault tolerance.

The majority quorum algorithm [15] is the first and a very simple algorithm of this kind. According to this algorithm, a node must obtain permission from a majority of nodes in the network. Since there can be only one majority at any point, ME is achieved easily. Maekawa presented an ME algorithm [5] by forming a *logical structure* on the network. In this scheme, a set of nodes is associated with each node, and this set has a nonempty intersection with all sets corresponding to the other nodes. As the size of each set is $\sqrt{n}$, the algorithm incurs $\sqrt{n}$ order of cost.

978-1-4244-6283-4/09/$26.00 ©2009 IEEE

Garcia-Molina and Barbara [16] have properly defined the concept of quorums with the notion of *coterie*. A coterie is a set of sets with the property that any two members of a coterie have a nonempty intersection. Combining the idea of logical structures and the notion of coteries, an efficient and fault tolerant quorum generation algorithm for ME is proposed by Agarwal and Abbadi [6]. Here the nodes form a logical binary tree to generate quorums. The quorum can be regarded as attempting to obtain permissions from nodes along a root–to–leaf path. If the root fails, then the obtaining permissions should follow two paths: one root–to–leaf path on the left subtree and one root-to-leaf path on the right subtree. This algorithm tolerates both node failures and network partitions. In the best case, this algorithm incurs logarithmic cost considering the size of the network. However, the cost increases with the increase of node failures.

At present, the number of distributed nodes has become very large. With the increasing importance of peer-to-peer computing [23] as well as grid computing [24], the distributed applications have been extended over a large number of nodes. The performance of these distributed applications depends on the number of participating nodes. Classical ME algorithms illustrated above do not consider these matters. Hence, we need scalable algorithms that reduce the number of participating nodes.

Sometimes the nodes in a network are divided into several groups where each group is often called a cluster. According to this concepts some hybrid ME solutions [8] [9] are proposed. Actual goal of these proposed algorithms was to combine two different approaches in different layers, intra-group (lower layer) and inter-group (upper layer). Two distributed ME solutions are presented by Erciyes [10] using a logical structure, where clusters are arranged on a ring. Bertier et al. proposed two token-based algorithms in [11] taking into account the hierarchical network topology, which reduce both latency cost and number of message. These three solutions are modification of Naimi's token-based algorithm [3] for proxy-based cluster. As these algorithms are basically token based, they suffer due to token failure. A two-layer permission based algorithm is presented by Rahman et al. in [12], where the coordinators (named as message routers) of the clusters form the upper layer. For quorum formation, tree-quorum algorithm [6] is used in each layer of the algorithm. Rahman and Akbar extended this algorithm in [13] for multi-level clustered network. However, the main problem of these algorithms [12] [13] is the failures of coordinators. Any failed coordinator has to be replaced using a leader election algorithm, which incurs extra cost.

In this paper, we propose a cluster-based two-layer distributed ME algorithm that uses no specific coordinator for a particular cluster, but improves the performance by reducing participating nodes. Fault tolerance of our proposed solution is much higher than the algorithm of Rahman et al. [12] and incurs less communication cost especially when failures occur. We also choose *tree-quorum* algorithm for selecting quorums in both of the layers, so that we can compare the performance of our algorithm with that of Rahman's algorithm. In Section II we describe the proposed network. Our proposed solution along, its proofs of correctness and liveness and analysis for optimality are presented in Section III. Next section includes the simulated comparison of the algorithm especially with Rahman et al. Finally a conclusion is given.

II. PROPOSED NETWORK

A. Description of the Environment

We consider an asynchronous distributed system, which follows the model proposed in [20]. Each pair of nodes is connected through a communication channel. Links may fail causing intermittent message drop. The message delays for communication and processing are finite. No assumption is made for the relative speeds of the nodes. A node may fail by stopping or crashing, in accordance with fail-stop model [19]. However, a failed node may restart afterwards (after a reasonably long time), which will be referred as recovery. When a process fails, it loses all its states. However, it may use local stable storage to save some information (that never changes throughout the execution of the algorithm), so that it can retrieve them later for proper execution of ME algorithm.

B. Network Architecture

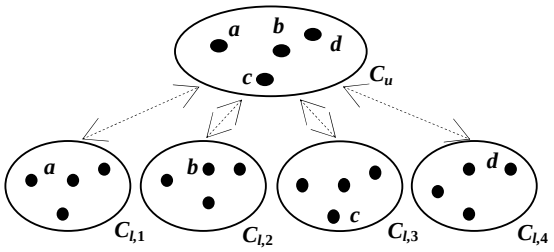

Fig. 1. Network architecture of the proposed algorithm

The nodes in a network are partitioned into several non-intersecting groups. Each group is called a cluster. The nodes inside the clusters form the lower layer of nodes. Though any number of arbitrary nodes forms the next (upper) layer, as a matter of guideline, from each of the clusters an arbitrary node is taken for the upper layer. Thus, the number of nodes of this layer is equal to the number of clusters. The upper layer can be considered as a single cluster. In Fig.1, $C_{l,1}$, $C_{l,2}$, $C_{l,3}$ and $C_{l,4}$ are four nonintersecting lower layer clusters. Four nodes a, b, c and d, taken from each of the lower layer clusters respectively, form the upper layer cluster C_u, which is

only cluster of the upper layer. Note that, each node is a member of a lower layer cluster; so each member of the upper layer cluster is also a member of one of the lower layer clusters.

Each node knows the members of its lower layer cluster as well as the members of the upper layer cluster. As the memberships to the clusters remain unchanged throughout the program, a node keeps this information in stable storage, so that it can retrieve this data after recovery.

III. PROPOSED ALGORITHM

A. Brief Outline

Two layers of nodes participate in our proposed algorithm: the members of a lower layer cluster and the members of the upper layer cluster. A coordination algorithm, as in [12] [13], communicates between these two layers of executions. In both layers, we use the tree-quorum algorithm [6] for quorum creation. When a node *x* wants to access the CS, first it requires to have the consensus from the nodes inside its lower layer cluster. When *x* gets permission at this layer, it needs to have permission from the upper layer. To get this permission, *x* selects an arbitrary node *y* among the members of the upper layer cluster as its *representing node*. To *y*, *x* is identified as the *represented node*. At the upper layer *y* executes the ME algorithm on behalf of *x*. If *y* gets consensus from the members of the upper layer cluster, it informs *x* about the consent. At this point, the node *x* has the total consensus, i.e., permissions from both layers, and can use the CS safely. We apply classical quorum based ME algorithm [5] [6] inside a cluster for collecting consensus.

B. Messages and States

As we apply quorum based ME algorithm inside the clusters, our ME algorithm uses *Request*, *Reply*, *Release*, *Inquire* and *Yield* messages. Since some nodes are members of two clusters of both layers, Layer No is added to the contents of these messages to identify the layer (i.e., the cluster) of executing ME algorithm. Possible values of Layer No are only 0 and 1, which identify the upper layer and the lower layer respectively.

The communication between the CS requesting node, a member of a lower layer cluster, and its representing node, a member of the upper layer cluster, is done through *Layer_Request*, *Layer_Reply* and *Layer_Release* messages, similar to [12] [13]. Functions of these messages are briefly described below:

- When a node *x* gets the consensus from a quorum of its lower layer cluster, it sends a *Layer_Request* message to an arbitrary node *y*, its representing node, to process the request in the upper layer cluster.
- If *y* receives consensus inside the upper layer cluster, it sends a *Layer_Reply* message to *x*.
- In order to release the consensus in the upper layer *x* sends a *Layer_Release* message to *y*.

Timestamp, a global logical time [14], consists in each message and denotes the time of sending the message. This timestamp is crucial for *Request* message. As multiple requests can come from different nodes to a single node, a node often needs to keep them in a queue to process afterward. A node keeps the incoming *Request* messages in a minimum priority queue, be identified as QUEUE, according to their timestamps. If timestamps of two *Request* messages are equal, then node identification numbers are used for this determination. This ordering is crucial for avoiding deadlock and starvation. A member node of the upper layer cluster also maintains a normal first-in first-out queue, be identified as FIFO, for *Layer_Request* messages.

Different nodes participate in the algorithm. At an instant, a node, according to its role, owns a state. As some nodes play at both layers, they possess same or different states at these two layers. To represent the proposed system, we define following arrays of states, where each element of an array represents the state of the corresponding node at a particular layer. Size of each array is only two with 0 and 1 indices: 0 for the upper layer and 1 for the lower layer.

- *REQUESTING*[0…1]: A node set this state to true if it sends *Request* messages to its fellow nodes (members of its cluster).
- *LOCKED*[0…1]: This state is set to true when a node sends *Reply* to a fellow *REQUESTING* node. Latter node is the *locking node* of the former.
- *BUSY*[0…1]: When a requesting node of the upper layer (Layer 0) cluster gets consensus from its cluster, its *BUSY*[0] state becomes true. In case of the lower layer (Layer 1), when a requesting node of a lower layer cluster gets consensus from its cluster as well as from the upper layer cluster, its *BUSY*[1] state is set to true.
- *INQUIRING*[0…1]: When a *LOCKED* node wants its consensus back, it sends an *Inquire* message to its locking node. At this point, the node sets the *INQUIRING* state to true.

State *LAYER_REQUESTING* is also defined for the nodes of the lower layer cluster. When a requesting node of a lower layer cluster gets necessary consensus from its cluster, it sends a *Layer_Request* message to its representing node. At this time, its *LAYER_REQUESTING* state is set to true. Initially, all the states are false. We will use ‘a state is set’ or similar languages to mean that the state is set to true. Similarly, we will use ‘a state is unset’ to mean that the state is false and ‘a state is reset’ to mean that the state is set to false.

C. Algorithm

In order to obtain consensus, a requesting node requires

consensus from two separate quorums. Firstly, the requesting node forms a quorum in its lower layer cluster and seeks consensus from the quorum. Next, its representing node seeks consensus by forming a quorum in the upper layer cluster.

A node, if its *LOCKED* state is unset, chooses the *Request* message at the head of its QUEUE and sends a *Reply* message, as its consensus, to the requesting node and sets its *LOCKED* state. Once a node exits from its critical section, it sends *Release* messages to all nodes of the lower layer quorum and, through the representing node, to all nodes of the upper layer quorum. After getting the release message, a node resets its *LOCKED* state and chooses another request residing at top of its QUEUE, if it is not empty, for next processing.

The following points briefly describe our proposed algorithm:

- Requests for the CS are generated at lower layer clusters. These requests are processed sequentially in both layers. The clusters $C_{l,1}$ and C_u in Fig. 1, for example, represent the participating clusters, if a node of $C_{l,1}$ places a request for the CS.
- The CS requesting node *x* first executes ME algorithm in its lower layer cluster C_l. It selects a quorum q_l and sends a *Request* message to each of the quorum members. Now, its *REQUESTING*[1] state is set. When *x* receives *Reply* messages from all members of q_l, it has the consensus in this layer. Now it picks an arbitrary node *y* (as representing node) from the members of the upper layer cluster C_u and sends a *Layer_Request* message to *y*. At this point, *x*'s *REQUESTING*[1] state is reset and *LAYER_REQUESTING* state is set.
- When *y* gets *Layer_Request* from *x* (as represented node), it queues the message into its FIFO, if it is already processing another *Layer_Request* (i.e., any of its states at this layer is true). Otherwise, it selects a quorum q_u inside C_u and executes ME algorithm on behalf of *x*. It's *REQUESTING*[0] state is set at this stage. When *y* gets *Reply* messages from all q_u members, it has the consensus in C_u. Now it resets *REQUESTING*[0] state and sets *BUSY*[0] state and sends a *Layer_Reply* message to *x*.
- When *x* receives the *Layer_Reply* message from *y*, it has the total consensus, i.e., permissions from both layers, and so it resets its *LAYER_REQUESTING* state and sets its *BUSY*[1] state and executes the CS. In this way, a node mutual exclusively enters the CS. After execution of the CS, *x* resets its *BUSY*[1] state and sends *Release* messages to the members of q_l. At the same time, it also sends a *Layer_Release* message to *y*.
- When *y* gets *Layer_Release* from *x*, it resets its *BUSY*[0] state and sends release messages to the members of q_u. If there is one or more *Layer_Request* message in *y*'s FIFO, *y* will take out one from the FIFO and will start processing by selecting a quorum q'_u inside C_u.

Inquire and *Yield* messages works to avoid deadlock, similarly as in [6] [12] [13]. Let a node *u* receives a request from node *v* that possesses an earlier timestamp than its currently processing request of a node *w*, to which it has already sent *Reply* message. Then *u* puts the request of *v* into QUEUE and sends an *Inquire* message to *w* and waits for either a *Yield* or *Release* message from *w*. At this time, its *LOCKED* state is reset and *INQUIRING* state is set. When *w* receives the *Inquire* message from *u*, it relinquishes the consensus of *u* as well as sends a *Yield* message to *u* if and only if it has not received all replies from its requesting quorum members. If *w* has already acquired all necessary replies to access the CS and may be already executing the CS, then it simply ignores the *Inquire* message and proceeds normally, that is, it continues to execute the CS. After finishing the execution, it sends a *Release* message to the inquiring node *u*. When *u* receives the *Yield* message, it resets it *INQUIRING* state and puts back the request of *w* into its QUEUE. Now it pop out the request from the top of QUEUE and accordingly sends a *Reply* message to corresponding node and gets into *LOCKED* state again. In the mean time, if no request with the earlier timestamp has come, the *Request* of *y* is the selected request message. If *u* receives *Release* message instead of *Yield* message from *w*, it does the same except reinserting the request of *w* into QUEUE, since the request has been served.

D. Proofs

D. 1. Correctness

A mutual exclusion solution is said to be correct if no more than one node gets simultaneous access to the CS. For quorum based algorithms, this condition holds, if there is at least one common node between any two quorums. In our proposed two-layer ME solution, we must get consensus at each layer: in a lower layer cluster and in the upper layer cluster. So, a quorum of our solution can be defined as $q = q_l \cup q_u$, where q_l and q_u are the quorums formed respectively with the members of a lower layer cluster and with the members of the upper layer cluster.

Similarly, another quorum could be $p = p_l \cup p_u$, where p_l and p_u are the quorums respectively of a lower layer cluster and of the upper layer cluster. Now,

$$p \cap q = (p_l \cap q_l) \cup (p_u \cap q_u)$$

Here, $p_u \cap q_u \neq \phi$, since these are the quorums selected from the members of the same cluster, the only cluster of the upper layer, and these are formed according to the tree-quorum algorithm, which ensures the intersection between any two quorums. So, we get $p \cap q \neq \phi$. Thus, the solution must maintain mutual exclusion for

accessing the CS.

D. 2. Liveness

To prove the liveness, we need to show that each request is served within a finite period. Let the C nodes of a cluster be N_1, N_2, … …, N_C. Consider the worst case scenario where the requests from each of the fellow nodes are queued at N_p. The timestamp of the queued request of N_i at N_p are T_i, where $1 \le i \le C$. The request sent by N_m contains the maximum timestamp. Thus, $T_{current} > T_m > T_i$, where $T_{current}$ is the current time and $i \neq m$. Let, the timestamp of the next request coming from N_j (after completion of its earlier request with timestamp T_j) is denoted by T_j^{next}. Definitely, $T_j^{next} \geq T_{current}$. Hence, $T_j^{next} > T_m$. Therefore, the request from N_m will be served in a finite duration (after C–1 outstanding requests are served) as it has the earlier timestamp than the next group of requests. So, any request of a node in a cluster of the lower layer or the upper layer must be served in a finite period.

In our two-layer architecture, a requesting node must have consensus at both layers. After getting consensus from its lower layer cluster, the node asks (by sending a *Layer_Request* message) its representing node to collect consensus in the upper layer cluster. Since the representing node processes the *Layer_Request* messages in FIFO manner, every *Layer_Request* will be processed in a finite time. Again, as the request of the representing node in the upper layer cluster must be served, ultimately the request is served in both layers within a finite period. So, liveness is proved.

E. Optimal Cluster Size

To find the optimal cluster size of the proposed solution, we do analysis in this section considering the tree-quorum algorithm [6] that is applied for quorum formation. According to the tree-quorum algorithm, the expected quorum size for a network with size n is expressed as $c_h = f(c_{h-1}+1)+(1-f)(2c_{h-1})$, where f denotes the fraction of the quorums that include the root of the binary tree with height h, while h is approximately $\log n - 1$. So, f is the probability of the root to be included in the quorum, when all the quorums are equally probable. As we assume that the root is included in the quorum if it is available, f is equivalent to the probability of the root being available. In the recursive equation of expected quorum size, each node becomes the root of a subtree in a particular level of the tree. Therefore, f denotes the probability that a node is available at a particular instant, simply, the availability of a node. The average number of messages needed against a single request of a node to enter the CS is proportional to quorum size. Thus c_h, expected quorum size, represents message cost function. Solving this recurrence, following equation is found:

$$c_h = \begin{cases} \dfrac{(2-f)^h - f}{1-f}, & \text{when } f \neq 1 \\ h+1, & \text{when } f = 1 \end{cases}$$

In our algorithm, there are participating clusters in two layers: a lower layer cluster and the upper layer cluster. We consider two parameters: n, the number of nodes in the network and C, cluster size of each lower layer cluster. Therefore, the number of lower layer clusters is n/C and this is the cluster size of the upper layer cluster. The height of the tree formed by the nodes inside a lower layer cluster is $h_l = \log C - 1$. Thus, the height of the tree formed by the nodes of the upper layer cluster is $h_u = h - h_l - 1$. Now, the total message cost of the proposed solution is:

$$c = c_{h_l} + c_{h_u} + 1$$

Here, c_{h_l} and c_{h_u} are the message costs at the lower layer and the upper layer respectively and lastly 1 is added for the representing node. Hence,

$$c = \frac{(2-f)^{h-h_l-1} - f}{1-f} + \frac{(2-f)^{h_l} - f}{1-f} + 1$$

Taking the derivative of c with respect to h_l and equating it to zero, we get $C = \sqrt{n}$ as the condition of optimality.

IV. SIMULATION

We simulate our proposed ME algorithm using PARSEC [21], which is a parallel C–based discrete–event simulation language. The aim of the simulation is to compare the performance of our algorithm with that of Rahman et al. [12]. For comparison *message cost* is taken as the performance metric. Message Cost is the average message complexity per request to enter into the CS, i.e., the average number of messages required for a node from request placing to getting consensus in order to execute the CS.

A. Simulation Environment

Our simulation is executed on a peer-to-peer network having an arbitrary number (up to 1200) of nodes randomly spread over the network. The network is assumed to ensure the ordered delivery of messages between a source and a destination. Communication latency between two specific nodes is taken constant. The times for message communication and message preparation/processing follows normal distribution with a mean of 12 and 8 time units respectively and a common variance of 50% of the mean. A node requests for the CS following a Poisson process with 0.0000002 request (arrival) rate. Node failures are modeled as a Poisson process with a failure rate calculated from the value of f and the recovery time. Recovery time is an exponential distribution with a mean of 1000000 time units.

In the simulation, initially we form the clusters arbitrari-

ly according to the optimal cluster size and select the nodes of the upper layer cluster by taking a random node from each cluster. Elections of the message routers are not simulated for [12]. Rather, a cost (both time and message) is assumed according to a leader election algorithm [22].

B. Performance Comparison

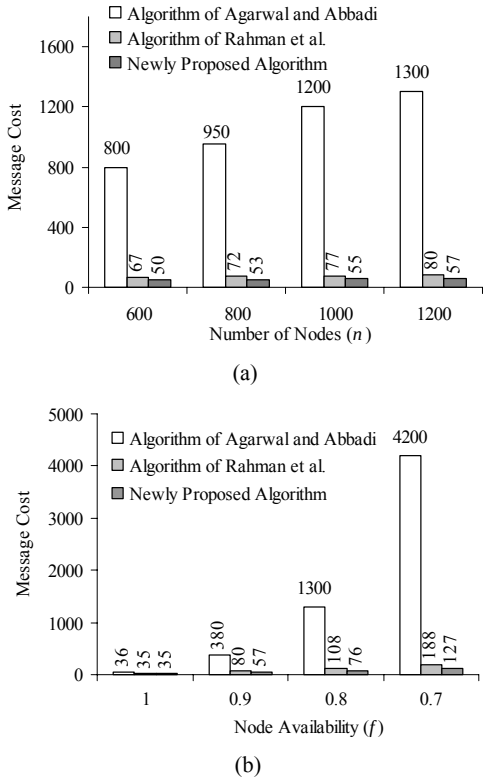

Fig. 2. Message cost of ME algorithms for (a) different n with f=0.9 and (b) different f with n=1200.

Message costs per CS entry for the classic tree-quorum based ME algorithm of Agarwal and Abbadi [6], the two-layer ME algorithm of Rahman et al. [12] and our proposed two-layer ME algorithm are plotted in Fig. 2(a) and 2(b) against different network sizes (n) and different availability of nodes (f) respectively. Both of the figures show that our algorithm simply outperforms the others especially when f decreases. According to the tree-quorum algorithm, the quorum size is inversely proportional to the value of f and varies from $\log V$ (for high values of f) to $V/2$ (for low values of f), where V is the number of participating nodes. Both of the two-layer algorithms reduce this size of participating nodes to C, i.e., $\sqrt{n}$, while the participating nodes in the classical algorithm is n. So, both algorithms outperforms the latter when f <1. Since Rahman et al. uses coordinators of the clusters, it needs to reelect new coordinator when any coordinator fails. For lower f, the rate of reelection increases. As each election of coordinator takes extra message cost, for lower f the message cost of Rahman et al. is significantly more than that of our proposed algorithm.

V. CONCLUSION

We have proposed a two-layer quorum based solution for distributed mutual exclusion. Though the proposed algorithm is cluster based, there is no use of specific coordinator (message router) for a cluster. Thus, no reelection of coordinator is required. We have devised the optimal cluster size taking message cost into consideration. At the end, we have presented a simulation result that demonstrates the noticeable improved performance of our algorithm comparing to other related algorithms. As our algorithm is sequential in nature, extended work on this research along with incorporating parallelism to the algorithm is left for future research publication.

REFERENCES

[1] K. Raymond, "A Tree based Algorithm for Distributed Mutual Exclusion", *ACM Transactions on Computer Systems*, Vol. 7, No. 1, February 1989, pp. 61–77.

[2] S. Nisho, K.F. Li and E.G. Manning, "A resilient mutual exclusion algorithm for computer networks", *IEEE Transactions on Parallel and Distributed Systems*, Vol. 1, No. 3, 1990 pp. 344–355.

[3] M. Naimi, M. Trehel, and A. Arnold, "A log (N) distributed mutual exclusion algorithm based on path reversal," *Journal of Parallel and Distributed Computing*, vol. 34, no. 1, April 1996, pp. 1–13.

[4] G. Ricart and A. K. Agrawala, "An Optimal Algorithm for Mutual Exclusion in Computer Networks", *Communications of the ACM*, Vol. 24, No. 1, January 1981, pp. 9–17.

[5] M. Maekawa, "A √*N* Algorithm for Mutual Exclusion in Decentralized Systems", *ACM Transaction on Computer Systems*, Vol. 3, No. 2, 1985, pp. 145–159.

[6] D. Agarwal and A. El Abbadi, "An Efficient and Fault–Tolerant Solution for Distributed Mutual Exclusion", *ACM Transactions on Computer Systems*, Vol. 9, No. 1, February 1991, pp. 1–20.

[7] P. C. Saxena and J. Rai, "A survey of permission-based distributed mutual exclusion algorithms", *Elsvier Science Publishers B. V.,* Vol. 25, No. 2, May 2003, pp. 159-181.

[8] Q. E. K. Mamun, M. Ali, S. M. Masum and M. A. R. Mustafa, "A Two–Layer Hybrid Algorithm for Achieving Mutual Exclusion In Distributed Systems", *WSEAS Transactions on Systems*, Vol. 3, No. 3, May 2004, pp. 1193–1198.

[9] Ahmed Housni and Michel Trelhel, "Distributed Mutual Exclusion Token-Permission based by Prioritized Groups", *Proceedings of the ACS/IEEE International Conference on Computer Systems and Applications*, June 2001, pp. 253–259.

[10] K. Erciyes, "Distributed Mutual Exclusion Algorithms on a Ring of Clusters", *ICCSA, SV-Lecture Notes in Computer Science,* 2004.

[11] M. Bertier, L. Arantes and P. Sens, "Distributed Mutual Exclusion Algorithms for Grid Applications: a Hierarchical Approach", *Journal of Parallel and Distributed Computing (JPDC)*, Elsevier, Vol. 66, 2006, pp. 128-144.

[12] Mohammad Ashiqur Rahman, Mohammad Shafiul Alam, M. M. Akbar, "A Two Layer Quorum Based Distributed Mutual Exclusion Algorithm", *The 9th International Conference on Computer and Information Technology (ICCIT)*, December 2006.

[13] Mohammad Ashiqur Rahman, M. M. Akbar, "A Quorum Based Distributed Mutual Exclusion Algorithm for Multi-Level Clustered Network Architecture", *Workshop on Algorithms and Computation (WALCOM), Dhaka*, February 2007.

[14] L. Lamport, "Time, clocks, and the ordering of events in a distributed system.", *Communications of the ACM*, Vol. 21, No. 7, July 1978, pp. 558-564.

[15] R. H. Thomas, "A majority consensus approach to concurrency control", *ACM Transaction on Database System*, Vol. 4, No. 2, June 1979, pp.180-209.

[16] H. Garcia-Molina and D. Barbara, "How to Assign votes in a Distributed System", *Journal of the Association for Computer Machinery*, Vol. 32, No. 4, 1985, pp. 841-860.

[17] J. Misra, "Detecting termination of distributed computations using markers", *Proceedings of the 2nd ACM Annual Symposium on Principles of Distributed Computing*, 1985, pp. 237–249.

[18] M. Raynal, "A simple taxonomy for distributed mutual exclusion algorithms", *ACM SIGOPS Operating Systems Review*, Vol. 25, No. 2, 1991, pp. 47-50.

[19] R. D. Schlichting and F. B. Schneider, "Fail-stop processors: an approach to designing fault-tolerant computing systems", *ACM Trans. on Computing Systems*, Vol. 1, No. 3, 1983, pp. 222–238.

[20] F. Cristian and C. Fetzer, "The timed asynchronous distributed system model", *IEEE Transactions on Parallel and Distributed Systems*, Vol. 10, No. 6, 1999, pp. 642–627.

[21] R. Bagrodia, R. Meyerr, and et al., "PARSEC: a parallel simulation environment for complex system", *UCLA Technical Report*, 1997.

[22] Scott D. Stoller, "Leader election in asynchronous distributed systems", *IEEE Transactions on Computers*, Vol. 49, No. 3, 2000, pp. 283–284.

[23] R. Steinmetz and K. Wehrle, "Peer-to-Peer Systems and Applications", *Lecture Notes in Computer Science*, Vol. 3485, 2005.

[24] Buyya and Rajkumar, "Grid Computing: Making the Global Cyber-infrastructure for e-Science a Reality". *CSI Communications*, Vol. 29, No. 1, 2005.

Proceedings of 2009 12th International Conference on Computer and Information Technology (ICCIT 2009)
21-23 December, 2009, Dhaka, Bangladesh

A Social Relation Aware Semantic Access Control

Mohammad M. R. Chowdhury, Josef Noll
UNIK-University Graduate Center, Kjeller, Norway
mohammad@unik.no, josef@unik.no

Abstract

Social relations are often used to identify an individual. In the digital world, such relations can be exploited to provide controlled access to private or community contents. This paper proposes an access control model that employs the social relations. Semantic technologies are used for formal specification of the model. The semantic access control model is composed of a knowledge base and access policies. The Web Ontology Language represents the knowledge base and the access policies are expressed through semantic rules. Execution of rules derives the access authorization decisions that state which user can access which contents with a specific privilege. The paper provides a detail evaluation of the proposed access control model.

Keywords: Access control, semantic technologies, ontology, rule, relation.

I. INTRODUCTION

A person's social environment includes his living and working environments, some of his social attributes such as income and educational background, and the communities he is part of. An individual has certain roles towards the social environment and maintain many relations with these social actors. Social science research identifies the roles and relations as identity of individuals [1], [2]. This research is concerned with making use of the social relations encompassing family, friends, relatives, neighbors, acquaintances, and social groups for securing access to the digital contents.

In this regard, an access control model is proposed which includes these social relations. The model is composed of a knowledge base and access policies. Semantics and semantic technologies act as the enabler to realize the access control model. Ontology is the cornerstone of the semantic technologies providing the formal specification of the knowledge base and access policies are represented through semantic rules. Execution of rules derives the access authorization decisions which state which user can access which resources with specific access rights or privileges.

The paper is organized as follows: chapter II presents the fundamentals of the access control; chapter III introduces semantics and semantic technologies; chapter IV provides the description of the proposed access control model including the implementation details and results of the implementation; chapter V contains the discussion aimed at evaluating the proposed model compared to the prominent access control models; the paper concludes with a summary in chapter VI.

II. ACCESS CONTROL

Access control can be achieved applying authentication and authorization processes. There exist two sets of identity attributes, the first set of attributes authenticates the user and the second set of information is applied to authorize the user [3]. In some systems, complete access is granted when a user subjects to successful authentication only. But most systems require enhanced control involving both authentication and authorization and authorization follows authentication. Access control often follows a standardized access control model.

A. Authentication

A user usually makes claims about him for identification towards a system. A part of the user's identity attribute is used to verify that the claims made by a person about himself are true. Authentication is the process of identifying an individual who wants to access a system. Access is granted when the presented claims are equal to the information stored in the system.

An authentication factor is the information or the process used to verify the identity. There are generally three types of authentication factors (listed from the weakest to the strongest): something a user knows (e.g. password), something a user has (e.g. security token), and something a user is or does (e.g. biometrics). The process of combining multiple authentication factors is called multi-factor authentication [4], [5]. Single factor authentication can be compromised quite easily. Hence, multiple factors are required to make the authentication process more secure.

B. Authorization

The second set of user's identity attribute is used to authorize a user. Authentication merely ensures that the individual is who he or she claims to be, but says nothing about access rights of individuals which is the responsibility of the authorization process. Authorization makes sure one accesses only what he is allowed to access. The process determines what a user can do in a system, such as read a document or write over a document. In this paper, we are only concerned with the authorization process as there exist numerous means of authentication.

C. Access Control Model

Access control models provide frameworks to realize access control functionalities in software and devices. Access control models deal with granting access per-

978-1-4244-6283-4/09/$26.00 ©2009 IEEE

missions based on the characteristics of subjects/objects. This section provides a thorough analysis of the requirements for designing access control models. Access control models are usually composed of subjects, objects and access rights. A subject is someone or something, for example, users, applications, or system processes. A subject is the one to which access to an object is granted or denied. Expressivity of a model measures the flexibility to support a wide range of access control policies. A flexible and tightly controlled security system needs to provide sufficient access granularity. However, there is a trade-off between granularity and usability. Scalability of a system is its ability to handle a growing number of components efficiently and effectively. There exist different aspects of scalability that include issues related to costs, performance, maintainability, changeability, robustness etc. The method of revoking access rights is one of the key scalability concerns in terms of efficiency and maintainability [6]. Access constraints should be designed with high level specification language to maintain interoperability and to make them human understandable.

Delegation is temporary transfer of access permissions or rights to one acting on behalf of another. Due to the delegation, the continuity of work is maintained even in the absence of the actual member of a role. The system allows access with specific rights when a user meets strict authentication requirements. Breach of security should result in revocation of access rights. Thus unauthorized actions by unreliable users or compromised machines can be prevented. Based on the discussions the requirements for designing access control models are listed as follows,

- The access control model should be generic and should have the necessary expressivity.
- It should support varying levels of granularity.
- The model should be scalable.
- It should support high level specification of access constraints.
- The delegation of access rights should be supported.
- The access control model should have provision for revocation of access rights.

Chapter V is going to evaluate the proposed access control model in light of these requirements.

III. INTRODUCTION TO SEMANTICS

This paper extensively uses semantic technologies for formal description of the social relations and access authorization policies. Semantics mean explicit interpretation of domain knowledge to make machine processing more intelligent, adaptive and efficient. The formal semantics provide machine understandability and manipulability of knowledge. Semantic technologies make use of the formal meaning of data and information for deriving new knowledge from the known facts. This is a cognitive process which is known as reasoning. The technology encompasses standards, methodologies and software aimed at providing more explicit meaning to the data.

Evolution of a Web that consists of machine understandable and manipulable knowledge was envisioned in 'Semantic Web', first introduced by Tim Berners-Lee [7]. Ontologies [8] are its cornerstone technology providing structured vocabularies to describe formal specification of domain knowledge. Ontology language is a formal language used to encode the ontology. Among the different ontology languages [9], this paper uses Web Ontology Language (OWL), which is proposed by World Wide Web Consortium (W3C) [10]. OWL builds on Resource Description Framework (RDF) [11] and RDF Schema (RDFS). OWL is selected because it has greater machine interpretability than that is supported by Extensible Markup Language (XML), RDF and RDFS by providing additional vocabulary. There are three variant of OWL listed according to their increasing expressiveness: OWL Lite, OWL DL and OWL Full. OWL DL is based on Description Logic which is the decidable segment of first order logic which is amenable to automated reasoning.

As the expressivity provided by the OWL is limited by tree like structures [11], the implicit knowledge cannot be inferred from the indirect relations between entities. However, the proposed access control framework spends most of its power to infer such relations that will determine the outcome of our restricted access scenarios. To be able to infer this knowledge, rule support and interworking with ontologies must be taken into account. One suitable rule language is the Semantic Web Rule Language, SWRL [12] supporting complimentary features for OWL DL. SWRL rules are written in terms of OWL classes, properties and individuals, and are defined as a set of antecedent and consequent parts. For example, a SWRL rule expressing that a person with a male sibling has a brother looks like as follows,

$$Person(?p) \wedge hasSibling(?p,?s) \wedge Man(?s) \rightarrow hasBrother(?p,?S)$$

It would require capturing the concepts: person, male and properties: *hasSibling* and *hasBrother* from OWL and p and s are variables.

This paper describes a home community scenario with OWL and access authorization policies with SWRL. The reasoning process derives the access authorization decisions by executing the policies.

IV. SEMANTIC ACCESS CONTROL

Access control can be realized through authentication and authorization. Authorization is achieved through the proposed access control model while users are assumed to be authenticated through any conventional authentication mechanism. The semantic access control model is specified using the ontology and semantic rules. This chapter provides the detail description of the proposed model.

A. Preliminaries

This section introduces the underlying formalisms of the ontology defined in this paper. The ontology is a set of *classes C*, *properties P* and *instances i*. The key concepts of the domain are defined through classes. In ontology a property establishes a relationship between the two instances. A property belongs to a domain and has a range. Syntactically, a domain links a property to a class and range links a property to either a class or a data range [10]. From an instance point of view, a property relates instances from the domain with the instances from the range. The real actors of a practical use case scenario (e.g. individuals) are defined through instances and they belong to the classes. In this research, concepts have two different relationships among them: *owl:subClassOf*, and *owl:disjointWith*. The semantic scope (SC) of a concept (class) C_i is represented as $SC(C_i)$. The definitions of these two relationships are,

- *owl:subClassOf:* $SC(C_1) \subseteq SC(C_2)$, the semantic scope of C_1 is narrower than that of C_2.
- *owl:disjointWith:* $SC(C_1) \subseteq SC(C_2)$, the semantic scope of C_1 is disjoint with that of C_2. Each *owl:disjointWith* statement asserts that C_1 and C_2 have no individuals in common.

Following are the definitions of several additional characteristics of OWL used in this paper,

- $\{i_1, i, ...i_n\} : SC(C_1)$, instances $i_1, i_2, ...i_n$ belong to class C_1.
- $P(i_1, i_2)$ states that i_1 relates with i_2 through the property P.
- *owl:symmetricProperty:* it states that if P relates i_1 & i_2 then P also relates i_2 & i_1 and can be represented as $P \equiv P^-$, where P is the inverse property of P^-.

B. Implementation

Suppose, there exists a community space in the network where there are two communities: Cycling and Rowing, each containing community and public resources. Alice, Bob, Katherin and Stefan are members of Cycling community, while Bill is a member of Rowing community. Alice, Bob, Stefan and Bill are friends to each other. Bob shares some of his private contents (videos and photos) in the community platform. Among his friends, Bob trusts Stefan and Bill more than Alice. When Alice, Stefan and Bill tries to access Bob's private contents, the following scenarios are expected:

- Though Alice and Bob are in the same community, Alice can only have limited access to Bob's private contents.
- Though Bill and Bob are not in the same community, Bill still can have limited access to Bob's private contents.
- As Stefan and Bob are in the same community, and Stefan is more trustworthy (to Bob) than the other friends, Stefan can have full access to Bob's private contents.

The proposed semantic access control model deal with these access scenarios.

The model (fig. 1) is composed of knowledge base and policy. The knowledge base consists of subject, object, privilege, attribute of subject/object, relation, and other optional entities. The knowledge base also contains properties to link the other ontology elements. This paper breaks down the component of the knowledge base as follows,

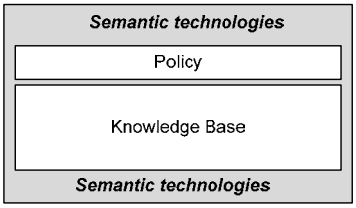

Fig. 1. The proposed semantic access control model.

$\{Identity,\ Role\} \subset Subject$
$\{Content, \mathrm{Re}source, Service\} \subset Object$
$\{FullAccess,\ LimitedAccess\} \subset \mathrm{Pr}ivilege$
$\{Age, ..., Trust\} \subset Attribute$
$\{Parents, Friends, \mathrm{Re}latives\} \subset \mathrm{Re}lation$
$\{Contexts\} \subset Option\,Entities$

The specific meaning of the privilege depends on the object types. For example, *FullAccess* refers to the streaming of a full movie whereas *LimitedAccess* refers to streaming trailer of a movie only. The knowledge base is represented through ontology using the Web Ontology Language (OWL). OWL language constructs and characteristics are already described in the preliminary (section IV.A). Fig. 2 illustrates the components (classes and properties) of the ontology.

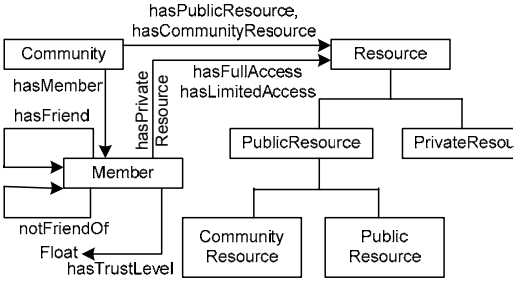

Fig. 2. The classes and properties of the ontology.

SQWRLQueryTab | Rule-1

Member Name	Limited Access to Contents
Alice	Captain_Nemo
Alice	KillBill
Alice	Alince_In_Wonderland

SQWRLQueryTab | Rule-2

Member Name	Limited Access to Contents
Bill	Captain_Nemo
Bill	KillBill
Bill	Alince_In_Wonderland

SQWRLQueryTab | Rule-3

Member Name	Full Access to Contents
Stefan	Captain_Nemo
Stefan	KillBill
Stefan	Alince_In_Wonderland

Fig. 3. Results derived executing the rules.

Following are the instances of the ontology:

- $\{Alice, Bill, Bob, Katherin, Stefan\}: Member$
- $\{Cycling, Rowing\}: Community$
- $\{KillBill\}: \Pr ivate \operatorname{Re} source$
- $\{CaptainNemo, AlineinWonderland\}: Community \operatorname{Re} source$

To realize these scenarios, access authorization policies are defined on top of the ontology. The policies are expressed through rules and rules are represented using SWRL. Following are the rule specifications that satisfy the three scenarios described earlier.

Rule 1 M_1 gets limited access to private resources of M_2, when they both belong to the same community but M_1 has trust level less than 0.7.

$$Member(?\,personA) \wedge Member(?\,personB) \wedge hasMember(?\,comm, ?\,personA) \wedge hasMember(?\,comm, ?\,personB) \wedge has \Pr ivate \operatorname{Re} source(?\,personA, ?\,resA) \wedge hasFriend(?\,personA, ?\,personB) \wedge hasTrustLevel(?\,personB, ?\,z) \wedge swrlb:lessThan(?\,z, 0.7) \rightarrow hasLimitedAccess(?\,personB, ?\,resA)$$

Rule 2 M_1 gets limited access to private resources of M_2, when they both belong to the different communities but M_1 has trust level greater than 0.7.

$$Member(?\,personA) \wedge Member(?\,personB) \wedge hasMember(?\,commA, ?\,personA) \wedge hasMember(?\,commB, ?\,personB) \wedge has \Pr ivate \operatorname{Re} source(?\,personA, ?\,resA) \wedge hasFriend(?\,personA, ?\,personB) \wedge hasTrustLevel(?\,personB, ?\,z) \wedge swrlb:greaterThan(?\,z, 0.7) \rightarrow hasLimitedAccess(?\,personB, ?\,resA)$$

Rule 3 M_1 gets full access to private resources of M_2, when they both belong to the same community and M_1 has trust level greater than 0.7.

$$Member(?\,personA) \wedge Member(?\,personB) \wedge hasMember(?\,comm, ?\,personA) \wedge hasMember(?\,comm, ?\,personB) \wedge has \Pr ivate \operatorname{Re} source(?\,personA, ?\,resA) \wedge hasFriend(?\,personA, ?\,personB) \wedge hasTrustLevel(?\,personB, ?\,z) \wedge swrlb:greaterThanOrEqual(?\,z, 0.7) \rightarrow hasLimitedAccess(?\,personB, ?\,resA)$$

B. Implementation results

The Protégé ontology editor platform was used to encode the ontology. Rules were edited using the SWRLTab (a SWRL plug-in to Protégé). It can check the validity of the rules while editing them. Jess rule engine executes the rules and derives the access authorization decisions. The decisions imply which users can access which contents through which rights or privileges. When the ontology is modified, the rules are going to be re-executed. If the re-execution of a rule generates incorrect decisions, the ontology is assumed to be inconsistent which requires a thorough review to maintain the consistency. Thus the execution of rule can also check the consistency of the ontology. However, SWRL brings in several design and use limitations, such as SWRL cannot support 'OR' clauses, explicit and universal quantifiers. Fig. 3 shows the results executing the rules defined in the previous section. It shows which resources Alice, Bill and Stefan can access with limited access and full access privileges.

V. EVALUATION

This chapter evaluates the proposed access control model in light of the requirements of access control model described in section II.C. Access Control List (ACL) is the most prominent but elementary access control model. It is an implementation mean of the access matrix model [14] which is mostly used in computer operating systems. An ACL is associated with an object. It specifies all the subjects that can access the object with a set of rights.

The model is quite generic and straightforward to design. ACL is not expressive enough to specify complex constraints. Therefore, it cannot support varying levels of granularity. It is necessary to examine all the subjects in the system to review access privileges. To revoke all rights of a subject, all ACLs must be checked one by one. Hence, troubleshooting is a tedious job. Its scalability is questionable from maintenance point of view. Delegation of access right is not clearly supported.

Capability list is another type of access list which is the inverse of ACL. Here access to an object is allowed if the subject possesses a capability for the object. The capability list has the similar limitations as the ACL.

In Role Based Access Control (RBAC) [15] users are grouped to roles and permissions are assigned to roles rather than to individual users. As seen in ACL, assigning permissions directly to users makes it difficult to control user-permission relationships. Roles categorize groups of users sharing common set of rights. There is a similarity between the role used here and traditional group. RBAC has two logical parts: assignment of roles, and assigning access rights for objects to roles.

Classical RBAC [15] is not a generic model and applied where the notion of role is involved. Classical RBAC

model cannot provide enhanced access granularity because it assigns access permissions to users through roles only. However, considerable efforts [16], [17], [18] have been made to extend RBAC to support wide range of access constraints. Scalability of various RBAC models is a concern in terms of maintainability and efficiency. Adding semantics to RBAC [19], [20], [21] facilitates high level specification of access rights and constraints. However, all these efforts were only limited to the formal specification of RBAC. The ability to delegate roles has been investigated in [22], [23]. These literatures presented frameworks supporting various forms of delegation extending the RBAC models. Classical RBAC supports revocation through revoking user-role assignment or permission-role assignment.

Fine-grained access control needs to extend beyond RBAC by including attribute or context based access control. In Attribute Based Access Control (ABAC) [24], access is granted based on the attributes of the related entities involved. Context-aware access control (CWAC) [25] incorporates factors that constitute surrounding contexts of a subject or an object as constraints to provide access. Both ABAC and context-aware access control models are quite generic but expressive enough to support varying levels of granularity. Scalability is again a design concern in terms of maintainability and efficiency. Semantic extension of these models [26], [27] can support high level specification of access rights and constraints. Delegation and revocation of access right are not clearly supported in ABAC and CWAC. In combination with roles and relationships, attributes or contexts of subjects/objects can be regarded as way to enhance granularity of access restrictions.

Even though the access control model design requirements suggest a generic approach for access control, the proposed solution is more application specific. It requires varying modifications (low to high) based on the domains where it will be applied. However it is expressive enough to derive access permission based on the formal specifications of user's roles, relationships and contexts. The model extends the basis of access permission by including additional attributes, such as age and trust besides user's the roles, relationships and contexts. Therefore varying levels of granularity is supported. OWL and SWRL facilitate high level specification of access constraints. The proposed model supports the delegation and revocation of access rights but scalability is a big concern.

VI. CONCLUSION

This paper introduces an access control model that includes social relations of people as the basis for controlled access to the digital contents. The formal representation of the model is realized through using semantic technologies. The evaluation of the semantic access control model shows that though it is not a generic model but it supports sufficient expressivity, varying levels of granularity, high level specification of constraints, and limited delegation and revocation of access rights. It is found to be comparable to the prominent RBAC model.

REFERENCES

[1] S. Stryker. "Symbolic Interactionism". Menlo Park, CA: Benjamin/Cummings, 1980.

[2] G. J. McCall and R. Simmons. "Identities and Interactions". NewYork: Free Press, 1966.

[3] Fulup Ar Foll, Jason Baragry. "Next Generation of Digital Identity". *Telektronikk 3/4 2007*, Telenor ASA, pp. 52-56.

[4] "Authentication in an Internet Banking Environment". *White paper, Federal Financial Institute Examination Council*, USA, October 2005.

[5] Abhilasha Bhargav-Spantzel, Anna Squicciarini, and Elisa Bertino. "Privacy Preserving Multi-factor Authentication with Biometrics". *In Proceedings of the second ACM workshop on Digital Identity Management*, Virginia, USA, 2006, pp. 63-72.

[6] Angelos D. Keromytis, Jonathan M. Smith. "Requirements for Scalable Access Control and Security Management Architectures". *ACM Transactions on Internet Technology (TOIT), Volume 7 , Issue 2*, May 2007.

[7] Tim Berners-Lee, J. Hendler, and O. Lassila. "The semantic web". *Scientific American Magazine*, 17 May, 2001.

[8] Dieter Fensel. "Ontologies: A Silver Bullet for Knowledge Management and Electronic Commerc", *2nd ed., Springer-Verlag*, 2004.

[9] Asunción Gómez-Pérez and Oscar Corcho, "Ontology languages for the Semantic Web", *IEEE Intelligent Systems*, Vol. 17, Issue 1, pp. 54–60, 2002.

[10] M. K. Smith, C. Welty, and D. L. McGuinness, "OWL Web Ontology Language Guide". *World Wide Web Consortium Recommendation*, 10 February 2004.

[11] Graham Klyne and Jeremy J. Carroll. "Resource Description Framework (RDF): Concepts and Abstract Syntax", *World Wide Web Consortium Recommendation*, February 2004.

[12] Boris Motik, Ulrike Sattler, and Rudi Studer. "Query answering for OWL-DL with rules", *In the proceeding of International Semantic Web Conference 2004*, 549-563, Hiroshima, Japan, pp.

[13] Ian Horrocks, Peter F. Patel-Schneider, Harold Boley, Said Tabet, Benjamin Grosof, and Mike Dean. "SWRL: A Semantic Web Rule Language

Combining OWL and RuleML", *W3C Member Submission*, 21 May 2004.

[14] Ravi S. Sandhu. "The Typed Access Matrix Model". *Proceedings of the IEEE Symposium on Security and Privacy 1992*, IEEE CS Press, USA.

[15] Ravi S. Sandhu, E. J. Coyne, H. L. Feinstein, and C. E. Youman. "Role-based Access Control Models". *IEEE Computer, 29, 2:38-47*, February 1996.

[16] Wook Shin, Jong-Youl Park, and Dong-Ik Lee. "Extended Role Based Access Control with Procedural Constraints for Trusted Operating Systems". *IEICE Transactions on Information and Systems 2005, Volume E88-D, Number 3*, pp. 619-627.

[17] Jianming Yong, Elisa Bertino, Mark Toleman, and Dave Roberts. "Extended RBAC with Role Attributes". *In Proceedings of th 10th Pacific Asia Conference on Information Systems (PACIS 2006)*, 6-9 July 2006, Kuala Lumpur, Malaysia.

[18] Anour F. A. Dafa-Alla, Eun Hee Kim, Keun Ho Ryu, and Yong Jun Heo. "PRBAC: An Extended Role Based Access Control for Privacy Preserving Data Mining". *In Proceedings of the Fourth Annual ACIS International Conference on Computer and Information Science (ICIS'05)*, 2005, pp. 68-73.

[19] M. A. Al-Kahtani and R. Sandhu. "Rule-based RBAC with Negative Authorization". *Proceedings of the 20th Annual Computer Security Applications Conference*, Tucson, AZ, 2004, pp. 405-415.

[20] T. Finin, A. Joshi, L. Kagal, J. Niu, R. Sandhu, and W. H. Winsborough and B. Thuraisingham. "Role based Access Control and OWL". *Proceedings of the Fourth OWL: Experiences and Directions Workshop 2008*.

[21] N. Heilili, Y. Chen, C. Zhao, Z. Luo and Z. Lin. "An OWL-based Approach for RBAC with Negative Authorization". *In Knowledge Science, Engineering and Management, J Lang, F Lin, and J Wang, Eds*. Springer, 2006.

[22] Ezedin S. Barka. "Framework for Role-Based Delegation Models". *Dissertation for Doctor of Philosophy,* George Mason University, Virgnia, 2002.

[23] Jason Crampton, Hemanth Khambhammettu. "Delegation in Role-Based Access Control". *In Proceedings of 11th European Symposium on Research in Computer Security, LNCS, Vol. 4189/2006*, Springer Berlin/Heidelberg, September, 2006, pp. 174-191.

[24] Hai-bo Shen, and Fan Hong. "An Attribute-Based Access Control Model for Web Services". *In Proceedings of Seventh International Conference on Parallel and Distributed Computing, Applications and Technologies (PDCAT)*, 2006, pp. 74-79.

[25] Young-Gab Kim, Chang-Joo Mon, Dongwon Jeong, Jeong-Oog Lee, Chee-Yang Song, and Doo-Kwon Baik. "Context-Aware Access Control Mechanism for Ubiquitous Applications". *Advances in Web Intelligence, LNCS, Volume 3528/2005*, pp. 236–242.

[26] Alessandra Toninelli, Rebecca Montanari, Lalana Kagal, and Ora Lassila. "A Semantic Context-Aware Access Control Framework for Secure Collaborations in Pervasive Computing Environments". *In Proceedings of the 5th International Semantic Web Conference 2006*.

[27] Hyuk Jin Ko, Dong HoWon, Dong Ryul Shin, Hyun Seung Choo, and Ung Mo Kim. "A Semantic Context-Aware Access Control in Pervasive Environments". *In Proceedings of the International Conference on Computational Science and Its Applications - ICCSA 2006*, Glasgow, UK, May 8-11, 2006, pp. 165-174.

Proceedings of 2009 12th International Conference on Computer and Information Technology (ICCIT 2009)
21-23 December, 2009, Dhaka, Bangladesh

Multicore Cluster Implementations of Hierarchical Bayesian Cortical Models

Pavan Yalamanchili, Tarek M. Taha†
Department of Electrical and Computer Engineering, Clemson University, Clemson, SC, USA
†Department of Electrical and Computer Engineering, University of Dayton, Dayton, OH, USA
pyalama@g.clemson.edu, ttaha@ieee.org

Abstract

We examine the parallelization of two recent biologically inspired hierarchical Bayesian cortical models onto two multicore processor based clusters. The models examined have been developed recently based on new insights from neuroscience and have several advantages over traditional neural network models. In particular, they need far fewer network nodes to simulate a biological scale cortical system than traditional neural network models, thus making them computationally more efficient. The two architectures examined are the Sony/Toshiba/IBM Cell BE and the Intel quad-core Xeon processors. Our results indicate that optimized implementations of the models on clusters of multicore processors can provide significant speedups and that such clusters are a promising approach for developing large scale simulations of the models. We show that for small scale implementations of the models, multicore clusters can provide speedups of about 850 times over serial implementations on the Cell Power Processor Unit.

Keywords: High performance computing, Artificial intelligence, Multicore architectures.

I. INTRODUCTION

The cortex constitutes the outer layer of the brain and utilizes a large collection of slow neurons operating in parallel to achieve very powerful cognitive capabilities. There has been a strong interest amongst researchers to develop large parallel implementations of cortical models on the order of animal or human brains [1][11][14][20]. At this scale, the models have the potential to provide much stronger inference capabilities than current generation computing algorithms [3]. A large domain of applications would benefit from the stronger inference capabilities including speech recognition, computer vision, textual and image content recognition, robotic control, and making sense of massive quantities of data. In this paper we explore the large scale implementation of two new cortical models that are currently attracting significant attention.

Recent scientific studies of the primate brain have led to new neuromorphic computational models [2][5][6][10] [13][21] of the information processing taking place in the cortex. The models differ significantly from traditional neural network models in that they are generally at a higher level of abstraction than neural network models and they consider several new biological details about the organization and processing in the cortex. Recently suggested properties of the neocortex include [13][15] a hierarchical structure of uniform computational elements, invariant representation and retrieval of patterns, auto associative recall, and sequence prediction through both feed-forward and feedback inference between layers in the hierarchy. Additionally, neuroanatomists have identified that a collection of about 80 to 100 neurons form into regular patterns of local cells running perpendicular to the cortical plane [9]. These collections of neurons are called mini-columns.

Cortical models based on hierarchical Bayesian networks [4][7] incorporate most of the recently suggested properties of the neocortex and have a significant computational advantage over traditional neural network models. Each node in the former models a cortical mini-column or a cortical column, while in the latter each node models only a single neuron. Mountcastle [15] states that the basic unit of cortical operation is the mini-column and that a collection of mini-columns are grouped into a cortical column. He also states that the mini-columns within a cortical column are bound together by a common set of inputs and short-range horizontal connections. Thus to model a large collection of neurons, a hierarchical Bayesian network based model would require far fewer nodes than a traditional neural network based model. Additionally, the number of node-to-node connections is greatly reduced in hierarchical Bayesian network based cortical models. Anatomical evidence suggests that most of neural connections in the cortex are within a column as opposed to being between columns.

In this paper we examine the MPI based parallel implementations of two recent hierarchical Bayesian network cortical models onto two high performance computing clusters. This is an important step towards the goal of biological scale implementations of these models. The two models examined are Hierarchical Temporal Memories (HTM) [10] and Dean's Hierarchical Bayesian model (to be referred to as the Dean model in the rest of the paper) [4]. At present we are not aware of any other hierarchical Bayesian cortical models (other than updates to these models and Lee and Mumford's work [13], on which Dean's model is based). In this study we examine the recognition phase of these models. The training of the models is generally carried out in a longer offline process.

Several research groups are examining large scale implementations of neuron based models [1][14] and cortical column based models [11][20]. Such large scale implementations require high performance resources to run the models at reasonable speeds. IBM is utilizing a 32,768 processor Blue Gene/L system to simulate a spiking network based model [1], while EPFL and IBM are utilizing a 8,192 processor Blue Gene/L system to simulate a sub-neuron based cortical model [14]. The PetaVision project announced at the Los Alamos National Laboratory in June 2008 is utilizing the Roadrunner supercomputer (currently ranked as

978-1-4244-6283-4/09/$26.00 ©2009 IEEE

the world's fastest supercomputer) to model the human visual cortex [17].

With the limited scaling in processor clock frequencies, multicore processors have become the standard industrial approach to improve processor performance. In this paper we compare the performance of hierarchical Bayesian cortical models on two recent multicore architecture clusters: one based on the Sony/Toshiba/IBM Cell processor [8] and the other based on the Intel quad-core Xeon processor (model E5345, also known as Clovertown). Lansner and Johannson [11] have shown that mouse sized cortical models developed on a cluster of commodity computers are computationally bound rather than communication bound. Therefore the acceleration of the computations of these models on multicore architectures can provide significant performance gains to enable large scale implementations. The two multicore clusters utilized were: 1) the Palmetto Cluster at Clemson University (USA) containing blades with two Intel quad-core Xeon processors, and 2) a cluster of Sony Playstation 3s at the Arctic Region Supercomputing Center (ARSC) in Fairbanks, Alaska, USA. The Cell processor has attracted significant attention recently because of its large number of high performance processing cores. The fastest supercomputer at present, the IBM Roadrunner supercomputer installed at Los Alamos National Laboratory, utilizes 12,240 Cell processors and 6,912 AMD Opteron processors. The PetaVision project at that laboratory is modeling "1 billion visual neurons and trillions of synapses" [17] on this machine. Details of the project are not publicly available yet, however, this appears to be a neuron level model.

The main contributions of this work are:

1. A comparison of the performance of these models on two recent multicore architectures.
2. A preliminary study of multicore cluster implementation of the models.

Our results indicate that clusters of multicore processors are a promising platform for large scale implementations of hierarchical Bayesian cortical models. We found that the Cell processor (utilizing only six of its eight cores on the Playstation 3) can provide about twice the performance of an Intel quad-core Xeon processor: the Cell provided speedups of about 80 while the quad-core Xeon provided speedups of about 40 over serial implementations of the models (on the Cell's Power Processor Unit). The MPI based cluster implementations show that the performances of the models scale linearly until serial factors start limiting performances (based on Amdahl's law). A cluster of 24 Intel Xeon processors provided a speedup of 809 times for the HTM model, while 32 Intel Xeon processors provided a speedup of 783 for the Dean model (over their serial implementations). Use of further processors did not provide significant improvements in speedups for the model configurations tested.

Section II of this paper reviews the models examined and outlines the network structures to be utilized to evaluate the models. Section III presents a description of the two multicore architectures utilized. Section IV discusses the parallelization of the two models onto the multicore clusters. Sections V and VI describe the experimental setup and results of the model, while section VII concludes the paper.

II. MODELS EXAMINED

A. Hierarchical Temporal Memory

George and Hawkins developed an initial mathematical model [7] of the neocortex based on the framework described by Hawkins in [9]. Their model utilizes a hierarchical collection of nodes that employ Pearl's Bayesian belief propagation algorithm [16]. As shown in Fig. 1, each node has one parent and multiple children. Input data is fed into the bottom layer of nodes (level 1) after undergoing some preprocessing. After a set of feed-forward and feedback belief propagations between nodes in the network, a final belief is available at the top level node. This belief is a distribution that indicates the degree of similarity between the input and the different items the network has been trained to recognize. The model is trained in a supervised manner by presenting the training data multiple times to the bottom layer of nodes.

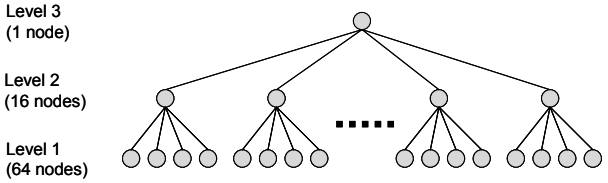

Fig. 1. Network structure of HTM model implemented.

The computational algorithm within each node of the model is identical and follows equations 1 through 6 below. The nodes send belief vectors to each other (π and λ) and utilize an internal probability matrix, Pxu (generated in an offline training phase).

$$\lambda_{product}[i] = \prod_{child} \lambda_{in}[child][i] \quad (1)$$

$$F_{xu}[j][k] = \pi_{in}[j] \times P_{xu}[j][k] \times \lambda_{product}[k] \quad (2)$$

$$m_{row}[j] = max(m_{row}[j], F_{xu}[j][k]) \quad (3)$$

$$m_{col}[k] = max(m_{col}[k], F_{xu}[j][k]) \quad (4)$$

$$\lambda_{out}[j] = m_{row}[j] / \pi_{in}[j] \quad (5)$$

$$\pi_{out}[child][k] = m_{col}[k] / \lambda_{in}[child][k] \quad (6)$$

B. Dean Model

Thomas Dean proposed a hierarchical Bayesian model [3][4] based on the work by Lee and Mumford [13] to model the invariant pattern recognition seen in the visual cortex. The example model examined in this study consists of a hierarchy of nodes with each node connected to a set of lower level nodes. There is a degree of overlap in the receptive field of the nodes in some of the layers (such as layer 2 in Fig. 2). Inputs to the layer 1 nodes are processed through a set of feed-forward and feedback processing steps through the network. A final inference based on this input is produced by the top layer node. The model is trained in a

supervised manner by presenting a set of training data to the bottom layer of nodes multiple times.

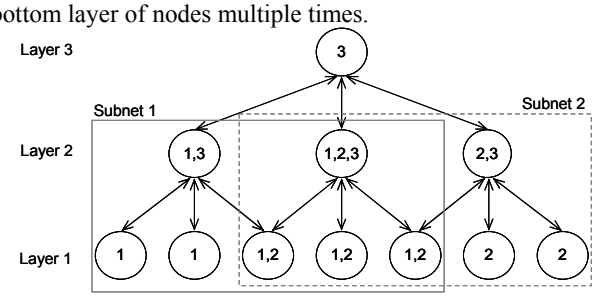

Fig. 2. A simple example of Thomas Dean's hierarchical Bayesian network model. This network can be divided into three subnets as shown. The nodes are numbered with the subnets they belong to.

Dean examined several approaches to process the hierarchical Bayesian network structure. The approach examined in this study is the one proposed by Dean where the network is decomposed into a set of subnets, and each subnet is evaluated individually. This decomposes the full tree into multiple subcomponents, thus simplifying the overall evaluation. A subnet can be defined as a node, its parents, and all the children of those parents in the same level as the original node [3], and as shown in Fig. 2, a node can belong to multiple subnets. Each subnet produces evidence to send to the next layer of subnets.

Algorithm 1. Processing in the Dean model

1. Preprocess inputs: find mixture of Gaussian for each 4×4 pixel patch
2. Repeat till output convergence:
3. Upward pass (from layers 1 to 3):
4. For all subnets in a layer:
5. Incorporate evidence from below (get image evidence or lambda values)
6. Process junction tree (collecting and distributing evidence)
7. Calculate evidence to send to upper layer of subnets (lambda values)
8. Downward pass (from layers 3 to 1):
9. For all subnets in a layer:
10. Incorporate evidence from above (get pi values)
11. Process junction tree (collecting and distributing evidence)
12. Calculate evidence to send to lower layer of subnets (pi values)
13. Read output

In order to process a subnet, it is first converted to its equivalent junction-tree representation. The Lauritzen and Spiegelhalter's junction-tree algorithm [12] is utilized for exact inference in the tree. Algorithm 1 lists the set of steps involved in the recognition phase of the Dean model.

III. ARCHITECTURES EXAMINED

The architectures examined in this study include the Intel quad-core Xeon E5345, and the STI Cell BE. The Intel Xeon E5345 processor contains four Intel Core based processing cores clocked at 2.33 GHz. The processor contains a 256 KB level one cache per core and an 8 MB shared level two cache. The processor can execute vector instructions (with four floating point operations) using the SSE3 instruction set. A cluster of dual socket Intel quad-core Xeon blades was utilized in this study (see Fig. 3 – further details are in Section V).

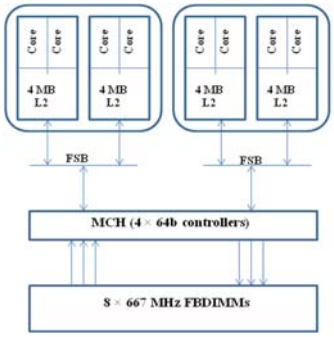

Fig. 3. Dual-socket, quad-core Intel Xeon E5345 (Clovertown) processor architecture

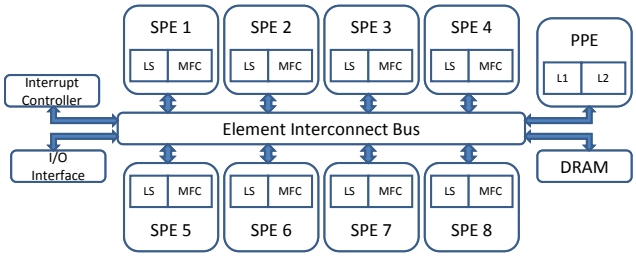

Fig. 4. STI Cell processor architecture

The Cell Broadband Engine developed by IBM, Sony, and Toshiba [8] is a multicore processor that heavily exploits vector parallelism. The current generation of the IBM Cell processor consists of nine processing cores: a PowerPC based Power Processor Unit (PPU) and eight Synergistic Processing Units (SPU). Fig. 4 shows the architecture diagram of this processor. The processor operates at 3.2 GHz. Each SPU is capable of processing up to four instructions in parallel each cycle (eight, if considering fused multiply-add instructions). The processing cores in the Cell utilize in-order execution with no branch prediction. This simplified hardware design means that several software level optimizations are necessary to achieve high performance on the SPUs (these are generally not needed on traditional processors, such as the Intel Xeon). The optimizations include use of vectorization, reducing the frequency of branch instructions through loop unrolling and function in-lining, and explicit memory optimizations. Instead of a processor controlled data cache, each SPU contains a programmer controlled local store to explicitly optimize memory operations. This enables several memory level optimizations not possible on most high performance processors. Since high compute-to-I/O ratios are needed

to achieve the full potential of the Cell processor [6], the programmer controlled memory stores are especially important. The Cell based Playstation 3 platform was utilized in this study.

IV. PARALLELIZATION OF MODELS

A. HTM Model

All the nodes in a particular layer are independent of each other and can therefore be evaluated in parallel. Therefore in this study, the HTM network was parallelized at two levels. In the clustered implementation, the nodes at the level 2 layer distributed to the different machines in the cluster. Each machine evaluates the level 2 nodes assigned to it, along with the level 1 nodes beneath the level 2 nodes. Every processor had a copy of the Pxu matrices it needed. MPI communication was needed to allow layer 2 nodes to communicate with the root node and to send the input image information to all the machines. On each processor, parallelization was done by assigning groups of nodes in a particular layer to separate processing cores. All computations in equations 1 through 6 were element-by-element matrix multiplies and divide, hence in order to accelerate the computations, the matrix values were converted into logarithmic form so that more expensive multiplies and divides could be replaced by less time consuming additions and subtractions. Details of the processor level optimizations on the Cell platform are presented in [18].

B. Dean Model

In case of the Dean model, a similar set of processing takes place. The threads are assigned a set of subnets or cliques depending on the level of parallelism implemented. Each thread then brings in the clique and node potentials needed along with any necessary subnet input beliefs. The outputs of a thread are the updated potentials and any subnet output beliefs generated.

For the subnet based parallelization approach, the three steps in each pass (shown in algorithm 1) are carried out serially for each subnet on a single core. Thus all of the equations related to a subnet are evaluated on a single core. In the clique based parallelization approach, all the cliques in a subnet are distributed across the cores available. Thus equations related to each clique are evaluated on an individual core.

In the clustered implementation, the distribution of the computations was carried out in a two step approach. In the first step, subnets were distributed in a round robin manner so that each machine had the same number of subnets to evaluate. MPI communication was needed to: 1) send the input image information to all the machines, 2) allow subnets to send beliefs to subnets above and below them in the hierarchy, and 3) allow cliques to communicate with each other in case of subnets that were split across multiple machines.

V. EXPERIMENTAL SETUP

Two hardware platforms were utilized in this study, one was Intel Xeon based, and the other was STI Cell based. The Intel Xeon platform utilized was the Palmetto Cluster at Clemson University. This system consists of about 257 blades, each containing two quad-core Intel Xeon processors running at 2.33 GHz (model E5345), and having 12 GB of DRAM. This cluster ran the CentOS 5 operating system. The STI Cell platform utilized was a cluster of nine Sony Playstation 3s at the Arctic Region Supercomputing Center (ARSC). The Playstation 3 has one Cell processor, on which six of the eight SPUs are available for use, and contains 256 MB of DRAM. This platform was running Fedora Core 9 with IBM Cell SDK 3.1. All the programs were compiled with -O3 optimizations using gcc. Since one of the nine Playstation 3s at the ARSC cluster was acting as a head node, the remaining eight Playstation 3s were used in the MPI study. Both clusters used MPICH2. The parameters of the networks implemented for each model are shown in Tables I and II. These networks were tested on the clusters while varying numbers of machines used in each cluster.

Table I. HTM model configurations evaluated

Network input size	32×32	48×48	64×64	80×80	96×96
Total Nodes	81	181	321	501	721
Layer 3 nodes	1	1	1	1	1
Layer 2 nodes	16	36	64	100	144
Layer 1 nodes	64	144	256	400	576

Table II. Dean model configurations evaluated

Network input size		28×28	36×36	40×40	52×52
Nodes	Total	59	98	110	186
	Layer 3	1	1	1	1
	Layer 2	9	16	9	16
	Layer 1	49	81	100	169
Subnets	Total	6	11	6	11
	Layer 3	1	1	1	1
	Layer 2	1	1	1	1
	Layer 1	4	9	4	9

VI. RESULTS

Fig. 5 presents the results of performance of the two models on the Xeon quad-core platform (with four and eight threads) and the STI Cell platform. The performance of the Xeon blade with four threads can be approximated to the performance of a single quad-core Xeon processor. The results indicate that the Cell processor running six threads provides about twice the throughput of the Xeon platform running four threads for the model configurations examined. Additionally, as the number of nodes is increased in both models, the Xeon eight thread performance approaches twice the Xeon four thread performance. This is likely due to the smaller versions of the models not having enough parallelism.

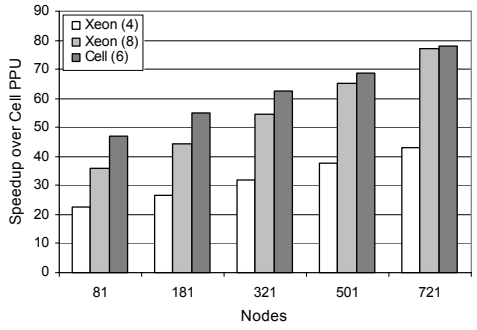

(a)

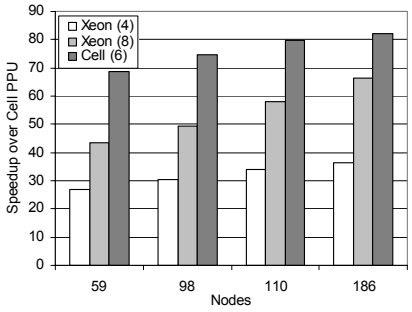

(b)

Fig. 5. Speedup over the Cell PPU for the (a) HTM, and (b) Dean models.

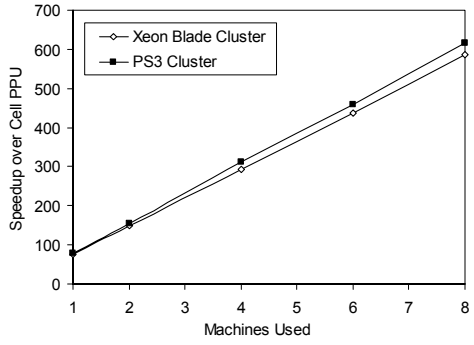

(a)

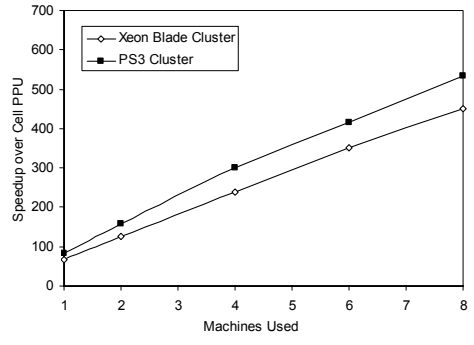

(b)

Fig. 6. Performance scaling of the MPI based implementations of the largest models examined.

Fig. 6 shows performance scaling of the MPI implementation of each model. Two clusters consisting of Playstation 3s and Xeon blades were utilized with all the cores on each machine being used. The largest network for each model was implemented (721 nodes for HTM and 186 nodes for Dean). The performance of both models scaled with the increase in the number of machines used. As expected from the Cell versus Xeon eight thread performance in Fig. 5, the Xeon cluster provided a lower speedup for the Dean model compared to the Cell cluster.

These results are quite significant, given the cost of each platform. Quad-core Xeon blades typically cost several times more than the Sony Playstation 3 (the latter currently sells for about $400 in the US). Additionally, each of the blades examined in this study contains two Xeon quad-core processors. Thus for developing large scale cortical simulations using column-level models, the Cell processor provides a more attractive platform.

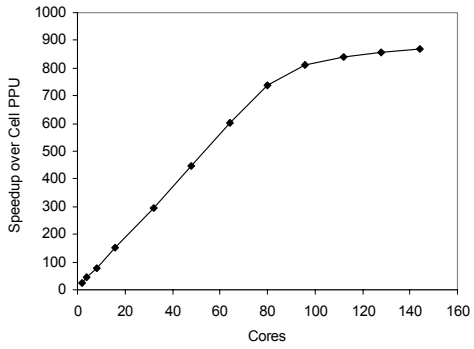

(a)

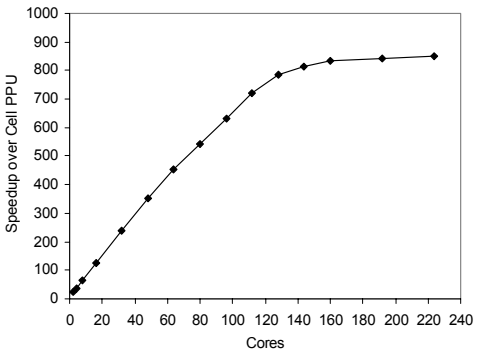

(b)

Fig. 7. Scaling the (a) HTM and (b) Dean models on a cluster of Xeon processors.

Since the Playstation 3 cluster utilized only had eight machines that could be utilized, the models were implemented on up to eight machines in Fig. 6. The Xeon cluster however had more machines available. Thus both models were scaled up on this cluster to the maximum number of cores they could be implemented on. In case of the HTM model, the maximum number of cores is given by the number of level two nodes (144 nodes for the model implemented). This is because each level two node and its four corresponding level 1 children are assigned to the same core. For the Dean model, the maximum number of cores is the total number of cliques in the level 1 subnet (225 for the model implemented).

Fig. 7 presents the results of the MPI based implementation on the Xeon cluster. It is seen that the HTM model performance scales up linearly with the number of cores until about 96 cores. At this point the runtime of the root node and the time for MPI communication between the level two nodes and the root node become a limiting factor, thus restraining the speedup (based on Amdahl's Law). The Dean model continues to scale almost linearly in performance until about 128 cores. There are 162 independent cliques in the level 1 subnets – thus adding more cores beyond this number provides limited performance gains.

VII. CONCLUSION

This paper presented the parallelization of two recent hierarchical Bayesian cortical column models on two multicore platforms. Additionally MPI based scaling of the models on two computing clusters were also investigated. The results indicate that the STI Cell processor can provide significant performance gains over the Intel quad-core Xeon processor. The cluster implementations indicate that Cell based Playstation 3 is a highly cost effective platform for developing large clusters to implement the models on the biological scale. The MPI based implementations on the Xeon cluster scaled well until serial components in the codes started to dominate the overall runtime and thus limit speedup (based on Amhdal's Law). For the models examined, these limits were reached at 96 and 128 cores (24 and 32 quad-core Xeon processors) for the HTM and Dean models respectively.

One of the limiting factors of the Playstation 3 over the Intel Xeon blade investigated is that it has significantly less system memory available. Although the smaller networks implemented did not run into the limits of this memory, it is possible that larger networks with more complex nodes could. As future work, we plan to investigate the use of the video memory on the platform to partially alleviate this issue. Possible areas of future work would be to: 1) develop mathematical models of performance scaling and performance limits on similar multicore clusters, 2) examine the parallelization of the training phase of the models, and 3) examine the applications of the large scale versions of these models to various domains (such as bioinformatics and security). Additionally, we plan to investigate the scaling of these models on the cluster of 336 Playstation 3s presented in [19].

ACKNOWLEDGEMENTS

This work is supported by an NSF CAREER Award and grants from the US Air Force. This work was also supported in part by a grant of computer time from the Arctic Region Supercomputing Center.

REFERENCES

[1] R. Ananthanarayan, D. Modha, "Anatomy of a cortical simulator", Proceedings of ACM/IEEE conference on Supercomputing, 2007.

[2] J. A. Anderson, "Arithmetic on a parallel computer: Perception versus logic," Brain and Mind, 4, 169–188, 2003.

[3] T. Dean, "A Computational Model of the Cerebral Cortex," Proceedings of the Twentieth National Conference on Artificial Intelligence (AAAI-05): 938-943, 2005.

[4] T. Dean, "Scalable inference in hierarchical generative models," Ninth International Symposium on Artificial Intelligence and Mathematics, 2006.

[5] T. Dean, "Learning invariant features using inertial priors," Annals of Mathematics and Artificial Intelligence, 47(3-4), 223–250, Aug. 2006.

[6] A. Felch, J. Moorkanikara-Nageswaran, A. Chandrashekar, J. Furlong, N. Dutt, A. Nicolau, A. Veidenbaum, R. H. Granger, "Accelerating Brain Circuit Simulations of Object Recognition with a Sony PlayStation 3," Proceedings of the International Workshop on Innovative Architectures, 2007.

[7] D. George and J. Hawkins, "A Hierarchical Bayesian Model of Invariant Pattern Recognition in the Visual Cortex," International Joint Conference on Neural Networks (IJCNN 2005), 2005.

[8] M. Gschwind, H. P. Hofstee, B. Flachs, M. Hopkins, Y. Watanabe, T. Yamazaki, "Synergistic Processing in Cell's Multicore Architecture," IEEE Micro, 26(2), 10–24, Mar. 2006.

[9] J. Hawkins and S. Blakeslee, "On Intelligence," Times Books, Henry Holt and Company, New York, NY 10011, Sept. 2004.

[10] J. Hawkins, D. George, "Hierarchical Temporal Memory: Concepts, Theory and Terminology", Numenta, http://www.numenta.com/Numenta_HTM_Concepts.pdf , 2006.

[11] C. Johansson, A. Lansner, "Towards Cortex Sized Artificial Neural Systems," Neural Networks, 20(1): 48-61, 2007.

[12] S. Lauritzen, D. Spiegelhalter, "Local computations with probabilities on graphical structures and their application to expert systems," Journal of the Royal Statistical Society, 50(2):157–194, 1988.

[13] T. S. Lee and D. Mumford, "Hierarchical bayesian inference in the visual cortex," Journal of the Optical Society of America A, 2(7), 1434–1448, 2003.

[14] H. Markram, "The Blue Brain Project," Nature Reviews Neuroscience, 7, 153–160, 2006.

[15] V. Mountcastle, "Introduction to the special issue on computation in cortical columns," Cerebral Cortex, 13(1):2–4, 2003.

[16] J. Pearl, "Probabilistic Reasoning in Intelligent Systems," Networks of Plausible Inference, Morgan Kaufmann, San Francisco, CA, 1988.

[17] J. Rickman, "Roadrunner supercomputer puts research at a new scale," Jun. 2008, http://www.lanl.gov/news/index.php/fuseaction/home.story/story_id/13602.

[18] T. Taha, P. Yalamanchili, M. Bhuyian, R. Jalasutram, and S. K. Mohan, "Parallelizing Two Classes of Neuromorhpic Models on the Cell Processor", International Joint Conference on Neural Networks (IJCNN), 2009.

[19] R. Linderman, "Early experiences with algorithm optimizations on clusters of playstation 3's," DoD HPCMP Users Group Conference, Jul. 2008.

[20] R. Zemel, "Cortical belief networks," in Hecht-Neilsen, R., ed., Theories of the Cerebral Cortex, New York, NY: Springer-Verlag, 2000.

Proceedings of 2009 12th International Conference on Computer and Information Technology (ICCIT 2009)
21-23 December, 2009, Dhaka, Bangladesh

On the Fast Computation of Decimal Logarithm

Ramin Tajallipour, Daniel Teng, Seok-Bum Ko, and Khan Wahid
Dept. of Electrical and Computer Engineering, University of Saskatchewan, Saskatoon, Saskatchewan, Canada
ramin.tajallipour@usask.ca, khan.wahid@usask.ca

Abstract

The paper presents a new and fast algorithm to efficiently compute radix-10 logarithm of a decimal number. The algorithm uses 32-bit floating-point arithmetic, and is based on a digit-by-digit iterative computation that does not require look-up tables, curve fitting, decimal-binary conversion, or division operations; the number of iterations depends on the user defined precision. The algorithm produces error-free (infinite precision) results up to 7 decimal digits. A numerical example is shown for the purpose of illustration. The accuracy is analyzed for several decimal digits showing compliance with the IEEE 754-2008 standard. When implemented on to the Xilinx VirtexII FPGA, the architecture costs only 1,053 logic cells, runs at a maximum frequency of 44 MHz, and consumes 79 mW of power.

Keywords: Decimal logarithm, radix-10 converter, floating point arithmetic, iterative computation, IEEE754-2008.

I. INTRODUCTION

In all computer systems, elementary functions play vital role - the logarithm and exponential operations are among those functions that have become very useful in many applications such as, financial analysis, tax calculation, internet based applications, and ecommerce [1], where these operations are performed to avoid hardware expensive multiplication and division operations. In the past, several hardware-efficient methods have been proposed for computing the base-2 logarithm of binary numbers [4][5][11]-[16]. However, after the inclusion of decimal floating point (FP) operation in the latest IEEE754-2008 standard [6], more researchers have been developing algorithms and architectures to efficiently compute decimal logarithms [7][17], as well as other decimal FP arithmetic units such as, exponentiation, trigonometric operations, etc.

There are other applications which require the direct computation of decimal (or radix-10) logarithm, such as, to measure the pH in chemistry, the earthquake intensity in Richter scale, the optical density in spectrometry and optics, the brightness of stars in astronomy, etc. [2]. The decimal encoded architecture has been implemented in IBM's recent POWER6 microprocessor [3]. Moreover, the base-10 logarithm is widely used in computing the ratio of voltage and power levels (called *bel*) in telecommunications, electronics and acoustics.

In most radix-10 logarithmic converters, the decimal input is first converted to binary followed by base-2 logarithm computation; after completion, the results are converted back to decimal radix – these back and forth conversions of bases introduce errors on the system. A generalized iterative algorithm to compute base-k logarithm has been presented in [8]; however, the division operation in that work yields erroneous computation. Moreover, the use of lookup tables and the lack of user control on the number of iteration make this algorithm very inefficient for hardware implementation.

In this paper, a new method for decimal logarithm (log, in short) computation is presented. The algorithm uses 32-bit floating-point arithmetic, and is based on a digit-by-digit iterative computation that does not require error correction circuitry, look-up tables, curve fitting, or division operations. The number of iterations of the log converter depends on the user defined precision. The performance analysis shows that the algorithm produces error-free computation for an internal precision width of 6 digits (24-bit) or more. The architecture is developed using 32-bit binary coded decimal (BCD) representation. The hardware implementation of the logarithmic converter on the Xilinx FPGA has also been presented.

II. BACKGROUND

The general form of any positive number, *L* can be expressed as:

$$\begin{aligned} L &= \sum_{i=-\infty}^{+\infty} C_i R^i \\ &= \ldots + C_2 R^2 + C_1 R^1 + C_0 R^0 + C_{-1} R^{-1} + C_{-2} R^{-2} + \ldots \end{aligned} \quad (1)$$

Where, *R* is the numerical base, and C_i is the coefficient for the i^{th} power of that base, ranging from 0 to $R-1$. For decimal base, *R* equals to 10.

According to the definition, the logarithm of any decimal number, *P* can be expressed as shown below:

$$L = \log_B P, \; P > 0 \quad (2)$$

Where, *B* is the log radix. Plugging (1) into (2) gives the following:

$$P = B^L = B^{\sum_{i=-\infty}^{+\infty} C_i R^i} \quad (3)$$

978-1-4244-6283-4/09/$26.00 ©2009 IEEE

For decimal number system, (3) leads to (4):

$$P = 10^{\sum_{i=-\infty}^{+\infty} C_i \times 10^i} \tag{4}$$

Now, (4) can be further expanded as shown below:

$$\begin{aligned} P = &...\times 10^{C_i \times 10^i} \times 10^{C_{i-1} \times 10^{i-1}} \times ... \times 10^{C_1 \times 10^1} \times 10^{C_0 \times 10^0} \\ &\times 10^{C_{-1} \times 10^{-1}} \times 10^{C_{-2} \times 10^{-2}} \times ... \end{aligned} \tag{5}$$

Taking the radix-10 log of (5) results in the following (6):

$$\begin{aligned} log_{10} P = &... + C_i \times 10^i + C_{i-1} \times 10^{i-1} ... + C_1 \times 10^1 \\ &+ C_0 \times 10^0 + C_{-1} \times 10^{-1} + C_{-2} \times 10^{-2} ... \end{aligned} \tag{6}$$

For simplicity, these coefficients of the final log result can be divided into two categories: integer (called "character": $..., C_i, C_{i-1}, ..., C_1, C_0$) and fraction (called "mantissa": $C_{-1}, C_{-2}, C_{-3}, ...$). In the following section, we describe the algorithm to evaluate these coefficients.

III. ALGORITHM FOR DECIMAL LOG

In order to calculate the log of a decimal positive number, *P*, as shown in (6), we first need to compute the upper limit for *i*, called $i_{\max}$, which is the number of mantissa digits in the final answer, set by the user.

Now, in order to perform the initial range reduction, let us define the range of *P:*

$$10^a \le P < 10^b, \; P > 1 \tag{7}$$

Where, the exponents *a* is the number of integers in $P - 1$ and *b* is the number of integers in P. By taking log at the left-hand side of (7), we find:

$$a \le \log_{10} P = L \tag{8}$$

Here, *a* is the character of *L*. Therefore, (8) can be expressed as shown below:

$$\log_{10} P = a + C_{-1} \times 10^{-1} + C_{-2} \times 10^{-2} + ... \tag{9}$$

Therefore,

$$P = 10^a \times 10^{C_{-1} \times 10^{-1}} \times 10^{\sum_{i=-\infty}^{-2} C_i \times 10^i} \tag{10}$$

Thus, after reducing the range, we store the input into a temporary variable, A, where $1 < A < 10$:

$$A = \frac{P}{10^a} = 10^{C_{-1} \times 10^{-1}} \times 10^{\sum_{i=-\infty}^{-2} C_i \times 10^i} \tag{11}$$

This division (by 10) operation can be easily implemented by right shifting the input digits. In order to determine the fractional parts (e.g., $C_{-1}, C_{-2}, C_{-3}, ...$), we follow the expression shown below:

$$\begin{aligned} A^{10} &= (10^{C_{-1} \times 10^{-1}} \times 10^{\sum_{i=-\infty}^{-2} C_i \times 10^i})^{10} \\ &= 10^{C_{-1}} \times 10^{\sum_{i=-\infty}^{-1} C_{i-1} \times 10^i} \end{aligned} \tag{12}$$

Then, the value of the first mantissa coefficient, C_{-1} can be computed by simply counting the number of integers in A^{10}. The temporary value stored in A^{10} undergoes power range reduction and is accumulated back in *A*. The process continues for the remaining mantissa coefficients until the number of iteration reaches $i_{\max}$, set earlier by the user.

For cases where the input ranges between 0 and 1, the log will produce negative result. Interestingly, the proposed algorithm is capable of handing such cases; the number is then converted to the scientific notation as shown below:

$$P = a \times 10^b, \text{ where } a > 1, \;\; b < 0 \tag{13}$$

Taking radix-10 log of both sides in (13) leads to the following (14):

$$L = \log_{10} P = -|b| + \log_{10} a \tag{14}$$

The algorithm of the digit-by-digit computation is illustrated in Fig. 1.

A. EXAMPLE

In order to better illustrate the algorithm, we present one example:

Determine the logarithm of decimal number, P = 124.23 up to three fractional digits.

The computation steps are as follows:

- Here the user sets the number of fractional digits; so, $i_{\max} = 3$; hence, the computation process will continue up to the computation of C_{-3}
- The number of integer in *P*: $N = 3$; hence, $C_0 = (3-1) = 2$
- Right shift the digits of *P* by two digits: $A \leftarrow (P >> 2) = 1.2423$
- Compute power-10 of *A* and accumulate the result: $A \leftarrow A^{10} = (1.2423)^{10} = 8.75517$
- Compute the number of integers in *A*: $N = 1$; hence, $C_{-1} = (1-1) = 0$
- Right shift the digits of *A* by zero digits: $A \leftarrow (8.75517 >> 0) = 8.75517$

- Compute power-10 of A and accumulate the result: $A \leftarrow A^{10} = (8.75517)^{10} = 2646341164$
- Compute the number of integers in A: $N = 10$; hence, $C_{-2} = (10-1) = 9$
- Right shift the digits of A by nine digits: $A \leftarrow (2646341164 >> 9) = 2.646341164$
- Compute power-10 of A and accumulate the result: $A \leftarrow A^{10} = (2.646341164)^{10} = 16844.50772$
- Once again, compute the number of integers in A: $N = 5$; hence, $C_{-3} = (5-1) = 4$
- The iteration stops, and the final answer is: $L = 2.094$

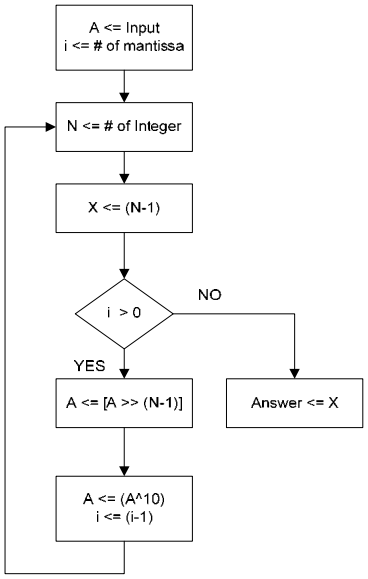

Fig. 1. Algorithm for the computation of decimal logarithm

Thus, it can be seen that the algorithm does not require any lookup tables, FP division operations, or error correction circuitry. The power-10 operation may incur some errors; however, it is shown in the next section (Fig. 4) that for an internal digit-width of 6 or higher, the algorithm produces error-free results. For the proposed implementation, a decimal precision of 10-digit has been used.

IV. HARDWARE IMPLEMENTATION

The architecture of the radix-10 log converter is shown in Fig. 2. The converter accepts two inputs: a 7-digit decimal number (P, in BCD) with the decimal point (inputted as hex 10) and the desired number of digits after the decimal radix point (i, fractions) of the log result. Depending on the user's selection of i, a counter is set which defines the number of iterations. The converter may take up to 40 clock cycles to output one fraction decimal digit.

The architecture is developed using unsigned BCD representation with an internal precision of 10 digits (40-bit binary). The DP (decimal point) separator module separates the decimal point and passed the unsigned magnitude to the temporary register, A. At the next clock, A is passed through the integer detector (ID) module to determine the number of integers, which is the first digit (or coefficient) of the final log answer. The shift operation to be performed on A is achieved at the same clock cycle by simply updating the DP locator which tracks the position of the decimal point. In next clock cycle, the power-10 operation is performed, and the intermittent results are passed to the ID block for integer number detection which is the second digit (or coefficient) of the final answer. The use of ID module is controlled by the controller through a 2x1 multiplexer. The process continues until the counter reaches to zero, when the controller stops the computation.

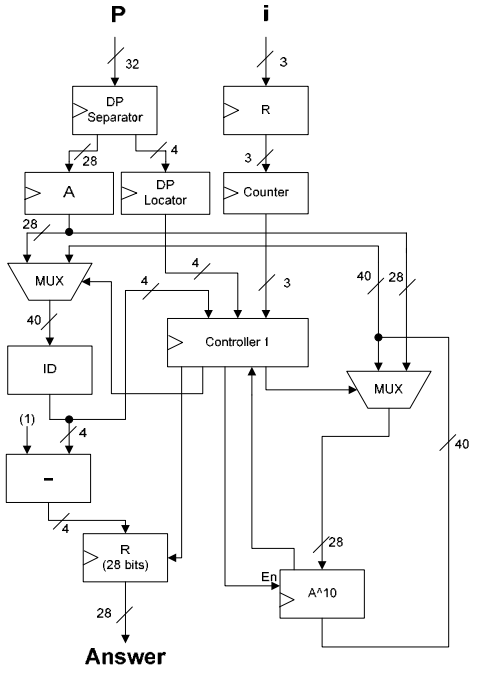

Fig. 2. Hardware architecture of the logarithmic converter

The architecture of the power-10 module is shown in Fig. 3. It is a key unit of the log converter and the accuracy of the final result greatly depends on its efficient implementation. Several efficient methods for decimal multiplication have been proposed in the past [9][10]. Here, the BCD-based multiplication algorithm as described in [9] is chosen for its low latency. The architecture to perform power-10 is based on successive squarer algorithm that takes as many as 10 clock cycles to complete ($A^2 \leftarrow A$, A is the 28-bit long intermittent input). The process is repeated three times to compute A^8, which is then multiplied by A^2 to compute A^{10} in the

next round. In each step of the computation, the most significant 10 digits are retained and passed to the next step. The controller tracks the position of the decimal point after each step and updates the DP locator.

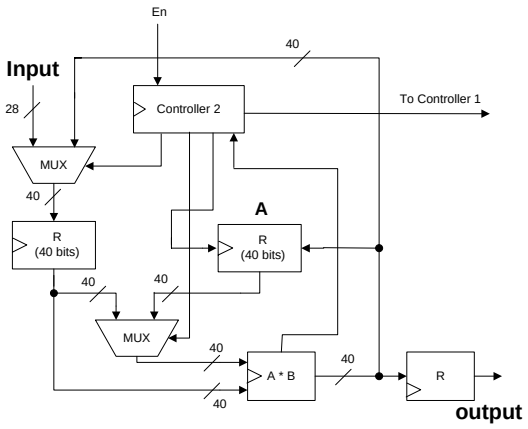

Fig. 3. Architecture of the Power-10 module

Fig. 4 shows the error incurred for various precision (number of digits) taken for the power-10 computation. It can be seen from the curve that for a precision of 6 digits of more, the algorithm produces error-free results. However, a key part of the proposed log algorithm is to count the number of integers before the decimal point to evaluate the coefficients, C_i (which may take any value between 0 and 9); hence, we retain the most significant 10 decimal digits (40-bit binary) that guarantees a lossless log computation.

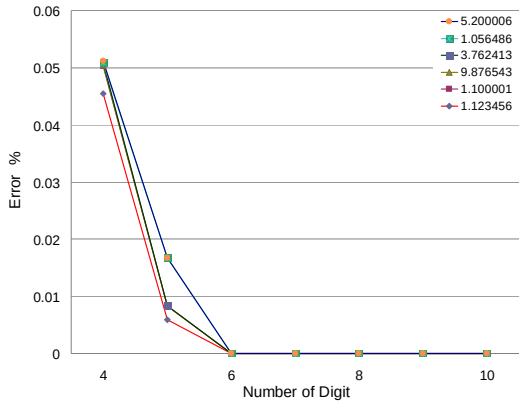

Fig. 4. Computation errors for different digit precision

The architecture of the log converter has been prototyped using Verilog onto Xilinx VirtexII FPGA (xc2v1000-6). The synthesized results show that the architecture costs 1,053 logic cells and 436 registers, and runs at a frequency of 44 MHz consuming 79 mW of power.

V. PERFORMANCE EVALUATION

Table I compares the results of the proposed log converter with other implementations. [7] and [17] present two decimal log converters which are based on curve fitting and digital recurrence algorithms respectively. Due to the use of LUT (i.e., ROM mapping), these two designs run a bit faster but cost more hardware resources and consume more power compared to our design.

Moreover, the proposed design outperforms other binary log designs [12][13] by a far margin. Note that, the proposed algorithm produces an error-free output for 32-bit precision. The power-10 module limits the operation frequency of our design; however, by using an efficient power-10 algorithm, the overall frequency of the converter can be vastly improved. The proposed architecture is scalable and can easily be extended for decimal64 and decimal128 formats, as defined in the IEEE 754-2008 standard [6].

Table I FPGA implementation of the decimal log converter

	Base	Scheme	Logic cells	Frequency (MHz)	Power (mW)
Detrey et al. [12]	2	ROM based	1,112	14.3	x
Detrey et al. [13]	2	ROM based	1,254	17.8	x
Dong-dong et al.[7]	10	Curve fitting	1,913	50.9	108
Dong-dong et al.[17]	10	Digit recurrence	2,842	47.7	x
Proposed	10	Iterative	1,053	44	79

X = not reported

VI. CONCLUSION

The paper presents a new and fast algorithm and efficient implementation for computing decimal logarithm using 32-bit floating point arithmetic that complies with the IEEE754-2008 standard. The algorithm is based on a digit-by-digit iterative computation that does not require look-up tables, curve fitting, decimal-binary conversion, or division algorithms, hence, can be easily implemented on software or hardware. The final logarithmic output is lossless where no correction circuitry is required; the hardware is scalable – can be extended to higher number of bits. Future research is directed towards the VLSI implementation of the algorithm.

VII. ACKNOWLEDGEMENT

The authors would like to acknowledge the Natural Science and Engineering Research Council of Canada (NSERC) for its support to this research work.

REFERENCES

[1] M. F. Cowlishaw, “Decimal Floating-Point: Algorism for Computers,” Proc. of the IEEE Symposium on Computer Arithmetic, pp. 104-111, 2003.

[2] http://en.wikipedia.org/wiki/Logarithm

[3] “IBM Power6”, IBM Corporation, May 2007.

[4] J.N. Mitchell, “Computer Multiplication and Division Using Binary Logarithms”, IRE Trans. Electron. Computer, pp. 512-517, 1962.

[5] D. Kostopoulos, “An Algorithm for the Computation of Binary Logarithms”, IEEE Trans. on Computers, vol. 40, no. 11, pp. 1267-1270, 1991.

[6] The IEEE Standard for Floating-Point Arithmetic (IEEE 754 2008).

[7] D. Chen, Y. Choi, Li Chen, D. Teng, K. Wahid, S. Ko, “A Novel Decimal-to-decimal Logarithmic Converter”, Proc. of the IEEE Symposium on Circuits and Systems, pp. 688-691, 2008.

[8] H. Lo and J. Chen, “A Hardwired Generalized Algorithm for Generating the Logarithm Base-k by Iteration,” IEEE Trans. Computer, vol. C-36, pp.1363 – 1367, 1987.

T. Lang and A. Nannarelli, “A Radix-10 Combinational Multiplier”, Proc. of the Asilomar Conference on Signals, Systems and Computers, pp. 313-317, 2006.

[9] H. C. Neto and M. P. Vestias, “Decimal Multiplier on FPGA Using Embedded Binary Multipliers”, Proc. of the International Conference on Field Programmable Logic and Applications, pp.197-202, 2008.

[10] M. Ercegovac, “Radix-16 Evaluation of Certain Elementary Functions”, IEEE Trans. on Computers, vol. C-22(6), pp. 561–566, 1973.

[11] J. Detrey, F. Dinechin, and X. Pujol, “Return of the Hardware Floating-Point Elementary Function”, Proc. of the 18th Arithmetic Conference, pp. 161-168, 2007.

[12] J. Detrey and F. de Dinechin, “A Parameterizable Floating-point Logarithm Operator for FPGAs”, Proc. of the 39th Asilomar Conference on Signals, Systems & Computers, pp. 1186-1190, 2005.

[13] P. T. P. Tang, “Table-driven Implementation of the Logarithm Function in IEEE Floating-point Arithmetic”, ACM Trans. on Mathematical Software, vol. 16(4), pp. 378 – 400, 1990.

[14] C. Wrathall and T. C. Chen, “Convergence Guarantee and Improvements for a Hardware Exponential and Logarithm Evaluation Scheme”, Proc. of the 4th IEEE Symposium on Computer Arithmetic, pp. 175–182, 1978.

[15] W. Wong and E. Goto, “Fast Hardware-based Algorithms for Elementary Function Computations using Rectangular Multipliers”, IEEE Trans. on Computers, vol. 43(3), pp. 278–294, 1994W.-K. Chen, *Linear Networks and Systems* (Book style).Belmont, CA: Wadsworth, 1993, pp. 123–135.

[16] Dongdong Chen, Yu Zhang, Younhee Choi, Moon Ho Lee, Seok-Bum Ko, “A 32-bit Decimal Floating-Point Logarithmic Converter,” Proceedings of the 19th IEEE Symposium on Computer Arithmetic, pp. 195-203, 2009.

Proceedings of 2009 12th International Conference on Computer and Information Technology (ICCIT 2009)
21-23 December, 2009, Dhaka, Bangladesh

Automated Fundamental Analysis for Stock Ranking and Growth Prediction

Ariful Islam, Hasib Zaman, Reaz Ahmed
Department of Computer Science and Engineering
Bangladesh University of Engineering and Technology, Dhaka-1000, Bangladesh
arif.tng@gmail.com, hasibcse04@gmail.com, reaz@cse.buet.ac.bd

Abstract

In this paper we present the Automated Ranking by Fundamental Analysis (ARFA), a new Fundamental Analysis (FA) tool developed for aiding the research of fundamental indicators. ARFA provides a flexible and easy to use yet powerful platform to create and test new fundamental indicators for analyzing and comparing fundamentals of the companies in a stock market. ARFAoffers a software interface for FA that is straight forward, easy to learn and at the same time exceptionally expressive without the need of any programming or customization.

In this work, we present a detailed description of ARFAs indicator creation platform with demonstration of its power by showing a number of well-known indicators written in ARFAs terminology. ARFA is intended for researcheras well as share market investors. It is web-based, free and open source. ARFA has a simple programming interface for future extensions of its terminology andability with easily pluggable modules.

Keywords: Automated ranking, Data Processor, Dynamic variable, Fundamental Analysis, Fundamental indicator, Parser .

I. INTRODUCTION

Fundamental analysis (FA) is the cornerstone of investing. FA of a business involves analyzing its financial statements and strength, its management and competitive advantages, and its competitors and markets. FA is performed on historical and present data, but with the goal of making financial forecasts. Fundamental investors look for stocks that are below their intrinsic value. FA is the examination of the underlying forces that affect the well being of the economy, investment sectors, and companies. This involves looking at revenues, expenses, assets, liabilities and other financial aspects of a company to gain insight on the company's future performance. To forecast future
stock prices, FA combines economic, industry and company analysis to derive a stocks current fair value and forecast future value. FA has less popularity than Technical Analysis (TA) as many people thinks FA is not suitable for short term investment and suitable analysis tools are not available to investors yet. But the
future prospect of a company can only be assesed by its financial fundamentals and the success of an investment depends highly on FA. Without FA an investment may suffer in the long run. There exists research on FA for long time and many mathematical models are derived but computer aided FA is not yet available to the investor.

For making FA easy to understand and user friendly we have developed ARFA. The basics of FA are examining some key ratios in business and developing an idea of the value of its stock. ARFA provides an open ground for investor and researcher to evaluate and compare the performance of new concept indicators as well as the existing ones. In order to provide this capability we have designed a recursive expression language in terms of commonly used company fundamental measure. To implement an indicator in ARFA one has to express the indicator in ARFA expression language. ARFA will then
output the result both in graphical and tabular format showing relative ranking of the companies. In ARFA, companies filtered by constraints like market sectors, market categories, company types etc. We believe that ARFA will assist the investors to test their ideas and to make profitable business decision.

The rest of this paper is organized as follows. Section 2 describes the overall system design. All Functional details and effect of using ARFA is presented in section 3. We have presented some related works in Section 4. Some future improvement and expansion of ARFA is given in Section 5 and finally we conclude in Section 6.

II. SYSTEM ANALYSIS AND DESIGN

In this section we present the overall system design. Figure 1 presents the use case diagram of the System.

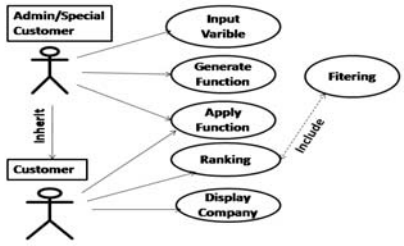

Fig.1 Usecase Diagram

978-1-4244-6283-4/09/$26.00 ©2009 IEEE

The functionality of these use case are as follows:

Input variable - Take variable as an input fromvariable list table.Two list is provided, one containing fundamental variables and other historical variables (see section III-B).
Generate function - Makes expression using input variables according to ARFA grammar (see section IIIA), output a new function and store it into function table.
Apply function - Show the list of available indicators or functions. selecting one, calculate function value from background data.
Ranking - Ranks companies or shares according to market catagory, sector, etc.
Display company - Show the ranked list to the customer or user of the system. (see example in section III-E)

Figure 2 presents the block diagram of System.

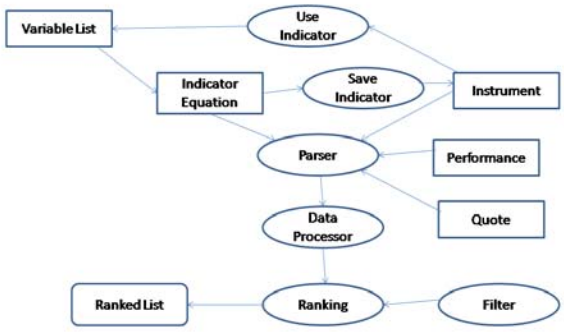

Fig.2 Block Diagram

ARFA produces the desired outcome representing the effect of a fundamental indicator. Three tables are provided: Performance, Instrument and Quote. *Performance* and *Quote* contains historical variable data, *Instrument* contains fundamental variable data. See details about variable list in section III-B. New variables can also be added in those tables. Sequence diagram of Figure 3 represents variable creation details.

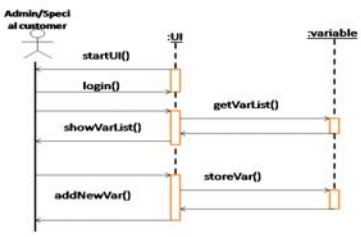

Fig.3 Sequence diagram –Variable Creation.

User writes an equation by using this variables.

Function name and its equation is stored in a new table named *indicator*. Sequence diagram of Figure 4 represents Function creation details.

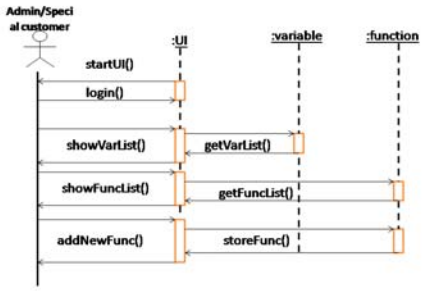

Fig.4 Sequence diagram-function creation

The new indicator data is added in *instrument* table and generates new variable to variable list. Details about indicator creation process is given in section III-C. Screen shot for adding new indicator is shown in Figure 5.

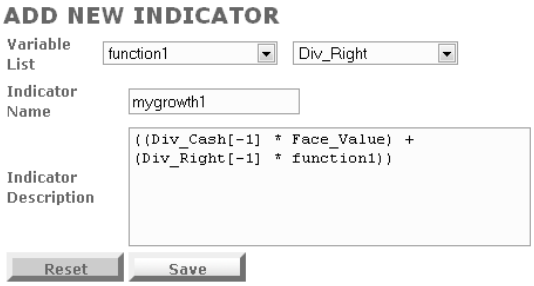

Fig.5 UI- Add new indicator.

A Parser then parses this expression and identifies the variables to be collected. We use the general equation parsing algorithom to find out the variables. Sequence diagram of how to use existing indicators to rank companies is given in Figure 6.

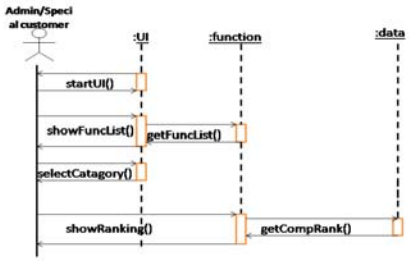

Fig.6 sequence diagram- ranking.

The Data processor subsequently collects the required data from current instrument table or from background tables like quote, performance.

Finally, the ranking algorithm process all this information and produces a ranked list (details in section III-D). Output filtering option is also available. An AI-based trading agent can use the data generated from ARFA, in conjunction with technical analysis and news, to produce automated buy or sell decisions.

We have used MySQL as database and both the Parser and the Data Processor are written in PHP.

III. FUNCTIONAL DESCRIPTION

A. Regular Expression Grammar

ARFA maintains the following grammar fragment:

Function → variable **operator** variable | *variable* operator num | variable
variable → **id** | **id** [**parameter**]

where the terminals **operator**, **id**, **num** and **parameter** generate sets of strings given by the following regular definitions:

letter→ [a – z A – Z]
digit → [0 – 9]
id → letter (letter |digit)*
digits → digit digit*
fraction → .digits | ε
num →digits fraction
operator → +| - | * | /
sign → +| -
parameter → sign* digits

B. Variables of System

ARFA uses two list of variables, one static and other dynamic. Static variables may be called as fundamental variables contained in *instrument* table. They have same value for every year. Some fundamental variables are – Market Capital, Share Capital, Face value, Market Lot, Num Security, Company Type, Last AGM Date, Reserve Surplus, Market Category etc.

Dynamic variables are historical variables contained in *performance* and *Quote* table. They have different values for different years. For example, EPS of current year is EPS[0], EPS of previous year EPS[-1], EPS of 2 years before current EPS[-2] etc. Some of historical variables are - EPS, Net Asset, Net Profit, PER, Div Bonus, Div Right, Div Cash, Dividend Yield, Diluted Net Asset, Diluted EPS etc. Quote table contains maximum close price (MaxCP), minimum close price (MinCP) and average close price (AvgCP).

C. Creating Various Indicators

ARFA gives the facility to create any new indicator. An example is given in Figure 5. A simple indicator of ARFA can be, (var1 + var2 / 2) - (var1 * var3)

For Example, Growth1 = (face value * cash div) + (avg price * stock div) + ((avg price - face value)* right share)

ARFA provides the facility to create various complex indicators. An indicator equation can have both static and dynamic variables. ARFA joins the current *instrument* table with available background tables *performance, quote* etc.

A complex indicator of ARFA can be,

(var1 + var[-1]) - (var[-1] - var[-2]) * 0.5

For example, function1 = (Share capital – Market Capital) / Net Asset[-1] + (EPS[-1] + EPS[0]) / 2

Another way to create complex indicators is to use multilevel indicators. Any output of an indicator in ARFA can be made available for use as an input in another indicator. This way the second indicator uses the output of the first indicator to produce its output.
That means, user can reuse his own indicators. The following indicator is possible.

function2 = (function1 * 2) + EPS[-2]

D. Ranking and Comparing Indicators Performance

New indicators can be used for Ranking. When user provides an indicator equation to ARFA, it is saved to *instrument* table as a new column. Next time, it is added to indicator list. ARFA gets function list from *indicator* table, one is selected. Filtering option such as market category, sector etc. is provided. ARFA gets company rank from processed data and ranked list is shown as output in both tabular and graphical form.

ARFA provides the facility of comparing various indicators performance on the same data. suppose, we want to compare between EPS and NAV. Then a ranked
list by EPS and another ranked list by NAV is produced.
ARFA measures performance of both and decides which
one is better.

E. Output Analysis

In this section ARFA output analysis is briefly described. Top 10 or Top N list can be produced easily by ARFA. Table I contains some top 10 lists generated by ARFA based on different indicators.

The summery table is shown in Table III.

TABLE I
TOP 10

Current	EPS	NAV	Net Prof	PER
ISLAMIBANK	ISLAMIBANK	ISLAMIBANK	TITASGAS	BSC
BEXIMCO	RENATA	1STICB	ISLAMIBANK	EASTRNLUB
BDTHAI	ABBANK	SONALIANSH	ABBANK	BEACHHATCH
ABBANK	1STICB	STYLECRAFT	PRIMEBANK	SAVAREFR
BLTC	DUTCHBANGL	MONNOJTX	SQURPHARM	KAY&QUE
ICB	APEXADELFT	RENATA	A	QSMDRYCELL
BXFISHERY	SQURPHARM	SQURPHARM	POWERGRID	HILLPLANT
RUPALIBANK	A	A	NBL	ICB1STNRB
PHARMACO	PHARMAID	DUTCHBANGL	SOUTHEASTB	GLAXOSMITH
LEGACYFOO	IFIC	BLTC	IFIC	UTTARABAN
T	AZADIPRIN	ABBANK	EXIMBANK	K

TABLE II
Current TOP 10

Current	Profit
ISLAMIBANK	0.927337382383485
BEXIMCO	0.858399993896484
BDTHAI	0.85248641872127
ABBANK	0.819056951810007
BLTC	0.814364640883978
ICB	0.796541611892001
BXFISHERY	0.793981481481482
RUPALIBANK	0.792667038898195
PHARMACO	0.792391304347826
LEGACYFOOT	0.791666663656331
Total	4.23547382939651

TABLE III
SUMMERY TABLE

Indicator	Common	Profit	Difference(%)
EPS	2	4.118	2.76
NAV	2	3.664	13.48
Net Prof	3	4.135	2.36
PER	0	3.675	13.22

Current column is based on percentage of

(MaxCP-MinCP)/MaxCP

where other columns are based on corresponding indicators. MaxCP means maximum close price and

MinCP means minimum close price. Current top 10 company with profit value is given in table II.

Profit = (*MaxCP-MinCP)/MaxCP*

Common means the number of common companies between *current* list and indicator based list. *Profit* column is calculated by the same way of table II.

Common means the number of common companies between *current* list and indicator based list. *Profit* column is calculated by the same way of table II.

Difference =
(*currentProfit - indicatorProfit) / currentProfit*

Current profit is found from last row of tableII. *Indicator profit* is found from *Profit* column of table III.

From table III we can see that, difference between current profit and indicator based profit is smallest for *Net Prof* and then for *EPS*. So EPS and Net Profit are better indicator than PER and NAV. Thus we can analysis any indicator's (existed or newly created) performance by ARFA system.

IV. RELATED WORK

Stock market prediction has always been one of the hottest topics in research, as well as a great challenge due to its complex and volatile nature. However, most of
the existing methods neglect the impact from fundamental analysis of stock market. A genetic programming based system is presented in [9] which specializes in taking some well known technical rules and adapting them to prediction problems. An evaluation of the performance of back propagation neural networks applied to the problem of predicting stock market prices can be found in [3]. Kim [7] has presented prediction mechanisms basedon support vector machines. In [2], a framework for a Multi-Agent System for Stock Trading is presented that addresses the issue of gathering and integrating diverse information sources with collaborating agents and providing decision-making for investors in the stock market. [11] presents a system that combines the information from both related news releases and technical indicators to enhance the predictability of the daily stock price trends. In [8] Least Squares Support Vector Machines are used for Stock Market Trend analysis. [6] finds Trading Patterns in Stock Market Data. [1] discussed about wireless investor. [10] discussed Trading With a Stock
Heuristic. A Multiagent Approach to Qlearning for Daily Stock Trading is described in [4]. Stock Trading Using RSPOP discussed in [5].

V. FUTURE RESEARCH

There exists various research sectors for extending the work presented in this paper. One of the major improvements can be to introduce Technical Analysis Tools like MACD (Moving Average Convergence-Divergence), RSI (Relative Strength Index) etc. as functions besides fundamental functions. Generally technical analysis is most effective in the short-term and less effective in the long-term, and fundamental analysis is effective for long- term investment decisions and less effective in the short-term. If Fundamental Analysis Tools can be joined with Technical Analysis tools, it will be strong enough to perform both analysis and thus give investors and traders flexibility to consider both short-term and longterm

VI. CONCLUSION

In this paper we presented a completely new tool for FA that help creating and experimenting new FA indicators. This web- based system is very expressive and provides complete support for wide range of indicators based on ratios used in FA. It also provides the framework for adding various indicators and using their out come in real life business decision making. It is in the early stage of development but still it is a powerful tool for Fundamental Analysis. If it is possible to combine FA with technical analysis then investor will highly be benefitted from this. In future we will find that this tool
is an important tool both to the researchers and investors
in business decision.

REFERENCES

[1] Peter Blakey. Wireless investor : Fundamental and technical analysis. *IEEE Microwave Magazine*,DECEMBER 2001.

[2] K. Liu Davis, D.N. and Y. Luo. A multi-agent framework for stock trading. Technical report, 16th IFIT World Computing Congress, Beijing, China, 2000.

[3] B. Freisleben. Stock market prediction with back propagation networks. In *Industrial and Engineering Applications of Artificial Intelligence and Expert System*, pages 451–460, Paderborn, Germany, June 1992. 5th International Conference.

[4] Member IEEE Jangmin O Jongwoo Lee Jae Won Lee, Jonghun Park and Euyseok Hong. A multiagent approach to q-learning for daily stock trading. *IEEE TRANSACTIONS ON SYSTEMS, MAN, AND CYBERNETICSPART A: SYSTEMS AND HUMANS*, 37(6), NOVEMBER 2007.

[5] IEEE Kai Keng Ang, Student Member and IEEE Chai Quek, Member. Stock trading using rspop: A novel rough set-based neuro-fuzzy approach. *IEEE TRANSACTIONS ON NEURAL NETWORKS*, 17(5), SEPTEMBER 2006.

[6] Stephen Barrass Keith V. Nesbitt. Finding trading patterns in stock market data. *IEEE Computer Graphics and Applications*, 2009.

[7] K. J. Kim. Financial time series forecasting using support vector machines. Technical report, Neurocomputing, 2003.

[8] Shouyang Wang Lean Yu, Huanhuan Chen and Kin Keung Lai. Evolving least squares support vector machines for stock market trend mining. *IEEE*

TRANSACTIONS ON EVOLUTIONARY COMPUTATION, 13(1), FEBRUARY 2009.

[9] Jin Li and Edward P.K. Tsang. Improving technical analysis predictions: An application of genetic programming. In *Proceedings of The 12th International Florida AI Research Society Conference*, pages 108–112, May 1-5 1999.

[10] Steven Hornik Russell L. Purvis William Leigh, Cheryl J. Frohlich and Tom L. Roberts. Trading with a stock chart heuristic. *IEEE TRANSACTIONS ON SYSTEMS, MAN, AND CYBERNETICSPART A: SYSTEMS AND HUMANS*, 38(1), JANUARY 2008.

[11] Arthur Hsu Yuzheng Zhai and Saman K Halgamuge. Combining news and technical indicators in daily stock price trends prediction. Masters thesis, University of Melbourne, Victoria, Australia, 2007.

Proceedings of 2009 12th International Conference on Computer and Information Technology (ICCIT 2009)
21-23 December, 2009, Dhaka, Bangladesh

Novel Objective Criteria for Perceptual Separation of Two Kinds of Distortion in Speech Enhancement Applications

Md. Jahangir Alam, Douglas O'Shaughnessy, Sid-Ahmed Selouani†
INRS-EMT, University of Quebec, Montreal QC, Canada
† University of Moncton, campus de shippigan, NB, Canada
alam@emt.inrs.ca, dougo@emt.inrs.ca, selouani@umcs.ca

Abstract

There is an increasing interest in the development of robust quantitative speech quality measures that correlate well with subjective measures. This paper presents two objective criteria-the Perceptual Signal to Audible Noise Ratio (PSANR) and the Perceptual Signal to Audible Distortion Ratio (PSADR), to characterize the two kinds of degradation (i.e., residual background noise, speech distortion or both) in speech enhancement applications. For performance evaluation of speech enhancement algorithms it is necessary to determine with accuracy the kind of degradation present in the enhanced signal. Experimental results for speech enhancement using different well-known approaches depict the usefulness of the proposed objective criteria.

Keywords: speech enhancement, masking threshold, objective quality measure, PSANDR.

I. INTRODUCTION

Quality assessment of the processed speech signal can be done using subjective listening tests or objective quality measures as shown in figure 1. Subjective listening tests such as Mean Opinion Score (MOS) or Degradation MOS (DMOS) provide perhaps the most reliable method for assessing speech quality. Subjective evaluation involves comparisons of original and processed speech signals by a group of listeners who are asked to rate the quality of speech signal along a pre-determined scale. These tests, however, can be time consuming, requiring in most cases access to the trained listeners. For these reasons, several researchers have investigated the possibility of devising objective, rather than subjective, measures of speech quality [5, 8-11].

The aim of the objective speech quality measures is to achieve high correlation with subjective speech quality measures such as Mean Opinion Score (MOS), or Degradation MOS (DMOS). An ideal objective speech quality measure would be able to assess the quality of the degraded or processed speech by simply observing the speech in question, without accessing the original speech. Much progress has been done in developing such an objective measure [5, 8-11]. Current objective measures are limited in that most require access to the original speech signal and some can only model the low-level processing (e.g., masking effects) of the auditory system. Yet, despite these limitations, some of these objective measures have been found to correlate well with subjective listening tests [11]. Objective speech quality measures can be classified according to the perceptual domain transformation module being used, and these are:

- Time domain measures
- Spectral domain measures and
- Perceptual domain measures

Perceptual domain measures are shown to have the best chance of predicting subjective quality of speech and other audio signals since they are based on the human auditory perception models.

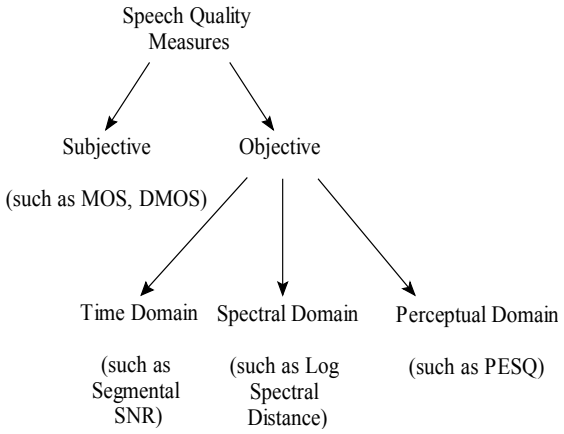

Figure 1. Classification of speech quality measures.

The common point of all objective criteria is their ability of evaluating speech quality using a single parameter which embeds all kind of degradations after any processing. Indeed, speech quality measures are basing their evaluation on both original and degraded speeches according to the following application

$$C: \begin{array}{l} \mathrm{E}^2 \to \mathbb{R} \\ (x, y) \to c \end{array}, \qquad (1)$$

where E denotes the time, frequency or perceptual domain, x and y denote the original speech and observed speech altered by noise or denoised speech after processing, respectively, and c is the score of the objective measure. Mathematically, C is not a bijection from E^2 to $\mathbb{R}$. It means that it is possible to find a signal y' which is perceptually different from y but has the same score than the one obtained with $\mathrm{y}\left(c(x, y) = c(x, y')\right)$.

The assessment of the denoised speech quality by means of two parameters permits to overcome the problem of non bijection of classic objective evaluation and to better characterize each kind of speech degradation.

Hence, instead of the application defined in (1), we develop a novel application from perceptual domain to $\mathbb{R}^2$

$$C: \quad \begin{aligned} \mathrm{E}^2 &\to \mathbb{R}^2 \\ (x, y) &\to (PSANR, PSADR) \end{aligned}, \tag{2}$$

where PSANR (Perceptual signal to audible noise ratio) and PSADR (Perceptual signal to audible distortion ratio) are two parameters related to the residual noise and the speech distortion, respectively. The definition of PSANR and PSADR is inspired from the SNR definition which is the ratio of signal energy to noise energy.

A masked signal is made inaudible by a masker if the masked signal magnitude is below the perceptual masking threshold MT. Residual noise and speech distortion can be audible or inaudible according to their position regarding the masking threshold. We propose to find decision rules to decide on the audibility of residual noise and speech distortion by using the masking threshold concept. If they are audible, the audibility rate will be quantified according to the proposed criterion.

This paper is organized as follows: Section 2 provides a description of the speech enhancement technique. In section 3, an overview of the proposed method is given. Performance evaluation is made in section 4 and in section 5 the paper is concluded.

II. SPEECH ENHANCEMENT METHOD

Basic speech enhancement methods involve estimating every frequency component of the clean speech spectrum $\hat{X}(m,k)$

$$\hat{X}(m,k) = H(m,k)Y(m,k), \tag{3}$$

where $m = 1, 2, ..., M$ is the frame index, $k = 1, 2, ..., K$ is the frequency bin index, M is the total number of frames and K is the frame length, $H(m,k)$ is the noise suppression filter chosen according to a suitable criterion, $Y(m,k)$ represent the short-time spectral components of the noisy signal. The error signal generated by this filter is

$$\begin{aligned} e(m,k) &= \hat{X}(m,k) - X(m,k) \\ &= \big(H(m,k) - 1\big) X(m,k) + H(m,k) D(m,k), \end{aligned} \tag{4}$$

where $D(m,k)$ denotes the noise power spectrum. The first term in equation (4) describes the speech distortion caused by the spectral weighting. The second term in the above equation is the residual noise distortion which is perceptually heard as background noise.

III. OVERVIEW OF THE PROPOSED METHOD

Figure 2 and Figure 3 depict the complete block diagram of our proposed method and block diagram to calculate the masking threshold, respectively. The following sections give a description of the proposed perceptual domain objective quality measure to quantify the two kinds of degradation, namely the residual noise and the speech distortion.

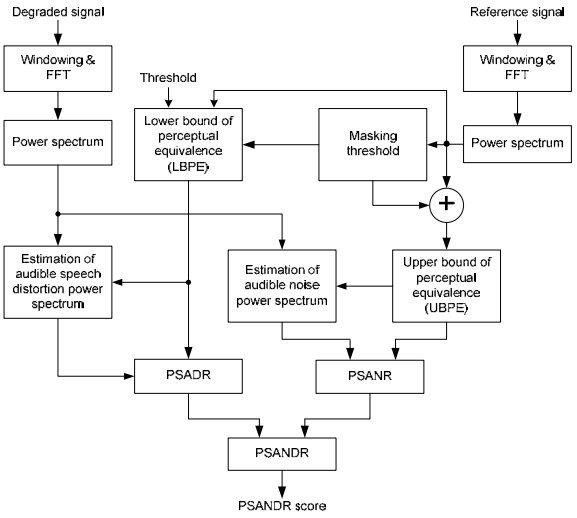

Figure 2. Block diagram of the PSANDR measure computation.

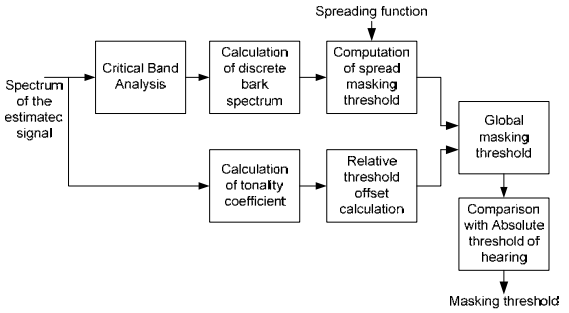

Figure 3. Block diagram for the calculation of the masking threshold

A. Computation of Masking Threshold (MT)

The masking threshold (MT) is obtained through modeling the frequency selectivity of the human auditory system and its masking properties. The estimation of the MT includes the preliminary estimation of the original clean speech, critical band analysis, the spread masking threshold, the relative threshold offset, the masking threshold normalization and comparison with the absolute threshold of hearing [7]. The steps involved in the computation of the MT are taken from the Johnston model [7] and is shown in figure 3.

B. Upper and Lower Bound of Perceptual Equivalence

According to MT definition, it is possible to add to the clean speech power spectrum, the MT curve so that the resulting signal (obtained by inverse FFT) has the same audible quality as the clean one. The resulting spectrum is called Upper Bound of Perceptual Equivalence (UBPE) and is defined as

$$UBPE(m,k) = \Gamma_x(m,k) + MT(m,k), \quad (5)$$

where $\Gamma_x(m,k)$ is the clean speech power spectrum. When some frequency components of the denoised speech are above UBPE, the resulting additive noise is heard. Thus, by analogy to UBPE, we propose to calculate a second curve which expresses the lower bound under which any attenuation of frequency components is heard as a distortion. We call it Lower Bound of Perceptual Equivalence (LBPE). To compute LBPE, we used the audible spectrum introduced in [12]. In such case, audible spectrum is calculated by considering the maximum between the clean speech spectrum and the masking threshold. When speech components are under MT, they are not heard and we can replace them by a chosen threshold $\sigma(m,k)$.

The proposed LBPE is defined as

$$LBPE(m,k) = \begin{cases} \Gamma_x(m,k) & \text{if } \Gamma_x(m,k) \geq MT(m,k) \\ \sigma(m,k) & \text{otherwise} \end{cases}. \quad (6)$$

The choice of $\sigma(m,k)$ obeys only one condition $\sigma(m,k) < MT(m,k)$. In this thesis we choose it equal to 0 dB.

Using UBPE and LBPE, we can define three regions characterizing the perceptual quantity of denoised speech: frequency components between UBPE and LBPE are perceptually equivalent to the original speech components, frequency components above UBPE contain a background noise and frequency components under LBPE are characterized by speech distortion. This characterization constitutes our idea to identify and detect audible additive noise and audible distortion. As an illustration, we present in figure 4 an example of speech frame power spectrum and its related curves UBPE and LBPE. The clean speech power spectrum is, for all frequencies index, between the two curves UBPE and LBPE. We remark that the two curves are the same for most peaks. It means that for these frequency intervals, any kind of degradation altering speech will be audible. If it quite over UBPE, it will be heard as background noise. In the opposite case, it will be heard as speech distortion.

C. Estimation of audible degradation

Estimation of audible noise power spectrum

Once UBPE calculated, the superposition of denoised signal power spectrum and UBPE leads to separate two cases. The First one corresponds to the regions of denoised speech power spectrum which are under UBPE. In such case, there is no audible residual noise. In the second case, some denoised speech frequency components are above UBPE, the amount above UBPE constitutes the audible residual noise. In term of listening tests, such residual noise is annoying and constitutes in some cases the musical noise. Such musical noise is well popular and constitutes the main drawback of spectral subtraction. Once the UBPE is calculated, it is possible to estimate the audible power spectrum density of residual noise using a simple subtraction when it exists. Hence, the residual noise power spectrum is written as

$$\Gamma_n^p(m,k) = \begin{cases} \Gamma_{\hat{x}}(m,k) - UBPE(m,k) & \text{if } \Gamma_{\hat{x}}(m,k) > UBPE(m,k) \\ 0 & \text{otherwise,} \end{cases} \quad (7)$$

where $\Gamma_{\hat{x}}(m,k)$ denotes the power spectrum of processed speech and the suffix p designs the perceptually sense of the power spectrum.

Audible speech distortion power spectrum estimation

Using the same methodology as the one used for residual background noise, it is possible to estimate the audible distortion power spectrum as

$$\Gamma_d^p(m,k) = \begin{cases} LBPE(m,k) - \Gamma_{\hat{x}}(m,k) & \text{if } \Gamma_{\hat{x}}(m,k) < LBPE(m,k) \\ 0 & \text{otherwise} \end{cases}. \quad (8)$$

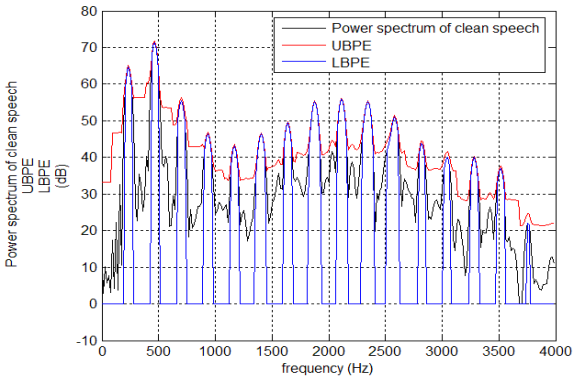

Figure 4. UBPE, LBPE and power spectrum of the original clean speech signal

D. Calculation of PSANR and PSADR

The perceptual residual noise criterion is defined as the ratio between the upper effective signal which is the UBPE and the audible residual noise. The Perceptual Signal to Audible Noise Ratio (PSANR) of *m*th frame is calculated in frequency domain and it is formulated as follows

$$PSANR(m) = 10 * \log_{10} \frac{\sum_{k=1}^{N} UBPE(m,k)}{\sum_{k=1}^{N} \Gamma_n^p(m,k)}. \quad (9)$$

The mean PSANR measure is computed by averaging the frame PSANR measures across the sentence as follows

$$PSANR_{mean} = \frac{1}{M} \sum_{m=1}^{M} PSANR(m) \quad (10)$$

Similarly, the Perceptual Signal to Audible Distortion Ratio (PSADR) of the *m*th frame is defined as a ratio between the lower effective signal which is LBPE and the audible distortion and is given as

$$PSADR(m) = 10 * \log_{10} \frac{\sum_{k=1}^{N} LBPE(m,k)}{\sum_{k=1}^{N} \Gamma_d^p(m,k)}. \quad (11)$$

The mean PSADR measure is computed by averaging the frame PSADR measures across the sentence as follows

$$PSADR_{mean} = \frac{1}{M} \sum_{m=1}^{M} PSADR(m) . \quad (12)$$

Next, the couple (PSANR, PSADR) defines the new criterion to evaluate both kinds of degradation. We call it Perceptual Signal to Audible Noise and Distortion Ratio (PSANDR). The higher the PSANDR score the better is the quality of the processed speech.

IV. PERFORMANCE EVALUATION

In order to evaluate performance of the proposed PSANDR measures to quantify the perceptual separation of the two kind of degradations (residual noise and speech distortion) we choose two well-known speech enhancement algorithms [1-5], namely, the spectral subtraction [2] and the Log MMSE algorithm incorporating speech-presence uncertainty (SPU) [4, 6]. Figure 5 depicts an example of denoised speech power spectrums and their related UBPE curve calculated from clean speech. Figure 5 (a) is obtained using the Log MMSE algorithm incorporating speech-presence uncertainty [4, 6]. We notice from this figure that excluding some frequency points (900, 1200, and 2300) the processed speech power spectrum is almost under the UBPE curve and hence they contain less (or not) residual audible noise. Figure 5 (b) is obtained using the spectral subtraction algorithm. It is observed from this figure that in the frequency regions between 800 Hz and 1800 Hz the processed speech power spectrum is above the UBPE and therefore they contain residual audible noise. In term of listening tests, such residual noise is annoying and constitutes in some cases the musical noise. Such musical noise is well popular and constitutes the main drawback of spectral subtraction.

Figure 6 (a) and (b) represent an example of power spectrum of the processed speech and its related curve LBPE calculated from the clean speech. Figure 6 (a) is obtained when the Log MMSE algorithm incorporating speech-presence uncertainty is used whereas figure 6 (b) is obtained when spectral subtraction algorithm is used. We notice from figure 6 (a) that excluding some specific frequency point almost all regions are above LBPE and hence they constitute little (or no) audible distortion of the clean speech. From figure 6 (b) it is observed that including the frequency regions between 3200 Hz- 3500 Hz there are other small frequency regions where the processed speech power spectrum is under the LBPE, which means that they constitute audible distortion of the clean speech. In term of listening tests, they are completely different from residual background noise. They are heard as a loss of speech tonality.

Table 1 shows the PSANDR (PSANR, PSADR) scores and the Segmental SNR values for the Log MMSE with SPU and the spectral subtraction methods when the clean signals are degraded with subway noise at global SNR levels of 5 dB and 10 dB. PSANR, giving idea about residual noise, depicts that the Log MMSE with SPU is the best one regarding noise attenuation. PSADR, determining the distortion of the denoised signals, illustrates that the important distortion is obtained using the Spectral Subtraction (SS) technique. These observations are confirmed by informal subjective listening tests.

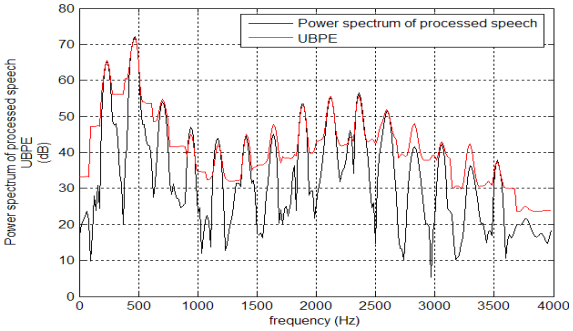

(a)

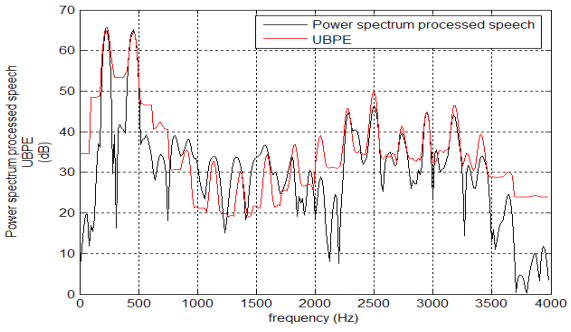

(b)

Figure 5. Power spectrums of the processed speech and its related clean speech UBPE. (a) for Log MMSE with SPU (b) for Spectral subtraction

V. CONCLUSION

Two parameters PSANR and PSADR characterizing the two kinds of degradation for speech enhancement applications are developed in this paper. We first propose two curves UBPE and LBPE to classify the audible residual noise and audible distortion. Simulation results comparing different well-known speech enhancement algorithms and classical objective measure (Segmental SNR) show a better characterization of degradation na-

ture of enhanced signal. The calculation of the degree of correlation of the proposed criteria with MOS criterion constitutes the perspectives of our future work.

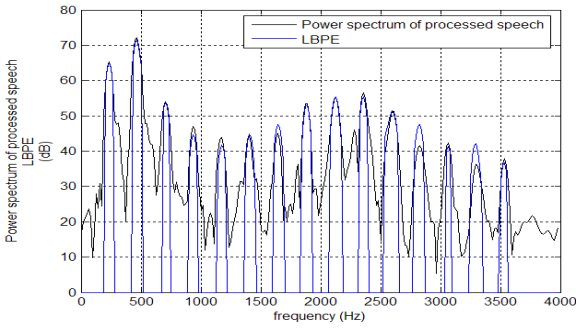

(a)

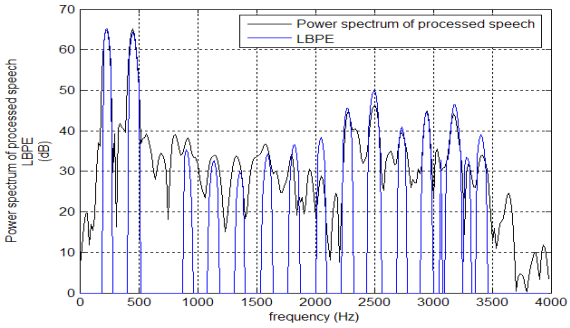

(b)

Figure 6. Power spectrums of the processed speech and its related clean speech LBPE, (a) for Log MMSE with SPU (b) for Spectral subtraction

Table 1 Experimental results

Algorithms	Input SNR (dB)	SegSNR	PSADR	PSANR
Log MMSE with SPU	5	**2.81**	**7.56**	**18.00**
	10	**4.85**	**16.65**	**7.115**
Spectral subtraction (Berouti)	5	1.40	6.94	10.764
	10	4.1	15.2	6.85

REFERENCES

[1] S. F. Boll, "Suppression of acoustic noise in speech using spectral subtraction," IEEE Trans. Acoustics, Speech, Signal Processing, vol. 27, pp. 113–120, Apr. 1979.

[2] M. Berouti, R. Schwartz, and J. Makhoul, "Enhancement of speech corrupted by acoustic noise," in Proc. IEEE Int. Conf. on Acoustics, Speech, Signal Processing, vol. 1, (Washington, DC), pp. 208–211, Apr. 1979.

[3] Y. Ephraim and D. Malah, "Speech enhancement using a minimum mean-square error short-time spectral amplitude estimation," *IEEE Trans. Acoust. Speech, Signal Processing*, vol. ASSP-32, no. 6, pp. 1109-1121, Dec. 1984.

[4] Y. Ephraim and D. Malah, "Speech enhancement using a minimum mean square error log-spectral amplitude estimator," IEEE Trans. Acoust., Speech, Signal Processing, vol. 33, pp. 443–445, 1985.

[5] Philipos C. Loizou, *Speech Enhancement Theory and Practice,* 1st edition, CRC press, June, 2007.

[6] Cohen, I., "Optimal speech enhancement under signal presence uncertainty using log-spectra amplitude estimator," IEEE Signal Processing Letters, vol. 9, no. 4, pp. 113-116, 2002.

[7] J. D. Johnston, "Transform coding of audio signals using perceptual noise criteria," IEEE J. on Selected Areas in Comm., vol. 6, pp. 314–323, Feb. 1988.

[8] E. Zwicker and H. Fastl, Psychoacoustics: Facts and Models. Springer-Verlag, 2nd ed., 1999.

[9] Yi Hu and Philipos C. Loizou, "Evaluation of Objective Quality Measures for Speech Enhancement," IEEE Trans. on Audio, Speech and Language Processing, vol. 16, No. 1, pp. 229-238, January 2008.

[10] Quackenbush S., T. Barnwell and M. Clements, *Objective Measures of Speech Quality*, Englewood Cliffs, NJ, USA, Prentice Hall, 1988.

[11] W. Yang, M. Benbouchta, and R. Yantorno, "Performance of a modified bark spectral distortion measure as an objective speech quality measure," IEEE ICASSP, pp.541-544, Seattle, 1998.

[12] D. E. Tsoukalas, J. Mourjopoulos and G. Kokkinakis, "Speech enhancement based on audible noise suppression," IEEE Trans. Speech and Audio Processing, vol. 5, no. 6, pp. 497- 514, November 1997.

Proceedings of 2009 12th International Conference on Computer and Information Technology (ICCIT 2009)
21-23 December, 2009, Dhaka, Bangladesh

Bayesian Networks Application for Representation and Structure Learning of Gene Regulatory Networks

Blagoj Ristevski, Suzana Loskovska†

Department of Information Systems Management, Faculty of Administration and Information Systems Management, St. Kliment Ohridski University – Bitola, Macedonia
†Department of Computer Science and Computer Engineering, Faculty of Electrical Engineering and Information Technologies, Ss. Cyril and Methodius University – Skopje, Macedonia
blagoj.ristevski@uklo.edu.mk, †suze@feit.ukim.edu.mk

Abstract

The cell functions and development are regulated by complex networks of genes, proteins and other components by means of their mutual interactions. These networks are called gene regulatory networks (GRNs). GRNs are used to reveal the fundamental gene regulatory mechanisms, to determine the reasons for many diseases and interactions between drugs and their targets. The introduction of experimental technologies such as microarrays, ChIP-chip which combines chromatin immunoprecipitation (ChIP) with microarrays and ChIP-Seq which combines ChIP with DNA sequencing, has provided a large number of available datasets related to gene expression and transcription factors (TFs) and their interactions. These datasets are basis for further analysis to reveal the gene regulation mechanisms. Many models have been applied to represent gene regulatory networks. We have used the dynamic Bayesian network model which is able to cope with missing data and can include a prior knowledge about transcription factors and their activation/inhibition of corresponding genes. We describe the obtained results and survey the common structure learning algorithms for learning of GRN's structure. We tested the obtained GRN for test datasets with different sizes and in the paper describe obtained dependencies between the ratio of Bayesian score and BIC and dataset size.

Keywords: gene regulatory networks, Bayesian networks, structure learning

I. INTRODUCTION

The living cells during their life span carry out many different tasks controlled by the cell genome which is encoded in the DeoxyriboNucleic Acid (DNA) molecule. The genes are transcribed into messenger RiboNucleic Acid (mRNA), and then translated in proteins.

Genes and their products – proteins work coordinately in complex networks. The cell functions and development are regulated by complex networks of genes, proteins and other components by means of their mutual interactions. These networks are called gene regulatory networks (GRNs). The proteins which activate or inhibit the transcription of the other genes by binding to specific DNA sequences are called transcription factors (TFs). Transcription factors are important components in gene regulatory networks. The GRNs are commonly used to study influences between cell components because they provide a clear and understandable notion for cell regulation as well as reveal the fundamental gene regulatory mechanisms and find out the reasons for many diseases.

Many destructive diseases such as cancer are related to different genetic disorders. The goal of many researches which includes the experimental and simulating methods is by studying the GRNs to reveal therapeutic and prognostic relevant knowledge about many diseases.

The necessity to generate, analyze and integrate the large scale expression data led to the development of microarray technology [9]. Besides microarray technology which gives data for genes' expression [13][14] other experimental technologies such as chromatin immunoprecipitation ChIP-chip and ChIP-Seq, provide a lot of available data about genome, transcriptome and interactome of different organisms. ChIP-chip gives information on interaction between transcription factors and promoter region of the gene when it is combined with microarray analysis [10]. ChIP-Seq technology uses DNA sequencing instead microarray [15]. Both technologies, ChIP-chip and ChIP-Seq provide data for protein-DNA interactions for a certain protein/transcription factor [15]. These different data types are basis for further analysis and they are means of revealing the gene regulation mechanisms and essential knowledge about cell processes on genomic and molecular level.

To represent GRNs, more models are used, such as state space model, Bayesian networks, dynamic Bayesian networks, Boolean networks, graphical Gaussian models, linear and nonlinear differential and difference equations model, fuzzy logic model, information theory model, and others models.

Finding out the most reliable and accurate structure of GRNs from high dimensional microarray data is a machine learning problem known as structure learning of graphical models. A subset of the data is used for model fitting and the residual data for the model validation [8]. Cross-validation methods are used for validation and training of regulatory networks. But, the obtained networks which fit the best to the training set are commonly overtrained [3]. Such overfitted networks lose their ability to generalize for the data outside the training set.

The rest of this paper is organized as follows. In the second section we present the models based on

978-1-4244-6283-4/09/$26.00 ©2009 IEEE

Bayesian networks and their advantages and disadvantages. The consequent section describes the dynamic Bayesian networks. A survey of structure learning algorithms of reconstructed gene regulatory networks is given in the Section 4. The following section is devoted to the reconstructed GRN using Bayes Net Toolbox (BNT) and obtained dependencies between the ratio of Bayesian score and BIC and dataset size. The concluding remarks are given in the last section.

II. BAYESIAN NETWORKS

The Bayesian networks are a special case of graph models that consist of two components and are based on statistical principles [6]. The first part is a directed acyclic graph *G=(V,E)* where $V = \{1,\cdots,n\}$ is a set of nodes and *E* is a set of edges. Each node $i \in V$ refers to random variable $x_i \in x$ that represents the gene expression in the GRNs. The set of edges corresponds to the conditional dependence among nodes. The second part of network is a set of conditional probability distributions that describe the conditional probability of each variable (the gene expression).

If $x = \{x_1,\cdots,x_n\}$ denotes a set of random variables, *G* - structure of graph, θ - set of parameters the joint probability distribution is given by (1).

$$p(x) = \prod_{i=1}^{n} p\left(x_i \middle| x_{\{1,\cdots,i-1\}}, \theta, G\right) \quad (1)$$

If pa_i denotes the parent nodes of the node x_i that means the state of each variable x_i depends on the states of its parent pa_i (2):

$$p(x) = \prod_{i=1}^{n} p\left(x_i \middle| pa_i, \theta, G\right) \quad (2)$$

Bayesian networks are suitable to show regulatory mechanisms between network components quantitatively as well as qualitatively. The qualitative description of regulatory mechanisms refers to presence/absence of an edge between network nodes whereas quantitative representation is made by a set of conditional probability distributions.

The modeling of the gene regulatory networks is made by structural and parameter learning. The goal of structural learning is to determine topology of network. For a given network structure, the parameter learning includes parameter estimation of unknown model for each gene. This is performed by determination of conditional dependencies between network components.

Bayesian networks can deal with noisy and stochastic nature of gene expression data and with incomplete knowledge about the system [17]. The small number of data points (samples) and the big number of genes are common problems for learning of Bayesian networks. Another disadvantage is that feedback loops cannot be modeled, although they exist in the gene regulatory networks.

III. DYNAMIC BAYESIAN NETWORKS

To overcome the problems of Bayesian networks, *dynamic Bayesian networks* are used to model gene regulations. The dynamic Bayesian networks are capable to deal with stochastic variables, time series gene expression data, to include prior knowledge obtained by literature, ChIP-chip and ChIP-Seq experiments [15], feedback loops, and to handle missing values and hidden variables. The hidden nodes (variables) can capture effects that cannot be directly measured in a microarray experiment.

The joint probability distribution is given by (3), where x_t^i is the *i*-th node at time *t*.

$$p\left(x_t \middle| x_{t-1}\right) = \prod_{i=1}^{n} p\left(x_t^i \middle| pa(x_t^i), \theta, G\right) \quad (3)$$

Dynamic Bayesian networks can apply to and learn from real biological data. There is a relationship between this kind of networks to Hidden Markov Model, Boolean networks, stochastic Boolean networks, dynamic Bayesian networks with continuous state and other probabilistic models [18]. The hidden nodes provide a way of linking similar data types and analysis of other network parameters. When some dependency exists between variables in the network, the hidden node can model that dependency.

Relatively low prediction accuracy and excessive computational time are two problems which reduce the performance of the dynamic Bayesian network model. To overcome these problems it is suggested a *dynamic Bayesian network approach* which limits the potential regulators to those genes with either earlier or simultaneous expression changes (up- or down-regulation) in regard to their target genes. Then, the genes with either earlier or simultaneous expression changes are assigned as possible regulators of those genes with a later expression change.

IV. STRUCTURE LEARNING

To choose the most appropriate structure of Bayesian network for a given dataset it is necessary to carry out a validation of the modeled networks. The precision and reliability of models predictions are commonly examined in respect with input experimental data during the process of model validation. Structure learning of Bayesian network consists of finding a directed acyclic graph (DAG) that the best fits the dataset. The structure learning consists of selecting scoring function that evaluates how well the DAG explains the data and then searching for the best DAG that optimizes the scoring function.

The number of directed acyclic graphs *G*(*n*) super-exponential depends on of the number of nodes *n*:

$$G(n) = \sum_{k=1}^{n} (-1)^{k+1} \binom{n}{k} 2^{k(n-k)} G(n-k) \quad (4)$$

After GRNs modeling, the model which provides a good fit to the data should be selected. The criteria such as Bayesian score [2], maximal likelihood, Bayesian

information criterion, minimum description length are used for model selection of gene regulatory networks.

Let M denotes the structure of a dynamic Bayesian network, D is the data set, $P(M)$ is the prior probability of the network structure and $P(D|M)$ is its marginal likelihood. θ is a parameter vector of the conditional probability distributions. The marginal likelihood is an average of the likelihood $P(D|M,\theta)$ over all possible parameters associated to the network. The Bayesian score is based on the marginal likelihood of the data defined as following:

$$P(D \mid M) = \int P(D \mid M, \theta) P(\theta \mid M) d\theta \quad (5)$$

It provides a matching between model complexity and the data size.

The goal of the Minimum Descriptive Length criterion (MDL) is to provide an optimal matching between the precision of the data fitting and the complexity of network model. The MDL score consists of model and data set encoding, hence the MDL criterion L is a sum of the network coding length L_M and data set coding lengths given by the following equation:

$$L = L_M + \sum_{j=1}^{m-1} H(x_{j+1} \mid x_j) = L_M - \sum_{j=1}^{m-1} \log(p(x_{j+1} \mid x_j)) \quad (6)$$

where $H(x_{j+1} \mid x_j)$ is the state transition conditional entropy, $p(x_{j+1} \mid x_j)$ is the transitional probability and m is the number of sample points [11].

At the Bayesian Information Criterion (BIC) n denotes the sample size, k – numbers of parameters and RSS is the residual sum of squares from estimated model. If it is assumed that the distribution of the model's errors is normal, then the aim is to minimize BIC, given by (7).

$$BIC = n \log\left(\frac{RSS}{n}\right) + k \log n \quad (7)$$

The Maximum Likelihood (ML) criterion expresses the likelihood $L(\theta)$ as a function of the unknown vector parameter θ and aims to find the parameters of all possible values which maximize $L(\theta)$. The solution can be a function of one or many parameters and this problem is often nonlinear optimization problem.

To obtain a good balance between the accuracy of data fitting and the complexity of gene network models, some of above mentioned criteria are applied. Their application infers GRNs with significant biological performances of inferred interactions between networks elements.

Because of super-exponential dependency between number of directed acyclic graphs and number of nodes, the local or global search algorithms are used (K2, Hill-climbing, MCMC, Structured EM). In addition to the search procedure, the scoring function should be specified.

The K2 algorithm is a greedy search algorithm that works as follows. In the beginning each node has no parents. The algorithm adds incrementally parent whose addition largely increases the score of the resulting structure. When there is no single parent that can increase the score, the adding parents to the node stops. K2 algorithm attempts to select the network structure that maximizes the posterior probability of network for given the experimental data [12].

Hill-climbing starts at a specific point in space, considers all nearest neighbors, and moves to the neighbor that has the highest score. If no neighbors have higher score than the current point (a local maximum is reached), the algorithm stops.

To evaluate the obtained results, the inferred network structure should be compared with the reference network. The Receiver Operator Characteristics (ROC) curves are used to evaluate inferred network structure quantitatively [5]. The ROC curve is a chart of the ratio between sensitivity and (1-specificity), where sensitivity corresponds to proportion of actual positives edges which are correctly identified and specificity is proportion of negatives edges which are correctly identified. The ROC curves can be summarized by computing the AUC (Area Under the ROC Curve).

Also, the n-cross validation is used for model validation, where the input set is divided to n parts. The n-1 parts are used as a training set, and the remaining one as a test set.

V. RESULTS

To implement dynamic Bayesian gene regulatory network we used insulin gene expression data, Bayes Net Toolbox [4] and Bayesian Network Structure Learning – software package [1]. From insulin data, we specified the interactions between genes (the gene number is 35) in regard to interactions transcription factors - target genes.

Also, we tested the obtained GRN for datasets with different sizes. Obtained dependencies between the ratio of Bayesian score and BIC are shown on Fig. 1- Fig. 3. For small dataset, the ratio of Bayesian score and BIC for observed gene network with 35 nodes has increasing tendency. To evaluate the statistical features of generated Bayesian network, re-sampling is utilized by generation of datasets with different sizes. Obtained result tendencies are shown on Fig. 2 and Fig. 3. They show that increasing of data samples improves the network inference, but the imbalance between large dataset and low variability can be avoided by decreasing of number of data samples [16].

VI. CONCLUSION

Besides the amount of microarray data sets, the reconstructing of GRNs is still a hard and challenging problem. Bayesian networks especially dynamic BNs are powerful tool which provides elucidation of interaction among genes. The main shortcoming of utilized Bayes Net Toolbox and Bayesian Network Structure Learning is their limitation to cope only with networks with small number of nodes, especially for structure learning.

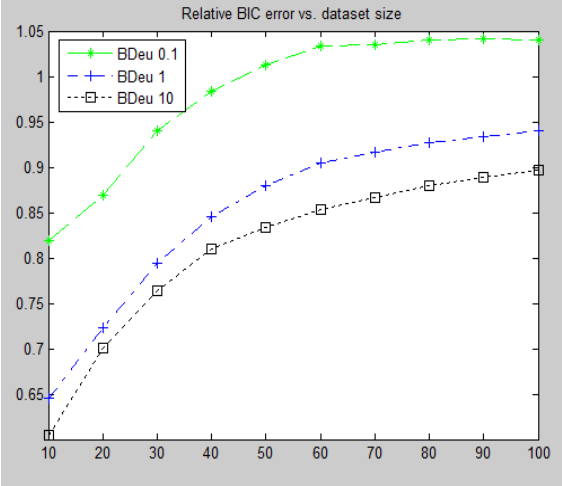

Fig. 1. Dependency between ratio of Bayesian score and BIC - and dataset size (10-100)

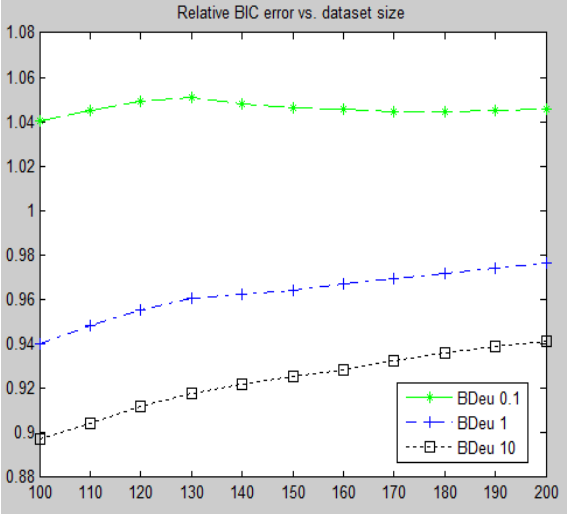

Fig. 2. Dependency between ratio of Bayesian score and BIC - and dataset size (100-200)

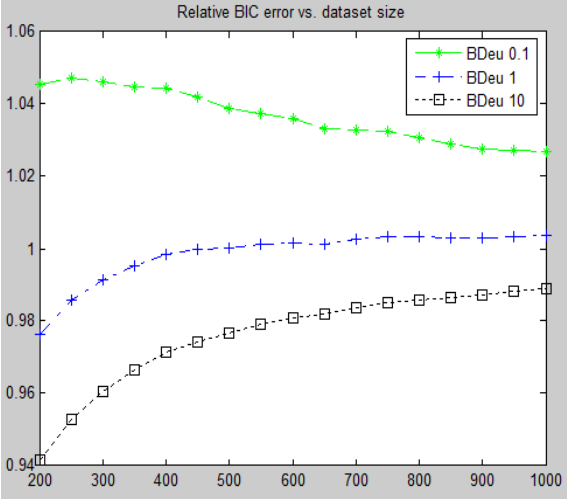

Fig. 3. Dependency between ratio of Bayesian score and BIC - and dataset size (200-1000)

Further efforts should be done toward dealing with larger gene networks and integrating heterogeneous biological data to improve the prediction and inference power of GRNs.

REFERENCES

[1] D. Eaton and K. Murphy, Bayesian Network Structure Learning - A Software Package for Matlab, www.cs.ubc.ca/~deaton/struct/bnsl.html

[2] G. F. Cooper and E. Herskovits, A Bayesian Method for the Induction of Probabilistic Networks from Data, *Machine Learning*, 9, 309-347, 1992.

[3] H. Lahdesmaki et *al*., On Learning Gene Regulatory Networks Under the Boolean Network Model, *Machine Learning*, 52, 147-167, 2003.

[4] K. Murphy, Bayes Net Toolbox for Matlab, www.cs.ubc.ca/~murphyk/Software/BNT/bnt.html

[5] L. Kaderali and N. Radde, Inferring Gene Regulatory Networks from Expression Data, *Computational Intelligence in Bioinformatics 2008*, 33-74, 2008 .

[6] N. Friedman and M. Goldszmidt, Learning Bayesian Networks with Local Structure, *Proceedings of the NATO Advanced Study Institute on Learning in graphical models*, 1998.

[7] F. R. Pinto A Probabilistic Approach to Study Yeast's Gene Regulatory Network, *Journal of Computer Science & Systems Biology*, JCSB/Vol.2 February 2009.

[8] P. Baldi and S. Brunak, *Bioinformatics:The Machine Learning Approach*.The MIT Press, Cambridge, 2001.

[9] S. Qing Ye, *Bioinformatics A Practical Approach*. Chapman & Hall/CRC, Taylor &Francis Group, Boca Raton, 2008.

[10] T. I. Lee et *al*., Chromatin immunoprecipitation and microarray-based analysis of protein location, *Nature protocols*, Vol.1 No.2, 2006.

[11] W. Zhao et *al*. Inferring gene regulatory networks from time series data using the minimum description length principle, *Bioinformatics*, Vol. 22 no. 17 2006, pp. 2219-2135.

[12] X.-Wen Chen, G. Anantha and X. Wang, An effective structure learning method for constructing gene networks, *Bioinformatics*, Vol. 22 no. 11, 2006.

[13] B. Ristevski, S. Loshkovska, S. Dzeroski, I. Slavkov, A Comparison of Validation Indices for Evaluation of Clustering Results of DNA Microarray Data, *The 2nd International Conference on Bioinformatics and Biomedical Engineering ICBBE 2008*, Shanghai, China.

[14] B. Ristevski, S. Loskovska, A Survey of Clustering Algorithms of Microarray Gene Expression Data Analysis, *The 10th International Multiconference Information Society – IS 2007*, Ljubljana, Slovenia

[15] E. J. Cooke, R. S. Savage, D. L. Wild, Computational approaches to the integration of gene expression, ChIP-chip and sequence data in the inference of gene regulatory networks, *Seminars in Cell & Developmental Biology*, 2009.

[16] N. Dojer, A. Gambin, A. Mizera, B. Wilczynsky and J. Tiuryn, Applying dynamic Bayesian networks to perturbed gene expression data, *BMC Bioinformatics*, 2006.

[17] B.-E. Perrin, L. Ralaivola, A. Mazurie, S. Bottani, J. Mallet, F. d'Alche-Buc, Gene network inference using dynamic Bayesian networks, *Bioinformatics*, vol. 19, 2003

[18] P. Li, C. Zhang, E. J. Perkins, P. Gong, Y. Deng, Comparison of probabilistic Boolean network and dynamic Bayesian network approaches for inferring gene regulatory networks, *BMC Bioinformatics*, 2007.

Proceedings of 2009 12th International Conference on Computer and Information Technology (ICCIT 2009)
21-23 December, 2009, Dhaka, Bangladesh

Extraction of Interesting Rules from Internet Search Histories

Md. Asaduzzaman, Md. Shahjahan
Department of Electrical & Electronic Engineering,
Khulna University of Engineering & Technology (KUET), Khulna-9203
milon01eee@yahoo.com, mdjahan8@yahoo.com

Abstract

Rule extraction aims to ultimately improve business performance through an understanding of past and present search histories of customers. A challenging task is to determine interesting rules from their heterogeneous search histories of shopping in the Internet. For this purpose Neural Network (NN) and Canonical Correlation Analysis (CCA) are used. Customers visit web pages one after another and leave their valuable search information behind. Firstly we produce a homogeneous data set from their heterogeneous search histories. It is difficult task to produce a homogeneous data from heterogeneous data without changing their characteristics of data. Secondly these data are trained by unsupervised NN to get their significant class. Thirdly we extract the maximally correlated customers by using CCA and then interesting rules are extracted among their maximally correlated customer. This is important for the traders, marketers and customers for making future business plan.

Keywords: Heterogeneous data, Rule Extraction, Neural networks, Statistics.

I. INTRODUCTION

THE Internet has has provided a tremendous level of excitement through its involvement with all kinds of businesses starting from e-commerce, e-business, e-supply, e-marketplace, e-payment, e-entertainment, e-learning, and so on. The e-commerce is now a hot and challenging topic. The growing interest in internet shopping encourages customers and organizations to know each other. Thus, organizations should understand their customer's behavior, preferences and future needs. This leads many companies to develop a lot of e-service systems. In recent years, e-commerce has grown dramatically in terms of volume and variety of goods and services [1]. It is predicted by American International Telecommunication Union and American International Data Group that Internet trade will account for 42% of the global trade volume by 2010 [2]. The internet based traders require knowing the customers interest to design their web pages that are attractive to the customers.

Now-a-days people feel easy to buy their goods from internet based shop without going to the shop physically. E-commerce has grown drastically and the scope of consumers has widened. A sick man who is unable to move can buy his necessary goods especially medicine through internet. Visitors do not need to use their cars and spend money for the gasoline. Also, they do not need to wear good cloths, he can purchase any commodity without maintaining time, he has no risk to bear money and goods, and so on. Our aims are to ultimately improve business performance through an understanding of past and present search histories of customers so as to determine and identify attitude of customers. Thus, organizations should understand their customer's behavior, preferences and future needs. This leads many companies to develop a lot of e-service systems.

Data mining is the term currently used for analyses which explore possible patterns or behaviors in datasets without utilizing classical hypothesis-driven statistical models [3]. Though it is very difficult to identify representative patterns of users' behaviors on the Web, previous studies have attempted to develop rigorous analytical tools to investigate web visit patterns. Huberman [4] demonstrated that Web visits have some unique and regular patterns, particularly those related to the number of clicks (hyperlink requests) [5] explored a tool to describe such patterns in a visual way and defined statistical models for use in analyzing the data. There is an another type of attempt that generates attributes considering various facts in the purchase patterns, such as length of pages, number of sub pages, mode of purchase etc. [6].

An organization generates log files that track the steps of visitors as they move around on the shop websites. Analyzing these web log files is very challenging, however, due to their huge size and the heterogeneity of the purchase patterns of each individual. Finding useful information buried in such large-scale datasets requires a rigorous analytical approach, yet the data are not very amenable to classical statistical models. We develop an algorithm that automatically generates equal size data from the heterogeneous data so that we can apply the data directly to the NN classifier.

The paper is organized as follows. Section II describes about the data patterns and the problems of heterogeneous data to analyze are discussed. We describe the proposed method in Sect. III. The rule extraction is reported in Sect. IV. We conclude the paper in Sect. V.

II. DESCRIPTION OF DATA

We collected visitors purchase patterns from the server of a software company in Japan, called "**Start Today Co Ltd",** http://www.starttoday.jp, WBG West 23F, 2-6 Nakase, Mihama-ku, Ciba 261-7123, and Japan. The data collection period was 12 July, 2006.

A. Examples of data

Here, we explain the visitors purchase patterns. In the first line of data, we see a series of numbers as follows.

591603924,01,26,01,26,01,26,01,34,01,25,46,17,46,17,01,25, 01,24,01,34,01,34,01,26,01,30,01,25,01,34,01,25,01,30,01,26, 01,34,01,30,01,25,46,17,46,17,46,19,45,02,45,02,46,19,46,19, 46,21,46,18,46,20,46,20,46,22. The first number 591603924 designates the customer ID. He went to a web shop called eproze at/shop/eproze/default.html. He looks at a commodity #21 at /shop/eproze/goods.html?gid=21. He looks at a commodity #19 at /shop/eproze/goods.html?gid=19. He looks at a commodity #66 at /shop/eproze/goods.html?gid=66.

In this case, the web page of the shop is (01,26). Since commodities 21, 19 and 66 are on the same page, the data shows that he moved as such (01,26) (01,26) (01,26). The final page he reached was (46,22) and purchased the commodity. He visited a total number of 33 pages in order to purchase the commodity. In this way, each customer searches a different number of pages. There are 153 lines of data – each line indicates the individual customer purchase pattern. All customers want to buy the commodity located at page (46,22). Our aim is to classify customer's time sequence through which they come to purchase the commodity, by using neural network.

B. Features of data

The data are very heterogeneous as shown in TABLE I. The page address is a pair of integer values. A customer visits continuously from one page to another. It is also possible to come back to the previously visited pages. The transition of pages of a customer is not the same with another customer. But the number of pages a customer visits may be same with others. The percentage of the same number of pages is about 3. The number of pair varies from 4 to 649. First 20 customers with their number of attribute are listed in TABLE I.

TABLE I
THE NUMBER OF ATTRIBUTES OF FIRST FIFTY CUSTOMERS

ID	Number of attributes	ID	Number of attributes
01	33	02	19
03	105	04	42
05	76	06	185
07	30	08	57
09	236	10	236
11	66	12	64
13	69	14	109
15	95	16	69
17	373	18	334
19	21	20	128

C. Problems of data to analyze

The main problem of the customer's purchase patterns is that they are heterogeneous. This is quite impossible to use these kinds of data in neural network and to make a decision about the category of data or customers. We need to make equal size data for using in neural network. Not only that, we need a single attribute data – not a pair data, since neural network can not use pair wise data. Moreover, first data point in a pair is more important than the second one. It is difficult to process such type of importance by a neural network.

II. METHODOLOGY

In this section we will describe the way to generate equal length data from heterogeneous data by three steps as shown in Fig. 1. It is very difficult to analyze these raw data. These raw data cannot be used directly in NN. So, it is necessary to create a standard data set that can be applied in NN and also can be used in CCA. There are two big problems face to create standard data set, which is 1). Data are paired and 2). Data sizes are different. In the next section, how to accumulate pair of data and also to create equal size data are explained.

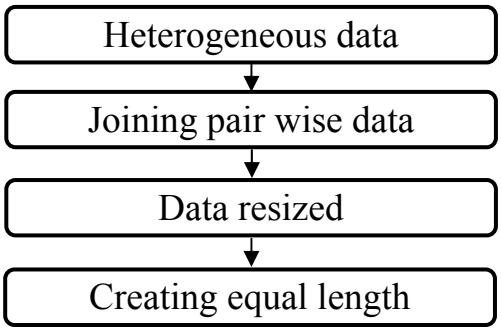

Figure 1: Data preprocessing

A. Joining pair wise data

We need to make a single attribute from a pair of attributes. But it is difficult to unite a simple arithmetic operation. Such as (02, 10) and (05, 07) are two different visited web pages. But by simple addition we get the same result (such 12). We just put a decimal point between two attributes. Therefore, they become new single attributes as 02.10 and 05.07. We combine pair wise data from heterogeneous data by adding a decimal point between them. We consider first part of the pair is more significant than the second part. Now, one can easily identify first part of the pair and second part also. So it is not unreasonable.

B. Data resized

The number of data varied from 4 to 699. We take a standard data length for creating equal length all the data set. In this research, we have taken target length (TL) or desired length is 80. If the numbers of raw data are too less from desired length and the number of raw data are too high from desired length, it becomes difficult to make desired length. For this reason, we consider the number of data from 21 to 300. We filter the customers with attributes less than 21 and greater than 300. At last we consider 116 purchased patterns from 153 purchased patterns. Then rescale the filtering data set. These new resized data set (RDS) are performed in the next section.

C. Creating equal length data from different length data

We need to make equal length data for using in NN and CCA. We create equal length from the total heterogeneous data. It is the core work in data preprocessing. Now we will describe how to generate equal length data from different length data. Firstly, a RDS is taken. The original data length (DL) and TL are compared. If DL is equal to or less than TL Attribute addition algorithm (AAA) is attempted, otherwise

Attribute reduction algorithm (ARA) is performed. Here this method will be described briefly [7]

Figure 2 shows the complete flow chart to create equal length data. AAA and ARA are explained in the following section. Store this data set in a file after performing AAA or ARA. Repeat the whole process for all filtering data set and store in a file. This file contains the training set for NN.

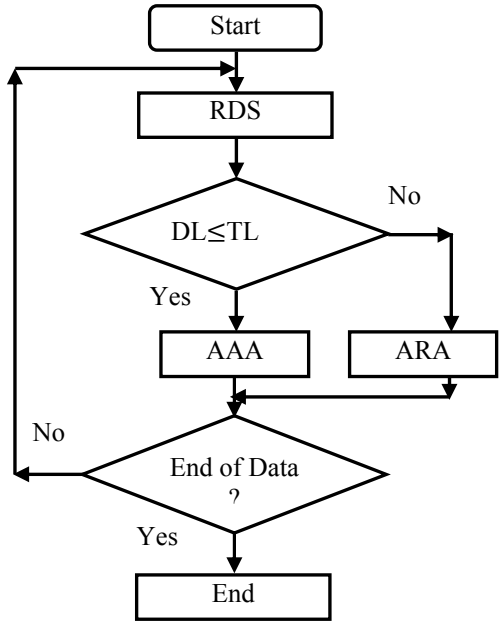

Figure 2: Flow of creating equal length data

i) Attribute addition algorithm (AAA)

AAA is shown in Fig. 3. If DL is equal to TL, data are stored, otherwise go to the next step. In this step, DL is checked for ten multiple (TM). If the DL is not equal to TM, some of intermediate data points are copied to make upper nearest TM numbers.

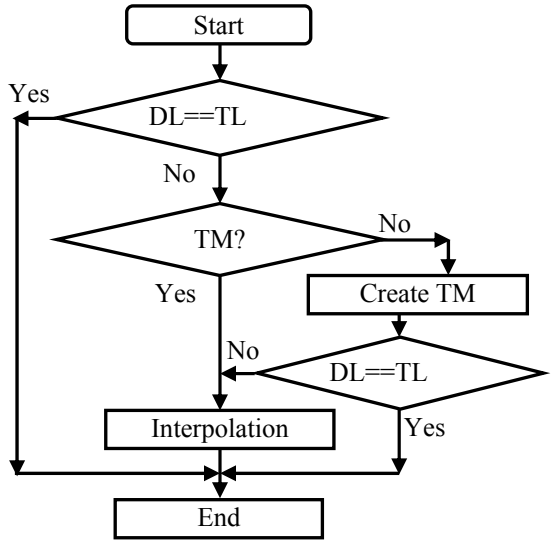

Figure 3: Attribute addition algorithm

In AAA, at first we create ten multiple data. It is not unreasonable because of some reasons: a) we repeat some intermediate data so that there is no need to create unknown attributes, b) we repeat data points for some intervals (not regular), c) we visualize raw data sets that many number of data have already repeated in every data set. So we can say that the data characteristics cannot be changed after performing TM. We create TM because of reduce computational complexity in the next section.

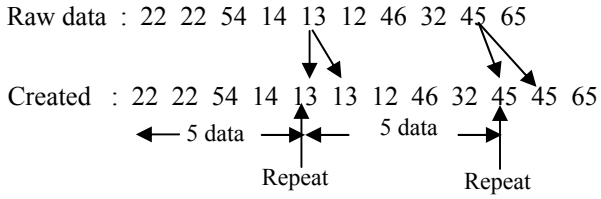

Figure 4: A hypothetical example to create 10 multiple data.

Again it is checked, DL is equal to TL. If DL is equal to TL, data are stored. Otherwise DL are performed the next stage. In this step, we create the additional data points by interpolation, using Newton's interpolation formula [8] for divided difference as described in below. A generalization of the formula is as follows .

$$f = f(x_0) + (x - x_0)f[x_0, x_1] + (x - x_0)(x - x_1)f[x_0, x_1, x_2] + \cdots + (x - x_0) \ldots (x - x_{n-1})f[x_0, x_1, \ldots x_n]$$

Figure 5 shows the sample of purchase pattern consisting of 30 attributes and Fig. 6 shows the generated 80 attributes using AAA from 30 attributes. the purchase pattern contain only 30 attributes, we have to generate additional 50 attributes using AAA. We see that Fig. 5.1 and Fig. 5.3 show similar shape. They are functionally approximately same.

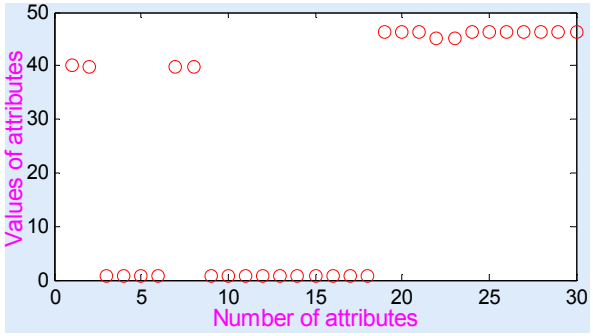

Figure 5: A sample of 30 attributes.

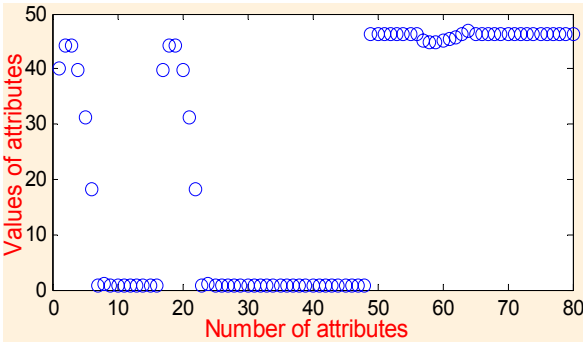

Figure 6: Generated 80 attributes by AAA for 30

ii) Attribute reduction algorithm (ARA)

ARA based on a comparison two neighboring data. In other word, it can be called comparison algorithm. A number of attributes are deleted comparing with a pre-specified threshold as shown in Fig. 7. Two neighboring attributes (say *m* & *n*) are compared. When the result does not exceed or equal the threshold value, attribute *n* is deleted, otherwise there is no deletion. The threshold value is not constant. Let's have 1,2,3,3.25,4,5,6 data points and the threshold value is 0.5. Since 3~3.25≤0.5, n=3.25 data point is deleted. This process will continue before the time when DL is equal to TL. If DL does not reach TL in beginning, this algorithm increases the threshold value of a step of 0.05 (or any suitable value).

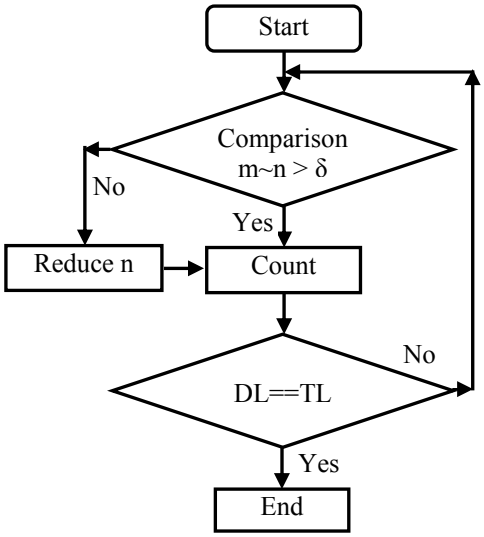

Figure 7: Attribute reduction algorithm

ARA has performed approximately unbiased because of some reasons, a). We select zero or very low threshold value. For this reason, repeated attributes or similar attributes are deleted. b). ARA compares two neighboring attributes (say *m* & *n*). When attribute *n* is deleted, the next comparison takes a new set. For this reason, a series of repeated data cannot be deleted at a time. It performs all over the data set. c). If DL does not reach TL, this algorithm increases the threshold value very small. Relatively same attribute or same information is deleted but different information exists in the data set. So, we can say that ARA is not unreasonable.

Figure 8 shows two samples of purchase pattern consisting of 200 attributes and Fig. 9 shows the generated 80 attributes by ARA from 200 attributes. Fig. 8 and Fig. 9 show approximately similar transition. In this case, 120 attributes reduce by ARA to produce 80 attribute. In this way, the algorithm creates equal length purchase patterns with equal size of 80. One can easily understand by visual inspection that both (raw data and created data) sets that generated data set are equivalent.

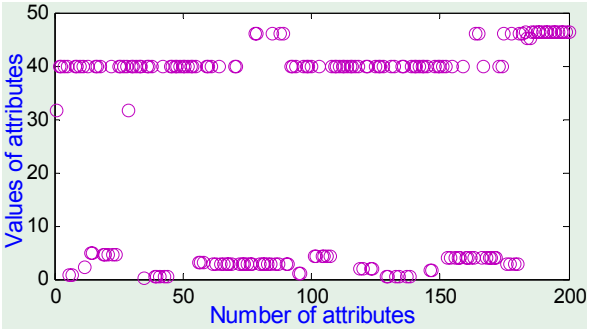

Figure 8: A sample of 200 attributes.

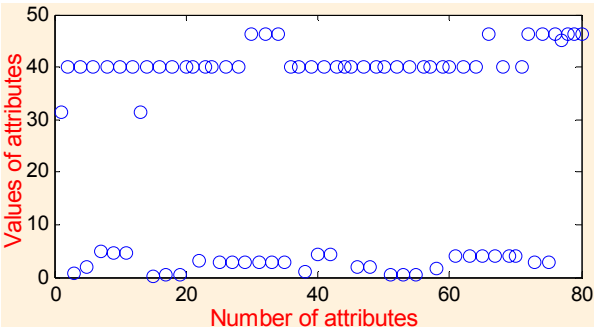

Figure 9: Generated 80 attributes by ARA for 200

D. Statistical validation

We have developed an algorithm that can automatically generate equal length data form heterogeneous data. Without data preprocessing, one cannot use it in NN and CCA or any suitable networks. The neural network needs equal length data. In order to apply CCA, the number of data points or attributes of the data sets must be always same. In order to prove that the generated data points are approximately unbiased, we test original and generated data using statistical tests. This will prove that the generated data is statistically sound and functionally same with original heterogeneous data. The generated data are validated by three statistical tests.

Z-test: A Z-test is any statistical test for which the distribution of the test statistic under the null hypothesis can be approximated by a normal distribution. Due to the central limit theorem, many test statistics are approximately normally distributed for large samples. Therefore, many statistical tests can be performed as approximate Z-tests if the sample size is not too small. The most general way to obtain a Z-test is to define a numerical test statistic that can be calculated from a collection of data, such that the sampling distribution of the statistic is approximately normal under the null hypothesis. Statistics that are averages (or approximate averages) of approximately independent data values are generally well-approximated by a normal distribution. An example of a statistic that would not be well-approximated by a normal distribution would be an extreme value such as the sample maximum [9].

We need to find the value of Z that will only be exceeded 5% of the time since we have set our alpha level at .05. Since the Z score is normally distributed (or has the Z distribution). For example, to get the Z for a 95% confidence interval, make the

shaded area 0.95. Then choose "between" and you will see that .95 of the area is between -1.96 and 1.96. For null hypothesis, it is seen that the Z value exceed this value or not. In TABLE II, first column shows the raw data, second column shows the degree of freedom, third column shows the two tailed Z-test value and finally we show that it is accepted or rejected. Here two data sets are taken for testing at a time, one is original raw data and second one is corresponding generated data.

TABLE II
SUMMARY OF Z-TEST

Number of raw data	Degree of freedom	Z-test values	Test hypothesis
30	108	0.0252	Accepted
57	135	0.0404	Accepted
42	120	0.0683	Accepted
76	154	0.0542	Accepted
95	173	0.1462	Accepted
139	217	0.1565	Accepted
200	278	0.0956	Accepted
227	305	0.1686	Accepted

III. RULE EXTRACTION

Rule induction is an area of machine learning in which formal rules are extracted from a set of observations. The rules extracted may represent a full scientific model of the data, or merely represent local patterns in the data. Some rule induction paradigms are: Association rule algorithms, Decision rule algorithms, Hypothesis testing algorithms, Horn clause induction, Version spaces, Rough set rules, Inductive Logic Programming, and so on. We use decision rule algorithm from these algorithms.

A. Clustering

After preprocess the data set it is usable for cluster analysis. Clustering is the classification of objects into groups (called clusters) so that objects from the same cluster are more similar to each other than objects from different clusters. Clustering is a common technique for statistical data analysis, which is used in many fields, including machine learning, data mining, pattern recognition, image analysis and bioinformatics [10].Neural networks are widely used for clustering data. An unsupervised competitive learning network (CLN) is used for clustering all customers.

After training these homogeneous data through the CLN a significant cluster are found. From this output six significant groups are extracted. The output neuron 4 wins the maximum number of customers. So this cluster contains the maximum information. On the other hand, the neuron 5 wins the minimum number of customers.

TABLE III
CHARACTERISTICS OF ESTIMATED CLUSTERS

Cluster name	*Winning neuron*	*Total customers*
A	1	23
B	4	36
C	6	16
D	7	18
E	8	11
F	5	8

TABLE III shows the summary of clusters. The maximum number of customers contributes in cluster B. Only four purchased patterns (one at output neuron 9 and three at 10) cannot occupy in any group. We ignored them for simplicity sake. There are no available statistical tools to get correlation among the clusters. For this purpose, CCA are used to find out the correlation. The weight values of weight vectors give the strength of relationship among attributes of two data sets. CCA finds the largest possible correlation between two data sets. There are maximum (15) possible combinations among six clusters. Such as Cluster A & Cluster B is an one combination. 24 distinct customers which have maximal canonical coefficients are obtained from these combinations.

B. Decision Rule

A set of decision rules is the verbal equivalent of a graphical decision tree, which specifies class membership based on a hierarchical sequence of (contingent) decisions. Each rule in a set of decision rules therefore generally takes the form of a Horn clause wherein class membership is implied by a conjunction of contingent observations.

IF condition1 AND condition2 AND/ OR ... AND condition THEN CLASS = class

Where condition is in general contingent on the choice of condition − 1. Decision rules can be transcribed from the corresponding decision tree, or can be induced directly from observations. Decision rules are commonly used in the medical field. For example, the Ottawa Ankle Rules guide obtaining radiographs for traumatic ankle pain.

Interesting rules are listed in Fig. 10. We find out these rules among the district customer, which are representing the total characteristic of data. Here it is seen that there are two major rules are i). Clustering rule and ii). General rule.

i. Clustering rule

If the data points (*(31.05 or 1.26 or 3.25) and (1.34 or 1.72 or 3.80 or 3.23) and 46.17 and 46.19 and 45.02 and/or 46.21 and 46.18 and 46.20 and 46.22)* follow this sequence this rules satisfied only the cluster A. similarly, if the data points *If ((31.50 or 0.54) and 46.17 and (44.97 or 44.91 or 44.79) and 46.19 and 45.02 and 46.18 and 46.20 and 46.22)* then its indicates only the cluster B. Similar way it is seen the rules 3,4,5, and 6.

ii. General rule

The rule number 3,4 are contributing the general rule. If the data points follow the following sequence it's contribute among the whole cluster:

If (31.50 and46.17 and 46.19 and 45.02 and 46.18 and/or 46.20 and 46.22) then cluster A (41, 93), B (20, 94, 107), C (42, 48, 101), D (15, 60, 78, 81), E (21, 30, 33, 55) F (67, 79)

Here we show the clusters with ID. In the same way we will explain the rule 7 and 8. It is seen that the most searching webpage are 31.50, 3.25, 46.17, 46.19, 45.02, 46.18, 46.20, and 46.22.

After getting these rules, it is necessary to determine which page number is most important or which products are demandable for customers. Now trader can determine which rule general sequence for all clusters and easily can be determined which is important for trader and customer. If trader can predict the customer demand, he can understand which product is more necessary or less necessary to store.

IV. CONCLUSION

This paper presents a new method that creates same length patterns from heterogeneous patterns and extraction the interesting rules for internet customers. The equal length patterns are generated with two ways - attribute addition and attribute reduction. We applied the generated equal length data in an unsupervised neural network in order to find the clusters. After getting the cluster, we extract the correlation through CCA. Maximally correlated customers are found out from correlation. 24 district customers are extracted. The most important rule is Rule 9. From these rules, the most important web pages are 31.50, 3.25, 46.17, 46.19, 45.02, 46.18, 46.20, and 46.22.

Online traders often want the interesting web sites which are attractive to their customers. The important search patterns of customers from their search histories are sorted out. There are other pages and commodities which may attract the customer's attention as well. The results are important for the policy makers of companies or organizations to adapt online customer's interest.

Clustering Rule

Rule 1:
If ((31.05 or 1.26 or 3.25) and (1.34 or 1.72 or 3.80 or 3.23) and 46.17 and 46.19 and 45.02 and/or 46.21 and 46.18 and 46.20 and 46.22) then cluster A

Rule 2:
If ((31.50 or 0.54) and 46.17 and (44.97 or 44.91 or 44.79) and 46.19 and 45.02 and 46.18 and 46.20 and 46.22) then cluster B

General Rule

Rule 3:
If (31.50 and46.17 and 46.19 and 45.02 and 46.21 and 46.18 and 46.20 and 46.22) then Cluster A (41), B (94), C (42), D (15, 78), E (21, 30, 55)

Rule 4:
If (3.25 or 0.54 or 1.26 or 2.79 and 46.17 and45.02 and 46.19 and/or 46.21 and 46.18 and 46.20 and 46.22) cluster A (1, 24,100), B (57), E (61), F (71).

Fig. 10: Interesting Rules

REFERENCES

[1] Kyootai Lee, and Kailash Joshi, "An empirical investigation of customer satisfaction with technology mediated service encounters in the context of online shopping," *Journal of Information Technology Management*, vol. XVIII, no. 2, pp. 18-37, 2007.

[2] Ranzhe Jing1, 2, Jianwei Yu2, Jiang Zuo2, "Exploring influence factors in e-commerce transaction behaviors," *IEEE International Symposium on Electronic Commerce and Security*, Guangzhou City, pp. 603-607, 2008

[3] David J. Hand, Heikki Mannila and Padhraic Smyth, *Principles of Data Mining*. MIT Press, Massachusetts, USA.

[4] Huberman, B. A., Pirolli, P. L. T., PitKow, J. E., Lukose, R. M., "Strong Regularity in World Wide Web Surfing," *Science*, 280(3) pp 95-97., 1998.

[5] Cadez I., Heckerman D., Meek C., Smyth P, and White S., "Visualization of Navigation Patterns on a Web Site Using Model-Based Clustering," *Technical Report MSR-TR-00-18*, *Microsoft Research, Redmond, WA* . 2000.

[6] Jeffrey Xu Yu, Yuming Ou, Chengqi Zhang, and Shichao Zhang "Identifying Interesting Customers through Web Log Classification" *IEEE trans. On Intelligent System*s, pp. 55-59, 2005.

[7] Md. Asaduzzaman, Md. Shahjahan, M.M. Kabir, M. Ohkura, K. Murase (2008), " Generation of Equal Length Patterns from Heterogeneous Patterns for Using in Artificial Neural Networks," *Proceedings of the International Joint Conference on Neural Networks (IJCNN2008*), Hong Kong, June 1-6, 2008, pp.3382-3387.

[8] Steven C. Chapra and R. P. Canale, *Numerical methods for engineers*. 3rd edition, McGrowHill, 1998.

[9] http://www.mnstate.edu/wasson/ed602ztestex.htm

[10] http://en.wikipedia.org/wiki/Data_clustering

[11] Simon Haykin, *Neural network: A comprehensive foundation*. 2nd edition, Pearson edition, 2005.

Proceedings of 2009 12th International Conference on Computer and Information Technology (ICCIT 2009)
21-23 December, 2009, Dhaka, Bangladesh

Design and Development of a Wall Climbing Robot and its Control System

Md. Akhtaruzzaman, Nurul Izzati Bt Samsuddin, Norsofiana Bt Umar, Mozasser Rahman
Department of Mechatronics Engineering, International Islamic University Malaysia, Kuala Lumpur, Malaysia
akhter900@yahoo.com, ixaty@yahoo.com, sofie_umar@yahoo.com, author4@net.edu

Abstract

The Robot, named as TRAIN WALL BOT, is designed to navigate on smooth vertical surfaces with the capability to avoid obstacles and overcome if the height is about 1cm. The design is inspired from train steel wheel movement that contains two actuated legs with rotary motion provided by a DC motor. The Robot uses pneumatic system and the suction force is supplied by an air compressor that turns on intermittently. The suction force ensures the attachment of the robot with the wall by using 3 vacuum valves and 6 vacuum pads. The robot is controlled using PIC 16F877A. Two limit switches are used to acknowledge the contact with its navigating surface. Vacuum suction is controlled based on the ON OFF priority of the limit switches. Though the design is quiet simple but it is capable to walk, climb vertical smooth surfaces and avoid obstacles. Forward and backward movements are also faster, smoother and more stable (because of the coupling design) than other existing wall climbing Robots. In this paper, various aspects of prototype design and development of the Climbing Robot are conveyed including the body, leg, feet design and gait dynamics.

Keywords: Train Wall Bot, Wall Climbing Robot, PIC 16F877A.

I. INTRODUCTION

Nowadays, wall climbing robot is widening up its versatility to stealth and range of exploration. For example, a small climbing robot can locate people trapped in the rubble of fallen buildings, or navigate difficult-to-access systems. A robot capable of functioning on any surface of a structure can be valuable for surface-based operations such as cleaning, painting, and inspection. Researchers have proposed a variety of climbing robots for various applications. In general these robots use three types of adhesion mechanism like vacuum suction (Wall Crawler Robot shown in figure 1.a), magnetic attraction (Tank Vert Robot shown in firuge 1.b) and gripping with claws or grasping mechanism (Wall Climbing Spider Robot in figure 1.c).

(a) (b) (c)

Fig. 1. Adhesion mechanism of different types of wall climbing robots.

Each of these mechanisms has some advantages and drawbacks. Magnetic adhesion can be very strong and has good power failure mitigation, but is only applicable for ferromagnetic surfaces. Suction adhesion requires an ambient pressure for attachment and is therefore not suitable for space applications. Micro-claws have shown good performance on brick buildings, but clawed and grasping robots cannot climb smooth surfaces, smooth metal or painted structures.

Technique of the constructed wall climbing robot, described in this paper, is similar to the train wheel mechanism where suction cups are attested to the bottom of the legs and body. It is capable to travel on smooth surfaces with certain inclinations, such as floors, walls, and ceilings. The usages of pneumatic system ensure the attachment of the robot with the surface of the wall while carrying onboard circuits, DC motor and some pneumatic equipment. The main objective is to develop a wall climbing robot that is simple in design, able to walk on smooth vertical surface, able to detect obstacles, able to navigate smoothly and faster compared to existing robots where the system must be cost wise and user friendly.

II. BACKGROUND OF EXISTING WALL CLIMBING ROBOT

A. GECKOBOT

This gecko-inspired robot [2], shown in figure 2a, uses PIC as its main controller and it is able to walk on flat surface, climb and steering. It uses peeling system on its feet to climb. Peeling is a very crucial and challenging task for climbing robots to improve their climbing ability and to minimize power consumption. The robot has a tail and the benefits of having a tail is preloading, holding the surface and maintaining balance in order to move. Pressing against the surface with a tail increases the normal force on the front toes leading secure climbing technique.

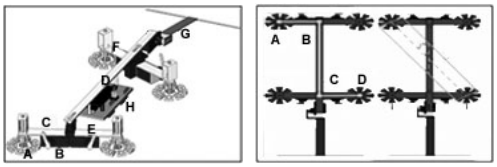

(a) (b)

Fig. 2. Design of Gakobot [2]

The robot body kinematics is composed of a four-bar mechanism as shown in Figure 2b. AB, BC, CD and ground are four linkages. It sequentially pulls two diagonally opposed feet up by using a motor on the four-

bar mechanism, propelling itself forward. Then, the feet that are aloft are attached to the ground and the opposite feet are lifted for the next forward motion. Steering is realized by controlling two servomotors on the four-bar mechanism separately when the other feet are aloft. While the robot is walking, the two motors rotate in a synchronized manner. When steering starts, its rear feet peel off the ground and Geckobot's tail presses harder against the surface. Then, the front motor rotates the whole body to reach the desired angle while the tail is sliding. At the same time, the back motor adjusts itself for the next step to the right angle while rear legs are aloft. PIC16F877A and H-bridges are used as its controller, ultrasonic sensor is used to avoid obstacles, adhesive footpads are used as a primary force that keeps the robot attach with the wall. 12V on board batteries are its power source.

B. WINDOW CLEANING ROBOT (URMAKAMI)

A lead pivoting support surface, such as a pivoting wheel and two or more traction drives, such as drive wheels are mounted on the base of the robotic device. Vacuum pads are mounted on the bottom of the base. The vacuum pads each have a low friction foot, designed for movement over a surface with minimal friction while vacuum is maintained. The robot can move over gaps without losing vacuum in all of the vacuum pads, using a fluid limiting valve at each vacuum pad. The main components of the robotic system are:

- The motor-pulley system to move the robot.
- The motor driver to control the robot's rotational direction and operation.
- The PIC microcontroller and the PCB board to control the robot.
- The solenoid valve and vacuum system to attach the robot to the window.
- Ultrasonic sensor to avoid obstacles.

Fig. 3. Window cleaning robot.

The concept of the Window Cleaning Robot has already been explored as an alternative to human employees, who run a safety risk in cleaning high rise buildings. However, a concept was needed which would not only guarantee a safe, reliable and efficient window cleaning robot but one that would also be cost-effective.

C. WAALBOT

The Waalbot [2], shown in the figure 4, is constructed with two sets of three-footed wheels that use rotary actuators for a single degree of freedom motion. Like Geckobot, Waalbot uses dry adhesion footpads. A PIC is used and it has onboard power. In addition, a spring-loaded tail ensures the robot will always push against the surface. The Waalbot is capable to walk and climb at any direction, avoid obstacles, steer (up to 180º of rotation) and plane transitions (from horizontal to vertical or vice versa).

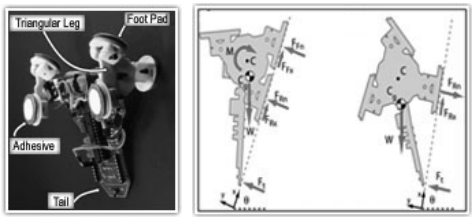

(a) (b)

Fig. 4. Waalbot

The principles of operation of the Waalbot are as follows:

- As the motors turn, the tail of the robot presses against the surface and the triangular legs rotate forward. The two feet which are adhered to the surface, supports the weight of the robot. At this position there are 5 contact points with the surface, 2 feet on each side and the tail.
- The motor torque provides an internal moment which presses the front feet onto the surface while pulling the rear feet away from the surface.
- When the rear foot reaches a critical peeling value, the adhesive peels away from the surface and the robot steps forward.

For the controller part, microcontroller and H bridge drivers are used to control the Waalbot. To detect the obstacles, ultrasonic sensors are mounted with the robot body. For the peeling system, adhesive footpads are used. Table I shows the summary of the described wall climbing robots components.

Table I Summary of the existing wall climbing robots.

	Geckobot	**Window Cleaning Robot**	**Waalbot**
Mechanical design	Gecko lizard inspired	4 feet and a body	Triangular legs inspired
Actuators	Electrical (servomotor)	Pneumatic	Electrical (servomotor)
Sensors	Accelerometer & ultrasonic sensor	Pressure Sensor	Ultrasonic sensor
Controller	Microcontroller (16F877A)	Microcontroller 16F877A	Microcontroller (16F877A)
Motor	DC Motor	Power Window Motor	DC Motor

III. MECHANICAL DESIGN OF THE TRAIN WALL BOT

The design is very simple having three main parts, the body or base, legs and coupling. Figure 5(a) shows the Train Wall Bot indicating its three basic parts.

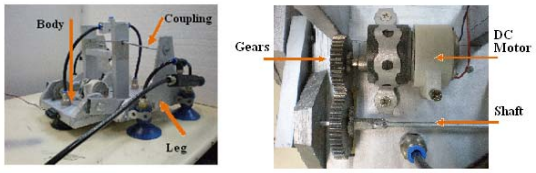

(a) (b)

Fig. 5. The Train Wall Bot (a) and some of its components (b).

The size of the body part is, 23 cm in length, 15 cm in width and 1.5 cm in thickness where the motor, gears and sensors are mounted on. The two vacuum pads are attested at the bottom part of the body. Two legs (each 23cm * 1.5cm * 1.5cm) have four vacuum pads attested at the bottom. The leg pair has one degree of freedom because of four bar linkage mechanism. The H shape coupling parts ensures the simultaneous rotation of both legs.

A. MATERIAL SELECTION

To ensure light weight and strong structure, aluminum is used to construct the body and leg of the Robot. For climbing and sticking to the wall, pneumatic system is used. Air compressor (30 bar or 340 psi) system is chosen to ensure the pneumatic system to work. Tube connectors are used to connect the vacuum pads with the air compressor which is a mechanical device that increases the pressure by reducing the volume of air. Three solenoid valves are used to control the air flow of the pneumatic system. The solenoid valves works as ON and OFF switch which is control by the PIC 16F877A. This PIC is chosen as the main controller of the whole system. The PIC also controls the rotational speed and direction of the DC motor having torque output approximately more than 500Nm. This DC motor generates the rotational movement (forward and backward) of the Robot. To transfer forces to the shafts, two gears are used with the motor. The shafts help to rotate the two legs simultaneously. The figure 5 (b) shows the DC motor, gears and shafts of the Robot. The interlocking of the teeth in a pair of meshing gears means that their circumferences necessarily move at the same rate of linear motion (meters per second). The smaller gear makes more revolutions in a given period of time; it turns faster. Here it is consider as, 30rpm = 1m/s.

B. CALCULATION OF FORCE AND TORQUE

For the rotational movement of the robot there are two different positions to attach with the climbing surface. One, leg is attested with the surface while body is moving, two, the body is attested with the wall while legs are moving. Figure 6 shows the two different and important positions of the Wall Bot which are related to its navigation mechanism. To determine the forces acting to move the robot during climbing action, it is necessary to consider the above two conditions. To calculate force, it needs to follow some steps like, finding volume, mass and weight.

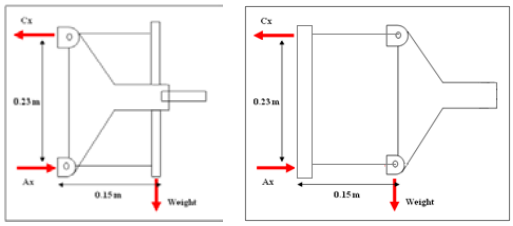

(a) (b)

Fig. 6. (a) Leg is attested with the wall, (b) Body is attested with the navigating surface.

The Train Wall Bot has two legs which moves simultaneously based on the only one motor which is mounted on the Robot Body. Based on this structure it is ensured that the Robot has one degree of freedom. The specification of the robot is given in the table II.

Table II Specification of Train Wall Bot.

Robot specification	
Mass	(1.81 + 0.68) = 2.49 kg
Length	23 cm
Height	15 cm
Width	15 cm
Turning radius	10 cm
Step length	10 cm
Vacuum pads area (per foot)	$Pi*r^2=Pi*4^2=50.24cm^2$
Force	25.48N, 9.572N
Torque	2.58 N.m, 0.96 N.m
Pressure (per foot)	$2.548*10^{-4}$ m², $0.957*10^{-4}$ m²
Speed	0.625m/s = 5.95 rpm

C. GAIT DESIGN OF TRAIN WALL BOT

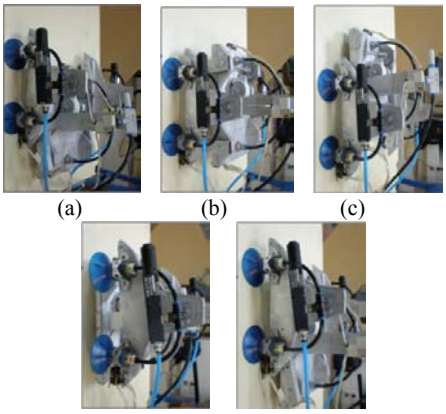

(a) (b) (c)

(d) (e)

Fig. 7. Steps of forward movement of the designed Robot.

TRAIN WALL BOT simultaneously rotates both legs by using a motor assisted with coupling system, propelling itself forward. At the beginning the robot starts from its rest position (considered as 0º), vacuum pads on the legs attaches to the wall (ON mode) while vacuum pads of the body is free from the wall (OFF mode). Hence, body rotates forward. At 180º and it touched the climbing surface. At this condition vacuum

pads of the body become attested with the surface (ON mode) and vacuum pads on the legs are become free (OFF mode). Hence, legs rotate forward. Following this technique the robot moves onward. For backward movement the robot will follow the same technique but in reverse order. Figure 6 shows the steps of forward movement of the robot.

IV. DESIGN OF CONTROLLER

Figure 8 shows the close loop diagram of the control system. The controller is activated when the input switch is on and it gives instruction to the motor to rotate in a certain speed to move the robot forward. The controller also gives the instruction to the system to continue the climbing mechanism by controlling the solenoid valves of the pneumatic device. If the IR distance sensor senses an obstacle, it will give feedback to PIC and the PIC will control the motor to move in reverse order for the backward movement of the robot.

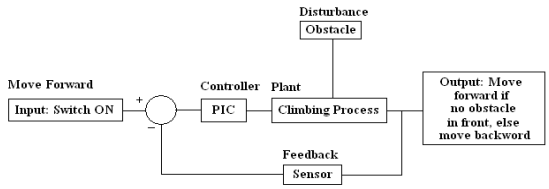

Fig. 8. Close loop diagram of control system, designed for the Train Wall Bot.

The Microchip's PIC16F877A, the 40 pin 8-bit CMOS Flash Microcontroller is targeted to provide single chip solution to control digital motion. The chip has 8 Kbytes of FLASH programmable memory, 360 byte of data memory (RAM), 256 byte of EEPROM Data Memory, 33 input or out put pins. The controller may receive analog signal input from up to 8 channels. The operating speed of the controller is provided by 20MHz clock input DC. The controller has two PWM outputs for each module from where only one is used to control the speed of the motor. In this project DC Geared Motor – SPG30 – 150K is used to control the rotary movement of the Robot. For DC motor it is easy task to reverse the rotational direction of the shaft by simply changing the polarity of the DC input. Another big advantage of DC motor is to control the variable speed of the motor shaft movement and can be achieved with just a suitable variable resistor or variable DC power supply. For more precise control to get the maximum efficiency, electronic PWM solution is the most preferable technique. The operating voltage of the Motor, used in this project, is 12V where power is 1.1W. The rotational speed and torque are 30 RPM and 588 mN.m respectively. The weight of the motor is 160 gram.

MD30B Enhanced 30A Motor Driver is used with the main controller because of its low cost and easy to use and capable to drive up to 30-Ampere peak motor current. This motor driver has 5V logic level inputs, bidirectional control for one motor, onboard PWM generation and PWM speed control up to 10KHz, Heat sink with fan for faster thermal release and pluggable connector for more user friendly design.

V. SENSORS AND SWITCHES

Infrared Sensor (SN GP2Y0A21 Sharp IR) is used to detect obstacles. The mechanism is simple where a pulse from IR sensor is emitted by the emitter. The light is travel out and in the case of no object, the light is never reflected and the reading shows no object in front of the robot. If the light reflects and returns to the detector, it creates a triangle with the point of reflection, the emitter and the detector. On this moment the reading can be detected as digital IO that indicates the presence of obstacles. The detection range of the sensor is about 10 to 80 cm and average current consumption is 30mA. Figure 8 (a) shows the triangular detection technique of IR Sensor.

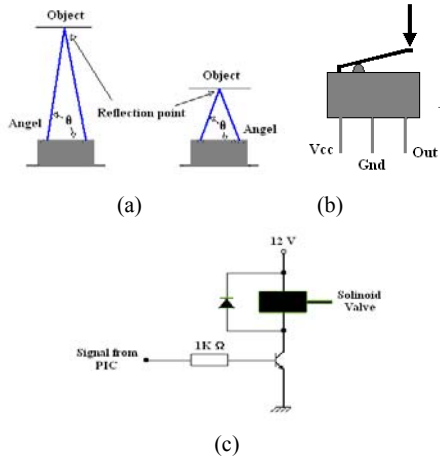

Fig. 9. (a) IR sensor triangulation technique, (b) Limit switch with digital I/O, (c) Valve control switch.

Two mechanical limit switches are used to detect the contact or touch of the climbing plane. The switch has the digital output signal that is sensed by the controller and it controls the electronic switches of the pneumatic device. Two transistors (2N3055) are used as the electronic switches that control the solenoid valve of the pneumatic device. The 2N3055 is a silicon Epitaxial-Base Planar NPN transistor mounted in Jedec TO-3 metal case. It is intended for power switching circuits, series and shunt regulators, output stages and high fidelity amplifiers. The output voltage, 5V, from PIC will switch ON the transistor, and 12V power supply will flow through the solenoid valve of the vacuum pump that causes the valve to become on and continuous air flow ensures the suction mechanism of the pneumatic device. Figure 9 (b) and (c) shows the diagram of limit switch and solenoid valve control switch of the whole system.

VI. ALGORITHM DESIGN

At the initial position when the robot starts to move, the both of the limit switches (legs and body limit switches) are on. In this position the solenoid valve for the leg must be on to make sure that the leg is attested with the

moving plane and the valve for the body part must be off which gives the capability to move the body. This action turns off the limit switch of the body and the switch is on again when the body touches the surface after completing first step. Now the solenoid valve for the body must be on and the valve for the leg must be off so that the robot can attach with wall and have the capacity to move its legs to keep its motion continuous. While the robot began to move its legs the limit switch attested with leg becomes off and it becomes on again at the moment of touching the wall for second time. In this position the robot comes to its initial state again from which it began to start moving. Here the limit switches are considered as sensors that send signals to the controller when it touches the surface of the wall. To maintain this moving process a truth table (shown in the figure 10) is formed and based on this truth table the main algorithm is designed and implemented to the device.

	Parameters			Actions	
	Limit Switch (Leg)	Limit Switch (Body)	State Flag	Valve (Leg)	Valve (Body)
1	1	1	0	1	0
2	1	0	1	1	0
3	1	1	1	0	1
4	0	1	0	0	1
5	1	1	0	1	0

Fig. 10. Truth table to control the suction valves.

After each five steps the Robot comes to its initial state. Here a State Flag variable is considered to indicate the state condition while moving forward or backward. First line shows the initial state of the robot where limit switches for both leg and body are on while flag is 0 (zero). When body starts moving and loses the contact with the surface, the condition is considered as the second stage of the moving procedure and the stage flag becomes 1 but the action remain same. At the moment of touching the plane with the body part the third condition will occur indicating the third line of the truth table. The next condition will appear while the leg is moving and finally it will reach to its initial stage indicating the 5th line of the truth table which is same as the line one. Figure 11 shows the flow diagram of the whole process.

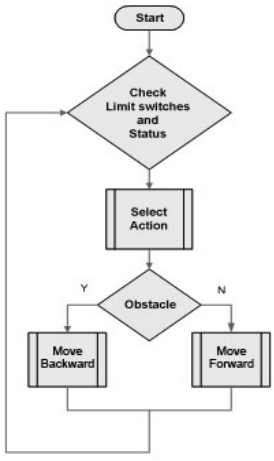

Fig. 11. Flow diagram of movement control algorithm.

VII. CONCLUSION

In terms of mechanical design, the motion is limited to climb only in the horizontal or vertical plane by its rotational stepping technique while it is capable to move over a certain height of obstacles. The design of the robot is very simple, cost wise, user friendly and it can move faster than other existing climbing robots. The designed robot has one degree of freedom, so it is not possible for the agent to move on zigzag path which can be considered as one of the limitations of the system. Multi directional movement and plane transition capability can be achieved by changing the design of the mobile agent by increasing the degree of freedom. The response of the robot to its environment can be increased by adding more sensors. In addition, the vision sensor can be installed which will be a great enhancement of this climbing robot. The implementation of wireless communication module (radio frequency or Infrared) will enhance the device one step forward for research and other uses that can be performed by the climbing robot. Robot to robot collaboration, multi agent communication system and remote tele-operation through a host computer, local and global localization for indoor navigation system may be one of the important applications of the designed robot. Furthermore, adding a gripper will allow implementing of algorithms for carrying objects (cooperatively by multiple robots if desired). As the early stages of the wall climbing robot development, the Train Wall Bot will play a great role in the research area of this field.

REFERENCES

[1] Bing L. Luka,*, David S. Cooke b, Stuart Galt c, Arthur A. Collie d, Sheng Chene, *Intelligent legged climbing service robot for remote maintenance applications in hazardous environments,* Department of Manufacturing Engineering and Engineering Management (MEEM), City University of Hong Kong

[2] Michael P. Murphy† *Geckobot and Waalbot: Small-Scale Wall Climbing Robots* mikemurphy@cmu.edu, †Department of Mechanical Engineering Carnegie Mellon University Pittsburgh, PA, USA

[3] William Tso, Michael Tanzini, Metin Sitti,Michael P. Murphy, *Waalbot: An Agile Small-Scale Wall Climbing Robot Utilizing Pressure Sensitive Adhesives* Department of Mechanical Engineering, Carnegie Mellon University, Pittsburgh, Pennsylvania 15213

[4] Weimin Shen and Jason Gu, *Permanent Magnetic System Design for the Wall-climbing Robot,* department of Electrical and Computer Engineering, Dalhousie University, 1360 Barrington St.,NS B3J2X4, Canada

[5] Yanjun Shen, *Permanent Magnetic System Design for the Wall-climbing Robot* College of Science, Three Gorges University, Yichang, Hubei Province 443002, China

Proceedings of 2009 12th International Conference on Computer and Information Technology (ICCIT 2009)
21-23 December, 2009, Dhaka, Bangladesh

Development of a Translation Model from HTML to WML using Component Based Information Extraction Technique

Md. Ashik Ali Khan, Md. Liakot Ali
Institute of Information and Communication Technology, BUET, Dhaka, Bangladesh
khan.ashik@gmail.com, liakot@iict.buet.ac.bd

Abstract

Now-a-days mobile is part of our daily life. So mobile browsing is becoming popular issue day by day. Today most web pages are written in HTML. Mobile Browsers are optimized for displaying web content. It has low-memory capacity and low-bandwidth. So, mobile browser cannot render all html documents in its limited area. Specific information of particular web page needs to visualize for mobile users. So the effective conversion from HTML to WML becomes a key issue for reducing tedious work. In this technique, not only convert static content, but also some sort of dynamic content will be converted and it improved the conversion effectively in speed and accurate rate, whilst presented the useful information conveniently to the users.

Keywords: Hierarchical Data Extraction, HTML-to-WML Converter, HTML Tree, HTML Parser.

I. INTRODUCTION

In a globalize-world where mobile commerce has attracted more and more users of all ages with its convenient and fast trading mode. However, mobile devices are the lack of Web content specifically designed for these types of devices.

To enable a web page for different mobile users, web pages are written twice. When a user requests a web server, web server checks HTTP USER AGENT to determine which type of browser requests.

At the moment, there are large numbers of resources that users are not concerned on the product pages of enterprises portal and electronic market places. As a consequence, users can only visualize a very small part of the Web and could not get what they need. Thus, the effective conversion from HTML to WML becomes a key issue for movable buyers. Previously, different solutions were proposed to convert HTML content to WML [1-2]. LazyWAP is a HTML to WML converter which converts HTML contents to WAP compatible format [1]. Liu and Shu proposed a method base on information extraction and discarding [2]. But these converters cannot satisfy the conversion demand. They take the whole HTML document as URL, and then converts based on corresponding rule and the arithmetic is too time- consuming to satisfy the demand of mobile commerce. The main problem, not at least, is that the large amount of html text and tags converts to corresponding WML tag and text and there is no guarantee that mobile browser render all the documents at a time. Because the structural difference between HTML and WML cannot support effective direct conversion. In HTML page, all the documents are combined and a few information of large page are suitable for certain user. On the other hand, information in WML pages is clustered. Mobile browsers display only one cluster at a time [3].

In this paper, we discuss about our developed Application Programming Interface (API) and extraction technique that will stay between web server and client and will be executed on HTTP- response. Our API absorbs the merits of information extraction and considers the structure features of commerce information.

II. RELATED ANALYSIS

A. COMPARATIVE ANALYSIS OF HTML AND WML

At present, most web pages are still compiled with HTML. They can't be displayed on mobile user's browsers directly. In order to make the conversion favorably, we must identify the relationships and distinctions between HTML and WML.

HTML and WML are both marked languages, and mark information with a pair of mutual tags. HTML is a subset of Standard Generalized Markup Language (SGML), which is an international publishing standard in existence since 1986. WML is a markup language based on eXtensible markup language (XML) and intended for use in specifying content and user interface for narrowband devices, including cellular phones and pagers [4]. WML tags are in some way logically subset of HTML tags. Therefore, it is not always possible to substitute an HTML tag of an HTML file with a corresponding WML tag [5]. As shown in Table I, there are many differences between HTML and WML.

Table I Differences between HTML and WML

	HTML	**WML**
Applied devices	Desktop computers.	Wireless devices, i.e., cellular phones, PDAs.
Scripting	JavaScript, VBScript	WMLScript.
Focus	Data format showed.	Data and its structure.
Feature	Content is integrated with presentation.	Content separate from presentation
Document Structure	·Loose. ·An HTML file con-	Well-formed. A WML file may

978-1-4244-6283-4/09/$26.00 ©2009 IEEE

	tains a single HTML page.	contains a single WML deck, and multiple WML cards constitute a single WML deck.
Language rules	Multiple white spaces are treated as the number of white spaces. No distinction between capital and lower case.	Multiple white spaces are treated as the single white space
Document Type Declaration (DTD)	<!DOCTYPE HTML PUBLIC" -//W3C// DTDHTML4.01//EN" "http://www.w3.org/TR/ html4/strict.dtd">	<?xml version ="1.0"?> <!doctype wml public "- //wapforum//dtd wml1.1//en">
Tags	Loose . Fixed, can't be extended artificially. Taking the first letter of abbreviation as a tag which is hard to understand its meaning. No distinction between capital and lowercase.	Strict. Extensible, users can define new tags, i.e. <name><name/> . Tags are easy to read and express the meaning of the data. Capital is different from lowercase. Start and end tags must be matching. ·Nested tags can't be covered by other labels

As is shown in Fig.1, the organization of a WML document largely varies from that of an HTML document.

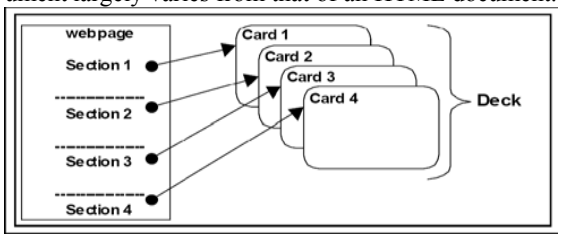

Fig. 1.Web document to card deck relation.

Since WML is an XML application, it is well-formed. But HTML is not well-formed. Rules for HTML tags nesting are loose and not always enforced by web browsers. At the very beginning of the translation process, the underlying HTML page has to be converted into well-formed HTML (i.e. XHTML) [6].

B. STRUCTURE FEATURES OF COMMODITIES WEB

Web pages about commodities usually appear in the product columns of the enterprise portal or the supplying information of electronic market places. The product's information what users focus on is generally presented in the form of a table. The tags <table>, <tr>, <td> always appear nested to make up of a table, so we seem them as a whole when deal with the tags. Then the entire product information is called an information block which can be expressed as an aggregate "B= {x|x=n, n belongs to A}, A represents the attribute domain". The attribute domain usually contains the product's name, style#, color, price and so on. The position of the information block is usually relatively fixed in a web page and the attribute domain in a block has the similar structure, without complex changes. Besides those, there are semantic relationships among different attributes [7]. Therefore, that creates advantageous conditions for conversion based on information extraction.

III. PROPOSED TRANSLATION MODEL

On those previous researches and the comparative analysis of HTML and WML, according to the features of Web pages about commodities, we propose a new translating model from HTML to WML. Its main idea is getting the useful commerce information effectively from a web page through information extraction, not translating all the tags directly. The specified area of a web will be marked by the developer. Then a web service will be called to transform that area into equivalent WML code when user requests to that web page. Figure 2 shows this architecture.

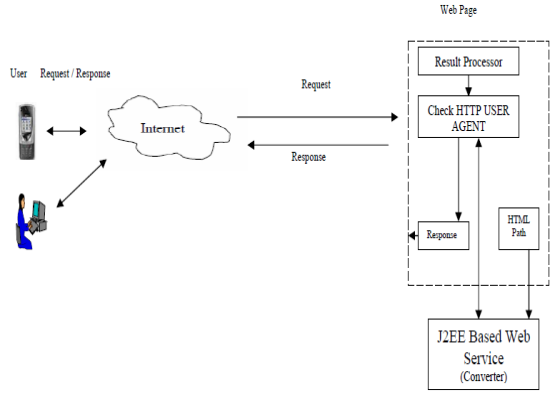

Fig. 2.Proposed Translation Model.

A. ACQUISITION OF WEB PAGE

When a user requests to a web page, then server side language in the web server process the request for that address and check the user agent to determine pc browser or mobile browser. If it is pc browser, corresponding web page will be sent to the client. If it is mobile browser then an API of web service will be called.

The contents of the web page and HTML path will be sent as parameter to that API. Web page about commodities information is shown in fig.3.

Fig. 3.A web page with the information of supplying commodities.

B. DOCUMENT ANALYSIS

HTML is a free type language. Our API transforms the HTML page into XHTML. Then it converts HTML into WML under the sub tree of HTML path. HTML path is written a log file by the developer for a particular web page. HTML path is based on XHTML tree. In this tree, all tags will be traversed recursively and binary search tree is applied for each sibling set will be indexed based on their repetition. A desktop application is developed for document analysis and generate HTML path using above concept.

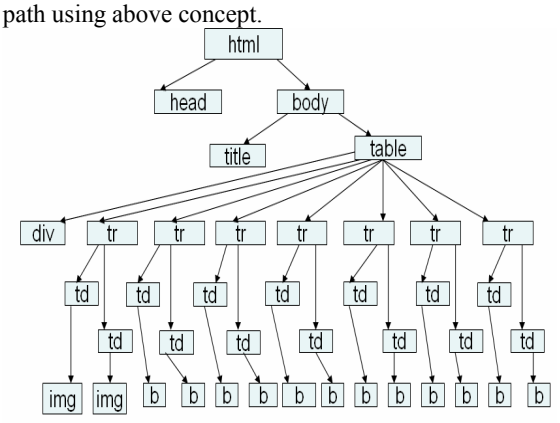

Fig. 4. HTML Tree Concept.

Figure 4 shows HTML tree. This tree will be transformed into another format as shown in figure 5.

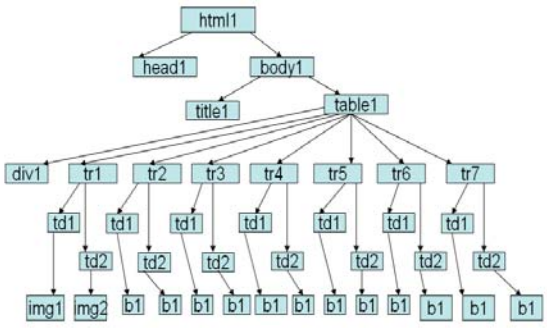

Fig. 5. HTML Path Concept.

HTML path is tree path. Tree is a connected acyclic graph. To extract the highlighted content, the HTML path would be html[1].body[1].table[1].tr[2]. We develop a desktop application for generate HTML path of any web page for developers to extract their necessary contents from a web page. This HTML path would be written in log file. The web service takes the source code of a web page and checks the log file for that URL to extract subtree of that HTML path. Figure 6 shows HTML path extractor.

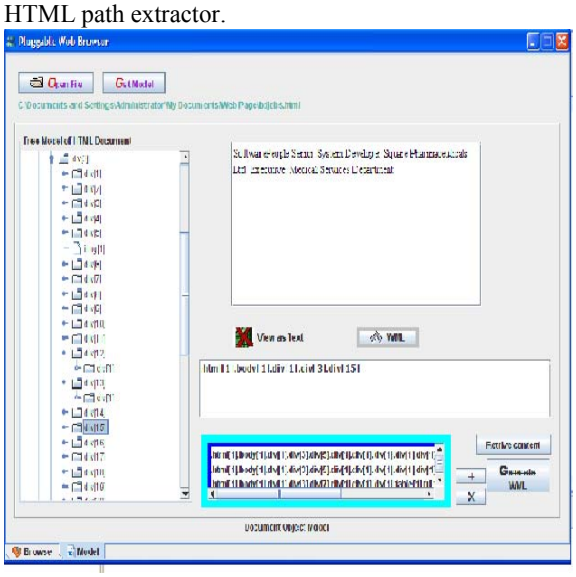

Fig. 6. HTML Path Extractor.

C. CONVERSION OF FORMAT

In the subtree, all tags having WML attribute, which our defined attribute, will be extract corresponding WML tags. All submit button and hyperlink tag would be translated into relative hyperlink tags in WML. We provide a context free grammar as script which translated into WMLScript for user validation. And For large document, we provide several cards and page heading will show “card 1 of n”. So users can navigate between several cards. As shown in figure7, the above page is translated into WML page.

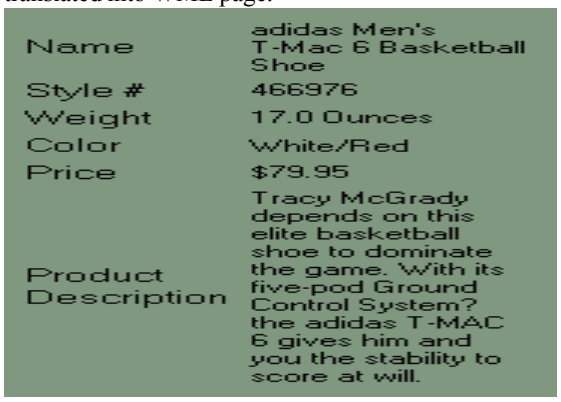

Fig. 7. The generated WML Page.

IV. CONCLUSION

The proposed translating model from HTML to WML appears to be a good solution for mobile commerce to obtain the useful information accurately and comprehensively. It does not only implement the conversion, but also bridge the gap between Hyper Text Transfer Protocol (HTTP) and Wireless Application Protocol (WAP). Therefore, we hope that the new conversion model would be a significant contribution to the ongoing revolution of Internet technology.

REFERENCES

[1] http://www.buzzle.com/editorials/3-12-2004-51586.asp.

[2] Jie L., Bo S. An effective method for translating HTML/XHTML into WML. Journal of Beijing Technology and Business University (Natural Science Edition), Nov, 2006 24(6), pp. 45-48.

[3] Mingqiu S., Bo Y. "A HTML to WML Translating model based on Information Extraction for Mobile Commerce", 4th International Conference on Wireless Communications, Networking and Mobile Computing, 12-14 Oct. 2008. WiCOM'08, pp. 1-4.

[4] WAP Wireless Markup Language specification (WML),http://www.oasis-open.org/cover/wap-wml.html, Nov19, 2002.

[5] Rahman, A. F. R., Alam, H., and Hartono, R., "Content Extraction from HTML Documents", 1st International Workshop on Web Document Analysis (WDA2001), 2001.

[6] ahman, A. F. R., Alam, H., and Hartono, R., "Understanding the Flow of Content in Summarizing HTML Documents", International Workshop on Document Layout Interpretation and its Applications (DLIA), 2001.

[7] WAP Forum, "Wireless Application Environment Overview.", http://www.wapforum.org/: WAP Forum Ltd, June16, 1999.